CHAIN VALLEY COLLIERY – MODIFICATION 2
Statement of Environmental Effects

2

Section 96 Modification to SSD-5465

Prepared for LakeCoal Pty Limited
June 2015

VOLUME 2 of 3 – Appendix D



LakeCoal

EMM
EMGA Mitchell McLennan

VOLUME 2 – Appendix D

Appendix D Subsidence assessment

Appendix D

Subsidence assessment



Appendix D — Subsidence assessment

D

Ditton Geotechnical Services Pty Ltd
82 Roslyn Avenue Charlestown NSW 2290
PO Box 5100 Kahibah NSW 2290

DgS
Ditton Geotechnical Services

LakeCoal Pty Ltd

Subsidence Impact Assessment for the Chain Valley Colliery - Modification 2

DGS Report No. CHV-002/4

Date: 25 May 2015

ABN 43 113 858 910 ACN 124 206 962
Ph: 02 4920 9798 Mob: 0413 094074
Email: steve.dgs@westnet.com.au

25 May 2015

Mr John Arnold
Senior Environmental Planner
EMM
Ground Floor, Suite
20 Chandos Street
St Leonards NSW 2065

DGS Report No. CHV-002/4

Dear John,

Subject: Subsidence Predictions and General Impact Assessment for the Chain Valley Colliery – Modification 2

This report has been prepared in accordance with the brief provided on the above project.

Please contact the undersigned if you have any questions regarding this matter.

For and on behalf of
Ditton Geotechnical Services Pty Ltd



Steven Ditton
Principal Engineer
BE (Civil) CPEng MIE(Aus) MAusIMM

Executive Summary

Chain Valley Colliery (CVC) is an underground coal mine located at the southern end of Lake Macquarie. The colliery is operated by LakeCoal Pty Limited (LakeCoal). Underground mining has occurred at CVC since 1962, with coal extraction undertaken using a combination of bord and pillar and miniwall mining methods. The colliery has extracted coal from three seams – the Wallarah Seam, the Great Northern Seam and the Fassifern Seam, with current extraction activities restricted to the Fassifern Seam as approved under the CVC's existing approval to extract up to 45 Miniwalls, Development Consent SSD-5465 (23/12/2013).

To-date, CVC has completed Approved Miniwalls (MWs) 1 to 8 and is currently extracting MW 9. LakeCoal is seeking an approval under Section 96(2) of the *Environmental Planning and Assessment Act 1979* (EP&A Act) to modify the mining layout by reducing the number of previously proposed miniwalls from 45 to 36 and re-orientating approved MWs 15 to 29 (now constituting MWs 13 to 25 in the modified layout) in the northern mining area.

The modifications to the approved mining layout are summarised in the table below.

Approved Mining Layout Panel No.	Modified Mining Layout Panel No.	Mining Geometry Modification
1 - 5	1 - 5	Extracted - No change except for some extracted panel length reductions
6	Deleted	Main heading access to modified MWs 26 to 31
7 - 8	6 - 7	Extracted - No change except for some extracted panel length reductions
9 - 10	8 - 9	Chain pillar width reduction from 56.4 & 32.6 m to 32.6 m
11 - 13	10 - 12	No change except for some extracted panel length reductions
14 - 19	Deleted	Main headings access to modified MWs 13 to 25
20 - 27	13 - 20	Panels re-orientated from NW-SE to E-W with some chain pillar widths reduced from 32.6 m to a range from 31.6 to 29.3 m. Panel lengths have all changed.
28 - 34	21 - 25	Panels re-orientated from NW-SE to E-W with Panel Widths increased to 97 m from between 89.8 m and 95.5 m and chain pillar widths reduced from 32.6 m to 29.3 m. Panel lengths have all changed. Mining height reduced to between 3.0 and 3.4 to allow for the panel width increase.
35 - 40	26 - 31	Panels re-orientated by 2^{o} with chain pillar widths increased from 30.6 m to 31.0 m. Panel lengths have all changed.
41 - 45	32 - 36	No change except for some panel length reductions to Modified MWs 34 to 36. *Note: Incorrect chain pillar width assumption of 32.6 m to be corrected to the approved width of 30.6 m in this study.*

In addition to the re-orientated panels, the changes to majority of the panel numbers and adjustments to some panel widths and chain pillar widths, albeit minor, have made it necessary to re-present the predictions for all of the miniwalls in the modified mining layout in this report.

Modelling completed for this assessment incorporated *"any relevant information obtained"* since the Development Consent was granted in 2013, including the outcomes of bathymetric surveys, to provide for robust predictions based on the data available.

The most recent bathymetric survey, completed in May 2015, also indicates that subsidence of 570 mm had developed above the tailgate chain pillars of MWs 3 and 6 after eight miniwalls had been extracted. This level exceeds the originally predicted subsidence of 460 mm in this area, but significantly, remains below the predicted maximum subsidence within the single seam mining areas which was used for the impact assessment. The measured tilts and strains and associated environmental impacts are still within the predicted ranges provided in the 2013 EIS.

Based on discussions with the Technical Services Manager at CVC, floor heave observations of 300 mm to 500 mm have occurred along MW3 and MW6 tailgate road ways. The additional subsidence of 110 mm appears, therefore, to be due to the on-going 'softening' and lateral 'squeezing' under increasing pillar load of several thin beds of claystone in the floor (and possibly the ribs and roof) of the Fassifern Seam.

The floor softening is caused by the 'swelling' of moisture-reactive claystone once it is exposed to humid mine air and then subject to the slow development of full pillar loading (16.4 MPa) from the deflecting conglomerate units in the overburden. This moisture (and strain) softening behaviour has been documented at several mines working the Fassifern Seam around Lake Macquarie to-date, as well as the possibility of lateral bearing failures of the softened claystone beds. The possible development of time-dependent subsidence mechanisms were discussed in the 2013 EIS:

"It should be noted that tuffaceous claystone beds associated with the Fassifern Seam and Awaba Tuff can soften to an undisturbed UCS of 2 to 3 MPa due to moisture sensitivity. The beds however are usually 'sandwiched' between stronger shaley coal units with strengths > 10 MPa, thus giving a higher average bearing capacity." and

" *The estimated pillar stresses of 9.75 MPa to 19.83 MPa give an FoS range of 1.51 to 3.08 and indicates that roof and floor strata with applied stresses of less than 15 MPa are likely to have an FoS > 2 and therefore behave elastically. Pillars with stresses greater than 15 MPa may experience local bearing or lateral squeezing failures in the roof or floor strata and increase surface subsidence due to strain softening behaviour.*"

Based on the observed pattern of subsidence to-date, which has been developing as a large bowl with the maximum subsidence occurring at the centre of the developing 'super panel', it is assessed that the additional subsidence is unlikely to be due to the thinning or presence of non-spanning conglomerate beds over the individual miniwalls (i.e. the previous assessment of High Subsidence Reduction Potential (SRP) still stands for these units, which make up more than 50% of the overburden.

The subsidence prediction model has therefore been adjusted to allow for time-dependent increases due to a moisture softened floor consolidation or local lateral bearing failures of thin claystone units.

A summary of the key changes in the mine design parameters and impacts associated with the modified layout are provided in the table below.

Element	Approved Mining Layout	Modified Mining Layout.
Maximum Miniwall Width	97m	97m
Minimum Chain Pillar Width	30.6m	29.3m
Maximum Extraction Height	3.5m	3.5m
Average Vertical Panel Subsidence (single seam mining area)	0.43m	0.66m
Maximum Vertical Panel Subsidence (single seam mining area)	0.62m	0.78m
Maximum Vertical Panel Subsidence (beneath existing workings)	0.89m (0.73m)	1.23m (0.94m)
Panel Tilt (single seam mining area)	2 to 17mm/m (average of 8mm/m)	2 to 15mm/m (average of 12mm/m)
Compressive Strain (single seam mining area)	1 to 6 mm/m (average of 3 mm/m)	1 to 6 mm/m (average of 3.5 mm/m)
Tensile Strain (single seam mining area)	1 to 6mm/m (average of 3 mm/m)	1 to 6 mm/m (average of 3.5 mm/m)

(brackets) - predicted subsidence excludes estimates of subsidence above previous mine working in WAL & GN Seams.

Assessment of Modified Miniwall Layout Subsidence Effects

The modified layout's MWs 9 to 36 are still located entirely beneath Lake Macquarie in areas where the depth of cover ranges from 148 m to 230 m. The miniwalls will still remain outside the High Water Mark Subsidence Barrier (HWMSB) and Seagrass Protection Barrier (SPB).

The interpreted rock cover depth ranges from 132 m to 214 m (average of 167 m) has been determined by subtracting the depth to bedrock contours from the cover depth below the lake bed.

The modified miniwalls will all have nominal void widths of 97 m with face extraction heights between 3.0 m to 3.5 m in the 4.5 m to 8 m thick Fassifern Seam. Chain pillar widths proposed now range from 29.3 m to 32.6 m with pillar lengths of 95 m (solid dimensions). Mine workings road ways (first workings) will be 5.4 m wide and 3.2 m high.

The panel width to full cover depth ratio (W/H) for the modified MWs 9 to 36 will range from 0.42 to 0.66, indicating 'sub-critical' subsidence behaviour. Based on a rock cover only, the W/H ratio increases slightly to a range of 0.45 to 0.74. The Upper and Lower Munmorah Conglomerate units are still considered to be the most likely units to span the modified miniwalls and range in thickness from 11 m to 57 m. Several other conglomerate units between the Vales Point, Wallarah and Great Northern Seams are also assessed to be thick enough to span or have High SRP.

The predicted Upper 95% Confidence Limit values for First and Final maximum incremental panel subsidence ranges from 210 mm to 780 mm (average of 570 mm) for MWs 9 to 31, compared to a maximum of 620 mm previously modelled (an overall increase of 160 mm). Average subsidence has been modelled to increase to 570 mm from the 430 mm previously predicted, i.e. an increase of 140 mm.

Final maximum chain pillar subsidence is estimated to range from 420 mm to 780 mm (average of 570 mm). Maximum panel tilt is estimated to range from 2 mm/m to 15 mm/m (average of 12 mm/m) with maximum compressive and tensile strains ranging from 1 to 6 mm/m (average of 3.5 mm/m). Measured tilt of 3 mm/m and strains of +/- 3 mm/m above MWs 1 to 8 indicates the prediction model is reasonable.

The final mean and U95%CL goaf edge subsidence predictions for the modified MWs 9 to 36 range from 0.04 to 0.25 m and from 0.07 to 0.36 m respectively and brackets the measured goaf edge subsidence of 42 mm to 88 mm above MWs 1 to 8. The measured angle of draw range of 0^o to 12^o above MWs 1 to 8 also indicates the prediction model is conservative with predicted values ranging from 8^o to 30.2^o for the modified layout.

Amended Subsidence Assessment for Chain Valley Bay

The cumulative subsidence (associated with corrected chain pillar widths) after MWs 32 to 36 are extracted is estimated to range between 600 mm and 1230 mm on the lake bed if all workings subsidence (WAL + GN + FAS) are included. The 2013 EIS estimated 495 mm to 886 mm of vertical subsidence would occur (and rounded these to 500 mm to 900 mm).

The increased prediction is associated with a number of factors, including; the 2 m reduction in the chain pillar width from 32.6 m to 30.6 for MWs 32 to 36, which has resulted in a 6% to 8% increase (30 mm to 70 mm) in the predicted subsidence effects previously provided for Chain Valley Bay in the 2013 EIS. A further 75 mm to 270 mm may also occur due to on-going subsidence of the thin claystone beds in the floor of the FAS (a total increase of 105 mm to 340 mm)

The corrected maximum tilt and strain predictions for the multiple seam mine workings area now range from 4 to 15 mm/m and +/- 6 mm/m respectively. The 2013 EIS predicted similar tilts ranging from 4 mm/m to 9 mm/m and strains between +3 to -4 mm/m (tensile strain is positive).

It is also noted that the Applicant has a conditional requirement to undertake and submit a further Multi-Seam Mining Feasibility Investigation prior to submission of an Extraction Plan covering these workings, which will further assess the potential subsidence and risks prior to any mining within the area of existing overlying workings.

Review of Subsidence Measurements To-date v. Predictions for the Updated DgS Modified ACARP, 2003 Model

Subsidence effect and impact predictions for the modified MWs 9 to 36 have been based on DgS modified **ACARP, 2003** model and subsidence effect data from CVCs MWs 1 to 8 and Mannering (Wyee) Colliery's LWs 17 to 23.

Bathymetric surveys above approved MWs 1 to 7 between 2012 and 2014 indicated subsidence of approximately 150 mm to 410 mm had developed after five panels had been completed. This was consistent with the final subsidence predictions presented in the 2013 EIS (i.e. 170 mm to 460 mm). The predicted values however, were exceeded by the 2015 survey with 570 mm occurring after the sixth miniwall had been extracted.

The empirical and analytical subsidence model predictions have now been modified as shown in the previous table and presented in **Table 17** of this report. As discussed earlier, measured tilt, strain, goaf edge subsidence and angle of draw above MWs 1 to 8 to-date have all been within the predicted ranges.

Assessment of Modified Miniwall Layout Subsidence Impacts

For completeness, this report has addressed all of the issues raised previously in relation to the Chain Valley Mining Extension 1 Project Environmental Impact Statement in the Director-General's Requirements (DGRs) and by government agencies relevant to mine subsidence.

As the modified miniwall layout is still wholly located outside a 35^{o} angle of draw to the High Water Mark (HWM), it is still unlikely there will be measureable impact on built features due to the modified mine plan.

The predicted angle of draw of 28.7^{o} from MWs 34 and 35 indicates that approximately 534 m^2 of seagrass bed (length of 95 m and maximum width of 8.5 m) may be subsided by up to 29 mm. It is not expected that this will result in any tilt or cracking impact to the lake bed or significantly increase the mean water depth at this location. The 2013 EIS estimated that up to 50 m^2 area of the seagrass beds may be subsided by up to 30 mm. In consideration of these projected impacts LakeCoal will revise the panel lengths to ensure that the seagrass communities are not subsided.

It is estimated that minor cracking of the rock head below the lake bed sediments of <120 mm width may occur within the goaf edge limits due to the predicted subsidence and strains. The depth of cracking is likely to occur within 10 m of the rock head. It is assessed that the surface zone cracks are unlikely to intersect any deeper strata fractures or bedding dilations associated with subsidence development, and therefore the cracks will naturally infill with lake bed sediments.

The change in subsidence effects due to the modified mining layout compared to the approved mining layout on the lake environment, including seagrass beds, benthic fauna, wave height changes and foreshore erosion will be assessed by specialist consultants.

Assessment of Sub-surface Fracturing for the Modified Mining Layout

The Approved MWs 28 to 32 that were presented in the 2013 EIS were reduced from 97 m to a range from 95.5 m to 89.8 m to maintain a minimum overburden buffer zone thickness (of 12T) between the continuous fracture network above the panels and the surface cracking zone immediately below the lake bed.

Based on a significant improvement to the height of fracturing prediction model applied in the 2013 EIS report (**Ditton and Merrick, 2014**), it is now proposed to maintain these panels at a constant void width of 97 m and reduce the mining height from 3.5 m to a range between 3.0 m and 3.5 m to maintain the 12T buffer thickness (refer **Li *et al* 2006**) and provide increased certainty to the development requirements for the mine plan (i.e. the panel widths to remain constant at 97 m).

The caving and subsidence development processes above a longwall panel usually result in sub-surface fracturing and shearing of sedimentary strata in the overburden. The disturbance to the overburden diminishes with distance above the workings with several distinct zones forming that may be characterised by their connectivity of cracking and hydraulic conductivity changes as described below (in descending order):

- Surface Zone (D-Zone)
- Elastic Constrained Zone (C-Zone)
- Discontinuous Fracture Constrained Zone (B-Zone)
- Continuous Fracture Zone (A-Zone)
- Caved Zone (included in the A-Zone)

Based on U95%CL values, the height of the A-Zone is now predicted to range from 85 m to 111 m for rock cover depths from 132 m to 214 m respectively (or 24T to 32T). The predicted heights of fracturing also coincides with the base heights of spanning Munmorah Conglomerate 'beams' above the modified miniwall layout.

The thickness of the Constrained Zone is estimated to range from 37 m to 93 m above the A-Horizon to the base of the surface D-Zone or 12T to 27T. The predicted Constrained Zone thicknesses above the proposed panel widths are therefore consistent with the minimum thickness recommended by **Forster, 1995** and **Li et al 2006** in similar geological conditions.

The presence of geological structure should, however, still be viewed with caution in regards to its potential interaction with the lake bed above the northern mining area.

Management strategies will continue to identify potential fault affected areas of the Site and deal with disproportionate water inflows into the workings should undermining of a smaller, undetected fault or structure occur. The potential for fault interaction with the multi-seam mine workings is probably lower for MWs 32 to 36, as the overlying seam workings did not encounter any faults of significance.

Monitoring

Due to the recent increased subsidence results from floor softening behaviour, it is recommended that consideration be given to increasing the frequency of the bathymetric surveys to allow the measured incremental and cumulative subsidence to be reviewed against the predictions if the revised model of floor softening needs to be confirmed earlier than the annual survey will allow (see below).

Any significant deviations or exceedances in measured subsidence or impact will need to be assessed and appropriate panel width and/or mining height reductions made to limit future impacts to acceptable levels. It should be understood however, that adjusting the mine plan requires a reasonable amount of forewarning due to the requirement that panels need to be developed several months in advance of miniwall extraction, however adjustments can more readily be made to the mining height, which could be utilised in the event unacceptable subsidence impacts have been detected and shorter term changes to reduce subsidence levels

are required. If the measured subsidence is within the predicted range it is not considered necessary to amend the modified mining layout assessed by this study.

Land based foreshore surveying will continue to be undertaken to confirm subsidence is not impacting the foreshore in the vicinity of the HWM.

Monitoring of groundwater chemistry changes and inflow rates should also be continued as an indirect measure of connectivity between the lake and mine workings and as part of the Extraction Plan or site Trigger Action Response Plan (TARP) requirements.

Underground inspections and monitoring of pillar, roof and floor stability and geological structure mapping should continue to be reviewed, together with groundwater inflow (water make) data.

As mentioned in the 2013 EIS, the presence of a fault, dyke or joint shear zones still have the potential to cause a hydraulic connection between sub-surface and surface fracture zones. It is therefore recommended that significant faults should not be undermined or at least assessed before doing so. The mapping of floor heave and rib spall locations should be routinely done as mining progresses to complement the additional subsidence data review requirement and future mine planning assessment work.

It is noted that Telstra cables are located within the proposed mining area, however these Telstra assets are already subject to an approved Management Plan between LakeCoal and Telstra (dated 16 February 2015) and are therefore not considered further within this report.

Table of Contents

Glossary of Terms

1.0 Introduction 1
1.1 Background 1
1.2 The Modification 1
1.3 Scope of Work 4
1.4 Performance Measure Requirements 6
2.0 Methodology 7
3.0 Available Information 9
4.0 Surface Conditions 10
5.0 Sub-Surface Conditions 11
5.1 Cover Depth 11
5.2 Geological Setting 11
5.3 Geological Model 12
5.4 Geotechnical Properties of Rock Mass 14
5.5 Geological Structure 15
6.0 Mining Geometry 17
7.0 Review of Subsidence Data 20
7.1 Chain Valley Colliery's Subsidence Data 20
7.2 Time Dependent Subsidence Mechanism 21
7.2.1 Pre-consolidation Pressure of Claystone Units 22
7.2.2 Primary and Secondary Consolidation 23
7.2.3 Time rate of Consolidation 24
7.3 Observed Floor Heave Considerations 24
7.4 Bearing Capacity of Roof and Floor Strata 25
7.5 Summary 26
8.0 Subsidence Predictions for the Modified Mining Layout 27
8.1 General 27
8.2 Geological Model and Subsidence Reduction Potential of Massive Units 27
8.3 Predicted Maximum Single Panel Subsidence 28
8.3.1 Empirical Model Assessment 28
8.3.2 Analytical Voussoir Beam Model Assessment 31
8.4 Maximum Predicted Subsidence above Chain Pillars 34
8.4.1 Chain Pillar Geometry 34

8.4.2 Empirical Model Pillar Stress 34
8.4.3 Empirical Model Pillar Strength and FoS 35
8.4.4 Empirical Model Results 35
8.4.5 Analytical Model Development 37
8.4.6 Analytical Model Results 40
8.5 Analytical Goaf Stiffness Model 42
8.6 Goaf Edge Subsidence Prediction 43
8.7 Angle of Draw Prediction 44
8.8 Multiple Panel Subsidence Prediction 46
8.9 Subsidence Profile Predictions 50
8.10 Predicted Subsidence Increases due to Multi-Seam Workings Stress Interaction from Modified MWs 32 to 36 50
8.11 Modified Mining Layout v. 2013 EIS Subsidence Effect Predictions 52
9.0 Prediction of Subsidence Impact Parameter Contours 56
9.1 Calibration of the SDPS® Model 56
9.2 Predicted Subsidence and Post-Mining Surface Level Contours 58
10.0 Subsidence Impacts and Management Strategies 59
10.1 General 59
10.2 Surface Cracking 60
10.2.1 Predicted Impacts 60
10.2.2 Impact Management Strategies 61
10.3 Sub-Surface Cracking 61
10.3.1 Sub-Surface Fracturing Zones 61
10.3.2 Sub-Surface Fracture Height and Constrained Zone Thickness Prediction Models 62
10.3.3 DgS, 2014 Geometry Pi-Term Model 64
10.3.4 DgS, 2014 Pi-Term Geology Model 65
10.3.5 Forster, 1995 T-Based Model 66
10.3.6 Panel Width-Based Models 66
10.3.7 Continuous and Discontinuous Sub-surface Fracture Height Predictions 67
10.3.8 Discussion of A-Zone Horizon Model Predictions 69
10.3.9 Discussion of B-Zone Horizon Model Predictions 70
10.3.10 Discussion of Constrained Zone Thickness Predictions 70
10.3.11 Discussion of D-Zone Horizon Model Predictions 70

10.3.12 Impact on Rock Mass Permeability 70
10.3.13 Review of Height of Fracturing above Wyee Longwalls..... 71
10.3.14 Discussion of Prediction Model Uncertainties and Spanning Strata 72
10.3.15 Discussion of Height of Fracturing Interaction with the Great Northern and Wallarah Seam Panels..... 73
10.3.16 Geological Structure Interaction Potential..... 73
10.3.17 Impact Management Strategies..... 74
10.4 Angle of Draw Effects on Seagrass Beds..... 75
10.5 Sea Level Rise and Subsidence Effects on Pillar Stability..... 75
10.6 Subsidence Effects on Wave Height and Foreshore Erosion 76
10.6.1 Potential Impacts..... 76
10.6.2 Impact Management Strategies..... 76
11.0 Monitoring Requirements 77
11.1 Subsidence Development 77
11.2 Surface Monitoring Plans..... 78
11.3 Sub-Surface Monitoring..... 78
12.0 Conclusions and Recommendations 79
13.0 References 81

Figures 1 to 32

Appendix A - Summary of the Modified ACARP, 2003 Empirical Subsidence and Height of Fracturing Prediction Models

Appendix B - Extract from SDPS® User Manual and Lam2D Model Details

Appendix C - Pillar Stability and Subsidence Calculations for Multi-seam Interaction

Glossary of Terms

Angle of Draw (AoD) — The angle to the vertical from the sides or ends of an extracted miniwall panel and the line drawn from the limits of extraction at seam level to the 20 mm subsidence contour at the surface. The 20 mm subsidence contour is an industry defined limit and represents the practical measurable limit of subsidence.

Barrier Pillar — The pillar of coal left beneath sensitive surface features (e.g. High Water Mark and seagrass beds) or significant geological structure (i.e. faults or dykes).

Chain Pillars — The pillar of coal left between adjacent miniwall panels. The pillars form a barrier that allows the goaf to be sealed off and facilitates tailgate roof stability during miniwall panel extraction. The height of the chain pillars is usually the same as the *development height*.

Compressive Strain — A decrease in the distance between two points on the surface. Compressive strains may cause shear cracking or steps at the surface if greater than 3 mm/m and are usually associated with concave curvatures near the middle of the panels.

Confidence Limits — A term used to define the level of confidence in a predicted *Subsidence Effect* (see definition below) subsidence impact parameter and based on a database of previously measured values above geometrically similar mining layouts.

Cover Depth (H) — The depth (H) from the surface to the mine workings roof horizon.

Critical Panels — Miniwall panels that are almost as deep as they are wide (W) (ie $0.6 < W/H < 1.4$) and is the point where failure of the overburden starts to occur if no massive strata is present (i.e. panel geometries are transitional between sub and super critical panels).

Massive strata may continue to span but the maximum subsidence will be greater due to the bending action rather than the natural arching mechanism. Maximum subsidence above panels with non-spanning strata will approach values that are proportional to the mining height.

Curvature — The rate of change of tilt between three points (A, B and C), measured at set distances apart (usually 10 m). The curvature is plotted at the middle point or point B and is usually concave in the middle of the panel and convex near the panel edges.

i.e. curvature = (tilt between points A and B - tilt between points B and C)/(average distance between points A to B and B to C) and usually expressed in 1/km.

	Radius of curvature is the reciprocal of the curvature and is usually measured in km (i.e. radius = 1/curvature). The curvature is a measure of surface 'bending' and is generally associated with cracking.
Credible Worst-Case	The Credible Worst-Case (CWC) prediction for a given *Subsidence Effect* and is normally the Upper 95% Confidence Limit determined from measured data and the line of 'best fit' or mean used to calculate the mean value. The CWC values are typically 1.5 to 2 times the mean values.
Design Angle of Draw (Design AoD)	The 'practical' angle of draw (AoD) used to define minimum or allowable distances from the sides and ends of an extracted pillar panel to sensitive surface features. It is considered to be an effective impact management tool in which to minimise impact from differential subsidence effects parameters such as tilt, curvature and strain, which may cause cracking or instability. A Design AoD of 26.5^{o} has been used with negligible impact to sensitive surface features at the Colliery to-date.
Development Height (h)	The height at which the first workings (i.e. the main headings & gateroads) are driven.
Extraction Height (T)	The height at which the seam is mined or extracted across a miniwall face.
Extraction Plan	The current approval system that is proposed to replace the **Subsidence Management Plan** (see below) and incorporates Project Approval Conditions that are used to define performance criteria and develop subsidence impact management plans.
Factor of Safety (FoS)	The ratio between the strength of a pillar divided by the load applied to the pillar.
Far-Field Displacement	Horizontal displacement outside of the AoD, is due to horizontal stress relief in the strata above an extracted panel of coal. The strains due to these movements are usually < 0.5 mm/m outside a 26.5^{o} AoD and do not cause damage directly. Such displacements have been associated with differential movement between bridge abutments and dam walls in the Southern Coalfield, but generally have not caused any damage to structures in the Newcastle Coalfield.
First Workings	The tunnels or roadways driven by a continuous mining machine to provide access to the production panels in a mine (i.e. main headings and gate roads). The roof of the roadways is generally supported by high strength steel rock bolts encapsulated in chemical resin. Subsidence above first workings pillars and roadways is generally < 20 mm.

Full Tributary Area Load	Refers to the full weight of the prism of rock directly above the pillar of coal supporting it. The prism area is defined by the line drawn half-way between the pillar and the adjacent pillars surrounding it. The volume of rock above the pillar is then determined by multiplying the Tributary Area by the depth of cover. The load is then determined by multiplying the volume by the density of rock (normally assumed to be 2.5 t/m^3).
Goaf	The extracted void behind a retreating longwall or miniwall that the immediate roof of the overburden collapses into soon after the coal has been extracted. The overburden above the 'goaf' then sags down and compresses it, resulting in a subsidence 'trough' developing at the surface.
Horizontal Displacement	Horizontal displacement of a point after subsidence has occurred above an underground mining area within the AoD. It can be predicted by multiplying the tilt by a factor derived for the near surface lithology at a site (e.g. a factor of around 7 to 15 is normally applied in the Newcastle Coalfield by DgS).
Inbye	An underground coal mining term used to describe the relative position of some feature or location in the mine that is closer to the working coal face than the reference location.
Inflexion Point (d)	The point above a subsided area where tensile strain changes to compressive strain along the deflected surface. It is also the point where maximum tilt occurs above an extracted miniwall panel. It is typically located between 0.25 and 0.4 x cover depth from the panel sides, depending on panel W/H ratio.
Longitudinal Subsidence Profile	Subsidence measured (or predicted) along a miniwall panel centre line.
Longwall Panels	Modern longwall panels are extracted using a coal shearer machine that cuts a slice of coal from the workings face as it moves back and forth across a panel between 150 m and 300 m wide. The panels are typically 1 to 3 km long and formed by twin-entry headings or tunnels along each side of the panel (i.e. gate roads). The immediate roof above the shearer is supported by a series of hydraulic supports (known as 'shields'). The shearer and supports move slowly forward at a rate of about 10 m/day.
Mean Values	The average value of a given *Subsidence Effect* (i.e. of subsidence, tilt, curvature or strain) predicted using a line of 'best fit' through a set of measured data points against key independent variables (e.g. panel width, cover depth, extraction height). The mean values are typically

	two-thirds to one half of the Credible Worst-Case values and sometimes lower.
Miniwall Panels	Miniwall panels are narrower versions of Longwall Panels (see Longwall Panels) and are extracted using similar techniques. The panel width is designed to minimise subsidence and impact to the overburden strata and are usually 60 m to 100 m wide, depending on the depth of cover needed to control subsidence and limit surface impact.
Outbye	An underground coal mining term used to describe the relative position of some feature or location in the mine that is closer to the point of mine entry than the reference location.
Outlier	A data point well outside the rest of the observations, representing an anomaly (e.g. a measurement related to a structural discontinuity or fault in the overburden that causes a compressive strain concentration at the surface, in an otherwise tensile strain field).
Panel Width (W)	The void width of an extracted miniwall between chain pillars.
Primary Subsidence	Subsidence that is caused directly by second workings or miniwall mining due to the sagging of overburden after coal is extracted and the immediate roof collapses into the void left behind by the retreating miniwall. Primary subsidence usually occurs soon after the undermining of a given surface location and continues for several weeks as the miniwall retreats further along the panel.
Residual Subsidence	The last 5% to 10% of subsidence that occurs after primary subsidence is complete, and is due to the re-consolidation or re-compaction of goaf and overburden and/or softening of the claystone floor units. It is a time dependent component of the total subsidence and is unlikely to cause further impact to surface features.
Rock Head	The geological boundary in the overburden between competent rock and unconsolidated sediments and weathered rock.
Secondary Subsidence	Indirect subsidence that is likely to occur above an extracted miniwall panel if another miniwall is extracted adjacent to it. The additional subsidence is caused by chain pillar compression and load transfer mechanisms to the goaf. These events can occur several times (at an exponentially decreasing rate) after the passing of at least three or four miniwall panels.
Second Workings	Refers to the removal of coal between first workings pillars and usually results in goaf formation as spans between pillars are significantly increased. Second workings are therefore performed on retreat in a miniwall panel that will no longer be required to provide access or ventilation to a given section of mine.

Shearing	The shortening and distorting effect of compressive strains and shear strains due to mine subsidence on surface terrain, which results in localised shear failures or movements and uplift of soils and rock.
Strain	The change in horizontal distance between two points at the surface after mining, divided by the pre-mining distance between the points. i.e. Strain = ((post-mining distance between A and B) - (pre-mining distance between A and B))/(pre-mining distance between A and B) and is usually expressed in mm/m. Strain can be estimated by multiplying the curvature by a factor derived for the near surface lithology at a site (e.g. a factor of around 7 to 20 is normally applied in the Newcastle Coalfield). Discontinuous overburden behaviour however, can result in local strain and curvature concentrations at cracks, making accurate predictions difficult. A rule of thumb is normally applied to allow for these effects, which is to increase smooth profile strains (and curvatures) by 2 to 4 times occasionally at a given location. The increase in strain also usually develops at locations with exposed rock profiles, as opposed to areas with deep soil profiles.
Sub-critical Panels	Miniwall panels that are much deeper than they are wide (i.e. W/H < 0.6) and cause lower magnitudes of subsidence than shallower and/or wider longwall panels. Subsidence is generally controlled by natural arching action of the overburden across the extracted coal seam.
Subsidence	The difference between the pre-mining surface level and the post-mining surface level at a point, after it settles above an underground mining area.
Subsidence Control Zone	Reducing the impact of subsidence on a feature by modifying the mining layout and set back distances from the feature (normally applied to sensitive natural features that can't be protected by mitigation or amelioration works).
Subsidence Effect	The term used to define the subsidence and differential subsidence parameters (i.e. subsidence, tilt, strain and horizontal displacement) that may or may not have an impact on natural or man-made surface and sub-surface features above a mining area.
Subsidence Impact	The impact that a subsidence effect has on natural or man-made surface and sub-surface features above a mining area.

Subsidence Management Plan	Refers to the approval process for managing mine subsidence impacts. Typically a colliery must prepare an Extraction Plan with specific management plans relevant to the mine to the satisfaction of the Director-General, Department of Planning and Infrastructure before the commencement of second workings.
Subsidence Mitigation/ Amelioration	Modifying or reducing the impact of subsidence on a feature, so that the impact is within safe, serviceable, and repairable limits (normally applied to moderately sensitive man-made features that can tolerate a certain amount of subsidence).
Subsidence Reduction Potential (SRP)	Refers to the potential reduction in subsidence due to massive strata in the overburden being able to either 'bridge' across an extracted panel with sub-critical or critical geometry, or have a greater bulking volume when it fails above super-critical panel geometry. The term was defined in an **ACARP, 2003** study into this phenomenon and is common in NSW Coalfields where massive sandstone / conglomerate units exist.
Super-Critical Panels	Miniwall panels that are not as deep (H) as they are wide (W) (ie W/H greater than 1.4) and will cause failure of the overburden and maximum subsidence that is proportional to the mining height (i.e. 0.5 to 0.6 T).
Tensile Strain	An increase in the distance between two points on the surface. Tensile strains greater than 2 mm/m are likely to cause cracking at the surface with shallow soil profiles over rock and are usually associated with convex curvatures near the sides (or ends) of the panels. Tensile strain also usually develops above chain pillars.
The Site	The area that will be affected by mine subsidence effects from the extraction of the proposed miniwall panels associated with the Chain Valley Mining Extension Area 1. LakeCoal has adopted an area defined by a line drawn at the 35^{o} Angle of Draw from the High Water Mark Level (RL 2.44m AHD) to define the limits of proposed miniwall extraction in most cases. The panels are also located outside the 26.5^{o} angle of draw limits from mapped seagrass beds.
Tilt	The rate of change of subsidence between two points (A and B), measured at set distances apart (usually 10 m). Tilt is plotted at the mid-point between the points and is a measure of the amount of differential subsidence. i.e. Tilt = (subsidence at point A - subsidence at point B)/(distance between the points) and is usually expressed in mm/m.

Transverse Subsidence Profile	Subsidence measured (or predicted) across a miniwall panel or cross line.
Valley Closure	The inward (or outward) movement of valley ridge crests due to subsidence trough deformations or changes to horizontal stress fields associated with miniwall mining. Measured movements have ranged between 10 mm and 400 mm in the NSW Coalfields and are usually visually imperceptible.
Valley Uplift	The phenomenon of upward movements along the valley floors due to **Valley Closure** and buckling of sedimentary rock units. Measured movements have ranged between 10 mm and 400 mm in the NSW Coalfields and may cause surface cracking in exposed bedrock on the floor of the valley (or gorge). The uplift due to valley closure is usually 0.5 to 1 times the closure magnitude.

1.0 Introduction

1.1 Background

Chain Valley Colliery (CVC) is an underground coal mine located at the southern end of Lake Macquarie, approximately 60 km south of Newcastle (**Figure 1.1**). The colliery is operated by LakeCoal Pty Limited (LakeCoal).

Underground mining has occurred at CVC since 1962, with coal extraction undertaken using a combination of bord and pillar and miniwall mining methods. The colliery has extracted coal from three seams - the Wallarah Seam, the Great Northern Seam and the Fassifern Seam, with current extraction activities restricted to the Fassifern Seam as approved under CVC's existing approval (Development Consent SSD-5465, approved 23/12/2013) to extract up to 45 miniwalls.

At the time of this assessment the Colliery had completed Miniwalls (MWs) 1 to 8 and about to commence MW9. LakeCoal is seeking an approval under Section 96(2) of the *Environmental Planning and Assessment Act 1979* (EP&A Act) to modify the mining layout by reducing the number of previously proposed miniwalls from 45 to 36 and re-orientating MWs 20 to 34 on an east-west direction (now constituting MWs 13 to 25) in the northern mining area. The nominal width of all proposed miniwalls is now 97 m, which will increase some of the currently approved panel widths of between 89.8 m and 95.5 m.

No changes are proposed in the multi-seam mining area (except for panel numbering and several minor length reductions) below Chain Valley Bay.

1.2 The Modification

The panel re-orientation and panel geometry modifications will result in a minor reduction of 3.8% to the spatial extent of the proposed mining activities. All secondary extraction, however, will continue to be limited to areas beneath Lake Macquarie with protection barriers for the foreshore and seagrass (see **Figures 1.2** and **1.3**). The approved and modified miniwall layouts are shown in **Figure 1.4**.

The modification to the approved MWs 9 to 45 are detailed in **Table 1** and summarised below:

- The approved MWs 9 and 10 (Modified MWs 8 and 9) will have the chain pillar widths between them reduced from 56.4 m to 32.4 m. The modified MW9 will have its length reduced by 466 m.

- The approved MWs 11 to 13 (modified MWs 10 to 12) will be shifted approximately 24 m south west due to the above chain pillar width reduction. The modified MWs 10 to 12 will have their lengths reduced by 2 m or increased by 7 to 29 m.

- The approved MWs 14 to 19 will be deleted. A portion of the area will now be used for first working access to the north western miniwalls in Myuna Bay (see below).

- The approved MWs 20 to 27 (modified MWs 13 to 20) in Myuna Bay will be re-oriented by 35^{o} from NW-SE to E-W with chain pillar widths reduced from 32.6 m to a range from 32.6 m to 29.3 m. The modified MWs 13 to 20 will have their lengths reduced by up to 355 m or increased by up to 1086 m.

- The approved MWs 28 to 32 (modified MWs 21 to 25) with panel widths between 89.8 m and 95.5 m, will all be increased to 97 m and re-oriented by 35^{o} from NW-SE to E-W. The chain pillar widths will be reduced from 32.6 m to a range from 32.6 m to 29.3 m. The modified MWs 21 to 25 will have their lengths reduced by up to 902 m or increased by up to 91 m. Mining heights for these panels will also be reduced from 3.5m to between 3.0m and 3.4m.

- The approved MWs 33 to 34 in Myuna Bay will be deleted due to the re-orientation of the preceding panels.

- The approved MWs 35 to 40 (modified MWs 26 to 31) will be re-oriented by 2^{o} anti-clockwise with chain pillar widths increased slightly from 30.6 m to 31.0 m. The modified MWs 26 to 31 will have their lengths increased by 23 m to 230 m.

- The approved MWs 41 to 45 (modified MWs 32 to 36) in Chain Valley Bay will generally remain unchanged with MWs 34 to 36 m shortened at their finishing ends by 53 m to 126 m. *Note: The subsidence predictions in the 2013 EIS Report incorrectly assumed the chain pillar widths were to 32.6 m instead of 30.6 m. This report has taken the opportunity to correct this oversight.*

Table 1 - Proposed Amendments to the Approved Mining Layout (SSD_5465)

Approved Miniwall #	Modified Miniwall #	Approved Panel Width (m)	Modified Panel Width (m)	Approved MG Chain Pillar Width (m)	Modified MG Chain Pillar Width (m)	Approved Panel Length (mined) (m)	Modified Panel Length (m)	Comment
1 - 2	1 - 2	72	-	30.5	-	920 (920)		Extracted
3	3	97	-	32.3	-	900 (900)		Extracted
4	4	97	-	39.8	-	868 (411)		Extracted
5	5	97	-	39.8	30.6	761 (761)		Extracted
6	Deleted - Proposed main headings corridor							
7	**6**	97	-	32.4	-	1272 (878)		Extracted
8	**7**	97	-	32.4	-	1191(1191)		Extracted
9	**8**	97	-	56.4	32.4	1152		Extracted
10	**9**	97	97	32.6	32.4	1731	1265	same orientation
11	**10**	97	97	-	-	1816	1814	
12	**11**	97	97	-	-	1906	1935	
13	**12**	97	97	-	-	721	729	

Bold - Proposed panel numbering change; Shaded - proposed geometry change;

Table 1 (cont…) - Proposed Amendments to the Approved Mining Layout (SSD_5465)

Approved Miniwall #	Modified Miniwall #	Approved Panel Width (m)	Modified Panel Width (m)	Approved MG Chain Pillar Width (m)	Modified MG Chain Pillar Width (m)	Approved Panel Length (mined) (m)	Modified Panel Length (m)	Comment
14	-	97	-	32.6	-	534	-	deleted
15	-	97	-	32.6	-	381	-	deleted
16	-	97	-	32.6	-	350	-	deleted
17	-	97	-	32.6	-	428	-	deleted
18	-	97	-	32.6	-	901	-	deleted
19	-	97	-	32.6	-	649	-	deleted
20	**13**	97	97	32.6	32.6	638	593	Re-orientate Panels 35° from NW-SE to E-W with chain pillar widths reduced
21	**14**	97	97	32.6	32.6	687	1513	
22	**15**	97	97	32.6	31.6	760	1740	
23	**16**	97	97	32.6	31.1	760	1846	
24	**17**	97	97	32.6	30.6	1287	1902	
25	**18**	97	97	32.6	29.9	1348	1902	
26	**19**	97	97	32.6	29.3	1348	1892	
27	**20**	97	97	32.6	29.3	1396	1041	
28	**21**	95.5	97	32.6	29.3	1434	908	Re-orientate Panels 35° from NW-SE to E-W. Panels widths increased, chain pillar widths and mining height reduced
29	**22**	93.8	97	32.6	29.3	1434	532	
30	**23**	92.5	97	32.6	29.3	555	542	
31	**24**	89.8	97	32.6	29.3	510	601	
32	**25**	89.8	97	32.6	29.3	510	404	
33	-	88.0	-	32.6	-	510	-	deleted
34	-	86.5	-	32.6	-	440	-	deleted
35	**26**	97	97	30.6	31.0	1508	1589	Small panel re-orientation (2°) & chain pillar width increase
36	**27**	97	97	30.6	31.0	1424	1477	
37	**28**	97	97	30.6	31.0	1253	1277	
38	**29**	97	97	30.6	31.0	510	740	
39	**30**	97	97	30.6	31.0	510	547	
40	**31**	97	97	30.6	31.0	395	418	
41	**32**	97	97	30.6	30.6	1550	1550	No change
42	**33**	97	97	30.6	30.6	1648	1648	
43	**34**	97	97	30.6	30.6	1575	1522	
44	**35**	97	97	30.6	30.6	1376	1292	
45	**36**	97	97	30.6	30.6	1079	950	

Bold - Proposed panel numbering change; Shaded - proposed geometry change;

All of the above geometry changes will result in minor modifications to the maximum subsidence effects and contours previously presented in the 2013 EIS. The change in panel lengths are not expected to cause an increase in the maximum subsidence effect predictions, only the areal extent of subsidence will be modified.

To avoid confusion between the previous and modified mining layouts, the predictions for the modified panels have been provided in their entirety in this report.

It is still possible that hazardous geological conditions or operational efficiency gains that can be achieved in the future may require further miniwall layout changes to be implemented.

However, as is the case with the current modification, the key design features will remain unchanged, i.e. underground mining will be undertaken in a manner that minimises the potential impacts to built features and sensitive environmental aspects as defined in the 2013 EIS (**EMM, 2013**).

1.3 Scope of Work

This report will be used for the purpose of preparing an application to modify development consent SSD-5465 which was approved in December 2013 following the assessment of an Environmental Impact Statement (the 2013 EIS) that was prepared under Part 4 of the *EP&A Act* for a State Significant Development (SSD).

This report has been prepared to include the following scope of work:

- A summary of the maximum predicted subsidence effects and surface / sub-surface impacts resulting from the mining layout to date (approved MWs 1 to 8). Note: The latest bathometric survey (dated 1/05/15) indicates that softening of the claystone floor and slow development of chain pillar load due to spanning conglomerate beds has resulted in greater than predicted subsidence beneath these panels (measured maximum of 570 mm v. predicted maximum of 460 mm above MWs 3 and 6); see **Section 7.1**.

- A summary of the maximum predicted subsidence effects and impacts resulting from the proposed panel geometry modifications defined in **Section 1.2** (i.e. modified MWs 9 to 31) and amended predictions for modified MWs 32 to 36 below Chain Valley Bay.

- Predicted cumulative subsidence effect profiles and contours resulting from the proposed mining layout modification (MWs 9 to 31) and amended predictions for modified MWs 32 to 36 below Chain Valley Bay.

- An assessment of the stability of the FAS floor and chain pillars in the proposed mining layout modification (see below).

- An assessment of the heights of sub-surface fracturing above the proposed mining layout modification (MWs 9 to 36).

The panel geometries for both the existing approved and re-oriented panels have been designed to control mine subsidence effects and impacts to Lake Macquarie and its environs in accordance with mining lease requirements and prior commitments by LakeCoal.

Miniwall face extraction heights will be up to 3.5 m in the 4.5 m to 8 m thick Fassifern Seam. As discussed in **Section 10.3**, the increase in panel width for the modified MWs 21 to 25 will

require the mining height to be limited to a range from 3.0 m to 3.5 m in order to maintain a minimum buffer zone thickness of 12 times the mining height (T) between sub-surface continuous fracture zones and surface cracking zones immediately below the lake bed.

The assessment of the modified mining layout has included a review of predictions against the measured subsidence effects to-date at CVC. The last bathymetric survey (01/05/15) indicated that maximum subsidence of the Lake bed had increased from 400 mm after MW6 to 570 mm after MW8 was completed. This was an increase of the predicted values above MWs 3 to 8.

The subsidence assessment has again considered the Department of Mineral Resources (now Division of Resources and Energy (DRE) within the Department of Trade & Investment, Regional Infrastructure & Services (DTIRIS)) *Guideline for Applications for Subsidence Management Approvals (December 2003).*

The surface and subsurface features of significance that exist within areas of predicted subsidence include:

- Lake Macquarie and its bed sediments;
- benthic fauna communities on the lake bed;
- seagrass beds and fish habitat;
- high water mark (RL 2.44 m, AHD) along the lake foreshore;
- Telstra submarine cables (fibre optic) from Summerland Point to Brightwaters;
- approved MWs 1 to 9 development headings and completed second workings (goaf) for MWs 1 to 8;
- CVC pillar extraction workings in the Wallarah Seam and bord and pillar workings in the Great Northern Seam exist above the modified MWs 32 to 36 in the Fassifern Seam below Chain Valley Bay;
- CVC pillar extraction workings in the Wallarah Seam above small areas of proposed first workings (main headings) in the Fassifern Seam;
- existing Myuna Colliery bord and pillar workings in the Fassifern Seam to the north east of the proposed MWs 13 to 25; and
- the extracted Mannering (Wyee Colliery) longwall panels 17 to 23 in the Fassifern Seam to the south west of the Proposal Area;

All of the modified miniwalls are located outside the High Water Mark Subsidence Barrier (HWMSB), which are defined by a 35^{o} Angle of Draw (AoD) line taken down from the High Water Mark Level at RL 2.44 m AHD to the Fassifern Seam and the Seagrass Protection Barrier (SPB).

As previously noted the Telstra assets are subject to an existing approved Management Plan between Telstra and LakeCoal and are not covered further in this report.

1.4 Performance Measure Requirements

The performance measures required by the current Development Consent are to ensure that built features remain 'safe and serviceable', 'negligible environmental consequences' occur to seagrass, threatened species or endangered populations and only 'minor environmental consequences' occur to benthic communities.

As the Site is wholly located outside a 35^{o} angle of draw to the HWM, it is unlikely there will be measureable impact to built features. No impacts to seagrass, threatened species, endangered populations or benthic communities have been observed to date and these aspects are to be considered further in separate studies based on the subsidence predictions.

LakeCoal will continue to implement an adaptive management approach to ensure the above performance measure is achieved. Adaptive management will involve the monitoring, remediation and periodic evaluation of the consequences of mining, with possible adjustment of the mining layout and/or methods through the Extraction Plan process to achieve the required measure of performance. Given the uncertainties associated with any proposed underground mine development, it is considered that the mine layout may need to be adjusted for adverse geological conditions that are associated with faults or structure encountered during first workings development in the mine.

2.0 Methodology

This report includes an assessment of subsidence effects and impacts of modified MWs 9 to 36 on the surface and subsurface features present within the Site.

Based on experience from CVC's current mining operations and other longwall mines in the Lake Macquarie Area, it is likely that the development of subsidence will be affected by the spanning potential of massive conglomerate and sandstone units that exist within the overburden. Available borehole data indicates that the Site is situated within the Triassic Narrabeen Group and Upper sequences of the Newcastle Coal Measures.

Subsidence effect and impact predictions for the modified miniwalls have therefore been based on the DgS modified **ACARP, 2003** Models, which allow the effects of massive, spanning strata or Subsidence Reduction Potential (SRP) to be included. The predictions made to-date indicate the upper and lower Munmorah Conglomerate units in the overburden are likely to have 'High' SRP above the 97 m wide panels. The predicted values have been validated with subsidence data from CVCs MWs 1 to 7 and Wyee (now Mannering Colliery) Longwalls (LWs) 17 to 23.

The subsidence prediction model curves used in **DgS, 2013** have also been improved upon and updated with additional data from other Newcastle Coalfield mines.

The height of sub-surface fracturing prediction models have also been updated with a new and improved empirical model (**Ditton and Merrick, 2014**) that includes a broad range of NSW longwall geometry and coalfield geology data and validated against Wyee longwalls (**Li et al, 2006**) plus CVC MWs 1 to 7 experience to-date.

Further details of the above models are provided in **Appendix A**.

It is considered that the above model modifications will provide greater certainty to the subsidence and sub-surface fracturing predictions for the northern area panels.

As was done in **DgS, 2013** for the 2013 EIS, the subsidence contour predictions for the modified miniwall layout presented in this study have been based on the DgS modified **ACARP, 2003** model-derived subsidence profiles and **SDPS, 2007**. SDPS is a US-developed 3-D influence function model that may be calibrated to the representative cross line profile predictions for the CVC miniwalls.

A 2-D numerical model (Lam-2D®) was used in **DgS, 2013** to assess the likely multi-seam stress interactions between the existing bord and pillar workings above the approved MWs 41 to 45 (modified MWs 32 to 36). The results of that analysis still apply for this modification assessment with the increase in subsidence derived from the ratio between the previous and current chain pillar width assumptions (i.e. 32.6/30.6 = 1.065 or a 6.5% increase to the previous subsidence assessment).

The empirical models are all based on regression analysis techniques with curves of 'best fit' used to estimate mean and residual measurement errors used to estimate Credible Worst-Case (Upper 95% Confidence Limits) values for the range of subsidence effects predicted.
The prediction models used therefore allow specialist consultants to assess the potential range of impacts to a given feature in a probabilistic manner.

Management plans and strategies may then be developed that allow the formulation of appropriate Trigger Action Responses Plans (TARPs) and adaptive mine planning adjustments or mitigation measures necessary to deliver satisfactory outcomes to the stakeholders.

3.0 Available Information

The following information was provided by LakeCoal to prepare this report:

(i) The mining layouts for the extracted MWs 1 to 8 and Modified MWs 9 to 36.

(ii) Cover depth contours and seam thickness isopachs for the Wallarah, Great Northern and Fassifern Seams.

(iii) Seventeen borehole lithology logs from the proposed extension area. Four of the boreholes were located over the lake and thirteen logs around the foreshore and Site boundary limits.

(iv) Inferred geological structure (fault and dyke) locations.

(v) Surface levels of lake bed and foreshore.

(vi) Locations of surface developments, seagrasses and infrastructure within the Site.

(vii) Subsidence results from Chain Valley MWs 1 to 7 and Wyee Colliery's LWs 17 to 23.

(viii) Foreshore subsidence monitoring data for Summerland Point and Trinity Point.

Data from boreholes within and adjacent to the Site have been referred to in order to develop a geotechnical model of the mining area. The location of the boreholes are shown in **Figure 2** and summarised in **Table 2**.

Table 2 - Borehole Log Summary

Borehole Number	Easting (MGA)	Northing (MGA)	Surface Level (AHD)	Fassifern Seam Cover Depth* (m)
EBU11	363951	6334150	0.70	183
EER32	366045	6335485	0.91	143
EER34	364390	6334794	17.74	176
EER38	362667	6333605	1.19	143
EVP6	363610	6331950	0.78	198
EWN2	368299	6334098	0.61	174
EWN7	365492	6334883	0.61	152
EWO2	367229	6335078	0.91	156
JCV1	366296	6331490	17.72	234
JCV13	366748	6332723	11.95	214
JCV3	365478	6333120	8.58	202
JCV5	365044	6331657	0.46	196
JCV8	366865	6330497	0.30	238
JCV9	366393	6329718	7.74	251
JMQ1	365447	6330157	0.91	237
JMQ2	365069	6330876	0.91	210
JMQ3	364670	6332397	0.91	214

* - Cover Depth = Lake Bed Level - Fassifern Seam C-Ply Level

4.0 Surface Conditions

The modified miniwalls are located wholly below the south western end of Lake Macquarie in near the communities of Mannering Park, Summerland Point, Morriset Park, Brightwaters and Sunshine. The communities are located on and around broad gently sloping peninsulas and quays associated with Myuna and Chain Valley Bays with surface levels ranging from 5 m to 30 m AHD; see **Figure 2**.

The lake foreshore consists of sandy to rocky shoreline with the high water mark defined at RL 2.44 m AHD. Seagrass communities have been mapped along the foreshore and extend below the low tide mark; see **Figure 1.2**.

There are no existing developments such as buildings, jetties, sea walls, boardwalks or known Aboriginal heritage sites within the 26.5^{o} angle of draw to the re-orientated miniwalls.

Further surface feature details are provided in **DgS, 2013**.

5.0 Sub-Surface Conditions

5.1 Cover Depth

The cover depth between the lake bed and Fassifern Seam C-Ply ranges from 148 m along the north and western boundaries of the Site and increases to 231 m in the south east. The average cover depth above the modified miniwalls is approximately 184 m; see **Figure 3.1**.

The maximum depth of water in the lake above the modified miniwalls ranges from 5.5 m to 9.1 m and the lake bed consists of silty sand and clay alluviual sediments with a thickness ranging from 6.1 m to 20.1 m. Weathered bedrock thickness below the lake ranges from 0.0 m to 11.9 m, giving a depth to 'rock head' (below the lake bed) of 6.1 m to 31 m; see **Figure 3.2**.

The interpreted rock cover depth ranges from 130 m to 214 m (average of 167 m) and has been determined by subtracting the depth to bedrock contours from the cover depth below the lake bed; see **Figure 3.3**.

5.2 Geological Setting

Reference to the 1:100,000 Geological Sheet for Newcastle - Gosford (**DMR, 1995**), indicates the Site is located within the Triassic Narrabeen Group and Permian Newcastle Coal Measures.

Based on the borehole logs within and adjacent to the Site, the lithology consists of thinly to massively-bedded sedimentary strata that belong to the Triassic Narrabeen Group and Late Permian Moon Island Beach Sub-group. The stratigraphy across the Site is summarised in **Table 3**.

Table 3 - Site Stratigraphy

Age	Group	Sub-Group	Coal Seams / Significant Units
Triassic	Narrabeen	Clifton	Munmorah Conglomerate
			Dooralong Shale
Permian	Newcastle Coal Measures	Moon Island Beach	Vales Point Seam
			Karignan Conglomerate
			Wallarah Seam
			Teralba Conglomerate
			Great Northern Seam
			Awaba Tuff
		Boolaroo	Karingal Conglomerate
			Fassifern Seam
			Pilot Seam

5.3 Geological Model

Reference to the exploration borehole logs within the Site indicates the following stratigraphic profile exists above and below the modified miniwalls:

Lake Macquarie:	Maximum depths range from 5.5m to 9.1m, overlying
Lake sediments & weathered rock:	Sand, silt and clay to a depth of 6.1m to 31m, overlying
Munmorah Conglomerate:	Conglomerate and sandstone; grey, medium to coarse grained with minor claystone / shale beds to a depth ranging from 24m to 156m, overlying
Dooralong Shale:	Interbedded shale and coal seams; dark grey brown to black with minor sandstone to a depth ranging from 30 m to 158m, overlying
Vales Point Seam:	Minor seam < 0.5m thick; with some shale and siltstone overlying
Karignan Conglomerate:	Conglomerate and sandstone; grey, medium to coarse grained to a depth ranging from 58m to 172m, overlying
Wallarah Seam:	Coal; 1m to 6m thick, to depths ranging from 63m to 178m, overlying
Teralba Conglomerate:	Conglomerate and sandstone; grey, medium to coarse grained and minor claystone and coal, to depths ranging from 86m to 202m, overlying
Great Northern Seam:	Coal with carbonaceous shale bands; 0.5m to 4.9m thick, to depths ranging from 87m to 205m, overlying
Awaba Tuff:	Tuffaceous claystone; 10m to 18m thick, overlying
Karingal Conglomerate:	Conglomerate and sandstone; grey, to depths ranging from 131m to 225m or is absent, overlying
Chain Valley Formation:	Interbedded shale, coal and claystone, 6m to 17m thick; to depths ranging from 148m to 231m, overlying
Fassifern Seam:	**Coal, shale & claystone; 4.5m to 8.0m to thick, overlying**
Lower Fassifern & Pilot Seam:	Shaley coal / claystone; 3m to 5m thick overlying
Croudace Bay Conglomerate:	Sandstone and conglomerate, grey.

The representative lithological profiles of the overburden and immediate mine workings roof, ribs and floor strata are presented in **Figures 4.1** to **4.3**.

Indicative conglomerate beam thicknesses and their location above the modified miniwalls have been presented in **Table 4A**, together with references to the figures presenting the contours of these units that were prepared using Surfer12® software.

The results are considered to be an improvement on the 2013 EIS, which only presented the range of beam thicknesses and their location assessed at the boreholes. The results in **Table 4A** show the interpreted values for the modified miniwalls as derived from the contours.

Table 4A - Massive Beam Thickness and Location Summary

Beam Unit	Effective Cover Depth H' (m)	Beam Thickness, t (m)	Beam Base Location above the Proposed Miniwalls, y (m)	Beam Location Factor (y/H)	Figure No.s for t and y
Munmorah Conglomerate (Upper)	148 - 232	20 - 35	106 - 190	0.58 - 0.92	5.1, 5.2
Munmorah Conglomerate (Lower)	148 - 232	7 - 57	78 - 128	0.40 - 0.74	6.1, 6.2
Karignan Conglomerate	148 - 232	3 - 22	63 - 95	0.30 - 0.55	7.1, 7.2
Teralba Conglomerate	148 - 232	10 - 28	26 - 80	0.13 - 0.47	8.1, 8.2
Karingal Conglomerate	148 - 232	0 - 55	11 - 23	0.07 - 0.13	9.1, 9.2

The thickness and location of the three seams of interest are presented in **Table 4B**, together with references to the figures presenting the contours of these units that were prepared using Surfer12® software.

Table 4B - Seam Thickness and Location Summary

Seam	Cover Depth H (m)	Seam Thickness, T (m)	Seam Base Location above the Proposed Miniwalls, y (m)	Figure No. for t, y & H
Wallarah	148 - 232	1.0 - 6.0	56 - 109	10.1, 10.2, 10.3
Great Northern	148 - 232	0.5 - 4.9	19 - 86	11.1, 11.2, 11.3
Fassifern	148 - 232	4.5 - 8.0	na	12.1,-, 3.1

5.4 Geotechnical Properties of Rock Mass

As mentioned previously, it is considered likely that the development of subsidence will be affected by the spanning potential of massive units or 'beams' within the Munmorah and Teralba Conglomerate Members. Similar behaviour has been observed at numerous adjacent underground coal mines in Lake Macquarie and in the Newcastle Coalfield generally.

These mines are also overlain by numerous sandstone channel and conglomerate members within the Permian Newcastle Coal measures and Triassic Narrabeen Group. The units are typically braided channel deposits with a bedding thickness range from 15 m to 80 m. The conglomerate beds are often separated into horizontal or wedge-shaped sub-units by thin mudstone and siltstone beds.

Geotechnical testing results of some of the Narrabeen Group and Permian Newcastle Coal Measures conglomerate and sandstone units have been summarised by **McNally, 1995** and **Ives, 1995** and are presented in **Table 5**.

Table 5 - Uniaxial Compressive Strength of the Stratigraphy in the Narrabeen Group and Newcastle Coal Measures

Formation/Unit	Mean (MPa)	Range (MPa)	No. of Tests
Munmorah Conglomerate*	40 / 55	27 - 53 / 37 - 73	26
Wallarah Coal	16	14 - 19	4
Teralba Conglomerate	67	12.5 - 175	68
Great Northern Coal	23	12 - 61	32
Awaba Tuff	66	20 - 254	54
Fassifern Seam	32	16 - 43	29
Australasian Coal	26	14 - 39	5

* - Conglomerate / Sandstone Units. MPa - Mega Pascals.

The test results indicate that the conglomerate and sandstone units typically have medium to high material strength (UCS between 25 MPa and 75 MPa) based on the International Society of Rock Mechanics (ISRM) Classification System (**ISRM, 1981**).

The CVC mining experiences with Awaba Tuff (or moisture sensitive claystone) in the roof and floor of the FAS prior to the extraction of MWs 1 to 8 was that minor heave (< 0.3 m) occurred in development headings around geologically structure affected areas, which are usually associated with wetter conditions.

Moderate floor heave and rib spall (0.3 m to 0.5 m) has also been recently observed in the tailgate roadways of MWs 3 and 6 to 8, where softening of tuffaceous claystone floor units are known to exist; see **Figure 12.2**. The total thickness of moisture sensitive claystone in the floor and ribs/ roof are estimated to be 0.9 m and 0.3 m respectively, based on borehole data and back analysis of available subsidence data (see **Section 7.3**).

Reference to borehole log data in the vicinity of the Chain Valley Bay area indicates that a 20 m to 30 m thick unit of Teralba Conglomerate exists immediately above the Great Northern Seam; see **Figure 4.2** and **4.3**. The interburden between these seams consists of several layers of moisture sensitive claystone that are hard when first cored and then swell and soften with

time due to stress relief and exposure to humid mine workings atmospheres and concentrated groundwater.

More recent experience obtained by the mine during the construction of a shaft between the GN and FAS seams in the south-eastern area of Chain Valley Bay confirmed the presence of swelling / puggy claystone in at least 15 m of the shot firing holes drilled upwards from the Fassifern Seam. Observed floor heave of first workings headings in the Great Northern and Fassifern Seams also indicates moisture sensitive claystone is present in the area.

There is anecdotal experience in the Lake Macquarie area where partial pillar extraction mine workings in the Fassifern Seam with moisture sensitive claystone floor units have developed 0.5 m of subsidence some 6 to 18 months after completion of mining (**DgS, 2012**).

5.5 Geological Structure

CVC is located to the west of the Macquarie Syncline, with Fassifern Seam bedding dipping towards the south east at 1^{o} to 3^{o}; see **Figure 12.3**.

Regional structure known to exist includes north-west and north-east striking normal faults with north-east and south-west downward throws of 0.5 m to 2 m. Low-angle thrust faults may also be present on a north-east strike (**Lohe & Dean-Jones, 1995**).

It is noted that, in general, miniwall panels have been extracted across the minor and moderate structures only (i.e. throws < half the mining height of 3.5 m). Major fault structures and hard dykes have been avoided by adjusting the miniwall layout to leave a stable barrier pillar of coal directly beneath these features. The points below list structures encountered during underground development in the current operations area.

- Minor to moderate north-west and north-east striking normal faults with throws ranging from 10 mm to 1.4 m (average of 0.5 m).

- A major north-west striking fault with a throw > 3 m.

- One to 2.5 m wide hard dykes (UCS of 80 MPa) striking north-west. The dykes were also encountered in the overlying workings in the Great Northern and Wallarah seams.

- A major fault (2.5 m throw) was encountered during development of MW4, which was initially encountered as a 0.5 m fault in the main headings. This subsequently required the miniwall length to be shortened back to 400 m. The miniwall was retreated through the fault (with a throw of ~1.8m) and the roof conditions were found to be manageable. After intersecting the fault in MW4, an exploration heading was driven across to MW5 and no further faulting was encountered within MW5.

- A 74 m wide barrier of coal was also originally proposed to avoid what was thought to be a significant dyke structure between approved MWs 3 and 8. Further investigation by horizontal drilling found a series of thinner structures < 1 m exist that enabled a 97 m wide panel (MW7) to be extracted.

It is likely that similar structures to those already encountered in the current operations area will exist within the limits of the Site. The detection of these structures and the assessment of the potential risks associated with undermining them are discussed in **Section 10.3.16**.

6.0 Mining Geometry

The following mine workings details have been used in this assessment of the modified miniwalls 9 to 36 in the Fassifern Seam:

- The modified miniwall layout will all have panel widths of 97 m and are aligned north-west to south-east and east-west below Lake Macquarie.

- The effective cover depth between the lake bed and Fassifern Seam C-Ply ranges from approximately 150 m to approximately 230 m with an average cover depth of approximately 184 m across the Site.

- The rock cover above the modified miniwall layout ranges from 132 m to 214 m.

- The Fassifern Seam thickness ranges from 4.5 m to 8.0 m.

- A face extraction height of 3.5 m. *Note: The mining heights for Modified MWs 20 to 25 have been reduced to a range from 3.0 to 3.4 m to meet minimum sub-surface fracturing constrained zone requirements immediately below the lake (i.e. 12T).*

- The first workings roadways will be nominally 5.4 m wide and 3.2 m high.

- Chain pillar widths will now range from 29.3 m to 32.6 m with pillar lengths of 95 m (solid dimensions).

The panel width to full cover depth ratio (W/H) for the modified miniwalls will range from 0.42 to 0.66, indicating 'sub-critical' subsidence behaviour for all overburden geologies. Based on a rock cover range from 132 m to 214 m (see **Figure 4**), the W/H increases to a range from 0.45 to 0.74 and still within the practical sub-critical limit range of 0.8 when massive, spanning conglomerate strata is present.

A summary of the mining geometry along the subsidence prediction cross lines (XL1 to 10) is presented in **Table 6**. The cross line locations are shown in **Figure 2**.

Old mine workings exist in the Wallarah Seam (circa 1960s - 1990s) and Great Northern Seam (circa 1970s - 2000s) above the modified location of MWs 32 - 36 beneath Chain Valley Bay. Details of the workings are provided in the assessment of multi-seam workings interaction in **Section 8.1**.

Table 6 - Modified Miniwall Layout Geometry

XL No.	Panel No.	Panel Width W (m)	Effective Cover Depth* H' (m)	Depth to Rock Head D_r (m)	Rock Cover^ (H_r)	Rock Cover W/H_r	Mining Height T (m)	Chain Pillar Width w_{cp} (m)
1	**1**	**72**	**200**	**20**	**180**	**0.40**	**3.4**	**30.6**
	2	**72**	**200**	**19**	**181**	**0.40**	**3.4**	**30.4**
	3	**97**	**200**	**18**	**182**	**0.53**	**3.5**	**32.6**
	6	**97**	**198**	**17**	**181**	**0.54**	**3.5**	**32.6**
	7	**97**	**195**	**15**	**180**	**0.54**	**3.5**	**32.6**
	8	97	193	14	179	0.54	3.5	32.6
	9	97	191	13	178	0.54	3.5	32.6
2	**4**	**97**	**196**	**18**	**178**	**0.54**	**3.5**	**40**
	5	**97**	**200**	**18**	**182**	**0.53**	**3.5**	**186**
3	7	97	190	16	174	0.56	3.5	32.6
	8	97	188	16	173	0.56	3.5	32.6
	9	97	185	15	171	0.57	3.5	32.6
	10	97	183	14	169	0.57	3.5	32.6
	11	97	178	13	165	0.59	3.5	32.6
	12	97	173	6	167	0.58	3.5	32.6
4	10	97	170	14	156	0.62	3.5	32.6
	11	97	184	15	169	0.57	3.5	300
5	13	97	188	8	180	0.54	3.5	32.6
	14	97	185	8	177	0.55	3.5	32.6
	15	97	182	9	173	0.56	3.5	31.6
	16	97	180	9	171	0.57	3.5	31.1
	17	97	175	10	165	0.59	3.5	30.6
	18	97	170	11	159	0.61	3.5	29.9
	19	97	165	11	154	0.63	3.5	29.3
	20	97	160	11	149	0.65	3.5	29.3
6	14	97	185	12	174	0.56	3.5	32.6
	15	97	178	12	166	0.58	3.5	31.6
	16	97	175	14	162	0.60	3.5	31.1
	17	97	173	13	160	0.61	3.5	30.6
	18	97	168	14	155	0.63	3.5	29.9
	19	97	163	14	149	0.65	3.5	29.3
	20	97	160	15	145	0.67	***3.4***	29.3
	21	97	158	24	135	0.72	***3.0***	29.3
	22	97	156	16	140	0.69	***3.3***	29.3
	23	97	153	16	137	0.71	***3.2***	29.3
	24	97	150	16	134	0.72	***3.1***	29.3
	25	97	148	17	132	0.74	***3.0***	300
7	26	97	167	12	155	0.63	3.5	31
	27	97	168	13	156	0.62	3.5	31
	28	97	169	13	156	0.62	3.5	300
8	26	97	187	16	171	0.57	3.5	31
	27	97	188	16	172	0.56	3.5	31
	28	97	189	17	173	0.56	3.5	31
	29	97	190	17	174	0.56	3.5	31
	30	97	190	17	173	0.56	3.5	31
	31	97	190	17	173	0.56	3.5	31

- see notes at bottom of table on next page

Table 6 (Cont…) - Modified Miniwall Layout Geometry

XL No.	Panel No.	Panel Width W (m)	Effective Cover Depth* H' (m)	Depth to Rock Head D_r (m)	Rock Cover^ (H_r)	Rock Cover W/H_r	Mining Height T (m)	Chain Pillar Width w_{cp} (m)
9	32	97	219	23	196	0.49	3.5	30.6
	33	97	218	21	197	0.49	3.5	30.6
	34	97	221	19	202	0.48	3.5	30.6
	35	97	220	17	203	0.48	3.5	30.6
	36	97	217	16	202	0.48	3.5	300
10	32	97	229	21	208	0.47	3.5	30.6
	33	97	230	20	210	0.46	3.5	30.6
	34	97	231	19	212	0.46	3.5	30.6
	35	97	232	18	214	0.45	3.5	30.6
	36	97	228	16	212	0.46	3.5	300

Bold - Extracted miniwalls.
italics - maximum allowable mining height to meet minimum constrained zone thickness in overburden.
* - Effective cover depth, H' = Lake Bed Level - Fassifern Seam C-Ply Level.
^ - Rock Cover, $H_r = H' - D_r$
shaded - Modified miniwalls below existing mine workings in the Great Northern and Wallarah Seams.

7.0 Review of Subsidence Data

7.1 Chain Valley Colliery's Subsidence Data

It was expected that final maximum subsidence would occur after three to five miniwalls have been extracted after a given panel and full loading has developed on the chain pillars (**DgS, 2013**).

A bathymetric survey in May, 2013 above the completed MWs 1 - 3 (three panels) indicated maximum subsidence of approximately 115 mm had developed above MWs 2 and 3; see **Figure 13.1**.The bathymetric survey in June, 2014 above the completed MWs 1 - 3 and 6 - 7 (5 panels) indicated subsidence of approximately 410 mm had developed and less than the predicted final subsidence of 460 mm in the 2013 EIS; see **Figure 13.2**. The most recent survey in May, 2015 however, measured 570 mm of subsidence above the tailgate chain pillars between MWs 6 and 7 after the completion of MW8 (the sixth panel); see **Figures 13.3** and **13.4**.

The measured longitudinal subsidence profiles above the tailgate chain pillars for MWs 3, 6 and 7 and panel centrelines for MWs 3 and 6 are presented in **Figures 13.5** to **13.9**.

Despite an increase of approximately ~110 mm above the predicted subsidence, the measured tilts and strains along XL1 are still within the predicted ranges provided in the 2013 EIS; see **Figures 13.10** and **13.11**. A summary of predicted v. measured subsidence effects along XL 1 (see **Figure 2** for its location) is presented in **Table 7**.

Table 7 - Summary of Predicted* v. Measured Final Maximum Subsidence based on Rock Cover Depth for CVC MWs 1-8

Panel No.s	Maximum Panel Subsidence S_{max} (m)		Maximum Pillar Subsidence S_p (m)		Maximum Tilt^ (mm/m)		Maximum Strain^ (mm/m)		Goaf Edge Subsidence (mm)		Angle of Draw (o)	
	Pred.	Meas.	Pred.	Meas.	Pred.	Meas.	Pred.	Meas.	Pred.	Meas.	Pred.	Meas.
MWs 1,2,3 & 7 (2014)	0.31 - 0.46	0.22 - 0.44	0.30 - 0.31	**0.34 - 0.40**	4 - 8	3 - 4	+/- 4	+1.5 -4.5	100 - 230	8 - 15	19.9 - 27.3	0 - 12
MWs 1,2,3, 7 & 8 (2015)	0.31 - 0.46	**0.52 - 0.54**	0.30 - 0.31	**0.43 - 0.57**	4 - 8	3 - 4	+/- 4	+/-3	100 - 230	6 - 44	19.9 - 27.3	0 - 25.9

Bold - measured data exceed predictions by >10%;* - Predicted values are U95%CLs based on DgS modified **ACARP, 2003** models for XL 1 from 2013 EIS;^ - Tilt, tensile & compressive strains derived from 'smooth profile' curvatures x 11 (tension is positive).

It was assessed in **DgS, 2013** that existing pillars in the workings at Chain Valley Colliery with stresses greater than 15 MPa may experience local bearing or lateral squeezing failures in the roof or floor strata and increase surface subsidence to between 200 mm and 900 mm.

The load acting on the MW3 and MW6 tailgate chain pillars also appears to have been relatively slow to develop due to four or five conglomerate 'beams' present within the overburden and making up 50% to 60% of the total rock cover thickness. The conglomerate units also appear to have been spanning across the extracted miniwalls in two directions, based on the subsidence observed and mine plan geometry.

The chain pillars have therefore been protected from double abutment loading of 16.3 MPa until the deflection of the spanning conglomerate units over the first four or five panels (MWs 1-3, 6 - 7) exceeded ~0.5 m; see **Figure 13.12**. It is also noted that measureable subsidence was not detected above the two miniwalls (MWs 6 and 7) with a total span of 200 m between the ribs; see **Figure 13.3**.

The development of a further 110 mm of subsidence above the chain pillars between June 2014 and May 2015 after maximum loading had been reached, suggests time-dependent subsidence has been occurring. Reference to **DgS, 2013** and **DgS, 2014** indicates there are several moisture-sensitive claystone beds between 150 mm and 300 mm thick sandwiched between non-sensitive coal and shale beds in the roof, ribs and floor of the FAS.

Further discussion on the subsidence development mechanism at CVC is presented in **Sections 7.2** and **7.3**.

7.2 Time Dependent Subsidence Mechanism

Several pillar panel mines in the Lake Macquarie area have claystone floors below the Wallarah, GN and FAS seams that are noted for their sensitivity to moisture content and stress changes (**Seedsman and Gordon, 1992**).

The changes in pillar stress that occur during first and second workings within a production panel generally cause an initial elastic response from the strata. The increases in pillar stress can also develop excess pore pressures in the previously exposed claystone, due to its low permeability. This usually results in consolidation settlements or time-dependent subsidence that decreases gradually as the load carried by the pore water initially, transfers to the soft rock matrix and compresses it as the water drains away.

The time taken for full load transfer or primary consolidation is dependent on the magnitude of stress and the length of the drainage pathway through the consolidating, softened claystone. The presence of permeable sandstone or fractured rock mass beds above and below the claystone unit could theoretically halve the time for the pore pressure to be relieved (i.e. two-way drainage).

As discussed in **DgS, 2014**, it is assessed that the de-stressed claystone floor beneath the road ways of the tailgates in FAS could lead to a 50% reduction of the rockmass strength and stiffness modulus after on-going exposure to humid mine workings conditions; see **Figure 13.13**. The softening behaviour is due to the swelling or volume increase of clay mineral rich rocks (usually smectite or montmorillonite).

At a cover depth of 198 m above MWs 3 and MW6 chain pillars, initial elastic subsidence of 0.48 m due to the applied load increment of 11.4 MPa (16.4 - 5.0 MPa) has been estimated in **Section 8.4,** based on the softened, material modulii values.

Based on consolidation theory below, an additional 0.10 m of subsidence is predicted due to the expulsion of pore water under applied loading (primary consolidation) and a further 0.14 m over 10 years due to plastic 'creep' (secondary consolidation). The final maximum subsidence is therefore estimated to be 0.72 m above MWs 3 and 6 based on soft floor consolidation theories.

An important factor in the assessment of primary consolidation is the maximum pressure the consolidating unit has been subject to in the past (also known as the pre-consolidation pressure).

7.2.1 Pre-consolidation Pressure of Claystone Units

If the applied stress is < the pre-consolidation pressure, the material is said to be 'Over-Consolidated', and the material will respond to the load in a similar fashion as a 'rebound' or unloading curve in a triaxial rock modulus test. On the other hand, if the material is stressed beyond the pre-consolidation curve, the material will behave as a 'Normally Consolidated' material and follow the loading curve.

The pre-consolidation pressure for the FAS claystone units have been estimated from horizontal stress testing results for the F3 Freeway in a ridge to the north west of the Chain Valley Colliery (refer to **Lohe & Dean Jones, 1995**). The test result at 24 m depth indicated a horizontal stress of 10.2 MPa for a vertical stress of 0.6 MPa. If the rock mass was overlain by a greater depth of soil and rock at some point in the past, then based on a horizontal to vertical stress ratio of 2 the pre-consolidation pressure at a depth of 24 m was approximately 5.2 MPa (due to a cover depth of 208 m). The over consolidation ratio (OCR) is the ratio between historical stress and the current applied stress and has been estimated below:

$$OCR = \sigma_{vo} / \sigma_v = 5.2/0.6 = 8.7 \text{ or } H_o/H = 208/24 = 8.7.$$

The pre-consolidation pressure (σ_p) at a depth of 198 m in FAS Seam may then be estimated as follows:

$$= \sigma_{vo\ (H=24m)} + \gamma(H - 24)$$

$$= 5.2 + 0.025(198 - 24) = 9.6 \text{ MPa}$$

To-date, the floor below the FAS chain pillars would have been subject to a pre-mining stress of ~ 5 MPa, followed by a pillar development load of 6.1 MPa, and finally a second workings load of approximately 16.4 MPa. Based on the above assessment, it is likely that the pre-consolidation pressure for the claystone units was exceeded, resulting in normally consolidated response above 9.6 MPa.

7.2.2 Primary and Secondary Consolidation

Primary consolidation displacements for the pillars have therefore been estimated using equations (1) and (2).

The development of subsidence due to primary consolidation in saturated, over-consolidated claystone is presented in **Das, 1998** as follows:

Primary Consolidation $= d/(1+e_o)\ [\ C_c \log(\sigma_p + d\sigma)/\sigma_p + C_s \log(\sigma_p/\sigma_o)]$

Secondary Consolidation or Creep $= C'_\alpha\, d \log(10 \text{ years}/1 \text{ year})$

where

e_o = initial void ratio of claystone $= wG_s = 0.18*2.65 = 0.48$ (for saturated clay)

C_c = compression index $= 0.2343\ (LL/100)G_s = 0.43$ (after **Nagaraj and Murty, 1985**)

C_s = swell index $= 0.0463\ (LL/100)G_s = 0.085$ (after **Nagaraj and Murty, 1985**)

σ_p = pre-consolidation pressure (estimated to be 9.6 MPa at 200 m cover in the Lake Macquarie area)

$d\sigma$ = increase in chain pillar stress from tributary area to double abutment loading conditions.

σ_o = initial pillar stress = tributary area stress $= 0.025H/(1-e)$

d = total thickness of claystone units = 1.2 m (within 3 m of the mine workings floor)

C'_α = secondary compression index = 0.105

Based on a maximum clay unit thickness of 1.2 m (0.9 m in the upper 1.5 m of the floor and 0.3 m in the pillar (refer **DgS, 2014**) with one-way or two-way drainage, a primary consolidation of 0.11 m is estimated after full loading is applied to the chain pillar. The subsidence is estimated due to a stress increase of 10.16 MPa and a pre-consolidation pressure of 9.6 MPa at 200 m cover depth.

Secondary consolidation or creep of 13 mm/a over 10 years results in a final subsidence above the panel as follows:

Final S_{max} = 0.48 m + 0.11 m + 0.13 m = **0.72 m**

7.2.3 Time rate of Consolidation

The time rate of primary consolidation may be estimated from the following formula:

$$t_{95\%} = T_v*(d/n)^2/C_v$$

where

n = 1 for one-way drainage and 2 for 2-way drainage.
C_v = coefficient of consolidation (1.5 m^2/a for Awaba Tuff from **Li and Smith, 1998**)
T_v = Dimensionless Time factor (1.125 for 95% of primary consolidation settlement)

The time for 95% of the primary consolidation phase to occur after completion of a mining stage ranges between 3 and 12 months. The C_v value is also affected by the permeability of the claystone and applied stress, and depending on the location and number of consolidating claystone units, could see a significant increase or decrease in primary consolidation time occurring in-situ.

For graphical presentation of the time-dependant subsidence process, the primary consolidation curve can be derived from the following equation which links the time factor to the % consolidation of the softened claystone units as follows:

$$U = S_t/S_{max} = 1 - (2/M^2)\, e^{-M2Tv}$$

where

U = average consolidation ratio

S_t = subsidence at time t

S_{max} = maximum subsidence due to primary consolidation

$M = \pi/2$

7.3 Observed Floor Heave Considerations

The mining experiences at Chain Valley Colliery to-date with GN and FAS Seam floor claystone indicate only minor floor heave has occurred in development headings around geologically structure affected areas, which are usually associated with wetter conditions. The development of floor heave does not necessarily indicate surface subsidence will develop and depends on the presence of massive spanning conglomerate and panel width as demonstrated in **Figure 13.12**.

As previously assess in **DgS, 2013**, the time-dependent subsidence development apparent above the foreshore of Chain Valley Bay without significant floor heave indicates that the GN and FAS claystone units probably have been (i) softening due to moisture ingress and volume change and then (ii) consolidating under applied loading for over 5 to 15 years since mining was completed.

Based on the above theories and anecdotal evidence of floor heave as discussed in **Section 5.4**, the primary and secondary consolidation curves have been reasonably fitted to the observed settlement plot to-date in **Figure 13.14** to suggest that lateral bearing failures of the claystone beds have not occurred due to the applied loading.

However, if the stresses applied to the materials did in fact exceed the softened strength of the claystone strata, then the increase in subsidence may in fact be due to lateral bearing failures of the thin claystone beds immediately below the chain pillars. The estimation of bearing capacity has therefore been addressed in **Section 7.4**.

7.4 Bearing Capacity of Roof and Floor Strata

It should be noted that tuffaceous claystone beds associated with the Fassifern Seam and Awaba Tuff may soften to an undisturbed UCS of 1 to 2 MPa due to moisture sensitivity; see **Figure 13.13**. The beds however are usually 'sandwiched' between stronger shaley coal units with strengths 8~10 MPa, thus giving a higher average strength and bearing capacity due to confining friction between the beds.

By applying the 2-layered bearing capacity theory presented in **Brown & Meyerhof, 1969** for a strip footing on a weak layer overlying a stronger one. The theory indicates that the overall bearing capacity of the weaker layer will be increased if the stronger unit is within 0.5 times the width of the pillar as follows:

$$q_u = N_{strip} \times UCS_1/2 = [4.14 + 0.5(w/t)]\ UCS_1/2$$

where

N_{strip} = Modified bearing capacity coefficient for a strip footing
w = 29.3 m to 32.6 m (proposed chain pillar widths)
UCS_1 = softened claystone strength = 1.5 MPa.
t = thickest weak layer thickness = 0.4 m.
q_u = thin weak layer bearing capacity = 20.3 - 33.7 MPa

The estimated maximum pillar stress range of 12.2 MPa to 20.7 MPa give an FoS range of 1.0 to 2.8 and indicates the floor strata may have experienced local bearing or lateral squeezing failures under worst-case softening conditions. The magnitude of final subsidence that is likely to develop due to is likely to be limited to a proportion of the sheared or failed layer(s).

Based on a similar case study of lateral bearing failures of softened claystone in the FAS at the nearby **Tasman Mine (DgS, 2013b)**, it is concluded that the final subsidence above MWs 3 and 6 are likely to be similar to the predicted values based on consolidation theory.

7.5 Summary

The assessment of the claystone bed properties, design loads, measured subsidence and development of underground floor heave up to 0.5 m suggests that the modified miniwall layout needs to consider that time dependent subsidence effects will occur again beneath the chain pillars of the future miniwalls at the Site.

However, it is concluded that regardless of which mechanism of time-dependent subsidence that occurs, it is assessed that the chain pillar subsidence with soft-floor conditions will be similar.

For the purposes of subsidence modelling and impact assessment of the modified mining layout, it is demonstrated in **Section 8.4**, that the empirical model for estimating chain pillar subsidence may still be used to estimate final subsidence affected by softened claystone floors if a multiplying factor of 1.5 is applied to the results.

8.0 Subsidence Predictions for the Modified Mining Layout

8.1 General

As was done in **DgS, 2013**, subsidence effect predictions for MWs 9 to 36 have been assessed across the Site after:

(i) each miniwall block has been extracted (i.e. First S_{max}), and

(ii) after mining of all of the proposed miniwall panels is complete (i.e. Final S_{max}).

The assessment requires consideration of the following:

- The subsidence reduction potential (SRP) of the overburden and the influence of proposed mining geometry on single panel subsidence development (i.e. whether the panels are likely to be sub-critical, critical or supercritical).

- The time-dependant behaviour of the chain pillars and immediate roof and floor system under double -abutment loading conditions when miniwalls have been extracted along both sides of the pillars with soft floor conditions.

- The combined effects of single panel and chain pillar subsidence to estimate Final Subsidence profiles and subsidence contours for subsequent environmental impact assessment.

The outcomes of the subsidence assessment are presented in the following sections.

8.2 Geological Model and Subsidence Reduction Potential of Massive Units

The SRP refers to the subsidence reducing effect that massive conglomerate / sandstone units may have above longwall and miniwall panels due to their inherent spanning or arching behaviour. The SRP is a function of the cover depth; the width of the panel (or span); the thickness of the massive unit and the distance of the unit above the workings.

The outcomes of the empirical model analysis for the massive conglomerate units within the overburden are summarised as follows:

- The thickness of the conglomerate beams most likely to span a range from 17 m to 35 m (mean of 27 m).

- The beams are located 82 m to 110 m above the proposed mine workings roof (mean of 97 m).

The minimum conglomerate beam thicknesses within the overburden likely to have ‘High’ and ‘Moderate’ SRP are presented in **Table 8**.

Table 8 - Minimum Beam Thickness Required for High and Moderate SRP above 97m Wide Miniwalls

Formation	Massive Unit No.	Cover Depth, H (m)	Location above Longwalls, y (m)	y/H	Minimum Beam Thickness for SRP, t_{min} (m)	Interpreted Beam Thickness from Bore Core t_{meas} (m)
High SRP						
Munmorah (Upper)	1	148 – 232	106 - 190	0.58 - 0.92	7 - 10	20 - 35
Munmorah (Lower)	2	148 – 232	75 - 122	0.38 - 0.72	10 - 12	8 - 55
Karignan	3	148 – 232	63 - 95	0.30 - 0.55	10 - 14	3 - 22
Teralba	4	148 – 232	26 - 80	0.13 - 0.47	11 - 19	10 - 28
Karingal	5	148 – 232	11 - 23	0.07 - 0.13	16 - 21	0 - 55
Moderate SRP						
Munmorah (Upper)	1	148 – 232	106 - 190	0.58 - 0.92	4 - 10	20 - 35
Munmorah (Lower)	2	148 – 232	75 - 122	0.38 - 0.72	5 - 11	8 - 55
Karignan	3	148 – 232	63 - 95	0.30 - 0.55	7 - 12	3 - 22
Teralba	4	148 – 232	26 - 80	0.13 - 0.47	8 - 14	10 - 28
Karingal	5	148 – 232	11 - 23	0.07 - 0.13	14 - 16	0 - 55

It is assessed that at least two of the five massive conglomerate units presented in **Table 8** will have 'High' SRP above the 97 m wide miniwalls (i.e. where the interpreted 'beam' thicknesses are greater than the minimum threshold limit values as shown in **Figures 14.1** to **14.5**).

It is also assessed that the presence of three or four massive strata units above the workings with 'High' SRP, indicates a low risk that the assumption of 'High' SRP for subsidence effect prediction will be incorrect. Measured subsidence above MWs 1 to 8 to-date (see **Section 7**) also confirms this assessment of 'High' SRP is valid.

8.3 Predicted Maximum Single Panel Subsidence

8.3.1 Empirical Model Assessment

The maximum subsidence above a single longwall (or miniwall) panel will depend upon its width (W), cover depth (H), extraction height (T), and the SRP of the overburden.

Based on reference to the DgS Modified **ACARP, 2003** model, the assessed SRP categories for the massive overburden strata units are used to select the appropriate subsidence prediction lines from one of three given depth categories (i.e. H=100 m, 200 m and 300 m +/- 50 m).

The depth categories were developed in the **ACARP, 2003** study to cater for the influence of scale on the spanning behaviour of the massive lithological units above panels of a given geometry. The categories derived are also consistent with the trends of the upper bound curves that were developed by the Department of Minerals Resources (now Resources and Energy) for the Newcastle and Southern Coalfields, in that measured subsidence generally increases with depth for a given panel width to cover depth ratio (W/H).

Based on a review of the subsidence data for Wyee longwalls 17 to 23 (see **DgS, 2013**) the model predictions are conservative if rock cover depth is used, but under predicts subsidence if the full cover depth below the lake bed surface is adopted (cover depth includes soil, alluvial sediments and weathered rock ranging between 6 m to 29 m thick).

The maximum subsidence, S_{max}, for single 97 m wide miniwall panels at 148 to 231 m depth with 'High' SRP overburden is summarised in **Table 9** for XLs 1 to 10 (see **Figure 3.1** for XL locations).

The relevant depth categories for the Modified MWs 9 to 36 are the 100 m and 200 m +/- 50 m categories, see **Figures 15.1** and **15.2** respectively. The **DMR, 1987** empirical model curve for the Newcastle Coalfield is also shown for comparative purposes.

Table 9 - Maximum Single Panel Subsidence Prediction Outcomes for High SRP

XL No.	MW No.	Massive Unit No.	Massive Unit Thickness (m)	Massive Unit Distance above Workings y (m)	Effective Cover Depth, H (m)	Unit Location Factor (y/H)	Extraction Height T (m)	Panel Width W (m)	Maximum Single Panel Subsidence S_{max} (m)	
									mean	U95% CL
1	**1**	**2**	**35**	**105**	**200**	**0.53**	**3.4**	**72**	**0.07**	**0.16**
	2	**2**	**34**	**108**	**200**	**0.54**	**3.4**	**72**	**0.07**	**0.16**
	3	**2**	**32**	**110**	**200**	**0.55**	**3.4**	**97**	**0.11**	**0.24**
	6	**2**	**30**	**112**	**198**	**0.57**	**3.4**	**97**	**0.11**	**0.25**
	7	**2**	**27**	**114**	**195**	**0.58**	**3.4**	**97**	**0.11**	**0.25**
	8	2	25	114	193	0.59	3.5	97	0.12	0.26
	9	2	22	114	191	0.60	3.5	97	0.12	0.26
2	**4**	**2**	**45**	**75**	**196**	**0.38**	**3.4**	**97**	**0.11**	**0.26**
	5	**2**	**45**	**78**	**200**	**0.39**	**3.4**	**97**	**0.11**	**0.24**
3	**7**	**2**	**17**	**105**	**190**	**0.55**	**3.5**	**97**	**0.12**	**0.28**
	8	2	17	110	188	0.59	3.5	97	0.13	0.28
	9	2	16	115	185	0.62	3.5	97	0.13	0.29
	10	2	16	102	183	0.56	3.5	97	0.13	0.29
	11	2	16	104	178	0.58	3.5	97	0.14	0.31
	12	2	17	110	173	0.64	3.5	97	0.14	0.30
4	10	1	20	106	170	0.62	3.5	97	0.16	0.35
	11	1	20	106	184	0.58	3.5	97	0.13	0.29
5	13	2	20	112	188	0.60	3.5	97	0.11	0.26
	14	3	20	111	185	0.60	3.5	97	0.12	0.27
	15	3	19	111	182	0.61	3.5	97	0.13	0.28
	16	2	19	110	180	0.61	3.5	97	0.13	0.29

+ - see bottom of table on next page for notes

Table 9 (Cont…) - Maximum Single Panel Subsidence Prediction Outcomes for High SRP

XL No	MW No	Strata Unit No.	Massive Unit Thickness (m)	Massive Unit Distance above Workings y (m)	Cover Depth H (m)	Unit Location Factor (y/H)	Extraction Height T (m)	Panel W (m)	Maximum Single Panel Subsidence S_{max} (m)	
									mean	U95% CL
5	17	2	18	110	175	0.63	3.5	97	0.14	0.31
	18	2	18	109	170	0.64	3.5	97	0.15	0.34
	19	2	17	108	165	0.65	3.5	97	0.17	0.36
	20	2	17	107	160	0.67	3.5	97	0.18	0.39
6	14	2	20	100	185	0.54	3.5	97	0.12	0.28
	15	2	19	99	178	0.56	3.5	97	0.14	0.30
	16	2	19	99	175	0.57	3.5	97	0.15	0.32
	17	2	18	98	173	0.57	3.5	97	0.15	0.33
	18	2	18	97	168	0.58	3.5	97	0.16	0.36
	19	2	17	96	163	0.59	3.5	97	0.18	0.39
	20	2	17	95	160	0.59	***3.4***	97	***0.19***	***0.41***
	21	2	17	94	158	0.59	***3.0***	97	***0.20***	***0.44***
	22	2	17	93	156	0.60	***3.3***	97	***0.20***	***0.43***
	23	2	16	92	153	0.60	***3.2***	97	***0.20***	***0.44***
	24	2	16	91	150	0.61	***3.1***	97	***0.21***	***0.45***
	25	2	17	90	148	0.61	***3.0***	97	***0.21***	***0.46***
7	26	2	12	108	167	0.65	3.5	97	0.16	0.36
	27	2	12	110	168	0.65	3.5	97	0.16	0.35
	28	1	20	135	169	0.80	3.5	97	0.16	0.35
8	26	2	24	102	187	0.55	3.5	97	0.13	0.29
	27	2	23	105	188	0.56	3.5	97	0.13	0.28
	28	2	22	110	189	0.58	3.5	97	0.13	0.28
	29	2	20	102	190	0.54	3.5	97	0.12	0.28
	30	2	20	105	190	0.55	3.5	97	0.13	0.28
	31	2	18	118	190	0.62	3.5	97	0.13	0.28
9	32	2	50	95	219	0.43	3.5	97	0.10	0.22
	33	2	50	100	218	0.46	3.5	97	0.10	0.22
	34	2	50	105	221	0.48	3.5	97	0.09	0.23
	35	2	50	110	220	0.50	3.5	97	0.09	0.22
	36	2	51	115	217	0.53	3.5	97	0.09	0.23
10	32	2	55	100	229	0.44	3.5	97	0.09	0.21
	33	2	55	104	230	0.45	3.5	97	0.09	0.21
	34	2	54	108	231	0.47	3.5	97	0.08	0.21
	35	2	54	112	232	0.48	3.5	97	0.08	0.21
	36	2	53	114	228	0.50	3.5	97	0.08	0.21

bold - extracted miniwalls; shaded - panel widths increased from **DgS, 2013**; *italics* – mining height reduced from **DgS, 2013**.

The results indicate that the maximum single panel subsidence for the 97 m wide panels are predicted to range between 0.07 and 0.46 m (2% to 13% of the mining height).

After the mining of several adjacent panels occurs the compression of the chain pillars will increase the maximum panel subsidence values. The assessment of multiple panel subsidence is presented in **Section 8.8**.

8.3.2 Analytical Voussoir Beam Model Assessment

The Voussoir Beam analysis has been completed again for the Modified miniwall layout with particular focus on the increased width panels (modified MWs 21 to 25).

Voussoir Beam theory allows a quantitative assessment of a jointed rock beam's spanning capability by arching action over an extracted miniwall panel. The **ACARP, 2003** empirical model of the subsidence reducing effect of spanning strata units was developed with reference to the Voussoir Beam analogue.

The Voussoir Beam model assesses the factor of safety against instability of the rock beam due to (i) abutment crushing, (ii) shear failure and (iii) buckling. The analytical model presented in **Diedrichs and Kaiser, 1999** also provides a statically admissible solution for the deflection of the spanning unit to be calculated for a given set of material strength and stiffness properties. The uncertainties inherent in the model include the effective span of the unit within the overburden, the uniformity or persistence of the 'beam', and the effective loading height acting on the beam.

Analytical models therefore allow the geo-mechanical properties of the Site strata to be used to (i) predict subsidence, and (ii) compare the outcomes to the empirical model, which has been based on measured subsidence data for a wide range of mining geometries and geomechanical properties in the Newcastle Coalfield.

Average rock mass elastic moduli for the conglomerate units were estimated based on the laboratory data and the relationship established by **Hoek and Diederichs, 2006** below:

$$E_{rockmass} = E_{laboratory}(0.02+1/(1+e^{(60-GSI)/11})$$

A Geological Strength Index (GSI) of 80 for 'Good' to 'Very Good' sandstone rock mass conditions has been estimated from **Marinos and Hoek, 2000** (blocky strata with good bedding parting surface quality (i.e. rough and slightly weathered). The Voussoir Beam model input assumptions have also been calibrated to geological conditions and subsidence data for the Wyee longwalls.

The rock mass properties assessed for the overburden conglomerate units above the mining geometries proposed are summarised in **Table 10** below.

Table 10 - Geo-mechanical Properties of the Conglomerate Beams

Parameter	Units	Magnitude
Rock Mass Density	t/m^3	2.5
Rock Mass UCS	MPa	40
E/UCS	-	250
Laboratory Youngs Modulus E_{lab}	GPa	10
Geological Strength Index+	Good Conglomerate / Sandstone	50 - 60 (mean 55)
E_{rm}/E_{lab}	-	0.4
Rock Mass Modulus, E_{rm}	GPa	3.9
Poissons Ratio	m/m	0.25
Abutment Angle for Beam Span*	degrees	12
Horizontal/Vertical Stress Factor	K	2
Intact Rock Mass Cohesion	MPa	5
Rock Mass Angle of Friction	^{o}	42

+ - as recommended in **Marinos and Hoek, 2000**; * - as estimated in **Seedsman, 2011**.

The Factor of Safety against arch abutment crushing and mid-span deflection for all of the panels (including empirical model predictions) are summarised in **Table 11**.

Table 11 - Summary of Voussoir Beam Analysis Outcomes for MWs 9 to 36

XL No.	MW No.	Panel Span W (m)	Effective Cover Depth H (m)	W/H	Conglomerate Beam Geometry			FoS Against Crushing	Predicted Mid-Span Deflection		
					No.	Thickness t (m)	Height above Workings, y (m)		Voussoir Beam (m)	ACARP, 2003 Single Panel (m) (mean-U95%CL)	
1	**1**	**200**	**72.0**	**0.36**	**1**	**20**	**160**	**12.60**	**0.14**	**0.07**	**0.16**
	2	**200**	**72.2**	**0.36**	**1**	**21**	**160**	**13.37**	**0.14**	**0.07**	**0.16**
	3	**200**	**97.0**	**0.49**	**1**	**22**	**160**	**9.39**	**0.16**	**0.11**	**0.24**
	6	**198**	**97.0**	**0.49**	**1**	**24**	**160**	**11.28**	**0.15**	**0.11**	**0.25**
	7	**195**	**97.0**	**0.50**	**1**	**25**	**160**	**12.97**	**0.14**	**0.11**	**0.25**
	8	193	97.0	0.50	1	26	160	14.51	0.14	0.12	0.26
	9	191	97.0	0.51	1	27	160	16.22	0.13	0.12	0.26
2	**4**	**196**	**97.0**	**0.49**	**1**	**20**	**150**	**7.03**	**0.18**	**0.11**	**0.26**
	5	**200**	**97.0**	**0.49**	**1**	**20**	**150**	**6.48**	**0.19**	**0.11**	**0.24**
3	**7**	**190**	**97.0**	**0.51**	**1**	**23**	**160**	**13.27**	**0.14**	**0.12**	**0.28**
	8	188	97.0	0.52	1	23	160	14.16	0.13	0.13	0.28
	9	185	97.0	0.52	1	23	160	15.73	0.13	0.13	0.29
	10	183	97.0	0.53	1	22	160	15.87	0.13	0.13	0.29
	11	178	97.0	0.54	1	21	160	18.43	0.12	0.14	0.31
	12	173	97.0	0.56	1	20	160	22.68	0.11	0.14	0.30
4	10	170	97.0	0.57	1	20	106	10.99	0.13	0.16	0.35
	11	184	97.0	0.53	1	20	106	11.36	0.12	0.13	0.29
5	13	188	97.0	0.52	1	30	150	15.34	0.13	0.11	0.26
	14	185	97.0	0.52	1	28	148	14.39	0.13	0.12	0.27
	15	182	97.0	0.53	1	25	148	13.33	0.13	0.13	0.28
	16	180	97.0	0.54	1	26	146	14.10	0.13	0.13	0.29

Table 11 (Cont…) - Summary of Voussoir Beam Analysis Outcomes for MWs 9 to 36

XL No.	MW No.	Panel Span W (m)	Effective Cover Depth H (m)	W/H	Conglomerate Beam Geometry			FoS Against Crushing	Predicted Mid-Span Deflection (m)		
					No.	Thickness t (m)	Height above Workings, y (m)		Voussoir Beam	ACARP, 2003 Single Panel (mean-U95%CL)	
5	17	175	97.0	0.55	1	25	144	14.56	0.12	0.14	0.31
	18	170	97.0	0.57	1	24	142	15.09	0.11	0.15	0.34
	19	165	97.0	0.59	1	22	140	14.70	0.11	0.17	0.36
	20	160	97.0	0.61	1	20	135	12.65	0.11	0.18	0.39
6	14	185	97.0	0.52	1	30	145	14.58	0.13	0.12	0.28
	15	178	97.0	0.54	1	30	143	16.61	0.12	0.14	0.30
	16	175	97.0	0.55	1	29	142	16.82	0.12	0.15	0.32
	17	173	97.0	0.56	1	28	140	16.06	0.12	0.15	0.33
	18	168	97.0	0.58	1	27	136	15.74	0.11	0.16	0.36
	19	163	97.0	0.60	1	26	133	15.87	0.11	0.18	0.39
	20	160	97.0	0.61	1	25	130	15.01	0.11	0.19	0.42
	21	158	97.0	0.61	1	24	125	12.92	0.11	0.23	0.51
	22	156	97.0	0.62	1	23	120	11.15	0.11	0.21	0.46
	23	153	97.0	0.63	1	22	116	10.14	0.12	0.22	0.48
	24	150	97.0	0.65	1	21	113	9.42	0.12	0.23	0.51
	25	148	97.0	0.66	1	20	110	7.51	0.13	0.24	0.54
7	26	167	97.0	0.58	1	20	135	10.01	0.13	0.16	0.36
	27	168	97.0	0.58	1	20	135	9.71	0.13	0.16	0.35
	28	169	97.0	0.57	1	20	135	9.44	0.13	0.16	0.35
8	26	187	97.0	0.52	1	20	150	8.70	0.16	0.13	0.29
	27	188	97.0	0.52	1	20	150	8.48	0.16	0.13	0.28
	28	189	97.0	0.51	1	20	148	7.87	0.16	0.13	0.28
	29	190	97.0	0.51	1	20	148	7.69	0.17	0.12	0.28
	30	190	97.0	0.51	1	20	148	7.69	0.17	0.13	0.28
	31	190	97.0	0.51	1	20	148	7.69	0.17	0.13	0.28
9	32	219	97.0	0.44	1	35	165	12.75	0.17	0.10	0.22
	33	218	97.0	0.44	1	32	165	11.77	0.18	0.10	0.22
	34	221	97.0	0.44	1	30	170	11.36	0.18	0.09	0.23
	35	220	97.0	0.44	1	26	175	10.71	0.18	0.09	0.22
	36	217	97.0	0.45	1	24	180	11.57	0.17	0.09	0.23
10	32	229	97.0	0.42	1	30	182	12.38	0.19	0.09	0.21
	33	230	97.0	0.42	1	30	183	12.38	0.19	0.09	0.21
	34	231	97.0	0.42	1	30	185	12.66	0.19	0.08	0.21
	35	232	97.0	0.42	1	28	188	12.12	0.19	0.08	0.21
	36	228	97.0	0.43	1	27	190	13.35	0.18	0.08	0.21

bold - extracted miniwalls; shaded - panel widths increased from **DgS, 2013**.

The results in **Table 11** are presented graphically in **Figures 15.3** and **15.4** for predicted subsidence v. FoS and W/H values respectively. Based on the subsidence data reviewed for Wyee LWs 17-23, the Voussoir beam analogy generally predicts subsidence for MWs 9 to 36 between the mean and U95%CL **ACARP, 2003** model values for 'good' to 'very good' rock mass conditions.

The Voussoir Beam model however, does not indicate a similar rate of increase in subsidence with W/H ratio as per the ACARP model; see **Figure 15.4**. The empirical model is therefore considered more likely to provide conservative estimates of single panel subsidence predictions than the Voussoir Beam model.

The compression of the chain pillars will increase the maximum panel subsidence values after the mining of several adjacent panels. The assessment of multiple panel subsidence is presented in **Section 8.8**.

8.4 Maximum Predicted Subsidence above Chain Pillars

8.4.1 Chain Pillar Geometry

The chain pillar geometries for the modified mining layout are summarised in **Table 12**.

Table 12 - Chain Pillar Geometries for the Modified Miniwall Layout

MW No.	MG Pillar Width w (m)	Development Height h (m)	w/h	Pillar Length (m)	Extraction Height T (m)	Effective Cover Depth H' (m)	Panel Width W (m)
8 - 9	32.6	3.2	10.2	95.3	3.5	200 - 173	97
13 - 20	32.6 - 29.3	3.2	10.2 - 9.2	95.3	3.5	188 - 160	97
21 - 25	29.3	3.2	9.2	95.3	3.5	160 - 148	97
26 - 31	31	3.2	9.7	95.3	3.5	187 - 190	97
32 - 36	30.6	3.2	9.6	95.3	3.5	217 - 232	97

MG = Maingate.

The predicted subsidence values above the chain pillars have been estimated in the following sub-sections based on empirical and analytical models of the roof-pillar-floor system.

8.4.2 Empirical Model Pillar Stress

The estimates of the total stress acting on the chain pillars on each side of the panel under double abutment loading conditions are presented in **Table 13** and were based on the abutment angle concept described in **ACARP, 1998a** for calibrating ALTS (Analysis of Longwall Tailgate Serviceability) to Australian coal mines; see **Figure 16**. The total stress (σ) acting on the chain pillars after mining is completed was estimated as follows:

σ = pillar load/area = $(P+A_1+A_2)/wl$

where:

P = full tributary area load of column of rock above each pillar;

= $(l+ r)(w + r).\rho.g.H$;

$A_{1,2}$ = total abutment load from each side of pillar in MN/m, and

$= (l+r)\rho g(0.5W'H - W'^2/8\tan\phi)$ (for sub-critical panel widths) or

$= (l+r)(\rho g H^2 \tan\phi)/2$ (for super-critical panel widths);

w = pillar width (solid);

l = pillar length solid;

r = roadway width;

H = depth of cover;

ϕ = abutment angle (normally taken to be 21°) and

ρ = rock mass density;

W' = effective panel width (rib to rib distance minus the roadway width).

A panel is deemed sub-critical when $W'/2 < H\tan\phi$.

8.4.3 Empirical Model Pillar Strength and FoS

The FoS of the chain pillars under double abutment loading conditions were calculated by dividing the pillar strength, S, with the pillar stress, σ. The pillar strength was based on the strength formula for "squat" pillars with w/h ratios greater than 5 from **ACARP, 1998b**, as follows:

$$S = 27.63\Theta^{0.51}(0.29((w/5h)^{2.5} - 1) + 1)/(w^{0.22}h^{0.11})$$

where:

h = pillar development height;

Θ = a dimensionless 'aspect ratio' factor or w/h ratio in this case.

8.4.4 Empirical Model Results

The predicted mean and Upper 95%CL Final Subsidence values above the proposed chain pillars (under double abutment loading conditions) are summarised for cross lines XL1 to 10 in **Table 13** for effective cover depths above the panels and pillars.

The results for all cases have been increased by a factor of 1.5 (based on the analytical assessment of time-dependant subsidence in **Section 7.2**) to allow for additional subsidence due to soft floor conditions. The adjusted values are plotted with the empirical model database in **Figure 17.1**. It is noted that the adjusted values are consistent with another case study where higher than normal subsidence above the chain pillars occurred at a mine with a weak shale roof.

Table 13 - Predicted Chain Pillar Subsidence based on Modified ACARP, 2003 Empirical Model

XL No.	MW No.	Panel Width W (m)	Effect-ive Cover Depth, H (m)	MG+ Chain Pillar Width w (m)	Pillar Height/ Width (w/h)	Chain Pillar Stress (MPa)	Pillar FoS under DA$ Loading Conditions	Adjusted Chain Pillar Subsidence S_p (m)*			
								First (mean- U95 %CL)		Final (mean - U95 %CL)	
1	**1**	**72.0**	**200**	**30.6**	**9.6**	**15.2**	**2.02**	0.25	0.50	0.31	0.55
	2	**72.2**	**200**	**30.4**	**9.5**	**16.3**	**1.87**	0.29	0.53	0.34	0.59
	3	**97.0**	**200**	**32.6**	**10.2**	**16.5**	**2.04**	0.30	0.55	0.36	0.61
	6	**97.0**	**198**	**32.6**	**10.2**	**16.3**	**2.07**	0.29	0.54	0.35	0.60
	7	**97.0**	**195**	**32.6**	**10.2**	**16.0**	**2.10**	0.28	0.53	0.34	0.59
	8	97.0	193	32.6	10.2	15.8	2.13	0.28	0.53	0.33	0.58
	9	97.0	191	32.6	10.2	-	3.13	0.16	0.41	0.19	0.45
2	**4**	**97.0**	**196**	**40**	**12.5**	**14.2**	**3.23**	0.24	0.49	0.28	0.54
	5	**97.0**	**200**	**-**	**-**	**-**	**-**	**-**	**-**	**-**	**-**
3	**7**	**97.0**	**190**	**32.6**	**10.2**	**15.5**	**2.18**	0.27	0.52	0.32	0.57
	8	97.0	188	32.6	10.2	15.2	2.21	0.26	0.51	0.31	0.57
	9	97.0	185	32.6	10.2	14.9	2.25	0.25	0.51	0.31	0.56
	10	97.0	183	32.6	10.2	14.6	2.30	0.25	0.50	0.30	0.55
	11	97.0	178	32.6	10.2	14.1	2.39	0.23	0.48	0.28	0.53
	12	97.0	173	-	-	-	-	-	-	-	-
4	10	97.0	170	32.6	10.2	13.9	2.41	0.23	0.48	0.28	0.53
	11	97.0	184	-	-	-	-	-	-	-	-
5	13	97.0	188	32.6	10.2	15.2	2.21	0.26	0.51	0.31	0.57
	14	97.0	185	32.6	10.2	14.9	2.26	0.25	0.51	0.30	0.56
	15	97.0	182	31.6	9.9	14.9	2.16	0.25	0.51	0.30	0.56
	16	97.0	180	31.1	9.7	14.7	2.13	0.25	0.50	0.30	0.55
	17	97.0	175	30.6	9.6	14.4	2.15	0.24	0.49	0.29	0.54
	18	97.0	170	29.9	9.3	14.0	2.13	0.23	0.48	0.28	0.53
	19	97.0	165	29.3	9.2	13.7	2.13	0.22	0.47	0.27	0.52
6	20	97.0	160	29.3	9.2	13.3	2.19	0.21	0.47	0.26	0.51
	14	97.0	185	32.6	10.2	14.7	2.28	0.25	0.24	0.30	0.55
	15	97.0	178	31.6	9.9	14.5	2.23	0.24	0.23	0.29	0.54
	16	97.0	175	31.1	9.7	14.3	2.20	0.24	0.23	0.29	0.54
	17	97.0	173	30.6	9.6	14.1	2.18	0.23	0.23	0.28	0.53
	18	97.0	168	29.9	9.3	13.8	2.16	0.23	0.22	0.27	0.52
	19	97.0	163	29.3	9.2	13.5	2.15	0.22	0.22	0.26	0.52
	20	97.0	160	29.3	9.2	13.3	2.19	0.21	0.22	0.25	0.49
	21	97.0	158	29.3	9.2	13.0	2.24	0.19	0.21	0.23	0.46
	22	97.0	156	29.3	9.2	12.7	2.29	0.19	0.21	0.23	0.47
	23	97.0	153	29.3	9.2	12.4	2.35	0.18	0.20	0.21	0.44
	24	97.0	150	29.3	9.2	12.1	2.41	0.17	0.20	0.21	0.44
	25	97.0	148	-	-	-	-	-	-	-	-
7	26	97.0	167	31	9.7	13.6	2.31	0.22	0.22	0.27	0.52
	27	97.0	168	31	9.7	13.7	2.29	0.22	0.22	0.27	0.52
	28	97.0	169	-	-	-	-	-	-	-	-

bold - extracted miniwalls

+ - The chain pillars are on the tailgate side of the panel.

* - Soft floor conditions assessed based on multiplying factor of 1.5.

Table 12 (Cont…) - Predicted Chain Pillar Subsidence based on Modified ACARP, 2003 Empirical Model

XL No.	MW No.	Panel Width W (m)	Effect-ive Cover Depth H (m)	MG+ Chain Pillar Width w (m)	Pillar Height/ Width (w/h)	Chain Pillar Stress (MPa)	Pillar FoS under DA$ Loading Conditions	Chain Pillar Subsidence, S_p (m)*			
								First (mean - U95%CL)		Final (mean - U95%CL)	
8	26	97.0	187	31	9.7	15.8	1.99	0.28	0.53	0.33	0.58
	27	97.0	188	31	9.7	15.9	1.97	0.28	0.53	0.34	0.59
	28	97.0	189	31	9.7	16.0	1.96	0.28	0.54	0.34	0.59
	29	97.0	190	31	9.7	16.1	1.95	0.29	0.54	0.34	0.59
	30	97.0	190	31	9.7	16.1	1.95	0.29	0.54	0.34	0.59
	31	97.0	190	-	-	-	-	-	-	-	-
9	32	97.0	219	30.6	9.6	19.4	1.59	0.39	0.64	0.47	0.72
	33	97.0	218	30.6	9.6	19.4	1.59	0.39	0.64	0.47	0.72
	34	97.0	221	30.6	9.6	19.6	1.57	0.40	0.65	0.48	0.73
	35	97.0	220	30.6	9.6	19.4	1.59	0.39	0.64	0.47	0.72
	36	97.0	217	-	-	-	-	-	-	-	-
10	32	97.0	229	30.6	9.6	20.5	1.50	0.43	0.68	0.52	0.77
	33	97.0	230	30.6	9.6	20.7	1.49	0.44	0.69	0.52	0.78
	34	97.0	231	30.6	9.6	20.8	1.48	0.44	0.69	0.53	0.78
	35	97.0	232	30.6	9.6	20.7	1.49	0.44	0.69	0.52	0.78
	36	97.0	228	-	-	-	-	-	-	-	-

$ - Double Abutment load.
+ - The chain pillars are on the tailgate side of the panel.
Shaded - pillars will be subject to multi-seam stress conditions (not included in table).
* - Soft floor conditions assessed based on multiplying factor of 1.5.

The predicted U95%CL values for Final Subsidence over the chain pillars (S_p) between the Modified MWs 9 to 36 are estimated to range from 0.45 m to 0.78 m for the 29.3 m to 32.6 m wide chain pillars (with time-dependent effects included).

The vertical stress acting on the chain pillars is estimated to range between 12.0 and 20.8 MPa with pillar FoS values from 1.48 to 3.23.

The pillar width/height ratio is a very important factor that indicates what the post-yield behaviour of the pillars is likely to occur when overloading occurs. Pillars with w/h ratios < 4 are likely to 'strain-soften' if overloading occurs and result in rapid failure and pillar runs; whereas pillars with w/h ratios > 7 are likely to 'strain-harden' and fail slowly or 'squeeze'.

The proposed chain pillars have w/h ratios > 9 and are therefore likely to strain-harden if they are over-loaded (see **Figures 17.2** to **17.4** for further demonstration of this phenomenon).

8.4.5 Analytical Model Development

The observed behaviour of the chain pillars and roof-floor system has also been used to develop a simple analytical model that includes elastic and post-yielded pillar responses to estimate subsidence above chain pillars based on laboratory testing data and observed time-dependant behaviour.

The compression of the chain pillars and immediate roof and floor strata has been estimated using the superimposition of two relatively simple analytical models. The purpose of this exercise is to check that the empirical model predictions are reasonable compared to analytical predictions, based on the range of measured physical parameters of the rock mass and coal seam. Floor softening effects may also be included in the analytical analysis.

Given that the stress on the chain pillars may exceed the in-situ strength of the coal and/or roof / floor materials, the analytical models needed to consider both the elastic and post-yield stiffness moduli of the pillar-roof-floor system.

As the FoS of the proposed chain pillars is generally > 1.5 under double abutment loading conditions it is likely that they will behave elastically in the long-term. The softening of the moisture sensitive claystone beds within the top 3 m below the floor, however, is likely to result in on-going settlement of the pillars over a period of at least 10 years after mining at a relatively constant rate of 13 mm/year.

Based on the equation for residual pillar modulus presented in **Zipf, 1999** (see **Figure 17.4**), the post-yield stiffness of the coal pillars has been estimated to equal ~15% of the peak Young's Modulus value of 2 GPa (i.e. 300 MPa).

The compression of the pillars in the elastic and post-yielded regimes has been calculated by assuming the pillar will behave like a spring under load, soften under initial yielding and then strain-harden as follows:

$$s_{pillar} = \sigma_{net} T_s / E_c + (\sigma_{max} - S_p) T_s / E_r \quad (1)$$

where:

s_{pillar} = pillar compression;

σ_{net} = pillar stress increase = maximum pillar stress - virgin stress;

T_s = Seam thickness;

E_c = Young's Modulus of Coal;

σ_{max} = maximum stress on pillar after load redistribution to the goaf (if applicable).

S_p = Pillar strength (**ACARP, 1998b**)

E_r = Residual Modulus of a 'squat' coal pillar in yield (**Zipf, 1999**)
= -0.175/(w/h) + 0.437 (GPa)

The analytical model used to estimate the immediate compression of the floor and roof was taken from Boussinesq's elastic pressure bulb theory beneath strip footings of varying aspect ratio, see **Das, 1998**:

$$s_{roof} = \sigma_{net}\, w(1-v^2)I\, [t_{roof1}/E_{roof1} + (w- t_{roof1})/E_{roof1}] \quad (2)$$

$$s_{floor} = \sigma_{net}\, w(1-v^2)I\, [t_{floor1}/E_{floor1} + (w- t_{floor1})/E_{floor1}] \quad (3)$$

where:

s_{roof} = roof compression above pillar;

s_{floor} = floor compression below pillar;

σ_{net} = net pillar stress increase (= total stress - effective pre-mining stress);

w = pillar width;

$E_{1,2\ roof}$ = Young's Modulus of roof materials 1 and 2 within a distance (w) above the pillar;

$E_{1,2\ floor}$ = Young's Modulus of floor materials 1 and 2 within a distance (w) below the pillar;

v = Poisson's Ratio;

I = Influence function for flexible rectangular footing shape geometries;
= 1 allowing for stiffness input uncertainty.

The estimate of analytical model surface subsidence (s_{total}) above a chain pillar subject to double abutment loading conditions may be estimated by summing equations (1), (2) and (3):

$$s_{total\ (mean)} = s_{pillar} + s_{roof} + s_{floor} \text{ (mean value)}$$

Worst-case subsidence ($S_{total\text{-}WC}$) has assumed the input parameters have been underestimated by 33% or $S_{total\text{-}WC} = 1.5 \times S_{total\ (mean)}$

Estimates of the mean laboratory and rock mass strength and stiffness properties for undrained, drained and softened conditions are presented in **Table 14** for the purposes of subsidence assessment.

Table 14 - Rock Mass Strength and Undrained and Softened Modulus Estimates (Mean Values)

Stratigraphic Units	GSI	E_{rm}/E_{lab}*	Rock Mass UCS Range+ [Average] (MPa)	Laboratory Youngs Moduli^ (GPa)	Undrained Rock Mass Moduli^ (GPa)	Drained Rock Mass Moduli* (GPa)	Softened Rock Mass Moduli* (GPa)
Conglomerate,	80	0.9	24 - 67 [60]	18	15	15	15
sandstone and siltstone	65	0.5	40	6	3	3	3
Awaba Tuff, mudstone and claystone floor	40	0.3	2 - 66 [16]	4	1.2	0.6	0.3
WAL, GN, & FAS Seams, Shaley Coal	50	0.37	16 - 32 [16]	4	1.5	1.5	0.75

\+ - UCS derived from laboratory testing on bore core samples from nearby mines.

^ - Laboratory Young's Modulus (E) derived from laboratory and sonic UCS data, E = 250 - 300 x UCS (units are in gigapascals [GPa]).

* - $E_{rockmass} = E_{laboratory}(0.02+1/(1+e^{(60-GSI)/11})$; **Hoek and Diederichs, 2006**.

8.4.6 Analytical Model Results

Analytical chain pillar subsidence predictions were determined for the modified mining layout (**Table 15**) and compared to the empirical model values in **Figures 18.1** and **18.2** for Wyee and Chain Valley Colliery data respectively.

Table 15 - Analytical Subsidence Model Predictions above the Modified Chain Pillars

XL No.	MW No.	Cover H (m)	Panel W (m)	Pillar Width w (m)	Pillar Stress (MPa)	Pillar FoS Under Final Loading	Subsidence Predictions Based on Analytical Pillar-Strata System Compression (m)*				
							Pillar	Roof	Floor	Total (mean)	1.5 x Total
1	**1**	**200**	**72.0**	**30.6**	**15.22**	**2.02**	**0.02**	**0.18**	**0.21**	**0.41**	**0.62**
	2	**200**	**72.2**	**30.4**	**15.31**	**2.00**	**0.02**	**0.18**	**0.20**	**0.41**	**0.61**
	3	**200**	**97.0**	**32.6**	**16.58**	**2.03**	**0.02**	**0.21**	**0.24**	**0.48**	**0.72**
	6	**198**	**97.0**	**32.6**	**16.37**	**2.05**	**0.02**	**0.21**	**0.24**	**0.47**	**0.70**
	7	**195**	**97.0**	**32.6**	**16.05**	**2.09**	**0.02**	**0.21**	**0.24**	**0.47**	**0.70**
	8	193	97.0	32.6	15.84	2.12	0.02	0.21	0.23	0.46	0.69
	9	191	97.0	32.6	15.63	2.15	0.02	0.20	0.23	0.46	0.68
2	**4**	**196**	**97.0**	**40**	**14.12**	**3.26**	**0.02**	**0.21**	**0.24**	**0.47**	**0.70**
	5	**200**	**97.0**	**186**	**-**	**-**	0.00	0.24	0.26	0.51	0.76
3	**7**	**190**	**97.0**	**32.6**	**15.53**	**2.17**	**0.02**	**0.20**	**0.23**	**0.45**	**0.68**
	8	188	97.0	32.6	15.32	2.20	0.02	0.20	0.23	0.45	0.67
	9	185	97.0	32.6	15.00	2.24	0.02	0.19	0.22	0.44	0.65
	10	183	97.0	32.6	14.79	2.27	0.02	0.19	0.22	0.43	0.64
	11	178	97.0	32.6	14.27	2.36	0.02	0.18	0.21	0.41	0.62
	12	173	97.0	32.6	13.74	2.45	0.02	0.18	0.20	0.40	0.59

Table 15 (Cont…) - Analytical Subsidence Model Predictions Above the Modified Chain Pillars

XL No.	MW No.	Cover H (m)	Panel W (m)	Pillar Width w (m)	Pillar Stress (MPa)	Pillar FoS Under Final Loading	Subsidence Predictions Based on Analytical Pillar-Strata System Compression (m)*				
							Pillar	Roof	Floor	Total (mean)	1.5 x Total
4	10	170	97.0	32.6	13.43	2.50	0.02	0.17	0.19	0.39	0.58
	11	184	97.0	300	-	-	0.00	0.23	0.25	0.49	0.73
5	13	188	97.0	32.6	15.32	2.20	0.02	0.20	0.23	0.45	0.67
	14	185	97.0	32.6	15.00	2.24	0.02	0.19	0.22	0.44	0.65
	15	182	97.0	31.6	15.00	2.15	0.02	0.19	0.22	0.43	0.64
	16	180	97.0	31.1	14.94	2.11	0.02	0.19	0.21	0.42	0.63
	17	175	97.0	30.6	14.56	2.12	0.02	0.18	0.20	0.40	0.61
	18	170	97.0	29.9	14.23	2.10	0.02	0.17	0.19	0.39	0.58
	19	165	97.0	29.3	13.86	2.10	0.02	0.16	0.19	0.37	0.56
	20	160	97.0	29.3	13.30	2.19	0.02	0.16	0.18	0.35	0.53
6	14	185	97.0	32.6	15.00	2.24	0.02	0.19	0.22	0.44	0.65
	15	178	97.0	31.6	14.57	2.21	0.02	0.18	0.21	0.41	0.62
	16	175	97.0	31.1	14.40	2.19	0.02	0.18	0.20	0.40	0.61
	17	173	97.0	30.6	14.34	2.15	0.02	0.18	0.20	0.40	0.60
	18	168	97.0	29.9	14.01	2.13	0.02	0.17	0.19	0.38	0.57
	19	163	97.0	29.3	13.63	2.13	0.02	0.16	0.18	0.36	0.55
	20	160	97.0	29.3	13.29	2.19	0.02	0.16	0.18	0.35	0.53
	21	158	97.0	29.3	13.06	2.23	0.02	0.15	0.17	0.35	0.52
	22	156	97.0	29.3	12.84	2.27	0.02	0.15	0.17	0.34	0.51
	23	153	97.0	29.3	12.50	2.33	0.02	0.15	0.17	0.33	0.50
	24	150	97.0	29.3	12.16	2.39	0.02	0.14	0.16	0.32	0.48
	25	148	97.0	300	-	-	0.00	0.17	0.19	0.36	0.54
7	26	167	97.0	31	13.56	2.31	0.02	0.17	0.19	0.38	0.56
	27	168	97.0	31	13.67	2.29	0.02	0.17	0.19	0.38	0.57
	28	169	97.0	300	-	-	0.00	0.21	0.23	0.43	0.65
8	26	187	97.0	31	15.74	1.99	0.02	0.20	0.22	0.44	0.67
	27	188	97.0	31	15.85	1.98	0.02	0.20	0.23	0.45	0.67
	28	189	97.0	31	15.96	1.96	0.02	0.20	0.23	0.45	0.68
	29	190	97.0	31	16.07	1.95	0.02	0.20	0.23	0.45	0.68
	30	190	97.0	31	16.07	1.95	0.02	0.20	0.23	0.45	0.68
	31	190	97.0	300	-	-	0.02	0.20	0.23	0.45	0.68
9	32	219	97.0	30.6	19.41	1.59	0.03	0.24	0.28	0.55	0.83
	33	218	97.0	30.6	19.30	1.60	0.03	0.24	0.28	0.55	0.82
	34	221	97.0	30.6	19.63	1.57	0.03	0.25	0.28	0.56	0.84
	35	220	97.0	30.6	19.52	1.58	0.03	0.25	0.28	0.56	0.83
	36	217	97.0	300	-	-	0.03	0.24	0.27	0.55	0.82
10	32	229	97.0	30.6	20.51	1.50	0.03	0.26	0.30	0.59	0.88
	33	230	97.0	30.6	20.62	1.49	0.03	0.26	0.30	0.59	0.88
	34	231	97.0	30.6	20.73	1.49	0.03	0.26	0.30	0.59	0.89
	35	232	97.0	30.6	19.94	1.69	0.03	0.26	0.30	0.60	0.89
	36	228	97.0	300	-	-	0.03	0.26	0.29	0.58	0.87

Shaded - pillars will be subject to multi-seam stress conditions.

* - t_{pillar} = 3.5 m; t_{roof1}=0.3 m;t_{roof2}=w-0.3; t_{floor1}= 0.9 m; t_{floor2} = w-0.9

The results of the analytical subsidence prediction analysis for the mean material properties and cover depth ranges indicate that the subsidence over the proposed chain pillars will range

between 0.32 m and 0.51 m after mining is completed. A 50% decrease in elastic modulus due to claystone unit softening will increase the predicted subsidence to 0.59 m and 0.89 m.

The mean and 1.5 x mean values of the analytical model also plot close to or just below the mean and Upper 95%CL values for the empirical model respectively (see **Figure 18.2**). The empirical model predictions are therefore considered reasonable for impact analysis purposes.

The analytical model also indicates that in the elastic range, approximately 5% of the surface subsidence is due to the compression of the pillar with 44% from the roof and 51% from the floor strata. The compression of the strata and chain pillars under double abutment loading conditions is also likely to result in a small proportion of the pillar stress transferring to the adjacent goaf.

8.5 Analytical Goaf Stiffness Model

Strain-hardening response of goaf between chain pillars will occur as the overburden strata compresses it, with Young's Moduli increasing exponentially up to and beyond the pre-mining stress (**Hardy and Heasley, 2004**). The stress-strain (σ-ε) curve for the strain-hardening goaf model used in this study is presented below:

$\sigma_g = a[e^{b\varepsilon} - 1]$

where

$a = E_i\sigma_v/(E_f-E_i)$

$b = (E_f-E_i)/\sigma_v$

σ_v= virgin vertical stress or a maximum vertical stress for a given cover depth.

E_i = initial Young's Modulus

E_f= final Young's Modulus

ε = rubble strain at seam level = c/nT

n = ratio of goaf or rubble thickness/seam thickness or mining height

T = mining height.

c = roof convergence at seam level

There is usually a small amount of void between the top of the collapsed roof rubble and overburden, which must be closed before the rubble starts to load up (i.e. system 'slackness'). The author of the LaModel® program suggests a typical initial Young's Modulus (E_i) of 0.7

MPa for the goaf and a maximum goaf stress limit to reasonably model the field conditions **Hardy and Heasley, 2004**.

The 'n' and Final Young's Modulus are the key variables required for calibrating the goaf model to measured maximum subsidence above extracted miniwall panels.

For an n = 4, the E_f values for the goaf in the Site with depths of cover from 148 m to 232 m, are estimated to range between 130 MPa and 222 MPa (see **Figure 19**).

Based on the premise that a proportion of the total pillar load will shed to the goaf as the overburden strata deflects and the chain pillar compresses, a simple beam and supporting spring analogy indicates that up to 50% of the pillar load may be supported by the goaf if it develops similar stiffness to the chain pillar that has an FoS of less than 1 and has gone into yield.

The empirical equation determined by **Zipf, 1999** gives a residual pillar stiffness E_r range of 250 to 300 MPa for pillars with a w/h ratios of 9.2 to 10.2, which is slightly higher for the goaf at the given cover depth range (see **Figure 19**).

The above analysis provides the mechanism to explain the strain hardening behaviour of the measured chain pillar subsidence curve, which is apparent for pillar stresses greater than 30 MPa in the empirical model (see **Figure 17.1**).

The load sharing mechanism between goaf and chain pillars is also influenced by the mining geometry (panel width and mining height) and affects the maximum subsidence predicted for multiple panels (see **Section 8.9**).

8.6 Goaf Edge Subsidence Prediction

Based on the DgS modified **ACARP, 2003** model, the final mean and U95%CL goaf edge subsidence predictions for the Modified MWs 9 to 36 range from 0.04 to 0.25 m and from 0.07 to 0.36 m respectively. The results have been derived from the prediction curves shown in **Figure 20.1** and the maximum final panel subsidence ranges with soft floor conditions (see **Section 8.8**).

The predictions are reasonably similar to the 2013 EIS (see **Section 8.11**) and measured values above MWs 1 to 8 to-date (see **Section 7.1**).

The predictions do not include the effects of multi-seam mining due to uncertainty in how the previous and additional subsidence has been or will be distributed above the miniwall layout.

8.7 Angle of Draw Prediction

The AoD predictions have been derived from the goaf edge subsidence predictions for MWs 9 to 36 assessed in **Section 8.6**.

The mean to U95%CL angle of draw (AoD) values around the limits of the proposed miniwall panels have been estimated from the prediction curves shown in **Figure 20.2** and range from 8.0^o to 30.2^o for cover depths from 148 m to 232 m.

The predictions are summarised in **Table 16A** and do not include the effects of multi-seam mining (see **Section 8.8**). The results are reasonably similar to the 2013 EIS (see **Section 8.11**) and measured values above MWs 1 to 8 to-date (see **Section 7.1**).

Multi-seam subsidence effects on angle of draw above MWs 32 - 36 are further discussed in **Section 9**.

Table 16A - Summary of Goaf Edge and Angle of Draw Predictions for Modified MWs 9 to 36

XL No.	MW No.	Goaf Edge Subsidence (m)		Angle of Draw (^{o})	
		mean	U95%CL	mean	U95%CL
1	**1**	0.21	0.28	**20.2**	***28.9***
	2	0.25	0.34	**21.7**	***30.4***
	3	0.16	0.26	**18.1**	***26.8***
	6	0.15	0.25	**18.0**	***26.7***
	7	0.15	0.25	**17.8**	**26.5**
	8	0.15	0.24	**17.5**	**26.2**
	9	0.11	0.17	15.1	23.8
2	**4**	0.11	0.18	**15.2**	**23.9**
	5	0.09	0.14	**13.6**	**22.3**
3	7	0.11	0.19	15.6	24.3
	8	0.13	0.22	16.8	25.5
	9	0.13	0.21	16.5	25.2
	10	0.12	0.21	16.2	24.9
	11	0.11	0.19	15.6	24.3
	12	0.09	0.15	13.7	22.4
4	10	0.09	0.16	13.6	22.3
	11	0.06	0.11	11.1	19.8
5	13	0.12	0.19	15.9	24.6
	14	0.13	0.22	16.9	25.6
	15	0.13	0.22	16.6	25.3
	16	0.13	0.21	16.4	25.1
	17	0.12	0.20	15.8	24.5
	18	0.11	0.19	15.1	23.8
	19	0.10	0.18	14.6	23.3
	20	0.09	0.17	14.0	22.7
6	14	0.11	0.18	15.2	23.9
	15	0.12	0.20	15.9	24.6
	16	0.11	0.19	15.5	24.2
	17	0.11	0.19	15.3	24.0

bold - extracted panels, *italics* **-** angle of draw above 26.5^o.

Table 16A (Cont…) - Summary of Goaf Edge and Angle of Draw Predictions for Modified MWs 9 to 36

XL No.	MW No.	Goaf Edge Subsidence (m)		Angle of Draw (°)	
		mean	U95%CL	mean	U95%CL
6	18	0.10	0.18	14.7	23.4
	19	0.09	0.17	14.2	22.9
	20	0.09	0.16	13.5	22.2
	21	0.07	0.14	12.1	20.8
	22	0.08	0.15	12.6	21.3
	23	0.07	0.14	12.1	20.8
	24	0.07	0.13	11.6	20.3
	25	0.04	0.08	8.0	16.7
7	26	0.08	0.15	13.3	22.0
	27	0.10	0.18	14.6	23.3
	28	0.06	0.10	10.5	19.2
8	26	0.11	0.19	15.6	24.3
	27	0.14	0.23	17.1	25.8
	28	0.14	0.23	17.2	25.9
	29	0.14	0.24	17.3	26.0
	30	0.14	0.24	17.3	26.0
	31	0.07	0.12	12.1	20.8
9	32	0.19	0.29	19.5	*28.2*
	33	0.19	0.29	19.6	*28.3*
	34	0.20	0.31	20.0	*28.7*
	35	0.20	0.31	20.0	*28.7*
	36	0.04	0.07	8.2	16.9
10	32	0.23	0.34	21.0	*29.7*
	33	0.24	0.35	21.2	*29.9*
	34	0.24	0.36	21.4	*30.1*
	35	0.25	0.36	21.5	*30.2*
	36	0.05	0.07	8.6	17.3

italics **-** angle of draw above 26.5°.

A review of the subsidence data above the old Wallarah Seam workings beneath Summerland Point indicates the predicted angles of draw for the proposed miniwalls are reasonable. A summary of the measured and inferred angles of draw outside the limits of areas of total extraction panels are presented in **Table 16B**.

Table 16B - Measured and Inferred Angles of Draw for Old Wallarah Seam Workings

Survey Line	Peg	Measured Subsidence (mm)	Distance from Goaf Edge (m)	Cover Depth (m)	Angle of Draw (o)
23	49	29	54	133	>22
	53	34	50	137	>20
	54	26	55	137	>21.9
	55	20	56	137	22.2
	56	8	57	137	<22.6
	60	17	63	137	<24.7

8.8 Multiple Panel Subsidence Prediction

Based on the predicted maximum single panel, chain pillar and goaf edge subsidence values derived from the **ACARP, 2003** model, the mean and worst-case first and final maximum subsidence predictions for multi-panels (and the associated impact parameters) are summarised for cross lines (XLs 1 to 10; see **Figure 2**) in the **Table 17** for MWs 9 to 36.

Multi-seam mining interaction will affect five of the proposed miniwalls (MWs 32-36) and will be further discussed in **Section 8.10**.

Table 17 - Predicted Maximum Subsidence Effects for Modified MWs 9 to 36 with High SRP

XL No	MW No.	Panel Width W (m)	Cover Depth H' (m)	Rock Cover Depth H_r (m)	W/H_r Ratio	Massive Unit Thickness (t) & Location above mine roof (y) (m)		Chain Pillar Width wcp (m)	Face Height T (m)	First S_{max*} (m)		Final S_{max*} (m)		First Pillar* S_p (m)		Final Pillar* S_p (m)		Tilt T_{max} (mm/m)		Horizontal Strain* (mm/m)	
																				Tensile	Comp-ressive
						t	y			*m*	*U95*	*m*	*U95*	*m*	*U95*	*m*	*U95*	*m*	*U95*	*U95*	*U95*
1	**1**	**72**	**200**	**180**	**0.40**	**20**	**160**	**30.6**	**3.4**	**0.07**	**0.33**	**0.27**	**0.54**	**0.25**	**0.50**	**0.31**	**0.55**	**8**	**12**	**4**	**3**
	2	**72**	**200**	**181**	**0.40**	**21**	**160**	**30.4**	**3.4**	**0.15**	**0.41**	**0.33**	**0.60**	**0.29**	**0.53**	**0.34**	**0.59**	**10**	**16**	**4**	**4**
	3	**97**	**200**	**182**	**0.53**	**22**	**160**	**32.6**	**3.5**	**0.21**	**0.50**	**0.44**	**0.72**	**0.30**	**0.55**	**0.36**	**0.61**	**10**	**15**	**6**	**5**
	6	**97**	**198**	**181**	**0.54**	**24**	**160**	**32.6**	**3.5**	**0.22**	**0.51**	**0.44**	**0.72**	**0.29**	**0.54**	**0.35**	**0.60**	**10**	**15**	**6**	**5**
	7	**97**	**195**	**180**	**0.54**	**25**	**160**	**32.6**	**3.5**	**0.22**	**0.50**	**0.43**	**0.72**	**0.28**	**0.53**	**0.34**	**0.59**	**10**	**15**	**6**	**5**
	8	**97**	**193**	**179**	**0.54**	**26**	**160**	**32.6**	**3.5**	**0.21**	**0.50**	**0.42**	**0.71**	**0.28**	**0.53**	**0.33**	**0.58**	**10**	**14**	**5**	**5**
	9	97	191	178	0.54	27	160	32.6	3.5	0.21	0.50	0.31	0.60	0.16	0.41	0.19	0.45	6	9	4	4
2	**4**	**97**	**196**	**178**	**0.54**	**20**	**150**	**40**	**3.5**	**0.12**	**0.41**	**0.31**	**0.61**	**0.24**	**0.49**	**0.28**	**0.54**	**6**	**9**	**4**	**4**
	5	**97**	**200**	**182**	**0.53**	**20**	**150**	**186**	**3.5**	**0.19**	**0.48**	**0.24**	**0.53**	**-**	**-**	**-**	**-**	**4**	**6**	**3**	**3**
3	7	97	190	174	0.56	23	160	32.6	3.5	0.12	0.42	0.35	0.65	0.27	0.52	0.32	0.57	7	11	5	4
	8	97	188	173	0.56	23	160	32.6	3.5	0.22	0.51	0.42	0.71	0.26	0.51	0.31	0.57	9	14	5	5
	9	97	185	171	0.57	23	160	32.6	3.5	0.22	0.52	0.41	0.71	0.25	0.51	0.31	0.56	9	14	5	5
	10	97	183	169	0.57	22	160	32.6	3.5	0.22	0.52	0.41	0.71	0.25	0.50	0.30	0.55	9	14	5	5
	11	97	178	165	0.59	21	160	32.6	3.5	0.23	0.53	0.40	0.71	0.23	0.48	0.28	0.53	9	13	5	5
	12	97	173	167	0.58	20	160	32.6	3.5	0.22	0.52	0.30	0.60	0.14	0.39	0.17	0.42	6	9	4	4
4	10	97	170	156	0.62	20	106	32.6	3.5	0.16	0.48	0.36	0.67	0.23	0.48	0.28	0.53	7	11	5	4
	11	97	184	169	0.57	20	106	300	3.5	0.21	0.37	0.21	0.37	-	-	-	-	3	5	3	3
5	13	97	188	180	0.54	30	150	32.6	3.5	0.11	0.40	0.33	0.62	0.26	0.51	0.31	0.57	7	10	4	4
	14	97	185	177	0.55	28	148	32.6	3.5	0.21	0.50	0.40	0.69	0.25	0.51	0.30	0.56	9	13	5	5
	15	97	182	173	0.56	25	148	31.6	3.5	0.21	0.51	0.41	0.70	0.25	0.51	0.30	0.56	9	13	5	5
	16	97	180	171	0.57	26	146	31.1	3.5	0.22	0.51	0.41	0.70	0.25	0.50	0.30	0.55	9	14	5	5
	17	97	175	165	0.59	25	144	30.6	3.5	0.23	0.53	0.41	0.71	0.24	0.49	0.29	0.54	9	14	5	5
	19	97	170	159	0.61	24	142	29.9	3.5	0.24	0.55	0.42	0.73	0.23	0.48	0.28	0.53	9	14	5	5
	20	97	165	154	0.63	22	140	29.3	3.5	0.25	0.57	0.42	0.74	0.22	0.47	0.27	0.52	9	14	5	5

Table 17 (cont…) - Predicted Maximum Subsidence Effects for MWs 9 to 36 for High SRP

XL No	MW No.	Panel Width W (m)	Cover Depth, H (m)	Rock Cover Depth Hr (m)	W/H_r Ratio	Massive Unit Thickness (t) & Location above mine roof (y) (m)		Chain Pillar Width (m)	Face Height T (m)	First S_{max}* (m)		Final S_{max}* (m)		First Pillar* S_p (m)		Final Pillar* S_p (m)		Tilt T_{max} (mm/m)		Horizontal Strain* (mm/m)	
																				Tensile	Comp-ressive
						t	y			*m*	*U95*	*m*	*U95*	*m*	*U95*	*m*	*U95*	*m*	*U95*	*U95*	*U95*
6	14	97	185	174	0.56	30	145	32.6	3.5	0.12	0.42	0.34	0.63	0.25	0.50	0.30	0.55	7	10	4	4
	15	97	178	166	0.58	30	143	31.6	3.5	0.22	0.53	0.41	0.71	0.24	0.49	0.29	0.54	9	13	5	5
	16	97	175	162	0.60	29	142	31.1	3.5	0.23	0.54	0.42	0.73	0.24	0.49	0.29	0.54	9	13	5	5
	17	97	173	160	0.61	28	140	30.6	3.5	0.23	0.54	0.42	0.73	0.23	0.49	0.28	0.53	9	13	5	5
	18	97	168	155	0.63	27	136	29.9	3.5	0.25	0.56	0.42	0.74	0.23	0.48	0.27	0.52	9	14	5	5
	19	97	163	149	0.65	26	133	29.3	3.5	0.26	0.59	0.43	0.76	0.22	0.47	0.26	0.52	9	14	6	5
	20	97	160	145	0.67	25	130	29.3	***3.4***	0.26	0.59	0.43	0.76	0.21	0.45	0.25	0.49	9	14	6	5
	21	97	158	135	0.72	24	125	29.3	***3.0***	0.27	0.60	0.43	0.76	0.19	0.42	0.23	0.46	9	14	6	5
	22	97	156	140	0.69	23	120	29.3	***3.3***	0.26	0.60	0.42	0.75	0.19	0.43	0.23	0.47	9	13	5	5
	23	97	153	137	0.71	22	116	29.3	***3.2***	0.27	0.60	0.41	0.74	0.18	0.41	0.21	0.44	9	13	5	5
	24	97	150	134	0.72	21	113	29.3	***3.1***	0.27	0.61	0.41	0.75	0.17	0.40	0.21	0.44	9	13	5	5
	25	97	148	132	0.74	20	110	300	***3.0***	0.24	0.52	0.27	0.52	-	-	-	-	5	7	3	3
7	26	97	167	155	0.63	20	135	31	3.5	0.16	0.48	0.35	0.67	0.22	0.47	0.27	0.52	7	11	5	4
	27	97	168	156	0.62	20	135	31	3.5	0.20	0.55	0.41	0.73	0.22	0.48	0.27	0.52	9	13	5	5
	28	97	169	156	0.62	20	135	300	3.5	0.20	0.43	0.24	0.43	-	-	-	-	4	6	3	3
8	26	97	187	171	0.57	20	150	31	3.5	0.13	0.43	0.37	0.66	0.28	0.53	0.33	0.58	7	11	5	5
	27	97	188	172	0.56	20	150	31	3.5	0.18	0.52	0.44	0.74	0.28	0.53	0.34	0.59	10	15	6	5
	28	97	189	173	0.56	20	148	31	3.5	0.18	0.52	0.44	0.74	0.28	0.54	0.34	0.59	10	15	6	6
	29	97	190	174	0.56	20	148	31	3.5	0.18	0.52	0.44	0.74	0.29	0.54	0.34	0.59	10	15	6	6
	30	97	190	173	0.56	20	148	31	3.5	0.18	0.52	0.45	0.74	0.29	0.54	0.34	0.59	10	15	6	6
	31	97	190	173	0.56	20	148	300	3.5	0.18	0.38	0.23	0.38	-	-	-	-	4	5	3	3

Table 17 (cont…) - Predicted Maximum Subsidence Effects for MWs 1 to 36 for High SRP (Single Seam Only)

XL No.	MW No.	Panel Width W (m)	Effective Cover Depth H (m)	Rock Cover Depth H' (m)	W/H' Ratio	Massive Unit Thickness (t) & Location above mine roof (y) (m)		Chain Pillar Width w_{cp} (m)	Face Height T (m)	First S_{max}* (m)		Final S_{max}* (m)		First Pillar* S_p (m)		Final Pillar* S_p (m)		Tilt T_{max} (mm/m)		Horizontal Strain* (mm/m)	
																				Tensile	Comp-ressive
						t	y			*m*	*U95*	*m*	*U95*	*m*	*U95*	*m*	*U95*	*m*	*U95*	*U95*	*U95*
9	32	97	219	196	0.49	35	165	30.6	3.5	0.10	0.38	0.43	0.71	0.39	0.64	0.47	0.72	9	14	6	5
	33	97	218	197	0.49	32	165	30.6	3.5	0.10	0.38	0.43	0.71	0.39	0.64	0.47	0.72	9	14	6	5
	34	97	221	202	0.48	30	170	30.6	3.5	0.09	0.38	0.43	0.72	0.40	0.65	0.48	0.73	9	14	6	5
	35	97	220	203	0.48	26	175	30.6	3.5	0.09	0.38	0.42	0.71	0.39	0.64	0.47	0.72	9	14	5	5
	36	97	217	202	0.48	24	180	300	3.5	0.09	0.23	0.09	0.23	-	-	-	-	1	2	1	1
10	32	97	229	208	0.47	30	182	30.6	3.5	0.09	0.37	0.45	0.74	0.43	0.68	0.52	0.77	10	15	6	6
	33	97	230	210	0.46	30	183	30.6	3.5	0.09	0.37	0.45	0.74	0.44	0.69	0.52	0.78	10	15	6	6
	34	97	231	212	0.46	30	185	30.6	3.5	0.08	0.37	0.46	0.74	0.44	0.69	0.53	0.78	10	15	6	6
	35	97	232	214	0.45	28	188	30.6	3.5	0.08	0.36	0.45	0.73	0.44	0.69	0.52	0.78	10	15	6	6
	36	97	228	212	0.46	27	190	300	3.5	0.08	0.21	0.08	0.21	-	-	-	-	1	2	1	1

Cover depth, H = cover below land surface and lake bed sediments to give equivalent soil and rock cover for estimating chain pillar subsidence.
Bold - MWs 1 - 8 have already been extracted; ***Bold italics*** - Face height reduced to meet minimum constrained zone thickness criteria below Lake.
* - Predictions based on Rock Cover Depth, H' = rock head cover below lake bed sediments and weathered rock to estimate overburden deflection.
Unit y = distance to base of massive strata unit above the mine workings.
SRP = refers to Subsidence Reduction Potential of the assumed strata unit for the purposes of subsidence prediction (i.e. Low, Moderate, High).
^ - Predicted strains are for a surface with deep soil cover and a 'smooth' subsidence profile. Near surface rock may cause strain concentrations which are 2 x 'smooth' profile strains.
mean = average or mean prediction. U*95* = Upper 95% Confidence Limit or Credible-Worst Case prediction for smooth profiles.
Shaded - pillars will be subject to multi-seam stress conditions (not included in **Table 17**).

The predicted credible worst-case (U95%CL) single seam only subsidence effect results for MWs 9 to 36 are summarised below:

- **First maximum panel subsidence** ranges from 0.21 m to 0.61 m (average of 0.48 m). Previously, **DgS, 2013** predicted ranges from 0.16 m to 0.57 m (average of 0.32 m).

- **Final maximum panel subsidence** ranges from 0.21 m to 0.76 m (average of 0.66 m). Previously, **DgS, 2013** predicted ranges from 0.23 m to 0.62 m (average of 0.43 m).

- **First maximum chain pillar subsidence** ranges from 0.39 m to 0.69 m (average of 0.52 m). Previously, **DgS, 2013** predicted ranges from 0.15 m to 0.34 m (average of 0.23 m).

- **Final maximum chain pillar subsidence** range from 0.42 m to 0.78 m (average of 0.57 m). Previously, **DgS, 2013** predicted ranges from 0.16 m to 0.41 m (average of 0.26 m).

- **Maximum panel tilt** ranges from 2 to 15 mm/m (average of 12 mm/m). Previously, **DgS, 2013** predicted ranges from 2 to 17 mm/m (average of 8 mm/m).

- **Maximum panel compressive strains** range from 1 to 6 mm/m (average of 3.5 mm/m). Previously, **DgS, 2013** predicted ranges from 1 to 6 mm/m (average of 3 mm/m).

- **Maximum panel tensile strains** range from 1 to 6 mm/m (average of 3.5 mm/m). Previously, **DgS, 2013** predicted ranges from 1 to 6 mm/m (average of 3 mm/m).

8.9 Subsidence Profile Predictions

Credible worst-case (Upper 95% Confidence Limit) subsidence effect profile predictions for Modified MWs 9 to 36 have been derived along cross lines XL1 to 10 after (i) each panel is extracted and (ii) on the completion of mining for SDPS model calibration purposes. The profiles are presented in **Figures 22.1** to **22.10**.

Based on the predicted subsidence profile exercise, credible worst case subsidence contours have subsequently been derived. Details of the predicted outcomes are presented and further discussed in **Section 10**.

8.10 Predicted Subsidence Increases due to Multi-Seam Workings Stress Interaction from Modified MWs 32 to 36

As discussed earlier **DgS, 2013** assumed 32.6 m wide chain pillars instead of 30.6 m wide pillars as intended for the miniwalls proposed beneath Chain Valley Bay. The difference in pillar width results in a slight increase in the pillar stresses of 6.5%, which has now been

corrected in this study, plus the additional subsidence to allow for softened claystone floor units.

Multi-seam pillar stress interaction potential and pillar stability for the proposed miniwalls in Chain Valley Bay were assessed in **DgS, 2013** using a combination of empirical, analytical and pseudo-numerical techniques (Lam-2D). Details of the assessment methodology are given in **DgS, 2013**.

The Lam2D model's results for the 32.6 m wide pillars have subsequently been multiplied by a pillar width ratio of 1.065 (i.e. 32.6/30.6) to estimate the increase in pillar stresses for 30.6 m wide pillars, and are presented in **Table 18**.

Table 18 - Estimated Subsidence increases due to Multi Seam Mine Workings Interaction in Chain Valley Bay due to 30.6 m wide Chain Pillars (MWs 32 to 36) based on pseudo-Numerical Modelling (Lam2D)

Location	Cover Depth H_i (m)	Typical Pillar Dimensions w x l (m)	Pillar Height h (m)	Increase in Pillar Stress (MPa)	Final Pillar Stress (MPa)	Final Pillar FoS	Subsidence Increase (mm)
Wallarah Seam Pillars	160	28 x 28 (SWs)	3.0	-2.5 to +2.5	10.3 - 15.3	1.64 - 2.44	46 - 68
	150	20 x 24 (FWs)	3.0	-2.5 to +2.5	3.4 - 8.4	2.03 - 5.01	1 - 17
Wallarah Seam Goaf	150	60 x 500 (SWs)	3.0	-1.7 to +1.7	0.8 - 3.9	Na	*17*
Great Northern	190	19 x 19 (FWs)	2.5	-3.4 to +6.6	4.5 - 14.5	4.51 - 1.39	92 - 137
Fassifern Pillars	220	30.6 x 95 (SWs)	3.2	-0.4 to +0.4	19.5 - 20.3	1.51 - 1.58	7 - 12
Fassifern Seam Goaf	220	97 (SWs)	3.2	-0.2 to +0.2	5.3 - 5.7	-	*4*
Multi-Seam Subsidence Increase Range for Wallarah Seam							1 - 68
Multi-Seam Subsidence Increase Range for Great Northern Seam							92 - 137
Multi-Seam Subsidence Increase Range for Fassifern Seam							7 - 12
Total Multi-Seam Subsidence Increase for Three Seams							**100 - 217**

Italics - subsidence range for goaf likely to be included in pillar subsidence increase range.

The change in pillar FoS and w/h ratios after multi-seam stress increases and worst-case pillar heights occur are plotted in **Figure 23**. The results indicate that some of the Great Northern Seam pillars FoS plot between 1.0 and 1.6 with others FoS exceeding 3. All pillars will have 'squat' pillar geometries and therefore are unlikely to cause a significant increase in subsidence should the pillars go into yield. Load transfer between yielding pillars and compressing goaf or non-yielded pillars is also likely to limit subsidence to the values shown above.

It is estimated that the pillar stress increases due to the multi-seam action effects will result in a further 100 mm to 217 mm of subsidence above Modified MWs 32 to 36 in addition to the predicted chain pillar subsidence range of 420 mm to 780 mm estimated due to single seam subsidence and softened claystone floor effects.

The incremental subsidence due to MWs 32 and 36 may range from 549 mm to 937 mm (including the multi-seam effects and soft floor conditions). The estimated subsidence does not include the estimated subsidence after the WAL and GN seams were mined.

The cumulative subsidence (including estimates of previous subsidence that occurred after the WAL and GN seams were originally completed) above MWs 32 to 36 has been estimated in **Table 19**.

Table 19 - Summary of Single Seam and Multi-Seam Subsidence Predictions

Subsidence Source	Case	Area Within WAL Seam First Workings Limits (XL10)		Area Within WAL Seam Second Workings Limits (XL9)	
		Incremental Subsidence (mm)	Cumulative Subsidence (mm)	Incremental Subsidence (mm)	Cumulative Subsidence (mm)
WAL Workings	Single seam Direct	*20 - 40*	*20 - 40*	*150 - 220*	*150 - 220*
GN Workings		*30 - 70*	*50 - 110*	*30 - 70*	*180 - 290*
FAS Workings		**450 - 740**	500 - 850	**420 - 720**	610 - 1010
WAL Workings	Multi-Seam Interaction with FAS workings	1 - 17	501 - 867	46 - 68	656 - 1078
GN Workings		92 - 137	592 - 1004	92 - 137	748 - 1218
FAS Workings	Multi-Seam Interaction with GN & WAL workings	7 - 12	**599 - 1011** (549 - 906)*	7 - 12	**755 - 1227** (575 - 937)*

WAL = Wallarah, GN = Great Northern, FAS = Fassifern; *Italics* - Estimate of subsidence that has already occurred; * - Cumulative subsidence range if previous subsidence above WAL and GN Seams is discounted.

Table 19 indicates that the corrected cumulative subsidence after the Modified MWs 32 to 36 are completed ranges between 755 mm and 1227 mm on the lake bed. The 2013 EIS Report estimated 495 mm to 886 mm (and rounded it up to 500 mm to 900 mm). The increase of 104 mm to 340 mm in the predicted multi-seam subsidence in this study compared to the 2013 EIS is mainly due to the soft floor conditions discussed herein.

The predicted subsidence contours in **Section 9** have included the potential subsidence increases for all workings to-date for impact assessment purposes.

8.11 Modified Mining Layout v. 2013 EIS Subsidence Effect Predictions

A comparison between the modified mining layout and the 2013 EIS subsidence effect predictions is summarised in **Table 20** and **21**.

The results indicate that the modified mining layout may have 104 mm to 340 mm higher subsidence than was predicted for the previous layout due to the development of soft floor conditions. While higher levels of subsidence are predicted, the level of subsidence expected at Chain Valley Colliery is significantly lower than the majority of underground mines employing secondary extraction methods, and as such is also unlikely that the modified layout

will cause a significant increase to the previously assessed impacts and therefore is unlikely to exceed the performance measures defined in the Development Consent for the Site.

Note: The predicted magnitudes of final subsidence will need to be confirmed with further bathymetric surveys, but at this stage, is considered to be conservative.

Table 20 - Summary of Comparison between Modified Mining Layout and 2013 EIS Predictions

Approved Mining Layout Panel No.	Modified Mining Layout Panel No.	Mine Layout Change	Final S_{max} (m)		Final Pillar S_p (m)		Tilt T_{max} (mm/m)		Horizontal Strain (mm/m)			
									Tension		Compression	
			2015 Mod	*2013 EIS*	*2015 Mod*	*2013 EIS*	*2015 Mod*	*2013 EIS*	*2015 Mod*	*2013 EIS*	*2015 Mod*	*2013 EIS*
1 - 5	1 - 5	No change	0.53-0.72	0.3-0.4	0.49-0.61	0.26-0.31	6-15	4 - 7	3 - 6	2 - 3	3 - 5	2 - 3
6	Deleted	FWs for access to MW 26 - 31	-	0.25	-	0.2	-	5	-	2	-	2
7 - 8	6 - 7	Panel lengths reduced	0.51	0.40	0.54	0.3	15	7	6	4	5	3
9 - 10	8 - 9	Chain pillar widths reduced to 32.4 m	0.71	0.32-0.42	0.57	0.21-0.28	9 - 14	4 - 8	5	2 - 4	3 - 5	2 - 4
11 - 13	10 - 12	Panel lengths reduced	0.37-0.71	0.38-0.44	0.42-0.55	0.18-0.25	5 - 14	6 - 9	3 - 5	3 - 4	4 - 5	3 - 4
14 - 19	Deleted	FWs for access to MWs 13 - 25	-	0.42-0.58	-	0.18-0.23	-	8 - 15	-	4 - 6	-	4 - 6
20 - 27	13 - 20	E-W Re-orientated Panels by 35^o & chain pillar widths reduced to 31.6 - 29.3 m	0.40-0.76	0.36-0.61	0.47-0.55	0.23-0.28	10 - 14	6-16	4 - 6	3 - 6	3 - 5	3 - 6
28 - 34	21 - 25	E-W Re-orientated Panels by 35^o, panel widths increased to 97 m & chain pillar widths reduced to 29.3 m. Mining height reduced.	0.52-0.76	0.45-0.62	0.44-0.47	0.16-0.23	7 - 14	6-17	3 - 6	3 - 6	3 - 5	3 - 6
35 - 40	26 - 31	Slight re-orientation of panels (2^o), panel widths increased to 97 m & chain pillars reduced to 29.3 m	0.38-0.74	0.37-0.43	0.53-0.54	0.19-0.30	6 - 13	3-8	3 - 5	2 - 4	2 - 5	2 - 4
41 - 45 (single-seam)	32 - 36	Some panel lengths reduced. Chain pillar width corrected from 32.6 m to 30.6 m in Modification Assessment	0.21-0.74	0.33-0.45	0.72-0.78	0.31-0.34	2 - 15	5-9	2 - 6	3 - 4	2 - 5	3 - 4
41 - 45 (multi-seam)	32 - 36		1.016-1.227	0.61-0.86	1.094-0.967	0.63-0.82	6 -15	7-13	2 - 4	3 - 4	2 - 5	3 - 4

Table 21 - Summary of Comparison between Modified Mining Layout and 2013 EIS Predictions

Approved Mining Layout Panel No.	Modified Mining Layout Panel No.	Mine Layout Change	Goaf Edge Subsidence S_{goe} (m)		Angle of Draw (o)	
			2015 Mod	*2013 EIS^*	*2015 Mod*	*2013 EIS^*
1 - 5	1 - 5	No change	0.14-0.34	0.11-0.22	22.3-30.4	20.3-27.1
6	Deleted	FWs for access to MW 26 - 31	-	0.14	-	23.3
7 - 8	6 - 7	Panel lengths reduced	0.24	0.15-0.16	26.5-26.1	22.8-23.2
9 - 10	8 - 9	Chain pillar widths reduced to 32.4 m	0.21	0.1-0.12	24.9-25.2	21.2-23.7
11 - 13	10 - 12	Panel lengths reduced	0.11-0.19	0.11-0.13	19.4-24.9	19.5-21.5
14 - 19	Deleted	FWs for access to MWs 13 - 25	-	0.12-0.16	-	20.5-22.3
20 - 27	13 - 20	E-W Re-orientated Panels by 35^o & chain pillar widths reduced to 31.6 - 29.3 m	0.08-0.22	0.11-0.17	22.7-25.6	20.3-22.6
28 - 34	21 - 25	E-W Re-orientated Panels by 35^o, panel widths increased to 97 m & chain pillar widths reduced to 29.3 m. Mining height reduced.	0.08-0.15	0.16-0.18	16.7-21.3	19.2-22.9
35 - 40	26 - 31	Slight re-orientation of panels (2^o), panel widths increased to 97 m & chain pillars reduced to 29.3 m	0.12-0.24	0.08-0.15	19.2-26.0	17.6-22.4
41 - 45 (single-seam)	32 - 36	Some panel lengths reduced. Chain pillar width corrected from 32.6 m to 30.6 m in Modification Assessment	0.07-0.36	0.11-0.25	16.9-30.2	23.2-27.4

^ - Predictions based on DgS modified **ACARP, 2013** models to allow comparison with modified mining layout.

9.0 Prediction of Subsidence Impact Parameter Contours

9.1 Calibration of the SDPS® Model

Credible worst-case subsidence contours for the modified miniwall panels have been generated using SDPS® influence function-based subsidence prediction software.

The SDPS® model was calibrated to the credible worst-case (U95%CL) profiles predicted by the **ACARP, 2003** empirical model. The outcome of the model calibration exercise is summarised in **Table 22**.

Table 22 - SDPS® Model Calibration Summary for the Modified MWs 9 - 36

Input Parameters from Modified ACARP, 2003	**Value**
Panel Nos. below XL s 1 - 10 shown in **Figure 2**	9 - 36
Panel Void Widths, W (m)	97
Effective Cover depth, H' (m)	148 - 232
Rock Cover Depth, H_r (m)	132 - 214
Seam Thickness (m)	4.5 - 8.0
Mining Height, T (m)	3.5
Roadway Development Height, h (m)	3.2
W/H_r range	0.45 - 0.74
SRP for Mining Area	High
Maximum Final Panel Subsidence*, S_{max} (m)	0.37 - 0.76 (MWs 32-36: 1.02 - 1.23)
Effective S_{max}/T Range	0.11 - 0.35
Chain Pillar Width, w_{cp} (m)	29.3 - 32.6
Roadway width (m)	5.4
Pillar Width/Height, w/h	12 - 17
Chain Pillar Subsidence* S_p (m)	0.38 - 0.78 (MWs 32-36: 1.02 - 1.23)
S_p/T Range	0.11 - 0.35
Distance to Influence Inflexion Point from Rib-Side (m) (d/H)	0.12 - 0.24
SDPS Calibration Results for 'Best Fit' Solution to the Modified ACARP, 2003 Model Predictions^	**Optimum Values**
Influence Angle (Tan(beta)) for internal and external panels	1.8 (internal) 2.0 (external)
Influence Angle (beta)	61 - 63
Supercritical Subsidence Factors (S_{max}/T)	0.6 (MWs 32-36: 0.66)
Distance to Influence Inflexion Point from Rib-Side (m) (d/H)	0.12 - 0.24

Notes:
* - Upper 95% Confidence Limits predicted from modified version of **ACARP, 2003**
^ - See SDPS manual extract in **Appendix B** for explanation of methodology and terms used.

The predicted SDPS® model was then calibrated to the modified **ACARP, 2003** model profiles along XLs 1 to 10. Representative subsidence effect profiles for MWs 14 to 25 have been compared in **Figures 24.1** to **24.3** along **XL6**. The predicted **ACARP, 2003** profiles are considered to be a worst-case representation of the modified mining layout. XLs 9 and 10 show the incremental subsidence effects of MWs 32 to 36 and do not include the multi-seam mining effects discussed in **Section 8.10**.

The predicted SDPS® subsidence and tilt profiles were generally located within +/- 10 to 20% of the predicted modified **ACARP, 2003** models U95%CL. This outcome is considered a reasonable fit considering that the **ACARP, 2003** profiles represent measured tilt profiles that are invariably affected by 'skewed' or kinked subsidence profiles.

The results of the analysis indicate that the majority of the predicted tensile and compressive strains predicted by the SDPS® model would fall within +/- 50% of the modified **ACARP, 2003** model predictions. This result is also considered reasonable in the context that the **ACARP, 2003** model represents measured profile data that includes strain concentration effects such as cracking and shearing. As mentioned earlier, this 'discontinuous' type of overburden behaviour can increase 'smooth' profile strains by 2 times 'occasionally'.

The SDPS® model was also calibrated to the predicted cumulative subsidence in **Table 20** and after mining of the three seams as shown in **Figures 25.1** to **25.3** along XL9 and **Figures 25.4** to **25.6** along XL10.

The results are summarised in **Table 23** and indicate that multiple seam affected panels will have maximum tilts increased from 7 to 12 mm/m, tensile strains from 2 to 4 mm/m and compressive strains from 3 to 5 mm/m.

Table 23 - Summary of Single v. Multiple Seam Effects above Modified MWs 32-36

XL	Panels	Maximum Final Subsidence (m)		Maximum Final Tilt (mm/m)		Maximum Final Tensile* Strain (mm/m)		Maximum Final Compressive* Strain (mm/m)	
		Single Seam	Multi-Seam*	Single Seam	Multi-Seam	Single Seam	Multi-Seam	Single Seam	Multi-Seam
9	32	0.71	1.15	8.5	14	2	3	3	4
	33	0.71	1.15	3	4	1	1	2	2
	34	0.71	1.14	1	2	1	1	1	2
	35	0.72	1.16	6	8	1	2	2	3
	36	0.25	0.53	3	6	1	2	1	2
10	32	0.75	1.07	9	12	1	2	4	5
	33	0.75	1.05	2	2	1	1	2	2
	34	0.73	1.05	1	1	1	1	1	1
	35	0.73	1.05	1	1	1	1	2	2
	36	0.23	0.39	6	7	8	10	1	1

It is assessed that the overall subsidence effect increases due to multi-seam effects will still be low in regards to environmental impact and are discussed further in **Section 10**.

9.2 Predicted Subsidence and Post-Mining Surface Level Contours

Based on the calibrated SDPS® model, predicted incremental subsidence effect contours (subsidence, tilt and horizontal strain) for the Modified MWs 9 to 36 in the Fassifern Seam, are presented in **Figures 26.1** to **26.3**.

Cumulative subsidence effect contours for Modified MWs 9 to 36 are presented in **Figures 27.1** to **27.3** and include the amended multi-seam mining effects above Modified MWs 32 to 36.

Pre-mining and post-mining surface levels for the proposed mining layout are shown in **Figures 28.1** and **28.2** for the incremental and cumulative cases respectively.

It is understood that the surface levels across the lake bed were derived from bathymetric surveys completed after mining in the Wallarah and Great Northern Seams. It is therefore considered that the post-mining contours in the areas of Modified MWs 32 - 36 are likely to be somewhere between the two sets of contours shown in the above figures.

10.0 Subsidence Impacts and Management Strategies

10.1 General

Based on the predicted maximum panel subsidence, tilt and strain values for the miniwall panel layouts, the potential for the following subsidence related impacts and their likely effect on the natural and man-made features within the Site have been assessed:

- changes to lake bed level;
- surface cracking beneath the lake bed, and
- height of sub-surface fracturing above the panels (direct and in-direct hydraulic connection zones).

Based on the observation that a finite range of subsidence effect values can occur at a given location above an extracted miniwall panel of known mining geometry and geology, it is possible to provide a range of predictions that are likely to occur within a nominal confidence limit (i.e. usually 95%). This approach allows specialist consultants and stakeholders to apply risk management principles in a practical way.

Discussions of likelihood of impact occurrence in the following sections generally refer to the qualitative measures of likelihood described in **Table 24**, and are based on terms used in **AGS, 2010** and **Vick, 2002**.

As explained in **Appendix A**, the terms 'mean' and 'Upper 95% Confidence Limit' (U95%CL) infer that the predicted maximum subsidence effect values may be exceeded on a small number of occasions, due to the presence of adverse geological or topographical conditions.

The selection of an appropriate 'credible worst-case' is normally defined by the U95%CL value. However, a higher confidence limit may need to be applied in consideration of the reliability of current survey technology, available mitigation techniques or likely response action times should an exceedance occur.

Conservative predictions of subsidence effects and sub-surface fracture heights have been made in this study due to the inaccessible surface locations below the lake and the sensitive ecological environment within the foreshore buffer zones.

Table 24 - Qualitative Measures of Likelihood

Likelihood of Occurrence	Event implication	Indicative relative probability of a single event
Almost Certain	The event is expected to occur.	90-99%
Very Likely	The event is expected to occur, although not completely certain.	75-90%
Likely+	The event will probably occur under normal conditions.	25-75%
Possible	The event may occur under normal conditions.	10-25%
Unlikely*	The event is conceivable, but only if adverse conditions are present.	5-10%
Very Unlikely	The event probably will not occur, even if adverse conditions are present.	1-5%
Not Credible	The event is inconceivable or practically impossible, regardless of the conditions.	<1%

Notes:
+ - Equivalent to the mean or line-of-best fit regression lines for a given impact parameter presented in **ACARP, 2003**.
* - Equivalent to the credible worst-case or U95%CL subsidence impact parameter in **ACARP, 2003**. The Likelihood of Occurrence refers to exceedance probability of the predicted value.

The predicted impacts and suggested management strategies for the natural and man-made features in the proposed extension area are presented in the following sections.

10.2 Surface Cracking

10.2.1 Predicted Impacts

The development of surface subsidence above longwall and miniwall extraction panels is caused by the bending of the overburden strata as it sags down into the newly created void in the workings. The sagging strata are supported in turn by the collapsed immediate roof, which then slowly compresses to a maximum subsidence limit.

Based on previous experience at nearby land based mines, it has been assumed that any surface cracking to the rock head below the lake bed sediments is likely to be minor for the predicted range of surface subsidence magnitudes from 0.37 m to 0.74 m for MWs 9 to 36.

Tensile strains associated with this magnitude of subsidence are predicted to range from 2 to 6 mm/m with occasional higher strains up to 12 mm/m possible due to strain concentration effects of surface joints in massive conglomerate beds.

Based on predicted maximum tensile strains of 2 mm/m to 12 mm/m, maximum crack widths are estimated to range from 20 mm to 120 mm wide at rock head. It is likely that any cracks that occur will be naturally ‘filled’ by lake bed sediments with no impact on the lake bed itself. The strains at the lake bed surface itself will also be more uniformly distributed and are therefore more likely to be absorbed by the plastic nature of the sediments.

Accordingly, no monitoring or remediation for the potential minor cracking would be required as may be undertaken for land based cracking. The cracks are also likely to be

tapered to depths ranging from 5 to 10 m below the rock head and should therefore be considered to be located within the Surface Zone.

Predicted compressive strains of 2 to 12 mm/m may cause low angle shear cracking and upward 'buckling' of near surface rock beds. The depth and 'plasticity' of the sediment however, is also likely to absorb the compressive strains, which will peak in the middle third area of the panels.

It should be understood that, occasionally, the measured crack widths would be expected to exceed the U95%CL indicated by the subsidence prediction model. These are generally found to be related to the presence of adverse or anomalous geological or topographical conditions.

In addition, tensile cracks of similar magnitudes to those mentioned above will probably develop up to 50 m behind the advancing goaf edge of the miniwall panels. The majority of these cracks are transient however, and some may partially or fully close in the central areas of the panels where permanent compressive strains develop after mining is completed.

10.2.2 Impact Management Strategies

As surface crack repair works in the lake are not feasible, monitoring for any changes to the lake bed, seagrass beds and foreshore characteristics should continue to be undertaken by techniques suitable for the potential impacts that may arise.

10.3 Sub-Surface Cracking

10.3.1 Sub-Surface Fracturing Zones

As noted in **Li *et al*, 2006**, "the transmission of water through the overburden strata may [occur] via a number of mechanisms such as (i) inter-granular porosity, (ii) mining induced voids, fractures and strata dilation/bed separations and (iii) structural discontinuities / geological defects [faults and dykes]".

The void created by extracting coal invariably results in the collapse of the immediate roof strata which is subject to bending and shearing stresses as the overburden tries to span the void. The extent of fracturing and shearing up through the strata is dependent on mining geometry and overburden geology.

International and Australian research on longwall mining interaction with groundwater systems indicates that the overburden may be divided into essentially four or five zones of surface and subsurface fracturing; see **Figures 29.1** and **29.2**. The zones are based on the **Forster, 1995** and **ACARP, 2007** models and are defined (in descending order) as follows:

- Surface Zone (D-Zone) - Unconstrained
- Elastic Zone (C-Zone) - Constrained
- Discontinuous Fracture Zone (B-Zone) - Constrained
- Continuous Fracture Zone (A-Zone) - Unconstrained

- Caved Zone (included in the A-Zone) - Unconstrained

Further details of the sub-surface fracture mechanics, including the strain and permeability increases in the A, B and C-Zones is presented in **Appendix A**.

10.3.2 Sub-Surface Fracture Height and Constrained Zone Thickness Prediction Models

The prediction of connective subsurface fracture network heights above longwall/miniwall panels over the past 40 years have been based on several simple empirical models that have allowed successful mining beneath permanent water bodies such as Lake Macquarie in the Newcastle Coalfield, water supply dams in the Southern Coalfield and relatively shallow depths of cover (< 150 m) below creeks and rivers without causing surface to seam or aquifer to seam connection.

Several instances of unanticipated cracking and drainage of near-surface alluvial and confined aquifers have occurred over the years in NSW (and internationally) however, and have led to further research into improving our understanding of the sub-surface crack development process and the height of fracture zone estimates above longwall and pillar extraction panels.

The research to-date has identified the following key parameters should be considered when making robust sub-surface fracture height predictions:

- Panel width (W)
- Mining height (T)
- Cover depth (H)
- Panel criticality (i.e. sub-critical or supercritical)
- Presence of massive sandstone or conglomerate strata that may control continuous fracture height development.
- Constrained Zone lithology and thickness required to control inter-connective cracking between surface and seam or aquifer and seam.
- Presence of geological structure (faults/dykes/joint swarms) that have an increased level of fracturing and therefore higher secondary conductivity.

Several of the current models in use in NSW consider only one or two of above parameters such as W or T because they were developed in a coalfield with a particular geometry and consistent geology, and generally provided satisfactory results. However, it is apparent that as mines are developed in other coalfields or mining geometries and/or geology changes within a coalfield, these models can significantly under-predict or over-predict the sub-surface fracture heights (if the key controlling factor or factors present at the new locations are no longer included in the simplified models).

All of the above factors have been considered by DgS for the Site using recently developed Pi-Term empirical models (**DgS, 2014**) which have been validated to measured NSW case studies with a broad range of mining geometries and geological conditions. Details of the *Geometry* and *Geology* Pi-Term Model's development are presented further below and in **Attachment A**.

The Pi-Term models are based on a conceptual model of the subsurface fracturing that develops above a longwall panel with varying mining geometry and geology; see **Figure 30.1**. The conceptual model demonstrates that longwall panel geometries and overburden geology determine the height of 'continuous' and 'discontinuous' fracturing. Continuous fractures above the mine workings tend to form up into the overburden at an angle of 12^o to 19^o from the rib sides, based on physical and numerical modelling observations and subsidence data; see **Figure 30.2**.

The extent of vertical fractures above the mine workings (i.e. the A-Zone) will also be dependent on the effective strata thickness that either (i) spans the goaf or (ii) sags down onto it with limited fracturing through the 'beam'.

A review of measured heights of A-Zone fracturing and borehole data above longwall panels in NSW and Queensland Coalfields in **Ditton and Merrick, 2014** demonstrates the overburden develops an effective strata unit thicknesses (t') that limits the A-Zone at a given height above a longwall; see **Figure 30.3**. The results indicate that the effective thickness of the strata units is influenced by the geology of the coalfield and the mining geometry.

When miniwall mining beneath water bodies and sensitive groundwater aquifers, it is essential that the mining geometry be controlled to provide an effective Constrained Zone (B or B+C) thickness to minimise the potential for a connective cracking zone to develop from the workings and up to the water body.

Reference to **Li *et al* 2006** and **Forster, 1995**, indicates that the minimum Constrained Zone thickness above the Continuous Fracture Zone to rock head (i.e. including the surface zone) should be a minimum of 12T beneath Lake Macquarie with a 10 m allowance for rock head variation (or surface cracking zone).

Based on a mining height of 3.5 m, a minimum Constrained Zone thickness of 42 m (i.e. 12T) was adopted for the the mining layouts in the Chain Valley Mining Extension 1 Area, the minimum constrained zone thickness continues to be applied under the proposed mining layout changes.

Continuous sub-surface fracture height predictions (A) for the Modified MWs 9 to 36 in a single seam mining environment have been made based on the following empirical prediction models developed in the NSW Coalfields:

- Geometry Pi-Term Model ($A = 2.215W'^{0.357}\ H'^{0.271}T^{0.372}$) (**Ditton & Merrick, 2014**)
- Geology Pi-Term Model ($A = 1.52W'^{0.4}H'^{0.535}T^{0.464}\ t'^{\ -0.4}$) (**Ditton & Merrick, 2014**.)
- A=1.0W to 1.5W **(SCT, 2008)**

- A= 21T to 33T **(Forster, 1995)**

Details of the development of each model and their limitations are provided in **Appendix A**

10.3.3 Geometry Pi-Term Model (Ditton & Merrick, 2014)

The model was developed in 2013-14 in response to several Planning Assessment Commission (PAC) concerns in regards to large apparent differences between established prediction methods that use only one parameter in a particular coalfield (eg the mining height v. panel void width models).

The Geometry Pi-term model considers the influence of the panel width, cover depth and mining height on the height of continuous fracturing above a longwall panel. A dimensionally consistent product and power rule has been derived using non-linear regression analysis of measured cases. The model considers the key mining geometries and indirectly includes the influence of a wide range of geological conditions.

The Pi-terms have been derived (by experiment) using Buckingham's Pi-term theorem and refer to the dimensionless ratios of key independent variables with a repeating variable of influence (the panel width) as follows:

$\underline{\text{Mean } A/W' = 2.215\,(H/W')^{0.271}(T/W')^{0.372}}$ $\qquad R^2 = 0.61$ (rmse=21%)

$\underline{\text{U95\%CL } A/W' = \text{Mean } A/W' + a}$

where

a = 0.16 for *sub-critical*, 0.16 - 0.085(W/H-0.7) for *critical* and 0.1 for *supercritical* panels

H = cover depth = maximum potential goaf load height

W' = effective panel width = minimum of W and 1.4H.

T = mining height.

Re-arranging the above equation in terms of A gives:

$\underline{A = 2.215W^{0.357}H'^{0.271}T^{0.372} \qquad +/- aW'}$

The heights of the B-Zone may also be estimated using a similar approach to the A-Zone methodology:

$\underline{\text{Mean } B/W' = 1.621\,(H'/W')^{0.55}(T/W')^{0.175}}$ $\qquad R^2 = 0.86$ & rsme = 0.12W' (13%)

U95% B/W' = Mean B/W' + b

where b = 0.16 for sub-critical panels, 0.16-0.085(W/H-0.7) for critical panels and 0.10 for supercritical panels.

Re-arranging the above equation in terms of B gives:

$$B = 1.621\ W'^{0.275} H^{0.55} T^{0.175} \quad +/- \ bW'$$

10.3.4 Pi-Term Geology Model (Ditton & Merrick, 2014)

Further to the Geometry Model, the Pi-term Geology model also considers the influence of the panel width, cover depth and mining height with the inclusion of the effective strata unit thickness. The effective strata unit thickness refers to the thickness of the beam that limits the height of continuous fracturing above a longwall panel. Using a product and power rule and non-linear regression analysis of measured cases, the range of effective beam thicknesses for a given mining geometry was derived for the NSW and Queensland Coalfields; see **Figure 30.3**.

The Pi-terms have been derived (by experiment) using Buckingham's Pi-term theorem and refer to the dimensionless ratios of key independent variables with a repeating variable of influence (the panel width) as follows:

$$\text{Mean } A/W' = 1.52\ (H/W')^{0.535} (T/W')^{0.464} (t'/W')^{-0.4} \qquad R^2 = 0.8 \text{ (rmse=15\%)}$$

$$\text{U95\%CL } A/W' = \text{Mean } A/W' + a$$

where

a = 0.15 for *sub-critical*, 0.15 - 0.0714(W/H-0.7) for *critical* and 0.1 for *supercritical* panels

H = cover depth = maximum potential goaf load height.

W' = effective panel width = minimum of W and 1.4H.

T = mining height.

t' = effective strata unit thickness in the overburden above the A-Zone and ranges between 16 m and 54 m across the Newcastle Coalfield with a median value of 20 m. (see *Section A11.4.4* in **Appendix A** for further details) .

Re-arranging the above equation in terms of A gives:

$$A = 1.52 W^{0.4} H'^{0.535} T^{0.464} t'^{-0.4} \quad +/- \ aW'$$

It is considered that the Geology Pi-Term model is superior to the Geometry Pi-Term Model as the t' factor may be back-analyzed to local height of A-Zone fracture height measurements once mining commences.

The two models are likely to provide conservative predictions if massive strata are present in the overburden with the capability to span the goaf and 'truncate' the A-Zone heights.

The heights of the B-Zone may also be estimated using a similar approach to the A-Zone methodology:

$$\text{Mean B/W'} = 1.873\,(H'/W')^{0.635}(T/W')^{0.257}(t'/W')^{-0.097} \quad R^2 = 0.86 \;\&\; \text{rmse} = 0.13W'(15\%)$$

$$\text{U95\% B/W'} = \text{Mean B/W'} + b$$

where b = 0.15 for sub-critical panels; 0.15-0.0714(W/H-0.7) for critical panels and 0.10 for supercritical panels.

Re-arranging the above equation in terms of B gives:

$$B = 1.873\,W'^{0.205}\,H^{0.635}T^{0.257}\,t'^{\,-0.097} \quad +/- \; bW'$$

10.3.5 T-Based Model (Forster, 1995)

The height of the A-Zone fracturing has been successfully predicted from relationships established with extensometer and piezometeric monitoring data above supercritical panels in the Newcastle Coalfield. A supercritical panel relationship between A and T was developed by **Forster, 1995** in the Lake Macquarie Region as follows:

A=21T to 33T above *supercritical* panel geometries

Massive conglomerate or sandstone strata units located at horizons just above the extracted coal seams where the continuous fracturing extended to. The model has been validated against Wyee LWs 17 to 23 in **Li et al, 2006** and provides a simple method by which to compare other model results. Caution is advised when making A-Zone predictions in other coalfields with less massive lithology present however.

10.3.6 Panel Width-Based Models (SCT, 2008)

The width-based model published in **SCT, 2008** was originally defined as a 'height of fracturing' models that did not distinguish between discontinuous and continuous zones of fracturing. The models were based on numerical Flac2-D outcomes and a FISH program that tracked tensile and compressive fracturing and bedding shear above a longwall goaf. The model is therefore likely to provide conservative estimates of the A-Zone and possibly includes the B-Zone fractures/dilated strata as well in some cases.

It is considered that whilst the program is a reasonable attempt at predicting fracture heights numerically, the model is still a 'continuous strata model' program that is trying to model part-discontinuous and part-continuous strata behaviour. Whilst the program appears to be able to identify caving zones and zones of large displacement (i.e. the A-Zone), the predicted heights of fracturing have only been related to one parameter, the panel width, W, as follows:

A = 1.0W to 1.5W

The width-based models do not consider the effect of cover depth or mining height and also assume the A-Zone will continue to increase above *supercritical* panel geometries. This usually means that surface to seam connectivity will always be predicted for critical and supercritical panel widths, which is at odds with industry experience.

A review of published industry experience of critical and supercritical panels presented in **Appendix A** indicate that only 2 or 3 cases out of 14 (15% - 20%) or 1 in 5 supercritical longwalls have resulted in surface to seam connectivity; see **Figure 30.3**.

This outcome suggests that factors such as cover depth, mining height and geological conditions should also be considered other than just the panel width alone when estimating heights of fracturing above longwall panels. The model may therefore indicate conservative A-Zone heights in some cases, and will depend on differences in mining height, cover depth and mining geology for a given panel width.

10.3.7 Continuous and Discontinuous Sub-surface Fracture Height Predictions

Out of the all the models assessed, it was concluded that the Geology Pi-Term and **Forster, 1995** models are most likely to provide a reasonable estimate the A-Zones and B-Zones above the proposed Chain Valley miniwalls. Where the constrained zone was estimated to be <12T, the mining height was subsequently reduced until this criteria was met. *Note: Alternatively, the width of the miniwalls could be reduced while maintaining a 3.5 m mining height.*

The predicted values for continuous (A-Zone) and discontinuous (B-Zone) sub-surface fracture heights and Constrained Zone thickness above the 97 m wide sub-critical miniwall panels are summarised in **Table 23**.

Predicted A-Zone horizons of 21T to 33T from **Forster, 1995** for 'critical' to 'supercritical' panel width geometries are also provided for comparison with the proposed sub-critical panel width outcomes in the Site.

An effective strata unit thickness t' = 19 m has been back-analysed from completed extraction at Wyee (Mannering) Colliery and Chain Valley Colliery that did not eventuate in a lake water inflows. The maximum height of A-Zone was assumed to result in a minimum constrained zone thickness of 12T below a surface cracking or D-Zone depth of 10 m. The results of the effective beam analysis are summarised in **Table 24A** (see **Section 10.3.14**).

The *continuous* sub-surface fracture heights (A-Horizon) have been plotted against depth of rock cover in **Figure 31.1** for the Modified MWs 9 to 36. The *discontinuous* sub-surface fracture heights (B-Horizon) have also been plotted against depth of rock cover in **Figure 31.2** for the modified miniwalls. Minimum Constrained Zone (B or B+C Zone) thicknesses are also indicated on the above figures.

Table 23 - Summary of Predicted Sub-Surface Fracturing Heights above Modified MWs 1 - 36

XL No.	MW No.	T (m)	W (m)	Rock Cover Depth H_r (m)	Spanning Munmorah Conglomerate Beam Location with High SRP			A-Zone Height (m)			B-Zone Height (m)	Confined Zone (Cz)# Thickness Between A & D Zones	
					Unit No.	Thick-ness (m)	Height above Panel (m)	Geology Pi-Term Model^	Forster 1995* 21T	Forster 1995* 33T	Geology Pi-Term Model^	Cz (m)	Cz/ T
1	***1***	***3.4***	***72.0***	***180***	***2***	***35***	***105***	***89***	***71***	***112***	***97***	***81***	***23.9***
	2	***3.4***	***72.2***	***181***	***2***	***34***	***108***	***89***	***71***	***112***	***97***	***82***	***24.2***
	3	***3.4***	***97.0***	***182***	***2***	***32***	***110***	***102***	***71***	***112***	***119***	***70***	***20.5***
	6	***3.4***	***97.0***	***181***	***2***	***30***	***112***	***102***	***71***	***112***	***119***	***69***	***20.4***
	7	***3.4***	***97.0***	***180***	***2***	***27***	***114***	***101***	***71***	***112***	***118***	***69***	***20.3***
	8	***3.5***	***97.0***	***179***	***2***	***25***	***114***	***102***	***74***	***116***	***119***	***67***	***19.2***
	9	3.5	97.0	178	2	22	114	101	74	116	119	67	19.1
2	***4***	***3.4***	***97.0***	***178***	***2***	***45***	***75***	***101***	***71***	***112***	***118***	***67***	***19.6***
	5	***3.4***	***97.0***	***182***	***2***	***45***	***78***	***102***	***71***	***112***	***119***	***70***	***20.5***
3	***7***	***3.5***	***97.0***	***174***	***2***	***17***	***105***	***101***	***74***	***116***	***119***	***63***	***18.0***
	8	***3.5***	***97.0***	***173***	***2***	***17***	***110***	***100***	***74***	***116***	***118***	***62***	***17.7***
	9	3.5	97.0	171	2	16	115	100	74	116	118	61	17.4
	10	3.5	97.0	169	2	16	102	99	74	116	118	60	17.1
	11	3.5	97.0	165	2	16	104	98	74	116	117	57	16.3
	12	3.5	97.0	167	2	17	110	97	74	116	117	60	17.2
4	10	3.5	97.0	156	1	20	106	96	74	116	116	50	14.3
	11	3.5	97.0	169	1	20	106	100	74	116	118	59	17.0
5	13	3.5	97.0	180	2	20	112	100	74	116	118	70	19.9
	14	3.5	97.0	177	2	20	111	100	74	116	118	67	19.2
	15	3.5	97.0	173	2	19	111	99	74	116	118	64	18.3
	16	3.5	97.0	171	2	19	110	99	74	116	117	62	17.9
	17	3.5	97.0	165	2	18	110	97	74	116	117	58	16.5
	18	3.5	97.0	159	2	18	109	96	74	116	116	53	15.1
	19	3.5	97.0	154	2	17	108	95	74	116	116	49	14.1
	20	3.5	97.0	149	2	17	107	93	74	116	115	46	13.0
6	14	3.5	97.0	174	2	20	100	100	74	116	118	64	18.2
	15	3.5	97.0	166	2	19	99	98	74	116	117	58	16.6
	16	3.5	97.0	162	2	19	99	97	74	116	117	54	15.5
	17	3.5	97.0	160	2	18	98	97	74	116	117	53	15.2
	18	3.5	97.0	155	2	18	97	95	74	116	116	49	14.0
	19	3.5	97.0	149	2	17	96	94	74	116	115	45	12.8
	20	**3.4**	97.0	145	2	17	95	92	71	112	114	43	12.6
	21	**3.0**	97.0	135	2	17	94	87	63	99	111	37	12.4
	22	**3.3**	97.0	140	2	17	93	90	69	109	113	40	12.1
	23	**3.2**	97.0	137	2	16	92	88	67	106	112	39	12.1
	24	**3.1**	97.0	134	2	16	91	87	65	102	111	37	12.1
	25	**3.0**	97.0	132	2	17	90	85	63	99	110	37	12.2
7	26	3.5	97.0	155	2	12	108	95	74	116	116	50	14.2
	27	3.5	97.0	156	2	12	110	95	74	116	116	50	14.3
	28	3.5	97.0	156	1	20	135	96	74	116	116	50	14.4

-see notes at bottom of table on next page.

Table 23 (Cont…) - Summary of Predicted Sub-Surface Fracturing Heights above Modified MWs 9 - 36

XL No.	MW No.	T (m)	W (m)	Rock Cover Depth H_r (m)	Spanning Munmorah Conglomerate Beam Location with High SRP			A-Zone Fracture Height (m)			B-Zone Fracture Height (m)	Confined Zone (Cz)# Thickness Between A & D-Zones	
					Unit No.	Thick-ness (m)	Height above Panel (m)	Geology Pi-Term Model^	Forster 1995*		Geology Pi-Term Model^	C_z (m)	C_z/T
									21T	33T			
7	26	3.5	97.0	155	2	12	108	95	74	116	116	50	14.2
	27	3.5	97.0	156	2	12	110	95	74	116	116	50	14.3
	28	3.5	97.0	156	1	20	135	96	74	116	116	50	14.4
8	26	3.5	97.0	171	2	24	102	100	74	116	118	61	17.4
	27	3.5	97.0	172	2	23	105	100	74	116	118	62	17.6
	28	3.5	97.0	173	2	22	110	101	74	116	118	62	17.6
	29	3.5	97.0	174	2	20	102	101	74	116	119	63	17.9
	30	3.5	97.0	173	2	20	105	101	74	116	119	62	17.7
	31	3.5	97.0	173	2	18	118	101	74	116	119	62	17.7
9	32	3.5	97.0	196	2	50	95	108	74	116	122	78	22.3
	33	3.5	97.0	197	2	50	100	108	74	116	122	79	22.7
	34	3.5	97.0	202	2	50	105	108	74	116	122	84	23.9
	35	3.5	97.0	203	2	50	110	108	74	116	122	85	24.3
	36	3.5	97.0	202	2	51	115	107	74	116	121	84	24.0
10	32	3.5	97.0	208	2	55	100	110	74	116	123	88	25.1
	33	3.5	97.0	210	2	55	104	110	74	116	123	90	25.6
	34	3.5	97.0	212	2	54	108	110	74	116	123	92	26.1
	35	3.5	97.0	214	2	54	112	111	74	116	123	93	26.7
	36	3.5	97.0	212	2	53	114	110	74	116	123	92	26.3

* - Constrained Zone Cz = H_r-A-10 (m);
Bold - Mining height reduced to maintain the minimum constrained zone thickness requirement of 12T.
Italics - Extracted panels 10m below rock head;
- Supercritical panel outcomes provided for comparison with proposed sub-critical panels.
Shaded - Recommended prediction outcomes for A, B Zone Horizons and Confined Zone thickness.
^ - U95%CL Geology PI-Term Model predictions assumes an Effective Strata unit thickness t'= 19 m (see **Table 23A**).

Discussion of the A to D-Zone cracking predictions is provided in the following sub-sections.

10.3.8 Discussion of A-Zone Horizon Model Predictions

The Geology Pi-term model predictions for the U95%CL A-Zone horizon above the proposed miniwall panels (see **Figure 31.1**) range from 85 m to 111 m for rock cover depths from 132 m to 214 m respectively. The results are consistent with and bracketed by **Forster, 1995** (A = 24T to 32T) and **SCT, 2008** (A = 1.14W to 1.18W). The height of fracturing is also consistent with the location of the spanning Munmorah Conglomerate units and is further discussed in **Section 12.3.14**.

The **Forster, 1995** model indicates connective cracking heights ranging from 71 m to 116 m above supercritical panel workings. These levels are considered to be conservative due to (i)

the proposed panels have sub-critical panel widths and (ii) the presence of spanning Munmorah Conglomerate units above the panels.

The corollary of the above assessment is that the depth below rock head to the A-Zone ranges from 47 m to 107 m (>12T+10 m). It is therefore considered 'very unlikely' that the A-Zone will interact with the Surface D-Zone cracks, unless a significant fault is undermined.

10.3.9 Discussion of B-Zone Horizon Model Predictions

The Pi-term model predicts that the U95%CL B-Zone horizon above the proposed miniwall panels (see **Figure 31.2**) ranges from 97 m to 123 m for rock cover depths of 132 m to 214 m (or 28T - 30T). The effective caving angle for the B-Zone fracture heights is ~ 13^{o} for mining heights of 3.4 m to 3.5 m.

The corollary of the above assessment is that the depth below rock head to the B-Zone ranges from 22 m to 91 m, which is also considered unlikely to interact with the Surface D-Zone cracks. The potential for drainage of sub-surface aquifers into the workings from the B-Zones is significantly reduced by the discontinuous nature of the cracking within the strata.

10.3.10 Discussion of Constrained Zone Thickness Predictions

The thickness of the Constrained Zone (B or B+C Zones) is estimated to range from 37 m to 93 m or 12T to 27T. The predicted Constrained Zone thicknesses above the proposed panel widths are therefore consistent with the minimum thickness recommended by **Li *et al,* 2006** and **Forster, 1995** in similar geological conditions.

The proposed mining height was reduced to a range from 3.5 m to 3.0 m to satisfy the 12T constrained zone thickness criteria above MWs 20 to 25 in the north western region of the Site where the rock head cover ranges from 145 m to 132 m.

10.3.11 Discussion of D-Zone Horizon Model Predictions

The D-Zone is usually affected by vertical fracturing due to unconfined strata bending within 10 m of the surface and may therefore re-route surface waters to dilated strata below it in the C or B-Zones if cracking in the lower zones intersect with the Surface D-Zone cracks.

This interaction however, is only likely to result in temporary adjustment of groundwater levels as newly formed voids become saturated or fill with sediment.

10.3.12 Impact on Rock Mass Permeability

In regards to changes to rock mass permeability, **Forster, 1995** indicates that horizontal permeability in the fractured A-Zone above longwall mines (see **Figure 29.2**) could increase by 2 to 4 orders of magnitude (e.g. pre-mining $k_h = 10^{-9}$ to 10^{-10} m/s; post-mining $k_h = 10^{-7}$ to 10^{-6} m/s). Similar outcomes are predicted in **ACARP, 2007** (see **Appendix A**).
Vertical permeability could not be measured directly from the boreholes discussed in the **Forster, 1995** model, but could be inferred by assuming complete pressure loss in the 'A-Zone', where direct hydraulic connection to the workings occurs.

The bedding separations and jointing in the Constrained Zone (B +C Zones) is unlikely to create a major change in vertical hydraulic conductivity, but are more likely to develop increased horizontal hydraulic conductivity and an increase in groundwater storage volumes. Groundwater is still able to 'leak' downwards through the Constrained Zone; however, the overall effect on the surface groundwater system is usually expected to be minimal, with re-charging of groundwater losses likely to occur from the surface hydrological system.

Overall, bedding parting separation would only be expected to increase rock mass storage capacity and horizontal permeability without direct hydraulic connection to the workings in the B-Zone or C-Zones. Rock mass hydraulic conductivity is also unlikely to increase significantly outside the angle of draw from the panel extraction limits up to the surface (see **Figure 29.2**).

10.3.13 Review of Height of Fracturing above Wyee Longwalls

The predicted Heights of A and B-Zone Fracturing have been determined for Wyee longwalls 1 (**Holla and Buizen, 1990**) and 17 to 23 (**Li *et al,* 2006**) in the Fassifern Seam and are presented in **Tables 24A** and **24B** respectively. Note that a review of Chain Valley MW 1 to 7 results have previously been provided in **Section 8.11**.

Table 24A - Predicted v. Measured A-Zone and Effective Strata Unit Thickness Summary for Wyee Mine's LWs 17 - 23

Panel No	Panel Width W (m)	Effective Cover Depth H (m)	W/H	T (m)	Depth to Rock (m)	Rock Cover Depth H' (m)	Predicted A-Zone Height (m)		Constrained Zone Thickness* (Cz) below Rock head - 10 m (m)			Effective Beam t' (m)
							Mean	U95%CL	Cz/T	Cz (m)	Meas. A m)	
Wyee LW Data												
1	216	206	1.05	3.4	4	202	124	151	**12.2**	42	126	**19**
17	130	174	0.75	3.2	14	160	89	108	13.0	42	<108	19
18	130	172	0.76	3.2	14	160	89	108	13.2	42	<108	19
19	130	170	0.76	3.2	14	156	88	107	12.1	39	<107	19
20	140	180	0.78	3.2	17	163	94	114	12.2	39	<114	19
21	140	175	0.80	3.2	14	161	92	112	12.1	39	<112	19
22	150	185	0.81	3.2	15	170	98	119	12.8	41	<119	19
23	150	195	0.77	3.2	16	179	101	122	14.6	47	<122	19

Bold - best-fit t' value for Geology Pi-Term Model; Meas. = Measured A-Zone height (published value);
* - Minimum constrained zone thickness based on rock cover and predicted U95%CL A-Zone height.

Based on the calibrated Geology Pi-Term Model (**Ditton and Merrick, 2014**). The worst-case predictions for the upper bound A-Zone horizon above the Wyee longwall panels range from 107 m to 151 m for rock cover depths from 156 m to 201 m respectively (or 33T to 44T). The effective caving angle for the A-Zone Fracture Heights is 16^{o}~20^{o} for a mining height of 3.2 m and 3.4 m.

Table 24B - Predicted B-Zone Summary for Wyee Mine's LWs 17 - 23

Panel No	Panel Width W (m)	Effective Cover Depth H (m)	W/H	T (m)	Depth to Rock (m)	Rock Cover Depth H' (m)	Predicted B-Zone Height (m)		Depth to B-Zone (dB) below Rock head (m)*		Effective Beam t' (m)
							Mean	U95%CL	Mean	U95%CL	
1	216	206	1.05	3.4	4	202	175	202	41	0	**19**
17	130	174	0.75	3.2	14	160	120	139	21	21	19
18	130	172	0.76	3.2	14	160	120	139	21	21	19
19	130	170	0.76	3.2	14	156	120	139	21	17	19
20	140	180	0.78	3.2	17	163	127	147	23	16	19
21	140	175	0.80	3.2	14	161	126	146	24	15	19
22	150	185	0.81	3.2	15	170	133	155	26	15	19
23	150	195	0.77	3.2	16	179	135	157	24	22	19

Bold - best-fit t' value for Geology Pi-Term Model; Meas. = Measured A-Zone height (published value);
* - Minimum constrained zone thickness based on rock cover and predicted U95%CL A-Zone height.

The predictions for the B-Zone horizon above the Wyee longwall panels range from 139 m to 202 m for rock cover depths from 170 m to 202 m respectively (or 50T to 53T).

The minimum predicted depths to the B-Zone below rock head are estimated to range from 0 m to 26 m. Potential interconnection with the D-Zone is assessed above Wyee LW1 only, with the rest of the Wyee longwalls likely to have had B-Zones > 15 m below rock head.

Overall, it is assessed that the Wyee longwall panels were satisfactory in regards to meeting the minimum Constrained Zone thickness requirements according to **Forster, 1995** and **Li *et al,* 2006**. The presence of 30 m thick spanning Munmorah Conglomerate Units above the panels may also have limited the fracture heights to ~80 m, which would have provided a Constrained Zone thickness of 70 m or 21T.

10.3.14 Discussion of Prediction Model Uncertainties and Spanning Strata

In regards to prediction model uncertainty, the DgS Pi-Term and **Forster, 1995** models are consistent in that they indicate surface-to-seam hydraulic connection is 'unlikely' to 'very unlikely' to occur for mining below rock cover depths greater than 132 m.

However, it is clear from the database on which the models were derived, that there is a high degree of variability in the data. This is probably due to the truncating effects of massive, spanning strata or geological structure interaction.

It is assessed that the A and B-Zone fracture heights are likely to be affected by the presence of spanning Munmorah Conglomerate units that are located above the three seams mine workings and approximately 90 m to 130 m above the Fassifern Seam. The predicted A and B-Zone horizons presented in **Section 10.3.7** therefore represent worst-case heights of fracturing for the Site.

This means that there will always be uncertainty in predicting the A and B-Zone horizons using any of the available models. The measurement of sub-surface fracturing and their impact on groundwater should therefore be undertaken in non-sensitive areas or cognisance made of all available local information at nearby mine sites. An adaptive management approach should be adopted to avoid continuous fracturing occurring beneath the lake bed to achieve the identified performance measure of no significant impact or surface to seam fracture connectivity.

10.3.15 Discussion of Height of Fracturing Interaction with the Great Northern and Wallarah Seam Panels

It is apparent from the height of fracturing assessment that the Great Northern Seam and Wallarah Seam mine workings are likely to be located within the A-Zone above the proposed miniwall panels.

The Great Northern Seam pillars will only be 25 m or 7T above the Fassifern Seam Goaf and may be subsided by up to 2 m for the proposed 3.5 m height miniwall panels. The potential for pillar instability is therefore possible; however, the extraction ratio of 36% in these workings suggests a worst-case subsidence of < 300 mm for old mine workings pillar heights of 2.5 m. As this result is similar to the previous multi-seam subsidence assessment, the potential instability of the pillars is not considered to represent a significant risk to the lake bed.

The impact of fracturing in the Wallarah Seam workings that are 60 to 70 m or 17T to 20T above the Fassifern Seam panels is likely to be minimal due to the presence of a 25 m thick spanning unit of Teralba Conglomerate above the Great Northern Seam.

10.3.16 Geological Structure Interaction Potential

The potential hydraulic connectivity of any structure to the surface will be controlled largely by the presence of spanning massive units and cover depth above the proposed miniwalls. The proposed panel widths and mining height will limit the height of fracturing above the workings and maintain a stable natural arch below the lake.

Major geological structures have produced increased (but manageable) groundwater inflows into the workings and are commonly known sites of poor roof conditions if undermined by continuous minor or miniwall shearer. Minor and moderate structures have not resulted in excessive mine water inflows.

As discussed in **Li *et al* 2006**, the high magnitude of horizontal stress in the overburden strata and north/north-east principal stress orientation will act positively on the north-west striking geological structure and reduce the opening potential of these structures. The north-west to east-west orientation of the proposed panels is also favourable in regards to vertical crack orientation and the regional horizontal stress.

As discussed earlier, LakeCoal will assess the potential risks in regards to undermining these features in regards to safety, operational and environmental hazards (e.g. high groundwater

inflows or in-rush events) when they are encountered and consider whether a mining layout change is necessary.

Further discussion on management strategies to identify geological structure of potential significance if undermined by the Modified miniwalls is presented in **Section 10.3.17**.

10.3.17 Impact Management Strategies

Based on **Table 23**, the prediction model outcomes indicate that the probability that continuous fracturing from the workings will intersect with surface zone cracks that extend 10 m depth below the surface is very unlikely to occur. It is also unlikely that significant leakage will occur from the lake due to interaction with B-Zone cracking or bed separations.

The presence of geological structure should be viewed with caution however, in regards to potential interaction with the lake bed generally.

Management strategies will need to identify potential fault-affected areas of the Site and deal with disproportionate water inflows into the workings should undermining of a smaller, undetected fault or structure occur. Undermining significant faults may result in higher continuous fracture connectivity and associated water makes and should be avoided. The potential for fault interaction with the multi-seam mine workings is probably lower for MWs 32 to 36, as the overlying seam workings did not encounter any faults of significance.

The significance of the geological structures encountered during development may be assessed in regards to their persistence and potential connectivity to the surface based on the following key parameters:

- Throw, trace, dip and dip direction
- Groundwater inflow rate change over time
- Groundwater inflow chemistry

However, it is unlikely that a significant structure will go undetected prior to the extraction of a miniwall as development headings will be formed on all sides of the panel prior to extraction (as was the case for the detection of the faulted area within the miniwall MW4 panel).

Recommendations for monitoring of sub-surface fracture heights above the proposed areas of secondary extraction are provided in **Section 11**.

10.4 Angle of Draw Effects on Seagrass Beds

LakeCoal currently adopts a 26.5^o angle of draw buffer zone from limits of extraction to seagrass beds around the foreshore. The predicted angle of draw to the 20 mm subsidence limits is estimated to range from 8^o to 28.7^o near the panels closest to the foreshores.

A review of the modified miniwall panel locations indicate that the angles of draw from the north-eastern goaf edge of MW 35 may result in a 534 m^2 area of the seagrass along the eastern foreshore of Chain Valley Bay and is summarised in **Table 26**. All other panels are located outside the predicted angles of draw from the seagrass areas.

Table 26 - Summary of Seagrass Encroachment Areas

Modified MW No.	XL	Cover Depth (m)	Predicted AoD (o)	Distance to 20 mm subsidence contour from goaf edge (m)	Maximum Distance inside Seagrass Bed Area, b (m)	Effected Length of Seagrass Bed (m)	Effected Area* A_e (m^2)
34	9	205	28.7	112	0	0	0
35	9	215	28.7	118	8.5	95	534
36	9	225	16.9 (26.5)	68 (112.5)	0	0	0
					Totals	95	534

* - Effected area is parabolic, A_e = 2bl/3; (bracket) - maximum predicted AoD < 26.5^o.

Based on a worst-case tilt range of 1 mm/m at the angle of draw of 26.5^o from the goaf edge, the affected areas may be subsided a further 8.5 mm (for a total subsidence of up to 28.5 mm). Horizontal strain magnitudes are also unlikely to exceed 1 mm/m outside a 26.5^o draw angle, nor cause cracking of the seagrass beds for the predicted angles of draw.

Given the above, it is therefore considered that the assumed AoD of 26.5^o from seagrass beds is unlikely to result in a significant change in bed levels if the AoD is exceeded slightly (by < 2^o) at some locations (and according to the prediction model only).

10.5 Sea Level Rise and Subsidence Effects on Pillar Stability

Reference to Lake Macquarie City Council website (www.lakemac.com.au) indicates that sea levels could rise between 0.59 and 0.90 m by 2100. Based on a predicted worst case subsidence of 1.23 m in Chain Valley Bay, pillars in the three seams will experience a slight increase in loading (<0.4%) due to an additional 1.48 m to 1.86 m of water depth by this time.

It is assessed that the projected sea level rise is very unlikely to cause pillar instability to occur.

10.6 Subsidence Effects on Wave Height and Foreshore Erosion

10.6.1 Potential Impacts

The predicted subsidence of the lake bed could increase the depth of water up to 780 mm above the modified MWs 9 to 31 and up to 1230 mm above MWs 32 to 36. An increase on the original 2013 assessment of 160 mm was predicted in the single seam areas and an increase of 340 mm was predicted in the multi seam areas.

The likely impacts of the proposed mining layout in regards to the above subsidence will be assessed by specialist coastal processes consultant to determine:

- Likely changes to wave form pattern and height due to increase in water depth.
- Potential foreshore erosion due to the wave form changes.

10.6.2 Impact Management Strategies

Strategies to manage the above potential impacts appropriately are beyond the scope of this report.

11.0 Monitoring Requirements

11.1 Subsidence Development

The development of subsidence above longwall and miniwall panels normally consists of three phases that are defined as ‘primary’, ‘secondary’ and ‘residual’ subsidence. Time dependant subsidence due to moisture softening is included in the residual subsidence category at CVC.

Maximum subsidence above a miniwall panel generally does not start to occur until the retreating miniwall face has moved at least a distance equal to the width of the panel from the start position, and is referred to as the 'square' position. The maximum panel subsidence will then continue for a given mining geometry and geological conditions until the miniwall retreats to within its square position from the finishing end of the panel.

Primary subsidence refers to the subsidence that occurs at a point as a direct result of a retreating miniwall passing beneath it (see **Figure 32**). The magnitude and rate of subsidence development is a function of the distance from the retreating miniwall face, the spanning behaviour of the overburden, and the time-dependent softening of the FAS claystone beds. Secondary subsidence is indirectly related to subsidence at a point due to subsequent adjacent miniwalls and is caused by compression of chain pillars and goaf movements. Secondary subsidence may occur each time another miniwall retreats past the point again, however, the magnitude and development rate of additional subsidence is likely to decrease exponentially as mining moves further away.

Residual subsidence, due to re-consolidation of goaf or softened claystone consolidation, may range widely and represents approximately 5 to 50% of maximum final subsidence and will be on-going for several months to years after primary or secondary subsidence ceases.

Approximately 90% to 95% of primary and secondary subsidence development will occur within 3 to 12 months after undermining occurs or subsequent miniwalls retreat past a given point. Final Maximum subsidence is not expected to occur above the first miniwall panel until four or five panels are completed in the group of panels.

On-going residual settlements of up to 230 mm due to claystone floor consolidation beneath the chain pillars may continue for a period of up to 10 years, however, these movements are unlikely to result in further impact occurring to the surface, due to their relatively uniform subsidence profile.

Multi-seam stress interaction may also affect the rates of subsidence development.

11.2 Surface Monitoring Plans

Subsidence effects may be determined using bathymetric surveys of the lake bed before and after mining of panels has occurred.

The surveys have been undertaken annually to-date, however, the development of additional time dependent subsidence below MW3 and MW6 tailgate chain pillars is not considered to be a significant deviation at this stage. However, it is recommended that the bathymetric survey frequency be increased to until the subsidence development mechanism and performance of the prediction model can be established.

If the measured subsidence is within the predicted range it is not considered necessary to amend the modified mining layout assessed by this study.

11.3 Sub-Surface Monitoring

Monitoring of sub-surface fracture heights above some of the miniwall panels would usually be recommended within the mining area to confirm the predictions of potential areas of connective surface cracking. Due to the presence of the lake however, no deep borehole extensometers have been installed above the Colliery's workings to monitor and measure heights of sub-surface fracturing due to the caving or goafing process during mining.

Furthermore, measurement of sub-surface fracture heights above the proposed miniwalls is not recommended due to the risks associated with the drilling from a barge and potential intersection with goafs from barge mounted drilling rigs after mining a given panel.

Monitoring of groundwater chemistry changes and inflow rates would probably provide an indirect measure of connectivity between the lake and mine workings and this should be considered as part of the Extraction Plan or site Trigger Action Response Plan (TARP) requirements.

The outcomes of inspections and monitoring of underground workings stability should also continue to be mapped and reviewed along with groundwater monitoring data. In particular, as the presence of a fault, dyke or joint shear zone has the potential to cause a hydraulic connection between the fracture zones, abnormal inflows may result if significant faults are undermined and should therefore be avoided.

12.0 Conclusions and Recommendations

It is concluded that softening of claystone beds below tailgate pillars and adjacent road ways along MW3 and MW6 has developed time-dependant subsidence with the originally predicted subsidence in this area of 460 mm being exceeded by 110 mm after MW8 was completed. Importantly, the subsidence to date has remained within the level of subsidence assessed in the 2013 EIS, being 620 mm in the single seam mining area.

The results indicate that the modified mining layout may have between 105 mm and 340 mm higher final subsidence than was predicted for the previous layout due mostly to the development of soft floor conditions and a minor chain pillar width correction (a 6% width reduction). It is also unlikely that the modified layout will cause a significant increase to the previously assessed impacts and therefore is unlikely to exceed the performance measures defined in the Development Consent for the Site.

Note: The predicted magnitudes of final subsidence will need to be confirmed with further bathymetric surveys, but at this stage, is considered to be conservative.

Where potential subsidence impacts to seagrass beds have been modelled, LakeCoal have committed to refining the mine design and panel lengths to ensure the subsidence impacts to the seagrass beds will be avoided.

It is recommended that the bathymetric survey frequency be increased until the subsidence development mechanism and performance of the prediction model can be established.

If the measured subsidence is within the predicted range it is not considered necessary to amend the modified mining layout assessed by this study.

LakeCoal will continue to implement an adaptive management approach which will involve the monitoring, periodic evaluation of the consequences of mining, with possible adjustment of the mining layout and/or methods through the Extraction Plan process to achieve the required measures of performance. It should be noted that the mine plan has already been adjusted in the north eastern area of the Site to meet height of subsurface fracturing criteria discussed in this report.

The prediction methods applied in this report will allow specialist consultants to assess the potential range of impacts to a given feature in a probabilistic manner. Management plans and strategies can then be developed that allow appropriate Trigger Action Responses and mine planning adjustments or mitigation measures necessary to deliver satisfactory outcomes to the feature and relevant stakeholders. The subsidence effect and impact assessment predictions have also been validated against surface and subsurface monitoring programs at CVC with similar geological conditions and mining methods elsewhere.

If the estimated worst-case impacts cannot be reasonably managed, or in the event that significant exceedances occur, then it will be necessary to adjust to the mining layout further to provide a more acceptable risk.

It is assessed that the proposed mining height above the modified MWs 20 to 25 will need to be reduced to maintain a minimum Constrained zone of 12T between the continuously fractured overburden (A-Zone) and the surface cracking zone beneath the lake bed sediments (D-Zone). The Pi-Term models that have been applied represent a significant improvement in our understanding of the interaction between mining geometry and geology on the extent of the fracture zones that are likely to develop above sub-critical panels.

Based on the analysis completed in **DgS, 2013**, it is still considered that the modified MWs 32 to 36 beneath Chain Valley Bay are unlikely to cause significant instability in the overlying mine workings and cause additional subsidence. Given the proposed timing for extraction of MWs 32 to 36 will be towards the end of the mining schedule, there remains substantial time to consider further refinement of mine layouts in this area based on subsidence monitoring data.

13.0 References

ACARP, 1998a. **Chain Pillar Design (Calibration of ALPS)**. Colwell, M., Mark, C.ACARP Report No. C6036 (October).

ACARP, 1998b. **ACARP Project No. C5024, Establishing the Strength of Rectangular and Irregular Pillars**. Galvin, J.M., Hebblewhite, B.K., Salamon, M.D.G., Lin, B.B.

ACARP, 2003. **ACARP Project No. C10023, Review of Industry Subsidence Data in Relation to the Impact of Significant Variations in Overburden Lithology and Initial Assessment of Sub-Surface Fracturing on Groundwater**, Ditton, S. and Frith, R.C. Strata Engineering Report No. 00-181-ACR/1 (Sep).

ACARP, 2005. **Systems Approach to Pillar Design**. Strata Control Technologies Pty Ltd, UNSW School of Mining, Coffey Geosciences Pty Ltd. ACARP Project No. C9018. (May).

ACARP, 2007. **Hydrological Response to Longwall Mining**. CSIRO Exploration & Mining. H. Guo, D. Adhikary, D. Gaveva. Report No. C14033 (October).

Brown & Meyerhof, 1969. **Experimental Study of Bearing Capacity in Layered Clays**. Proceedings of 7th International Conference on Soil Mechanics and Foundation Engineering, Mexico.

Das, 1986. **Influence of Width/Height Ratio on Post Failure Behaviour of Coal**. M.N. Das. Institution Journal of Mining and Geological Engineering Vol 4.

Das, 1998. **Principles of Geotechnical Engineering** (4th Edition). Braja M. Das. PWS Publishing Company.

DgS, 2012. **Addendum to Main Report - Review of the Subsidence Predictions for the Proposed Partial Pillar Extraction of 3-West Panel (Panel 13) at the Tasman Mine, George Booth Drive, Seahampton**. DgS Report No. TAS-004/10a (25 April 2012).

DgS, 2013. **Subsidence Impact Assessment for the Chain Valley Colliery Mining Extension 1 Project**. DGS Report No. CHV-002/1. Ditton Geotechnical Services (25 April 2013).

DgS, 2014. **Subsidence Assessment for the Proposed Underground Headings between Chain Valley Colliery and Mannering Colliery**. DGS Report No. CHV-002/3 (27/1/14).

Diedrichs and Kaiser, 1999. **Stability of Large Excavations in Laminated Hard Rock Masses: the Voussoir Analogue Revisited**. M.S. Diedrichs and P.K. Kaiser. International Journal of Rock Mechanics and Mining Sciences 36.

Ditton and Merrick, 2014. **A New Sub-Surface Fracture Height Prediction Model for Longwall Mines in the NSW Coalfields**. Presentation given at Australian Earth Sciences Convention, Newcastle (04/07/2014).

DMR, 1987. **Mining Subsidence in NSW. 2. Surface Subsidence Prediction in the Newcastle Coalfield**. L. Holla. Department of Mineral Resources (January).

DMR, 1995. **The Newcastle Coalfield**. Geological Sheet Series. NSW Department of Minerals Resources.

EMM, 2013. Chain Valley Colliery Mining Extension 1 Project Environmental Impact Statement. EMGA Mitchell McLennan.

Holla and Buizen, 1990. **Strata Movement due to Shallow Longwall Mining and the Effect on Ground Permeability**. Proceedings of Australian Institution of Minerals and Metallurgy. Vol 295, No. 1 (1986).

Forster, 1995.**Impact of Underground Coal Mining on the Hydrogeological Regime, Central Coast, NSW**. Forster, I. Published in Australian Geomechanics Society (AGS) Conference Proceedings (February), Engineering Geology of Newcastle – Gosford Region, University of Newcastle.

Hardy and Heasley, 2004. **Enhancements to the LaModel Stress Analysis Program**. R.Hardy and K.A. Heasley. SME Publications.

Hoek and Diederichs, 2006. **Empirical Estimation of Rock Mass Modulus**. Hoek, E. and Diederichs, M.S. International Journal of Rock Mechanics and Mining Science, 43 (2).

Ives, 1995. **Stratigraphy and Engineering Properties of the Newcastle and Tomago Coal Measures**. M.J. Ives. Published in Australian Geomechanics Society (AGS) Conference Proceedings (February), Engineering Geology of Newcastle – Gosford Region, University of Newcastle.

ISRM, 1981. **Basic Geotechnical Description of Rock Masses**. International Society For Rock Mechanics, Commission on Classification of Rocks and Rock Masses. ISRM Journal, Vol 18 pp 85 to 110.

Li and Smith, 1998. **Planning for Time-Dependant Subsidence**. Published Proceedings of 4th Triennial MSTS Conference, University of Newcastle, July.

Li *et al.,* 2006. **A Case Study on Longwall Mining Under the Tidal Waters of Lake Macquarie**. G. Li, I. Forster, M. Fellowes and A. Myors, 2006. Proceedings of Coal 2006 Conference, University of Wollongong.

Li *et al.*, 2010. **A Case Study on Mine Subsidence Due to Multi-Seam Longwall Extraction**. G. Li, P. Steuart, R. Paquet, R. Ramage. Submitted to AusIMM Conference " The 2nd Australasian Ground Control in Mining 2010".

Lohe & Dean-Jones, 1995. **Structural Geology of the Narrabeen Group in the Newcastle-Gosford Region**. Published in Australian Geomechanics Society (AGS) Conference Proceedings (February), Engineering Geology of Newcastle – Gosford Region, University of Newcastle.

McNally, 1995. **Engineering Geology of the Narrabeen Group in the Gosford-Newcastle Region**. G.H. McNally. Published in Australian Geomechanics Society (AGS) Conference Proceedings (February), Engineering Geology of Newcastle – Gosford Region, University of Newcastle.

Marinos and Hoek, 2000. **GSI: A Geologically Friendly Tool for Rock Mass Strength Estimation**. P. Marinos, E. Hoek. Proceedings of GeoEng 2000 Conference, Melbourne.

Marino and Choi, 1999. **Softening Effects on Bearing Capacity of Mine Floors**. G.G. Marino & S. Choi. Journal of Geotechnical and Geoenvironmental Engineering (Dec 1999).

Nagaraj and Murty, 1985. **Prediction of Pre-consolidation Pressure and Recompression Index of Soils**. Geotechnical Testing Journal Vol 8 No. 4.

Peng and Chiang, 1984. **Longwall Mining**. S.S. Peng & H.S. Chiang. Wiley.

SCT, 2008. **Assessment of Longwall Panel Widths and Potential Hydraulic Connection to Bowmans Creek – Ashton Mine**. SCT Operations Pty Ltd Report to Ashton Coal, September.

Seedsman, 2011. **Assessment of Subsidence in Domains 1 & 2**. Seedsman Geotechnics Report No. CV28 May 2011.

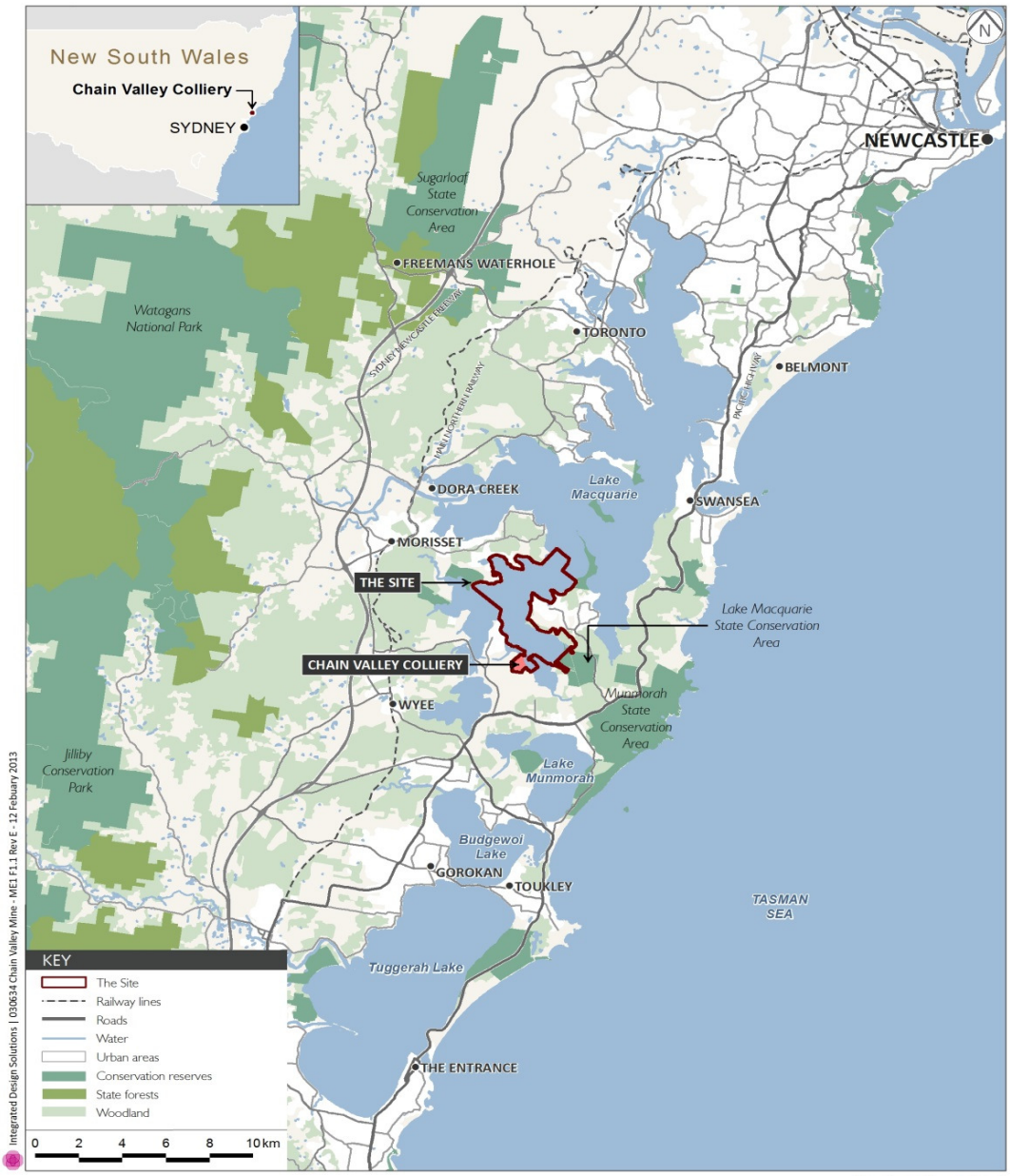
Seedsman & Gordon, 1992. **Weak Claystone Floors and their Implications to Pillar Design and Settlement**. 11th International Conference on Ground Control In Mining, University of Wollongong, NSW (July).

SDPS, 2007. **Subsidence Deformation Prediction System - Quick Reference Guide and Working Examples**. Agioutantis, Z., Karmis, M. Department of Mining and Minerals Engineering, Virginia Polytechnic Institute and State University, Virginia.

Vick, 2002. **Degrees of Belief: Subjective Probability and Engineering Judgement**. Vick, S.G. ASCE Press.

Whittaker and Reddish, 1989. **Subsidence Occurrence, Prediction and Control**. B.N. Whittaker and D.J. Reddish. Developments in Geotechnical Engineering, 56, Elsevier.

Zipf, 1999. **Using a Post-Failure Stability Criterion in Pillar Design**. R. Karl Zipf, Jnr. Proceedings of Second International Workshop on Coal Pillar Mechanics, NIOSH IC 9448 (June).



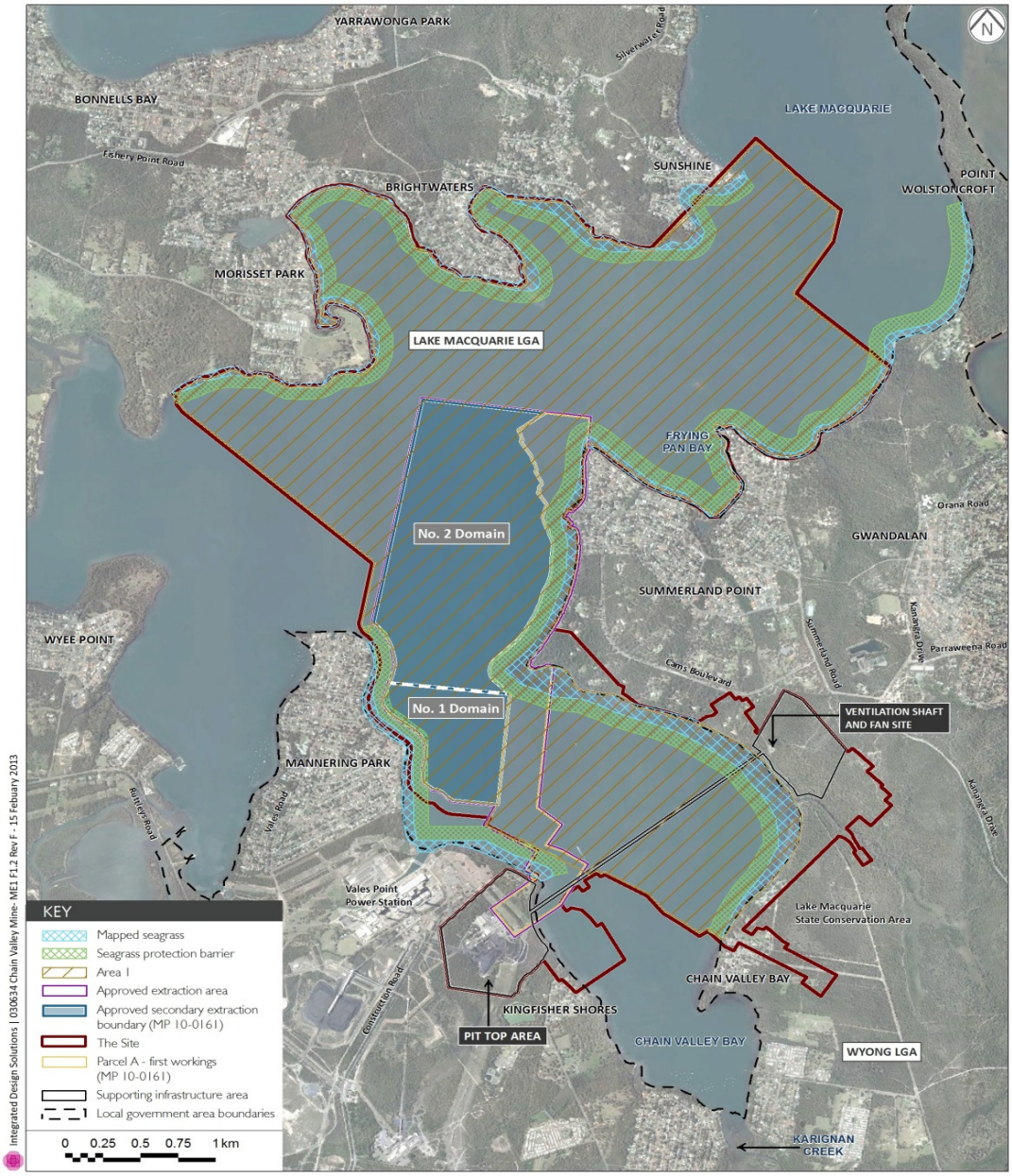
Regional context

Chain Valley Colliery Mining Extension | Project - Environmental Impact Statement

Figure 1.1

EMM

DgS	Engineer:	S.Ditton	Client:	LakeCoal - Chain Valley Colliery	
	Drawn:	S.Ditton		CHV-002/4	
	Date:	20.03.15	Title:	Regional Context for the Modified Mine Layout at CVC	
	Ditton Geotechnical Services Pty Ltd		Scale:		Figure No: 1.1



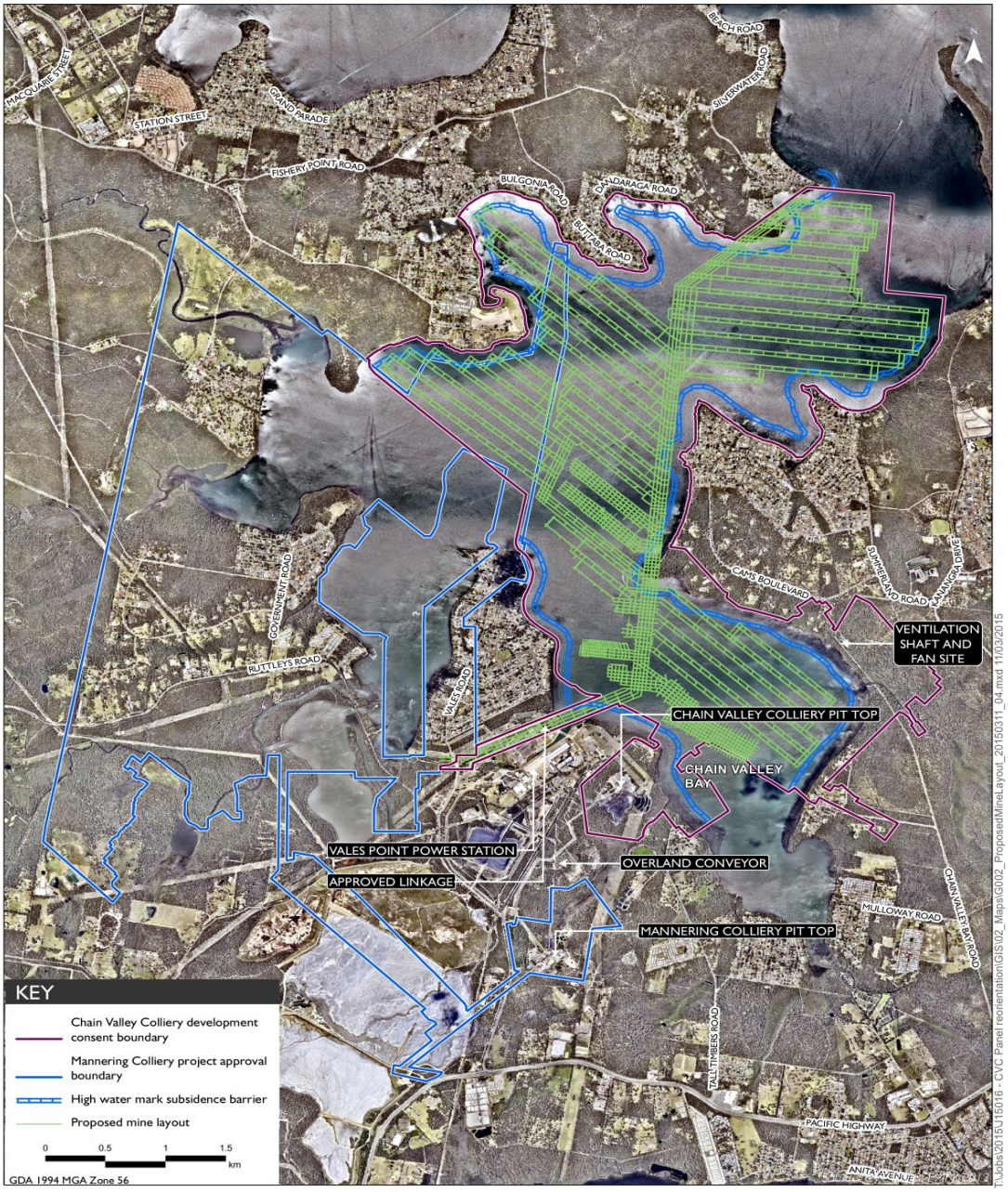
The Site

EMM

Chain Valley Colliery Mining Extension 1 Project - Environmental Impact Statement

Figure 1.2

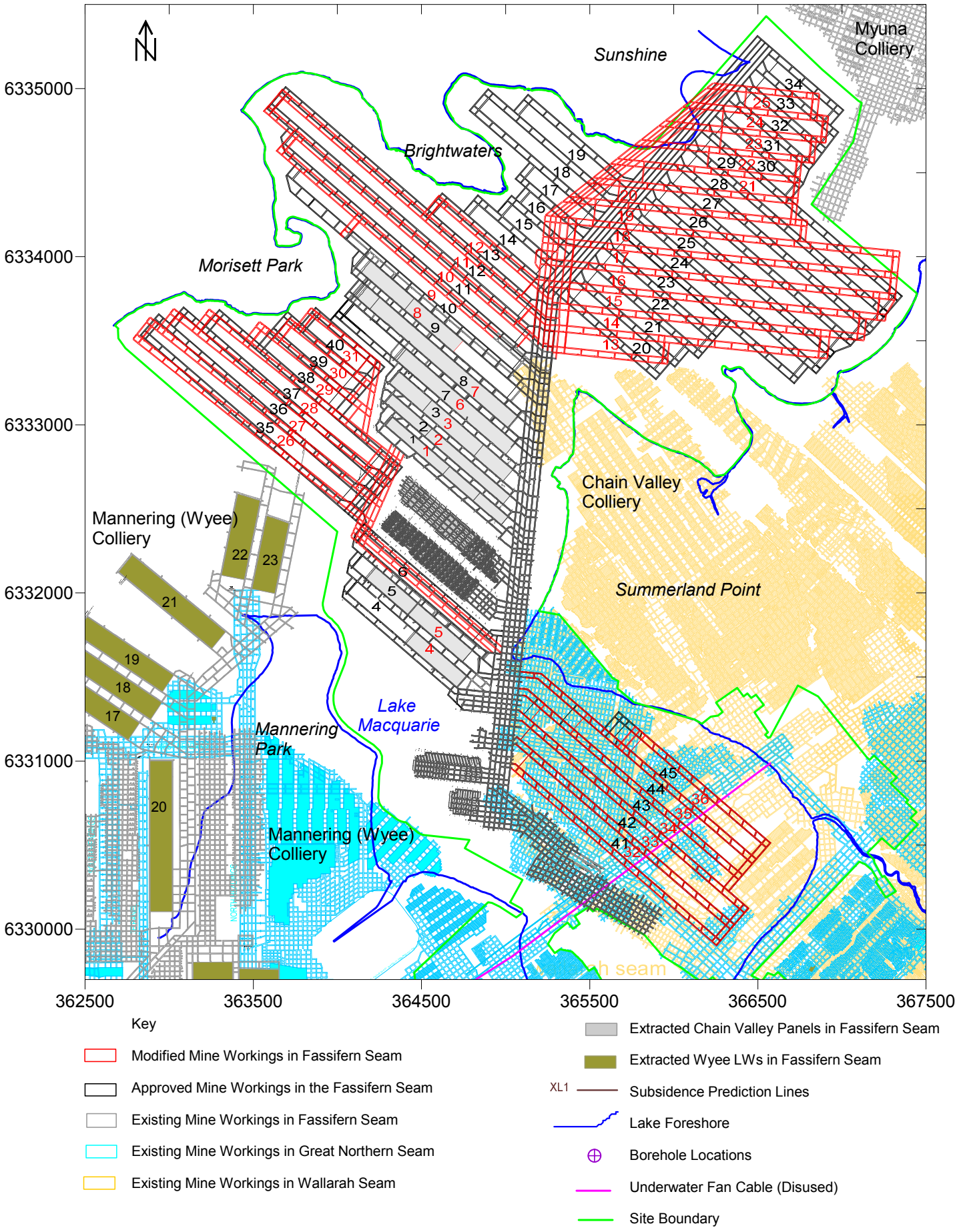
DgS	Engineer:	S.Ditton	Client:	LakeCoal - Chain Valley Colliery	
	Drawn:	S.Ditton		CHV-002/4	
	Date:	20.03.15	Title:	Site Boundary for the Approved Mining Area at CVC	
	Ditton Geotechnical Services Pty Ltd		Scale:		Figure No: 1.2



EMM
EMGA Mitchell McLennan

Proposed mine layout
Figure 2

DgS	Engineer:	S.Ditton	Client:	LakeCoal - Chain Valley Colliery	
	Drawn:	S.Ditton		CHV-002/4	
	Date:	20.03.15	Title:	Modified Miniwall Layout & HWMSB Location	
	Ditton Geotechnical Services Pty Ltd		Scale:		Figure No: 1.3



DgS

Ditton Geotechnical Services Pty Ltd

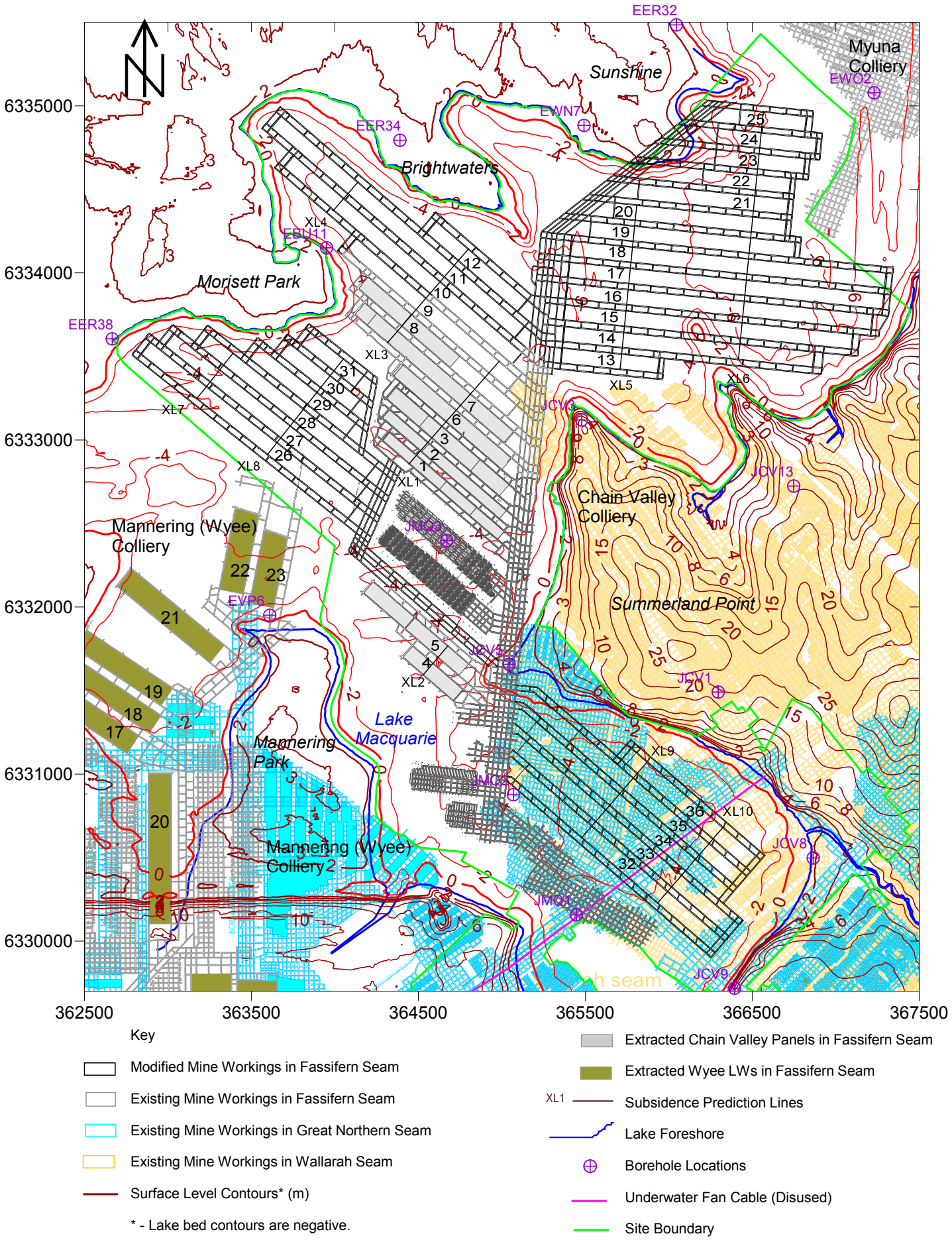
Engineer:	S.Ditton
Drawn:	S.Ditton
Date:	20.03.15

Client: LakeCoal - Chain Valley Colliery
CHV-002/4

Title: Proposed Mining Layout Modification for MWs 9 to 36 in the Fassifern Seam

Scale: 1:12,000 (A4)

Figure No: 1.4



DgS

Ditton Geotechnical Services Pty Ltd

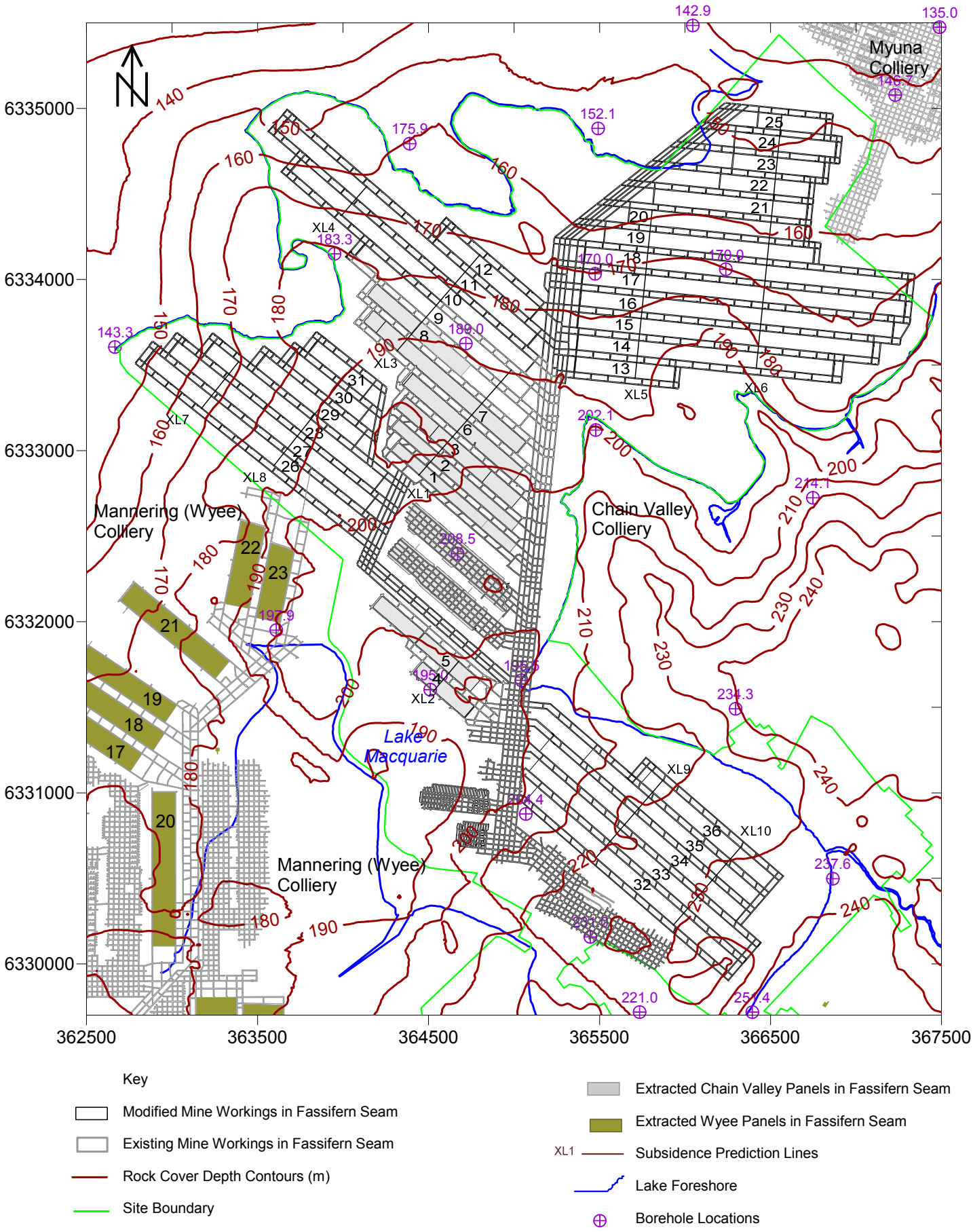
Engineer:	S.Ditton
Drawn:	S.Ditton
Date:	20.03.15

Client: LakeCoal - Chain Valley Colliery
CHV-002/4

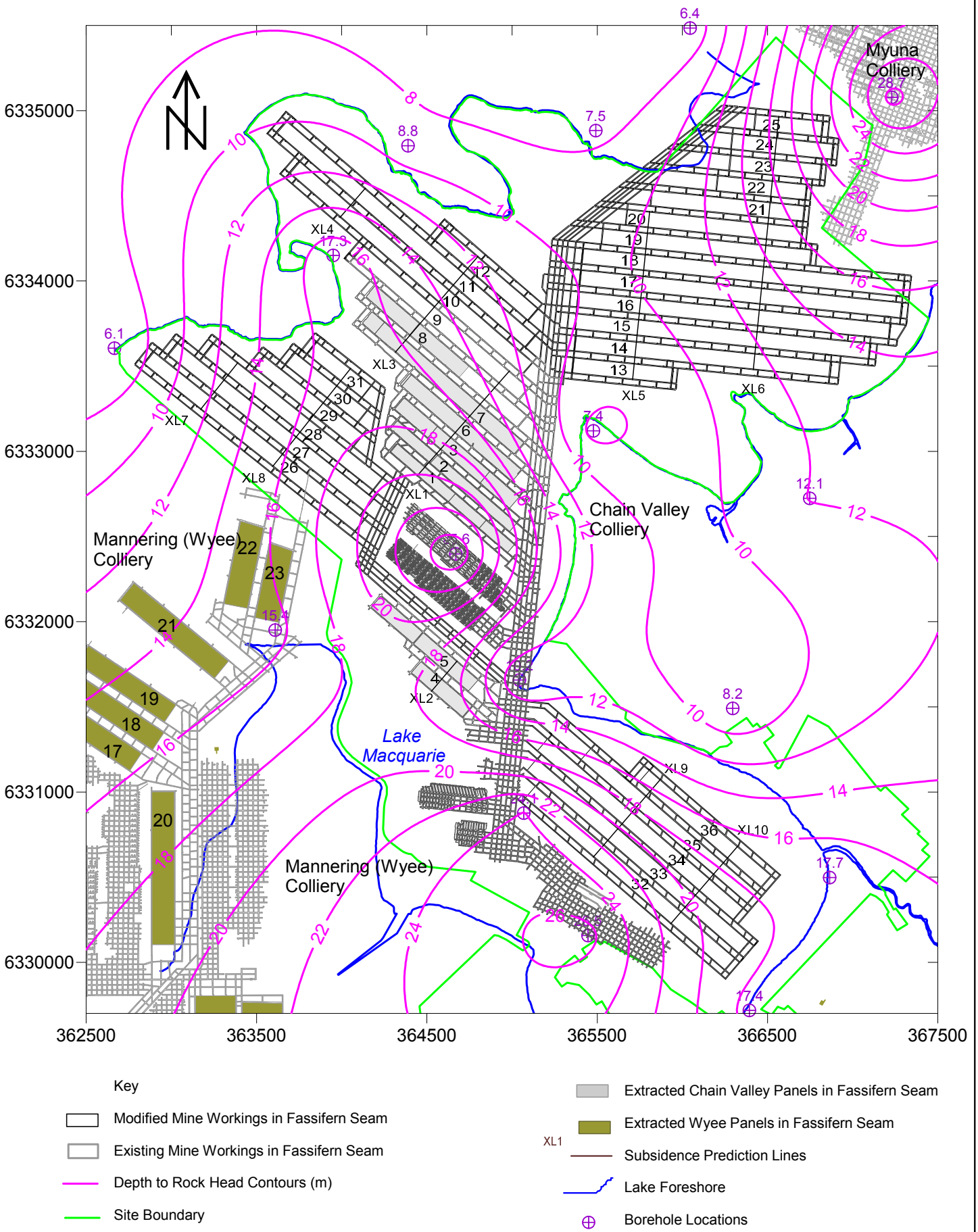
Title: Surface Level Contours above the Modified Mine Layout and Existing Mine Workings in the Wallarah, Great Northern and Fassifern Seams

Scale: 1:12,000 (A4)

Figure No: 2



DgS	Engineer:	S.Ditton	Client:	LakeCoal - Chain Valley Colliery CHV-002/4	
	Drawn:	S.Ditton			
	Date:	20.03.15	Title:	Effective Cover Depth Contours (below lake bed) above the Modified Mine Layout	
Ditton Geotechnical Services Pty Ltd			Scale:	1:12,000 (A4)	Figure No: 3.1



Key

- Modified Mine Workings in Fassifern Seam
- Existing Mine Workings in Fassifern Seam
- Depth to Rock Head Contours (m)
- Site Boundary
- Extracted Chain Valley Panels in Fassifern Seam
- Extracted Wyee Panels in Fassifern Seam
- XL1 Subsidence Prediction Lines
- Lake Foreshore
- Borehole Locations

DgS

Ditton Geotechnical Services Pty Ltd

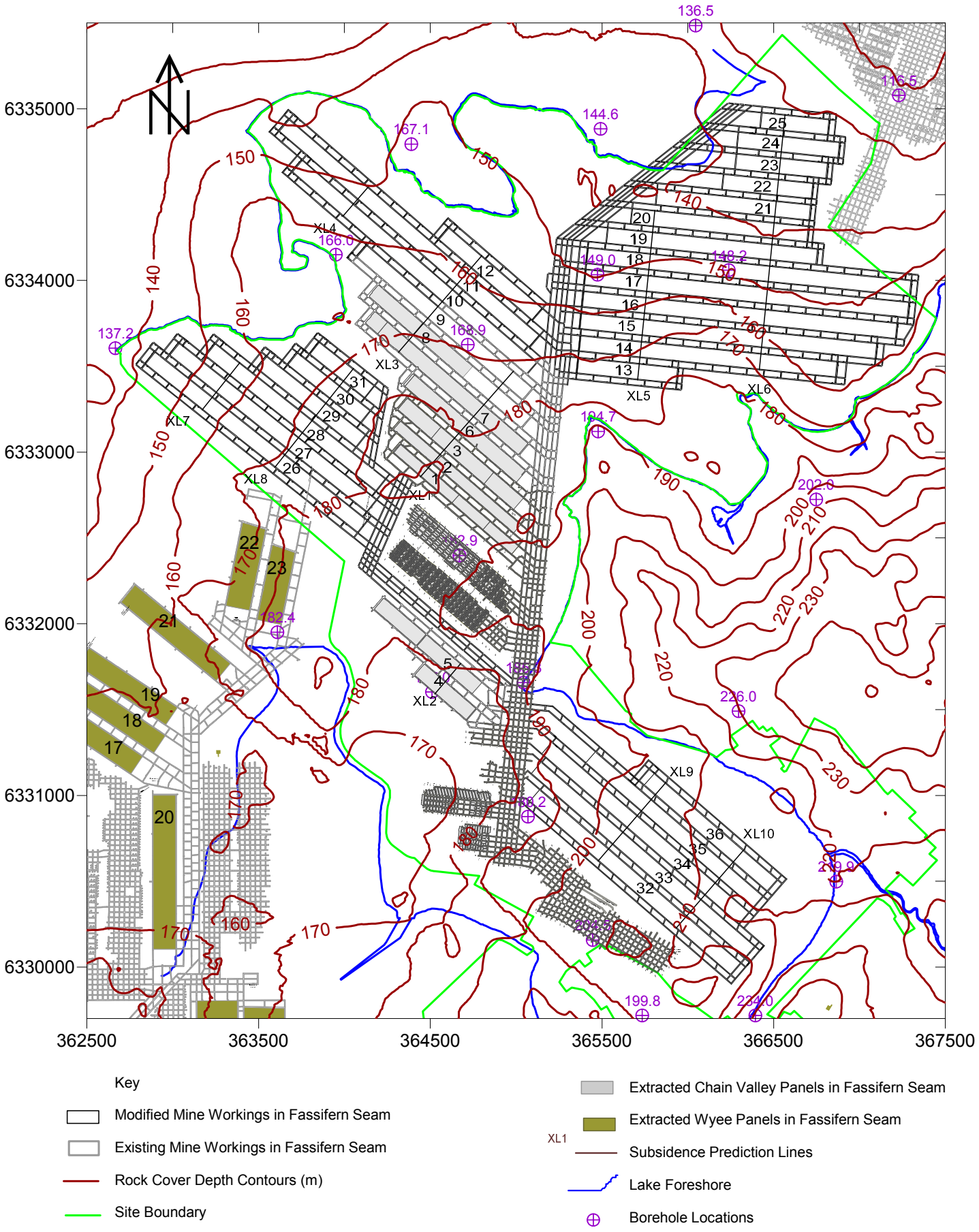
Engineer:	S.Ditton
Drawn:	S.Ditton
Date:	20.03.15

Client: LakeCoal - Chain Valley Colliery
CHV-002/4

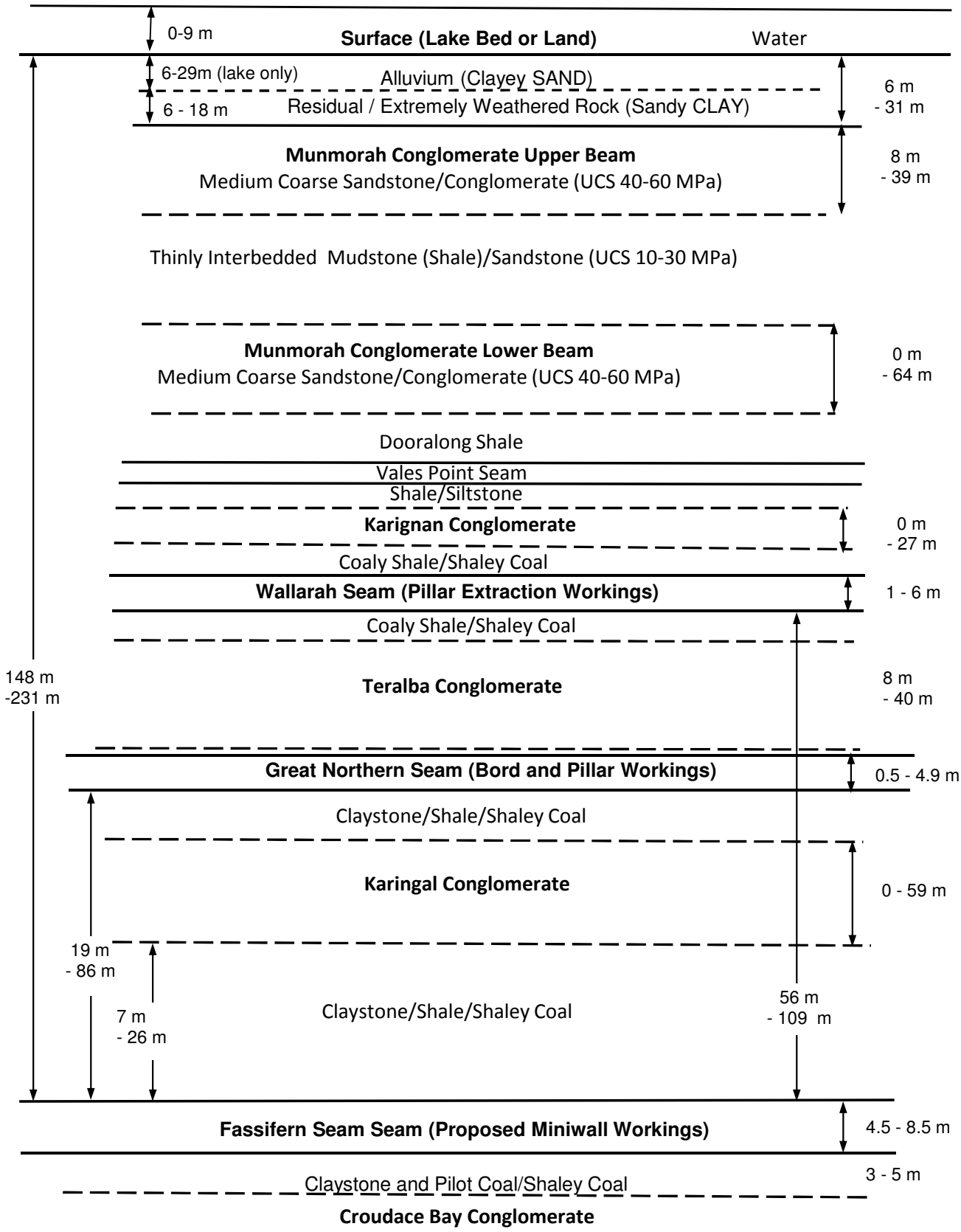
Title: Depth to Rock Head Contours above the Modified Mine Layout

Scale: 1:12,000 (A4)

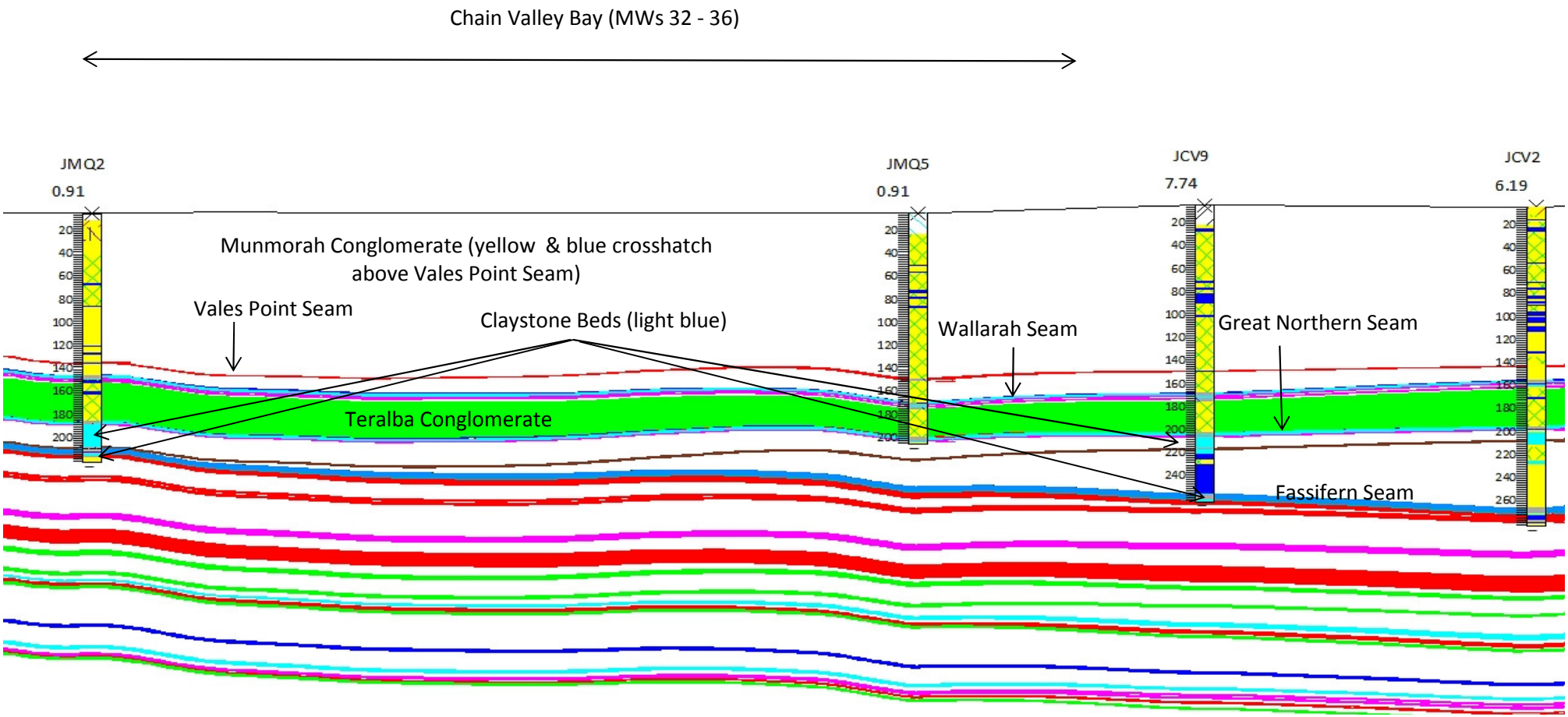
Figure No: 3.2



DgS	Engineer:	S.Ditton	Client:	LakeCoal - Chain Valley Colliery CHV-002/1	
	Drawn:	S.Ditton			
	Date:	05.12.12	Title:	Interpreted Rock Cover Contours above the Modified Mine Layout	
Ditton Geotechnical Services Pty Ltd			Scale:	1:12,000 (A4)	Figure No: 3.3

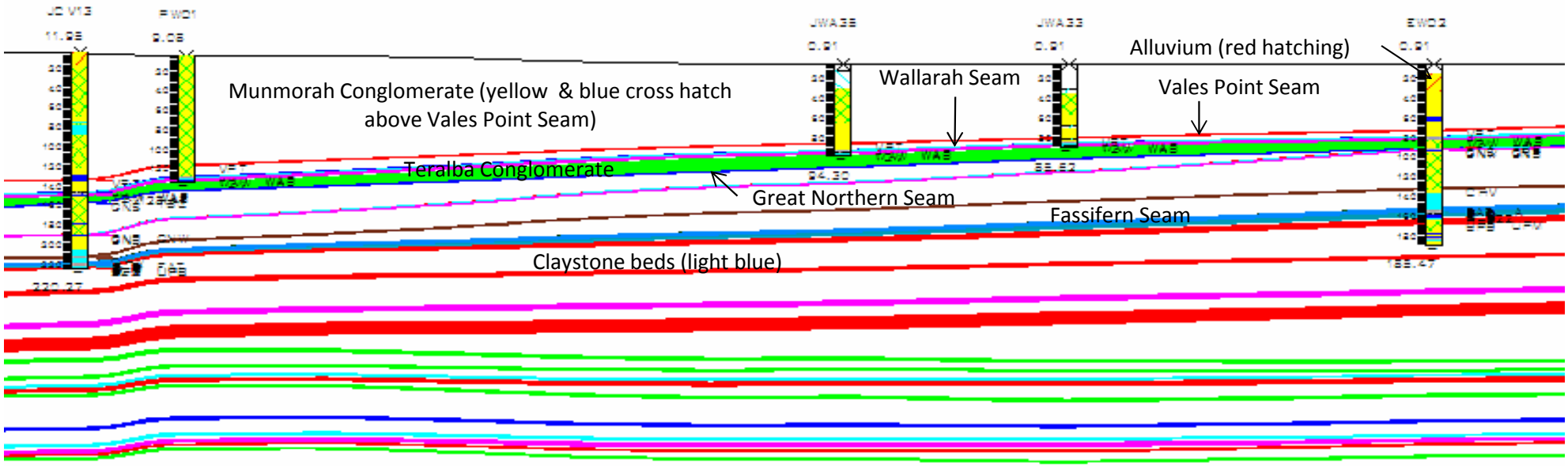


DgS	Engineer: S.Ditton	Client:	LakeCoal - Chain Valley Colliery		
	Drawn: S.Ditton		CHV-002/4		
	Date: 20.03.15	Title:	Geotechnical Model of the Strata above the Modified Mine Layout		
	Ditton Geotechnical Services Pty Ltd	Scale:	NTS	Figure No:	4.1

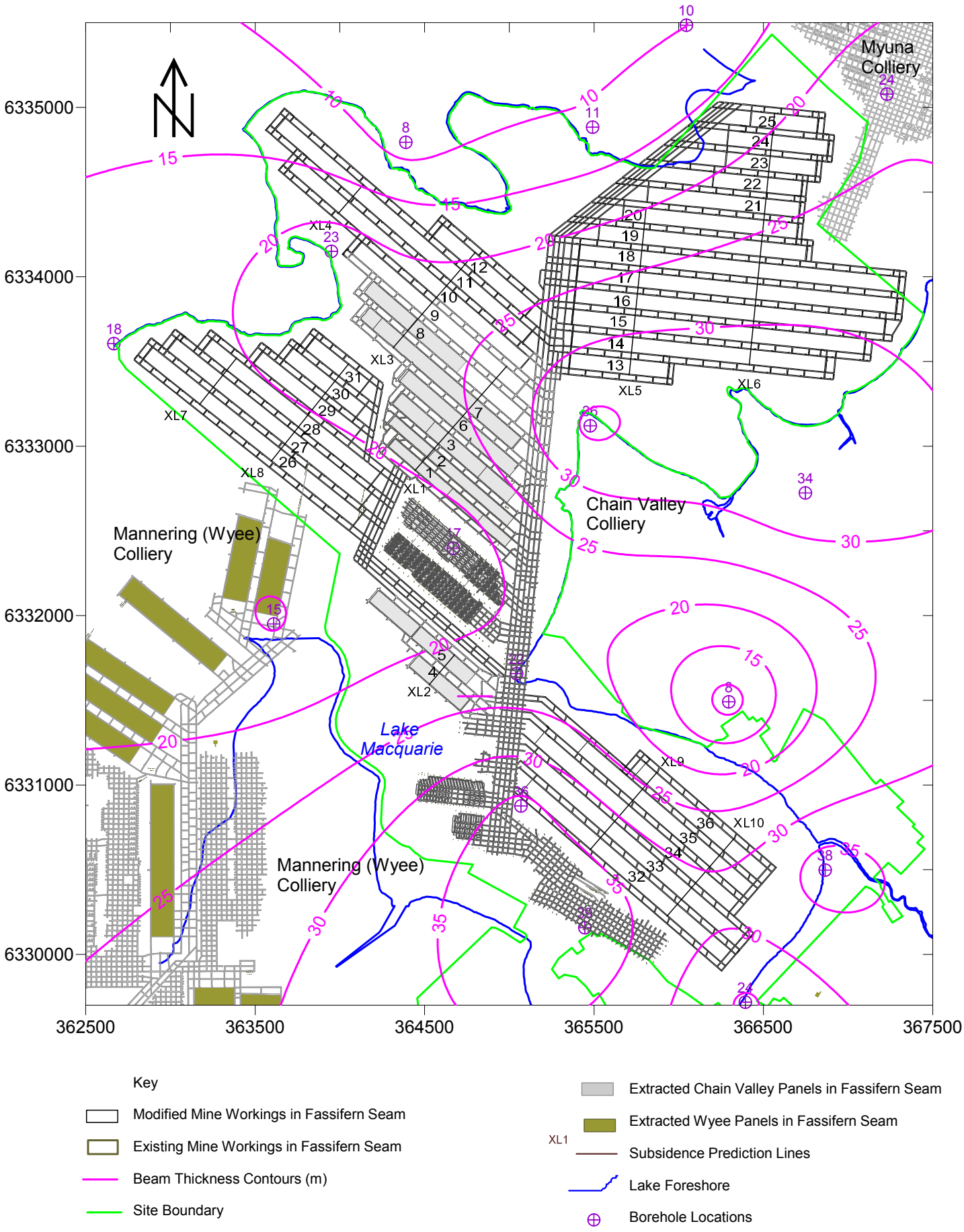


DgS	Engineer:	S.Ditton	Client:	LakeCoal - Chain Valley Colliery CHV-002/4	
	Drawn:	S.Ditton			
	Date:	15.05.15	Title:	Geological Section Through Chain Valley Bay	
	Ditton Geotechnical Services Pty Ltd		Scale:	NTS	Figure No: 4.2

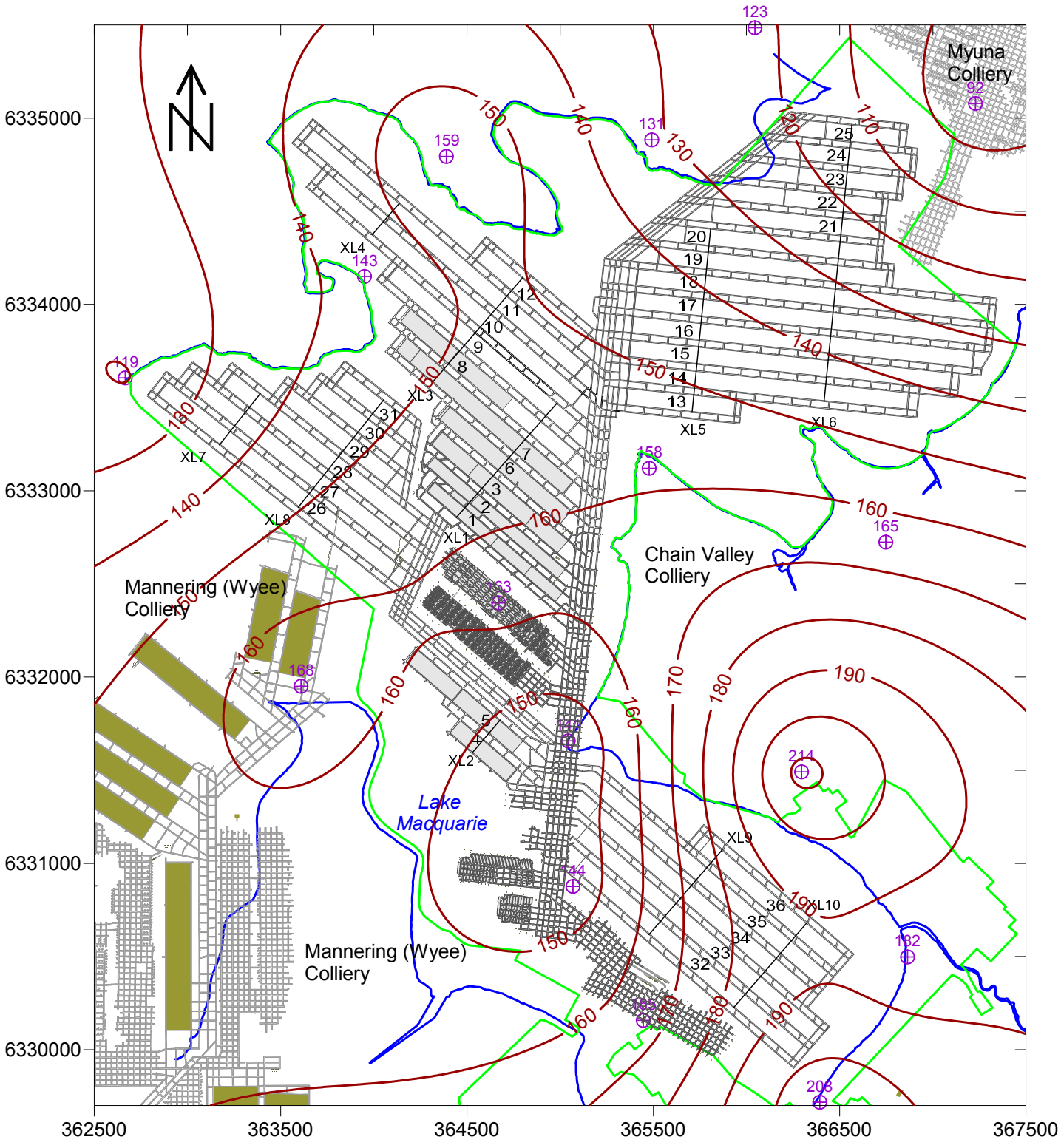
Myuna Bay (MWs 13 - 25)



DgS	Engineer:	S.Ditton	Client:	LakeCoal - Chain Valley Colliery CHV-002/4	
	Drawn:	S.Ditton			
	Date:	15.05.15	Title:	Geological Section Through Myuna Bay	
	Ditton Geotechnical Services Pty Ltd		Scale:	NTS	Figure No: 4.3



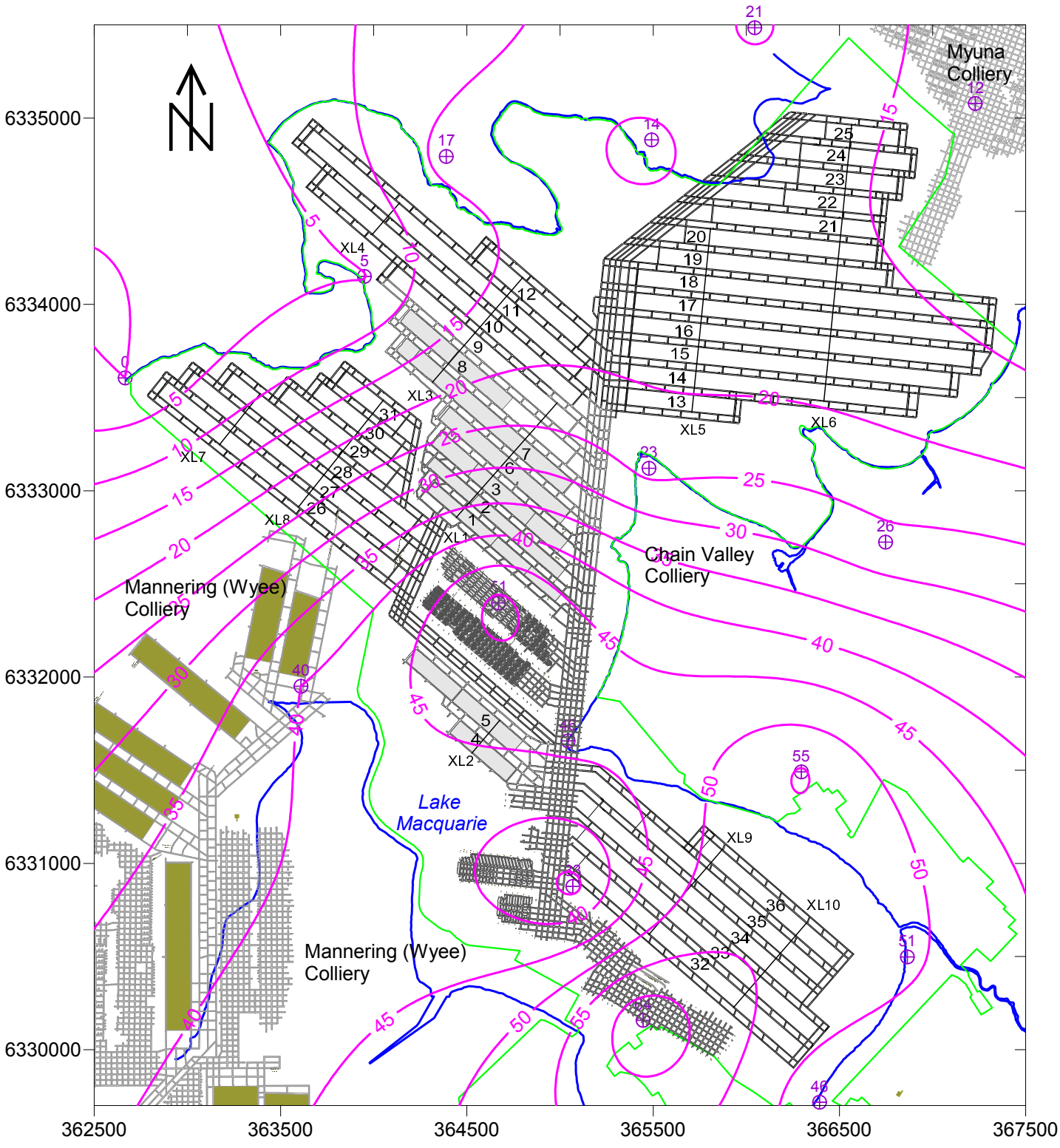
DgS	Engineer:	S.Ditton	Client:	LakeCoal - Chain Valley Colliery CHV-002/4	
	Drawn:	S.Ditton			
	Date:	20.03.15	Title:	Munmorah Conglomerate Upper Beam Thickness Contours above the Modified Mine Layout for MWs 9 to 36	
	Ditton Geotechnical Services Pty Ltd		Scale:	1:12,000 (A4)	Figure No: 5.1



Key

- Modified Mine Workings in Fassifern Seam
- Existing Mine Workings in Fassifern Seam
- Beam Distance above Workings Contours (m)
- Site Boundary
- Extracted Chain Valley Panels in Fassifern Seam
- Extracted Wyee Panels in Fassifern Seam
- XL1 Subsidence Prediction Lines
- Lake Foreshore
- Borehole Locations

DgS Ditton Geotechnical Services Pty Ltd	Engineer:	S.Ditton	Client:	LakeCoal - Chain Valley Colliery CHV-002/4	
	Drawn:	S.Ditton			
	Date:	20.03.15	Title:	Munmorah Conglomerate Upper Beam Distance Contours above the Modified Mine Layout for MWs 9 to 36	
			Scale:	1:12,000 (A4)	Figure No: 5.2



Key

- Modified Mine Workings in Fassifern Seam
- Existing Mine Workings in Fassifern Seam
- Beam Thickness Contours (m)
- Site Boundary
- Extracted Chain Valley Panels in Fassifern Seam
- Extracted Wyee Panels in Fassifern Seam
- XL1 Subsidence Prediction Lines
- Lake Foreshore
- Borehole Locations

DgS

Ditton Geotechnical Services Pty Ltd

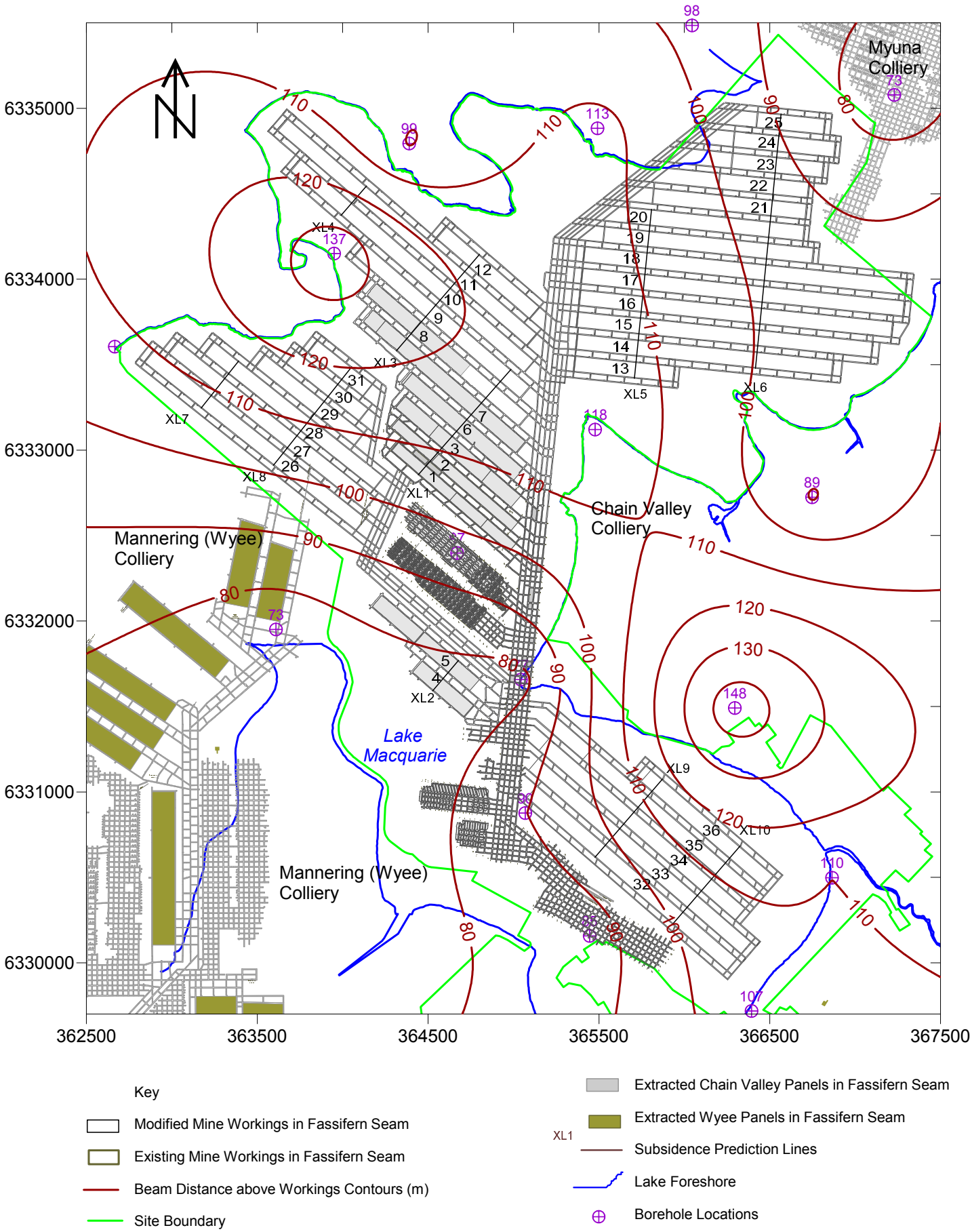
Engineer:	S.Ditton
Drawn:	S.Ditton
Date:	20.03.15

Client: LakeCoal - Chain Valley Colliery CHV-002/4

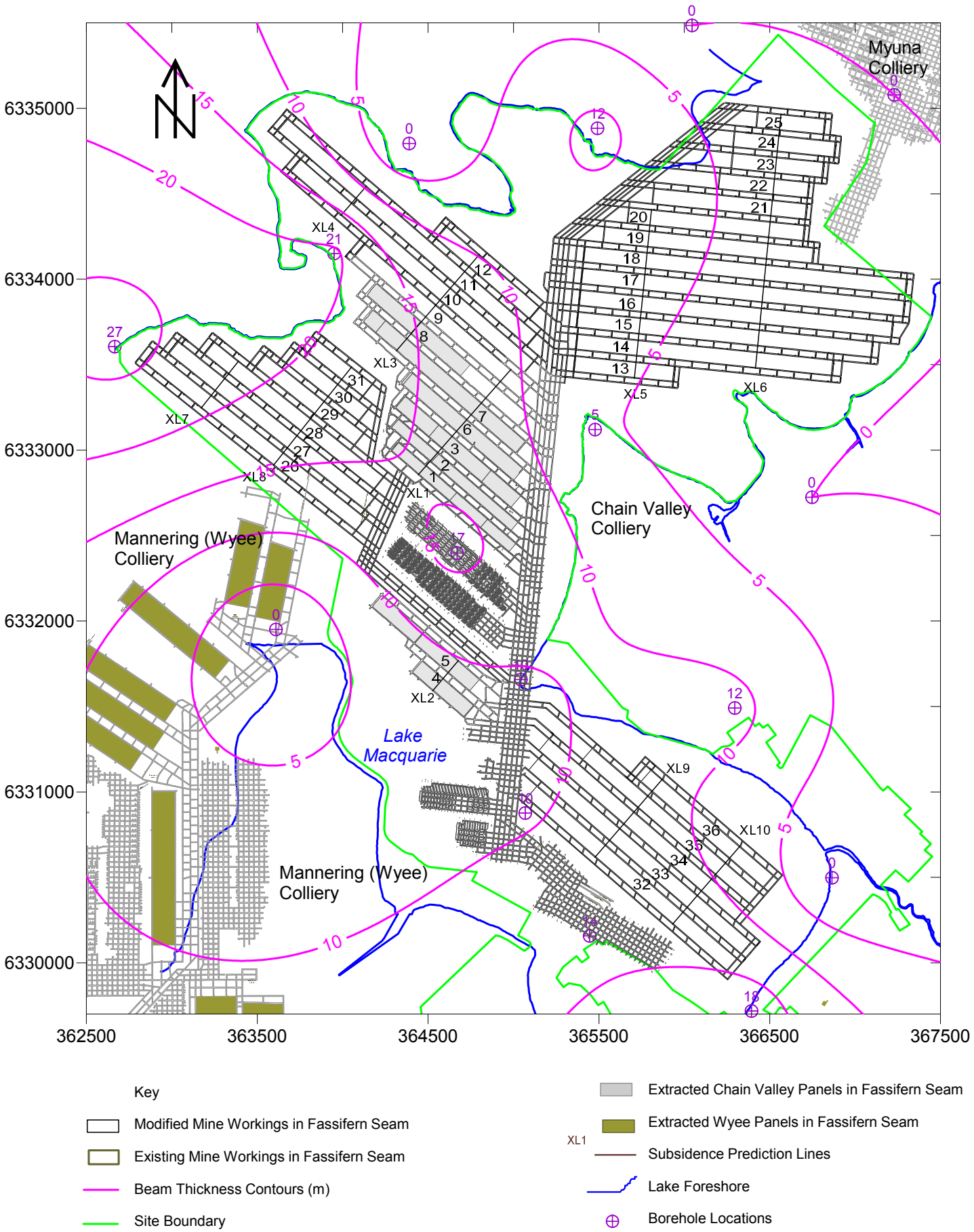
Title: Munmorah Conglomerate Lower Beam Thickness Contours above the Modified Mine Layout for MWs 9 to 36

Scale: 1:12,000 (A4)

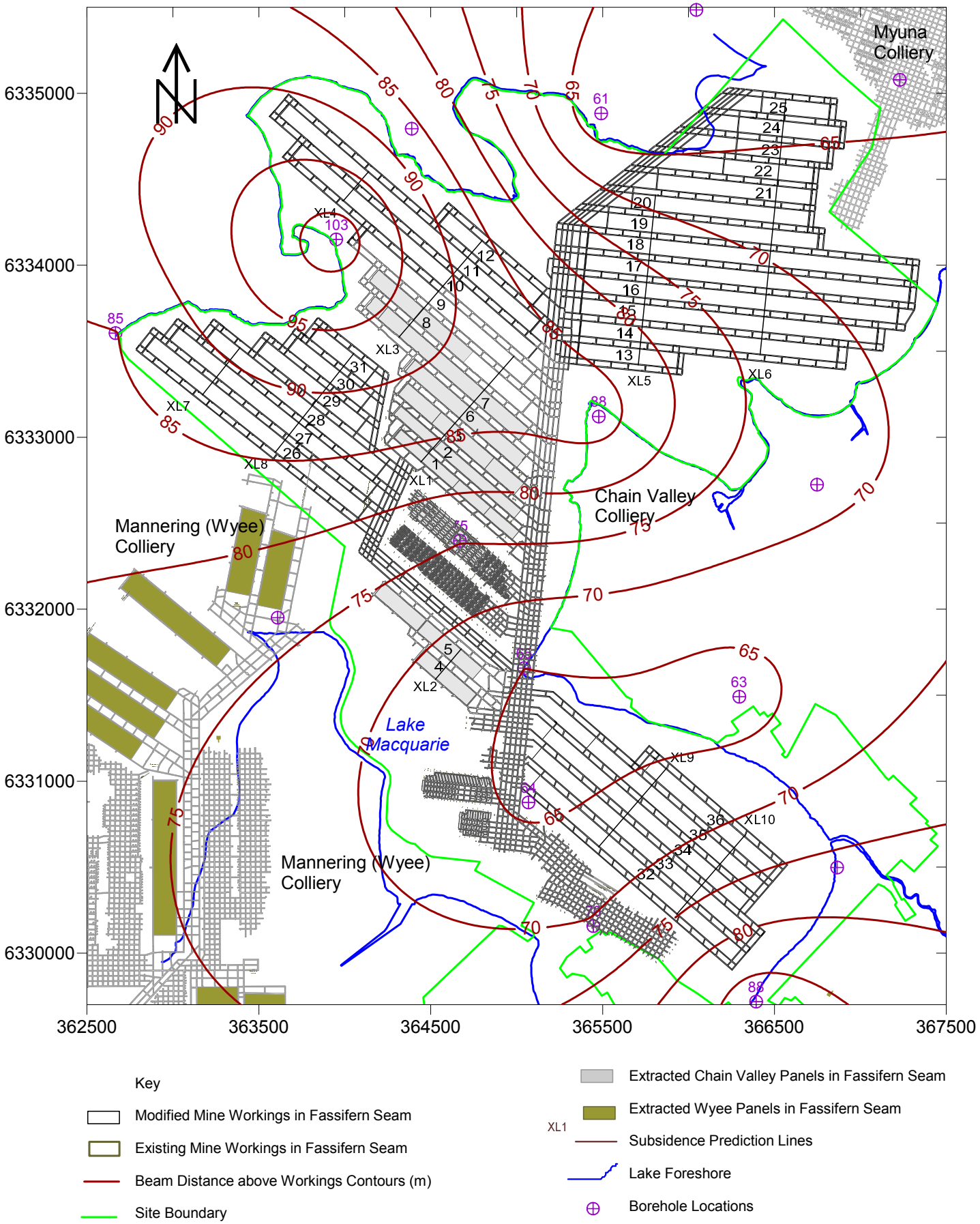
Figure No: 6.1



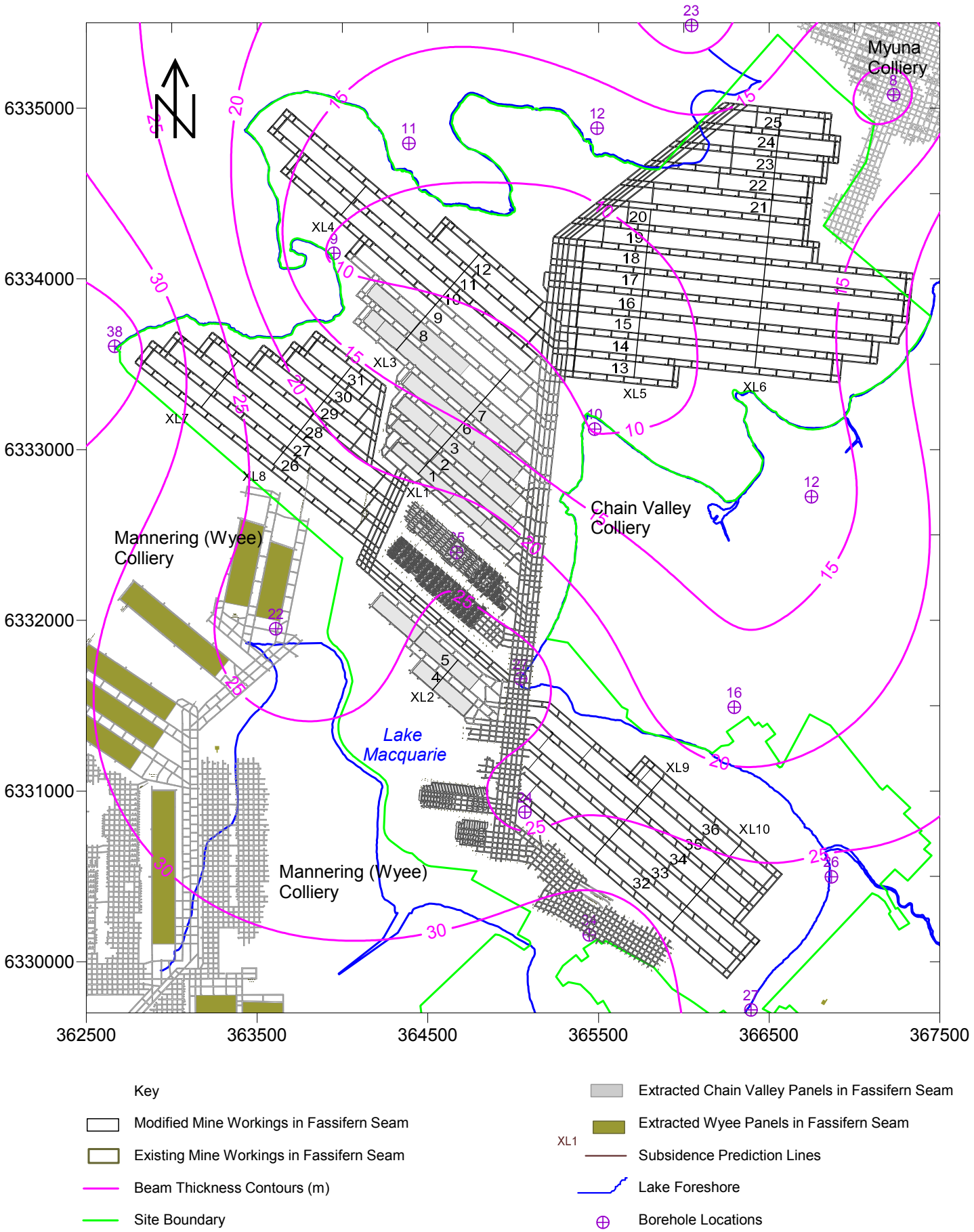
DgS	Engineer:	S.Ditton	Client:	LakeCoal - Chain Valley Colliery CHV-002/4	
	Drawn:	S.Ditton			
	Date:	20.03.15	Title:	Munmorah Conglomerate Lower Beam Distance Contours above the Modified Mine Layout for MWs 9 to 36	
	Ditton Geotechnical Services Pty Ltd		Scale:	1:12,000 (A4)	Figure No: 6.2



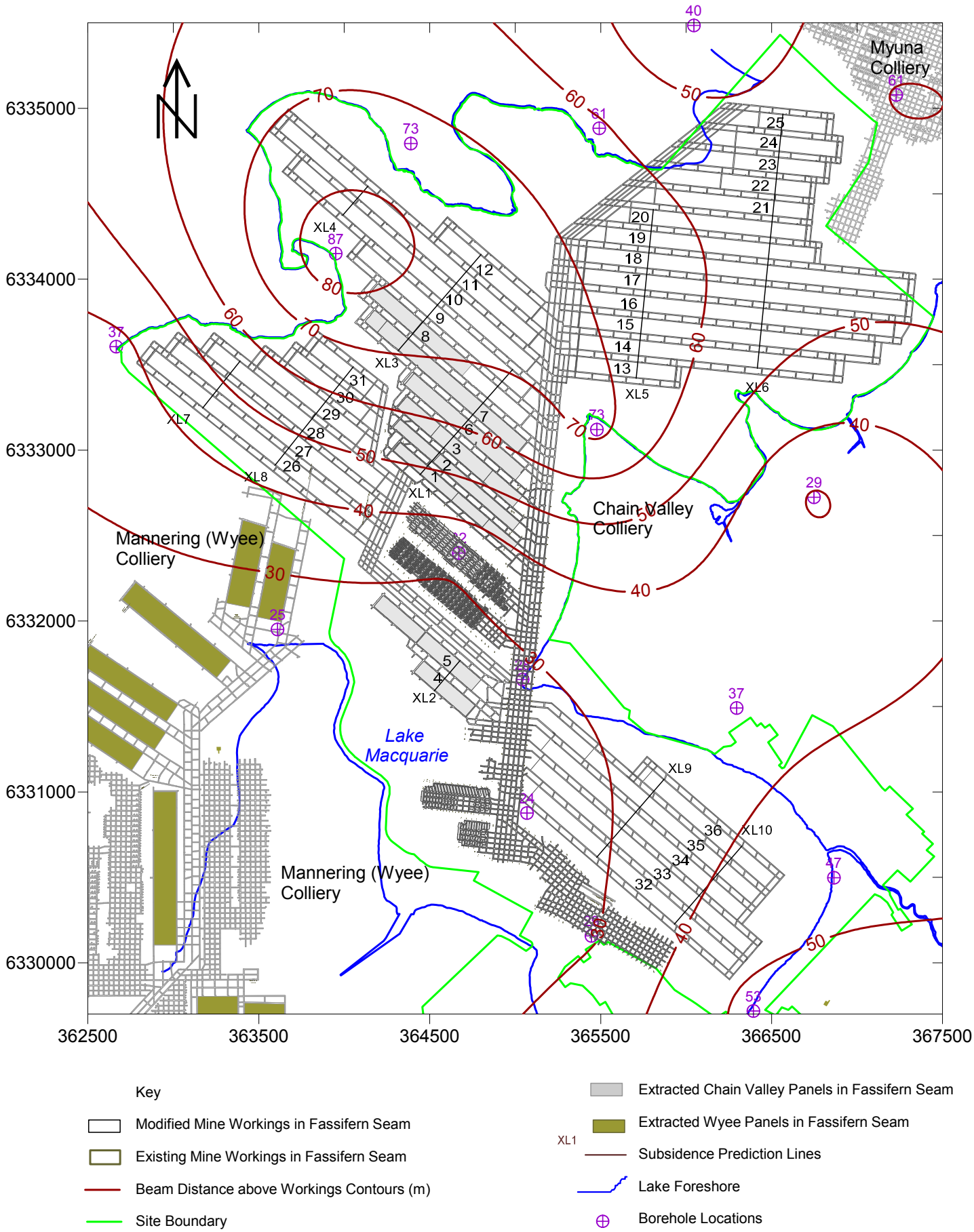
DgS	Engineer:	S.Ditton	Client:	LakeCoal - Chain Valley Colliery CHV-002/4	
	Drawn:	S.Ditton			
	Date:	20.03.15	Title:	Karignan Conglomerate Beam Thickness Contours above the Modified Mine Layout for MWs 9 to 36	
	Ditton Geotechnical Services Pty Ltd		Scale:	1:12,000 (A4)	Figure No: 7.1



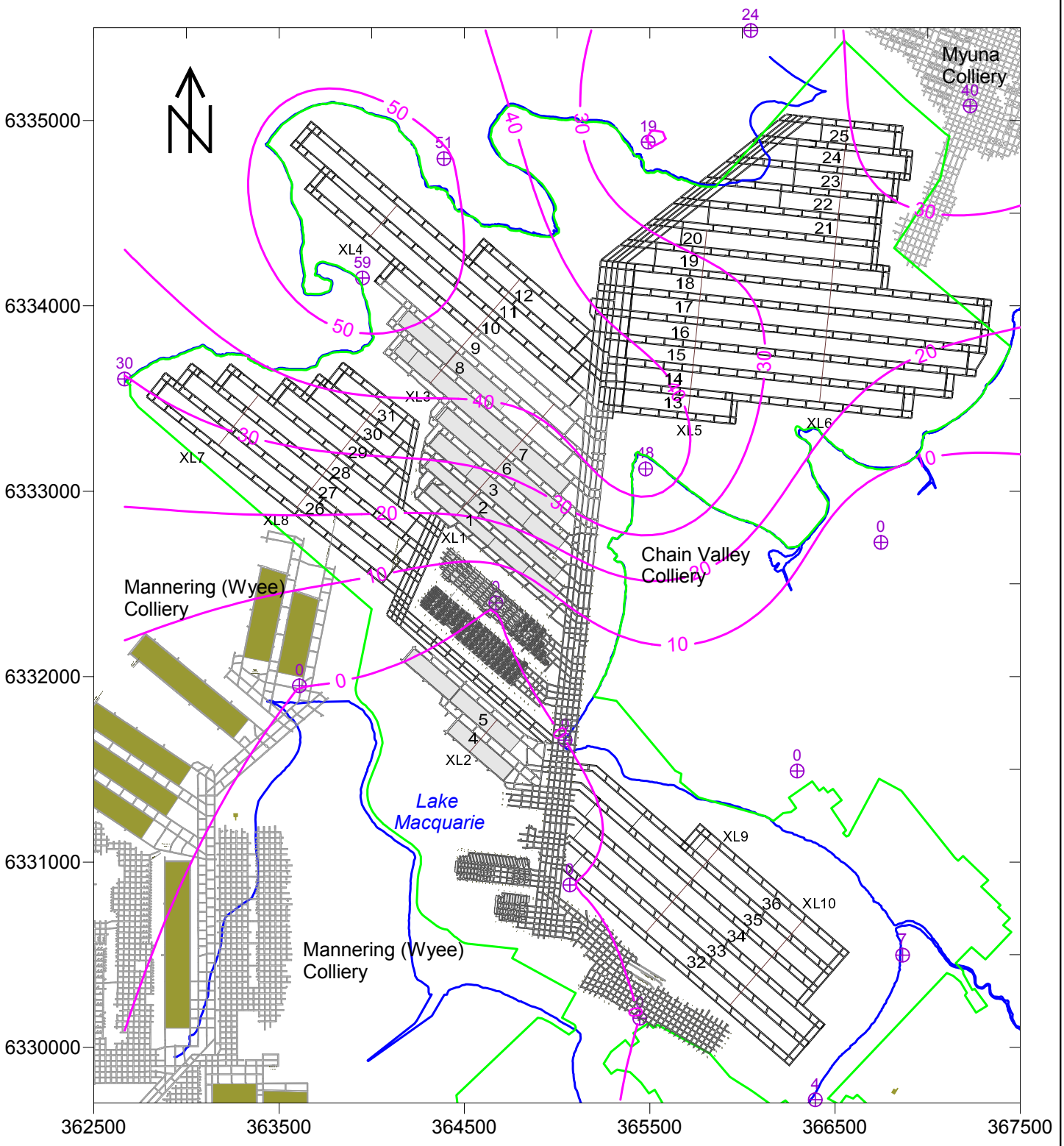
DgS	Engineer:	S.Ditton	Client:	LakeCoal - Chain Valley Colliery CHV-002/4	
	Drawn:	S.Ditton			
	Date:	20.03.15	Title:	Karignan Conglomerate Beam Distance Contours above the Modified Mine Layout for MWs 9 to 36	
Ditton Geotechnical Services Pty Ltd			Scale:	1:12,000 (A4)	Figure No: 7.2



DgS	Engineer:	S.Ditton	Client:	LakeCoal - Chain Valley Colliery CHV-002/4	
	Drawn:	S.Ditton			
	Date:	20.03.15	Title:	Teralba Conglomerate Beam Thickness Contours above the Modified Mine Layout for MWs 9 to 36	
Ditton Geotechnical Services Pty Ltd			Scale:	1:12,000 (A4)	Figure No: 8.1



DgS	Engineer:	S.Ditton	Client:	LakeCoal - Chain Valley Colliery CHV-002/4	
	Drawn:	S.Ditton			
	Date:	20.03.15	Title:	Teralba Conglomerate Beam Distance Contours above Modified Mine Layout MWs 9 to 36	
Ditton Geotechnical Services Pty Ltd			Scale:	1:12,000 (A4)	Figure No: 8.2



Key

- Modified Mine Workings in Fassifern Seam
- Existing Mine Workings in Fassifern Seam
- Beam Thickness Contours (m)
- Site Boundary
- Extracted Chain Valley Panels in Fassifern Seam
- Extracted Wyee Panels in Fassifern Seam
- XL1 Subsidence Prediction Lines
- Lake Foreshore
- Borehole Locations

DgS

Ditton Geotechnical Services Pty Ltd

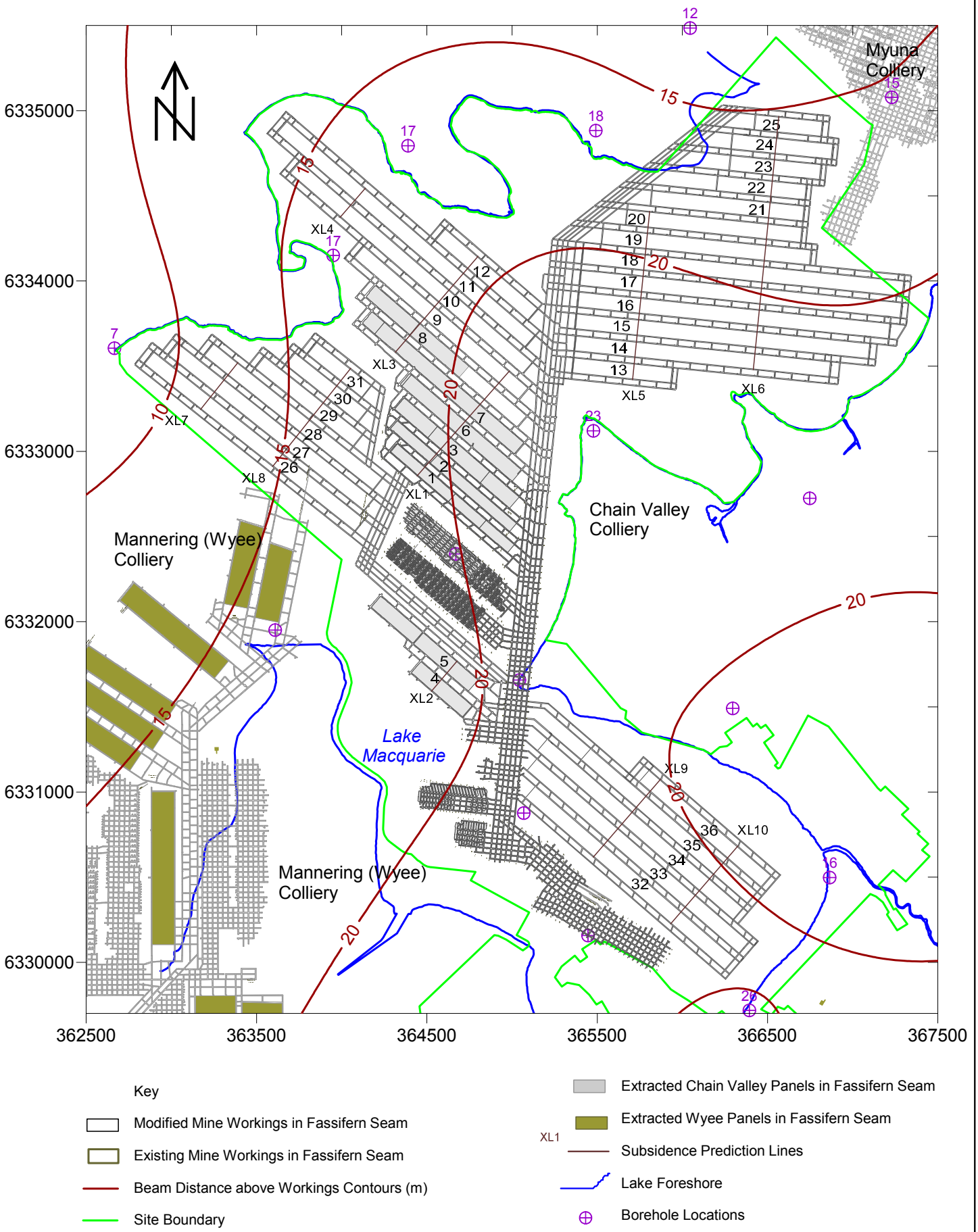
Engineer:	S.Ditton
Drawn:	S.Ditton
Date:	05.12.12

Client: LakeCoal - Chain Valley Colliery CHV-002/1

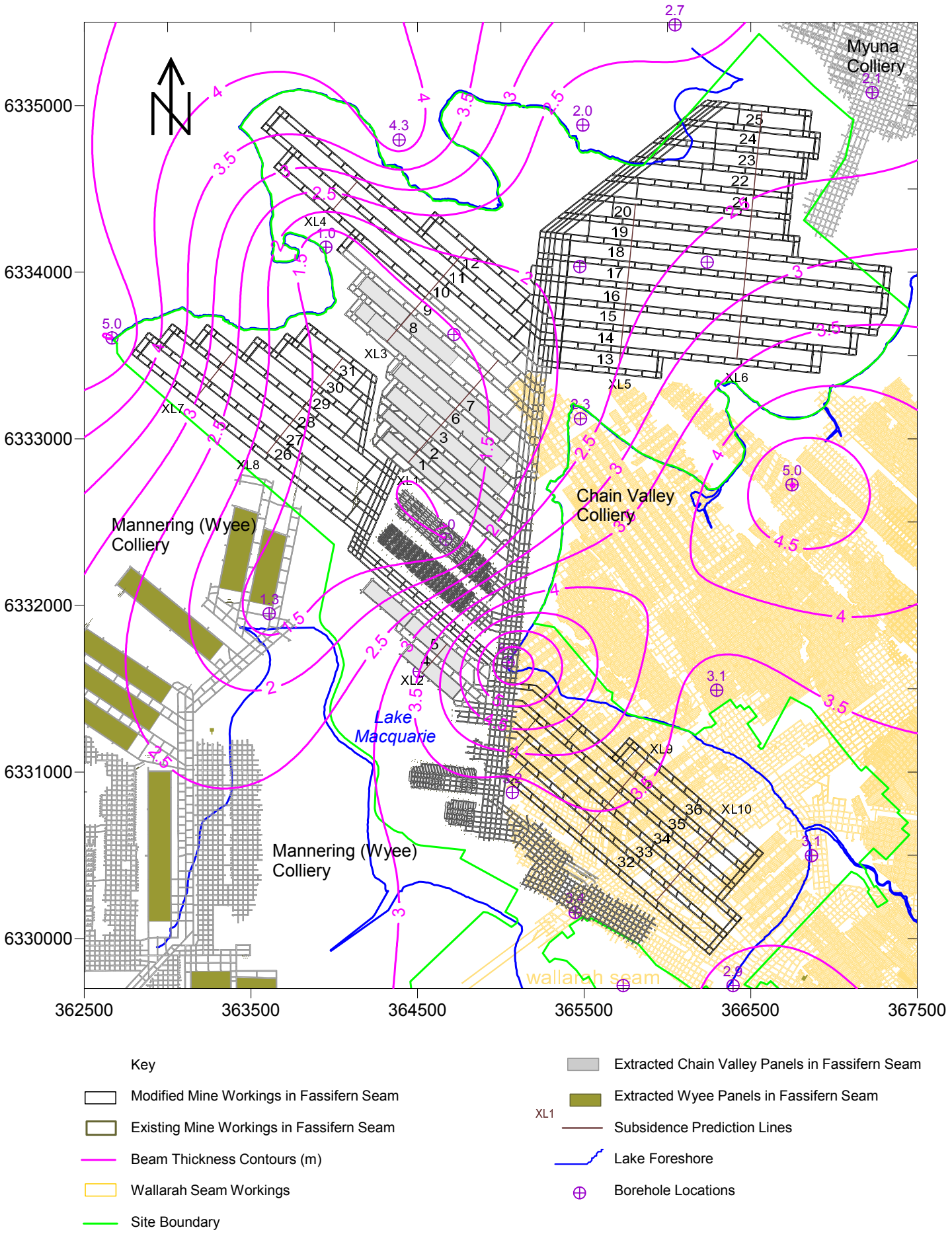
Title: Karingal Conglomerate Beam Thickness Contours above the Modified Mine Layout MWs 9 to 36

Scale: 1:12,000 (A4)

Figure No: 9.1



DgS	Engineer:	S.Ditton	Client:	LakeCoal - Chain Valley Colliery CHV-002/4	
	Drawn:	S.Ditton			
	Date:	20.03.15	Title:	Karingal Conglomerate Beam Distance Contours above Modified Mine Layout MWs 9 to 36	
Ditton Geotechnical Services Pty Ltd			Scale:	1:12,000 (A4)	Figure No: 9.2



Key

- Modified Mine Workings in Fassifern Seam
- Existing Mine Workings in Fassifern Seam
- Beam Thickness Contours (m)
- Wallarah Seam Workings
- Site Boundary
- Extracted Chain Valley Panels in Fassifern Seam
- Extracted Wyee Panels in Fassifern Seam
- XL1 Subsidence Prediction Lines
- Lake Foreshore
- Borehole Locations

DgS

Ditton Geotechnical Services Pty Ltd

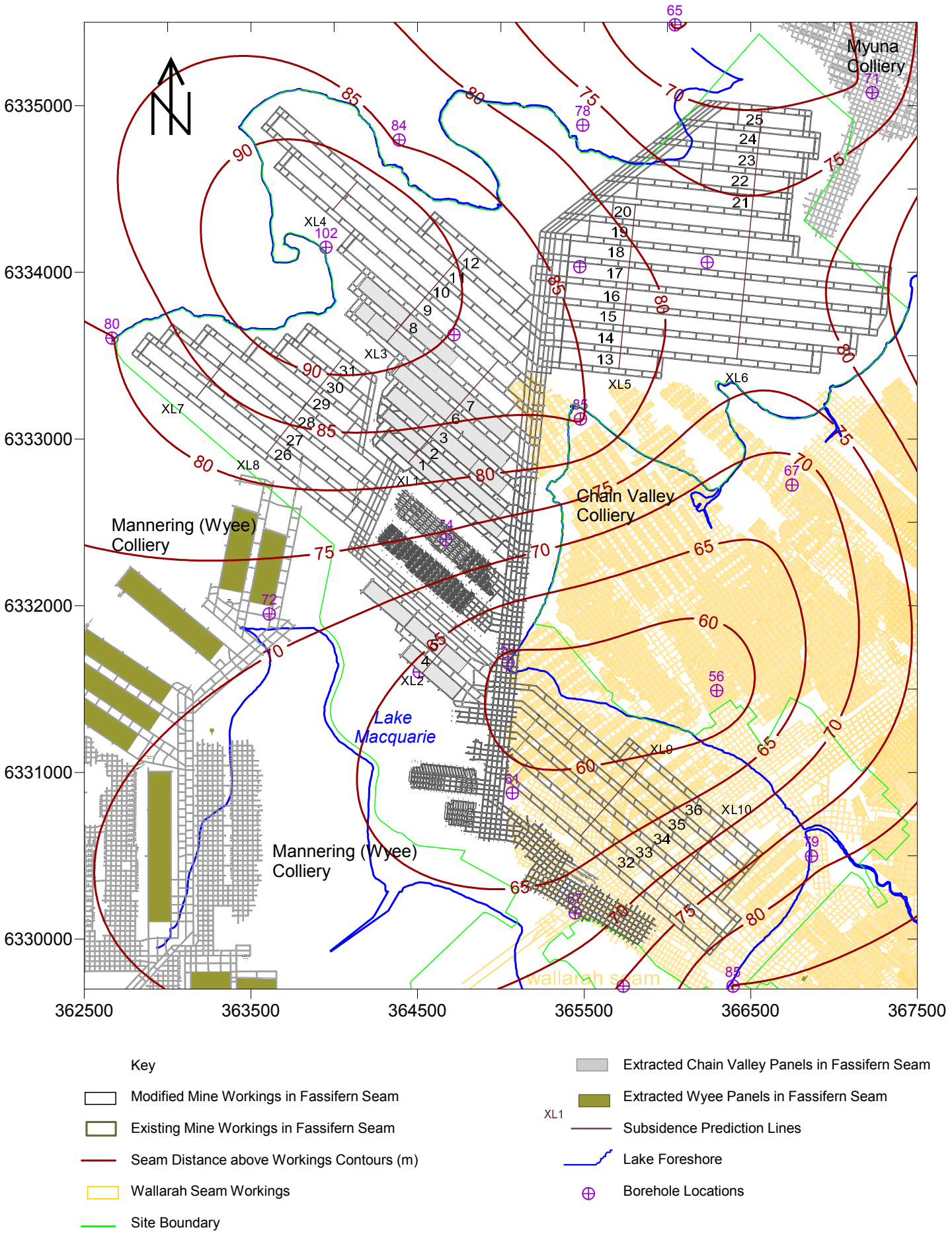
Engineer:	S.Ditton
Drawn:	S.Ditton
Date:	20.03.15

Client: LakeCoal - Chain Valley Colliery CHV-002/4

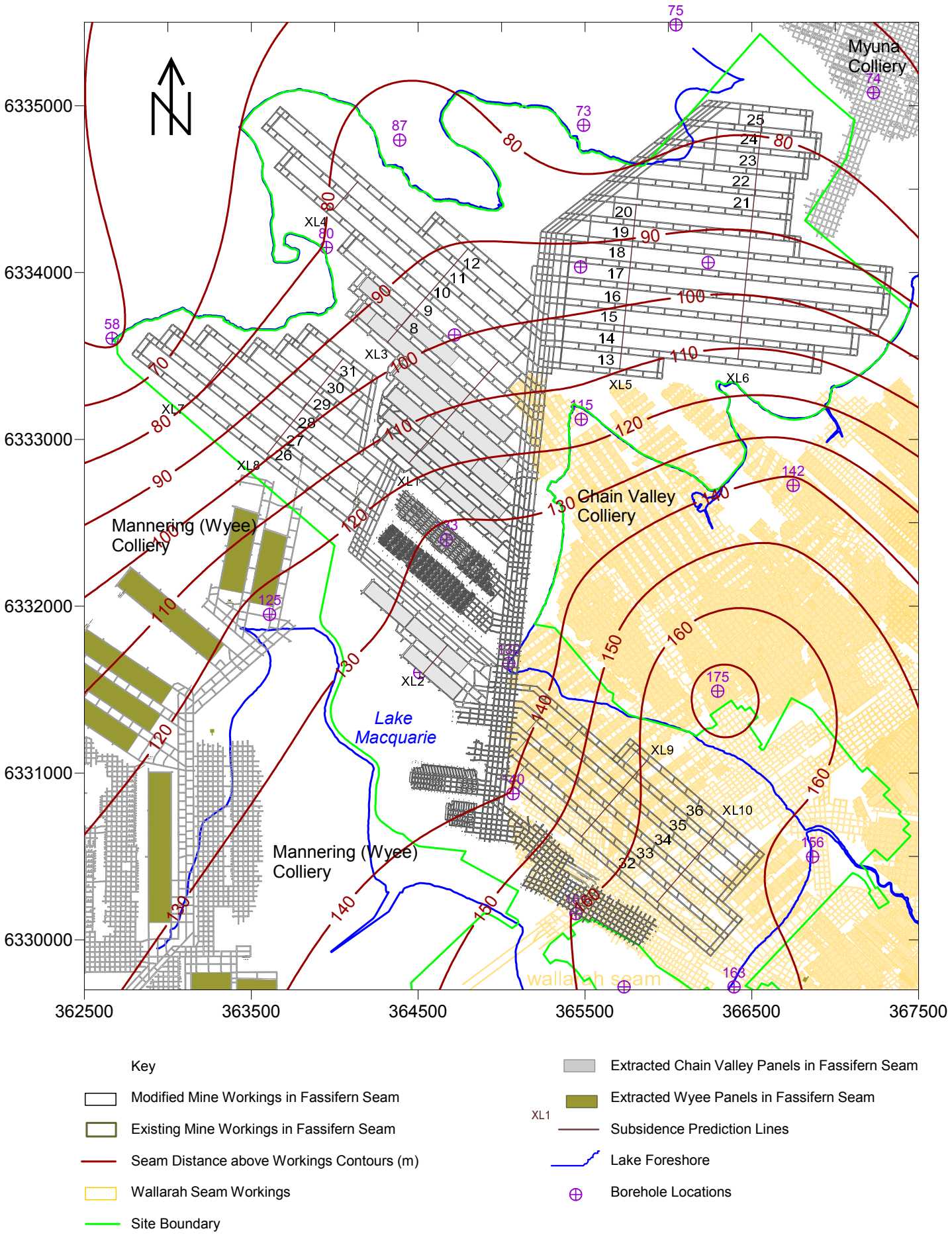
Title: Wallarah Seam Thickness Contours above the Modified Mine Layout for MWs 9 to 36

Scale: 1:12,000 (A4)

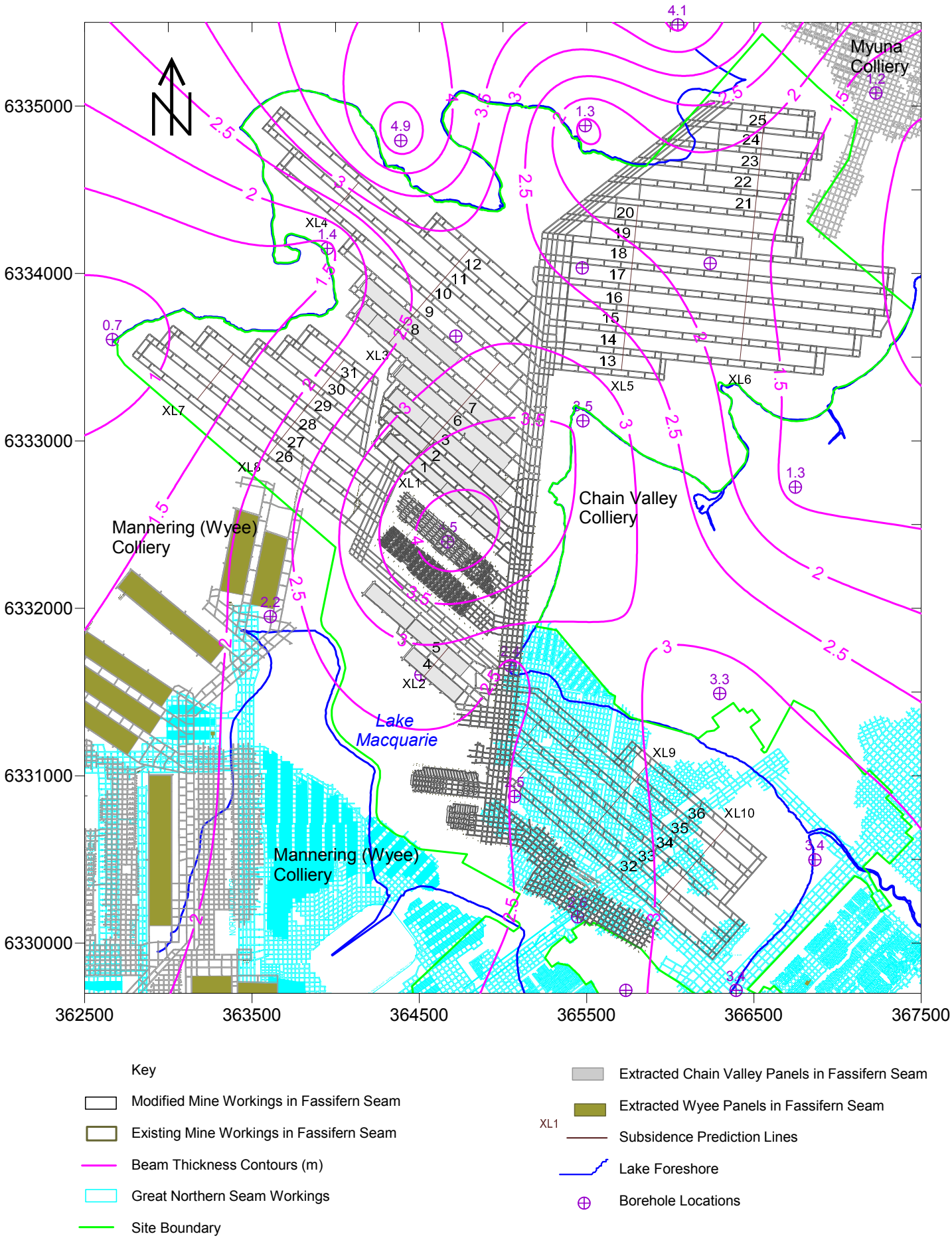
Figure No: 10.1



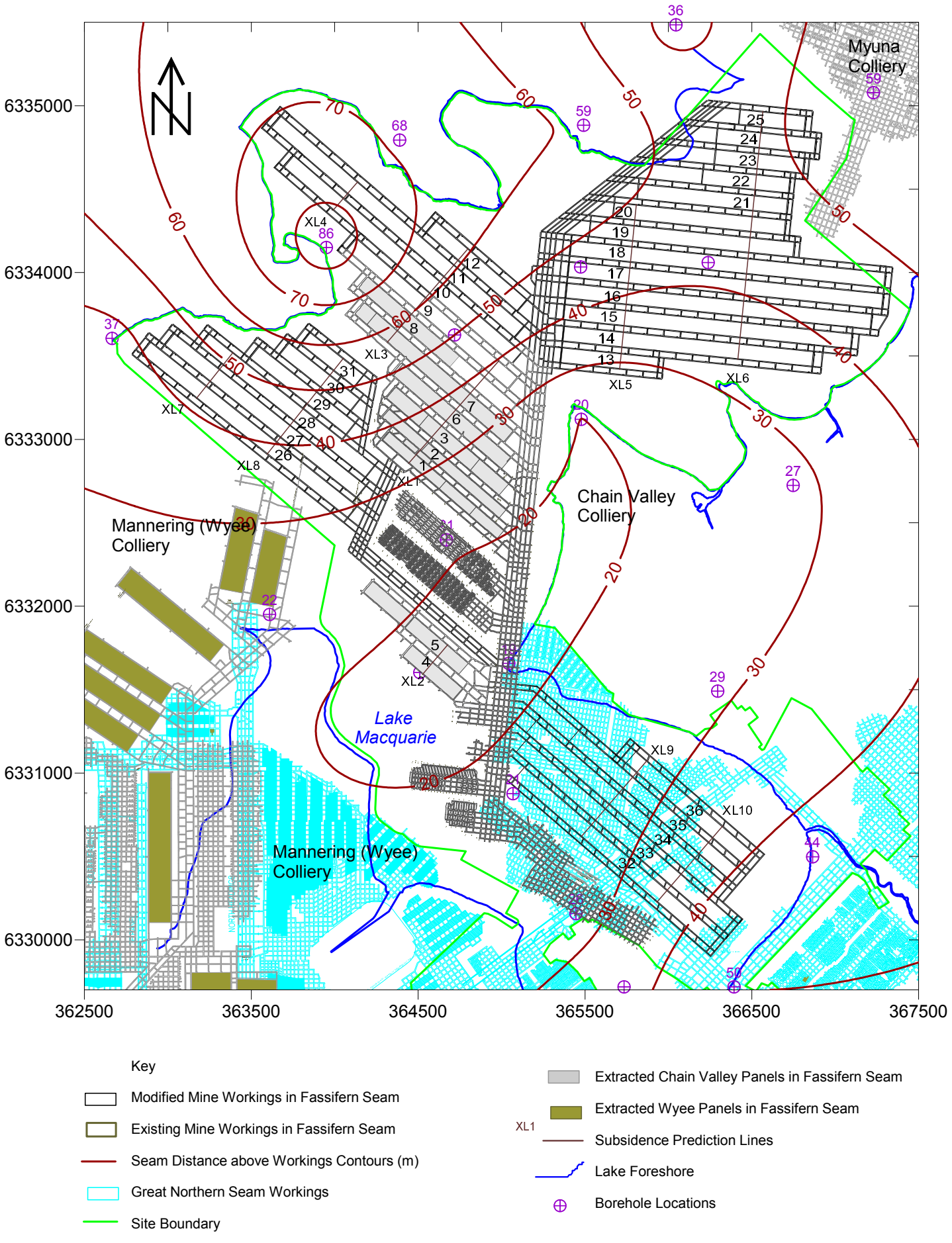
DgS	Engineer:	S.Ditton	Client:	LakeCoal - Chain Valley Colliery CHV-002/4	
	Drawn:	S.Ditton			
	Date:	20.03.15	Title:	Wallarah Seam Distance Contours above the Modified Mine Layout for MWS 9 to 36	
	Ditton Geotechnical Services Pty Ltd		Scale:	1:12,000 (A4)	Figure No: 10.2



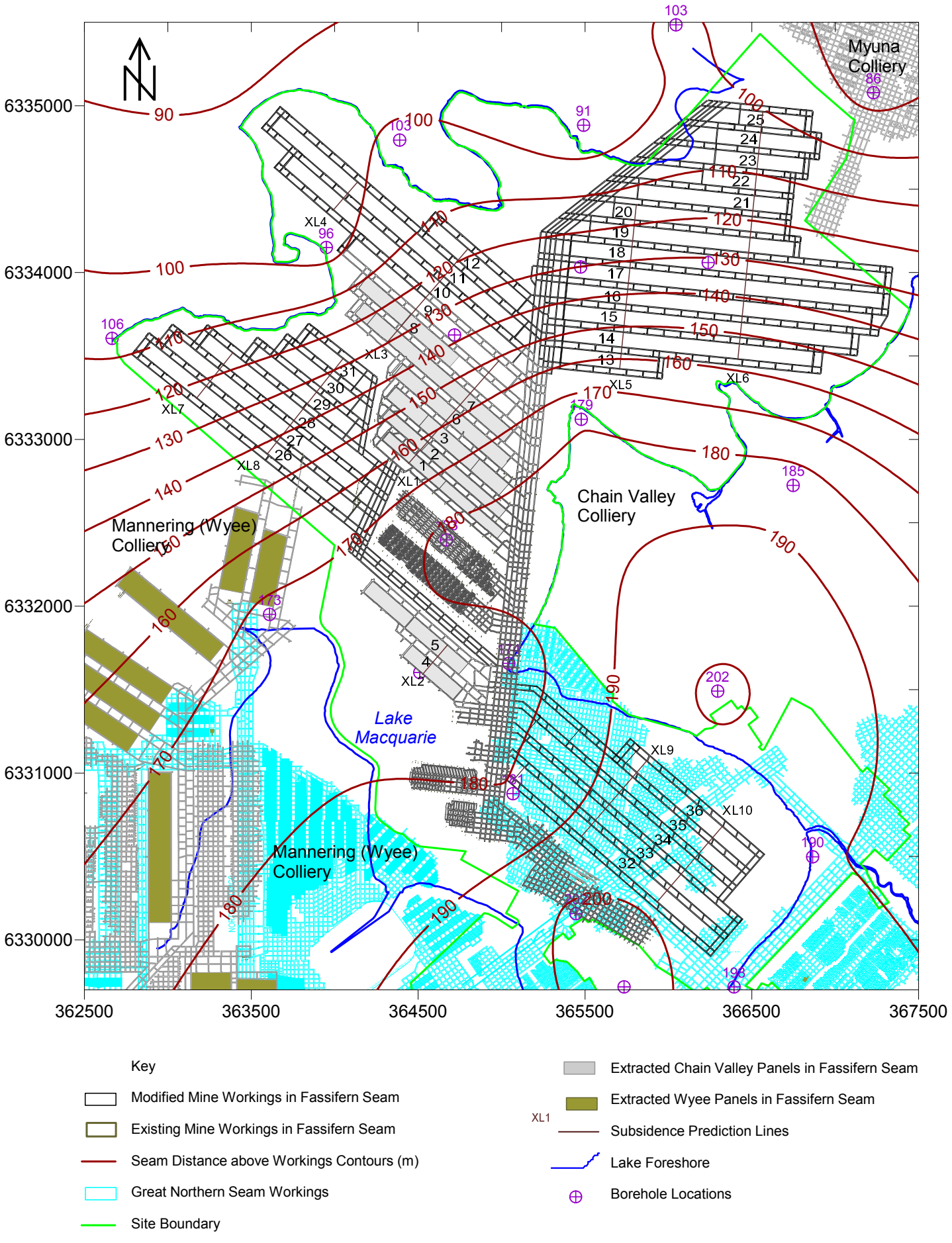
DgS	Engineer:	S.Ditton	Client:	LakeCoal - Chain Valley Colliery CHV-002/4	
	Drawn:	S.Ditton			
	Date:	20.03.15	Title:	Wallarah Seam Cover Depth Contours above the Modified Mine Layout for MWs 9 to 36	
Ditton Geotechnical Services Pty Ltd			Scale:	1:12,000 (A4)	Figure No: 10.3



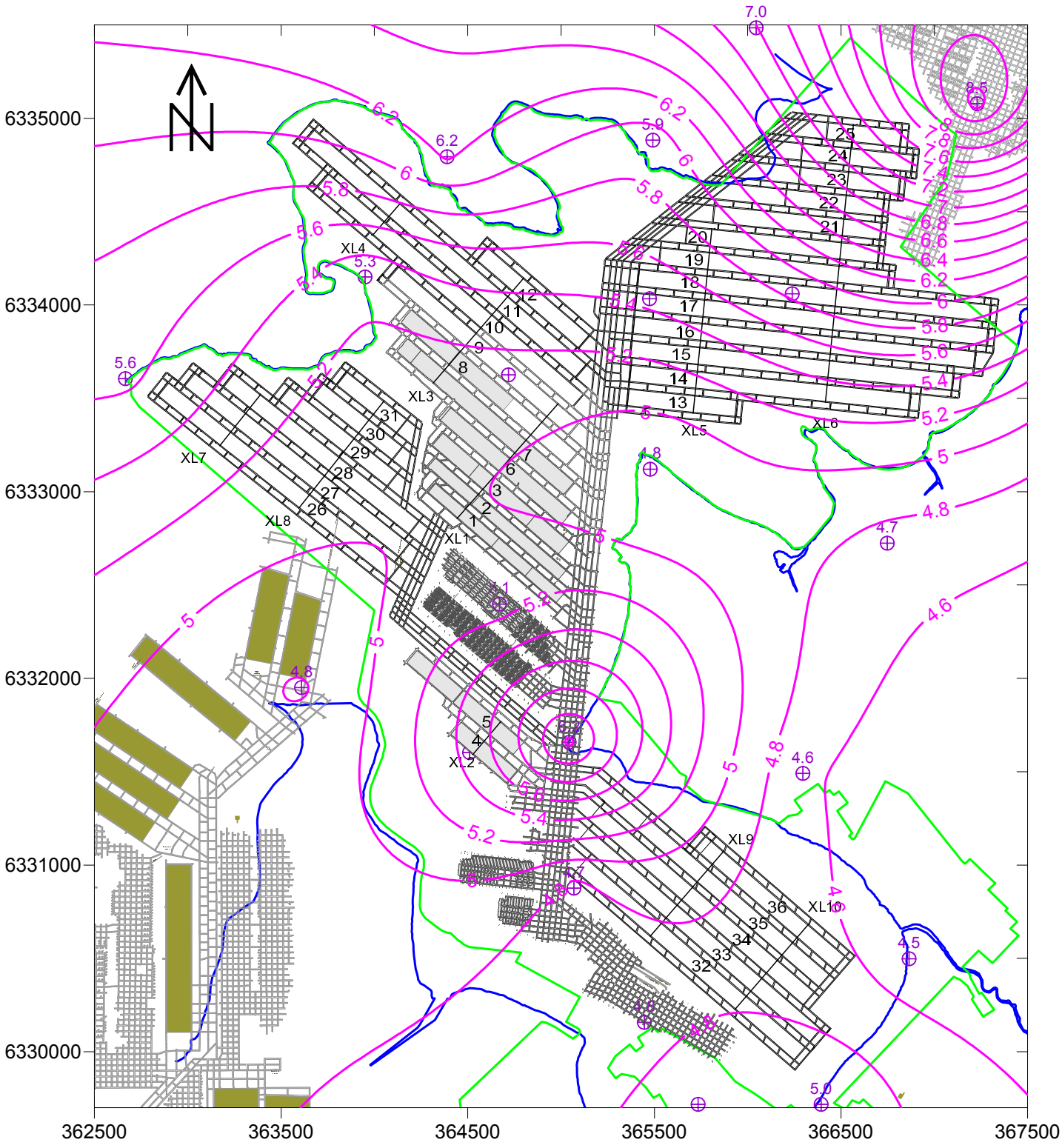
DgS	Engineer:	S.Ditton	Client:	LakeCoal - Chain Valley Colliery CHV-002/4	
	Drawn:	S.Ditton			
	Date:	20.03.15	Title:	Great Northern Seam Thickness Contours above the Modified Mine Layout for MWs 9 to 36	
	Ditton Geotechnical Services Pty Ltd		Scale:	1:12,000 (A4)	Figure No: 11.1



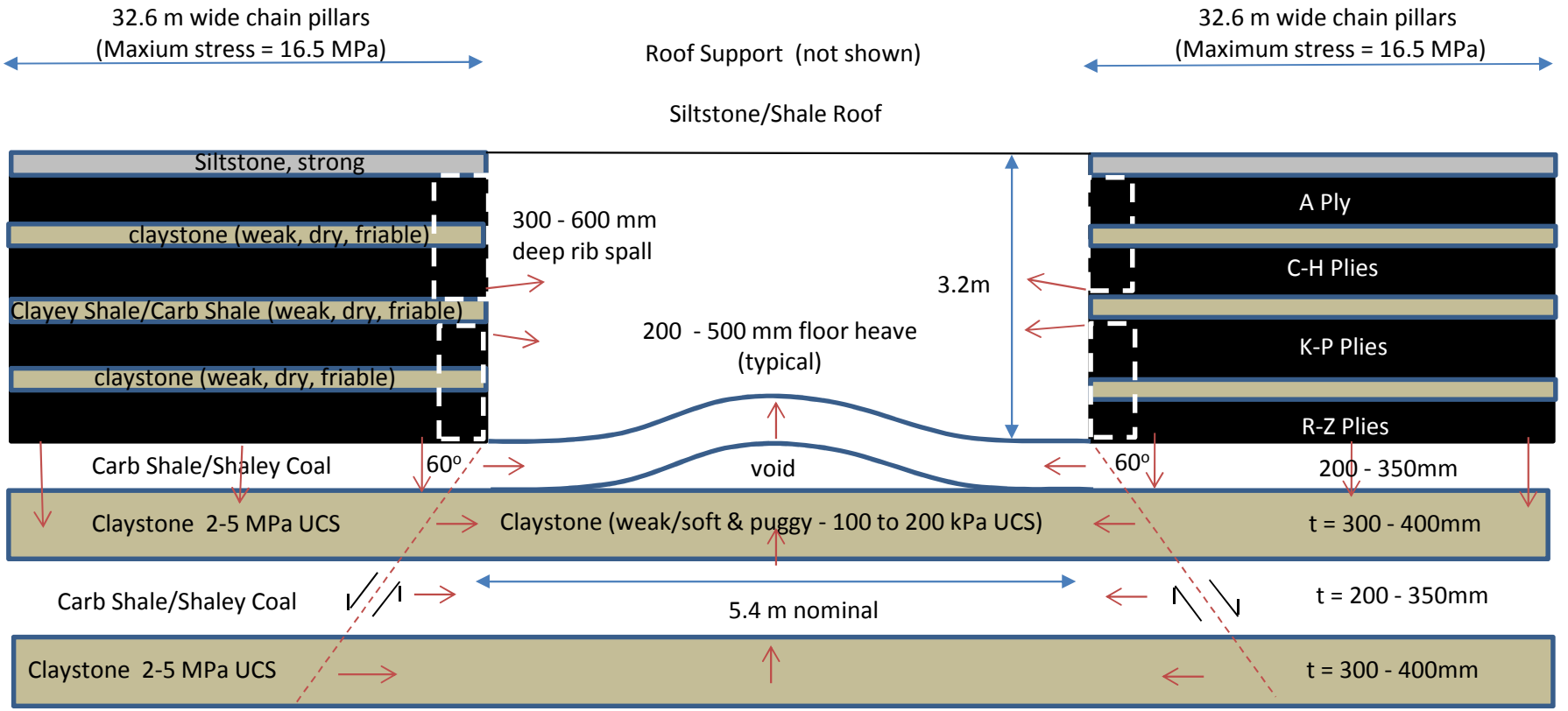
DgS	Engineer:	S.Ditton	Client:	LakeCoal - Chain Valley Colliery CHV-002/4	
	Drawn:	S.Ditton			
	Date:	20.03.15	Title:	Great Northern Seam Distance Contours above the Modified Mine Layout for MWs 9 to 36	
	Ditton Geotechnical Services Pty Ltd		Scale:	1:12,000 (A4)	Figure No: 11.2



DgS	Engineer:	S.Ditton	Client:	LakeCoal - Chain Valley Colliery CHV-002/4	
	Drawn:	S.Ditton			
	Date:	20.03.15	Title:	Great Northern Seam Cover Depth Contours above the Modified Mine Layout for MWs 9 to 36	
Ditton Geotechnical Services Pty Ltd			Scale:	1:12,000 (A4)	Figure No: 11.3



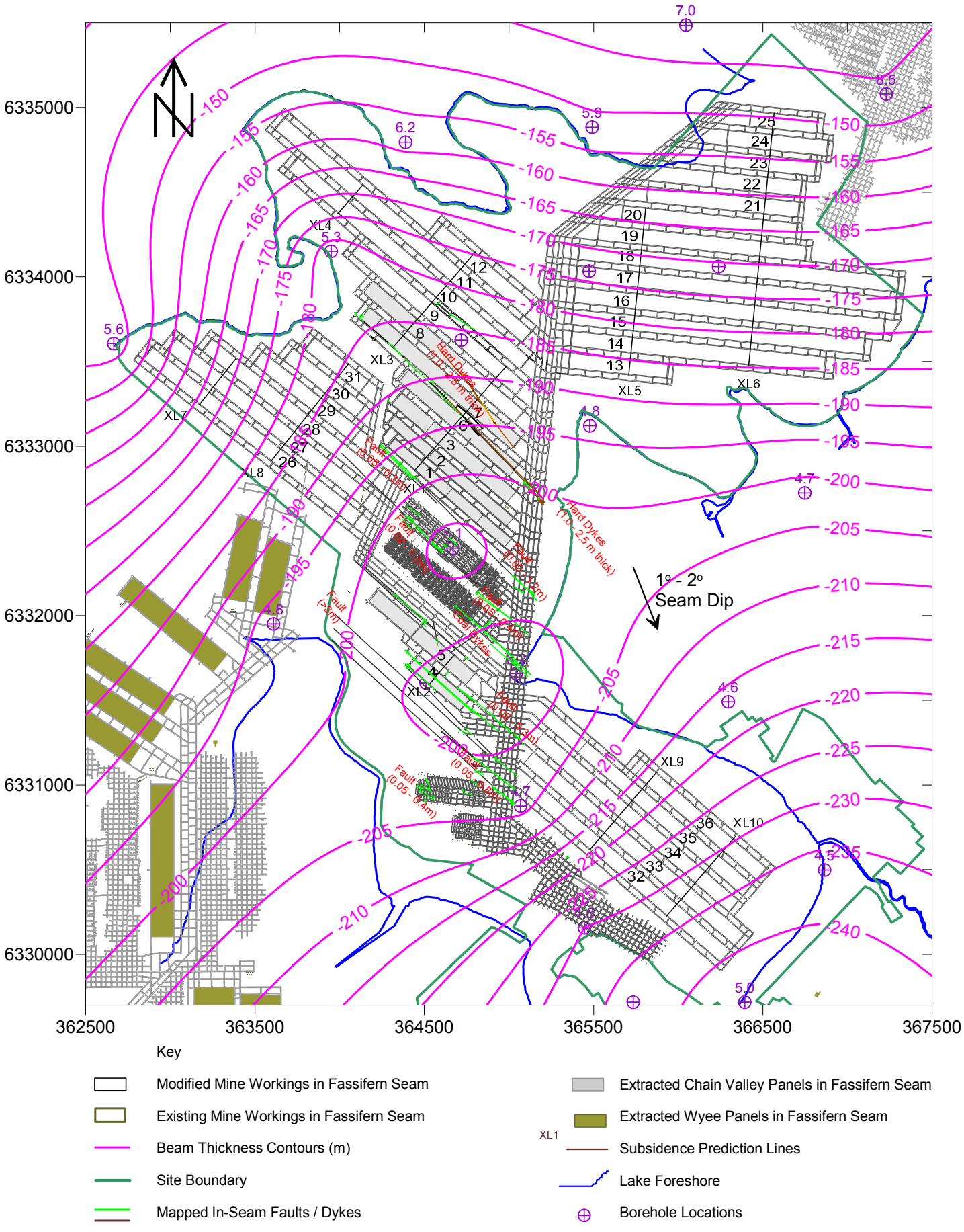
DgS	Engineer:	S.Ditton	Client:	LakeCoal - Chain Valley Colliery CHV-002/4	
	Drawn:	S.Ditton			
	Date:	20.03.15	Title:	Fassifern Seam Thickness Contours and the Modified Mine Layout for MWs 9 to 36	
	Ditton Geotechnical Services Pty Ltd		Scale:	1:12,000 (A4)	Figure No: 12.1



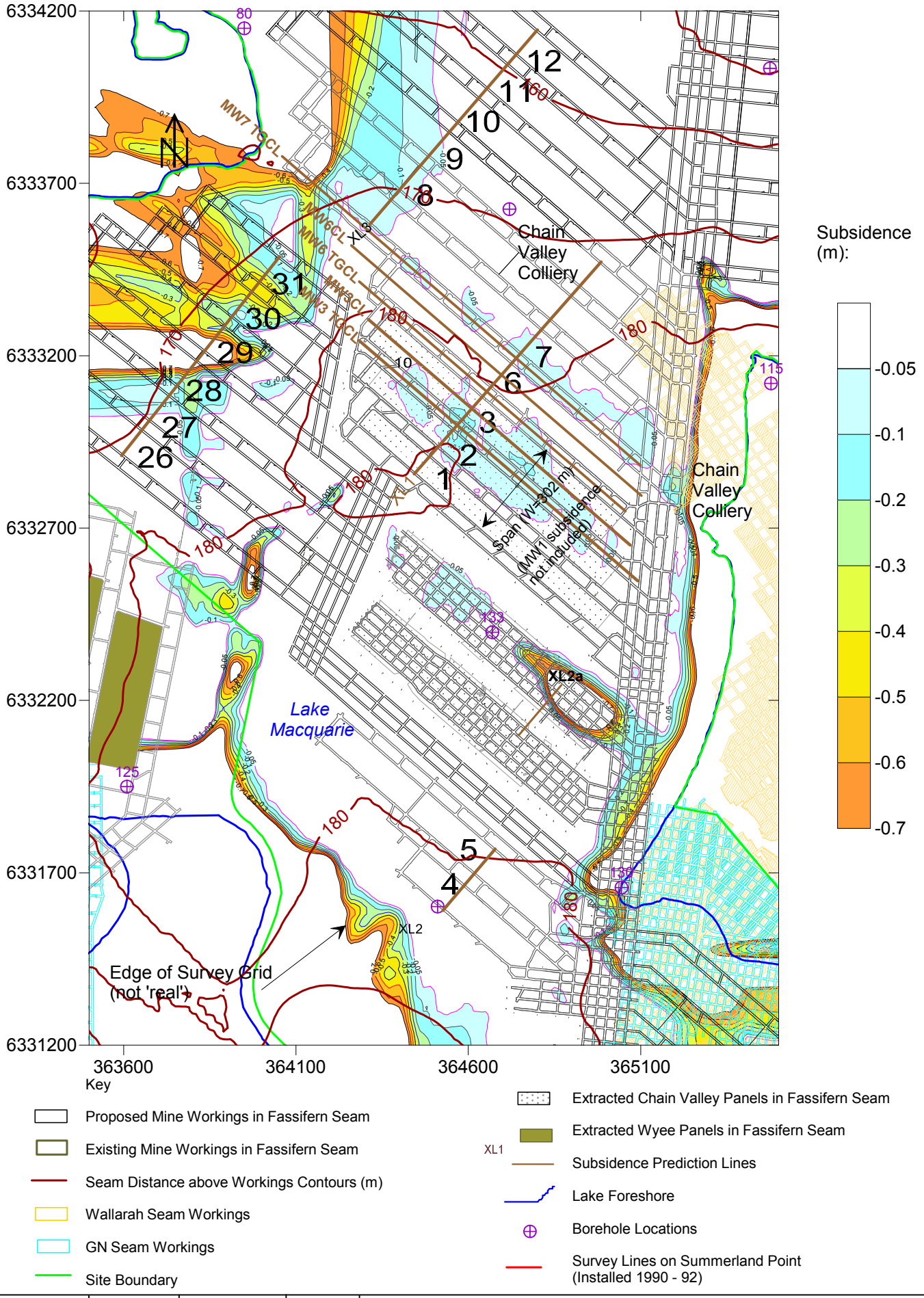
Notes: → Displacement vectors

1. Headings driven at 3.2 m height on development. MW face extraction height = 3.5 m.
2. Floor heave typically starts to occur after development and miniwall extraction due to softening of claystone when unconfined and exposed to humid mine air.
3. Moisture ingress likely to increase, causing further softening and swelling of claystone in headings and settlement of pillars.
4. Rib spall occurs due to lateral pillar and floor displacement/shear failures along mid-height pillar claystone bands.

DgS	Engineer:	S.Ditton	Client:	LakeCoal - Chain Valley Colliery CHV-002/4	
	Drawn:	S.Ditton			
	Date:	15.05.15	Title:	Typical Roadway Conditions that occur in FAS Mine Workings Floor due to Softening Claystone Units	
	Ditton Geotechnical Services Pty Ltd		Scale:	NTS	Figure No: 12.2



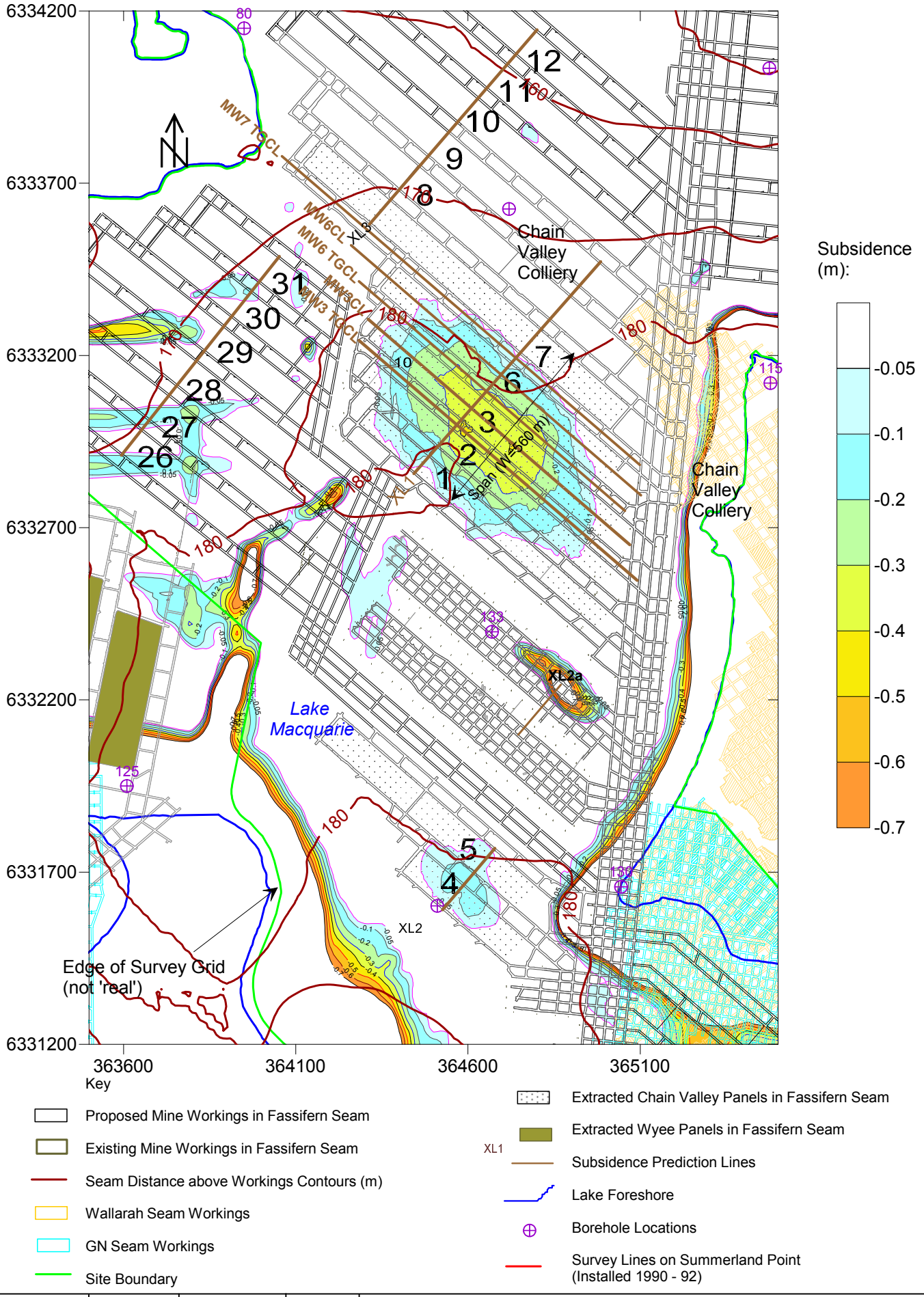
DgS	Engineer:	S.Ditton	Client:	LakeCoal - Chain Valley Colliery CHV-002/4	
	Drawn:	S.Ditton			
	Date:	20.03.15	Title:	Top of Fassifern Seam Level Contours and the Modified Mine Layout for MWs 9 to 36 with Mapped In-seam Geological Structure	
	Ditton Geotechnical Services Pty Ltd		Scale:	1:12,000 (A4)	Figure No: 12.3



Key

- Proposed Mine Workings in Fassifern Seam
- Existing Mine Workings in Fassifern Seam
- Seam Distance above Workings Contours (m)
- Wallarah Seam Workings
- GN Seam Workings
- Site Boundary
- Extracted Chain Valley Panels in Fassifern Seam
- Extracted Wyee Panels in Fassifern Seam
- XL1 Subsidence Prediction Lines
- Lake Foreshore
- Borehole Locations
- Survey Lines on Summerland Point (Installed 1990 - 92)

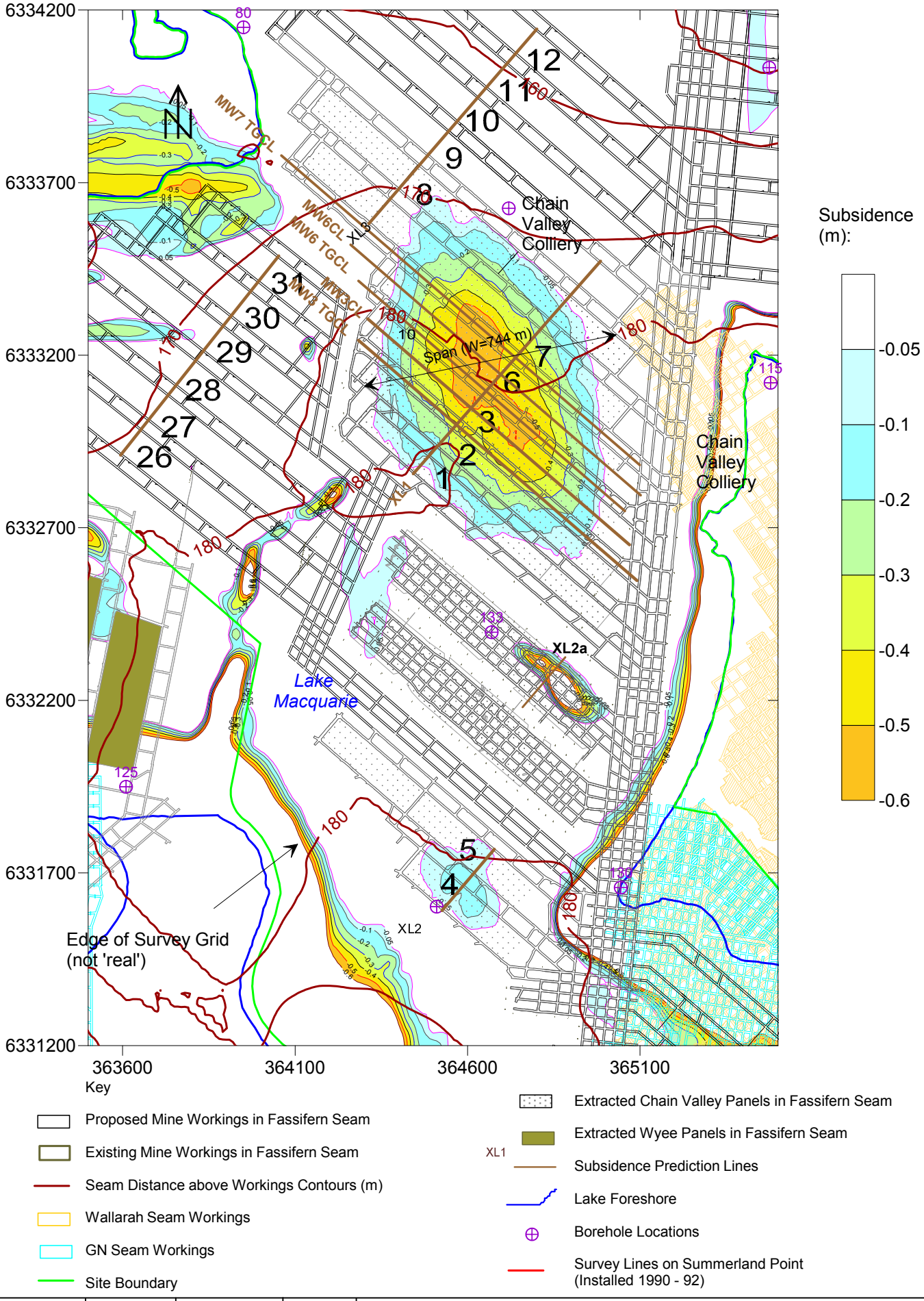
DgS	Engineer:	S.Ditton	Client:	LakeCoal - Chain Valley Colliery CHV-002/4	
	Drawn:	S.Ditton			
	Date:	20.03.15	Title:	Measured Bathymetric Subsidence above MWs 1 to 3 in the Fassifern Seam at Chain Valley Colliery (Survey Date: 01/06/13)	
Ditton Geotechnical Services Pty Ltd			Scale:	1:1,500 (A4)	Figure No: 13.1



DgS

Ditton Geotechnical Services Pty Ltd

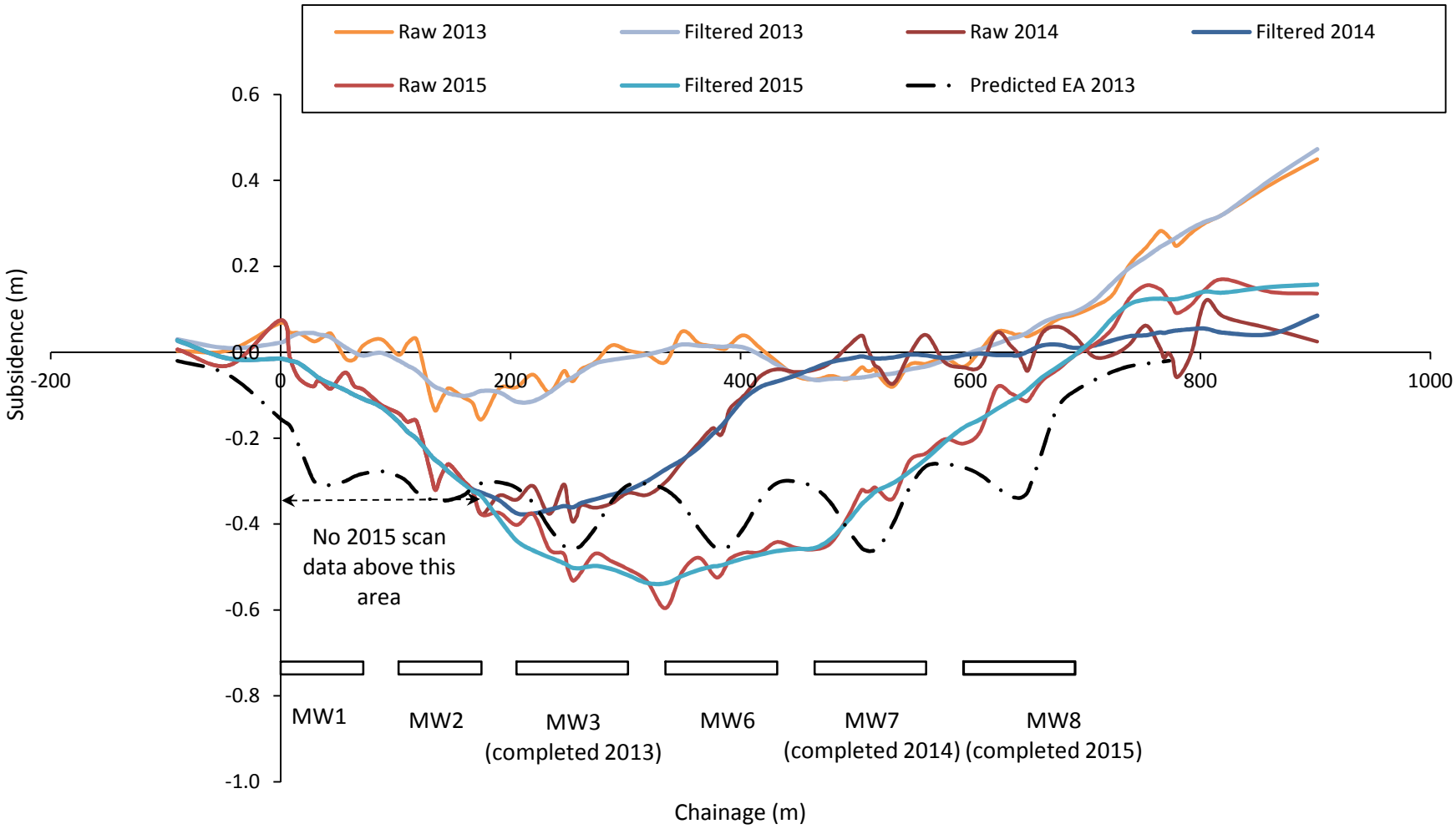
Engineer:	S.Ditton	Client:	LakeCoal - Chain Valley Colliery CHV-002/4		
Drawn:	S.Ditton				
Date:	20.03.15	Title:	Measured Bathymetric Subsidence above MWs 1 to 7 in the Fassifern Seam at Chain Valley Colliery (Survey Date: 01/06/14)		
		Scale:	1:1,500 (A4)	Figure No:	13.2



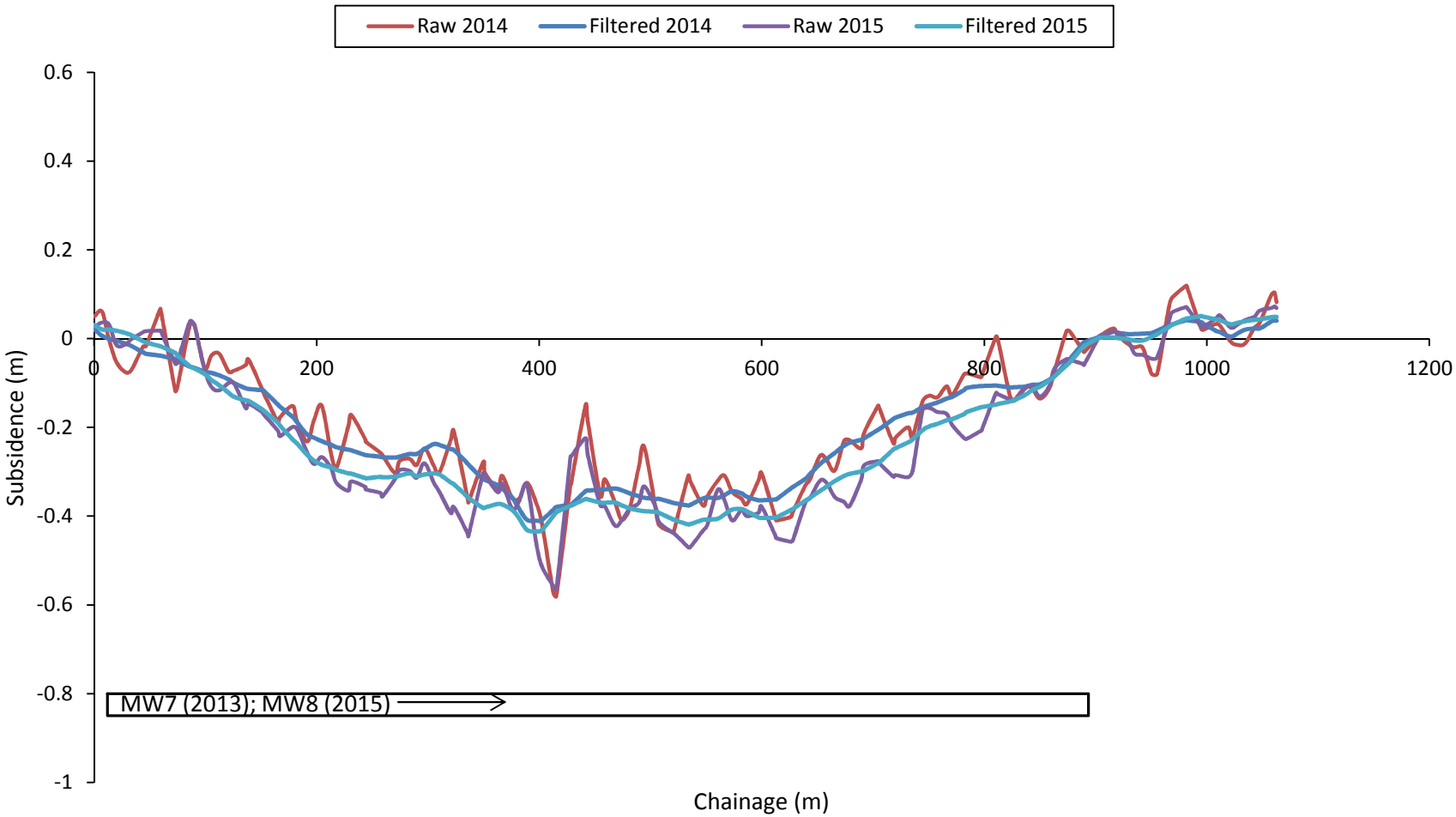
Key

- Proposed Mine Workings in Fassifern Seam
- Existing Mine Workings in Fassifern Seam
- Seam Distance above Workings Contours (m)
- Wallarah Seam Workings
- GN Seam Workings
- Site Boundary
- Extracted Chain Valley Panels in Fassifern Seam
- Extracted Wyee Panels in Fassifern Seam
- Subsidence Prediction Lines
- Lake Foreshore
- Borehole Locations
- Survey Lines on Summerland Point (Installed 1990 - 92)

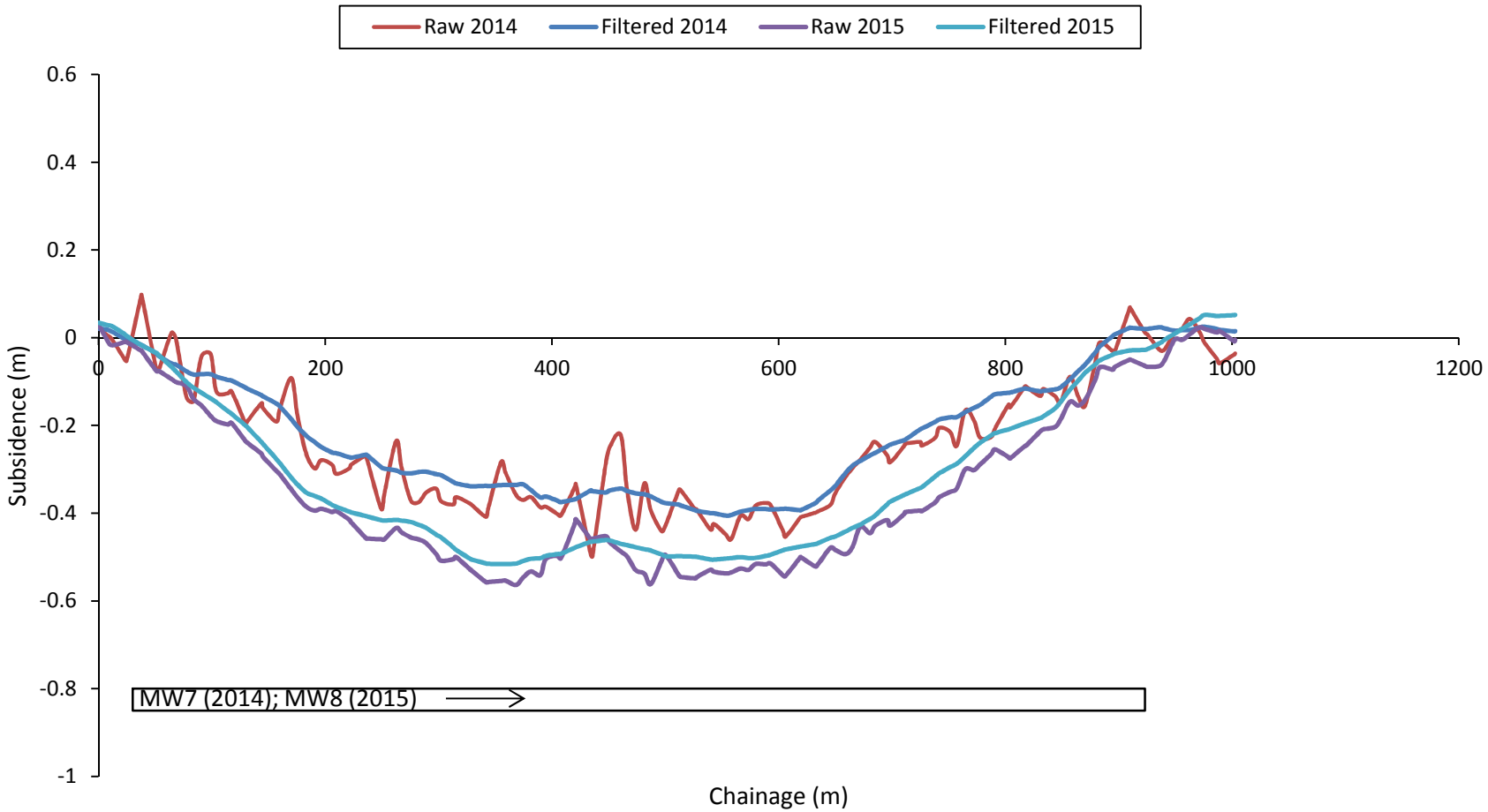
DgS	Engineer:	S.Ditton	Client:	LakeCoal - Chain Valley Colliery CHV-002/4	
	Drawn:	S.Ditton			
	Date:	20.03.15	Title:	Measured Bathymetric Subsidence above MWs 1 to 8 in the Fassifern Seam at Chain Valley Colliery (Survey Date: 01/05/15)	
Ditton Geotechnical Services Pty Ltd			Scale:	1:1,500 (A4)	Figure No: 13.3



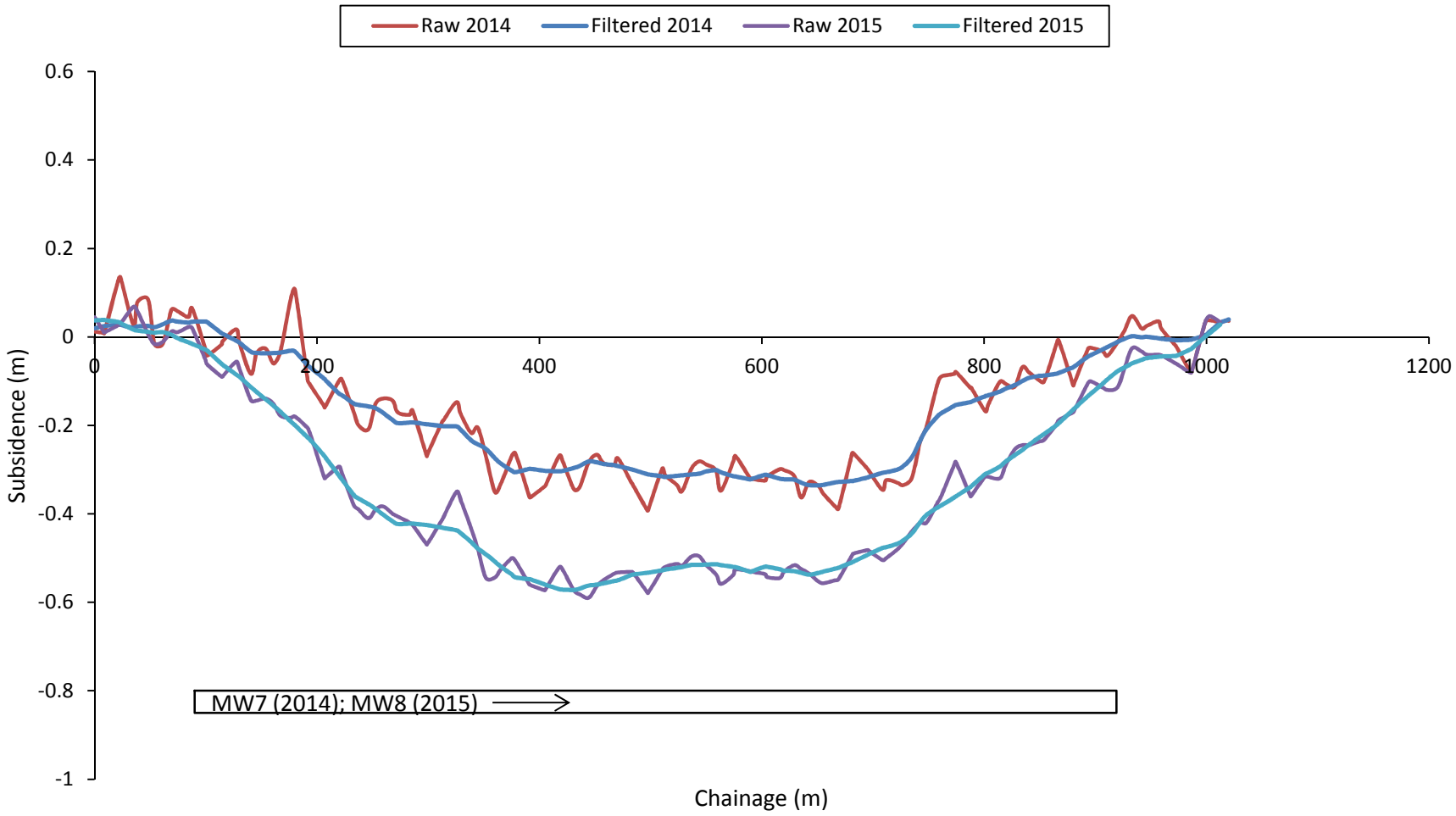
DgS	Engineer:	S.Ditton	Client:	LakeCoal - Chain Valley Colliery CHV-002/4	
	Drawn:	S.Ditton			
	Date:	15.05.15	Title:	Measured Subsidence Along XL1 (based on Bathymetric Surveys) with Predicted EA, 2013 Report Profile (see prediction line location in Figures 13.1-13.3)	
	Ditton Geotechnical Services Pty Ltd		Scale:	NTS	Figure No: 13.4



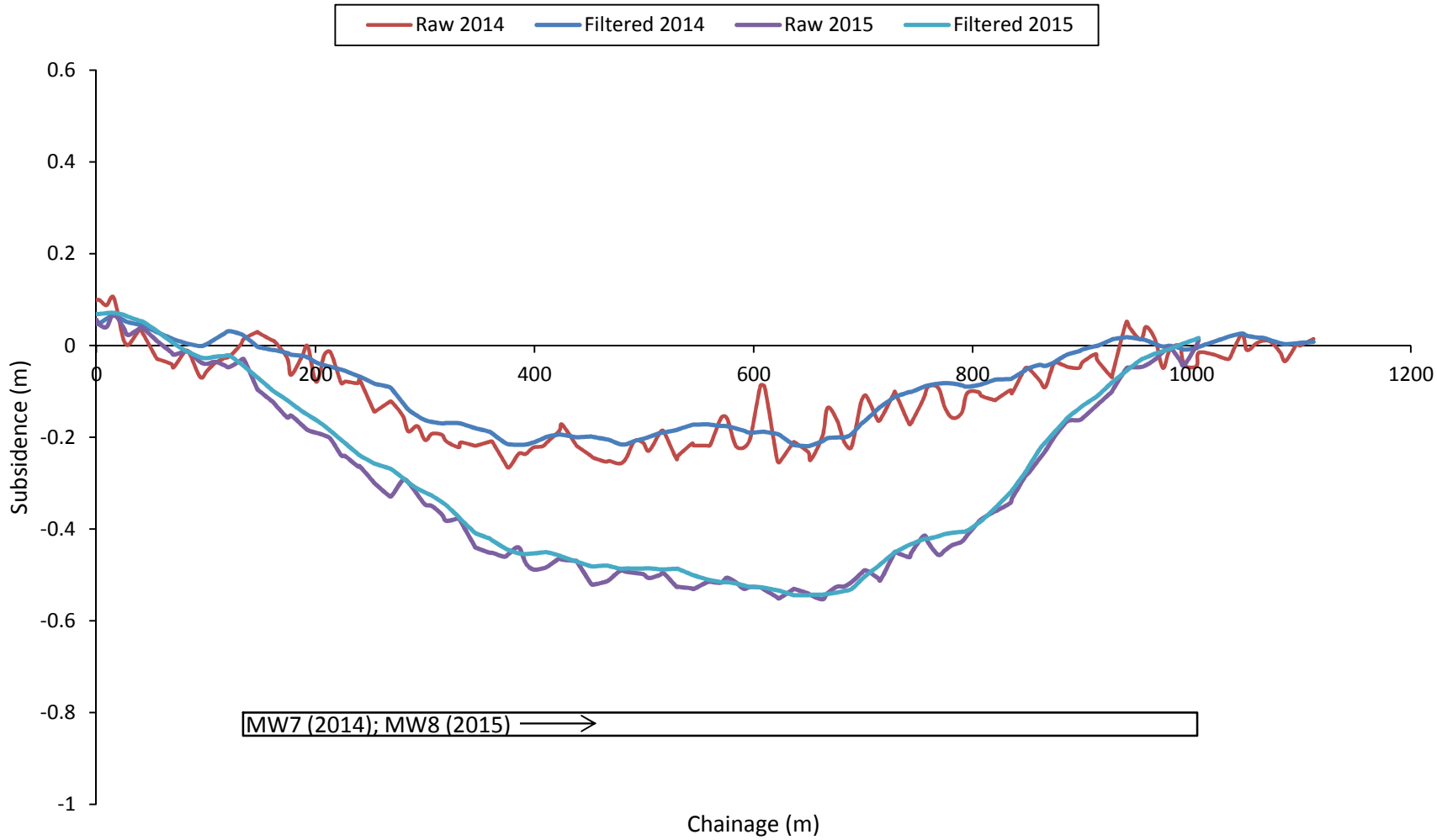
DgS	Engineer:	S.Ditton	Client:	LakeCoal - Chain Valley Colliery CHV-002/4	
	Drawn:	S.Ditton			
	Date:	15.05.15	Title:	Measured Subsidence Along MW3 Tailgate Chain Pillars (based on Bathymetric Surveys) (see Figures 13.1-13.3 for Location)	
	Ditton Geotechnical Services Pty Ltd		Scale:	NTS	Figure No: 13.5



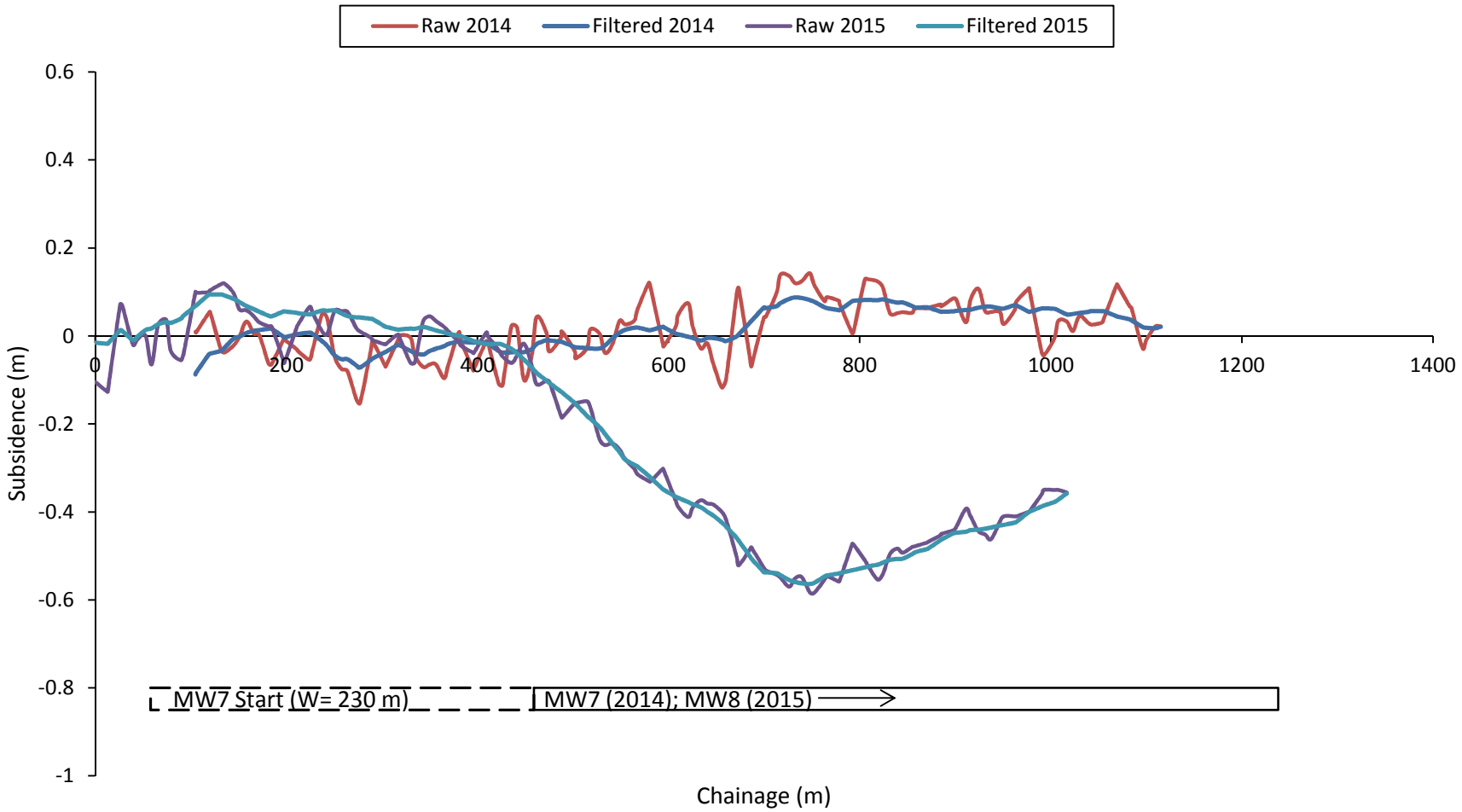
DgS	Engineer:	S.Ditton	Client:	LakeCoal - Chain Valley Colliery CHV-002/4	
	Drawn:	S.Ditton			
	Date:	15.05.15	Title:	Measured Subsidence Along MW3 Panel Centreline (based on Bathymetric Surveys) (see Figures 13.1-13.3 for Location)	
	Ditton Geotechnical Services Pty Ltd		Scale:	NTS	Figure No: 13.6



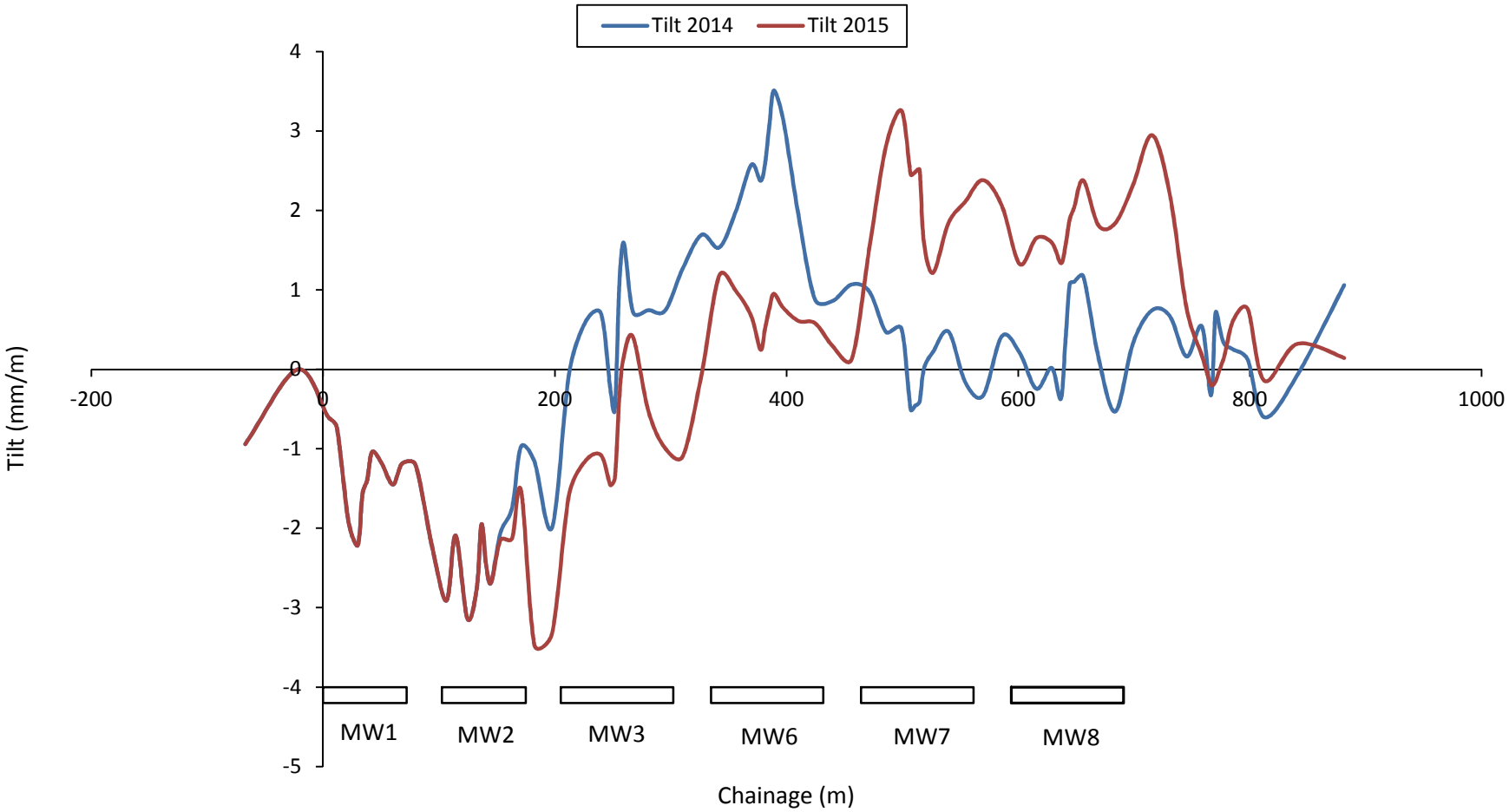
DgS	Engineer:	S.Ditton	Client:	LakeCoal - Chain Valley Colliery CHV-002/4	
	Drawn:	S.Ditton			
	Date:	15.05.15	Title:	Measured Subsidence Along MW6 Tailgate Chain Pillars (based on Bathymetric Surveys) (see Figures 13.1-13.3 for Location)	
	Ditton Geotechnical Services Pty Ltd		Scale:	NTS	Figure No: 13.7



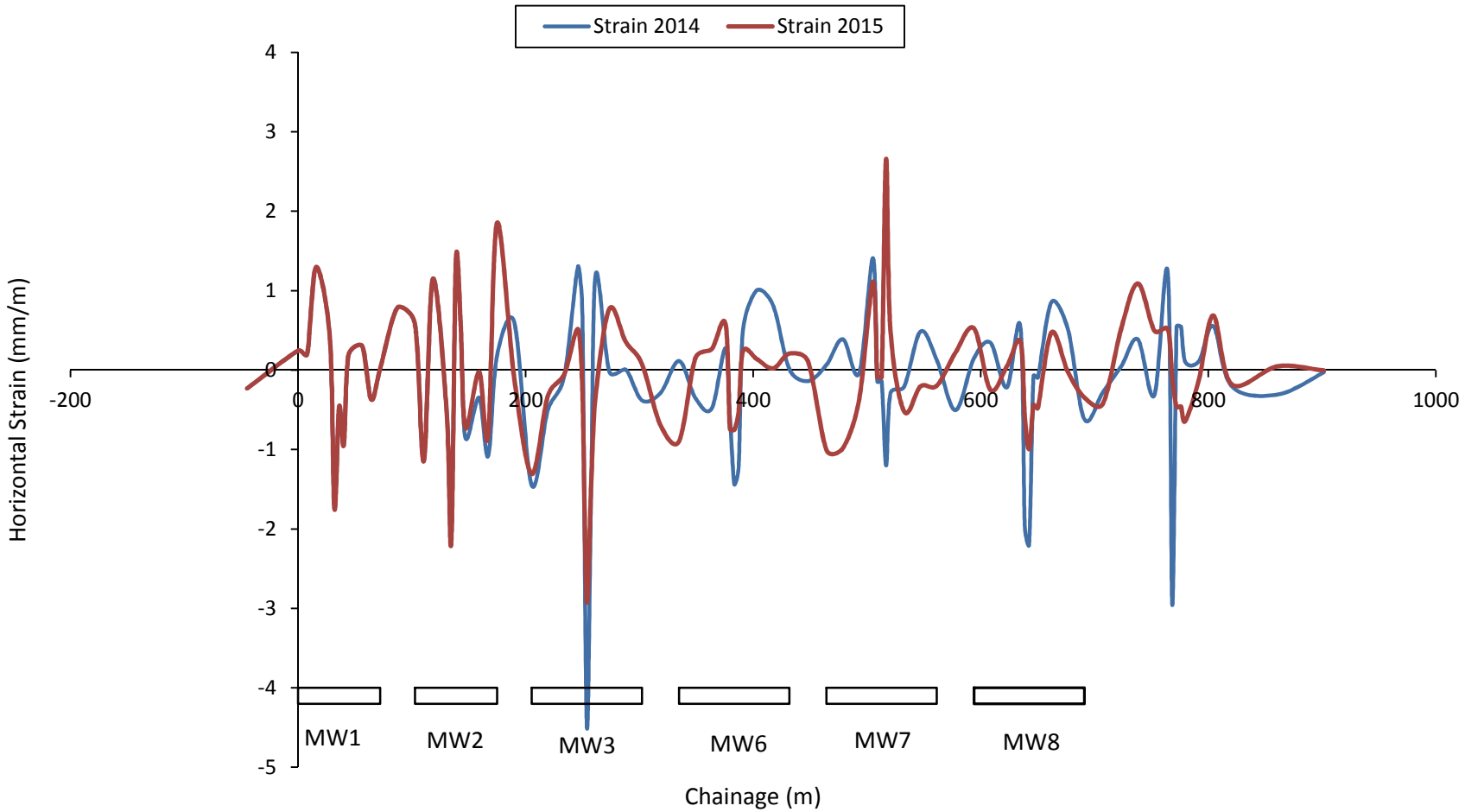
DgS	Engineer:	S.Ditton	Client:	LakeCoal - Chain Valley Colliery CHV-002/4	
	Drawn:	S.Ditton			
	Date:	15.05.15	Title:	Measured Subsidence Along MW6 Panel Centreline (based on Bathymetric Surveys) (see Figures 13.1-13.3 for Location)	
	Ditton Geotechnical Services Pty Ltd		Scale:	NTS	Figure No: 13.8



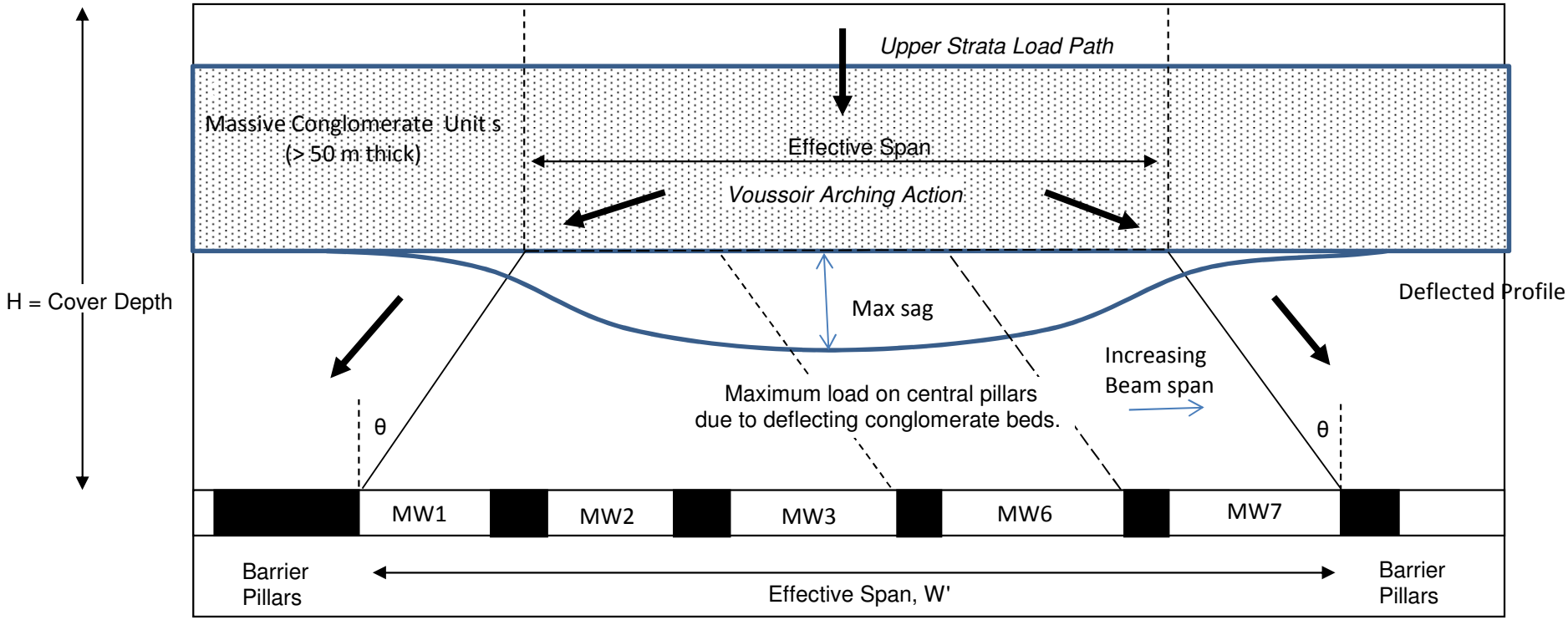
DgS	Engineer:	S.Ditton	Client:	LakeCoal - Chain Valley Colliery CHV-002/4	
	Drawn:	S.Ditton			
	Date:	15.05.15	Title:	Measured Subsidence Along MW7 Tailgate Chain Pillars (based on Bathymetric Surveys) (see Figures 13.1-13.3 for Location)	
	Ditton Geotechnical Services Pty Ltd		Scale:	NTS	Figure No: 13.9



DgS	Engineer:	S.Ditton	Client:	LakeCoal - Chain Valley Colliery CHV-002/4	
	Drawn:	S.Ditton			
	Date:	20.03.15	Title:	Measured Tilt based on Bathymetric Surveys in 2012 and 2015 above MW1-7 Cross line (see Figure 23.5 for Location)	
	Ditton Geotechnical Services Pty Ltd		Scale:	NTS	Figure No: 13.10



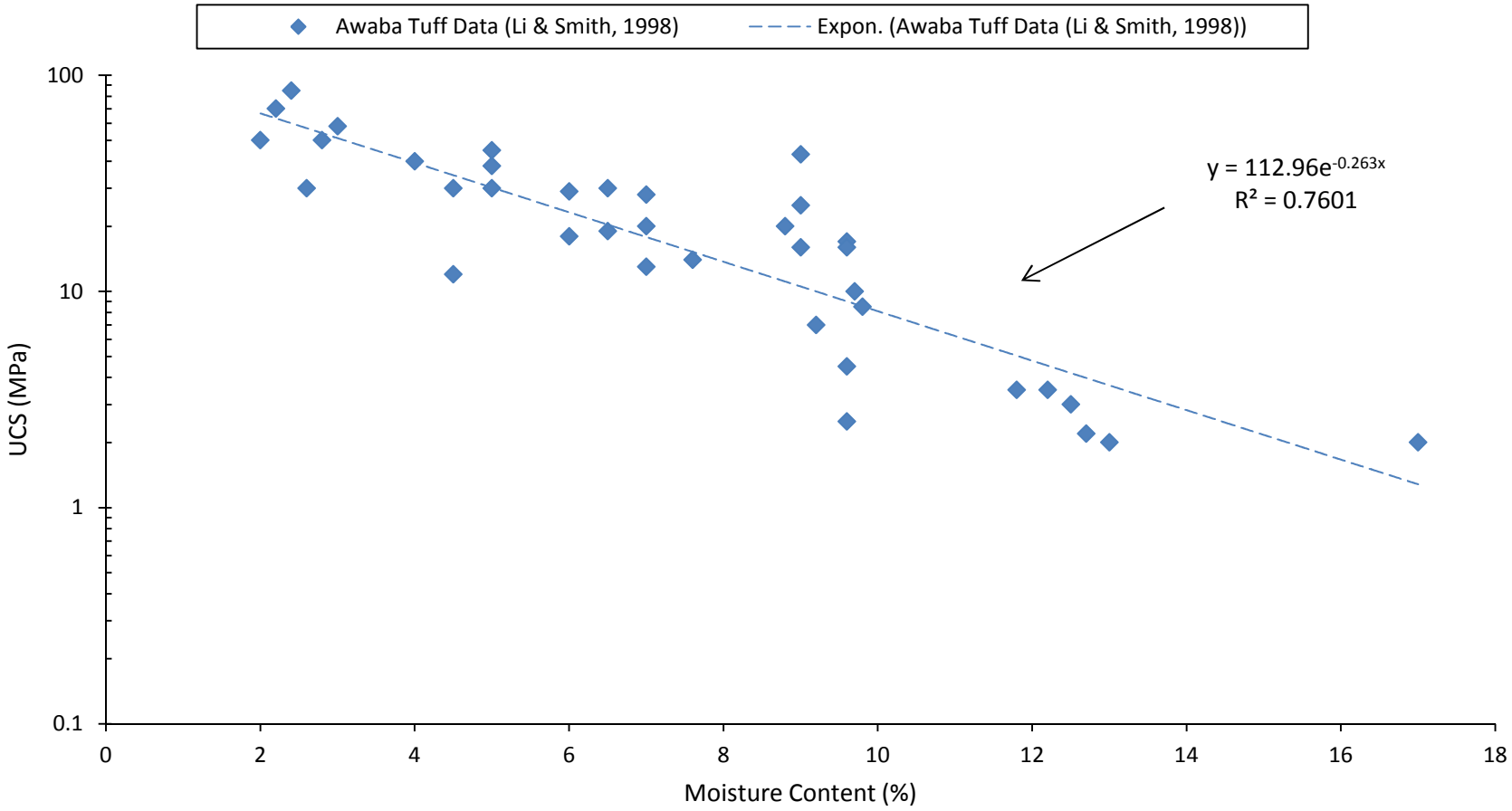
DgS	Engineer:	S.Ditton	Client:	LakeCoal - Chain Valley Colliery CHV-002/4	
	Drawn:	S.Ditton			
	Date:	20.03.15	Title:	Measured Strain based on Bathymetric Surveys in 2012 and 2015 above MW1-7 Crossline (see Figure 23.5 for Location)	
	Ditton Geotechnical Services Pty Ltd		Scale:	NTS	Figure No: 13.11



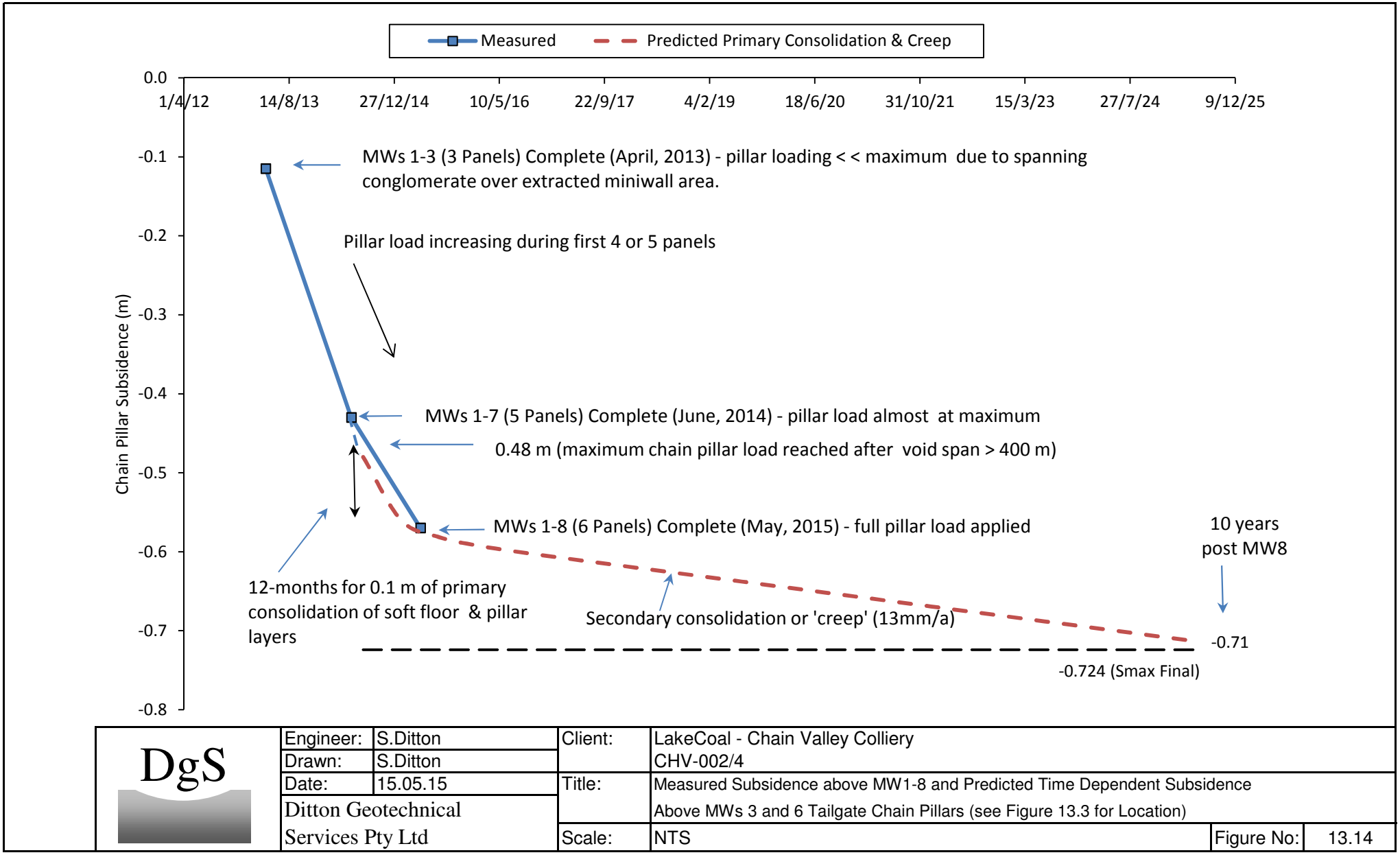
θ = abutment angle = 12º - 19º depending on W'/H ratio of 'super panel'

DgS	Engineer:	S.Ditton	Client:	LakeCoal - Chain Valley Colliery CHV-002/4	
	Drawn:	S.Ditton			
	Date:	15.05.15	Title:	Conceptual Strata Spanning Model for Panels with Spanning Conglomerate over MWs	
	Ditton Geotechnical Services Pty Ltd		Scale:	NTS	Figure No: 13.12

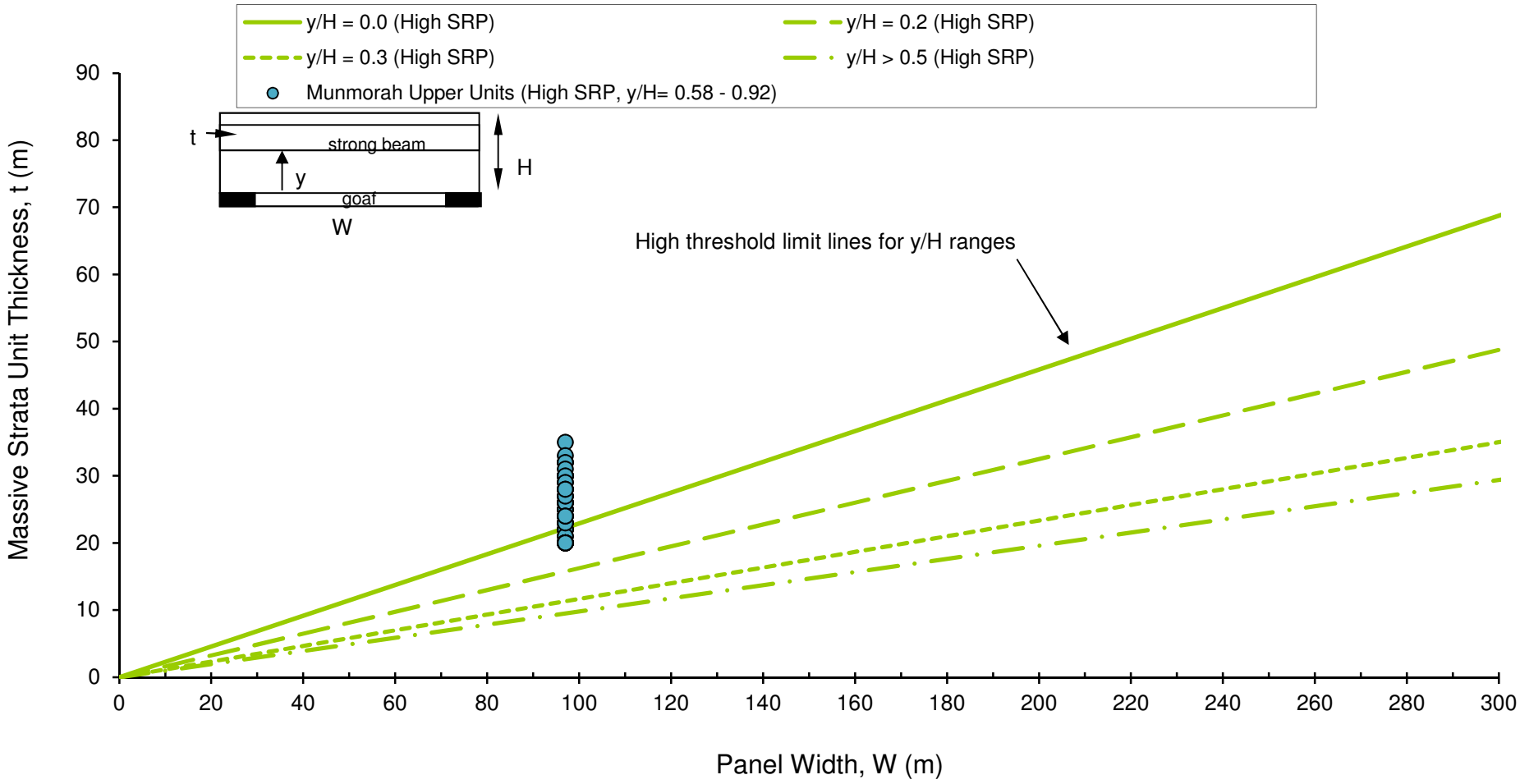
Awaba Tuff Data (Li & Smith, 1998)



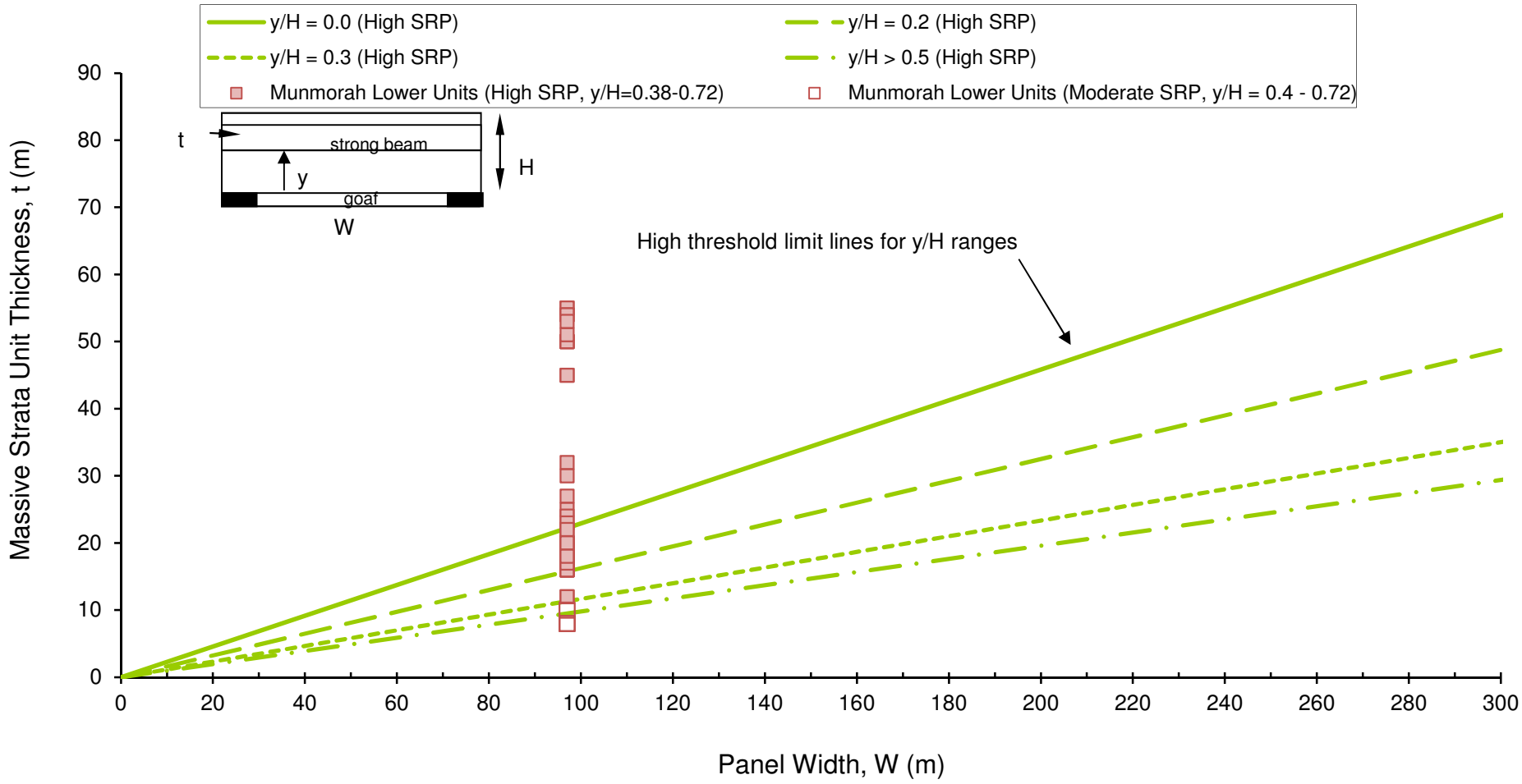
DgS	Engineer:	S.Ditton	Client:	LakeCoal - Chain Valley Colliery CHV-002/4	
	Drawn:	S.Ditton			
	Date:	15.05.15	Title:	Awaba Tuff Claystone UCS Tests v. Moisture Content	
	Ditton Geotechnical Services Pty Ltd		Scale:	NTS	Figure No: 13.13



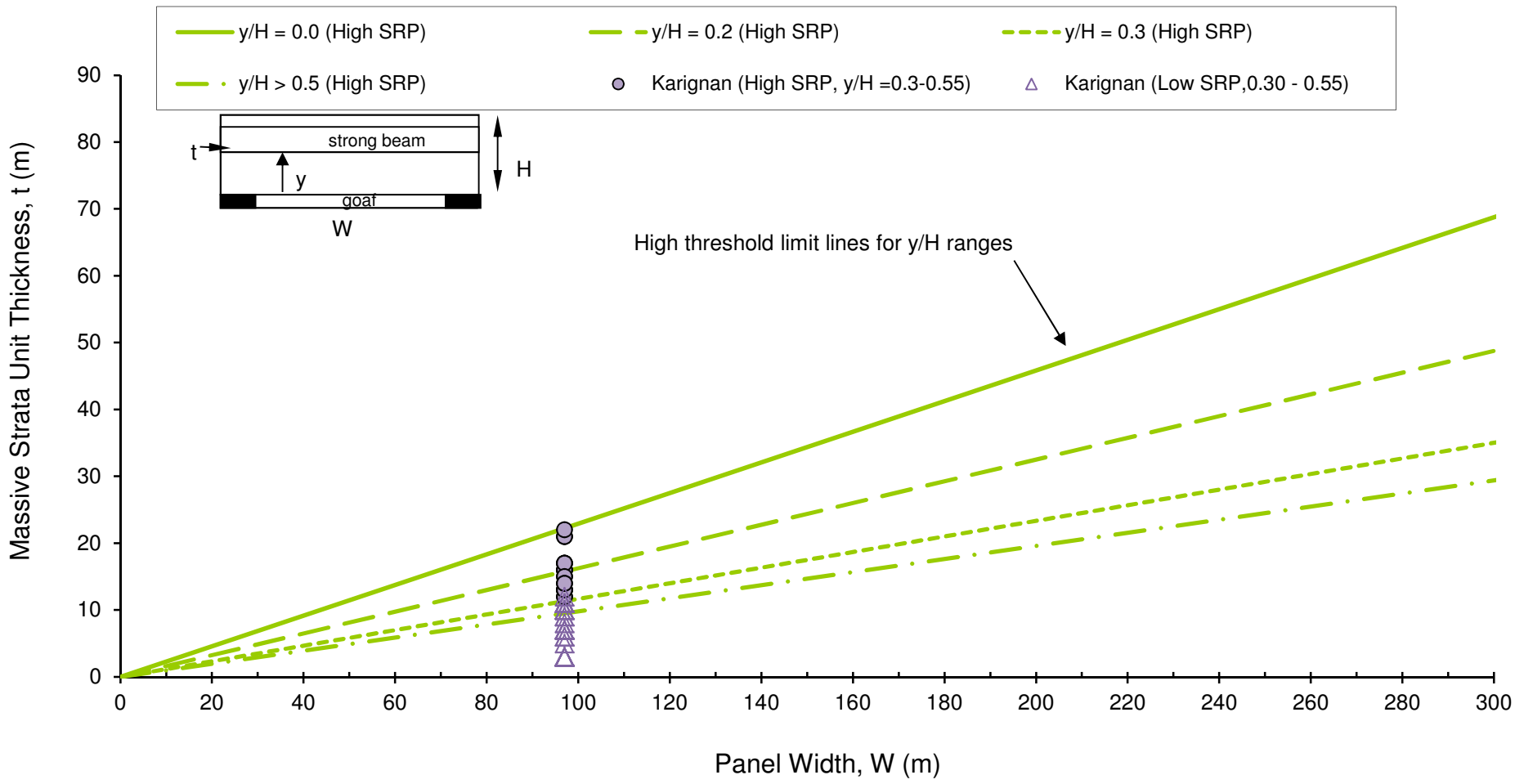
DgS	Engineer:	S.Ditton	Client:	LakeCoal - Chain Valley Colliery CHV-002/4	
	Drawn:	S.Ditton			
	Date:	15.05.15	Title:	Measured Subsidence above MW1-8 and Predicted Time Dependent Subsidence Above MWs 3 and 6 Tailgate Chain Pillars (see Figure 13.3 for Location)	
	Ditton Geotechnical Services Pty Ltd		Scale:	NTS	Figure No: 13.14



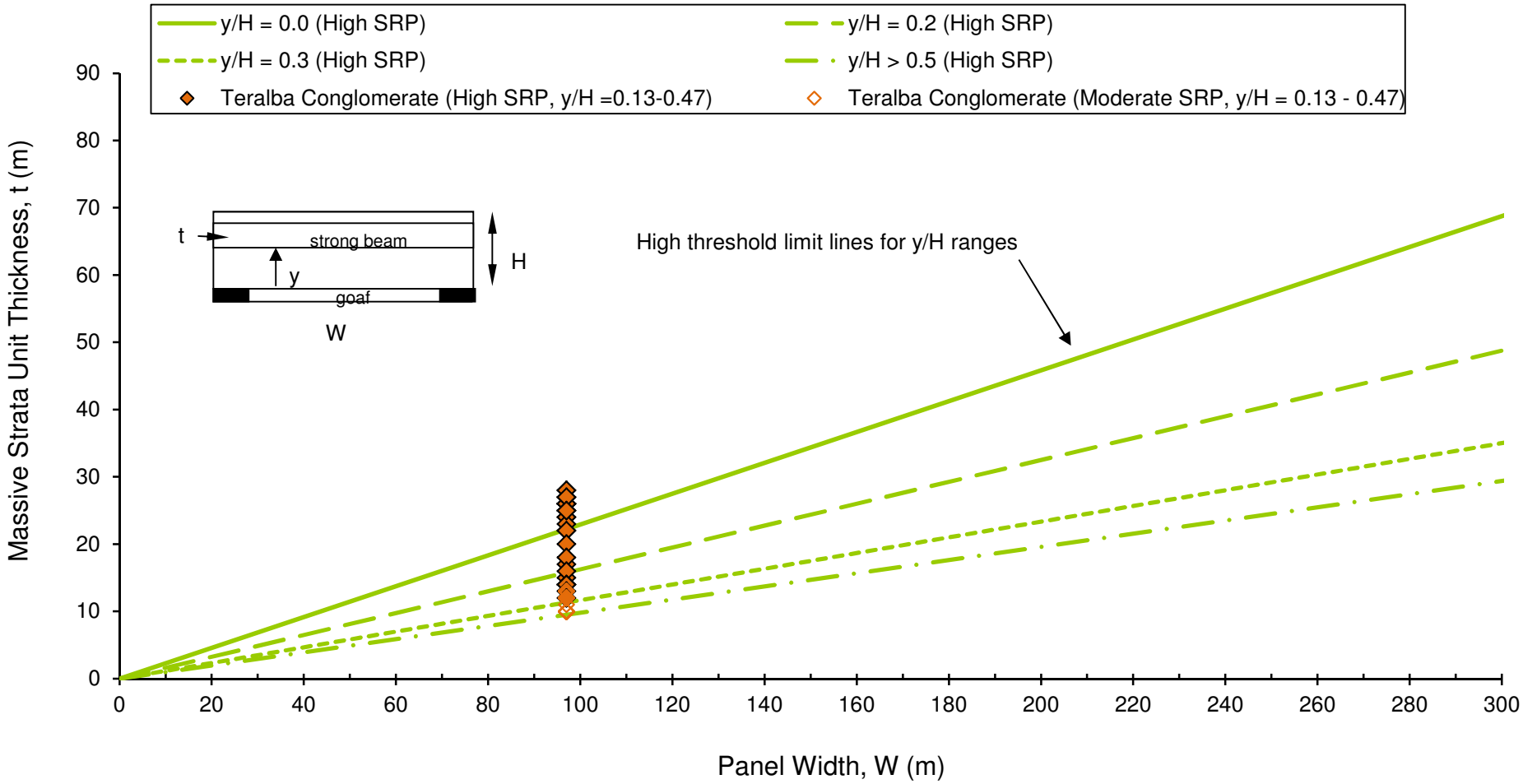
DgS	Engineer:	S.Ditton	Client:	LakeCoal - Chain Valley Colliery CHV-002/4	
	Drawn:	S.Ditton			
	Date:	20.03.15	Title:	Predicted Subsidence Reduction Potential of the Upper Munmorah Conglomerate Units Above Miniwalls 9 - 36 with Cover Depths between 150 and 250 m	
	Ditton Geotechnical Services Pty Ltd		Scale:	NTS	Figure No: 14.1



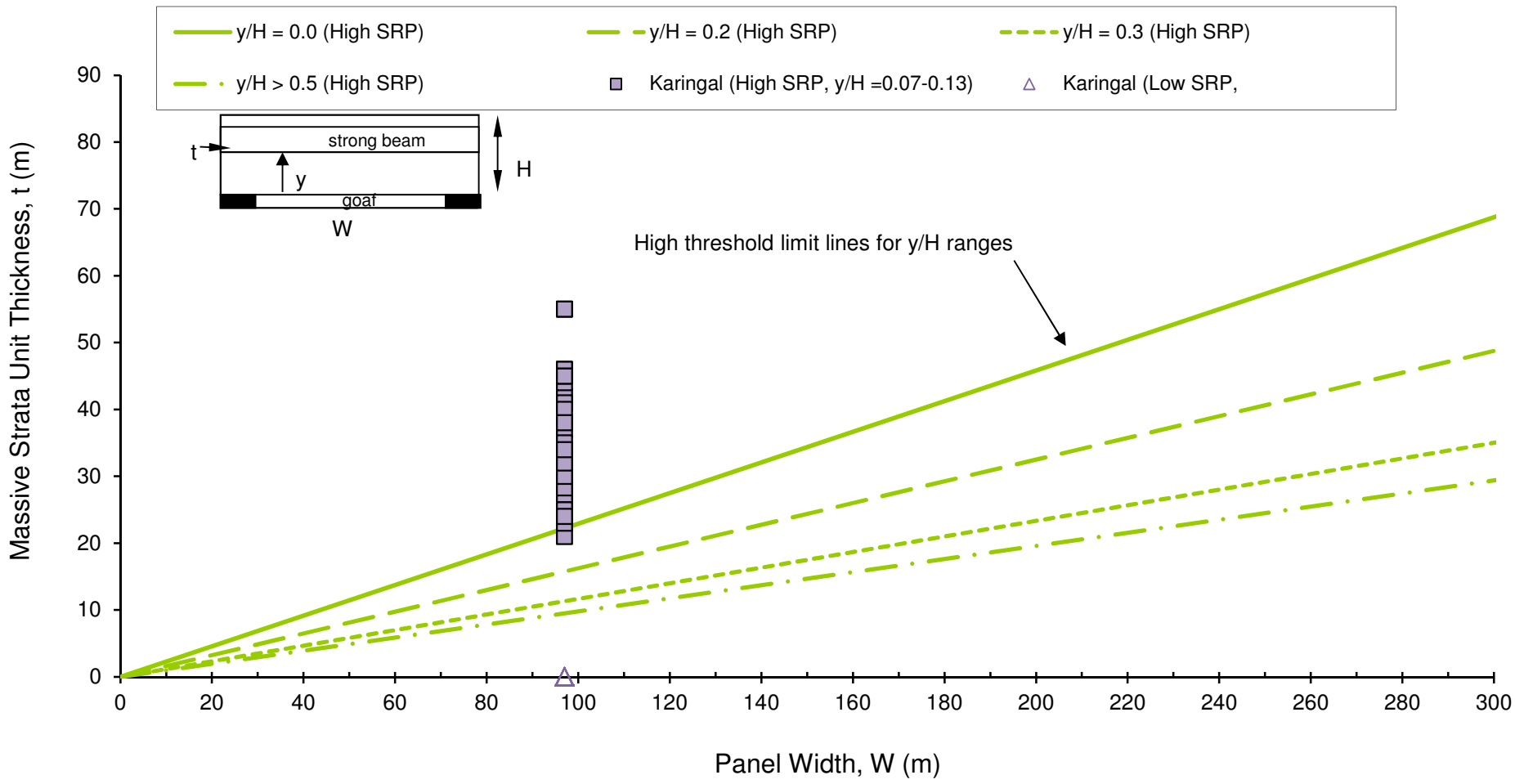
DgS	Engineer:	S.Ditton	Client:	LakeCoal - Chain Valley Colliery CHV-002/4	
	Drawn:	S.Ditton			
	Date:	20.03.15	Title:	Predicted Subsidence Reduction Potential of the Lower Munmorah Conglomerate Units Above Miniwalls 9 - 36 with Cover Depths between 150 and 250 m	
	Ditton Geotechnical Services Pty Ltd		Scale:	NTS	Figure No: 14.2



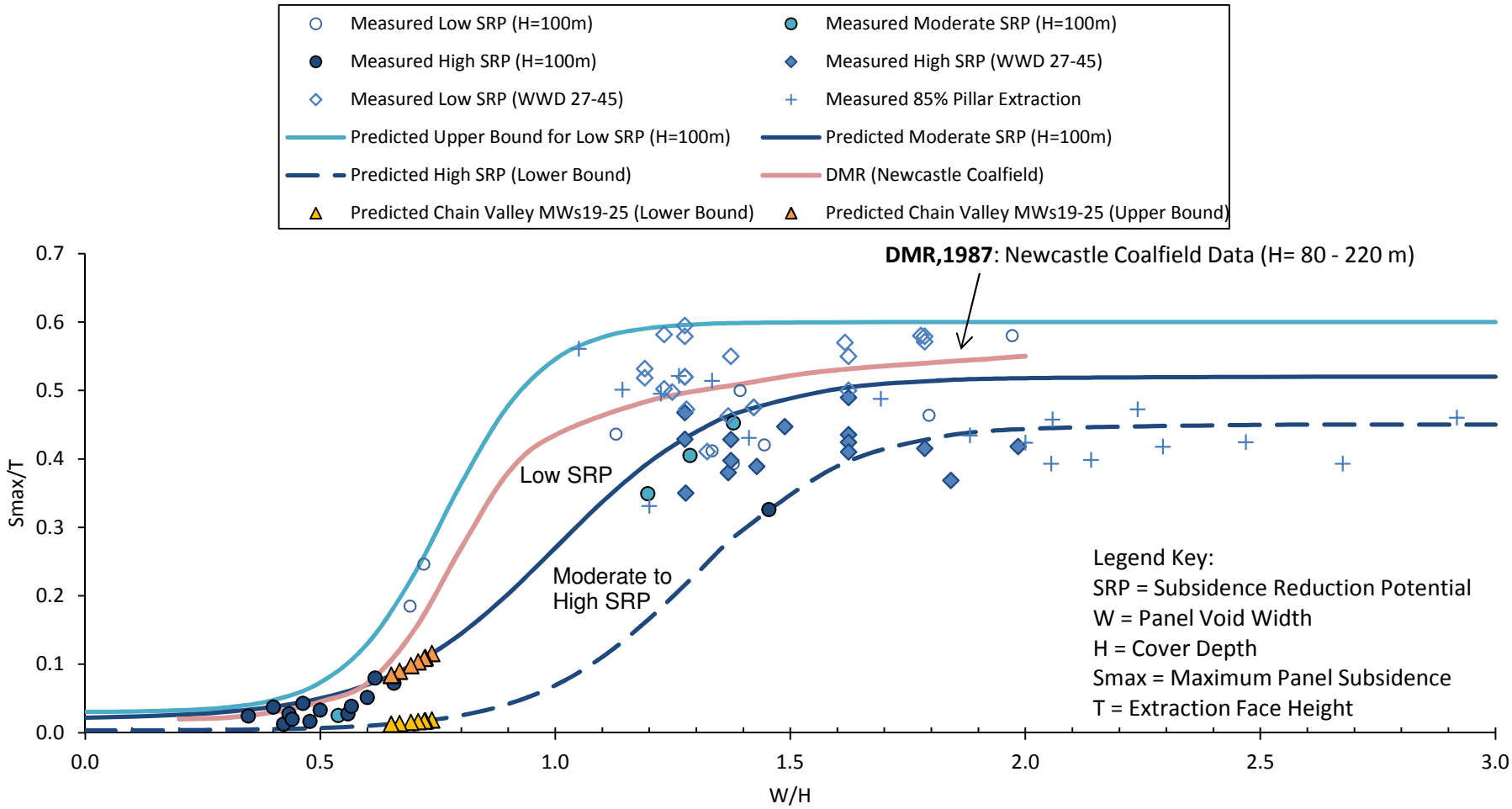
DgS	Engineer:	S.Ditton	Client:	LakeCoal - Chain Valley Colliery CHV-002/4	
	Drawn:	S.Ditton			
	Date:	20.03.15	Title:	Predicted Subsidence Reduction Potential of the Karignan Conglomerate Units Above Miniwalls 9 - 36 with Cover Depths between 150 and 250 m	
	Ditton Geotechnical Services Pty Ltd		Scale:	NTS	Figure No: 14.3



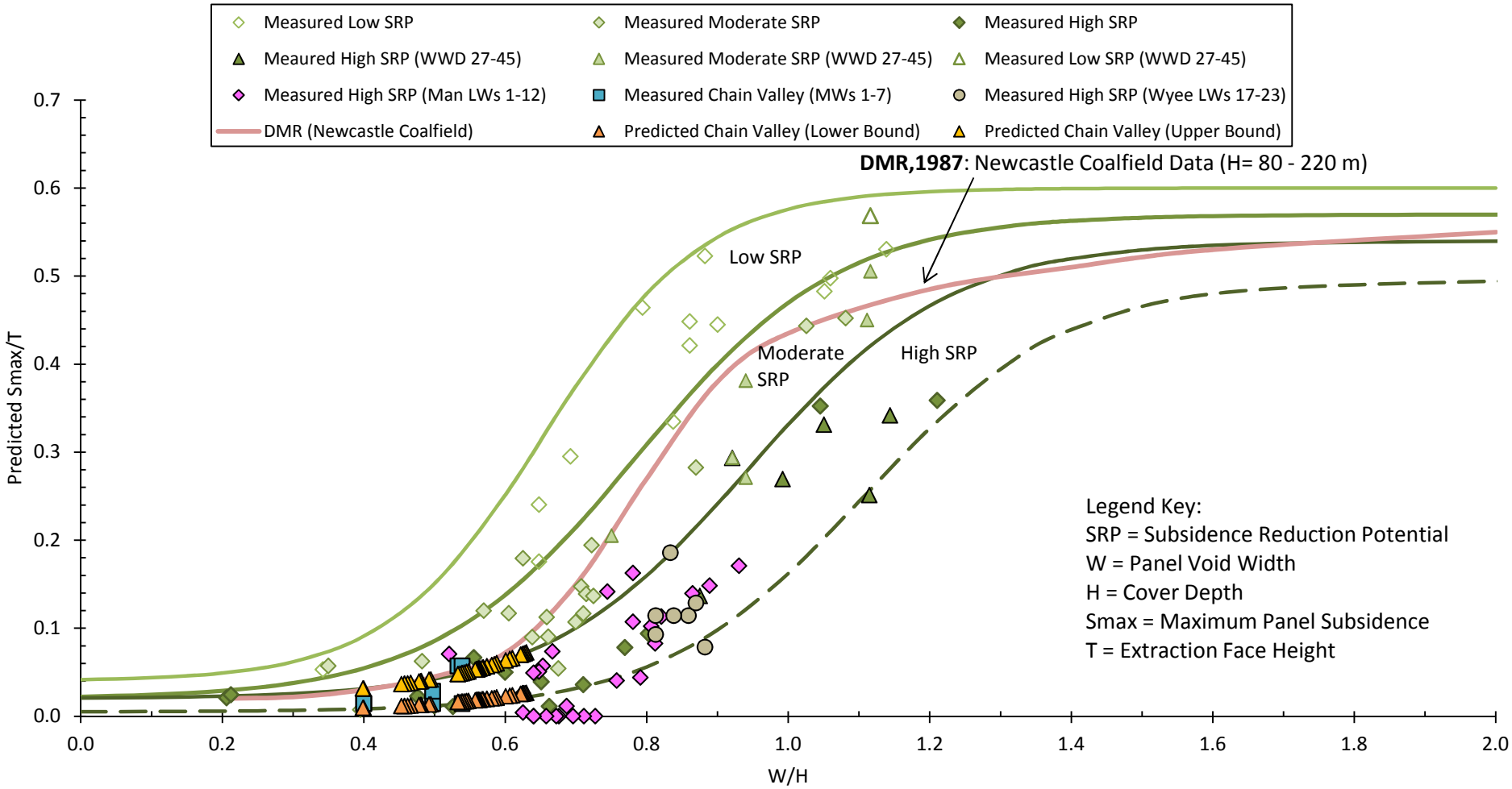
DgS	Engineer:	S.Ditton	Client:	LakeCoal - Chain Valley Colliery CHV-002/4	
	Drawn:	S.Ditton			
	Date:	20.03.15	Title:	Predicted Subsidence Reduction Potential of the Teralba Conglomerate Units Above Miniwalls 9 - 36 with Cover Depths between 150 and 250 m	
	Ditton Geotechnical Services Pty Ltd		Scale:	NTS	Figure No: 14.4



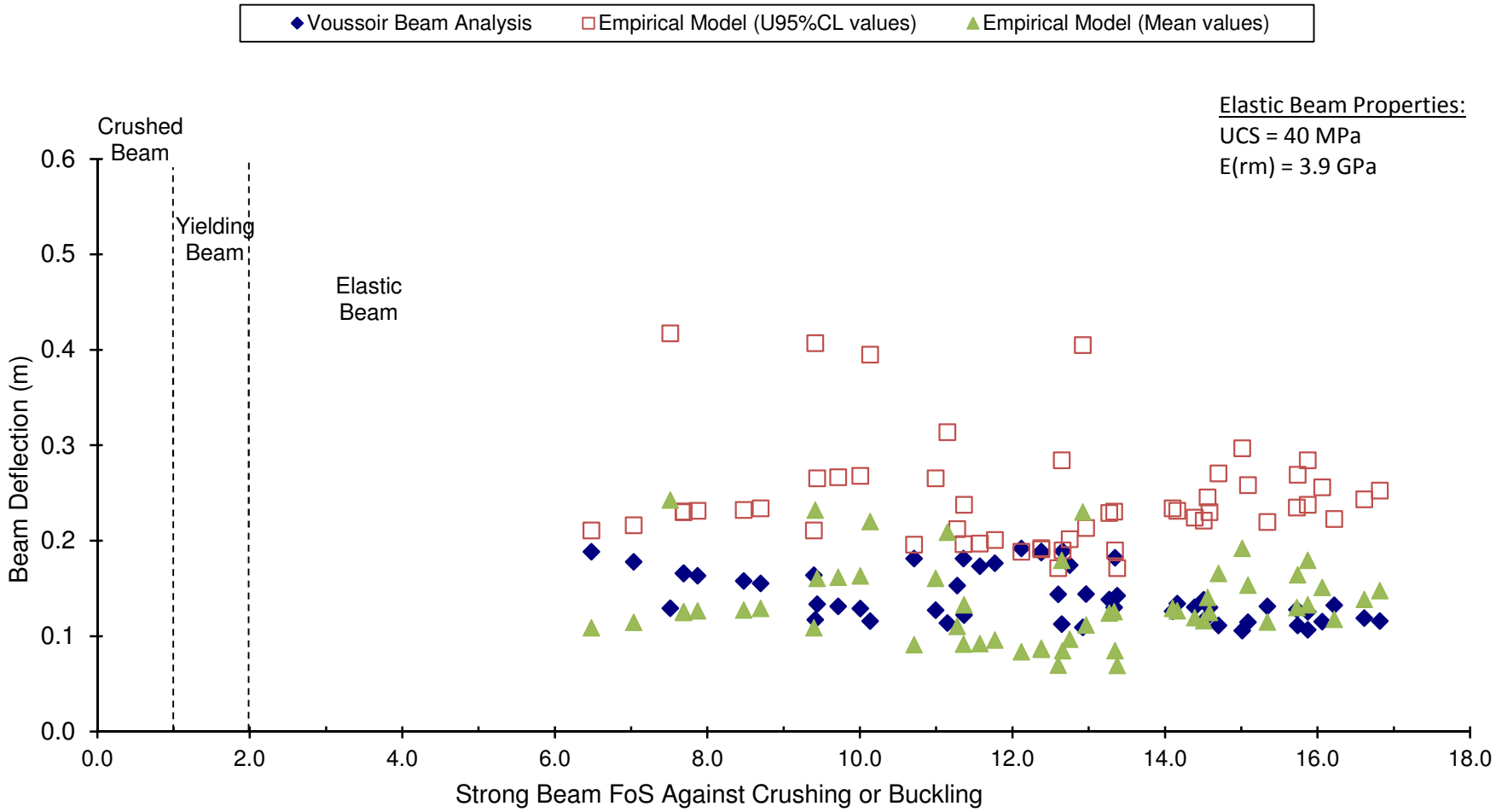
DgS	Engineer:	S.Ditton	Client:	LakeCoal - Chain Valley Colliery CHV-002/4	
	Drawn:	S.Ditton			
	Date:	20.03.15	Title:	Predicted Subsidence Reduction Potential of the Karingal Conglomerate Units Above Miniwalls 9 - 36 with Cover Depths between 150 and 250 m	
	Ditton Geotechnical Services Pty Ltd		Scale:	NTS	Figure No: 14.5



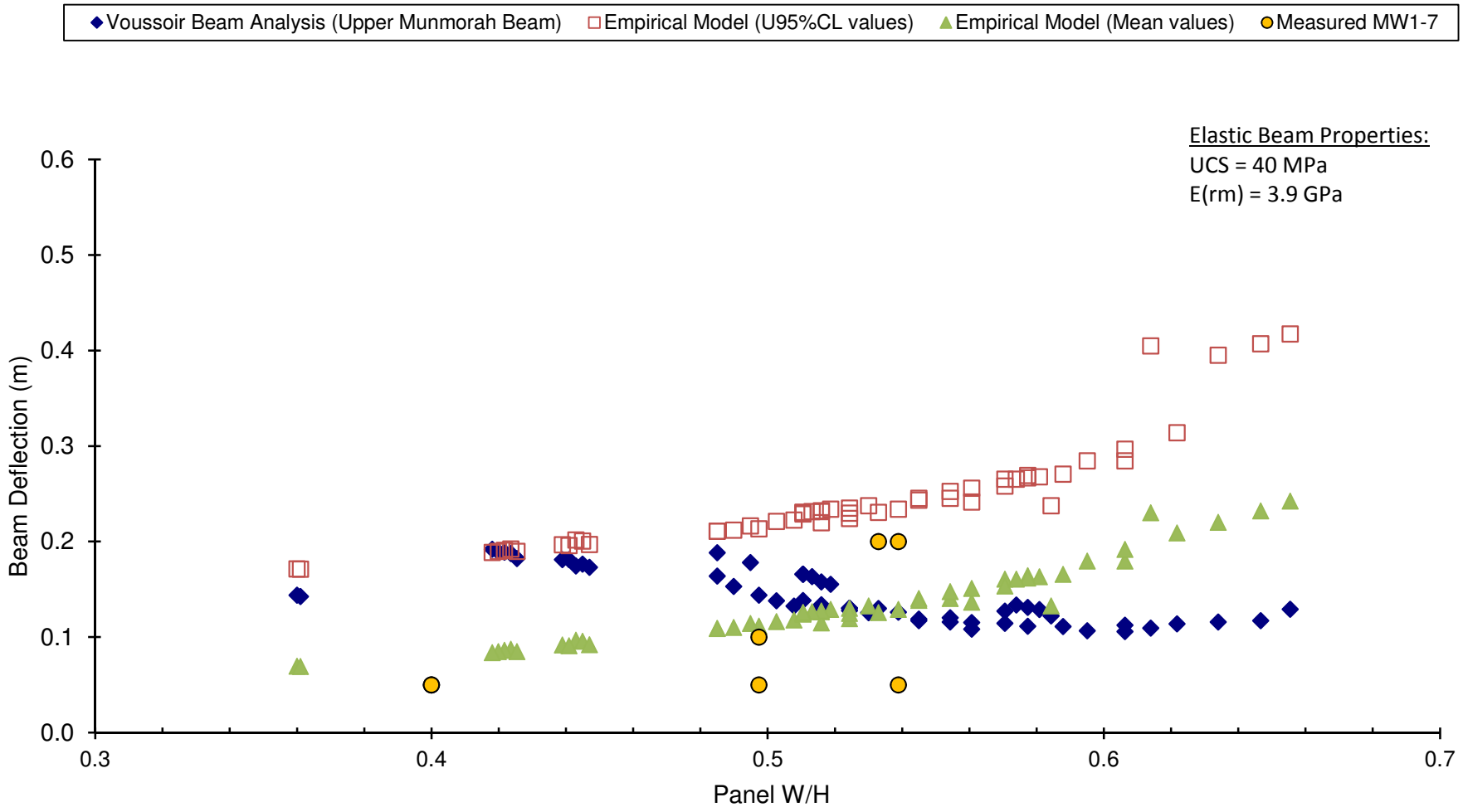
DgS	Engineer:	S.Ditton	Client:	LakeCoal - Chain Valley Colliery CHV-002/4	
	Drawn:	S.Ditton			
	Date:	20.03.15	Title:	Predicted Maximum Single Panel Subsidence for Miniwalls 1 to 36 with Cover Depths between 50 m and 150 m	
	Ditton Geotechnical Services Pty Ltd		Scale:	NTS	Figure No: 15.1



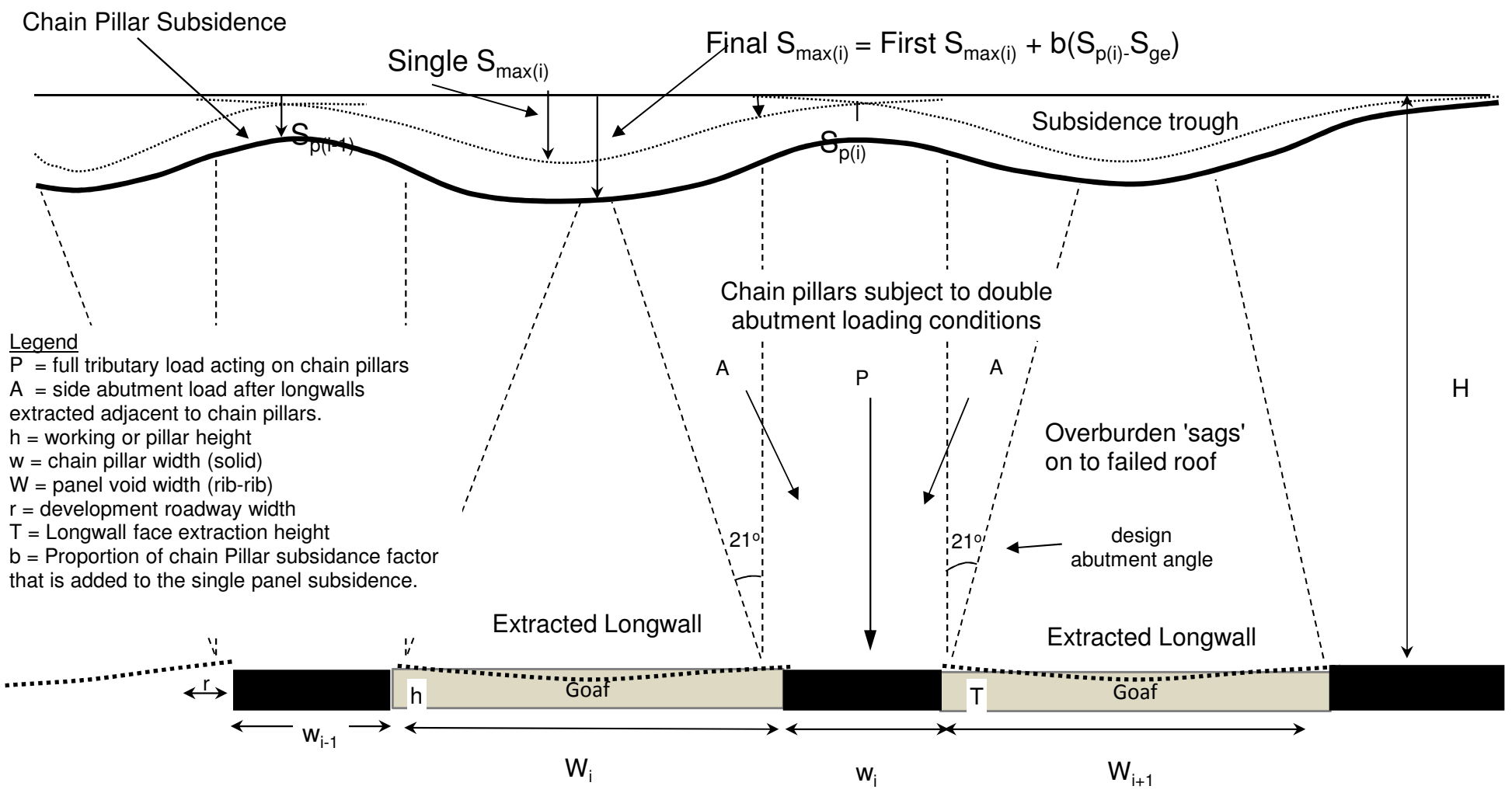
DgS	Engineer:	S.Ditton	Client:	LakeCoal - Chain Valley Colliery CHV-002/4	
	Drawn:	S.Ditton			
	Date:	20.03.15	Title:	Predicted Maximum Single Panel Subsidence for Miniwalls 1 to 36 with Cover Depths between 150 m and 250 m	
	Ditton Geotechnical Services Pty Ltd		Scale:	NTS	Figure No: 15.2



DgS	Engineer:	S.Ditton	Client:	LakeCoal - Chain Valley Colliery CHV-002/4	
	Drawn:	S.Ditton			
	Date:	20.03.15	Title:	Predicted v. Measured Maximum Single Panel Subsidence for Chain Valley MWs 9 - 36 against Factor of Safety for Upper Munmorah Conglomerate Beam Failure	
	Ditton Geotechnical Services Pty Ltd		Scale:	NTS	Figure No: 15.3

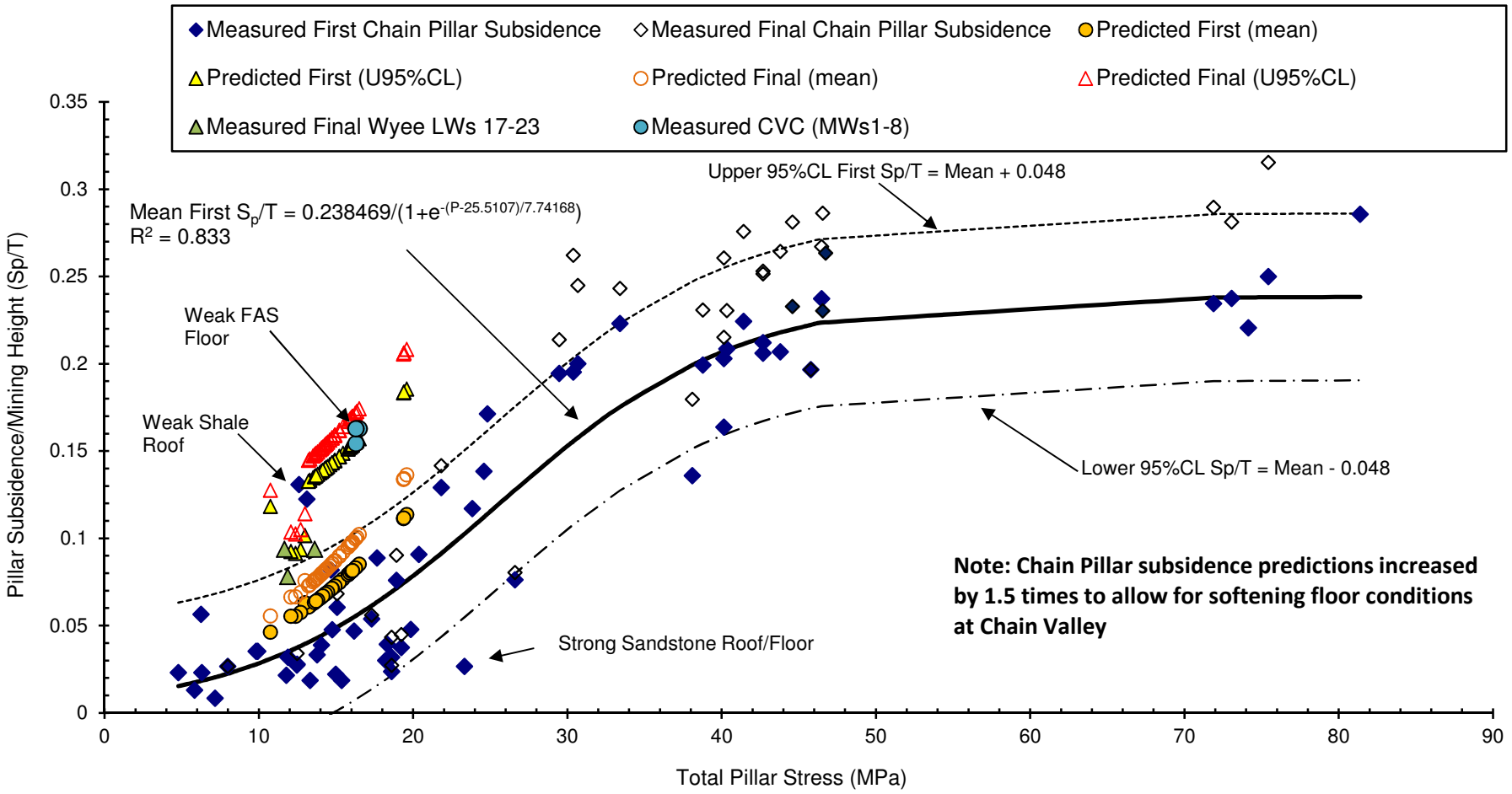


DgS	Engineer:	S.Ditton	Client:	LakeCoal - Chain Valley Colliery CHV-002/4	
	Drawn:	S.Ditton			
	Date:	20.03.15	Title:	Predicted v. Measured Maximum Single Panel Subsidence for Chain Valley MWs 9 - 36 against Panel Width / Cover Depth	
	Ditton Geotechnical Services Pty Ltd		Scale:	NTS	Figure No: 15.4

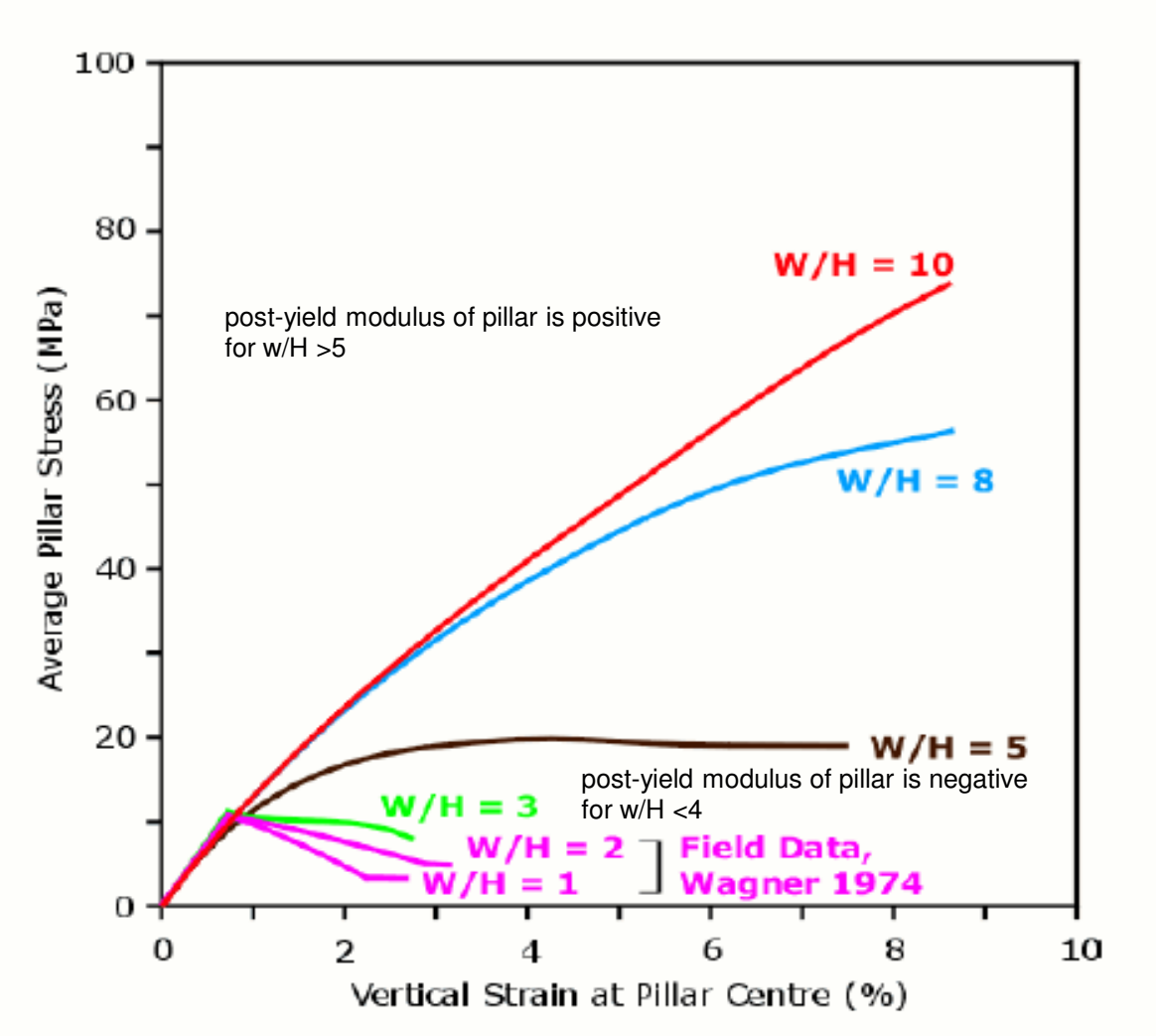


Legend
P = full tributary load acting on chain pillars
A = side abutment load after longwalls extracted adjacent to chain pillars.
h = working or pillar height
w = chain pillar width (solid)
W = panel void width (rib-rib)
r = development roadway width
T = Longwall face extraction height
b = Proportion of chain Pillar subsidance factor that is added to the single panel subsidence.

DgS	Engineer:	S.Ditton	Client:	LakeCoal - Chain Valley Colliery CHV-002/4	
	Drawn:	S.Ditton			
	Date:	20.03.15	Title:	Multiple Longwall Panel Subsidence Mechanism Concepts	
	Ditton Geotechnical Services Pty Ltd		Scale:	NTS	Figure No: 16



DgS	Engineer:	S.Ditton	Client:	LakeCoal - Chain Valley Colliery CHV-002/4	
	Drawn:	S.Ditton			
	Date:	15.05.15	Title:	Chain Pillar Subsidence Prediction Model based on the ACARP, 2003 and the Predicted Outcomes for Modified MWs 9 to 36	
	Ditton Geotechnical Services Pty Ltd		Scale:	NTS	Figure No: 17.1



Ref: ACARP, 2005

DgS	Engineer:	S.Ditton	Client:	LakeCoal - Chain Valley Colliery	
	Drawn:	S.Ditton		CHV-002/4	
	Date:	20.03.15	Title:	In-situ Pillar Stress v. Strain Behaviour for a Range of Pillar Width/Height Ratios	
	Ditton Geotechnical Services Pty Ltd		Scale:	NTS	Figure No: 17.2

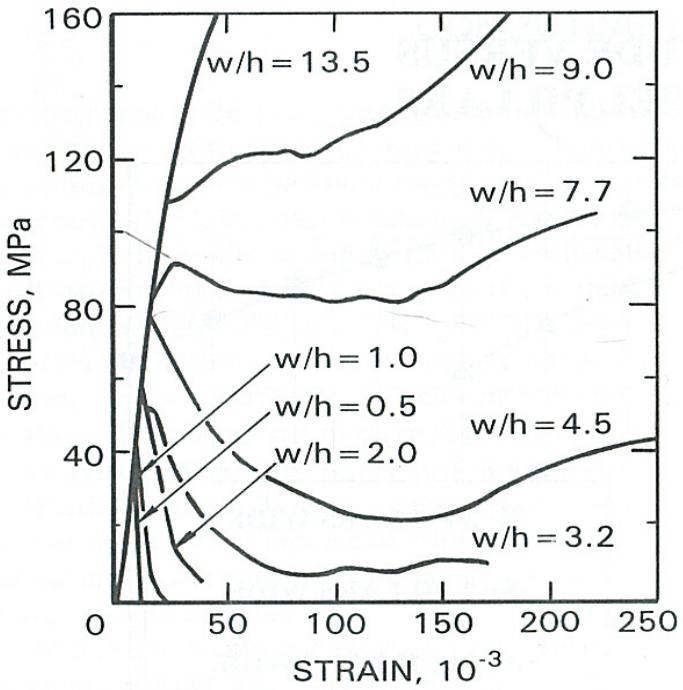


Figure 4.—Complete stress-strain curves for Indian coal specimens showing increasing residual strength and postfailure modulus with increasing w/h (after Das [1986]).

Ref: Das**, 1996**

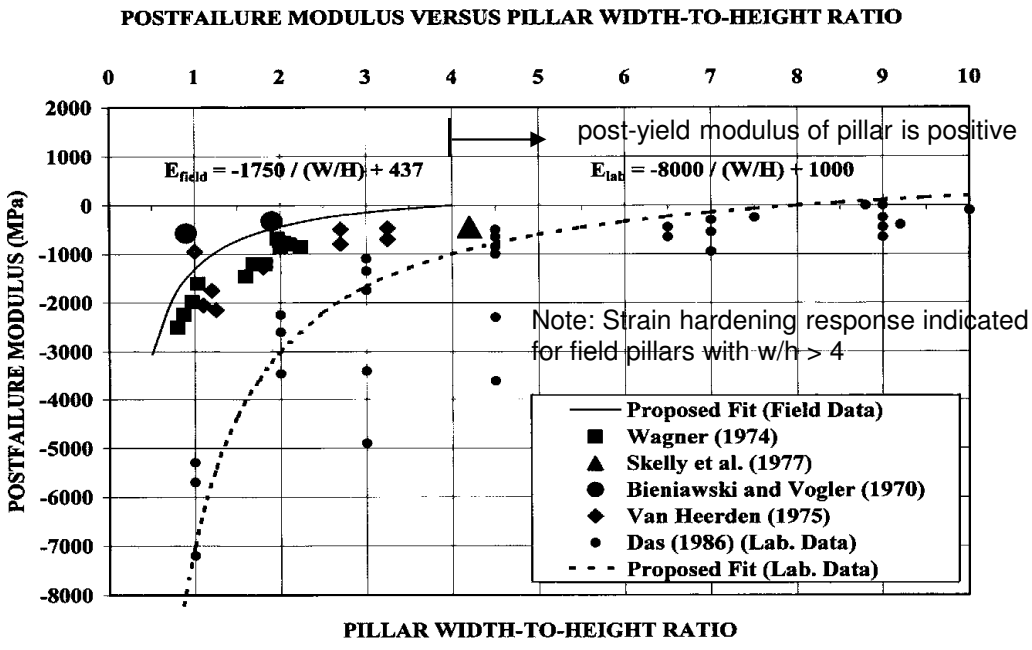
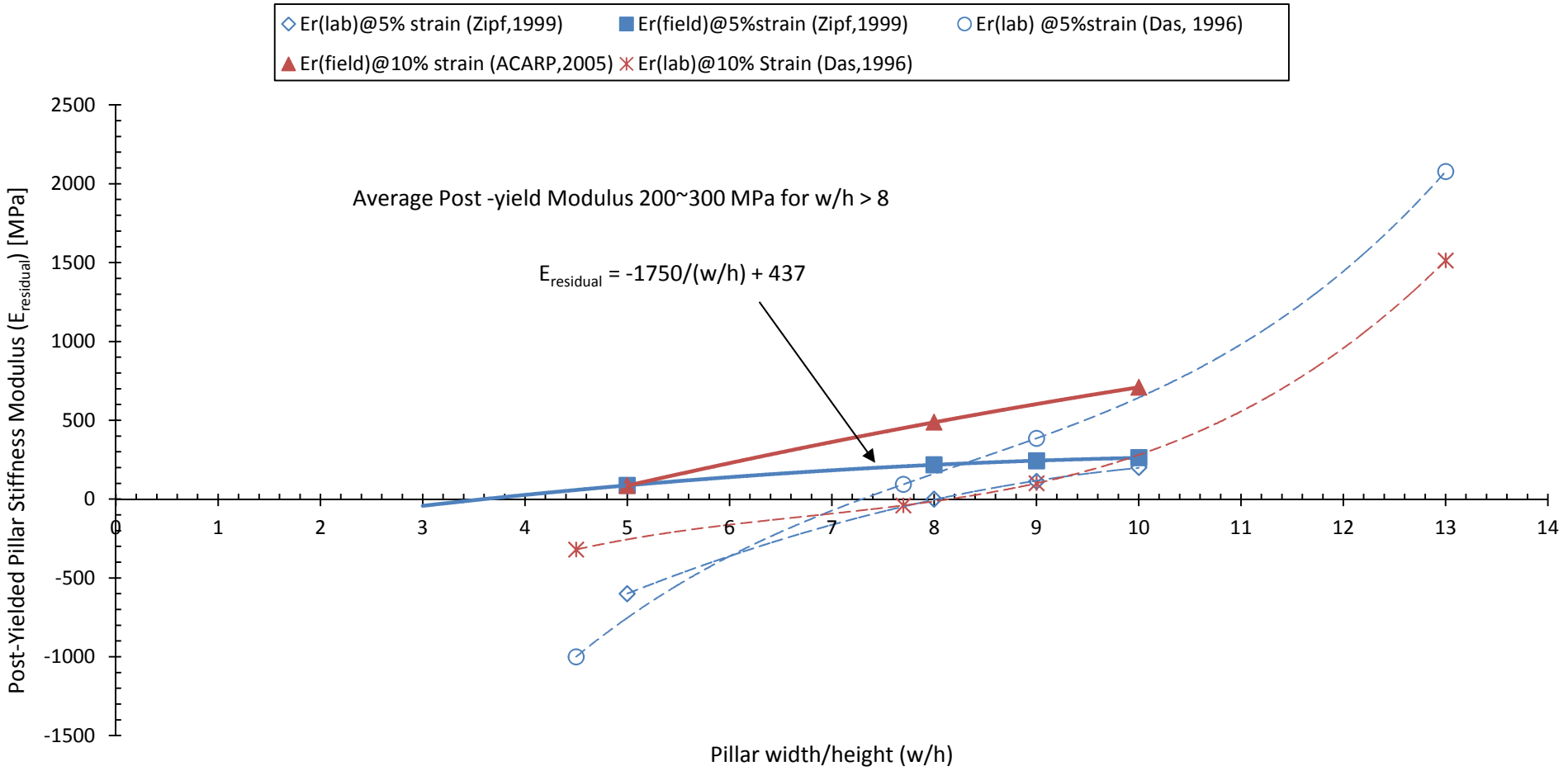


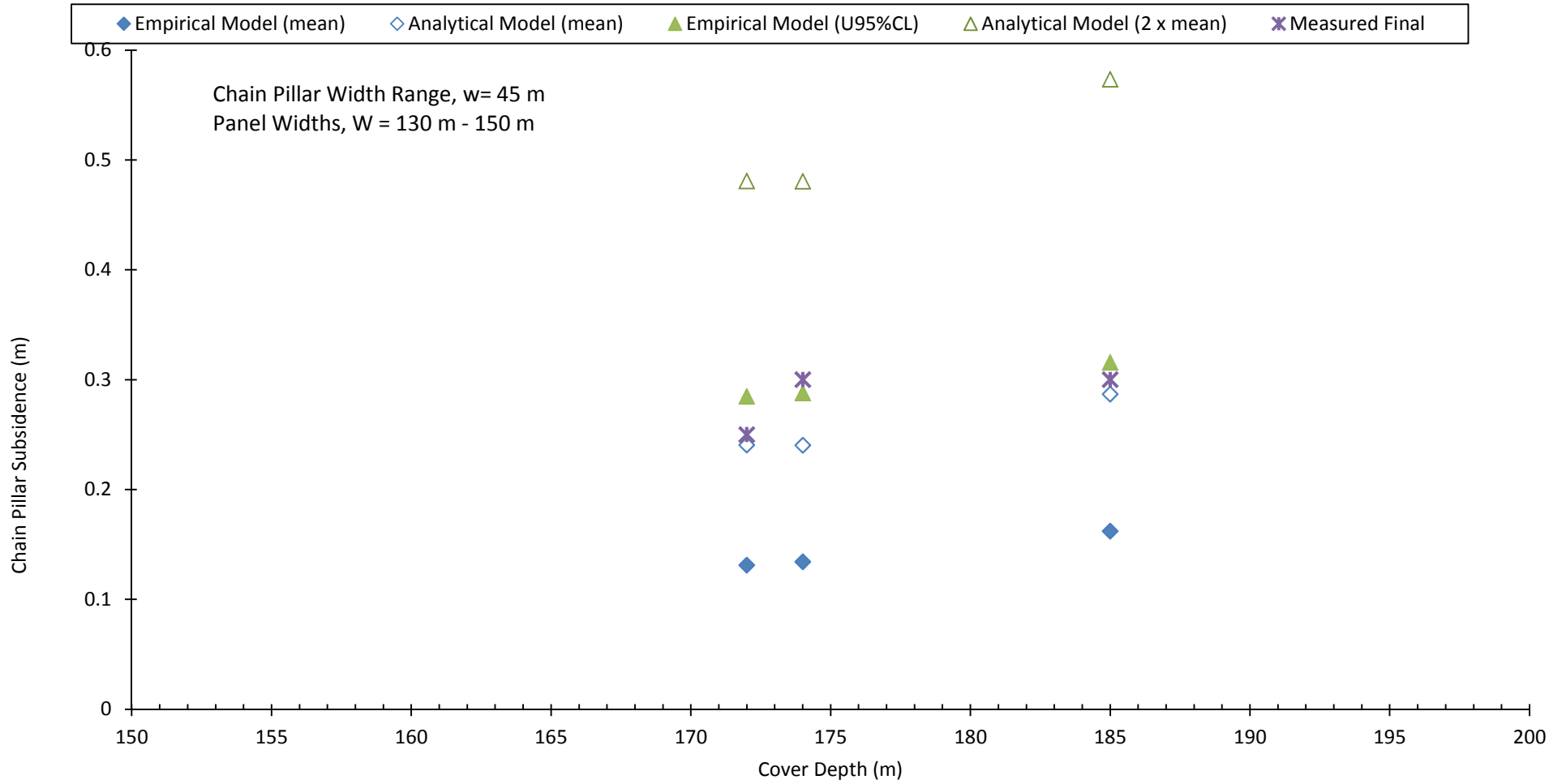
Figure 5.—Summary of postfailure modulus data for full-scale coal pillars and laboratory specimens. Also shown is proposed approximate equation for E_p.

Ref: **Zipf, 1999**

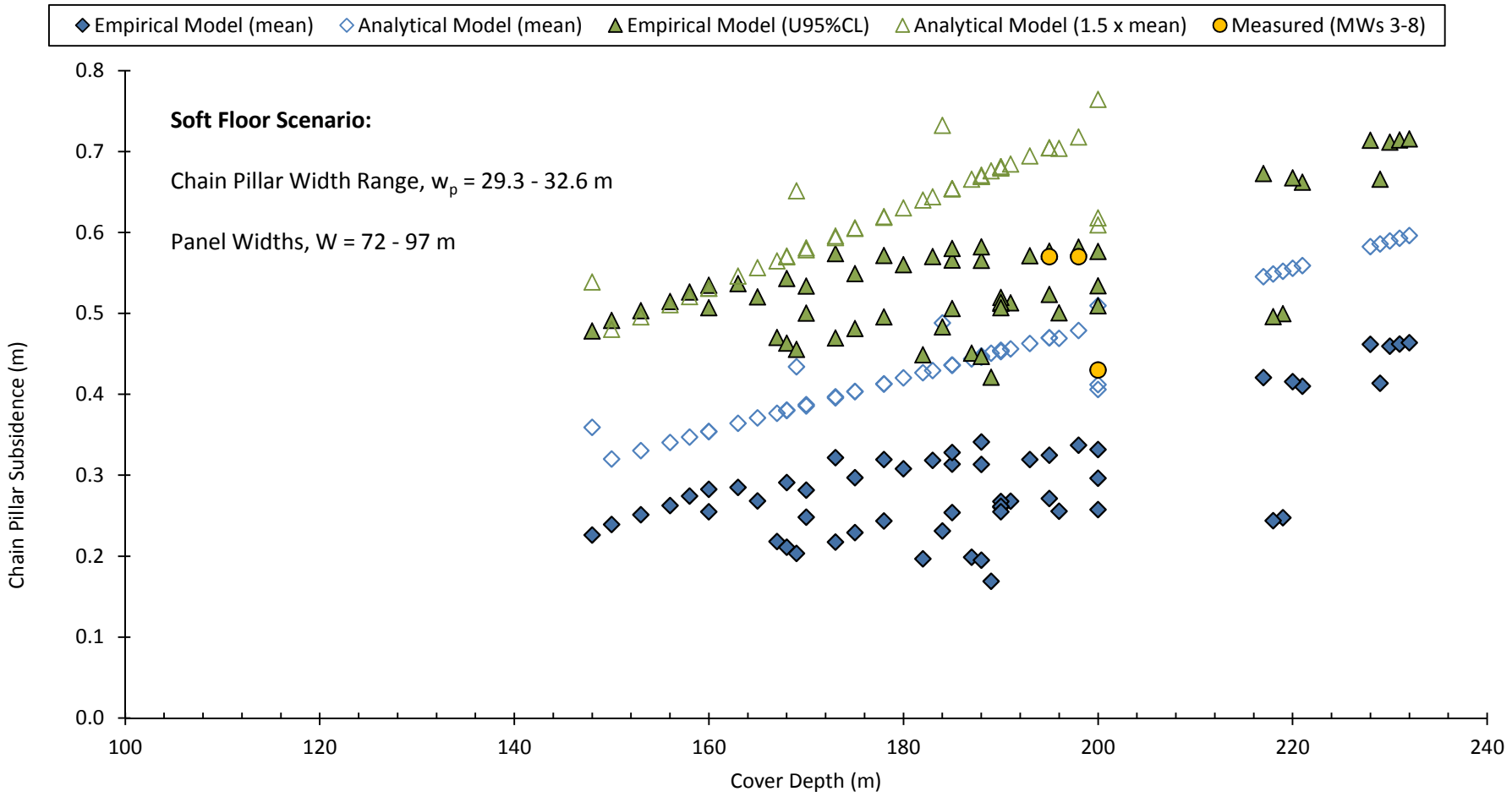
DgS	Engineer:	S.Ditton	Client:	LakeCoal - Chain Valley Colliery	
	Drawn:	S.Ditton		CHV-002/4	
	Date:	20.03.15	Title:	Post-yielded Modulus & Laboratory Stress - Strain Curves for a range of pillar w/h Ratios	
	Ditton Geotechnical Services Pty Ltd		Scale:	NTS	Figure No: 17.3



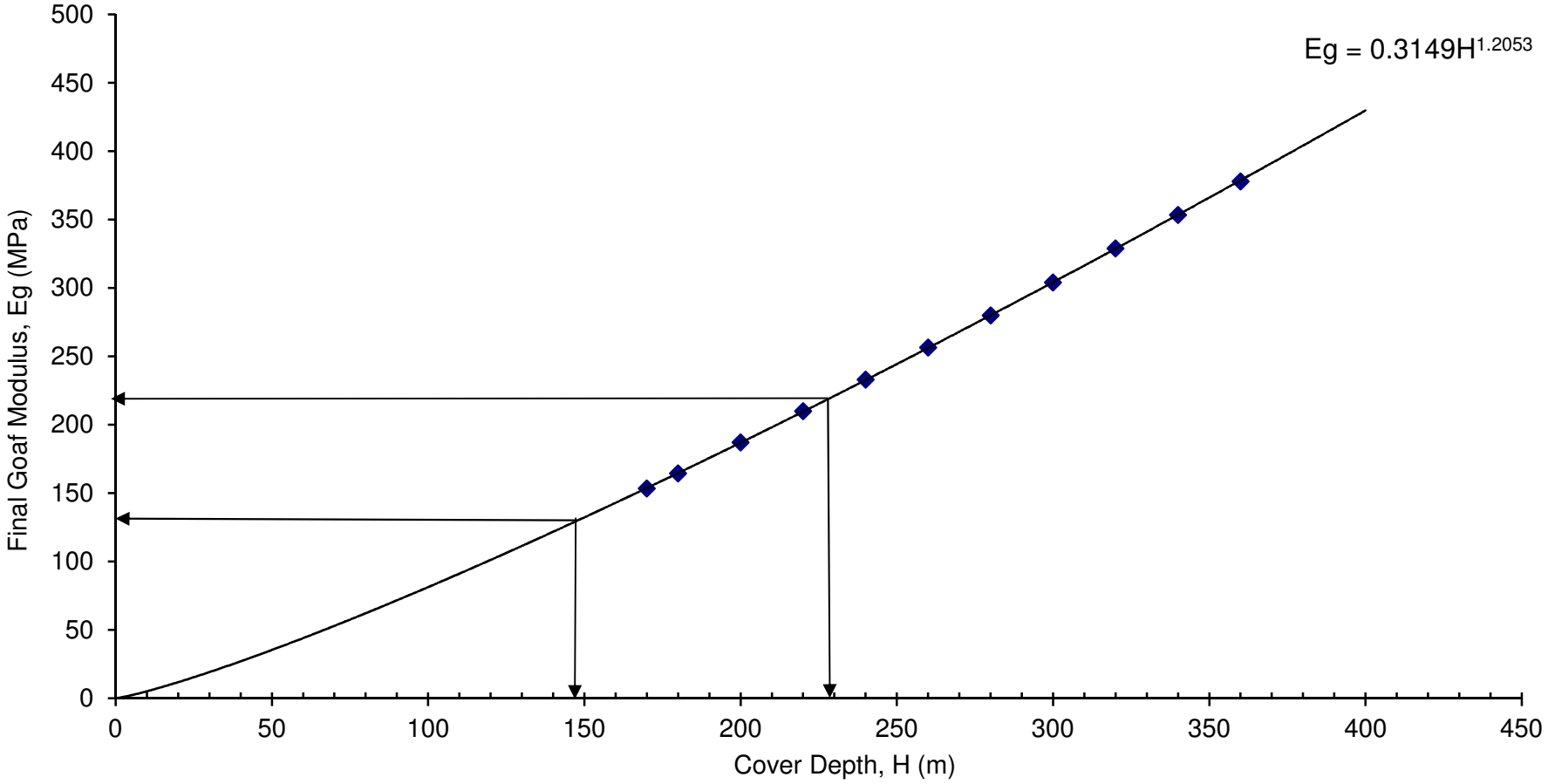
DgS	Engineer:	S.Ditton	Client:	LakeCoal - Chain Valley Colliery CHV-002/4	
	Drawn:	S.Ditton			
	Date:	20.03.15	Title:	In-situ and Laboratory Post-yielded Modulii for a Range of Pillar Width/Height Ratios according to Zipf, 1999; Das, 1996 and ACARP, 2005	
	Ditton Geotechnical Services Pty Ltd		Scale:	NTS	Figure No: 17.4



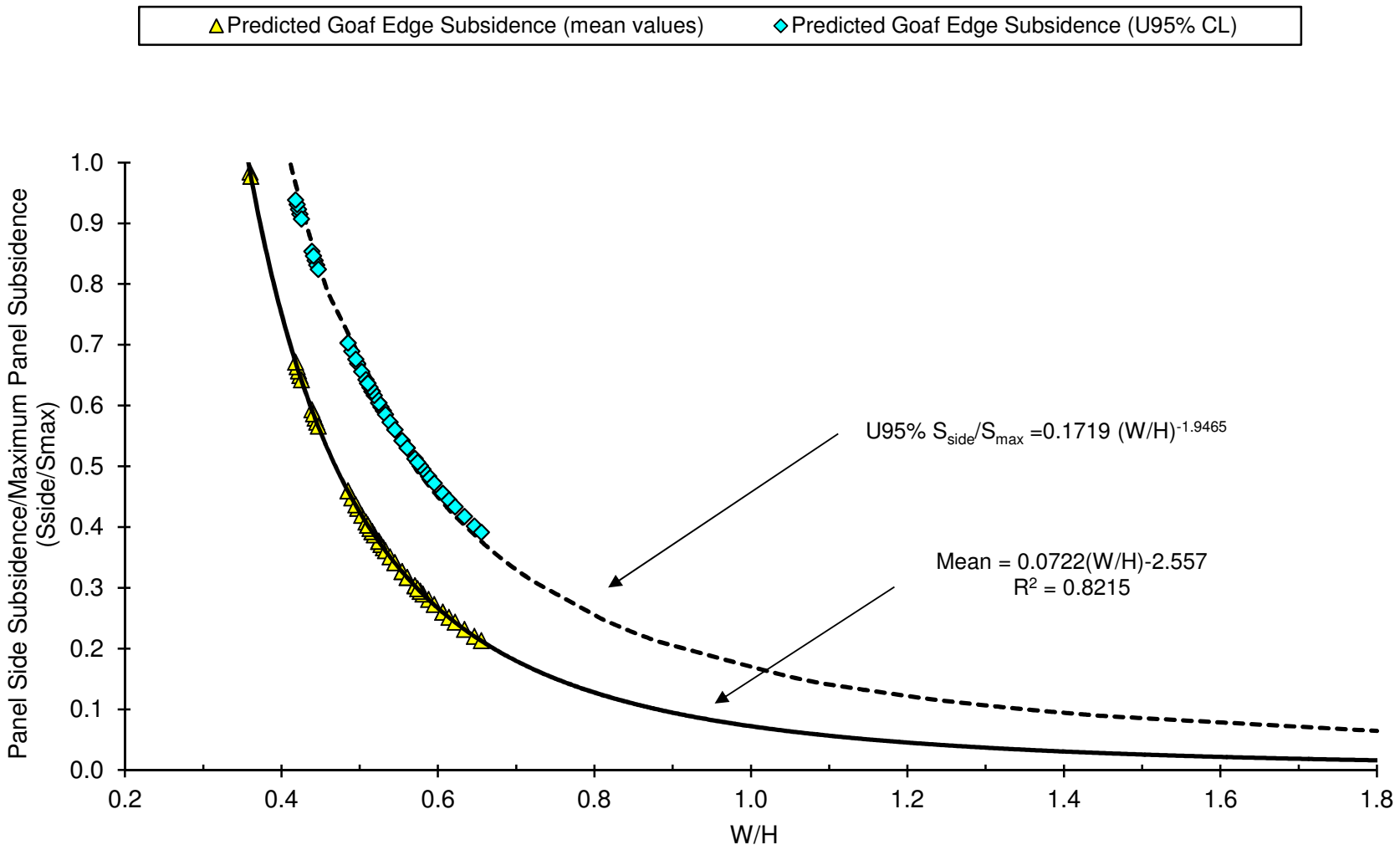
DgS	Engineer:	S.Ditton	Client:	LakeCoal - Chain Valley Colliery CHV-002/4	
	Drawn:	S.Ditton			
	Date:	20.03.15	Title:	Predicted Analytical Model v. Empirical Model Outcomes for Wyee Colliery LWs 17 to 23 Chain Pillar Subsidence based on Effective Cover Depth	
Ditton Geotechnical Services Pty Ltd			Scale:	NTS	Figure No: 18.1



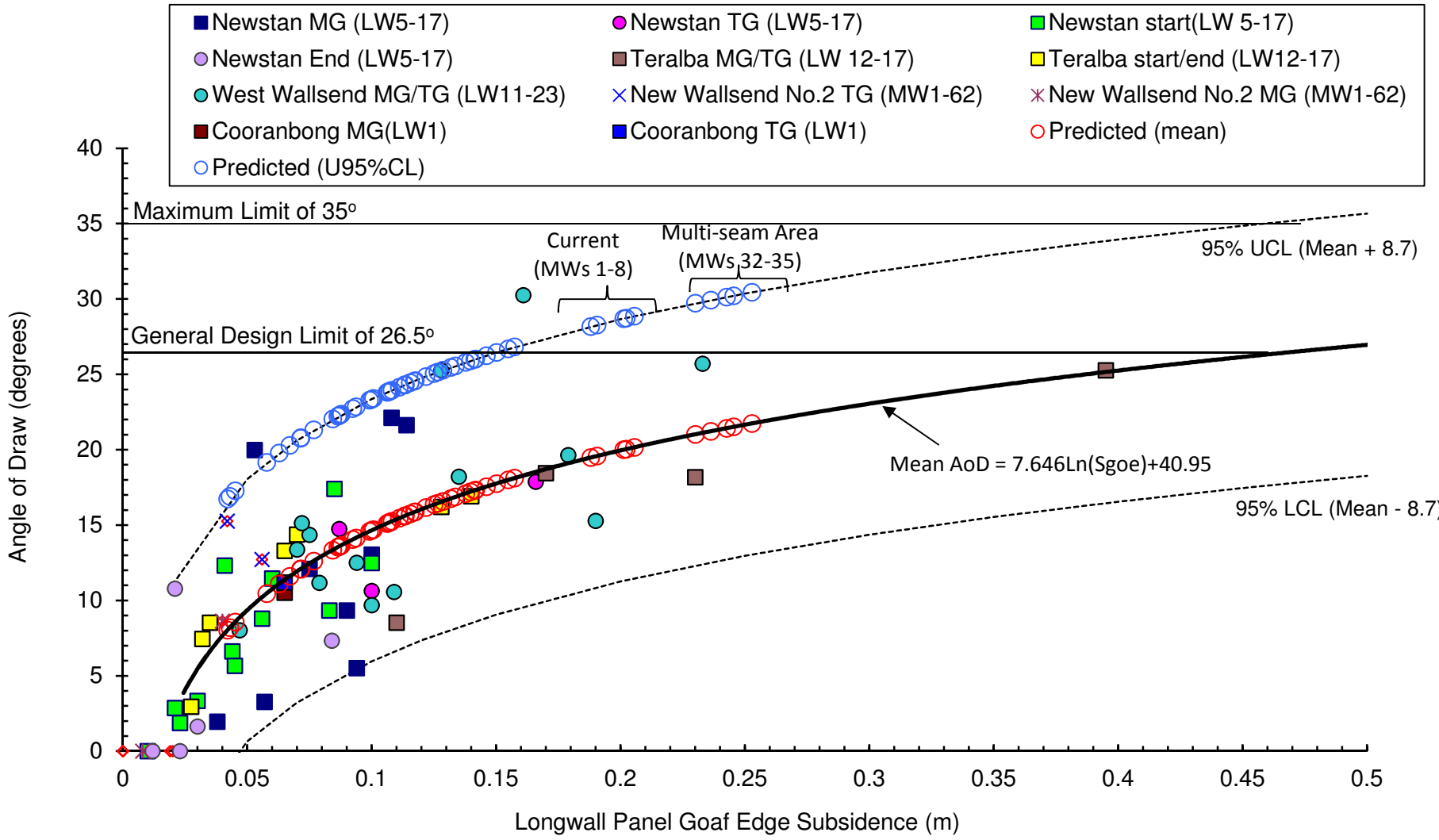
DgS	Engineer:	S.Ditton	Client:	LakeCoal - Chain Valley Colliery CHV-002/4	
	Drawn:	S.Ditton			
	Date:	15.05.15	Title:	Predicted Analytical Model v. Empirical Model Outcomes for CVC Modified MWs 9 to 36 Chain Pillar Subsidence based on Effective Cover Depth	
	Ditton Geotechnical Services Pty Ltd		Scale:	NTS	Figure No: 18.2



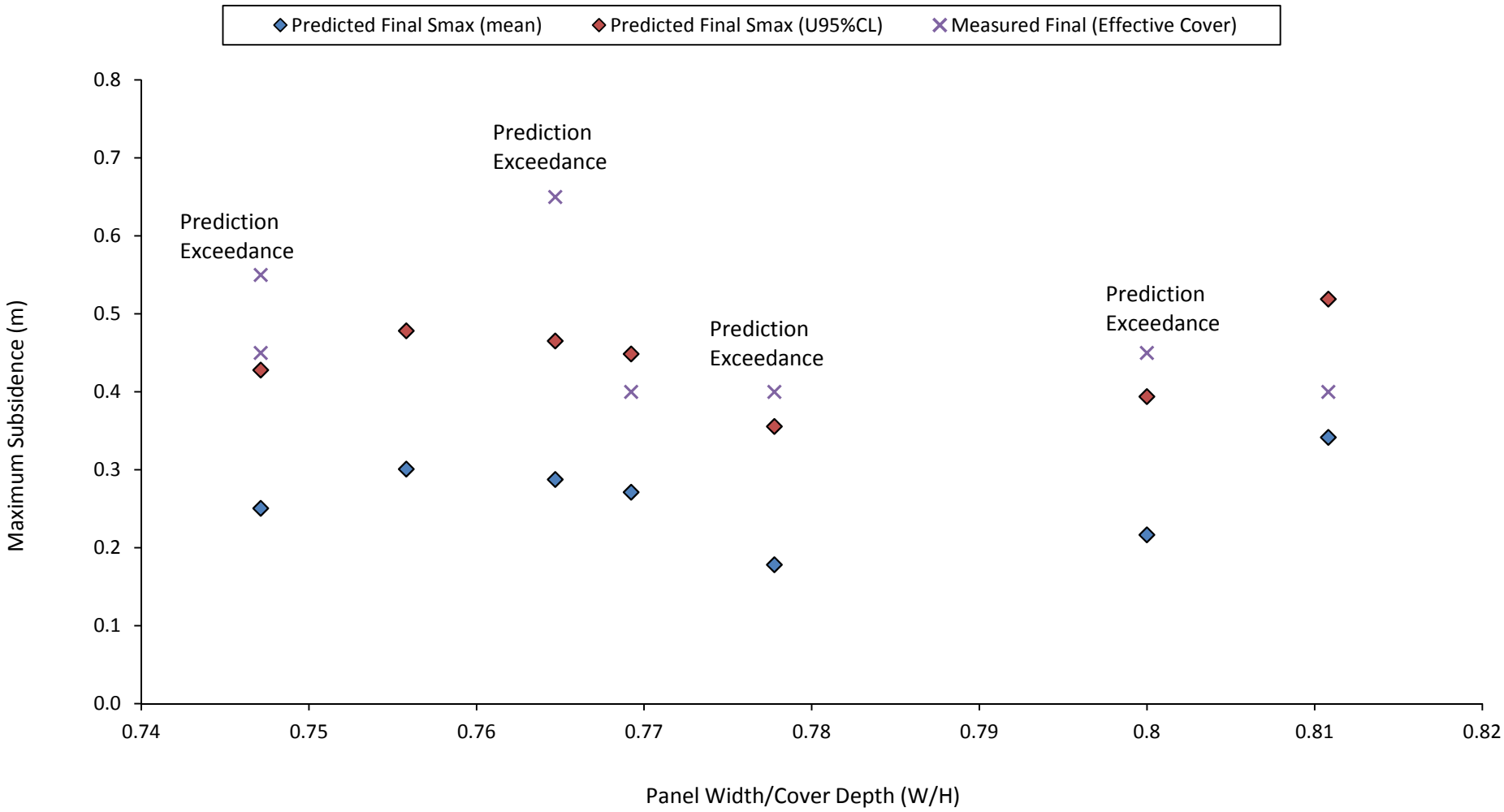
DgS	Engineer:	S.Ditton	Client:	LakeCoal - Chain Valley Colliery CHV-002/4	
	Drawn:	S.Ditton			
	Date:	20.03.15	Title:	Strain Hardening Goaf Model for Estimating Minimum Cover Depth Required for Load on Yielding Chain Pillar to be Transferred to Goaf	
Ditton Geotechnical Services Pty Ltd			Scale:	NTS	Figure No: 19



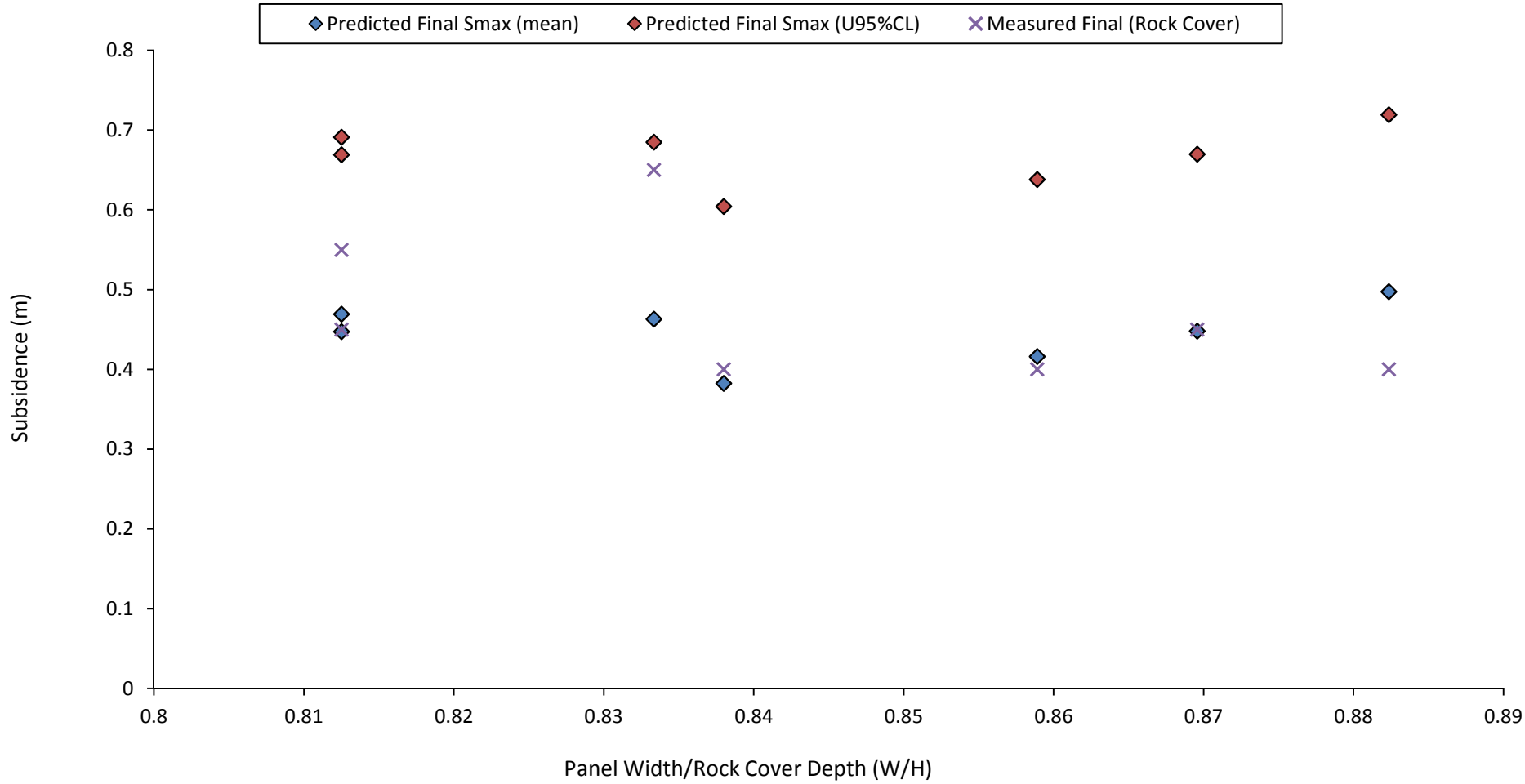
DgS	Engineer:	S.Ditton	Client:	LakeCoal - Chain Valley Colliery	
	Drawn:	S.Ditton		CHV-002/4	
	Date:	20.03.15	Title:	Empirical Model for Goaf Edge Subsidence Prediction Above Miniwall Panels in the	
	Ditton Geotechnical Services Pty Ltd			Newcastle Coalfield and Modified MW 9 to 36 Outcomes	
			Scale:	NTS	Figure No: 20.1



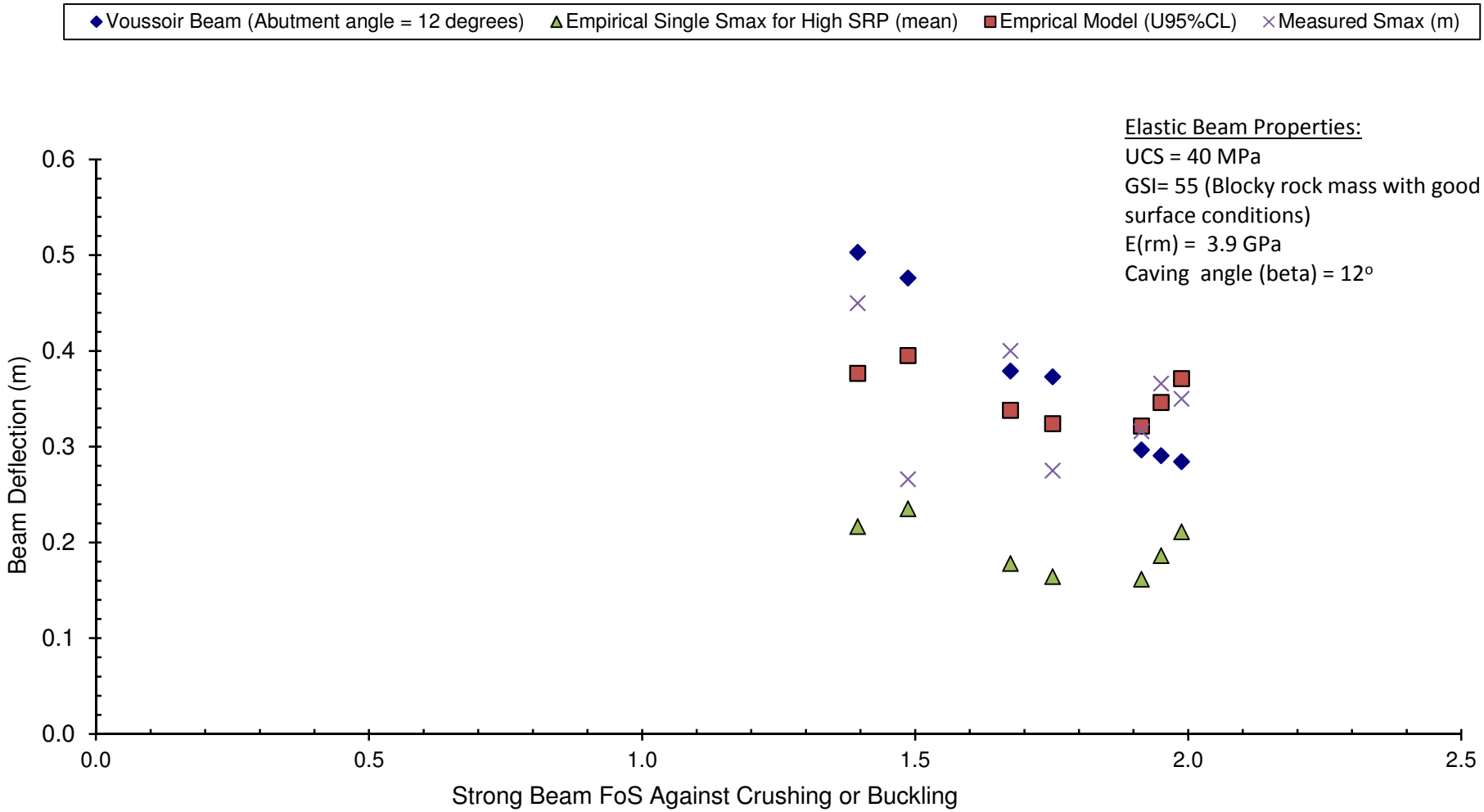
DgS	Engineer:	S.Ditton	Client:	LakeCoal - Chain Valley Colliery CHV-002/4	
	Drawn:	S.Ditton			
	Date:	15.05.5	Title:	Empirical Model for Predicting the Angle of Draw from Longwall Panel Limits in the Newcastle Coalfield (ACARP, 2003) and Modified MWs 9 to 36	
	Ditton Geotechnical Services Pty Ltd		Scale:	NTS	Figure No: 20.2



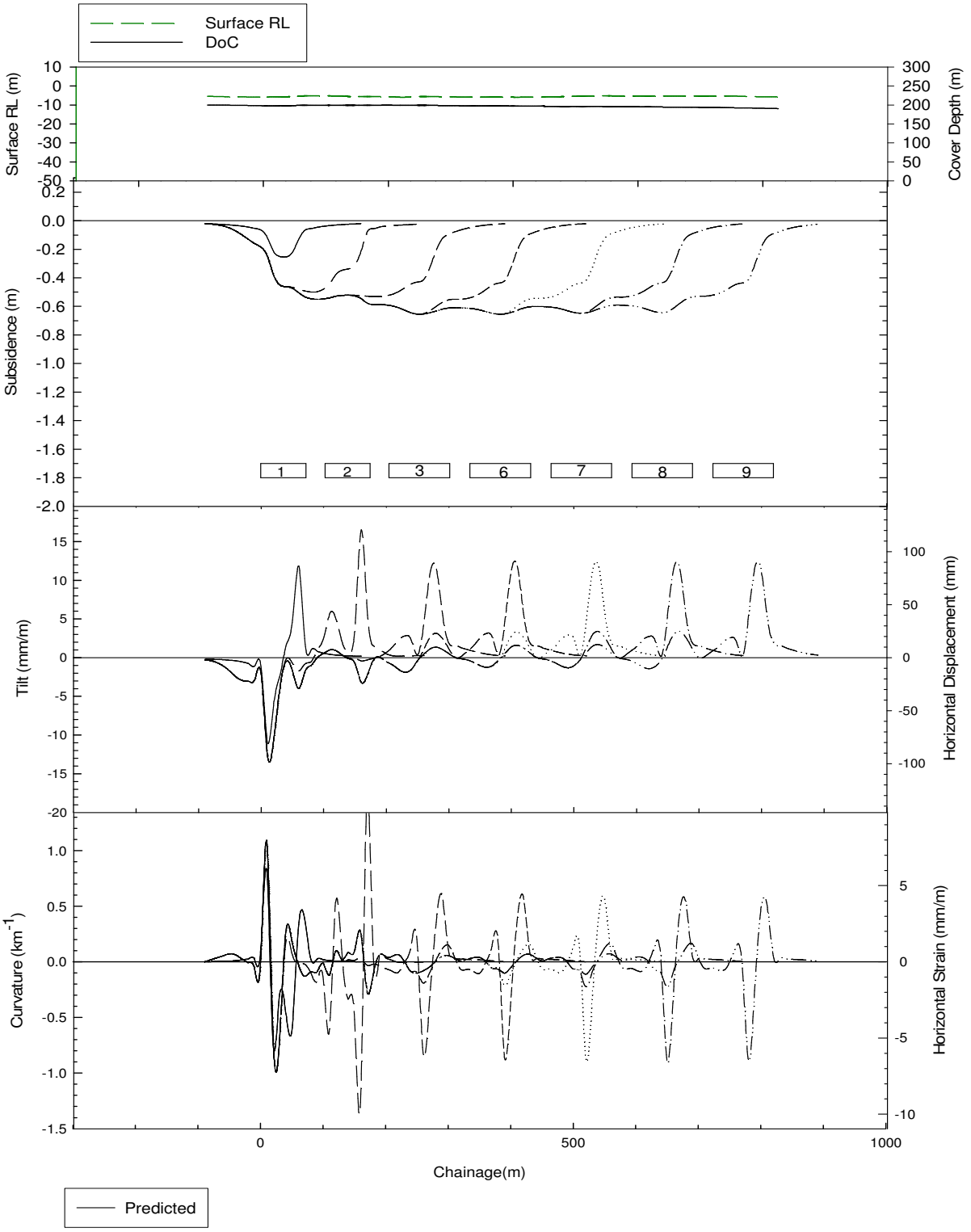
DgS	Engineer:	S.Ditton	Client:	LakeCoal - Chain Valley Colliery CHV-002/4	
	Drawn:	S.Ditton			
	Date:	20.03.15	Title:	Predicted v. Measured Maximum Final Subsidence above Wyee LWs 17 to 23 based on Total Cover Depth	
	Ditton Geotechnical Services Pty Ltd		Scale:	NTS	Figure No: 21.1



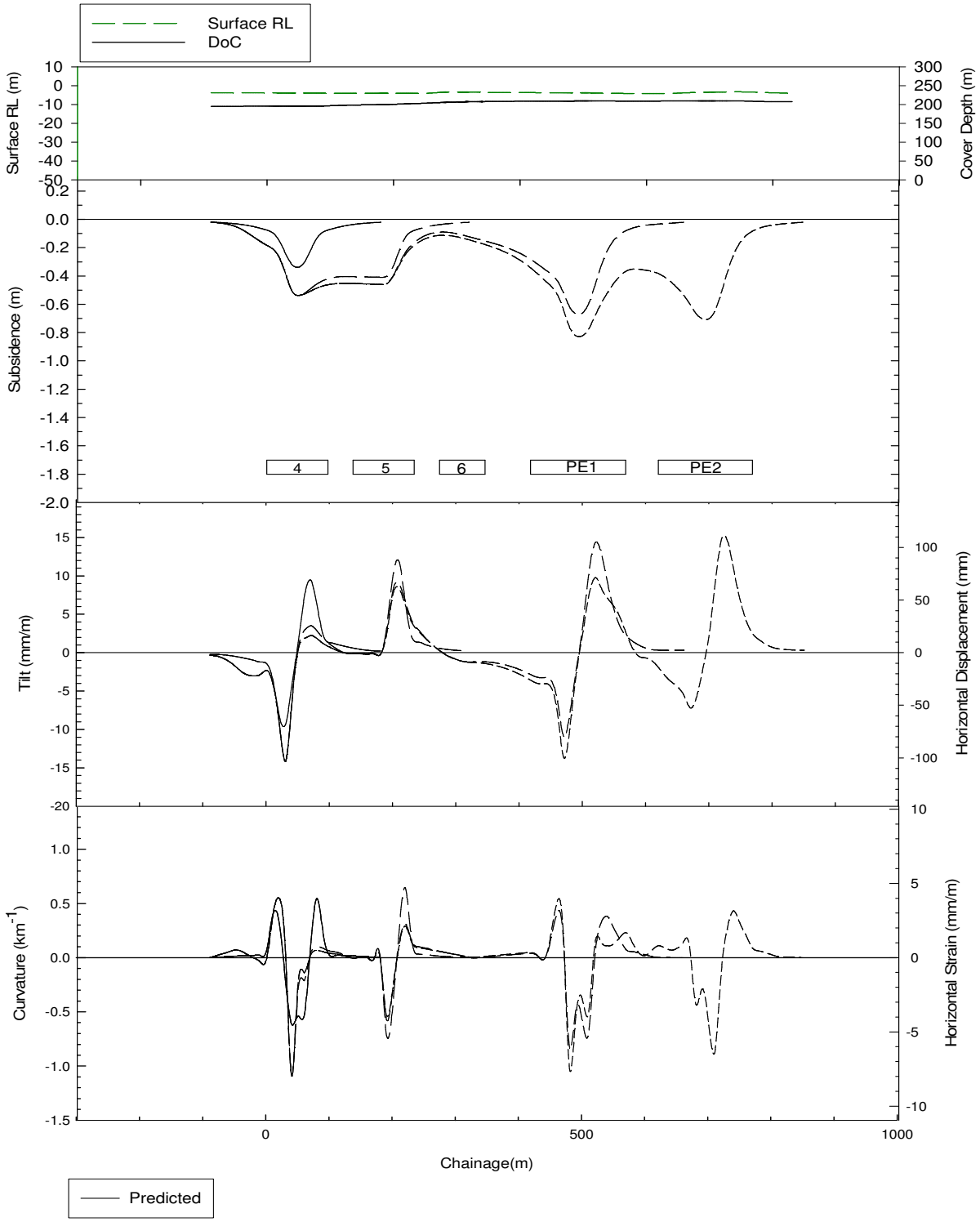
DgS	Engineer:	S.Ditton	Client:	LakeCoal - Chain Valley Colliery CHV-002/4	
	Drawn:	S.Ditton			
	Date:	20.03.15	Title:	Predicted v. Measured Maximum Final Subsidence above Wyee LWs 17 to 23 based on Rock Cover Depth	
	Ditton Geotechnical Services Pty Ltd		Scale:	NTS	Figure No: 21.2



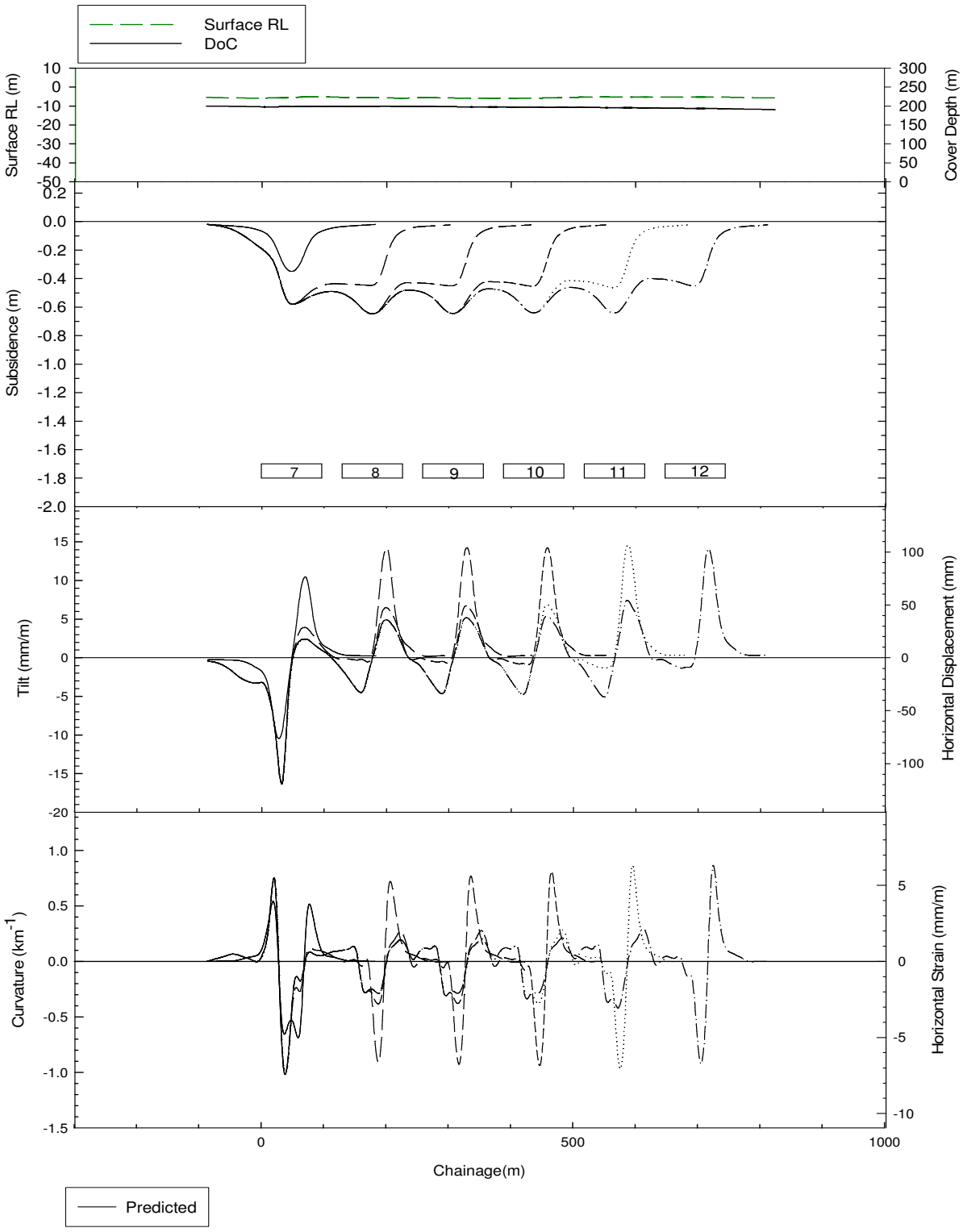
DgS	Engineer:	S.Ditton	Client:	LakeCoal - Chain Valley Colliery CHV-002/4	
	Drawn:	S.Ditton			
	Date:	20.03.15	Title:	Predicted v. Measured Maximum Final Subsidence above Wyee LWs 17 to 23 based on Voussoir Beam Model Analogue	
	Ditton Geotechnical Services Pty Ltd		Scale:	NTS	Figure No: 21.3



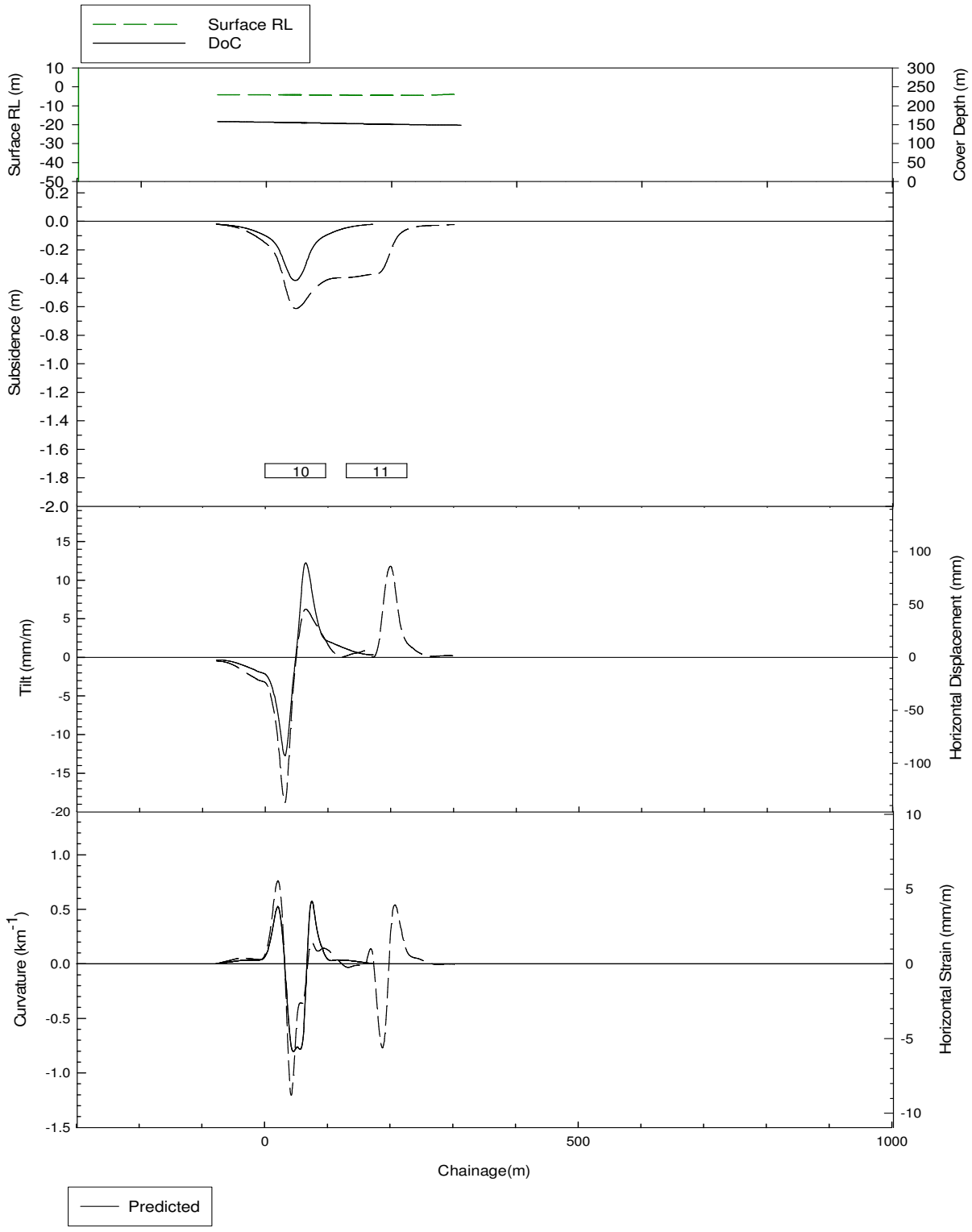
DgS	Engineer:	S.Ditton	Client:	LakeCoal - Chain Valley Colliery	
	Drawn:	S.Ditton		CHV-002/4	
	Date:	15.05.15	Title:	Predicted Subsidence Effects along XL1	
	Ditton Geotechnical			(see Figure 2 for Location)	
	Services Pty Ltd		Scale:		Figure No: 22.1



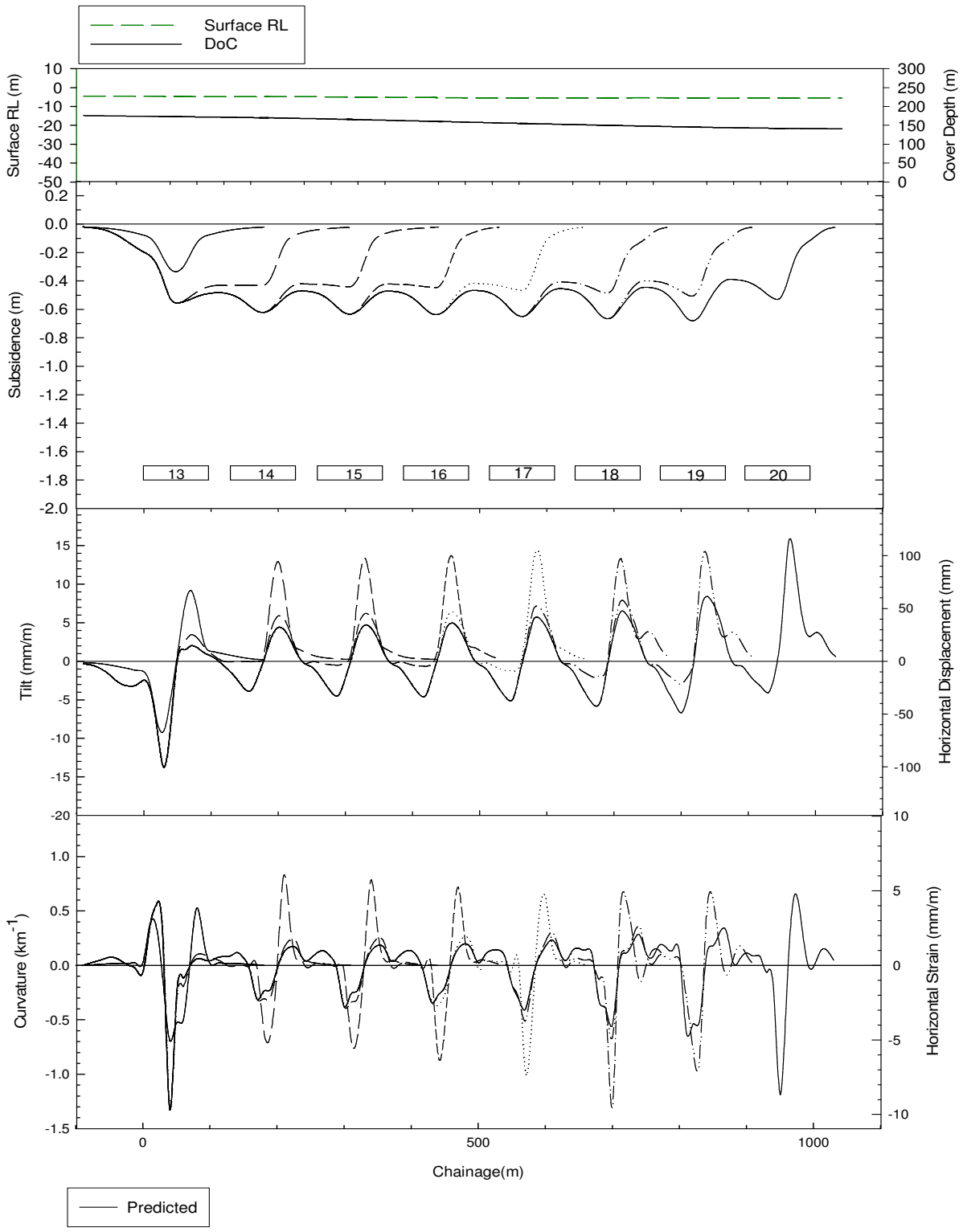
DgS	Engineer:	S.Ditton	Client:	LakeCoal - Chain Valley Colliery	
	Drawn:	S.Ditton		CHV-002/4	
	Date:	15.05.15	Title:	Predicted Subsidence Effects along XL2	
	Ditton Geotechnical			(see Figure 2 for Location)	
	Services Pty Ltd		Scale:	NTS	Figure No: 22.2



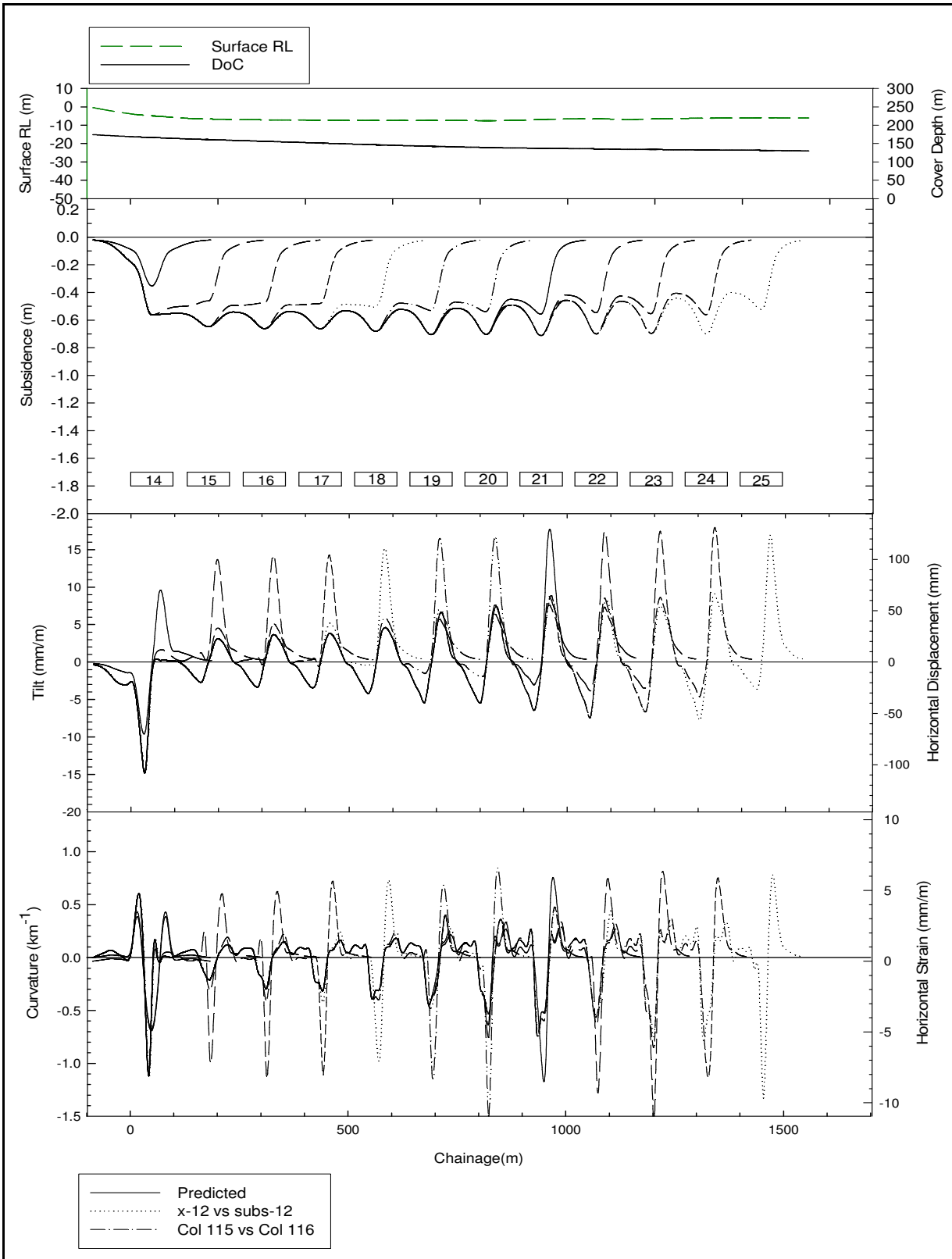
DgS	Engineer:	S.Ditton	Client:	LakeCoal - Chain Valley Colliery	
	Drawn:	S.Ditton		CHV-002/4	
	Date:	15.05.15	Title:	Predicted Subsidence Effects along XL3	
	Ditton Geotechnical			(see Figure 2 for Location)	
	Services Pty Ltd		Scale:		Figure No: 22.3



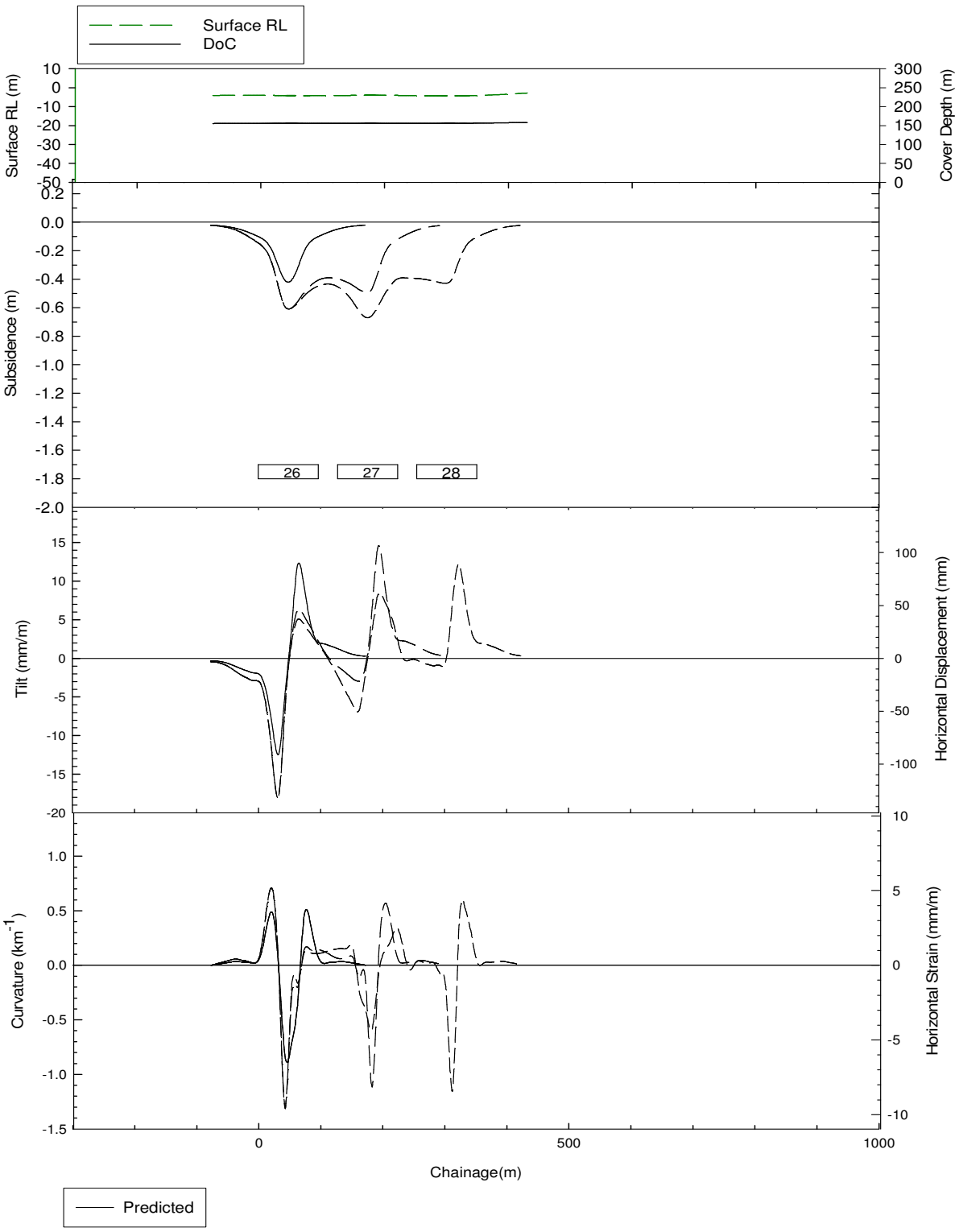
DgS	Engineer:	S.Ditton	Client:	LakeCoal - Chain Valley Colliery	
	Drawn:	S.Ditton		CHV-002/4	
	Date:	15.05.15	Title:	Predicted Subsidence Effects along XL4	
	Ditton Geotechnical Services Pty Ltd			(see Figure 2 for Location)	
			Scale:		Figure No: 22.4



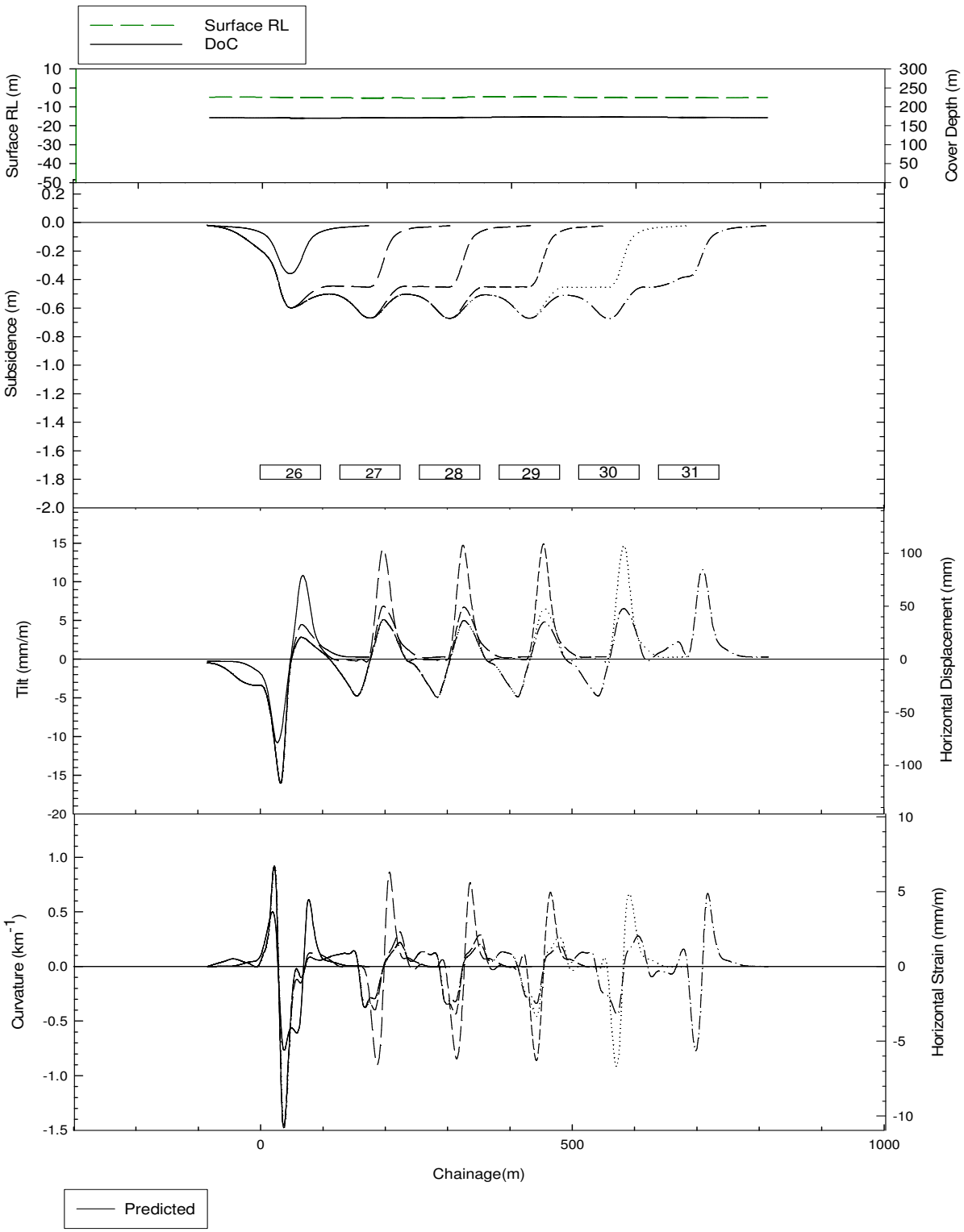
DgS	Engineer:	S.Ditton	Client:	LakeCoal - Chain Valley Colliery	
	Drawn:	S.Ditton		CHV-002/4	
	Date:	15.05.15	Title:	Predicted Subsidence Effects along XL5	
	Ditton Geotechnical			(see Figure 2 for Location)	
	Services Pty Ltd		Scale:		Figure No: 22.5



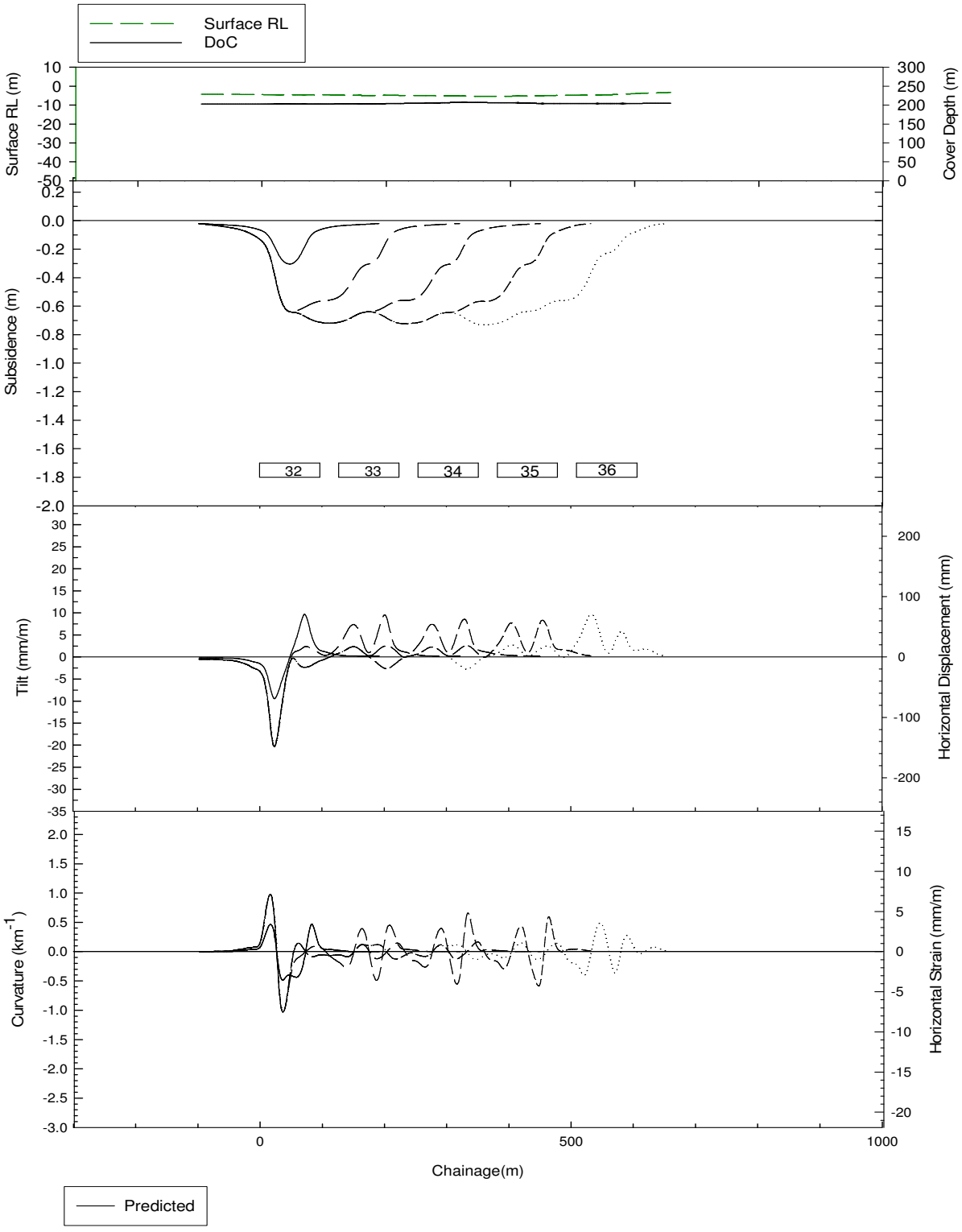
DgS	Engineer:	S.Ditton	Client:	LakeCoal - Chain Valley Colliery	
	Drawn:	S.Ditton		CHV-002/4	
	Date:	15.05.15	Title:	Predicted Subsidence Effects along XL6	
	Ditton Geotechnical			(see Figure 2 for Location)	
	Services Pty Ltd		Scale:		Figure No: 22.6



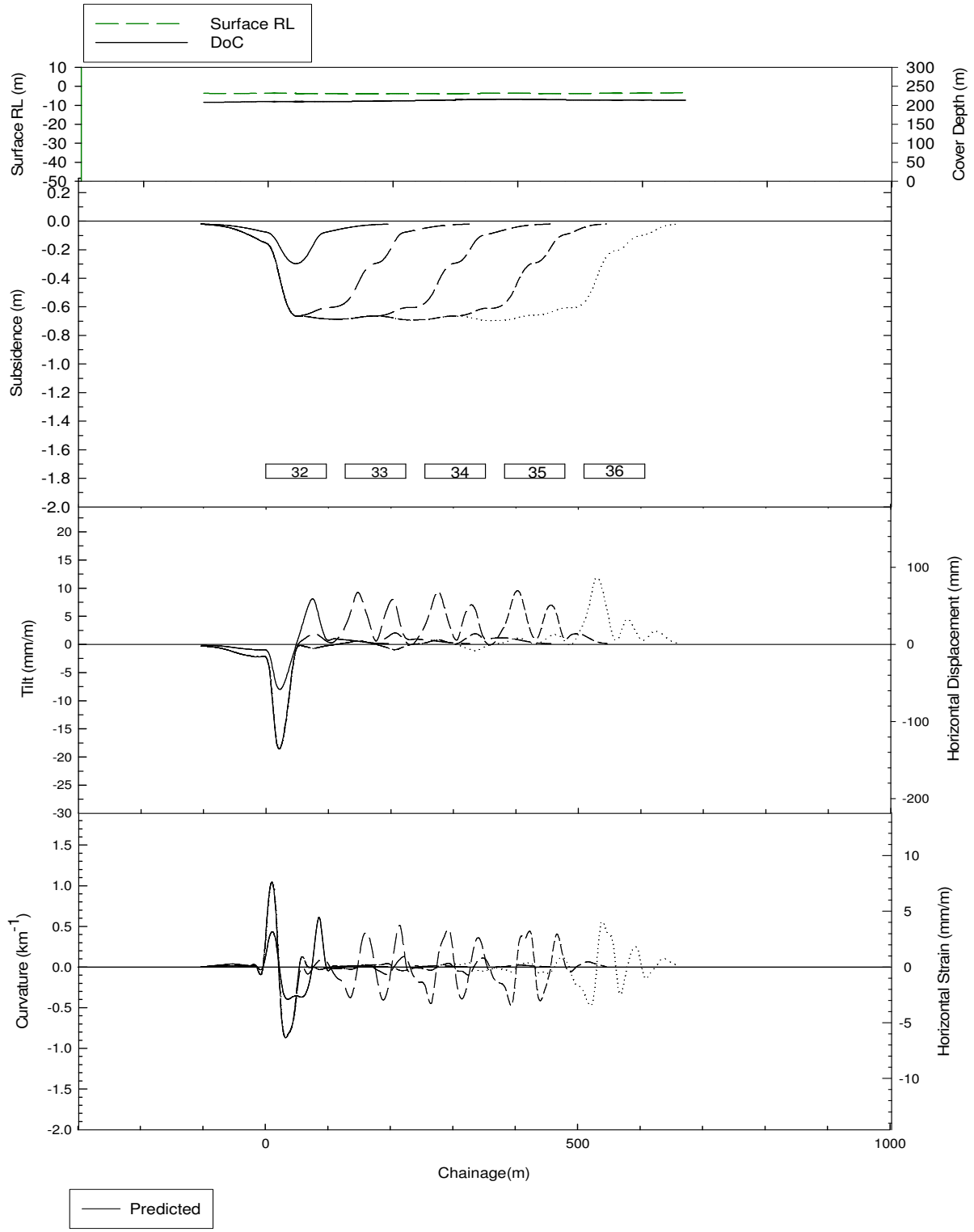
DgS	Engineer:	S.Ditton	Client:	LakeCoal - Chain Valley Colliery	
	Drawn:	S.Ditton		CHV-002/4	
	Date:	15.05.15	Title:	Predicted Subsidence Effects along XL7	
	Ditton Geotechnical			(see Figure 2 for Location)	
	Services Pty Ltd		Scale:		Figure No: 22.7



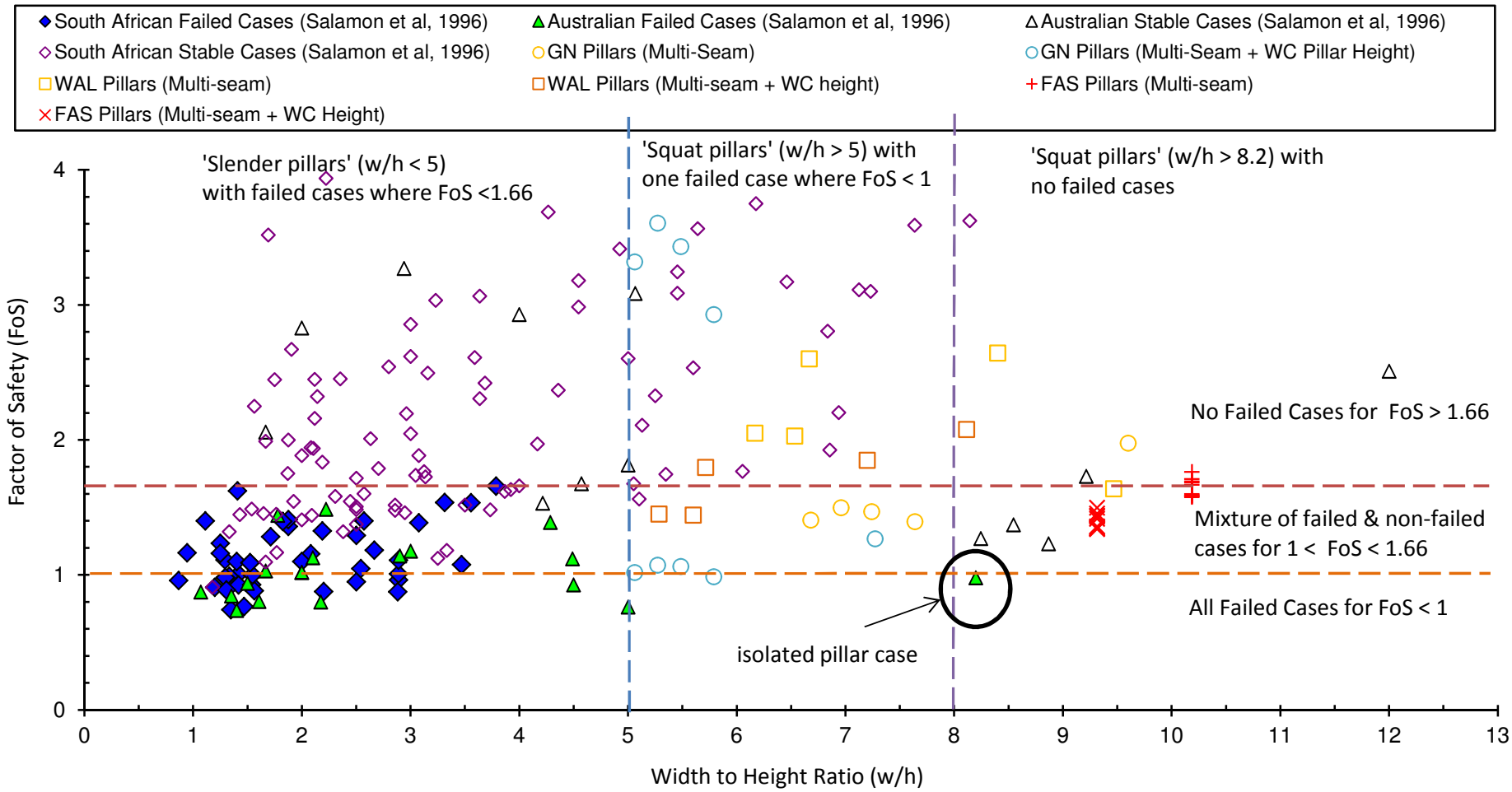
DgS	Engineer:	S.Ditton	Client:	LakeCoal - Chain Valley Colliery	
	Drawn:	S.Ditton		CHV-002/4	
	Date:	15.05.15	Title:	Predicted Subsidence Effects along XL8	
	Ditton Geotechnical			(see Figure 2 for Location)	
	Services Pty Ltd		Scale:		Figure No: 22.8



DgS	Engineer:	S.Ditton	Client:	LakeCoal - Chain Valley Colliery	
	Drawn:	S.Ditton		CHV-002/4	
	Date:	15.05.15	Title:	Predicted Subsidence Effects along XL9	
	Ditton Geotechnical			(see Figure 2 for Location)	
	Services Pty Ltd		Scale:		Figure No: 22.9

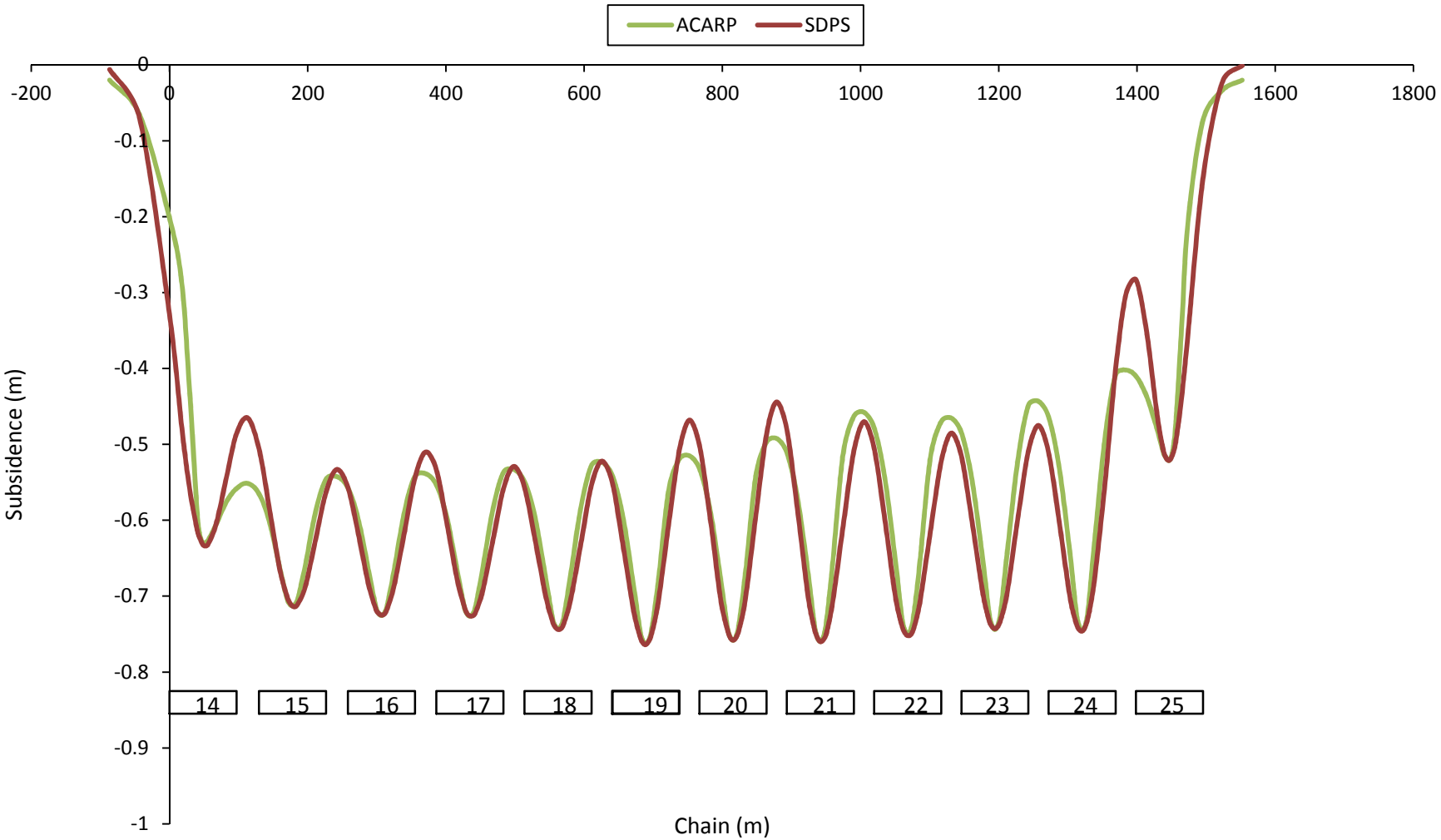


DgS	Engineer:	S.Ditton	Client:	LakeCoal - Chain Valley Colliery	
	Drawn:	S.Ditton		CHV-002/4	
	Date:	15.05.15	Title:	Predicted Subsidence Effects along XL10	
	Ditton Geotechnical			(see Figure 2 for Location)	
	Services Pty Ltd		Scale:		Figure No: 22.10

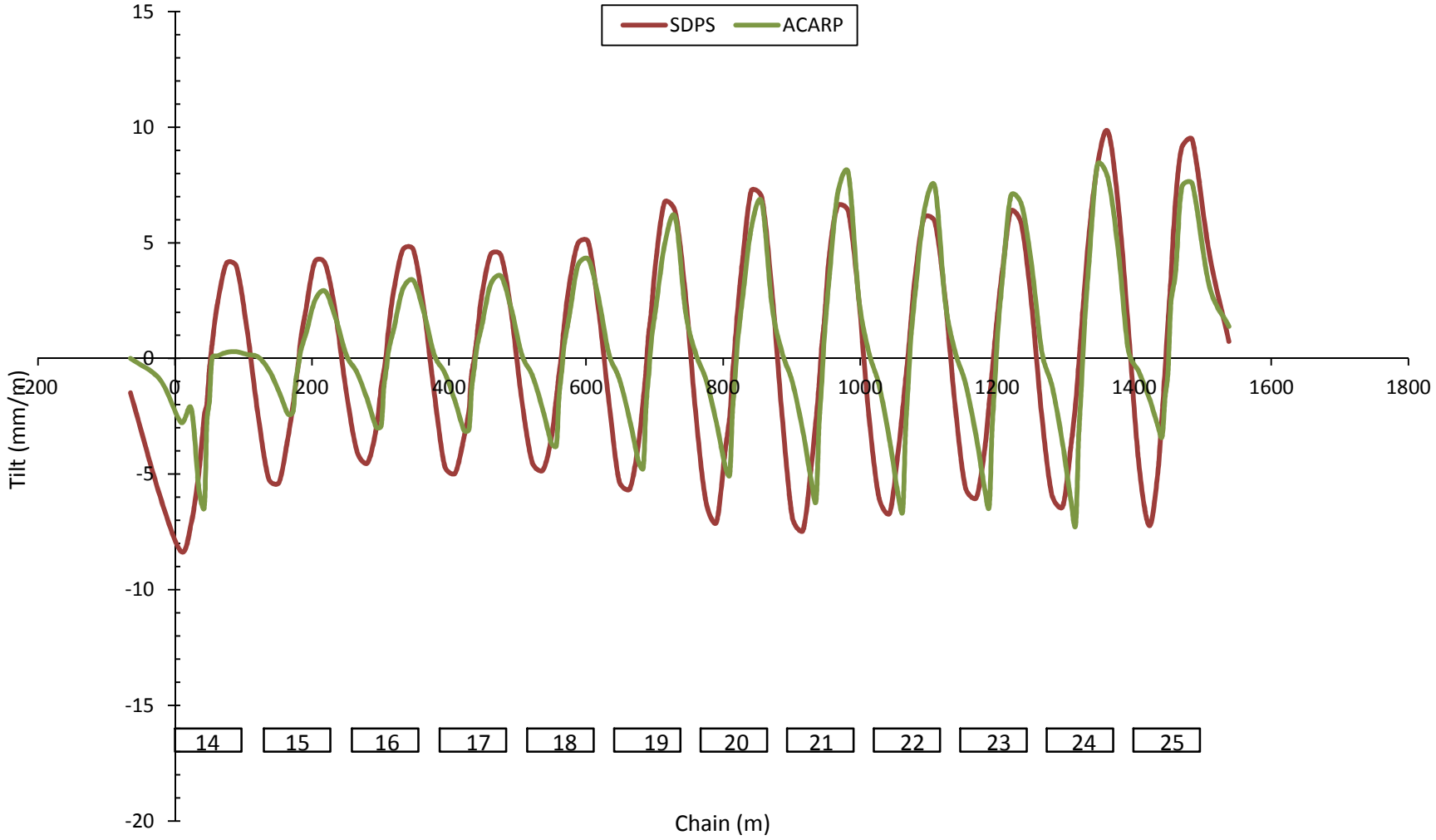


Data extracted from Salamon, *et al* 1996.

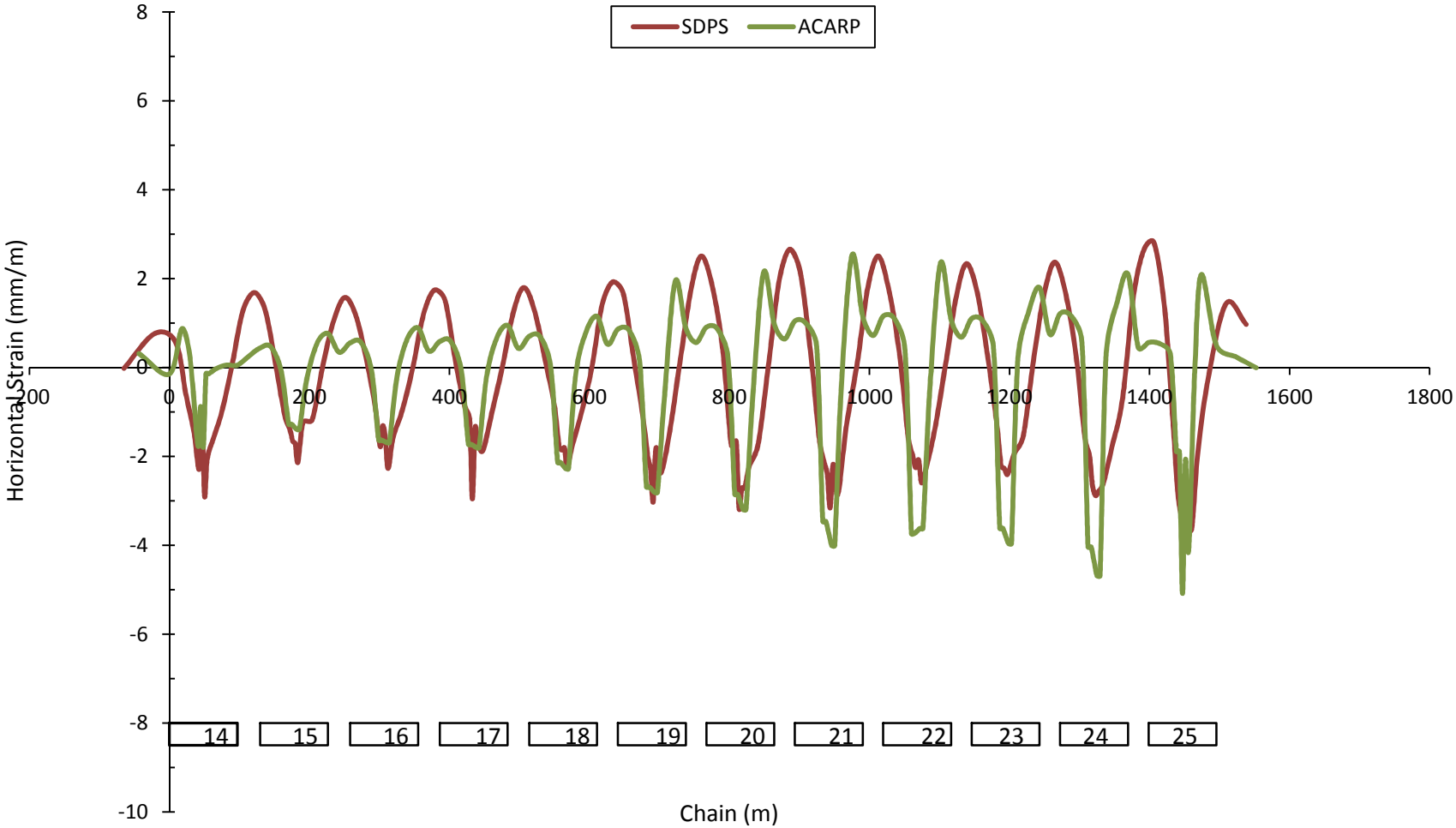
DgS	Engineer:	S.Ditton	Client:	LakeCoal - Chain Valley Colliery CHV-002/4	
	Drawn:	S.Ditton			
	Date:	20.03.15	Title:	Database of Failed and Stable Bord and Pillar Panels from Australian and South African Coal Mines with Proposed MW32-36 Pillars	
	Ditton Geotechnical Services Pty Ltd		Scale:	NTS	Figure No: 23



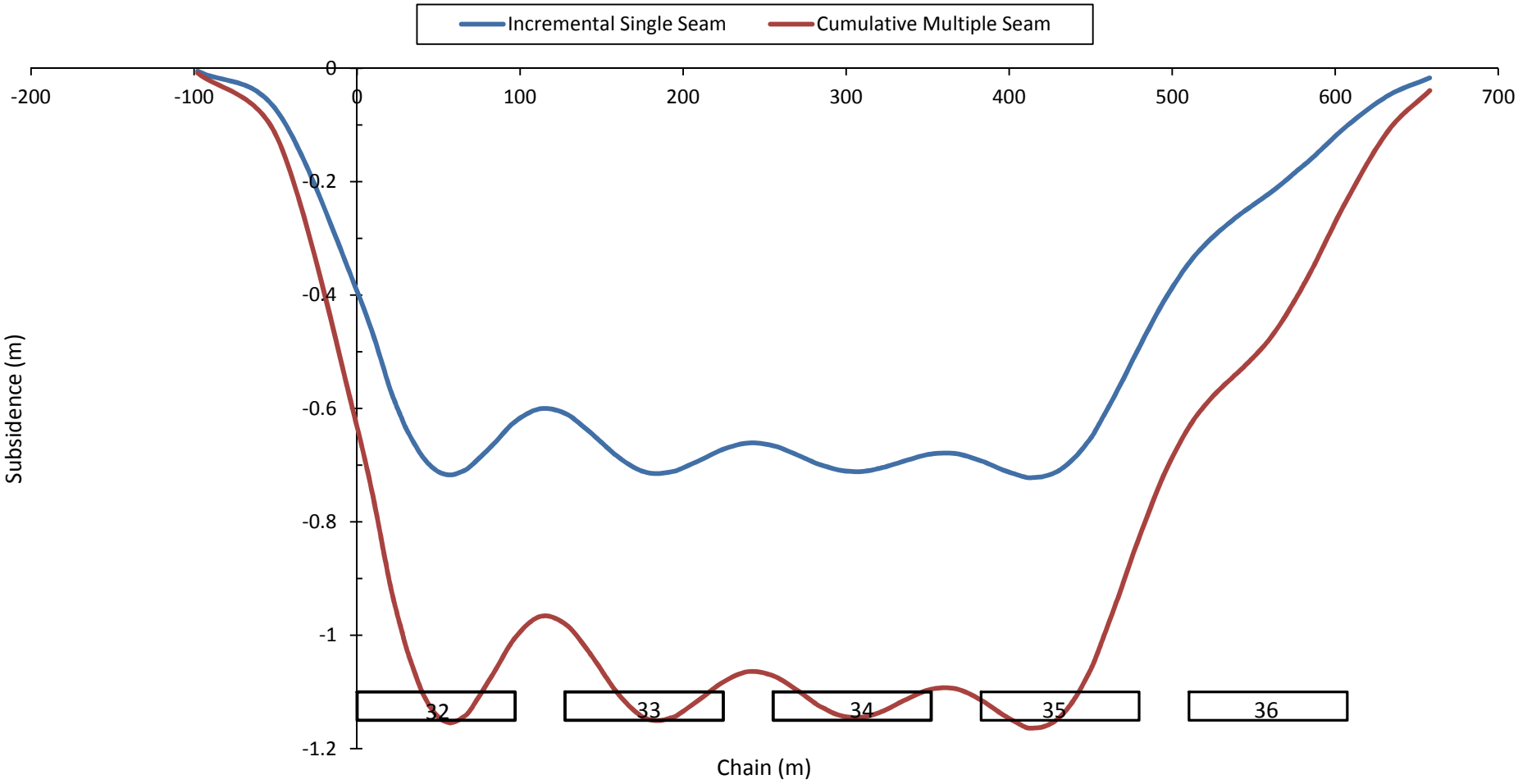
DgS	Engineer:	S.Ditton	Client:	LakeCoal - Chain Valley Colliery CHV-002/4	
	Drawn:	S.Ditton			
	Date:	15.05.15	Title:	Calibrated SDPS v. ACARP, 2003 Model Subsidence Profiles along XL6	
	Ditton Geotechnical Services Pty Ltd		Scale:	NTS	Figure No: 24.1



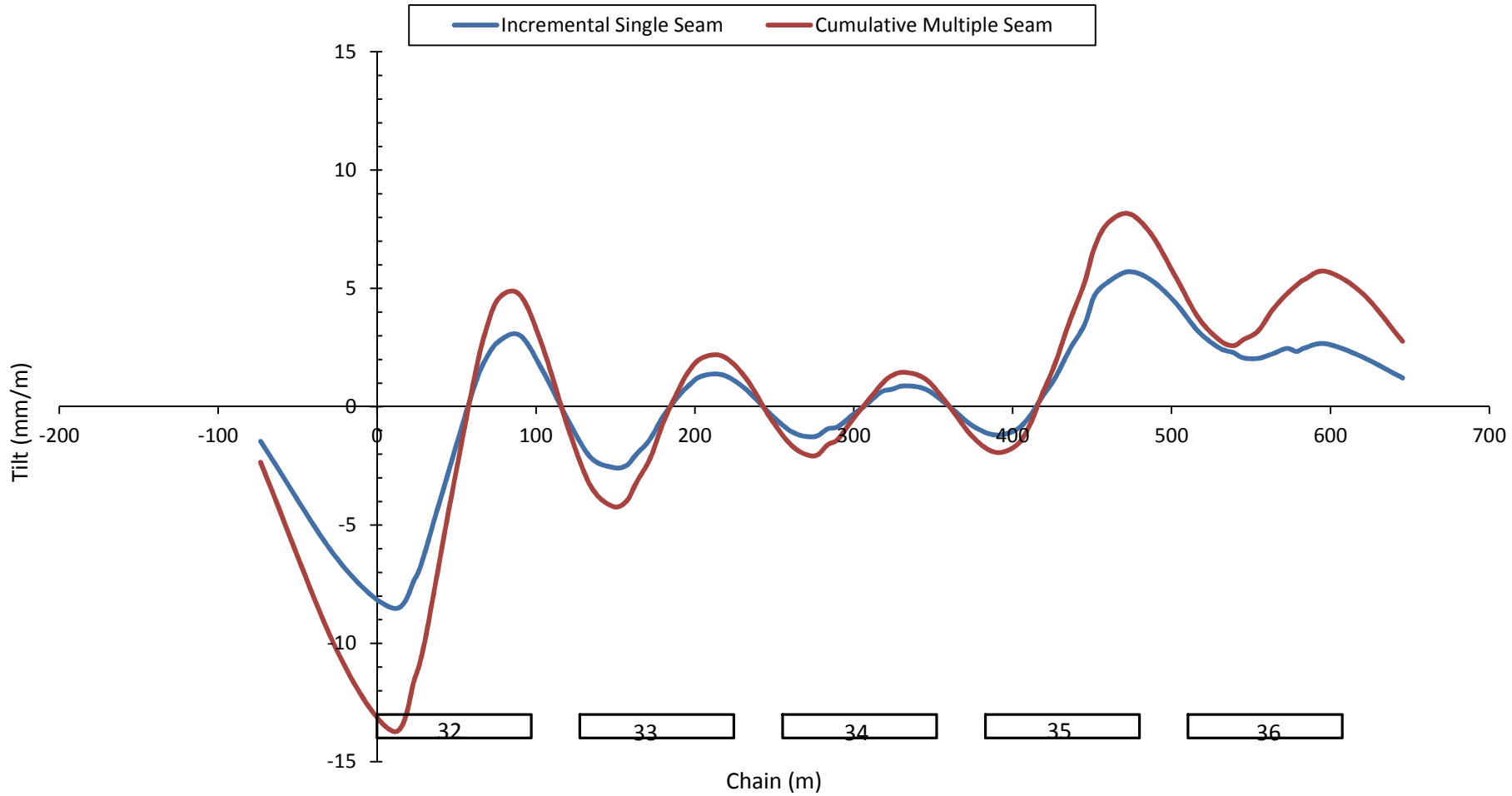
DgS	Engineer:	S.Ditton	Client:	LakeCoal - Chain Valley Colliery CHV-002/4	
	Drawn:	S.Ditton			
	Date:	15.05.15	Title:	Calibrated SDPS v. ACARP, 2003 Model Tilt Profiles along XL6	
	Ditton Geotechnical Services Pty Ltd		Scale:	NTS	Figure No: 24.2



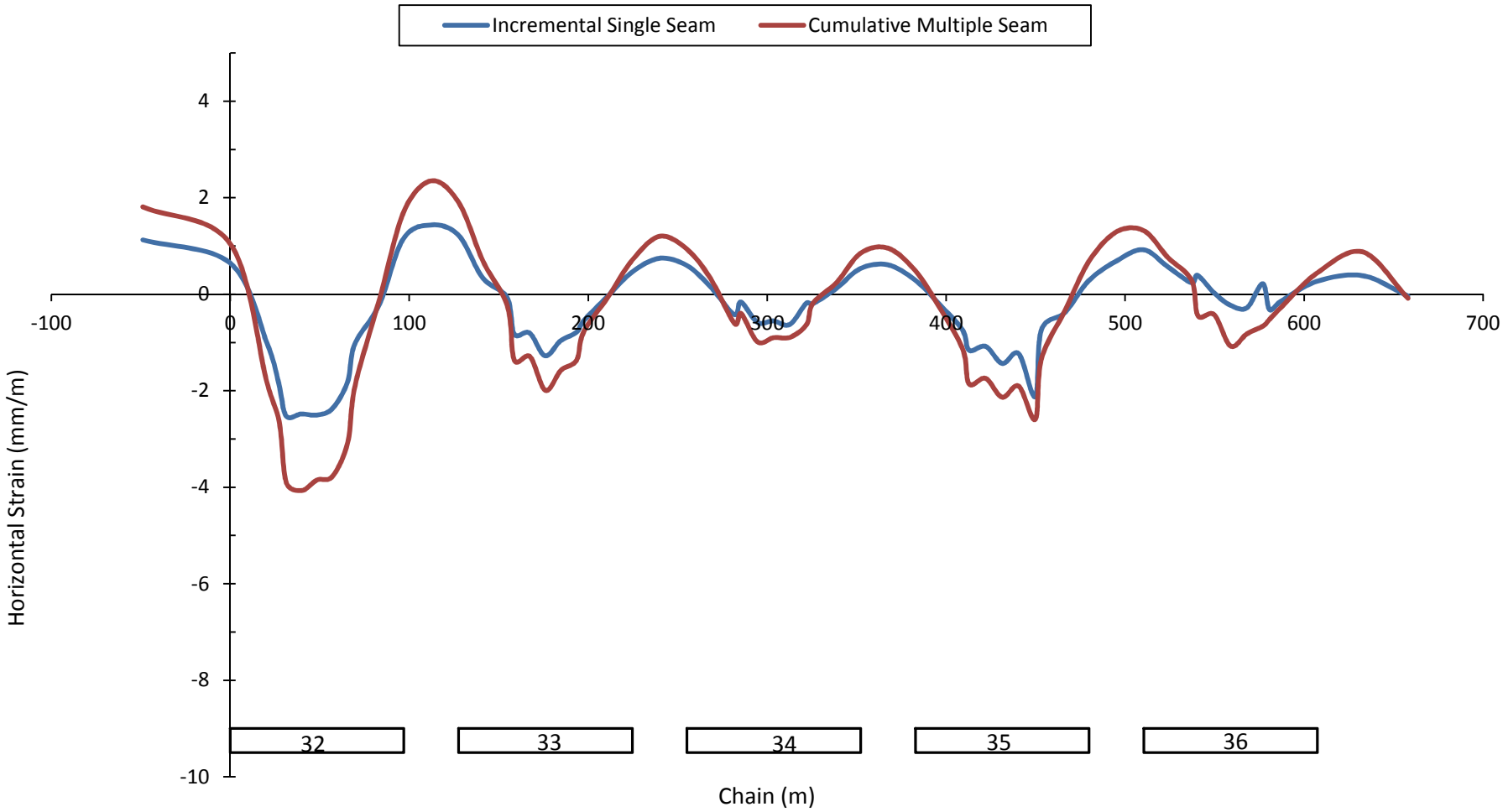
DgS	Engineer:	S.Ditton	Client:	LakeCoal - Chain Valley Colliery CHV-002/4	
	Drawn:	S.Ditton			
	Date:	15.05.15	Title:	Calibrated SDPS v. ACARP, 2003 Model Strain Profiles along XL6	
	Ditton Geotechnical Services Pty Ltd		Scale:	NTS	Figure No: 24.3



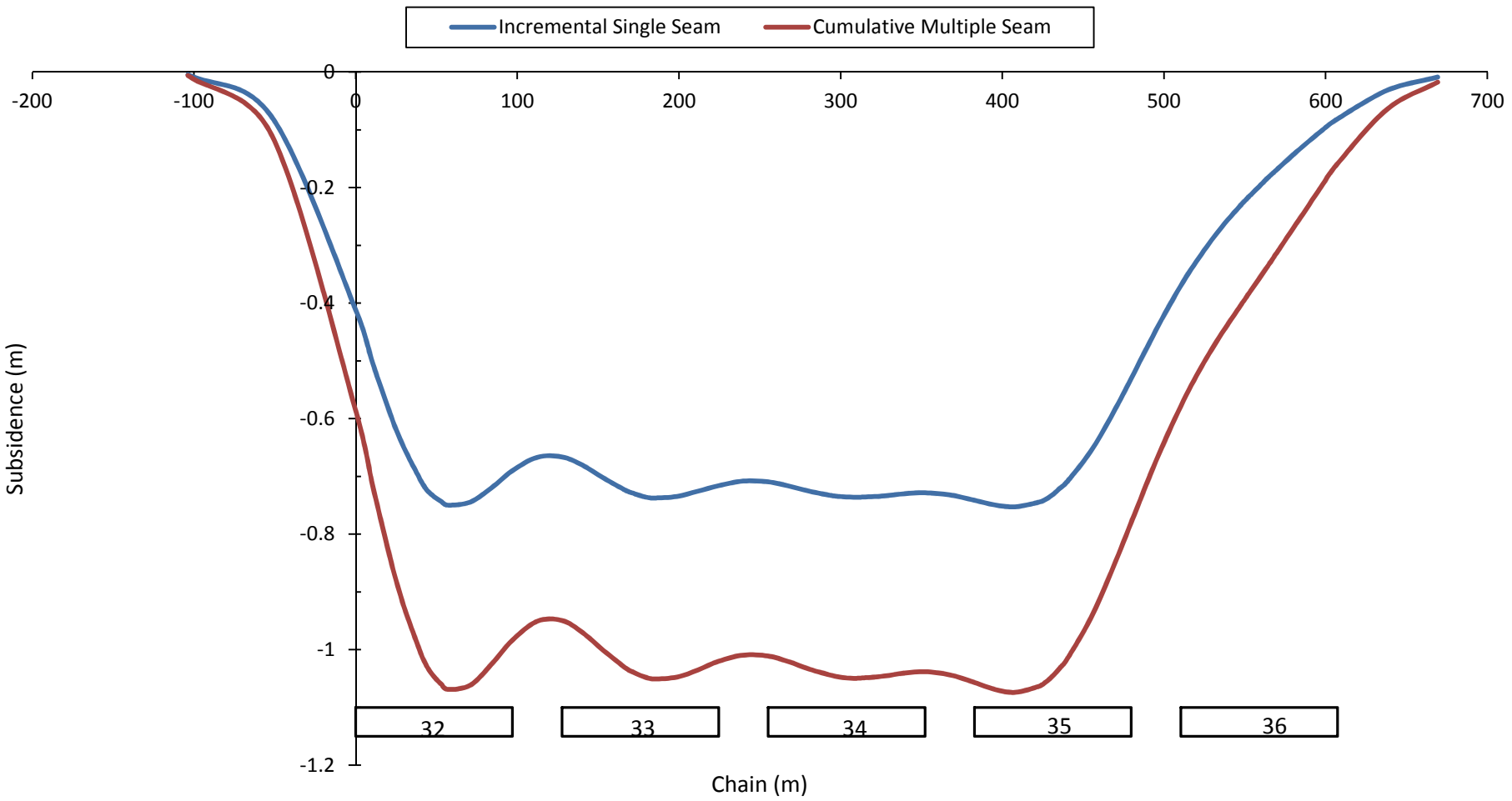
DgS	Engineer:	S.Ditton	Client:	LakeCoal - Chain Valley Colliery CHV-002/4	
	Drawn:	S.Ditton			
	Date:	15.05.15	Title:	Calibrated SDPS Single and Multi-Seam Model Subsidence Profiles along XL9 above Modified MWs 32 to 36	
	Ditton Geotechnical Services Pty Ltd		Scale:	NTS	Figure No: 25.1



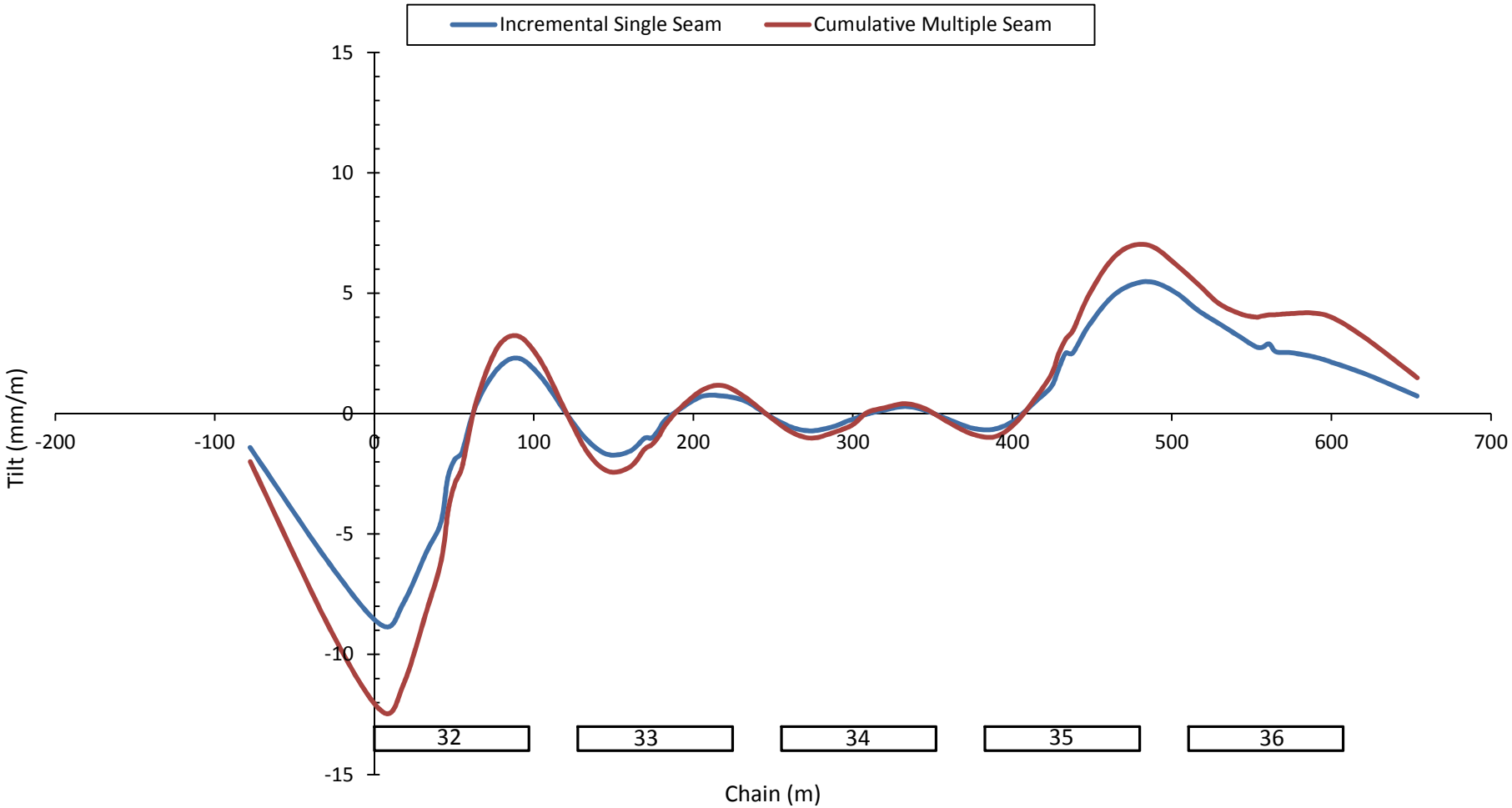
DgS	Engineer:	S.Ditton	Client:	LakeCoal - Chain Valley Colliery CHV-002/4	
	Drawn:	S.Ditton			
	Date:	15.05.15	Title:	Calibrated SDPS Single and Multi-Seam Model Tilt Profiles along XL9 above Modified MWs 32 to 36	
	Ditton Geotechnical Services Pty Ltd		Scale:	NTS	Figure No: 25.2



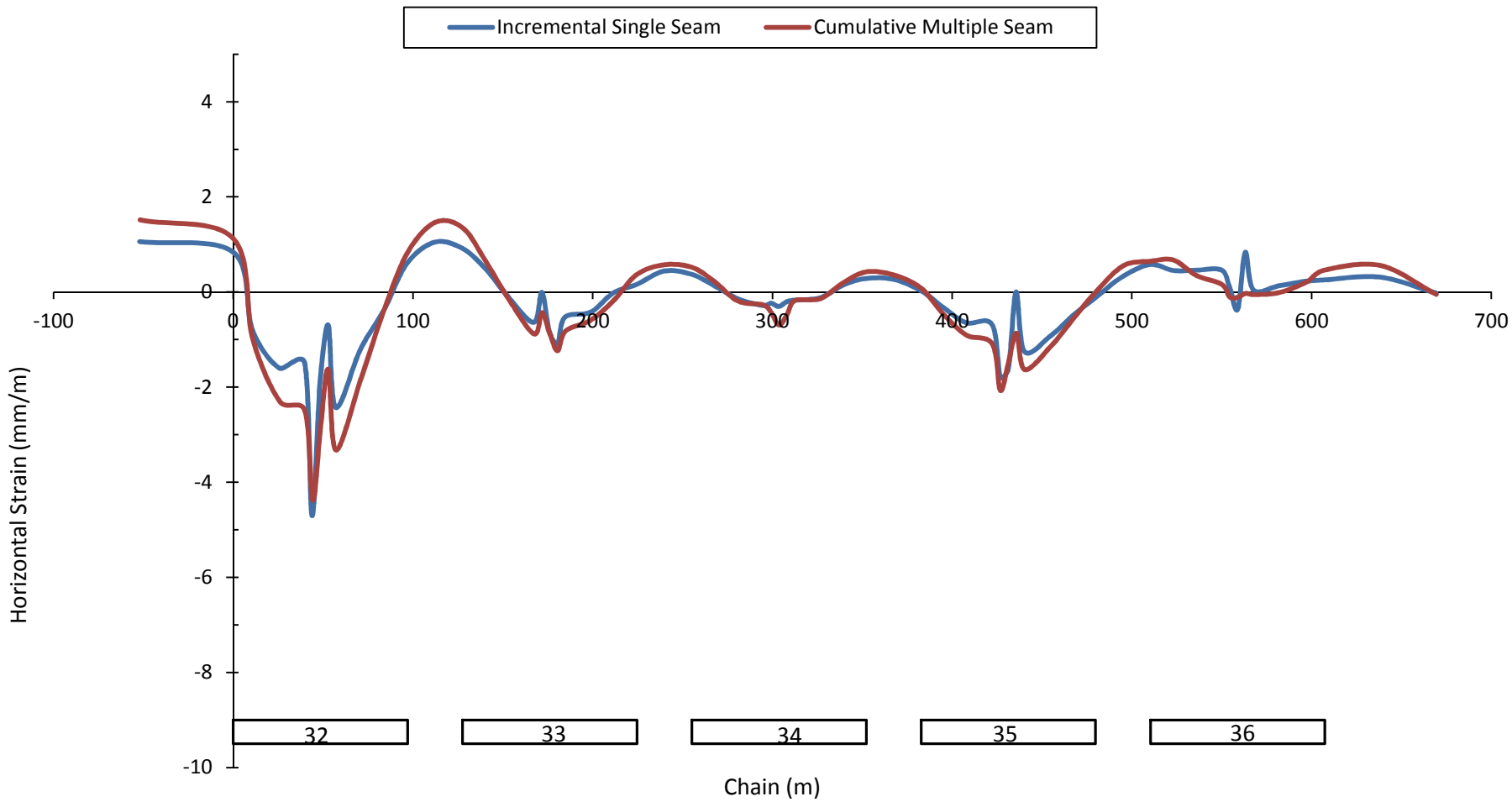
DgS	Engineer:	S.Ditton	Client:	LakeCoal - Chain Valley Colliery CHV-002/4	
	Drawn:	S.Ditton			
	Date:	15.05.15	Title:	Calibrated SDPS Single and Multi-Seam Model Strain Profiles along XL9 above Modified MWs 32 to 36	
	Ditton Geotechnical Services Pty Ltd		Scale:	NTS	Figure No: 25.3



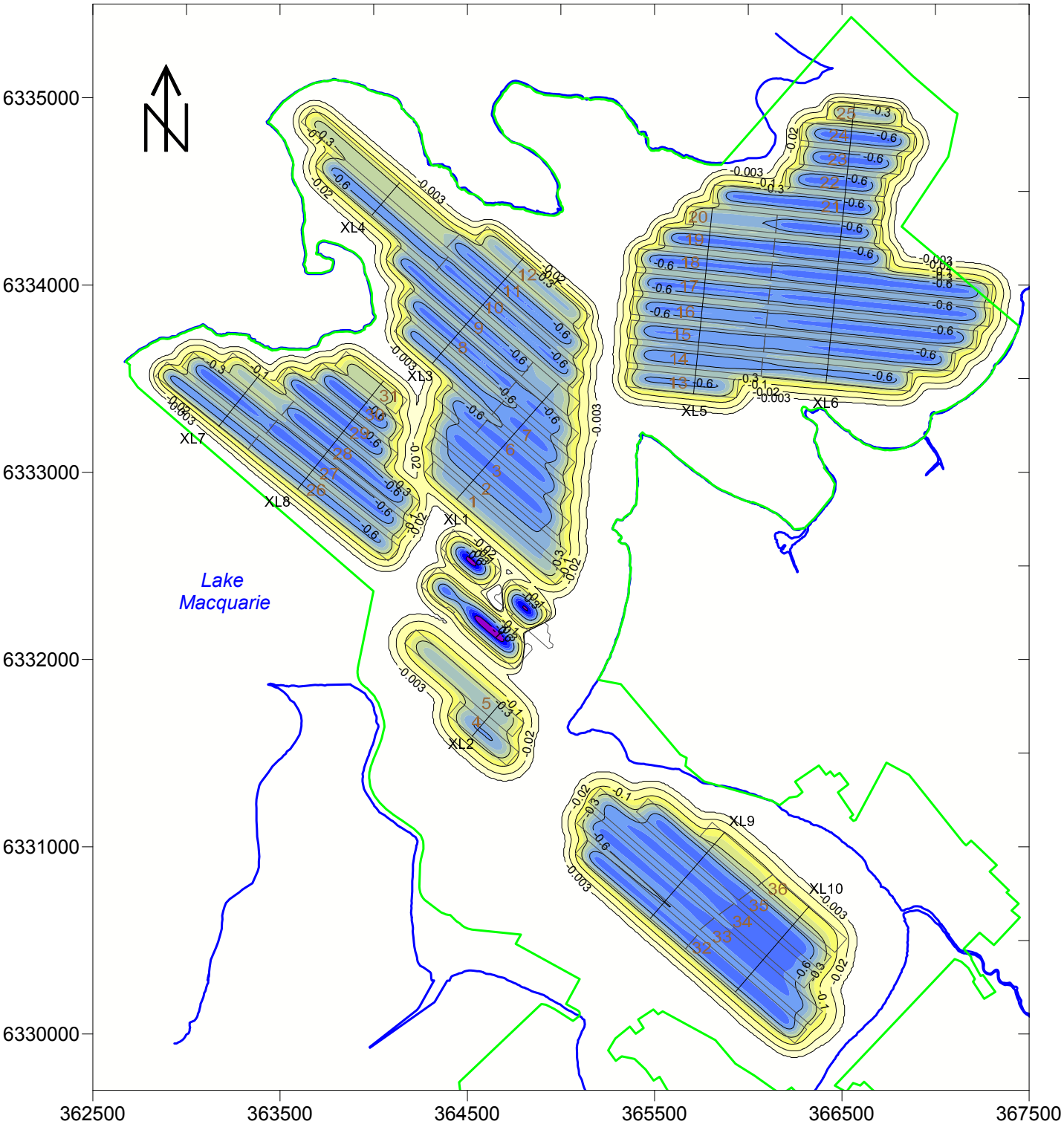
DgS	Engineer:	S.Ditton	Client:	LakeCoal - Chain Valley Colliery CHV-002/4	
	Drawn:	S.Ditton			
	Date:	20.03.15	Title:	Calibrated SDPS Single and Multi-Seam Model Subsidence Profiles along XL10 above Modified MWs 32 to 36	
	Ditton Geotechnical Services Pty Ltd		Scale:	NTS	Figure No: 25.4



DgS	Engineer:	S.Ditton	Client:	LakeCoal - Chain Valley Colliery CHV-002/4	
	Drawn:	S.Ditton			
	Date:	20.03.15	Title:	Calibrated SDPS Single and Multi-Seam Model Tilt Profiles along XL10 above Modified MWs 32 to 36	
	Ditton Geotechnical Services Pty Ltd		Scale:	NTS	Figure No: 25.5



DgS	Engineer:	S.Ditton	Client:	LakeCoal - Chain Valley Colliery CHV-002/4	
	Drawn:	S.Ditton			
	Date:	20.03.15	Title:	Calibrated SDPS Single and Multi-Seam Model Strain Profiles along XL10 above Modified MWs 32 to 36	
	Ditton Geotechnical Services Pty Ltd		Scale:	NTS	Figure No: 25.6



Key:

- Proposed Miniwalls in Fassifern Seam
- Pillar Extraction Panels in Fassifern Seam
- XL1 — Subsidence Prediction Lines
- Lake Foreshore
- Site Boundary

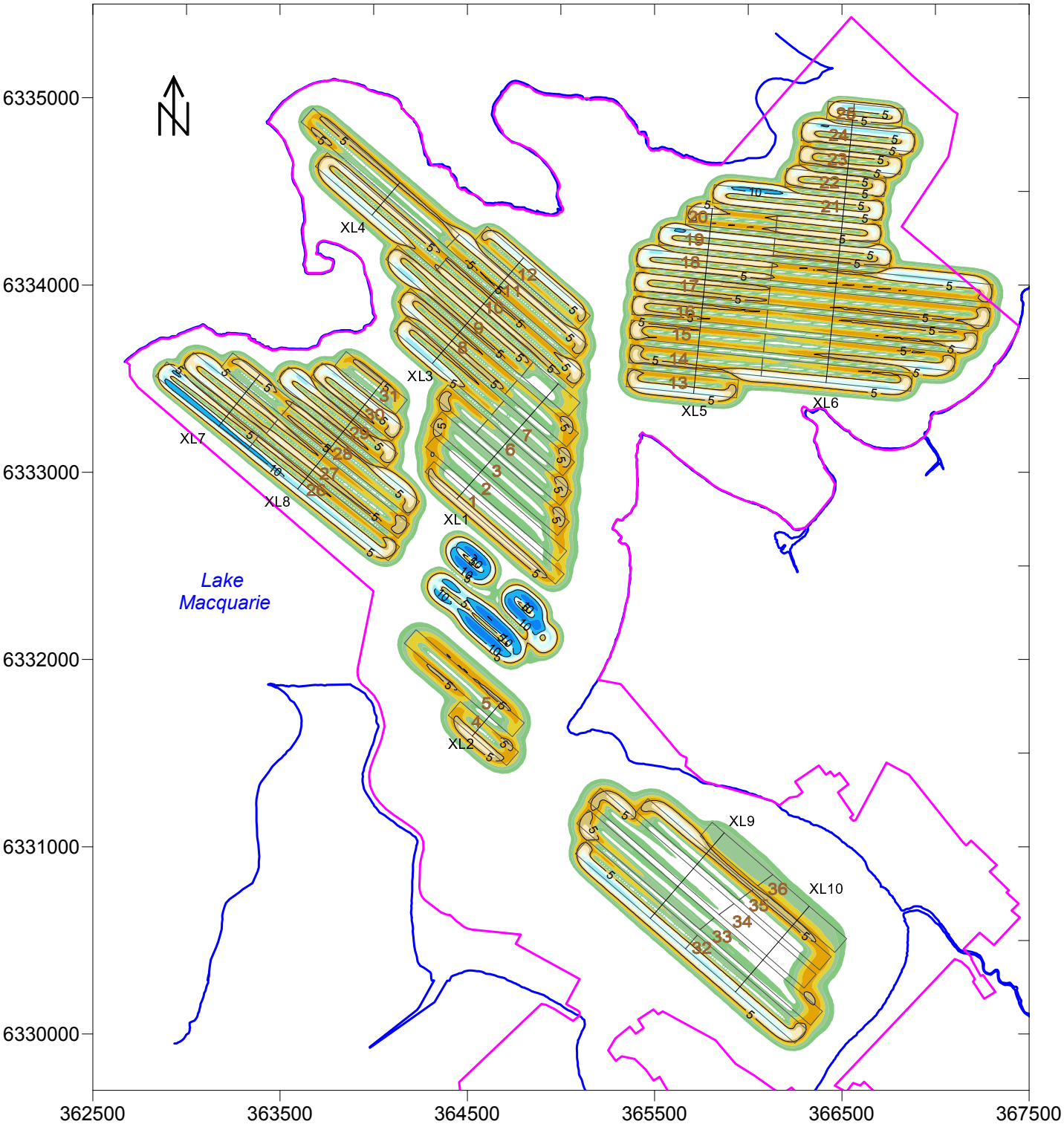
Subsidence (m):

-0.003 0.02 -0.1 -0.2 -0.3 -0.4 -0.5 -0.6 -0.7 -0.8 -0.9 -1 -1.1

DgS

Ditton Geotechnical Services Pty Ltd

Engineer:	S.Ditton	Client:	LakeCoal - Chain Valley Colliery CHV-002/4
Drawn:	S.Ditton		
Date:	15.05.15	Title:	Predicted Incremental Subsidence Contours above the Modified Mine Layout without Multi-Seam Mining Effects above MWs 32-36
		Scale:	1:12,000 (A4)
		Figure No:	26.1



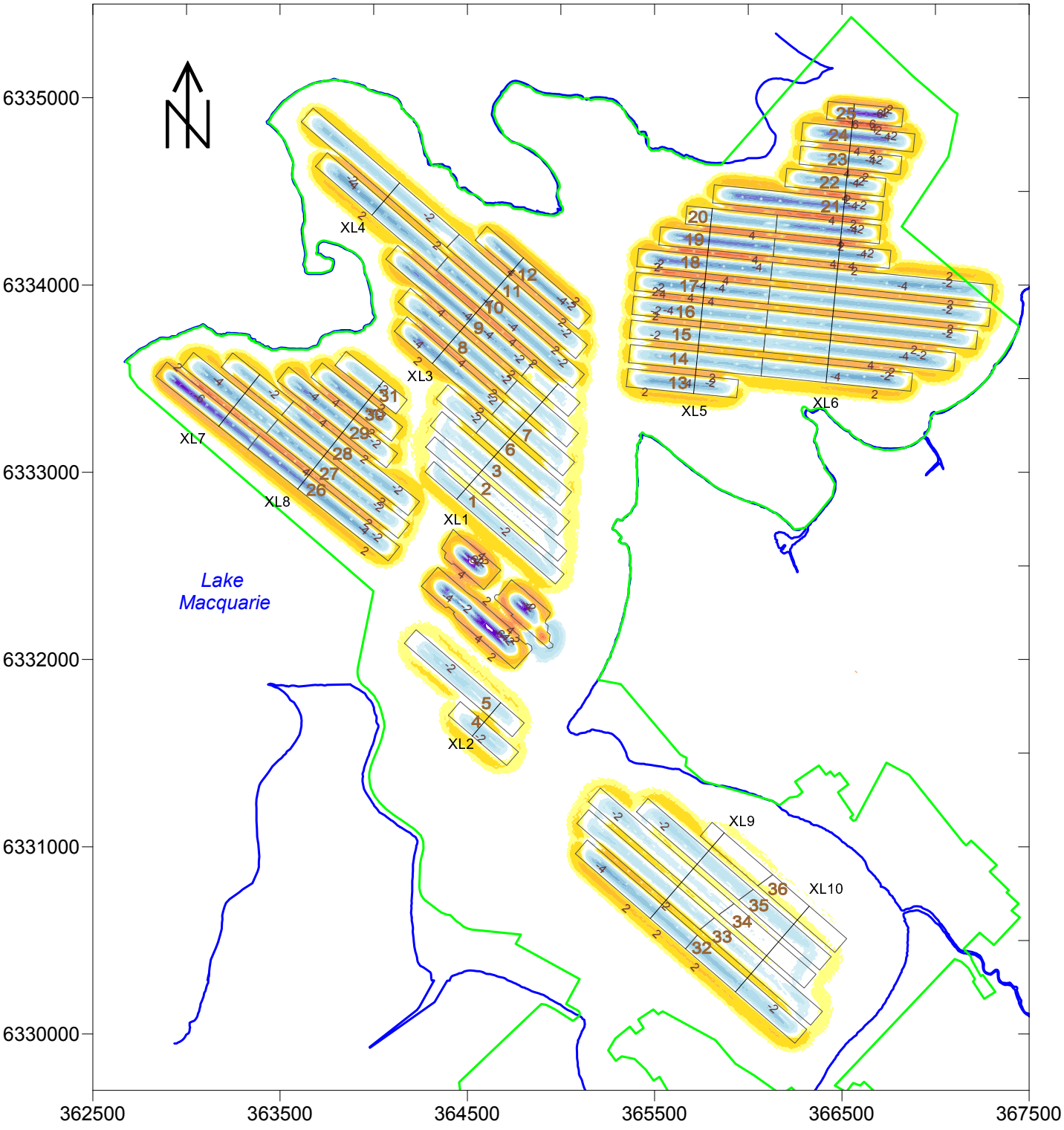
Key:

- Proposed Miniwalls in Fassifern Seam
- Pillar Extraction Panels in Fassifern Seam
- XL1 — Subsidence Effect Prediction Lines
- Lake Foreshore
- Site Boundary

Tilt (mm/m):

16 13 10 9 8 7 6 5 4 3 2 1

DgS	Engineer:	S.Ditton	Client:	LakeCoal - Chain Valley Colliery CHV-002/4	
	Drawn:	S.Ditton			
	Date:	15.05.15	Title:	Predicted Incremental Tilt Contours above the Modified Mine Layout without Multi-Seam Mining Effects above MWs 32-36	
Ditton Geotechnical Services Pty Ltd			Scale:	1:12,000 (A4)	Figure No: 26.2



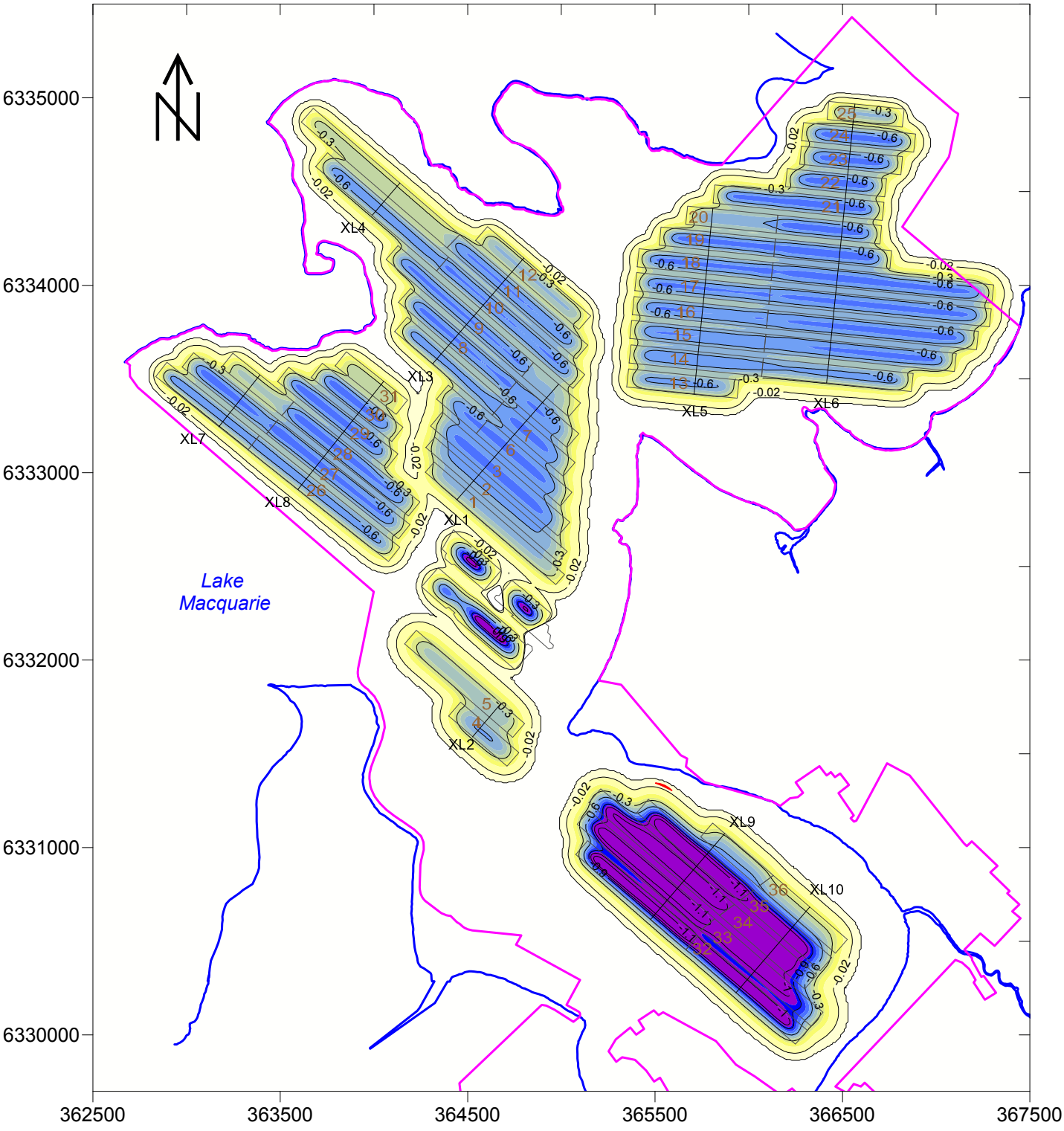
Key:

- Proposed Miniwalls in Fassifern Seam
- Pillar Extraction Panels in Fassifern Seam
- XL1 — Subsidence Prediction Lines
- Lake Foreshore
- Site Boundary

Horizontal Strain (mm/m):

7 6 5 4 3 2 1 0.5 0 -0.5 -1 -2 -3 -4 -5 -6 -7 -8 -9

DgS	Engineer:	S.Ditton	Client:	LakeCoal - Chain Valley Colliery CHV-002/4	
	Drawn:	S.Ditton			
	Date:	20.03.15	Title:	Predicted Incremental Strain Contours above the Modified Mine Layout without Multi-Seam Mining Effects above MWs 32-36	
Ditton Geotechnical Services Pty Ltd			Scale:	1:12,000 (A4)	Figure No: 26.3



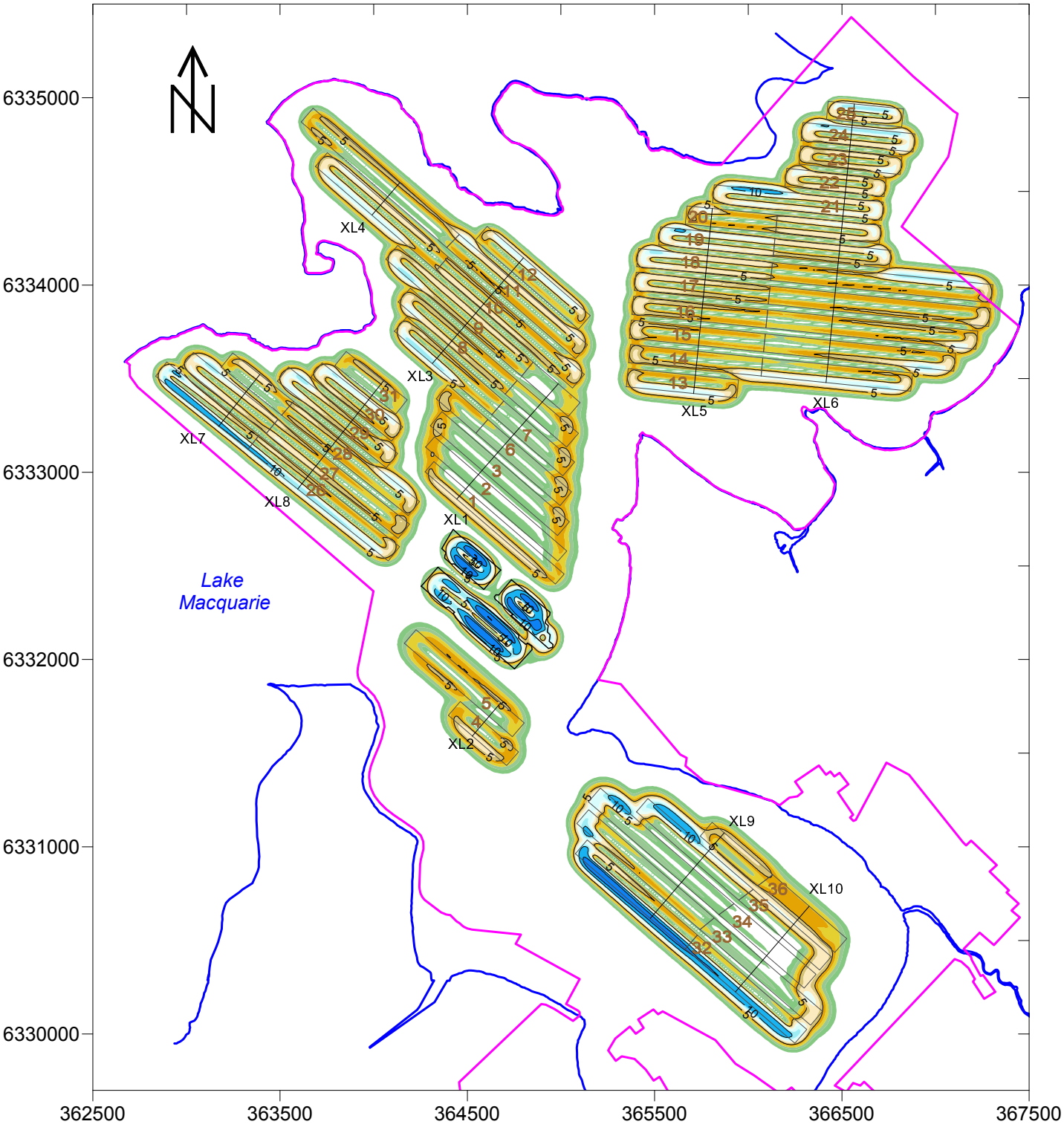
Key:

- Proposed Miniwalls in Fassifern Seam
- Pillar Extraction Panels in Fassifern Seam
- XL1 — Subsidence Prediction Lines
- Lake Foreshore
- Site Boundary
- Seagrass area that may be subsided up to 30 mm.

Subsidence (m):

-0.002 -0.02 -0.1 -0.2 -0.3 -0.4 -0.5 -0.6 -0.7 -0.8 -0.9 -0.95 -1 -1.1 -1.2

DgS	Engineer:	S.Ditton	Client:	LakeCoal - Chain Valley Colliery CHV-002/4	
	Drawn:	S.Ditton			
	Date:	15.05.15	Title:	Predicted Worst-case Cumulative Subsidence Contours above the Modified Mine Layout with Multi-Seam Mining Effects included above MWs 32-36	
	Ditton Geotechnical Services Pty Ltd		Scale:	1:12,000 (A4)	Figure No: 27.1



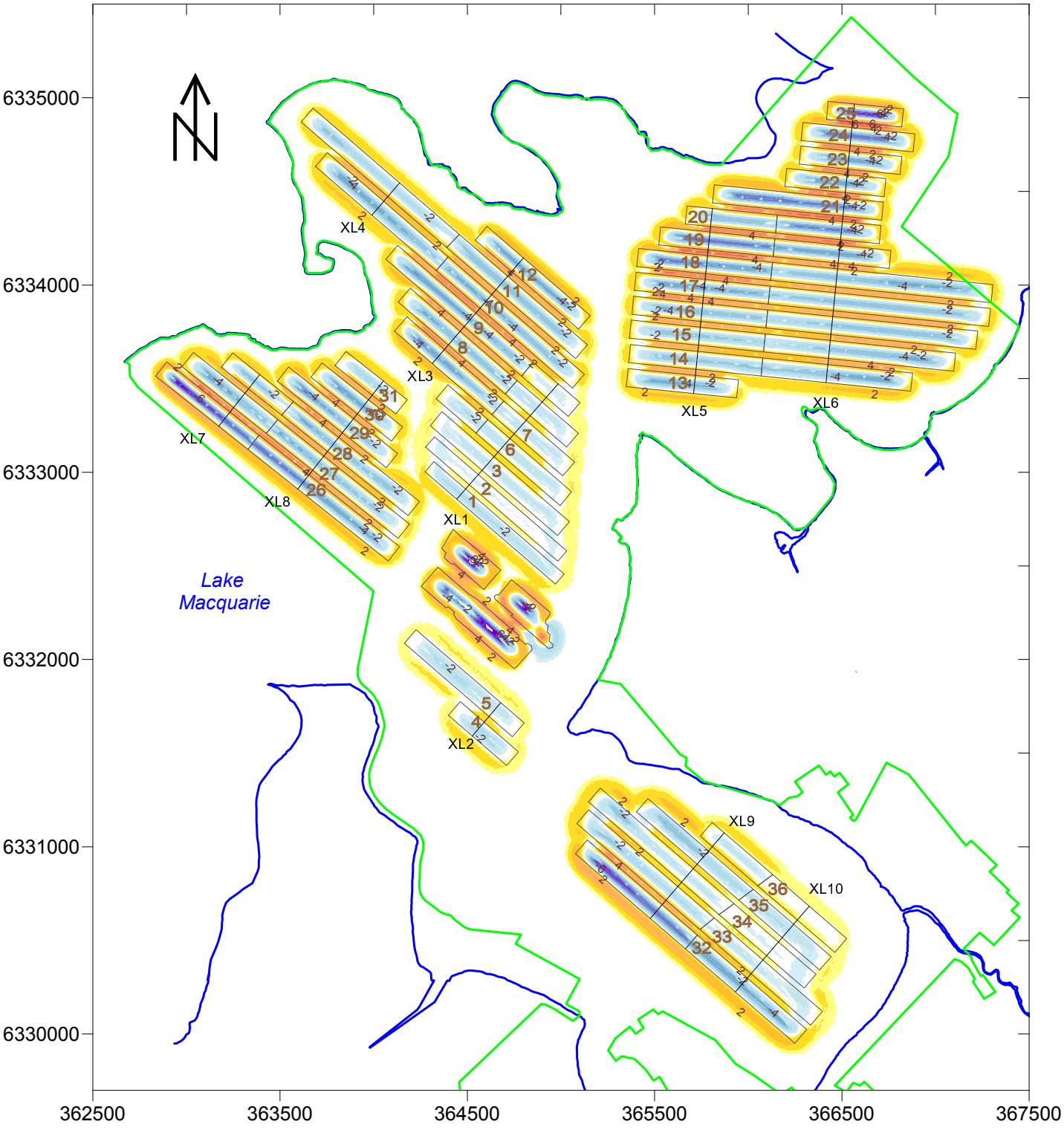
Key:

- Proposed Miniwalls in Fassifern Seam
- Pillar Extraction Panels in Fassifern Seam
- XL1 — Subsidence Prediction Lines
- Lake Foreshore
- Site Boundary

Tilt (mm/m):

16 13 10 9 8 7 6 5 4 3 2 1

DgS	Engineer:	S.Ditton	Client:	LakeCoal - Chain Valley Colliery CHV-002/4	
	Drawn:	S.Ditton			
	Date:	15.05.15	Title:	Predicted Cumulative Tilt Contours above the Modified Mine Layout with Multi-Seam Mining Effects above MWs 32-36	
Ditton Geotechnical Services Pty Ltd			Scale:	1:12,000 (A4)	Figure No: 27.2



Key:

- Proposed Miniwalls in Fassifern Seam
- Pillar Extraction Panels in Fassifern Seam
- XL1 — Subsidence Prediction Lines
- Lake Foreshore
- Site Boundary

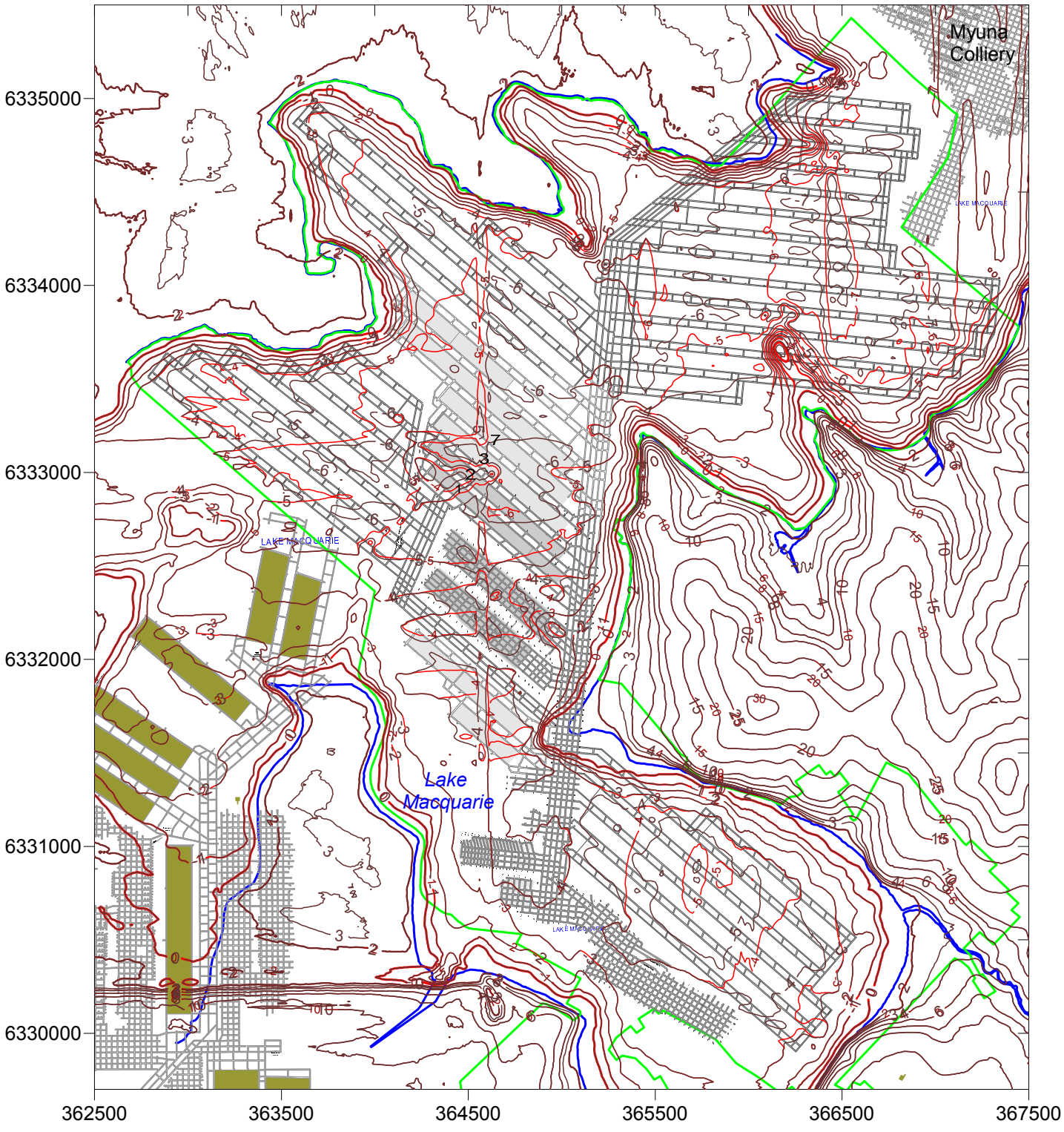
Horizontal Strain (mm/m):

7 6 5 4 3 2 1 0.5 0 -0.5 -1 -2 -3 -4 -5 -6 -7 -8 -9

DgS

Ditton Geotechnical Services Pty Ltd

Engineer:	S.Ditton
Drawn:	S.Ditton
Date:	15.05.15
Client:	LakeCoal - Chain Valley Colliery CHV-002/4
Title:	Predicted Cumulative Strain Contours above the Modified Mine Layout with Multi-Seam Mining Effects above MWs 32-36
Scale:	1:12,000 (A4)
Figure No:	27.3



Key

- Proposed Mine Workings in Fassifern Seam
- Existing Mine Workings in Fassifern Seam
- Pre-Fassifern Seam Mining Surface Level Contours* (m)
- * - Lake bed contours are negative.
- Site Boundary
- Extracted Chain Valley Panels in Fassifern Seam
- Extracted Wyee Panels in Fassifern Seam
- Lake Foreshore
- Predicted Pos-Fassifern Seam Mining Surface Levels^
- ^ - excludes all multi-seam mining effects.

DgS

Ditton Geotechnical Services Pty Ltd

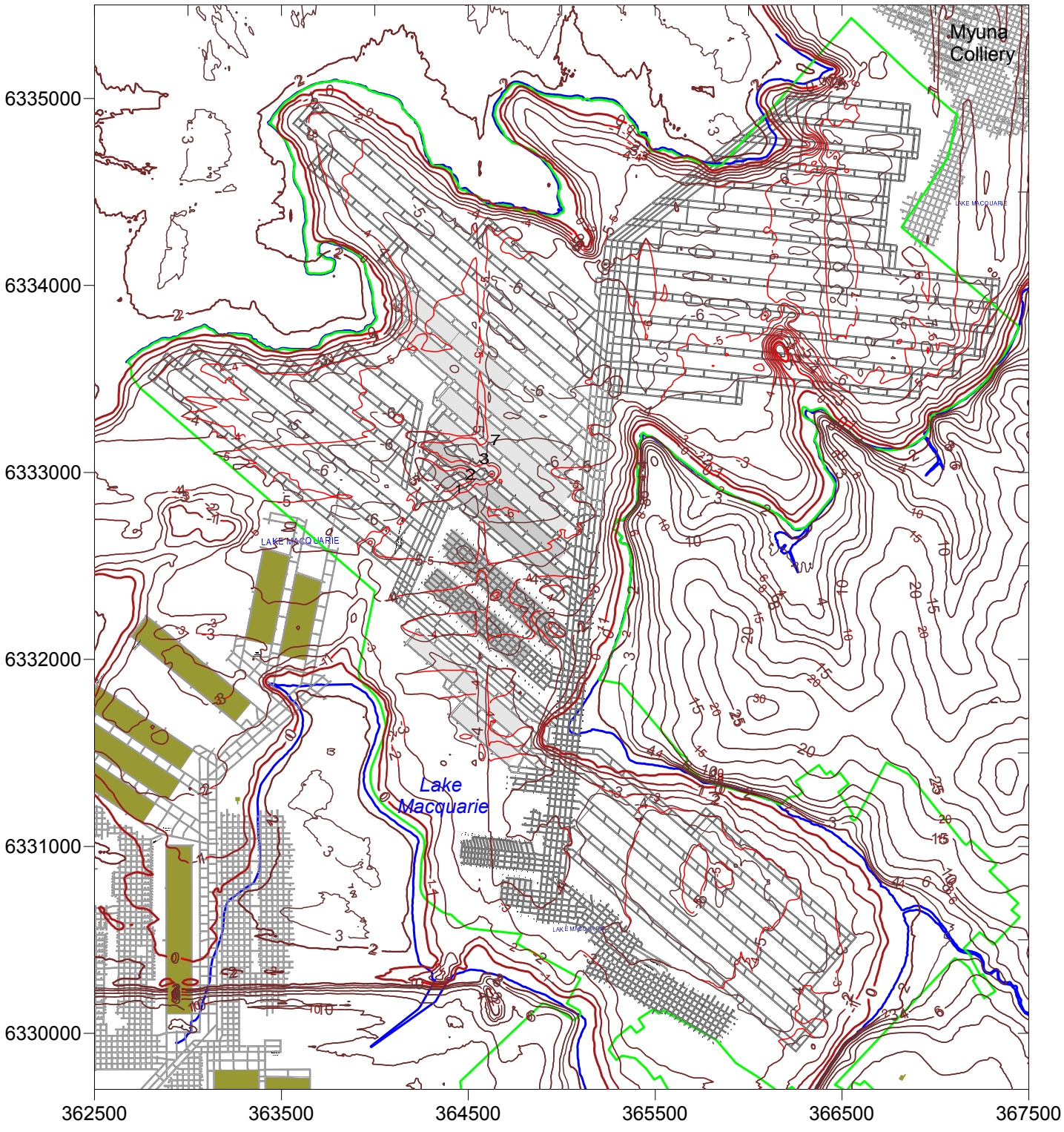
Engineer:	S.Ditton
Drawn:	S.Ditton
Date:	15.05.15

Client: LakeCoal - Chain Valley Colliery CHV-002/4

Title: Predicted Surface Level Contours after Mining the Modified Mine Layout in the Fassifern Seam (excludes Multi-Seam Effects)

Scale: 1:12,000 (A4)

Figure No: 28.1



Key

- Proposed Mine Workings in Fassifern Seam
- Existing Mine Workings in Fassifern Seam
- Pre-Fassifern Seam Mining Surface Level Contours* (m)
- * - Lake bed contours are negative.
- Site Boundary
- Extracted Chain Valley Panels in Fassifern Seam
- Extracted Wyee Panels in Fassifern Seam
- Lake Foreshore
- Predicted Pos-Fassifern Seam Mining Surface Levels^
- ^ - excludes all multi-seam mining effects.

DgS

Ditton Geotechnical Services Pty Ltd

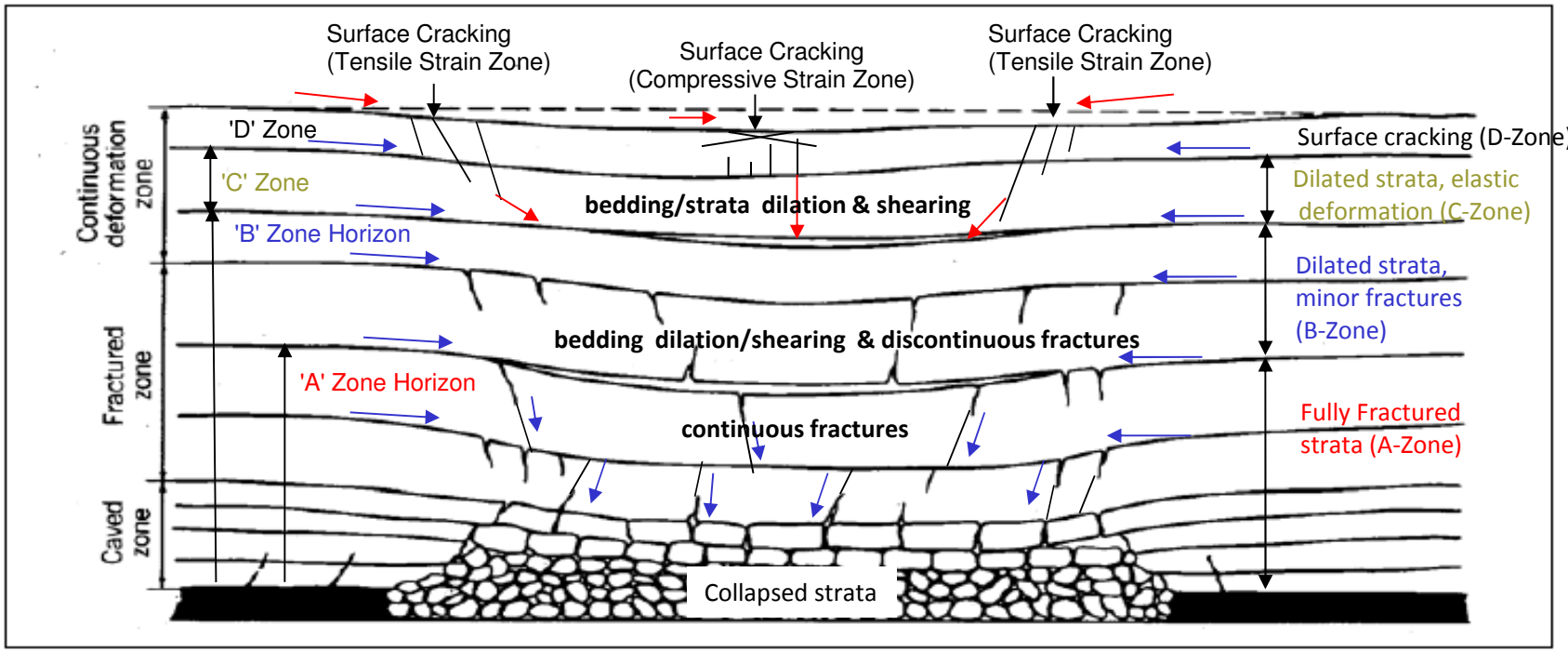
Engineer:	S.Ditton
Drawn:	S.Ditton
Date:	15.05.15

Client: LakeCoal - Chain Valley Colliery CHV-002/4

Title: Predicted Surface Level Contours after Mining the Modified Mine Layout in the Fassifern Seam (includes Multi-Seam Effects)

Scale: 1:12,000 (A4)

Figure No: 28.2



Zones in the Overburden According to Peng and Chiang (1984)

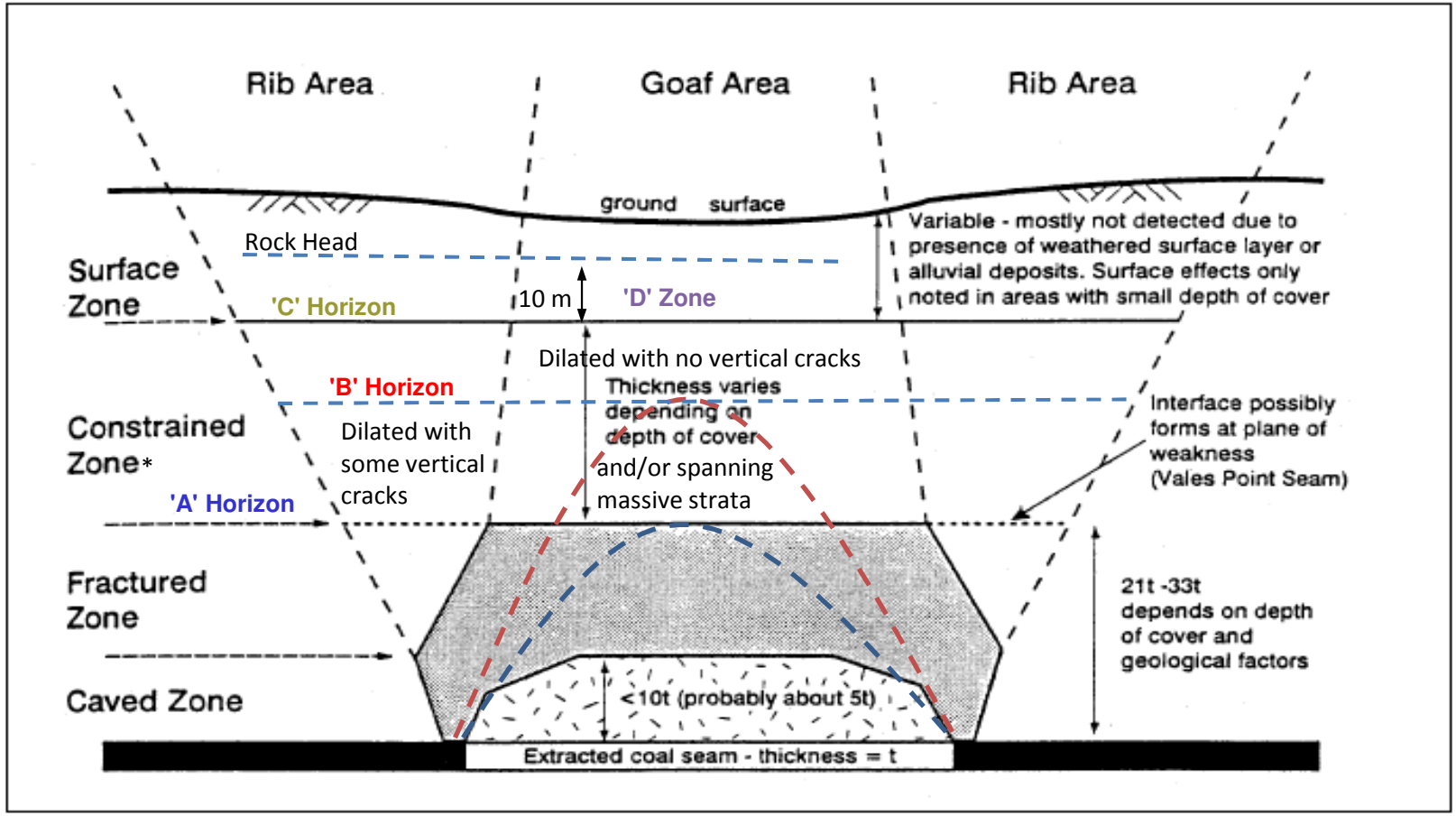
Key

'A' Horizon - Zone of Continuous Crack Connection to Workings (**Whittaker and Reddish,1989**)

'B" Horizon - Zone Of Discontinuous Crack Connection to Workings (**Whittaker and Reddish, 1989**)

→ Surface water flow path → Sub-surface water flow path

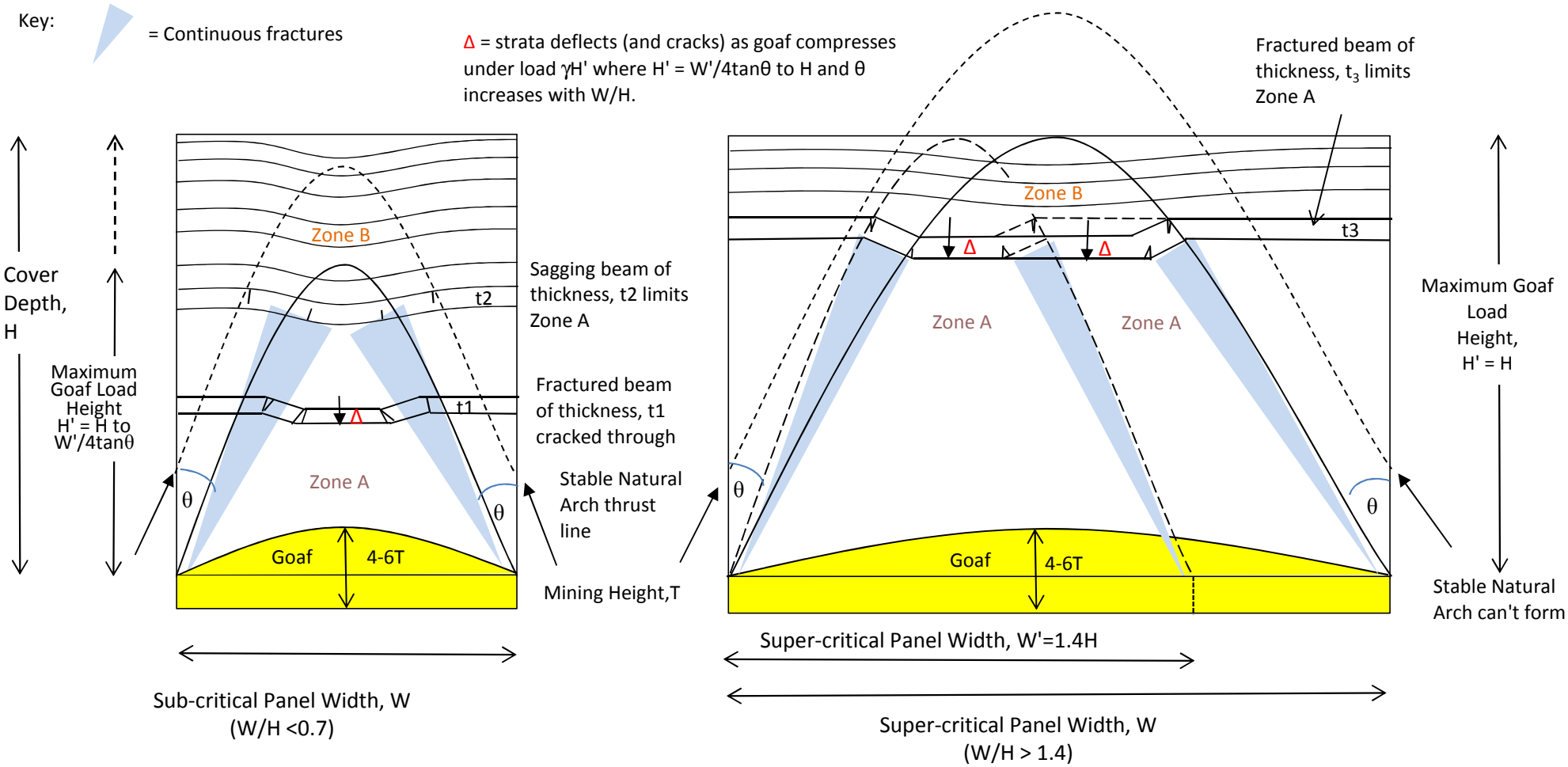
DgS	Engineer:	S.Ditton	Client:	LakeCoal - Chain Valley Colliery CHV-002/4	
	Drawn:	S.Ditton			
	Date:	20.03.15	Title:	Schematic Model of Overburden Fracture Zones Above Longwall Panels	
	Ditton Geotechnical Services Pty Ltd		Scale:	NTS	Figure No: 29.1



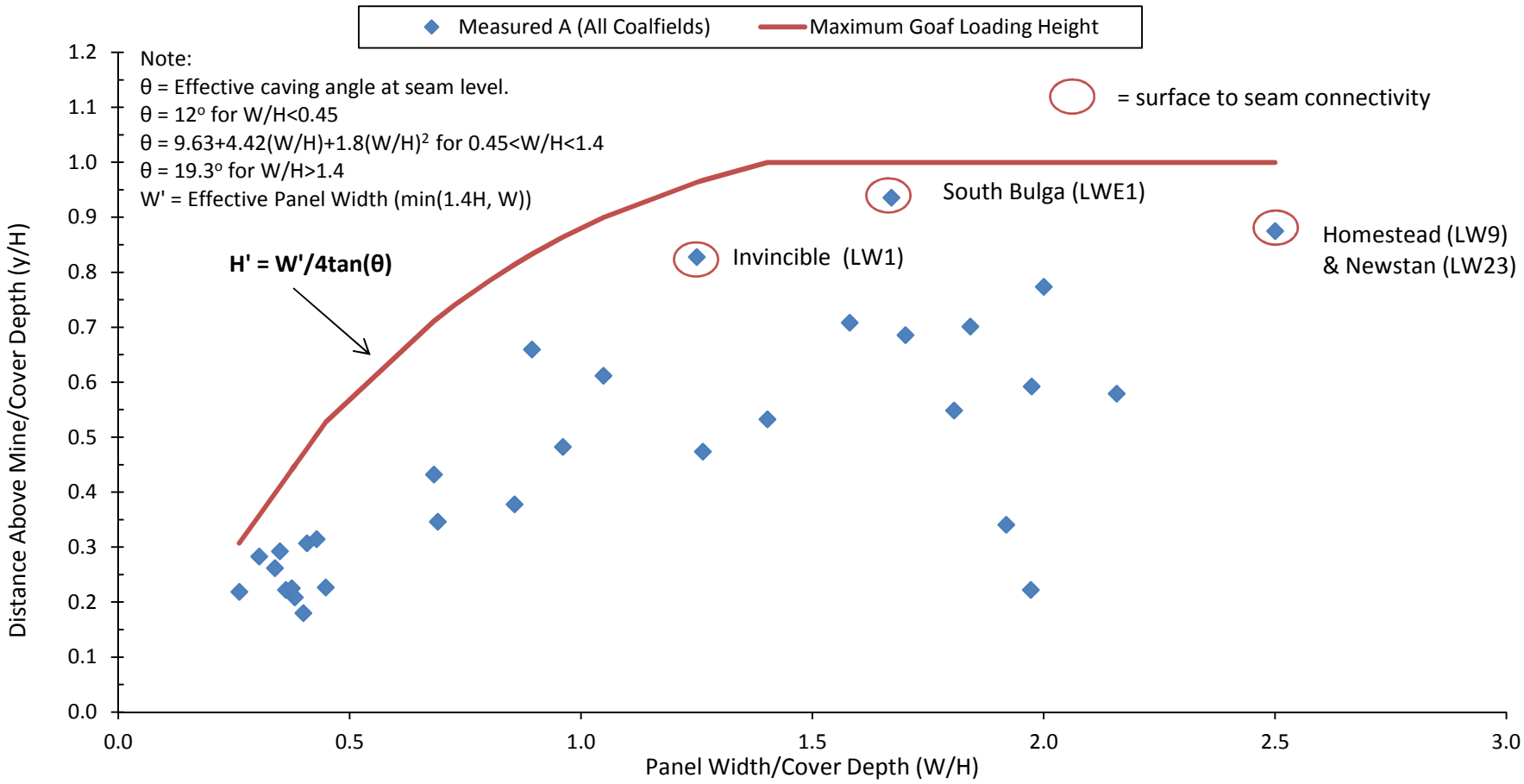
Zones in the Overburden according to Forster (1995)

* - Constrained Zone generally means B-Zone, but may include C-Zone , depending on W/H ratio and geology

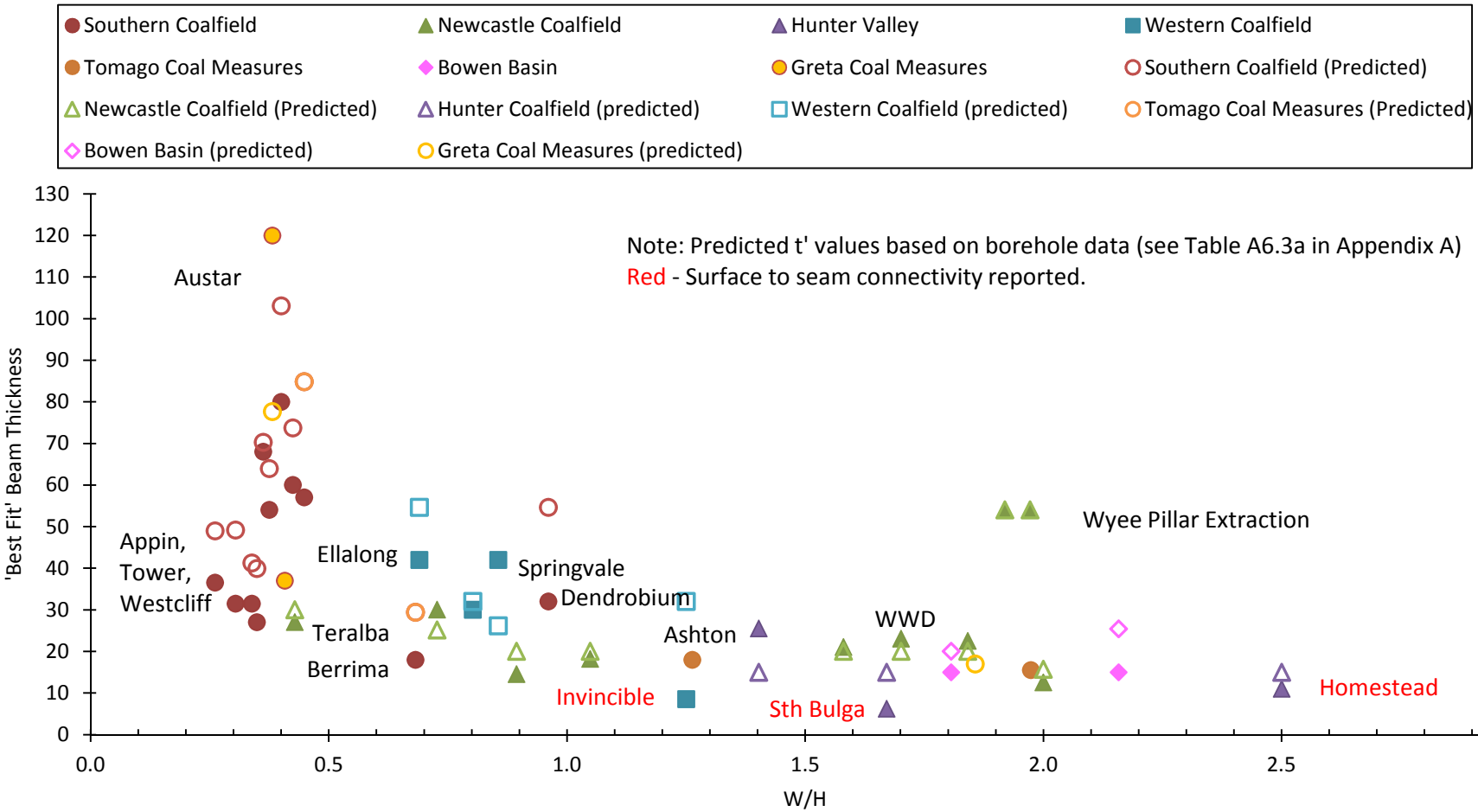
DgS	Engineer:	S.Ditton	Client:	LakeCoal - Chain Valley Colliery CHV-002/4	
	Drawn:	S.Ditton			
	Date:	20.03.15	Title:	Schematic Model of Overburden Fracture Zones in **Forster, 1995** Model (based on Piezometric Data Above High Extraction Panels in the Newcastle Coalfield)	
	Ditton Geotechnical Services Pty Ltd		Scale:	NTS	Figure No: 29.2



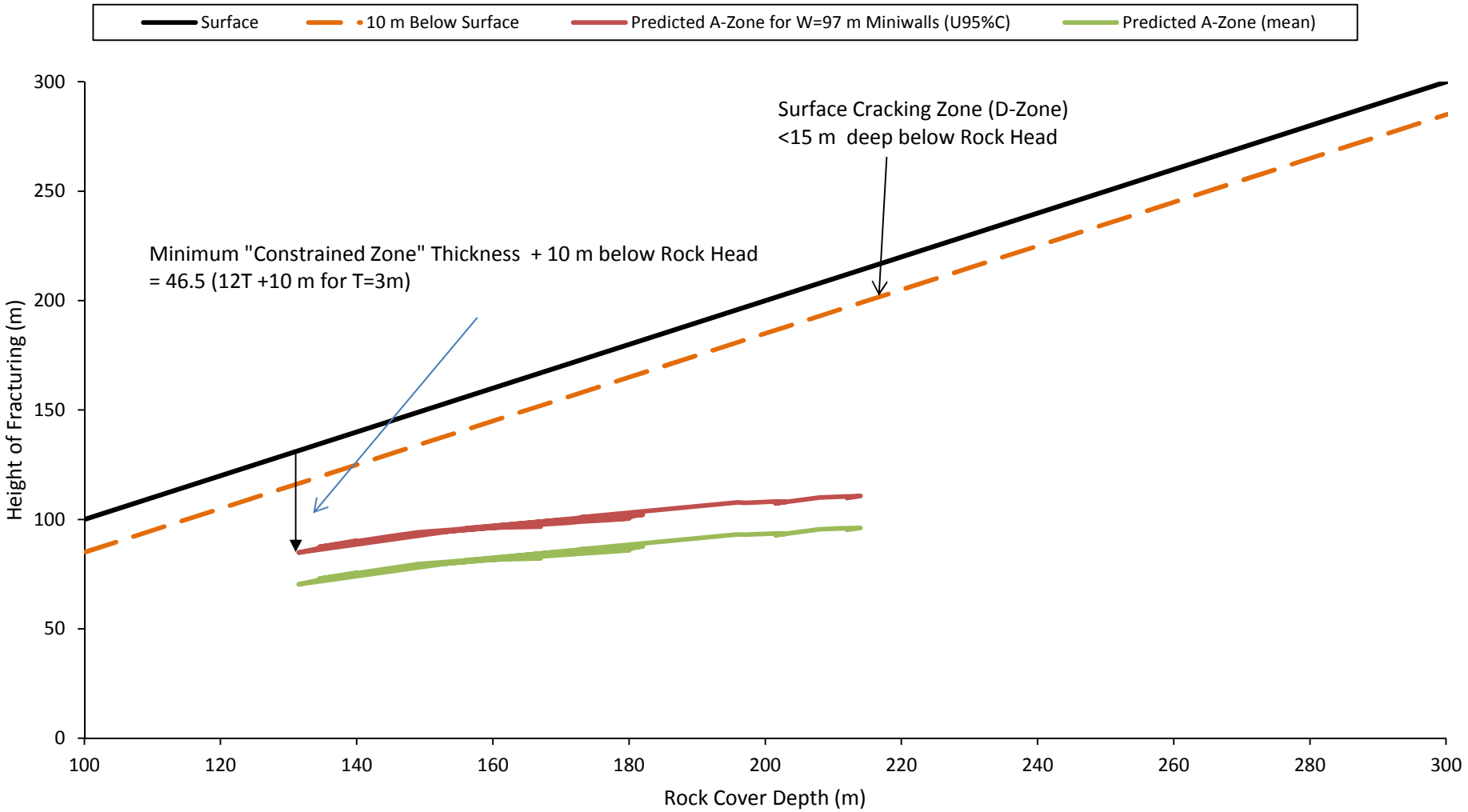
DgS	Engineer:	S.Ditton	Client:	LakeCoal - Chain Valley Colliery CHV-002/4	
	Drawn:	S.Ditton			
	Date:	20.03.15	Title:	Conceptual Model for Development of Height of Continuous Fracturing Zone for a range of Longwall Panel Geometries	
	Ditton Geotechnical Services Pty Ltd		Scale:	NTS	Figure No: 30.1



DgS	Engineer:	S.Ditton	Client:	LakeCoal - Chain Valley Colliery CHV-002/4	
	Drawn:	S.Ditton			
	Date:	20.03.15	Title:	Measured Heights of Continuous Fracturing in NSW and QLD Coalfields with Reported Surface to Seam Connectivity Cases, caving angles and theoretical Goaf Loading Height	
Ditton Geotechnical Services Pty Ltd			Scale:	NTS	Figure No: 30.2

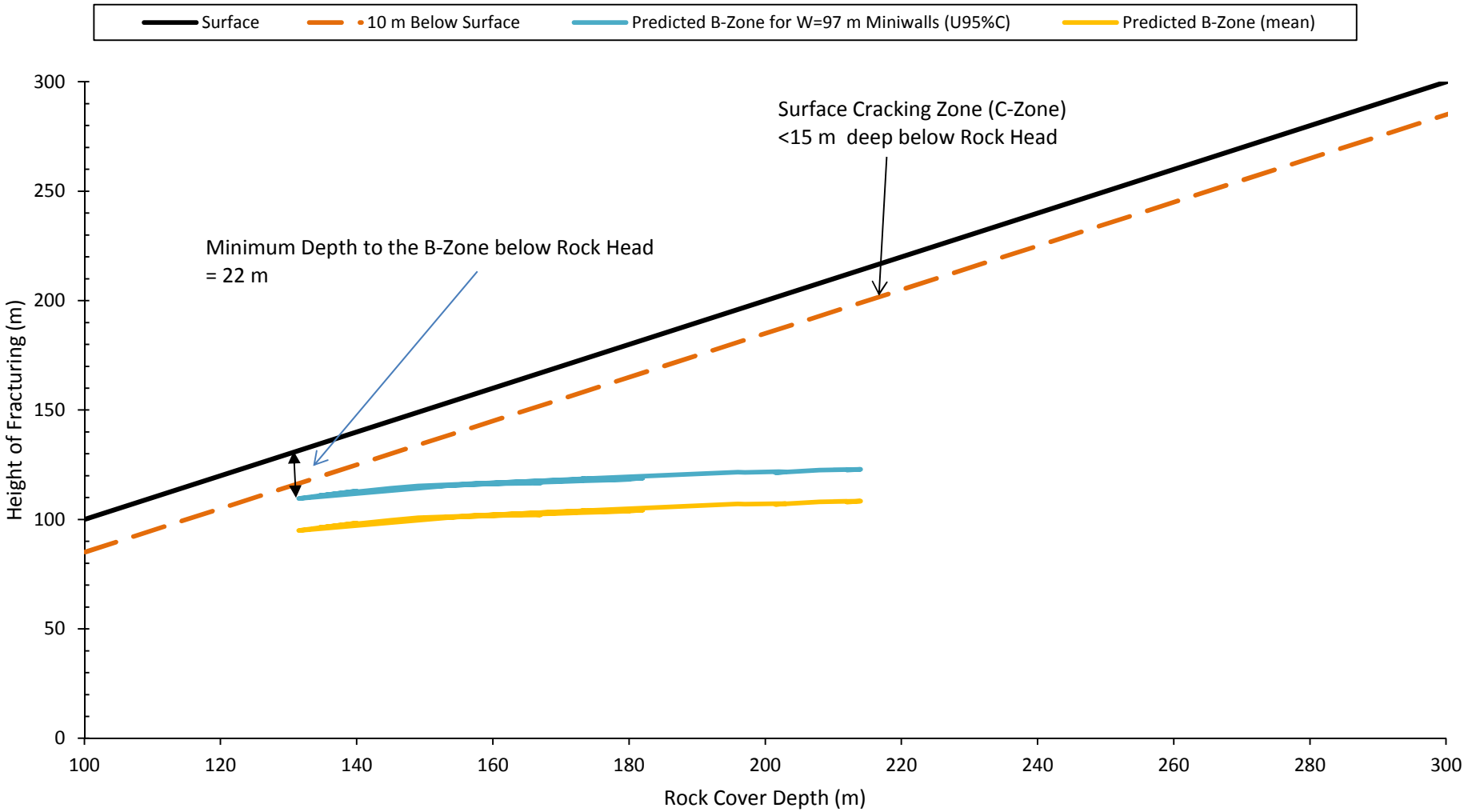


DgS	Engineer:	S.Ditton	Client:	LakeCoal - Chain Valley Colliery CHV-002/4	
	Drawn:	S.Ditton			
	Date:	20.03.15	Title:	Results of Back-analysis of Effective Strata Units required to Match the Observed A-Zone Heights above Longwall Panel Goafs using the Geology Pi-Term Model	
	Ditton Geotechnical Services Pty Ltd		Scale:	NTS	Figure No: 30.3



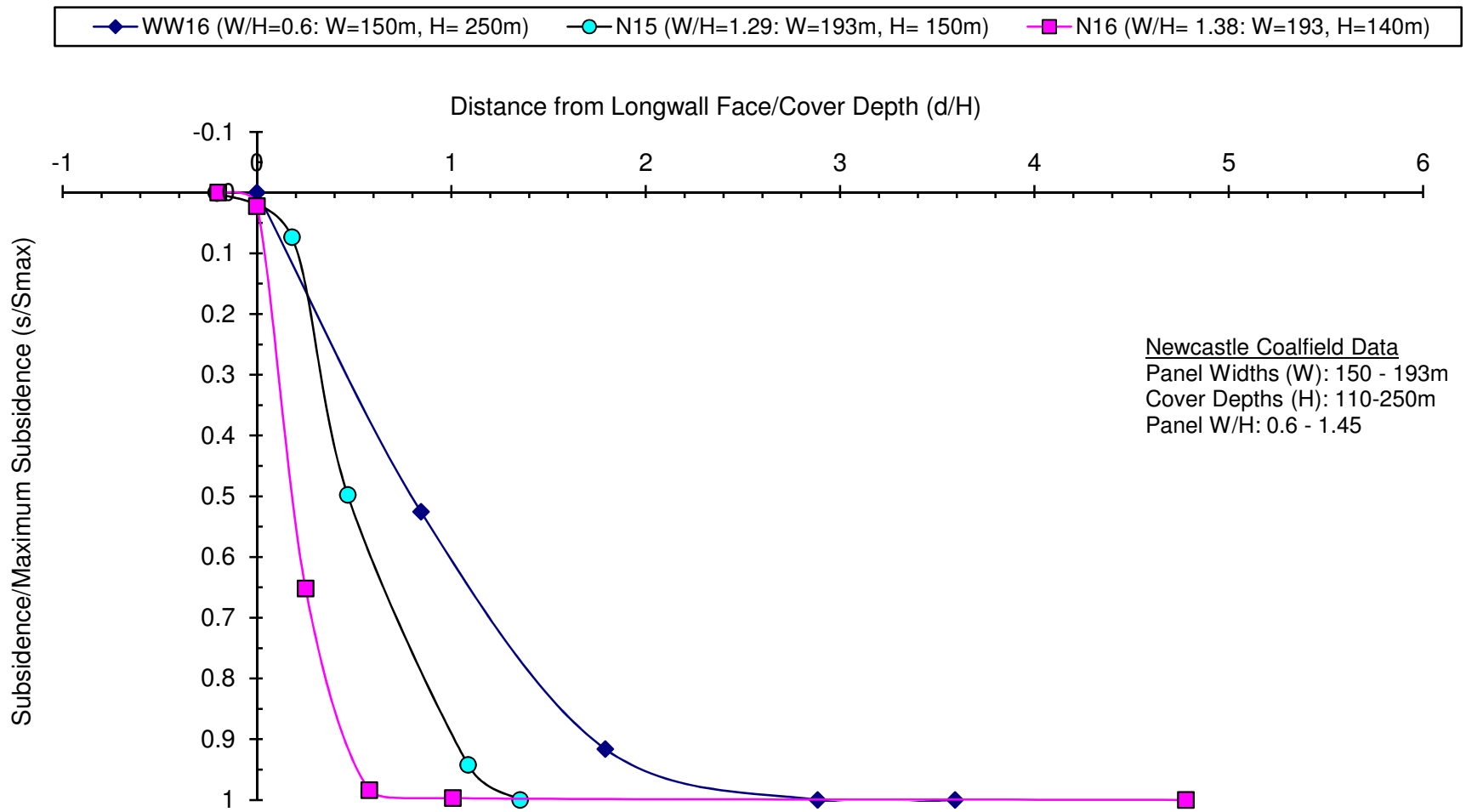
Reference: DgS Modified 2012 Sub-surface Fracture Model Outcomes based on **ACARP,2003**

DgS	Engineer:	S.Ditton	Client:	LakeCoal - Chain Valley Colliery	
	Drawn:	S.Ditton		CHV-002/4	
	Date:	20.03.15	Title:	Continuous (A-Zone) Sub-Surface Fracture Heights and Constrained Zone Thickness above the Proposed 97 m Wide MWs 1 to 36 in the Fassifern Seam	
	Ditton Geotechnical Services Pty Ltd		Scale:	NTS	Figure No: 31.1



Reference: DgS Modified 2012 Sub-surface Fracture Model Outcomes based on **ACARP,2003**

DgS	Engineer:	S.Ditton	Client:	LakeCoal - Chain Valley Colliery	
	Drawn:	S.Ditton		CHV-002/4	
	Date:	20.03.15	Title:	Discontinuous (B-Zone) Sub-Surface Fracture Heights in Constrained Zone	
	Ditton Geotechnical Services Pty Ltd			Thickness above the Proposed 97 m Wide MWs 1 to 36 in the Fassifern Seam	
			Scale:	NTS	Figure No: 31.2



DgS	Engineer:	S.Ditton	Client:	LakeCoal - Chain Valley Colliery CHV-002/4	
	Drawn:	S.Ditton			
	Date:	20.03.15	Title:	Empirical Single Longwall Centreline Subsidence Development Prediction Model (based on Newcastle Coalfield Measurements)	
	Ditton Geotechnical Services Pty Ltd		Scale:	NTS	Figure No: 32

Appendix A - Summary of the Modified ACARP, 2003 Empirical Model

DGS MODIFIED ACARP, 2003 EMPIRICAL SUBSIDENCE AND HEIGHT OF FRACTURING PREDICTION MODEL

A1 Introduction

This appendix provides a description of how subsidence and sub-surface fracturing develops above longwall panels and provides a summary of the empirical subsidence prediction models used in this study.

The **ACARP, 2003** model was originally developed by Strata Engineering (Australia) Pty Ltd under ACARP funding with the goal of providing the industry with a robust and reliable technique to utilise the significant amount of geological and testing information already gathered by mining companies.

Over the past six years the **ACARP, 2003** model has been used successfully by the model's author, Steven Ditton, at several longwall mines in the Newcastle, Hunter Valley, Western and Southern Coalfields of NSW and the Bowen Basin, Queensland.

Subsidence prediction work for Stage 1 of the Moolarben Coal Project in 2006 resulted in further external scrutinization of the model and the robustness of the methodology by an Independent Hearing and Assessment Panel (IHAP), which was set up to assess Environmental Impact Assessments for new coal mining projects by NSW Department of Planning (DoP).

The outcomes of the IHAP for Moolarben resulted in several refinements to the model, as requested by the independent subsidence expert, Emeritus Professor J M Galvin, UNSW School of Mining and Director of Galvin and Associates Pty Ltd.

The refinements generally included several technical adjustments and clarification of the terminology used to enable a better understanding of the model by the wider technical community.

Over the past 7 years, Ditton Geotechnical Services Pty Ltd (DgS) has modified the **ACARP, 2003** model to be able to use it to calibrate an influence function model (SDPS®) that was developed by the Polytechnical Institute for the US Coalfields. The SDPS® program allows a wider range of topographic and complex mining layouts (including longwall and pillar extraction panels) to be assessed.

This appendix summarises the **ACARP, 2003** model in its current format and explains the refinements made to the original model. Details of the **SDPS®** model itself are provided at the back of this appendix.

A2 Description of Subsidence Development Mechanisms above Longwalls

After the extraction of a single longwall panel, the immediate mine roof usually collapses into the void left in the seam. The overlying strata or overburden then sags down onto the collapsed material, resulting in settlement of the surface.

The maximum subsidence occurs in the middle of the extracted panel and is dependent on the mining height, panel width, cover depth, overburden strata strength and stiffness and bulking characteristics of the collapsed strata. For the case of single seam mining, maximum panel subsidence has not exceeded 60% of the mining height (T) in over 95% of the published cases for the Newcastle, and Southern Coalfields (refer **ACARP, 2003** and **Holla and Barclay, 2000**). For the 5% of cases, which did exceed 58%T, the maximum subsidence did not exceed 65%T (i.e. 2.7 m for a 4.2m mining height). The actual subsidence may also be lower than this value due to the spanning or bridging capability of the strata above the collapsed ground (or the goaf).

The combination of the above factors determines whether a single longwall panel will be *sub-critical, critical,* or *supercritical* in terms of maximum subsidence.

Sub-critical subsidence refers to panels that are narrow and deep enough for the overburden to bridge or 'arch' across the extracted panel regardless of geology. It is therefore termed 'deep arching' in the context of the subsidence model.

Beyond the *sub-critical* range, the overburden becomes *critical*, and is unable to develop deep arching behaviour. Spanning of the overburden is dependent on 'shallow beam' bending or Voussoir arching behaviour and the presence of massive, competent strata. Cracking or breakdown of the overburden strata may therefore start to develop above *critical* panel geometries as the spanning mechanism transitions from 'deep arching' to 'shallow beam' behaviour.

Supercritical panels refer to panel geometries that cause complete collapse of the overburden. In the case of super-critical panels, maximum panel subsidence does not usually continue to increase significantly with increasing panel width.

In the Newcastle Coalfields, *sub-critical* or (deep arching) behaviour generally occurs when the panel width (W) is <0.7 times the cover depth (H) and supercritical when W/H > 1.4. Critical behaviour usually occurs between W/H ratios of 0.7 and 1.4. In the deeper areas of the Southern Coalfield, critical subsidence behaviour may start to occur when W/H is > 0.5. As the cover depth averages at about 250 m in the Newcastle Coalfield and 450 m in the Southern Coalfield and both areas have massive strata units in the overburden, this indicates that the cover depth is likely to be a key factor when assessing subsidence.

The transition point from sub-critical to critical behaviour in a particular coalfield is also influenced by the 'bridging' capability of the strata if it can develop a spanning Voussoir Arch. In the Newcastle Coalfield, the commencement of critical panel behaviour can effectively increase up to W/H ratios of 0.9.

The maximum subsidence for sub-critical and critical panel widths is generally < 60% of the longwall extraction height (T) and could range between 5% and 40% T, depending on the thickness of massive sandstone or conglomerate strata.

The surface effect of extracting several adjacent longwall panels is dependent on the stiffness of the overburden and the chain pillars left between the panels. Invariably, 'extra' subsidence occurs above a previously extracted panel and is caused primarily by the compression of the chain pillars and adjacent strata between the extracted longwall panels.

A longwall chain pillar undergoes the majority of life-cycle compression when subject to double abutment loading (i.e. the formation of goaf on both sides of it, after two adjacent panels have been extracted). Surface survey data indicates that an extracted panel can affect the chain pillars between three or four previously extracted panels. The stiffness of the overburden and chain pillar system will determine the extent of load transfer to the preceding chain pillars. If the chain pillars go into yield, the load on the pillars will be mitigated to some extent by load transfer to adjacent fallen roof material or goaf.

The surface subsidence usually extends outside the limits of extraction for a certain distance (i.e. the angle of draw). The angle of draw distance is usually less than or equal to 0.5 to 0.7 times the depth of cover (or angles of draw to the vertical of 26.5^{o} to 35^{o}) in the NSW and QLD Coalfields.

A3 ACARP Project Overview

The original **ACARP, 2003** model was originally developed for the Newcastle Coalfield to deal with the issue of making reliable subsidence predictions over longwall panels by using both geometrical and geological information.

The project was initially focused on the behaviour of massive sandstone and conglomerate strata in the Newcastle Coalfield, but has now been successfully used in other coalfields since development over the past six years. This has occurred naturally due to the expansion of the model's database with data from other coalfields and has resulted in generic refinements to the model to deal with the wider range of geometrical and geological conditions.

In regards to geometry, the subsidence above a series of longwalls is strongly influenced by the panel width, the cover depth, the extraction height and the stiffness of the interpanel pillars (i.e. the chain pillars) and immediate roof and floor strata.
In regards to geology, the presence of massive strata units, such as conglomerate and sandstone channels above longwall panels, has resulted in reduced subsidence compared to that measured over longwall panels with similar geometry and thinner strata units.

Geological structure, such as faults and dykes, can cause increases in subsidence due to their potential to adversely affect the spanning capability of the overburden.

During the original development of the model, a database of maximum single and multi longwall panel subsidence and associated massive strata units was compiled for the

Newcastle Coalfield. The database draws on subsidence data from over fifty longwall panels and covers a panel width to cover depth (W/H) ratio from 0.2 to 2.0 (cover depth ranges between 70 m and 351 m), as shown in **Figure A1**.

The original project database includes single seam longwall mining data from eleven collieries within the Newcastle Coalfield, as presented in **Table A1**.

Table A1 - Empirical Database Sources from Newcastle Coalfield

Colliery	Colliery	Colliery
Cooranbong	Lambton	Wyee
New Wallsend No. 2 (Gretley)	Teralba	
Moonee	Burwood	
Stockton Borehole	West Wallsend	
Newstan	John Darling	

The wide range of single longwall panel W/H ratios in the database was considered unique compared to the other Australian coalfields and enabled the study to focus on overburden and chain pillar behaviour effects separately.

Pillar extraction or multiple seam data was not used to produce the subsidence prediction curves, as it invariably makes the assessment of geological influences more difficult. Other NSW and QLD longwall and high pillar extraction mine data that have been added to the model database over the past seven years as shown in **Table A2**.

Table A2 - Empirical Longwall Database from Other Mines

Coalfield	Colliery	Colliery
Newcastle	West Wallsend	Newstan
	Mandalong	Chain Valley
Hunter Valley	United	Wollemi
	Austar	North Wambo
Southern	Berrima	Appin
	Elouera	Dendrobium
	Metropolitan	
Western	Springvale	Angus Place
	Ulan	
Queensland	Cook	Oaky Creek
	Moranbah North	

In summary, the key features of the **ACARP, 2003** model are that it:

- Is derived from a comprehensive database of measured subsidence, strain, tilt and curvature above longwalls in the Newcastle, Hunter Valley, Western and Southern Coalfields.

- Has been validated with measured subsidence profile data.

- Adds to the **DMR, 1987** model for the Newcastle Coalfield, as it addresses multiple panels and contains a significantly larger data base.

- Includes the effects of massive sandstone/conglomerate lithology on subsidence.

- Allows reliable predictions of maximum single panel subsidence, chain pillar subsidence, tilt, curvature, strain and the angle of draw within a 95% Confidence Limit.

- Enables 'greenfield' sites (i.e. where there is no subsidence data) to be assessed rapidly and accurately.

- Provides maximum subsidence predictions based on Upper 95% Confidence Limits (or 5% Probability of Exceedence limits), which in practice have rarely been exceeded.

- The confidence limits have been derived by the application of central limit theory and the likely normal distribution of residuals about lines of best fit or regression lines determined for the model database.

- Utilises historical information directly - predictions are based on actual data.

- Enables prediction of secondary tilt, curvature and strain magnitudes. Effects such as 'skewing' due to rapid surface terrain variations, surface 'hump' or step development and cracking can result in tilt, curvature and strain magnitudes significantly greater than predicted 'smooth' profile values.

  This issue has been addressed empirically by linking measured impact parameters with key mining geometry variables. Strain concentration factors and database confidence limits have been developed to estimate the likely range of subsidence impact parameters.

- Is amenable to subsidence contouring and allows the impacts on surface features to be assessed, including post-mining topography levels for watercourse impact assessment.

- Predictions of subsidence at specific locations can be done to provide an indication of likely subsidence magnitude; however, depending on the sensitivity of the feature, it may be prudent to adopt maximum predicted subsidence for a given panel.

- Incorporates an empirical model of sub-surface fracturing and far-field displacements.

  Note: Recent far-field horizontal displacement model work in the Newcastle Coalfield indicates the empirical model is conservative.

The following key input parameters are required to make subsidence predictions using the model:

- Panel Width (W)
- Cover Depth (H)
- Seam Working Height (T)
- Overburden lithology details, specifically the thickness and location of massive strata units (t, y).
- Chain Pillar Height (h), Width (w_{cp}) and Length (l) [solid dimensions]
- Roadway width (r)

The statistical inferences and estimates of the model uncertainty associated with the prediction methodology are presented in the following sections.

A4 Single Panel Subsidence Predictions

A4.1 Geometrical Factors

The major finding of the **ACARP, 2003** project in regards to mining geometry was that the historical relationship between subsidence and panel width to cover depth ratio (W/H) is not a constant for the range of cover depths (H) involved.

Figure A2.1 shows the range of maximum subsidence that can occur above longwall panels with similar mining geometries and a range of cover depths. The apparent differences between the DMR's Southern NSW and Newcastle Coalfield curves and laminated overburden theory (**Heasley, 2000**) also support the above finding.

For an overburden consisting of sedimentary rock layers or plates, **Heasley, 2000** applied laminated beam theory by **Salamon, 1989** to form the basis of the pseudo-numerical subsidence prediction program LAMODEL ("LAyered MODEL" of overburden) that has been found to have reasonable success in the US Coalfields.

According to LAMODEL theory, the maximum seam roof convergence (C_{max}) above a longwall panel of mining height (T), width (W) and cover depth (H), with an idealised overburden of uniform lamination thickness (t), Youngs Modulus (E), unit weight (γ) and Poisson's Ratio (v) is:

$C_{max} = [\sqrt{12(1-v^2)}]/t\ (\gamma H/E)\ (W^2/4)$ or T (whichever gives the lower value)

Several points can be made about this equation:

- The γH term represents the vertical stress acting on the plates at seam level and assumes spanning strata (i.e. sub-critical to critical panels).

- For completely collapsed strata, C_{max} may be assumed to equal T at seam level.

- The surface subsidence may then be estimated as the minimum of $0.5C_{max}$ and 0.6T for sub-critical/critical and supercritical panel geometries.

- In terms of traditional empirical models of estimating subsidence, the above equation indicates that the maximum single panel subsidence is a function of W^2/t and γH/E for sub-critical W/H ratios < 0.7 or T for super-critical W/H ratios >1.4. The influence of the panel width and mining height will therefore change with W/H.

Clamped elastic beam theory indicates that strata beam deflections, that are located at a distance y above the mine workings, are a function of γ(H-y)/E and W^4/t^3 before cracking at the abutments and mid-span. The deflection of the beam will generate higher tensile stresses in the top of the beam at the abutments than in the bottom of the beam at mid-span. The cracking results in a transition from continuous elastic beam behaviour to a cracked beam of separate blocks or 'voussoirs' under simply supported loading conditions.

The Voussoir beam supports the load through the formation of a compressive arch, which develops as the individual blocks or Voussoirs rotate towards the goaf below it (i.e. the voussoirs cannot sustain tensile stresses, however, the deformed beam will span if the blocks have sufficient strength, stiffness and geometry. The elastic and Voussoir beam cases are shown in **Figure A2.2**.

If the rotated blocks are able to support the load, then the deflection of the cracked Voussoir beam is a function of γ(H-y)/E and W^2/t, which is consistent with the laminated beam model theory; see **Figure A2.3**.

The **ACARP, 2003** model surmised that single panel subsidence normalised by mining height T, was a function of W/H, γH/E or H, W/t and y/H in accordance with Buckingham's Pi theory.

The first three parameters above are related to panel geometry (i.e. the panel width, W, cover depth, H, and mining height, T, whilst the last two parameters (strata unit thickness, t, and distance, y, to the unit above the workings) infer geological influences of massive strata units.

Based on the above equations, surface subsidence is expected to increase with increasing cover depth (H) for the same W/H ratio, and is primarily a function of the increasing panel width (W) as $S_{max} = f(W^2/H)$ according to beam theory. For constant single panel width (W), subsidence will therefore decrease with increasing cover depth (H). The subsidence data was subsequently separated into three cover depth categories of H = 100, 200 and 300 m +/-50 m and is presented in **Figures A3** to **A5**.

The influence of overburden lithology was found to be readily apparent once the database was filtered using the above cover depth ranges.

A4.2 Geological Factors

Once the first stage in the development of the subsidence prediction model had addressed the influence of cover depth the effect of “significant” overburden lithology above single longwall / miniwall panels could be addressed. **Figure A6** illustrates a physical model, showing the subsidence reducing effects of a massive strata unit.

Borehole data was used to derive the thickness and location of massive strata units considered to be critically important for surface subsidence prediction, for a given panel width and depth. The methodology takes into account the maximum massive strata unit thickness (t) at each location and the height to the base of the unit above the longwall panel (y).

The subsidence above a panel, given cover depth (H) and panel width (W) decreases significantly when a massive strata unit is thicker than a certain minimum limit value. The thickness is also reduced when the unit is closer to the surface. The strata unit is considered to have a 'high' subsidence reduction potential (SRP) when it exceeds a minimum thickness for a given y/H ratio, as shown in **Figures A7.1** to **A7.3** for each cover depth category.

For a thin strata unit located relatively close to a panel, the ‘Subsidence Reduction Potential (SRP) will be 'low'. However, there is also an intermediate zone, where a single strata unit (or several thinner units) below the 'high' subsidence reduction thickness can result in a 'moderate' reduction in subsidence. A second limit line can therefore be drawn, which represents the threshold between 'moderate' and 'low' SRP.

It is considered that the ‘high’ SRP limit line represents the point between elastic and yielding behaviour of a spanning beam. The ‘moderate’ SRP limit line represents the point between yielding behaviour and collapse or failure of a spanning beam (which has been yielding).

The limit lines have been determined for the strata units located at various heights (y) above the workings in each depth category, as shown in **Figures A8** to **A10**.

A4.3 Summary of Model Concepts

The **ACARP, 2003** model introduces several new parameters, to improve the definition of various types of overburden behaviour and the associated mechanics.

As outlined in **Section A4.2**, the ‘Subsidence Reduction Potential’ (SRP) of massive or thickly bedded geological units above single longwall panels for the Newcastle Coalfield has been introduced to describe the influence that a geological unit may have on subsidence magnitudes. The massive geological units are defined in terms of 'high', 'moderate' or 'low' SRP.

Massive unit thickness, panel width, depth of cover and height of unit above the workings are considered to be key parameters for assessing overburden stiffness and spanning capability over a given panel width, controlling surface subsidence. A conceptual model for overburden behaviour is illustrated in **Figure A11**.

Variation in subsidence along the length of a panel may therefore be due to the geometry and / or SRP variation of geological units within the overburden.

For W/H ratios <0.7, the overburden spans across the extracted panel like a 'deep' beam or linear arch, whereby the mechanics of load transfer to the abutments is governed by axial compression along an approximately parabolic shaped line of thrust, see **Figure A12**.

For W/H ratios >0.7 the overburden geometry no longer allows axially compressive structural behaviour to dominate, as the natural line of thrust now lies outside of the overburden. Bending action due to subsequent block rotation occurs. Provided that the abutments are able to resist this rotation, flatter lines of thrust still develop within the overburden, but the structural action is now dominated by bending action. This type of overburden behaviour has been defined as 'shallow' beam behaviour, which in structural terms is fundamentally less stiff than 'deep' beam behaviour. This results in a significant increase in subsidence or sag across an extracted longwall panel (all other factors being equal), as shown **Figure A12**.

"Voussoir beam" or "fractured linear arch" theory can be used to explain both types of overburden behaviour, as deep seated or flatter arches develop in the strata in an attempt to balance the disturbing forces.

The database also indicates the presence of a 'Geometrical Transition Zone', whereby subsidence increases significantly, regardless of the SRP of the geological units, as shown in **Figure A13**. This behaviour occurs when panel width to cover height ratio (W/H) ranges from 0.6 to 0.9. This phenomenon can be simply explained as a point of significant shift in structural behaviour and the commencement of overburden breakdown.

The model therefore allows the user to determine the range of expected subsidence magnitudes and the location of geology related SRP and/or 'geometrical transition zones' along a panel. Identification of the transition zones is an important factor in assessing potential damage risks of differential subsidence to important infrastructure, buildings and natural surface features, such as rivers, lakes and cliff lines etc.

The 'strata unit location factor' (y/H) was developed to assist in assessing the behaviour of massive strata units above the workings. The y/H factor is a simple way to include the influence of the unit location above the workings in terms of the effective span of the unit and the stresses acting upon it.

The key elements of this factor and their influence on the behaviour of the strata unit are:

- y, the height of the beam above the workings, which determines the effective span of the beam, and

- H, cover depth over the workings, which exerts a strong influence on the stress environment and, hence, the propensity for buckling or compressive failure of the beam.

Essentially beam failure due to the action of increasing horizontal stress (i.e. crushing or buckling) appears more likely as y decreases and H increases. The ratio of y/H may therefore be used to differentiate between the SRP of a beam of similar thickness, but at varying heights above the workings. The model also demonstrates that as the depth of cover increases, a thicker beam is required to produce the same SRP above a given panel width. This phenomenon may also be simply due to greater vertical load acting upon the massive strata 'beam'.

A5 Multiple Longwall Panel Subsidence Prediction

A5.1 General

The effect of extracting several adjacent longwall panels is governed by the stiffness of the overburden and the chain pillars left between the panels. Invariably, 'extra' subsidence occurs above a previously extracted panel and is caused primarily by cracking of the overburden and the compression of the chain pillars and adjacent strata between the extracted longwall panels.

A conceptual model of subsidence mechanisms above adjacent longwall panels in a single seam is shown in **Figure A14**.

A5.2 Predicting Subsidence above Chain Pillars (ACARP, 2003 Model)

A chain pillar undergoes the majority of life-cycle compression when subject to double abutment loading (i.e. the formation of goaf on either side, after two adjacent panels have been extracted). Surface survey data indicates that an extracted panel can affect the chain pillars of up to three or four previously extracted panels. The stiffness of the overburden and chain pillar system will determine the extent of load transfer to preceding chain pillars.

Multiple-panel effects have therefore been included in the model by adding empirical estimates of surface subsidence over chain pillars to the maximum subsidence predictions for single panels.

The empirical model presented in **ACARP, 2003** for estimating the subsidence above a chain pillar, was based on the regression equation presented in **Figure A15**. The model compares the ratio of chain pillar subsidence (Sp) over the extraction height (T), to the width of the chain pillar divided by the cover depth multiplied by the total extracted width (1000w/W'H).

A regression analysis on the data indicates a strong exponential relationship for 1000wcp/W'H values up to 0.543. For values > 0.543, the relationship becomes constant.

$S_p/T = 7.4044e–10.329F$ ($R^2 = 0.92$) for $F< 0.543$, and

$S_p/T = 0.023$ for $F > 0.543$

where

$F = 1000w/W'H$

W' = The total extracted width which includes the width of the panels extracted on both sides of the subject chain pillar, and the width of the chain pillar itself (i.e. $W' = W_i + w_i + W_{i+1}$).

Note that the final subsidence for a longwall panel with several subsequent extracted panels was then determined empirically by adding 50% of the predicted chain pillar subsidence (S_p) to the single panel S_{max} estimate.
This approach however, did not include an abutment angle to estimate pillar loads, which are likely to vary significantly between sub-critical and supercritical panel layouts.

*The chain pillar model has now been amended to include better predictions of chain pillar load that are consistent with ALTS methodology (refer **ACARP, 1998a**) and has resulted in the modified version presented in Section A5.2.*

A5.2 Predicting Subsidence above Chain Pillars (DgS, 2008 Model)

After the **ACARP, 2003** model was published; further studies on chain pillar subsidence measurements were undertaken at several mine sites in the Western (Springvale, Angus Place and Ulan) and Southern Coalfields (Appin and Elouera). The measured subsidence above the chain pillars was significantly greater than the Newcastle Coalfield pillars and considered to be linked to the stress acting on the pillars and the longwall mining height.

Maximum subsidence above the chain pillars invariably occurred after the pillars were subject to double abutment loading conditions (i.e. goaf on both sides).

The **ACARP, 2003** model for estimating chain pillar subsidence was subsequently superseded by the pillar stress v. strain type approach presented in **Figure A16**. The chain pillar stress was estimated by assuming a design abutment angle of 21^o for the pillar load, according to the methodology presented in **ACARP, 1998a** for sub-critical and supercritical longwall panels.

Prediction of subsidence above the chain pillars (S_p) was determined based on the following regression equation using the mining height, T and pillar stress, σ:

$$S_p/T = 0.238469/(1+e^{-[(\sigma-25.5107)/7.74168]}) \qquad (R^2 = 0.833)$$

The uncertainty of the predictions was estimated by calculating the variance of the residuals about the regression lines and calculating 90% Confidence Limits for the database as follows:

90% CL S_p error = 0.048T

It was also considered necessary to test if the above stress v. strain type approach was adequate for reliable predictions, by comparing the subsidence outcomes with the pillar Factor of Safety; see **Figure A17**.

The strength of the chain pillars was estimated using the rectangular pillar strength formulae presented in **ACARP, 1998b**. The FoS was derived by dividing the pillar strength by the pillar load (i.e. stress).

Generally it has been found that significant surface subsidence above the chain pillar (i.e. 10 - 30% of pillar height) starts to occur when the pillar FoS is < 2. For FoS values greater than 2, subsidence above the pillars is virtually independent of FoS and the pillars generally perform elastically under load.

The database indicates that when the FoS is < 2, the stiffness of the pillar starts to decrease, due to the development of load induced fracturing within the pillar and surrounding strata. FoS values of < 2 represent pillar stresses that exceed 50% of the pillar strength. Laboratory testing of coal and sandstone samples also show sample 'softening' as the ultimate load carrying capacity of the sample is approached.

For pillars with FoS values < 1, the subsidence above the chain pillars tend to a maximum limit of approximately 25 to 30% of the mining height. This type of behaviour is expected for chain pillars that have width to height ratios w/h > 5, which is the point where 'strain hardening' deformation starts to develop with increased confinement of the 'pillar core'.

A5.3 Calculation of First and Final Subsidence for Multiple Longwall Panels

Multiple panel predictions can be made by adding the predicted single panel subsidence to a proportion of the chain pillar subsidence (including the residual subsidence) to estimate first and final subsidence above a given longwall panel.

The definition of first and final S_{max} is as follows:

First S_{max} = the first maximum subsidence after the extraction of a longwall panel, including the effects of previously extracted longwall panels adjacent to the subject panel.

Final S_{max} = the final maximum subsidence over an extracted longwall panel, after at least three more panels have been extracted, or when mining is completed.

In the Newcastle Coalfield, First and Final S_{max} values for a panel are predicted by adding 50% and 100% of the predicted subsidence over the chain pillars respectively (i.e. between the previous and current panel) less the goaf edge subsidence (see **Section A5**).

Residual subsidence above chain pillars and longwall blocks tends to occur after extraction due to (i) increased overburden loading on pillars and (ii) on-going goaf consolidation or creep effects. Based on the final chain pillar subsidence measurements presented in **Figure A16**, the residual movements can increase subsidence by a further 10 to 30%.

An example of measured multiple longwall subsidence behaviour is presented in **Figure A18**.

Final subsidence is normally estimated by assuming a further 20% of the chain pillar subsidence will occur. However, this may be increased or decreased, depending on local experience.

The prediction of first and final subsidence originally presented in **ACARP, 2003** involved the use of several empirical coefficients, which have proven to be difficult to apply in practice. The interested reader may refer to this methodology, however, the above method is considered easier to apply and likely to result in a similar outcome.

In summary, the mean values of the First S_{max} and Final S_{max} are calculated as:

$$\text{First } S_{max} = \text{Single } S_{max} + 0.5(S_{p(i-1)} - S_{goe(i-1)})$$

$$\text{Final } S_{max} = \text{First } S_{max} + 1.0(\text{Final } S_{p(i)} - \text{First } S_{goe(i)})$$

The U95% Confidence Limits or Credible Worst Case Values are then:

$$\text{U95\% First } S_{max} = \text{mean First } S_{max} + 1.64\ (\text{U95\% } S_{max} \text{ error} + \text{U95\% } S_p \text{ error})^{1/2}.$$

$$\text{U95\% Final } S_{max} = \text{mean Final } S_{max} + 1.64\ (\text{U95\% } S_{max} \text{ error} + \text{U95\% } S_p \text{ error})^{1/2}.$$

It should also be understood that the terms ‘mean' and ‘Upper 95% Confidence Limit’ used in the model generally infer that the predicted maximum values will be exceeded by 50% and 5% respectively of the panels mined with similar geometry and geology etc.

Using lower probability of exceedence values (e.g. U99%CL) may be justified for particularly sensitive features, however, the magnitude of the maximum values does not usually increase significantly above the U95%CL values.

When local subsidence data is available for multiple longwall panels, the relationship between the multiple and single panel subsidence predictions can be determined as follows:

$$\text{First } S_{max} = \text{Single } S_{max} + 0.5b(S_{p(i-1)} - S_{goe(i-1)})$$

$$\text{Final } S_{max} = \text{First } S_{max} + b(\text{Final } S_{p(i)} - \text{First } S_{goe(i)})$$

The ‘b’ factor may be estimated from measured subsidence profiles, and allows the load transfer effect between the goaf and the chain pillars to be included in the model if necessary.

It has been observed at deeper NSW Coalfield Mines (i.e. the Western and Southern Coalfields) where the proportion of subsidence over the chain pillars to be added to the single panel subsidence decreased when the cover depth exceeded 350 m.

A6 Subsidence Profile and Impact Parameter Predictions

Part of the **ACARP, 2003** project included the development of several models to predict the maximum panel deformation parameters and surface profiles associated with subsidence. The following models were developed:

- panel goaf edge or rib subsidence,
- angle of draw,
- maximum transverse and longitudinal tilt, curvature and strain,
- the locations of the above parameters over the longwall panel for the purposes of subsidence profile development, and
- heights of continuous and discontinuous fracturing above the longwall, based on measured surface tensile strains and fracture limit horizons over extracted panels (see **Section A7** for details).

A conceptual model of surface deformation profiles that develop above longwall panels is given in **Figure A19**.

All of the above subsidence parameters have been statistically linked to key geometrical parameters such as the cover depth (H), panel width (W), working height (T) and chain pillar width (w_{cp}) and shown in **Figures A20** to **A27**.

A summary of all the empirical model relationships between the key subsidence profile parameters that were developed in **ACARP, 2003** and DgS are presented in **Table A3**.

Table A3 - Summary of Subsidence Impact Parameter Prediction Models Developed from ACARP, 2003

Parameter	Regression Equation and +/- 90% Confidence Limits or Upper95%CL	Coefficient of Determination (R^2)	Figure No.
Subsidence Reduction Potential (SRP) of Strata Unit in Overburden with thickness t, panel width, W and location factor, y/H above workings for Cover Depth Category	**High** SRP t for a given panel W plots above line for given strata unit y/H. **Moderate** SRP t plots between High SRP line and next y/H line below it. **Low** SRP t plots below Moderate SRP limit line.	N/A - curve location determined by successful re-prediction of >90% of cases I databases	**Figure A8** for H<150m; **Figure A9** for H< 250m; **Figure A10** for H< 350m
Single Maximum Longwall Panel Subsidence (Single S_{max}) for Assessed Strata Unit SRP of Low, Moderate or High	Upper and Lower bound prediction lines for a given SRP are used to estimate range of S_{max}/T for a given Panel W/H. Average of limit lines value is mean Single S_{max} value +/- 0.03T for W/H < 0.6; +/- 0.1T for 0.6<W/H<0.9; +/-0.05T for W/H>0.9	N/A - curve location determined by successful re-prediction of >90% of cases I databases	**Figure A3** for H<150m; **Figure A4** for H< 250m; **Figure A5** for H< 350m
Chain Pillar Subsidence, S_p (m)	Mean $S_p/T = 0.238469/(1+e^{-[(\sigma DAL-25.5107)/7.74168]})$ +/- 0.048T	$R^2 = 0.833$	**Figure A16**
Goaf Edge Subsidence	Mean $S_{goe}/S_{max} = 0.0722(W/H)^{-2.557}$ U95%CL $S_{goe}/S_{max} = 0.0719(W/H)^{-1.9465}$	$R^2 = 0.82$	**Figure A20**
Angle of Draw	Mean AoD = $7.646Ln(S_{goe})+32.259$ U95%CL = Mean AoD + 8.7^o	$R^2 = 0.56$	**Figure A21**
Maximum Tilt T_{max} (mm/m)	$T_{max} = 1.1925(S_{max}/W')^{1.3955}$ +/- $0.4T_{max}$ (W' = lesser of W and 1.4H)	$R^2 = 0.94$	**Figure A22**
Maximum Convex Curvature C_{max} (km^{-1})	Mean $C_{max} = 15.60(S_{max}/W'^2)$ +/- 0.5Mean	$R^2 = 0.79$	**Figure A23**
Maximum Concave Curvature C_{min} (km^{-1})	Mean $C_{min} = 19.79(S_{max}/W'^2)$ +/- 0.5Mean	$R^2 = 0.79$	**Figure A24**
Maximum Tensile Strain E_{max} (mm/m)	Mean 'smooth' $E_{max} = 5.2C_{max}$ +/- 0.5 Mean Mean 'Cracked' $E_{max} = 14.4C_{max}$	$R^2 = 0.72$ $R^2 = 0.32$	**Figure A25**
Maximum Compressive E_{min} (mm/m)	Mean $E_{max} = 5.2(C_{min})$ +/- 0.5 Mean Mean 'Cracked' $E_{min} = 14.4C_{min}$	$R^2 = 0.72$ $R^2 = 0.32$	**Figure A25**
Critical Panel Width	W_{crit} = 1.4H where H = cover depth	N/A	**ACARP, 2003**

Table A3 (Continued) - Summary of Subsidence Impact Parameter Prediction Models Developed from ACARP, 2003

Subsidence at Inflexion Point or Maximum Tilt S_{Tmax}	Mean S_{Tmax}/S_{max} = -0.0925(W/H)+0.7356 +/- 0.2	R^2 = 0.5	**ACARP, 2003**
Distance to Inflexion Point, d/H	d/H = 0.2425Ln(W/H) + 0.3097	R^2 = 0.73	**Figure A27**
Distance to Peak Tensile Strain (mm/m)	d_t/H = 0.1643Ln(W/H) + 0.2203 for W/H >0.6; d_t/H = 0.2425Ln(W/H) + 0.2387 for W/H <0.6;	R^2 = 0.28	**Figure A27**
Distance to Peak Compressive Strain (mm/m)	d_c/H = 0.3409Ln(W/H) + 0.3996 for W/H >0.6; d_c/H = 0.2425Ln(W/H) + 0.3767 for W/H <0.6	R^2 = 0.59	**Figure A27**

* - If H within 25 m of depth category boundary, then average result with overlying or underlying depth category value.
- Centreline profile parameters are not presented here (refer to **ACARP, 2003**).

A7 Subsidence Profile Predictions above Longwall Panels

Predicted 'smooth' subsidence profiles above single and multiple longwall panels have been determined based on cubic spline curve interpolation through seven key points along the subsidence trough (i.e. maximum in-panel subsidence, inflexion point, maximum tensile and compressive strain, goaf edge subsidence, subsidence over chain pillars and 20 mm subsidence or angle of draw limit).

The locations of these points have been determined empirically, based on regression relationships between the variables and the geometry of the panels (see **Table A3**). Both transverse and longitudinal profiles have been derived in this manner.

First and second derivatives of the fitted spline curves provide 'smooth' or continuous subsidence profiles and values for tilt and curvature. Horizontal displacement and strain profiles were derived by multiplying the tilt and curvature profiles by an empirically derived constant associated with the bending surface beam thickness (based on the linear regression relationship between the variables, as discussed in **ACARP, 2003**).

An allowance for the possible horizontal shift in the location of the inflexion point (within the 95% Confidence Limits of the database) has also been considered, for predictions ofsubsidence at features located over the goaf or extracted area.

A8 Subsidence Contour Predictions above Longwall Panels

Subsidence contours can be derived with geostatistical kriging techniques over a 10 m square grid using Surfer 10® software and the empirically derived subsidence profiles along cross lines, centre lines and corner lines around the ends of the longwall panels. Vertical 'slices' may taken through the contours to (i) determine subsidence profiles along creeks or infrastructure, and (ii) assess the likely impacts on the relevant surface features.

A8.1 Subsidence Contours

Subsidence contour predictions have been made in this study using SPDS®, which is an influence function based model that firstly calculates seam convergence and pillar displacements empirically around the workings. The influence of an extracted element of coal is transmitted to the surface via a 3-D influence function, which also takes varying topography into account.

The model is usually calibrated to measured maximum subsidence values by adjusting key parameters such as influence angles and inflexion point location from extracted panel sides.

A8.2 Tilt and Curvature Contours

The predicted principal tilt and curvature contours were derived using the calculus module of the Surfer10® program and the predicted subsidence contours from the SPDS® runs. The subsidence contours were based on a 10 m grid.

Principal tilts (i.e. surface gradient or slope) were calculated by taking the first derivative of the subsidence contours in x and y directions as follows:

$$T_p = [(\partial s/\partial x)^2 + (\partial s/\partial y)^2]^{0.5}$$

where ∂s = subsidence increment over distances ∂x and ∂y along x and y axes.

Principal curvatures (i.e. rate of change in slope or surface bending) were calculated by taking the second derivative of the subsidence contours in x and y directions as follows:

$$C_p = [(\partial^2 s/\partial x^2)(\partial s/\partial x)^2 + 2(\partial^2 s/\partial x \partial y)(\partial s/\partial x)(\partial s/\partial y) + (\partial^2 s/\partial y^2)(\partial s/\partial y)^2]/pq^{2/3}$$

where $p = (\partial s/\partial x)^2 + (\partial s/\partial y)^2$ and $q = 1+p$

A8.3 Strain

Before predictions of strain can be made, the relationship between the measured curvatures and strain must be understood. As discussed in **NERDDP, 1993b** and **ACARP, 2003**, structural and geometrical analysis theories indicate that strain is linearly proportional to the curvature of an elastic, isotropic bending 'beam'; see **Figure A28**. This proportionality actually represents the depth to the neutral axis of the beam, or in other words, half the beam

thickness. **NERDDP, 1993b** studies returned strain over curvature ratios ranging between 6 and 11 m for NSW and Queensland Coalfields. Near surface lithology strata unit thickness and jointing therefore dictate the magnitude of the proportionality constant between curvature and strain.

ACARP, 2003 continued with this approach and introduced the concept of secondary curvature and strain concentration factors due to cracking. The peak strain / curvature ratio for 'smooth' subsidence profiles in the Newcastle Coalfield was assessed to equal 5.2 m (mean) and 7.8 m (U95%CL) with the possibility that surface cracking could increasing the 'smooth-profile' strains to 10 or 15 times the curvature. The above values may also be affected by the thickness of near surface geology.

Reference to **DMR, 1987** also suggests a curvature to strain multiplier of 10 for high pillar extraction and longwall panels in the Newcastle Coalfield.

Attempts by others to reduce the variability in strain and curvature data by introducing additional parameters, such as the radius of influence, r, by **Karmis et al, 1987** and cover depth, H, by **Holla and Barclay, 2000**, appear to have achieved moderate success in the coalfields in which they were applied. However, when these models were applied to the Newcastle Coalfield data presented in **ACARP, 2003**, the results did not appear to improve things unfortunately; see **Figures A29.1** and **A29.2**.

It is therefore considered that the variability in behaviour is probably due to other parameters, which are very difficult to measure (such as the thickness and flexural, buckling and shear strengths of the near surface strata).

Provided that the likelihood of cracking can be ascertained from the strain predictions, then appropriate subsidence management plans can still be implemented.

A9 Prediction Of Subsidence Impact Parameters And Uncertainty Using Regression Analysis Techniques

A9.1 Regression Analysis

Key impact parameters have been predicted using normalised longwall subsidence data from the Newcastle Coalfield. This approach allows a reasonable assessment of the uncertainty involved using statistical regression techniques. A linear or non-linear regression line has been fitted to the database for each impact parameter, normalised to easily measured parameters, such as maximum subsidence, panel width and cover depth. The quality or significance of the regression line is influenced by the following parameters:

(i) the size of the database,

(ii) the presence of outliers, and

(iii) the physical relationship between the key parameters.

The regression curves were reviewed carefully, as such curves can be (i) affected by outliers, and (ii) misleading, in that by adopting a mathematical relationship which gives the best fit (i.e. R^2) the curves are controlled by the database and may not reflect the true underlying physical dependencies or mechanisms that the data represents.

These issues are inherent in all prediction modelling techniques because, for example, all models must be calibrated to field observations to validate their use for prediction or back analysis purposes.

The regression techniques presented in the **ACARP, 2003** was done by firstly assessing conceptual models of the mechanics and key parameter dependencies (based on established solid mechanics and structural analysis theories), before generating the regression equations.

Several outliers in the model databases were excluded in the final regression equations, but only when a reasonable explanation could be given for each anomaly (i.e. multiple seam subsidence, geological faults / dykes and surface cracking effects).

The regression equations in **ACARP, 2003** have R^2 (i.e. Coefficients of Determination) values generally greater than 50%; indicating that the relationships between the variables are significant. For cases where the R^2 values are < 50%, the regression lines are almost horizontal (i.e. the parameter doesn't change significantly over the range of the database), and the use of the regression line will be close to the mean of the database anyway.

A9.2 Prediction Model Uncertainty

The level of uncertainty in the model predictions has been assessed using statistical analysis of the residuals or differences between the measured data and regression lines (i.e. lines of best fit). The *Standard Error* of the prediction has been derived from the residuals, which has then been multiplied by the appropriate 'z' or 't' statistic for the assumed normal probability distribution to define Upper (and Lower) Confidence Limits.

The residual population errors for the single panel subsidence model are shown in **Figure A30**.

The empirical database therefore allows an assessment of variance and standard error such that the required subsidence parameter's mean and upper 95% Confidence Limit (Credible Worst Case) values can be determined for a given mining geometry and geology.

Provided there are (i) more than 10 data points in the data sets covering the range of the prediction cases, and (ii) the impact parameter and independent variables have an established physical relationship based on solid or structural mechanics theories, then it is considered unlikely that the regression lines will be significantly biased away from the underlying physical relationship between the variables by any limitations of the data set.

On-going review of each of the regression equations over the past six years by DgS has not required significant adjustment of the equations to include new measured data points. The

regression equations derived are also amenable to spreadsheet calculation and program automation.

It is also important to make the distinction between the terms confidence *limit* and confidence *interval*. The Credible Worst Case terminology used in the model is **not** the upper limit of the 95% Confidence **Interval** - which would encompass 95% of the data. Since the lower 95% Confidence Limit is rarely used in practice, it was considered appropriate to adopt the 5% Probability of Exceedence values instead (this by definition represents the upper limit of the **90% Confidence Interval**).

Further, the term *Upper 95% Confidence Limit* used in the **ACARP, 2003** model is considered acceptable in the context of 'one-tailed' probability distribution limits (i.e. the Lower 95% Confidence Limit is generally of little practical interest).

A10 Subsidence Model Validation Studies

A10.1 Model Development

The **ACARP, 2003** model was developed so that it could re-predict > 90% of the database on which it is based. Validation studies also included comparison of measured and predicted subsidence, tilt and strain profiles above several longwall panel crosslines and centrelines. Examples of predicted and measured profiles above multiple panels for the Newcastle Coalfield are shown in **Figures A31** to **A34** using the **ACARP, 2003** model. Subsequent predictions v. measured subsidence profiles are presented in **Figures A35** to **A38** using the updated version of the model discussed herein.

DgS is usually required to review predicted v. measured subsidence profiles after the completion of a longwall panel and report the results to mines and government departments. Over the past nine years, the model has usually over predicted measured subsidence, with the data falling somewhere between the mean and U95%CL values. Prediction exceedances have occurred less than 5% of the time and where the assessment of the overburden SRP was found to be incorrect.

The predictions of curvature and strain, however, are generally problematic due to the common effects of discontinuous or cracking behaviour (i.e. lithological variation and cracking), resulting in measured strains that can be two to four times greater than predicted 'smooth' profile strains. This issue is discussed further in **Section A10.2**.

A10.2 Field Testing of Strain Predictions

Strain and curvature concentrations can increase 'smooth' profile strains by 2 to 4 times in the Newcastle Coalfield, when the panel width to cover depth ratio (W/H) exceeds 0.8 or radius of curvature is less than 2 km, see **ACARP, 2003**.

Where cracking occurs, measured strains will be highly dependent on the bay-length. Rock exposures with widely spaced or adversely orientated jointing can also result in much larger crack widths than for a location with deep soil profiles.

For example, a measured strain of 3 to 6 mm/m along a cross line above a longwall panel in the Newcastle Coalfield caused several cracks in soil that ranged in width from 10 mm to 30 mm and a single 100 mm wide crack in a sandstone rock exposure with medium strength and widely spaced jointing, see **Figure A39**.

At the moment, it is not possible to predict the magnitude of strains from 'smooth profile' models confidently, however, it is possible to make reasonable predictions that strains > 2 mm/m will cause cracking within the tensile strain zones. Shearing and buckling is also likely to occur within the compressive zones above a longwall with shallow surface rock.

Overall, strains and cracking can be managed effectively by assuming cracks will occur within the limits of a longwall panel and may need to be repaired after each panel is completed.

A11 Sub-Surface Fracturing Model

A11.1 Sub-Surface Fracturing Zones

The caving and subsidence development processes above a longwall panel usually result in sub-surface fracturing and shearing of sedimentary strata in the overburden, according to **Peng and Chiang, 1984** (see **Figure A40a**) and **Whittaker and Reddish, 1989** (see **Figure A40b**). The height of fracturing (HoF) is dependent on mining geometry and overburden geology.

International and Australian research on longwall mining interaction with groundwater systems indicates that the overburden may be divided into essentially four or five zones of surface and subsurface fracturing. The zones are defined in **Table A4** (in descending order):

Table A4 - Sub-Surface Fracture Zone Summary

Zone Type	Zone	Fracture and Groundwater Response Description	Typical Vertical Strain (mm/m)
Surface Cracking Zone (un-constrained)	D	Vertical cracking due to horizontal strains extending to maximum depths of 10 - 15 m. Surface waters may be diverted below affected area and resurface downstream where interaction with B & C Zones occur.	<3
Elastic Deformation Zone (dilated bedding & constrained)	C	Generally unaffected by strains with some bedding parting dilation. Horizontal strains constrained by overlying/underlying strata. Groundwater levels may be lowered temporarily due to new storage volume in voids between beds, but likely to recover at a rate dependant on climate. Elastic Zone may not be present if B or A Zones extend up to Surface Zone.	<3
Discontinuous Fracture Zone (dilated bedding & constrained)	B	Minor vertical cracking due to bending that do not extend through strata units. Increased bedding parting dilation and similar groundwater response to Zone C. Some groundwater leakage may occur to B Zone, however, losses likely to be recharged by surface hydro-geological system.	<8
Continuous Fracture Zone (unconstrained)	A	Major vertical cracking due to bending that pass through strata units and allow a direct hydraulic connection to workings below. Full depressurisation of groundwater occurs in the Zone that may recover in the long term once mining is completed.	>8
Caved (included in the A-Zone)	A	Caved strata up to 3 to 5 x Mining Height above the workings. Collapsed roof bulks in volume to provide some support to overlying strata.	>80

The characteristics of each HoF zone are further described below:

Starting from the seam level, the **Caved Zone** (included in the **A-Zone**) refers to the immediate mine workings roof above the extracted panel, which has collapsed into the void left after the coal seam has been extracted. The Caved Zone usually extends for 3 to 5 times the mining height, T, above the roof of the mine workings due to bulking factors of 1.3 to 1.5, and sometimes from 10 to 15T if the strata have low bulking properties (e.g. bulking factors of 1.10 to 1.15). Thinly bedded and laminated strata are likely to have lower bulking factors than thickly bedded or massive units within the Caved Zone.

The **Continuous Fracture Zone (A-Zone)** has been affected by a high degree of bending deformation, resulting in significant fracturing and bedding parting separation and shearing of the rock mass. Vertical tensile strains range from -10 to 140 mm/m with strata dilation in excess of 1 m. Compressive strains tend to develop at horizontal bedding separations after initial fracturing and overlying strata deflections occur resulting in re-compaction of the goaf and disturbed strata.

Continuous sub-surface fracturing refers to the zone of cracking above a longwall panel that is likely to result in a direct flow-path or hydraulic connection to the workings. All groundwater (or surface waters) within this Zone would be expected to drain vertically into the mine workings goaf.

The **Strata Dilation Zone (B-Zone)** refers to the section of overburden immediately above the A-Zone that has also been deformed by bending action, but to a lesser degree than the A-Zone. The B-Zone will have bedding parting separations and discontinuous fractures through bending strata units due to vertical strains ranging from -2 to 8 mm/m and strata dilation from 30 mm to 400 mm, depending on the panel width. An increase to horizontal rock mass permeability (hydraulic conductivity) is expected in the B-Zone with groundwater flowing horizontally into dilated strata.

Only minor vertical permeability increases are expected in the B-Zone due to alternating horizontal tensile and compression zones associated with Voussoir Beam action above the A-Zone. It is noted in **Whittaker and Reddish, 1989**, that some groundwater leakage from the B-Zone to the A-Zone is possible due to limited crack or joint interaction between the zones.

Overall, the majority of the B-Zone is considered to be a ‘constrained’ and ‘dilated’ zone with low connectivity potential to the mine workings. The B-Zone therefore represents a sub-surface fracturing zone that causes temporary groundwater system disturbance.

The **Elastic Deformation Zone (C-Zone)** is located above the B Zone and is the zone where the strata may have suffered minor bending and disturbance. Impacts include horizontal shearing and minor bed separations or dilation of up to 30 mm due to vertical tensile strains between 1 and 2 mm/m. The bedding separations may result in minor increases to horizontal hydraulic conductivity and negligible changes to vertical hydraulic conductivity. Groundwater system disturbance is expected to be negligible in this zone.

The development of the Elastic Deformation Zone (C-Zone) will depend on the mining geometry and the presence of spanning strata. The C-Zone is probably only likely to develop above critical to sub-critical mining geometries (i.e. W/H < 1.4) but may also be present above super-critical panels also if favourable geological conditions exist.

The strata in the B and C-Zones are also likely to be in compression due to natural arch formation (above sub-critical and critical panels). The arch will also act as barrier to vertical drainage of groundwater despite the presence of naturally occurring vertical joints in the rock mass. Low permeability strata such as claystone, tuff and mudstone will also limit rock mass 'gaps' and further retard vertical flow rates through these zones.

In the absence of significant geological structure (i.e. faults and dykes), the overall effect on the surface groundwater system due to leakage through the B and C-Zones will be minimal, with re-charging of groundwater losses likely to occur from the surface hydrological system. The presence of significant geological structure may increase the drainage rates through these strata zones however. Monitoring of mine groundwater makes v. rainfall - runoff data will determine the rate of leakage that is occurring through these zones.

The **Surface Cracking Zone (D-Zone)** includes the vertical cracking due to horizontal tensile and compressive strains caused by mine subsidence deformation. The D-Zone may extend to depths ranging from 5 m to 20 m (typically < 15 m) in the Newcastle Coalfield, and is dependent on near-surface geology and surface topography.

For mine design purposes, typical D-Zone depths in relatively flat terrain may be assumed to range from 10 m to 12 m (i.e. < 15m). *Note: **Forster and Enever, 1992** adopted a D-Zone thickness of <15 m based on data from Wyee and Cooranbong Collieries, and included it in the minimum cover depth formula of 45T+10 m for designing supercritical panels below tidal waters of Lake Macquarie in the Newcastle Coalfields.*

A11.2 Impact on Rock Mass Permeability

In regards to changes to rock mass permeability, **Forster, 1995** indicates that horizontal permeabilities in the fractured zones above longwall mines could increase by 2 to 4 orders of magnitude (e.g. pre-mining $k_h = 10^{-9}$ to 10^{-10} m/s; post-mining $k_h = 10^{-7}$ to 10^{-6} m/s).

Vertical permeability's could not be measured directly from the boreholes but could be inferred by assuming complete pressure loss in the 'A Zone', where direct hydraulic connection to the workings occurs. Only a slight increase in the 'B zone' or indirect / discontinuous fracturing develops (mainly due to increase in storage capacity) from bedding parting separation. It is possible that minor vertical flows will occur from B zone into A zone (and workings) as well.

Discontinuous fracturing would be expected to increase rock mass storage capacity and horizontal permeability without direct hydraulic connection to the workings. Rock mass permeability is unlikely to increase significantly outside the limits of extraction.

A11.3 Mine Design Criteria for Sub-Surface Fracture Height Control

When designing mining layouts for sub-surface fracture control, the A-Zone is the most significant in regards to groundwater and surface water interaction as it represents the region of broken ground whereby a hydraulic connection to the mine workings will most certainly occur.

The B-Zone is probably just as important as it represents the transition zone between the continuously fractured ground and elastic deformation or surface zones. The B-Zone also includes strata which are confined and where bedding parting separations (i.e. dilations) occur in the sagging rock mass above the caved and broken strata units in the A-Zone.

The C-Zone has been deformed as well, but not to the same extent as the B-Zone.

Note: It is difficult to define the boundary between the B and C-Zones without vertical strain measurements from extensometers. Both zones are considered to be 'constrained' and 'dilated' and will act as an effective barrier between the A-Zone and near surface groundwater and surface watercourses.

The formation and thickness of the HoF Zones will firstly be dependent on the 'criticality' of the proposed longwall panel. The same terms used for subsidence prediction are also referred to below and are based on the ratio between panel width (W) and the cover depth (H):

- Subcritical refers to panels with W/H < 0.7;
- Critical refers to panels with W/H > 0.7 and < 1.4; and
- Supercritical refers to panels with W/H > 1.4.

Several case studies have been referred to below which consider super-critical and sub-critical panel geometries separately due to their fundamental differences in spanning behaviour.

Conceptual models of the A and B-Zones above supercritical panels are presented in **Whittaker & Reddish, 1998** and are based on physical modelling results. **Forster and Enever, 1992** indicated similar strata zoning from field monitoring (**Figure A40c**) above supercritical, total pillar extraction panels in the Lake Macquarie Area of the Newcastle Coalfield.

A conceptual model that includes the B and C-Zones was presented in **ACARP, 2007** (**Figure A40d**) for sub-critical mining geometries in the Western Coalfield. A similar sub-surface fracture zoning is also suggested by **Mark, 2007** (**Figure A40e**) for the US Coalfields and **Kendorski, 1993** for the UK Coalfields (**Figure A40f**).

From the above conceptual height of fracturing models, several simple empirical models have been developed over the years to estimate the thicknesses of the A, B and C-Zones for the purpose of avoiding groundwater and surface water connectivity with underground mines.

The suite of HoF prediction models that probably represent the state-of-the-art are summarised in the following sections.

A11.3.1 Wardell, 1975, Reynolds, 1977 and Singh and Kendorski, 1981

Wardell, 1975 recommended a minimum rock cover depth of 50T - Surface Zone thickness above total extraction or longwall panels when mining under tidal waters in the Newcastle Coalfield. The minimum cover depth (H) was based on a maximum horizontal tensile strain limit of 7.5 mm/m and the Newcastle Holla curves. It is noted that a maximum horizontal tensile strain of 10 mm/m has been specified in the UK when mining below permanent waters.

Wardell has also recommended a minimum cover depth of 60T (which included a Surface Zone thickness ranging from 12 m to 15 m) for mining below stored waters with longwalls in the Southern Coalfield.

The Wardell Guidelines recommended that panel widths should be limited to <0.4H to maximize the thickness of the Constrained Zone (i.e. B and C-Zones) beneath tidal waters. **Reynolds, 1977** recommended 0.33H for maximum panel widths at depths more than 120 m below the reservoirs in the Southern Coalfield.

The height of continuous fracturing was not estimated in the Wardell Guidelines, but probably assumed to be significantly lower than 50T - the 15 m thick surface cracking zone. **Holla, 1991** noted that the 60T value is dependent on the S_{max} and K ratio (and hence W/H ratio) and should not be applied blindly to all mining geometries.

Singh and Kendorski, 1981 adopted a general height of A-Zone Fracturing of $56T^{0.5}$ based on a review of international case studies with a minimum Constrained plus Surface Zone thickness of 45 m for mudstone and 57 m for sandstone strata conditions when mining below tidal waters. The model recognizes that fracturing may extend further through massive strata than thinly bedded units due to their propensity to carry greater load.

A11.3.2 Whittaker and Reddish Physical Model, 1989

It is considered that the published physical modeling work in **Whittaker and Reddish, 1989** provides valuable insight into the mechanics of sub-surface fracturing over longwall panels. The outcomes included specific guidelines (over and above such work as the Wardell, 1975 Guidelines) for the prevention of inundation of mine workings beneath surface and sub-surface water bodies.

The **Whittaker and Reddish, 1989** height of fracturing model was developed in response to the water ingress problems associated with early longwall extraction at the Wistow Mine in Selby, UK. The longwall panel was located at 350 m depth and experienced groundwater inflows of 121 to 136 litres/sec when sub-surface fracturing intersected a limestone aquifer 77 m above the seam.

The physical model is a scaled down version of the real-world, and therefore requires compatible material strength properties (i.e. plaster) to generate fracturing from the laboratory-sized void widths and mining heights being simulated. The pattern of cracking and heights of fracturing observed should therefore not be dismissed because of the materials used to create the model.

The Whittaker and Reddish model identifies two distinct zones of fracturing above super-critical width extractions (continuous A-Zone and discontinuous B-Zone fracturing) and indicates the height of each is a function of maximum tensile strain at the surface. As such, its use is also based upon being able to make credible subsidence and strain predictions. The mechanical concepts of the model are shown in **Figure A40b**.

The definition of the 'continuous' height of fracturing refers to the height in which a zone of direct hydraulic connection for groundwater inflows to the mine workings develops (i.e. the A-Zone).

The definition of the extent of 'discontinuous' height of fracturing refers to the height at which the horizontal permeability increases as a result of strata de-lamination and incomplete fracturing through the strata beds (i.e. the B-Zone). Minor occurrences of direct connection of fractures to the workings is considered possible, but will depend on the geology (e.g. the presence of persistent vertical structure such as faults and dykes).
The outcomes of the modeling work resulted in two logarithmic type curves that relate the surface horizontal strain to the measured A and B fracture heights normalized to the cover depth (see **Figure A40b**).

The physical modeling work that was completed to derive the prediction curves is summarised below:

- The physical model was constructed from multiple 1.25 cm thick layers of coloured sand and plaster with sawdust bond breakers placed between each successive layer. Based on a real world/model ratio of 92, the model layers represented 1.15 m thick layers in the real world. The model was initially devoid of vertical joints or cracks.

- The scale and mechanical properties of the model satisfied dimensional analysis and similitude laws. *Note: This aspect of mechanical models is very important, as overburden strength properties will not fracture if they are too high for the model's mining geometry.*

- The plaster layers for the model were equivalent to a rock mass with a density of 2.35 t/m^3, a UCS of 10.94 MPa and Youngs Modulus, E, of 984 MPa.

- The model was used to simulate the overburden behaviour of a panel with a W/H ratio of 1.31 and a progressively increasing working height range that commenced at 1.2 m and finished at 10.8 m. The advancing longwall face was simulated by removing timber blocks at the base of the model in 1.2 m to 2.0 m lift stages.

- The extent or heights of 'continuous' and 'discontinuous' fracturing above the longwall 'face' were measured and plotted with the associated peak tensile strain predictions at the surface. The subsidence and strains were measured from a grid and calculated using the method provided in the **UK Subsidence Engineers Handbook, 1975**.

- The fracturing path progressed up at an inward angle of approximately 18^o to 19^o from the solid rib and increased towards the centre of the panel higher up into the strata. Continuous fracturing occurred in the cantilever bending zone close to the rib-side only, as fracturing in the overburden above the middle portion of the panel tended to 'close' and did not appear to represent an area where groundwater inflows into the workings would eventuate.

- Surface cracks extended down from the surface for a depth up to 7.5 m.

- Other similar models were also prepared and used to demonstrate the "ability of strong overburden at the surface to cause bridging of the strata in this manner is dependent upon the strength and general competence of the rocks near to the surface, in addition to the width of the extracted region."

- Any groundwater inflow conditions were therefore considered to be "mainly associated with the longwall rib-side fracture zone [or tensile strain zone]" above longwall panels.

The findings above are considered reasonable for super-critical longwall geometries where panel widths are greater than the critical width (i.e. 1.2 - 1.4H) and the height of fracturing is likely to be controlled primarily by the mining height and strata properties.

Using the analytical model equations derived in **Section A11.4.2**, the progression of the height of continuous fracturing was back analysed by DgS using the maximum compressive beam stress for spanning strata units under full loading conditions (Equation 1) and goaf supported strata units (Equation 2):

$$\sigma_c = 0.75\gamma(H - A)(W - 2A\tan\theta)^2/t_i^2 \qquad \text{(Lower Beam)} \qquad (1)$$

$$\sigma_c = 4\Delta E t_i/(W - 2A\tan\theta)^2 \qquad \text{(Upper Beams)} \qquad (2)$$

It was noted that the goaf did not 'bulk' in the model, resulting in no reduction in subsidence between the seam and surface (i.e. $S_{max} = T$) and measured surface strain/curvature ratio indicated $\Delta = 0.5T$ over the effective span, $W_i = W - 2y\tan\theta$ above the goaf.

The results of the model are summarized in **Table A5** below:

Table A5 - Physical Model Results Summary for the Height of Continuous Fracturing Development above a Supercritical Longwall Panel

Lift No	Mining Height T (m)	S_{max} (m)	E_{max} (mm/m)	A (m)	Effective Beam Span W_i (m)	Measured Beam Curvature in Spanning Strata (km^{-1})	Measured Effective Beam Thickness t_i (m)	Stress in Lowest Beam after Lift & Prior to Collapse (MPa)	Stress in Spanning Unit above Goaf (MPa)	Predicted Minimum Beam Thickness Required to Span Goaf (m)
1	1.2	1.2	7.6	23.96	137.55	0.51	105 (47.9)	12.0	4.82	**56.7**
2	2.4	2.4	15.3	43.26	120.77	0.66	81 (38.6)	12.5	7.81	**43.6**
3	4.2	4.2	26.8	67.38	107.25	1.46	62 (24.1)	17.3	6.55	*26.6*
4	6.0	6.0	38.2	85.60	90.36	2.94	38 (18.2) (9.1)	13.8	10.10	*10.8*
5	8.4	8.4	53.5	99.57	77.60	5.58	19.4 (14) (7)	19.2	7.45	*5.6*
6	10.8	10.8	68.8	105.0	67.81	9.39	5.4 (2.7)	12.5	-	*3.0*

Wi = Effective Span above mine workings at A-Zone Limit Horizon (W - 2Atanθ).
(9.1) - Bedding thickness halved as bedding sheared under load > it's shear strength during test.
Bold - stress limited to UCS based on full cover load (Equation 1).
italics - stress limited to UCS based on deflecting strata curvature (Equation 2).
UCS = 10.94 MPa; E = 984 MPa; θ=19.3°.

The measured strata unit thickness (t_i) required to span the goaf voids and limit the height of continuous fracturing (A) after each successive lift were back-analysed using the measured A-Zone heights and Equation (2); see **Figure A40g**. The minimum beam thickness required to span the goaf was also estimated based on the two analytical model Equations (1) and (2) and compared to the measured beam thickness at the A-Horizon in **Figure A40h**.

Several further salient points are apparent from the results as follows:

- After extraction of the panel, all of the spanning units deflected under gravity loading until the tensile, shear and compressive stresses in some of the rock mass bedding units were exceeded.

- It was apparent from the modelling data that the overburden above each mining stage resulted in the beam shearing into two or three separate beams, with the lower beam collapsing and the upper beam(s) left to span the void. It is noted that the maximum shear stress acting on the initial beam would have developed on the bedding surface near the middle of the beam section, so it would be expected to shear or slip there first.

- If the strata unit separated from the overlying rock mass, it either collapsed into the void below (if the stress exceeded the UCS of the beam) or it was thick enough to span under its own self weight. The sagging beam units were also supported by the underlying goaf to some degree.

- The rock mass units caved up into the overburden at an angle of break (θ) and effectively reduced the span of overlying units to $W_i = W-2ytan(\theta)$.The potential load acting on the strata units also decreased linearly with the reduction in overlying cover.

- The height of continuous fracturing (i.e. the A-Zone) was defined as the point where the overlying strata were spanning the cracked and collapsed strata below it.

- The A-Zone height increased after the mining height T was increased, with no change to panel width or cover depth.

- The strata units continued to deflect after each incremental increase in mining height, with the lower units collapsing when the UCS of the beam was exceeded. In some of the lifts, it is apparent that the spanning strata units sheared into units that were approximately half the thickness of the original spanning beam. The beam stress was also subsequently decreased if shearing occurred. Estimates of shear stress at mid-beam thickness exceeded the shear strength of the strata unit (or bedding plane surface) in these instances, assuming a friction angle of 20^o along the bedding planes.

- The spanning strata lost stiffness when their thickness was decreased, resulting in further deflection (and stress acting in the beam).

- Collapsed strata units provided support to the sagging strata above and ultimately controlled the deflection of the overlying units.

- The A/T ratio ranged from 20 to 10 as the mining height increased from 1.2 m to 10.8 m. For real world mining heights of 2.4 m to 6 m, the A/T ranged from 18 to 14.

Further discussion on the analytical height of fracturing models for real world conditions is presented in **Section A11.4.2**.

A11.3.3 Forster and Enever, 1992

A comprehensive monitoring program above two supercritical pillar extraction and one longwall panel in the Great Northern Seam was presented in **Forster and Enever, 1992**.

The outcomes of the work was to recommend a reduction in the minimum rock cover limit required to extract coal beneath Lake Macquarie to 45T + 10 m, and was based on borehole piezometric and rock mass permeability testing before and after total extraction mining. The 10 m was not added to account for the surface cracking zone, but to allow for localized depressions that could reduce the rock cover thickness to < 45T. The surface cracking zone of <15 m was therefore included in the 45T+10 m criterion.

The height of continuous fracture zone was assessed to have ranged between 21T and 33T above the mine workings. The thickness of the Constrained Zone was defined as being dependent on the cover depth, but should be > 12T + 10 m below tidal waters.

The thickness of the 'Constrained Zone' above the 'Fractured Zone' was also considered to have greater importance in regards to providing a groundwater drainage path barrier than the tensile strain limit of 7.5 mm/m set by **Wardell, 1975**. It was considered that the thickness of the Constrained Zone and the presence of low permeability lithologies, such as mudstone and claystone, were more likely to influence the performance of the strata barrier above the A-Zone than putting a limit on surface strain. The strain limit criterion has subsequently been left out of sub-aqueous mine design criteria in NSW Coalfields.

A11.3.4 ACARP, 2006

This report reviews the impacts of shallow longwall mining on the groundwater systems based on fieldwork conducted in the Hunter Valley, NSW (Beltana Mine) and Bowen Basin, Queensland (Gregory Crinum Mine).

The **ACARP, 2006** report suggests that continuous cracking is likely to occur through the strata beams within the Fractured Zone defined by an "angle of break" of 12^o to the vertical and extending inwardly from the rib-sides. International research suggests a range between 10^o and 15^o.

A complementary set of fractures would also be expected to develop further inside the panel on the undersides of the bending units where full subsidence develops in the strata. The angle to full subsidence ranges from 25^o to the vertical according to **ACARP, 2006** and from 32^o to 45^o in **Li and Cairns, 2000**.

Back analysis of the angles of break suggest that surface to seam cracking could theoretically reach the surface above panels that are wide enough to prevent the opposing cantilevering abutments to interact together and limit fracturing. For a panel width of 200 m, this would occur where cover depths are < 370 m to 470 m (due to angles of break of 12^o to 15^o). It is also noted that the inferred height of fracturing is very sensitive to the assumed angle of break.

Note: The panel geometry discussed is actually still in the sub-critical range (i.e. W/H < 0.7) and it is considered by DgS that theoretical fracturing to the surface can only occur in the critical to supercritical panel width range.

ACARP, 2006 also notes an absence of surface to seam fracturing connection or groundwater inflows in the literature, where sub-aqueous mining has occurred below a depth of cover of 120 m to 160 m (for assumed critical to super-critical panel widths). The reason for this phenomenon is considered to be related to the observation that cracked and rotated blocks may still interact and provide low permeability regions in the zones of compressive strain above and below tensile cracking in the deflected beams. It was assessed that the reduction in effective span due to the cantilever effect over the ribs and increase in support that develops to overlying strata units may also allow strata units as thin as 10 m or so span across the fractured zone.

The report concluded that the height of continuous fracturing is therefore likely to be controlled by either spanning strata units or units that are not spanning which are thick enough to stop fracturing occurring right through the unit.

In the case of the non-spanning strata mechanism, **ACARP, 2006** did not have the resources available to fully evaluate what the minimum strata thickness range is likely to be in order to limit the continuous fracturing height.

Note: A similar conclusion was reached by DgS after a case by case review by DgS of supercritical longwall geometries in the NSW Coalfields in this study. It is also considered likely that this phenomenon would require the compressive stress in the deformed rock mass units to exceed their unconfined compressive strength for complete break-through to occur. However, it is also apparent that the presence of thin strata units that deform predominately in shear along slipping bedding partings, can also limit vertical cracking developing to the surface cracking zones.

A11.3.5 MSEC, 2011 and SCT, 2001

The MSEC and SCT models are based on several published case-studies for mining impacts in the NSW Coalfields and their own internal analytical and numerical modeling results. The 'heights of fracturing' are predicted based on longwall and total pillar extraction panel widths and indicate maximum values ranging from 1W to 1.5W (SCT) and 1.374 (W-30) (MSEC). The database of 'observed heights of fracturing' and the above panel width models are presented in **Figure A40i**.

Based on a review by DgS of the database from which the MSEC and SCT models are derived, and extensometer and vertical strain measurements at other mines, it is apparent that the models include cases of both A and B-Zone fracture heights (see **Figure A40j** and **Section 11.4** for further details). DgS concludes that the MSEC and SCT 'height of fracturing' models are probably conservative.

It is also apparent that there are three reported cases in the database which indicate 'fracturing through to the surface' has occurred (LW1 at Invincible, LW11 at Angus Place and LWE1 at South Bulga). A review of the extensometer data published by **Holla, 1991** for the Invincible case study, DgS concurs with the assessment that continuous fracturing has probably extended to the surface cracking zone (or to within 10 m below the surface). No data is available for the latter two cases, however, based on the above discussion, it is considered possible that surface to seam connectivity of the B-Zone (and not the A-Zone) occurred at these sites (further discussion on these sites are included in the following sections).

A11.3.6 Bulli Seam PAC, 2010

The NSW Government Planning and Assessment Commission (PAC) for the Bulli Seam Project Application in 2010 identified several apparent deficiencies in the commonly used 'height of sub-surface fracturing' models as follows:

- It is apparent that the prediction models based on panel width only indicated significantly greater sub-surface fracture heights than the models based on mining height.

- The panel width only-based models did not distinguish between continuous and discontinuous fracture heights.

- The authors and reviewers of the prediction models all recognize the deficiencies in the height of fracturing models that are based solely on panel width or mining height. They also indicate that more thorough analysis is probably required to determine a 'more definitive' function that relates the height of connective cracking to the mining geometry.

Based on the PAC report and review of available published data the following comments are made by DgS:

- The data on which the Panel Width-Only models are based are likely to include both A and B type fracturing zones (hence the review of MSEC and SCT database presented in **Figures A40i** & **A40j**).

- The Panel Width only models appear to have been developed mainly from data obtained at deep, sub-critical mines of the Southern and Western Coalfields.

- The height of fracturing is considered unlikely to extend further up into the strata once the critical panel width is reached (for a given mining height) and no further deformation of the overburden can occur.

- The behaviour of the overburden is more likely to be influenced by panel width for sub-critical panels and mining height for supercritical panels.

A11.3.7 State of the Art Summary and Gap Analysis for Alternative Models

In summary, the literature review outcomes indicate the following:

- The A-Zone is assessed to range from 21T to 33T above supercritical panels and up to 43T above critical and sub-critical panels. The B and C-Zone thicknesses will generally depend on the cover depth less the A-Zone Horizon estimate.

- The models that are based on the longwall panel widths only indicate maximum 'heights of fracturing' that range from 1.0W to 1.5W (SCT) and 1.374(W-30). These models however, probably include both A and B-Zone fracture heights in some instances and are therefore likely to be conservative.

- It is apparent that the published height of fracturing models based on mining height alone varies significantly for supercritical, critical and sub-critical mining geometries. The A-Zone could (and does) extend higher up into the overburden above sub-critical

panel geometries as the fracturing due to strata deformation is also influenced by the panel width.

- It is also reasonable to assume that the maximum height of the A-Zone will probably occur above the centre of a sub-critical longwall panel with a naturally spanning catenary arch.

- Surface drilling investigations above subsided longwall panels in NSW and QLD have found the maximum height of fracturing is in fact 'dome-shaped' and develops somewhere between the point of maximum tensile strain and the centre of the panels.

- In order to distinguish between A and B-Zones it is considered best-practice to install borehole extensometers and multiple-piezometers (deep and shallow) above longwall panels and measure the various fracture and dilated zones based on anchor displacements, vertical strain and the short to medium term impacts to established groundwater regimes.

- When longwall mining beneath lakes and sensitive groundwater aquifers, it is essential that the mining geometry be controlled to provide an effective B/C-Zone or Constrained Zone thickness to minimise the potential for connective cracking to develop up to the feature. The presence of geological structure should also be considered as it may act as a potential groundwater conduit between the A and B-Zones.

- Based on **Forster and Enever, 1992**, the minimum Constrained Zone (B/C Zone) thickness above the Fractured A-Zone should be >12T + 10 m and include the surface cracking zone thickness of <15 m beneath Lake Macquarie. The minimum B/C Zone thickness does not include weathered material and/or alluvial sediments.

- For cases where permanent water bodies do not exist, but surface to seam hydraulic connection is not desirable, it is recommended that the continuous height of fracturing zone should not encroach within the surface cracking zone (ie. A minimum of 10 m to 12 m below the surface should be assumed generally, but may need to be increased up to 20 m for steep topography affects).

- As mentioned earlier, the height of A-Zone fracturing is strongly dependant on the presence of the bridging capability of massive conglomerate or sandstone units above a given panel. Therefore, estimating the height of A and B-Zone fracturing also requires a review of the overburden lithology and the presence of geological structure.

- It is also apparent from a case by case review, that the height of fracturing may be controlled by strata that is not actually spanning, but may be thick enough or flexible enough to stop fracturing occurring right through the strata unit. For this scenario, it is considered the height of fracturing will be controlled by (i) the thickness and/or flexibility of the strata unit relative to the panel width and its location above the workings, (ii) the thickness of compressible goaf material that will induce curvature in

the overlying strata units as the goaf is compressed, and (iii) the presence of confined, semi-impermeable strata units such as mudstone and claystone in the B and C-Zones that will swell in the presence of groundwater and effectively seal off small width cracks.

- For the case of sub-critical panels, the maximum non-spanning strata height and load acting on the goaf may be limited by the 'natural' or catenary arch that can form across the mined void width. It is noted that the A-Zone has not intersected the surface above any of the 13 sub-critical longwall panels in the NSW Coalfields.

- For super-critical panels however, the height of fracturing could theoretically reach the surface and the maximum load acting on the goaf will probably equal the cover depth. It is noted that the A-Zone has not intersected the surface above critical and supercritical panels at 17 out of 20 longwalls (85%) in NSW and Queensland Coalfields.

- Near surface geology will affect the potential for surface cracking to intersect the sub-surface fractures above supercritical longwall panels. Based on physical modelling results and mine site case studies, thinner and weaker strata units may actually reduce the likelihood of cracking zone interconnection compared to thicker and stronger units.

- Subsidence effect data (i.e. Horizontal strain/curvature ratios or K Factors) also suggest that the near surface strata will behave like a beam with a thickness equal to twice this ratio or the observed cracking depths (i.e. the depth to the neutral axis of bending). For the Newcastle Coalfield, the effective beam thickness ranges from 10 m to 30 m (i.e. K Factors of 5 to 15). The Western and Southern Coalfields have effective beam thickness ranges from 30 m to 60 m (i.e. K Factors of 15 to 30).

Based on the HoF prediction model review, it was considered necessary in this study to:

(i) review and expand the database of continuous and discontinuous cracking to include a representative range of mining geometries on which to base the empirical models on;

(ii) update and re-evaluate the **ACARP, 2003** models;

(iii) attempt to develop further subsurface fracturing models that included the panel width, mining height, cover depth and lithology (effective strata unit thicknesses and their properties).

(iv) provide a clearer definition of the surface cracking depth (D-Zone).

A11.4 Expansion of the Database and Review of Sub-Surface Fracturing Prediction Models Presented in ACARP, 2003

A recent review of the **ACARP, 2003** database and the inclusion of new HoF data has recently been undertaken by DgS in 2012 and 2013 for various projects in the Newcastle/Lake Macquarie and Hunter Valley Coalfields. The up-dated database is presented in **Table A6.1** and includes a greater number of cases where A and B-Zone fracture heights have been determined from borehole extensometer and piezometeric data collected over a reasonable period of time (i.e. > 12 months after mining impacts). Surface and groundwater interaction may also be established by other means in the absence of piezometers and extensometer results (e.g. mine water make increases several days or weeks (instead of months) after rainfall events, would indicate direct hydraulic connection to the surface).

The measured coalfield data base presented in **ACARP, 2003** was based mainly on a dataset of post-mining drilling data to estimate heights of fracturing for the A and B-Zones (except for the **Forster and Enever, 1992** data). The updated model database now includes further extensometer and/or piezometric data from the Southern, Western and Hunter Valley Coalfields in NSW, including Newcastle (West Wallsend, Mandalong, Wyee, Cooranbong, Teralba), Lower Hunter Valley (Abel, Austar, Ellalong); the Upper Hunter Valley (Homestead, Ashton, South Bulga), Southern Coalfield (Berrima, Metropolitan, Kemira, Belambi West, West Cliff, Tahmoor, Dendrobium, Appin) and the Western Coalfield (Springvale, Invincible). Two cases for Queensland (Oaky Creek and Crinum) were also included in the database.

Based on a review of published extensometer results presented in **Holla, 1991**, **Frith, 2006, MSEC, 2011** and **ACARP, 2007**, it is assessed that there are six cases in the database presented in **MSEC, 2011** that appear to include the A and B-Zones and four cases whereby the 'height of fracturing' are claimed to have reached the surface at distances above the workings of 21T (Homestead Mine, LWs 9/9A), 39T (Invincible Colliery, LW1), 57T (South Bulga, LWE1) and 106T (Angus Place, LW11).

In order to use the height of fracturing data presented in **MSEC, 2011** with the **ACARP, 2003** data, it was necessary to identify the likely A-Zone cases and B-Zone cases based on the following fracture zoning criteria:

(i) A-Zones are likely to have vertical strains > 20 mm/m and large strata dilations > 200 mm; and

(ii) B-Zones are likely to have vertical strains of < 8 mm/m and strata dilations < 200 mm, based on measured values for cases with piezometer-established B-Zone strains measured at other mines.

Note: it does not necessarily follow that uniform vertical strains throughout the strata mean the height of continuous fracturing is likely to have reached the surface. The uniform strains may also be due to strata bedding dilations if strains are < 8 mm/m. Rock mechanics theory also indicates that a vertical tensile strain of 8 - 9 mm/m will induce a horizontal tensile strain of 2 - 3 mm/m in the rock mass due to

Poisson's ratio effect. The theoretical strain to fracture a joint-free sample of rock is 0.3 to 0.6 mm/m. It has been observed in the field that existing joints and bedding in the rock mass allow it to 'absorb' higher levels of tensile strain before developing fresh cracks at around 2 - 3 mm/m. The use of the proposed vertical strain of 8 mm/m is therefore considered to be a reasonable indicator that fresh cracking is likely to occur in the rock mass.

The following cases were changed from A to B-Zone fracturing horizons or reinterpreted by DgS based on the above criteria:

- Tahmoor LW3 (extensometer interpretation by **Holla & Buizen, 1991**)
- Westcliff / Endeavour Drift BH3 (post-mining bore interpretation by **MSEC, 2006**)
- Angus Place LW11 (fractures to surface interpreted by **Kay, 1990**)
- Springvale LW411 (extensometer & piezometer interpretation by **CSIRO, 2007**)
- Springvale LW409 (piezometer interpretation by **CSIRO, 2007**)
- Ellalong LW2 (extensometer interpretation by **Holla, 1986**)

The height of continuous fracturing for LWE1 at South Bulga (**SCT, 2000**) has been assumed to extend to within 10 m of the surface and into the surface cracking zone as the extensometer or piezometric data is not available to review at this stage.

The assessment in **Kay, 1990** that the height of fracturing above LW11 at Angus Place extended to the surface was well above previous ranges (106T) measured at the mine to-date. Further discussions by the mine with the author recently indicates that a 100 m high cliff face probably affected the overburdens spanning capability, resulting in a greater than normal level of subsidence and near surface cracking. Although the surface flows in the creeks may have been re-routed into near surface cracks at the time, it is not likely that a surface to seam connection occurred.

It has also been decided to remove two case study points (Central and Southern German Creek Mines) from the original **ACARP, 2003** data base as they appear to be much lower than other cases with similar geology and geometry and were based on drilling data only.

The results of the database review and re-assignment of A- to B-Zones are shown in **Figure A40j** with the reinterpreted values summarised in **Table 6.1.** A summary of several representative extensometer results that were used to review the published heights of fracturing data presented in **Table A6.1** are provided in **Table A6.2**.

The expanded database presented in **Table A6.1** has subsequently been used to (i) update the strain and curvature index-based models presented in **ACARP, 2003** and (ii) develop more technically concise models that allow variations in geology and geometry to be assessed in each coalfield. The results are presented in the following sections.

Table A6.1 - Updated HoF Model Database for Australian Coalfields

Site	Panels	Mine	Seam	W (m)	H (m)	W/H	T (m)	A (m)	B (m)	A/T	ACARP 2003 Model Predictions				
											t^ (m)	y^ (m)	Unit SRP*	U95% CL S_{max} (m)	U95% CL E_{max} (mm/m)
1	MW508	Bellambi W.	Bulli	110	421	0.26	2.50	92	-	37	100	90	High	0.30	2
2	LW10	Metropolitan	Bulli	140	460	0.30	3.40	130	-	38	100	130	High	0.29	3
3	LW1-4	South Coast	Bulli	110	325	0.34	2.50	85	-	34	100	85	High	0.24	3
4	LW6	Kemira	Wong.	117	335	0.35	2.75	98	-	36	100	98	High	0.16	2
5	LW20	Metropolitan	Bulli	163	450	0.36	3.40	100	-	29	100	100	High	0.34	2
6	LWA1	Austar	Greta	159	417	0.38	6.00	*87*	277	15	100	80	High	0.56	4
7	LW514	Bellambi W.	Bulli	150	400	0.38	2.70	90	-	33	100	90	High	0.29	2
8	LW28	Appin	Bulli	200	500	0.40	2.30	90	-	39	120	90	*High*	0.27	1
9	*LW2*	*Ellalong*	*Greta*	*150*	*368*	*0.41*	*3.50*	*113*	*210*	*32*	100	113	*High*	*0.40*	*3*
10	*LW3*	*Tahmoor*	*Bulli*	*180*	*424*	*0.42*	*2.18*	-	204	-	100	100	*High*	*0.29*	*2*
11	LW9	Teralba	YW	150	350	0.43	2.70	*110*	150	41	34	110	High	0.32	2
12	*TE*	*West Cliff*	*Bulli*	*200*	*446*	*0.45*	*2.50*	*101*	*245*	40	100	101	*High*	*0.30*	*1*
13	TE	Berrima	Wong.	120	176	0.68	2.3	76	112	33	100	76	High	0.50	3
14	*LW409*	*Springvale*	*Lithgow*	*265*	*385*	*0.69*	*3.25*	*133*	*254*	41	55	133	High	*0.6*	*3*
15	LW9	Mandalong	WW	160	220	0.73	4.50	-	-	-	30	160	High	0.5	3
16	***LW11***	***Angus Place***	***Lithgow***	***211***	***263***	***0.80***	***2.47***	***-***	***253***	***-***	100	***253***	High	***0.5***	***3***
17	*411*	*Springvale*	*Lithgow*	*315*	*368*	*0.86*	*3.25*	139	288	43	55	139	High	*0.68*	*5*
18	LW5	Mandalong	WW	160	179	0.89	3.70	118	154	32	25	83	*Mod*	1.38	3
19	LW5	Dendrobium	Wong.	245	255	0.96	3.75	123	-	33	80	123	High	1.25	5
20	LW1	Wyee	Fassifern	216	206	1.05	3.44	126	-	37	30	126	High	1.09	5
21	**LW1**	**Invincible**	**Lithgow**	**145**	**116**	**1.25**	**2.70**	**106**	***111***	**39**	**15**	**106**	**Low**	**1.62**	**16**
22	TE1	Abel	U. Don.	120	95	1.26	2.55	45	*75*	20	15	41	Low	1.51	22
23	LWs	Ashton	Pikes Gully	216	154	1.40	2.55	82	*130*	32	30	82	Low	1.5	15
24	LW40	WWC	WBH	179	113	1.58	3.80	80	*108*	21	20	80	Low	2.28	21
25	**LWE1**	**Sth Bulga**	**Whybrow**	**259**	**155**	**1.67**	**2.55**	**145**	**150**	**57**	**20**	**145**	**Low**	**1.53**	**8**
26	LW41	WWC	WBH	179	105	1.70	3.80	72	100	19	20	72	Low	2.28	24
27	LW9	Crinum	Lillyvale	280	155	1.81	3.50	85	*150*	24	35	105	High	1.82	8
28	LW39	WWC	WBH	179	97	1.84	3.90	68	92	17	20	68	Low	2.18	25
29	TE-3D	Wyee North	GN	355	185	1.92	1.90	63	*143*	33	50	63	High	1.14	4
30	TE-355	Wyee North	GN	355	180	1.97	1.90	40	-	21	50	40	High	1.14	4
31	Panel2	Abel	U. Don	150	76	1.97	1.88	45	71	24	15	33	Low	1.13	23
32	TE-Nth B	Cooranbong	G.N	150	75	2.00	2.80	58	*70*	21	20	58	Low	1.68	33
33	LW1	Oaky Ck	German Ck.	205	95	2.16	3.20	55	*90*	17	30	55	Low	1.92	25
34	**LW9/9a**	**Homestead**	**Whybrow**	**200**	**80**	**2.50**	**3.40**	**75**	**75**	**23**	**15**	**65**	**Low**	**1.98**	**29**

- = not available; **bold** - surface to seam fracturing assessed by others; *italics* - Continuous Fracture Zone heights (A-Zone) was originally reported by others and included the Discontinuous Fracture and Dilated Zone (B-Zone). A and B- Zone height of the B-Zone heights were re-assessed by DgS based on a review of available measured vertical strains and piezometric data (see **Figure A40i and A40j**); No shade - Sub-critical panels (W/H<0.7); Light grey shade - Critical panels (0.7<W/H<1.4); Grey shade - Supercritical panels (W/H>1.4).
* - SRP = Subsidence Reduction Potential for strata unit with thickness t and distance y above the workings. The SRP may be due to spanning or bulking behavior over the range of W/H and is also considered to be an indicator of whether a strata unit will limit the height of continuous fracturing; ^ - likely values assessed from borehole and subsidence data; Wong. = Wongawilli; YW= Young Wallsend; WW = West Wallarah; U. Don = Upper Donaldson; WBH = West Borehole; GN - Great Northern.

Table A6.2 - Summary of Measured A, B, C & D Zone Strains in Extensometers*

Parameter	**Underground Coal Mines**									
	Angus Place$		**West Wallsend**				**Abel^**			
Panel No.	LW11		LW39		LW40		Panel 1		Panel 2	
Cover Depth H (m)	211		97		113		95		76	
Panel Width W (m)	263		179		179		120		150	
W/H	0.8		1.84		1.58		1.26		2.0	
Mining Height, T	2.5		3.8		3.9		2.1		2.1	
Fracture Zone	Dilat-ion (mm)	**Strains# (mm/m)**	Dilat-ion (mm)	**Strains# (mm/m)**	Dilat-ion (mm)	**Strains# (mm/m)**	Dilat-ion (mm)	**Strains# (mm/m)**	Dilat-ion (mm)	**Strains# (mm/m)**
D-Zone	-	***3 - 5***	-	***25***	-	***24***	-	***24***	-	***23***
C-Zone	-	**-**	-	**-**	-	**-**	-	**-**	-	**-**
B-Zone	~60 - 120	**5 - 6**	8 - 17	**1 - 2**	25 - 50	**5 - 8**	14 - 19	**1 - 2**	<20	**-1 - 0**
A-Zone	~1000	**100**	234 - 957	**115 - 139**	390 - 769	**39 - 77**	279 - 1289	**28 - 129**	158 - 185	**16 - 19**
Parameter	**Mandalong**		**Austar**		**Ellalong**		**Invincible**		**Tahmoor**	
Panel No.	LW5		LWA1		LW2		LW1		LW3	
Cover Depth H (m)	179		453		368		116		424	
Panel Width W (m)	160		159		150		145		180	
W/H	0.89		0.35		0.41		1.25		0.42	
Mining Height, T	3.7		6.0		3.5		1.26		2.2	
Fracture Zone	Dilat-ion (mm)	**Strains# (mm/m)**	Dilat-ion (mm)	**Strains# (mm/m)**	**Strains# (mm/m)**		**Strains# (mm/m)**		**Strains# (mm/m)**	
D-Zone	-	***5***	-	***3***	***3***		***10***		***1***	
C-Zone	<20	**<1**	<10	**<1**	**<1**		**-**		**<1**	
B-Zone	19 - 29	**2 - 5**	24 - 133	**1 - 7**	**1 - 5**		**<5**		**1 - 4**	
A-Zone	73 - 672	**80**	222 - 1177	**11 - 59**	**>10**		**10 - 75**		**N/A**	

* - A, B & C-Zone strains are vertical and approximately 3 to 4 times the horizontal strain due to Poisson's ratio effect; *italics* - D-Zone strains are horizontal.
# - tensile strains are positive. Negative strains or compression develops after full subsidence occurs and goaf compresses under load from sagging overburden strata; ^ - Effective mining height for total pillar extraction (Te = 0.85T); $ - Strain data not available and quoted from published literature.

Table A6.2 (Cont…) - Summary of Measured A, B, C & D Zone Strains in Extensometers*

Parameter	Underground Coal Mine			
	Springvale			
Panel No.	LW411		LW412	
Cover Depth H (m)	368		400	
Panel Width W (m)	315		315	
W/H	0.90		0.79	
Mining Height, T	3.25		3.25	
Fracture Zone	**Dilation (mm)**	**Strains# (mm/m)**	**Dilation (mm)**	**Strains# (mm/m)**
D-Zone	-	*3*	-	*3*
C-Zone	<42	<5	<33	<5
B-Zone	39 - 410	4 - 10 (**17**)	2 - 505	4 - 8 (**25**)
A-Zone	194 - 1441	14 - 42	174 - 1571	5 - 42

* - A, B & C-Zone strains are vertical and approximately 3 to 4 times the horizontal strain due to Poisson's ratio effect; *italics* - D-Zone strains are horizontal.
# - tensile strains are positive. Negative strains or compression develops after full subsidence occurs.
^ - Effective mining height for total pillar extraction (Te = 0.85T).
bold - measure strain near the top of the B-Zone where a bedding separation occurred. Piezometer data indicates the height of continuous fracturing is further below this point.

A11.4.1 Updated Tensile Strain Model

The physical model presented in **Whittaker and Reddish, 1989** related the ratio of the height of continuous and discontinuous fracturing (A and B) above longwall panels over cover depth (H) with the maximum tensile strain (E_{max}) at the surface due to mine subsidence. Actual drilling data over extracted longwall panel goaf was subsequently used to define a real-world relationship between these variables at several Australian Coalfield mines in **ACARP, 2003**.

The additional data presented in **Table A6.1** has been added to the original database and the regression equations have been revised below:

{A-Line} Mean A/H = $0.180\ Ln(E_{max}) + 0.1405$, $R^2 = 0.70$

U95%CL A/H* = $0.180\ Ln(E_{max}) + 0.3742$.

{B-Line} Mean B/H = $0.146\ Ln(E_{max}) + 0.5315$, $R^2 = 0.47$

U95%CL B/H* = $0.146\ Ln(E_{max}) + 0.8426$.

* - Maximum A/H and B/H = 1.

where

A, B = height above workings to A and B-Zone horizons,
H = cover depth,

E_{max} = the maximum predicted tensile strain for a 'smooth' subsidence profile.

The new tensile strain model is presented in **Figure A41a** and has a much stronger fit to the new database for the A-Zone than the **ACARP, 2003** model, with only a slight improvement for the B-Zone horizon. The R^2 value for the logarithmic regression curve fitted to the revised A-Zone data was previously 0.44 and is now 0.70. The R^2 value for the B-Zone was previously 0.46 and is now 0.47.

The measured database model still appears to indicate a similar height of fracturing trend to the **Whittaker and Reddish, 1989** physical model. However, as was concluded in **ACARP, 2003**, the predicted heights of 'continuous' and 'discontinuous' fracturing in the real world were again higher for a given tensile strain at the surface, and probably due to the influence of jointing in the rock mass (compared to none in the physical model).

The real world database indicates that the tensile strain probably needs to be >32 mm/m for surface to seam connection to occur, and is approximately 50% of the physical model value of 60 mm/m. It should also be noted that if connective cracking is likely to extend into the Surface Cracking Zone (a depth of 10~15 m below the surface), then the maximum tensile strain for surface to seam connection reduces to 25 mm/m. It is assessed however, that the predicted strains are also dependent on surface crack width development and should therefore not be used to assess surface to seam connectivity directly without considering the near surface B and C-Zone lithologies.

Considering the potential difficulties with predicting strains after the onset of cracking, it is still assessed that it is unlikely that the tensile strain-based model will be reliable. **ACARP, 2003** attempted to modify the strain-based model to a curvature-based approach. The resulting regression equations however, did not improve the correlation between the adopted variables (i.e. both methods had R^2 values of 0.44). The curvature-based model of height of sub-surface fracture prediction was subsequently revised with the expanded model database in **Section A11.4.2** to see if the regression equations could be improved upon.

A11.4.2 Updated Overburden Curvature Index Model

The Overburden Curvature Index or S_{max}/W'^2 term was introduced in **ACARP, 2003** in an attempt to provide a readily measurable field parameter that would not be compromised as much by surface strain concentration effects (i.e. cracking). The logarithmic regression lines were re-derived using the expanded database to give new predictions of the mean and U95%CL values for both A and B-Zones as follows:

{A-Line} Mean A/H $= 0.198\ \mathrm{Ln}(S_{max}/W'^2) + 1.1518, \qquad R^2 = 0.66$

U95%CL A/H* $= 0.198\ \mathrm{Ln}(S_{max}/W'^2) + 1.3915.$

{B-Line} Mean B/H $= 0.152\ \mathrm{Ln}(S_{max}/W'^2) + 1.3265, \qquad R^2 = 0.52;$

U95%CL B/H* $= 0.152\ \mathrm{Ln}(S_{max}/W'^2) + 1.5928.$

* - Maximum A/H and B/H = 1.

where

A, B = height above workings to A and B Horizons,
H = cover depth (m).
S_{max}/W'^2 = Overburden Curvature Index,
W' = lesser of W and 1.4H

Note: It is reasonable to assume the effective mining width (W') and height of fracturing (A/B) will be limited beyond the point where the maximum subsidence or strata deformation has been reached above supercritical mining geometries (i.e. W/H > 1.4).

The revised regression results are shown in **Figure A41b**.

Despite the apparent improvement in the regression equations, the same apparent differences still remain between the Australian height of fracturing database and the UK physical modelling results. One obvious difference is that the UK physical model represents a supercritical case study where the panel width and cover depth was constant (i.e. W/H = 1.34). The Australian database however, has a significant range of sub-critical, critical and super-critical panel geometries and further investigation of this difference is therefore required (see **Section A11.4.4)**.

A11.4.3 Influence of Lithology on Sub-Surface Fracture Heights

An assessment was made in **ACARP, 2003** on whether massive lithology had the potential to control or limit the height of fracturing above a longwall panel. The expanded model database presented in **Table A6.1** still indicates that it does, with the A-Horizon likely to have coincided with the base of the massive strata units in 17 out of 21 cases with 'Moderate' to 'High' SRP strata units.

The potential for massive strata units to mitigate the height of continuous fracturing above the workings should therefore not be ignored where subsidence magnitudes and HoF are clearly being controlled by spanning strata.

Overall, the HoF results suggest that the presence of massive sandstone or conglomerate lithology can control the height of hydraulic fracturing due to their spanning capability or thickness generally. However, as has been observed at Mandalong and Springvale Mines, the presence of geological structure (faults, dykes, seam rolls and shear zone or joint swarms) has resulted in a weakening of the overburden by the tectonic activity and there has been increased subsidence due to the breakdown of massive sandstone / conglomerate into several thinner units and (ii) increased shearing and tensile stress acting on the discontinuities has resulted in groundwater conduits developing deeper into the overburden.

It is therefore usually recommended that a mine undertake a sub-surface fracture-monitoring program which includes a combination of borehole extensometer and piezometer measurements during extraction in non-sensitive areas of the mining lease. Mitigation strategies for longwall mining are generally limited to (i) reducing the extraction height, (ii) decreasing the panel width and (iii) panel location adjustment. On-going monitoring of

surface alluvium and near surface rock mass aquifers is also undertaken with standpipe piezometers to check the post-mining integrity of ground water dependent ecosystems (GDE) and surface water systems generally.

A11.4.4 Height of Fracturing Angle Model, DgS 2012

Due to the currently held belief in the Australian mining industry that the sub-surface fracture heights are strongly influenced by panel width and mining height, an alternative model was developed by DgS in 2012 using a different approach to analysing the UK model data presented in **ACARP, 2003**.

Predictions of the heights of continuous and discontinuous fracturing (the A and B-Zone horizons) were re-analysed using the panel width, the mining height and a simple parabolic profile formula to estimate A and B-Zone fracture heights from a calibrated abutment angle at seam level (θ_A and θ_B) as follows:

- Continuous Fracture Zone Height, $A = W'/(4\tan(\theta_A))$
- Discontinuous Fracture Zone Height, $B = W'/(4\tan(\theta_B))$

where,

W' = Effective Panel width or minimum of W and 1.4H.

θ_A = abutment angle to estimate height of A-Zone

θ_B = abutment angle to estimate height of B-Zone

When the UK model's fracture height data is plotted as a height of fracturing angle (estimated from an assumed parabolic fracturing profile between rib abutments), a strong correlation is apparent between the mining height for a given panel width and cover depth (W/H = 1.34); see **Figures A41c** and **A41d** for A and B-Zone Horizons respectively.

The regression analysis indicates the following fracture height angles (in degrees) apply for estimating A and B-Zone fracture heights in the real world:

$\theta_A = 41.617T^{-0.467}$ (mean) and $25.083T^{-0.401}$ (lower 95%CL)

$\theta_B = 21.806T^{-0.233}$ (mean) and $17.295T^{-0.238}$ (lower 95%CL)

Real world fracture height data measured with piezometers and borehole extensometers indicates a similar trend as the physical model results, although there is more scatter in the data that is probably due to both mining geometry (W/H) and geological variability.

The UK physical model assessed mining heights of 1.2 m to 10.8 m, and generated fracture height angles at the abutments ranging from 55^o to 18^o for the A-Zone and from 37^o to 18^o for

the B-Zone horizon. The fracture height angle tends to follow a decaying power law as the mining height increases.

For real-world mining heights of 1.9 m to 6.0 m (median of 3.0 m), the calibrated fracture height angles range from 34^o to 18^o for the A-Zone, and from 22^o to 13^o for the B-Zone. One A-Zone case had a fracture height angle of 58^o due to the apparent 'truncating' effect of a 40 m thick conglomerate strata unit 40 m to 60 m above a supercritical panel in the Great Northern Seam (Wyee Colliery's North-3D Panel).

As was found in the strain and curvature-based model's, the presence of pre-existing jointing in the rock mass is likely to have contributed to greater fracture heights determined from the field data compared to the laboratory model.

The effect of massive strata units is apparent in the database (see **Figure A41c**) and further measurements are necessary to develop a more discerning prediction model that allows 'Low' and 'High' SRP strata to be assessed separately using this model. The height of fracturing model proposed at the time was considered likely to be conservative for greenfields sites if based on the lower bound fracture height angles and to give upper bound fracture height predictions.

Further review of sub-critical, critical and supercritical panel case studies in 2013 has found that the A and B-Zone fracture height angle model could also be further divided into sub-critical, critical and supercritical panel geometries (see **Figure A41e** and **A41f**) as follows:

$\theta_A = 32.448T^{-0.241}$ for the mean fracture height angle.

Upper 95%Confidence limits for the A-Zone were estimated by reducing the mean angle by 5^o, 7^o and 10^o for supercritical, critical and sub-critical longwalls respectively.

$\theta_B = 31.5T^{-0.373}$ for the mean fracture height angle for supercritical panels
$= 25.4T^{-0.373}$ for the mean fracture height angle for critical/sub-critical panels

Upper 95%Confidence limits for the B-Zone were estimated by reducing the mean angle by 3.5^o, 7^o and 7^o for supercritical, critical and sub-critical longwalls respectively.

The review outcomes suggest that heights of subsurface fracturing appear to increase above sub-critical panels for a given mining height, but are also likely to be due to the panel width and changes in macro-scale structural behaviour of the overburden as well.

Whilst the trend from sub-critical to supercritical panel geometries appears reasonably consistent across the abutment angle model database (with a few cases where thick strata has clearly limited the fracture heights) it is noted that the predicted heights of fracturing are highly sensitive to the selected value of theta. It was therefore considered that a new modelling approach based on Dimensional Analysis and Buckingham's Pi-Theorem would be

needed to reasonably establish definitive relationships between the key variables over a broader range of mining geometries and geological conditions.

A11.5 Alternative Sub-surface Fracture Model Development

Starting with the influence of mining height (T) on the height of A-Zone fracturing, if we firstly consider a supercritical panel of a given width (W) and cover depth (H), **Whittaker and Reddish, 1989** and **Singh & Kendorski, 1991** each demonstrated that the height of continuous fracturing (A) will increase with the square root of the mining height, $T^{\sim 0.5}$, or a power rule of the form $A = aT^b$, as shown in **Figure A41g**. It is apparent that the database of real-world fracture heights with W/H range from 0.3 to 2.22 has greater scatter than the UK model curve for supercritical panel geometry, and therefore indicates that other factors such as the panel width and geology should probably be considered. The apparent under prediction of A-Zone fracture heights by the **Forster and Enever, 1992** model, also supports this view.

If the fracture heights are plotted against panel width (W) only, a similar 'scattered' outcome results as shown in **Figure A41h**. The conservative nature of the height of fracturing models presented by SCT and MSEC is also demonstrated in the figure and suggests that both A and B-Zones are included in their models.

A slightly improved regression analysis results if A is plotted against W/H in **Figure A41i** or when normalized to the panel width (A/W) and is plotted against T in **Figure A41j** for sub-critical, critical and super-critical panel geometries.

Based on these plots, it is clear that consideration needs to be given to the structural behavior of the overburden across the full range of mining geometries, its constituent strata units (or 'beams') and the influence of mining height, T on the development of fracture heights above longwall panels.

A11.5.1 Strata Behaviour Mechanisms that Influence Fracture Heights above Longwalls

Based on structural analysis theories, a conceptual model of the macro-scale and micro-scale mechanisms of sub-surface fracture height development are described below and shown graphically in **Figure A42a**:

Macro-Scale Mechanisms:

- For sub-critical panels, a natural catenary will probably form and transfer the weight of the top half to 2/3 of the overburden to the abutments. The strata below the arch will be subject to sagging or bending forces caused by the void formation. Depending on the span and thickness of individual strata units, the strata in the immediate roof will bend, separate, crack and ultimately cave into the extracted coal void (see *Micro-scale Mechanisms* below).

- Natural catenary arching action infers that the spanning overburden can remain entirely in compression and there is an absence of tensile and shear or 'bending'

stresses. Subsidence data indicates that catenary arching stops occurring once W/H exceeds 0.7.

- Once W/H exceeds 0.7, the overburden will still attempt to span, however, the geometry of the arch will be too shallow for a catenary arch to develop, resulting in bending and cracking of the rock mass.

- The load will still be able to be carried over the void by the overburden, provided the rock mass has adequate strength and stiffness to resist the applied bending moments and shear and tensile stresses (along with increased compressive stresses from inward strata block rotation). This type of behaviour is known as Voussoir or 'cracked beam' behaviour, and is basically a flatter, but a less stiff version of a catenary arch.

- Shallow arching or Voussoir beam action will continue across the panel until it can no longer support the span or weight of the shallow arch. This is usually assumed to have occurred once W/H reaches 1.2 to 1.4H. The weight of the overburden will then be fully supported by the goaf beyond this point and subsidence will be a function of the mining height and cover depth or goaf load.

- The above macro-mechanisms will influence the behavior of the overburden strata units and subsequent development of the sub-surface fracture heights as follows:

Micro-scale Mechanisms:

- Soon after the coal seam is extracted from beneath the overburden, its constituent 'beams' in the immediate roof will generally deflect and behave elastically until the tensile and shear stresses within the rock mass units exceed the material and/or bedding parting strength of the units.

- The strata units will subsequently crack at the abutments and mid-span and the confinement will be partially lost. The cracked beam segments will then rotate inwardly and create a shallow compression arch within the beams (Voussoir action) that may or may not support the load.

- The cracks in the beams at this stage are likely to be discontinuous, with the beam continuing to behave pseudo-elastically with zones of compressive stress above and below the tensile cracks.

- The beam will continue to span and deflect under the applied loading until the compressive strength of the beam is reached, where the beam will then either collapse into the available void, or yield and load the previously failed strata units and goaf below it.

- Based on the physical model results presented in **Whittaker and Reddish, 1989**, the beams may also shear into two or three thinner units before the lower units ultimately crush if their UCSs are exceeded. Bending beam theory indicates that the maximum

shear stress will occur at mid-beam thickness. The beams are therefore likely to break down into half their thickness units each time shearing occurs along bedding partings.

- The goaf will compress and cause further overlying strata units to deflect, shear and crack. The goaf load will continue to increase as cracking continues up into the strata.

- The curvature induced in the beams will probably not cause complete fracture to develop through the beam until the compressive strength of the beam materials is reached. The induced curvature will therefore be a function of the stiffness of the goaf, the stiffness (and thickness) of the deflecting beam and the load acting on it.

- The goaf stiffness will initially be a function of the mining height and the bulking properties of the collapsed roof materials. The goaf stiffness will also increase as the load acting upon it increases (i.e. strain hardening behavior).

- The goaf load will be a function of the rock mass density and effective height of rock above it. The effective goaf load height is likely to be somewhere between the height to the underside of the spanning arch (above sub-critical and critical panels) and the full cover depth. Full load spanning of strata units above supercritical panel geometries are unlikely to occur and full cover depth load may be assumed to act upon the goaf.

A11.5.2 Analytical Height of Fracturing Model

An analytical model of how sub-surface fracturing develops in the overburden is described below in an attempt to define the likely relationships between the mining geometry and overburden as described in the previous section.

Initial Conditions - Elastic Beam Response to Longwall Mining

The maximum horizontal tensile stress before fracturing (σ_t) in a beam of thickness (t) with an effective span of W_i at a distance (y) above the workings will be:

$$\sigma_t = 6M/t^2 = 3\gamma(H-y)W_i^2/4t^2$$

where

M = surcharge load x span^2 /12 = $\gamma DW_i^2/12 = \gamma(H-y)\ W_i^2/12$

γ = unit weight of the rock mass

D = the depth to the base of the spanning beam (or H-y)

The equation shows that the tensile stress in a stack of beams will be greatest near the roof of the mine workings and then decrease linearly towards the surface. The effective span W_i of the beam will decrease as a function of the angle of break of the collapsing strata in the

Caving Zone. The angles of break (θ) are likely to range between 12^o and 19^o according to the literature and underground observations.

Elastic Beam Cracking and Voussoir Beam Development

The fracturing will continue to progress higher up into the strata until a beam of a certain critical thickness is reached that can either span the distance between the naturally occurring abutments or is thick enough not to fracture right through the beam after it has failed. It is also important to note that the angle of break is not the same as the height of fracturing angles (θ_A and θ_B) discussed in **Section A11.3.4**, as the latter angles were back-calculated from measured heights of continuous fracturing and assumed parabolic fracture limit profiles.

As discussed earlier, the cracking of the strata will lead to the development of Voussoir arching or 'cracked beam' behaviour. The stability of the Voussoir beam will depend upon the compressive stress (σ_c) developed in the beam of thickness (t) that is located a distance, y, above the workings with an effective span (W_i) as follows:

$$\sigma_c = \gamma(H'-y)W_i^2/(4nt^2(1-0.667n))$$

where

n = the proportion of the beam t in compression and may be determined iteratively by minimizing σ_c as the arch shortens under load and develops a new equilibrium (and provided the stress remains in the elastic region or is less than the UCS). Voussoir analysis results based on the method presented in **Diedrichs and Kaiser, 1999**, indicate that 'n' can range from 0.5 and 0.75 in spanning beams, and will be closer to 0.5 when beam crush conditions are reached.

W_i = W - 2ytanθ = effective span of the bending beam at distance, y above the mine workings.

H' = Effective Goaf Load Height, H' or Cover Depth, H.

Voussoir Beam Crushing and Height of Continuous Fracturing

It follows then, that the height of continuous fracturing, A, is likely to develop up to the point where the beam crushes or σ_c = UCS and infers the following relationship exists at the point where the beam starts to yield or crush:

$$UCS = \gamma(H'- A)(W-2A\tan\theta)^2/(4nt^2(1-0.667n))$$

$$= 0.75\gamma(H'- A)(W-2A\tan\theta)^2/t^2 \quad (1)$$

where

θ = the angle of break that subtended to vertical from the rib side and ranges from 12^o - 19^o based on subsidence data and underground observations.

H'- A = thickness of rock supported by the beam and may decrease to t (the beam thickness) if the strata beds shear and dilate during subsidence development.

n = 0.5 (conservative).

Equation (1) indicates that the height of A-Zone fracturing is likely to be a cubic function that is dependent on the following variables:

- Panel width, W
- Effective Goaf Load Height, H' or Cover Depth, H.
- Thickness, location and strength and stiffness of the strata units within the overburden (t, y, UCS, E)
- Angle of break, tanθ

Stresses in Overlying Beams Supported by Collapsed/Fractured Beams

It is noted that Equation (1) ignores the presence of collapsed and fractured material within the A-Zone itself. The formation of the goaf will provide support to overlying fractured units, but also influence the magnitude of curvature and bending stress in the overlying beams as the goaf is compacted and the beams deflect. The curvature of the overlying 'beams' (p_i) may be estimated as follows:

$$p_i = 8\Delta/(y+W_i)^2 = 8(S_{max})/(y+W_i)^2 = 8(\varepsilon_g\ 4T)/(y+W_i)^2 = 32(\sigma_g/E_g)T/(y+Wi)2 = 32(\gamma H'/E_g)T/(y+W_i)^2$$

where

Δ = mid-span deflection of beam with an effective span, $W_i = W - 2y\tan\theta$.
ε_g = vertical strain of goaf with thickness of 4T (T+3T) and a bulking factor of 1.3.
σ_g = maximum vertical stress acting on the goaf = $\gamma H'$.
H' = effective goaf load height = minimum of H and W'/(4tanθ)).
E_g = stiffness of the goaf, which is likely to be a function of H, W, T and t.

From the estimated curvature of the strata units above the compacting goaf, the bending stress in the beam may be estimated as follows:

$$\sigma_c = 2M/(Znt) = 2p_i E't^3/[12(nt^2(1-0.667n))] = 16(\gamma H)T\ t\ E'/(E_g(A+W_i^2)) \quad (2)$$

where

E' = rock mass Young's Modulus = 100 - 300UCS (depending on rock mass Geological Strength Index (**Hoek & Diderichs, 2006**));

n = 0.5 for beam at the yield point (i.e. σ_c = UCS)

As before, if σ_c exceeds the UCS, the cracking may extend right through the beam and the height of fracturing, A, may then continue to develop up to the next strata unit. The following relationship will therefore exist at the A horizon:

$$\sigma_c = UCS = 16(\gamma H')T\ t\ E' / E_g\ (W+A(1-2\tan\theta))^2$$

Overall, the equations represent the physical relationships for either spanning strata (Equation (1)) or non-spanning strata (Equation (2) that are of sufficient thickness to limit fracture continuation through it for a given UCS and mining geometry. As discussed in the following sections, the goaf modulus is likely to be dependent on the mining geometry (W, T and H').

The above equation indicates a complex system with a significant number of independent variables that will influence the height of fracturing outcomes.

Considering the complexity of the above equation and uncertainty in regards to assigning the rock mass and goaf properties, the physical relationship between the variables may also be assessed practically with Dimensional Analysis, a commonly used tool by hydraulics engineers (see **Section A11.5.3**).

A11.5.3 Dimensional Analysis and Buckingham's Pi Theory

According to **Vennard and Street, 1982**, Dimensional Analysis is "the mathematics of dimensions of quantities" built on Fourier's 1882 "principle of dimensional homogeneity". The underlying principle states that "an equation expressing a physical relationship between quantities must be dimensionally homogeneous" i.e. the dimensions of each side of the equation must be the same. It is a valuable means of determining physical relationships between variables in complex systems that defy analytical solution and must be solved by empirical means (i.e. observation, intuition or experiment).

Buckingham's Pi-theory accomplishes this by the formation of dimensionless groups of independent variables that are measureable in the field. For the theory to work, the Pi-terms together must represent all of the three fundamental or primary dimensions of Mass (M), Distance (L) and Time (T), be independent of each other, and not break down into further dimensionless groups.

Buckingham's Pi theory states that in order to determine the physical relationship between a set of 'n' independent parameters in a complex system, it follows that n-3 dimensionless parameters (known as Pi-terms) will be required to reasonably define the dependent variable.

The final equations obtained are in the form of:

$$\pi_1 = f(\pi_2, \pi_3 \ldots \pi_{n-3}) \text{ or } f'(\pi_1, \pi_2 \ldots \pi_{n-3}) = 0$$

From the previous analytical equations derived in **Section A11.5.2**, it is assessed that up to 10 variables may influence the height of Continuous Fracturing (A) and Discontinuous Fracturing (B) as follows:

$$A, B = f(W, H, T, t, \rho, UCS, E, E_g, \tan\theta)$$

The above variables may then be expressed as a combination of products and powers:

$$A, B = aW^b H^c T^d t^e UCS^f, \rho^g E^h E_g^i \tan\theta^j$$

Seven dimensionless Pi-terms will therefore be necessary to describe the relationships between ten variables identified in a system driven by horizontal and vertical stress, panel width, cover depth, mining height, rock mass density, rock mass strength and stiffness, goaf stiffness, caving angle or angle of break and the location of competent or relatively thick strata units in the overburden.

Notes:
1. The y term may be ignored as it corresponds with the dependent variable (A or B).
2. The goaf modulus (E_g) and caving angle (θ) are considered to be dependent on the mining geometry and may therefore be precluded from the regression analysis.
3. The beam thickness, t refers to the thickness likely to exist just above the fracture height location (t is the most difficult of the parameters to assess, as the strata units may 'break down' into thinner units during subsidence development. The assignment of the appropriate t value therefore requires engineering judgment and analysis that includes a review of borehole logs and rock mass properties with extensometer and piezometer data (if available).

The first step in the analysis is to select a suitable set of recurring variables that cannot themselves be formed into a dimensionless group and can be used to represent one or more of the fundamental dimensions. The recurring variable set selected included the panel width, W, rock mass strength, UCS, and density, ρ, and were used to express the fundamental variables as follows:

Length, L: W; Mass, M: ρW^3; Time, T: $\rho^{0.5} W / UCS^{0.5}$

The dimensionless π terms for the remaining independent variables were then assessed using the recurring variable set as follows:

π_1: $A \cdot L^{-1} = A/W$ (Height of Fracturing Term)

π_2: $H \cdot L^{-1} = H/W$ (Goaf Load Index Term)

π_3: $T \cdot L^{-1} = T/W$ (Strata Curvature Index Term)

π_4: $t \cdot L^{-1} = t/W$ (Strata Unit Thickness Term)

π_5: $E \cdot M^{-1} L^1 T^2 = E/UCS$ (Strata Unit Stiffness Term)

which gives:

$$A/W = a\,(H'/W)^b (T/W)^c\,(t/W)^d\,(E/UCS)^e$$

The constants and powers for each Pi-term can now be determined using measured values in the field and non-linear regression techniques.

If we assume for the moment that the last π term representing the ratio of rock mass stiffness over strength for all cases in the database will be constant (E is typically 250 to 300 times the UCS), then the full equation of dimensionless π terms may be simplified as follows:

$$A/W = a\,(H/W)^b\,(T/W)^c\,(t/W)^d \text{ and } B/W = e\,(H'/W)^f\,(T/W)^g\,(t/W)^h$$

The form of the dimensionless π term equations will be explained in the following sections.

Note: Some of the published literature recommends that the super-critical panel width W' = 1.4H should be used instead of the Panel Width, W, for estimating the height of fracturing above super-critical panels. This is because it was argued that the height of fracturing would probably not continue to develop higher into the strata once the overburden had reached the critical width and had already completely failed. The author agrees with this view and considers the height of continuous fracturing beyond this point would then be controlled by the mining height, cover depth (or goaf load) and geological conditions only.

A11.5.4 Pi-Term Model for Predicting Height of Continuous Fracturing (A) above Longwalls based Mining Geometry Only (i.e. Geometry Model)

For the purposes of demonstrating that height of fracturing prediction models need to consider the influence of geology, a regression analysis was completed without the strata unit thickness Pi-term (t'/W') included. Based on the empirical database presented in **Table A6.1**, the statistics software XLSTAT® was used to complete a multi-nonlinear regression analyses on the first three Pi-terms defined earlier as follows:

$$\underline{\text{Mean } A/W' = 2.215\,(H/W')^{0.271}(T/W')^{0.372}} \qquad R^2 = 0.61 \text{ \& r.m.s.e.} = 0.12W' \text{ (21\%)}$$

$$\underline{\text{U95\% } A/W' = \text{Mean } A/W' + a}$$

where a = 0.16 for subcritical panels; 0.16 - 0.085(W/H - 0.7) for critical panels; and 0.10 for supercritical panels.

W' = Effective Panel Width = minimum of W and 1.4H.

T = Mining Height.

Re-arranging the above equation in terms of A gives:

$$\underline{A = 2.215W'^{0.357}H^{0.271}\,T^{0.372} \quad +/- aW'}$$

The regression results suggest that the height of continuous fracturing (A) will increase with effective panel width (W'), the cover depth or goaf load (H) and the mining height (T) all raised to powers ranging from 0.27 to 0.37.

The above equation(s) may be used to estimate A-Zone fracture heights in the absence of specific geological information (i.e. borehole data). The predicted v. measured outcomes using the "geometry" Pi-terms only model are presented in **Figures A42b** to **A42d**.

The plots indicate that the 'geometry only' Pi-term model is likely to provide reasonably conservative predictions, provided that the geology is not too dissimilar to the conditions that were present for the given mining geometry. For cases where the geology is significantly different above a proposed mining geometry, the above equation may underestimate or overestimate the fracture heights by a significant amount.

The development of a Pi-term model that considers the influence of overburden geology is subsequently addressed in **Section A11.5.5**.

A11.5.5 Pi-Term Model for Predicting Height of Continuous Fracturing (A) above Longwalls with the Geology Pi-Term Included

The presence of massive strata units such as sandstone, conglomerate and igneous rock that may span the fractured strata in the A-Zone is likely to limit the potential range of continuous fracture height development above the mine workings. Based on the analytical models (Equations (1) and (2)), the minimum thickness required to span the A-Zone or limit its development will depend on a number of factors, including span, thickness and rock mass axial and diametric strength. The minimum strata unit thickness required to span the A-Zone may be estimated using empirical and analytical methods, and are described in **Sections A11.5.6** and **A11.5.7** respectively.

If no obvious strata unit thickness is present in the overburden, then it will be necessary to adopt an appropriate minimum value based on subsidence data and typical or atypical geological conditions. The minimum effective t' values are also defined in **Section A11.5.6**.

Based on the empirical database presented in **Table A6.1**, the statistics software XLSTAT® was used to complete a multi-nonlinear regression analyses on the first four Pi-terms defined earlier as follows:

$$\text{Mean } A/W' = 1.52\,(H/W')^{0.535}(T/W')^{0.464}(t'/W')^{-0.4} \qquad R^2 = 0.81 \;\&\; \text{rmse} = 0.09W'(15\%)$$

$$\text{U95\% } A/W' = \text{Mean } A/W' + a$$

where a = 0.15 for subcritical panels; 0.15 - 0.0714(W/H - 0.7) for critical panels; and 0.10 for supercritical panels.
H = cover depth = the maximum potential goaf load height.
W' = effective panel width = minimum of W and 1.4H.
T = mining height.
t' = effective strata unit thickness; see **Sections A11.5.6**.

Re-arranging the above equation in terms of A, gives:

$$A = 1.52W'^{0.4}H^{0.535}T^{0.464}t'^{-0.4} \quad +/- \; aW'$$

The regression results indicate that the height of continuous fracturing (A) will increase with effective panel width (W'), the cover depth or goaf load (H) and mining height (T), all raised to powers ranging from to 0.4, 0.54 and 0.46 respectively and decrease with effective strata unit thickness (t') raised to the power of -0.4. The form of the power rule equation requires the powers to sum to unity to achieve dimensional consistency. The back-analysed powers are also similar in magnitude to the analytical models previously discussed.

A11.5.6 Effective Strata Unit Thickness Estimates for the Geology Pi-Term Model using Empirical Modelling Techniques

In order to calibrate the geological Pi-term model, it was necessary to use back-analysis techniques to estimate the likely strata unit thicknesses that existed immediately above the measured heights of continuous fracturing for a given mining geometry.

One of the difficulties in estimating the effective strata thickness from borehole data is the uncertainty in regards to the response of the 'bedded' strata under bending forces and whether they will break down into thinner units.

For example, a 33 to 40 m thick unit of Munmorah Conglomerate existed 80 m above LW5 at the Mandalong Mine and extensometer data measured the beam shearing into 15 m and 20 m thick units, which reduced the effective thickness of the conglomerate beam by approximately 50% (i.e. 15 m to 20 m). The height of continuous fracturing was estimated to occur at 118 m or near the top of the conglomerate, based on piezometer data.

Other longwalls with similar geometry at Mandalong did not break down into thinner units (based on measured subsidence data). The presence of a seam roll and thrust fault to the near the panel was identified in the mine workings and indicates that the strata may have been significantly 'worked' and weakened by tectonic activity prior to mining. It is suggested that assessments in greenfields sites should consider the outcome of massive units shearing into two beams for worst-case geological condition scenarios.

Initial values of t' were therefore estimated from borehole log and extensometer data to derive the general form of the equation presented in **Section A11.5.5**. The resulting regression equation indicated the strata unit thickness should be raised to a power of -0.4 to -0.5. A single iteration was then required to re-define the coefficients and remaining Pi-term powers. The results of the analysis are summarized in **Table A6.3a** and **Figure A42e**.

The results indicate that the back-analysed (or measured) t' values ranged between 18 m and 80 m (median of 46 m) for the *sub-critical* panels; from 8.5 m to 42 m (median of 25 m) for the *critical* panels and between 6 m and 34 m (median of 23 m) for the *supercritical* panel geometries. The measured t' values for the deeper panels appear to be generally thicker than the panels at lower depth of cover in areas with similar geological conditions (i.e. massive sandstones and conglomerate units capable of spanning the longwall voids were present in both cases). Further review of the geomechnical properties of the overburden is necessary to increase our understanding of this phenomenon.

Table A6.3a - Effective Strata Unit Thicknesses (t') Back Analysed from HoF Model Database for Australian Coalfields

Site	Panels	Mine	W (m)	H (m)	W/H	A (m)	Back Analysed t' (m)	Bore log t_{log} (m)	t_{max} 95% goaf span probability	Rock Mass Conditions (see TA6.3b)	t_{min} from subsidence data (m)	Effective Strata unit thickness* t' (m)
1	MW508	Bellambi W.	110	421	0.26	92	36.5	100	49	Normal	30	49
2	LW10	Metropolitan	140	460	0.30	130	31.5	100	49	Normal	30	49
3	LW1-4	South Coast	110	325	0.34	85	31.5	100	41	Normal	20	41
4	LW6	Kemira	117	335	0.35	98	27	100	40	Normal	20	40
5	LW20	Metropolitan	163	450	0.36	100	68	100	70	Normal	30	70
6	LWA1	Austar	159	417	0.38	*87*	160	100	78	Normal	30	78
7	LW514	Bellambi W.	150	400	0.38	90	54	100	64	Normal	30	64
8	LW28	Appin	200	500	0.40	90	80	120	103	Normal	40	103
9	LW2	Ellalong	150	368	0.41	113	37	100	49	Normal	30	49
10	LW3	Tahmoor	180	424	0.42	-	60	100	74	Normal	30	74
11	LW9	Teralba	150	350	0.43	*110*	27	34	48	Normal	30	30
12	TE	West Cliff	200	446	0.45	*101*	57	100	85	Normal	30	85
13	TE	Berima	120	176	0.68	*76*	18	100	29	Normal	20	29
14	LW409	Springvale	265	384	0.69	*133*	42	55	78	Normal	32	32
15	LW9(11)	Mandalong	160	220	0.73	-	30	30	25	Normal	20	25
16	LW11	Angus Place	211	263	0.80	-	30	100	26	Normal	10	26
17	411	Springvale	315	368	0.86	139	42	55	86	Normal	32	32
18	LW5	Mandalong	160	179	0.89	118	14.5	25	37	Normal	20	20
19	LW5	Dendrobium	245	255	0.96	123	32	80	55	Normal	20	55
20	LW1	Wyee	216	206	1.05	126	18.2	30	39	Normal	20	20
21	**LW1**	**Invincible**	**145**	**116**	**1.25**	**96**	**8.5**	**15**	19	**Adverse**	**10**	**10**
22	TE 1	Abel	120	95	1.26	45	18	15	29	Normal	15	15
23	LWs	Ashton	216	154	1.40	82	25.5	30	44	Normal	15	15
24	LW40	WWD	179	113	1.58	80	21	20	25	Normal	20	20
25	**LWE1**	**Sth Bulga**	**259**	**155**	**1.67**	**145**	**6.2**	**15**	28	**Adverse**	**10**	**10**
26	LW41	WWD	179	105	1.70	72	23	20	24	Normal	20	20
27	LW9	Crinum	280	155	1.81	85	34	35	36	Normal	20	20
28	LW39	WWD	179	97	1.84	68	22.5	20	22	Normal	20	20
29	TE (3D)	Wyee North	355	185	1.92	63	54	50	78	Normal	20	20
30	TE(LW4)	Wyee North	355	180	1.97	40	>54	50	109	Normal	20	20
31	TE	Abel	150	76	1.97	45	15.5	15	26	Normal	15	15
32	TE(NthB)	Cooranbong	150	75	2.00	58	12.5	20	16	Normal	20	16
33	LW1	Oaky ck	205	95	2.16	55	29	30	25	Normal	15	25
34	**LW9/9a**	**Homestead**	**200**	**80**	**2.50**	**70**	**11**	**15**	16	**Normal**	**15**	**15**

W' = minimum (W, 1.4H); t_{min} - minimum beam thickness values at A-Horizon based on subsidence and borehole extensometer data; t' = effective beam thickness above A-Zone derived from back analysis techniques; * - t' is selected by consideration of tlog, t_{max} and t_{min} (see text below).

Bold - surface to seam fracturing reported by others; *italics* - Continuous Fracture Zone heights (A-Zone) was originally reported and included the Discontinuous Fracture and Dilated Zone (B-Zone). The A and B- Zone heights were re-assessed by DgS based on a review of available measured vertical strains and piezometric data (see **Figure A40i and A40j**).

In order to be able to make credible height of continuous fracturing predictions at a 'green fields' site based on borehole data alone, it was necessary to identify strata unit thicknesses that did and did not stop the height of fracturing.

To do this, the effective strata unit thicknesses from the database that appeared to have stopped the height of fracturing were normalized to the effective panel width (t'/W') and plotted against the unit's location factor (y/H); see **Figure A42f**. A similar exercise was completed for the strata units that did not stop the height of fracturing development, and are plotted on the above figure as well.

The two strata thickness categories were subsequently used in a logistic regression analysis to define the probabilistic power line equation below to indicate whether a strata unit is likely to span the goaf and limit the development of the height of fracturing at a given horizon above the workings:

$$P(i=1)=50\% \text{ for } t_{max} = W'[0.035(y/H)^{-1.3}]$$

where

i = 1 for a spanning unit, and

$P(i=1)=50\%$ for t_{max} refers to a 50% probability that a beam of a given thickness will span the fractured zone at a given location in the overburden.

A similar exercise was completed in order to define for the 95% probability of spanning equation:

$$P(i=1)=95\% \text{ for } t_{max} = W'[0.12(y/H)^{-0.85}]$$

where

i = 1 for a spanning unit, and

$P(i=1)=95\%$ for t_{max} refers to a 95% probability that a beam of a given thickness will span the fractured zone at a given location in the overburden.

The two above equations above are shown in **Figure A42f** with the database of 'goaf spanning' and 'non-goaf spanning' units.

For conservative or worst-case height of fracturing prediction, subsidence data was also reviewed to indicate the minimum effective beam thickness values (t_{min}) when massive strata units are not obviously present to span and limit the height of the A-Zone.

For this scenario, it is considered that t_{min} is likely to equal twice the measured peak surface strain to curvature ratios or twice the depth of observed cracking (whichever is the greater). For the Newcastle and Hunter Coalfields, a t_{min} range from 15 m to 20 m is indicated from subsidence monitoring data, with a t' range from 30 m to 40 m indicated for the Western and Southern Coalfields.

The t_{min} values for the likely cover depths are provided in **Table A6.3b**.

Table A6.3b - Minimum Effective Strata Thickness Based on Subsidence Data for Normal and Adverse Rock Mass Conditions in Australian Coalfields

Cover Depth H (m)	Minimum Effective t_{min}					
	Normal*					Adverse**
	Southern	Western	Newcastle/ Greta	Tomago/Hunter Valley/Narrabri	Bowen Basin	All Coalfields
>450	40	-	-	30	30	15
350 - 450	40	40	30	20	20	15
250 - 350	20	20	20	20	20	10
150 - 250	20	20	20	15	15	10
<150	20	15	20	15	15	10

* - Normal conditions refer to rock mass behaviour that is unlikely to be adversely affected by geological structure or atypical rock mass conditions (e.g. deep weathering or a lack of low permeability units in the B-Zone).
** - Adverse are likely to be affected by geological structure or atypical rock mass conditions (see definition above).

Validation of the model involved the application of the following algorithm to check that the predicted beam thickness values (t') from the available borehole data (t_{log}) were consistent with the back-analysed results and the maximum (t_{max}) and minimum thicknesses (t_{min}) derived from borehole and subsidence data that is required to span the goaf:

- If $t_{log} > t_{max\ (for\ 95\%\ spanning\ probability)}$ then $t' = t_{max\ (for\ 95\%\ spanning\ probability)}$

  (so as not to bias the database above the required t' to span the goaf at a given horizon);

- If $t_{log} < t_{max\ for\ 95\%\ spanning\ probability}$ then $t' = t_{min\ based\ on\ subsidence\ data}$

  (see below).

A summary of the back analysis v. predicted effective strata unit thickness presented in **Table A6.3a** are compared graphically in **Figure A42g**. It is assessed that the proposed algorithm to estimate the likely strata unit thickness for the Pi-Term model is reasonable to give an R^2 value of 0.8 and root mean square area of 15%.

The predicted v. measured outcomes using the "Geology" Pi-term model are presented in **Figures A42h** to **A42j**. Further validation of the Geology Pi-term model outcomes are presented in **Sections A11.5.7** and **A11.5.8**.

A11.5.7 Analytical Models of Goaf Spanning Strata Unit Thickness

The minimum thicknesses of the strata units required to limit the height of continuous fracturing have also been estimated analytically for the following scenarios:

(i) Strata units that can support the full overburden load.

(ii) Single goaf spanning units, which are single strata units that have sheared / dilated away from the overlying rock mass but are able to support their own weight and span any partial voids immediately below.

For Scenario (i) the minimum strata unit thickness to fully support the overburden above it was assessed using Voussoir Beam theory presented in **Diedrichs and Kaiser, 1999**. For a factor of safety against crushing of 2:

$$t_{min,\ full} = \sqrt{(1.5\gamma(H-y)(W-2y\tan\theta)^2/UCS)}$$

For Scenario (ii) the minimum strata unit thickness to support its self-weight only was also assessed using Voussoir Beam theory presented in **Diedrichs and Kaiser, 1999**. For a factor of safety against crushing of 2:

$$t_{min,\ single} = 1.5\gamma(W-2y\tan\theta)^2/UCS$$

Note: The above equations were derived from Equation (1) and assume that the compression arch forms within 50% of the beam thickness (conservative).

Back analysis of the database indicated the angle of break increases with W/H and ranges from $\theta = 12^o$ for sub-critical panels and 19.3^o for supercritical panels. The following equations give the best fit to the geology model presented in **Section A11.5**:

$\theta = 12^o$	or W/H <0.45
$\theta = 9.63^o + 4.42(W/H) + 1.8(W/H)^2$	for 0.45 < W/H < 1.4
$\theta = 19.3^o$	for W/H > 1.4

Published laboratory UCS testing data on sandstone / conglomerate / igneous core samples from each coalfield were adopted as shown in **Table A6.4**.

A summary of the analytical goaf spanning equation results and back analysed strata unit thicknesses and beam stresses are presented in **Table A6.4**. It is considered that the minimum beam stress will govern the loading/spanning scenario for a given mining geometry. The results again demonstrate the complexity of how the fracture zone heights develop and the difficulties involved with using analytical or numerical techniques v. empirical methods.

The analytical beam thicknesses estimated for the goaf spanning scenarios are also plotted in **Figure A42f**. It is apparent the minimum thicknesses determined for the full rock mass loading case scenario and single spanning unit scenario generally plot above and below the logistic regression line for a 50% Probability of Spanning respectively. This would suggest that the Scenario (i) model is more likely to reflect the loading behaviour of the rock mass compared to Scenario (ii) (assuming the rock mass properties adopted are reasonable).

The predicted v. observed A values for the proposed Geology Pi-term model are presented in **Figures A42f** and **Figure A42g** respectively. The residual errors reasonably follow a normal probability distribution about the regression curve according to Central Limit Theory in statistics (see **Figure A42h**).

Table A6.4 - Minimum Strata Unit Thicknesses Required for Spanning the Goaf based on Analytical Models of the Overburden

Site	Panels	Mine	W (m)	H (m)	W_i	UCS (MPa)	t (m)	y (m)	y/H	Back analysed t, (m)	Full Load t_{min} (m)	Single Beam t_{min} (m)	Full Beam Load Stress (MPa)	Goaf Supported Beam Stress (MPa)
1	MW508	Bellambi W.	110	421	71	70	100	90	0.21	36.5	30	3	23	72
2	LW10	Metropolitan	140	460	85	70	100	130	0.28	31.5	36	4	45	49
3	LW1-4	South Coast	110	325	74	70	100	85	0.26	31.5	26	3	25	66
4	LW6	Kemira	117	335	75	70	100	98	0.29	27	27	3	35	52
5	LW20	Metropolitan	163	450	120	70	100	100	0.22	68	52	8	21	100
6	LWA1	Austar	159	417	122	70	100	80	0.19	160	51	8	18	208
7	LW514	Bellambi W.	150	400	112	70	100	90	0.23	54	46	7	25	75
8	LW28	Appin	200	500	162	70	120	90	0.18	80	76	14	31	61
9	LW2	Ellalong	150	368	102	70	100	113	0.31	37	38	6	36	59
10	LW3	Tahmoor	180	424	180	70	100	100	0.24	60	75	17	72	85
11	LW9	Teralba	150	350	103	70	34	110	0.31	27	37	6	66	34
12	TE	West Cliff	200	446	157	70	100	101	0.23	57	68	13	49	45
13	TE	Berima	120	176	84	70	100	76	0.43	18	19	4	40	34
14	LW409	Springvale	265	384	201	70	55	133	0.27	78	74	22	108	26
15	LW9(11)	Mandalong	160	220	160	67	30	160	0.73	30	29	14	-	-
16	LW11	Angus Place	211	263	211	70	100	*253*	0.96	30	15	24	-	-
17	411	Springvale	315	368	242	70	100	139	0.38	42	85	31	142	20
18	LW5	Mandalong	160	179	97	67	25	83	0.46	14.5	18	5	51	23
19	LW5	Dendrobium	245	255	177	70	80	123	0.48	32	47	17	75	28
20	LW1	Wyee	216	206	143	70	30	126	0.61	18.2	30	11	92	18
21	**LW1**	**Invincible**	**145**	**116**	**83**	**70**	**15**	**106**	**0.91**	8.5	9	**4**	36	15
22	TE 1	Abel	120	95	91	30	15	41	0.43	18	23	10	24	20
23	LWs	Ashton	216	154	158	30	30	82	0.53	25.5	47	31	52	10
24	LW40	WWD	179	113	102	30	20	80	0.71	21	21	13	15	22
25	**LWE1**	**Sth Bulga**	**259**	**155**	**115**	**30**	**20**	**145**	**0.94**	6.2	13	**17**	65	2
26	LW41	WWD	179	105	97	30	20	72	0.69	23	20	12	11	28
27	LW9	Crinum	280	155	157	130	35	105	0.68	34	22	7	28	79
28	LW39	WWD	179	97	88	30	20	68	0.70	22.5	17	10	8	32
29	TE (3D)	Wyee North	355	185	215	70	50	63	0.34	54	55	25	36	28
30	TE(LW4)	Wyee North	355	180	224	70	50	40	0.22	<u>156</u>	61	27	37	34
31	TE	Abel	150	76	75	30	15	33	0.43	15.5	15	7	14	18
32	TE(NthB)	Cooranbong	150	75	64	67	20	58	0.77	12.5	8	2	8	47
33	LW1	Oaky ck	205	95	94	30	30	55	0.58	29	21	11	8	37
34	**LW9/9a**	**Homestead**	**200**	**80**	63	**30**	**15**	**65**	**0.81**	11	8	5	6	18

W' = minimum (W, 1.4H); t_{min} - minimum beam thickness values at A-Horizon based on subsidence and borehole extensometer data; t' = effective beam thickness above A-Zone derived from back analysis techniques;
Bold - surface to seam fracturing reported by others;
<u>Underlined</u> - Conservative estimate of t' returned.
italics - Continuous Fracture Zone heights (A-Zone) was originally reported and included the Discontinuous Fracture and Dilated Zone (B-Zone). The A and B- Zone heights were re-assessed by DgS based on a review of available measured vertical strains and piezometric data (see **Figure A40i** and **A40j**).

A11.5.8 Pi-Term Model for Predicting Heights of Discontinuous Fracturing (B) Above Longwalls using Geometry Pi-Terms Only (Geometry Model)

Based on the empirical database presented in **Table A6.1**, the statistics software XLSTAT® was used to complete a multi-nonlinear regression analysis as follows for estimating the height of the dilated B-Zone :

$$\text{Mean } B/W' = 1.621\,(H'/W')^{0.55}(T/W')^{0.175} \qquad R^2 = 0.86 \text{ \& rsme} = 0.12W' \text{ (13\%)}$$

$$U95\%\ B/W' = \text{Mean } B/W' + b$$

where b = 0.16 for subcritical panels, 0.16-0.085(W/H-0.7) for critical panels and 0.10 for supercritical panels.

H' = Goaf Load Height = H

W' = Effective Panel Width = minimum of W and 1.4H.

T = Mining Height.

Re-arranging the above equation in terms of B gives:

$$B = 1.621\,W'^{0.275}H^{0.55}T^{0.175} \quad +/- bW'$$

The predicted v. observed B/W' and B' values are presented in **Figure A42k** and **Figure A42l** respectively. The residual errors follow a normal probability distribution about the regression curve as expected according to Central Limit Theory in statistics (see **Figure A42m**). The regression indicates a relatively weaker relationship exists between the height of B-Zone fracturing and the mining height compared to the A-Zone relationship.

A11.5.9 Pi-Term Model for Predicting Heights of Discontinuous Fracturing (B) Above Longwalls using the Geology Pi-Term

Based on the empirical database presented in **Table A6.1**, the statistics software XLSTAT® was used to complete a multi-nonlinear regression analysis as follows for estimating the height of the dilated B-Zone :

$$\text{Mean } B/W' = 1.873\,(H'/W')^{0.635}(T/W')^{0.257}(t'/W')^{-0.097} \qquad R^2 = 0.86 \text{ \& rmse} = 0.13W'(15\%)$$

$$U95\%\ B/W' = \text{Mean } B/W' + b$$

where b = 0.15 for subcritical panels; 0.15-0.0714(W/H-0.7) for critical panels and 0.10 for supercritical panels.

H' = Goaf Load Height = H

W' = Effective Panel Width = minimum of W and 1.4H.

T = Mining Height.

t' = Effective strata unit thickness; see **Section A11.5.6**.

Re-arranging the above equation in terms of B gives:

$$B = 1.873\ W'^{0.205}\ H^{0.635} T^{0.257}\ t'^{-0.097} \quad +/-\ bW'$$

The predicted v. observed B/W' and B' values are presented in **Figure A42n** and **Figure A42o** respectively. The residual errors follow a normal probability distribution about the regression curve as expected according to Central Limit Theory in statistics (see **Figure A42p**). The regression indicates a relatively weaker relationship exists between the height of B-Zone fracturing, the mining height and strata unit thickness compared to the A-Zone relationship.

A11.5.10 Pi-Term Model Validation

Validation of the proposed Pi-Term model has been completed as follows:

(i) A review of the range of independent variables within the database to check if the model is likely to be biased towards a particular parameter or mining geometry.

(ii) Comparison of predicted v. measured A and B-Horizons for each model to check model reliability.

(iii) Sensitivity analysis of the model to the assumed input parameters (based on method applied in **Hydrosimulations, 2013**).

(iv) Comparison of model results with other models over a representative range of mining geometries and overburden geologies.

(i) Database Variable Review

In regards to the data base, the following parameters from **Table A6.1** were plotted against the W/H ratio in **Figures A43a** to **43d** to test for sample bias:

- Panel Width (W)
- Cover Depth (H)
- Mining Height (T)
- Height of A-Zone Fracturing (A)
- Height of B-Zone Fracturing/Strata Dilation (B)

It is assessed that the database has sufficient coverage in regards to panel width, cover depth and mining height to reliably estimate HoF Zones above sub-critical to super-critical panels with W/H values ranging from 0.3 to 2.2.

(ii) Model Reliability

In regards to prediction model reliability, the minimum effective strata unit thickness assessed for each site has used to estimate the height of A and B-Zones and the residual areas subjected to a Normality test. The distributions of model residual errors should follow the Central Limit theorem for regression analysis. That is, a normal distribution of errors would be expected to occur about the regression line of 'best-fit'. If the regression lines are deemed to meet this requirement, the assessment of predicted confidence limits will then be possible. It would then be expected that < 5% of measured values would exceed the predicted U95%CL values on average.

The regression results for the A-Zone Geological model are summarised in **Table A6.5** and **Figure A42j**. The results demonstrate the model errors satisfy normality tests with 61% of the measured values below the predicted mean values and 97% of the measured values below the Upper 95%CL predictions. A slightly lower reliability outcome was achieved for the Geometry Model for the B-Zone with 55% of measured values below the mean and 90% below the U95%CL (see **Table A6.6**).

It is therefore considered that the reliability of the Pi-Term geology model is acceptable for worst-case estimates of A-Zone fracture heights at new or existing coal mines in Australia until local performance data either confirms or supersedes it.

The results for the B-Zone geology model checks also indicate the model errors satisfy normality tests as shown in **Figure A42p** and are summarised in **Table A6.7**. The proposed mean and U95%CL model satisfactorily over predicts 52% and 95% of the measured B-Zone data (i.e. within 5% of the expected values). A slightly lower reliability outcome was achieved for the Geometry Model for the B-Zone (see **Table A6.8**).

Overall, it is considered that the reliability of both the Pi-Term Models is acceptable for estimates of B-Zone discontinuous fracture height assessments at new or existing coal mines in the NSW Coalfields and should be confirmed or re-calibrated with local measurement data.

The above results indicate that the model is likely to provide reasonably conservative estimates of the height of continuous fracturing for the full range of mining geometries, based on the effective panel width, effective goaf load height (cover depth), mining height and effective strata unit thickness in the A or B-Zones.

Table A6.5 - Summary of Measured v. Predicted Height of Continuous Fracture A-Zones for the Geology Model

Site	Panel	Mine	Panel Width W (m)	Cover Depth H (m)	W/H	Mining Height T (m)	Predicted t' (m)	Predicted A (m)		Measured A (m)	Pass = 1; Fail = 0	
								mean	U95%CL		m	U95
1	MW508	Bellambi W	110	421	0.26	2.50	49	82	98	**92**	0	**1**
2	LW10	Metropolitan	140	460	0.30	3.40	49	109	130	**130**	0	**1**
3	LW1-4	South Coast	110	325	0.34	2.50	41	76	93	**85**	0	**1**
4	LW6	Kemira	117	335	0.35	2.75	40	84	102	**98**	0	**1**
5	LW20	Metropolitan	163	450	0.36	3.40	70	99	124	**100**	0	**1**
6	LWA1	Austar	159	417	0.38	6.00	78	118	142	***87***	1	**1**
7	LW514	Bellambi W	150	400	0.38	2.70	64	84	106	**90**	0	**1**
8	LW28	Appin	200	500	0.40	2.30	103	81	111	**90**	0	**1**
9	LW2	Ellalong	150	368	0.41	3.50	49	101	123	**113**	0	**1**
10	LW3	Tahmoor	180	424	0.42	2.18	74	80	107	**-**	-	**-**
11	LW9	Teralba	150	350	0.43	2.70	30	106	128	***110***	0	**1**
12	TE	West Cliff	200	446	0.45	2.50	85	86	116	***101***	0	**1**
13	TE-SW1	Berrima	120	176	0.68	2.3	29	63	81	***76***	0	**1**
14	LW409	Springvale	265	384	0.69	3.25	32	148	188	**133**	0	**1**
15	LW9	Mandalong	160	220	0.73	4.50	25	115	139	**-**	-	**-**
16	LW11	Angus Place	211	263	0.80	2.47	16	129	159	**-**	-	**-**
17	411	Springvale	315	368	0.86	3.25	32	156	199	**139**	0	**1**
18	LW5	Mandalong	160	179	0.89	3.70	20	103	125	**118**	0	**1**
19	LW5	Dendrobium	245	255	0.96	3.75	55	100	132	**123**	0	**1**
20	LW1	Wyee	216	206	1.05	3.44	20	121	148	**126**	0	**1**
21	*LW1*	*Invincible*	*145*	*116*	*1.25*	*2.70*	*15*	90	106	*96*	**0**	**1**
22	TE1	Abel	120	95	1.26	2.30	15	59	72	**45**	1	**1**
23	LWs	Ashton	216	154	1.40	2.55	15	101	123	**82**	1	**1**
24	LW40	WWD	179	113	1.58	3.80	20	81	97	**80**	1	**1**
25	*LWE1*	*South Bulga*	*259*	*155*	*1.67*	*2.55*	*15*	120	142	*145*	**0**	**0**
26	LW41	WWD	179	105	1.70	3.80	20	76	91	**72**	1	**1**
27	LW9	Crinum	280	155	1.81	3.50	20	105	127	**85**	1	**1**
28	LW39	WWD	179	97	1.84	3.90	20	71	85	**68**	1	**1**
29	TE-3D	Wyee North	355	185	1.92	1.90	20	60	86	**63**	0	**1**
30	TE-355	Wyee North	355	180	1.97	1.90	20	59	84	**40**	1	**1**
31	Panel2	Abel	150	76	1.97	1.88	15	45	56	**45**	1	**1**
32	TE - North B	Cooranbong	150	75	2.00	2.80	16	53	64	**58**	0	**1**
33	LW1	Oaky Ck	205	95	2.16	3.20	25	58	71	**55**	1	**1**
34	*LW9/9a*	*Homestead*	*200*	*80*	*2.50*	*3.30*	*15*	62	73	***70***	0	**1**
Percentage of Measured < Predicted Value											39	97

italics - Surface to seam connection reported by authors.

Table A6.6 - Summary of Measured v. Predicted Height of Continuous Fracture A-Zones for the Geometry Model

Site	Panel	Mine	Panel Width W (m)	Cover Depth H (m)	W/H	Mining Height T (m)	Predicted A (m)		Measured A (m)	Pass = 1; Fail = 0	
							mean	U95%CL		m	U95
1	MW508	Bellambi W	110	421	0.26	2.50	86	103	**92**	0	1
2	LW10	Metropolitan	140	460	0.30	3.40	107	130	**130**	0	1
3	LW1-4	South Coast	110	325	0.34	2.50	80	98	**85**	0	1
4	LW6	Kemira	117	335	0.35	2.75	85	104	**98**	0	1
5	LW20	Metropolitan	163	450	0.36	3.40	113	139	**100**	1	1
6	LWA1	Austar	159	417	0.38	6.00	135	161	***87***	1	1
7	LW514	Bellambi W	150	400	0.38	2.70	97	121	**90**	1	1
8	LW28	Appin	200	500	0.40	2.30	108	140	**90**	1	1
9	LW2	Ellalong	150	368	0.41	3.50	105	129	**113**	0	1
10	LW3	Tahmoor	180	424	0.42	2.18	97	126	**-**	-	-
11	LW9	Teralba	150	350	0.43	2.70	94	118	***110***	0	1
12	TE	West Cliff	200	446	0.45	2.50	108	140	***101***	1	1
13	TE	Berrima	120	176	0.68	2.3	68	87	***76***	0	1
14	LW409	Springvale	265	384	0.69	3.25	126	169	**133**	0	1
15	LW9	Mandalong	160	220	0.73	4.50	102	128	**-**	-	-
16	LW11	Angus Place	211	263	0.80	2.47	95	127	**-**	-	-
17	411	Springvale	315	368	0.86	3.25	133	179	**139**	0	1
18	LW5	Mandalong	160	179	0.89	3.70	90	113	**118**	0	0
19	LW5	Dendrobium	245	255	0.96	3.75	116	150	**123**	0	1
20	LW1	Wyee	216	206	1.05	3.44	101	129	**126**	0	1
21	*LW1*	*Invincible*	*145*	*116*	*1.25*	*2.70*	69	85	**96**	**0**	**0**
22	TE1	Abel	120	95	1.26	2.30	57	71	**45**	1	1
23	LWs	Ashton	216	154	1.40	2.55	84	105	**82**	1	1
24	LW40	WWD	179	113	1.58	3.80	80	105	**80**	0	1
25	*LWE1*	*South Bulga*	*259*	*155*	*1.67*	*2.55*	84	119	**145**	**0**	**0**
26	LW41	WWD	179	105	1.70	3.80	76	100	**72**	1	1
27	LW9	Crinum	280	155	1.81	3.50	95	129	**85**	1	1
28	LW39	WWD	179	97	1.84	3.90	73	95	**68**	1	1
29	TE-3D	Wyee North	355	185	1.92	1.90	84	126	**63**	1	1
30	TE-355	Wyee North	355	180	1.97	1.90	83	123	**40**	1	1
31	Panel2	Abel	150	76	1.97	1.88	48	65	**45**	1	1
32	TE-NthB	Cooranbong	150	75	2.00	2.80	55	72	**58**	0	1
33	LW1	Oaky Ck	205	95	2.16	3.20	67	88	**55**	1	1
34	*LW9/9a*	*Homestead*	*200*	*80*	*2.50*	*3.30*	61	79	***70***	0	1
Percentage of Measured < Predicted Value										45	90

italics - Surface to seam connection reported by authors.

Table A6.7 - Summary of Measured v. Predicted Height of Dilated B-Zones for the Geology Model

Site	Panel	Mine	Panel Width W (m)	Cover Depth H (m)	W/H	Mining Height T (m)	t' (m)	Predicted B (m)		Measured B (m)	Pass = 1; Fail = 0	
								mean	U95%CL		m	U95
1	MW508	Bellambi West	110	421	0.26	2.50	49	198	214	-	-	-
2	LW10	Metropolitan	140	460	0.30	3.40	49	238	259	-	-	-
3	LW1 to 4	South Coast	110	325	0.34	2.50	41	170	187	-	-	-
4	LW6	Kemira	117	335	0.35	2.75	40	181	198	-	-	-
5	LW20	Metropolitan	163	450	0.36	3.40	70	234	258	-	-	-
6	LWA1	Austar	159	417	0.38	6.00	78	254	278	**277**	0	1
7	LW514	Bellambi West	150	400	0.38	2.70	64	203	225	-	-	-
8	LW28	Appin	200	500	0.40	2.30	103	227	257	-	-	-
9	LW2	Ellalong	150	368	0.41	3.50	49	211	233	**210**	1	1
10	LW3	Tahmoor	180	424	0.42	2.18	74	204	231	**204**	0	1
11	LW9	Teralba	150	350	0.43	2.70	30	200	223	**150**	1	1
12	TE	West Cliff	200	446	0.45	2.50	85	220	250	***245***	0	1
13	TE SW1	Berrima	120	176	0.68	2.3	29	119	137	**112**	1	1
14	LW409	Springvale	265	384	0.69	3.25	32	249	289	***254***	0	1
15	LW9	Mandalong	160	220	0.73	4.50	25			-	-	-
16	LW11	Angus Place	211	263	0.80	2.47	16	177	208	***253***	0	0
17	411	Springvale	315	368	0.86	3.25	32	251	295	**288**	0	1
18	LW5	Mandalong	160	179	0.89	3.70	20	150	171	**154**	0	1
19	LW5	Dendrobium	245	255	0.96	3.75	55	186	218	-	-	-
20	LW1	Wyee	216	206	1.05	3.44	20	171	198	-	-	-
21	LW1	Invincible	145	116	1.25	2.70	**10**	110	116	***111***	**0**	**1**
22	TE1	Abel	120	95	1.26	2.30	15	86	95	***75***	1	1
23	LWs	Ashton	216	154	1.40	2.55	15	135	154	***130***	1	1
24	LW40	WWD	179	113	1.58	3.80	20	112	113	***108***	**1**	1
25	LWE1	South Bulga	259	155	1.67	2.55	**10**	141	155	**150**	**0**	**1**
26	LW41	WWD	179	105	1.70	3.80	20	100	105	**100**	1	1
27	LW9	Crinum	280	155	1.81	3.50	20	143	155	***150***	0	1
28	LW39	WWD	179	97	1.84	3.90	20	92	97	**92**	0	1
29	TE-3D	Wyee North	355	185	1.92	1.90	60	128	154	***143***	0	1
30	TE-355	Wyee North (LW4)	355	180	1.97	1.90	60	125	150	-	-	-
31	Panel2	Abel	150	76	1.97	1.88	15	69	76	**71**	0	1
32	TE-North B	Cooranbong	150	75	2.00	2.80	16	70	75	***70***	1	1
33	LW1	Oaky Ck	205	95	2.16	3.20	25	91	95	***90***	1	1
34	LW9/9a	Homestead	200	80	2.50	3.30	15	75	80	**75**	**1**	1
Percentage of Measured < Predicted Value											**43**	**96**

Table A6.8 - Summary of Measured v. Predicted Height of Dilated B-Zones for the Geometry Model

Site	Panel	Mine	Panel Width W (m)	Cover Depth H (m)	W/H	Mining Height T (m)	Predicted B (m)		Measured B (m)	Pass = 1; Fail = 0	
							mean	U95%CL		m	U95
1	MW508	Bellambi West	110	421	0.26	2.50	192	210	**-**	-	-
2	LW10	Metropolitan	140	460	0.30	3.40	228	250	**-**	-	
3	LW1 to 4	South Coast	110	325	0.34	2.50	167	184	**-**	-	-
4	LW6	Kemira	117	335	0.35	2.75	175	194	**-**	-	-
5	LW20	Metropolitan	163	450	0.36	3.40	235	261	**-**	-	-
6	LWA1	Austar	159	417	0.38	6.00	247	272	**277**	0	0
7	LW514	Bellambi West	150	400	0.38	2.70	206	230	**-**	-	-
8	LW28	Appin	200	500	0.40	2.30	246	278	**-**	-	-
9	LW2	Ellalong	150	368	0.41	3.50	206	230	**210**	0	1
10	LW3	Tahmoor	180	424	0.42	2.18	216	245	**204**	1	1
11	LW9	Teralba	150	350	0.43	2.70	192	216	**150**	1	1
12	TE	West Cliff	200	446	0.45	2.50	234	266	***245***	0	1
13	TE SW1	Berrima	120	176	0.68	2.3	120	139	**112**	1	1
14	LW409	Springvale	265	384	0.69	3.25	244	286	***254***	0	1
15	LW9	Mandalong	160	220	0.73	4.50	165	191	**-**	-	-
16	LW11	Angus Place	211	263	0.80	2.47	177	209	***253***	0	0
17	411	Springvale	315	368	0.86	3.25	250	296	**288**	0	1
18	LW5	Mandalong	160	179	0.89	3.70	143	166	**154**	0	1
19	LW5	Dendrobium	245	255	0.96	3.75	195	229	**-**	-	-
20	LW1	Wyee	216	206	1.05	3.44	165	193	**-**	-	-
21	LW1	Invincible	145	116	1.25	2.70	104	116	***111***	0	1
22	TE1	Abel	120	95	1.26	2.30	86	95	***75***	1	1
23	LWs	Ashton	216	154	1.40	2.55	134	154	***130***	1	1
24	LW40	WWD	179	113	1.58	3.80	111	113	***108***	1	1
25	LWE1	South Bulga	259	155	1.67	2.55	134	155	**150**	0	1
26	LW41	WWD	179	105	1.70	3.80	104	105	**100**	1	1
27	LW9	Crinum	280	155	1.81	3.50	142	155	***150***	0	1
28	LW39	WWD	179	97	1.84	3.90	92	97	**92**	0	1
29	TE-3D	Wyee North	355	185	1.92	1.90	148	174	***143***	1	1
30	TE-355	Wyee North (LW4)	355	180	1.97	1.90	144	170	-	-	-
31	Panel2	Abel	150	76	1.97	1.88	71	76	**71**	0	1
32	TE-North B	Cooranbong	150	75	2.00	2.80	70	75	***70***	1	1
33	LW1	Oaky Ck	205	95	2.16	3.20	93	95	***90***	1	1
34	LW9/9a	Homestead	200	80	2.50	3.30	75	80	**75**	1	1
Percentage of Measured < Predicted Value										**48**	**91**

(iv) Parameter Sensitivities

A review of the sensitivity of the Pi-Term Models has been completed in **Merrick, 2014** and demonstrates that the model is not overly sensitive to changes to the input parameters, W, H and T. The influence of the effective strata thickness t' has a greater impact on the height of fracturing for values < 20 m than the cases with t'> 20 m. This is not surprising as the spanning capabilities of the strata units will probably decrease rapidly below this thickness range as it corresponds with the point where the bending beam stress starts to exceed the UCS of the rock mass.

The model variable sensitivity charts are presented in **Figures A43e** to **A43h**.

(v) Comparison with other models

Three critical cases were identified in the analysis where the A-Zone extended to within 10 m of the surface (Invincible, South Bulga, and Homestead Mines) with a minimum t' value of 10 m assumed. Adopting a minimum beam thickness of 10 m will generally indicate the maximum likely height of continuous fracturing for all cases in the database (see **Figure A42g**).

For completeness, four case studies have been selected from the sub-critical, critical and supercritical panel geometries and plotted with varying panel widths in **Figures A43i** to **A43l** to demonstrate the sensitivity of the models to changes in mining geometry. Several sub-surface fracture height models (**Foster, 1995; SCT, 2008; ACARP, 2007** and **Tammetta, 2013**) that have been referred to by OEH and PACs during recent project approval applications are also plotted with the Pi-term model results. It is apparent that the models are based on a smaller number of key variables and some were developed from data in a particular coalfield only. The application of the models in other coalfields with significantly different geological conditions and mining geometries are considered to have resulted in a larger range of 'error' compared to the Pi-term models.

Finally, the width-based models also do not consider the effect of cover depth or mining height and assume the A-Zone will continue to increase above *supercritical* panel geometries. This usually means that surface to seam connectivity will always be predicted for critical and supercritical panel widths. It is noted that only 2 or 3 cases out of 14 (15% - 20%) or 1 in 5 supercritical longwalls have resulted in surface to seam connectivity; see **Figure 43m**.

This outcome suggests that other factors such as cover depth, mining height and geological conditions should also be considered than just the panel width alone when estimating heights of fracturing above longwall panels.

A11.5.11 Definition of Surface Cracking Zone

During the development of the Pi-term model it has also been necessary to better define the surface cracking zone depth. The depth of the surface cracking zone has been estimated from subsidence data, surface crack observations and published measurements as follows:

- The literature review findings presented in **Section A11.3** indicate that surface cracking depths above longwalls are likely to be < 15 m generally.

- The Mean and median strain/curvature ratios of 5.3 m and 7.4 m mentioned earlier in Section derived from subsidence data measurements for Newcastle Coalfield (see **Figures A43n** and **A43o**) indicates the ***average surface cracking depth***. The ratio is considered to be a direct measurement of the depth to the neutral axis of bending where tensile strains cross over to compressive strain. This also suggests near surface strata beam thicknesses are twice the depth to the neutral axis of bending or 11 m to 15 m. It is apparent that these values are consistent with near surface beam thicknesses assumed in the Pi-Term Geology Model.

- Borehole measurement devices measured depths of cracking at the base of sandstone valleys in the Southern Coalfield of up to 12 m after mine subsidence effects (refer **Mills, 2007**).

- Measured crack depths of up to 20 m have been measured along the crests of steep slopes above LW41 (ref to **RCA, 2013**).

Based on the above information, it is assessed that the following conservative crack depths presented in **Table A6.9** may be assumed when assessing surface to seam connectivity potential above longwalls beneath varying topography:

Table A6.9 - Suggested Maximum Cracking Depths for Impact Assessment

Location and Topography	Surface Cracking Depth (m)
	Newcastle/Hunter Valley - Southern/Western Coalfield
Flat Terrain with Moderate Slopes up to 18^o	7.5 - 12
Bases of Valleys	12 - 15
Low side of panel beneath steep slopes > 18^o (not valley floor)	3.5 - 5
Crests or high side of panel beneath steep slopes > 18^o	15 - 20

A11.5.12 Summary

The geometry and geology Pi-term models presented in **Section A11.5** for estimating the A-Zone and B-Zone fracture horizons are generally consistent with the prevailing view that the panel width, cover depth and mining height will have the greatest influence on fracture development heights above longwall panels. The Pi-term models for A and B-Zone Fracture

Heights are also generally consistent with **Whittaker and Reddish, 1990**, **Singh & Kendorski, 1991** and the analytical models presented earlier.

The spanning or non-spanning capability of strata units in the overburden cannot be ignored however, when assessing the potential fracturing heights above a longwall panel. Where local extensometer and piezometric data are available, the influence of spanning strata may be used to calibrate the Geology Pi-term model to a given site.

Predictions based on the up-dated Strain, Overburden Curvature Index and Fracture Height Angle Models are still also considered relevant and will provide similar, if not more conservative outcomes. These models may be used to provide a range of predictions at a greenfields site for risk assessment purposes. It should be understood however, that only the Geology Pi-term model will allow the influence of strata unit thickness or local site geology to be included directly in the predictions of sub-surface fracture height.

It should be understood that the vagaries of the rock mass do not usually allow the strata unit thickness term to be assessed directly from borehole data without back analysis of overburden performance measurements. The database presented in this appendix has been used to derive a minimum beam thickness of 10 m to estimate worst-case heights of fracturing for adverse rock mass conditions. A thickness of 15 m to 20 m corresponds to the minimum beam thicknesses assessed from surface strain and curvature measurements (and a cracking depth of 7.5 m to 10 m).

Subsequent measurements of continuous heights of fracturing may require a thinner strata unit thickness to be used to calibrate the model. At this stage, there are three cases in the database that have been reported to have fractured through to the surface, which required a beam thickness of 6 to 11 m to match the Pi-term model exactly and intersect the surface cracking zone (or D-Zone). One of the cases (South Bulga LWE1) however, may have included the B-Zone in the interpretation of the 'height of fracturing' at the time it was assessed.

It is assessed that the assumptions that the height of fracturing will be limited when either:

- critical panel widths exceed 1.4H;
- spanning strata exists that can bridge the fractured zone or the presence of plastic, low strength strata that tends to shear along bedding partings when deformed through bending action, rather than crack vertically, may also limit continuous cracking heights.

All of these outcomes are intuitively correct and correlate well with observed behaviour across sub-critical to supercritical mining geometries. It is also noted that the strata unit thickness term enables all of the database and subsequent regression equations to be used with a reasonable level of confidence, such that the predicted worst-case values will not be unduly biased by the database itself. The geology Pi-term t'/W' was back analysed for each of the 34 case studies to give an exact fit between the predicted and measured fracture heights. The set of measured t' values were correlated with the predicted t' with a high R^2 of 0.9. The

predicted v. measured heights of continuous fracturing were also correlated and returned an R^2 value of 0.8, which is also a good fit.

For estimates of HoF above partial pillar extraction panels, the HoF zones may be based on the effective mining height, T_e (if remnant pillars are likely to fail) or the maximum span between stable remnant pillars.

The use of the Pi-term models for multi-seam mining environments will also require consideration of the interburden thicknesses and cumulative effects of the A-Zones if they likely to intersect overlying longwall goafs. The multi-seam affect may be estimated for an overlying seam by converting the multi-seam subsidence increase to an effective mining height.

A12 Far-Field Displacements and Strain Predictions

A12.1 Background

The term far-field displacements (FFD) generally refer to the horizontal surface movements that occur outside the vertical subsidence limit or angle of draw to an extracted pillar panel or longwall block. It is currently understood that FFDs are a phenomenon caused by the reduction of horizontal stress when collapse of overburden rock (i.e. goafing) occurs above an extracted area. There also appears to be a strong correlation between the FFDs and the surface subsidence magnitude (which is also an indicator of horizontal stress relief). A conceptual model of the mechanics of FFDs is presented in **Figure A44a**.

Horizontal stress in rock is normally greater than the vertical stress at a given depth of cover; it has been 'locked' into the strata by tectonic movements and over-consolidation pressures (i.e. stress). Over-consolidation stresses occur in sedimentary rock after uplift and erosion over millennia has gradually removed the overlying material since the time of formation. Tectonic induced stress usually results in strong directional bias between the major and minor principal stress magnitudes, with variation due to stiffness of the lithological units as well (refer to **Nemcik et al, 2005**, **Pells, 2004**, **McQueen, 2004, Enever, 1999** and **Walker, 2004**).

It is considered that both of the abovementioned horizontal stress development mechanisms are likely to be present in the near surface rocks in the western area of the Newcastle Coalfield.

FFD's have only recently become an issue in the Newcastle Coalfield because of adverse surface impact experiences in the Southern Coalfield (e.g. horizontal movements of around 25 mm have been measured over 1.5 km away from extracted longwall panels on a concrete dam wall. No cracking damage occurred to the dam wall because of these movements however).

The strains associated with FFDs are usually very low, however, there is one case in the Southern Coalfield where a bridge was subject to lateral shearing of approximately 50 mm along the river bed axis.

To-date, it is understood that there are no precedents in the Newcastle Coalfield where similar FFD effects (measured or inferred via damage) have occurred around longwalls or total extraction panels. Horizontal movements have been measured outside the angle of draw limits from mine workings however, albeit at smaller distances and magnitudes (eg. 20 mm of horizontal movement has been measured in undulating terrain at 250 m from one longwall block where the cover depth was 135 m).

The horizontal stress in the Newcastle Coal Measures has been measured at several locations along the F3 Freeway to the west of Wyong and Newcastle (**Lohe and Dean-Jones, 1995**). The magnitude of the measured horizontal stress indicates that it is relatively high, with magnitudes that are 1.5 to >5 times the vertical stress, in relatively flat or moderately undulated terrain.

The major principal horizontal stress is usually orientated N to NE in the Western Newcastle Coalfield, but it can be re-orientated parallel to the axis of a ridge due to natural weathering processes near the surface (which cause lateral unloading towards the gullies); refer to **Lohe and Dean Jones, 1995**.

A12.2 In-situ Stress Field

Reference to stress measurement data in **Lohe and Dean-Jones, 1995** indicates that the 'shallow' (ie < 100 m below the surface) regional stress field in the undulating terrain along the eastern and eastern sides of Lake Macquarie is likely to have its major principal horizontal stress > 5 x vertical stress (and assuming horizontal stress is zero at the surface). Deeper strata at depths > 150 m is likely to have its major principal horizontal stress <2 x vertical stress.

The stress data from the above reference was measured using over-coring / HI-Cell techniques and is presented in Table A4.

Table A6 - Horizontal Stress Field Measurements in Newcastle Coalfield Relevant to Tasman

Location	Depth (m)	In-situ Stress Measurements*			
		Major Sigma 1 (MPa)	Minor Sigma 2 (MPa)	Vertical Sigma 3 (MPa)	Sigma1+/ Sigma 3
Wakefield	24	10.4	0.42	0.6	17.3
Wallsend Borehole	100	13.3	9.7	2.5	5.3
West Wallsend No. 2	190	27.4	20.3	4.75	5.8
Kangy Angy	70	11.8	4.2	1.75	6.7
Moonee	90	11.7	8.3	2.25	5.2
West Wallsend	170	6.4	n/a	4.25	1.5
Ellalong	320	6.5	4.6	8.0	0.8

* - All measurements in medium strength sandstone.
+ - ratio assumes horizontal stress is zero at the surface (which is not always correct).

The shallow stress data is plotted in **Figure A44b** and indicates that the major principal horizontal stress could be as high as 6 MPa at the surface (unless weathered rock and soil is present) with the Major and Minor Principal Horizontal stresses equal to approximately 4 times the vertical stress for depths up to 250 m.

This high Sigma 1 reading, however, may be associated with a sandstone / conglomerate ridgeline and not typical for the areas away from ridgelines (although a residual 'surface' horizontal stress range from 1.5 to 6.5 MPa has also been assessed for the Sydney Metropolitan area in **McQueen, 1999** and **Pells, 2002**).

Another commonly used assumption in the NSW Coalfields is that the major principal horizontal stress is approximately 2 x the vertical stress and the minor principal horizontal stress is 1.4 ~ 1.5 x the vertical stress (or the Major Principal Horizontal Stress is 1.33~1.4 x the Minor Principal Horizontal Stress). It is also acknowledged that the horizontal stress in the

Newcastle and Sydney areas can be 4 to 5 times the vertical stress, based on shallow rock mass data at depths < 50 m; refer to **Lohe and Dean Jones, 1995**. The sources of this stress field imbalance has been explained in **Enever, 1999**, **Pells, 2002** and **Fell *et al*, 1992** as being due to:

(i) the 'over consolidation' ratio; where the vertical pressure due to ancient surface at the time of consolidation has since been eroded away, leaving a 'locked' in horizontal stress component in today's sedimentary rock mass. The OCR can be shown to decrease exponentially with depth and is equal in all directions at a given point.

(ii) Tectonic strain; where crustal plate movements apply a strain to the rock mass and the resultant stress is dependent on the stiffness of the individual beds and direction of movement.

(iii) Geological structure (faults/dykes); where discontinuities can change the magnitude and orientations of the regional stress field significantly.

(iv) Topographic relief (ridges/valleys/gorges); where the magnitude and direction of the regional stress field can vary due to geometric affects.

The influence of underground mining can also result in changes (both increases and decreases) in horizontal and vertical stress field magnitudes as the rock mass adjusts to a new equilibrium state.

Based on the measured stress conditions, the horizontal stress magnitudes may be estimated based on the equations presented in **Nemcik et al, 2005**:

$\sigma_H = K\sigma_v + E\varepsilon = \sigma_v [(\upsilon/1-\upsilon)OCR] + E\varepsilon$

$\sigma_h = f(\sigma_H)$ and $\sigma_v = 0.025H$ (MPa)

where,

σ_H = Major Horizontal Principal Stress;

σ_h = Minor Horizontal Principal Stress;

σ_v = Vertical Stress;

υ = Poisson's Ratio (normally ranges between 0.15 and 0.4 in coal measure rocks);

$(\upsilon/1-\upsilon)$ = Horizontal to vertical stress ratio factor (K_o) due to Poisson's Ratio effect on its own;

OCR = The over-consolidation ratio, which relates vertical pre-consolidation pressure (σ_{vo}) with current vertical pressure (σ_v) as follows, $OCR = \sigma_{vo}/\sigma_v = H_o/H$.

(*Note: This is an additional term that has been introduced by DgS, and has been mentioned (but not derived) in* **Pells, 2002** *and calculated in* **Fell et al, 1992**).

E = Young's Modulus for rock-mass unit;

ε = Tectonic Stress Factor (TSF) or Tectonic Strain.

Due to the wide range of horizontal stress values noted in the literature, it is recommended that the horizontal stress magnitudes be measured in-situ at several lithological horizons before high extraction mining commences.

Based on the apparent complexity and large variation between the interpretations of published stress field data, it was considered necessary to conduct a sensitivity analysis on the stress field profiles during the calibration of Map-3D® using the flat terrain data (see **Section A12.3** for details).

Total horizontal displacement measurements outside the ends and corners of several longwall panels in the Newcastle Coalfield (Newstan and West Wallsend Collieries), have been plotted against distance from the panel goaf edge / cover depth at the panel; refer to **Figure A45**.

Curves of best fit have been fitted to identify data trends from various locations from the ends and corners of the panels (note: the movements outside the corners of a longwall are typically smaller than the panel ends). The data has been obtained using GPS / EDM traverse techniques with quoted accuracy limits of +/- 7 to 10 mm.

The data in **Figure A45** has also been normalised to maximum measured subsidence (S_{max}) above a given panel and is presented in **Figure A46**. It is considered that presenting the data in this format allows all of the available data to be used appropriately to make subsequent FFD predictions.

The data presented in **Figures A47** was measured from the sides of several longwall panels using in-line, steel tape measurements. This method is considered more accurate than the EDM techniques, however, they do not capture all of the displacement. The measured values have subsequently been adjusted to absolute movements, based on the EDM measurements presented in **Figures A45** and **A46**.

A combined graph of normalised total displacement data from the ends and sides of the longwall panels is presented in **Figure A48** with worst-case design curves from ends, corners and sides of a longwall panel for flat terrain conditions.

The empirical models may be used for calibrating the numerical models input parameters when proposed mining layouts and topographical conditions are considered to be well outside the available database (see **DgS, 2007**).

A12.3 Numerical Far-Field Displacement Modelling

The numerical modelling program Map-3D® has been applied at several mines in the Newcastle Coalfield to-date for the purposes of estimating FFD movements. The model was chosen mainly due to its suitability for modelling large-scale rock masses.

The program is a 3-dimensional elastic, isotropic, boundary-element model, which essentially starts with an infinite solid space and calculates the effects of excavations, geological structure, varying material types, and free-surfaces on the regional stresses and strains. Further details about the software can be found at the Map-3D® web site.

The model is firstly calibrated to measured displacement data for a given mining geometry, regional horizontal stress field and surface topography. The Young's Modulus or stiffness of the overburden is then adjusted above an extracted panel (or panels) and assumed caving zone until a reasonable match is achieved.

Although the empirical models indicate that subsidence is a key parameter for predicting FFDs, numerical modelling of horizontal stress relief effects does not require the subsidence above the panels to be matched (by the model) because the extraction of coal and subsequent goafing behaviour can be calibrated to measured far-field displacements instead. Therefore, the modelling outcomes are not linked to the modelled subsidence directly.

Non-linearity can be introduced into the model to analyse the effects of fault planes and bedding using displacement-discontinuity elements with normal and shear stiffness and Mohr-Coulomb friction and cohesive strength properties.

Multiple mining stages and irregular topography can also be defined to enable mechanistic extrapolation of existing empirical databases with a reasonable degree of confidence.

An example of a predicted far-field displacement pattern around a high extraction pillar panel mine is presented in **Figure A49**.

A12.5 Empirical Strain Prediction Model

Strain measurements from the side of several longwall panels from West Wallsend and Newstan Collieries and were also normalised to maximum panel subsidence. The data are presented in **Figure A50**.

Several curves are shown with the data in the above figure, one is the best-fit or mean curve and two are upper limit confidence limit curves for the data (U95%CL and U99%CL). The confidence limit curves have been defined using weighted non-linear statistical techniques and the residual errors about the mean curve.

A13 References

ACARP, 1998a. **Chain Pillar Design (Calibration of ALPS)**. ACARP Project No. C6036, Colwell, M. Colwell Geotechnical Services.

ACARP, 1998b, **Project No. C5024, Establishing the Strength of Rectangular and Irregular Pillars**. J.M.Galvin, B.K. Hebblewhite, M.D.G. Salamon and B.B.Lin. School of Mining, UNSW.

ACARP, 2003. **Review of Industry Subsidence Data in Relation to the Impact of Significant Variations in Overburden Lithology and Initial Assessment of Sub-Surface Fracturing on Groundwater**. ACARP Project No. C10023. S. Ditton and R. Frith, Strata Engineering Report No. 00-181-ACR/1.

ACARP, 2006. **Techniques to Predict and Measure Subsidence & its Impacts on the Groundwater Regime above Shallow Longwalls**. ACARP Project No. C23920 Report by Seedsman Geotechnics Pty Ltd and Geoterra Pty Ltd (March).

ACARP, 2007. **Hydrological Response to Longwall Mining**. CSIRO Exploration & Mining. H. Guo, D. Adhikary, D. Gaveva. Report No. C14033 (October).

Bulli Seam PAC, 2010. **Bulli Seam Operations Review Report**. NSW Government Planning Assessment Commission (10 July).

Colwell,1993. **Water Inflow Investigation for a Longwall Operation**. M. Colwell. Published in Queensland Coal Geology Groups Conference Proceedings, New Developments in Coal Geology, Brisbane.

Diedrichs and Kaiser, 1999. **Stability of Large Excavations in Laminated Hard Rock Masses: the Voussoir Analogue Revisited**. M.S. Diedrichs and P.K. Kaiser. International Journal of Rock Mechanics and Mining Sciences 36.

DgS, 2007. **Prediction of Far-Field Displacements Due to Pillar Extraction or Longwall Mining in Mountainous Terrain**. S. Ditton. Proceedings of the 7th Triennial MSTS Conference on Mine Subsidence, University of Wollongong (November 26-27)

DMR, 1987. **Mining Subsidence in NSW: 2. Surface Subsidence Prediction in the Newcastle Coalfield**. L. Holla. Department of Minerals Resources (June).

Enever, 1999. **Near Surface In-situ Stress and its Counterpart at Depth in the Sydney Metropolitan Area**. Enever, J.R. Published in Australian Geomechanics Society (AGS) Conference Proceedings of the 8th Annual Conference on Geomechanics, Hobart.

Fell *et al*, 1992. **Geotechnical Engineering of Embankment Dams**. Fell, R., MacGregor, P. and Stapledon, D.A.A. Balkema.

Forster and Enever, 1992. **Hydrogeological Response of Overburden Strata to Underground Mining, Central Coast, NSW**. I.R. Forster (Pacific Power) and J. Enever (CSIRO).

Forster, 1995. **Impact of Underground Coal Mining on the Hydrogeological Regime, Central Coast, NSW**. I.R. Forster. Published in Australian Geomechanics Society (AGS) Conference Proceedings (February), Engineering Geology of Newcastle – Gosford Region, University of Newcastle.

Frith, 2006. **Geotechnical Assessment of Overburden Fracturing Related to the Bulli Seam Extraction along the Line of the Proposed Endeavour Drift**. Frith Consulting Pty Ltd. Internal Report to BHP Billiton (October).

Holla, 1991. **Some Aspects of Strata Movement relating to Mining Under Water Bodies in NSW, Australia**. L. Holla. Published proceedings of 4th Int. Water Congress, Ljubljana, Slovenia, Yugoslavia (September).

Holla and Barclay, 2000. **Mine Subsidence in the Southern Coalfield**. L.Holla and E.Barclay. Department of Minerals Resources (June).

Karmis, et al, 1987. **Surface Deformation Characteristics Above Undermined Areas: Experiences from the Eastern United States Coalfields**. M. Karmis, A. Jarosz, P. Schilizzi & Z. Agioutantis. Published in Civil Engineering Transactions Journal, Institution of Engineers, Australia.

Kendorski, F.S., 1993. **Effect of High Extraction Coal Mining on Surface and Ground Water**. Proceedings of the 12th Conference on Ground Control in Mining, Morgantown, WV.

Li and Cairns, 2000. **Strata control experiences in longwall mining over old mine workings**. Li, G. and Cairns, R. AJM 3rd Annual Longwall Mining Summit, Yeppoon.

Lohe and Dean-Jones, 1995. **Structural Geology of the Newcastle-Gosford Region**. E.M. Lohe and G.L. Dean-Jones. Published in Australian Geomechanics Society (AGS) Conference Proceedings (February), Engineering Geology of Newcastle - Gosford Region, University of Newcastle.

McQueen, 2004. **In-situ Rock Stress and Its Effect in Tunnels and Deep Excavations in Sydney**. McQueen. L.B. Article presented in Australian Geomechnics Journal Vol 39. No. 3 (September).

MSEC, 2011. **Review of Under Surface and Groundwater Resources at Shallow Depths of Cover for the Proposed LWs 41 to 50, West Wallsend Colliery**. MSEC Report No. 519 (Rev A) - August.

Nemcik et al, 2005. **Statistical Analysis of Underground Stress Measurements in Australian Coal Mines**. Nemcik, J., Gale, W. and Mills, K. Published in proceedings of the Bowen Basin Geology Symposium.

Pells, 2002. **Developments in the Design of Tunnels and Caverns in the Triassic Rocks of the Sydney Region**. International Journal of Rock Mechanics and Mining Sciences No. 39. Pells, P.J.N.

Pells, 2004. **Substance and Mass Properties for the Design of Engineering Structures in the Hawkesbury Sandstone**. Article presented in Australian Geomechnics Journal Vol 39. No. 3 (September).

Peng and Chiang, 1984. **Longwall Mining**. S.S. Peng & H.S. Chiang. Wiley.

RCA, 2013. **End of Panel Longwall 41, Surface Subsidence Mapping Report, West Wallsend Colliery**. Robert Carr and Associates Pty Ltd. *Report Pending*.

Reynolds, 1977. **Coal Mining Under Stored Water**. Report on an Inquiry into Coal Mining Under or in the Vicinity of Stored Waters of the Nepean, Avon, Cordeaux, Cataract and Woronora Reservoirs, NSW for the NSW Government.

SCT, 2001. **Geotechnical Assessment for the Dendrobium Project**. SCT Operations Pty Ltd Report No. DEN1950 (5th June).

SCT, 2008. **Assessment of Longwall Panel Widths and Potential Hydraulic Connection to Bowmans Creek – Ashton Mine**. SCT Operations Pty Ltd Report to Ashton Coal, September.

Seedsman, 2010. **Calibrated Parameters for the Prediction of Subsidence at Mandalong Mine**. R.W. Seedsman. Coal Operators' Conference, University of Wollongong (February).

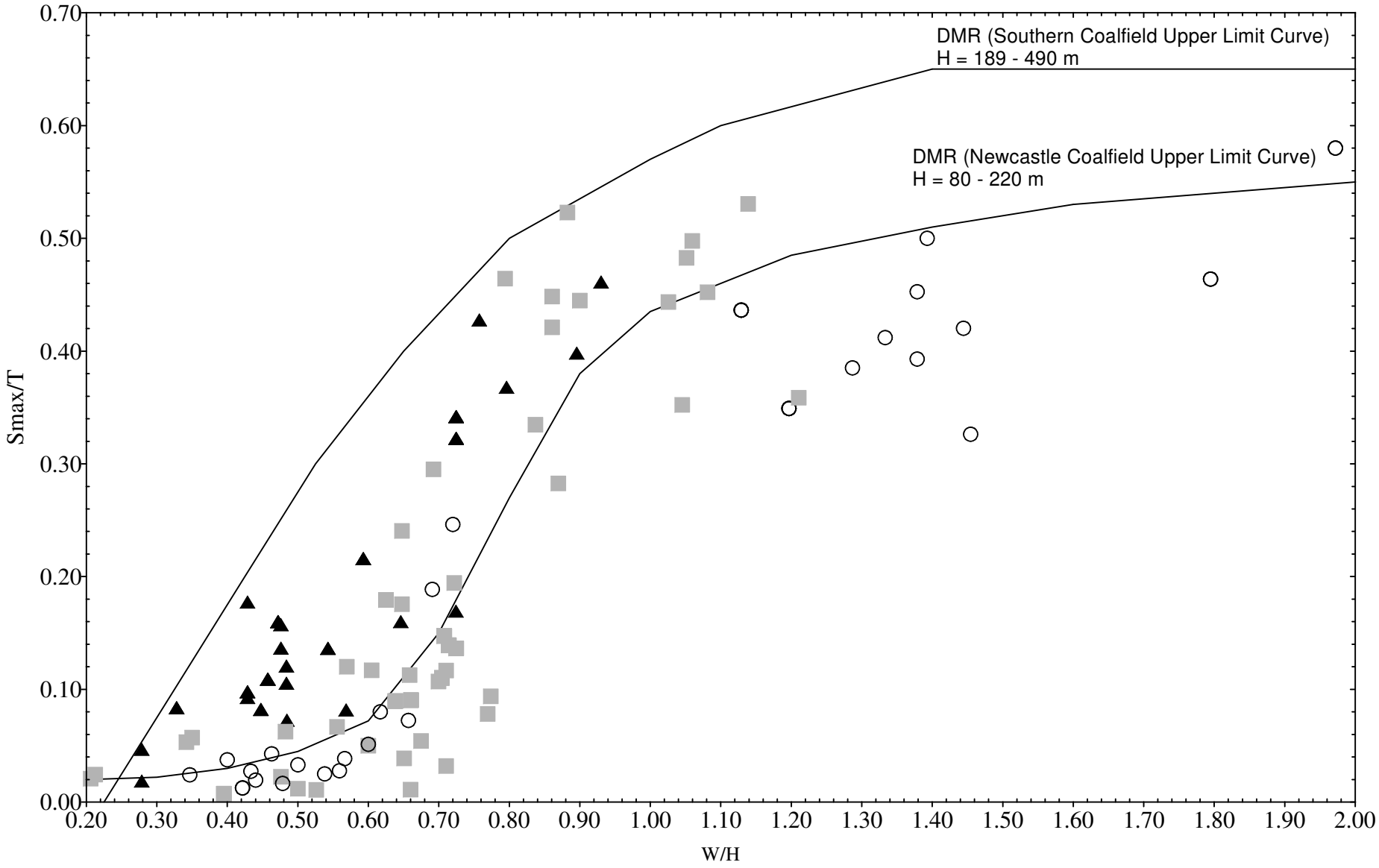
Singh and Kendorski, 1981. **Strata Disturbance Prediction for Mining Beneath Surface Water and Waste Empoundments**. M.M. Singh and F.S Kendorski. First Conference in Ground Control in Mining, West Virginia University, 76-89.

Tammetta, 2013. **Estimation of the Height of Complete Groundwater Drainage Above Mined Longwall Panels**. Paul Tammetta. Paper published in Groundwater Journal (Vol 51, No. 5, Sep-Oct 2013).

Walker, 2004. **Stress Relief on Hillsides and Hillside Excavations**. Walker, B.F. Article presented in Australian Geomechnics Journal Vol 39. No. 3 (September).

Wardell, 1975. **Mining Under Tidal Waters**. Wardell and Partners Report prepared for NSW Government.

Whittaker & Reddish, 1989. **Subsidence, Occurrence, Prediction and Control**. B. N. Whittaker and D.J. Reddish. Department of Mining Engineering, University of Nottingham, UK.



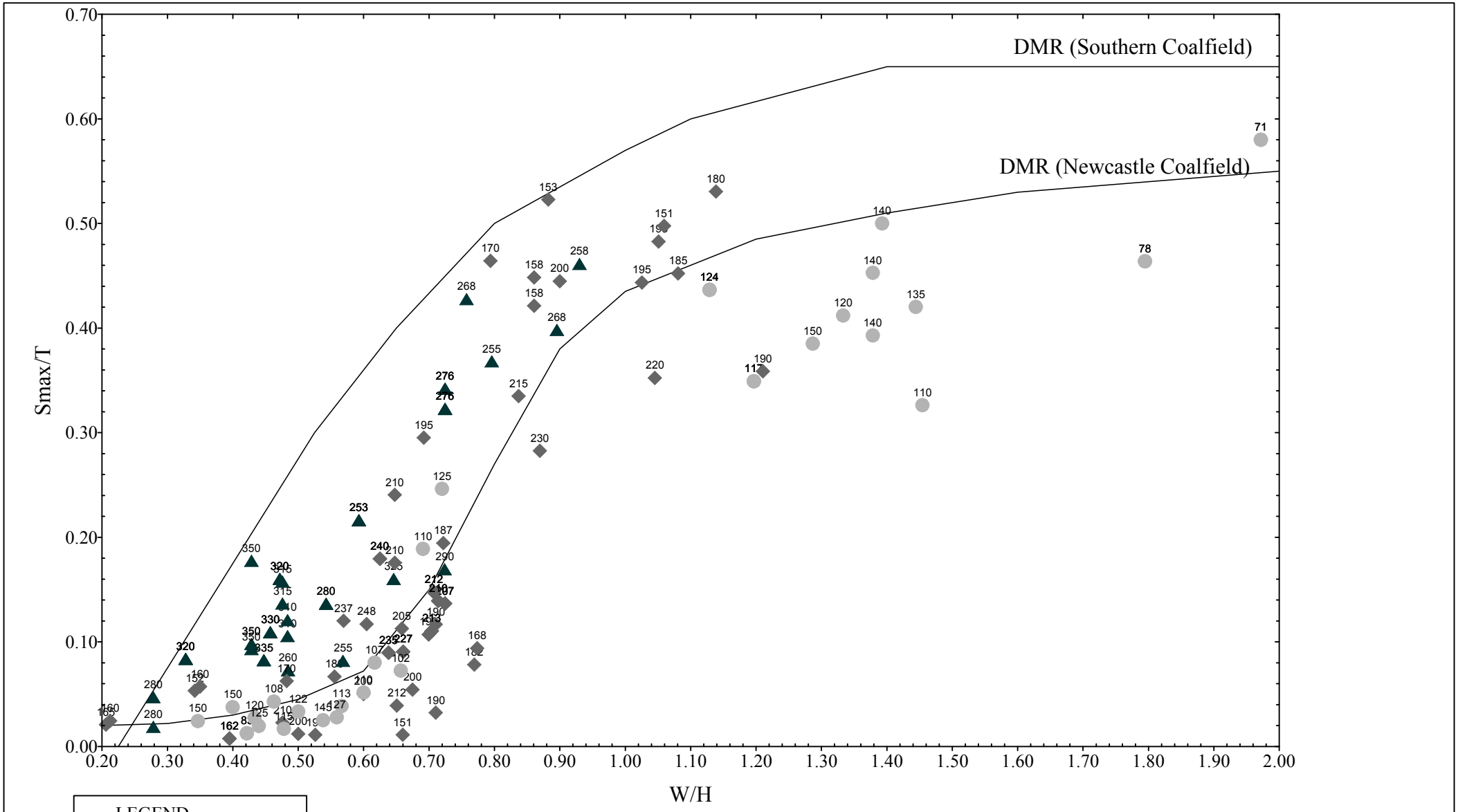
LEGEND
Cover Depth, H (m)
- ○ H = 70m to H = 151m
- ■ H = 151m to H = 251m
- ▲ H = 251m to H = 350m

DgS

Ditton Geotechnical Services Pty Ltd

Engineer:	S.Ditton
Drawn:	S.Ditton
Date:	08.06.08

Client:	Adapted from ACARP, 2003
Title:	Project Database and DMR Subsidence Prediction Curves for Single Longwall Panels in Newcastle Coalfield
Scale:	NTS
Figure No:	A1



LEGEND
Data Point
Cover Depth, H (m)

- H = 70m to H = 151m
- H = 151m to H = 251m
- H = 251m to H = 350m

DgS

Ditton Geotechnical Services Pty Ltd

Engineer:	S.Ditton
Drawn:	S.Ditton
Date:	08.06.08

Client:	Adapted from ACARP, 2003		
Title:	Project Database for Single Longwall Panels in Newcastle Coalfield showing Cover Depth for Each Point		
Scale:	NTS	Figure No:	A2.1

Continuous or clamped elastic beam in overburden with horizontal stress.

Simply supported beam analogy for cracked beam analysis

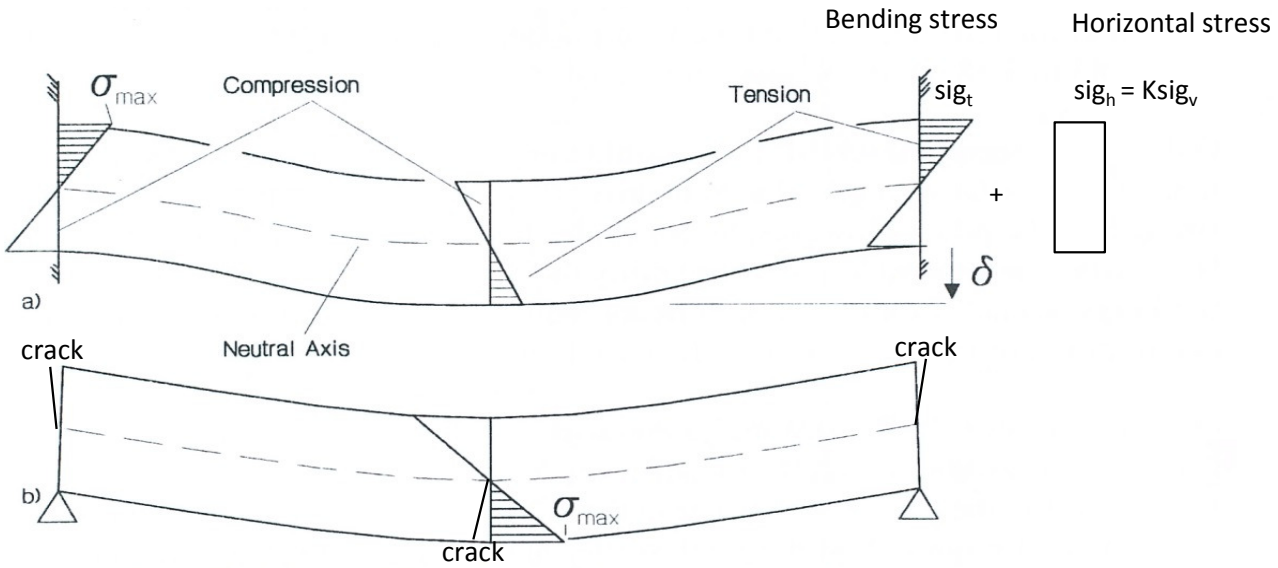


Fig. 4. Elastic beam with (a) fixed ends and (b) simple (pin) supports.

Note: Elastic beam cracks if $sig_t + sig_h > 0$, where tensile stress is positive.

Ref: Diedrichs & Kaiser, 1999

DgS	Engineer:	S.Ditton	Client:	Adapted from ACARP, 2003	
	Drawn:	S.Ditton			
	Date:	03.06.13	Title:	Internal Compressive Stress Arch Geometry	
	Ditton Geotechnical Services Pty Ltd		Scale:	NTS	Figure No: A2.2

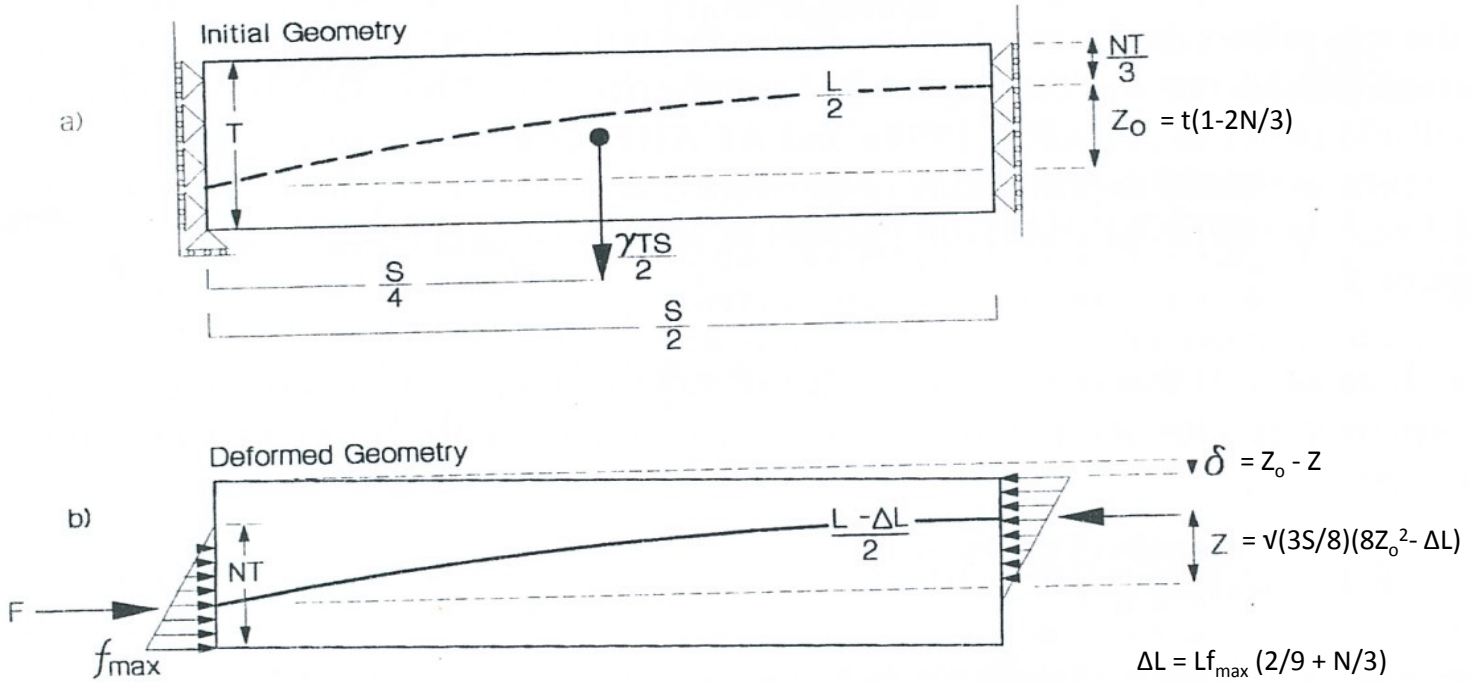
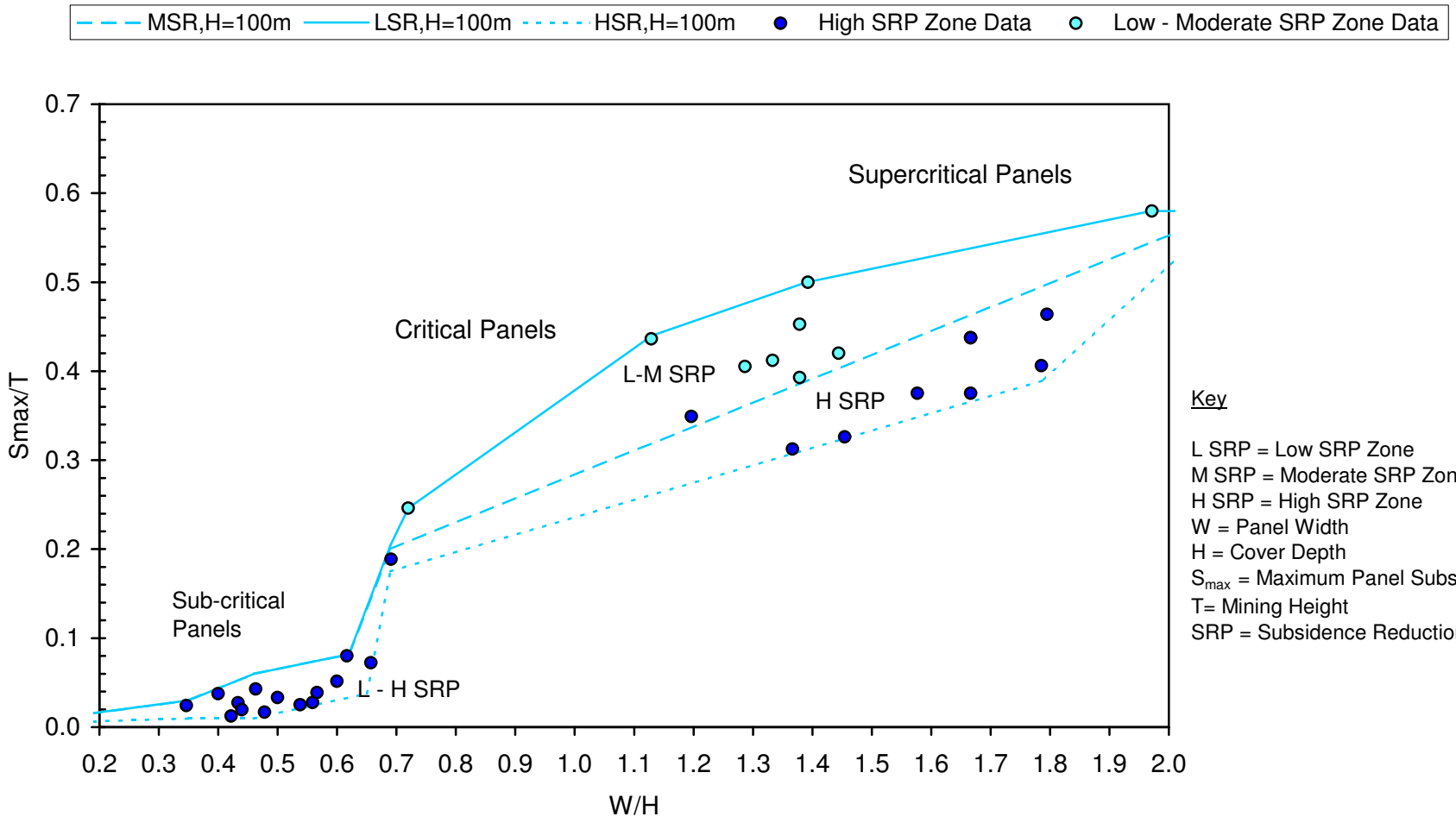


Fig. 5. Voussoir beam (half-span shown) and nomenclature.

Ref: Diedrichs & Kaiser, 1999

DgS	Engineer: S.Ditton	Client:	Adapted from ACARP, 2003		
	Drawn: S.Ditton				
	Date: 03.06.13	Title:	Internal Compressive Stress Arch Development in Simply Supported Beam (i.e. Voussoir Beam Analogy)		
	Ditton Geotechnical Services Pty Ltd	Scale:	NTS	Figure No:	A2.3

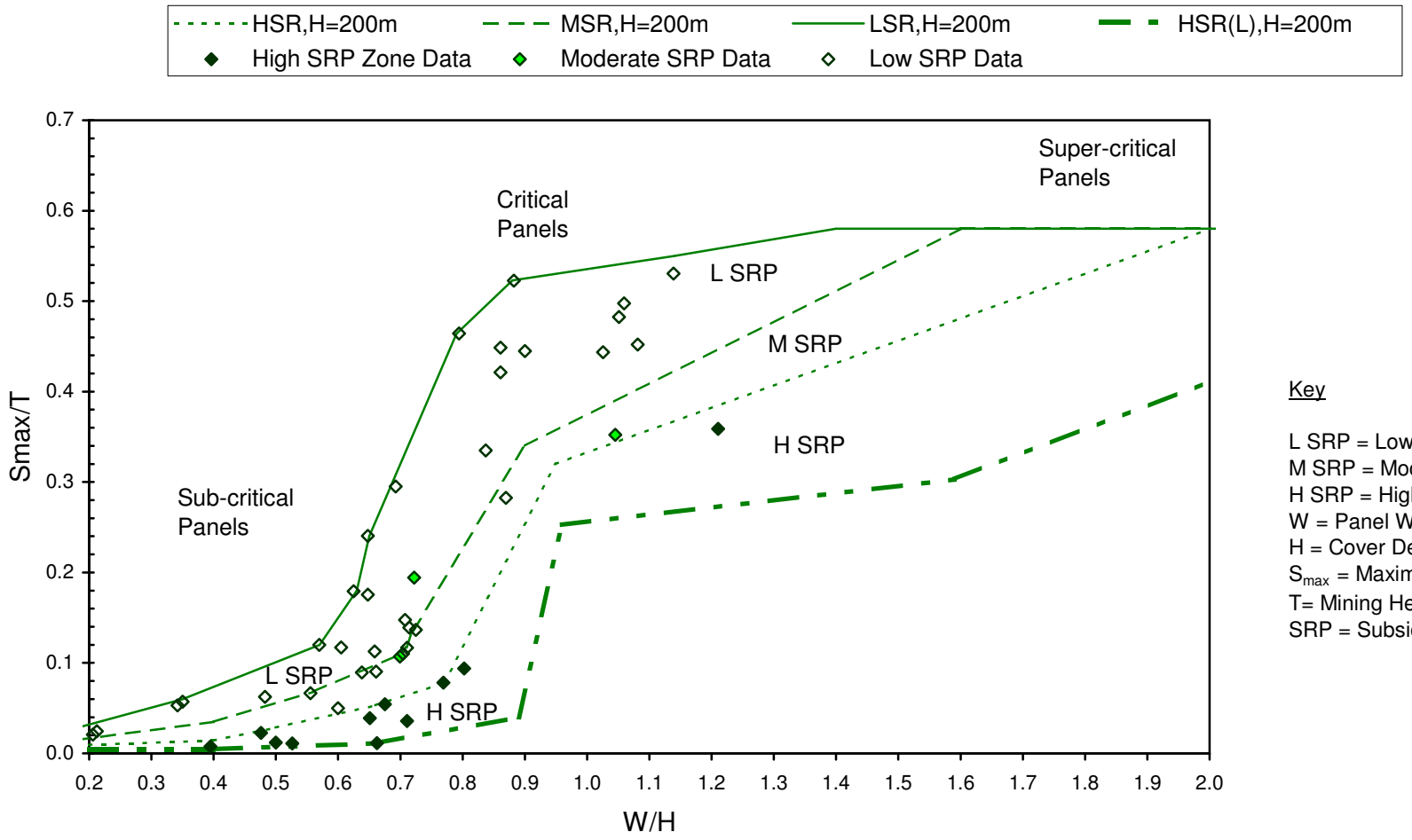


Key

L SRP = Low SRP Zone
M SRP = Moderate SRP Zone
H SRP = High SRP Zone
W = Panel Width
H = Cover Depth
S_{max} = Maximum Panel Subsidence
T= Mining Height
SRP = Subsidence Reduction Potential

Note: No SRP distinguishment for panels with W/H<0.65

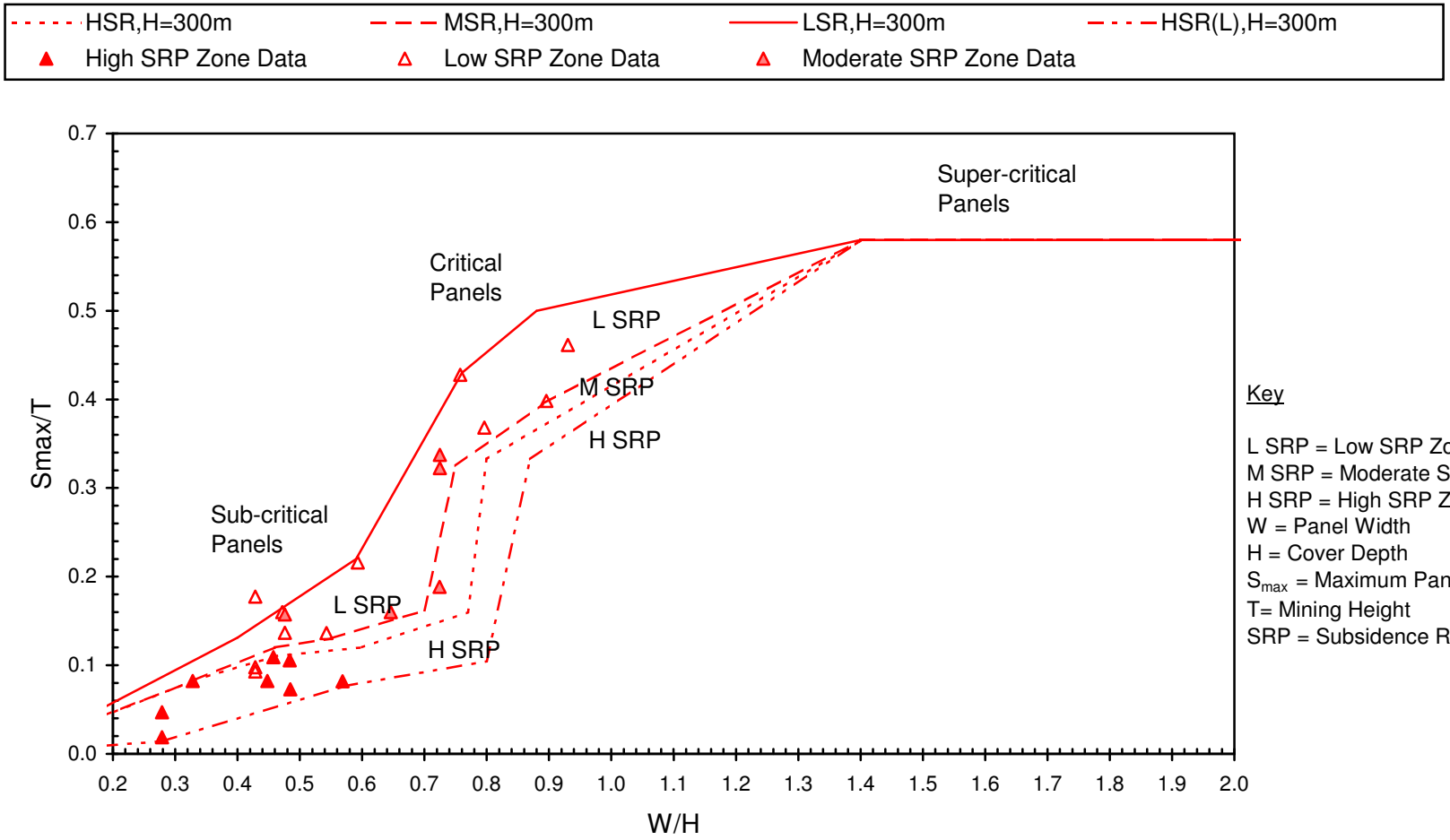
DgS	Engineer: S.Ditton	Client:	Adapted from ACARP, 2003
	Drawn: S.Ditton		
	Date: 08.08.08	Title:	Empirical Model for Predicting Subsidence Above Panels with Cover Depths Between 50 and 150 m and Low to High SRP Zones
	Ditton Geotechnical Services Pty Ltd	Scale:	NTS — Figure No: A3



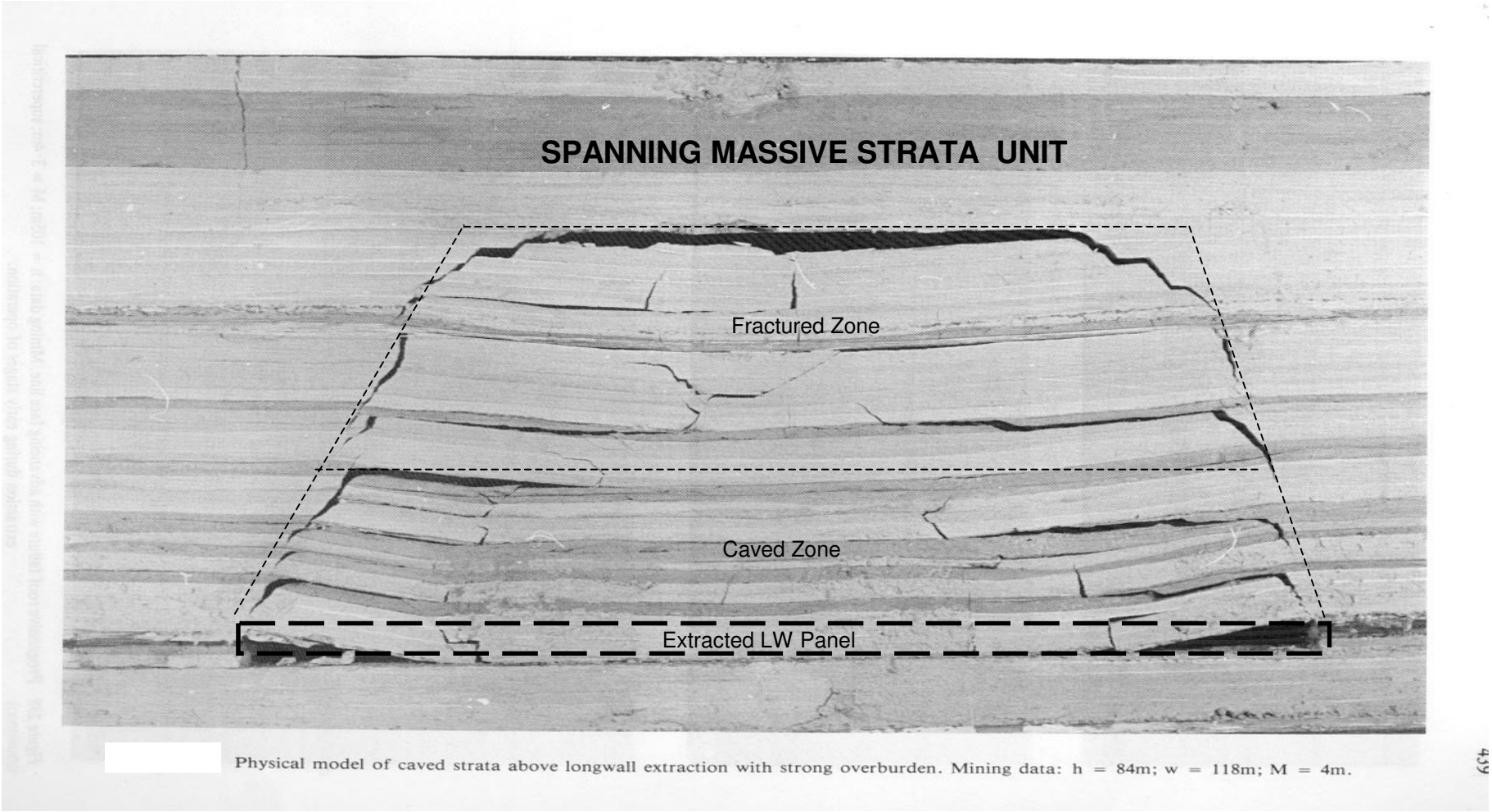
Key

L SRP = Low SRP Zone
M SRP = Moderate SRP Zone
H SRP = High SRP Zone
W = Panel Width
H = Cover Depth
S_{max} = Maximum Panel Subsidence
T= Mining Height
SRP = Subsidence Reduction Potential

DgS	Engineer:	S.Ditton	Client:	Adapted from ACARP, 2003	
	Drawn:	S.Ditton			
	Date:	08.08.08	Title:	Empirical Model for Predicting Subsidence Above Panels with Cover Depths Between 250 and 350 m and Low to High SRP Zones	
	Ditton Geotechnical Services Pty Ltd		Scale:	NTS	Figure No: A4



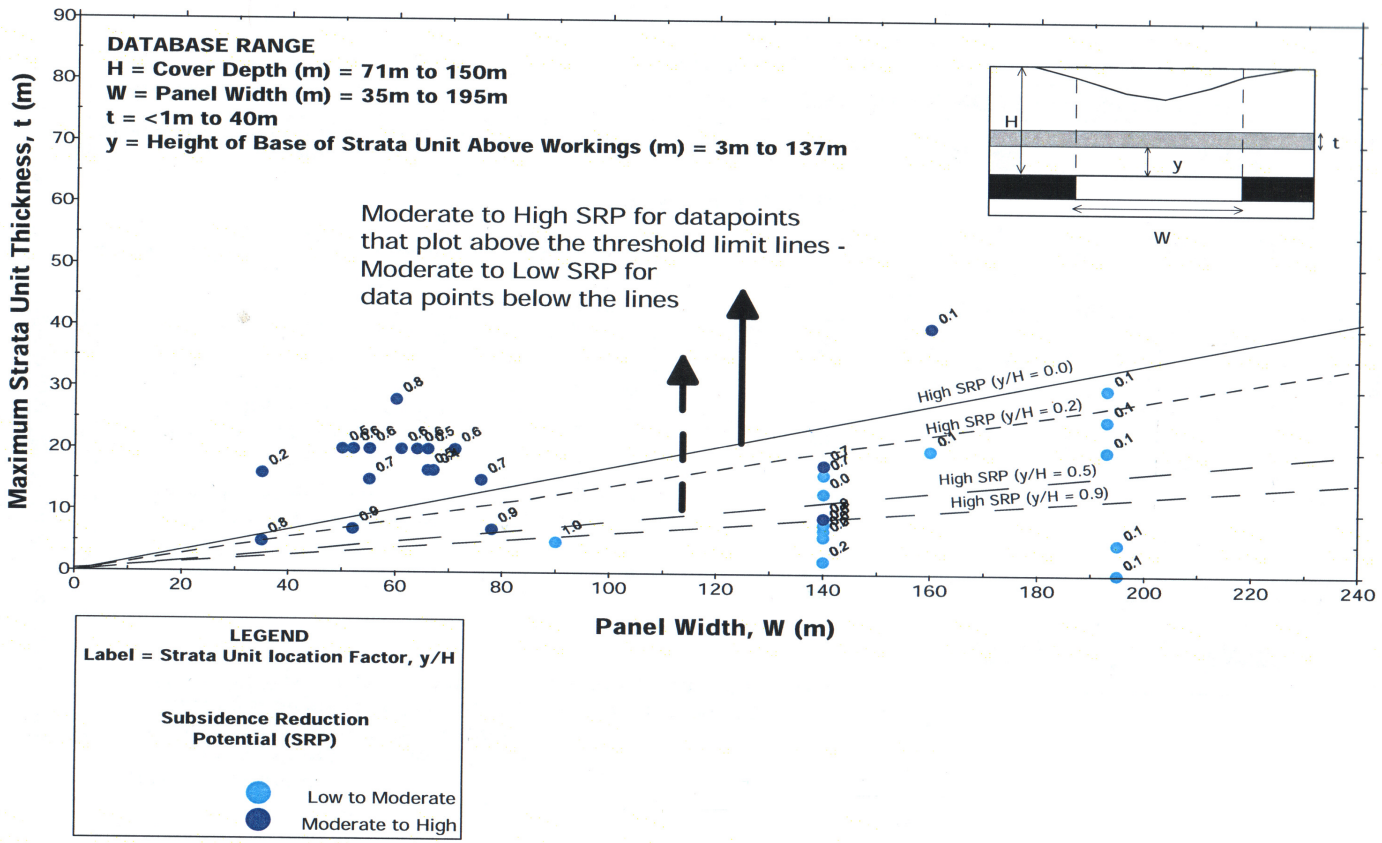
DgS	Engineer:	S.Ditton	Client:	Adapted from ACARP, 2003	
	Drawn:	S.Ditton			
	Date:	08.08.08	Title:	Empirical Model for Predicting Subsidence Above Panels with Cover Depths Between 250 and 350 m and Low to High SRP Zones	
	Ditton Geotechnical Services Pty Ltd		Scale:	NTS	Figure No: A5



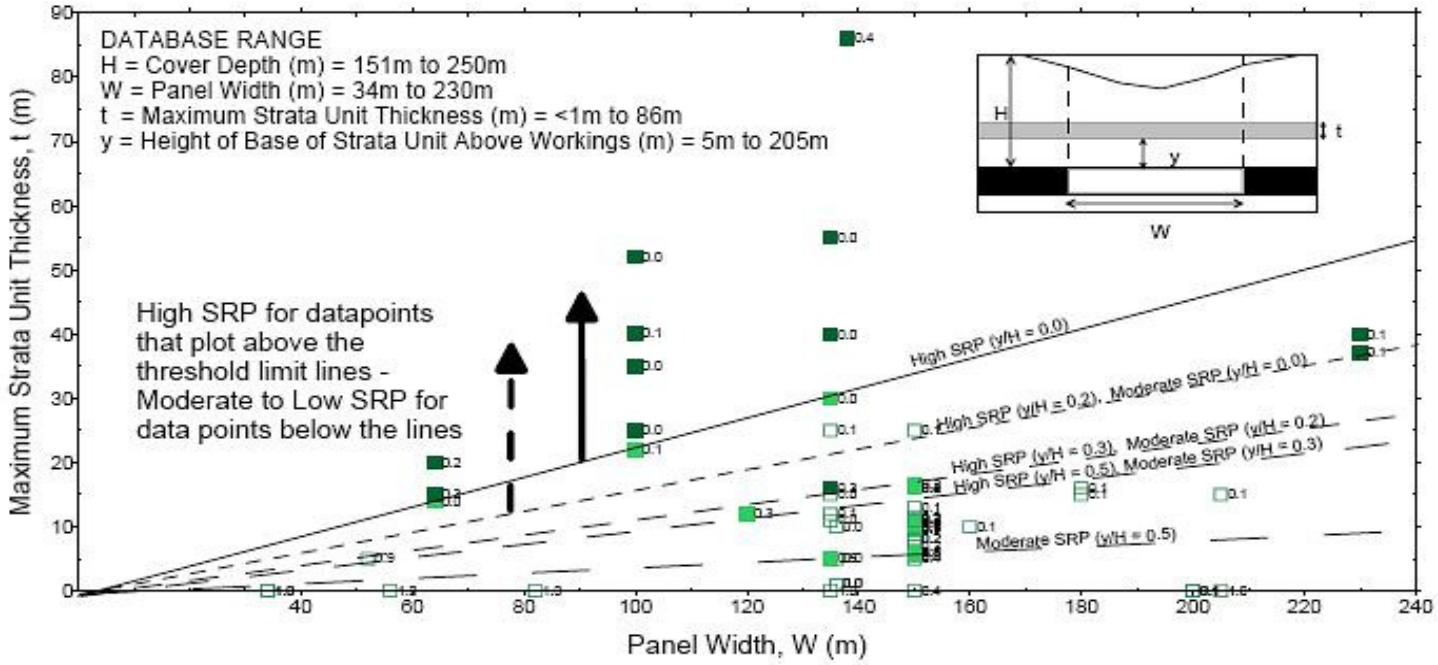
Physical model of caved strata above longwall extraction with strong overburden. Mining data: h = 84m; w = 118m; M = 4m.

439

DgS	Engineer:	S.Ditton	Client:	Adapted from ACARP, 2003	
	Drawn:	S.Ditton			
	Date:	08.08.08	Title:	Physical Overburden Model Showing the Subsidence Reducing Effect of a Massive Strata Unit At the Surface	
	Ditton Geotechnical Services Pty Ltd		Scale:	NTS	Figure No: A6

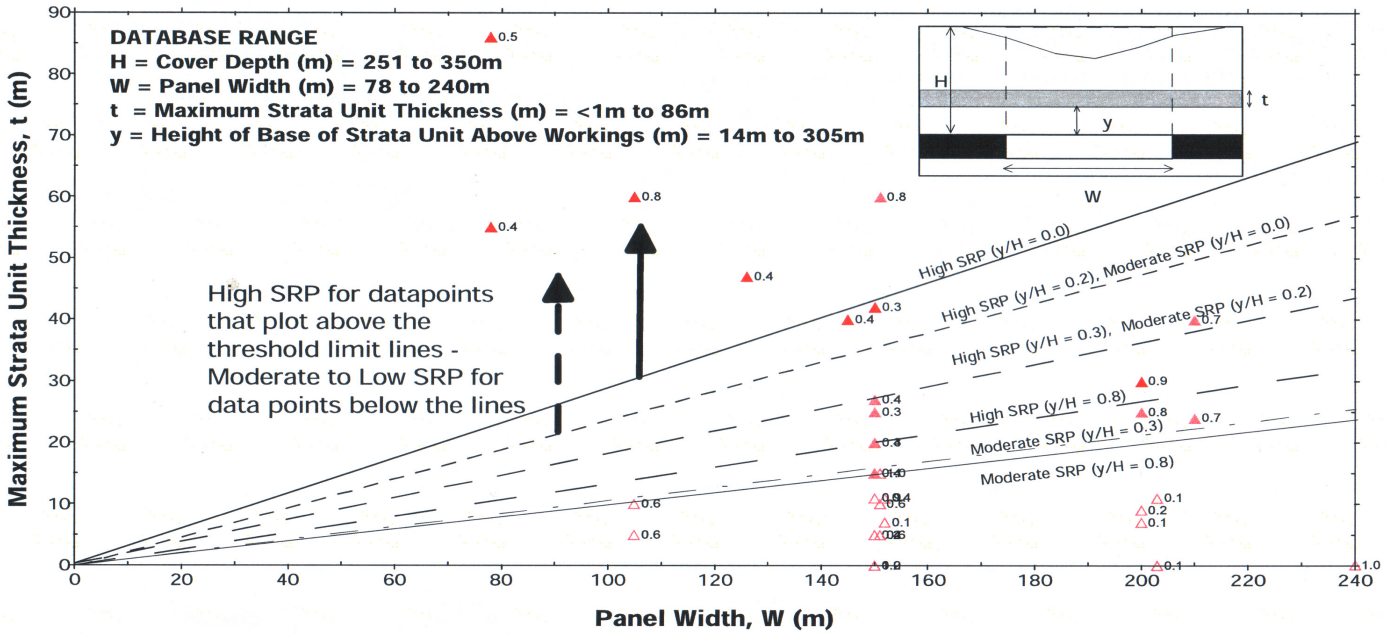


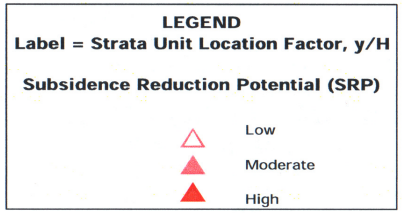
DgS	Engineer:	S.Ditton	Client:	Extract from ACARP, 2003	
	Drawn:	S.Ditton			
	Date:	08.08.08	Title:	Project Database of Maximum Strata Unit Thickness and SRP Threshold Limit Lines for H=50 m to 150 m	
	Ditton Geotechnical Services Pty Ltd		Scale:	NTS	Figure No: A7.1



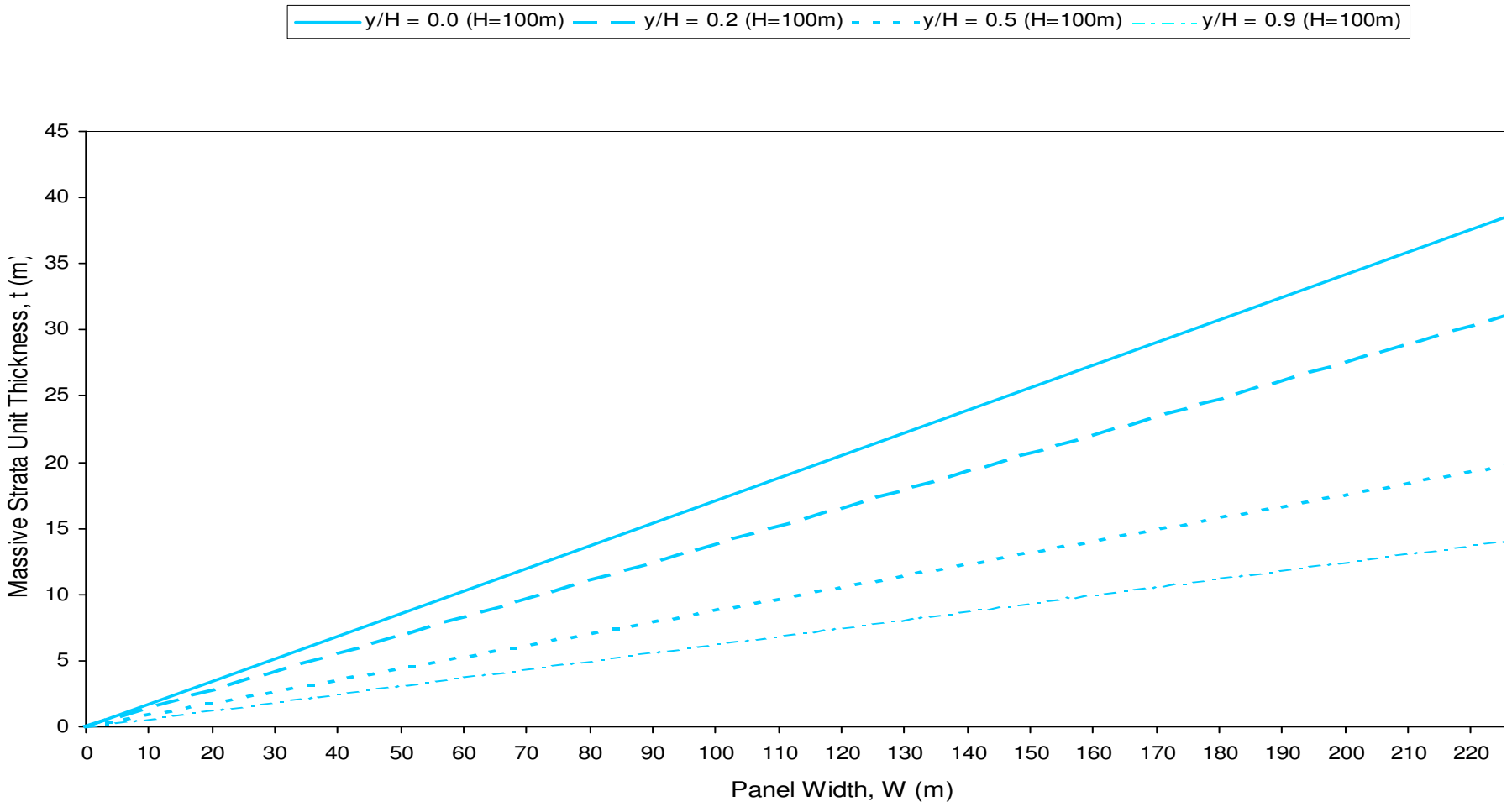


DgS	Engineer:	S.Ditton	Client:	Extract from ACARP, 2003	
	Drawn:	S.Ditton			
	Date:	08.08.08	Title:	Project Database of Maximum Strata Unit Thickness and SRP Threshold Limit Lines for H=150 m to 250 m	
	Ditton Geotechnical Services Pty Ltd		Scale:	NTS	Figure No: A7.2

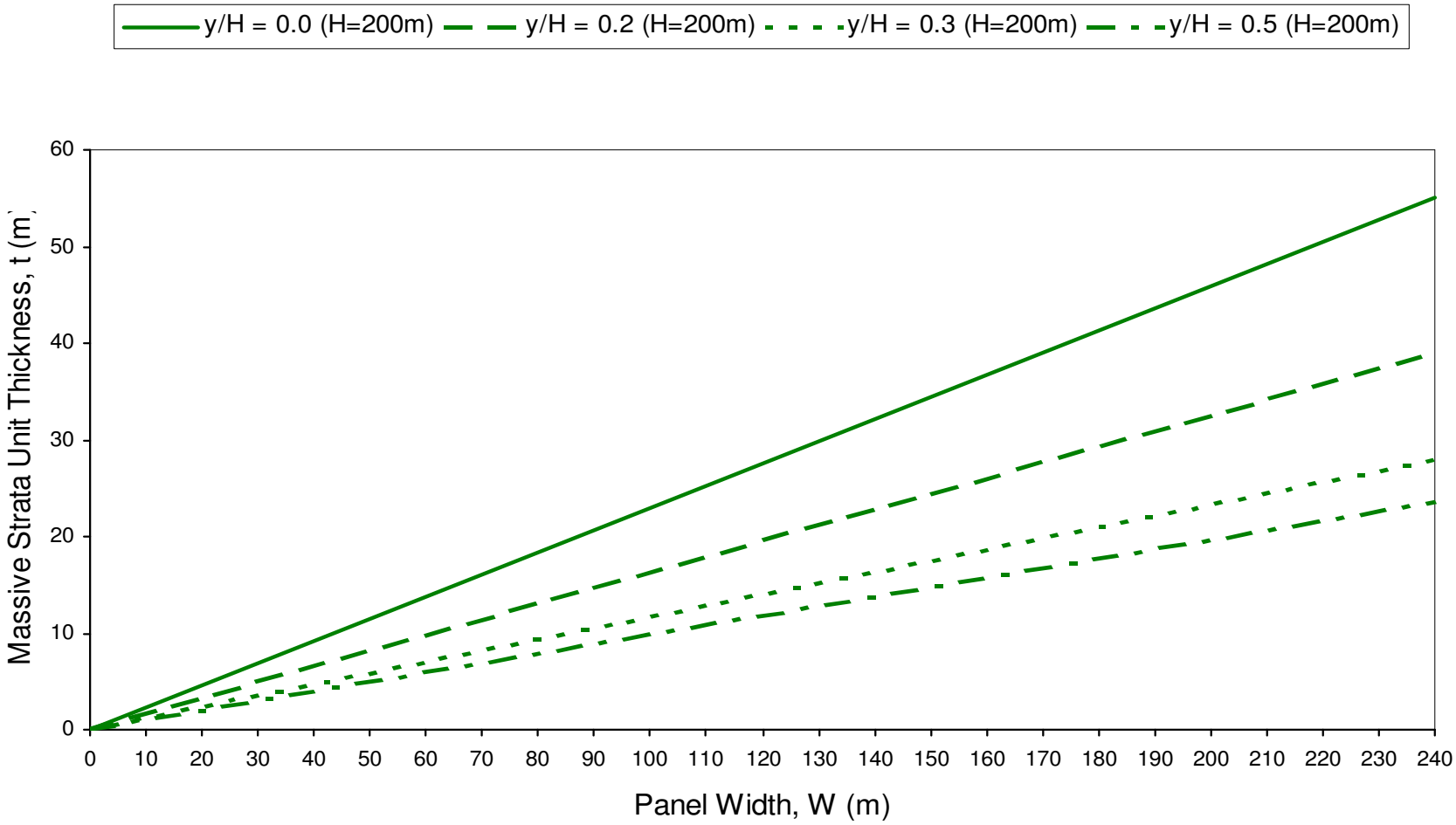




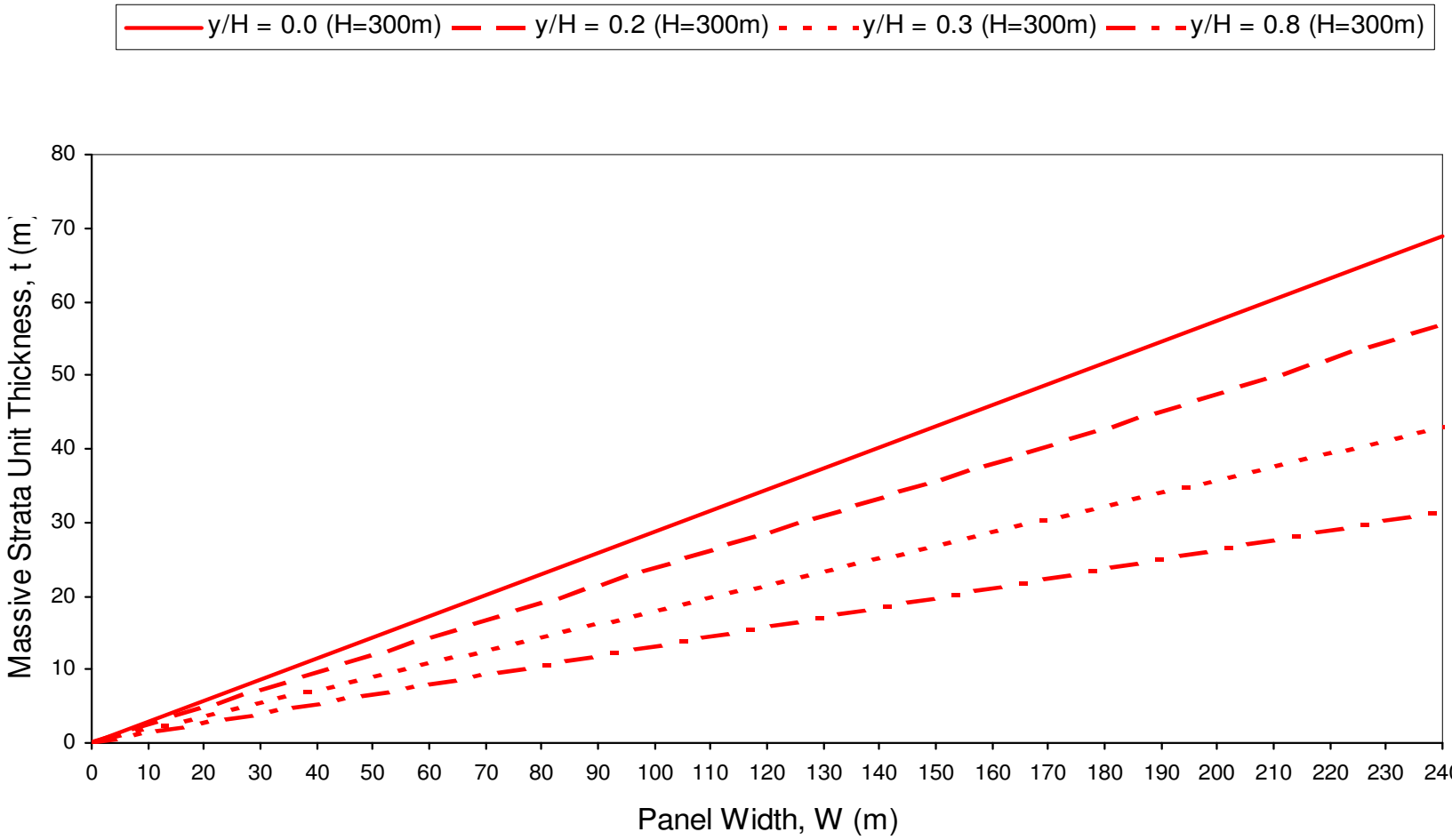
DgS	Engineer:	S.Ditton	Client:	Extract from ACARP, 2003	
	Drawn:	S.Ditton			
	Date:	08.08.08	Title:	Project Database of Maximum Strata Unit Thickness and SRP Threshold Limit Lines for H=250 m to 350 m	
	Ditton Geotechnical Services Pty Ltd		Scale:	NTS	Figure No: A7.3



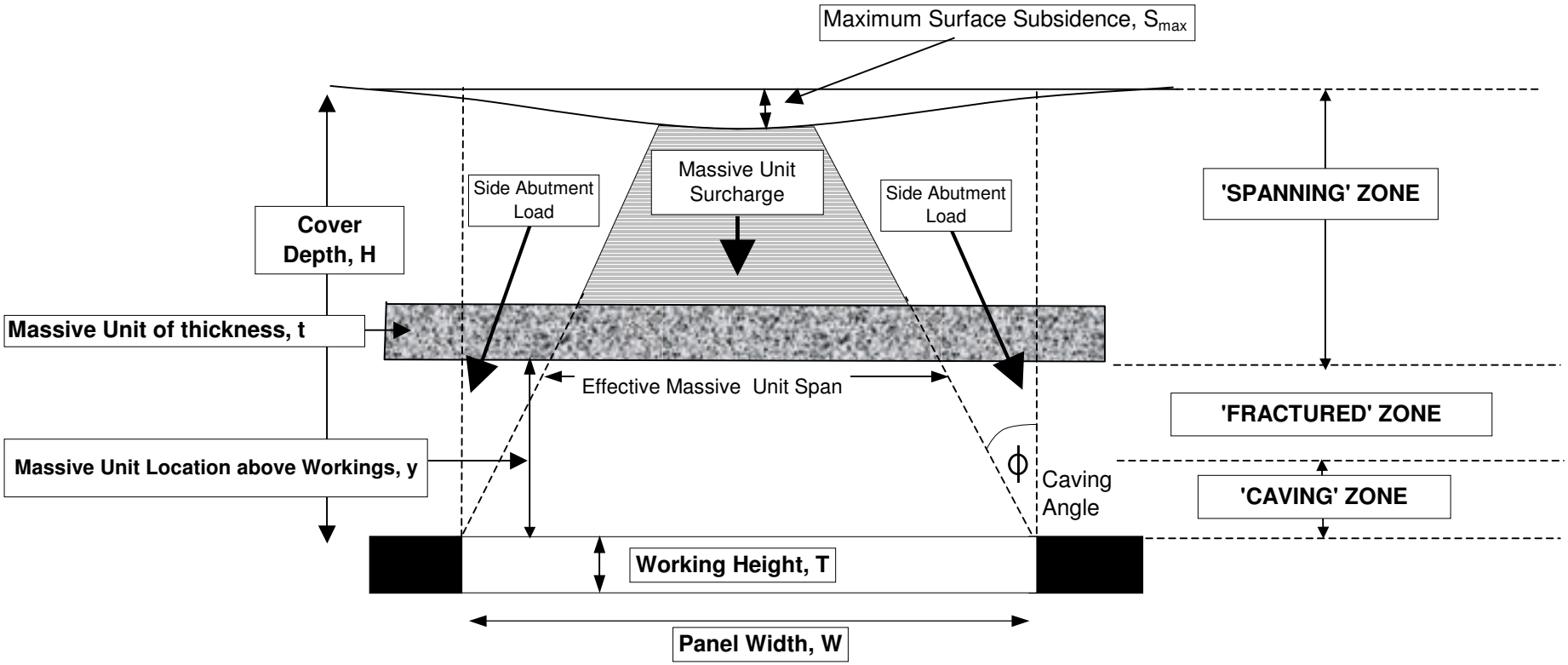
DgS	Engineer:	S.Ditton	Client:	Adapted from ACARP, 2003	
	Drawn:	S.Ditton			
	Date:	08.08.08	Title:	Empirical Model for Predicting Subsidence Reduction Potential Above Panels with Cover Depths Between 50 and 150 m	
	Ditton Geotechnical Services Pty Ltd		Scale:	NTS	Figure No: A8



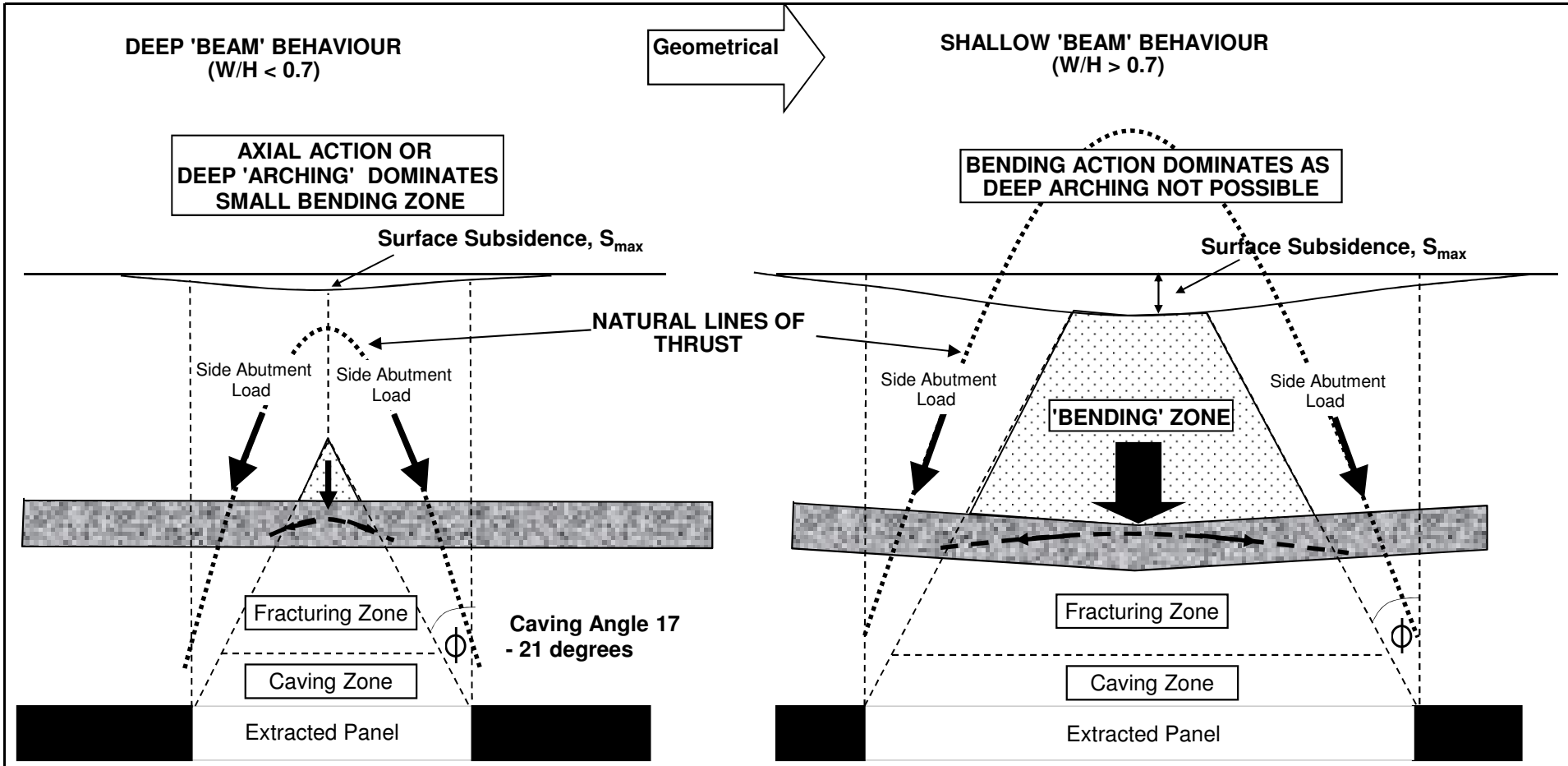
DgS	Engineer:	S.Ditton	Client:	Adapted from ACARP, 2003	
	Drawn:	S.Ditton			
	Date:	08.08.08	Title:	Empirical Model for Predicting Subsidence Reduction Potential Above Panels with Cover Depths Between 150 and 250 m	
	Ditton Geotechnical Services Pty Ltd		Scale:	NTS	Figure No: A9



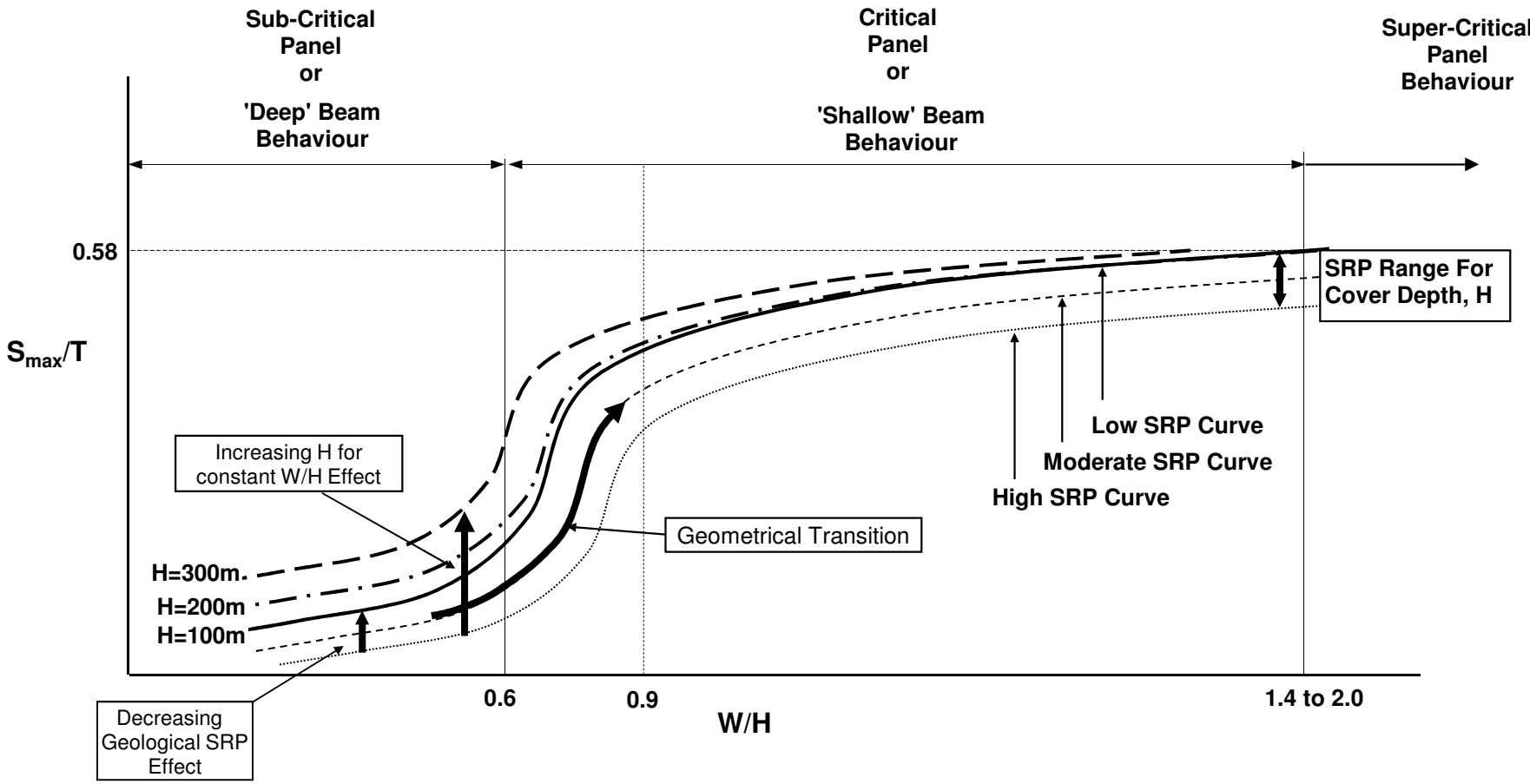
DgS	Engineer:	S.Ditton	Client:	Adapted from ACARP, 2003	
	Drawn:	S.Ditton			
	Date:	08.08.08	Title:	Empirical Model for Predicting Subsidence Reduction Potential Above Panels with Cover Depths Between 250 and 350 m	
	Ditton Geotechnical Services Pty Ltd		Scale:	NTS	Figure No: A10



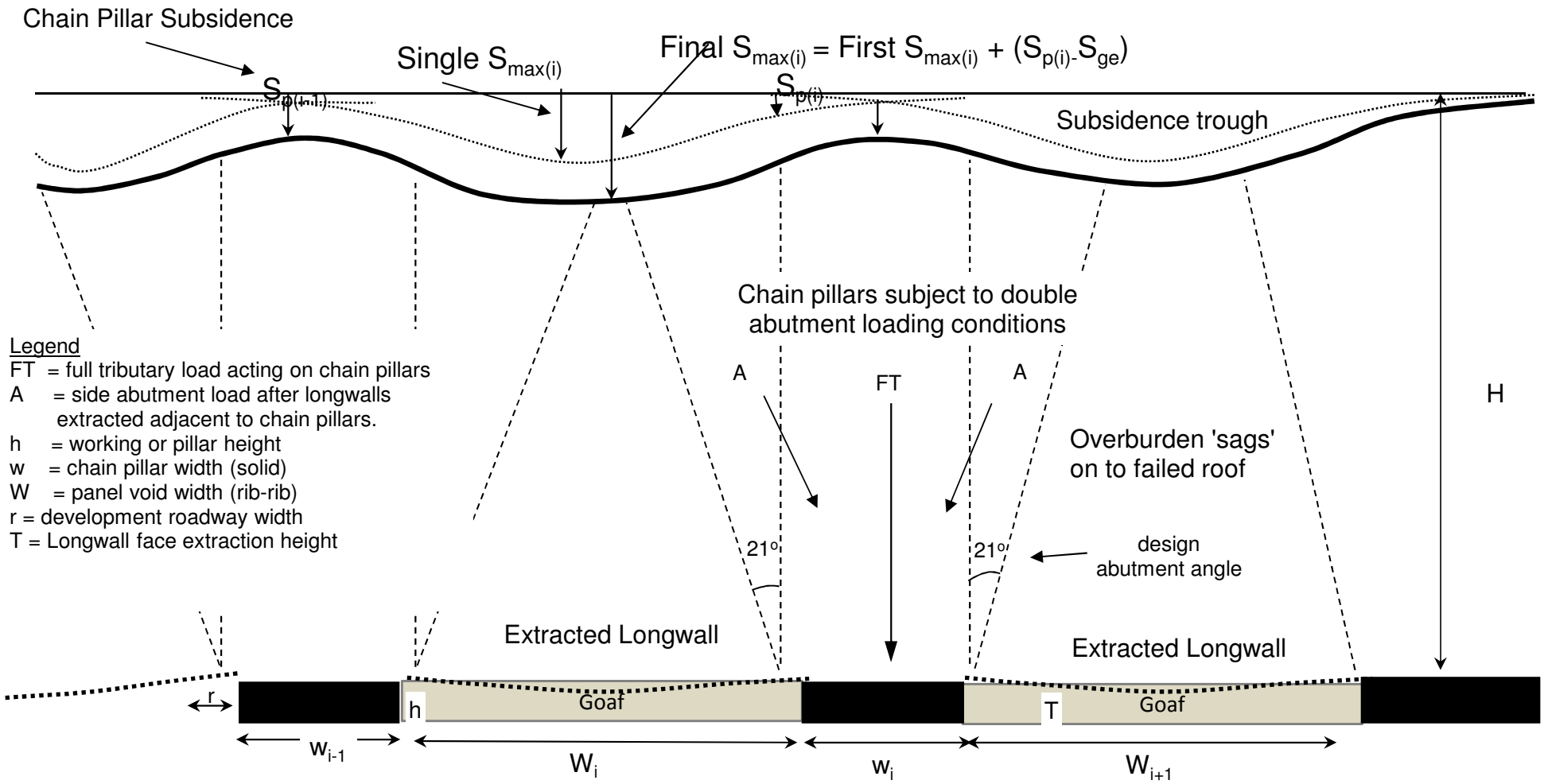
DgS	Engineer:	S.Ditton	Client:	Adapted from ACARP, 2003	
	Drawn:	S.Ditton			
	Date:	08.08.08	Title:	Overburden with Massive Strata Unit Behaviour Concept Model and Key Parameter Definitions	
	Ditton Geotechnical Services Pty Ltd		Scale:	NTS	Figure No: A11



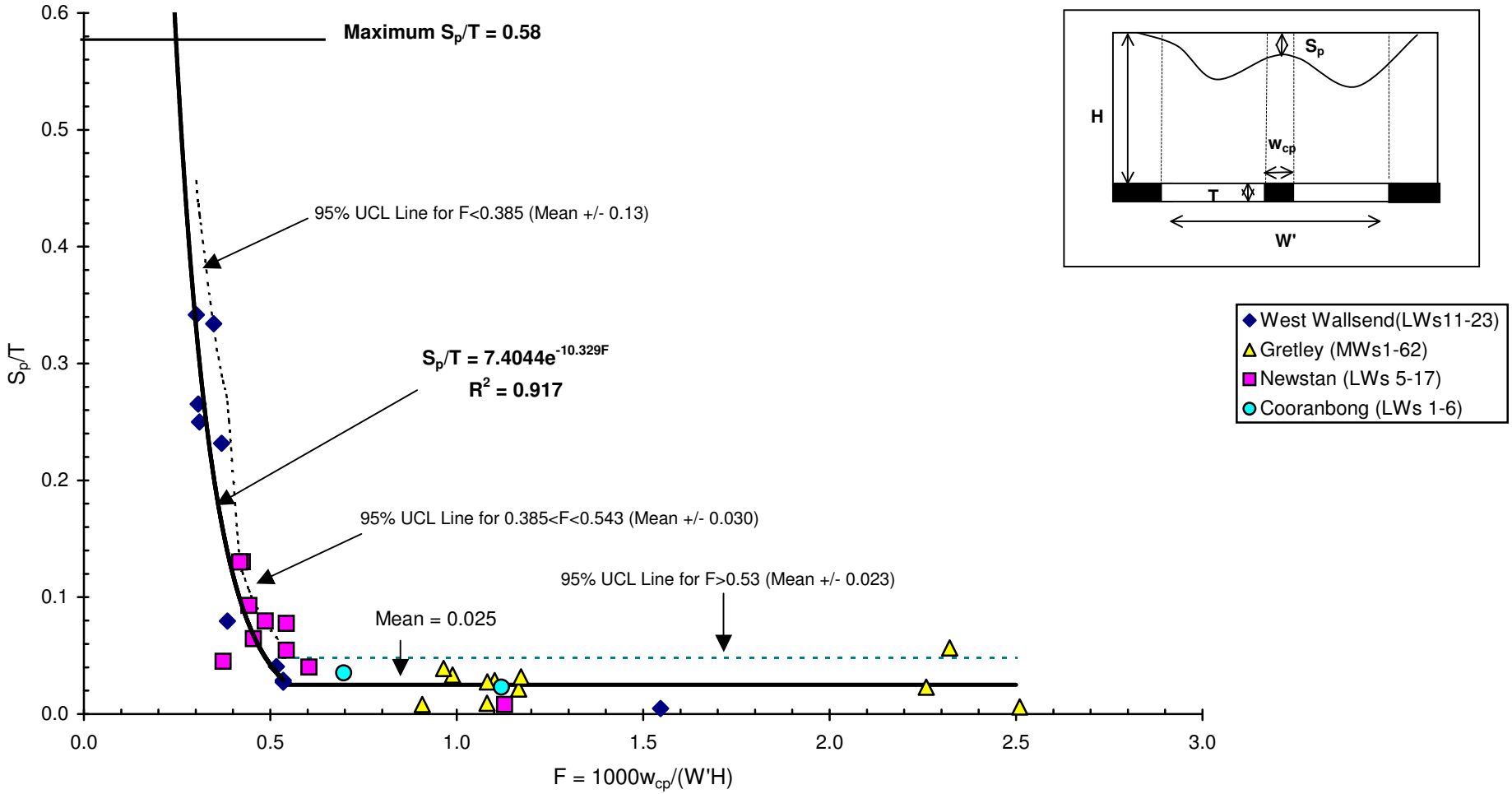
DgS	Engineer:	S.Ditton	Client:	Adapted from ACARP, 2003	
	Drawn:	S.Ditton			
	Date:	08.08.08	Title:	Overburden with Massive Strata Units Behaviour Concept Models of Beam Action Types for Subcritical and Supercritical Longwall Panels	
	Ditton Geotechnical Services Pty Ltd		Scale:	NTS	Figure No: A12



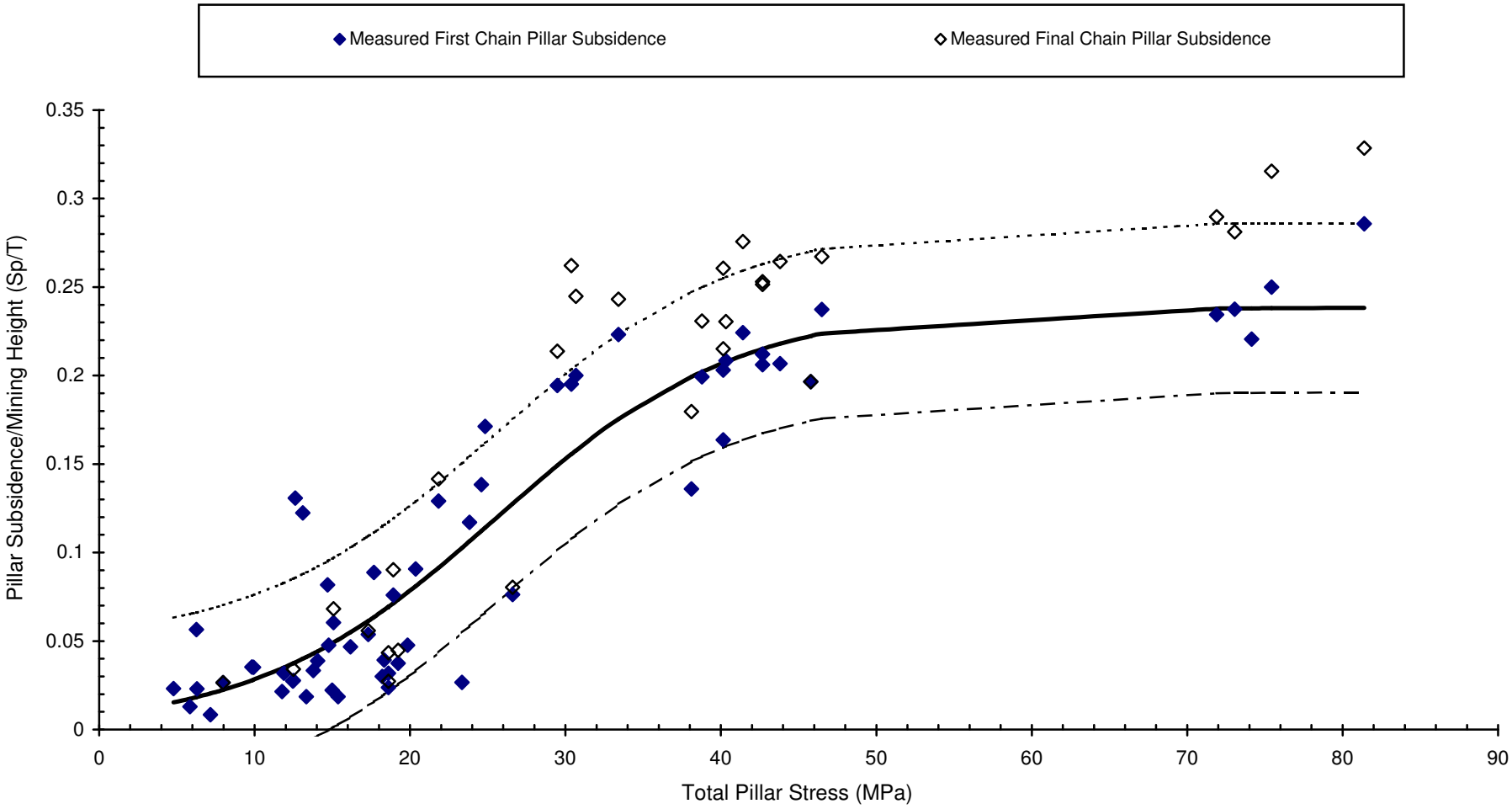
DgS	Engineer:	S.Ditton	Client:	Adapted from ACARP, 2003	
	Drawn:	S.Ditton			
	Date:	08.08.08	Title:	Geomechnical and Geological Effects of Overburden Behaviour on Maximum Subsidence for Single Panels	
	Ditton Geotechnical Services Pty Ltd		Scale:	NTS	Figure No: A13



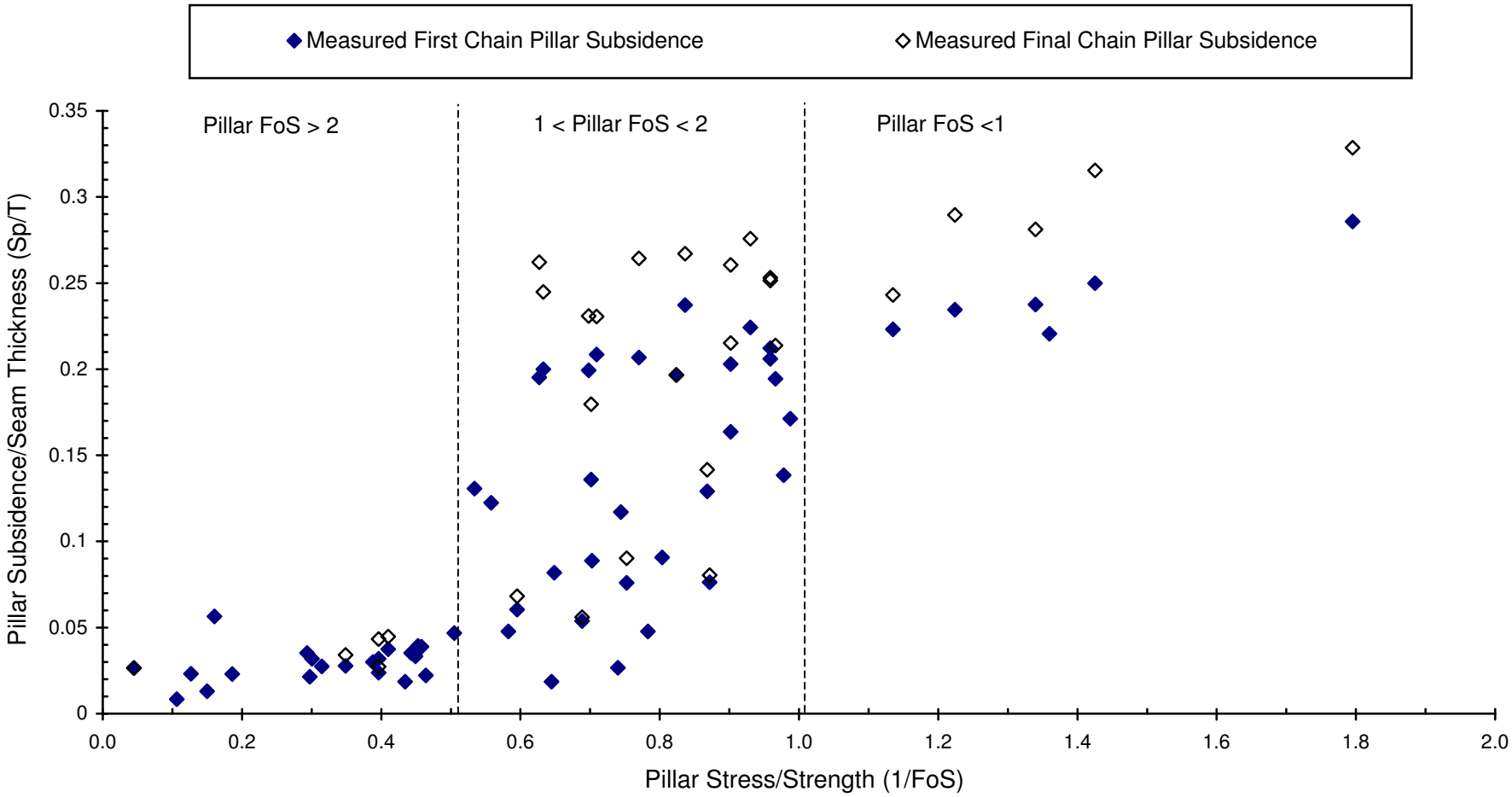
DgS	Engineer:	S.Ditton	Client:	Adapted from ACARP, 2003	
	Drawn:	S.Ditton			
	Date:	19.07.12	Title:	Multiple Longwall Panel Subsidence Mechanism Concepts	
	Ditton Geotechnical Services Pty Ltd		Scale:	NTS	Figure No: A14



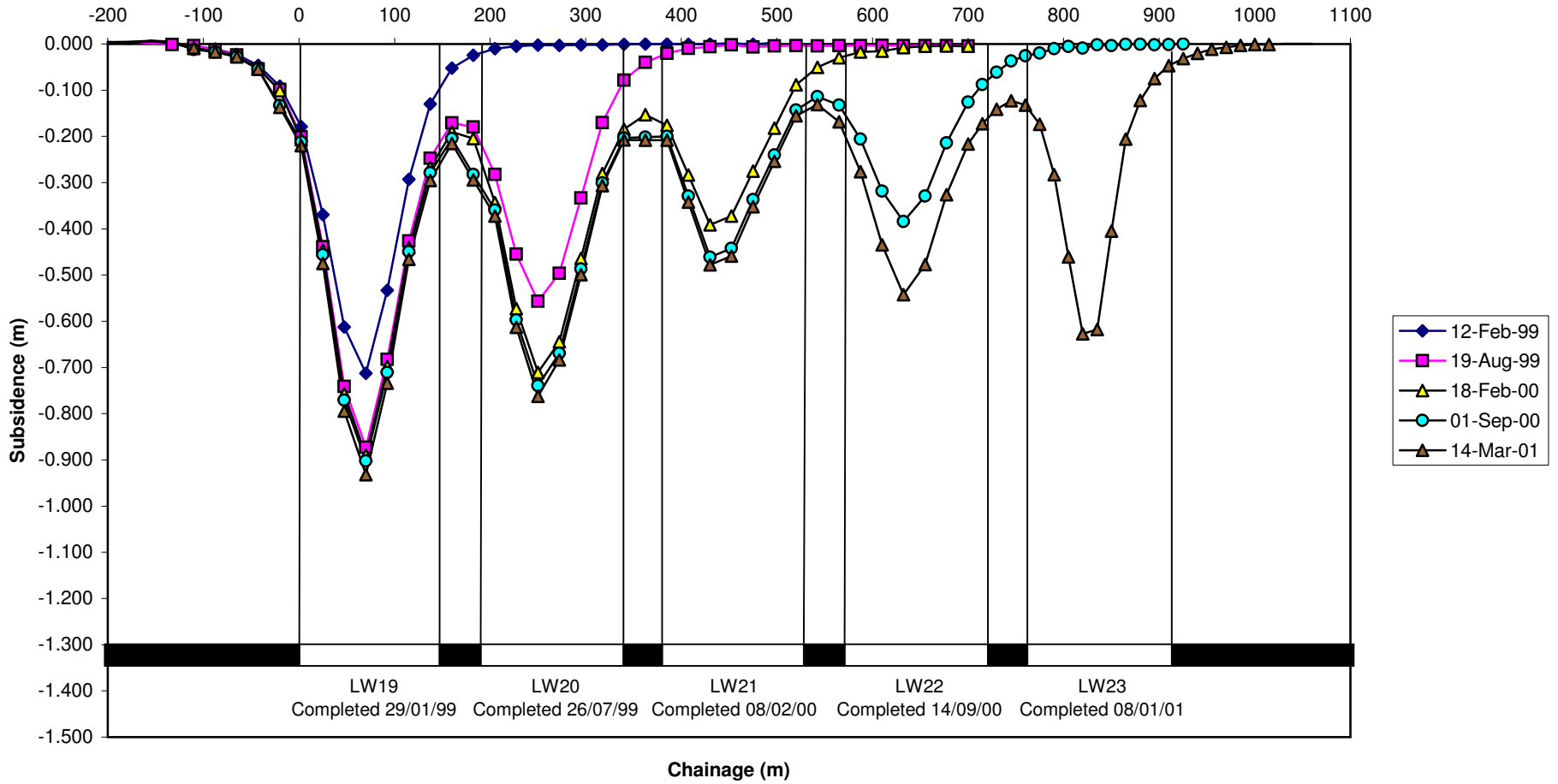
DgS	Engineer:	S.Ditton	Client:	Extract from ACARP, 2003	
	Drawn:	S.Ditton			
	Date:	08.08.08	Title:	2003 Empirical Model for Predicting Subsidence above Chain Pillars Subject to Double Abutment Loading	
	Ditton Geotechnical Services Pty Ltd		Scale:	NTS	Figure No: A15



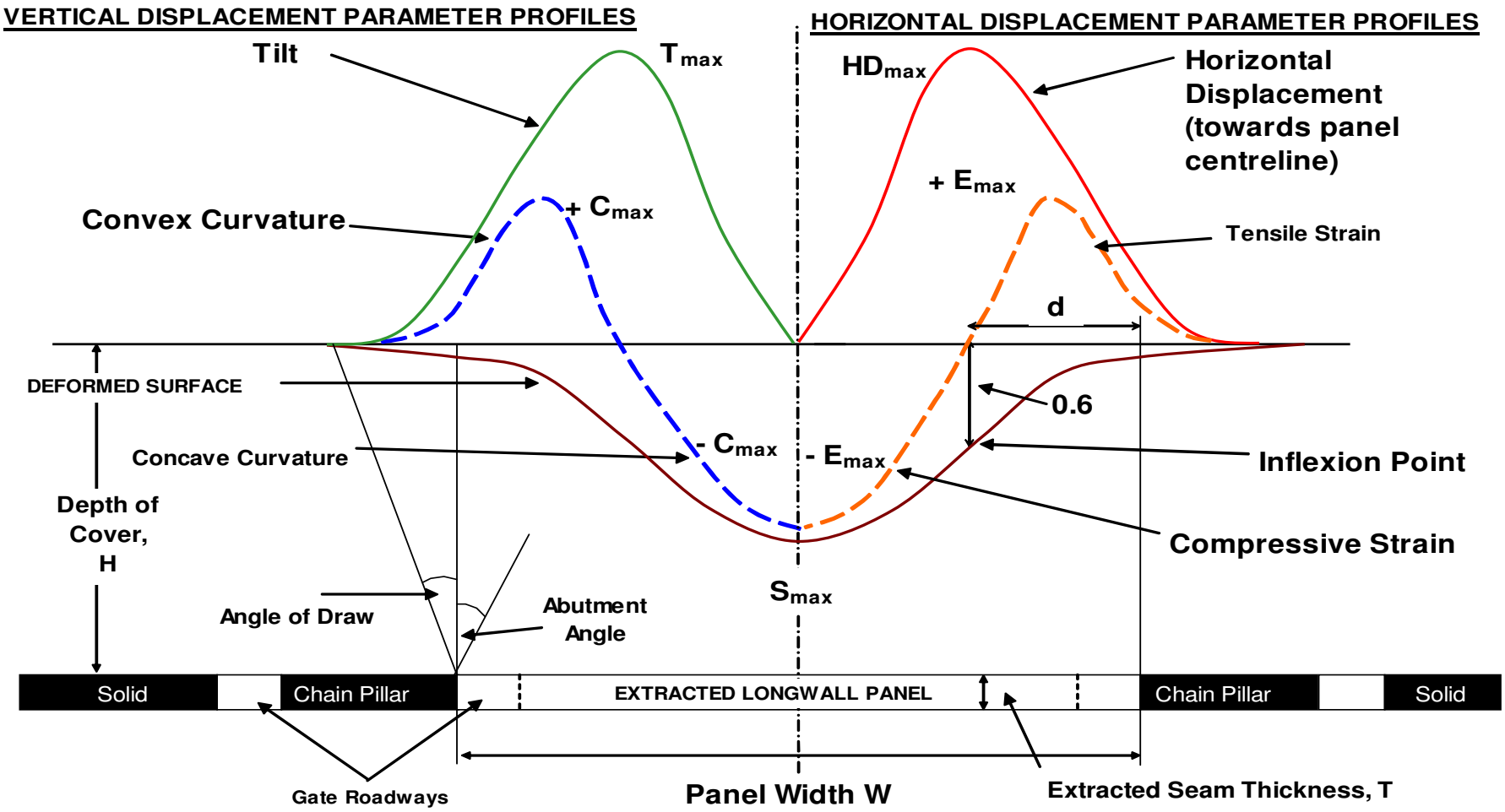
DgS	Engineer:	S.Ditton	Client:	Adapted from ACARP, 2003	
	Drawn:	S.Ditton			
	Date:	08.08.08	Title:	2008 Empirical Model (DgS) for Predicting Subsidence above Chain Pillars Subject to Double Abutment Loading	
	Ditton Geotechnical Services Pty Ltd		Scale:	NTS	Figure No: A16



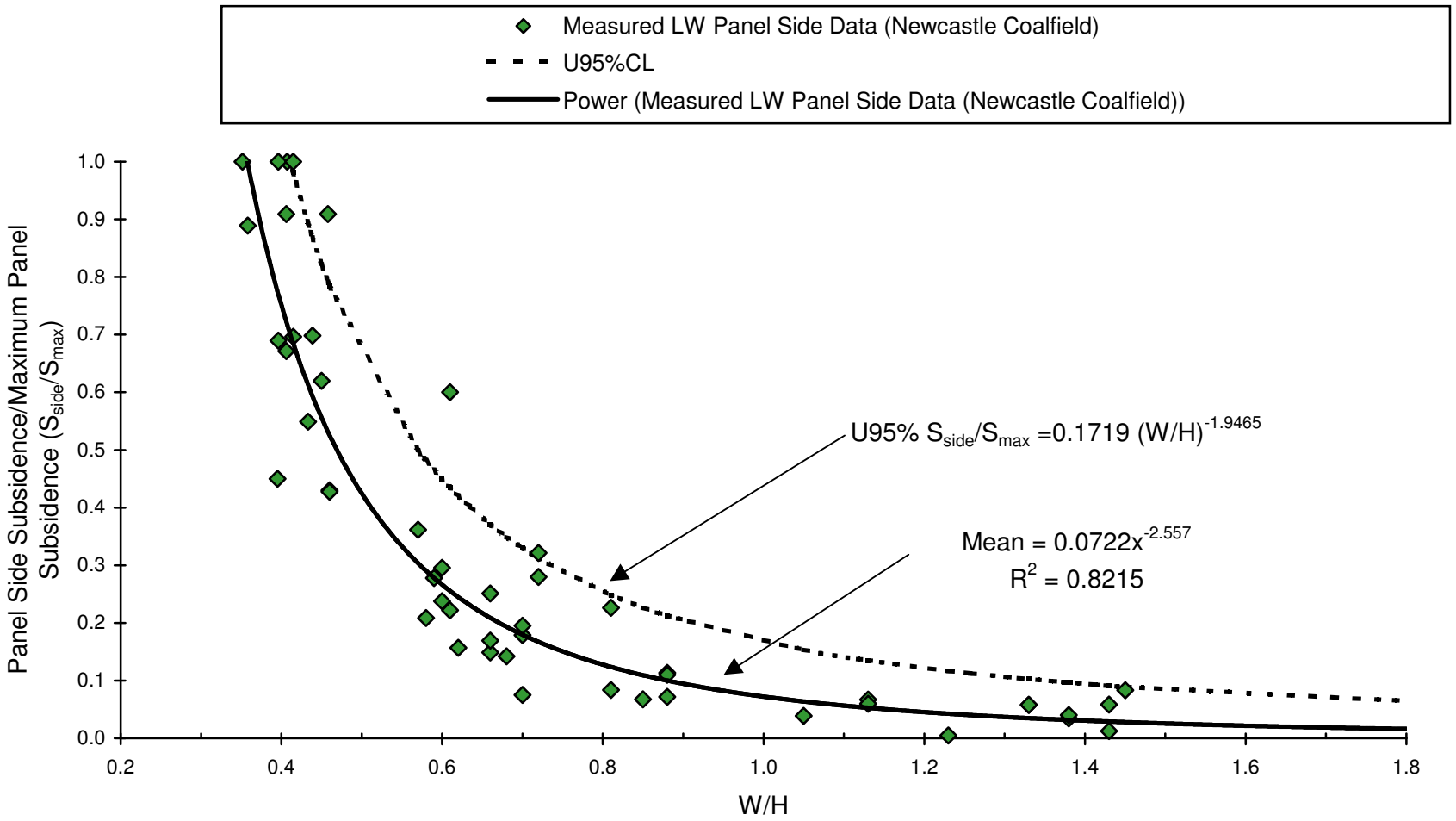
DgS	Engineer:	S.Ditton	Client:	Adapted from ACARP, 2003	
	Drawn:	S.Ditton			
	Date:	08.08.08	Title:	Empirical DgS, 2008 Model Data of 1/FoS v. Subsidence above Chain Pillars Subject to Double Abutment Loading	
	Ditton Geotechnical Services Pty Ltd		Scale:	NTS	Figure No: A17



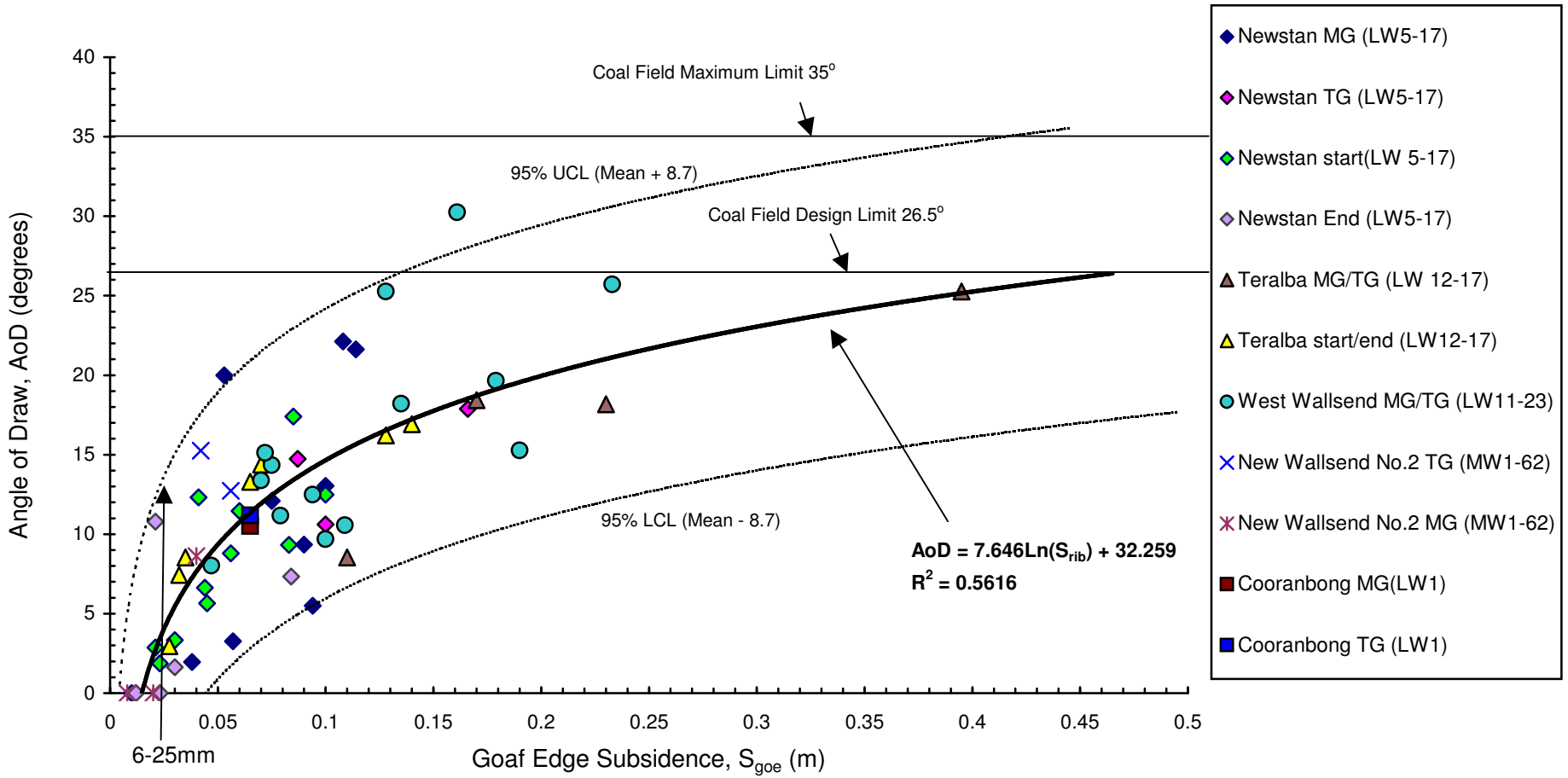
DgS	Engineer:	S.Ditton	Client:	Adapted from ACARP, 2003	
	Drawn:	S.Ditton			
	Date:	08.08.08	Title:	Measured Multiple Longwall Panel Subsidence in Newcastle Coalfield	
	Ditton Geotechnical Services Pty Ltd		Scale:	NTS	Figure No: A18



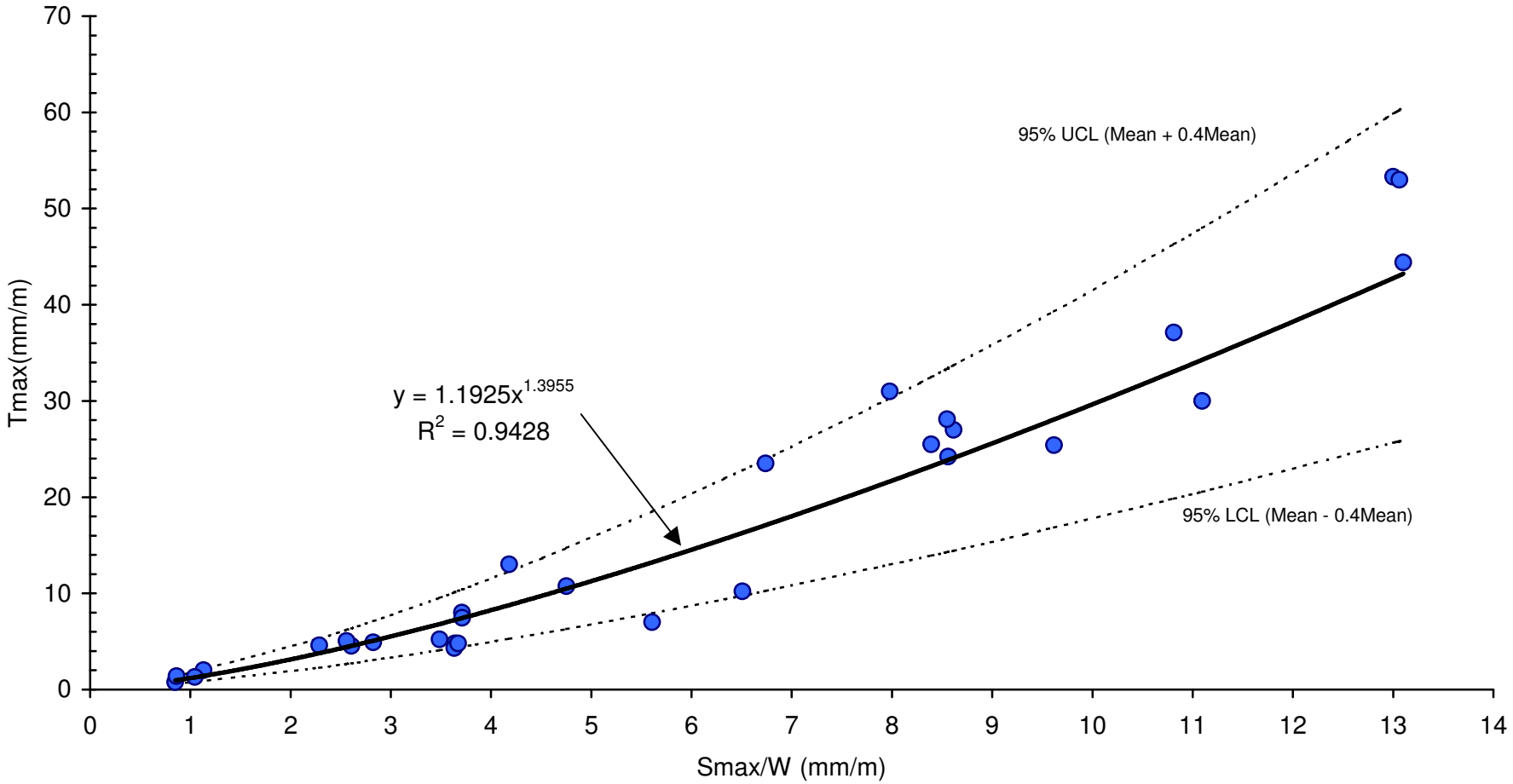
DgS	Engineer:	S.Ditton	Client:	Extract from ACARP, 2003	
	Drawn:	S.Ditton			
	Date:	08.08.08	Title:	Mine Subsidence Trough Deformation Parameters (adapted from Holla, 1987)	
	Ditton Geotechnical Services Pty Ltd		Scale:	NTS	Figure No: A19



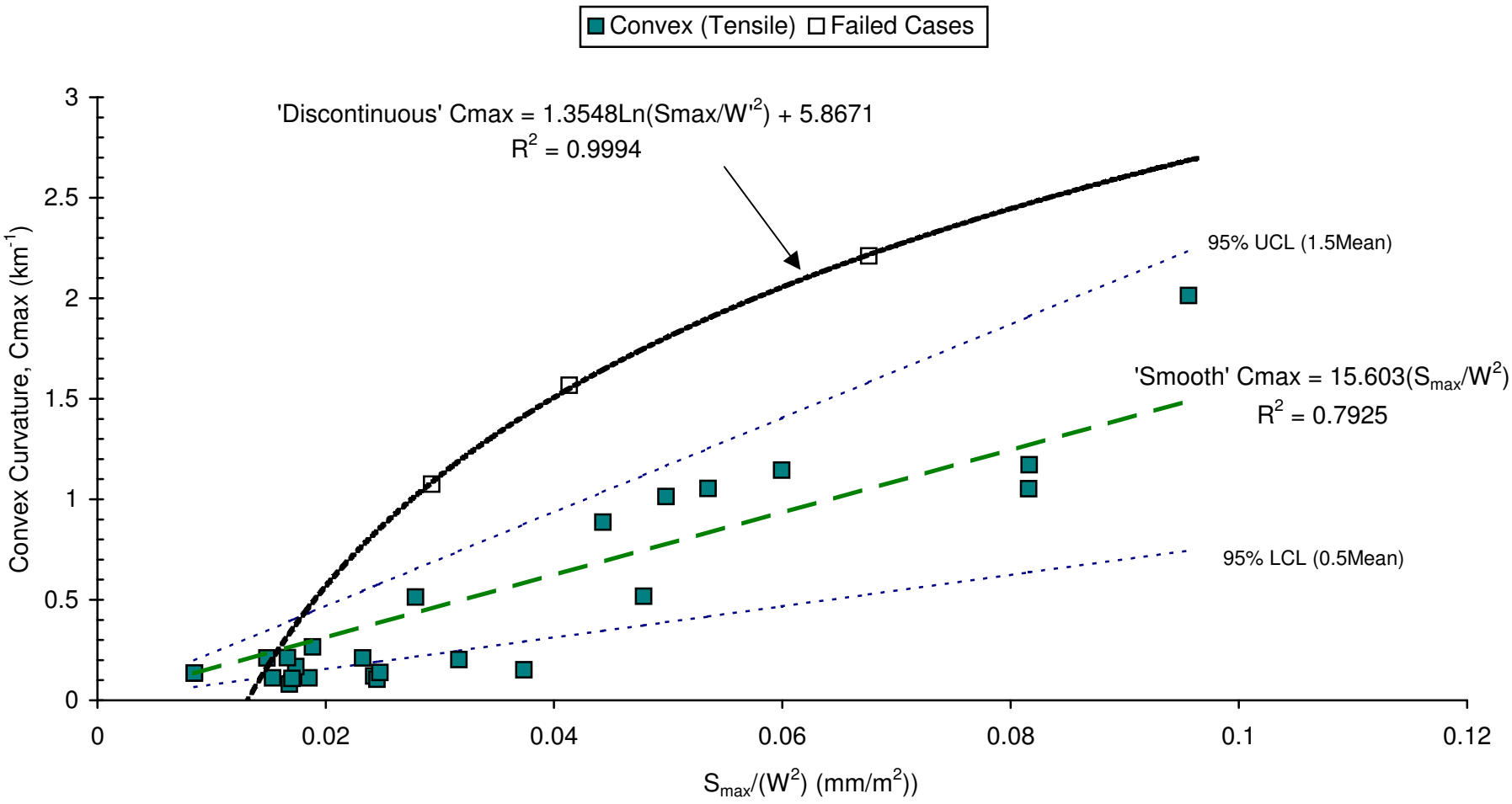
DgS	Engineer:	S.Ditton	Client:	Adapted from ACARP, 2003	
	Drawn:	S.Ditton			
	Date:	08.08.08	Title:	Empirical Model for Goaf Edge Subsidence Prediction Above Longwall Panels	
	Ditton Geotechnical Services Pty Ltd		Scale:	NTS	Figure No: A20



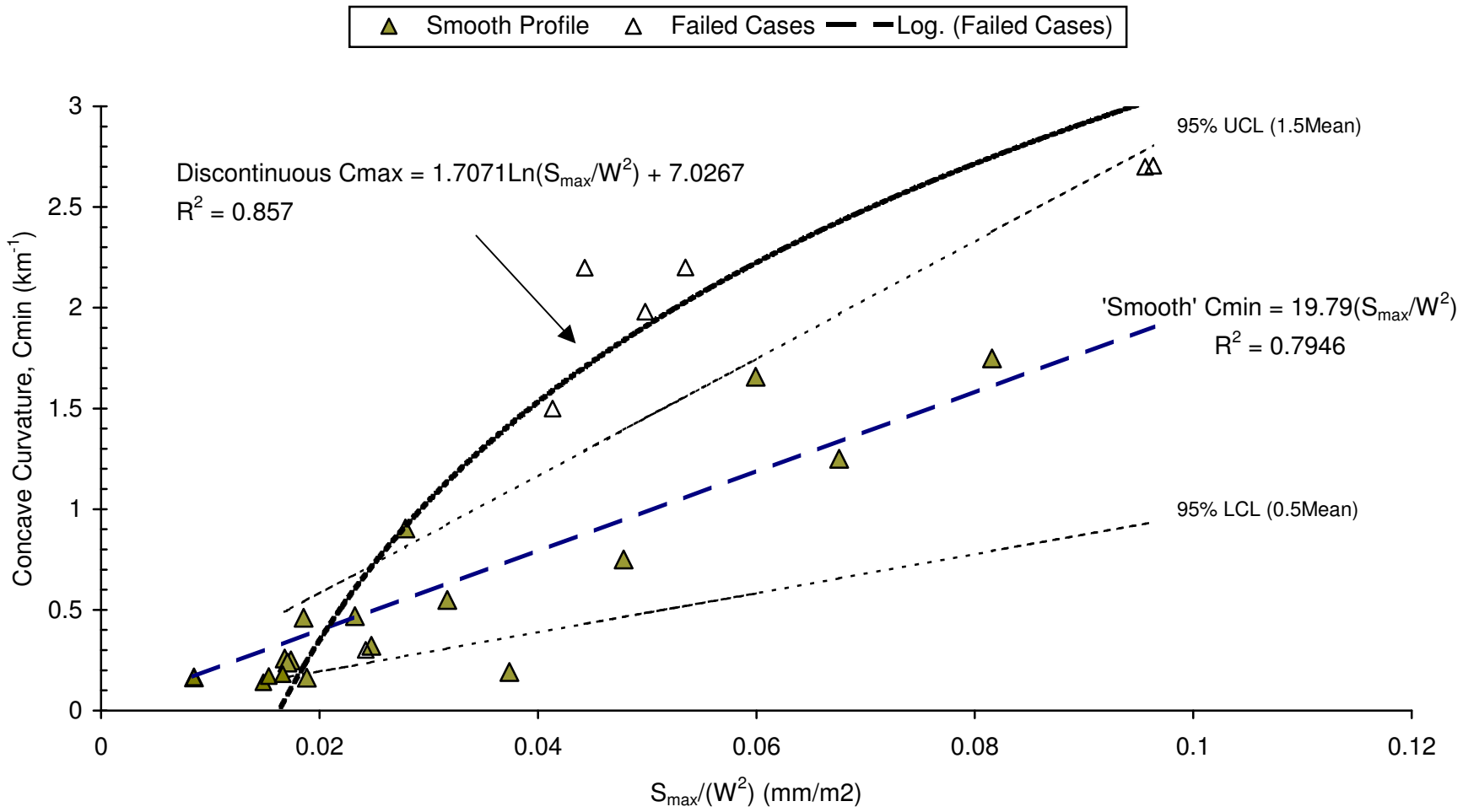
DgS	Engineer:	S.Ditton	Client:	Extracted from ACARP, 2003	
	Drawn:	S.Ditton			
	Date:	08.08.08	Title:	Empirical Prediction Model for Longwall Panel Angle of Draw	
	Ditton Geotechnical Services Pty Ltd		Scale:	NTS	Figure No: A21



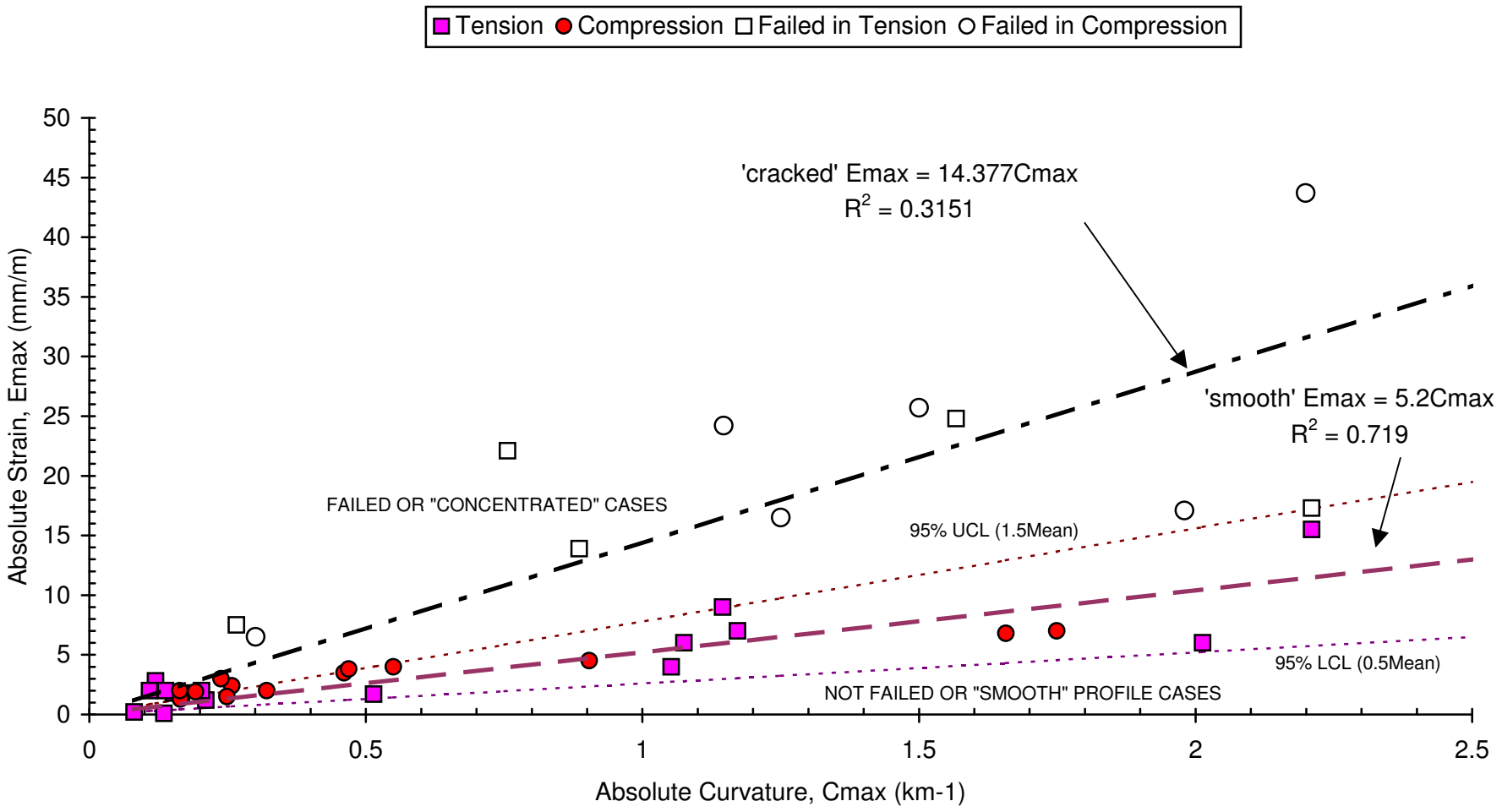
DgS	Engineer:	S.Ditton	Client:	Extract from ACARP, 2003	
	Drawn:	S.Ditton			
	Date:	08.08.08	Title:	Empirical Model for Maximum Panel Tilt Prediction Above Longwall Panels	
	Ditton Geotechnical Services Pty Ltd		Scale:	NTS	Figure No: A22



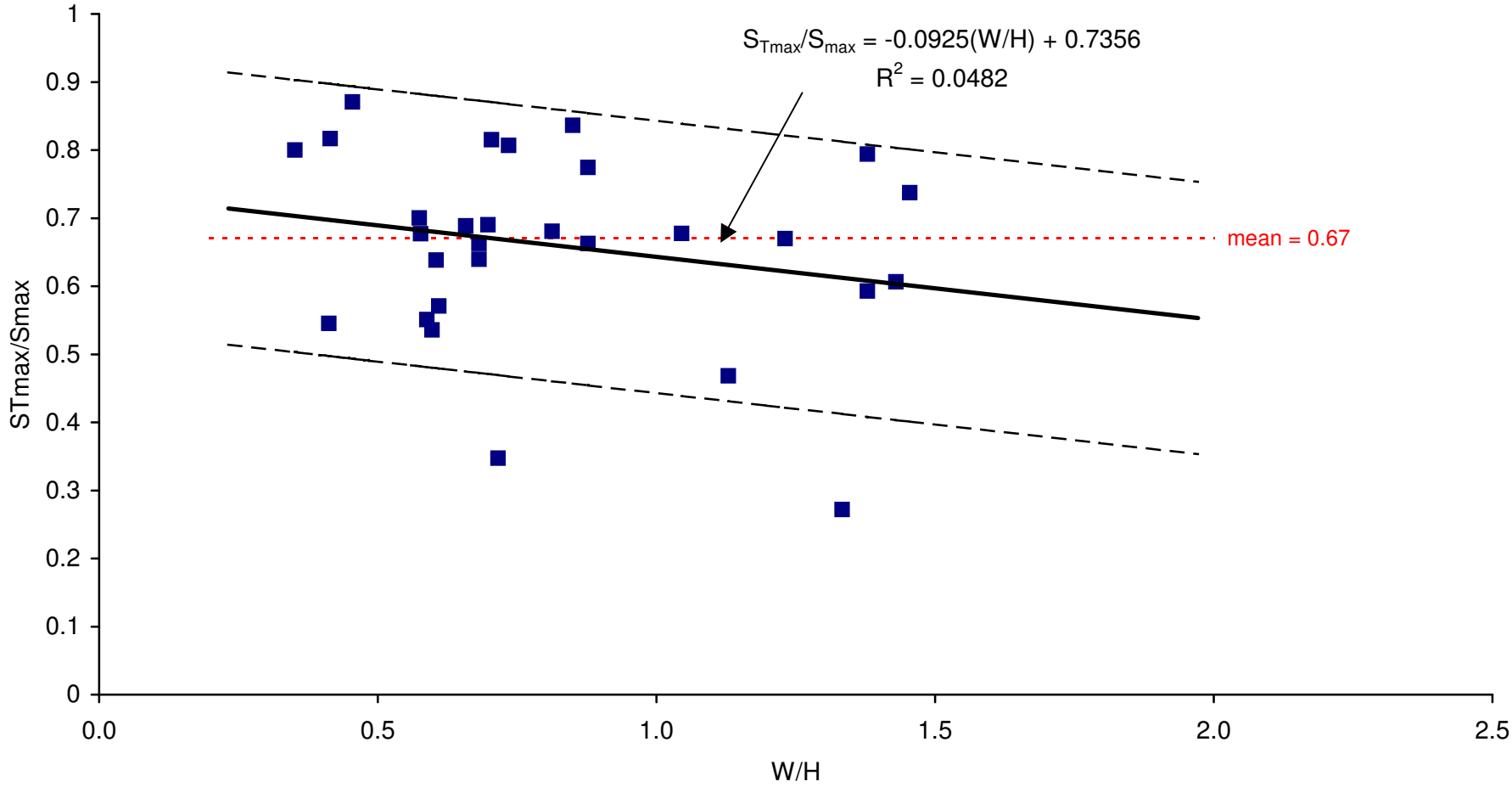
DgS	Engineer:	S.Ditton	Client:	Extract from ACARP, 2003	
	Drawn:	S.Ditton			
	Date:	08.08.08	Title:	Empirical Model for Maximum Panel Convex Curvature Prediction Above Longwall Panels for Smooth and Discontinuous Profiles	
	Ditton Geotechnical Services Pty Ltd		Scale:	NTS	Figure No: A23



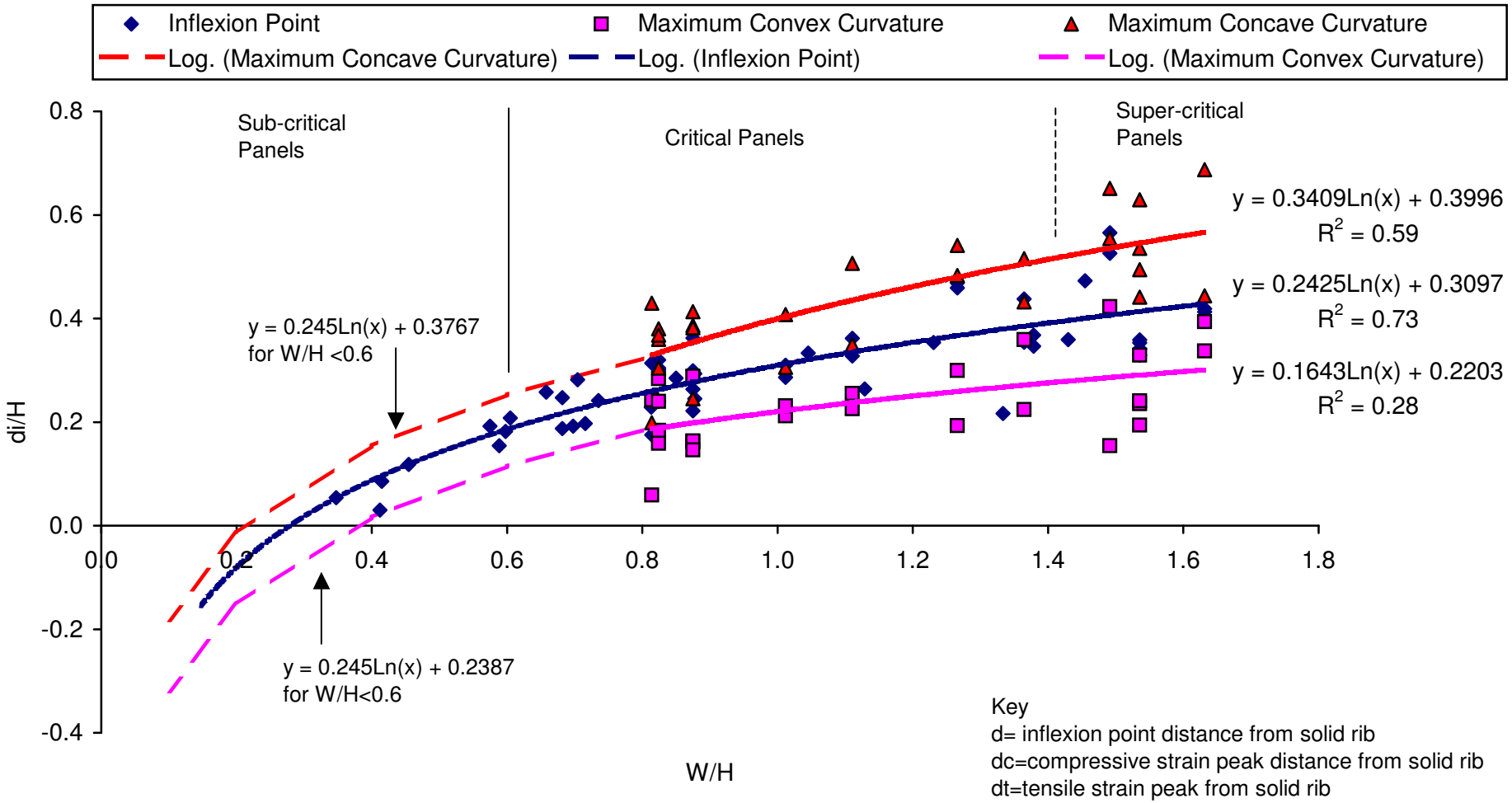
DgS	Engineer:	S.Ditton	Client:	Extract from ACARP, 2003	
	Drawn:	S.Ditton			
	Date:	08.08.08	Title:	Empirical Model for Maximum Panel Concave Curvature Prediction Above Longwall Panels for Smooth and Discontinuous Profiles	
	Ditton Geotechnical Services Pty Ltd		Scale:	NTS	Figure No: A24



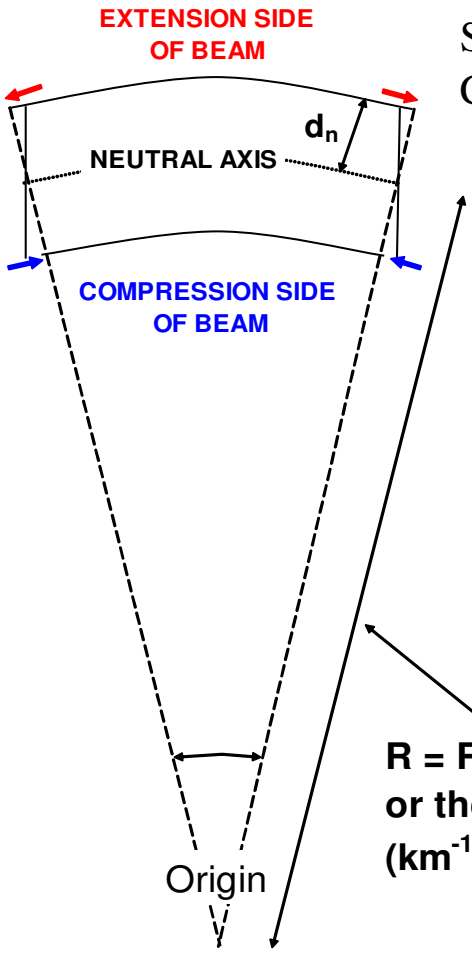
DgS	Engineer:	S.Ditton	Client:	Extract from ACARP, 2003	
	Drawn:	S.Ditton			
	Date:	08.08.08	Title:	Empirical Model for Maximum Panel Strain Prediction Above Longwall Panels for Smooth and Cracked Profiles	
	Ditton Geotechnical Services Pty Ltd		Scale:	NTS	Figure No: A25



DgS	Engineer:	S.Ditton	Client:	Extract from ACARP, 2003	
	Drawn:	S.Ditton			
	Date:	08.08.08	Title:	Empirical Model for Subsidence at Maximum Tilt Above Longwall Panels	
	Ditton Geotechnical Services Pty Ltd		Scale:	NTS	Figure No: A26



DgS	Engineer:	S.Ditton	Client:	Adapted from ACARP, 2003	
	Drawn:	S.Ditton			
	Date:	08.08.08	Title:	Empirical Model for Predicting the Location of Inflexion Point, Maximum Tensile and Compressive Strain Peaks due to Longwall Panel Subsidence in the Newcastle Coalfield	
	Ditton Geotechnical Services Pty Ltd		Scale:	NTS	Figure No: A27



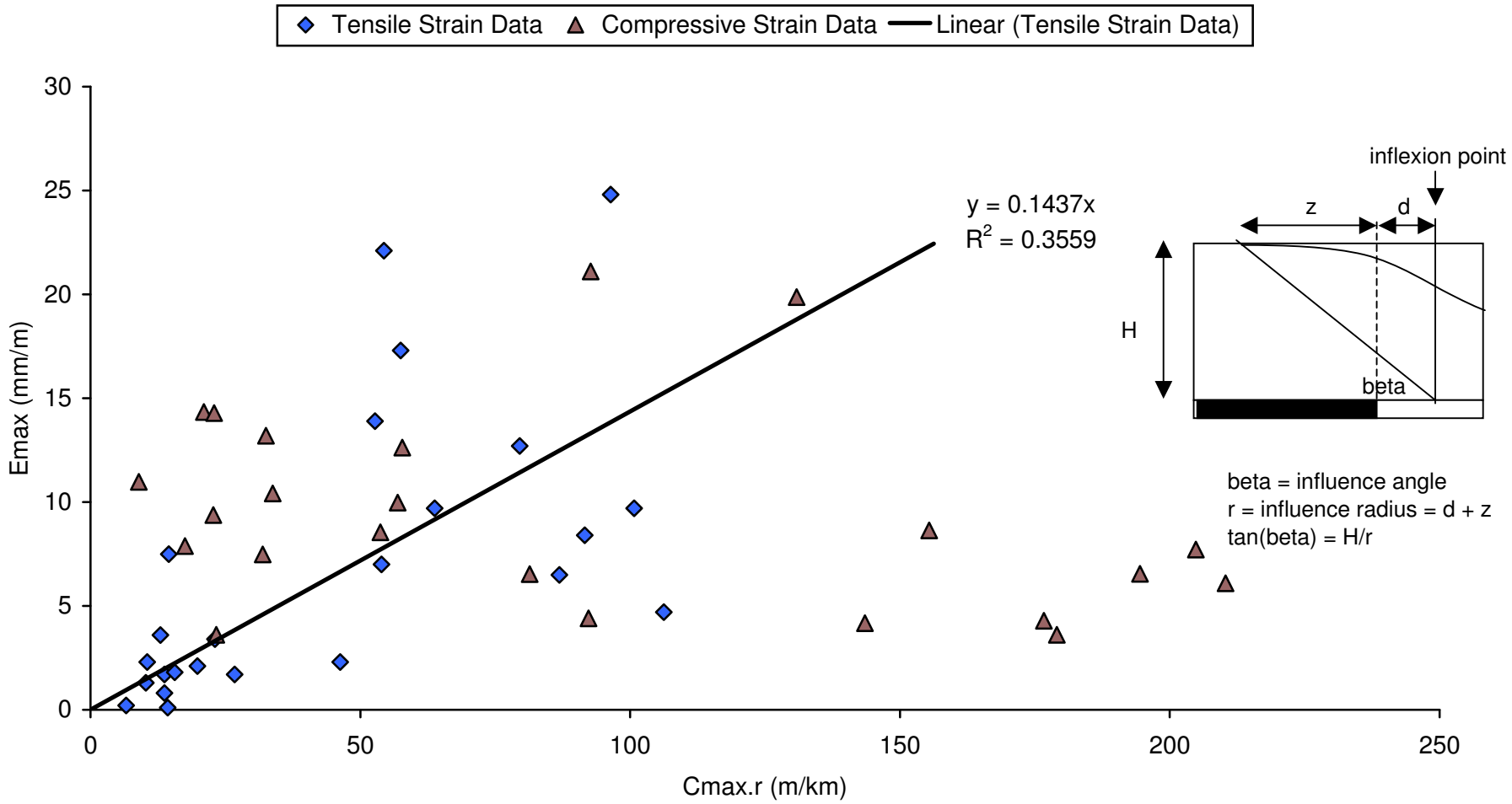
Strain E = (mm/m)
Curvature C = km-1

E = C x dn

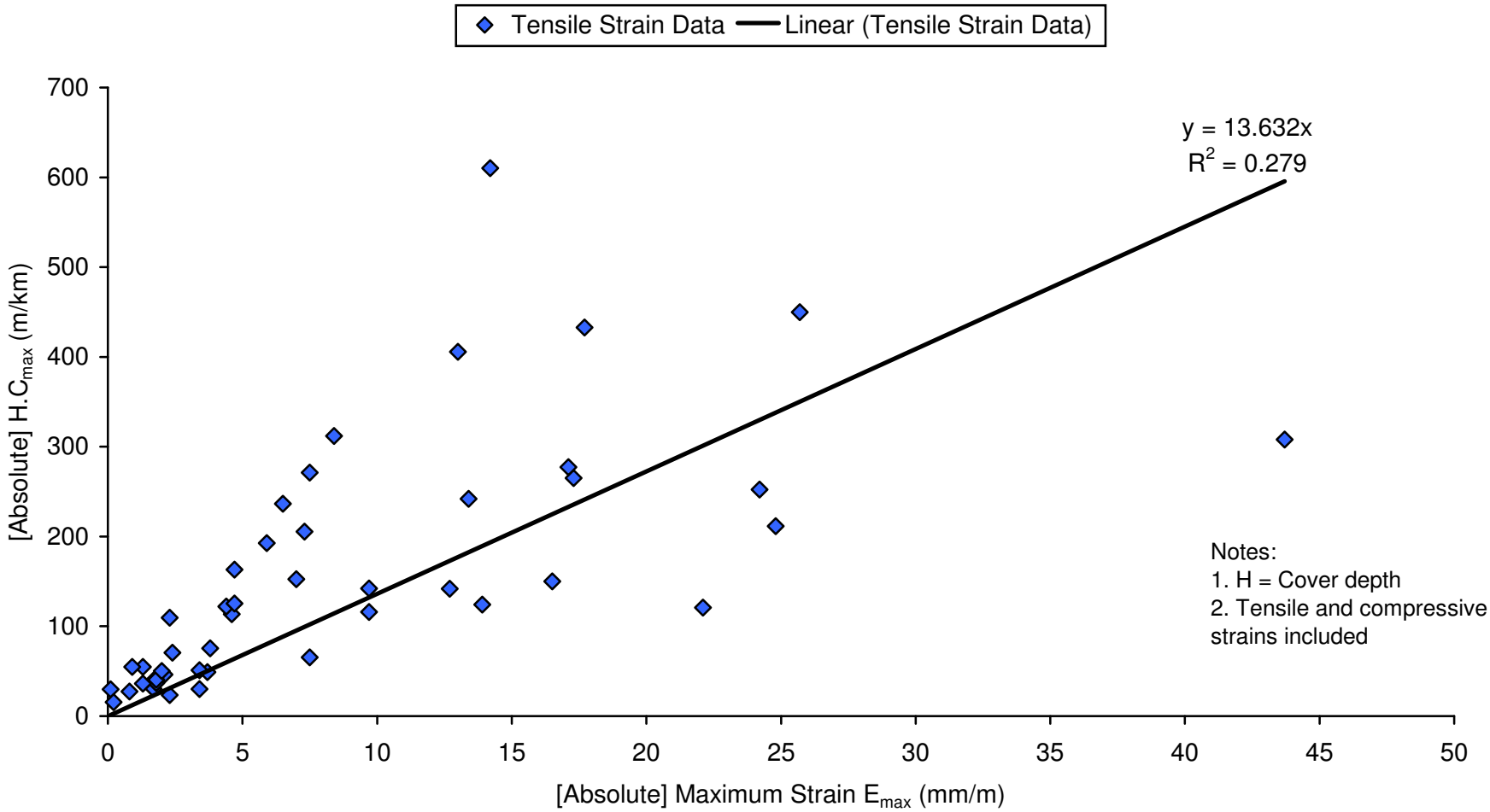
Average
dn = 5.2 m
for database

R = Radius of curvature or the curvature, C = 1/R (km^{-1})

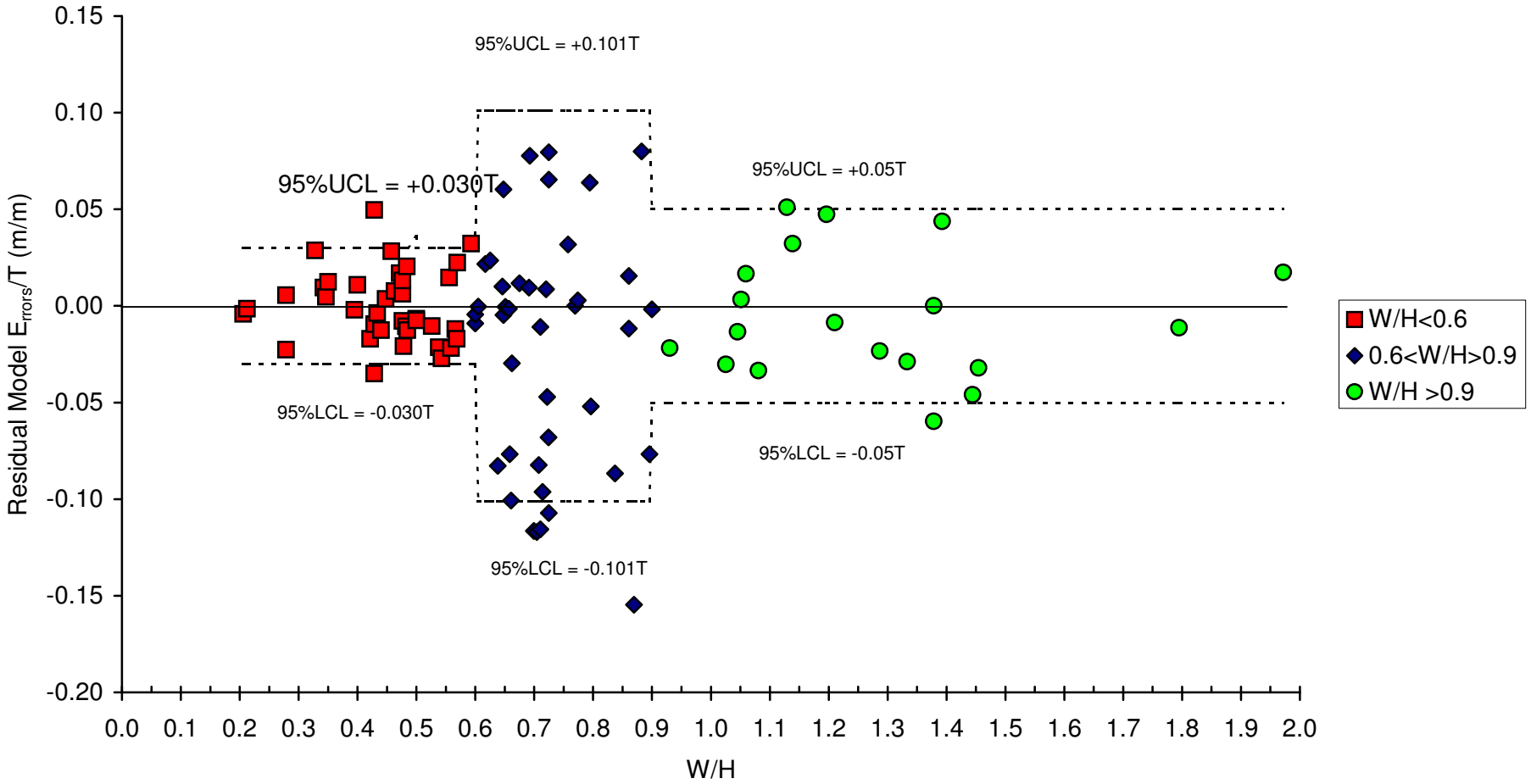
DgS	Engineer:	S.Ditton	Client:	Extract from ACARP, 2003	
	Drawn:	S.Ditton			
	Date:	08.08.08	Title:	Bending Beam Theory for Strain Prediction from Curvature Measurements	
	Ditton Geotechnical Services Pty Ltd		Scale:		Figure No: A28



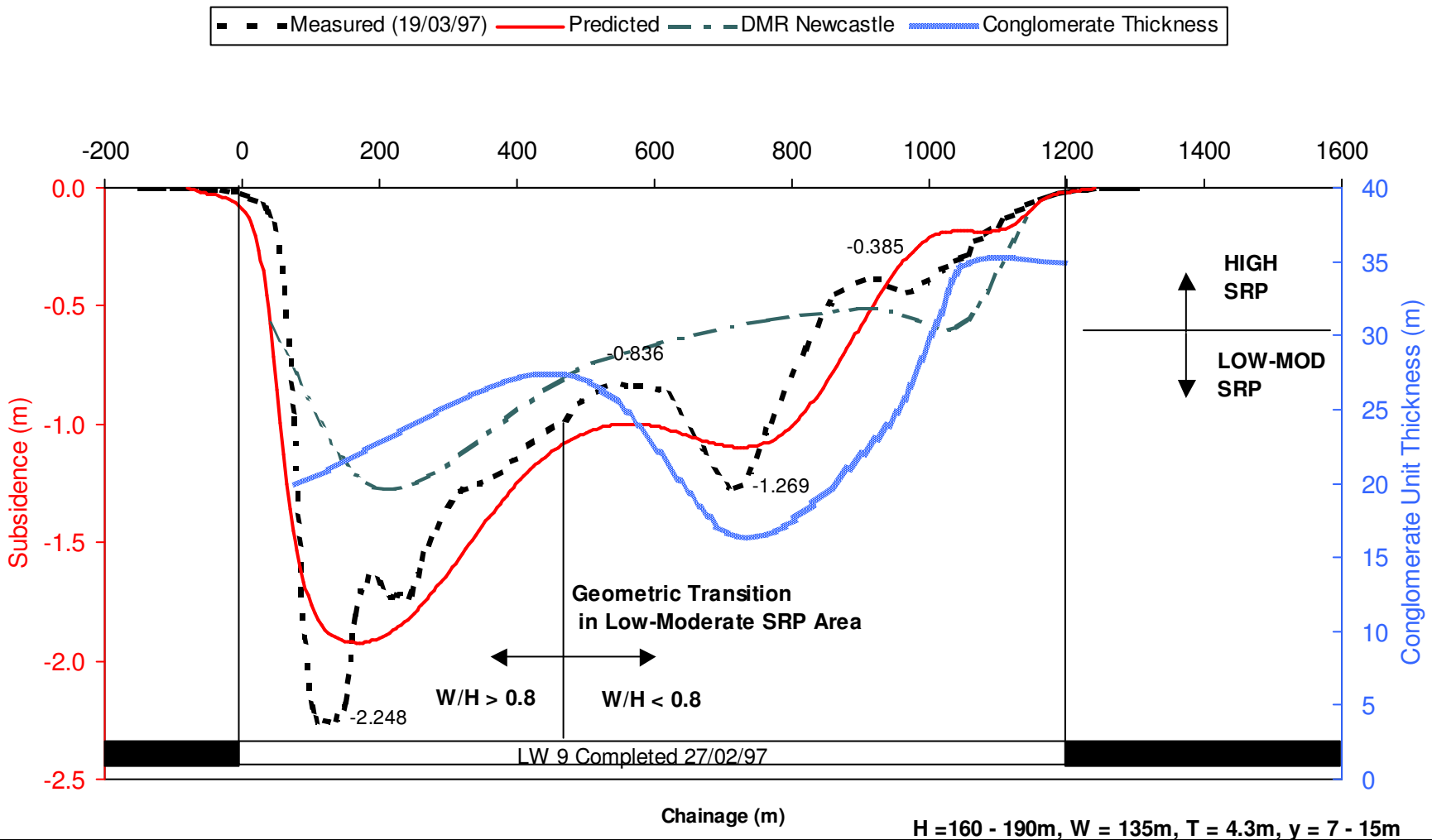
DgS	Engineer:	S.Ditton	Client:	Karmis, 1987 Adapted for ACARP, 2003	
	Drawn:	S.Ditton			
	Date:	08.08.08	Title:	Empirical Model Recommended by Karmis et al, 1987 for Predicting Strain from Curvature Above Longwall Panels in Newcastle Coalfield	
	Ditton Geotechnical Services Pty Ltd		Scale:	NTS	Figure No: A29.1



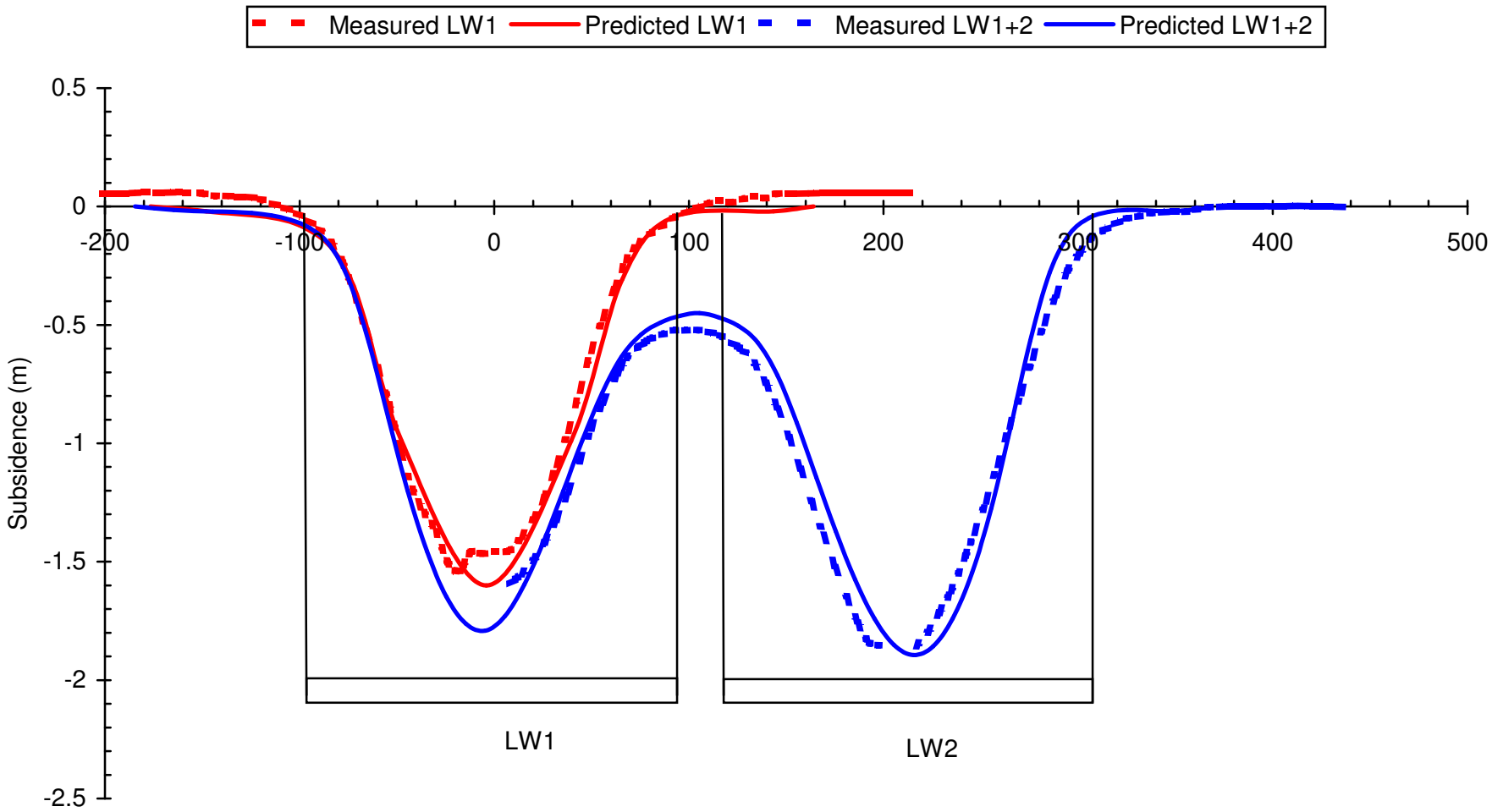
DgS	Engineer:	S.Ditton	Client:	Holla and Barclay, 2000 Adapted for ACARP, 2003	
	Drawn:	S.Ditton			
	Date:	08.08.08	Title:	Empirical Model Recommended by Holla and Barclay, 2000 for Predicting Curvature from Maximum Strain Above Longwall Panels in the Newcastle Coalfield	
	Ditton Geotechnical Services Pty Ltd		Scale:	NTS	Figure No: A29.2



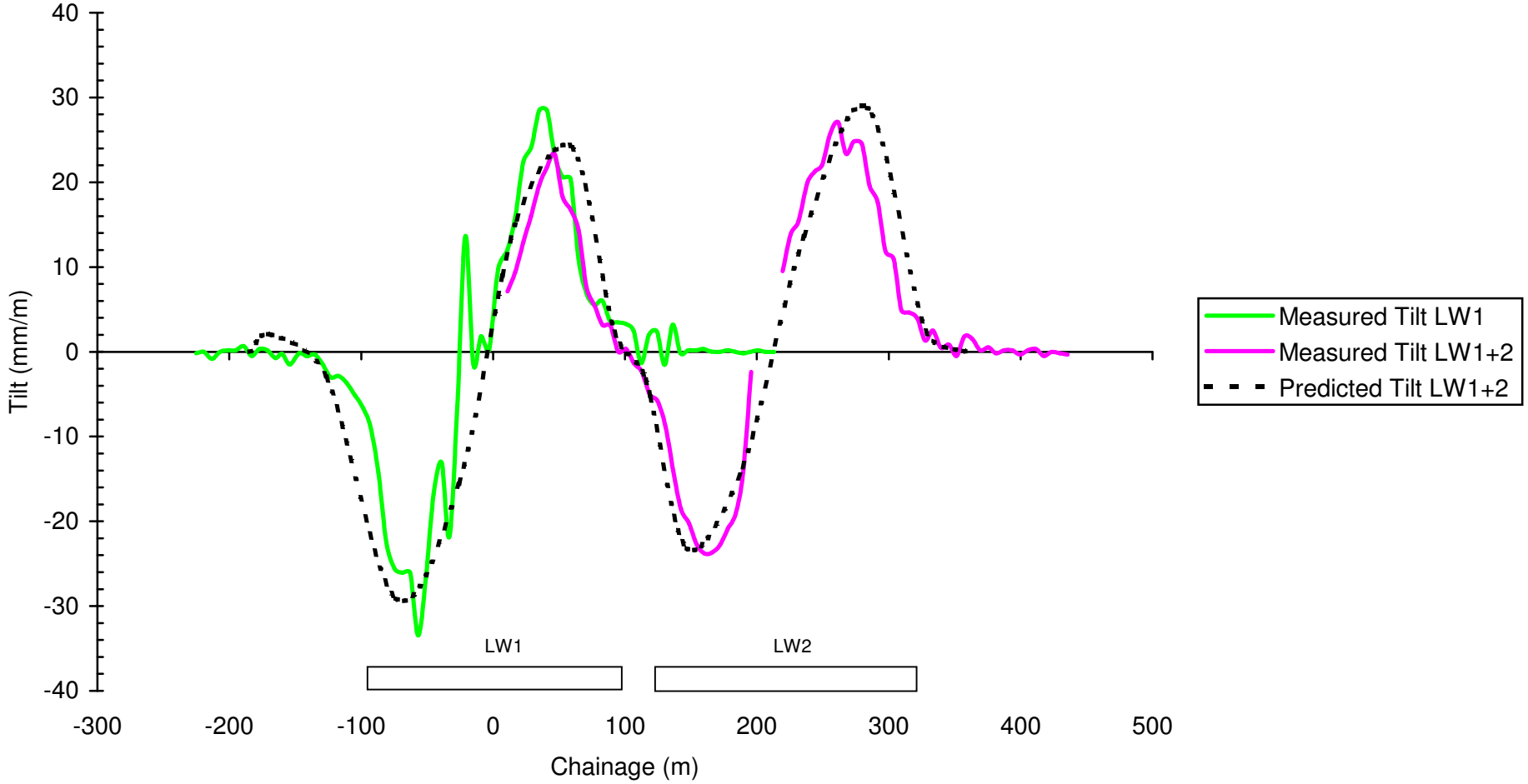
DgS	Engineer:	S.Ditton	Client:	Extract from ACARP, 2003	
	Drawn:	S.Ditton			
	Date:	08.08.08	Title:	Residual Errors of Database for Single Panel Prediction Model above Longwalls in the Newcastle Coalfield	
	Ditton Geotechnical Services Pty Ltd		Scale:	NTS	Figure No: A30



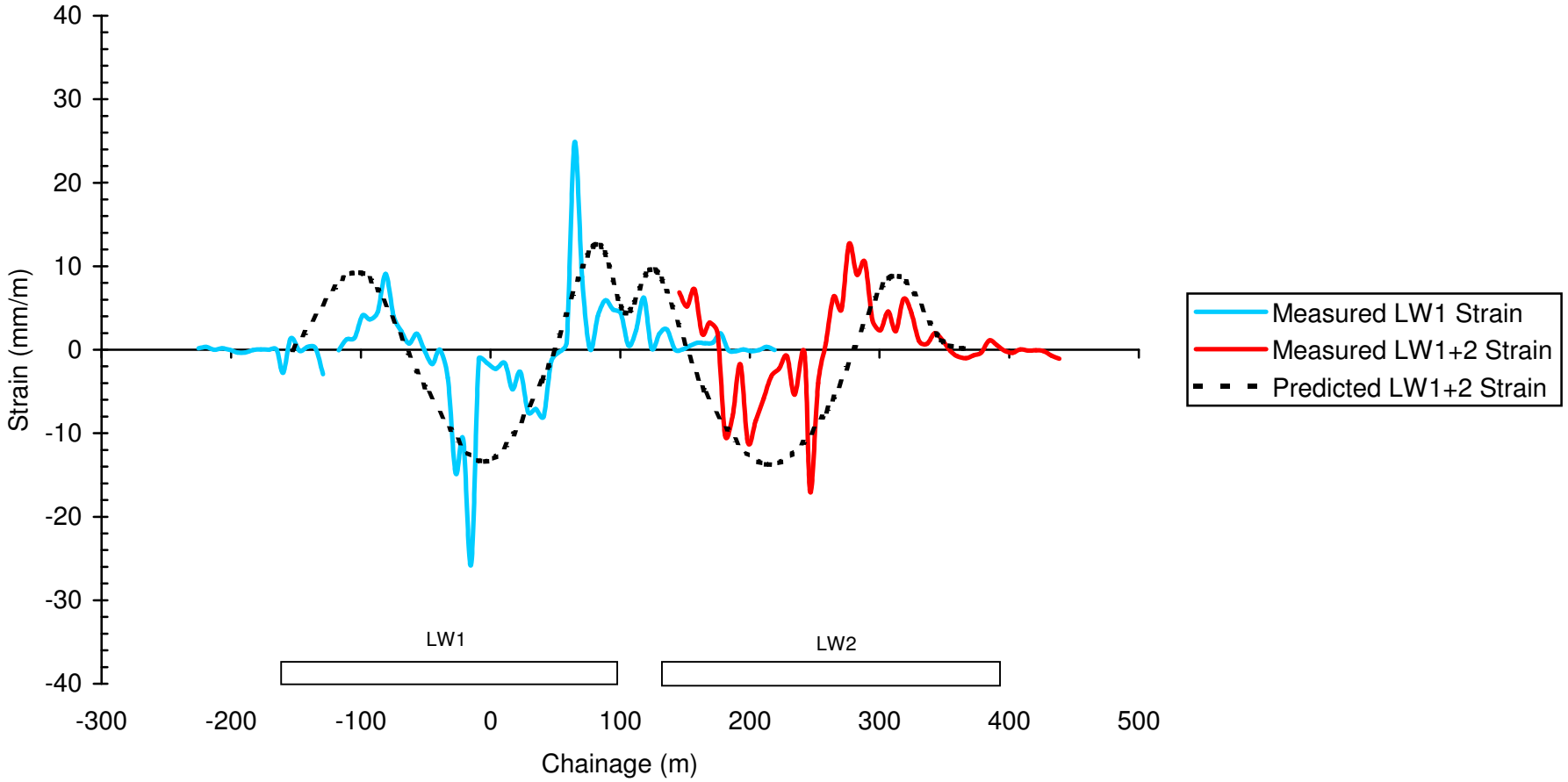
DgS	Engineer:	S.Ditton	Client:	Extract from ACARP, 2003	
	Drawn:	S.Ditton			
	Date:	08.08.08	Title:	Predicted v. Measured Centreline Subsidence Profiles for a Newcastle Coalfield Longwall with Massive Conglomerate Strata and Sub-Critical to Supercritical Transition	
	Ditton Geotechnical Services Pty Ltd		Scale:	NTS	Figure No: A31



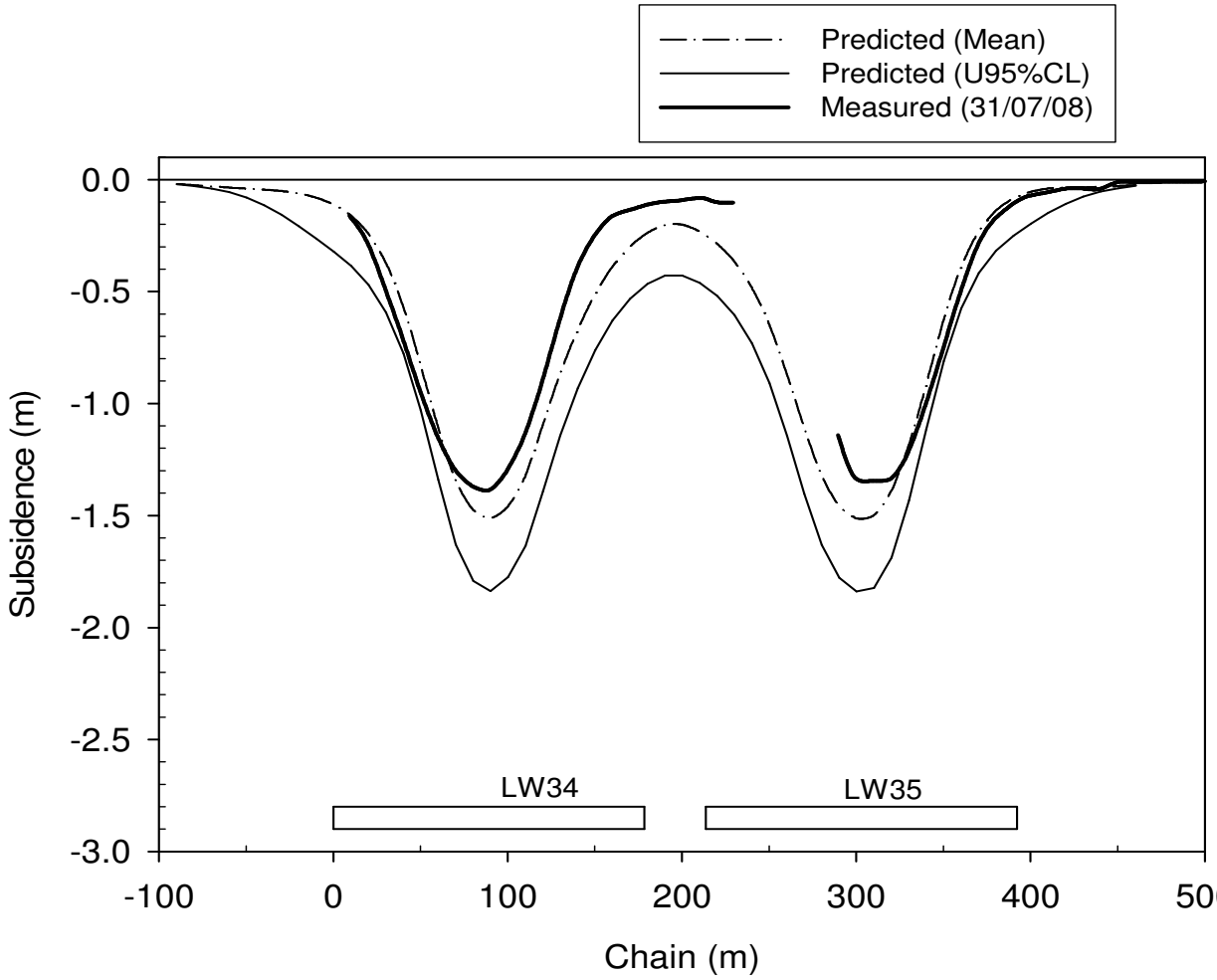
DgS	Engineer:	S.Ditton	Client:	Extract from ACARP, 2003	
	Drawn:	S.Ditton			
	Date:	08.08.08	Title:	Predicted v. Measured Crossline Subsidence Profiles for a Newcastle Coalfield Longwall Mine	
	Ditton Geotechnical Services Pty Ltd		Scale:	NTS	Figure No: A32



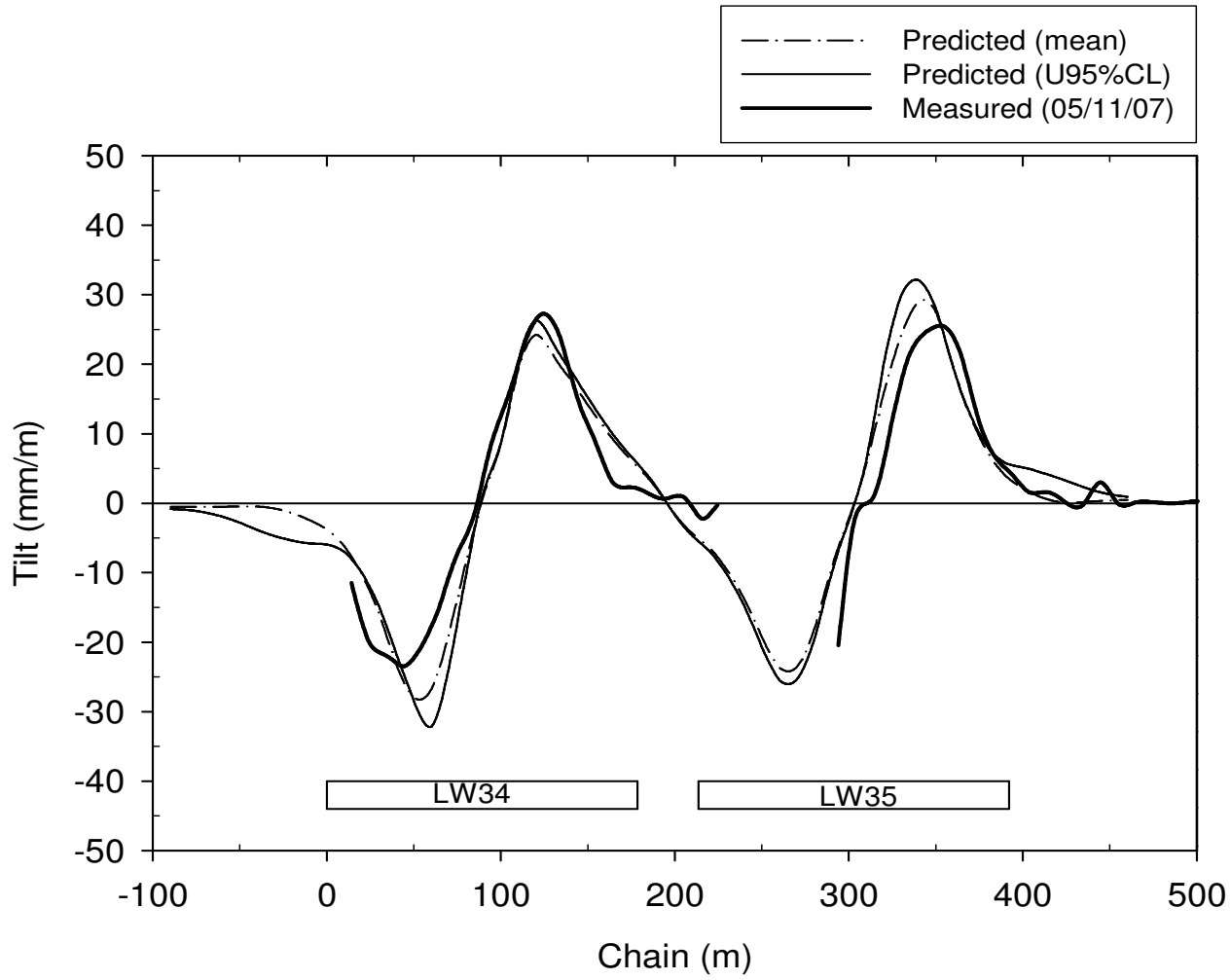
DgS	Engineer:	S.Ditton	Client:	Extract from ACARP, 2003	
	Drawn:	S.Ditton			
	Date:	08.08.08	Title:	Predicted v. Measured Crossline Tilt Profiles for a Newcastle Coalfield Longwall Mine	
	Ditton Geotechnical Services Pty Ltd		Scale:	NTS	Figure No: A33



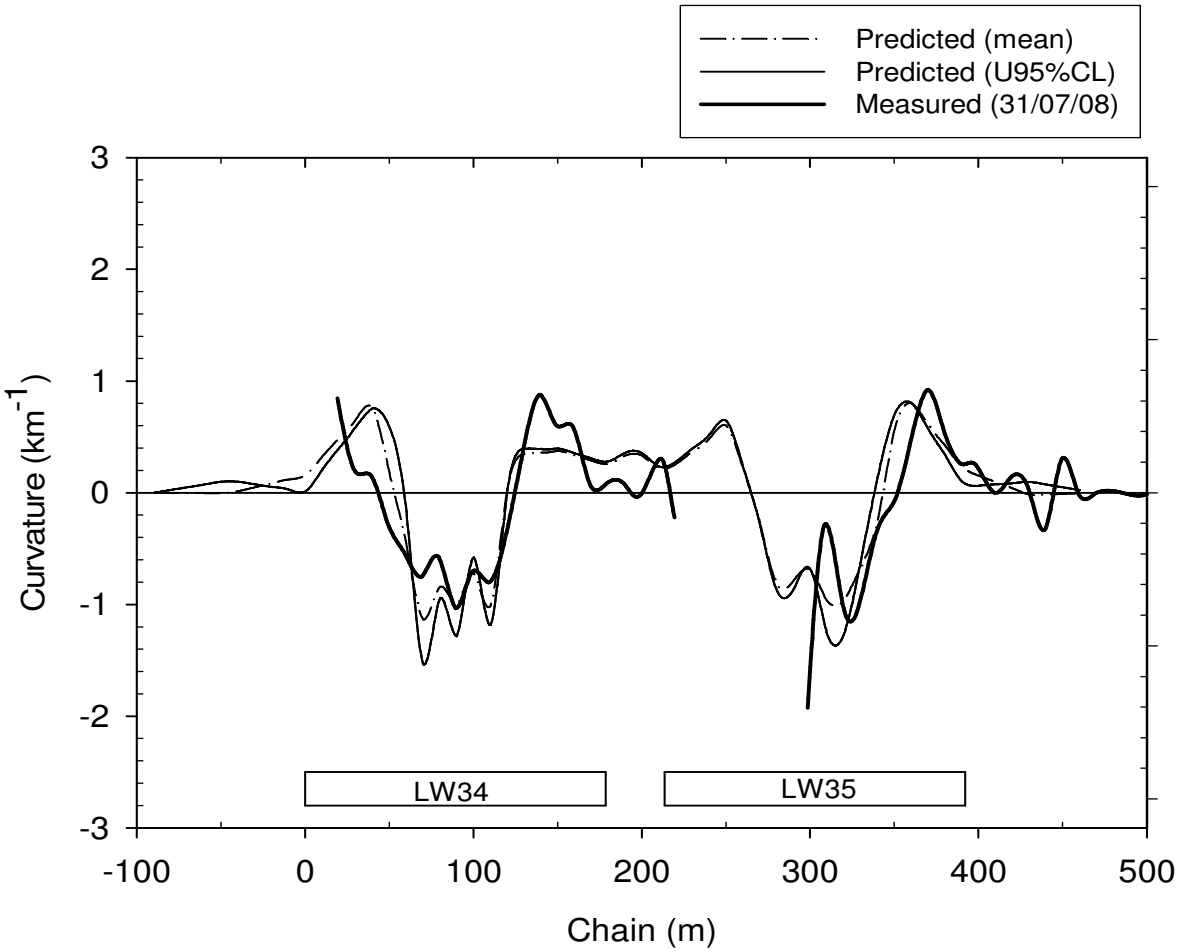
DgS	Engineer:	S.Ditton	Client:	Extract from ACARP, 2003	
	Drawn:	S.Ditton			
	Date:	08.08.08	Title:	Predicted v. Measured Crossline Strain Profiles for a Newcastle Coalfield Longwall Mine	
	Ditton Geotechnical Services Pty Ltd		Scale:	NTS	Figure No: A34



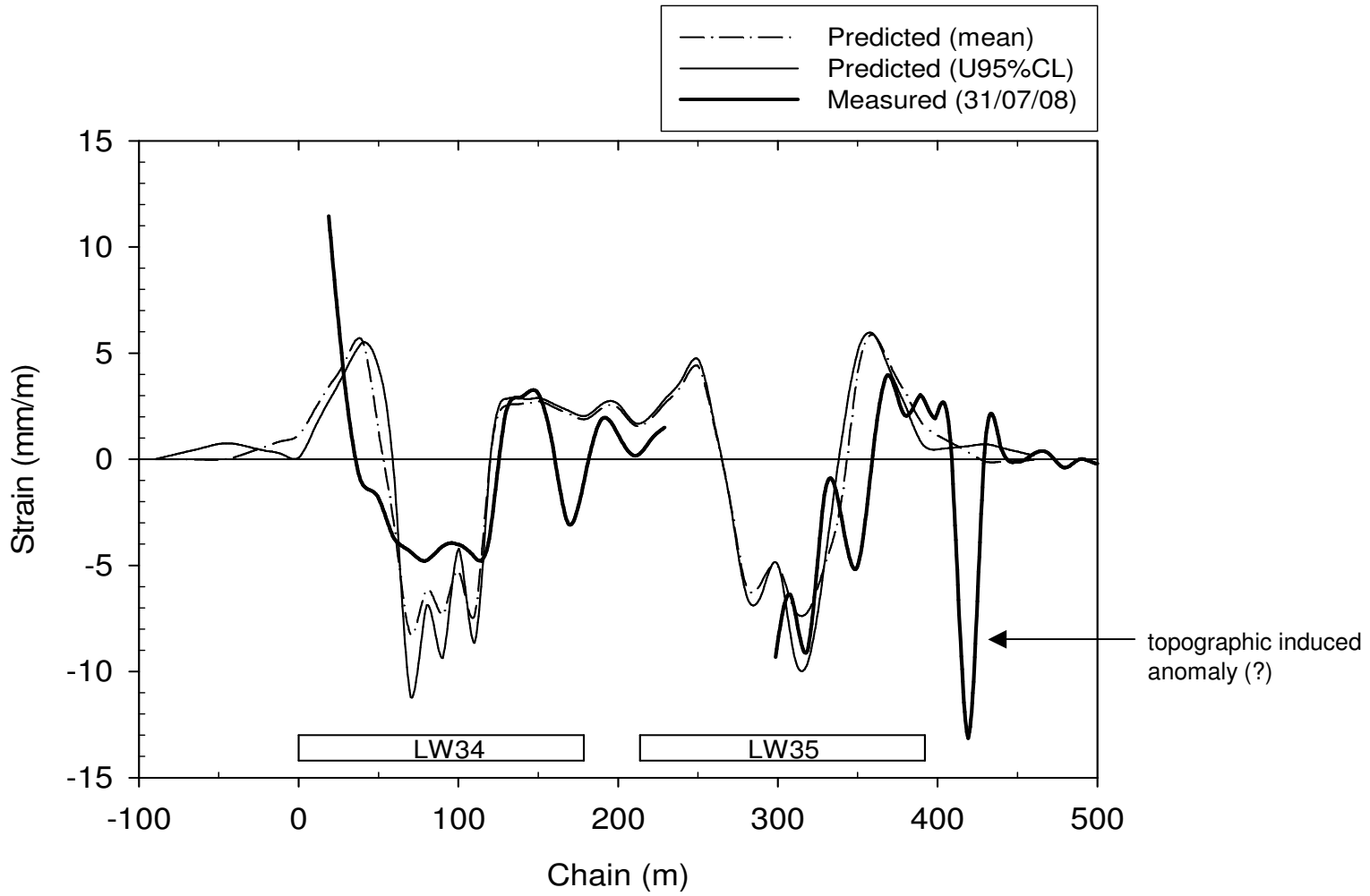
DgS	Engineer:	S.Ditton	Client:	DgS, 2008 Modified ACARP, 2003 Model Outcomes	
	Drawn:	S.Ditton			
	Date:	07.09.08	Title:	Predicted v. Measured Crossline Subsidence Profiles for a Newcastle Coalfield Longwall Longwall Panel	
	Ditton Geotechnical Services Pty Ltd		Scale:	NTS	Figure No: A35



DgS	Engineer:	S.Ditton	Client:	DgS, 2008 Modified ACARP, 2003 Model Outcomes	
	Drawn:	S.Ditton			
	Date:	07.09.08	Title:	Predicted v. Measured Crossline Tilt Profiles for a Newcastle Coalfield Longwall Mine	
	Ditton Geotechnical Services Pty Ltd		Scale:	NTS	Figure No: A36



DgS	Engineer:	S.Ditton	Client:	DgS, 2008 Modified ACARP, 2003 Model Outcomes	
	Drawn:	S.Ditton			
	Date:	07.09.08	Title:	Predicted v. Measured Crossline Curvature Profiles for a Newcastle Coalfield Longwall Mine	
	Ditton Geotechnical Services Pty Ltd		Scale:	NTS	Figure No: A37



DgS	Engineer:	S.Ditton	Client:	DgS, 2008 Modified ACARP, 2003 Model Outcomes	
	Drawn:	S.Ditton			
	Date:	08.09.08	Title:	Predicted v. Measured Crossline Strain Profiles for a Newcastle Coalfield Longwall Mine	
	Ditton Geotechnical Services Pty Ltd		Scale:	NTS	Figure No: A38



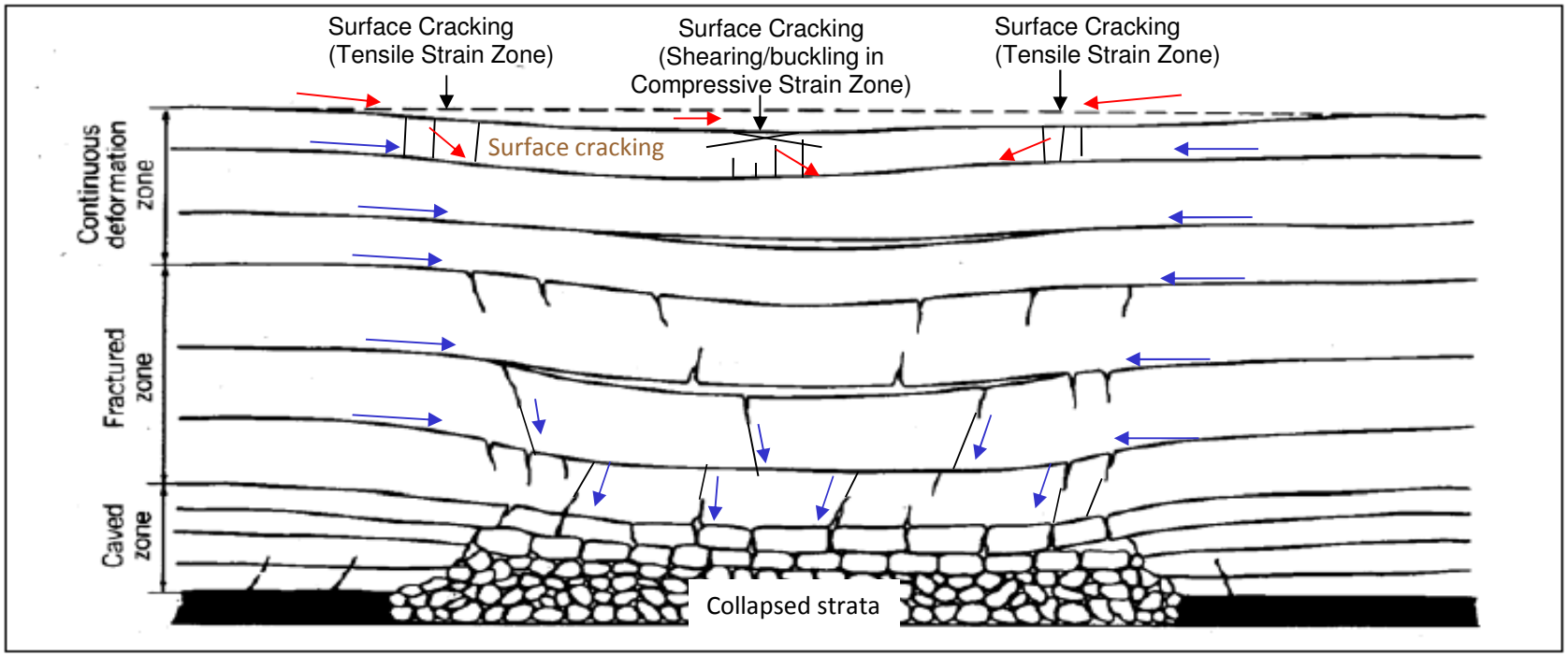
Strain Concentration Factor Calculation for 10 m Baylength^

- Measured crack width = 100 mm.
- Measured crack depth >5 m
- Location = 27 m from solid rib.
  Smax = 1.4 m.
- Cover depth, H = 180 m.
- LW panel width, W= 175 m.
  (W/H = 0.97)
- Measured curvature,
  C = 1.15 km-1
  (radius of 867 m)
- Measured strain over 10 m,
  E = 5.8 mm/m*
- Concentrated strain = crack width/bay-length = 100/10 = 10 mm/m.

Therefore, concentrated strain = 10/5.8 = 1.7 x uniform strain.

*- peak strains measured 10 m to south of crack at same distance from rib.
^ - It is likely that strain concentration includes strain from adjacent 'bays'.

DgS	Engineer:	S.Ditton	Client:	Adapted from ACARP, 2003	
	Drawn:	S.Ditton			
	Date:	08.08.08	Title:	Example of Strain Concentration Effect Above Longwall with Shallow Surface Rock	
	Ditton Geotechnical Services Pty Ltd		Scale:	NTS	Figure No: A39



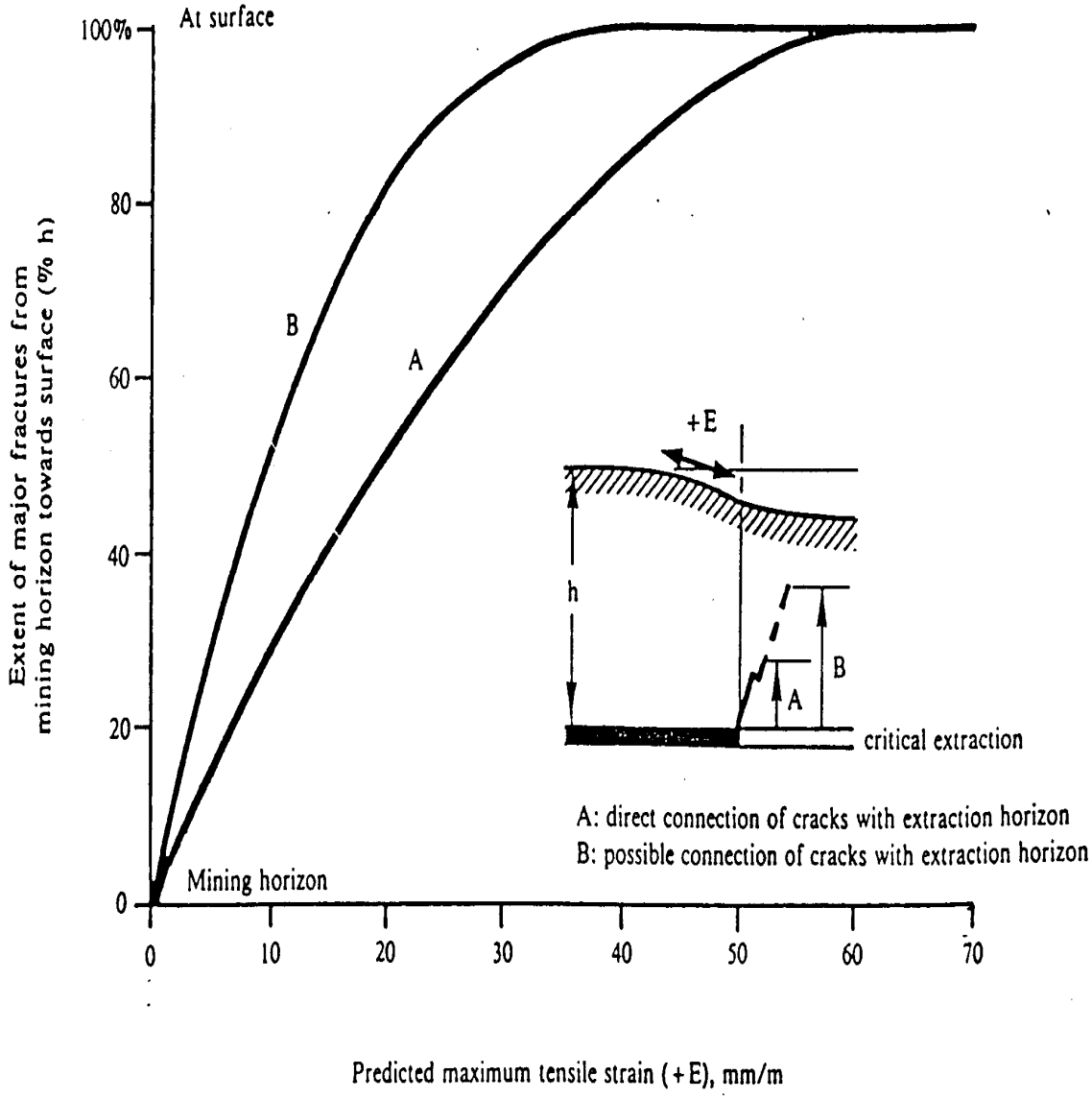
Zones in the Overburden According to Peng and Chiang (1984)

Key

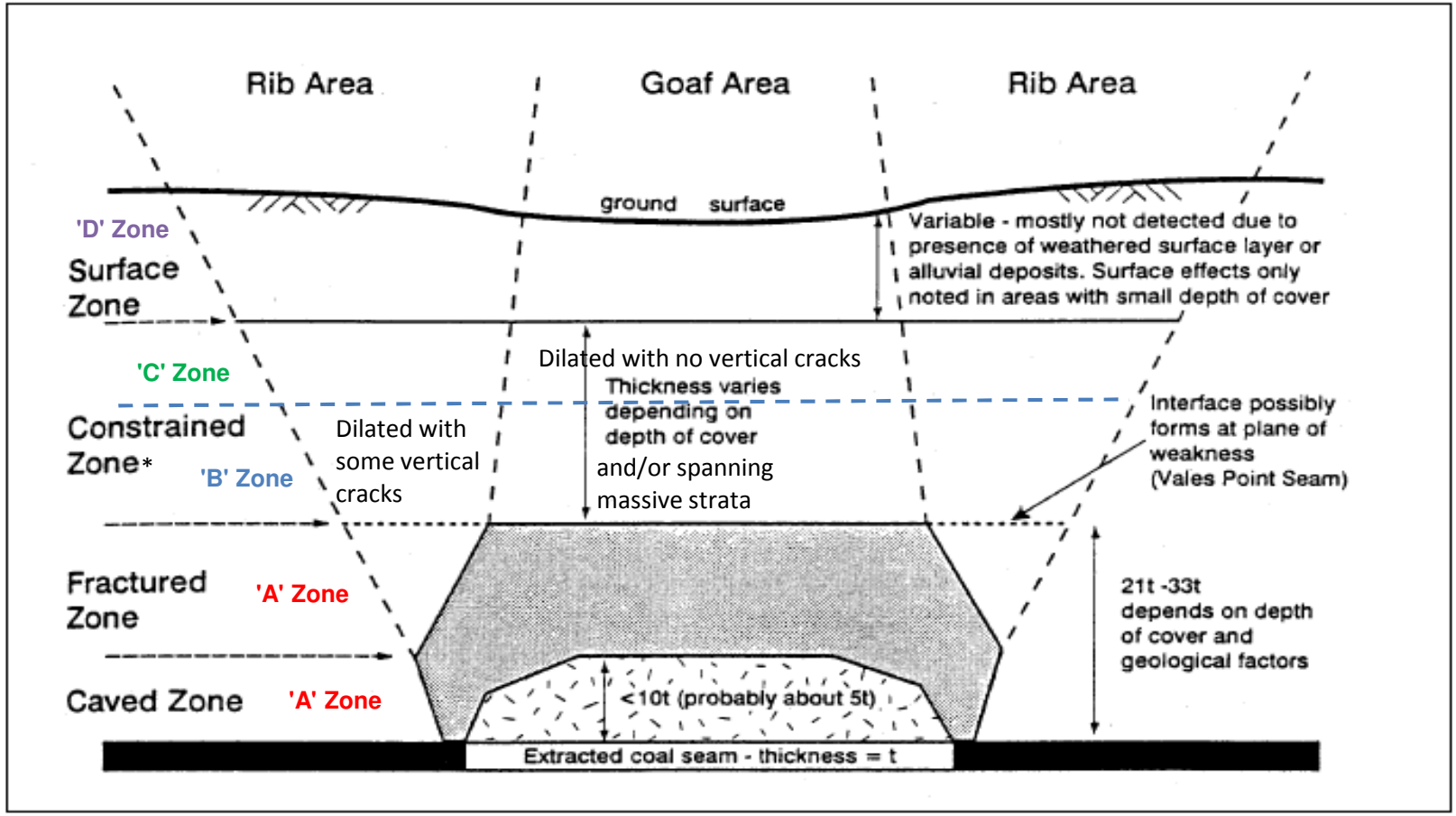
Surface water flow path

Sub-surface water flow path

DgS	Engineer:	S.Ditton	Client:	Appendix A	
	Drawn:	S.Ditton			
	Date:	23.11.12	Title:	Schematic Model of Overburden Fracture Zones Above Longwall Panels	
	Ditton Geotechnical Services Pty Ltd		Scale:	NTS	Figure No: A40a



DgS	Engineer:	S.Ditton	Client:	Extract from ACARP, 2003	
	Drawn:	S.Ditton			
	Date:	30.04.07	Title:	Enpirically Based Sub-Surface Fracturing Model Presented in Whittaker & Reddish, 1989	
	Ditton Geotechnical Services Pty Ltd		Scale:	NTS	Figure No: A40b



Zones in the Overburden according to Forster (1995)

* - Constrained Zone generally means B-Zone, but may include C-Zone , depending on W/H ratio and geology

DgS	Engineer:	S.Ditton	Client:	Appendix A	
	Drawn:	S.Ditton			
	Date:	23.11.12	Title:	Schematic Model of Overburden Fracture Zones in **Forster, 1995** Model (based on Piezometric Data Above High Extraction Panels in the Newcastle Coalfield)	
	Ditton Geotechnical Services Pty Ltd		Scale:	NTS	Figure No: A40c

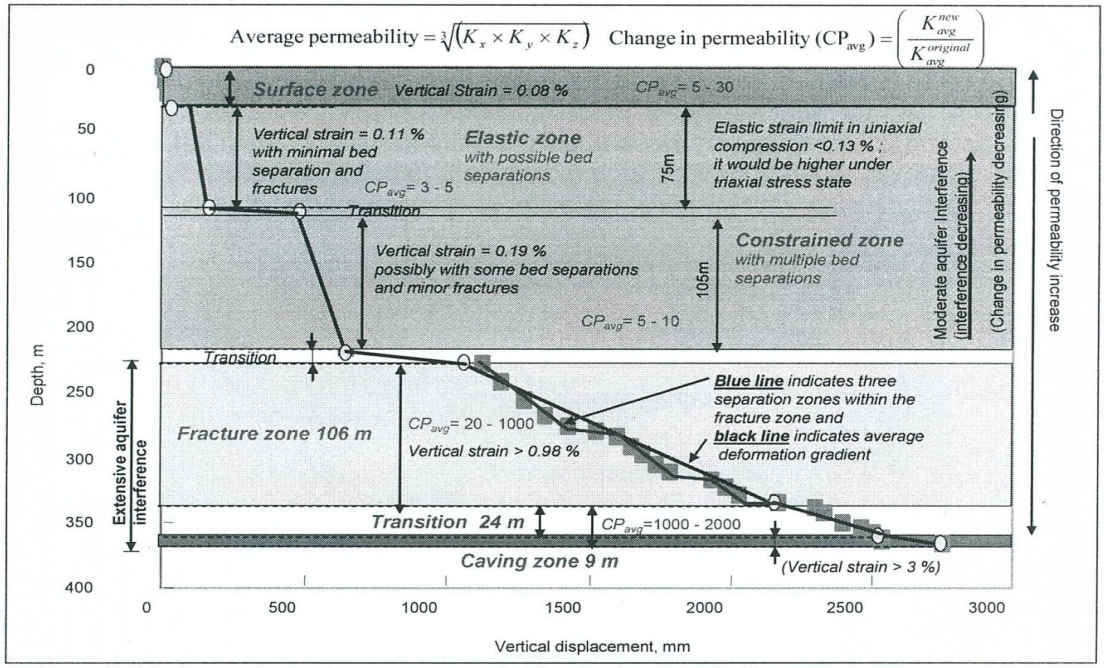


Figure H. Hydrogeological response model for Springvale Colliery

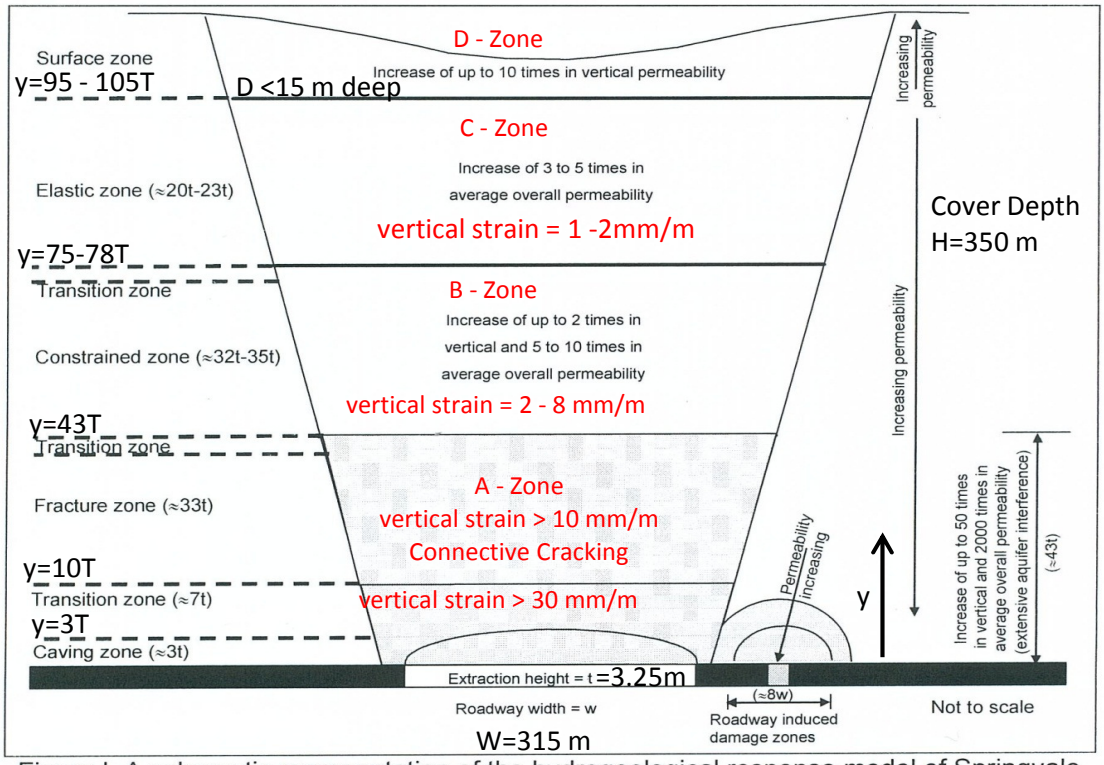


Figure I. A schematic representation of the hydrogeological response model of Springvale Colliery

DgS	Engineer:	S.Ditton	Client:	Appendix A	
	Drawn:	S.Ditton			
	Date:	23.11.12	Title:	Schematic Model of Overburden Fracture Zones **in ACARP, 2007**	
	Ditton Geotechnical Services Pty Ltd		Scale:		Figure No: A40d

Figure 6 is a conceptual model that illustrates the type of damage that can be expected within the overburden due to subsidence above a full-extraction panel. Five broad zones can be identified [Singh and Kendorski 1981; Peng and Chiang 1984; Kendorski 1993, 2006]:

1. The *complete caving zone*, in which the roof rock is completely disrupted as it falls into the gob, normally extends two to four times the extracted seam height (h).
2. The *partial caving zone,* in which the beds are completely fractured but never lose contact with one another, extends up to 6–10 h.
3. The *fracture zone,* within which the subsidence strains are great enough to cause new fracturing in the rock and create direct hydraulic connections to the lower seam. The top of this zone can be as high as 24 h above the lower seam.
4. The *dilated zone,* where the permeability is enhanced but little new fracturing is created, extends up to 60 h.
5. The *confined zone,* where subsidence normally causes no change in strata properties other than occasional bed slippage. This zone extends from the top of the dilated zone to about 50 ft below the surface.

6. D - Zone (<15 m)

5. C - Zone

4. B - Zone

3. A - Zone

1, 2. A - Zone

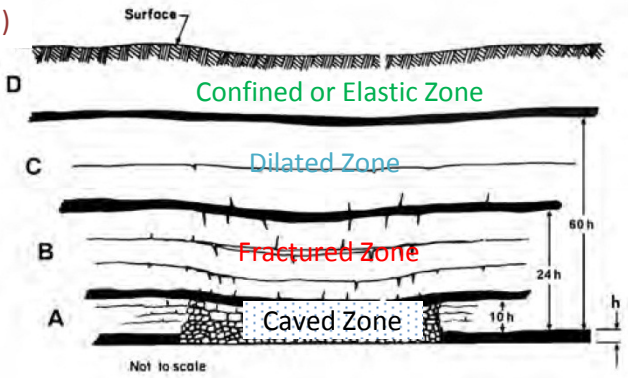


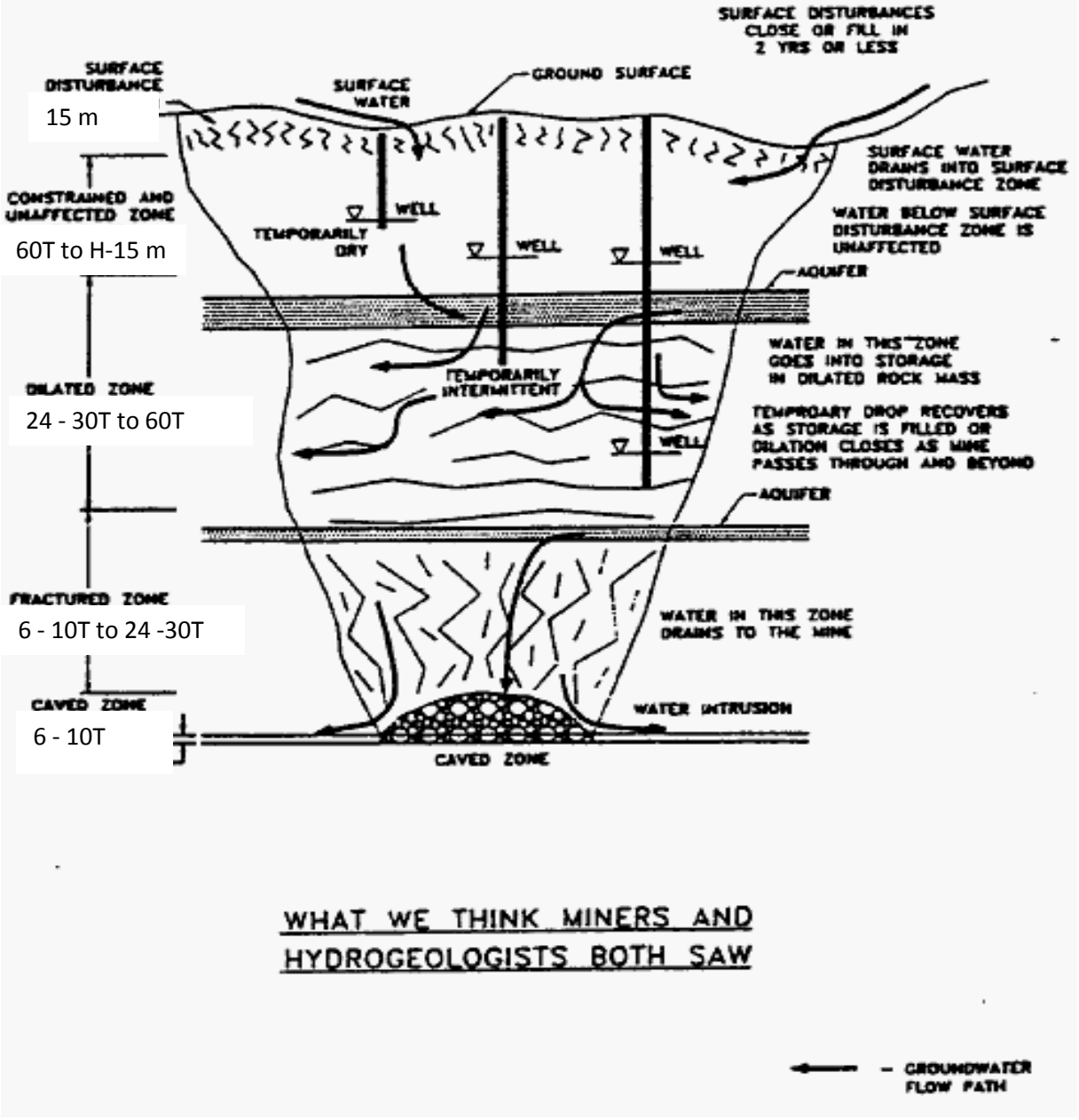
Figure 6.—Overburden response to full-extraction mining: (A) caving zones, (B) fracture zone, (C) dilated zone, and (D) confined zone.

The dimensions of these zones vary from panel to panel because of differences in geology and panel geometry. The implication of this model for multiple-seam mining is that when the interburden thickness exceeds approximately 6–10 times the lower seam thickness, the upper seam should be largely intact, although the roof may be fractured or otherwise damaged.

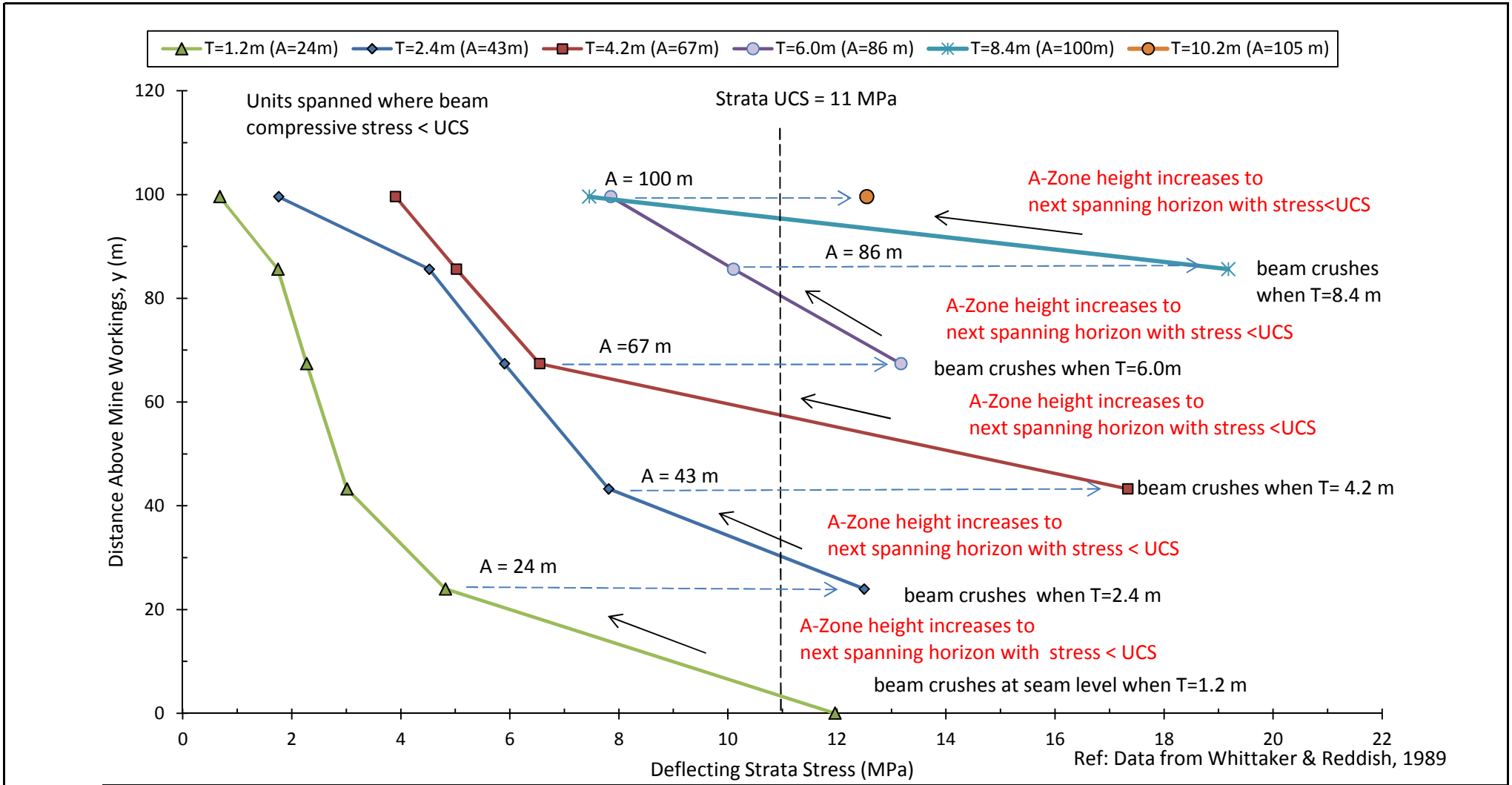
Note: Equivalent **ACARP, 2007** model zones A to D also shown down the left side.

DgS	Engineer:	S.Ditton	Client:	Appendix A	
	Drawn:	S.Ditton			
	Date:	03.06.13	Title:	Model of Overburden Fracture Zones above US Longwall Mines According to Mark, 2007	
	Ditton Geotechnical Services Pty Ltd		Scale:		Figure No: A40e

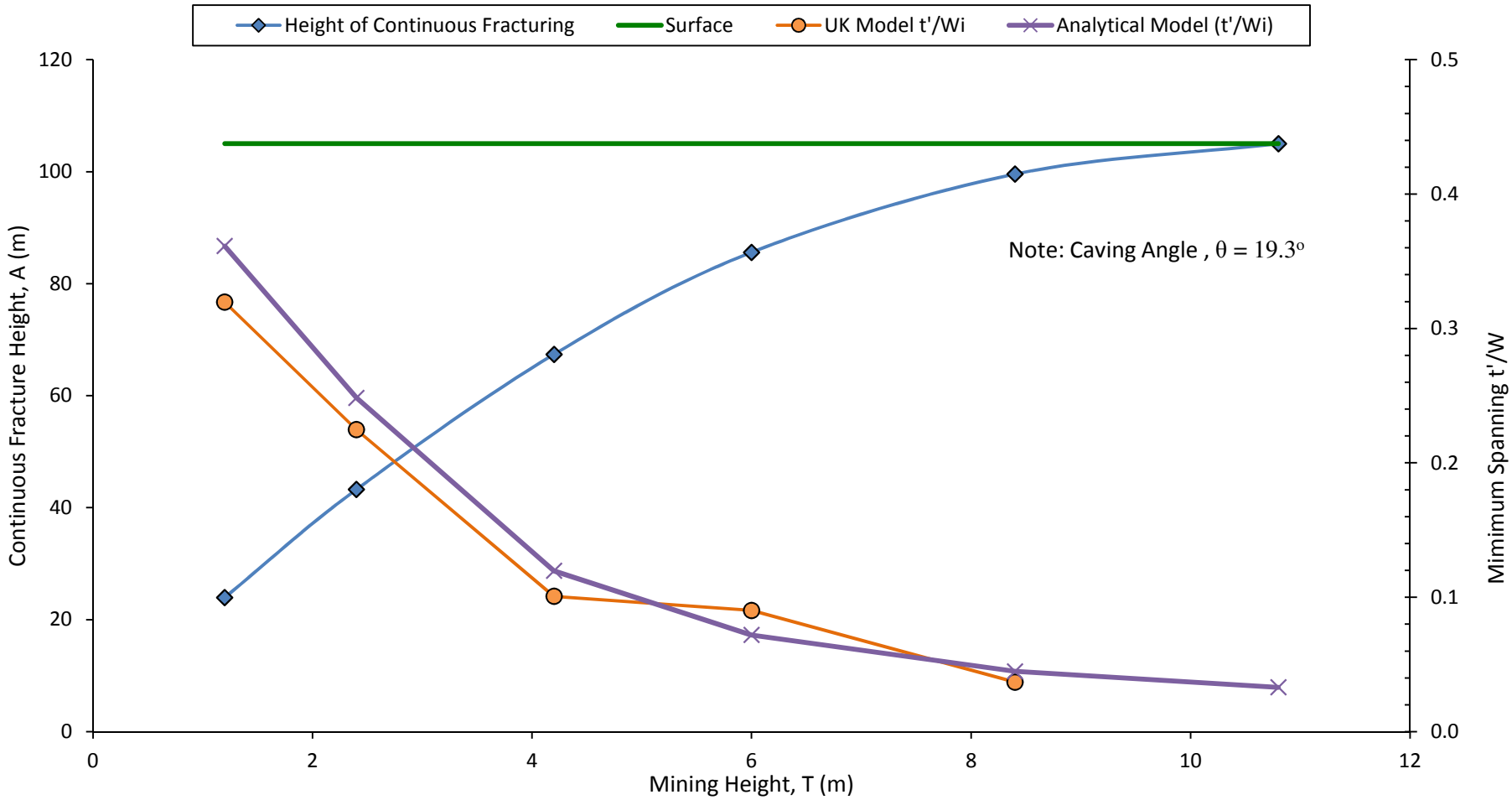
Zone and Thickness Ranges
(based on Mining Height, T)



DgS	Engineer:	S.Ditton	Client:	Appendix A	
	Drawn:	S.Ditton			
	Date:	03.06.13	Title:	Model of Overburden Fracture Zones above UK Longwall Mines According to Kendorski, 1993	
	Ditton Geotechnical Services Pty Ltd		Scale:		Figure No: A40f

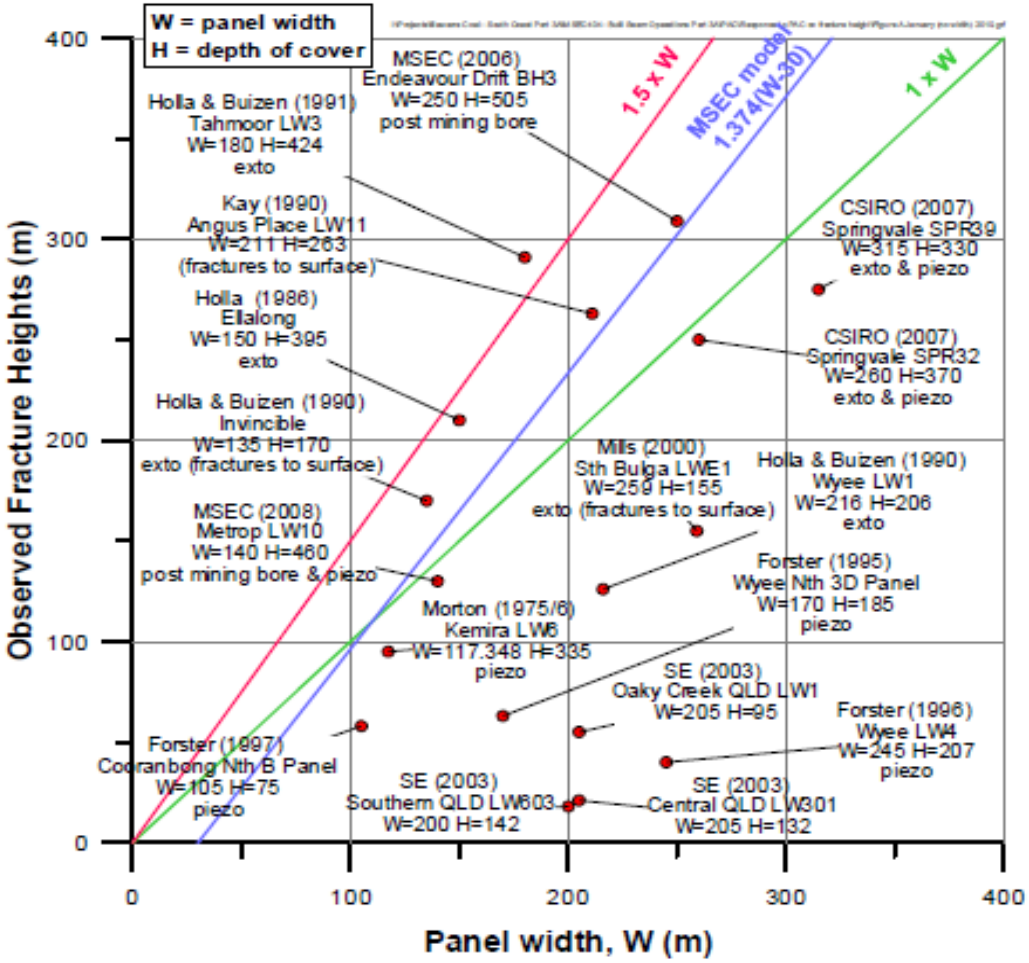


DgS	Engineer:	S.Ditton	Client:	Review of Height of Fracturing Data	
	Drawn:	S.Ditton			
	Date:	07.06.13	Title:	Interpreted Beam Stress in Spanning Units of Physical Model of Laminated Overburden above a Longwall	
	Ditton Geotechnical Services Pty Ltd		Scale:	NTS	Figure No: A40g



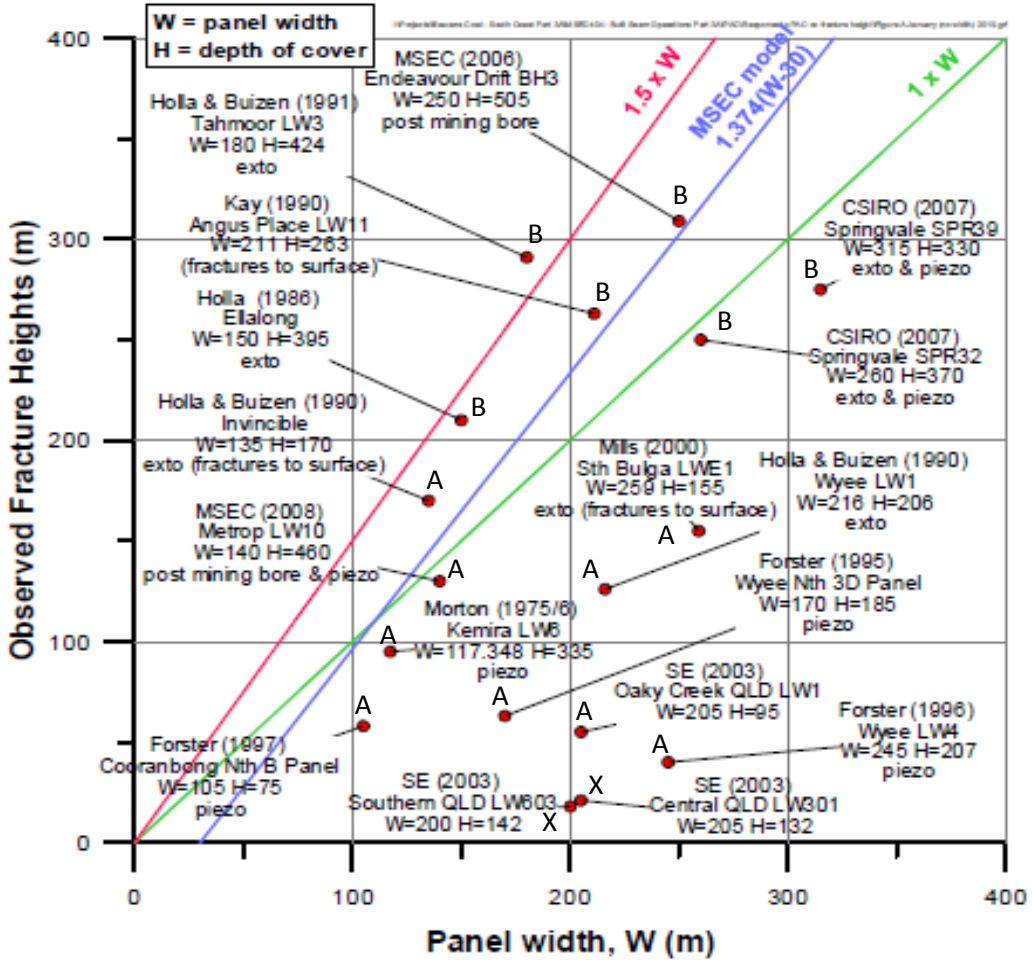
Ref: Data from Whittaker & Reddish, 1989

DgS	Engineer:	S.Ditton	Client:	Review of Height of Fracturing Data	
	Drawn:	S.Ditton			
	Date:	07.06.13	Title:	Analytical v. Physical HoF Model Mimimum Beam Thickness Required to Span the Continuous Fracture Zone	
	Ditton Geotechnical Services Pty Ltd		Scale:	NTS	Figure No: A40h



Ref: MSEC, 2011

DgS	Engineer:	S.Ditton	Client:	Review of Height of Fracturing Data	
	Drawn:	S.Ditton			
	Date:	07.06.13	Title:	Observed Fracture Height Models presented by SCT and MSEC	
	Ditton Geotechnical Services Pty Ltd		Scale:	NTS	Figure No: A40i



Key

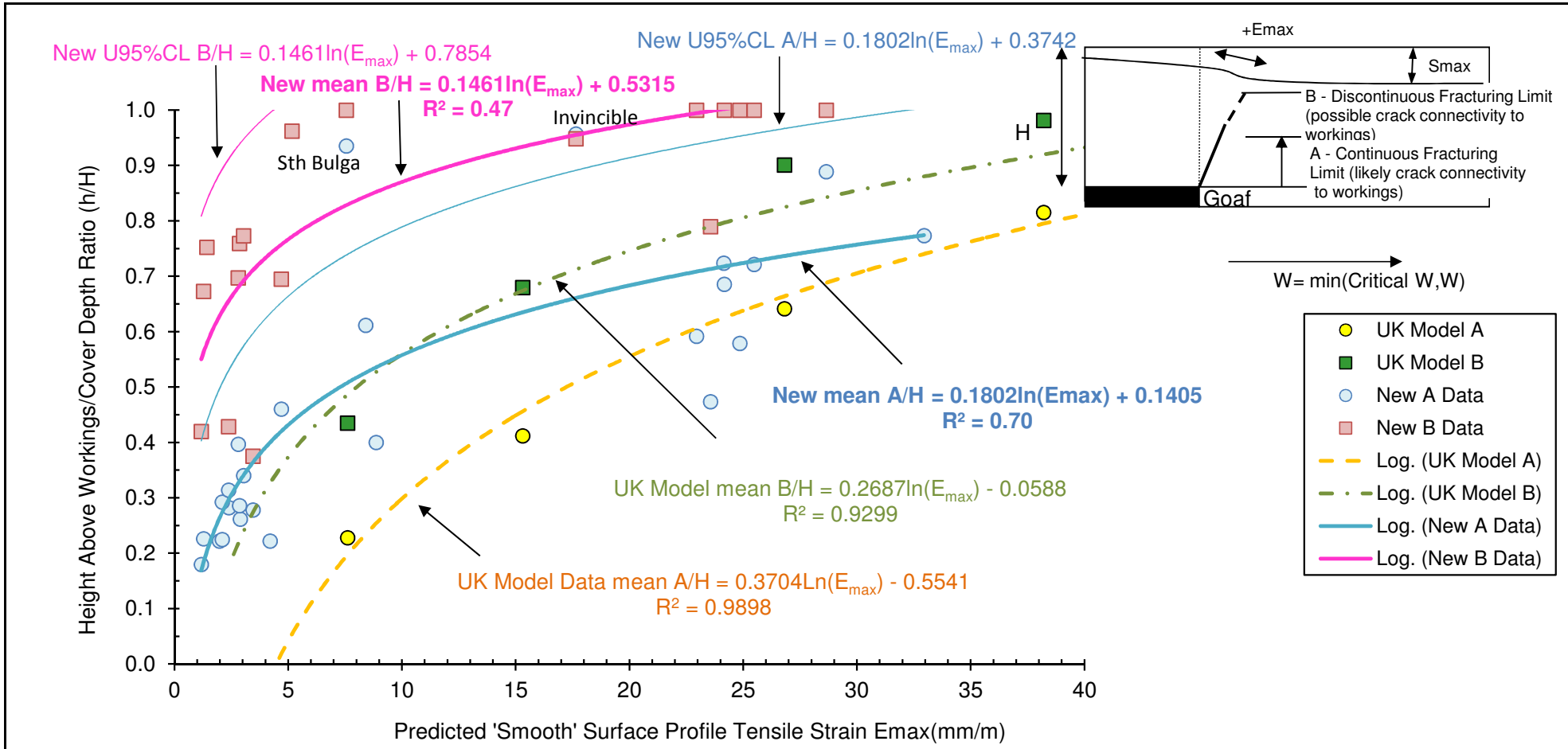
A: A-Zone Horizon

B: B-Zone Horizon

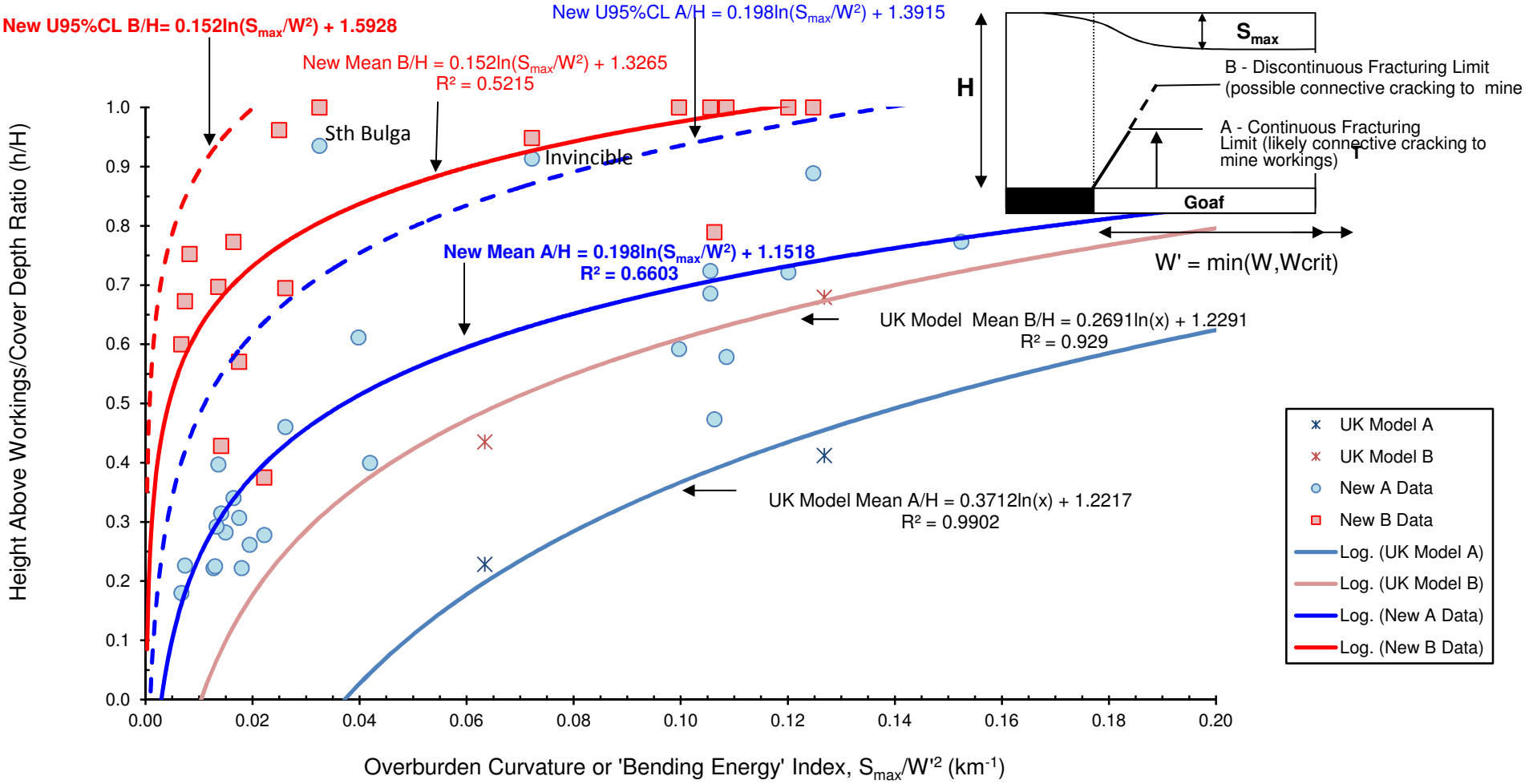
X: In-conclusive data

Ref: MSEC, 2011

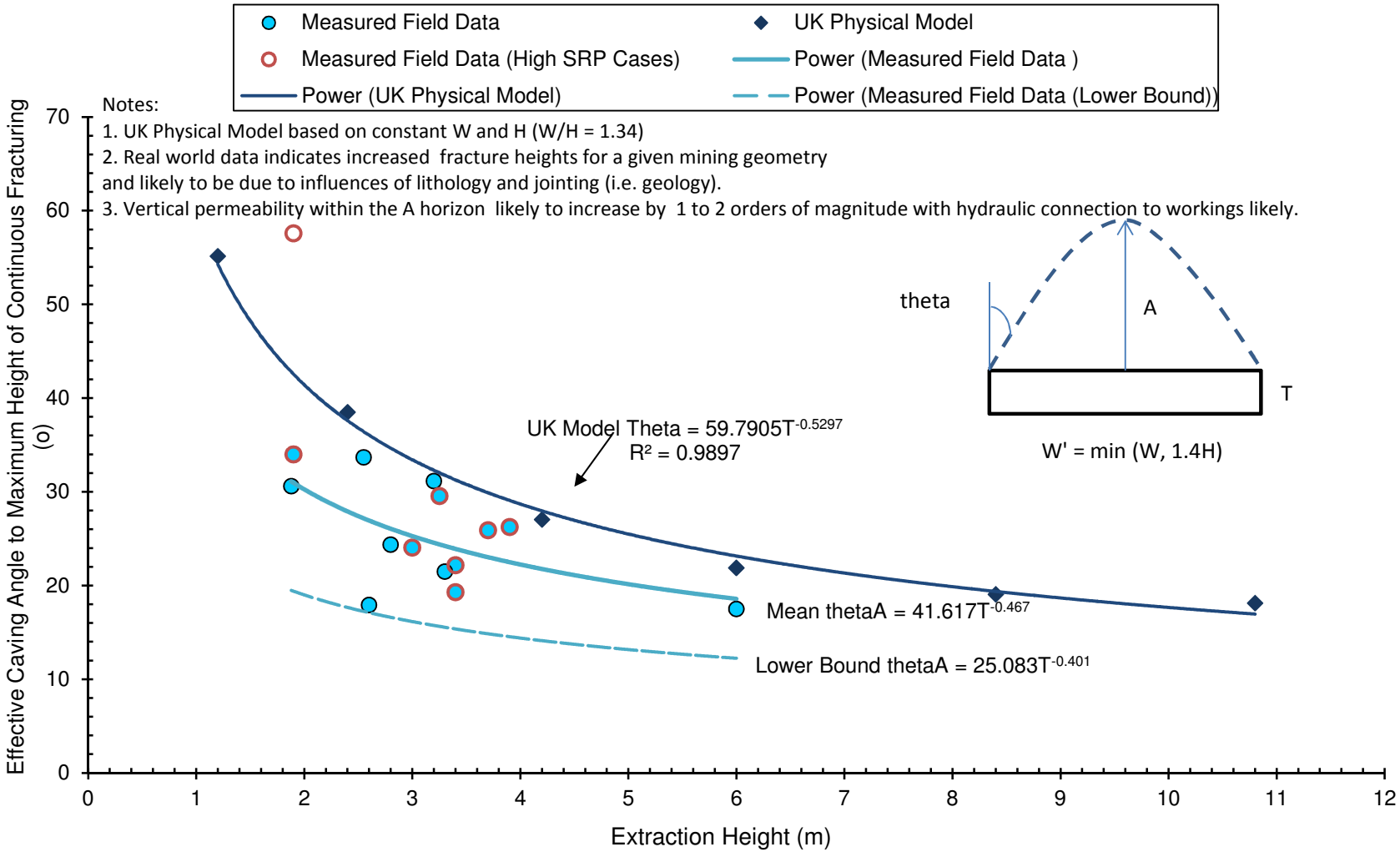
DgS	Engineer:	S.Ditton	Client:	Review of Height of Fracturing Data	
	Drawn:	S.Ditton			
	Date:	07.06.13	Title:	Review of Observed Fracture Height Models presented by SCT and MSEC v. Whittaker & Reddish Sub-Surface Fracture Model Zoning	
	Ditton Geotechnical Services Pty Ltd		Scale:	NTS	Figure No: A40j



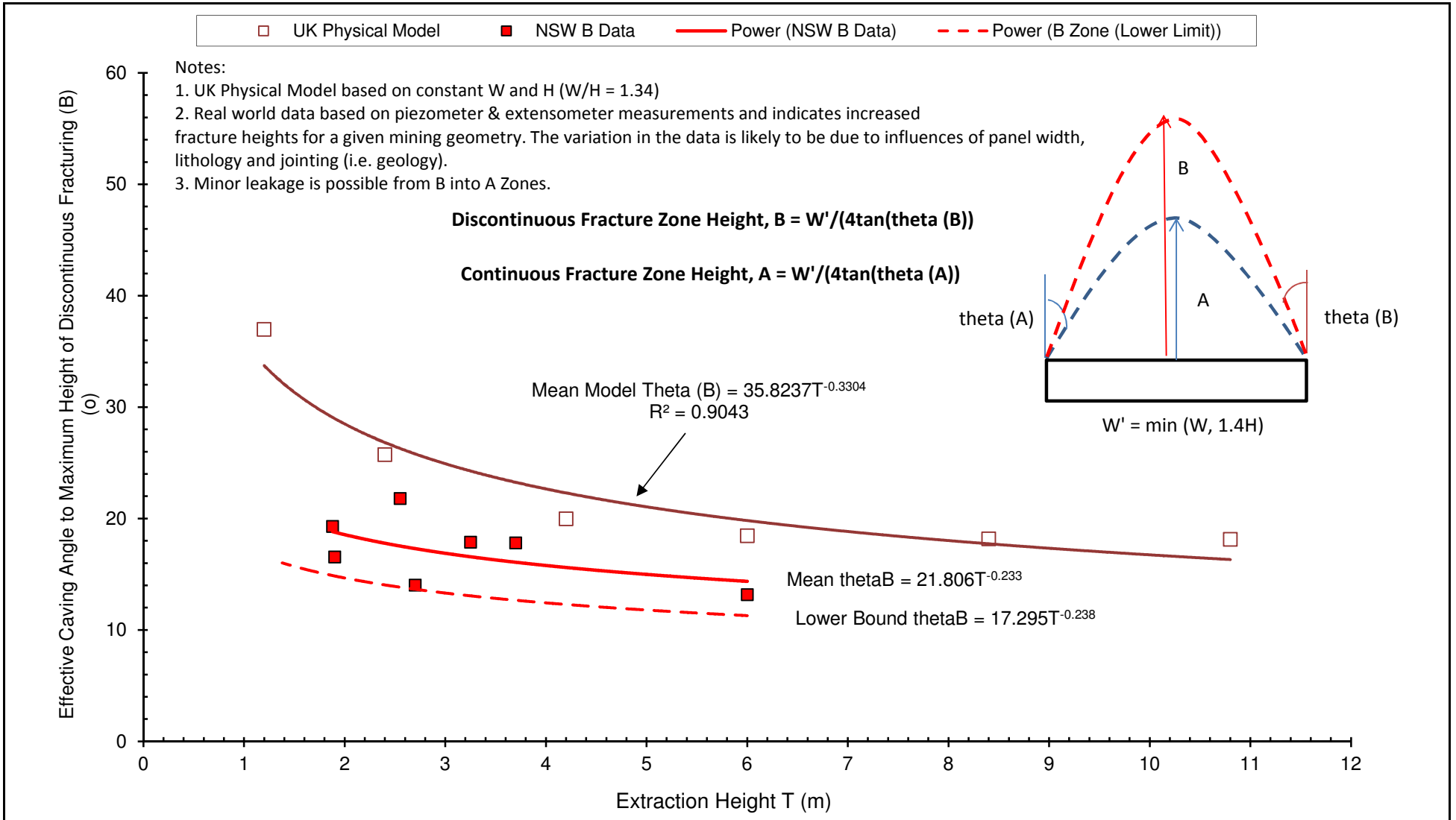
DgS	Engineer: S.Ditton	Client:	Updated Whittaker and Reddish Model presented in ACARP, 2003	
	Drawn: S.Ditton			
	Date: 18.11.12	Title:	Continuous and Discontinuous Sub-Surface Fracture Height Model above Longwalls using Surface Tensile Strains as the Key Indicator	
	Ditton Geotechnical Services Pty Ltd	Scale:	NTS	Figure No: A41a



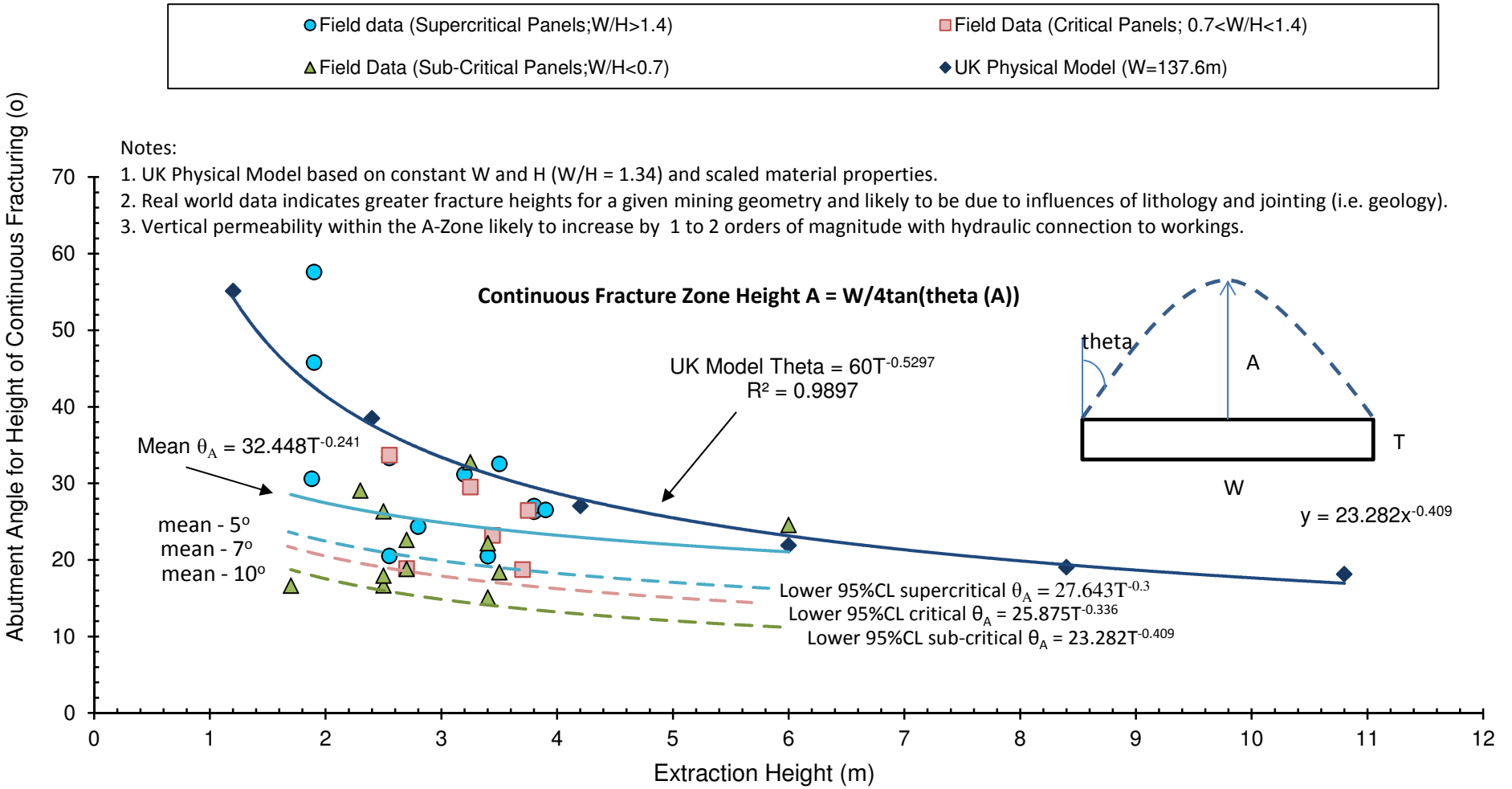
DgS	Engineer:	S.Ditton	Client:	Updated from ACARP, 2003	
	Drawn:	S.Ditton			
	Date:	03.12.12	Title:	Continuous and Discontinuous Sub-Surface Fracture Heights above Longwalls (based on ACARP, 2003)	
	Ditton Geotechnical Services Pty Ltd		Scale:	NTS	Figure No: A41b



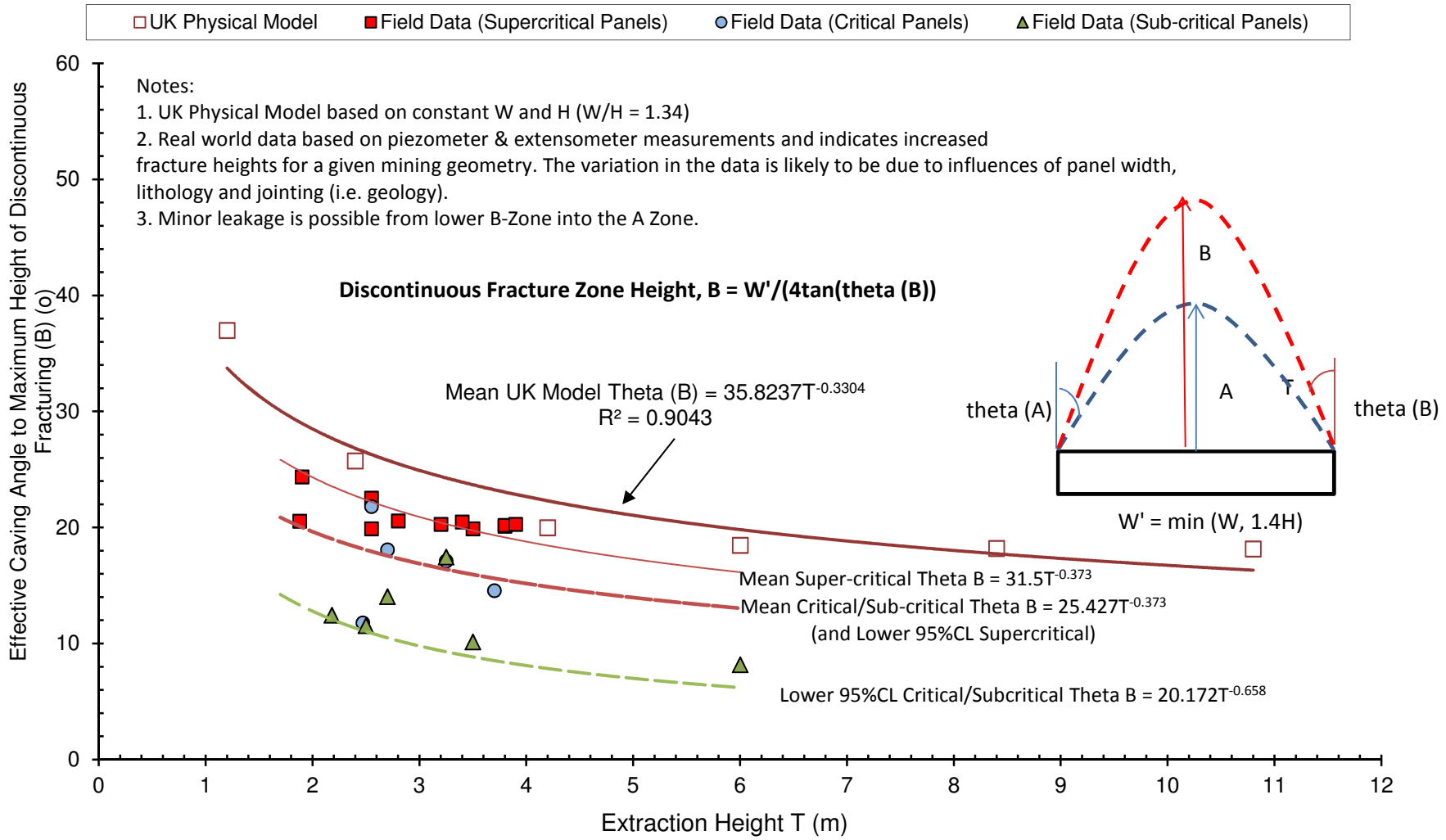
DgS	Engineer:	S.Ditton	Client:	Modified from ACARP, 2003 (DgS,2012)	
	Drawn:	S.Ditton			
	Date:	15.11.12	Title:	Alternative ACARP, 2003 A-Zone Sub-Surface Fracture Height Model based on Panel Width and Mining Height as Key Parameters	
	Ditton Geotechnical Services Pty Ltd		Scale:	NTS	Figure No: A41c



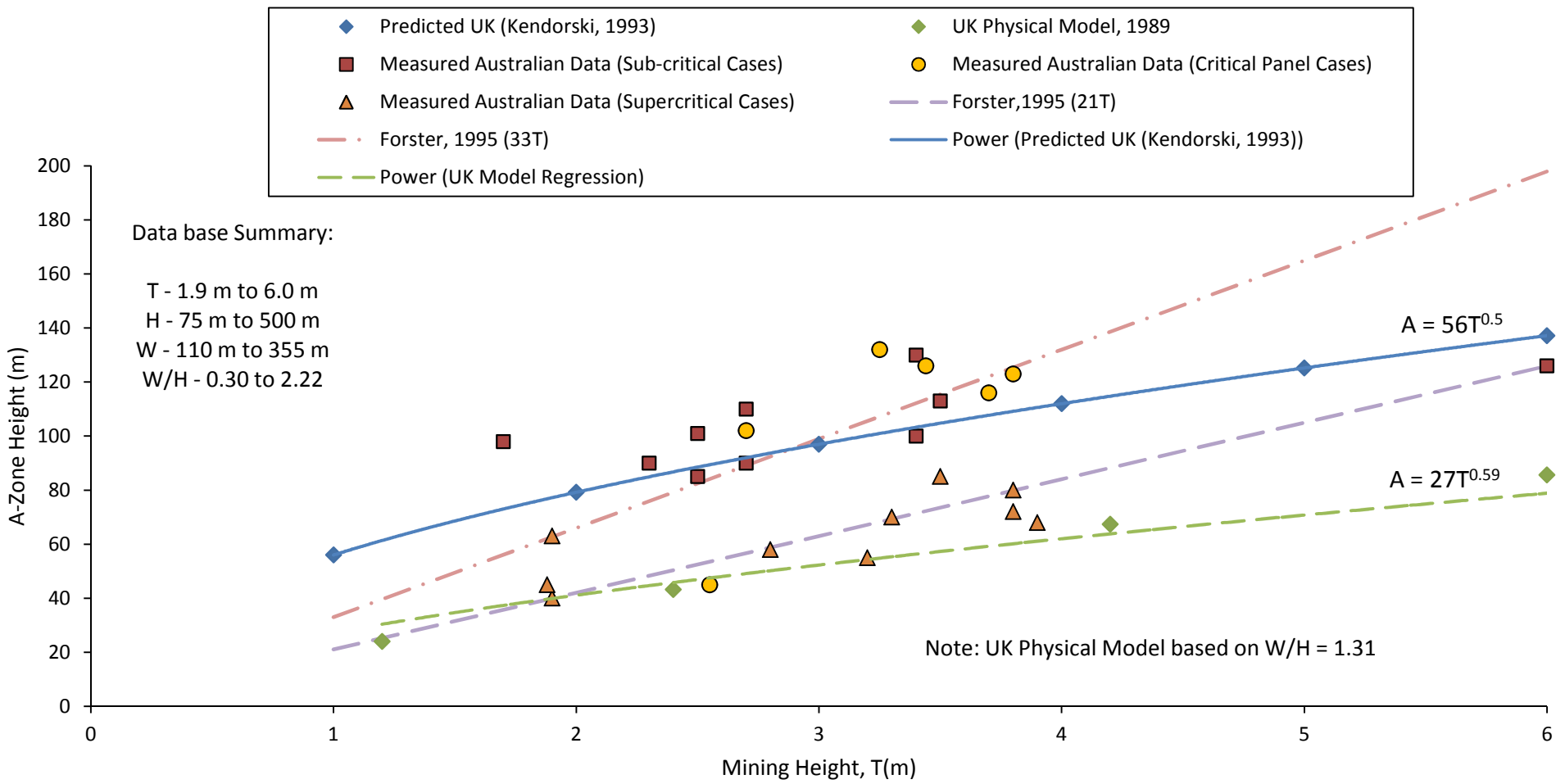
DgS	Engineer:	S.Ditton	Client:	Modified from ACARP, 2003 (DgS,2012)	
	Drawn:	S.Ditton			
	Date:	15.11.12	Title:	Alternative ACARP, 2003 B-Zone Sub-Surface Fracture Height Model based on Panel Width and Mining Height as Key Parameters	
	Ditton Geotechnical Services Pty Ltd		Scale:	NTS	Figure No: A41d



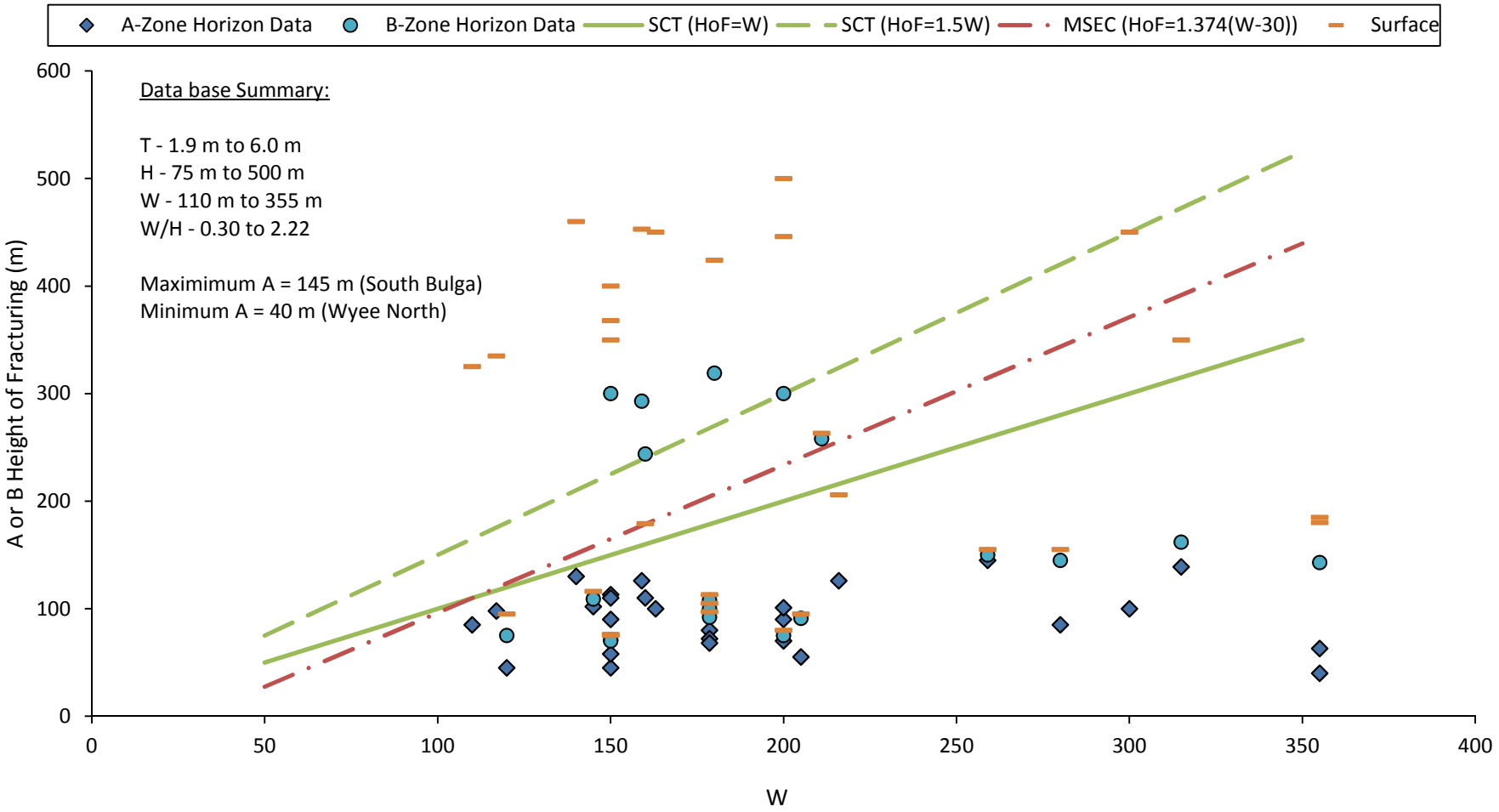
DgS	Engineer:	S.Ditton	Client:	Modified from ACARP, 2003	
	Drawn:	S.Ditton			
	Date:	10.06.13	Title:	Predicted Height of Continuous Fracturing Based on HoF Angle and Mining Height	
	Ditton Geotechnical Services Pty Ltd		Scale:	NTS	Figure No: A41e



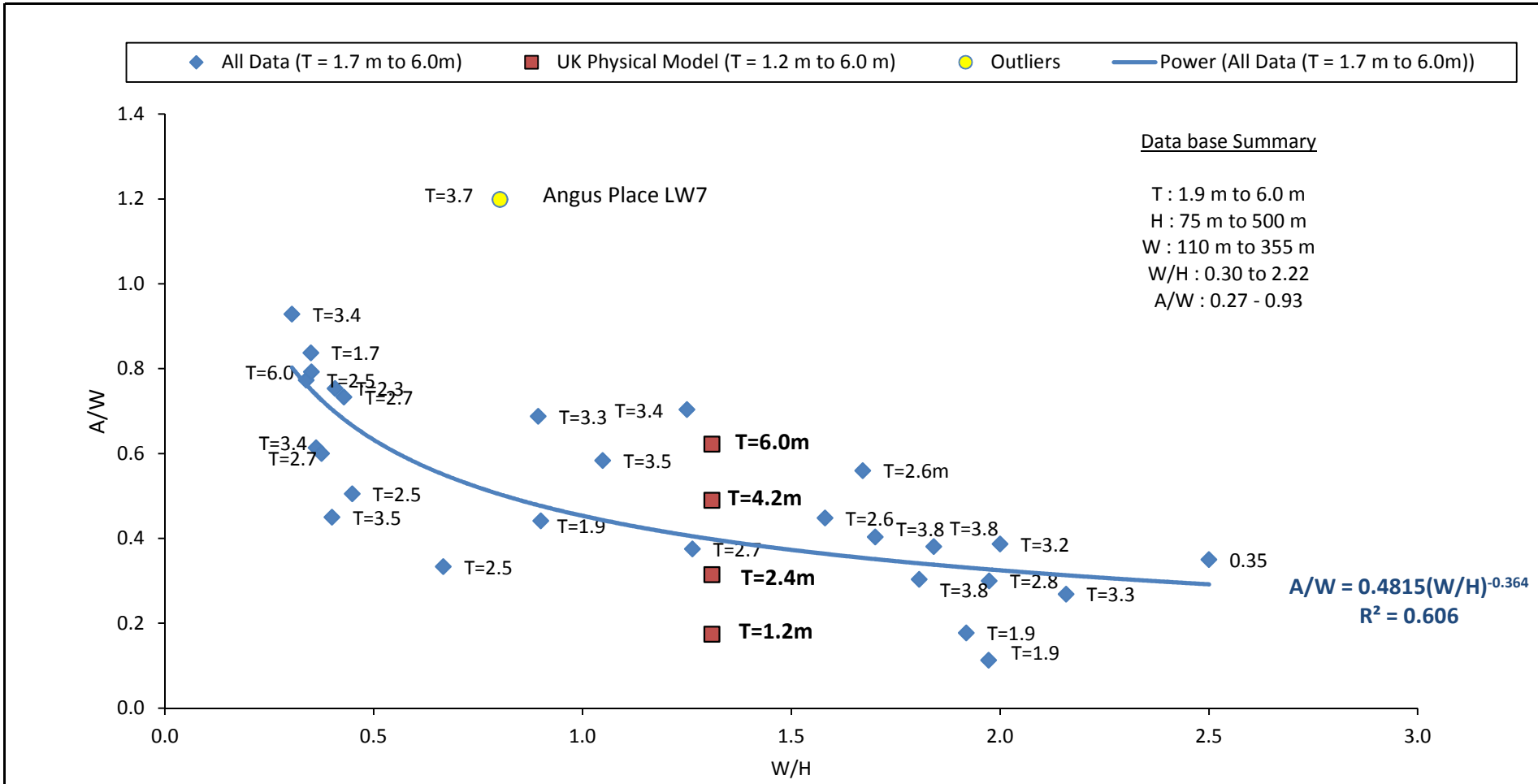
DgS	Engineer:	S.Ditton	Client:	Modified from ACARP, 2003	
	Drawn:	S.Ditton			
	Date:	10.06.13	Title:	Predicted Height of Discontinuous Fracturing Based on Measured Heights of Discontinuous Fracture Angles and Mining Height	
	Ditton Geotechnical Services Pty Ltd		Scale:	NTS	Figure No: A41f



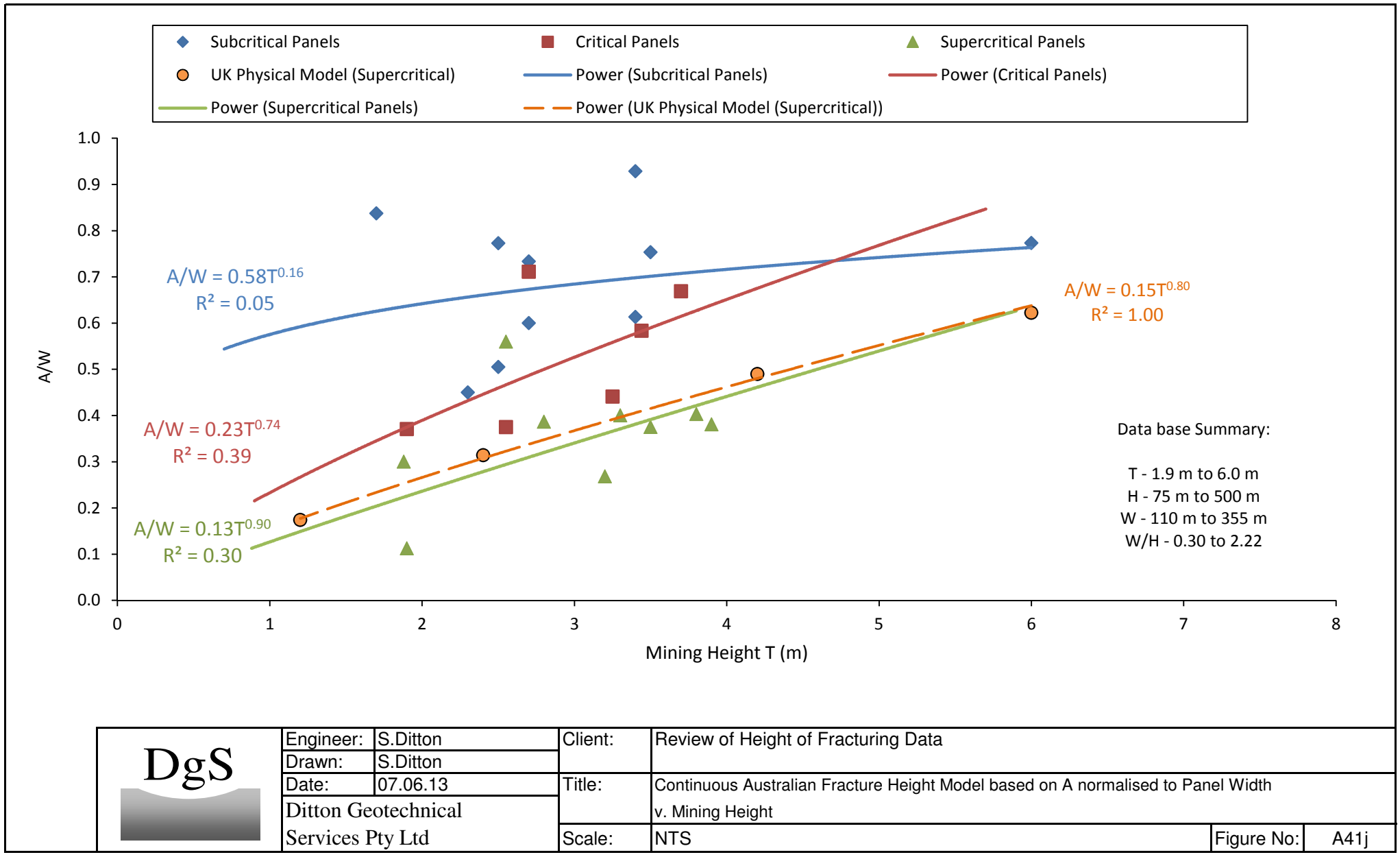
DgS	Engineer:	S.Ditton	Client:	Review of Height of Fracturing Data	
	Drawn:	S.Ditton			
	Date:	07.06.13	Title:	Continuous UK Fracture Height Models based on Mining Height Only v. Measured Australian Database	
	Ditton Geotechnical Services Pty Ltd		Scale:	NTS	Figure No: A41g



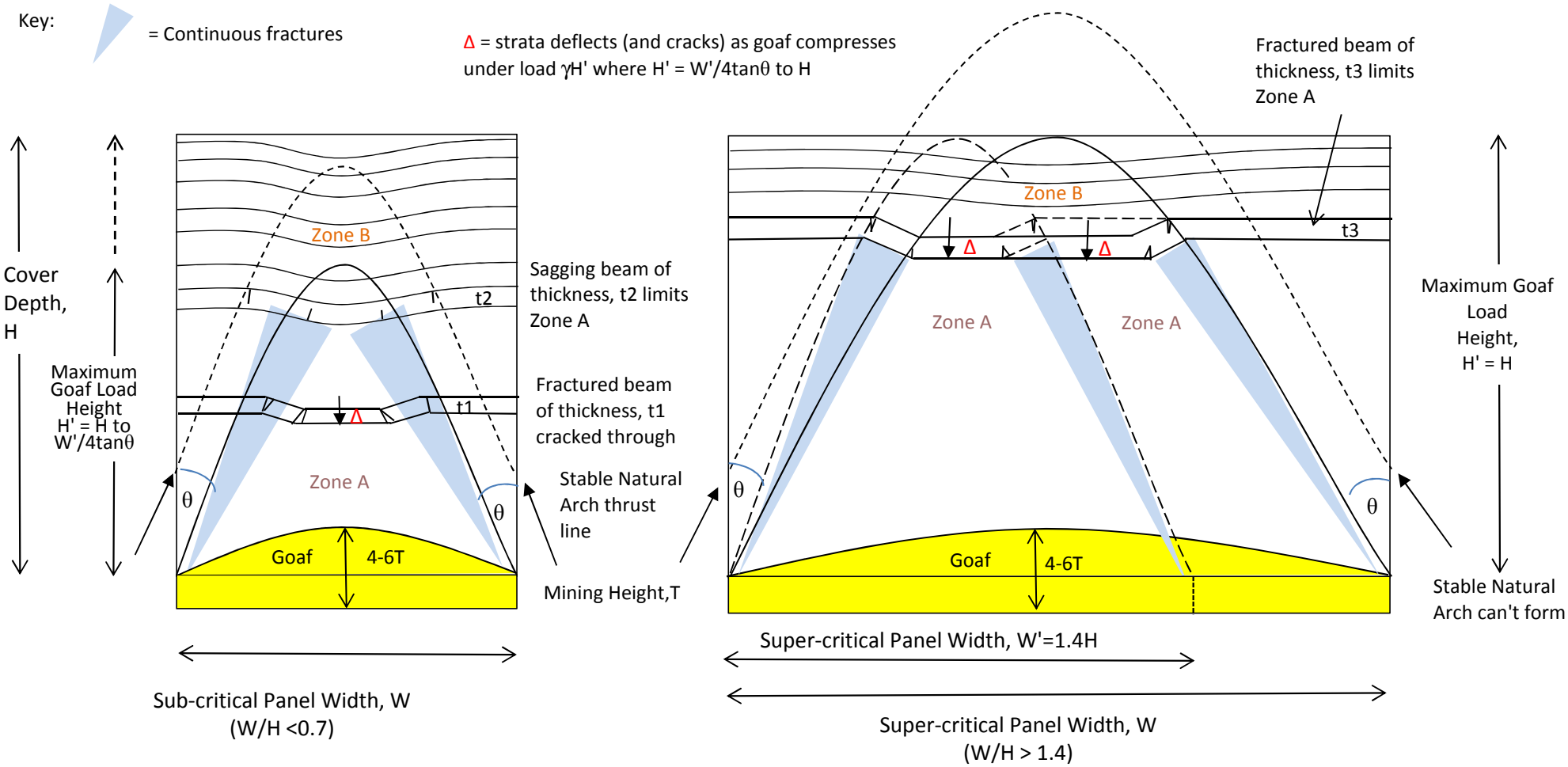
DgS	Engineer:	S.Ditton	Client:	Review of Height of Fracturing Data	
	Drawn:	S.Ditton			
	Date:	07.06.13	Title:	Continuous Australian Fracture Height Model based on Panel Width Only Database	
	Ditton Geotechnical Services Pty Ltd		Scale:	NTS	Figure No: A41h



DgS	Engineer:	S.Ditton	Client:	Review of Height of Fracturing Data	
	Drawn:	S.Ditton			
	Date:	07.06.13	Title:	Continuous Australian Fracture Height Model based on A normalised to Panel Width with Influence of Mining Height Included	
Ditton Geotechnical Services Pty Ltd			Scale:	NTS	Figure No: A41i

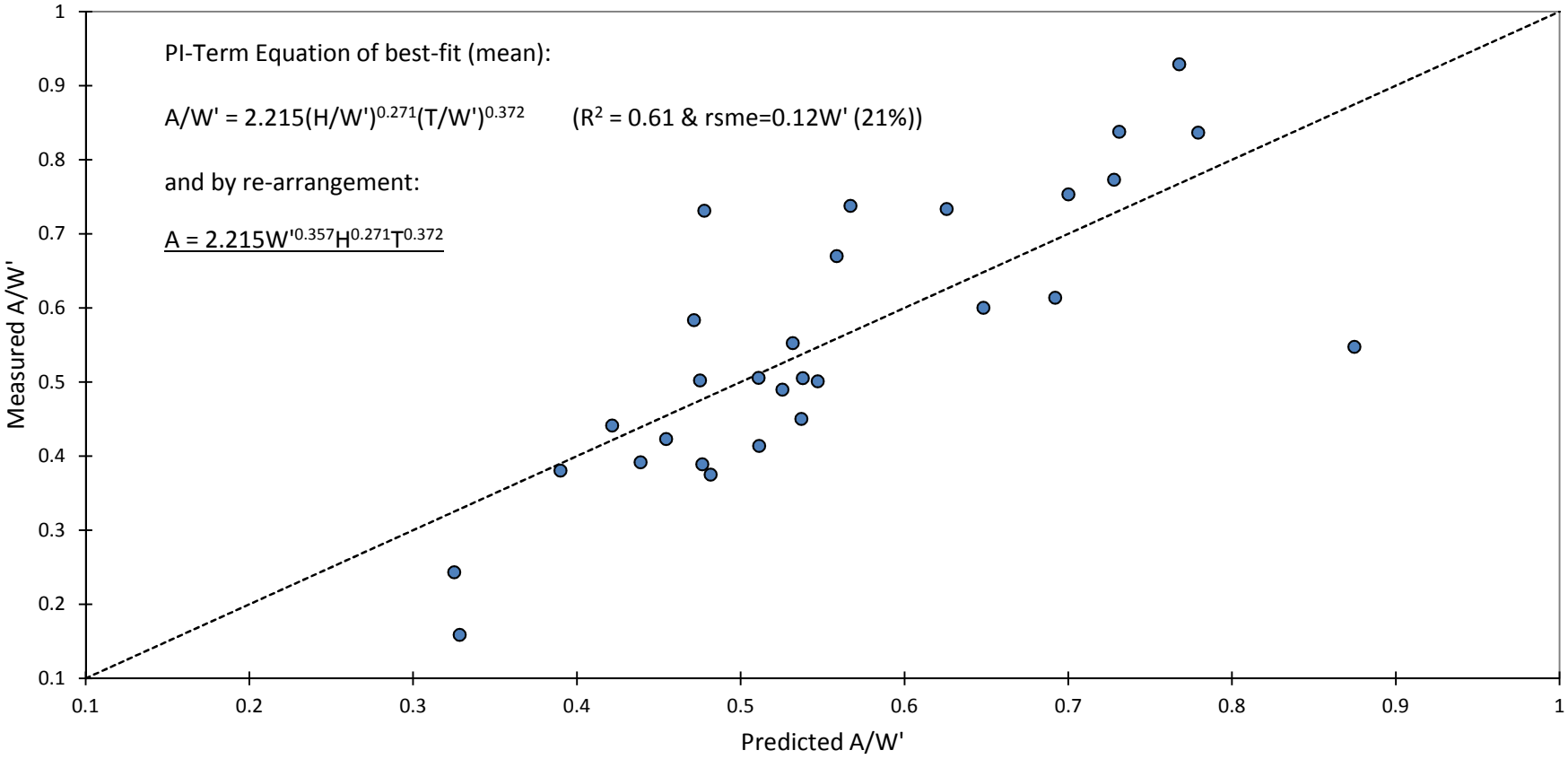


DgS	Engineer: S.Ditton	Client:	Review of Height of Fracturing Data	
	Drawn: S.Ditton			
	Date: 07.06.13	Title:	Continuous Australian Fracture Height Model based on A normalised to Panel Width v. Mining Height	
	Ditton Geotechnical Services Pty Ltd	Scale:	NTS	Figure No: A41j

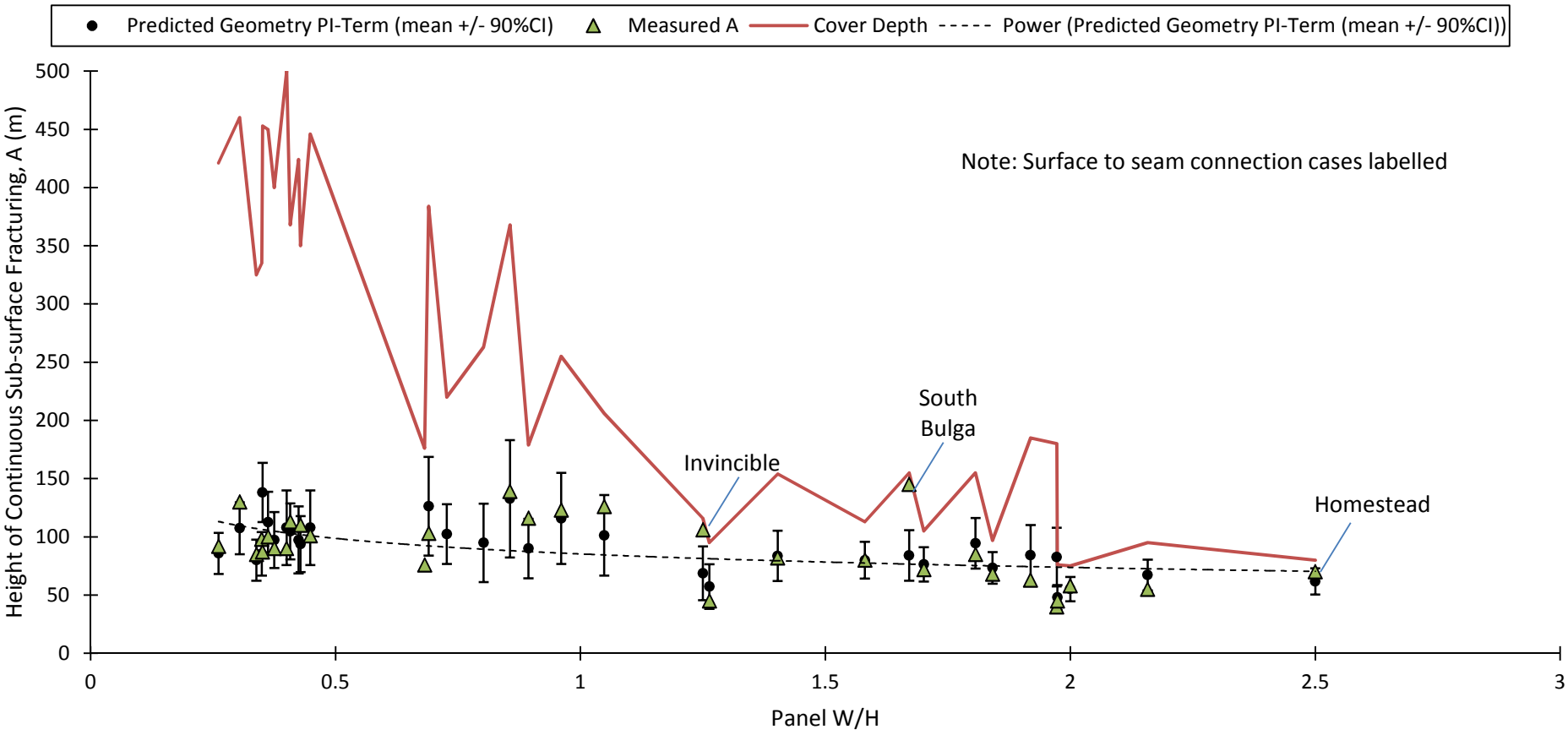


DgS	Engineer:	S.Ditton	Client:	Review of Height of Fracturing Data
	Drawn:	S.Ditton		
	Date:	26.08.13	Title:	Conceptual Model for Development of Height of Continuous Fracturing Zone for a range of Longwall Panel Geometries
Ditton Geotechnical Services Pty Ltd			Scale:	NTS — Figure No: A42a

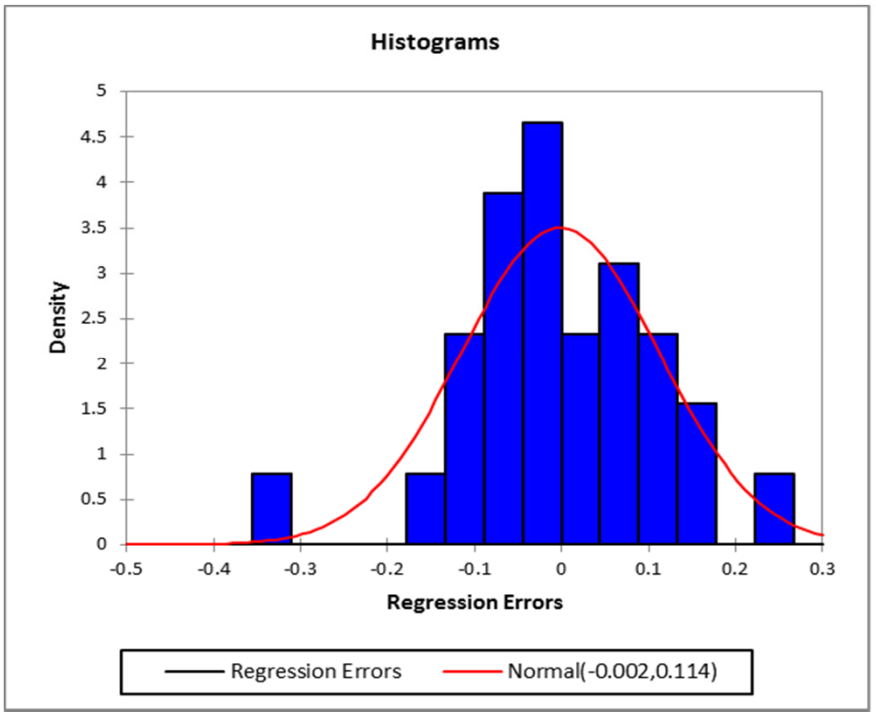
Mine Geometry Only PI-Term Model

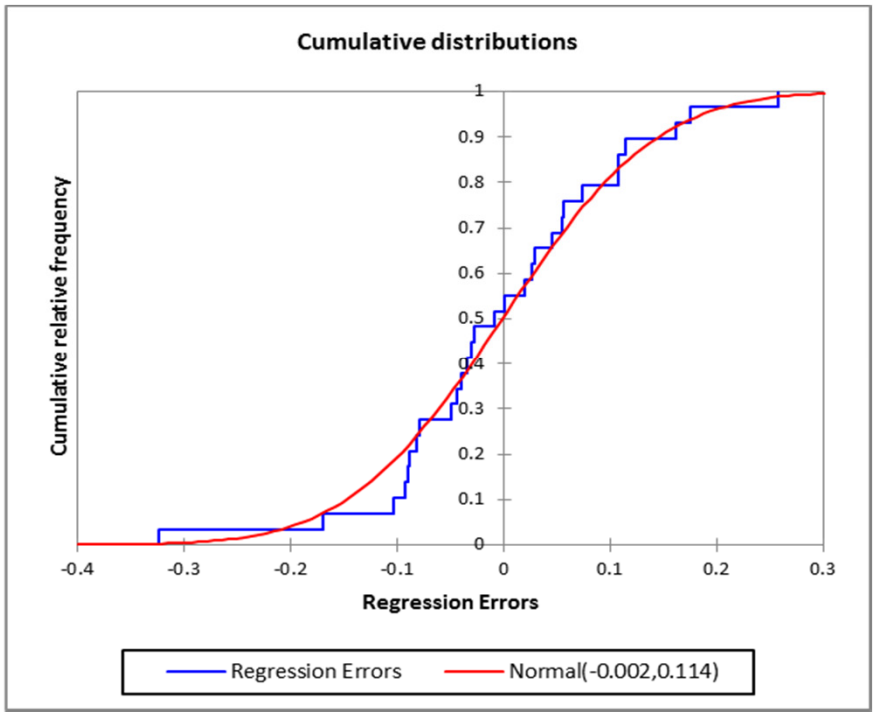


DgS	Engineer:	S.Ditton	Client:	Review of Height of Fracturing Data	
	Drawn:	S.Ditton			
	Date:	01.05.14	Title:	Results of Non-Linear Regession Analysis: Predicted v. Measured Value Analysis for Height of A-Zone Fracturing for the Geometry PI-Term Model	
	Ditton Geotechnical Services Pty Ltd		Scale:	NTS	Figure No: A42b



DgS	Engineer:	S.Ditton	Client:	Review of Height of Fracturing Data	
	Drawn:	S.Ditton			
	Date:	01.05.14	Title:	Results of Non-Linear Regession Error analysis for Geometry PI-Terms Only Height of A-Zone Prediction Model (Geology Pi-Term Not Included)	
	Ditton Geotechnical Services Pty Ltd		Scale:	NTS	Figure No: A42c



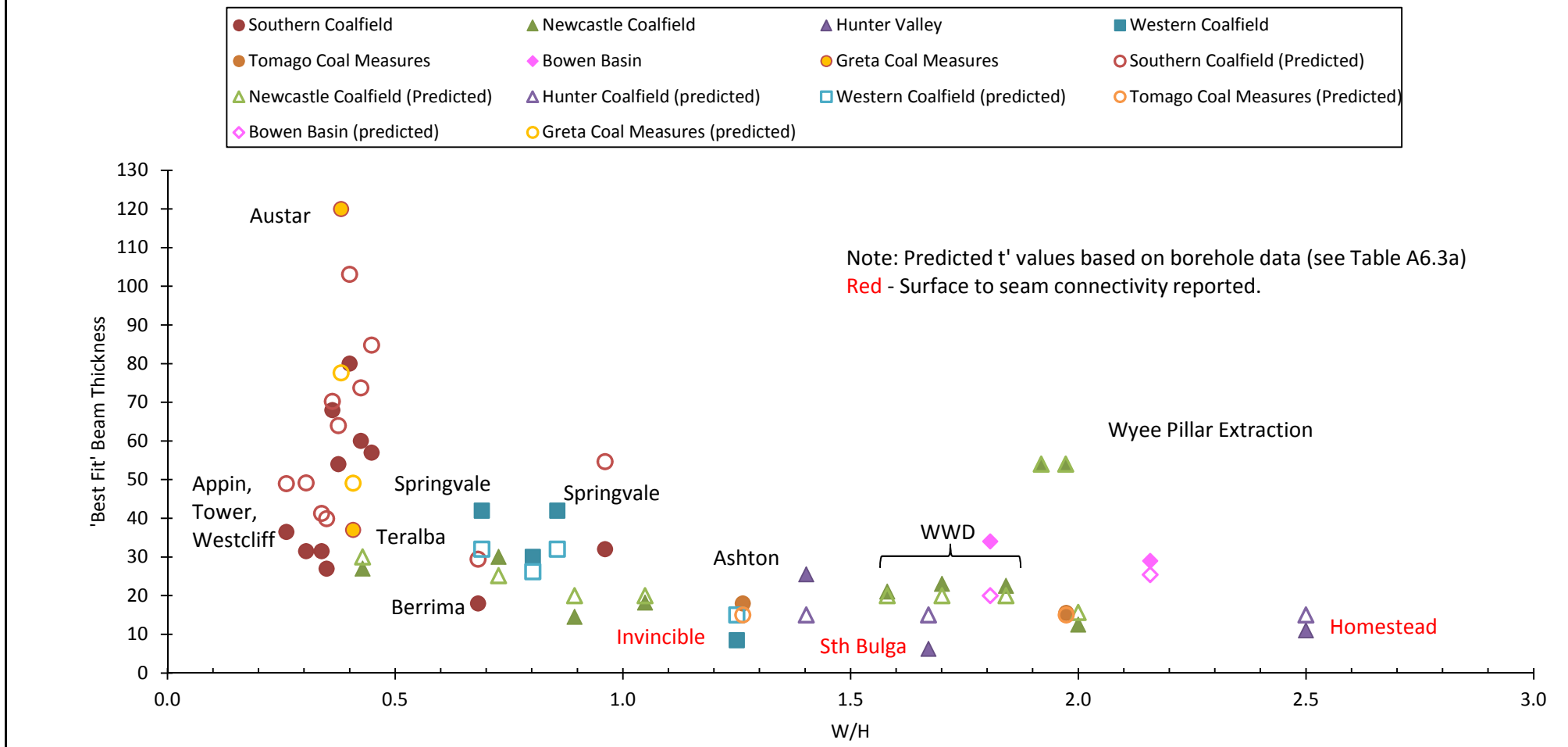


Kolmogorov-Smirnov test:

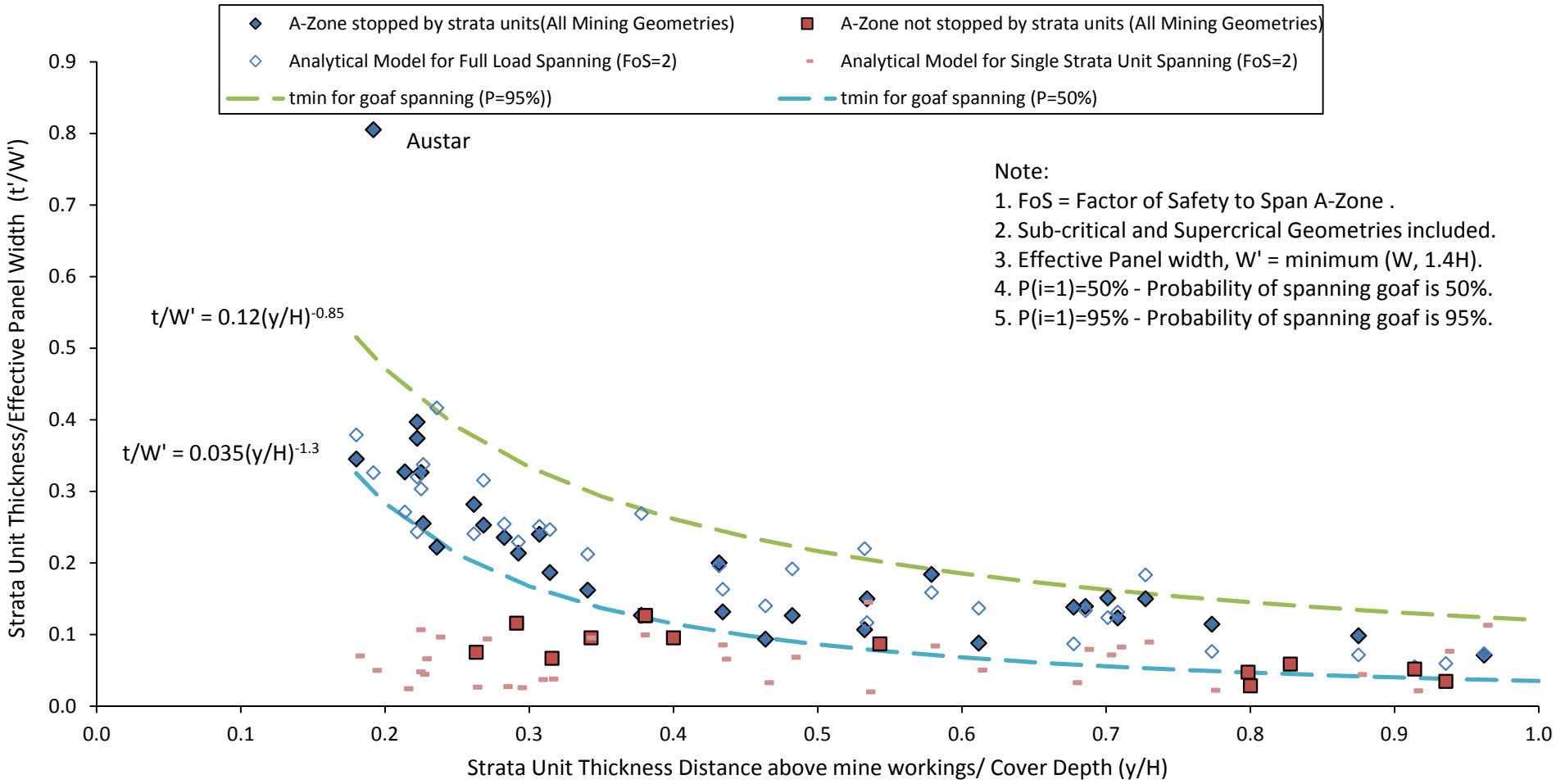
D	0.117
p-value	0.798
alpha	0.05

Test interpretation:
H0: The sample follows a Normal distribution
Ha: The sample does not follow a Normal distribution
As the computed p-value is greater than the significance level alpha=0.05, one cannot reject the null hypothesis H0.
The risk to reject the null hypothesis H0 while it is true is 79.75%.

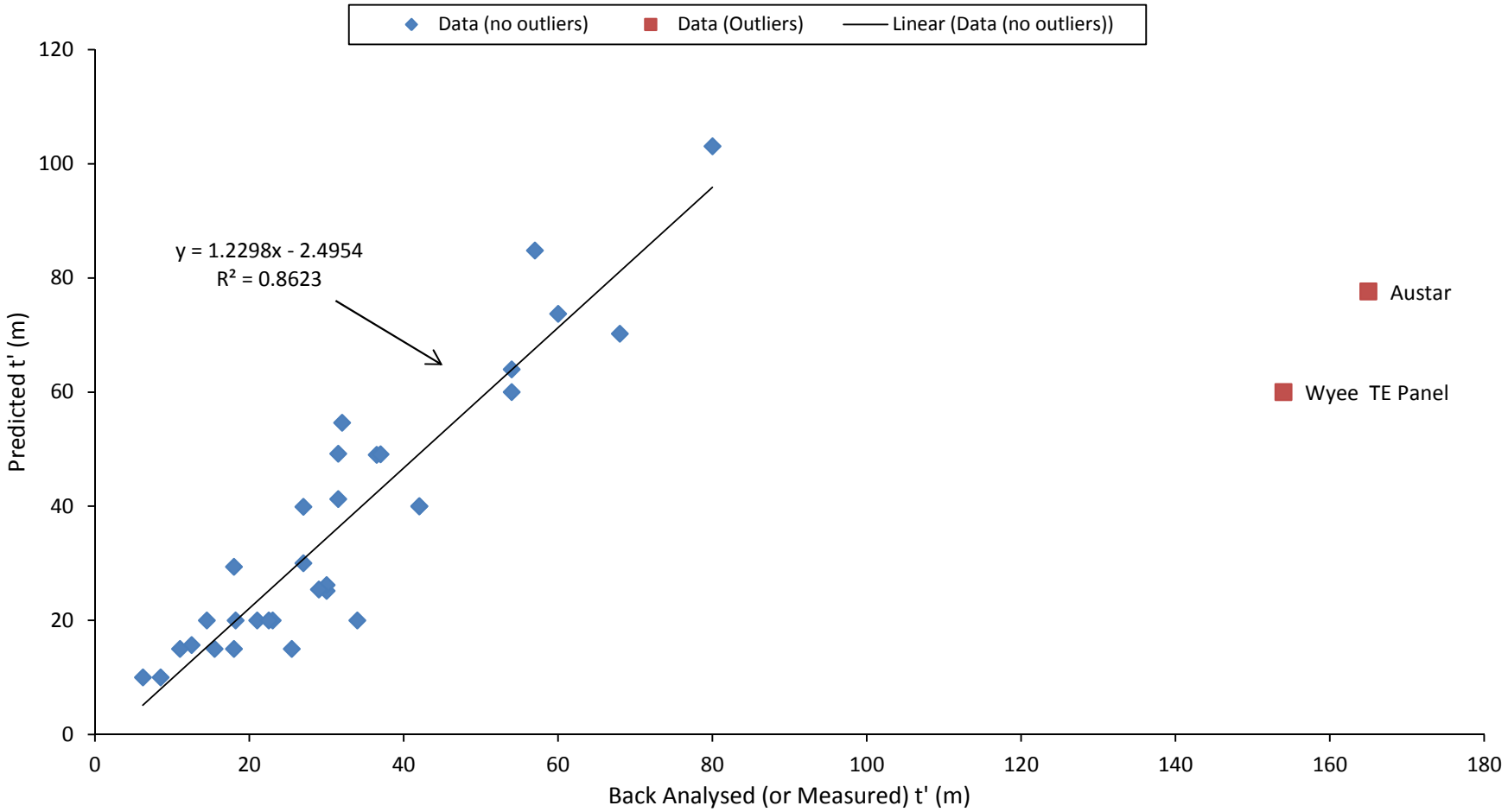
DgS	Engineer:	S.Ditton	Client:	Review of Height of Fracturing Data
	Drawn:	S.Ditton		
	Date:	01.05.14	Title:	Results of Non-Linear Regession Error analysis for Geometry Pi-Term Height of A-Zone Prediction Model: Regression Error Normal Distribution Test
	Ditton Geotechnical Services Pty Ltd		Scale:	NTS — Figure No: A42d



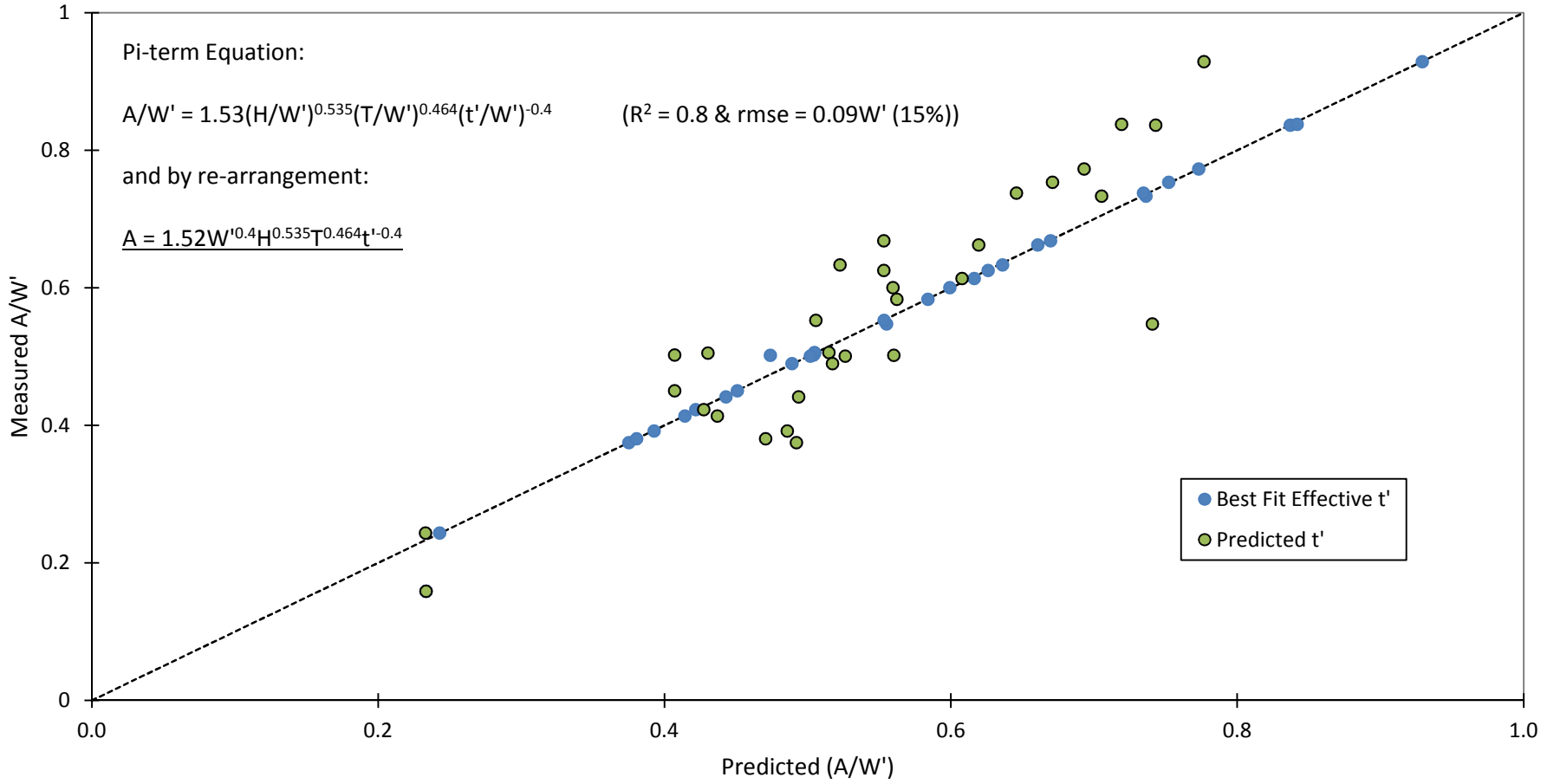
DgS	Engineer: S.Ditton	Client:	Review of Height of Fracturing Data	
	Drawn: S.Ditton			
	Date: 01.05.14	Title:	Results of Back-analysis of Effective Strata Units required to Match the Observed A-Zone Heights above Longwall Panel Goafs using the Geology Pi-Term Model	
	Ditton Geotechnical Services Pty Ltd	Scale:	NTS	Figure No: A42e



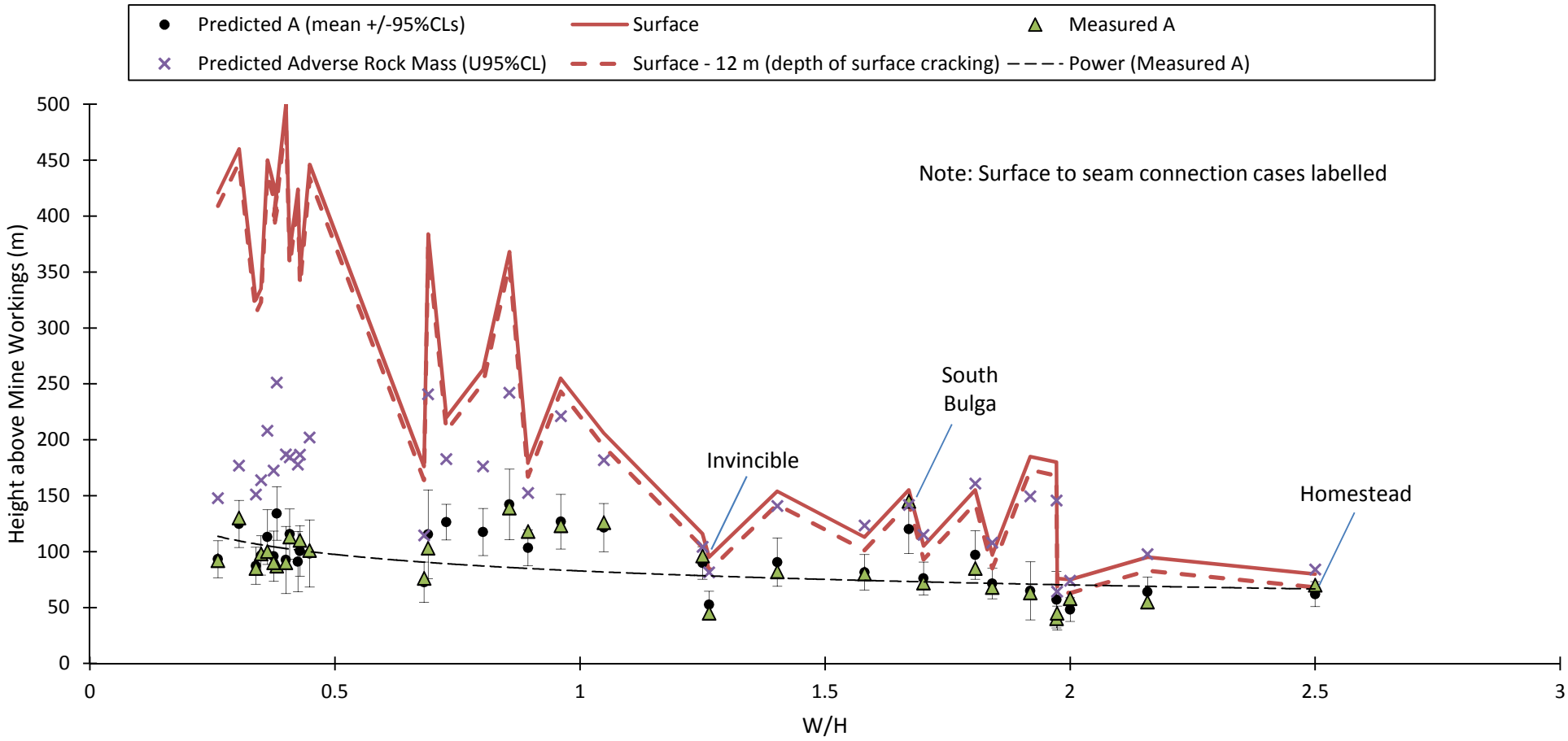
DgS	Engineer: S.Ditton	Client:	Review of Height of Fracturing Data
	Drawn: S.Ditton		
	Date: 01.05.14	Title:	Minimum Effective beam Thickness Required to Span the A-Zone, based on Back Analysis Results for the Geology Pi-Term Model (see Figure A42e)
	Ditton Geotechnical Services Pty Ltd	Scale:	NTS — Figure No: A42f



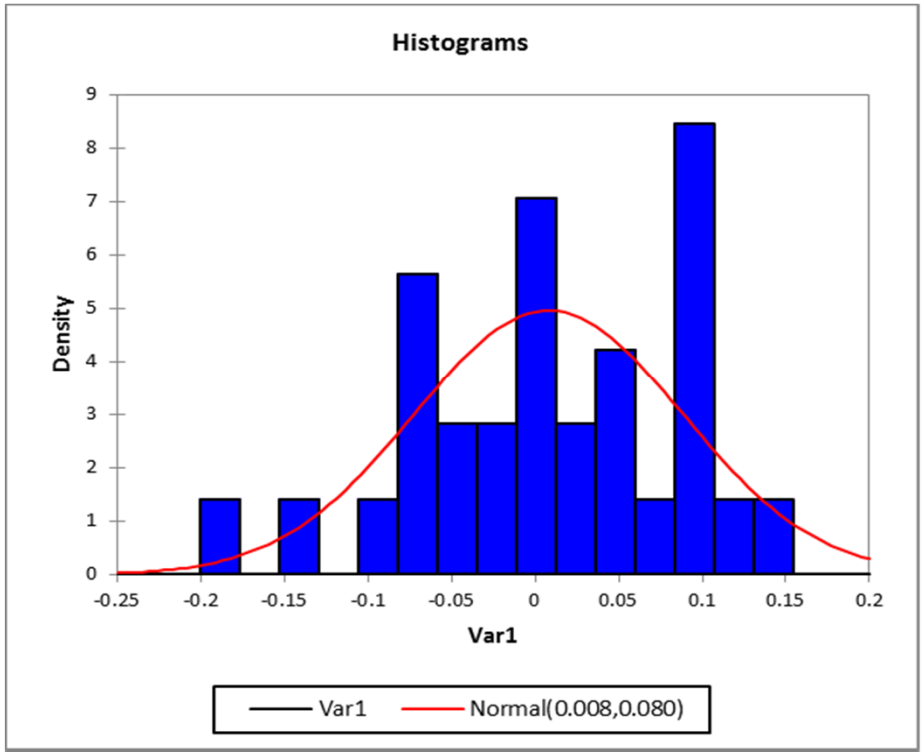
DgS	Engineer:	S.Ditton	Client:	Review of Height of Fracturing Data	
	Drawn:	S.Ditton			
	Date:	01.05.14	Title:	Comparison of Back-Analysed (or measured (t') v. Predicted t' for the Geological PI-Term	
	Ditton Geotechnical Services Pty Ltd		Scale:	NTS	Figure No: A42g

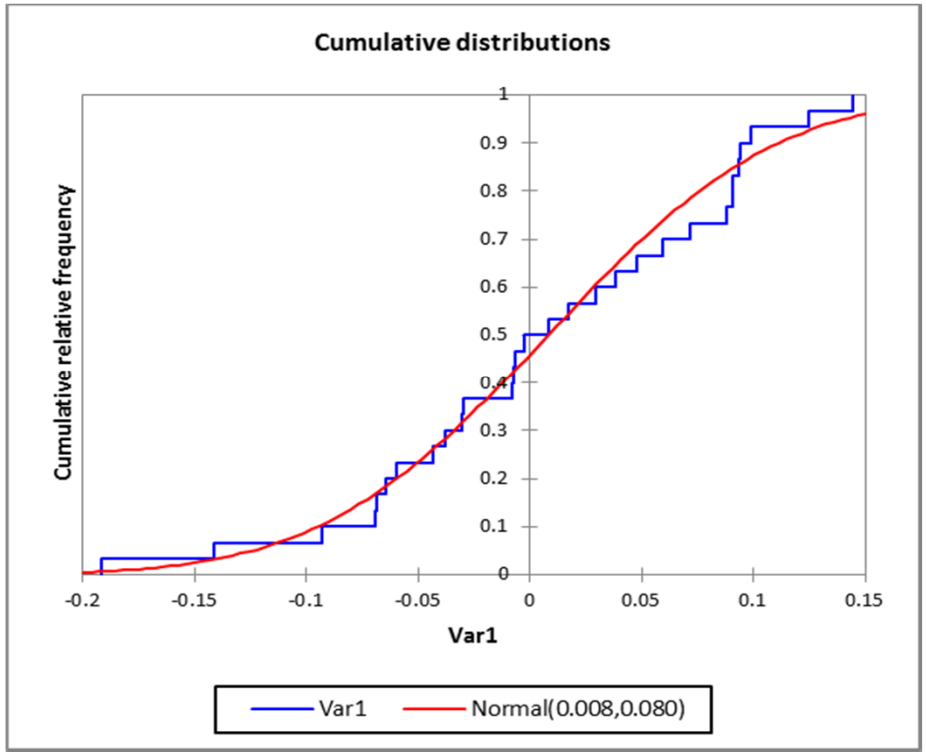


DgS	Engineer:	S.Ditton	Client:	Review of Height of Fracturing Data	
	Drawn:	S.Ditton			
	Date:	01.05.14	Title:	Results of Non-Linear Regession Analysis: Predicted v. Measured Value Analysis for Height of A-Zone Fracturing for Geology Pi-Term Model	
Ditton Geotechnical Services Pty Ltd			Scale:	NTS	Figure No: A42h



DgS	Engineer:	S.Ditton	Client:	Review of Height of Fracturing Data	
	Drawn:	S.Ditton			
	Date:	01.05.14	Title:	Results of Non-Linear Regession Error analysis for Height of A-Zone Prediction Model with Geology Included	
	Ditton Geotechnical Services Pty Ltd		Scale:	NTS	Figure No: A42i



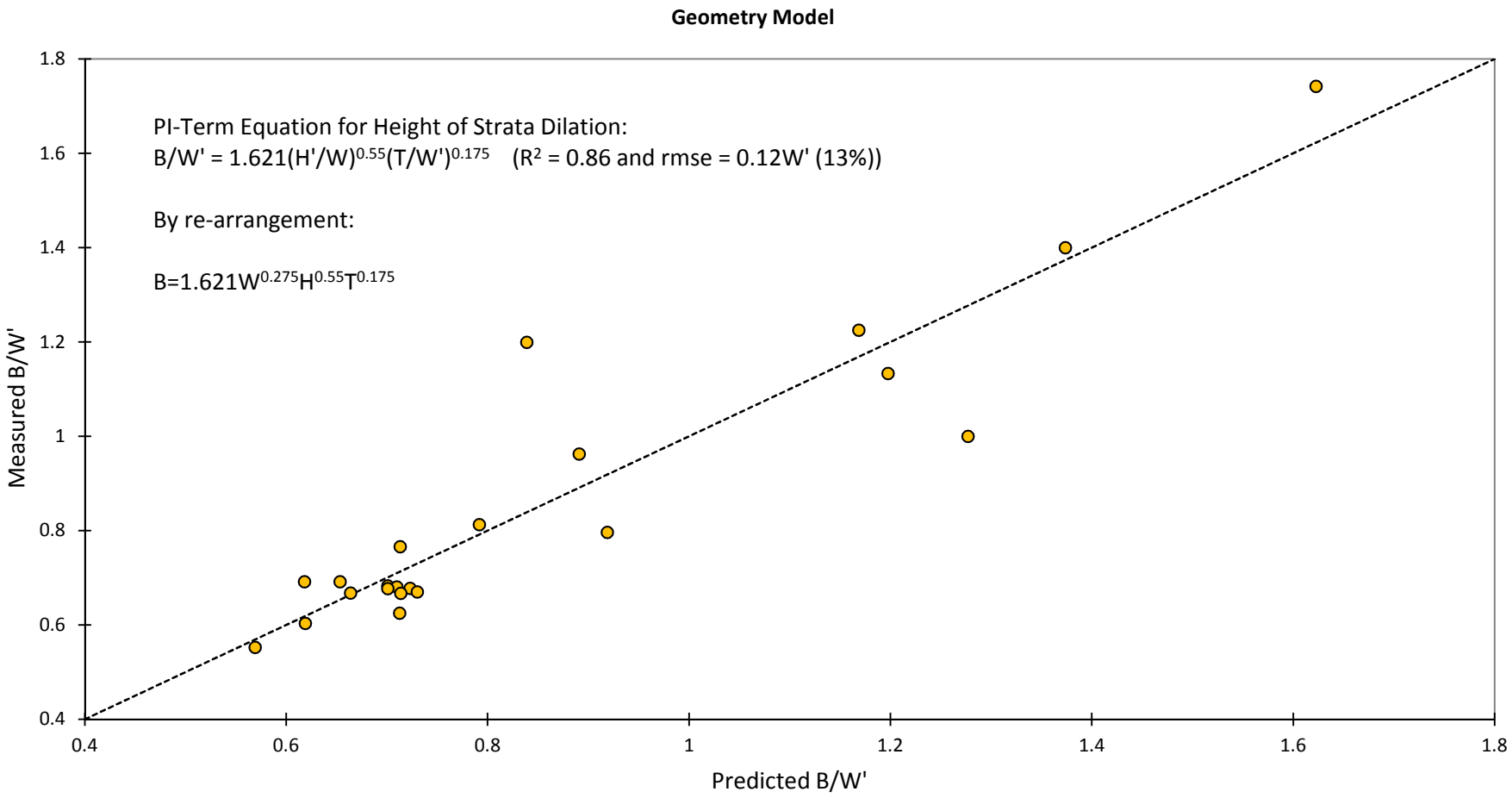


Kolmogorov-Smirnov test:

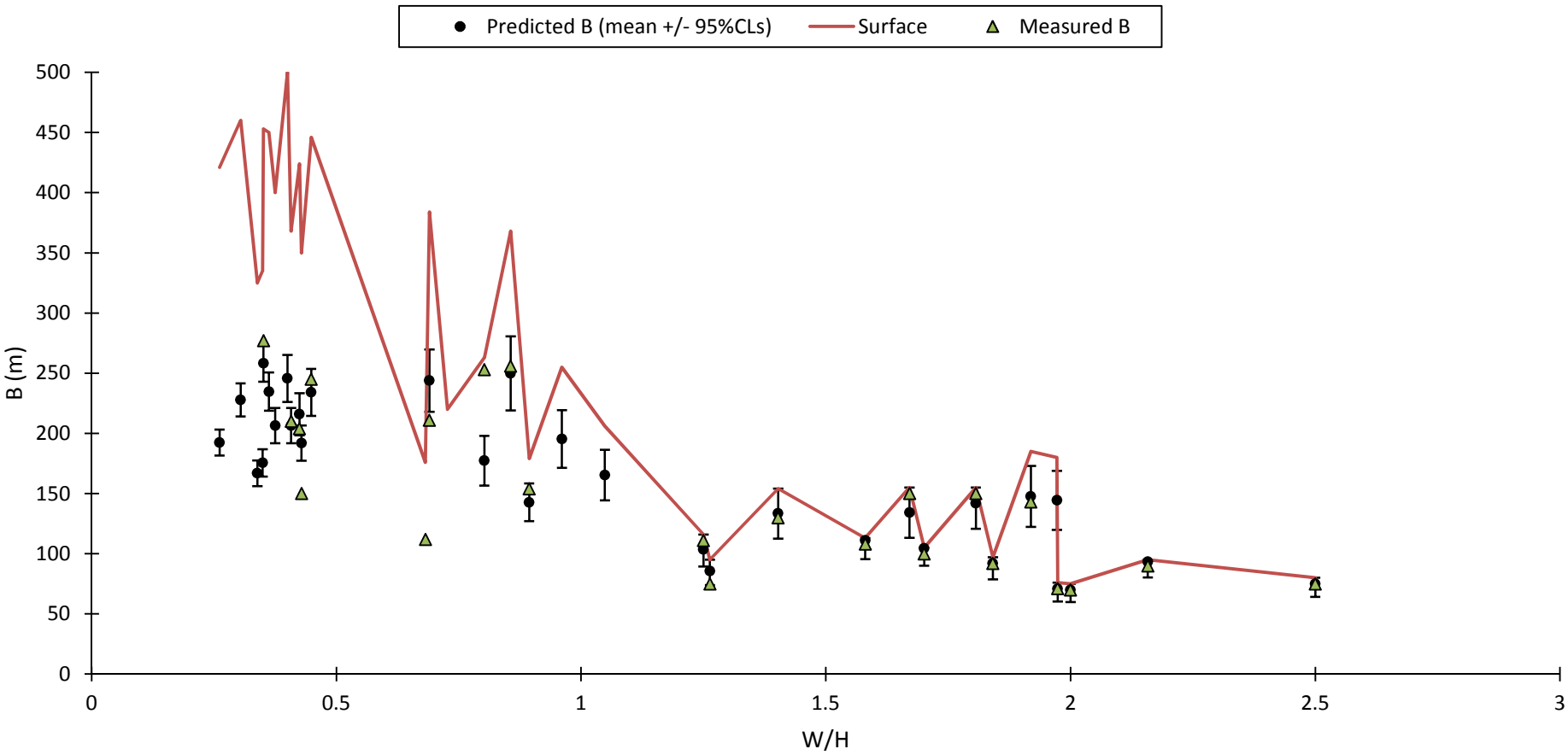
D	0.107
p-value	0.866
alpha	0.05

Test interpretation:
H0: The sample follows a Normal distribution
Ha: The sample does not follow a Normal distribution
As the computed p-value is greater than the significance level alpha=0.05, one cannot reject the null hypothesis H0.
The risk to reject the null hypothesis H0 while it is true is 86.6%.

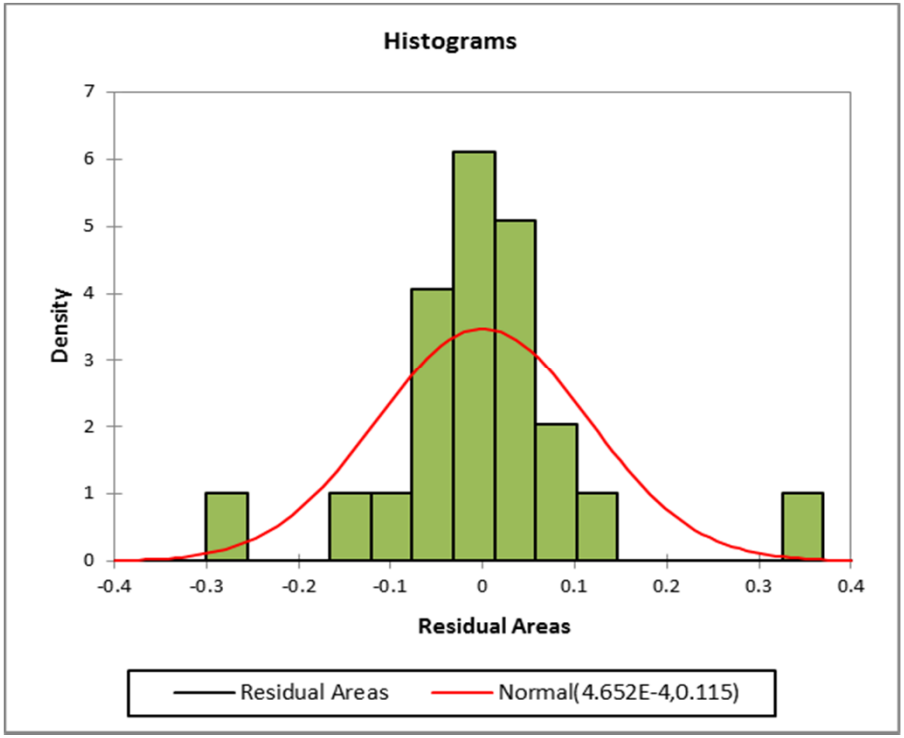
DgS	Engineer:	S.Ditton	Client:	Review of Height of Fracturing Data	
	Drawn:	S.Ditton			
	Date:	01.05.14	Title:	Results of Non-Linear Regession Error analysis for Geology Pi-Term Height of A-Zone	
	Ditton Geotechnical Services Pty Ltd			Prediction Model: Regression Error Normal Distribution Test	
			Scale:	NTS	Figure No: A42j

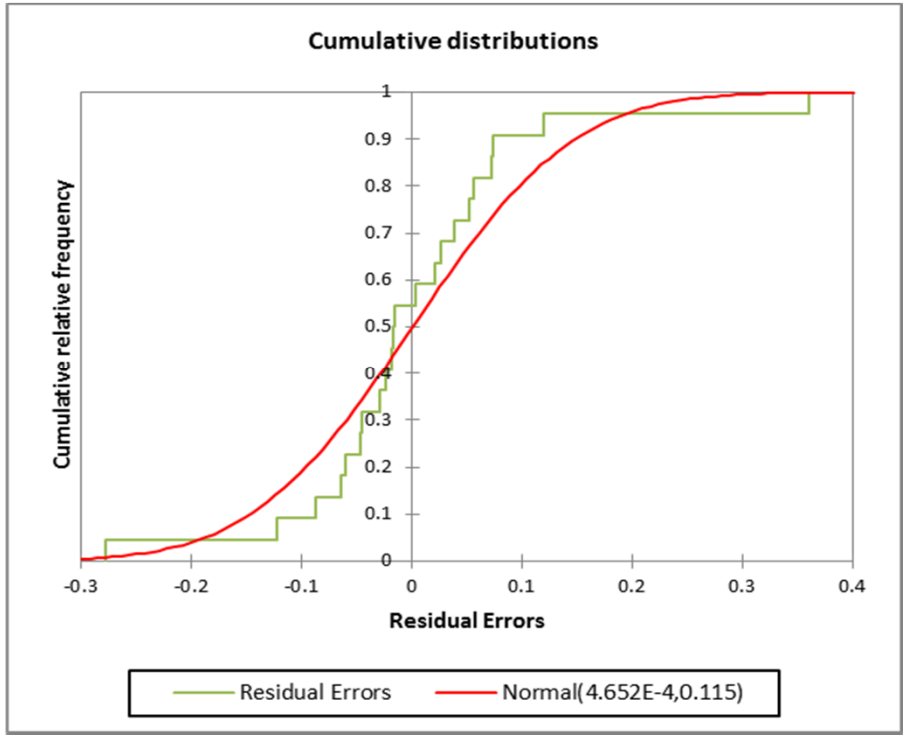


DgS	Engineer:	S.Ditton	Client:	Review of Height of Fracturing Data	
	Drawn:	S.Ditton			
	Date:	01.02.14	Title:	Results of Non-Linear Regession Error analysis for Height of B-Zone Predictions for Geometry Only Pi-Term Model	
	Ditton Geotechnical Services Pty Ltd		Scale:	NTS	Figure No: A42k



DgS	Engineer:	S.Ditton	Client:	Review of Height of Fracturing Data	
	Drawn:	S.Ditton			
	Date:	01.02.14	Title:	Results of Non-Linear Regession Error analysis for Height of B-Zone Predictions for Geometry Only Pi-Term Model	
	Ditton Geotechnical Services Pty Ltd		Scale:	NTS	Figure No: A42l





Kolmogorov-Smirnov test:

D	0.173
p-value	0.487
alpha	0.05

Test interpretation:

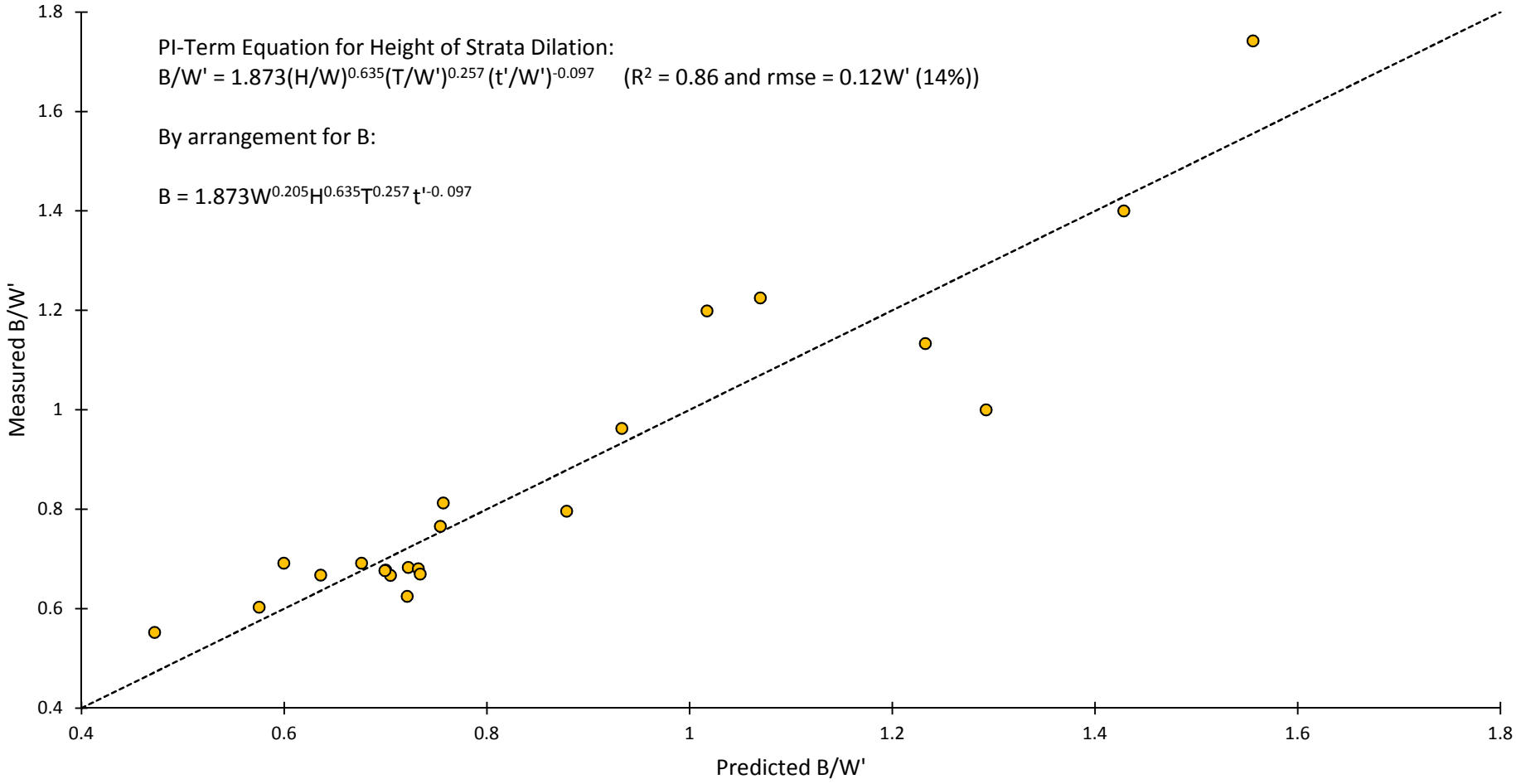
H0: The sample follows a Normal distribution

Ha: The sample does not follow a Normal distribution

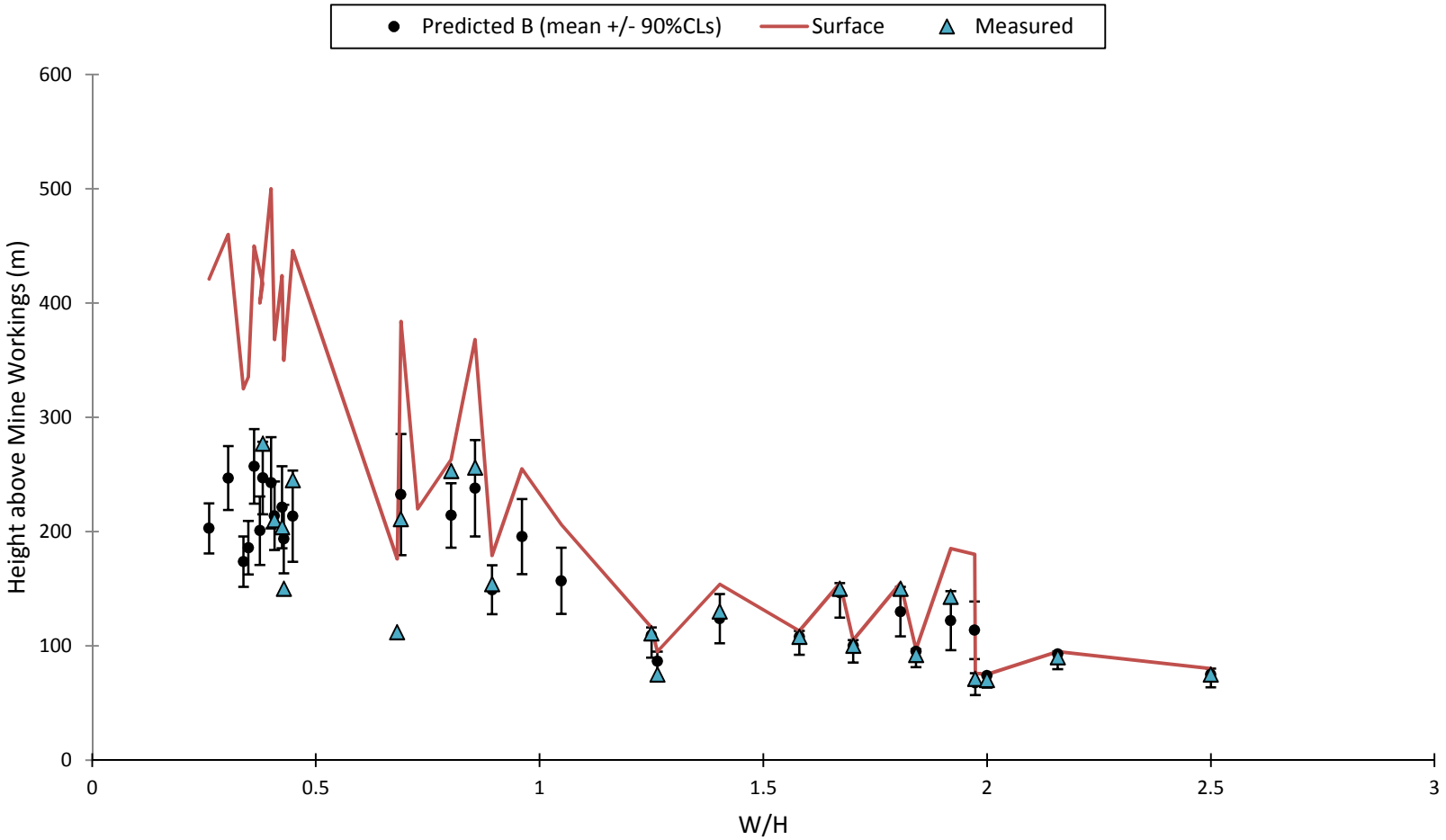
As the computed p-value is greater than the significance level alpha=0.05, one cannot reject the null hypothesis H0.

The risk to reject the null hypothesis H0 while it is true is 48.70%.

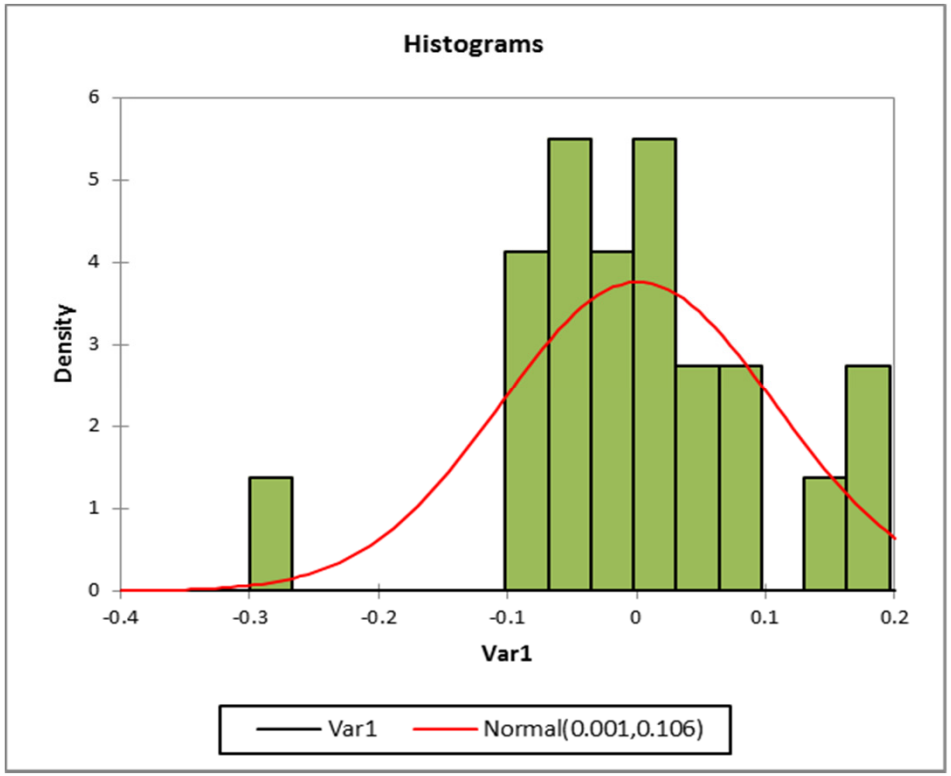
DgS	Engineer:	S.Ditton	Client:	Review of Height of Fracturing Data	
	Drawn:	S.Ditton			
	Date:	01.02.14	Title:	Results of Non-Linear Regession Error analysis for Height of B-Zone Predictions for Geometry Only Pi-Term Model	
	Ditton Geotechnical Services Pty Ltd		Scale:	NTS	Figure No: A42m

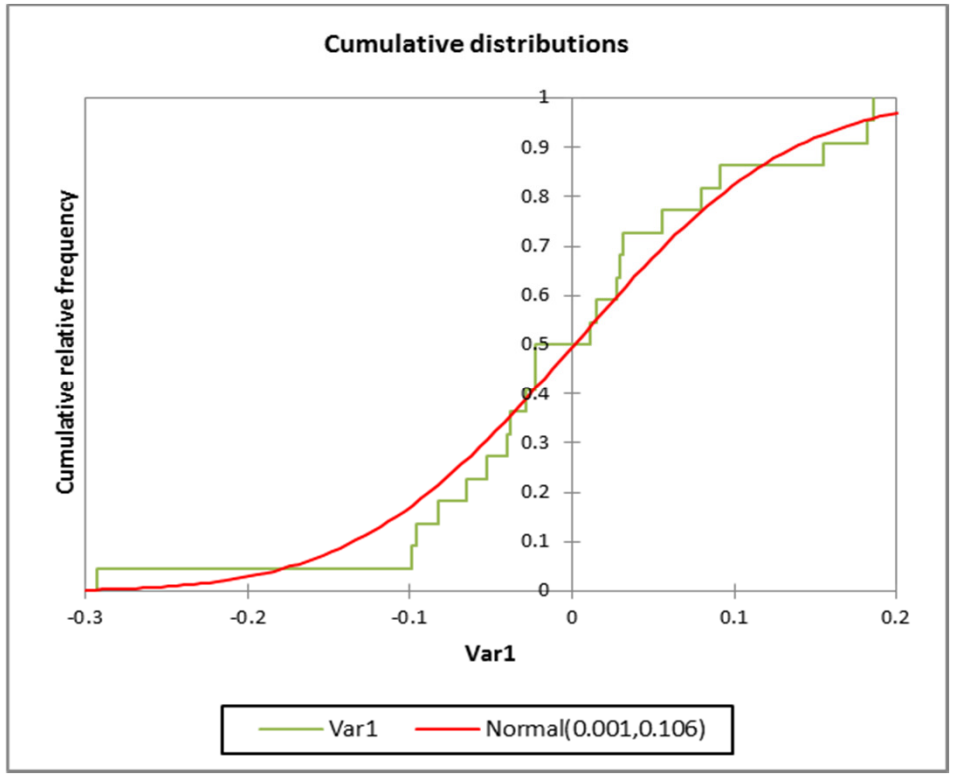


DgS	Engineer:	S.Ditton	Client:	Review of Height of Fracturing Data	
	Drawn:	S.Ditton			
	Date:	01.02.14	Title:	Results of Non-Linear Regession Error analysis for Height of B-Zone Predictions for Geology Pi-Term Model	
	Ditton Geotechnical Services Pty Ltd		Scale:	NTS	Figure No: A42n



DgS	Engineer:	S.Ditton	Client:	Review of Height of Fracturing Data	
	Drawn:	S.Ditton			
	Date:	01.02.14	Title:	Results of Non-Linear Regession Error analysis for Height of B-Zone Predictions for Geology Pi-Term Model	
	Ditton Geotechnical Services Pty Ltd		Scale:	NTS	Figure No: A42o





Kolmogorov-Smirnov test:

D	0.126
p-value	0.849
alpha	0.05

Test interpretation:

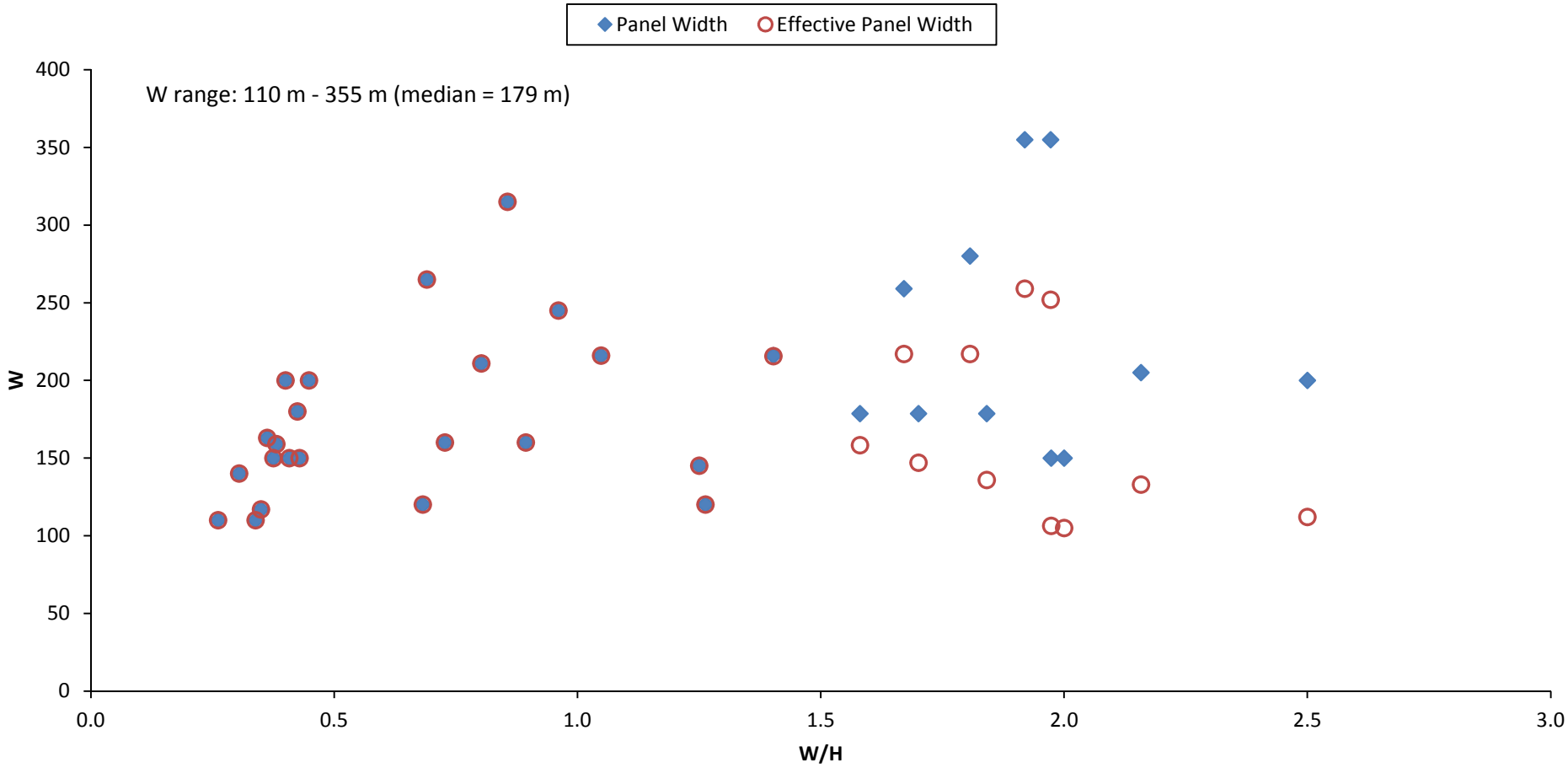
H0: The sample follows a Normal distribution

Ha: The sample does not follow a Normal distribution

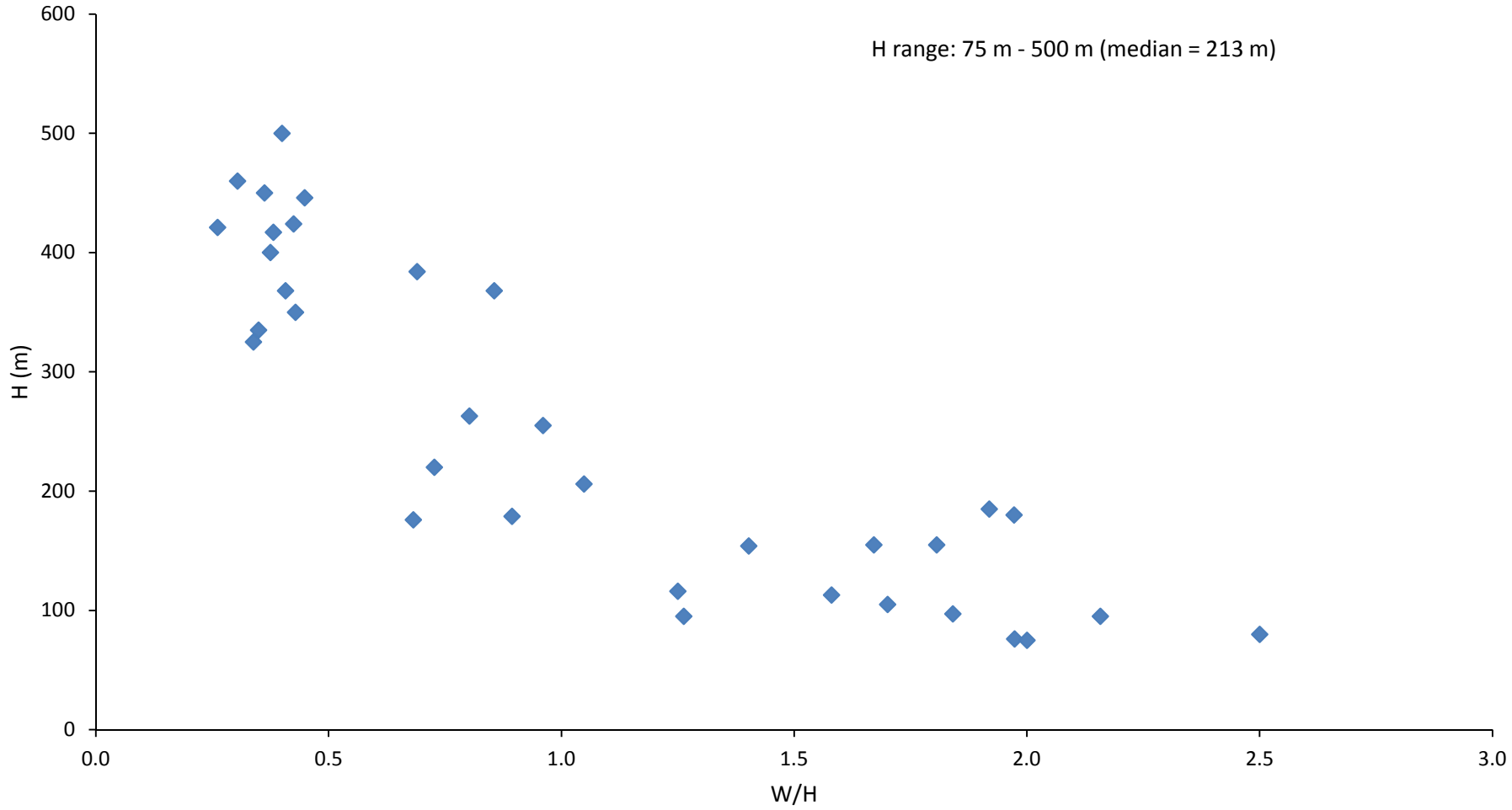
As the computed p-value is greater than the significance level alpha=0.05, one cannot reject the null hypothesis H0.

The risk to reject the null hypothesis H0 while it is true is 84.89%.

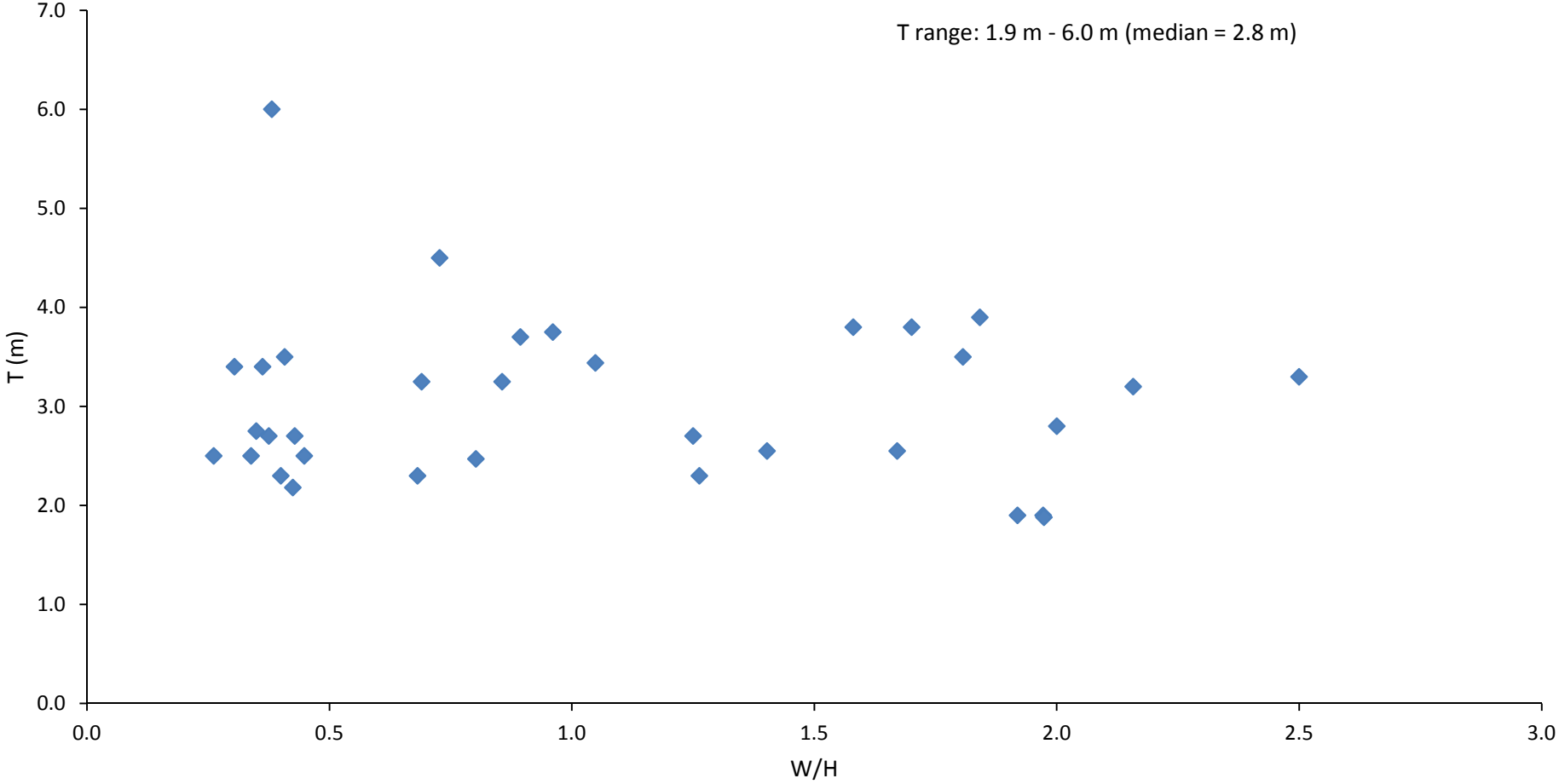
DgS	Engineer:	S.Ditton	Client:	Review of Height of Fracturing Data	
	Drawn:	S.Ditton			
	Date:	01.02.14	Title:	Results of Non-Linear Regession Error analysis for Height of B-Zone Predictions for Geology Pi-Term Model	
	Ditton Geotechnical Services Pty Ltd		Scale:	NTS	Figure No: A42p



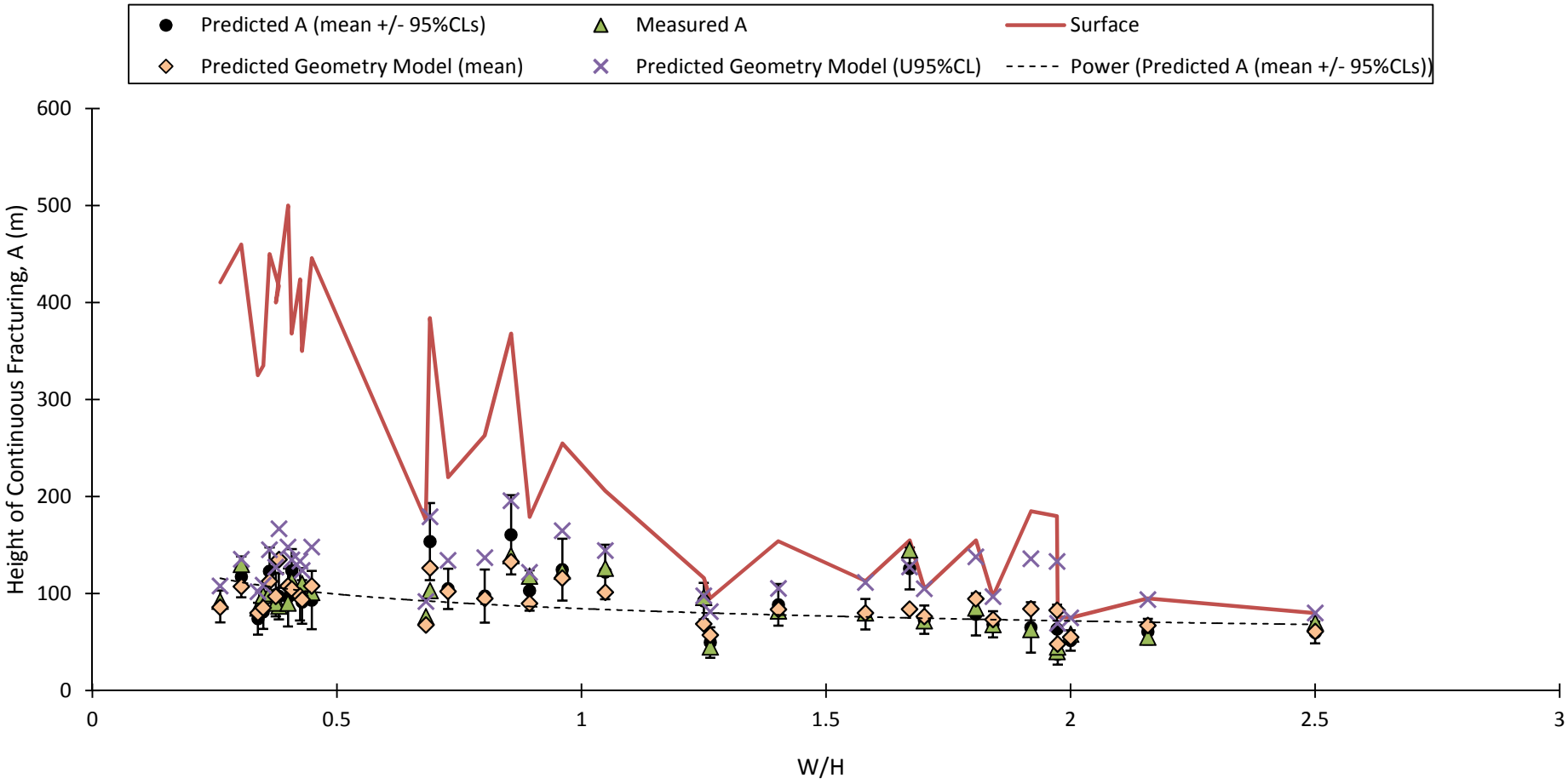
DgS	Engineer:	S.Ditton	Client:	Modified from ACARP, 2003	
	Drawn:	S.Ditton			
	Date:	03.12.12	Title:	Panel Width v. W/H Database for Sub-surface Fracturing Model	
	Ditton Geotechnical Services Pty Ltd		Scale:	NTS	Figure No: A43a



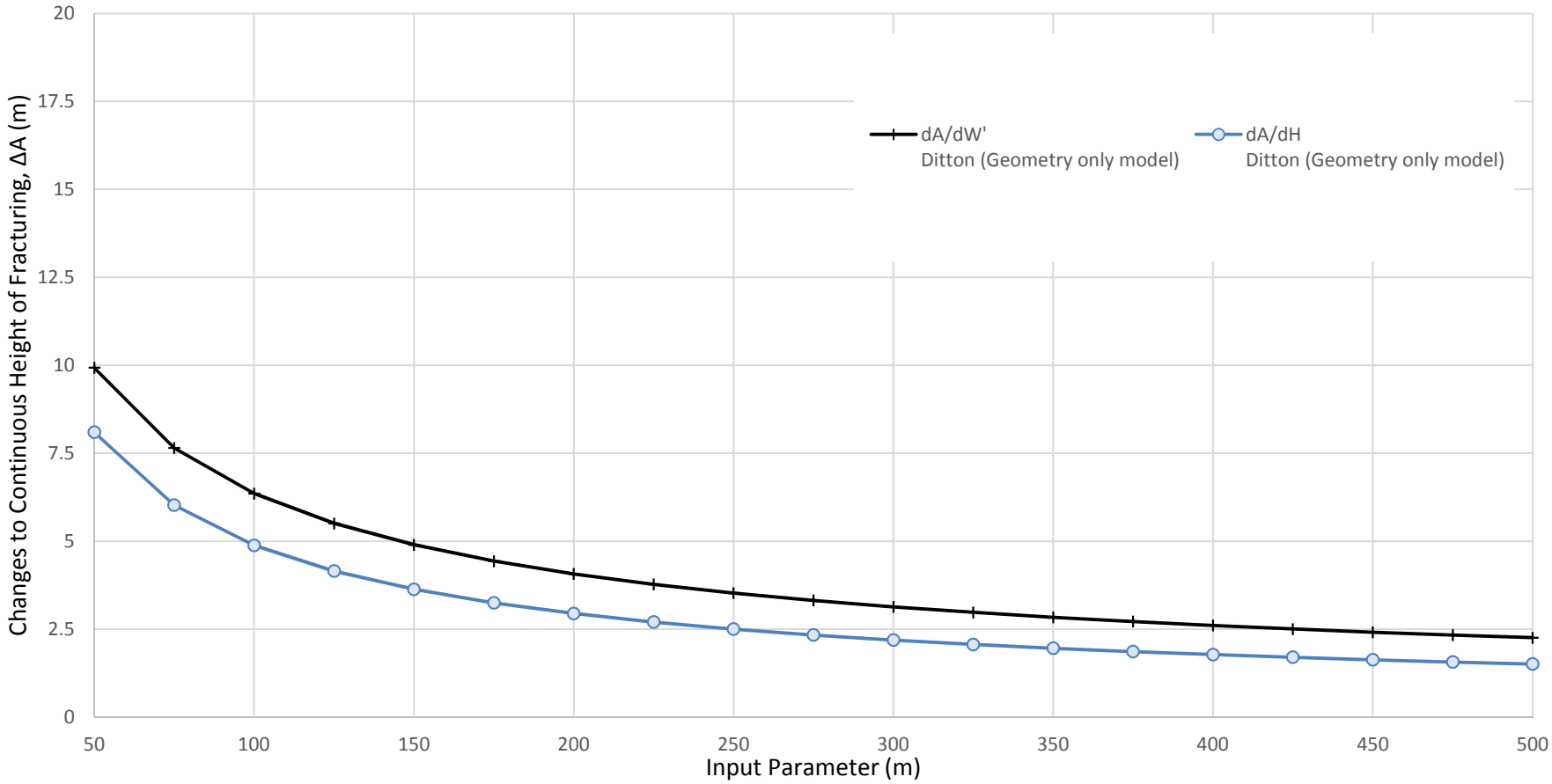
DgS	Engineer:	S.Ditton	Client:	Modified from ACARP, 2003	
	Drawn:	S.Ditton			
	Date:	03.12.12	Title:	Cover Depth v. W/H Database for Sub-surface Fracturing Model	
	Ditton Geotechnical Services Pty Ltd		Scale:	NTS	Figure No: A43b



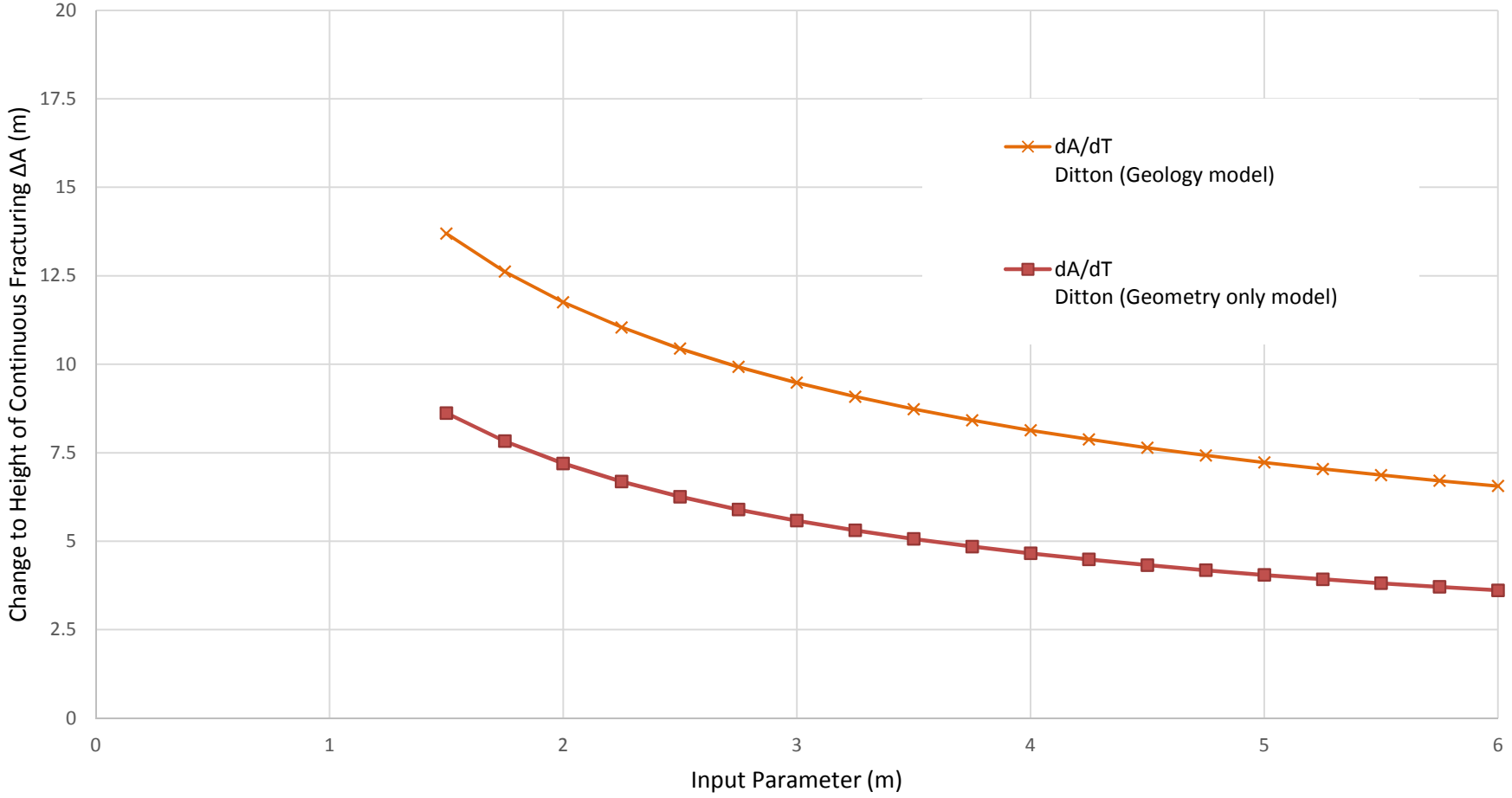
DgS	Engineer:	S.Ditton	Client:	Modified from ACARP, 2003	
	Drawn:	S.Ditton			
	Date:	03.12.12	Title:	Mining Height v. W/H Database for Sub-surface Fracturing Model	
	Ditton Geotechnical Services Pty Ltd		Scale:	NTS	Figure No: A43c



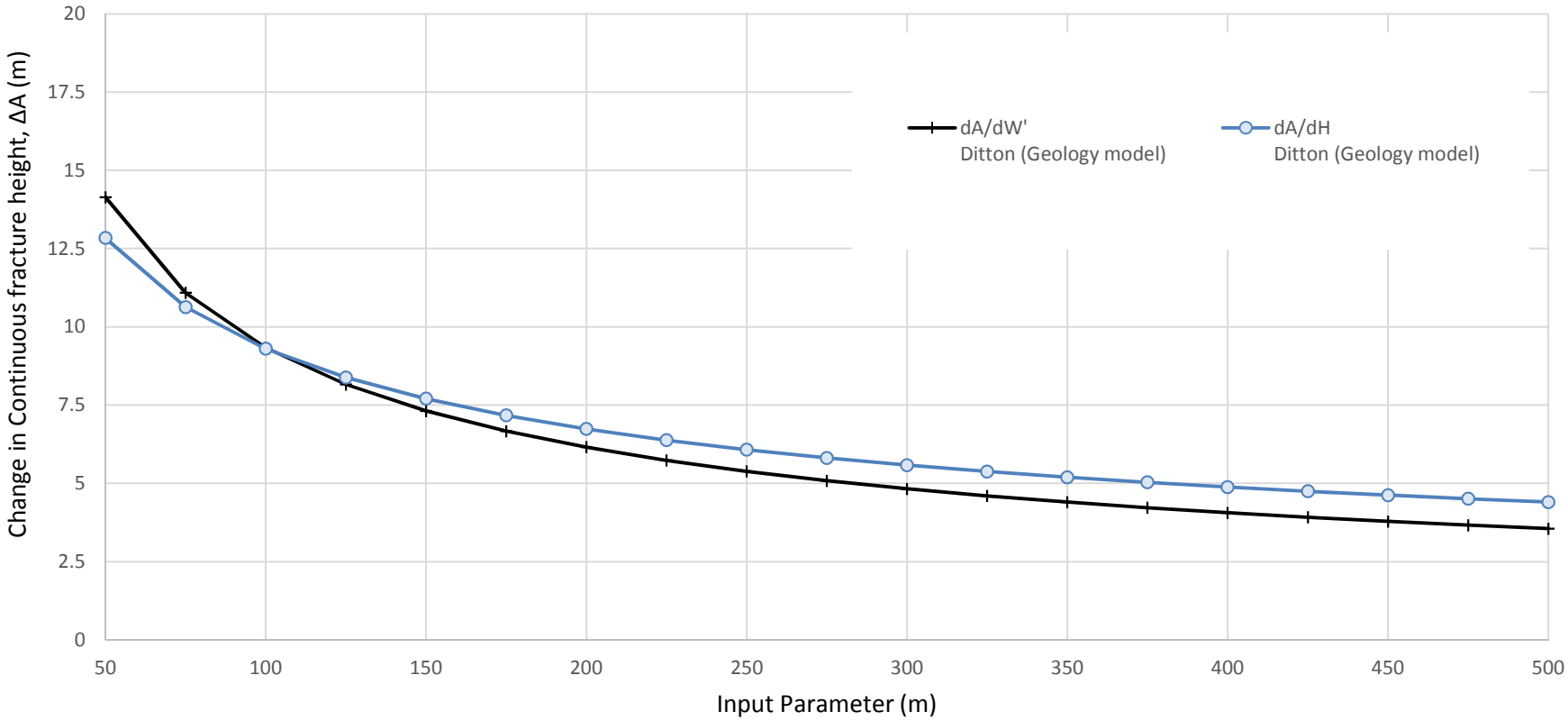
DgS	Engineer:	S.Ditton	Client:	Review of Height of Fracturing Data	
	Drawn:	S.Ditton			
	Date:	01.05.14	Title:	Heights of Continuous Fracturing Predictions for the Geometry and Geology Pi-Term Models	
	Ditton Geotechnical Services Pty Ltd		Scale:	NTS	Figure No: A43d



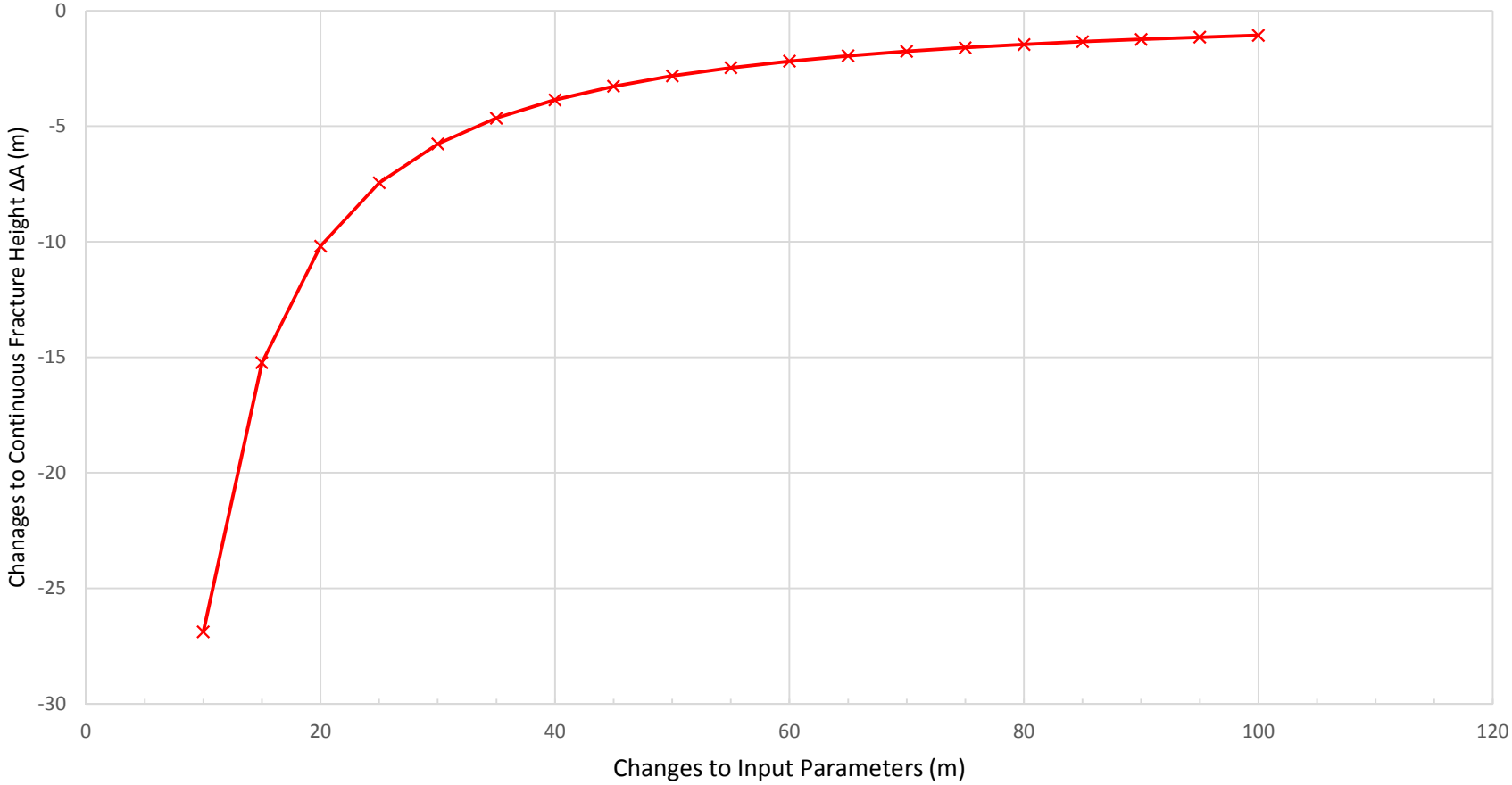
DgS	Engineer:	S.Ditton	Client:	Modified from ACARP, 2003	
	Drawn:	S.Ditton			
	Date:	25.05.14	Title:	Sensitivity Analysis of Geometry Only Pi-Term Model Input Parameters on Predicted Height of Continuous Fracturing: W' and H (as per Merrick, 2014)	
	Ditton Geotechnical Services Pty Ltd		Scale:	NTS	Figure No: A43e



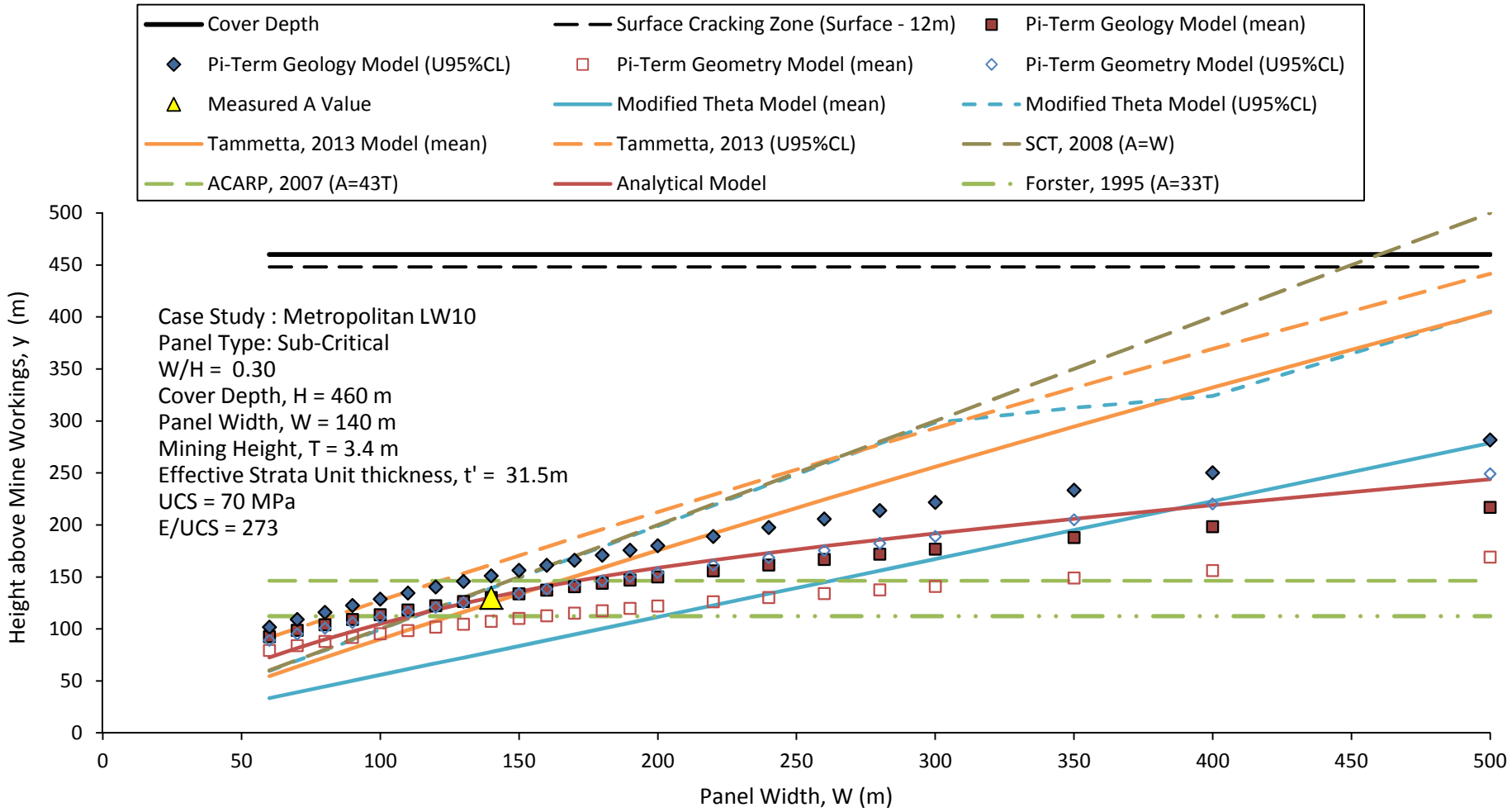
DgS	Engineer:	S.Ditton	Client:	Modified from ACARP, 2003	
	Drawn:	S.Ditton			
	Date:	25.05.14	Title:	Sensitivity Analysis of Geology & Geometry Pi-Term Model Input Parameters on Predicted Height of Continuous Fracturing: T (as per Merrick, 2014)	
	Ditton Geotechnical Services Pty Ltd		Scale:	NTS	Figure No: A43f



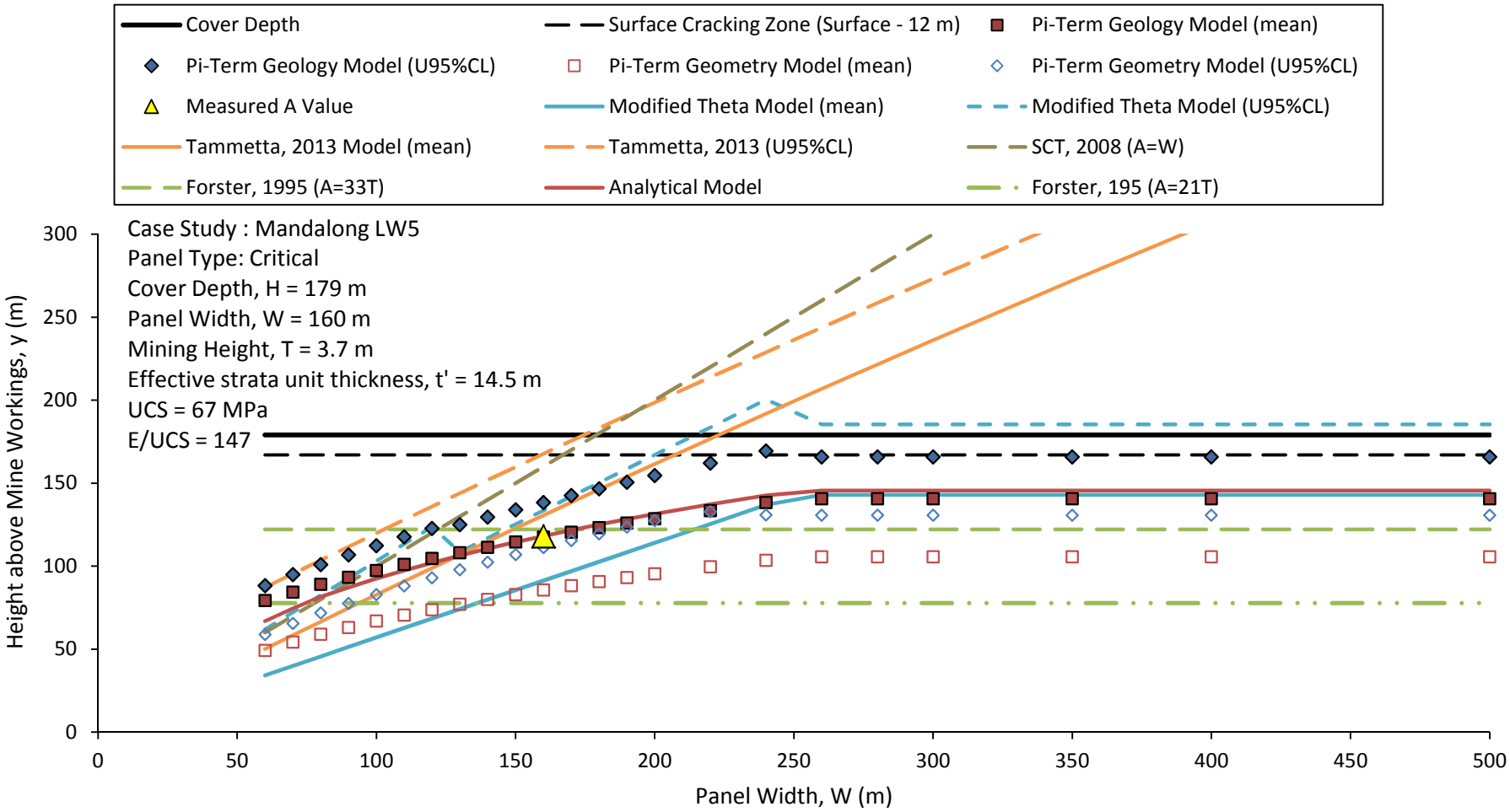
DgS	Engineer:	S.Ditton	Client:	Modified from ACARP, 2003	
	Drawn:	S.Ditton			
	Date:	25.05.14	Title:	Sensitivity Analysis of Geology Pi-Term Model Input Parameters on Predicted Height of Continuous Fracturing: W' and H (as per Merrick, 2014)	
	Ditton Geotechnical Services Pty Ltd		Scale:	NTS	Figure No: A43g



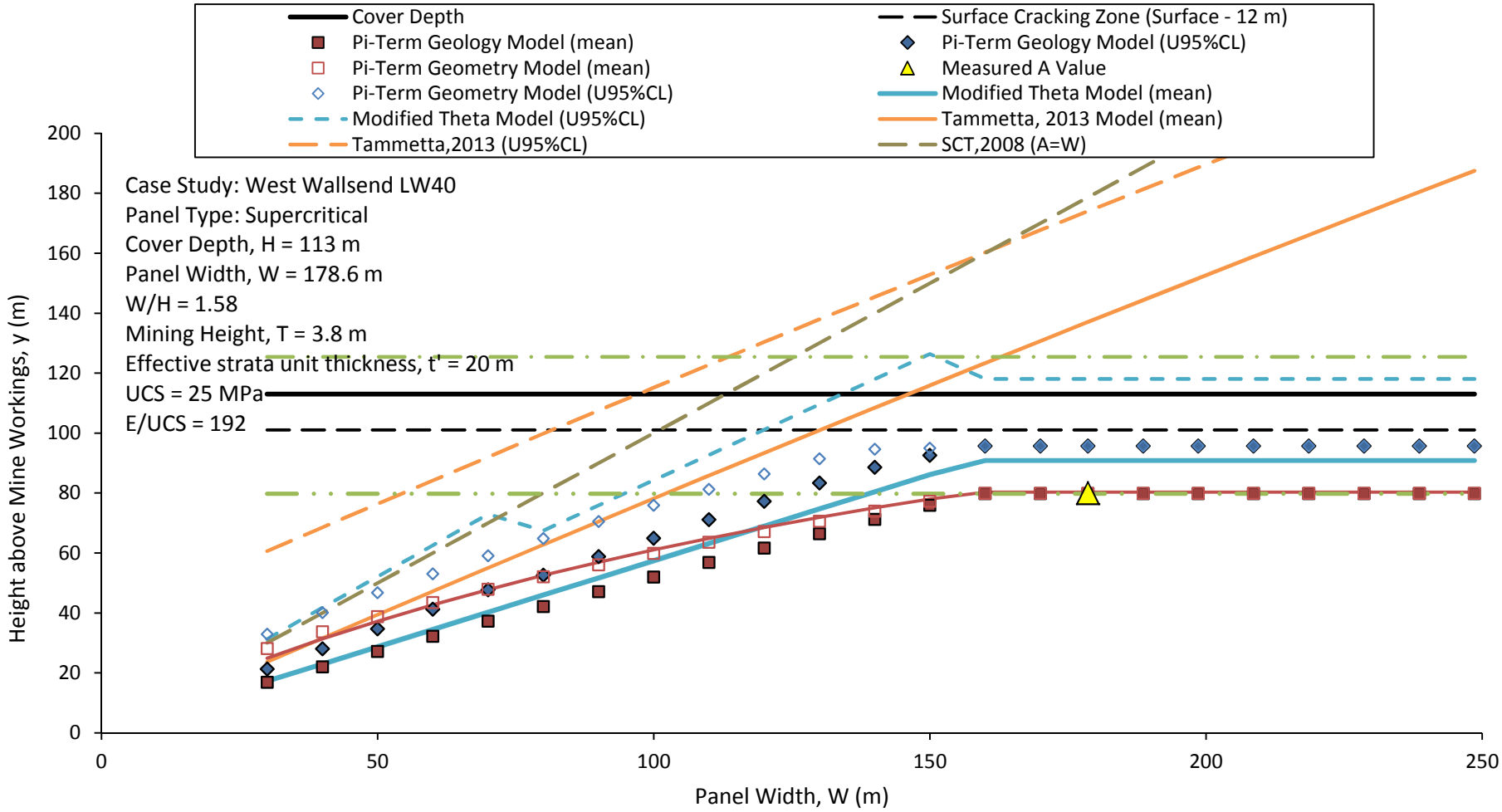
DgS	Engineer:	S.Ditton	Client:	Modified from ACARP, 2003	
	Drawn:	S.Ditton			
	Date:	25.05.14	Title:	Sensitivity Analysis of Geology Pi-Term Model Input Parameters on Predicted Height of Continuous Fracturing: t' (as per Merrick, 2014)	
	Ditton Geotechnical Services Pty Ltd		Scale:	NTS	Figure No: A43h



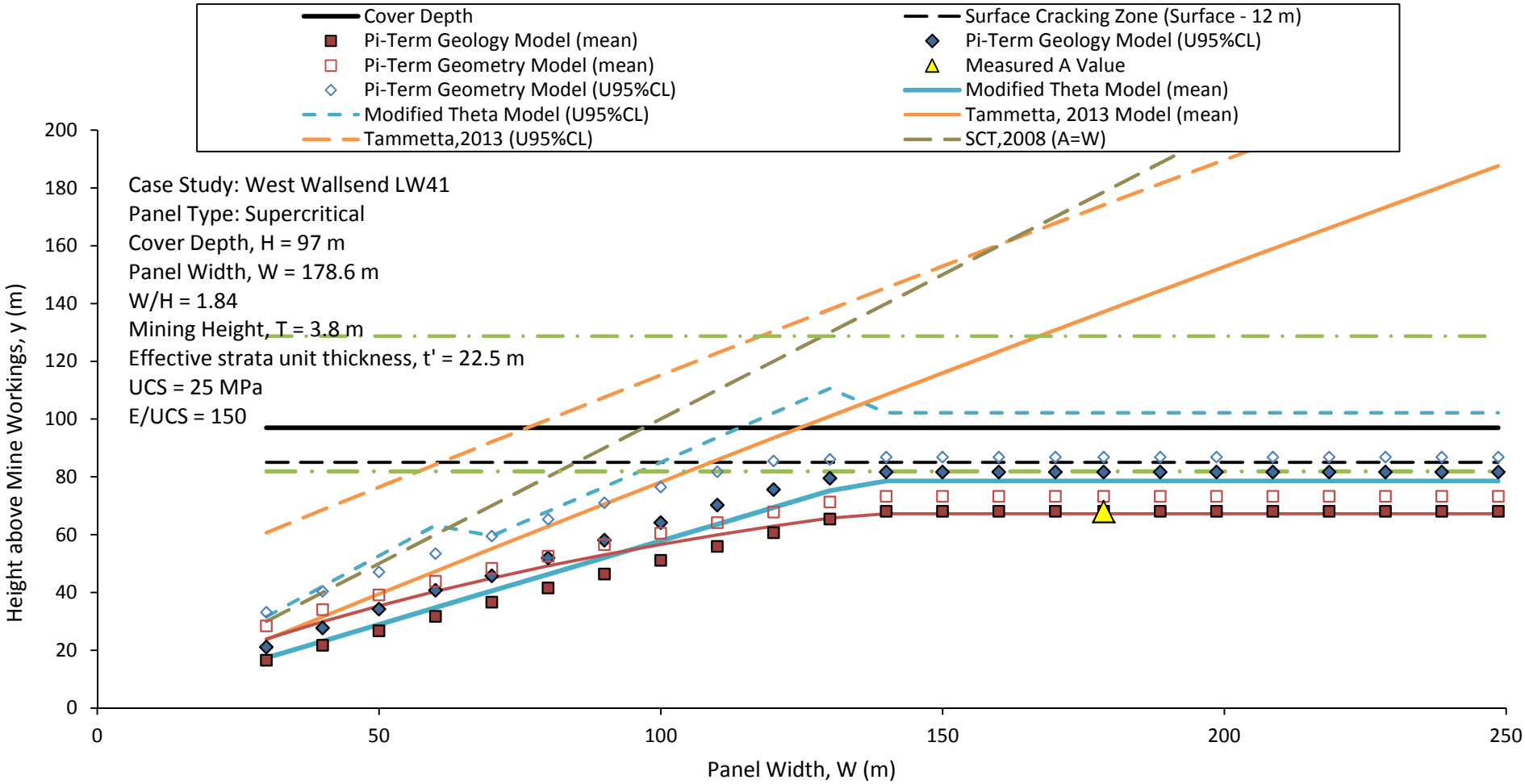
DgS	Engineer:	S.Ditton	Client:	Modified from ACARP, 2003	
	Drawn:	S.Ditton			
	Date:	16.03.14	Title:	Predicted A-Zone Fracture Heights for Varying Panel Widths using Pi-Term Geometry and Geology Models and Current State of the Art Models	
Ditton Geotechnical Services Pty Ltd			Scale:	NTS	Figure No: A43i



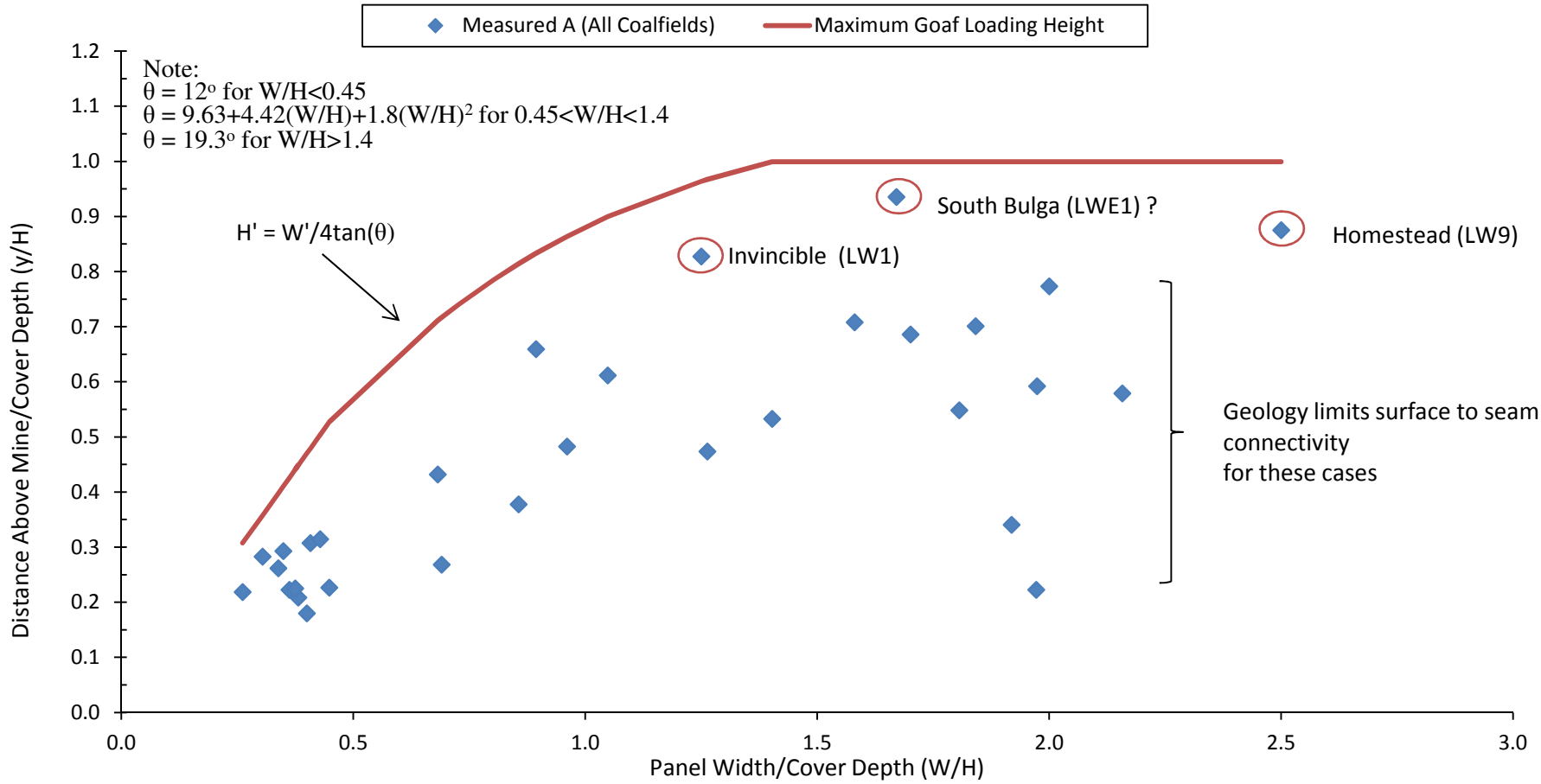
DgS	Engineer:	S.Ditton	Client:	Modified from ACARP, 2003	
	Drawn:	S.Ditton			
	Date:	16.03.14	Title:	Predicted A-Zone Fracture Heights for Varying Panel Widths using Pi-Term Geometry and Geology Models and Current State of the Art Models	
	Ditton Geotechnical Services Pty Ltd		Scale:	NTS	Figure No: A43j



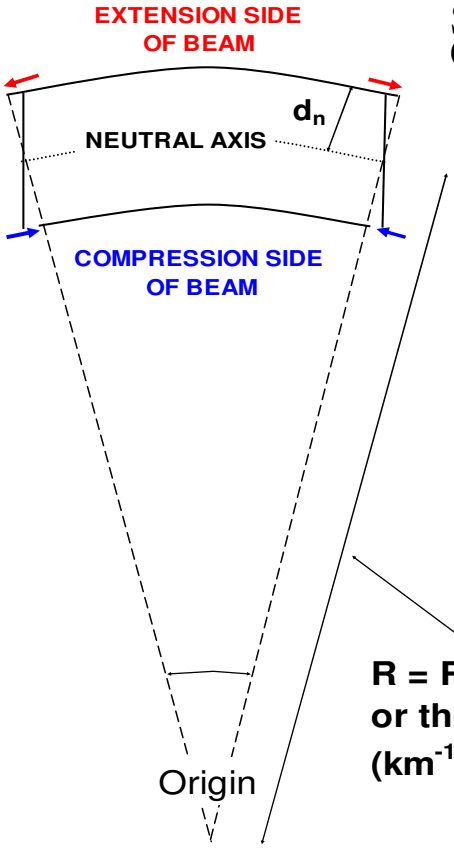
DgS	Engineer:	S.Ditton	Client:	Modified from ACARP, 2003	
	Drawn:	S.Ditton			
	Date:	16.03.14	Title:	Predicted A-Zone Fracture Heights for Varying Panel Widths using Pi-Term Geometry and Geology Models and Current State of the Art Models	
	Ditton Geotechnical Services Pty Ltd		Scale:	NTS	Figure No: A43k



DgS	Engineer:	S.Ditton	Client:	Modified from ACARP, 2003	
	Drawn:	S.Ditton			
	Date:	16.03.14	Title:	Predicted A-Zone Fracture Heights for Varying Panel Widths using Pi-Term Geometry and Geology Models and Current State of the Art Models	
	Ditton Geotechnical Services Pty Ltd		Scale:	NTS	Figure No: A43l



DgS	Engineer:	S.Ditton	Client:	Review of Height of Fracturing Data	
	Drawn:	S.Ditton			
	Date:	01.05.14	Title:	Measured Heights of Continuous Fracturing in NSW and QLD Coalfields with Reported Surface to Seam Connectivity Cases and Theoretical Goaf Loading Height	
	Ditton Geotechnical Services Pty Ltd		Scale:	NTS	Figure No: A43m



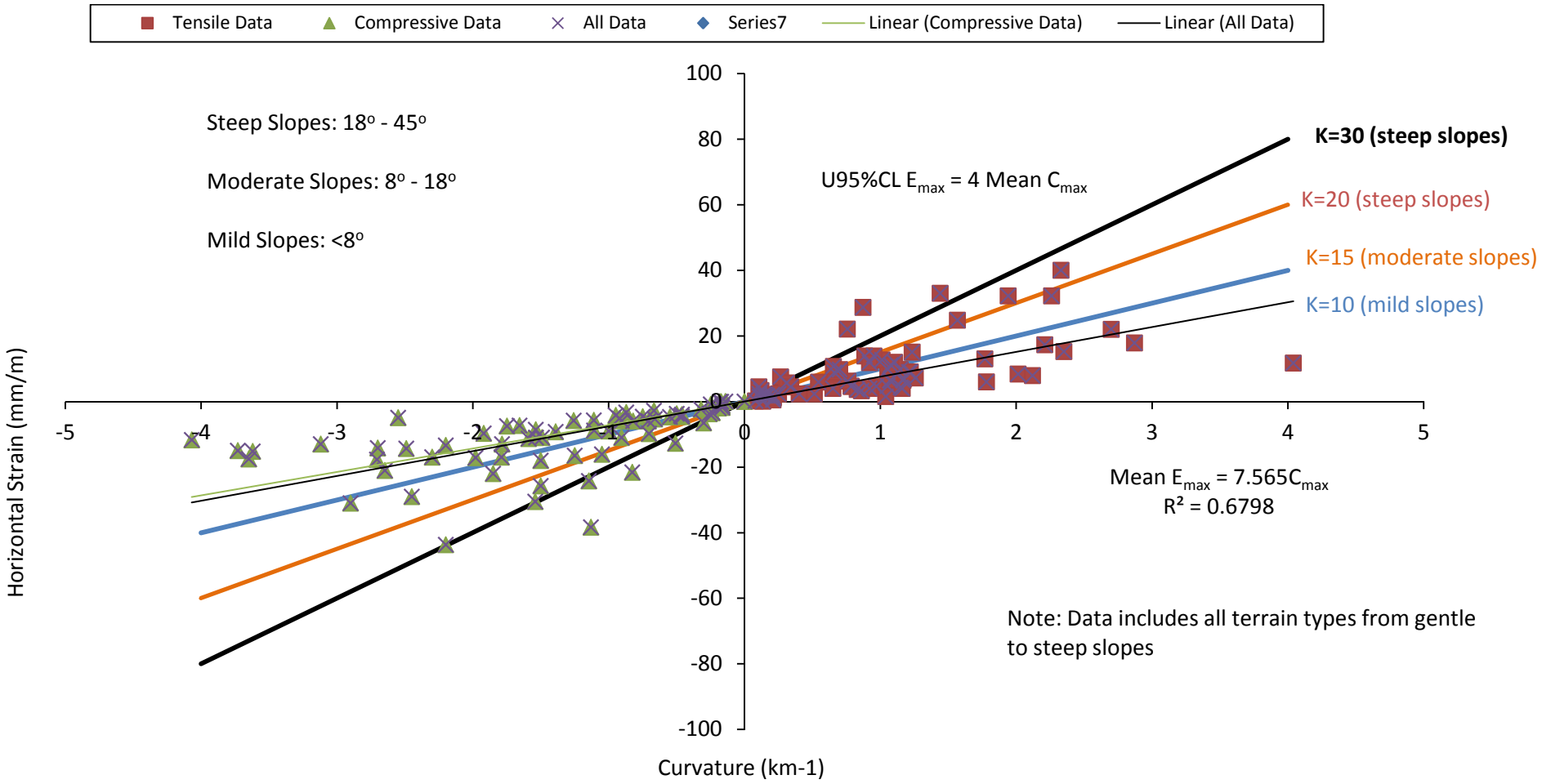
Strain E = (mm/m)
Curvature C = km^{-1}

$E = C \times d_n$

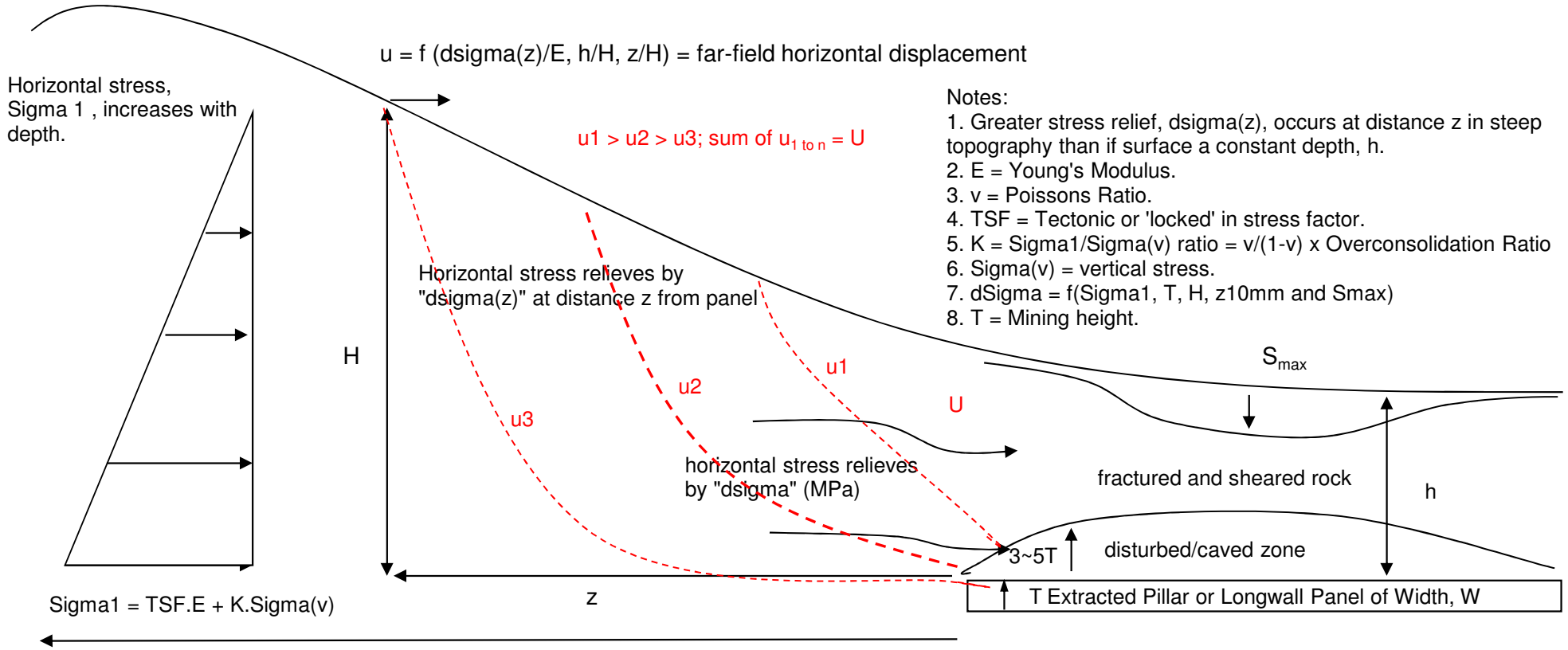
= Depth of Cracking

R = Radius of curvature or the curvature, C = 1/R (km^{-1})

DgS	Engineer:	S.Ditton	Client:	Extract from ACARP, 2003	
	Drawn:	S.Ditton			
	Date:	08.08.08	Title:	Bending Beam Theory for Strain Prediction from Curvature Measurements	
	Ditton Geotechnical Services Pty Ltd		Scale:	NTS	Figure No: A43n

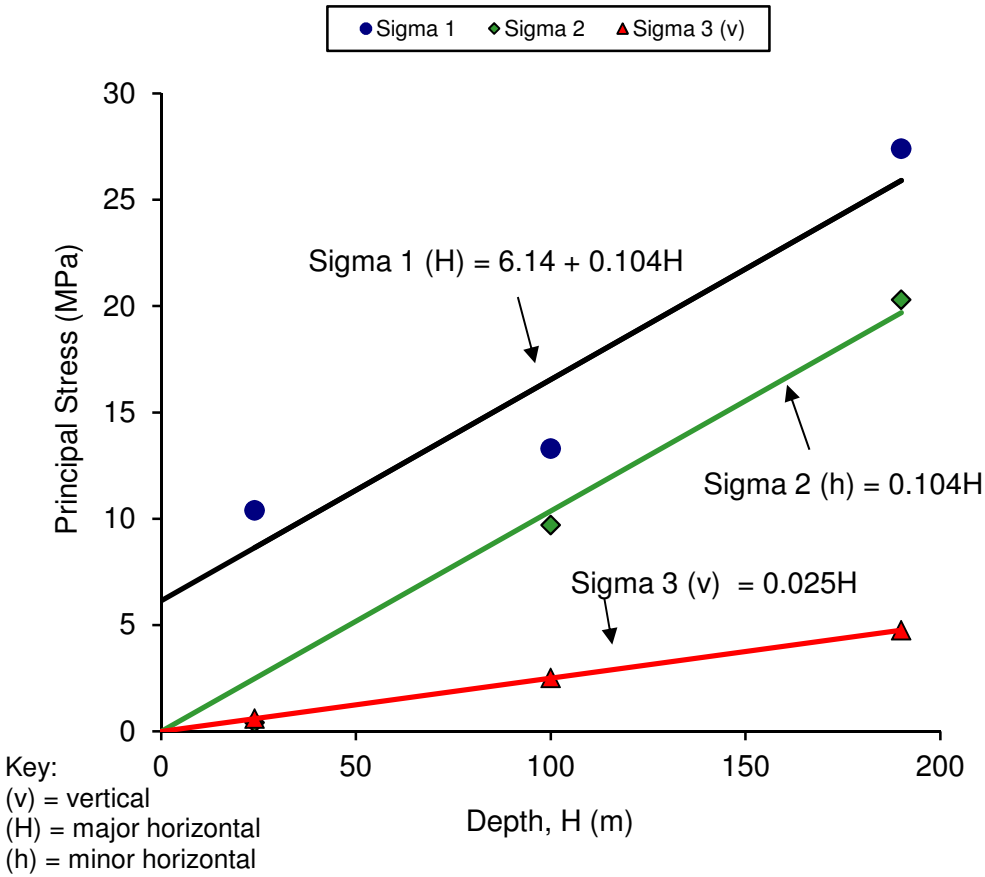


DgS	Engineer:	S.Ditton	Client:	Extract from ACARP, 2003	
	Drawn:	S.Ditton			
	Date:	08.08.08	Title:	Empirical Model for Maximum Panel Strain Prediction Above Longwall Panels for Smooth and Cracked Profiles in the Newcastle Coalfield	
	Ditton Geotechnical Services Pty Ltd		Scale:	NTS	Figure No: A43o

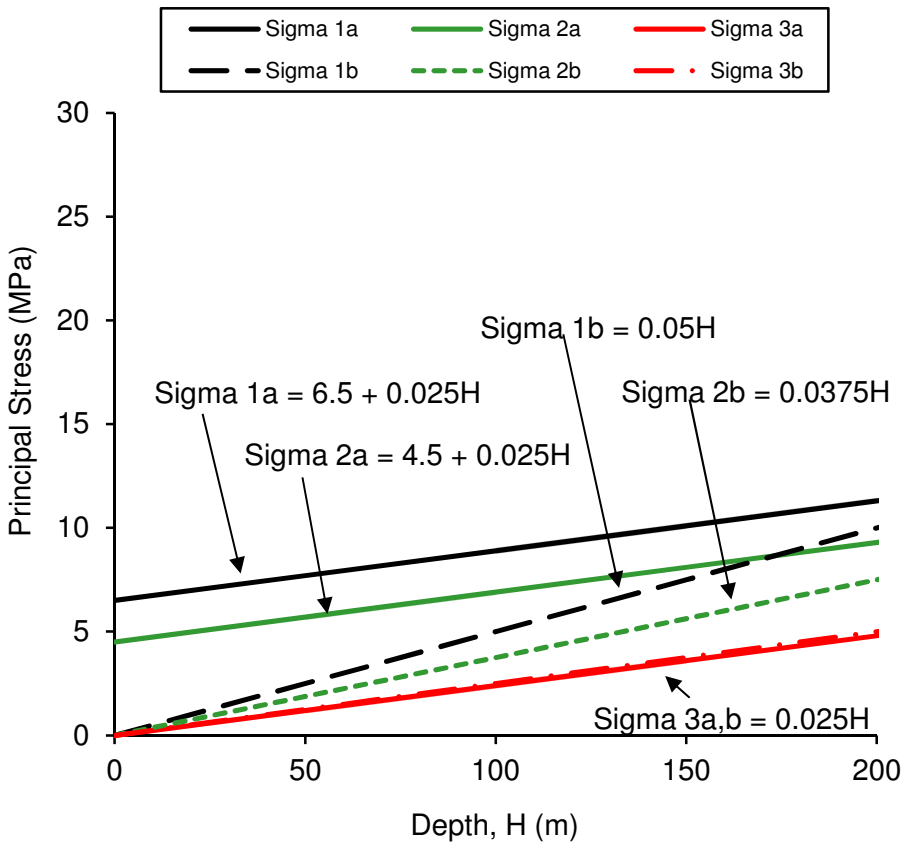


Simple Analytical Model for Predicting Total FFD : U = 0.5(Sigma1 x 12.3/2)z10mm/[E(H+h)/2] + 'tail' of 10mm + Smax component (refer to text)

DgS	Engineer:	S.Ditton	Client:	DgS, 2007	
	Drawn:	S.Ditton			
	Date:	22.05.07	Title:	Conceptual Model of Far-Field Displacement Outside Angle of Draw Limits from Pillar Extraction or Longwall Panels	
	Ditton Geotechnical Services Pty Ltd		Scale:	NTS	Figure No: A44a

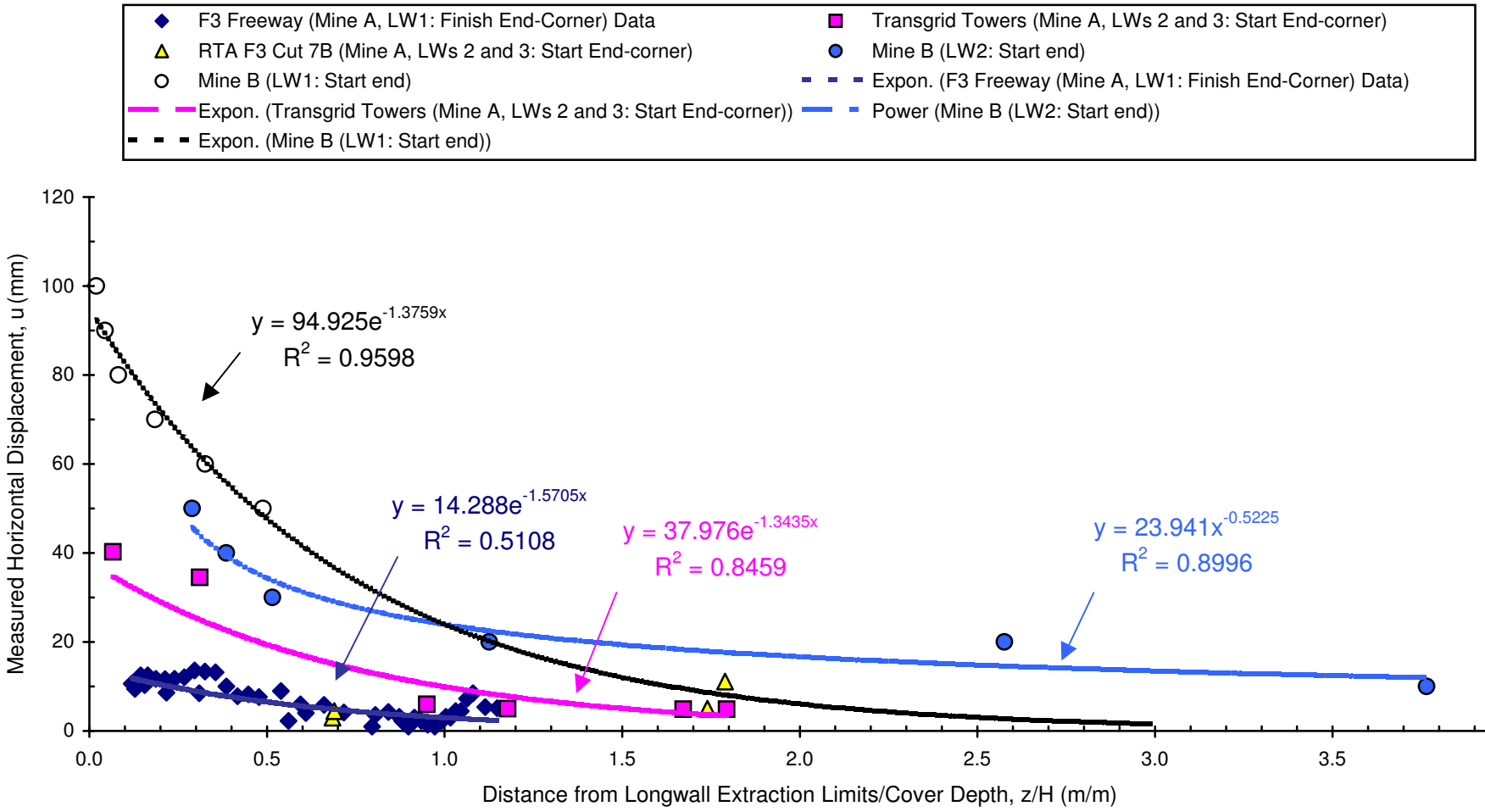


Measured Stress Field for F3 Freeway, West of Newcastle (Lohe & Dean Jones, 1995)

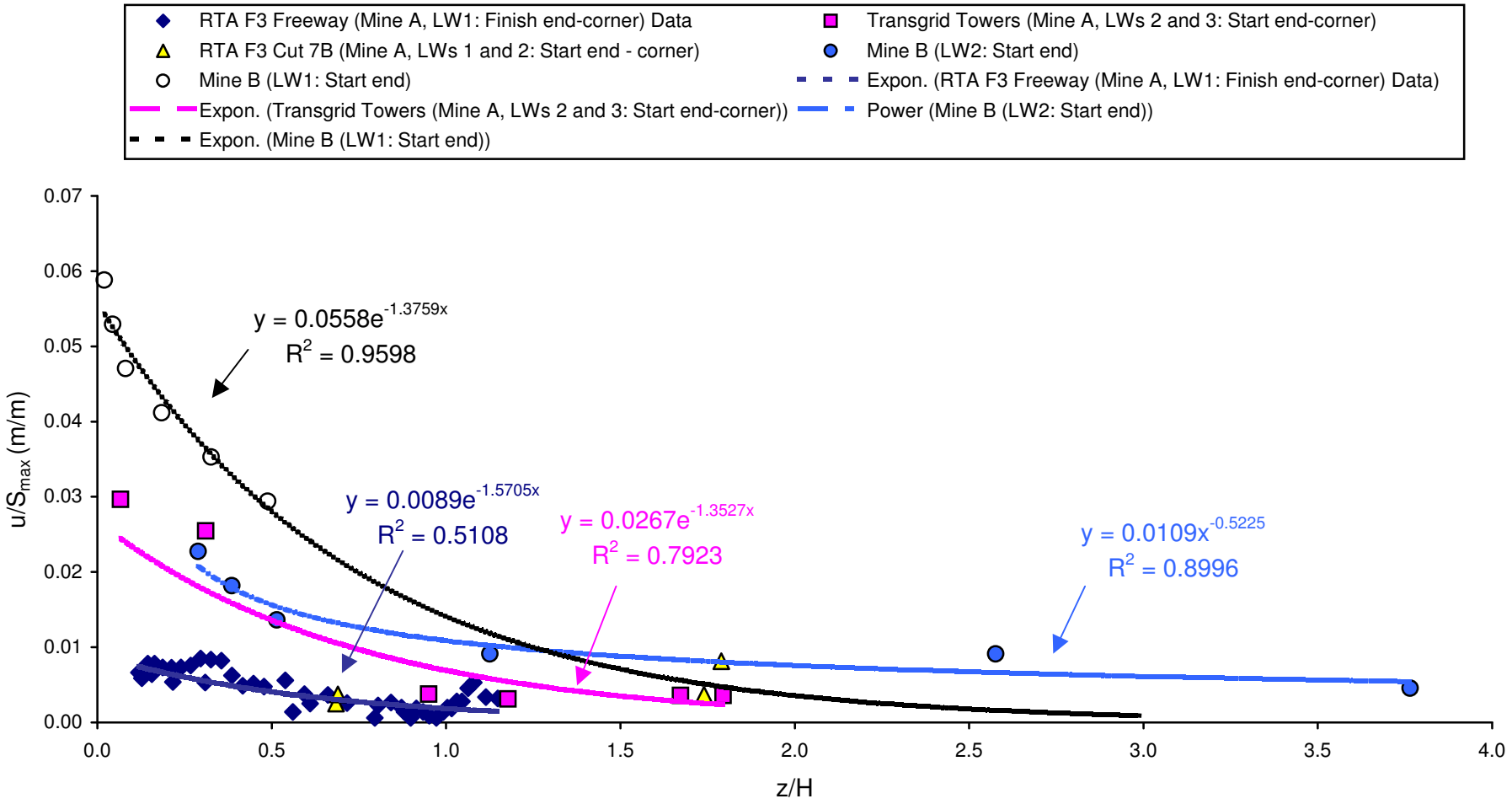


Typical Stress Field Models for Sydney Basin Overburden a) McQueen, 2004; b) Lohe & Dean Jones, 1995; c) Pells, 2002 not shown for clarity (refer to text).

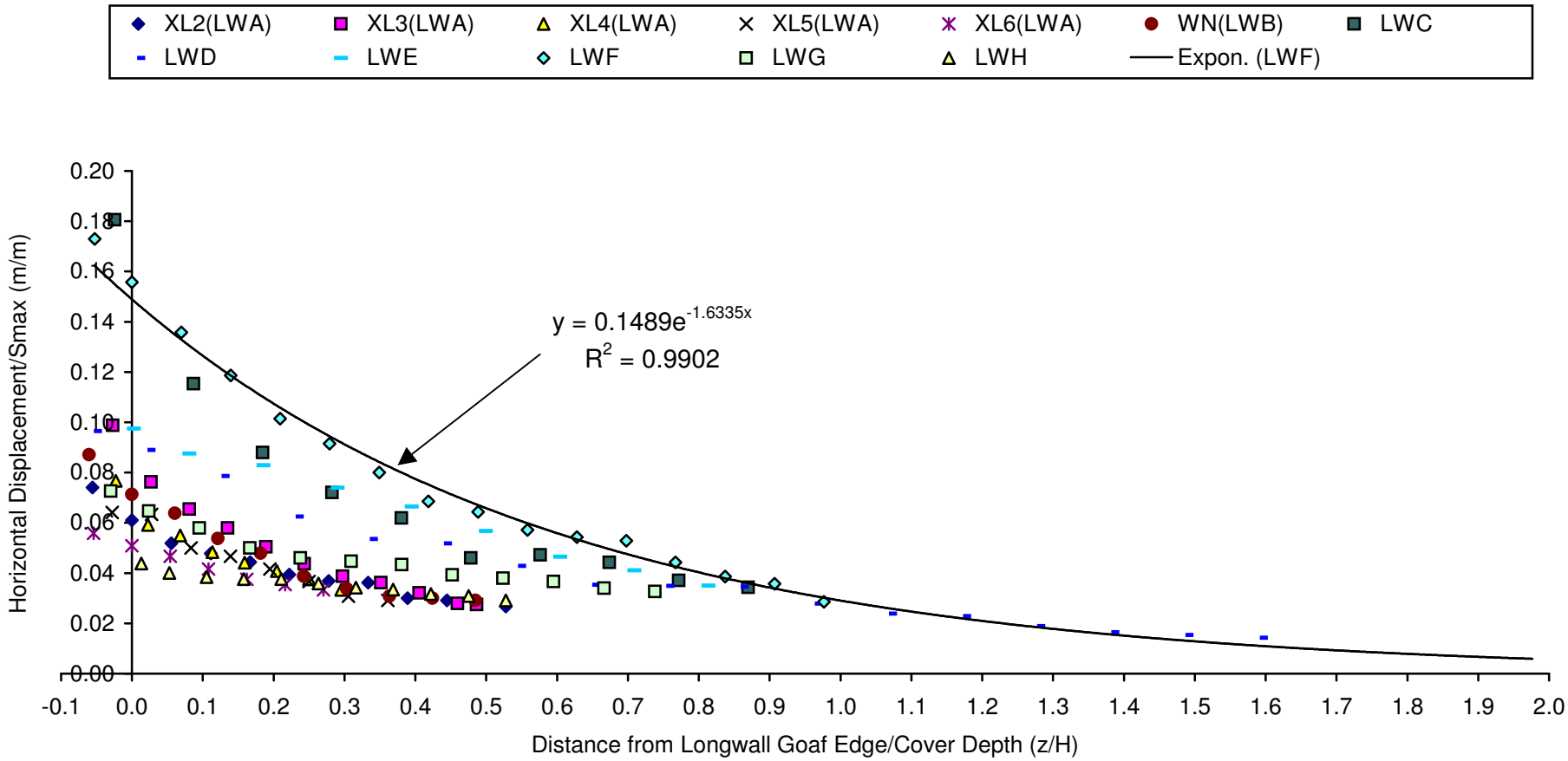
DgS	Engineer:	S.Ditton	Client:	DgS, 2007	
	Drawn:	S.Ditton			
	Date:	12.07.07	Title:	Published Principal Stress Field Models for Sydney Basin and Western Area of Newcastle Coalfield	
	Ditton Geotechnical Services Pty Ltd		Scale:	NTS	Figure No: A44b



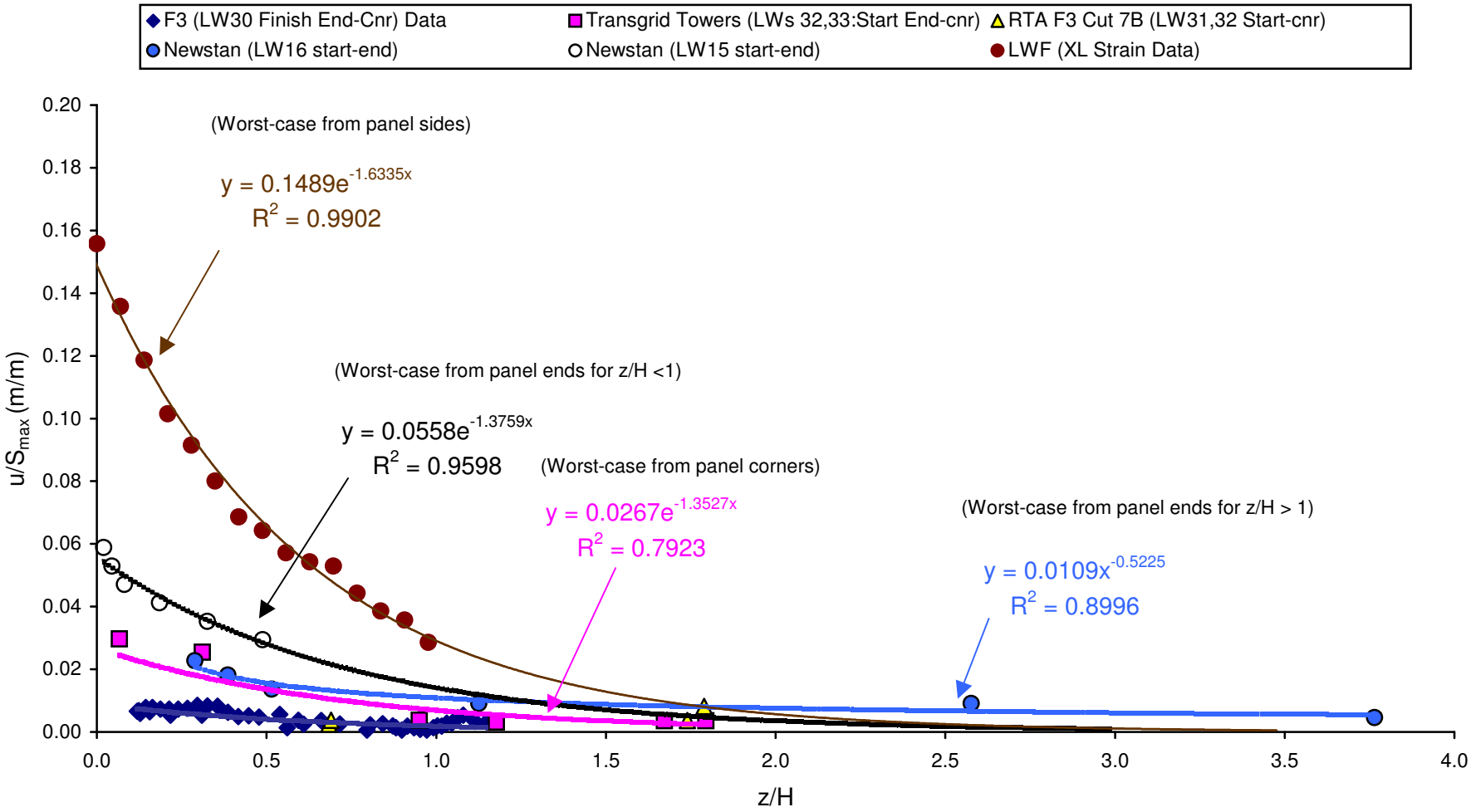
DgS	Engineer:	S.Ditton	Client:	DgS, 2007	
	Drawn:	S.Ditton			
	Date:	22.05.07	Title:	Empirical far-field displacement prediction model using total station electronic distance measurements from longwall panel ends	
	Ditton Geotechnical Services Pty Ltd		Scale:	NTS	Figure No: A45



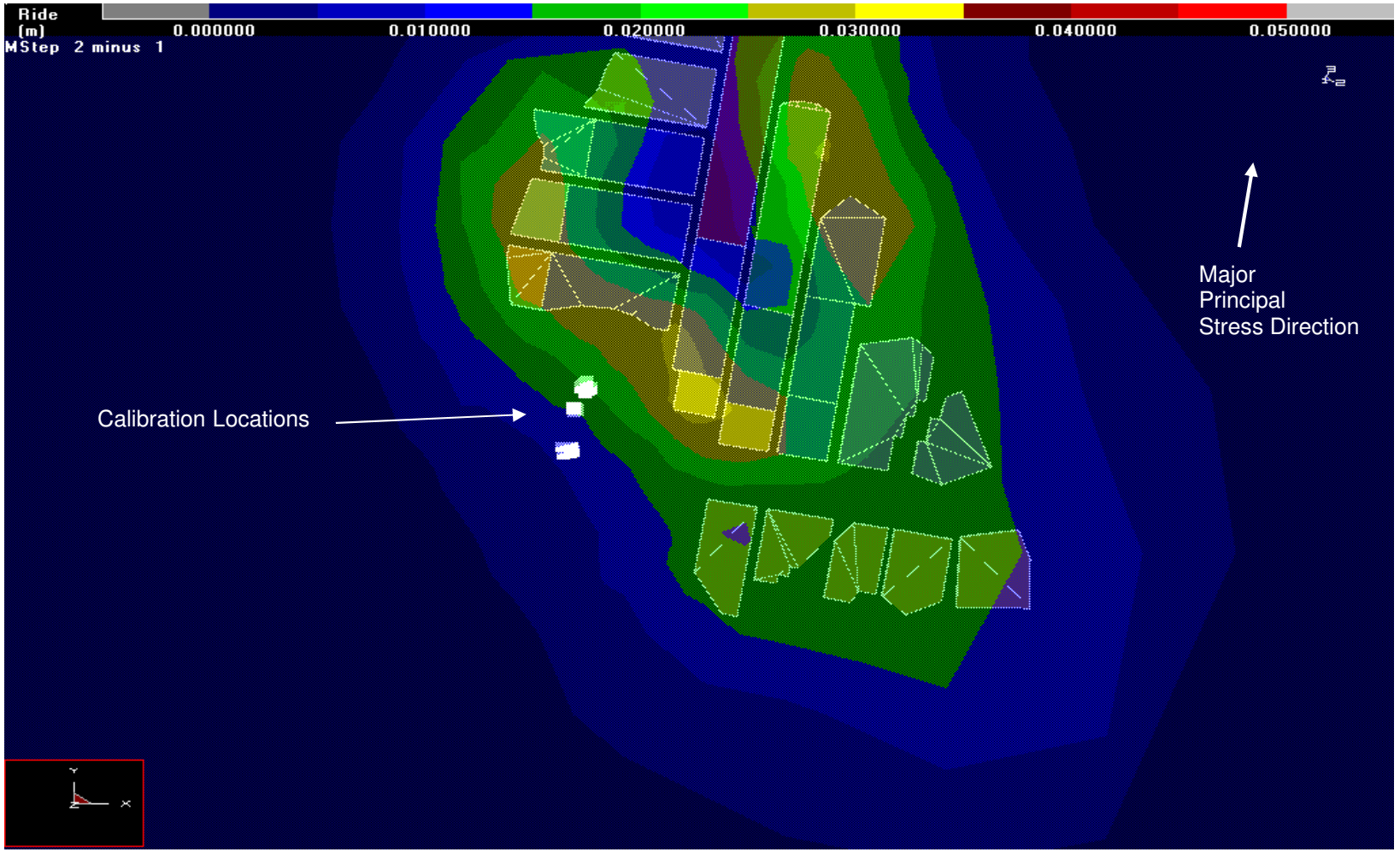
DgS	Engineer:	S.Ditton	Client:	DgS, 2007	
	Drawn:	S.Ditton			
	Date:	22.05.07	Title:	Empirical far-field displacement prediction model using total station electronic distance measurements from longwall panel ends and normalised to maximum panel subsidence	
	Ditton Geotechnical Services Pty Ltd		Scale:	NTS	Figure No: A46



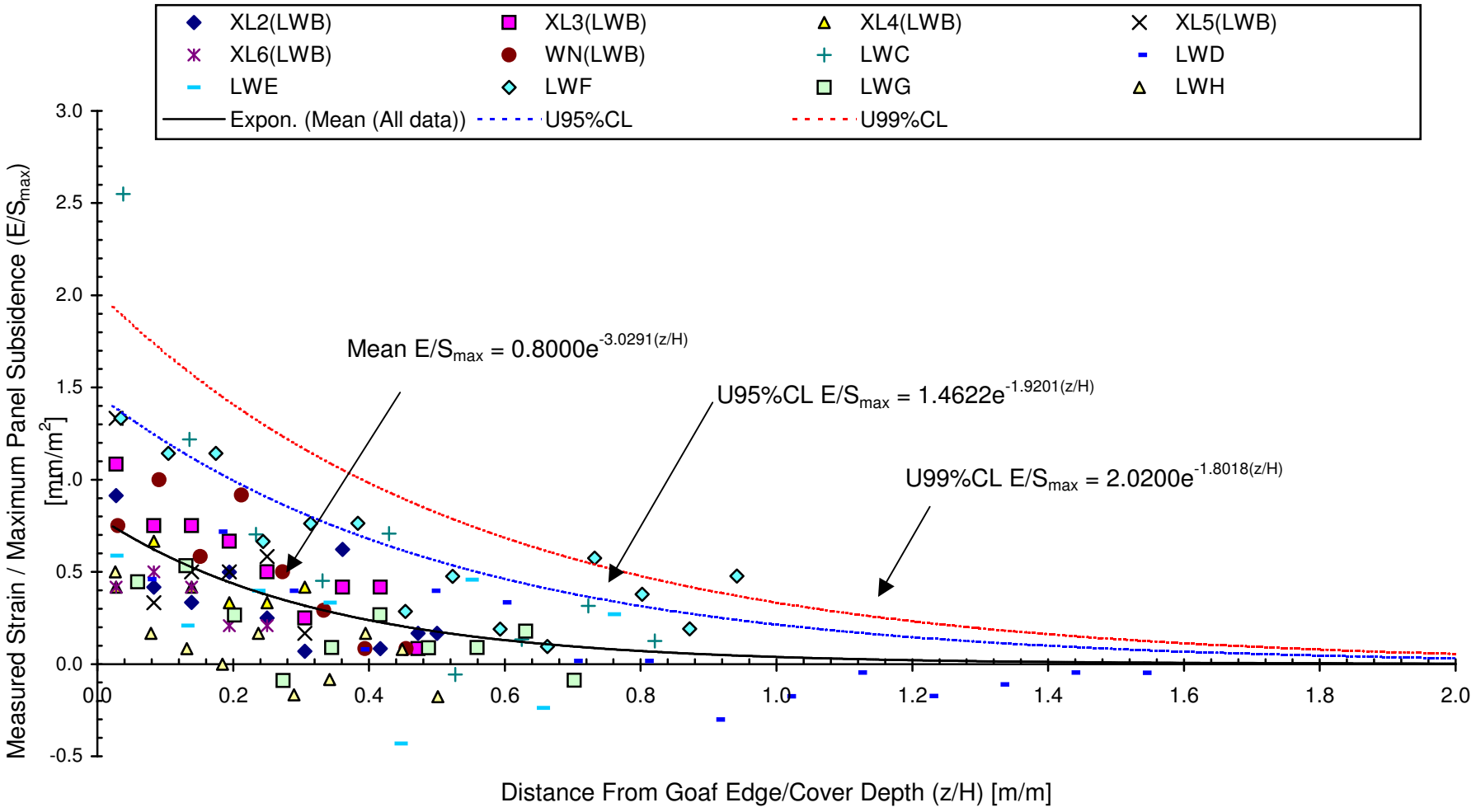
DgS	Engineer:	S.Ditton	Client:	DgS, 2007	
	Drawn:	S.Ditton			
	Date:	22.05.07	Title:	Empirical far-field displacement prediction model using cummulative steel tape measurements from longwall sides and normalised to maximum panel subsidence	
	Ditton Geotechnical Services Pty Ltd		Scale:	NTS	Figure No: A47



DgS	Engineer:	S.Ditton	Client:	DgS, 2007	
	Drawn:	S.Ditton			
	Date:	22.05.07	Title:	Combined empirical far-field displacement prediction models for longwall panel sides, ends and corners.	
	Ditton Geotechnical Services Pty Ltd		Scale:	NTS	Figure No: A48



DgS	Engineer:	S.Ditton	Client:	DgS, 2007	
	Drawn:	S.Ditton			
	Date:	22.05.07	Title:	Example of Map-3D Elastic Boundary Element Model Far-Field Displacement Contours Around a Complex Pillar Extraction Mining Layout	
	Ditton Geotechnical Services Pty Ltd		Scale:	NTS	Figure No: A49



DgS	Engineer:	S.Ditton	Client:	DgS, 2007	
	Drawn:	S.Ditton			
	Date:	22.05.07	Title:	Empirical far-field strain prediction model using cummulative steel tape measurements from longwall sides and normalised to maximum panel subsidence	
	Ditton Geotechnical Services Pty Ltd		Scale:	NTS	Figure No: A50

Appendix B - Extract from SDPS® User Manual and Lam2D Model Details

S D P S

Surface Deformation Prediction System
for Windows
version 5.2

Quick Reference Guide and Working Examples

by

Dr. Zacharias Agioutantis and Dr. Michael Karmis
Department of Mining and Minerals Engineering
Virginia Polytechnic Institute and State University
Blacksburg, Virginia 24061-0239

This software package is the property of the Department of Mining and Minerals Engineering, VPI & SU. It has been licensed and may be distributed only to O.S.M.R.E. and State Regulatory Agencies. The SDPS software can be purchased by individuals and/or companies through Carlson Software.

February 2002

List of Symbols

w	the panel width; the minimum dimension of a panel
h	panel depth; the vertical distance between the mining horizon and the surface; also known as the overburden thickness
m	the seam thickness; the extraction thickness (note that the extraction thickness may be different than the seam thickness)
R	the extraction ratio
R*	the adjusted extraction ratio
d	the distance of the inflection point from the rib (a positive value indicates that the position of the inflectionpoint is inby); also referred to as the “edge effect”
β	the influence angle
r	the influence radius
Smax	the maximum subsidence
a	the maximum subsidence factor
Bs	the strain coefficient
%HR	the percent hardrock in the overburden
Wp	the pillar width
Hp	the pillar height
Wo	the opening width

1.7 Overview of Subsidence Parameters

Maximum Subsidence Factor
The values of maximum subsidence factor, as function of the width-to-depth ratio and the percent hardrock in the overburden, are shown in the supercritical subsidence factor tables for longwall panels and for room-and-pillar panels respectively. When using the profile function method, the subsidence factor is calculated for the actual width-to-depth ratio of the panel. For example, for a panel with W/h = 0.8 (subcritical) and %HR = 50% the subsidence factor is equal to 0.38.

When using the influence function method, the technique requires knowledge of the supercritical subsidence factor, which will subsequently be adjusted through the superposition concept by the program itself. For example, for a panel with W/h = 0.8 (subcritical) and %HR = 50% the subsidence factor is found for W/h = 1.5 (supercritical) and equal to 0.40.

Notes:
A panel is considered supercritical for W/h greater than 1.2. Due to numerical approximations there may be slight variations to the supercritical subsidence factors presented in the supercritical subsidence factor tables.

Inflection Point
The location of the inflection point from the rib, with respect to overburden depth (d/h), can be estimated based on two empirical curves (see the Inflection Point Diagram). Both curves were statistically generated from the available field data. The first is an average curve based on a least squares estimator, while the second is considered an envelope or conservative curve in the sense that it tends to overpredict the surface impact of a given excavation area. In essence, this means that for average data the predicted subsidence profile could be either inside or outside of the measured subsidence line, whereas for conservative (envelope) data, an attempt is made to keep the prediction lines outside the measured ones, i.e. overestimate the influence of the mined area to the surface.

From experience and constant validation of the programs, the authors recommend that, for Appalachian predictions, improved accuracy is obtained by using the following rule:
determine the d/h ratio using the conservative curve for subcritical panels (W/h < 1.2)
determine the d/h ratio using the average curve for supercritical panels (W/h >= 1.2).

Notes:
Always use the actual width-to-depth ratio.

Angle of Influence
The angle of principal influence (β, beta) is one of the basic parameters used in the influence function method since it has a major impact on the distribution of the deformations on the surface. It is measured in degrees from the horizontal and the

average value determined for the Appalachian coalfields is beta=67 deg. The parameter required for these calculations is the tangent of this angle (i.e. tanβ = 2.31). The angle of influence is related to the radius of influence as shown in the equation:

$$\tan\beta = \frac{h}{r}$$

where
h = the overburden depth
r = the radius of influence

This value should be determined for each site by fitting a calculated subsidence profile to a measured subsidence profile. If this is not possible, the influence angle can be approximately set as the complementary angle to the angle of draw.

Supercritical Subsidence Factor Tables
The supercritical subsidence factors used in the calculations are presented in Tables 1.7.1 and 1.7.2.

Table 1.7.1: Calculation of maximum subsidence factors (Smax/m) for longwall panels

	Percent Hardrock in the Overburden							
W/h	10%	20%	30%	40%	50%	60%	70%	80%
0.6	0.64	0.59	0.51	0.42	0.34	0.26	0.21	0.16
0.7	0.69	0.63	0.55	0.46	0.36	0.28	0.22	0.18
0.8	0.71	0.65	0.57	0.47	0.38	0.29	0.23	0.18
0.9	0.72	0.66	0.58	0.48	0.38	0.30	0.23	0.19
1.0	0.73	0.67	0.58	0.49	0.39	0.30	0.24	0.19
1.1	0.74	0.68	0.59	0.49	0.39	0.31	0.24	0.19
1.2	0.74	0.68	0.59	0.49	0.39	0.31	0.24	0.19
1.3	0.74	0.68	0.60	0.49	0.40	0.31	0.24	0.19
1.4	0.75	0.69	0.60	0.50	0.40	0.31	0.24	0.19
1.5	0.75	0.69	0.60	0.50	0.40	0.31	0.24	0.19
1.6	0.75	0.69	0.60	0.50	0.40	0.31	0.24	0.19
1.7	0.75	0.69	0.60	0.50	0.40	0.31	0.24	0.19
1.8	0.75	0.69	0.60	0.50	0.40	0.31	0.24	0.19
1.9	0.76	0.69	0.60	0.50	0.40	0.31	0.24	0.19
2.0	0.76	0.69	0.60	0.50	0.40	0.31	0.24	0.19

Table 1.7.2: Calculation of maximum subsidence factors (Smax/(m R*)) for high extraction room-and-pillar panels

	Percent Hardrock in the Overburden							
W/h	10%	20%	30%	40%	50%	60%	70%	80%
0.6	0.52	0.48	0.42	0.35	0.28	0.22	0.17	0.13
0.7	0.57	0.53	0.46	0.38	0.30	0.24	0.19	0.15
0.8	0.60	0.55	0.48	0.40	0.32	0.25	0.19	0.15
0.9	0.61	0.56	0.49	0.41	0.32	0.25	0.20	0.16
1.0	0.62	0.57	0.49	0.41	0.33	0.26	0.20	0.16
1.1	0.62	0.57	0.50	0.41	0.33	0.26	0.20	0.16
1.2	0.63	0.58	0.50	0.42	0.33	0.26	0.20	0.16
1.3	0.63	0.58	0.51	0.42	0.34	0.26	0.20	0.16
1.4	0.64	0.58	0.51	0.42	0.34	0.26	0.21	0.16
1.5	0.64	0.59	0.51	0.42	0.34	0.26	0.21	0.16
1.6	0.64	0.59	0.51	0.42	0.34	0.26	0.21	0.16
1.7	0.64	0.59	0.51	0.43	0.34	0.27	0.21	0.16
1.8	0.64	0.59	0.51	0.43	0.34	0.27	0.21	0.17
1.9	0.64	0.59	0.51	0.43	0.34	0.27	0.21	0.17
2.0	0.64	0.59	0.52	0.43	0.34	0.27	0.21	0.17

Horizontal Strain Factor

The value of this factor is directly related to the magnitude of the calculated strains and curvatures over an undermined area. It can be empirically estimated by the average ratio of measured strain and curvature over a set of surface points.

The average value determined for the Appalachian coalfields is:

$$Bs = (0.35 \pm 0.05)\ \frac{h}{\tan\beta}$$

where h is the excavation depth and tanβ is the influence angle. The horizontal strain factor is expressed in units of length. The horizontal strain coefficient is unitless and its default value is 0.35.

Note: The higher the value for this coefficient, the larger the predicted strains and displacements.

Chapter 3: The Influence Function Method

3.1 Overview of the Influence Function Method

Influence function methods for subsidence prediction have the ability to consider any mining geometry, to negotiate superposition of the influence from a number of excavated areas having different mining characteristics and, also, to calculate horizontal strains as well as other related deformation indices. The function utilized in SDPS is the bell-shaped Gaussian function. This method assumes that the influence function for the two-dimensional case is given by:

$$g(x,s) = \frac{S_o(x)}{r}\exp\left[-\pi\frac{(x-s)^2}{r^2}\right]$$

where:

r	=	the radius of principal influence = h / tan(beta);
h	=	the overburden depth;
beta	=	the angle of principal influence;
s	=	coordinate of the point P, where subsidence is considered;
x	=	coordinate of the infinitesimal excavated element; and
So(x)	=	convergence of the roof of the infinitesimal excavated element.

Subsidence at any point P(s), therefore, can be expressed by the following equation:

$$S(x,s) = \frac{1}{r}\int_{-\infty}^{+\infty} s_o(x)\exp\left[-\pi\frac{(x-r)^2}{r^2}\right]$$

where:

So(x)	=	m(x) a(x);
m(s)	=	extraction thickness; and
a(x)	=	roof convergence (subsidence) factor.

The influence function formulation can thus be applied to calculate surface deformations (subsidence, strain, slope, curvature, displacements) above longwall and room-and-pillar panels, given the geometry of the excavation, information on the overburden geology, as well as the location of the prediction points on the surface. More specifically, the required data include:

- the geometry of the mine plan and the associated properties (extraction thickness, subsidence factor for supercritical conditions)

- the location (coordinates) of the points on the surface for which prediction of the deformation indices (subsidence, strain, slope, curvature, horizontal displacement) is to be performed
- the empirical parameters that numerically represent the behavior of the overburden

The typical steps required to calculate surface deformations using the influence function method, are shown below. The corresponding flowchart is also shown in Figure 3.1.1. Figure 3.1.2 presents a schematic diagram for creating the input data. Figure 3.1.3 presents typical distributions for the deformation indices that can be calculated by the influence function method. Table 3.1.1 shows all the indices that can be calculated by the influence function method.

✓ Load the Influence Function Program
✓ Input Data
✓ Mine Plan Data
  - Prediction Point Data
  - Empirical Parameters
✓ Select calculation options
  - Subsidence
  - Horizontal Strain
  - Horizontal Displacement
  - Slope
  - Curvature
✓ Save Project File
✓ Calculate Surface Deformations
✓ Load Graphing Program
✓ View Calculated Deformations

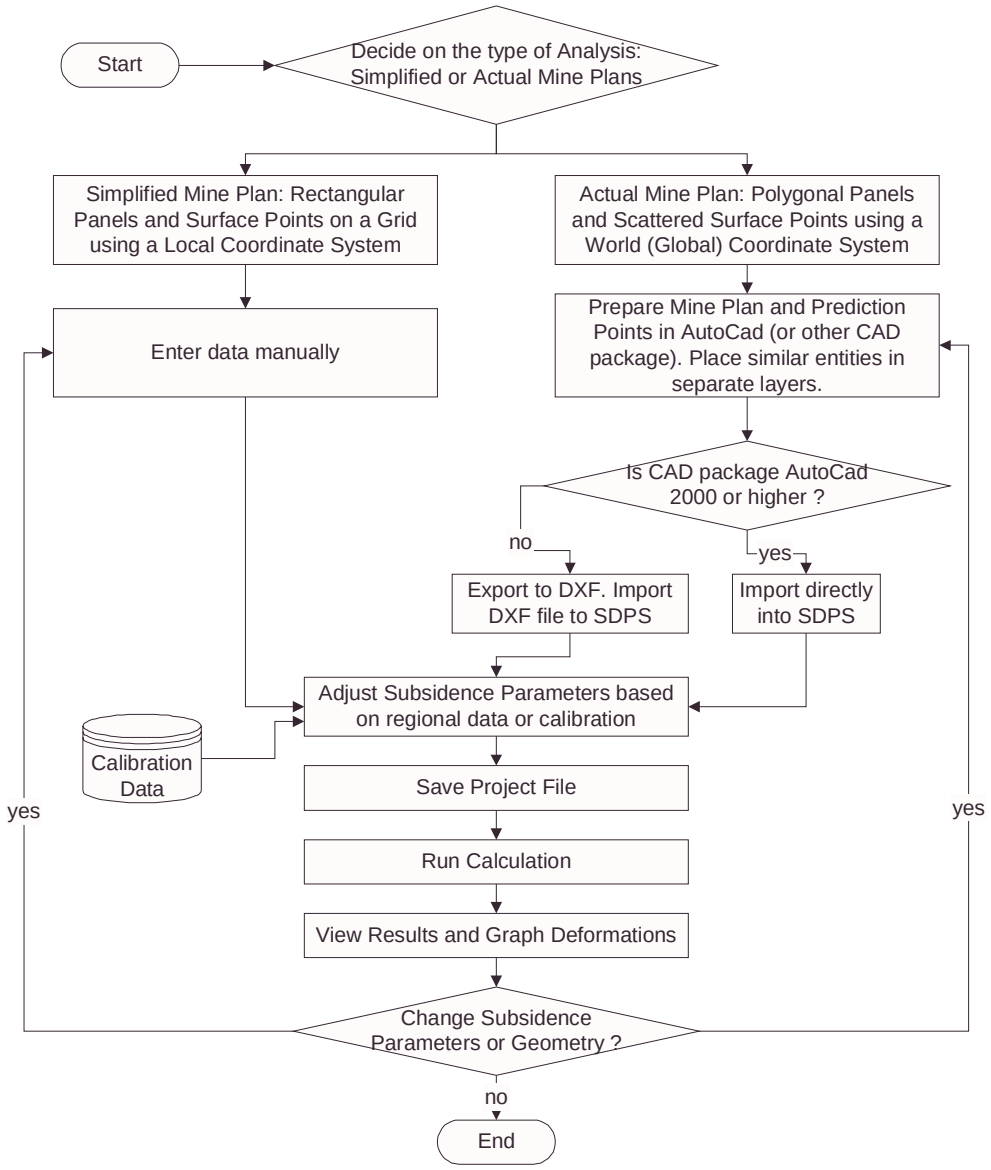
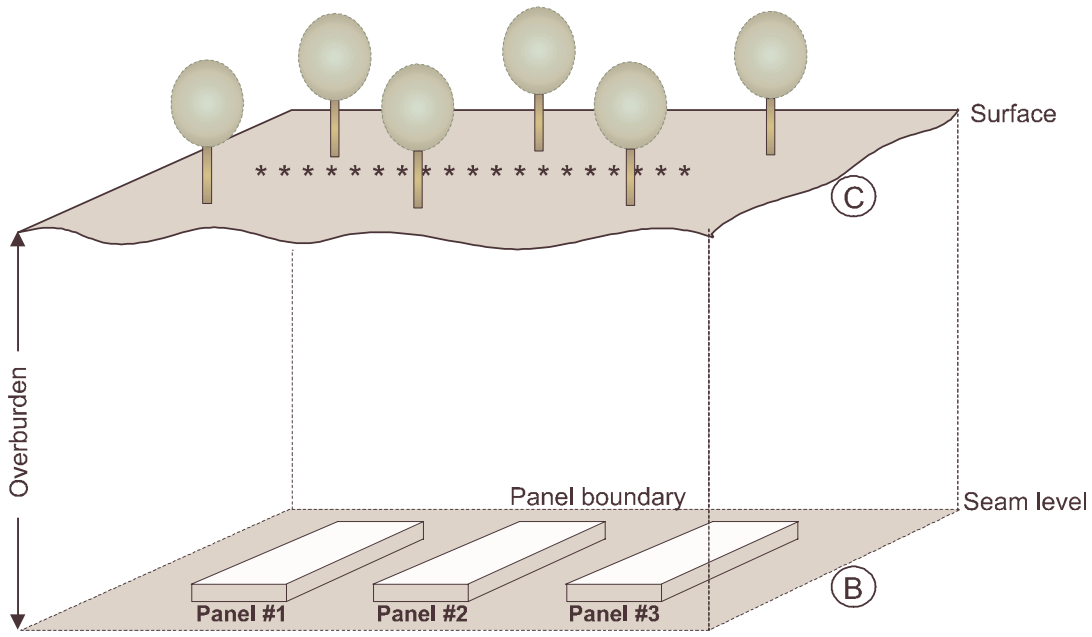


Figure 3.1.1: Flowchart diagram for using the influence function module



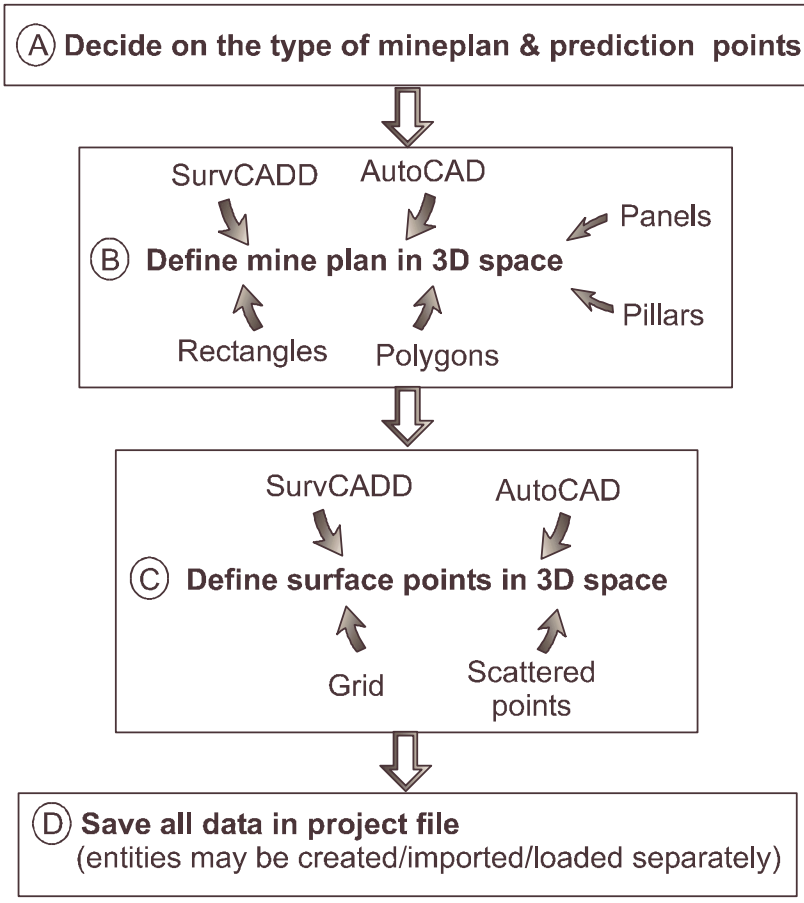
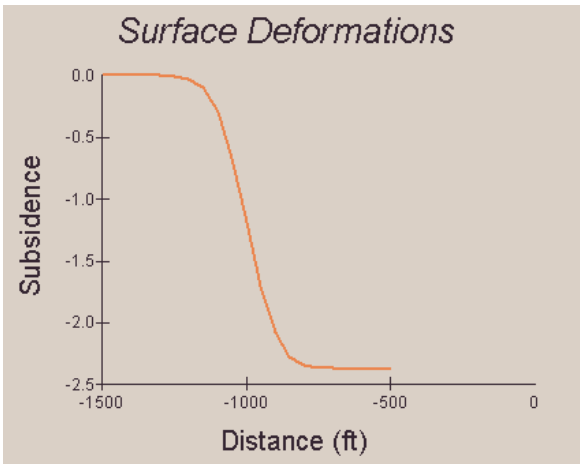
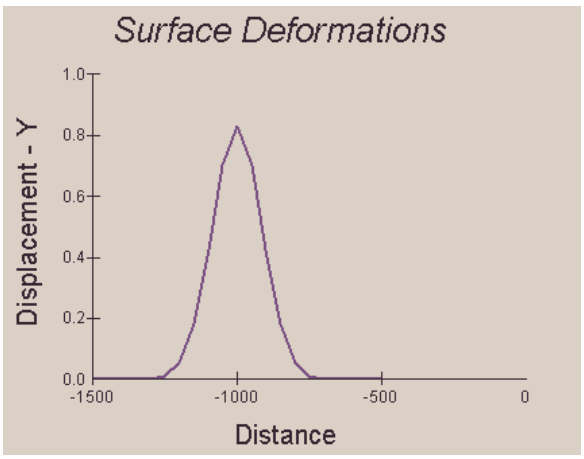
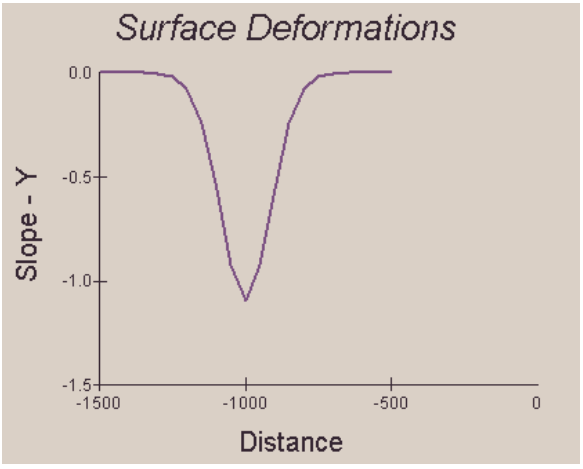


Figure 3.1.2: Steps in defining a project file







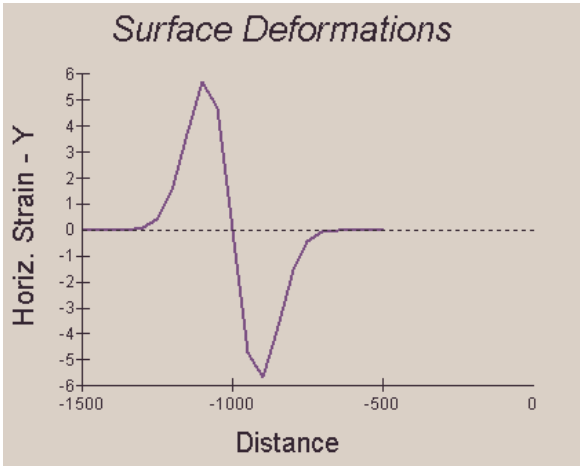


Figure 3.1.3: Typical deformation distributions

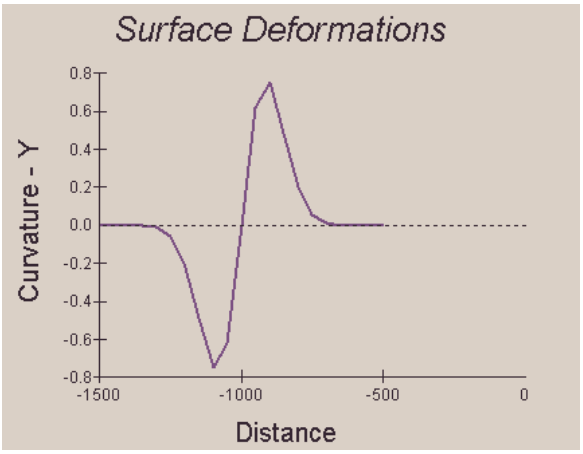


Table 3.1.1: Identification codes for deformation indices

Number	Deformation Index Name	Code	Units
1	Subsidence	SU	ft or m
2	Slope in the X-direction	TX	%
3	Slope in the Y-direction	TY	%
4	Directional Slope	TA	%
5	Maximum (Total) Slope	TM	%
6	Angle[1] of Maximum Slope	TE	deg
7	Horizontal Displacement in the X-direction	VX	ft or m
8	Horizontal Displacement in the Y-direction	VY	ft or m
9	Directional Horizontal Displacement	VA	ft or m
10	Maximum (Total) Horizontal Displacement	VM	ft or m
11	Angle[1] of Maximum Horizontal Displacement	VE	deg
12	Curvature in the X-direction	KX	1/ft or 1/m [2]
13	Curvature in the Y-direction	KY	1/ft or 1/m [2]
14	Directional Curvature	KA	1/ft or 1/m [2]
15	Maximum Principal Curvature	K1	1/ft or 1/m [2]
16	Minimum Principal Curvature	K2	1/ft or 1/m [2]
17	Maximum Curvature	KM	1/ft or 1/m [2]
18	Angle[1] of Maximum Principal Curvature	KE	deg
19	Horizontal Strain in the X-direction	EX	- [3]
20	Horizontal Strain in the Y-direction	EY	- [3]
21	Directional Horizontal Strain	EA	- [3]
22	Maximum Strain	EM	- [3]
23	Maximum Principal Strain	E1	- [3]
24	Minimum Principal Strain	E2	- [3]
25	Angle[1] of Maximum Principal Strain	EE	deg

[1] This angle is calculated in degrees from the positive x-axis in a counter-clockwise direction. It gives the direction of the maximum value of the corresponding index on the x-y plane.

[2] expressed in tenths of ppm (divide by 10.000 to obtain result)

[3] expressed in millistrains (divide by 1000 to obtain result)

3.2 Definition of the Mine Plan in the Influence Function Program

Mine plan data describe the extraction area under consideration using various conventions. An extraction area is always defined in three-dimensional space by specifying the X,Y,Z coordinates of the points defining that area. Mine panels and pillars are referred to as excavation parcels. A parcel can be either active or not active. A parcel, which is not active, is not deleted from the file, but it does not participate in the calculations.

Geometry and Boundary Adjustment:

The geometry of a mine plan is determined by the geometry of the excavation panels adjusted by the edge effect. This parameter represents the distance between the actual rib of the excavation and the position of the inflection point, as determined by panel geometry and site characteristics. The location of the inflection point, which defines the transition between horizontal tensile and compressive strain zones, is very important for the application of the influence function method. The distance of the inflection point from the rib using either an average and a conservative estimate as a function of the width-to-depth ratio of a panel can be estimated using this graph.

Thus, the magnitude of the edge effect can be determined as follows:

- ✓ from the graph estimating the location of the inflection point for the conservative or average estimate (Figure 3.1.1),
- ✓ by clicking on the *Subs.Parm* button in the rectangular mine plan form of the influence function program,
- ✓ by analyzing subsidence curves measured at a specific site or region.

Panel Representation:

- ✓ Simple mine layouts can usually be approximated using sets of rectangular extraction areas. In this case, the input required for every parcel includes the parcel number; the coordinates of the west, east, south, and north borders; the seam elevation; the extraction thickness (mining height); and the average supercritical subsidence factor (in percent) associated with it. These coordinates can be specified in a local or a global coordinate system with axes parallel to the parcel sides. In the Influence function module, this option is implemented as **Rectangular Mine Plans.**

- ✓ Complex mine layouts can usually be approximated by a closed polygon (i.e. a piece-wise linear shape). In this case, the input required for every point within a parcel includes the point reference number; the northing (Y), easting (X), and elevation (Z); the extraction thickness (mining height); and the supercritical subsidence factor (in percent) associated with it. The mine plan editor can

provide access to all points in a parcel, add new points, and add new parcels provided that the current parcel is defined by three or more points. The points should be entered in a counter-clockwise fashion. The location of each point should be adjusted to reflect the edge effect, or the relative position of the inflection point. The maximum number of parcels and points per parcel can be adjusted within the limits of the available memory. In the Influence function module, this option is implemented as Polygonal Mine Plans.

Warning:

Pillars can not exist outside extracted areas. If a pillar is defined outside an extracted area the results are unpredictable. Currently, the parcel definition module of the program can not check for such inconsistencies. Examples of erroneous panel definitions are given in Appendix 3.

Notes:

- ✓ If no adjustments are made to the geometry of the mine plan, the program assumes that the inflection point is over the rib of the excavation.
- ✓ The user must specify whether each parcel represents an extracted panel or a pillar within an extracted panel. A pillar is mathematically represented as a parcel with a negative subsidence factor. Setting the pillar option on a parcel will reset the subsidence factor associated with this parcel. In that sense, an extraction area can be either positive (i.e. longwall panel) or negative (i.e. pillar in the middle of a panel). Thus, a mine plan that consists only of pillars (without an extraction boundary) will produce a mathematically positive! subsidence.
- ✓ It should be emphasized that the subsidence factor used here is the subsidence factor for supercritical conditions.
- ✓ The reason for supporting more than one format for input data is for the user's convenience. For example, certain panels or pillars can be easily represented as rectangles and can be entered as single entities, compared to four or more entries required if these panels are digitized point by point. Additionally, calculations for rectangular parcels are much faster compared to calculations for parcels defined by individual points.

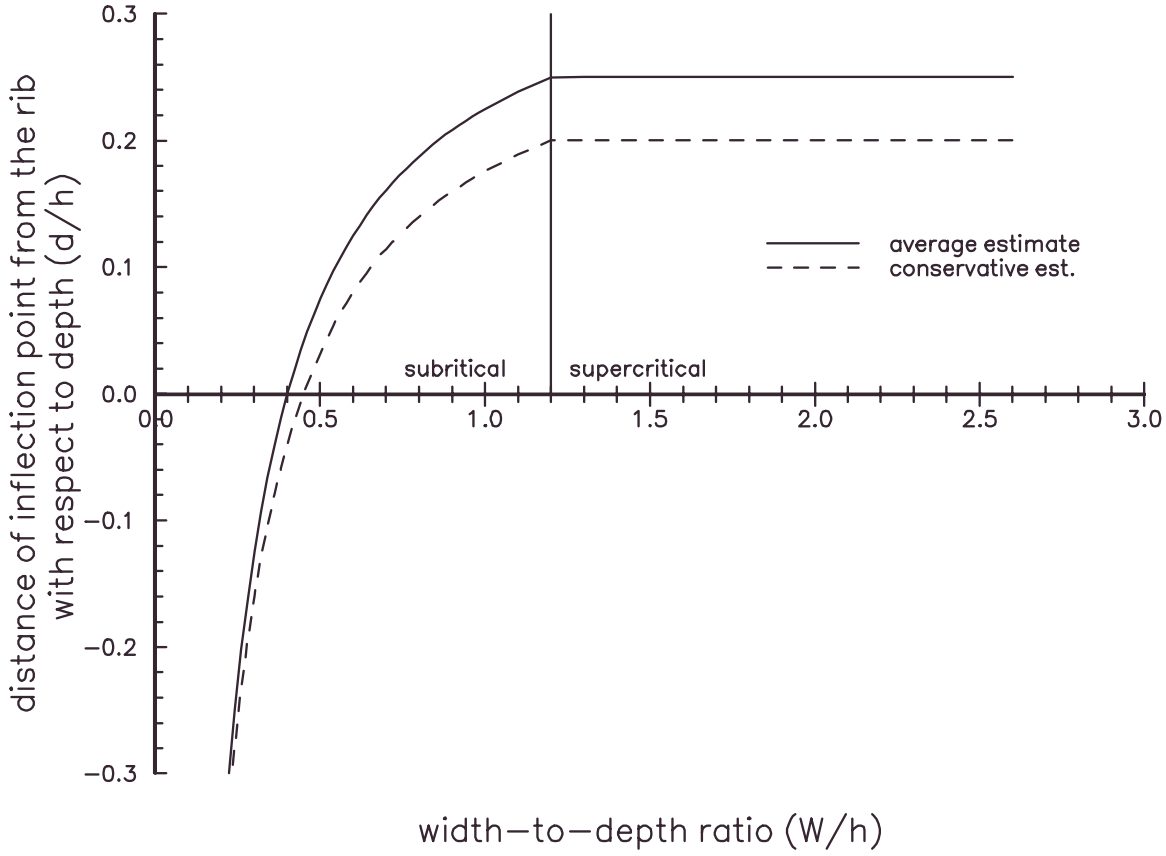


Figure 3.2.1: Determination of the offset of the inflection point.

3.3 Definition of the Prediction Points in the Influence Function Program

Prediction point data describe the surface points where the deformation indices will be calculated. Prediction points are always defined in three-dimensional space, by specifying the X,Y,Z coordinates of these points. A point can be either active or not active. A point which is not active is not deleted from the file but will not be included in the calculations.

Scattered Points

A scattered point set may consist of any number of points that are randomly located on the surface. If such points can be specified as part of a grid, then the Grid Points option should be used. Required parameters for each point include:

- ✓ the point reference code which can be any alphanumeric string,
- ✓ the easting, northing and elevation of each point,
- ✓ the point status, i.e. active or not active (an inactive point will not be displayed in the View option and will not participate in any of the calculations)

Grid Points

A grid point set may consist of any number of points in a window. This window is defined by minima and maxima in the X- and Y- directions as well as the cell size in each direction.

The grid can only be oriented parallel to the current coordinate system. If the grid needs to be oriented at an angle to the current coordinate system, the grid points should be generated by a different tool and imported as scattered points into the Influence Function module.

The user has two options regarding grid elevations.

- ✓ to consider a flat surface and specify a uniform elevation for all points, and
- ✓ to consider each point on an individual basis and specify individual point elevations.

Surface Deformation Characteristics Above Undermined Areas: Experiences from the Eastern United States Coalfields

M. KARMIS, A. JAROSZ, P. SCHILIZZI & Z. AGIOUTANTIS*

SUMMARY Damage resulting from surface movements due to underground mining may range from simple land settlement to severe structural damage. Since subsidence prevention is not feasible, it is important that accurate ground movement prediction techniques are developed, so that damage due to underground mining as well as the amount of coal lost due to the protection of surface structures can be minimized.

To facilitate the mitigation of the deleterious effects of subsidence in the Eastern U.S. region, empirical subsidence prediction techniques for longwall mining were developed from 45 case studies collected within the coalfield. From these subsidence prediction techniques a strain prediction model was also formulated. These subsidence and strain prediction methods can be used to predict ground movements as part of the mining plan and to evaluate the impacts of underground mining on the surface.

1 INTRODUCTION

Surface subsidence is rapidly gaining emphasis as an important environmental consequence of underground coal mining in the United States. Its impact has been witnessed in both rural and urban areas, and can be associated with active as well as abandoned mining operations. The damage associated with this phenomenon may include land settlement and fracturing, structural damage to surface buildings or facilities and disruption or contamination of ground water supplies.

As the need for energy increases, coal production will undoubtedly be accelerated, and since over 99 percent of all subsidence recorded in the United States arises from underground mining, it is evident that the incidence of subsidence will increase. With this increase in production and as underground mining moves into more populous areas, the prediction of surface subsidence, horizontal displacements, strains, and associated damages will surely become a requisite.

To exemplify the significance of this problem, a recent U.S. Bureau of Mines report indicated that over 32,000 km^2 have been undermined in the United States in extracting coal, metals and nonmetallic ores. Over one-fourth of this area, or approximately 8100 km^2, has been disturbed by subsidence, with underground mining of bituminous coal accounting for 7700 km^2 and metal and nonmetallic ores accounting for 68 km^2 of disturbed land. Thus, over 99 percent of all subsidence incidents are attributed to underground coal mining. Moreover, the Bureau of Mines estimates that an additional 10,000 km^2 will be undermined in the United States by the year 2000 (Chen et al., 1982), thus increasing considerably the number of areas in the country affected by subsidence.

Even though, under present technological and economic conditions, subsidence prevention is not feasible, it has been demonstrated in many coalfields that surface subsidence can be predicted and controlled, thus minimizing the deleterious effects of ground movement. Therefore, it is imperative that reliable methods of surface movement prediction and control be established for the United States. With such techniques available, ground movements can be predicted as part of the mining plan, and if environmentally, economically or legally unacceptable situations are foreseen, remedial measures can be implemented.

2 TYPES OF MINING SUBSIDENCE EXPERIENCED IN THE UNITED STATES

Underground excavations disturb the natural equilibrium of the rock mass, causing redistribution of loads in the medium and thus producing horizontal and vertical displacements. Subsidence occurs when these displacements propagate from the mine opening, through the overlying strata, to the surface and can manifest two principle modes of ground settlement: sinkhole and trough subsidence (Figure 1).

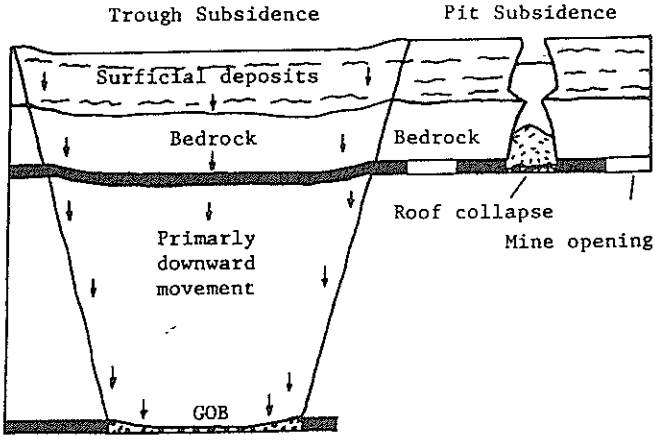


Figure 1 Trough and pit subsidence (after Wildanger et al., 1980).

2.1 Sinkholes, or Pit Subsidence

Sinkholes, or pit subsidence, are characterized by a sudden and sometimes violent collapse of the surface and usually occur above shallow, abandoned room and pillar mines with incompetent overburden; in rare instances, however, this type of subsidence

can also occur over active mines, given the proper mining and geological conditions. Pit subsidence is expressed by an abrupt drop in the surface and has vertical to bell-shaped walls. The washing of bedrock and surficial deposits into the mine void may cause the depth of sinkhole to exceed the mining height.

Obviously, the effects of pit subsidence can be serious. The damage caused is the result of a loss of support over all or part of the structure. Also, due to the uncertainty of mine and geologic parameters, the time, location and extend of such a subsidence event is very difficult to predict. Since the goal of subsidence and strain prediction is to minimize the cost of extracting coal in active mines that are below structures, the characteristics of trough subsidence have been studied more extensively than those of sinkholes.

2.2 Trough Subsidence

Trough subsidence is expressed by a gradual and general movement over an observed area with a subsidence basin being formed. Trough theory considers the phenomenon of subsidence to be represented by a complicated combination of material movement and interaction, as depicted in Figure 2. Caving occurs above the mine opening (zone a). The strata above the caving zone moves toward the excavation, experiencing fracturing (zone b) and beam bending phenomena (zone c). This representation of ground movement around a mining excavation is considerably complex to analyze and model; therefore, this concept is simplified by treating only the effects of underground excavation on the surface, or other strata levels within the bending zone.

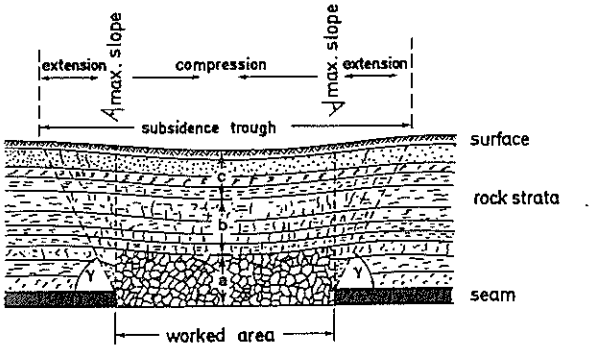


Figure 2 Strata movements above an extracted area (after Kratzsch, 1983)

Trough theory considers a zone of influence in which movement occurs and which spreads from the excavation to the surface, forming a subsidence trough. When an excavation is made at depth, the movement of the strata extends to the surface and manifests itself as vertical displacement (subsidence) and horizontal displacement within a zone of influence. The zone of influence is bounded by a plane that extends from the edge of extraction to the line on the surface where movement ceases. A vertical cross-section of the subsidence trough along with its associated parameters is shown in Figure 3. The angle defined by the vertical from the rib and the line of influence is the angle of draw (or limit angle).

3 DEVELOPMENT OF SUBSIDENCE PREDICTION METHODS

A number of different methods have been proposed for or applied to prediction of surface ground movements due to underground mining. These

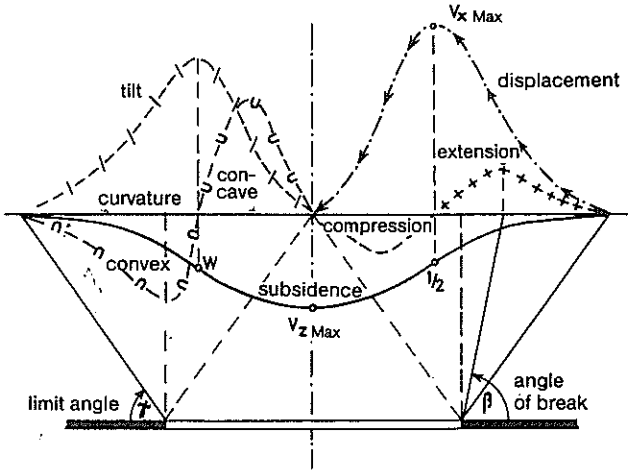


Figure 3 Components of ground movement (after Kratzsch, 1983)

approaches can be broadly divided into three groups. The first two are:

- Theoretical models based on the elastic, plastic, viscoelastic or other phenomenological models which are widely used in other engineering fields (Voight and Pariseau, 1970).

- Numerical methods, mostly used as solutions to complex situations involving the phenomenological methods.

Both these approaches assume that the strata in the overburden behaves in a specific and predictable manner. In using these models, considerable information describing the behavior of the overburden is required, which has often limited the applicability of these methods. Furthermore, in order to adapt their results to field data, a large number of adjusting coefficients may have to be determined.

The third approach can be defined as:

- Empirical or semi-empirical methods such as profile functions, influence functions, the zone area method (Brauner, 1973; Karmis et al., 1981b and 1983).

In this research, the latter approach was pursued since empirical methods are realistic, flexible, and easy to use. Their application, however, requires that a significant number of field measurements be made in order to determine the essential input parameters of the equations.

3.1 Data Collection and Analysis

During the initial stages of this research effort, a large number of subsidence case studies were collected from literature, the coal industry and government agencies. In total, data from 45 longwall panels and 70 room and pillar panels were collected. The limitations of the collected case studies data, i.e. accuracy of surveys, frequency of monitoring, lack of horizontal movement measurements, etc, led Virginia Polytechnic Institute and State University to the initiation of a detailed subsidence and strain monitoring program

above a number of active mines, located in three major coal producing counties of Virginia. The aim of this program was to enhance the data base with accurate and complete measurements of surface movements and to subsequently allow the refinement of the prediction techniques.

In this major monitoring effort, a total of sixteen room and pillar sections and seven longwall panels, in nine mines, were instrumented. Above each panel or section a number monument lines were installed. The lines were extended on either side of the panel well beyond the maximum expected area of influence. The final effort included approximately 1,200 stations over 35,000 feet of monitoring lines (Schilizzi et al., 1986).

This data bank was used to determine some basic ground movement relationships between the basic mining and subsidence parameters, in order to allow the evaluation of the various prediction methods for the Appalachian coal region.

Analysis of the subsidence information has revealed some interesting subsidence characteristics for Appalachian longwall panels. The observed angles of draw varied considerably; however, the angle of draw appears to approach a constant value of approximately 30 degrees at width-to-depth (W/h) ratios in excess of 1.2 (Figure 4). The range of maximum subsidence factors for the collected case studies is shown in Figure 5. It shows two lines constructed from the data. Line (1) represents the average values S_{max}/m, whereas line (2) is an envelope line, covering all data points. The figure also shows that this parameter asymptotes to a constant value at a width-to-depth ratios greater than 1.2. These results suggest that critical conditions are reached for W/h ratios of about 1.2,

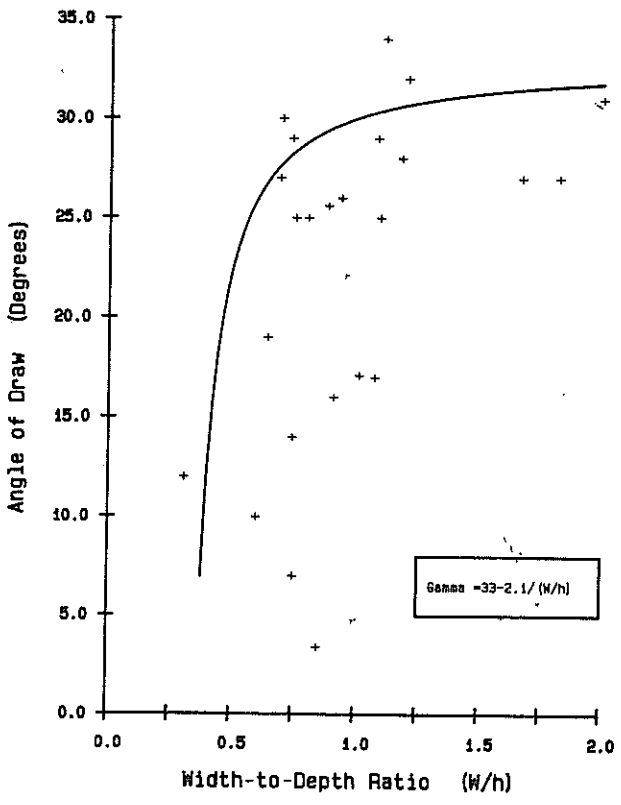


Figure 4 Observed angles of draw for various case studies

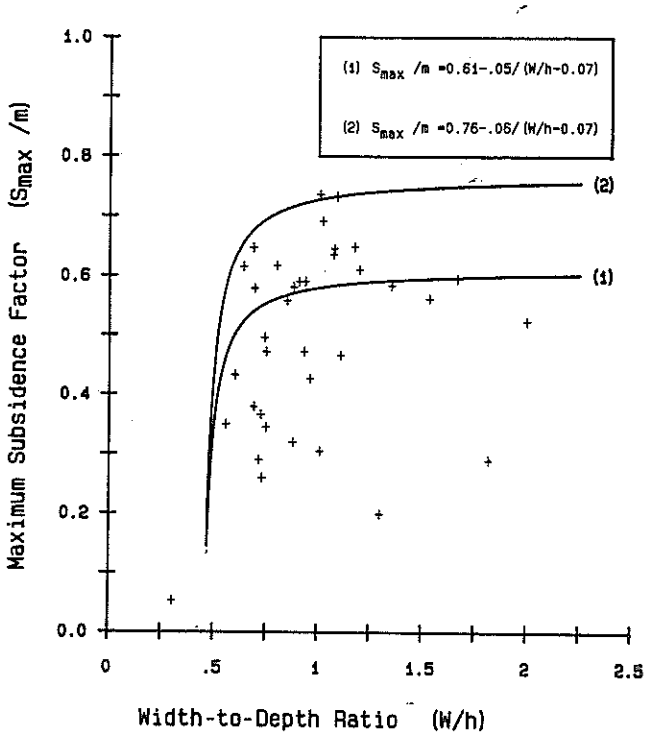


Figure 5 Influence of W/h ratio on maximum subsidence factor

as confirmed by the relationship between the position of the inflection point and the width-to-depth ratio of the panel shown on Figure 6.

According to the collected data and their dispersion, it was hypothesized that two factors influenced the subsidence: geology of the overburden and geometry of the panel. In order to establish the relationship between geology (lithology) and subsidence, the subsidence factor was plotted against the percent of hardrock (percent of limestone and sandstone) in the overburden for critical and supercritical panels only (Figure 7). Since the effect of panel geometry was thus eliminated, a relationship between subsidence and geological conditions was established. Once this correlation was possible, a complete relationship between subsidence and panel geometry was developed for varying lithologies (Figure 8).

To determine characteristic subsidence profiles, different empirical or semi-empirical methods were tested and adopted. Data collected during the monitoring program were primarily used, because of their completeness and accuracy.

3.2 Profile Function Methods

A profile function method defines the distribution of subsidence or strain values on the surface along a profile, orthogonal to the boundary of (theoretically) an infinitely long underground excavation. In general, a function which is tangent or asymptotic to two horizontal lines is required. The parameters to be used for this equation must be determined from field data.

The advantage of such a method is that it can be implemented easily through the use of a computer, or of pre-calculated tables. The main disadvantage is that it cannot negotiate excavations of complex shape or significant variations in mining

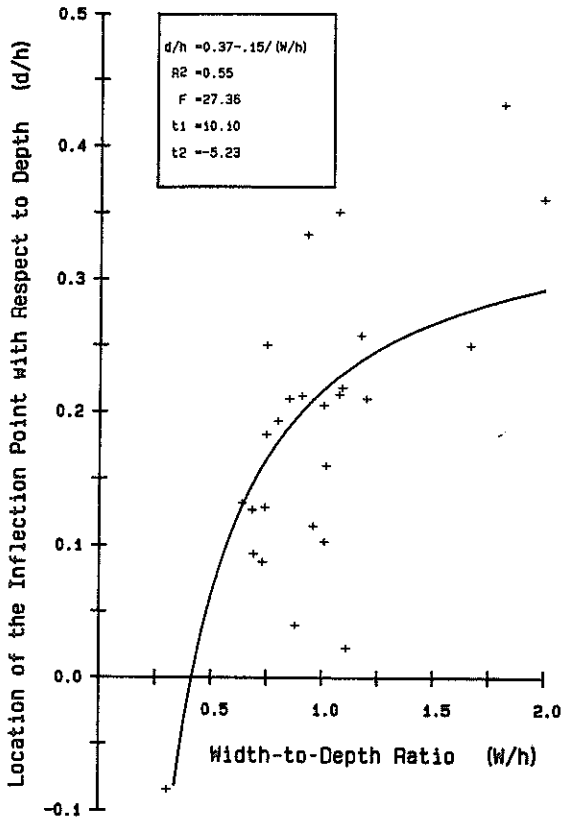


Figure 6 Effect of W/h ratio on inflection point location

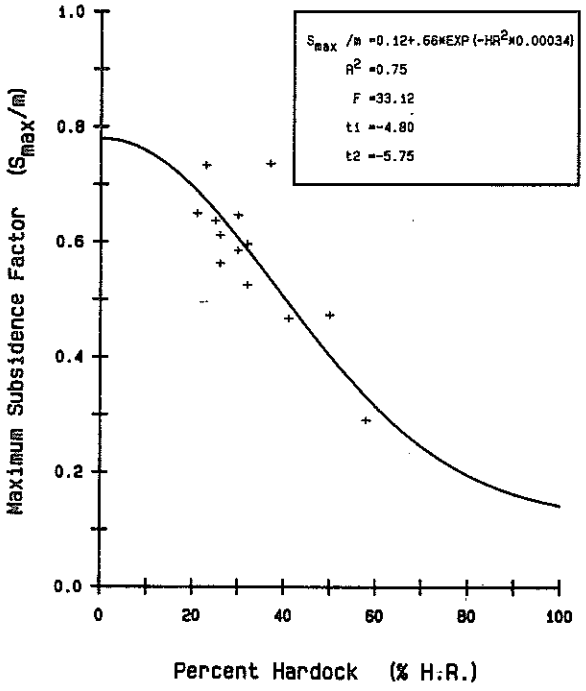


Figure 7 Effect of lithology on maximum subsidence factor

Parameters such as mining height, percent of extraction, and depth of the excavation (Brauner, 1973; Karmis et al., 1981a).

In this approach, a number of accepted profile functions were fitted to the subsidence profiles

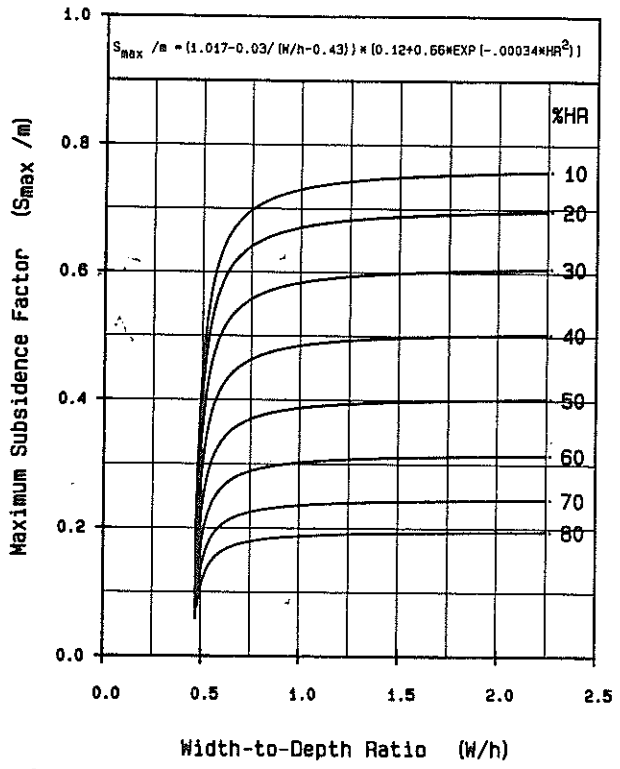


Figure 8 Nomograms for maximum subsidence prediction

developed from collected case studies. This analysis demonstrated that the hyperbolic tangent function given by the following equation, provided the best fit curve (Karmis et al., 1981b and 1984):

$$S(x) = 0.5\ S_{max}[1-\tanh(cx)/B] \qquad (1)$$

where,

S(x) = subsidence at a given point on the surface;
S_{max} = maximum subsidence (obtained from a table [Table 1] or nomogram [Figure 8]);
c = constant, calculated as 1.8 for critical or supercritical panels and 1.4 for subcritical panels;
x = distance from the inflection point to the point in question; and,
B = distance from the inflection point to S_{max} (which can be assessed from tables or nomograms [Figure 6] as a function of panel geometry and width-to-depth ratio).

The latter equation can be used in conjunction with predictions of S_{max} (Figure 8) and position of the inflection point (Figure 6) to allow for complete subsidence pre-calculation.

3.3 Influence Function Methods

This approach to subsidence prediction was initially developed by Dutch and German engineers (Bals, 1932) and has been extensively used in the Central and Eastern European coalfields. An influence function describes the distribution of vertical ground movement, i.e. subsidence, on the surface or other levels of the overburden, caused by an infinitesimal underground excavation. Considering the two dimensional situation:

$$dS(x_1,z) = f(x_1-x_2,z)dV \qquad (2)$$

where,

$dS(x_1,z)$ = subsidence at point $P(x_1,z)$;
dV = infinitesimal underground excavation (void);
$f(x_1-x_2,z)$ = influence function;
x_1 = coordinate of surface point;
x_2 = coordinate of infinitesimal excavation; and,
z = vertical distance from excavation to prediction point $P(x_1,z)$.

The Budryk-Knothe influence function method (Knothe, 1957), developed in Poland, was selected for this research as the most appropriate function for use in the Eastern U.S. coalfields. Initially, a two-dimensional situation was considered for the analysis of data obtained from panels of an almost orthogonal shape and with uniform mining conditions i.e. mining height, percent extraction, depth. The equation used is as follows:

$$f(x,z) = -\frac{1}{r}\exp(-\pi\frac{x^2}{r^2}) \qquad (3)$$

where,

r = the radius of influence (r=z/tan(b));
b = angle of influence; and,
x,z = coordinates of surface point on a system where the origin is located at the infinitesimal excavation.

For the three-dimensional approach:

$$f(x,y,z) = \frac{1}{r^2}\exp[-\pi\frac{(x^2+y^2)}{r^2}] \qquad (4)$$

where,

r = the radius of influence; and,
x,y,z = coordinates of a surface point on a system where the origin is located at the infinitesimal excavation.

Subsidence at any point will be:

$$S(x,y,z) = \frac{S_{max}}{r^2}\iint_A \exp[-\frac{\pi}{r^2}(x^2+y^2)]dxdy \qquad (5)$$

where,

$S(x,y,z)$ = subsidence at a point having coordinates x,y,z;
S_{max} = maximum subsidence for supercritical excavation;
r = the radius of influence; and,
A = the area of excavation.

The above integral was transformed and solved in polar coordinates, for polygonal excavations.

For this method, as with most mathematical models, the inflection point of the subsidence profile is located above the rib of the excavation. In practice, however, the inflection point is displaced at a distance, d, from the rib. In order to accommodate this, the outer boundaries of the excavation have been adjusted accordingly.

3.4 Zone Area Method

This method was initially developed in Britain for irregular longwall or room and pillar panels (Marr, 1975). It assumes that movement at a specific point on the surface is affected by the excavation of a circular underground area which is further sub-divided into a series of angular rings. To determine the amount of movement caused by each ring, the extracted area of the ring is calculated and multiplied by the zone factor of the respective ring. Appropriate zone factors for Appalachia have been calculated from the field data (Goodman, 1980; Karmis et al., 1981b and 1984). The same procedure is followed for all rings, and the superimposed results will yield total movement.

4 DEVELOPMENT OF STRAIN PREDICTION METHODS

One of the most damaging manifestations of surface subsidence is the development of horizontal strains. As noted previously, subsidence measured in Appalachia is smaller than that found in certain other coalfields, such as the U.K. However, the strains experienced in the U.S. often appear to be greater than those predicted for British conditions. Thus, an effort was directed toward the identification of the cause of these higher strains and toward the subsequent formulation of an acceptable strain prediction model for Appalachia.

As a first step, the relationship between strain and curvature had to be determined. Factor B was used to calculate horizontal strain as a function of curvature, i.e.:

$$\text{Horizontal Strain} = -B * \text{Curvature} \qquad (6)$$

In the original stages of this research a direct relationship between strain and curvature was sought which could describe B independent of any other mining parameters (Karmis et al., 1983). As more case studies were made available through this project, it became apparent that such a relationship will be difficult to establish (Figure 9). As a result, a different approach was adopted, based on the work of Awershin (1947), Budryk (1953) and Akimov and Zemicev (1970), which suggested that the magnitude of the horizontal strain factor (B) is a function of the excavation depth or the radius of principal influence (r).

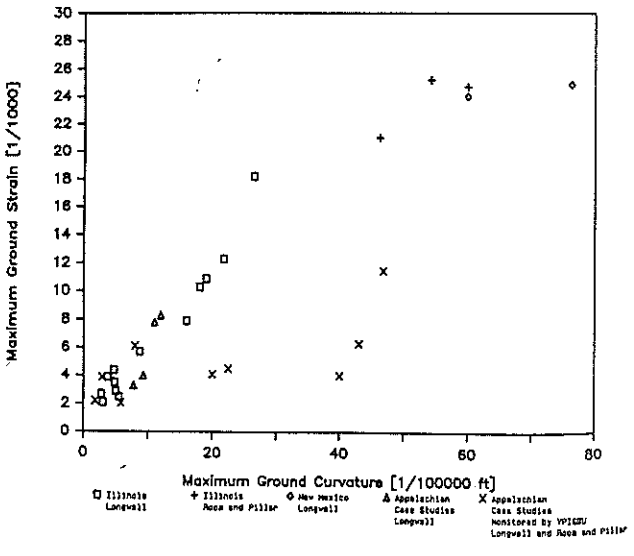


Figure 9 Maximum ground strain and curvature data

For each of the collected case studies, factor B was determined by comparing the measured strains and the fitted curvature profiles.

Using the established values of parameter B and the corresponding values of excavation depth (h), radius of influence (r), and angle of principal influence (b), a statistical relationship was found (Figure 10) as expressed by the equation:

$$B = (0.35 \pm 0.05)\ r \qquad (7)$$

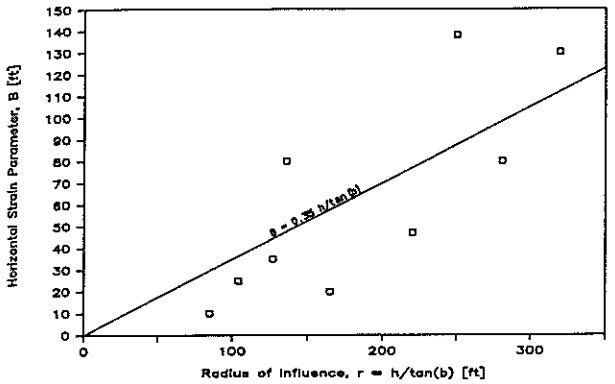


Figure 10 Effect of radius of influence on the horizontal strain parameter

or

$$B = (0.35 \pm 0.05)\ h/\tan(b) \qquad (8)$$

where,

r = radius of the principal influence;
h = depth of the excavation; and,
b = angle of the principal influence.

5 DEVELOPMENT OF COMPUTER SOFTWARE

The development of a comprehensive software package was necessary in order to facilitate the analysis of the field measurements. All field data were stored in an 880-line memory incorporated in the surveying instrument, and then transferred to magnetic diskettes for further processing on an HP micro-computer system. Stored field data included coordinates, sometimes on a localized system, elevations and the values of subsidence and strain for individual stations on the monitoring lines for each date.

Computer software for the application of the prediction methods under consideration was developed for two widely used personal computer systems.

For the profile function, the program is rather simple and involves the calculation of subsidence values along a line orthogonal to the rib of the excavation. The parameters used for this calculation depend on the given geologic conditions, width-to-depth ratio and mining height, and must be obtained from tables or nomograms and entered manually. The origin of the coordinates can be adjusted manually if necessary.

For the application of the influence function method, a number of programs were developed, each of them for specific conditions. For general cases involving complex mining conditions, where the mining section under consideration must be divided into polygons of uniform conditions, the influence function equation was converted to polar coordinates and was used in the program in this form. The computer program calculates subsidence at any point along a polygonal line or on a grid. For mine sections of irregular shape or where areas of different mining height, extraction ratio or seam elevation exist, the section is separated into homogeneous polygonal sub-sections. Subsidence and other related indices of deformation, in any given direction, caused by each of these sub-sections is calculated and their total value is determined by superposition. This procedure, however, requires considerable computational time for each point.

For simple conditions, however, where areas of different mining height, extraction ratio or seam elevation can be described by rectangular homogeneous sub-sections, different programs have been written for considerably faster execution on a microcomputer, yielding comparable results. Furthermore, a program using the two dimensional approach has been written for single panels of uniform overall parameters.

The program for the zone area method was initially developed for mainframe computers (Karmis et al., 1982); however, it is currently being adapted for use with personal computers.

It should be noted that these programs also produce data compatible with commercially available plotting and contouring software packages. Mine plan coordinates and the corresponding parameters can be entered manually or by a digitizer or by a plotter with digitizing capabilities.

6 APPLICATION OF PREDICTION METHODS

In this paper, data obtained from three case studies are presented to demonstrate and compare the prediction methods. The first two are from room and pillar mining operations, whereas the last one is from a longwall case study.

In the first example, the two dimensional approach was used. Predicted and fitted subsidence curves, using the profile and influence function methods, are presented in Figure 11.

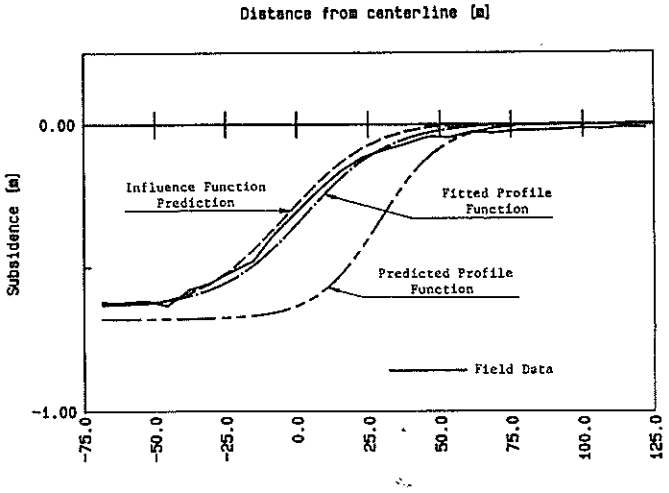


Figure 11 Example #1: Field data and prediction curves

In the second example (Figure 12), a three dimensional influence function approach was used to take into account a number of pillars left in place for roof control purposes. This case demonstrates the accuracy which can be obtained through adjustment of the influence function parameters, especially for subsidence predictions.

In the last example (Figure 13), a three dimensional influence function method was used for a longwall operation with considerable variation in overburden depth. Subsidence and horizontal strain values, calculated using this technique, show excellent correlation with the corresponding measured values.

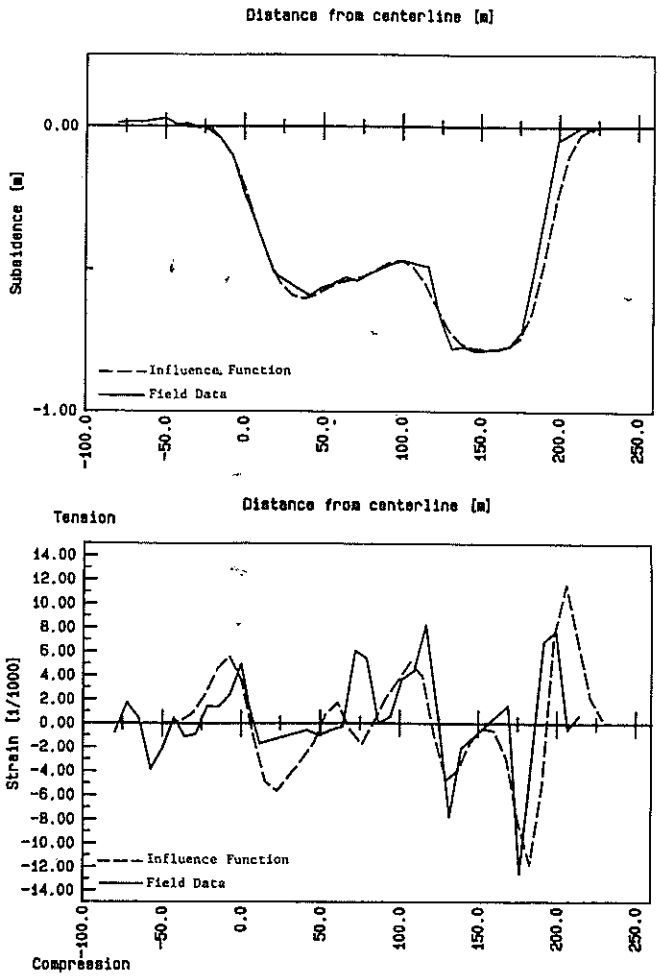


Figure 12 Example #2: Field data and prediction curves for subsidence and horizontal strain

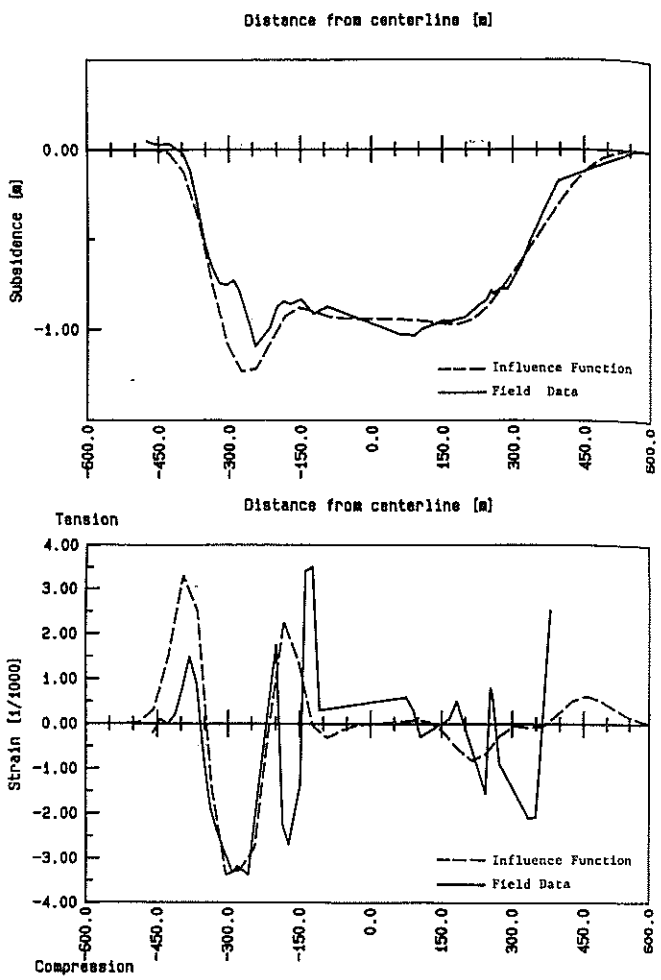


Figure 13 Example #3: Field data and prediction curves for subsidence and horizontal strain

7 CONCLUSIONS

The expansion of underground mining into more populous areas, and the resultant increase in the potential for surface and structural damage, have rendered the formulation of accurate surface deformation models an important requisite. To meet this demand, accurate subsidence and strain prediction techniques have been formulated for the Eastern U.S. coalfield. The semi-empirical subsidence prediction techniques discussed in this paper were developed from a substantial number of case studies collected within the Appalachian coalfield. Using the subsidence model as a base, the strain model was formulated using empirically and mathematically derived relationships. These models can greatly facilitate mine planning and allow the amount of coal lost due to the protection of surface structures to be minimized.

8 ACKNOWLEDGEMENTS

This research is based upon work sponsored by the Office of Surface Mining, Reclamation and Enforcement, the U.S. Department of the Interior and the Powell River Project. Any opinions, findings, conclusions or recommendations expressed in this paper are those of the authors and do not necessarily reflect the views of the sponsors. Finally, the cooperation, encouragement, and discussions offered by the technical personnel of numerous coal companies involved in this project are gratefully acknowledged.

9 REFERENCES

1. Akimov, A. and B. Zemicev, 1970, Subsidence of the Rock Strata Caused by the Underground Excavation of Coal and Lead Ores, Nedra Publishing, Moscow, (in Russian).

2. Awershin, S. G., 1947, Subsidence of the Rock Strata Caused by Underground Excavation, Ugletekhizdat Press, Moscow, (in Russian), 245 p.

3. Bals, R., 1932, "A Contribution to the Problem of Precalculating Mining Subsidence," Milteilungen aus dem Markscheidewesen, Vol. 42/43, pp. 98-111 (in German).

4. Brauner, G., 1973, "Subsidence Due to Underground Mining (in two parts)," U.S.B.M. Info. Circ. 8571, 8572.

5. Budryk, W., 1953, "Determination of the Magnitude of Horizontal Strains," Archives of Mining and Metallurgy, Vol. I, Part 1, (in Polish).

6. Chen, C. Y., D. E. Jones and D. K. Hunt, 1982, "Government Regulation of Surface Subsidence due to Underground Mining," Proceedings, International Symposium on the State of the Art of Ground Control in Longwall Mining and Mining Subsidence, Honolulu, Hawaii, pp. 245-252.

7. Goodman, G., 1980, "Computer Modeling of Mining Subsidence Using the Zone Area Method," M.S. Thesis, VPI&SU.

8. Karmis, M., C. Haycocks, I. Eitani and B. Webb, 1981a, "A Study of Longwall Subsidence in the Appalachian Coal Region Using Field Measurements and Computer Modeling Techniques," Proceedings, 1st Conference for Ground Control in Mining, West Virginia University, July 27-29, pp. 220-229.

9. Karmis, M., C. Haycocks, B. Webb and T. Triplett, 1981b, "The Potential of the Zone Area Method for Mining Subsidence Prediction in the Appalachian Coalfield," Proceedings, Workshop on Surface Subsidence Due to Underground Mining, Morgantown, West Virginia, November 30-December 2, pp. 48-62.

10. Karmis, M., G. Goodman, C. Haycocks and T. Triplett, 1982, "The Development and Testing of a Regional Subsidence Prediction Model," Proceedings, 17th Inter. Symposium on Computer Applications to the Mineral Industry, APCOM, Denver, Colorado, pp. 240-252.

11. Karmis, M., T. Triplett, C. Haycocks and G. Goodman, 1983, "Mining Subsidence and Its Prediction in the Appalachian Coalfield," Proceedings, 24th U.S. Symp. on Rock Mech., College Station, Texas, June, pp. 665-675.

12. Karmis, M., G. Goodman and G. Hasenfus, 1984, "Subsidence Prediction Techniques for Longwall and Room and Pillar Panels in Appalachia," Proceedings, Second International Conference on Stability in Underground Mining, Lexington, Kentucky, August 6-8, pp. 541-553.

13. Knothe, S., 1957, "Observations of Surface Movements Under Influence of Mining and the Theoretical Interpretation," Proceedings, European Congress on Ground Movement, The University of Leeds, April 9-12.

14. Kratzsch, H., 1983, "Mining Subsidence Engineering," Springer-Verlag, Berlin, Heidelberg, New York.

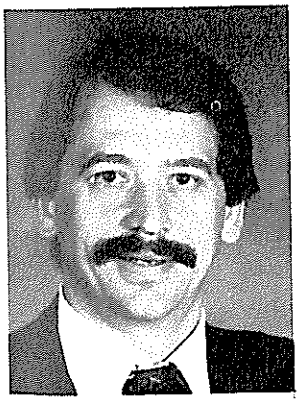
15. Marr, J. E., 1975, "The Application of the Zone Area System to the Prediction of Mining Subsidence," Min. Eng., Vol. 135, No. 176, pp. 53-62.

16. Schilizzi, P., M. Karmis and A. Jarosz, 1986, "Development of Subsidence Prediction Technology from an Extensive Monitoring Program," Proceedings, 2nd Workshop on Surface Subsidence Due to Underground Mining, Morgantown, West Virginia, June 9-11, in press.

17. Voight, B. and W. Pariseau, 1970, "State of Predictive Art in Subsidence Engineering," Journal of the Soil Mechanics and Foundations Div., Proc., ASCE, Vol. 96, No. SM2.

18. Wildanger, E. G., J. Mahar and A. Nieto, 1980, "Sinkhole-type Subsidence Over Abandoned Coal Mines in St. David, Illinois," Illinois Abandoned Mined Lands Reclamation Council, 88 p.

* (Paper C1570 originally presented at the Fourth Australia - New Zealand Conference on Geomechanics, Perth, May 1984)



M KARMIS

Michael Karmis is Professor of Mining Engineering at Virginia Polytechnic Institute and State University, where he has been a member of the faculty since 1978. Previously he was with the faculty of the National Technical University of Athens, Greece. Dr Karmis is a graduate of the University of Strathclyde, Glasgow, Scotland, where he received the B.Sc. (Honors) and Ph.D. degrees in Mining Engineering.

Dr Karmis' research interest is in the area of rock mechanics and ground control and he is particularly interested in the application of such principles to the design and optimization of mining systems. He has authored or co-authored numerous technical papers and reports on this subject.

Dr Karmis is a Fellow of the Institution of Mining and Metallurgy, a Member of many professional societies, a Chartered and Professional Engineer, and serves as an independent consultant to the mining industry.

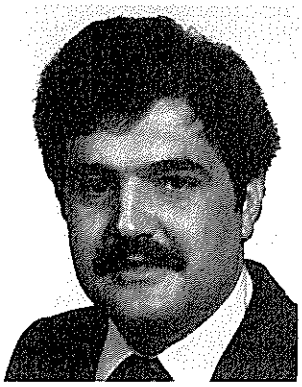


A P JAROSZ

Andrzej P Jarosz has been a Research Associate at the Department of Mining and Minerals Engineering, Virginia Polytechnic Institute and State University, since 1984. Previously he worked for the Mining and Metallurgy Academy in Cracow, Poland, as a faculty member and for the Central Mining Institute in Katowice, Poland, as head of the Mine Pillar Control Laboratory.

Dr Jarosz is a graduate of the Mining and Metallurgy Academy, Cracow, Poland, where he received his M.S. (Honors) and Ph.D. degrees in Mining Surveying.

Dr Jarosz's research interest is in the areas of subsidence monitoring and prediction as well as the practical applications of ground control principles in mining. He has authored or co-authored many technical papers on this subject.



P P G SCHILIZZI

Paul P G Schilizzi received his education at the National Technical University, Athens, Greece, and graduated in July, 1980, with a Diploma in Mining and Metallurgical Engineering. Mr Schilizzi attended graduate school in the Department of Mining and Minerals Engineering, Virginia Polytechnic Institute and State University, where he completed his M.S. degree in July, 1982. He received an assistantship to continue his education leading to a Ph.D. degree in the same department and completed his work for this degree in January, 1987.



Z AGIOUTANTIS

Zacharias Agioutantis graduated from the National Technical University, Athens, Greece, in November, 1982, with a Diploma in Mining and Metallurgical Engineering. He was then admitted to the graduate program at Virginia Polytechnic Institute and State University, Blacksburg, Virginia, under an assistantship, and received his M.S. degree in Mining Engineering. Since September, 1984, he has been pursuing a Ph.D. degree at the same school while working on different research projects. His research work is reflected in several publications in the fields of Rock Mechanics and Ventilation.

THE NEW TWO-DIMENSIONAL LAMODEL PROGRAM (LAM2D)

By Olayemi O. Akinkugbe[1] and Keith A. Heasley, Ph.D.[2]

ABSTRACT

The safe, productive exploitation of coal in multiple-seam situations requires specific design technology. At present, there are two general design approaches that the mining engineer can use to analyze the multiple-seam problem in question: simple empirical relationships or complex numerical models. Often, the empirical approaches are too general for the specific problem, and the numerical models require too much time and expertise for the practicing engineer. In this paper, a new program designed for quickly and easily calculating the stresses, strains, and safety factors associated with basic multiple-seam mining situations is presented. The program implements a simplified two-dimensional (2–D) boundary-element method in order to model the complex multiple-seam stress and displacement interactions. The program incorporates automatic coal and gob property generation to simplify the input and inherently calculates pillar safety factors to enhance the output.

INTRODUCTION

Numerical modeling as a tool for engineering design has been used for decades. During this time, the awareness of its relevance has greatly increased and, at the same time, considerable developments have been made at improving its accuracy. Presently, there are several general numerical techniques for solving engineering problems; one may choose to use finite-element, boundary-element, discrete-element, finite difference, and/or a hybrid combination of the above to solve the problem at hand. Based on the mathematical approximations involved, numerical methods can be classified into two categories: domain methods and boundary methods. The domain methods are characterized by area and volume discretization of the problem domain. They use relatively large numbers of elements, resulting in large systems of equations that usually consume large amounts of computer resources and require lengthy times for solution. The boundary-element method, on the other hand, requires only the discretization of the boundaries of the domain of interest. Relative to subsurface mineral extraction, only the planar area of the seam is discretized in order to obtain a solution for the desired problem. The boundary-element method usually leads to smaller systems of equations, faster computing times, and a reduced need for computing resources.

The displacement-discontinuity method, a version of the boundary-element method promoted early by Salamon [1963], is usually the method of choice for analyzing stresses and displacement distribution in slitlike or thin-seam openings. In this approach, the relative movement between the roof and floor of a mine is treated mathematically as a discontinuity in the displacement field of the surrounding media, in other words, a crack/slit in a continuum. The displacement-discontinuity method has been used to create several well-known computer packages for solving geomechanical problems in underground mines.

The first implementation of the displacement-discontinuity method into a personal computer code for calculating stress and displacement from multiple seams was done by the U.S. Bureau of Mines. The program was called MULSIM/BM. In 1992, MULSIM/BM was upgraded to MULSIM/NL [Zipf 1992a,b] by the addition of nonlinear seam material models, calculations for determining the mechanical strain energy changes associated with the seam materials, and a capability for "stepping" though a series of mining sequences. A new displacement-discontinuity program called LaModel was later introduced by the National Institute for Occupational Safety and Health [Heasley and Chekan 1999]. LaModel implemented the same nonlinear seam material models in MULSIM/NL, but introduced a laminated overburden model. This model assumes the overburden to be a stack of horizontally lying strata, which naturally increases the flexibility of the overburden. As a result, LaModel estimation of the stresses, displacements, and surface subsidence is considered more accurate compared to the homogeneous overburden model implemented in MULSIM/NL.

In this paper, a new 2–D boundary-element program, LaM2D, is introduced. This program implements the laminated overburden model [Heasley 1998; Salamon 1991, 1962] used in the three-dimensional (3–D) LaModel program into a greatly simplified 2–D program. This 2–D implementation of the laminated boundary-element program was specifically developed in order to provide a fast, simple, multiple-seam analysis program for the practicing engineer. LaM2D only requires that the user input the minimum geometric parameters from the multiple-seam mining situation. The program automatically incorporates default overburden, coal, and gob properties to simplify the input and inherently calculates pillar safety factors for the program output.

[1]Research assistant.
[2]Associate professor.
West Virginia University, Department of Mining Engineering, Morgantown, WV.

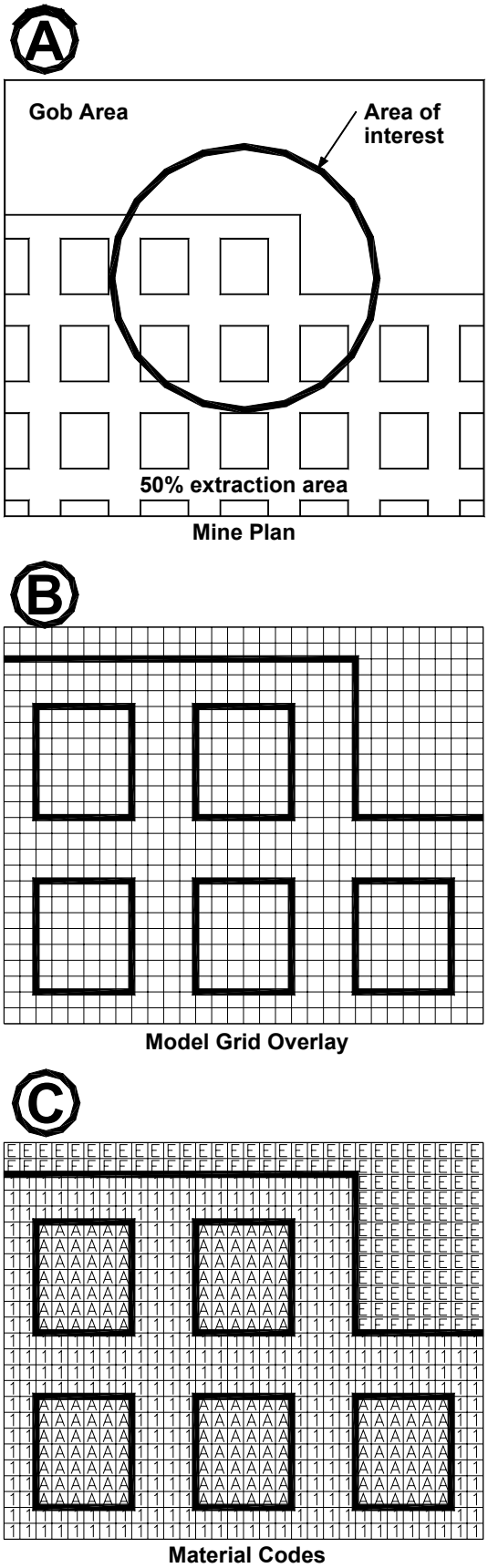


Figure 1.—Schematic of LaModel mine grid.

2–D LAMINATED OVERBURDEN MODEL

In the 3–D MULSIM and LaModel programs, the horizontal plan of the seam was used to determine a grid of elements from which the vertical (out-of-plane) stresses and displacements were determined. For example, given the mine plan in Figure 1A, a square grid (with an element size optimized to best fit the entry and pillar dimensions and large enough to cover the intended modeling area) was superimposed on the mining plan, as shown in Figure 1B. Each element of the grid was then designated as a particular material using a letter code (Figure 1C). (In this case, the pillar material is "A", the open entries are "1", and the gob material is "E".) This grid of materials was then used as the representation of the mine for which the vertical stresses and displacements were determined.

In the 2–D laminated model, a cross-section of the pillars in the seam is used to determine a linear array of elements from which the vertical stresses and displacements are determined. For example, given the cross-section of pillars in Figure 2A, a linear array of elements (with an element size optimized to best fit the entry and pillar dimensions and large enough to cover the intended modeling area) is superimposed on the mining plan, as shown in Figure 2B. Each element of the material array is then designated as a particular material using a letter code (Figure 2C). (In this case, the pillar material is "A", and the open entries are "1".) This array of material properties is then used as the representation of the mine for which the vertical stresses and displacements are determined.

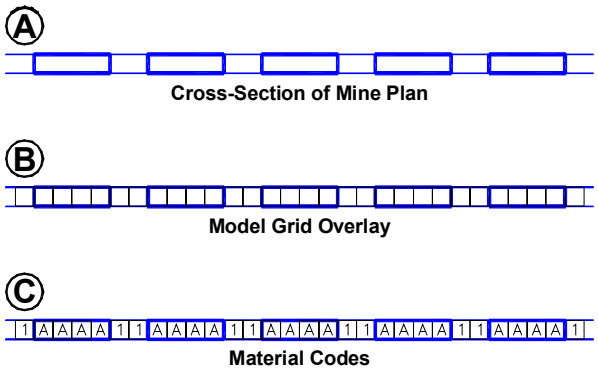


Figure 2.—Schematic of LaM2D mine grid.

Advantages

The big advantages of the LaM2D program over the previous 3–D programs are that the mine grid is much simpler and faster to input (minutes instead of hours) and the solution times are much quicker, in fact, almost instantaneous (seconds instead of minutes or hours). To further speed the input process, LaM2D (in default mode) only requires that the user input the minimum geometric

parameters to define the seam geometries. Default properties for overburden, coal, and gob are automatically generated. (In the advanced mode, the user has complete control over all of the input parameters.) This ease of input and instantaneous solution enables the user to quickly analyze and compare many different design variations or perform parametric studies.

Disadvantages

The main disadvantage of LaM2D is that it is only a 2–D plane strain analysis. Therefore, the variation in the mine plan in the out-of-plane direction is ignored, and only mining plans that can be reasonably represented in 2–D can be accurately simulated. The plane strain approximation means that the pillars and entries in the cross-section are essentially assumed to be infinitely long in the out-of-plane direction. Therefore, mining plans that change dramatically in the out-of-plane direction will not be modeled properly. However, LaM2D does have a capability for inputting an out-of-plane extraction ratio, which can be used to accurately simulate the crosscuts in the "infinitely" long pillars (see below). With the out-of-plane extraction ratio, not only infinitely long pillars, but also mining plans that are reasonably continuous and symmetric across the plane of the cross-section can be accurately simulated.

Stability Analysis in LaM2D

In addition to its capability to quickly analyze basic multiple-seam interactions, LaM2D also provides several practical stability indices for the affected mine and pillars. The presently available computer programs for analyzing seam interactions in single- or multiple-seam mining situations typically produce only seam displacement and stress values as output. The new LaM2D program goes several steps further by using the seam displacement and convergence values to determine pillar safety factors, multiple-seam subsidence, and multiple-seam horizontal strain values for output.

Safety Factors

To ensure overall mine stability, the general approach is to size the pillars large enough, and therefore strong enough, to support the applied loads. In classical engineering, this generally requires a pillar safety factor greater than 1.0, with some reasonable margin for error. In situations where seam interactions exist as a result of a superjacent or a subjacent seam, simple empirical methods for calculating pillar safety factors are not generally applicable. Also, computer programs based on the single-seam empirical methods are not recommended for multiple-seam interaction analysis; rather, more complex numerical methods are often required. However, most practicing mining engineers are accustomed to working with pillar safety factors, and the stresses and displacements generated by the complex numerical modeling programs are not generally as useful or as comparable. In order to provide the customary safety factors and enhance the practical functionality of the LaM2D program, an automatic calculation of pillar safety factors has been incorporated into the program.

The primary safety factor implemented in the LaM2D program is stress-based and uses the typical safety factor calculation:

$$SF = \frac{S_p}{B} \tag{1}$$

where SF = the pillar safety factor;
S_p = the pillar strength;
and B = the pillar load.

In order to incorporate realistic pillar strengths into the program, the Mark-Bieniawski pillar strength formula [Mark and Chase 1997] was used to determine pillar strengths because of its strong empirical basis and long successful history of application in the U.S. coalfields:

$$S_p = S_i \left[0.64 + 0.54\left(\frac{w}{h}\right) - 0.18\left(\frac{w^2}{lh}\right) \right] \tag{2}$$

where S_i = the in situ coal strength;
w = the pillar width;
h = the pillar height;
and l = the pillar length.

In the program, the height of the pillar is determined from the input seam height, and the width of the pillar is automatically determined from the number of elements across the pillar. For calculating the pillar load, LaM2D averages the values of all of the calculated element stresses across the pillar. The safety factor is then determined by dividing the Mark-Bieniawski pillar strength by the average pillar stress. Ultimately, the pillar safety factors can be displayed in a colored-square or line plot (see the subsequent case study).

Multiple-seam Subsidence and Strain

When a seam is undermined, it experiences multiple-seam stress transfer similar to an overmining situation. However, a seam that is undermined by total extraction mining can also be subjected to subsidence and the associated horizontal tensile and compressive strains. The multiple-seam subsidence effects are an important ground control consideration and can result in serious roof and floor instability and damages in the overlying seam. For

instance, field studies of room-and-pillar operations [Chekan and Listak 1994] showed that severe roof conditions are typically experienced within the tension and compression zones of a subsidence trough.

In previous multiple-seam analysis programs, the upper-seam subsidence and strain were never explicitly determined, although these calculations can be critical to analyzing the overlying mine stability. In order to provide the expected multiple-seam subsidence and strain values to the practicing engineer and increase the information available for design, the LaM2D program specifically calculates these values and provides them to the user. In the program, the upper-seam subsidence is calculated using the lower-seam convergence distribution and a laminated influence function. Once the seam subsidence is known, the resulting horizontal strains are determined using the method promoted by the National Coal Board in the *Subsidence Engineers Handbook* [National Coal Board 1975]. A demonstration of these strain calculations is presented later in the case study.

Out-of-plane Extraction Ratio

Because of the 2–D plane-strain formulation of LaM2D, the pillars and entries in the cross-sectional mine plan are essentially assumed to be infinitely long in the out-of-plane direction. This assumption is typically unrealistic for many pillar geometries in practical applications, where the pillars have a finite length in the out-of-plane direction. In many 2–D cross-sections, such as across a longwall gate road or through a room-and-pillar section, the pillar plan in the out-of-seam direction is fairly continuous (although not infinite). In these situations, an "out-of-plane extraction ratio" can be used to get a more accurate calculation of the true 3–D stress and displacements in the modeled mine plan.

In LaM2D, the in-plane extraction ratio is inherently provided through the specification of pillar material and openings in the input material properties (see Figure 2C). To specify the out-of-plane extraction ratio, the functional extraction ratio for the noninfinitely long pillars needs to be input. For example, consider a room-and-pillar section with 40- by 80-ft pillars and 20-ft-wide entries. The 2–D cross-section in LaM2D goes through the 80-ft length of the pillar; therefore, the input mine plan shows 80 ft of pillar material coupled with 20 ft of opening (an in-plane extraction ratio of 20%). In the out-of-plane direction for this situation, there is 40 ft of pillar coupled with 20 ft of opening. This results in an out-of-plane extraction ratio of 33%.

If the user inputs an out-of-seam extraction ratio, the stress from the infinitely long simulation will be adjusted to account for the limited pillar length. Essentially, the material stress and convergence values calculated for the infinitely long pillar are increased by a factor of:

$$\frac{1}{1-e} \tag{3}$$

where e = the out-of-plane extraction ratio. Thus, the practical result of using the out-of-plane extraction ratio is that the calculated stress values will realistically represent the average stress on the finite pillar, while the convergence values will represent an out-of-plane average across the finite pillar and the adjacent opening. Therefore, the 2–D simulation can give realistic 3–D pillar stress when the out-of-plane extraction ratio is used.

However, using the out-of-plane extraction ratio does not provide realistic 3–D safety factors. Without using the out-of-plane extraction ratio, the program calculates accurate pillar stresses, pillar strengths, and safety factors for the plane strain (infinitely long pillar) situation. When the out-of-plane extraction ratio is used, the program accurately adjusts the pillar stress values up to account for the limited length of the pillar; however, the pillar strength is still calculated based on an infinite-length pillar (for lack of sufficient information on the true pillar size). Therefore, the safety factor is realistically decreased from the 2–D situation, but is still not an accurate safety factor for the 3–D situation implied by the out-of-plane extraction ratio.

LAM2D INPUT

Compared to most numerical modeling programs, the input and output for the LaM2D program were simplified as much as possible to make it very user-friendly. Typical numerical modeling programs involve parameter input, solution of the model based on the input parameters, and an output or plot of the solution values. In many cases, three separate programs are used to perform the parameter input, solution, and the output (e.g., LaModel); however, the full-featured LaM2D program incorporates all of the numerical modeling steps into a single program.

Furthermore, the many material property input parameters necessary for modeling often seem daunting for practicing engineers who do not have the time to gather and verify specific material properties for both the seam and its surrounding rocks. In the LaM2D program, realistic average coal seam and overburden parameters are automatically defined. In fact, if the program is run in the standard mode, the only parameters required from the user are: the general model information, which includes model title, number of seams, and the system of units to be used (Figure 3); the seam geometry information, which includes element size, grid size, seam depths, and thicknesses (Figure 4); and the seam material grids (Figure 5). In standard mode, all of the seam and overburden properties are automatically entered with average values. However, if the user desires and the program is run in advanced mode,

the program allows the user the total flexibility of adjusting any or all parameters in the program, including the rock mass parameters (Figure 6), in-seam element parameters (Figure 7), boundary conditions (Figure 8), and program control values (Figure 9).

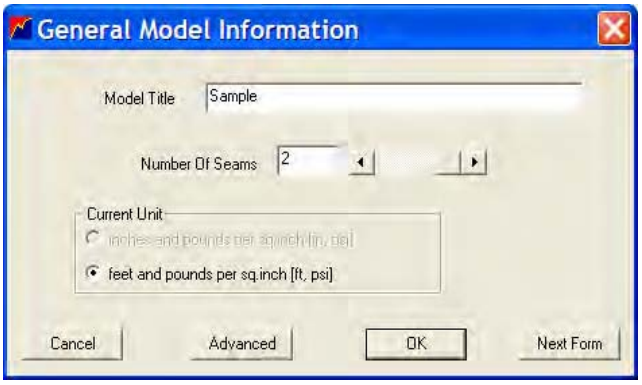


Figure 3.—General model information form.

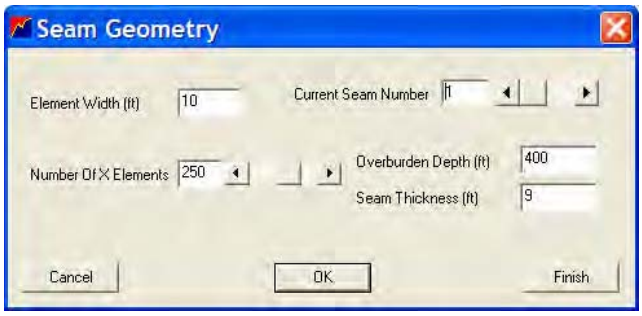


Figure 4.—Seam geometry form.

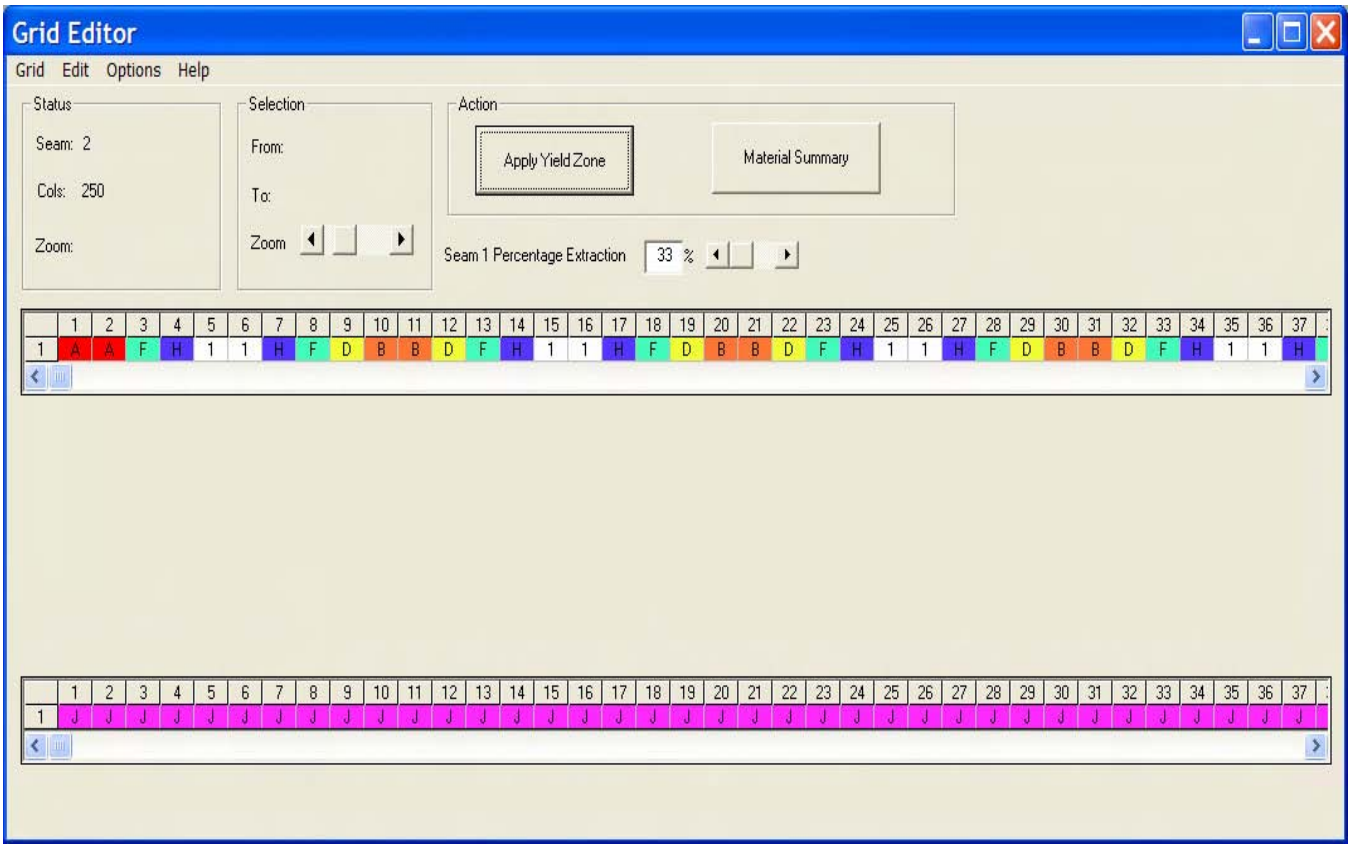


Figure 5.—Grid editor form.

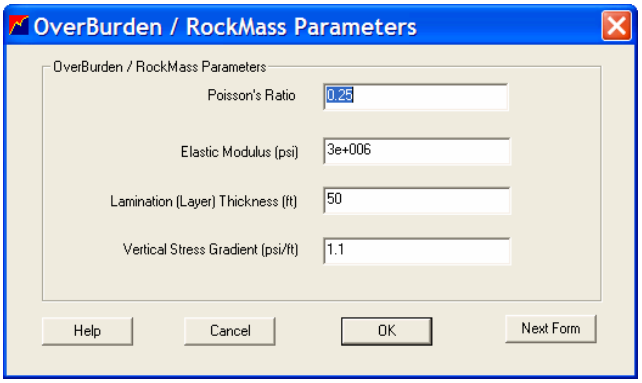


Figure 6.—Overburden and rock mass parameters form.

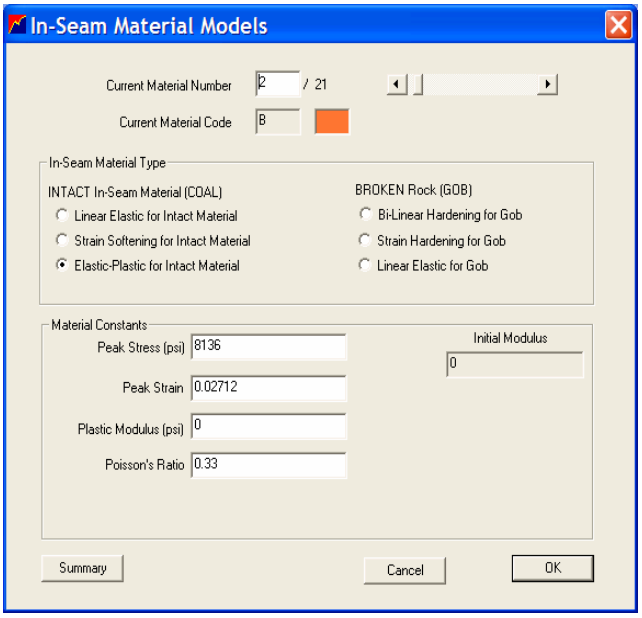


Figure 7.—In-seam material form.

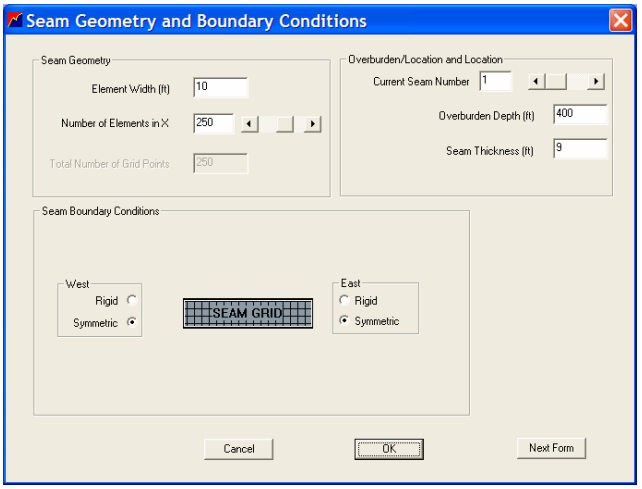


Figure 8.—Seam geometry and boundary condition form.

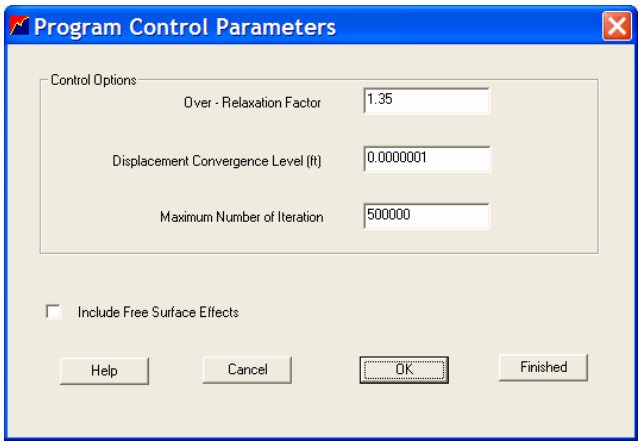


Figure 9.—Program control form.

Grid Editor

The grid editor is used for inputting the seam material codes. It contains a simulated cross-section for each of the modeled mining seams (Figure 5) where the user can enter the appropriate letter codes into the proper grid location in order to represent the 2–D mine layout. The letter codes are entered using a mouse-driven interface similar to an Excel spreadsheet. The user only needs to input the primary coal letter code for each seam, and the program automatically generates appropriate yield zones based on a Bieniawski pillar strength. Also, the grid editor is where the user inputs the out-of-plane extraction ratio.

Running the Model

Once all of the input has been completed, the LaM2D program typically runs in just a few seconds. Then, the output can be viewed using a number of plotting routines. The values output from the program include: seam convergence, seam stress, multiple-seam stress, multiple-seam displacement, and horizontal strain. Any of these values can be plotted separately using the traditional "colored-square" plot or line graph. Also, a new "comparison plot" can be used to visualize, compare, and analyze the interacting effect of different values from one seam to the other.

CASE STUDY

In order to test the accuracy and utility of using the new, simplified multiple-seam program, LaM2D, a comparative case study was performed using both LaModel and LaM2D. The case study was taken from the literature [Ellenberger et al. 2003] and documents a situation where a longwall panel undermined an active room-and-pillar mainline development. The upper mine operates in the 9-ft-thick Coalburg Seam and has driven a seven-entry mainline with 40- by 80-ft pillars. The lower mine operates in the 5.6-ft-thick No. 2 Gas Seam and was

retreating a 1,000-ft-wide longwall panel directly under the overlying mains. The interburden at this site averaged 560 ft, and the maximum overburden over the upper mine was about 400 ft. The idealized mine map for this site, as used in the comparative study, is shown in Figure 10.

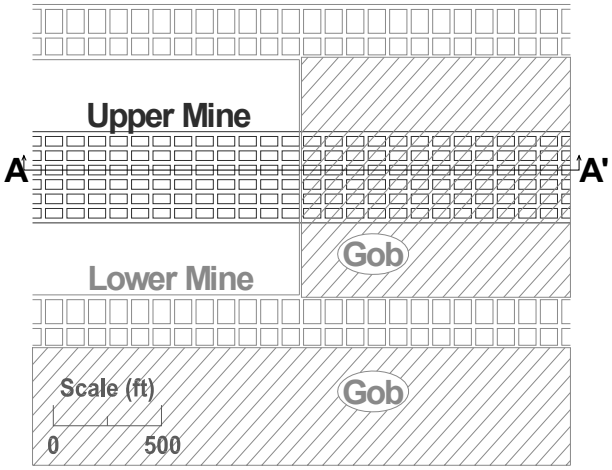


Figure 10.—Idealized mine plan for the case study analysis.

For the idealized comparative study in this paper, the mains are modeled as perfectly aligned with the middle of the longwall panel, and all of the pillars in the mains and the gate roads are modeled with consistent sizes. In reality, the mains were somewhat offset from the center of the longwall panel and slightly skewed to the longwall advance. Also, the pillars in both the mains and the longwall gate roads have some variations in dimension due to practical and operational considerations [Ellenberger et al. 2003].

In the field, when the upper seam was undermined by the longwall, tension cracks began to develop in the roof when the underlying face approached to within 70 ft. Roof and rib control problems intensified as the longwall moved under and continued beyond the upper seam. The sandstone roof in the upper mine was extensively fractured, with some apertures measured at 4 in. Several roof falls occurred and severe rib spalling was experienced. As the dynamic subsidence settled and reached equilibrium, the roof fractures mostly closed and conditions significantly improved.

For the mine plan in Figure 10, a 3–D LaModel model was developed. This model used 10-ft elements on a 250-by-250 grid to represent the mine plan shown. Entering the material parameters and the mine grid in order to build this simplified model took about 1 hr (for the real mine plan with variable size pillars and off-angle pillar, more than a day was used to build the model). The program then took another hour to solve the model for the seam stresses and displacements. Overall, LaModel took about 2 hr to build and solve the model.

Using LaM2D, a 2–D cross-section from the critical area (section A–A′) in Figure 10 was modeled. This cross-section essentially consists of the upper-seam pillars and the lower-seam longwall, as shown in Figure 11. With the simplified 2–D LaM2D, a linear array of 250 10-ft elements was used to represent each seam. The minimum parameter input for the model was used, as shown in Figures 3 and 4, and only took a minute or two to enter. Also, the material grids were entered into the program using the grid editor (Figure 5) and took another few minutes. After all of the parameters and grids were entered, the program solved for the seam stresses, displacements, safety factors, and strains in a few seconds. Overall, the total parameter input and solution required less than 10 min using LaM2D.



Figure 11.—Cross-section used in the LaM2D program.

Figure 12 compares the stresses calculated with the 3–D LaModel program with those calculated with the simplified LaM2D program. For all practical purposes, the vertical stresses calculated by the two models are the same. Both models show the stress abutment in front of the advancing longwall face and the reduced stress in the gob behind the longwall. Further, the LaM2D program can be used to determine the pillar safety factors and the subsidence-induced strain. For instance, the pillar safety factors for the case study are shown in Figure 13. It can be seen in this figure that the safety factors are generally high and pillar failure would not be expected. This is consistent with observations in the field, which reported pillar spalling but no pillar failure. The horizontal strain was also calculated for the case study, as shown in Figure 14. The tensile stress in front of the moving longwall and the compressive stress behind the longwall on the order of 250 microstrains are clearly evident. Based on the National Coal Board experience with surface strains [National Coal Board 1975], the 250 microstrains should only cause "slight damage." However, the correlation between strain and underground roof damage is not very well defined, and 250 microstrains could be consistent with the observed roof cracking and roof falls.

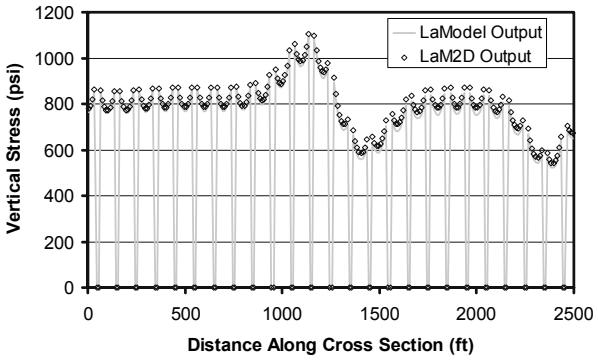


Figure 12.—Comparison of LaModel and LaM2D stresses.

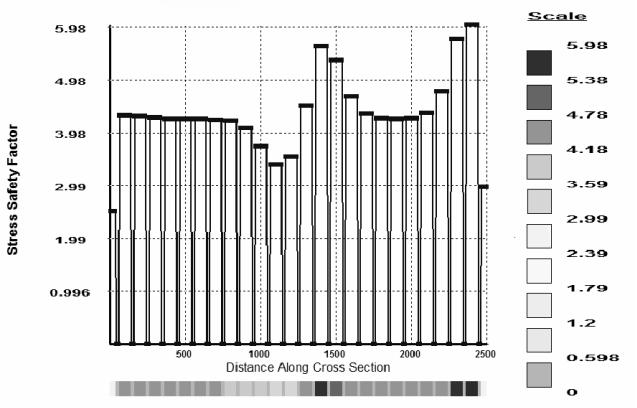


Figure 13.—LaM2D safety factor output.

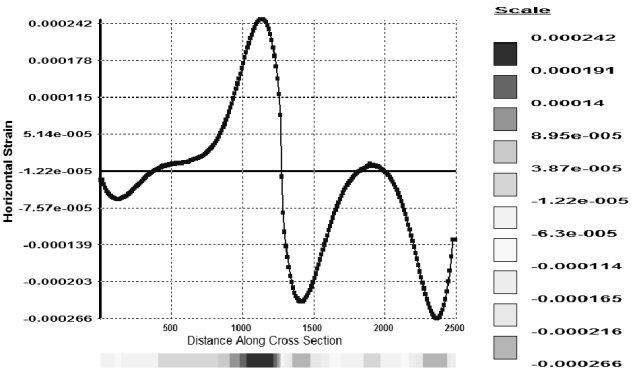


Figure 14.—LaM2D horizontal strain output.

SUMMARY AND CONCLUSIONS

A simplified 2–D boundary-element method designed to model the complex multiple-seam stress and displacement interactions has been implemented into the LaM2D program. This new program allows the user to quickly and easily calculate the stresses, displacements, safety factors, and strains associated with basic multiple-seam mining situations that can be accurately represented in two dimensions. The input to LaM2D has been greatly simplified by incorporating automatic overburden, interburden, coal, and gob property generation. Also, the program is the first multiple-seam analysis package to inherently calculate pillar safety factors and multiple-seam-induced subsidence and strain. In a practical comparison with the full-featured multiple-seam program LaModel, the simplified LaM2D provided comparable stress and displacement calculations in minutes instead of hours. Further, the unique safety factor and strain calculations of the LaM2D program provided practical accurate assessments of the observed pillar and roof behavior in the modeled mine.

REFERENCES

Chekan GJ, Listak JM [1994]. Design practices for multiple-seam room-and-pillar mines. Pittsburgh, PA: U.S. Department of the Interior, Bureau of Mines, IC 9403.

Ellenberger JL, Chase FE, Mark C, Heasley KA, Marshall JK [2003]. Using site case histories of multiple-seam coal mining to advance mine design. In: Peng SS, Mark C, Khair AW, Heasley KA, eds. Proceedings of the 22nd International Conference on Ground Control in Mining. Morgantown, WV: West Virginia University, pp. 59–64.

Heasley KA [1998]. Numerical modeling of coal mines with a laminated displacement-discontinuity code [Dissertation]. Golden, CO: Colorado School of Mines, Department of Mining and Earth Systems Engineering.

Heasley KA, Chekan GJ [1999]. Practical boundary-element modeling for mine planning. In: Mark C, Heasley KA, Iannacchione AT, Tuchman RJ, eds. Proceedings of the Second International Workshop on Coal Pillar Mechanics and Design. Pittsburgh, PA: U.S. Department of Health and Human Services, Public Health Service, Centers for Disease Control and Prevention, National Institute for Occupational Safety and Health, DHHS (NIOSH) Publication No. 99–114, IC 9448, pp. 73–87.

Mark C, Chase FE [1997]. Analysis of retreat mining pillar stability (ARMPS). In: Mark C, Tuchman RJ, eds. Proceedings: New technology for ground control in retreat mining. Pittsburgh, PA: U.S. Department of Health and Human Services, Public Health Service, Centers for Disease Control and Prevention, National Institute for Occupational Safety and Health, IC 9446, pp. 17–34.

National Coal Board [1975]. Subsidence engineers handbook. London: National Coal Board, Mining Department.

Salamon MDG [1962]. The influence of strata movement and control on mining development and design [Dissertation]. Durham, U.K.: University of Durham, King's College, Department of Mining.

Salamon MDG [1963]. Elastic analysis of displacements and stresses induced by the mining of seam or reef deposits, part 1. J S Afr Inst Min Metall *64*(4):128–149.

Salamon MDG [1991]. Deformation of stratified rock masses: a laminated model. J S Afr Inst Min Metall *91*(1): 9–26.

Zipf RK Jr. [1992a]. MULSIM/NL application and practitioner's manual. Pittsburgh, PA: U.S. Department of the Interior, Bureau of Mines, IC 9322.

Zipf RK Jr. [1992b]. MULSIM/NL theoretical and programmer's manual. Pittsburgh, PA: U.S. Department of the Interior, Bureau of Mines, IC 9321.

This paper was previously published as:

Heasley KA, Akinkugbe OO [2004]. A simple program for estimating multiple-seam interactions. SME preprint 04–137. Littleton, CO: Society for Mining, Metallurgy, and Exploration, Inc.

Appendix C - Pillar Stability and Subsidence Calculations for Multi-seam Interaction

UNSW Pillar Design Spreadsheet	30.6	30.4	32.6	32.6	32.6	32.6	32.6	40.0	186.0	32.6	32.6
	1.1	**1.2**	**1.3**	**1.4**	**1.5**	**1.6**	**1.7**	**2.1**	**2.2**	**3.1**	**3.2**
Chain Valley XL.Panel#	MW1	MW2	MW3	MW6	MW7	MW8					
INPUT DATA	95.3	95.3	95.3	95.3	95.3	95.3	95.3	95.3	95.3	95.3	95.3
Depth of Cover (m)	**200**	**200**	**198**	**195**	**195**	**193**	**191**	**196**	**200**	**190**	**188**
Mining Height (m)	**3.5**	**3.5**	**3.5**	**3.5**	**3.5**	**3.5**	**3.5**	**3.5**	**3.5**	**3.5**	**3.5**
Pillar Length - centres (m)	100.7	100.7	100.7	100.7	100.7	100.7	100.7	100.7	100.7	100.7	100.7
Pillar Width - centres (m)	36.0	35.8	38.0	38.0	38.0	38.0	38.0	45.4	191.4	38.0	38.0
Roadway Width for maximum pillar dimension	5.4	5.4	5.4	5.4	5.4	5.4	5.4	5.4	5.4	5.4	5.4
Roadway Width for minimum pillar dimension	5.4	5.4	5.4	5.4	5.4	5.4	5.4	5.4	5.4	5.4	5.4
Cut-Through Angle (degrees)	**90**	**90**	**90**	**90**	**90**	**90**	**90**	**90**	**90**	**90**	**90**
Average Panel Span (m) {rib-rib width}	74	72	97	97	97	97	**97**	**97**	**97**	**97**	**97**
SG (tonnes/m^3)	2.5	2.5	2.5	2.5	2.5	2.5	2.5	2.5	2.5	2.5	2.5
Conversion (tonnes to N)	10000	10000	10000	10000	10000	10000	10000	10000	10000	10000	10000
Abutment Angle (^{0})	21	21	21	21	21	21	21	21	21	21	21
W/H	0.37	0.36	0.49	0.50	0.50	0.50	0.51	0.49	0.49	0.51	0.52
PRELIMINARY CALCULATIONS											
Maximum Rib to Rib Pillar Length (w_2)	**95.3**	**95.3**	**95.3**	**95.3**	**95.3**	**95.3**	**95.3**	**95.3**	**95.3**	**95.3**	**95.3**
Minimum Rib to Rib Pillar Width (w_1)	**30.6**	**30.4**	**32.6**	**32.6**	**32.6**	**32.6**	**32.6**	**40.0**	**186.0**	**32.6**	**32.6**
w, Minimum Rib to Rib Pillar Width (ie $w_1 \sin\theta$)	**30.6**	**30.4**	**32.6**	**32.6**	**32.6**	**32.6**	**32.6**	**40.0**	**186.0**	**32.6**	**32.6**
Minimum Pillar Width/Height Ratio	**8.7**	**8.7**	**9.3**	**9.3**	**9.3**	**9.3**	**9.3**	**11.4**	**27.2**	**9.3**	**9.3**
Extraction Ratio (%)	**19.6%**	**19.6%**	**18.8%**	**18.8%**	**18.8%**	**18.8%**	**18.8%**	**16.6%**	**8.0%**	**18.8%**	**18.8%**
Abutment Angle (Radians)	0.367	0.367	0.367	0.367	0.367	0.367	0.367	0.367	0.367	0.367	0.367
Cut-Through Angle (Radians)	1.571	1.571	1.571	1.571	1.571	1.571	1.571	1.571	1.571	1.571	1.571
Is the Panel Super-Critical?	No	No	No	No	No	No	No	No	No	No	No
D (Peng & Chiang Loading Factor)	72.549	72.549	72.185	71.637	71.637	71.268	70.898	71.820	72.549	70.712	70.339
R (Pillar 2nd Abutment Component)	0.87	0.87	0.89	0.90	0.90	0.90	0.90	0.95	1.00	0.90	0.90
Dimensionless Pillar 'Rectangularity'	1.51	1.52	1.49	1.49	1.49	1.49	1.49	1.41	0.68	1.49	1.49
Width/Height Ratio Exponent	1.00	1.00	1.00	1.00	1.00	1.00	1.00	1.00	1.00	1.00	1.00
Effective Width Factor (Omega)	1.51	1.52	1.49	1.49	1.49	1.49	1.49	1.41	0.68	1.49	1.49
Effective Width Interim	46.33	46.10	48.58	48.58	48.58	48.58	48.58	56.35	126.03	48.58	48.58
Effective Pillar Width (m)	46.33	46.10	48.58	48.58	48.58	48.58	48.58	56.35	126.03	48.58	48.58
Effective Pillar Loading Height (m)	200.00	200.00	198.00	195.00	195.00	193.00	191.00	196.00	200.00	190.00	188.00
RESULTS											
Tributary Area Loading (MPa)	**6.22**	**6.22**	**6.10**	**6.00**	**6.00**	**5.94**	**5.88**	**5.88**	**5.44**	**5.85**	**5.79**
Pillar Strength (UNSW Squat Pillar 1999)	**26.38**	**26.17**	**28.56**	**28.56**	**28.56**	**28.56**	**28.56**	**38.21**	**672.19**	**28.56**	**28.56**
Pillar Strength (UNSW w/h<5)	**N/A**	**N/A**	**N/A**	**N/A**	**N/A**	**N/A**	**N/A**	**N/A**	**N/A**	**N/A**	**N/A**
Safety Factor under FTA Loading (Squat Pillar)	**4.24**	**4.21**	**4.68**	**4.76**	**4.76**	**4.81**	**4.86**	**6.50**	**123.64**	**4.88**	**4.93**
Safety Factor under FTA Loading (w/h<5)	**N/A**	**N/A**	**N/A**	**N/A**	**N/A**	**N/A**	**N/A**	**N/A**	**N/A**	**N/A**	**N/A**
Single Abutment Loading (3D) - full	4.59	4.54	5.13	5.02	5.02	4.95	4.87	4.12	0.91	4.84	4.76
Single Abutment Loading (3D) - pillar	**4.00**	**3.95**	**4.59**	**4.50**	**4.50**	**4.45**	**4.39**	**3.92**	**0.91**	**4.36**	**4.30**
Single Abutment Loading (3D) - solid	0.59	0.59	0.55	0.52	0.52	0.50	0.49	0.21	0.00	0.48	0.46
Design Abutment Load Multiplier	1.00	1.00	1.00	1.50	1.50	1.00	1.00	1.00	1.00	1.00	1.00
Total Pillar Loading with Single Abutment Loading	11.22	11.17	11.69	12.01	12.01	11.39	11.27	10.80	7.35	11.21	11.09
Safety Factor (under Single Abutment Loading)	**2.35**	**2.34**	**2.44**	**2.38**	**2.38**	**2.51**	**2.53**	**3.54**	**91.46**	**2.55**	**2.58**
Total Pillar Loading @ nA	10.81	10.76	11.23	13.54	13.54	10.89	10.76	10.00	6.35	10.69	10.55
Safety Factor @ nA	**2.44**	**2.43**	**2.54**	**2.11**	**2.11**	**2.62**	**2.66**	**3.82**	**105.86**	**2.67**	**2.71**
Total Pillar Loading under Double Abutment Loading	15.39	15.31	16.37	16.05	16.05	15.84	15.63	14.12	7.26	15.53	15.32
Safety Factor (under Double Abutment Loading)	**1.71**	**1.71**	**1.75**	**1.78**	**1.78**	**1.80**	**1.83**	**2.71**	**92.56**	**1.84**	**1.86**
Elastic Model Subsidence											
Ecoal(GPa)	**0.75**	**0.75**	**0.75**	**0.75**	**0.75**	**0.75**	**0.75**	**0.75**	**0.75**	**0.75**	**0.75**
E1floor(GPa)	**0.30**	**0.30**	**0.30**	**0.30**	**0.30**	**0.30**	**0.30**	**0.30**	**0.30**	**0.30**	**0.30**
E2floor(GPa)	**1.50**	**1.50**	**1.50**	**1.50**	**1.50**	**1.50**	**1.50**	**1.50**	**1.50**	**1.50**	**1.50**
E1roof(GPa)	**1.00**	**1.00**	**1.00**	**1.00**	**1.00**	**1.00**	**1.00**	**1.00**	**1.00**	**1.00**	**1.00**
E2roof(GPa)	**1.20**	**1.20**	**1.20**	**1.20**	**1.20**	**1.20**	**1.20**	**1.20**	**1.20**	**1.20**	**1.20**
Poissons Ratio floor/roof	**0.25**	**0.25**	**0.25**	**0.25**	**0.25**	**0.25**	**0.25**	**0.25**	**0.25**	**0.25**	**0.25**
initial vertical stress (MPa)	**5.00**	**5.00**	**4.95**	**4.88**	**4.88**	**4.83**	**4.78**	**4.90**	**5.00**	**4.75**	**4.70**
increase in vertical stress for DA (MPa)	**10.39**	**10.31**	**11.42**	**11.18**	**11.18**	**11.02**	**10.86**	**9.22**	**2.26**	**10.78**	**10.62**
Roof t1	**0.30**	**0.30**	**0.30**	**0.30**	**0.30**	**0.30**	**0.30**	**0.30**	**0.30**	**0.30**	**0.30**
Roof t2	**30.30**	**30.10**	**32.30**	**32.30**	**32.30**	**32.30**	**32.30**	**39.70**	**185.70**	**32.30**	**32.30**
Roof sig1	**10.39**	**10.31**	**11.42**	**11.18**	**11.18**	**11.02**	**10.86**	**9.22**	**2.26**	**10.78**	**10.62**
Roof sig2	**9.44**	**9.36**	**10.37**	**10.15**	**10.15**	**10.01**	**9.86**	**8.38**	**2.06**	**9.79**	**9.64**
Floor t1	**0.90**	**0.90**	**0.90**	**0.90**	**0.90**	**0.90**	**0.90**	**0.90**	**0.90**	**0.90**	**0.90**
Floor t2	**29.7**	**29.5**	**31.7**	**31.7**	**31.7**	**31.7**	**31.7**	**39.1**	**185.1**	**31.7**	**31.7**
Floor sig1	**10.39**	**10.31**	**11.42**	**11.18**	**11.18**	**11.02**	**10.86**	**9.22**	**2.26**	**10.78**	**10.62**
Floor sig2	**10.39**	**10.30**	**11.41**	**11.17**	**11.17**	**11.01**	**10.85**	**9.22**	**2.26**	**10.77**	**10.61**
Pillar Compression (m)	**0.045**	**0.045**	**0.050**	**0.049**	**0.049**	**0.048**	**0.047**	**0.040**	**0.010**	**0.047**	**0.046**
Roof Compression (m)	**0.226**	**0.223**	**0.265**	**0.259**	**0.259**	**0.256**	**0.252**	**0.263**	**0.299**	**0.250**	**0.246**
Floor Compression (m)	**0.222**	**0.219**	**0.258**	**0.253**	**0.253**	**0.249**	**0.246**	**0.251**	**0.268**	**0.244**	**0.240**
Total FTA Compression (m)	**0.494**	**0.487**	**0.573**	**0.561**	**0.561**	**0.553**	**0.545**	**0.554**	**0.577**	**0.541**	**0.533**
Total Effective Compression (m)	**0.494**	**0.487**	**0.573**	**0.561**	**0.561**	**0.553**	**0.545**	**0.554**	**0.577**	**0.541**	**0.533**
1.5 times Effective Compression (m)	**0.741**	**0.731**	**0.860**	**0.842**	**0.842**	**0.830**	**0.818**	**0.832**	**0.866**	**0.812**	**0.799**
Total Yielded Panel Subs (m)	**1.64**	**1.63**	**1.76**	**1.74**	**1.74**	**1.73**	**1.72**	**1.73**	**1.77**	**1.71**	**1.70**
Measured			**0.570**	**0.570**							
Bearing Capacity											
Upper Floor Unit UCS, 2*cu1 (MPa)	**2.0**	**2.0**	**1.0**	**2.0**	**2.0**	**2.0**	**2.0**	**2.0**	**2.0**	**2.0**	**2.0**
Upper Unit Thickness, H (m)	**0.9**	**0.9**	**0.3**	**0.9**	**0.9**	**0.9**	**0.9**	**0.9**	**0.9**	**0.9**	**0.9**
Lower Floor Unit UCS, 2*cu2 (MPa)	**40.0**	**40.0**	**40.0**	**40.0**	**40.0**	**40.0**	**40.0**	**40.0**	**40.0**	**40.0**	**40.0**
cu1/cu2	**0.1**	**0.1**	**0.0**	**0.1**	**0.1**	**0.1**	**0.1**	**0.1**	**0.1**	**0.1**	**0.1**
H/B	**0.03**	**0.03**	**0.01**	**0.03**	**0.03**	**0.03**	**0.03**	**0.02**	**0.00**	**0.03**	**0.03**
N*1	**21.73**	**21.61**	**58.47**	**22.88**	**22.88**	**22.88**	**22.88**	**27.13**	**111.04**	**22.88**	**22.88**
N*2	**1.09**	**1.08**	**1.46**	**1.14**	**1.14**	**1.14**	**1.14**	**1.36**	**5.55**	**1.14**	**1.14**
Floor Bearing Capacity (MPa)	**21.7**	**21.6**	**29.2**	**22.9**	**22.9**	**22.9**	**22.9**	**27.1**	**111.0**	**22.9**	**22.9**
Eff Pillar Stress (MPa)	**15.4**	**15.3**	**16.4**	**16.1**	**16.1**	**15.8**	**15.6**	**14.1**	**7.3**	**15.5**	**15.3**
Eff Floor Bearing Failure FoS	**1.41**	**1.41**	**1.79**	**1.43**	**1.43**	**1.44**	**1.46**	**1.92**	**15.29**	**1.47**	**1.49**
FTA Floor Bearing Failure FoS	**3.50**	**3.47**	**4.80**	**3.81**	**3.81**	**3.85**	**3.89**	**4.62**	**20.42**	**3.91**	**3.95**
Immediate Roof Unit UCS, 2*cu1 (MPa)	**2.0**	**2.0**	**2.0**	**2.0**	**2.0**	**2.0**	**2.0**	**2.0**	**2.0**	**2.0**	**2.0**
Immediate Roof Unit Thickness, H (m)	**3.0**	**3.0**	**3.0**	**3.0**	**3.0**	**3.0**	**3.0**	**3.0**	**3.0**	**3.0**	**3.0**
Upper Roof Unit UCS, 2*cu2 (MPa)	**40.0**	**40.0**	**40.0**	**40.0**	**40.0**	**40.0**	**40.0**	**40.0**	**40.0**	**40.0**	**40.0**
cu1/cu2	**0.1**	**0.1**	**0.1**	**0.1**	**0.1**	**0.1**	**0.1**	**0.1**	**0.1**	**0.1**	**0.1**
H/B	**0.10**	**0.10**	**0.09**	**0.09**	**0.09**	**0.09**	**0.09**	**0.08**	**0.02**	**0.09**	**0.09**
N*1	**9.24**	**9.21**	**9.57**	**9.57**	**9.57**	**9.57**	**9.57**	**10.81**	**35.14**	**9.57**	**9.57**
N*2	0.46	0.46	0.48	0.48	0.48	0.48	0.48	0.54	1.76	0.48	0.48
Roof Bearing Capacity (MPa)	9.2	9.2	9.6	9.6	9.6	9.6	9.6	10.8	35.1	9.6	9.6
Pillar Stress (MPa)	**15.4**	**15.3**	**16.4**	**16.1**	**16.1**	**15.8**	**15.6**	**14.1**	**7.3**	**15.5**	**15.3**
Effective Roof Bearing Failure FoS	**0.60**	**0.60**	**0.59**	**0.60**	**0.60**	**0.60**	**0.61**	**0.77**	**4.84**	**0.62**	**0.63**
FTA Roof Bearing Failure FoS	**1.49**	**1.48**	**1.57**	**1.59**	**1.59**	**1.61**	**1.63**	**1.84**	**6.46**	**1.64**	**1.65**
Voussoir Beam Deflection (m)	**0.004**	**0.004**	**0.004**	**0.001**	**0.001**	**0.419**	**0.006**	**0.011**	**0.282**	**0.005**	**0.065**
System Settlement at Base of beam (m)	0.000	0.000	0.000	0.000	0.000	0.000	0.000	0.000	0.000	0.000	0.000
Applied Pillar Stress/FTA Stress Ratio (Mpa)	1.00	1.00	1.00	1.00	1.00	1.00	1.00	1.00	1.00	1.00	1.00
Effective Pillar Stress (Mpa)	15.39	15.31	16.37	16.05	16.05	15.84	15.63	14.12	7.26	15.53	15.32
Multi-Seam Stress Inc (min)											
Multi-Seam Stress Inc (max)											
Effective Pillar FoS	**1.71**	**1.71**	**1.75**	**1.78**	**1.78**	**1.80**	**1.83**	**2.71**	**92.56**	**1.84**	**1.86**
Eresidual coal(GPa)	**0.24**	**0.24**	**0.25**	**0.25**	**0.25**	**0.25**	**0.25**	**0.28**	**0.37**	**0.25**	**0.25**

UNSW Pillar Design Spreadsheet	32.6	32.6	32.6	32.6	32.6	300.0	32.6	32.6	31.6	31.1	30.6
	3.3	**3.4**	**3.5**	**3.6**	**4.1**	**4.2**	**5.1**	**5.2**	**5.3**	**5.4**	**5.5**
Chain Valley XL.Panel#											
INPUT DATA	95.3	95.3	95.3	95.3	95.3	95.3	95.3	95.3	95.3	95.3	95.3
Depth of Cover (m)	**185**	**183**	**178**	**173**	**170**	**184**	**188**	**185**	**182**	**180**	**175**
Mining Height (m)	**3.5**	**3.5**	**3.5**	**3.5**	**3.5**	**3.5**	**3.5**	**3.5**	**3.5**	**3.5**	**3.5**
Pillar Length - centres (m)	100.7	100.7	100.7	100.7	100.7	100.7	100.7	100.7	100.7	100.7	100.7
Pillar Width - centres (m)	38.0	38.0	38.0	38.0	38.0	305.4	38.0	38.0	37.0	36.5	36.0
Roadway Width for maximum pillar dimension	5.4	5.4	5.4	5.4	5.4	5.4	5.4	5.4	5.4	5.4	5.4
Roadway Width for minimum pillar dimension	5.4	5.4	5.4	5.4	5.4	5.4	5.4	5.4	5.4	5.4	5.4
Cut-Through Angle (degrees)	**90**	**90**	**90**	**90**	**90**	**90**	**90**	**90**	**90**	**90**	**90**
Average Panel Span (m) {rib-rib width}	**97**	**97**	**97**	**97**	**97**	**97**	**97**	**97**	97	97	97
SG (tonnes/m^3)	2.5	2.5	2.5	2.5	2.5	2.5	2.5	2.5	2.5	2.5	2.5
Conversion (tonnes to N)	10000	10000	10000	10000	10000	10000	10000	10000	10000	10000	10000
Abutment Angle (^{0})	21	21	21	21	21	21	21	21	21	21	21
W/H	0.52	0.53	0.54	0.56	0.57	0.53	0.52	0.52	0.53	0.54	0.55
PRELIMINARY CALCULATIONS											
Maximum Rib to Rib Pillar Length (w_2)	**95.3**	**95.3**	**95.3**	**95.3**	**95.3**	**95.3**	**95.3**	**95.3**	**95.3**	**95.3**	**95.3**
Minimum Rib to Rib Pillar Width (w_1)	**32.6**	**32.6**	**32.6**	**32.6**	**32.6**	**300.0**	**32.60**	**32.60**	**31.60**	**31.10**	**30.60**
w, Minimum Rib to Rib Pillar Width (ie $w_1 \sin\theta$)	**32.6**	**32.6**	**32.6**	**32.6**	**32.6**	**300.0**	**32.60**	**32.60**	**31.60**	**31.10**	**30.60**
Minimum Pillar Width/Height Ratio	**9.3**	**9.3**	**9.3**	**9.3**	**9.3**	**27.2**	**9.3**	**9.3**	**9.0**	**8.9**	**8.7**
Extraction Ratio (%)	**18.8%**	**18.8%**	**18.8%**	**18.8%**	**18.8%**	**7.0%**	**18.8%**	**18.8%**	**19.2%**	**19.4%**	**19.6%**
Abutment Angle (Radians)	0.367	0.367	0.367	0.367	0.367	0.367	0.367	0.367	0.367	0.367	0.367
Cut-Through Angle (Radians)	1.571	1.571	1.571	1.571	1.571	1.571	1.571	1.571	1.571	1.571	1.571
Is the Panel Super-Critical?	No	No	No	No	No	No	No	No	No	No	No
D (Peng & Chiang Loading Factor)	69.776	69.397	68.443	67.475	66.887	69.587	70.339	69.776	69.207	68.826	67.864
R (Pillar 2nd Abutment Component)	0.91	0.91	0.91	0.92	0.92	1.00	0.90	0.91	0.90	0.90	0.90
Dimensionless Pillar 'Rectangularity'	1.49	1.49	1.49	1.49	1.49	0.48	1.49	1.49	1.50	1.51	1.51
Width/Height Ratio Exponent	1.00	1.00	1.00	1.00	1.00	1.00	1.00	1.00	1.00	1.00	1.00
Effective Width Factor (Omega)	1.49	1.49	1.49	1.49	1.49	0.48	1.49	1.49	1.50	1.51	1.51
Effective Width Interim	48.58	48.58	48.58	48.58	48.58	144.65	48.58	48.58	47.46	46.90	46.33
Effective Pillar Width (m)	48.58	48.58	48.58	48.58	48.58	144.65	48.58	48.58	47.46	46.90	46.33
Effective Pillar Loading Height (m)	185.00	183.00	178.00	173.00	170.00	184.00	188.00	185.00	182.00	180.00	175.00
RESULTS											
Tributary Area Loading (MPa)	**5.70**	**5.63**	**5.48**	**5.33**	**5.23**	**4.95**	**5.79**	**5.70**	**5.63**	**5.58**	**5.44**
Pillar Strength (UNSW Squat Pillar 1999)	**28.56**	**28.56**	**28.56**	**28.56**	**28.56**	**1672.92**	**28.56**	**28.56**	**27.45**	**26.91**	**26.38**
Pillar Strength (UNSW w/h<5)	**N/A**	**N/A**	**N/A**	**N/A**	**N/A**	**N/A**	**N/A**	**N/A**	**N/A**	**N/A**	**N/A**
Safety Factor under FTA Loading (Squat Pillar)	**5.01**	**5.07**	**5.21**	**5.36**	**5.46**	**338.09**	**4.93**	**5.01**	**4.88**	**4.82**	**4.85**
Safety Factor under FTA Loading (w/h<5)	**N/A**	**N/A**	**N/A**	**N/A**	**N/A**	**N/A**	**N/A**	**N/A**	**N/A**	**N/A**	**N/A**
Single Abutment Loading (3D) - full	4.65	4.58	4.39	4.21	4.10	0.50	4.76	4.65	4.68	4.68	4.56
Single Abutment Loading (3D) - pillar	**4.21**	**4.15**	**4.01**	**3.86**	**3.77**	**0.50**	**4.30**	**4.21**	**4.21**	**4.20**	**4.09**
Single Abutment Loading (3D) - solid	0.44	0.42	0.39	0.35	0.33	0.00	0.46	0.44	0.47	0.49	0.47
Design Abutment Load Multiplier	1.00	1.00	1.00	1.00	1.00	1.00	1.00	1.00	1.00	1.00	1.00
Total Pillar Loading with Single Abutment Loading	10.91	10.79	10.49	10.18	10.00	6.45	11.09	10.91	10.84	10.78	10.53
Safety Factor (under Single Abutment Loading)	**2.62**	**2.65**	**2.72**	**2.80**	**2.86**	**259.38**	**2.58**	**2.62**	**2.53**	**2.50**	**2.51**
Total Pillar Loading @ nA	10.35	10.21	9.87	9.53	9.33	5.45	**10.55**	**10.35**	**10.31**	**10.26**	**10.00**
Safety Factor @ nA	**2.76**	**2.80**	**2.89**	**3.00**	**3.06**	**306.98**	**2.71**	**2.76**	**2.66**	**2.62**	**2.64**
Total Pillar Loading under Double Abutment Loading	15.00	14.79	14.27	13.74	13.43	5.95	15.32	15.00	15.00	14.94	14.56
Safety Factor (under Double Abutment Loading)	**1.90**	**1.93**	**2.00**	**2.08**	**2.13**	**281.11**	**1.86**	**1.90**	**1.83**	**1.80**	**1.81**
Elastic Model Subsidence											
Ecoal(GPa)	**0.75**	**0.75**	**0.75**	**0.75**	**0.75**	**0.75**	**0.75**	**0.75**	**0.75**	**0.75**	**0.75**
E1floor(GPa)	**0.30**	**0.30**	**0.30**	**0.30**	**0.30**	**0.30**	**0.30**	**0.30**	**0.30**	**0.30**	**0.30**
E2floor(GPa)	**1.50**	**1.50**	**1.50**	**1.50**	**1.50**	**1.50**	**1.50**	**1.50**	**1.50**	**1.50**	**1.50**
E1roof(GPa)	**1.00**	**1.00**	**1.00**	**1.00**	**1.00**	**1.00**	**1.00**	**1.00**	**1.00**	**1.00**	**1.00**
E2roof(GPa)	**1.20**	**1.20**	**1.20**	**1.20**	**1.20**	**1.20**	**1.20**	**1.20**	**1.20**	**1.20**	**1.20**
Poissons Ratio floor/roof	**0.25**	**0.25**	**0.25**	**0.25**	**0.25**	**0.25**	**0.25**	**0.25**	**0.25**	**0.25**	**0.25**
initial vertical stress (MPa)	**4.63**	**4.58**	**4.45**	**4.33**	**4.25**	**4.60**	**4.70**	**4.63**	**4.55**	**4.50**	**4.38**
increase in vertical stress for DA (MPa)	**10.38**	**10.22**	**9.82**	**9.42**	**9.18**	**1.35**	**10.62**	**10.38**	**10.45**	**10.44**	**10.18**
Roof t1	**0.30**	**0.30**	**0.30**	**0.30**	**0.30**	**0.30**	**0.30**	**0.30**	**0.30**	**0.30**	**0.30**
Roof t2	**32.30**	**32.30**	**32.30**	**32.30**	**32.30**	**299.70**	**32.30**	**32.30**	**31.30**	**30.80**	**30.30**
Roof sig1	**10.38**	**10.22**	**9.82**	**9.42**	**9.18**	**1.35**	**10.62**	**10.38**	**10.45**	**10.44**	**10.18**
Roof sig2	**9.43**	**9.28**	**8.92**	**8.55**	**8.34**	**1.23**	**9.64**	**9.43**	**9.49**	**9.49**	**9.25**
Floor t1	**0.90**	**0.90**	**0.90**	**0.90**	**0.90**	**0.90**	**0.90**	**0.90**	**0.90**	**0.90**	**0.90**
Floor t2	**31.7**	**31.7**	**31.7**	**31.7**	**31.7**	**299.1**	**31.7**	**31.7**	**30.7**	**30.2**	**29.7**
Floor sig1	**10.38**	**10.22**	**9.82**	**9.42**	**9.17**	**1.35**	**10.62**	**10.38**	**10.45**	**10.44**	**10.18**
Floor sig2	**10.37**	**10.21**	**9.81**	**9.41**	**9.17**	**1.35**	**10.61**	**10.37**	**10.45**	**10.44**	**10.18**
Pillar Compression (m)	**0.045**	**0.045**	**0.043**	**0.041**	**0.040**	**0.006**	**0.046**	**0.045**	**0.046**	**0.046**	**0.045**
Roof Compression (m)	**0.241**	**0.237**	**0.228**	**0.219**	**0.213**	**0.288**	**0.246**	**0.241**	**0.235**	**0.231**	**0.222**
Floor Compression (m)	**0.235**	**0.231**	**0.222**	**0.213**	**0.208**	**0.256**	**0.240**	**0.235**	**0.230**	**0.226**	**0.218**
Total FTA Compression (m)	**0.521**	**0.513**	**0.493**	**0.473**	**0.461**	**0.551**	**0.533**	**0.521**	**0.511**	**0.503**	**0.484**
Total Effective Compression (m)	**0.521**	**0.513**	**0.493**	**0.473**	**0.461**	**0.551**	**0.533**	**0.521**	**0.511**	**0.503**	**0.484**
1.5 times Effective Compression (m)	**0.781**	**0.769**	**0.739**	**0.709**	**0.691**	**0.826**	**0.799**	**0.781**	**0.766**	**0.755**	**0.726**
Total Yielded Panel Subs (m)	**1.68**	**1.67**	**1.64**	**1.61**	**1.59**	**1.73**	**1.70**	**1.68**	**1.67**	**1.66**	**1.63**
Measured											
Bearing Capacity											
Upper Floor Unit UCS, 2*cu1 (MPa)	**2.0**	**2.0**	**2.0**	**2.0**	**2.0**	**2.0**	**2.0**	**2.0**	**2.0**	**2.0**	**2.0**
Upper Unit Thickness, H (m)	**0.9**	**0.9**	**0.9**	**0.9**	**0.9**	**0.9**	**0.9**	**0.9**	**0.9**	**0.9**	**0.9**
Lower Floor Unit UCS, 2*cu2 (MPa)	**40.0**	**40.0**	**40.0**	**40.0**	**40.0**	**40.0**	**40.0**	**40.0**	**40.0**	**40.0**	**40.0**
cu1/cu2	**0.1**	**0.1**	**0.1**	**0.1**	**0.1**	**0.1**	**0.1**	**0.1**	**0.1**	**0.1**	**0.1**
H/B	**0.03**	**0.03**	**0.03**	**0.03**	**0.03**	**0.00**	**0.03**	**0.03**	**0.03**	**0.03**	**0.03**
N*1	**22.88**	**22.88**	**22.88**	**22.88**	**22.88**	**176.56**	**22.88**	**22.88**	**22.30**	**22.02**	**21.73**
N*2	**1.14**	**1.14**	**1.14**	**1.14**	**1.14**	**8.83**	**1.14**	**1.14**	**1.12**	**1.10**	**1.09**
Floor Bearing Capacity (MPa)	**22.9**	**22.9**	**22.9**	**22.9**	**22.9**	**176.6**	**22.9**	**22.9**	**22.3**	**22.0**	**21.7**
Eff Pillar Stress (MPa)	**15.0**	**14.8**	**14.3**	**13.7**	**13.4**	**6.0**	**15.3**	**15.0**	**15.0**	**14.9**	**14.6**
Eff Floor Bearing Failure FoS	**1.53**	**1.55**	**1.60**	**1.66**	**1.70**	**29.67**	**1.49**	**1.53**	**1.49**	**1.47**	**1.49**
FTA Floor Bearing Failure FoS	**4.02**	**4.06**	**4.17**	**4.29**	**4.37**	**35.68**	**3.95**	**4.02**	**3.96**	**3.94**	**4.00**
Immediate Roof Unit UCS, 2*cu1 (MPa)	**2.0**	**2.0**	**2.0**	**2.0**	**2.0**	**2.0**	**2.0**	**2.0**	**2.0**	**2.0**	**2.0**
Immediate Roof Unit Thickness, H (m)	**3.0**	**3.0**	**3.0**	**3.0**	**3.0**	**3.0**	**3.0**	**3.0**	**3.0**	**3.0**	**3.0**
Upper Roof Unit UCS, 2*cu2 (MPa)	**40.0**	**40.0**	**40.0**	**40.0**	**40.0**	**40.0**	**40.0**	**40.0**	**40.0**	**40.0**	**40.0**
cu1/cu2	**0.1**	**0.1**	**0.1**	**0.1**	**0.1**	**0.1**	**0.1**	**0.1**	**0.1**	**0.1**	**0.1**
H/B	**0.09**	**0.09**	**0.09**	**0.09**	**0.09**	**0.01**	**0.09**	**0.09**	**0.09**	**0.10**	**0.10**
N*1	**9.57**	**9.57**	**9.57**	**9.57**	**9.57**	**54.14**	**9.57**	**9.57**	**9.41**	**9.32**	**9.24**
N*2	0.48	0.48	0.48	0.48	0.48	2.71	0.48	0.48	0.47	0.47	0.46
Roof Bearing Capacity (MPa)	9.6	9.6	9.6	9.6	9.6	54.1	9.6	9.6	9.4	9.3	9.2
Pillar Stress (MPa)	**15.0**	**14.8**	**14.3**	**13.7**	**13.4**	**6.0**	**15.3**	**15.0**	**15.0**	**14.9**	**14.6**
Effective Roof Bearing Failure FoS	**0.64**	**0.65**	**0.67**	**0.70**	**0.71**	**9.10**	**0.63**	**0.64**	**0.63**	**0.62**	**0.63**
FTA Roof Bearing Failure FoS	**1.68**	**1.70**	**1.75**	**1.80**	**1.83**	**10.94**	**1.65**	**1.68**	**1.67**	**1.67**	**1.70**
Voussoir Beam Deflection (m)	**0.011**	**0.021**	**0.010**	**0.038**	**0.887**	**0.913**	**0.691**	**1.072**	**0.957**	**0.957**	**0.957**
System Settlement at Base of beam (m)	0.000	0.000	0.000	0.000	0.000	0.000	0.000	0.000	0.000	0.000	0.000
Applied Pillar Stress/FTA Stress Ratio (Mpa)	1.00	1.00	1.00	1.00	1.00	1.00	1.00	1.00	1.00	1.00	1.00
Effective Pillar Stress (Mpa)	15.00	14.79	14.27	13.74	13.43	5.95	15.32	15.00	15.00	14.94	14.56
Multi-Seam Stress Inc (min)											
Multi-Seam Stress Inc (max)											
Effective Pillar FoS	**1.90**	**1.93**	**2.00**	**2.08**	**2.13**	**281.11**	**1.86**	**1.90**	**1.83**	**1.80**	**1.81**
Eresidual coal(GPa)	**0.25**	**0.25**	**0.25**	**0.25**	**0.25**	**0.37**	**0.25**	**0.25**	**0.24**	**0.24**	**0.24**

UNSW Pillar Design Spreadsheet	29.9	29.3	29.3	32.6	31.6	31.1	30.6	29.9	29.3	29.3	29.3
	5.6	**5.7**	**5.8**	**6.1**	**6.2**	**6.3**	**6.4**	**6.5**	**6.6**	**6.7**	**6.8**
Chain Valley XL.Panel#											
INPUT DATA	95.3	95.3	94.8	95.3	95.3	95.3	95.3	95.3	95.3	95.3	95.3
Depth of Cover (m)	**170**	**165**	**160**	**185**	**178**	**175**	**173**	**168**	**163**	**160**	**158**
Mining Height (m)	**3.5**	**3.5**	**3.5**	**3.5**	**3.5**	**3.5**	**3.5**	**3.5**	**3.5**	**3.5**	**3.5**
Pillar Length - centres (m)	100.7	100.7	100.2	100.7	100.7	100.7	100.7	100.7	100.7	100.7	100.7
Pillar Width - centres (m)	35.3	34.7	34.7	38.0	37.0	36.5	36.0	35.3	34.7	34.7	34.7
Roadway Width for maximum pillar dimension	5.4	5.4	5.4	5.4	5.4	5.4	5.4	5.4	5.4	5.4	5.4
Roadway Width for minimum pillar dimension	5.4	5.4	5.4	5.4	5.4	5.4	5.4	5.4	5.4	5.4	5.4
Cut-Through Angle (degrees)	**90**	**90**	**90**	**90**	**90**	**90**	**90**	**90**	**90**	**90**	**90**
Average Panel Span (m) {rib-rib width}	97	97	97	97	97	97	97	97	97	97	97
SG (tonnes/m^3)	2.5	2.5	2.5	2.5	2.5	2.5	2.5	2.5	2.5	2.5	2.5
Conversion (tonnes to N)	10000	10000	10000	10000	10000	10000	10000	10000	10000	10000	10000
Abutment Angle (^{0})	21	21	21	21	21	21	21	21	21	21	21
W/H	0.57	0.59	0.61	0.52	0.54	0.55	0.56	0.58	0.60	0.61	0.61
PRELIMINARY CALCULATIONS											
Maximum Rib to Rib Pillar Length (w_2)	**95.3**	**95.3**	**94.8**	**95.3**	**95.3**	**95.3**	**95.3**	**95.3**	**95.3**	**95.3**	**95.3**
Minimum Rib to Rib Pillar Width (w_1)	**29.90**	**29.30**	**29.30**	**32.60**	**31.60**	**31.10**	**30.60**	**29.90**	**29.30**	**29.30**	**29.30**
w, Minimum Rib to Rib Pillar Width (ie $w_1 \sin\theta$)	**29.90**	**29.30**	**29.30**	**32.60**	**31.60**	**31.10**	**30.60**	**29.90**	**29.30**	**29.30**	**29.30**
Minimum Pillar Width/Height Ratio	**8.5**	**8.4**	**8.4**	**9.3**	**9.0**	**8.9**	**8.7**	**8.5**	**8.4**	**8.4**	**8.4**
Extraction Ratio (%)	**19.8%**	**20.1%**	**20.1%**	**18.8%**	**19.2%**	**19.4%**	**19.6%**	**19.8%**	**20.1%**	**20.1%**	**20.1%**
Abutment Angle (Radians)	0.367	0.367	0.367	0.367	0.367	0.367	0.367	0.367	0.367	0.367	0.367
Cut-Through Angle (Radians)	1.571	1.571	1.571	1.571	1.571	1.571	1.571	1.571	1.571	1.571	1.571
Is the Panel Super-Critical?	No	No	No	No	No	No	No	No	No	No	No
D (Peng & Chiang Loading Factor)	66.887	65.896	64.890	69.776	68.443	67.864	67.475	66.492	65.495	64.890	64.483
R (Pillar 2nd Abutment Component)	0.89	0.89	0.90	0.91	0.90	0.90	0.90	0.90	0.90	0.90	0.90
Dimensionless Pillar 'Rectangularity'	1.52	1.53	1.53	1.49	1.50	1.51	1.51	1.52	1.53	1.53	1.53
Width/Height Ratio Exponent	1.00	1.00	1.00	1.00	1.00	1.00	1.00	1.00	1.00	1.00	1.00
Effective Width Factor (Omega)	1.52	1.53	1.53	1.49	1.50	1.51	1.51	1.52	1.53	1.53	1.53
Effective Width Interim	45.52	44.82	44.76	48.58	47.46	46.90	46.33	45.52	44.82	44.82	44.82
Effective Pillar Width (m)	45.52	44.82	44.76	48.58	47.46	46.90	46.33	45.52	44.82	44.82	44.82
Effective Pillar Loading Height (m)	170.00	165.00	160.00	185.00	178.00	175.00	173.00	168.00	163.00	160.00	158.00
RESULTS											
Tributary Area Loading (MPa)	**5.30**	**5.16**	**5.01**	**5.70**	**5.51**	**5.43**	**5.38**	**5.24**	**5.10**	**5.01**	**4.94**
Pillar Strength (UNSW Squat Pillar 1999)	**25.66**	**25.06**	**25.04**	**28.56**	**27.45**	**26.91**	**26.38**	**25.66**	**25.06**	**25.06**	**25.06**
Pillar Strength (UNSW w/h<5)	**N/A**	**N/A**	**N/A**	**N/A**	**N/A**	**N/A**	**N/A**	**N/A**	**N/A**	**N/A**	**N/A**
Safety Factor under FTA Loading (Squat Pillar)	**4.84**	**4.85**	**5.00**	**5.01**	**4.99**	**4.96**	**4.91**	**4.90**	**4.91**	**5.01**	**5.07**
Safety Factor under FTA Loading (w/h<5)	**N/A**	**N/A**	**N/A**	**N/A**	**N/A**	**N/A**	**N/A**	**N/A**	**N/A**	**N/A**	**N/A**
Single Abutment Loading (3D) - full	4.46	4.35	4.14	4.65	4.53	4.49	4.48	4.38	4.27	4.14	4.06
Single Abutment Loading (3D) - pillar	**3.99**	**3.89**	**3.73**	**4.21**	**4.09**	**4.04**	**4.03**	**3.93**	**3.82**	**3.73**	**3.66**
Single Abutment Loading (3D) - solid	0.47	0.46	0.42	0.44	0.44	0.44	0.45	0.45	0.44	0.42	0.40
Design Abutment Load Multiplier	1.00	1.00	1.00	1.00	1.00	1.00	1.00	1.00	1.00	1.00	1.00
Total Pillar Loading with Single Abutment Loading	10.30	10.05	9.73	10.91	10.60	10.47	10.40	10.17	9.92	9.73	9.60
Safety Factor (under Single Abutment Loading)	**2.49**	**2.49**	**2.57**	**2.62**	**2.59**	**2.57**	**2.54**	**2.52**	**2.53**	**2.57**	**2.61**
Total Pillar Loading @ nA	**9.77**	**9.51**	**9.15**	**10.35**	**10.04**	**9.91**	**9.86**	**9.62**	**9.37**	**9.15**	**9.00**
Safety Factor @ nA	**2.63**	**2.63**	**2.74**	**2.76**	**2.73**	**2.71**	**2.68**	**2.67**	**2.68**	**2.74**	**2.78**
Total Pillar Loading under Double Abutment Loading	14.23	13.86	13.30	15.00	14.57	14.40	14.34	14.01	13.63	13.29	13.06
Safety Factor (under Double Abutment Loading)	**1.80**	**1.81**	**1.88**	**1.90**	**1.88**	**1.87**	**1.84**	**1.83**	**1.84**	**1.89**	**1.92**
Elastic Model Subsidence											
Ecoal(GPa)	**0.75**	**0.75**	**0.75**	**0.75**	**0.75**	**0.75**	**0.75**	**0.75**	**0.75**	**0.75**	**0.75**
E1floor(GPa)	**0.30**	**0.30**	**0.30**	**0.30**	**0.30**	**0.30**	**0.30**	**0.30**	**0.30**	**0.30**	**0.30**
E2floor(GPa)	**1.50**	**1.50**	**1.50**	**1.50**	**1.50**	**1.50**	**1.50**	**1.50**	**1.50**	**1.50**	**1.50**
E1roof(GPa)	**1.00**	**1.00**	**1.00**	**1.00**	**1.00**	**1.00**	**1.00**	**1.00**	**1.00**	**1.00**	**1.00**
E2roof(GPa)	**1.20**	**1.20**	**1.20**	**1.20**	**1.20**	**1.20**	**1.20**	**1.20**	**1.20**	**1.20**	**1.20**
Poissons Ratio floor/roof	**0.25**	**0.25**	**0.25**	**0.25**	**0.25**	**0.25**	**0.25**	**0.25**	**0.25**	**0.25**	**0.25**
initial vertical stress (MPa)	**4.25**	**4.13**	**4.00**	**4.63**	**4.45**	**4.38**	**4.33**	**4.20**	**4.08**	**4.00**	**3.95**
increase in vertical stress for DA (MPa)	**9.98**	**9.74**	**9.30**	**10.38**	**10.12**	**10.02**	**10.01**	**9.81**	**9.56**	**9.29**	**9.11**
Roof t1	**0.30**	**0.30**	**0.30**	**0.30**	**0.30**	**0.30**	**0.30**	**0.30**	**0.30**	**0.30**	**0.30**
Roof t2	**29.60**	**29.00**	**29.00**	**32.30**	**31.30**	**30.80**	**30.30**	**29.60**	**29.00**	**29.00**	**29.00**
Roof sig1	**9.98**	**9.74**	**9.30**	**10.38**	**10.12**	**10.02**	**10.01**	**9.81**	**9.56**	**9.29**	**9.11**
Roof sig2	**9.07**	**8.84**	**8.44**	**9.43**	**9.19**	**9.11**	**9.10**	**8.91**	**8.68**	**8.44**	**8.28**
Floor t1	**0.90**	**0.90**	**0.90**	**0.90**	**0.90**	**0.90**	**0.90**	**0.90**	**0.90**	**0.90**	**0.90**
Floor t2	**29.0**	**28.4**	**28.4**	**31.7**	**30.7**	**30.2**	**29.7**	**29.0**	**28.4**	**28.4**	**28.4**
Floor sig1	**9.98**	**9.74**	**9.30**	**10.38**	**10.12**	**10.02**	**10.01**	**9.81**	**9.56**	**9.29**	**9.11**
Floor sig2	**9.98**	**9.74**	**9.30**	**10.37**	**10.12**	**10.02**	**10.01**	**9.81**	**9.56**	**9.29**	**9.11**
Pillar Compression (m)	**0.044**	**0.043**	**0.041**	**0.045**	**0.044**	**0.044**	**0.044**	**0.043**	**0.042**	**0.041**	**0.040**
Roof Compression (m)	**0.212**	**0.203**	**0.194**	**0.241**	**0.228**	**0.222**	**0.218**	**0.209**	**0.199**	**0.194**	**0.190**
Floor Compression (m)	**0.209**	**0.200**	**0.191**	**0.235**	**0.223**	**0.217**	**0.214**	**0.205**	**0.197**	**0.191**	**0.187**
Total FTA Compression (m)	**0.465**	**0.446**	**0.426**	**0.521**	**0.494**	**0.483**	**0.476**	**0.457**	**0.438**	**0.426**	**0.417**
Total Effective Compression (m)	**0.465**	**0.446**	**0.426**	**0.521**	**0.494**	**0.483**	**0.476**	**0.457**	**0.438**	**0.426**	**0.417**
1.5 times Effective Compression (m)	**0.698**	**0.669**	**0.639**	**0.781**	**0.742**	**0.725**	**0.714**	**0.686**	**0.657**	**0.638**	**0.626**
Total Yielded Panel Subs (m)	**1.60**	**1.57**	**1.54**	**1.68**	**1.64**	**1.62**	**1.61**	**1.59**	**1.56**	**1.54**	**1.53**
Measured											
Bearing Capacity											
Upper Floor Unit UCS, 2*cu1 (MPa)	**2.0**	**2.0**	**2.0**	**2.0**	**2.0**	**2.0**	**2.0**	**2.0**	**2.0**	**2.0**	**2.0**
Upper Unit Thickness, H (m)	**0.9**	**0.9**	**0.9**	**0.9**	**0.9**	**0.9**	**0.9**	**0.9**	**0.9**	**0.9**	**0.9**
Lower Floor Unit UCS, 2*cu2 (MPa)	**40.0**	**40.0**	**40.0**	**40.0**	**40.0**	**40.0**	**40.0**	**40.0**	**40.0**	**40.0**	**40.0**
cu1/cu2	**0.1**	**0.1**	**0.1**	**0.1**	**0.1**	**0.1**	**0.1**	**0.1**	**0.1**	**0.1**	**0.1**
H/B	**0.03**	**0.03**	**0.03**	**0.03**	**0.03**	**0.03**	**0.03**	**0.03**	**0.03**	**0.03**	**0.03**
N*1	**21.33**	**20.98**	**20.98**	**22.88**	**22.30**	**22.02**	**21.73**	**21.33**	**20.98**	**20.98**	**20.98**
N*2	**1.07**	**1.05**	**1.05**	**1.14**	**1.12**	**1.10**	**1.09**	**1.07**	**1.05**	**1.05**	**1.05**
Floor Bearing Capacity (MPa)	**21.3**	**21.0**	**21.0**	**22.9**	**22.3**	**22.0**	**21.7**	**21.3**	**21.0**	**21.0**	**21.0**
Eff Pillar Stress (MPa)	**14.2**	**13.9**	**13.3**	**15.0**	**14.6**	**14.4**	**14.3**	**14.0**	**13.6**	**13.3**	**13.1**
Eff Floor Bearing Failure FoS	**1.50**	**1.51**	**1.58**	**1.53**	**1.53**	**1.53**	**1.52**	**1.52**	**1.54**	**1.58**	**1.61**
FTA Floor Bearing Failure FoS	**4.02**	**4.06**	**4.19**	**4.02**	**4.05**	**4.06**	**4.04**	**4.07**	**4.11**	**4.19**	**4.24**
Immediate Roof Unit UCS, 2*cu1 (MPa)	**2.0**	**2.0**	**2.0**	**2.0**	**2.0**	**2.0**	**2.0**	**2.0**	**2.0**	**2.0**	**2.0**
Immediate Roof Unit Thickness, H (m)	**3.0**	**3.0**	**3.0**	**3.0**	**3.0**	**3.0**	**3.0**	**3.0**	**3.0**	**3.0**	**3.0**
Upper Roof Unit UCS, 2*cu2 (MPa)	**40.0**	**40.0**	**40.0**	**40.0**	**40.0**	**40.0**	**40.0**	**40.0**	**40.0**	**40.0**	**40.0**
cu1/cu2	**0.1**	**0.1**	**0.1**	**0.1**	**0.1**	**0.1**	**0.1**	**0.1**	**0.1**	**0.1**	**0.1**
H/B	**0.10**	**0.10**	**0.10**	**0.09**	**0.09**	**0.10**	**0.10**	**0.10**	**0.10**	**0.10**	**0.10**
N*1	**9.12**	**9.02**	**9.02**	**9.57**	**9.41**	**9.32**	**9.24**	**9.12**	**9.02**	**9.02**	**9.02**
N*2	0.46	0.45	0.45	0.48	0.47	0.47	0.46	0.46	0.45	0.45	0.45
Roof Bearing Capacity (MPa)	9.1	9.0	9.0	9.6	9.4	9.3	9.2	9.1	9.0	9.0	9.0
Pillar Stress (MPa)	**14.2**	**13.9**	**13.3**	**15.0**	**14.6**	**14.4**	**14.3**	**14.0**	**13.6**	**13.3**	**13.1**
Effective Roof Bearing Failure FoS	**0.64**	**0.65**	**0.68**	**0.64**	**0.65**	**0.65**	**0.64**	**0.65**	**0.66**	**0.68**	**0.69**
FTA Roof Bearing Failure FoS	**1.72**	**1.75**	**1.80**	**1.68**	**1.71**	**1.72**	**1.72**	**1.74**	**1.77**	**1.80**	**1.83**
Voussoir Beam Deflection (m)	**0.957**	**0.957**	**0.957**	**0.957**	**0.957**	**0.957**	**0.957**	**0.957**	**0.957**	**0.957**	**0.957**
System Settlement at Base of beam (m)	0.000	0.000	0.000	0.000	0.000	0.000	0.000	0.000	0.000	0.000	0.000
Applied Pillar Stress/FTA Stress Ratio (Mpa)	1.00	1.00	1.00	1.00	1.00	1.00	1.00	1.00	1.00	1.00	1.00
Effective Pillar Stress (Mpa)	14.23	13.86	13.30	15.00	14.57	14.40	14.34	14.01	13.63	13.29	13.06
Multi-Seam Stress Inc (min)											
Multi-Seam Stress Inc (max)											
Effective Pillar FoS	**1.80**	**1.81**	**1.88**	**1.90**	**1.88**	**1.87**	**1.84**	**1.83**	**1.84**	**1.89**	**1.92**
Eresidual coal(GPa)	**0.23**	**0.23**	**0.23**	**0.25**	**0.24**	**0.24**	**0.24**	**0.23**	**0.23**	**0.23**	**0.23**

UNSW Pillar Design Spreadsheet	29.3	29.3	29.3	300.0	31.0	31.0	300.0	31.0	31.0	31.0	31.0
	6.9	6.1	6.11	6.12	7.1	7.2	7.3	8.1	8.2	8.3	8.4
Chain Valley XL.Panel#											
INPUT DATA	95.3	94.8	94.8	94.8	95.3	95.3	95.3	95.3	95.3	95.3	95.3
Depth of Cover (m)	156	153	150	148	167	168	169	187	188	189	190
Mining Height (m)	3.5	3.5	3.5	3.5	3.5	3.5	3.5	3.5	3.5	3.5	3.5
Pillar Length - centres (m)	100.7	100.2	100.2	100.2	100.7	100.7	100.7	100.7	100.7	100.7	100.7
Pillar Width - centres (m)	34.7	34.7	34.7	305.4	36.4	36.4	305.4	36.4	36.4	36.4	36.4
Roadway Width for maximum pillar dimension	5.4	5.4	5.4	5.4	5.4	5.4	5.4	5.4	5.4	5.4	5.4
Roadway Width for minimum pillar dimension	5.4	5.4	5.4	5.4	5.4	5.4	5.4	5.4	5.4	5.4	5.4
Cut-Through Angle (degrees)	90	90	90	90	90	90	90	90	90	90	90
Average Panel Span (m) {rib-rib width}	97	97	97	97	97	97	97	97	97	97	97
SG (tonnes/m^3)	2.5	2.5	2.5	2.5	2.5	2.5	2.5	2.5	2.5	2.5	2.5
Conversion (tonnes to N)	10000	10000	10000	10000	10000	10000	10000	10000	10000	10000	10000
Abutment Angle (^{0})	21	21	21	21	21	21	21	21	21	21	21
W/H	0.62	0.63	0.65	0.66	0.58	0.58	0.57	0.52	0.52	0.51	0.51
PRELIMINARY CALCULATIONS											
Maximum Rib to Rib Pillar Length (w_2)	**95.3**	**94.8**	**94.8**	**94.8**	**95.3**	**95.3**	**95.3**	**95.3**	**95.3**	**95.3**	**95.3**
Minimum Rib to Rib Pillar Width (w_1)	**29.30**	**29.30**	**29.30**	**300.00**	**31.00**	**31.00**	**300.00**	**31.00**	**31.00**	**31.00**	**31.00**
w, Minimum Rib to Rib Pillar Width (ie $w_1 \sin\theta$)	**29.30**	**29.30**	**29.30**	**300.00**	**31.00**	**31.00**	**300.00**	**31.00**	**31.00**	**31.00**	**31.00**
Minimum Pillar Width/Height Ratio	**8.4**	**8.4**	**8.4**	**27.1**	**8.9**	**8.9**	**27.2**	**8.9**	**8.9**	**8.9**	**8.9**
Extraction Ratio (%)	**20.1%**	**20.1%**	**20.1%**	**7.1%**	**19.4%**	**19.4%**	**7.0%**	**19.4%**	**19.4%**	**19.4%**	**19.4%**
Abutment Angle (Radians)	0.367	0.367	0.367	0.367	0.367	0.367	0.367	0.367	0.367	0.367	0.367
Cut-Through Angle (Radians)	1.571	1.571	1.571	1.571	1.571	1.571	1.571	1.571	1.571	1.571	1.571
Is the Panel Super-Critical?	No	No	No	No	No	No	No	No	No	No	No
D (Peng & Chiang Loading Factor)	64.074	63.455	62.829	62.409	66.294	66.492	66.690	70.152	70.339	70.526	70.712
R (Pillar 2nd Abutment Component)	0.90	0.91	0.91	1.00	0.91	0.91	1.00	0.89	0.89	0.89	0.89
Dimensionless Pillar 'Rectangularity'	1.53	1.53	1.53	0.48	1.51	1.51	0.48	1.51	1.51	1.51	1.51
Width/Height Ratio Exponent	1.00	1.00	1.00	1.00	1.00	1.00	1.00	1.00	1.00	1.00	1.00
Effective Width Factor (Omega)	1.53	1.53	1.53	0.48	1.51	1.51	0.48	1.51	1.51	1.51	1.51
Effective Width Interim	44.82	44.76	44.76	144.07	46.78	46.78	144.65	46.78	46.78	46.78	46.78
Effective Pillar Width (m)	44.82	44.76	44.76	144.07	46.78	46.78	144.65	46.78	46.78	46.78	46.78
Effective Pillar Loading Height (m)	156.00	153.00	150.00	148.00	167.00	168.00	169.00	187.00	188.00	189.00	190.00
RESULTS											
Tributary Area Loading (MPa)	**4.88**	**4.79**	**4.69**	**3.98**	**5.18**	**5.21**	**4.54**	**5.80**	**5.83**	**5.86**	**5.89**
Pillar Strength (UNSW Squat Pillar 1999)	**25.06**	**25.04**	**25.04**	**1669.52**	**26.80**	**26.80**	**1672.92**	**26.80**	**26.80**	**26.80**	**26.80**
Pillar Strength (UNSW w/h<5)	**N/A**	**N/A**	**N/A**	**N/A**	**N/A**	**N/A**	**N/A**	**N/A**	**N/A**	**N/A**	**N/A**
Safety Factor under FTA Loading (Squat Pillar)	**5.13**	**5.23**	**5.33**	**419.36**	**5.17**	**5.14**	**368.10**	**4.62**	**4.60**	**4.57**	**4.55**
Safety Factor under FTA Loading (w/h<5)	**N/A**	**N/A**	**N/A**	**N/A**	**N/A**	**N/A**	**N/A**	**N/A**	**N/A**	**N/A**	**N/A**
Single Abutment Loading (3D) - full	3.98	3.86	3.73	0.36	4.19	4.23	0.44	4.97	5.01	5.05	5.09
Single Abutment Loading (3D) - pillar	**3.59**	**3.50**	**3.40**	**0.36**	**3.81**	**3.84**	**0.44**	**4.42**	**4.45**	**4.48**	**4.51**
Single Abutment Loading (3D) - solid	0.38	0.36	0.33	0.00	0.38	0.39	0.00	0.55	0.56	0.57	0.58
Design Abutment Load Multiplier	1.00	1.00	1.00	1.00	1.00	1.00	1.00	1.00	1.00	1.00	1.00
Total Pillar Loading with Single Abutment Loading	9.48	9.28	9.09	5.34	9.99	10.05	5.99	11.22	11.28	11.34	11.40
Safety Factor (under Single Abutment Loading)	**2.64**	**2.70**	**2.75**	**312.79**	**2.68**	**2.67**	**279.48**	**2.39**	**2.38**	**2.36**	**2.35**
Total Pillar Loading @ nA	**8.86**	**8.64**	**8.43**	**4.34**	**9.37**	**9.44**	**4.99**	**10.77**	**10.84**	**10.91**	**10.98**
Safety Factor @ nA	**2.83**	**2.90**	**2.97**	**384.90**	**2.86**	**2.84**	**335.54**	**2.49**	**2.47**	**2.46**	**2.44**
Total Pillar Loading under Double Abutment Loading	12.84	12.50	12.16	4.69	13.56	13.67	5.43	15.74	15.85	15.96	16.07
Safety Factor (under Double Abutment Loading)	**1.95**	**2.00**	**2.06**	**355.68**	**1.98**	**1.96**	**308.28**	**1.70**	**1.69**	**1.68**	**1.67**
Elastic Model Subsidence											
Ecoal(GPa)	**0.75**	**0.75**	**0.75**	**0.75**	**0.75**	**0.75**	**0.75**	**0.75**	**0.75**	**0.75**	**0.75**
E1floor(GPa)	**0.30**	**0.30**	**0.30**	**0.30**	**0.30**	**0.30**	**0.30**	**0.30**	**0.30**	**0.30**	**0.30**
E2floor(GPa)	**1.50**	**1.50**	**1.50**	**1.50**	**1.50**	**1.50**	**1.50**	**1.50**	**1.50**	**1.50**	**1.50**
E1roof(GPa)	**1.00**	**1.00**	**1.00**	**1.00**	**1.00**	**1.00**	**1.00**	**1.00**	**1.00**	**1.00**	**1.00**
E2roof(GPa)	**1.20**	**1.20**	**1.20**	**1.20**	**1.20**	**1.20**	**1.20**	**1.20**	**1.20**	**1.20**	**1.20**
Poissons Ratio floor/roof	**0.25**	**0.25**	**0.25**	**0.25**	**0.25**	**0.25**	**0.25**	**0.25**	**0.25**	**0.25**	**0.25**
initial vertical stress (MPa)	**3.90**	**3.83**	**3.75**	**3.70**	**4.18**	**4.20**	**4.23**	**4.68**	**4.70**	**4.73**	**4.75**
increase in vertical stress for DA (MPa)	**8.94**	**8.67**	**8.41**	**0.99**	**9.38**	**9.47**	**1.20**	**11.07**	**11.15**	**11.23**	**11.32**
Roof t1	**0.30**	**0.30**	**0.30**	**0.30**	**0.30**	**0.30**	**0.30**	**0.30**	**0.30**	**0.30**	**0.30**
Roof t2	**29.00**	**29.00**	**29.00**	**299.70**	**30.70**	**30.70**	**299.70**	**30.70**	**30.70**	**30.70**	**30.70**
Roof sig1	**8.94**	**8.67**	**8.41**	**0.99**	**9.38**	**9.47**	**1.20**	**11.07**	**11.15**	**11.23**	**11.32**
Roof sig2	**8.12**	**7.88**	**7.64**	**0.90**	**8.53**	**8.60**	**1.09**	**10.05**	**10.13**	**10.21**	**10.28**
Floor t1	**0.90**	**0.90**	**0.90**	**0.90**	**0.90**	**0.90**	**0.90**	**0.90**	**0.90**	**0.90**	**0.90**
Floor t2	**28.4**	**28.4**	**28.4**	**299.1**	**30.1**	**30.1**	**299.1**	**30.1**	**30.1**	**30.1**	**30.1**
Floor sig1	**8.94**	**8.67**	**8.41**	**0.99**	**9.38**	**9.47**	**1.20**	**11.07**	**11.15**	**11.23**	**11.32**
Floor sig2	**8.94**	**8.67**	**8.41**	**0.99**	**9.38**	**9.47**	**1.20**	**11.06**	**11.15**	**11.23**	**11.32**
Pillar Compression (m)	**0.039**	**0.038**	**0.037**	**0.004**	**0.041**	**0.041**	**0.005**	**0.048**	**0.049**	**0.049**	**0.050**
Roof Compression (m)	**0.186**	**0.181**	**0.175**	**0.212**	**0.207**	**0.209**	**0.256**	**0.244**	**0.246**	**0.248**	**0.250**
Floor Compression (m)	**0.184**	**0.178**	**0.173**	**0.189**	**0.203**	**0.205**	**0.228**	**0.239**	**0.241**	**0.243**	**0.245**
Total FTA Compression (m)	**0.409**	**0.397**	**0.385**	**0.405**	**0.451**	**0.455**	**0.490**	**0.532**	**0.536**	**0.540**	**0.544**
Total Effective Compression (m)	**0.409**	**0.397**	**0.385**	**0.405**	**0.451**	**0.455**	**0.490**	**0.532**	**0.536**	**0.540**	**0.544**
1.5 times Effective Compression (m)	**0.614**	**0.596**	**0.578**	**0.608**	**0.677**	**0.683**	**0.735**	**0.798**	**0.804**	**0.810**	**0.816**
Total Yielded Panel Subs (m)	**1.51**	**1.50**	**1.48**	**1.51**	**1.58**	**1.58**	**1.63**	**1.70**	**1.70**	**1.71**	**1.72**
Measured											
Bearing Capacity											
Upper Floor Unit UCS, 2*cu1 (MPa)	**2.0**	**2.0**	**2.0**	**2.0**	**2.0**	**2.0**	**2.0**	**2.0**	**2.0**	**2.0**	**2.0**
Upper Unit Thickness, H (m)	**0.9**	**0.9**	**0.9**	**0.9**	**0.9**	**0.9**	**0.9**	**0.9**	**0.9**	**0.9**	**0.9**
Lower Floor Unit UCS, 2*cu2 (MPa)	**40.0**	**40.0**	**40.0**	**40.0**	**40.0**	**40.0**	**40.0**	**40.0**	**40.0**	**40.0**	**40.0**
cu1/cu2	**0.1**	**0.1**	**0.1**	**0.1**	**0.1**	**0.1**	**0.1**	**0.1**	**0.1**	**0.1**	**0.1**
H/B	**0.03**	**0.03**	**0.03**	**0.00**	**0.03**	**0.03**	**0.00**	**0.03**	**0.03**	**0.03**	**0.03**
N*1	**20.98**	**20.98**	**20.98**	**176.56**	**21.96**	**21.96**	**176.56**	**21.96**	**21.96**	**21.96**	**21.96**
N*2	**1.05**	**1.05**	**1.05**	**8.83**	**1.10**	**1.10**	**8.83**	**1.10**	**1.10**	**1.10**	**1.10**
Floor Bearing Capacity (MPa)	**21.0**	**21.0**	**21.0**	**176.6**	**22.0**	**22.0**	**176.6**	**22.0**	**22.0**	**22.0**	**22.0**
Eff Pillar Stress (MPa)	**12.8**	**12.5**	**12.2**	**4.7**	**13.6**	**13.7**	**5.4**	**15.7**	**15.8**	**16.0**	**16.1**
Eff Floor Bearing Failure FoS	**1.63**	**1.68**	**1.73**	**37.61**	**1.62**	**1.61**	**32.53**	**1.39**	**1.39**	**1.38**	**1.37**
FTA Floor Bearing Failure FoS	**4.30**	**4.38**	**4.47**	**44.35**	**4.24**	**4.21**	**38.85**	**3.79**	**3.77**	**3.75**	**3.73**
Immediate Roof Unit UCS, 2*cu1 (MPa)	**2.0**	**2.0**	**2.0**	**2.0**	**2.0**	**2.0**	**2.0**	**2.0**	**2.0**	**2.0**	**2.0**
Immediate Roof Unit Thickness, H (m)	**3.0**	**3.0**	**3.0**	**3.0**	**3.0**	**3.0**	**3.0**	**3.0**	**3.0**	**3.0**	**3.0**
Upper Roof Unit UCS, 2*cu2 (MPa)	**40.0**	**40.0**	**40.0**	**40.0**	**40.0**	**40.0**	**40.0**	**40.0**	**40.0**	**40.0**	**40.0**
cu1/cu2	**0.1**	**0.1**	**0.1**	**0.1**	**0.1**	**0.1**	**0.1**	**0.1**	**0.1**	**0.1**	**0.1**
H/B	**0.10**	**0.10**	**0.10**	**0.01**	**0.10**	**0.10**	**0.01**	**0.10**	**0.10**	**0.10**	**0.10**
N*1	**9.02**	**9.02**	**9.02**	**54.14**	**9.31**	**9.31**	**54.14**	**9.31**	**9.31**	**9.31**	**9.31**
N*2	0.45	0.45	0.45	2.71	0.47	0.47	2.71	0.47	0.47	0.47	0.47
Roof Bearing Capacity (MPa)	9.0	9.0	9.0	54.1	9.3	9.3	54.1	9.3	9.3	9.3	9.3
Pillar Stress (MPa)	**12.8**	**12.5**	**12.2**	**4.7**	**13.6**	**13.7**	**5.4**	**15.7**	**15.8**	**16.0**	**16.1**
Effective Roof Bearing Failure FoS	**0.70**	**0.72**	**0.74**	**11.53**	**0.69**	**0.68**	**9.98**	**0.59**	**0.59**	**0.58**	**0.58**
FTA Roof Bearing Failure FoS	**1.85**	**1.88**	**1.92**	**13.60**	**1.80**	**1.79**	**11.91**	**1.60**	**1.60**	**1.59**	**1.58**
Voussoir Beam Deflection (m)	**0.957**	**0.957**	**0.957**	**0.957**	**0.957**	**0.957**	**0.957**	**0.957**	**0.957**	**0.957**	**0.957**
System Settlement at Base of beam (m)	0.000	0.000	0.000	0.000	0.000	0.000	0.000	0.000	0.000	0.000	0.000
Applied Pillar Stress/FTA Stress Ratio (Mpa)	1.00	1.00	1.00	1.00	1.00	1.00	1.00	1.00	1.00	1.00	1.00
Effective Pillar Stress (Mpa)	12.84	12.50	12.16	4.69	13.56	13.67	5.43	15.74	15.85	15.96	16.07
Multi-Seam Stress Inc (min)											
Multi-Seam Stress Inc (max)											
Effective Pillar FoS	**1.95**	**2.00**	**2.06**	**355.68**	**1.98**	**1.96**	**308.28**	**1.70**	**1.69**	**1.68**	**1.67**
Eresidual coal(GPa)	**0.23**	**0.23**	**0.23**	**0.37**	**0.24**	**0.24**	**0.37**	**0.24**	**0.24**	**0.24**	**0.24**

UNSW Pillar Design Spreadsheet	31.0	31.0	30.6	30.6	30.6	30.6	30.6	30.6	30.6	30.6	30.6
	8.5	8.6	9.1	9.2	9.3	9.4	9.5	10.1	10.2	10.3	10.4
Chain Valley XL.Panel#											
INPUT DATA	95.3	95.3	95.3	95.3	95.3	95.3	95.3	95.3	95.3	95.3	95.3
Depth of Cover (m)	190	190	219	218	221	220	217	229	230	231	232
Mining Height (m)	3.5	3.5	3.5	3.5	3.5	3.5	3.5	3.5	3.5	3.5	3.5
Pillar Length - centres (m)	100.7	100.7	100.7	100.7	100.7	100.7	100.7	100.7	100.7	100.7	100.7
Pillar Width - centres (m)	36.4	36.4	36.0	36.0	36.0	36.0	36.0	36.0	36.0	36.0	36.0
Roadway Width for maximum pillar dimension	5.4	5.4	5.4	5.4	5.4	5.4	5.4	5.4	5.4	5.4	5.4
Roadway Width for minimum pillar dimension	5.4	5.4	5.4	5.4	5.4	5.4	5.4	5.4	5.4	5.4	5.4
Cut-Through Angle (degrees)	90	90	90	90	90	90	90	90	90	90	90
Average Panel Span (m) {rib-rib width}	97	97	97	97	97	97	97	97	97	97	97
SG (tonnes/m^3)	2.5	2.5	2.5	2.5	2.5	2.5	2.5	2.5	2.5	2.5	2.5
Conversion (tonnes to N)	10000	10000	10000	10000	10000	10000	10000	10000	10000	10000	10000
Abutment Angle (^{0})	21	21	21	21	21	21	21	21	21	21	21
W/H	0.51	0.51	0.44	0.44	0.44	0.44	0.45	0.42	0.42	0.42	0.42
PRELIMINARY CALCULATIONS											
Maximum Rib to Rib Pillar Length (w_2)	95.3	95.3	95.3	95.3	95.3	95.3	95.3	95.3	95.3	95.3	95.3
Minimum Rib to Rib Pillar Width (w_1)	31.00	31.00	30.60	30.60	30.60	30.60	30.60	30.60	30.60	30.60	30.60
w, Minimum Rib to Rib Pillar Width (ie $w_1 \sin\theta$)	31.00	31.00	30.60	30.60	30.60	30.60	30.60	30.60	30.60	30.60	30.60
Minimum Pillar Width/Height Ratio	8.9	8.9	8.7	8.7	8.7	8.7	8.7	8.7	8.7	8.7	8.7
Extraction Ratio (%)	19.4%	19.4%	19.6%	19.6%	19.6%	19.6%	19.6%	19.6%	19.6%	19.6%	19.6%
Abutment Angle (Radians)	0.367	0.367	0.367	0.367	0.367	0.367	0.367	0.367	0.367	0.367	0.367
Cut-Through Angle (Radians)	1.571	1.571	1.571	1.571	1.571	1.571	1.571	1.571	1.571	1.571	1.571
Is the Panel Super-Critical?	No	No	No	No	No	No	No	No	No	No	No
D (Peng & Chiang Loading Factor)	70.712	70.712	75.917	75.744	76.263	76.090	75.570	77.631	77.800	77.969	78.138
R (Pillar 2nd Abutment Component)	0.89	0.89	0.85	0.86	0.85	0.85	0.86	0.85	0.84	0.84	0.84
Dimensionless Pillar 'Rectangularity'	1.51	1.51	1.51	1.51	1.51	1.51	1.51	1.51	1.51	1.51	1.51
Width/Height Ratio Exponent	1.00	1.00	1.00	1.00	1.00	1.00	1.00	1.00	1.00	1.00	1.00
Effective Width Factor (Omega)	1.51	1.51	1.51	1.51	1.51	1.51	1.51	1.51	1.51	1.51	1.51
Effective Width Interim	46.78	46.78	46.33	46.33	46.33	46.33	46.33	46.33	46.33	46.33	46.33
Effective Pillar Width (m)	46.78	46.78	46.33	46.33	46.33	46.33	46.33	46.33	46.33	46.33	46.33
Effective Pillar Loading Height (m)	190.00	190.00	219.00	218.00	221.00	220.00	217.00	229.00	230.00	231.00	232.00
RESULTS											
Tributary Area Loading (MPa)	5.89	5.89	6.81	6.78	6.87	6.84	6.74	7.12	7.15	7.18	7.21
Pillar Strength (UNSW Squat Pillar 1999)	26.80	26.80	26.38	26.38	26.38	26.38	26.38	26.38	26.38	26.38	26.38
Pillar Strength (UNSW w/h<5)	N/A	N/A	N/A	N/A	N/A	N/A	N/A	N/A	N/A	N/A	N/A
Safety Factor under FTA Loading (Squat Pillar)	4.55	4.55	3.88	3.89	3.84	3.86	3.91	3.71	3.69	3.67	3.66
Safety Factor under FTA Loading (w/h<5)	N/A	N/A	N/A	N/A	N/A	N/A	N/A	N/A	N/A	N/A	N/A
Single Abutment Loading (3D) - full	5.09	5.09	6.30	6.26	6.38	6.34	6.22	6.70	6.74	6.77	6.81
Single Abutment Loading (3D) - pillar	4.51	4.51	5.38	5.36	5.44	5.41	5.33	5.66	5.69	5.72	5.75
Single Abutment Loading (3D) - solid	0.58	0.58	0.92	0.90	0.94	0.93	0.89	1.03	1.04	1.06	1.07
Design Abutment Load Multiplier	1.00	1.00	1.00	1.00	1.00	1.00	1.00	1.00	1.00	1.00	1.00
Total Pillar Loading with Single Abutment Loading	11.40	11.40	13.19	13.13	13.31	13.25	13.07	13.78	13.84	13.90	13.96
Safety Factor (under Single Abutment Loading)	2.35	2.35	2.00	2.01	1.98	1.99	2.02	1.91	1.91	1.90	1.89
Total Pillar Loading @ nA	10.98	10.98	13.11	13.04	13.25	13.18	12.97	13.81	13.88	13.95	14.02
Safety Factor @ nA	2.44	2.44	2.01	2.02	1.99	2.00	2.03	1.91	1.90	1.89	1.88
Total Pillar Loading under Double Abutment Loading	16.07	16.07	19.41	19.30	19.63	19.52	19.19	20.51	20.62	20.73	20.84
Safety Factor (under Double Abutment Loading)	1.67	1.67	1.36	1.37	1.34	1.35	1.37	1.29	1.28	1.27	1.27
Elastic Model Subsidence											
Ecoal(GPa)	0.75	0.75	0.75	0.75	0.75	0.75	0.75	0.75	0.75	0.75	0.75
E1floor(GPa)	0.30	0.30	0.30	0.30	0.30	0.30	0.30	0.30	0.30	0.30	0.30
E2floor(GPa)	1.50	1.50	1.50	1.50	1.50	1.50	1.50	1.50	1.50	1.50	1.50
E1roof(GPa)	1.00	1.00	1.00	1.00	1.00	1.00	1.00	1.00	1.00	1.00	1.00
E2roof(GPa)	1.20	1.20	1.20	1.20	1.20	1.20	1.20	1.20	1.20	1.20	1.20
Poissons Ratio floor/roof	0.25	0.25	0.25	0.25	0.25	0.25	0.25	0.25	0.25	0.25	0.25
initial vertical stress (MPa)	4.75	4.75	5.48	5.45	5.53	5.50	5.43	5.73	5.75	5.78	5.80
increase in vertical stress for DA (MPa)	11.32	11.32	13.93	13.85	14.10	14.02	13.76	14.78	14.87	14.95	15.04
Roof t1	0.30	0.30	0.30	0.30	0.30	0.30	0.30	0.30	0.30	0.30	0.30
Roof t2	30.70	30.70	30.30	30.30	30.30	30.30	30.30	30.30	30.30	30.30	30.30
Roof sig1	11.32	11.32	13.93	13.85	14.10	14.02	13.76	14.78	14.87	14.95	15.04
Roof sig2	10.28	10.28	12.66	12.58	12.81	12.73	12.50	13.43	13.51	13.58	13.66
Floor t1	0.90	0.90	0.90	0.90	0.90	0.90	0.90	0.90	0.90	0.90	0.90
Floor t2	30.1	30.1	29.7	29.7	29.7	29.7	29.7	29.7	29.7	29.7	29.7
Floor sig1	11.32	11.32	13.93	13.85	14.10	14.02	13.76	14.78	14.87	14.95	15.04
Floor sig2	11.32	11.32	13.93	13.85	14.10	14.02	13.76	14.78	14.87	14.95	15.04
Pillar Compression (m)	0.050	0.050	0.061	0.061	0.062	0.061	0.060	0.065	0.065	0.065	0.066
Roof Compression (m)	0.250	0.250	0.304	0.302	0.307	0.305	0.300	0.322	0.324	0.326	0.328
Floor Compression (m)	0.245	0.245	0.298	0.296	0.301	0.300	0.294	0.316	0.318	0.320	0.321
Total FTA Compression (m)	0.544	0.544	0.662	0.658	0.670	0.666	0.654	0.703	0.707	0.711	0.715
Total Effective Compression (m)	0.544	0.544	0.662	0.658	0.670	0.666	0.654	0.703	0.707	0.711	0.715
1.5 times Effective Compression (m)	0.816	0.816	0.993	0.987	1.005	0.999	0.981	1.054	1.060	1.066	1.072
Total Yielded Panel Subs (m)	1.72	1.72	1.89	1.89	1.91	1.90	1.88	1.95	1.96	1.97	1.97
Measured											
Bearing Capacity											
Upper Floor Unit UCS, 2*cu1 (MPa)	2.0	2.0	2.0	2.0	2.0	2.0	2.0	2.0	2.0	2.0	2.0
Upper Unit Thickness, H (m)	0.9	0.9	0.9	0.9	0.9	0.9	0.9	0.9	0.9	0.9	0.9
Lower Floor Unit UCS, 2*cu2 (MPa)	40.0	40.0	40.0	40.0	40.0	40.0	40.0	40.0	40.0	40.0	40.0
cu1/cu2	0.1	0.1	0.1	0.1	0.1	0.1	0.1	0.1	0.1	0.1	0.1
H/B	0.03	0.03	0.03	0.03	0.03	0.03	0.03	0.03	0.03	0.03	0.03
N*1	21.96	21.96	21.73	21.73	21.73	21.73	21.73	21.73	21.73	21.73	21.73
N*2	1.10	1.10	1.09	1.09	1.09	1.09	1.09	1.09	1.09	1.09	1.09
Floor Bearing Capacity (MPa)	22.0	22.0	21.7	21.7	21.7	21.7	21.7	21.7	21.7	21.7	21.7
Eff Pillar Stress (MPa)	16.1	16.1	19.4	19.3	19.6	19.5	19.2	20.5	20.6	20.7	20.8
Eff Floor Bearing Failure FoS	1.37	1.37	1.12	1.13	1.11	1.11	1.13	1.06	1.05	1.05	1.04
FTA Floor Bearing Failure FoS	3.73	3.73	3.19	3.21	3.16	3.18	3.22	3.05	3.04	3.03	3.01
Immediate Roof Unit UCS, 2*cu1 (MPa)	2.0	2.0	2.0	2.0	2.0	2.0	2.0	2.0	2.0	2.0	2.0
Immediate Roof Unit Thickness, H (m)	3.0	3.0	3.0	3.0	3.0	3.0	3.0	3.0	3.0	3.0	3.0
Upper Roof Unit UCS, 2*cu2 (MPa)	40.0	40.0	40.0	40.0	40.0	40.0	40.0	40.0	40.0	40.0	40.0
cu1/cu2	0.1	0.1	0.1	0.1	0.1	0.1	0.1	0.1	0.1	0.1	0.1
H/B	0.10	0.10	0.10	0.10	0.10	0.10	0.10	0.10	0.10	0.10	0.10
N*1	9.31	9.31	9.24	9.24	9.24	9.24	9.24	9.24	9.24	9.24	9.24
N*2	0.47	0.47	0.46	0.46	0.46	0.46	0.46	0.46	0.46	0.46	0.46
Roof Bearing Capacity (MPa)	9.3	9.3	9.2	9.2	9.2	9.2	9.2	9.2	9.2	9.2	9.2
Pillar Stress (MPa)	16.1	16.1	19.4	19.3	19.6	19.5	19.2	20.5	20.6	20.7	20.8
Effective Roof Bearing Failure FoS	0.58	0.58	0.48	0.48	0.47	0.47	0.48	0.45	0.45	0.45	0.44
FTA Roof Bearing Failure FoS	1.58	1.58	1.36	1.36	1.35	1.35	1.37	1.30	1.29	1.29	1.28
Voussoir Beam Deflection (m)	0.957	0.957	0.957	0.957	0.957	0.957	0.957	0.957	0.957	0.957	0.957
System Settlement at Base of beam (m)	0.000	0.000	0.000	0.000	0.000	0.000	0.000	0.000	0.000	0.000	0.000
Applied Pillar Stress/FTA Stress Ratio (Mpa)	1.00	1.00	1.00	1.00	1.00	1.00	1.00	1.00	1.00	1.00	1.00
Effective Pillar Stress (Mpa)	16.07	16.07	19.41	19.30	19.63	19.52	19.19	20.51	20.62	20.73	20.84
Multi-Seam Stress Inc (min)											
Multi-Seam Stress Inc (max)											
Effective Pillar FoS	1.67	1.67	1.36	1.37	1.34	1.35	1.37	1.29	1.28	1.27	1.27
Eresidual coal(GPa)	0.24	0.24	0.24	0.24	0.24	0.24	0.24	0.24	0.24	0.24	0.24

UNSW Pillar Design Spreadsheet	300.0										
	10.5	9.1	9.2	9.3	9.4	9.5	10.1	10.2	10.3	10.4	10.5
Chain Valley XL.Panel#											
INPUT DATA	95.3	95.3	95.3	95.3	95.3	95.3	95.3	95.3	95.3	95.3	95.3
Depth of Cover (m)	228	219	218	221	220	217	229	230	231	232	228
Mining Height (m)	3.5	3.5	3.5	3.5	3.5	3.5	3.5	3.5	3.5	3.5	3.5
Pillar Length - centres (m)	100.7	100.7	100.7	100.7	100.7	100.7	100.7	100.7	100.7	100.7	100.7
Pillar Width - centres (m)	36.0	36.0	36.0	36.0	36.0	36.0	36.0	36.0	36.0	36.0	36.0
Roadway Width for maximum pillar dimension	5.4	5.4	5.4	5.4	5.4	5.4	5.4	5.4	5.4	5.4	5.4
Roadway Width for minimum pillar dimension	5.4	5.4	5.4	5.4	5.4	5.4	5.4	5.4	5.4	5.4	5.4
Cut-Through Angle (degrees)	90	90	90	90	90	90	90	90	90	90	90
Average Panel Span (m) {rib-rib width}	97	97	97	97	97	97	97	97	97	97	97
SG (tonnes/m^3)	2.5	2.5	2.5	2.5	2.5	2.5	2.5	2.5	2.5	2.5	2.5
Conversion (tonnes to N)	10000	10000	10000	10000	10000	10000	10000	10000	10000	10000	10000
Abutment Angle (^{0})	21	21	21	21	21	21	21	21	21	21	21
W/H	0.43	0.44	0.44	0.44	0.44	0.45	0.42	0.42	0.42	0.42	0.43
PRELIMINARY CALCULATIONS											
Maximum Rib to Rib Pillar Length (w_2)	95.3	95.3	95.3	95.3	95.3	95.3	95.3	95.3	95.3	95.3	95.3
Minimum Rib to Rib Pillar Width (w_1)	30.60	30.60	30.60	30.60	30.60	30.60	30.60	30.60	30.60	30.60	30.60
w, Minimum Rib to Rib Pillar Width (ie $w_1 \sin\theta$)	30.60	30.60	30.60	30.60	30.60	30.60	30.60	30.60	30.60	30.60	30.60
Minimum Pillar Width/Height Ratio	8.7	8.7	8.7	8.7	8.7	8.7	8.7	8.7	8.7	8.7	8.7
Extraction Ratio (%)	19.6%	19.6%	19.6%	19.6%	19.6%	19.6%	19.6%	19.6%	19.6%	19.6%	19.6%
Abutment Angle (Radians)	0.367	0.367	0.367	0.367	0.367	0.367	0.367	0.367	0.367	0.367	0.367
Cut-Through Angle (Radians)	1.571	1.571	1.571	1.571	1.571	1.571	1.571	1.571	1.571	1.571	1.571
Is the Panel Super-Critical?	No	No	No	No	No	No	No	No	No	No	No
D (Peng & Chiang Loading Factor)	77.461	75.917	75.744	76.263	76.090	75.570	77.631	77.800	77.969	78.138	77.461
R (Pillar 2nd Abutment Component)	0.85	0.85	0.86	0.85	0.85	0.86	0.85	0.84	0.84	0.84	0.85
Dimensionless Pillar 'Rectangularity'	1.51	1.51	1.51	1.51	1.51	1.51	1.51	1.51	1.51	1.51	1.51
Width/Height Ratio Exponent	1.00	1.00	1.00	1.00	1.00	1.00	1.00	1.00	1.00	1.00	1.00
Effective Width Factor (Omega)	1.51	1.51	1.51	1.51	1.51	1.51	1.51	1.51	1.51	1.51	1.51
Effective Width Interim	46.33	46.33	46.33	46.33	46.33	46.33	46.33	46.33	46.33	46.33	46.33
Effective Pillar Width (m)	46.33	46.33	46.33	46.33	46.33	46.33	46.33	46.33	46.33	46.33	46.33
Effective Pillar Loading Height (m)	228.00	219.00	218.00	221.00	220.00	217.00	229.00	230.00	231.00	232.00	228.00
RESULTS											
Tributary Area Loading (MPa)	7.09	6.81	6.78	6.87	6.84	6.74	7.12	7.15	7.18	7.21	7.09
Pillar Strength (UNSW Squat Pillar 1999)	26.38	26.38	26.38	26.38	26.38	26.38	26.38	26.38	26.38	26.38	26.38
Pillar Strength (UNSW w/h<5)	N/A	N/A	N/A	N/A	N/A	N/A	N/A	N/A	N/A	N/A	N/A
Safety Factor under FTA Loading (Squat Pillar)	3.72	3.88	3.89	3.84	3.86	3.91	3.71	3.69	3.67	3.66	3.72
Safety Factor under FTA Loading (w/h<5)	N/A	N/A	N/A	N/A	N/A	N/A	N/A	N/A	N/A	N/A	N/A
Single Abutment Loading (3D) - full	6.66	6.30	6.26	6.38	6.34	6.22	6.70	6.74	6.77	6.81	6.66
Single Abutment Loading (3D) - pillar	5.64	5.38	5.36	5.44	5.41	5.33	5.66	5.69	5.72	5.75	5.64
Single Abutment Loading (3D) - solid	1.02	0.92	0.90	0.94	0.93	0.89	1.03	1.04	1.06	1.07	1.02
Design Abutment Load Multiplier	1.00	1.00	1.00	1.00	1.00	1.00	1.00	1.00	1.00	1.00	1.00
Total Pillar Loading with Single Abutment Loading	13.72	13.19	13.13	13.31	13.25	13.07	13.78	13.84	13.90	13.96	13.72
Safety Factor (under Single Abutment Loading)	1.92	2.00	2.01	1.98	1.99	2.02	1.91	1.91	1.90	1.89	1.92
Total Pillar Loading @ nA	13.74	13.11	13.04	13.25	13.18	12.97	13.81	13.88	13.95	14.02	13.74
Safety Factor @ nA	1.92	2.01	2.02	1.99	2.00	2.03	1.91	1.90	1.89	1.88	1.92
Total Pillar Loading under Double Abutment Loading	20.40	19.41	19.30	19.63	19.52	19.19	20.51	20.62	20.73	20.84	20.40
Safety Factor (under Double Abutment Loading)	1.29	1.36	1.37	1.34	1.35	1.37	1.29	1.28	1.27	1.27	1.29
Elastic Model Subsidence											
Ecoal(GPa)	0.75	0.75	0.75	0.75	0.75	0.75	0.75	0.75	0.75	0.75	0.75
E1floor(GPa)	0.30	0.30	0.30	0.30	0.30	0.30	0.30	0.30	0.30	0.30	0.30
E2floor(GPa)	1.50	1.50	1.50	1.50	1.50	1.50	1.50	1.50	1.50	1.50	1.50
E1roof(GPa)	1.00	1.00	1.00	1.00	1.00	1.00	1.00	1.00	1.00	1.00	1.00
E2roof(GPa)	1.20	1.20	1.20	1.20	1.20	1.20	1.20	1.20	1.20	1.20	1.20
Poissons Ratio floor/roof	0.25	0.25	0.25	0.25	0.25	0.25	0.25	0.25	0.25	0.25	0.25
initial vertical stress (MPa)	5.70	5.48	5.45	5.53	5.50	5.43	5.73	5.75	5.78	5.80	5.70
increase in vertical stress for DA (MPa)	14.70	13.93	13.85	14.10	14.02	13.76	14.78	14.87	14.95	15.04	14.70
Roof t1	0.30	0.30	0.30	0.30	0.30	0.30	0.30	0.30	0.30	0.30	0.30
Roof t2	30.30	30.30	30.30	30.30	30.30	30.30	30.30	30.30	30.30	30.30	30.30
Roof sig1	14.70	13.93	13.85	14.10	14.02	13.76	14.78	14.87	14.95	15.04	14.70
Roof sig2	13.35	12.66	12.58	12.81	12.73	12.50	13.43	13.51	13.58	13.66	13.35
Floor t1	0.90	0.90	0.90	0.90	0.90	0.90	0.90	0.90	0.90	0.90	0.90
Floor t2	29.7	29.7	29.7	29.7	29.7	29.7	29.7	29.7	29.7	29.7	29.7
Floor sig1	14.70	13.93	13.85	14.10	14.02	13.76	14.78	14.87	14.95	15.04	14.70
Floor sig2	14.70	13.93	13.85	14.10	14.02	13.76	14.78	14.87	14.95	15.04	14.70
Pillar Compression (m)	0.064	0.061	0.061	0.062	0.061	0.060	0.065	0.065	0.065	0.066	0.064
Roof Compression (m)	0.320	0.304	0.302	0.307	0.305	0.300	0.322	0.324	0.326	0.328	0.320
Floor Compression (m)	0.314	0.298	0.296	0.301	0.300	0.294	0.316	0.318	0.320	0.321	0.314
Total FTA Compression (m)	0.699	0.662	0.658	0.670	0.666	0.654	0.703	0.707	0.711	0.715	0.699
Total Effective Compression (m)	0.699	0.662	0.658	0.670	0.666	0.654	0.703	0.707	0.711	0.715	0.699
1.5 times Effective Compression (m)	1.048	0.993	0.987	1.005	0.999	0.981	1.054	1.060	1.066	1.072	1.048
Total Yielded Panel Subs (m)	1.95	1.89	1.89	1.91	1.90	1.88	1.95	1.96	1.97	1.97	1.95
Measured											
Bearing Capacity											
Upper Floor Unit UCS, 2*cu1 (MPa)	2.0	2.0	2.0	2.0	2.0	2.0	2.0	2.0	2.0	2.0	2.0
Upper Unit Thickness, H (m)	0.9	0.9	0.9	0.9	0.9	0.9	0.9	0.9	0.9	0.9	0.9
Lower Floor Unit UCS, 2*cu2 (MPa)	40.0	40.0	40.0	40.0	40.0	40.0	40.0	40.0	40.0	40.0	40.0
cu1/cu2	0.1	0.1	0.1	0.1	0.1	0.1	0.1	0.1	0.1	0.1	0.1
H/B	0.03	0.03	0.03	0.03	0.03	0.03	0.03	0.03	0.03	0.03	0.03
N*1	21.73	21.73	21.73	21.73	21.73	21.73	21.73	21.73	21.73	21.73	21.73
N*2	1.09	1.09	1.09	1.09	1.09	1.09	1.09	1.09	1.09	1.09	1.09
Floor Bearing Capacity (MPa)	21.7	21.7	21.7	21.7	21.7	21.7	21.7	21.7	21.7	21.7	21.7
Eff Pillar Stress (MPa)	20.4	19.4	19.3	19.6	19.5	19.2	20.5	20.6	20.7	20.8	20.4
Eff Floor Bearing Failure FoS	1.07	1.12	1.13	1.11	1.11	1.13	1.06	1.05	1.05	1.04	1.07
FTA Floor Bearing Failure FoS	3.07	3.19	3.21	3.16	3.18	3.22	3.05	3.04	3.03	3.01	3.07
Immediate Roof Unit UCS, 2*cu1 (MPa)	2.0	2.0	2.0	2.0	2.0	2.0	2.0	2.0	2.0	2.0	2.0
Immediate Roof Unit Thickness, H (m)	3.0	3.0	3.0	3.0	3.0	3.0	3.0	3.0	3.0	3.0	3.0
Upper Roof Unit UCS, 2*cu2 (MPa)	40.0	40.0	40.0	40.0	40.0	40.0	40.0	40.0	40.0	40.0	40.0
cu1/cu2	0.1	0.1	0.1	0.1	0.1	0.1	0.1	0.1	0.1	0.1	0.1
H/B	0.10	0.10	0.10	0.10	0.10	0.10	0.10	0.10	0.10	0.10	0.10
N*1	9.24	9.24	9.24	9.24	9.24	9.24	9.24	9.24	9.24	9.24	9.24
N*2	0.46	0.46	0.46	0.46	0.46	0.46	0.46	0.46	0.46	0.46	0.46
Roof Bearing Capacity (MPa)	9.2	9.2	9.2	9.2	9.2	9.2	9.2	9.2	9.2	9.2	9.2
Pillar Stress (MPa)	20.4	19.4	19.3	19.6	19.5	19.2	20.5	20.6	20.7	20.8	20.4
Effective Roof Bearing Failure FoS	0.45	0.48	0.48	0.47	0.47	0.48	0.45	0.45	0.45	0.44	0.45
FTA Roof Bearing Failure FoS	1.30	1.36	1.36	1.35	1.35	1.37	1.30	1.29	1.29	1.28	1.30
Voussoir Beam Deflection (m)	0.957	0.957	0.957	0.957	0.957	0.957	0.957	0.957	0.957	0.957	0.957
System Settlement at Base of beam (m)	0.000	0.000	0.000	0.000	0.000	0.000	0.000	0.000	0.000	0.000	0.000
Applied Pillar Stress/FTA Stress Ratio (Mpa)	1.00	1.00	1.00	1.00	1.00	1.00	1.00	1.00	1.00	1.00	1.00
Effective Pillar Stress (Mpa)	20.40	19.41	19.30	19.63	19.52	19.19	20.51	20.62	20.73	20.84	20.40
Multi-Seam Stress Inc (min)											
Multi-Seam Stress Inc (max)											
Effective Pillar FoS	1.29	1.36	1.37	1.34	1.35	1.37	1.29	1.28	1.27	1.27	1.29
Eresidual coal(GPa)	0.24	0.24	0.24	0.24	0.24	0.24	0.24	0.24	0.24	0.24	0.24

UNSW Pillar Design Spreadsheet											
Chain Valley XL.Panel#	1.1	1.2	1.3	1.4	1.5	1.6	1.7	2.1	2.2	2.3	3.1
INPUT DATA											
Depth of Cover (m)	**200**	**200**	**200**	**198**	**195**	**193**	**191**	**196**	**200**	**190**	**188**
Mining Height (m)	**3.2**	**3.2**	**3.2**	**3.2**	**3.2**	**3.2**	**3.2**	**3.2**	**3.2**	**3.2**	**3.2**
Pillar Length - centres (m)	100.7	100.7	100.7	100.7	100.7	100.7	100.7	100.7	100.7	100.7	100.7
Pillar Width - centres (m)	36.0	35.8	38.0	38.0	38.0	38.0	38.0	45.4	191.4	38.0	38.0
Roadway Width for maximum pillar dimension	5.4	5.4	5.4	5.4	5.4	5.4	5.4	5.4	5.4	5.4	5.4
Roadway Width for minimum pillar dimension	5.4	5.4	5.4	5.4	5.4	5.4	5.4	5.4	5.4	5.4	5.4
Cut-Through Angle (degrees)	**90**	**90**	**90**	**90**	**90**	**90**	**90**	**90**	**90**	**90**	**90**
Average Panel Span (m) {rib-rib width}	72	72	97	97	97	97	97	97	97	97	97
SG (tonnes/m^3)	2.5	2.5	2.5	2.5	2.5	2.5	2.5	2.5	2.5	2.5	2.5
Conversion (tonnes to N)	10000	10000	10000	10000	10000	10000	10000	10000	10000	10000	10000
Abutment Angle (^{0})	21	21	21	21	21	21	21	21	21	21	21
W/H	0.36	0.36	0.49	0.49	0.50	0.50	0.51	0.49	0.49	0.51	0.52
PRELIMINARY CALCULATIONS											
Maximum Rib to Rib Pillar Length (w_2)	**95.3**	**95.3**	**95.3**	**95.3**	**95.3**	**95.3**	**95.3**	**95.3**	**95.3**	**95.3**	**95.3**
Minimum Rib to Rib Pillar Width (w_1)	**30.6**	**30.4**	**32.6**	**32.6**	**32.6**	**32.6**	**32.6**	**40.0**	**186.0**	**32.6**	**32.6**
w, Minimum Rib to Rib Pillar Width (ie $w_1 \sin\theta$)	**30.6**	**30.4**	**32.6**	**32.6**	**32.6**	**32.6**	**32.6**	**40.0**	**186.0**	**32.6**	**32.6**
Minimum Pillar Width/Height Ratio	**9.6**	**9.5**	**10.2**	**10.2**	**10.2**	**10.2**	**10.2**	**12.5**	**29.8**	**10.2**	**10.2**
Extraction Ratio (%)	**19.6%**	**19.6%**	**18.8%**	**18.8%**	**18.8%**	**18.8%**	**18.8%**	**16.6%**	**8.0%**	**18.8%**	**18.8%**
Abutment Angle (Radians)	0.367	0.367	0.367	0.367	0.367	0.367	0.367	0.367	0.367	0.367	0.367
Cut-Through Angle (Radians)	1.571	1.571	1.571	1.571	1.571	1.571	1.571	1.571	1.571	1.571	1.571
Is the Panel Super-Critical?	No	No	No	No	No	No	No	No	No	No	No
D (Peng & Chiang Loading Factor)	72.549	72.549	72.549	72.185	71.637	71.268	70.898	71.820	72.549	70.712	70.339
R (Pillar 2nd Abutment Component)	0.87	0.87	0.89	0.89	0.90	0.90	0.90	0.95	1.00	0.90	0.90
Dimensionless Pillar 'Rectangularity'	1.51	1.52	1.49	1.49	1.49	1.49	1.49	1.41	0.68	1.49	1.49
Width/Height Ratio Exponent	1.00	1.00	1.00	1.00	1.00	1.00	1.00	1.00	1.00	1.00	1.00
Effective Width Factor (Omega)	1.51	1.52	1.49	1.49	1.49	1.49	1.49	1.41	0.68	1.49	1.49
Effective Width Interim	46.33	46.10	48.58	48.58	48.58	48.58	48.58	56.35	126.03	48.58	48.58
Effective Pillar Width (m)	46.33	46.10	48.58	48.58	48.58	48.58	48.58	56.35	126.03	48.58	48.58
Effective Pillar Loading Height (m)	200.00	200.00	200.00	198.00	195.00	193.00	191.00	196.00	200.00	190.00	188.00
RESULTS											
Tributary Area Loading (MPa)	**6.22**	**6.22**	**6.16**	**6.10**	**6.00**	**5.94**	**5.88**	**5.88**	**5.44**	**5.85**	**5.79**
Pillar Strength (UNSW Squat Pillar 1999)	**30.81**	**30.54**	**33.62**	**33.62**	**33.62**	**33.62**	**33.62**	**45.99**	**848.18**	**33.62**	**33.62**
Pillar Strength (UNSW w/h<5)	**N/A**	**N/A**	**N/A**	**N/A**	**N/A**	**N/A**	**N/A**	**N/A**	**N/A**	**N/A**	**N/A**
Safety Factor under FTA Loading (Squat Pillar)	**4.96**	**4.91**	**5.46**	**5.51**	**5.60**	**5.66**	**5.72**	**7.83**	**156.01**	**5.75**	**5.81**
Safety Factor under FTA Loading (w/h<5)	**N/A**	**N/A**	**N/A**	**N/A**	**N/A**	**N/A**	**N/A**	**N/A**	**N/A**	**N/A**	**N/A**
Single Abutment Loading (3D) - full	4.50	4.54	5.21	5.13	5.02	4.95	4.87	4.12	0.91	4.84	4.76
Single Abutment Loading (3D) - pillar	**3.93**	**3.95**	**4.65**	**4.59**	**4.50**	**4.45**	**4.39**	**3.92**	**0.91**	**4.36**	**4.30**
Single Abutment Loading (3D) - solid	0.58	0.59	0.56	0.55	0.52	0.50	0.49	0.21	0.00	0.48	0.46
Design Abutment Load Multiplier	1.00	1.00	1.00	1.50	1.50	1.00	1.00	1.00	1.00	1.00	1.00
Total Pillar Loading with Single Abutment Loading	11.14	11.17	11.80	12.19	12.01	11.39	11.27	10.80	7.35	11.21	11.09
Safety Factor (under Single Abutment Loading)	**2.76**	**2.73**	**2.85**	**2.76**	**2.80**	**2.95**	**2.98**	**4.26**	**115.41**	**3.00**	**3.03**
Total Pillar Loading @ nA	10.72	10.76	11.37	13.80	13.54	10.89	10.76	10.00	6.35	10.69	10.55
Safety Factor @ nA	**2.87**	**2.84**	**2.96**	**2.44**	**2.48**	**3.09**	**3.13**	**4.60**	**133.58**	**3.15**	**3.19**
Total Pillar Loading under Double Abutment Loading	15.22	15.31	16.58	16.37	16.05	15.84	15.63	14.12	7.26	15.53	15.32
Safety Factor (under Double Abutment Loading)	**2.02**	**2.00**	**2.03**	**2.05**	**2.09**	**2.12**	**2.15**	**3.26**	**116.79**	**2.17**	**2.20**
Elastic Model Subsidence											
Ecoal(GPa)	**0.75**	**0.75**	**0.75**	**0.75**	**0.75**	**0.75**	**0.75**	**0.75**	**0.75**	**0.75**	**0.75**
E1floor(GPa)	**0.30**	**0.30**	**0.30**	**0.30**	**0.30**	**0.30**	**0.30**	**0.30**	**0.30**	**0.30**	**0.30**
E2floor(GPa)	**1.50**	**1.50**	**1.50**	**1.50**	**1.50**	**1.50**	**1.50**	**1.50**	**1.50**	**1.50**	**1.50**
E1roof(GPa)	**1.00**	**1.00**	**1.00**	**1.00**	**1.00**	**1.00**	**1.00**	**1.00**	**1.00**	**1.00**	**1.00**
E2roof(GPa)	**1.20**	**1.20**	**1.20**	**1.20**	**1.20**	**1.20**	**1.20**	**1.20**	**1.20**	**1.20**	**1.20**
Poissons Ratio floor/roof	**0.25**	**0.25**	**0.25**	**0.25**	**0.25**	**0.25**	**0.25**	**0.25**	**0.25**	**0.25**	**0.25**
initial vertical stress (MPa)	**5.00**	**5.00**	**5.00**	**4.95**	**4.88**	**4.83**	**4.78**	**4.90**	**5.00**	**4.75**	**4.70**
increase in vertical stress for DA (MPa)	**10.22**	**10.31**	**11.58**	**11.42**	**11.18**	**11.02**	**10.86**	**9.22**	**2.26**	**10.78**	**10.62**
Roof t1	**10.00**	**2.00**	**2.00**	**2.00**	**2.00**	**2.00**	**2.00**	**2.00**	**2.00**	**2.00**	**2.00**
Roof t2	**20.60**	**28.40**	**30.60**	**30.60**	**30.60**	**30.60**	**30.60**	**38.00**	**184.00**	**30.60**	**30.60**
Roof sig1	**10.18**	**10.31**	**11.58**	**11.42**	**11.18**	**11.02**	**10.86**	**9.22**	**2.26**	**10.78**	**10.62**
Roof sig2	**8.49**	**9.23**	**10.38**	**10.24**	**10.02**	**9.88**	**9.74**	**8.30**	**2.05**	**9.67**	**9.52**
Floor t1	**6.00**	**6.00**	**6.00**	**6.00**	**6.00**	**6.00**	**6.00**	**6.00**	**6.00**	**6.00**	**6.00**
Floor t2	**24.6**	**24.4**	**26.6**	**26.6**	**26.6**	**26.6**	**26.6**	**34.0**	**180.0**	**26.6**	**26.6**
Floor sig1	**10.21**	**10.30**	**11.57**	**11.41**	**11.17**	**11.01**	**10.85**	**9.22**	**2.26**	**10.77**	**10.61**
Floor sig2	**9.99**	**10.07**	**11.36**	**11.20**	**10.96**	**10.81**	**10.65**	**9.13**	**2.26**	**10.57**	**10.42**
Pillar Compression (m)	**0.041**	**0.041**	**0.046**	**0.046**	**0.045**	**0.044**	**0.043**	**0.037**	**0.009**	**0.043**	**0.042**
Roof Compression (m)	**0.232**	**0.224**	**0.270**	**0.266**	**0.261**	**0.257**	**0.253**	**0.264**	**0.300**	**0.251**	**0.248**
Floor Compression (m)	**0.345**	**0.347**	**0.406**	**0.400**	**0.392**	**0.386**	**0.380**	**0.367**	**0.297**	**0.378**	**0.372**
Total Compression (m)	**0.618**	**0.612**	**0.722**	**0.712**	**0.697**	**0.687**	**0.677**	**0.667**	**0.606**	**0.672**	**0.662**
Total Effective Compression (m)	**0.618**	**0.612**	**0.722**	**0.712**	**0.697**	**0.687**	**0.677**	**0.667**	**0.606**	**0.672**	**0.662**
1.5 times Effective Compression (m)	**0.927**	**0.918**	**1.083**	**1.068**	**1.045**	**1.030**	**1.016**	**1.001**	**0.908**	**1.008**	**0.993**
Total Yielded Panel Subs (m)	**0.70**	**0.69**	**0.80**	**0.79**	**0.77**	**0.76**	**0.75**	**0.73**	**0.65**	**0.74**	**0.73**
5 x Effective Predictions (m)	**3.090**	**3.060**	**3.610**	**3.560**	**3.485**	**3.435**	**3.385**	**3.337**	**3.028**	**3.360**	**3.310**
Bearing Capacity											
Upper Floor Unit UCS, 2*cu1 (MPa)	**20.0**	**20.0**	**20.0**	**20.0**	**20.0**	**20.0**	**20.0**	**20.0**	**20.0**	**20.0**	**20.0**
Upper Unit Thickness, H (m)	**6.0**	**6.0**	**6.0**	**6.0**	**6.0**	**6.0**	**6.0**	**6.0**	**6.0**	**6.0**	**6.0**
Lower Floor Unit UCS, 2*cu2 (MPa)	**40.0**	**40.0**	**40.0**	**40.0**	**40.0**	**40.0**	**40.0**	**40.0**	**40.0**	**40.0**	**40.0**
cu1/cu2	**0.5**	**0.5**	**0.5**	**0.5**	**0.5**	**0.5**	**0.5**	**0.5**	**0.5**	**0.5**	**0.5**
H/B	**0.20**	**0.20**	**0.18**	**0.18**	**0.18**	**0.18**	**0.18**	**0.15**	**0.03**	**0.18**	**0.18**
N*1	**6.69**	**6.67**	**6.86**	**6.86**	**6.86**	**6.86**	**6.86**	**7.47**	**19.64**	**6.86**	**6.86**
N*2	**3.35**	**3.34**	**3.43**	**3.43**	**3.43**	**3.43**	**3.43**	**3.74**	**9.82**	**3.43**	**3.43**
Floor Bearing Capacity (MPa)	**66.9**	**66.7**	**68.6**	**68.6**	**68.6**	**68.6**	**68.6**	**74.7**	**196.4**	**68.6**	**68.6**
Eff Pillar Stress (MPa)	**15.2**	**15.3**	**16.6**	**16.4**	**16.1**	**15.8**	**15.6**	**14.1**	**7.3**	**15.5**	**15.3**
Eff Floor Bearing Failure FoS	**4.40**	**4.36**	**4.14**	**4.19**	**4.27**	**4.33**	**4.39**	**5.29**	**27.05**	**4.42**	**4.48**
FTA Floor Bearing Failure FoS	**10.77**	**10.73**	**11.14**	**11.25**	**11.42**	**11.54**	**11.66**	**12.72**	**36.13**	**11.72**	**11.85**
Immediate Roof Unit UCS, 2*cu1 (MPa)	**40.0**	**40.0**	**40.0**	**40.0**	**40.0**	**40.0**	**40.0**	**40.0**	**40.0**	**40.0**	**40.0**
Immediate Roof Unit Thickness, H (m)	**10.0**	**10.0**	**10.0**	**10.0**	**10.0**	**10.0**	**10.0**	**10.0**	**10.0**	**10.0**	**10.0**
Upper Roof Unit UCS, 2*cu2 (MPa)	**40.0**	**40.0**	**40.0**	**40.0**	**40.0**	**40.0**	**40.0**	**40.0**	**40.0**	**40.0**	**40.0**
cu1/cu2	**1.0**	**1.0**	**1.0**	**1.0**	**1.0**	**1.0**	**1.0**	**1.0**	**1.0**	**1.0**	**1.0**
H/B	**0.33**	**0.33**	**0.31**	**0.31**	**0.31**	**0.31**	**0.31**	**0.25**	**0.05**	**0.31**	**0.31**
N*1	**5.14**	**5.14**	**5.14**	**5.14**	**5.14**	**5.14**	**5.14**	**5.14**	**5.14**	**5.14**	**5.14**
N*2	5.14	5.14	5.14	5.14	5.14	5.14	5.14	5.14	5.14	5.14	5.14
Roof Bearing Capacity (MPa)	102.8	102.8	102.8	102.8	102.8	102.8	102.8	102.8	102.8	102.8	102.8
Pillar Stress (MPa)	**15.2**	**15.3**	**16.6**	**16.4**	**16.1**	**15.8**	**15.6**	**14.1**	**7.3**	**15.5**	**15.3**
Effective Roof Bearing Failure FoS	**6.75**	**6.72**	**6.20**	**6.28**	**6.40**	**6.49**	**6.58**	**7.28**	**14.15**	**6.62**	**6.71**
FTA Roof Bearing Failure FoS	**16.54**	**16.52**	**16.69**	**16.86**	**17.12**	**17.30**	**17.48**	**17.49**	**18.91**	**17.57**	**17.76**
Voussoir Beam Deflection (m)	**0.004**	**0.004**	**0.004**	**0.001**	**0.001**	**0.419**	**0.042**	**0.006**	**0.011**	**0.821**	**0.282**
System Settlement at Base of beam (m)	0.000	0.000	0.000	0.000	0.000	0.000	0.000	0.000	0.000	0.000	0.000
Applied Pillar Stress/FTA Stress Ratio (Mpa)	1.00	1.00	1.00	1.00	1.00	1.00	1.00	1.00	1.00	1.00	1.00
Effective Pillar Stress (Mpa)	15.22	15.31	16.58	16.37	16.05	15.84	15.63	14.12	7.26	15.53	15.32
Multi-Seam Stress Inc (min)											
Multi-Seam Stress Inc (max)											
Effective Pillar FoS	**2.02**	**2.00**	**2.03**	**2.05**	**2.09**	**2.12**	**2.15**	**3.26**	**116.79**	**2.17**	**2.20**
Eresidual coal(GPa)	**0.25**	**0.25**	**0.27**	**0.27**	**0.27**	**0.27**	**0.27**	**0.30**	**0.38**	**0.27**	**0.27**

UNSW Pillar Design Spreadsheet											
Chain Valley XL.Panel#	3.2	3.3	4.1	4.2	4.3	4.4	4.5	4.6	5.1	5.2	5.3
INPUT DATA											
Depth of Cover (m)	**185**	**183**	**178**	**173**	**170**	**184**	**188**	**185**	**182**	**180**	**175**
Mining Height (m)	**3.2**	**3.2**	**3.2**	**3.2**	**3.2**	**3.2**	**3.2**	**3.2**	**3.2**	**3.2**	**3.2**
Pillar Length - centres (m)	100.7	100.7	100.7	100.7	100.7	100.7	100.7	100.7	100.7	100.7	100.7
Pillar Width - centres (m)	38.0	38.0	38.0	38.0	38.0	305.4	38.0	38.0	37.0	36.5	36.0
Roadway Width for maximum pillar dimension	5.4	5.4	5.4	5.4	5.4	5.4	5.4	5.4	5.4	5.4	5.4
Roadway Width for minimum pillar dimension	5.4	5.4	5.4	5.4	5.4	5.4	5.4	5.4	5.4	5.4	5.4
Cut-Through Angle (degrees)	**90**	**90**	**90**	**90**	**90**	**90**	**90**	**90**	**90**	**90**	**90**
Average Panel Span (m) {rib-rib width}	**97**	**97**	**97**	**97**	**97**	**97**	**97**	**97**	**97**	**97**	**97**
SG (tonnes/m^3)	2.5	2.5	2.5	2.5	2.5	2.5	2.5	2.5	2.5	2.5	2.5
Conversion (tonnes to N)	10000	10000	10000	10000	10000	10000	10000	10000	10000	10000	10000
Abutment Angle (^{0})	21	21	21	21	21	21	21	21	21	21	21
W/H	0.52	0.53	0.54	0.56	0.57	0.53	0.52	0.52	0.53	0.54	0.55
PRELIMINARY CALCULATIONS											
Maximum Rib to Rib Pillar Length (w_2)	**95.3**	**95.3**	**95.3**	**95.3**	**95.3**	**95.3**	**95.3**	**95.3**	**95.3**	**95.3**	**95.3**
Minimum Rib to Rib Pillar Width (w_1)	**32.6**	**32.6**	**32.6**	**32.6**	**32.6**	**300.0**	**32.6**	**32.6**	**31.6**	**31.1**	**30.6**
w, Minimum Rib to Rib Pillar Width (ie $w_1 \sin\theta$)	**32.6**	**32.6**	**32.6**	**32.6**	**32.6**	**300.0**	**32.6**	**32.6**	**31.6**	**31.1**	**30.6**
Minimum Pillar Width/Height Ratio	**10.2**	**10.2**	**10.2**	**10.2**	**10.2**	**29.8**	**10.2**	**10.2**	**9.9**	**9.7**	**9.6**
Extraction Ratio (%)	**18.8%**	**18.8%**	**18.8%**	**18.8%**	**18.8%**	**7.0%**	**18.8%**	**18.8%**	**19.2%**	**19.4%**	**19.6%**
Abutment Angle (Radians)	0.367	0.367	0.367	0.367	0.367	0.367	0.367	0.367	0.367	0.367	0.367
Cut-Through Angle (Radians)	1.571	1.571	1.571	1.571	1.571	1.571	1.571	1.571	1.571	1.571	1.571
Is the Panel Super-Critical?	No	No	No	No	No	No	No	No	No	No	No
D (Peng & Chiang Loading Factor)	69.776	69.397	68.443	67.475	66.887	69.587	70.339	69.776	69.207	68.826	67.864
R (Pillar 2nd Abutment Component)	0.91	0.91	0.91	0.92	0.92	1.00	0.90	0.91	0.90	0.90	0.90
Dimensionless Pillar 'Rectangularity'	1.49	1.49	1.49	1.49	1.49	0.48	1.49	1.49	1.50	1.51	1.51
Width/Height Ratio Exponent	1.00	1.00	1.00	1.00	1.00	1.00	1.00	1.00	1.00	1.00	1.00
Effective Width Factor (Omega)	1.49	1.49	1.49	1.49	1.49	0.48	1.49	1.49	1.50	1.51	1.51
Effective Width Interim	48.58	48.58	48.58	48.58	48.58	144.65	48.58	48.58	47.46	46.90	46.33
Effective Pillar Width (m)	48.58	48.58	48.58	48.58	48.58	144.65	48.58	48.58	47.46	46.90	46.33
Effective Pillar Loading Height (m)	185.00	183.00	178.00	173.00	170.00	184.00	188.00	185.00	182.00	180.00	175.00
RESULTS											
Tributary Area Loading (MPa)	**5.70**	**5.63**	**5.48**	**5.33**	**5.23**	**4.95**	**5.79**	**5.70**	**5.63**	**5.58**	**5.44**
Pillar Strength (UNSW Squat Pillar 1999)	**33.62**	**33.62**	**33.62**	**33.62**	**33.62**	**2112.89**	**33.62**	**33.62**	**32.18**	**31.49**	**30.81**
Pillar Strength (UNSW w/h<5)	**N/A**	**N/A**	**N/A**	**N/A**	**N/A**	**N/A**	**N/A**	**N/A**	**N/A**	**N/A**	**N/A**
Safety Factor under FTA Loading (Squat Pillar)	**5.90**	**5.97**	**6.13**	**6.31**	**6.42**	**427.01**	**5.81**	**5.90**	**5.72**	**5.64**	**5.66**
Safety Factor under FTA Loading (w/h<5)	**N/A**	**N/A**	**N/A**	**N/A**	**N/A**	**N/A**	**N/A**	**N/A**	**N/A**	**N/A**	**N/A**
Single Abutment Loading (3D) - full	4.65	4.58	4.39	4.21	4.10	0.50	4.76	4.65	4.68	4.68	4.56
Single Abutment Loading (3D) - pillar	**4.21**	**4.15**	**4.01**	**3.86**	**3.77**	**0.50**	**4.30**	**4.21**	**4.21**	**4.20**	**4.09**
Single Abutment Loading (3D) - solid	0.44	0.42	0.39	0.35	0.33	0.00	0.46	0.44	0.47	0.49	0.47
Design Abutment Load Multiplier	1.00	1.00	1.00	1.00	1.00	1.00	1.00	1.00	1.00	1.00	1.00
Total Pillar Loading with Single Abutment Loading	10.91	10.79	10.49	10.18	10.00	6.45	11.09	10.91	10.84	10.78	10.53
Safety Factor (under Single Abutment Loading)	**3.08**	**3.12**	**3.21**	**3.30**	**3.36**	**327.60**	**3.03**	**3.08**	**2.97**	**2.92**	**2.93**
Total Pillar Loading @ nA	10.35	10.21	9.87	9.53	9.33	5.45	10.55	10.35	10.31	10.26	10.00
Safety Factor @ nA	**3.25**	**3.29**	**3.41**	**3.53**	**3.60**	**387.71**	**3.19**	**3.25**	**3.12**	**3.07**	**3.08**
Total Pillar Loading under Double Abutment Loading	15.00	14.79	14.27	13.74	13.43	5.95	15.32	15.00	15.00	14.94	14.56
Safety Factor (under Double Abutment Loading)	**2.24**	**2.27**	**2.36**	**2.45**	**2.50**	**355.04**	**2.20**	**2.24**	**2.15**	**2.11**	**2.12**
Elastic Model Subsidence											
Ecoal(GPa)	**0.75**	**0.75**	**0.75**	**0.75**	**0.75**	**0.75**	**0.75**	**0.75**	**0.75**	**0.75**	**0.75**
E1floor(GPa)	**0.30**	**0.30**	**0.30**	**0.30**	**0.30**	**0.30**	**0.30**	**0.30**	**0.30**	**0.30**	**0.30**
E2floor(GPa)	**1.50**	**1.50**	**1.50**	**1.50**	**1.50**	**1.50**	**1.50**	**1.50**	**1.50**	**1.50**	**1.50**
E1roof(GPa)	**1.00**	**1.00**	**1.00**	**1.00**	**1.00**	**1.00**	**1.00**	**1.00**	**1.00**	**1.00**	**1.00**
E2roof(GPa)	**1.20**	**1.20**	**1.20**	**1.20**	**1.20**	**1.20**	**1.20**	**1.20**	**1.20**	**1.20**	**1.20**
Poissons Ratio floor/roof	**0.25**	**0.25**	**0.25**	**0.25**	**0.25**	**0.25**	**0.25**	**0.25**	**0.25**	**0.25**	**0.25**
initial vertical stress (MPa)	**4.63**	**4.58**	**4.45**	**4.33**	**4.25**	**4.60**	**4.70**	**4.63**	**4.55**	**4.50**	**4.38**
increase in vertical stress for DA (MPa)	**10.38**	**10.22**	**9.82**	**9.42**	**9.18**	**1.35**	**10.62**	**10.38**	**10.45**	**10.44**	**10.18**
Roof t1	**2.00**	**2.00**	**2.00**	**2.00**	**2.00**	**2.00**	**2.00**	**2.00**	**2.00**	**2.00**	**2.00**
Roof t2	**30.60**	**30.60**	**30.60**	**30.60**	**30.60**	**298.00**	**30.60**	**30.60**	**29.60**	**29.10**	**28.60**
Roof sig1	**10.37**	**10.21**	**9.81**	**9.41**	**9.17**	**1.35**	**10.62**	**10.37**	**10.45**	**10.44**	**10.18**
Roof sig2	**9.31**	**9.16**	**8.80**	**8.45**	**8.23**	**1.23**	**9.52**	**9.31**	**9.37**	**9.36**	**9.13**
Floor t1	**6.00**	**6.00**	**6.00**	**6.00**	**6.00**	**6.00**	**6.00**	**6.00**	**6.00**	**6.00**	**6.00**
Floor t2	**26.6**	**26.6**	**26.6**	**26.6**	**26.6**	**294.0**	**26.6**	**26.6**	**25.6**	**25.1**	**24.6**
Floor sig1	**10.37**	**10.21**	**9.81**	**9.41**	**9.17**	**1.35**	**10.61**	**10.37**	**10.44**	**10.43**	**10.18**
Floor sig2	**10.18**	**10.02**	**9.63**	**9.24**	**9.00**	**1.35**	**10.42**	**10.18**	**10.23**	**10.22**	**9.96**
Pillar Compression (m)	**0.042**	**0.041**	**0.039**	**0.038**	**0.037**	**0.005**	**0.042**	**0.042**	**0.042**	**0.042**	**0.041**
Roof Compression (m)	**0.242**	**0.238**	**0.229**	**0.220**	**0.214**	**0.288**	**0.248**	**0.242**	**0.236**	**0.232**	**0.223**
Floor Compression (m)	**0.364**	**0.358**	**0.344**	**0.330**	**0.322**	**0.274**	**0.372**	**0.364**	**0.359**	**0.356**	**0.344**
Total Compression (m)	**0.647**	**0.637**	**0.612**	**0.587**	**0.572**	**0.567**	**0.662**	**0.647**	**0.637**	**0.630**	**0.608**
Total Effective Compression (m)	**0.647**	**0.637**	**0.612**	**0.587**	**0.572**	**0.567**	**0.662**	**0.647**	**0.637**	**0.630**	**0.608**
1.5 times Effective Compression (m)	**0.971**	**0.956**	**0.918**	**0.881**	**0.858**	**0.851**	**0.993**	**0.971**	**0.956**	**0.945**	**0.911**
Total Yielded Panel Subs (m)	**0.72**	**0.71**	**0.68**	**0.65**	**0.64**	**0.61**	**0.73**	**0.72**	**0.71**	**0.70**	**0.68**
5 x Effective Predictions (m)	**3.235**	**3.185**	**3.061**	**2.936**	**2.861**	**2.837**	**3.310**	**3.235**	**3.187**	**3.151**	**3.038**
Bearing Capacity											
Upper Floor Unit UCS, 2*cu1 (MPa)	**20.0**	**20.0**	**20.0**	**20.0**	**20.0**	**20.0**	**20.0**	**20.0**	**20.0**	**20.0**	**20.0**
Upper Unit Thickness, H (m)	**6.0**	**6.0**	**6.0**	**6.0**	**6.0**	**6.0**	**6.0**	**6.0**	**6.0**	**6.0**	**6.0**
Lower Floor Unit UCS, 2*cu2 (MPa)	**40.0**	**40.0**	**40.0**	**40.0**	**40.0**	**40.0**	**40.0**	**40.0**	**40.0**	**40.0**	**40.0**
cu1/cu2	**0.5**	**0.5**	**0.5**	**0.5**	**0.5**	**0.5**	**0.5**	**0.5**	**0.5**	**0.5**	**0.5**
H/B	**0.18**	**0.18**	**0.18**	**0.18**	**0.18**	**0.02**	**0.18**	**0.18**	**0.19**	**0.19**	**0.20**
N*1	**6.86**	**6.86**	**6.86**	**6.86**	**6.86**	**29.14**	**6.86**	**6.86**	**6.77**	**6.73**	**6.69**
N*2	**3.43**	**3.43**	**3.43**	**3.43**	**3.43**	**14.57**	**3.43**	**3.43**	**3.39**	**3.37**	**3.35**
Floor Bearing Capacity (MPa)	**68.6**	**68.6**	**68.6**	**68.6**	**68.6**	**291.4**	**68.6**	**68.6**	**67.7**	**67.3**	**66.9**
Eff Pillar Stress (MPa)	**15.0**	**14.8**	**14.3**	**13.7**	**13.4**	**6.0**	**15.3**	**15.0**	**15.0**	**14.9**	**14.6**
Eff Floor Bearing Failure FoS	**4.57**	**4.64**	**4.81**	**4.99**	**5.11**	**48.97**	**4.48**	**4.57**	**4.52**	**4.51**	**4.60**
FTA Floor Bearing Failure FoS	**12.04**	**12.17**	**12.51**	**12.87**	**13.10**	**58.89**	**11.85**	**12.04**	**12.03**	**12.07**	**12.30**
Immediate Roof Unit UCS, 2*cu1 (MPa)	**40.0**	**40.0**	**40.0**	**40.0**	**40.0**	**40.0**	**40.0**	**40.0**	**40.0**	**40.0**	**40.0**
Immediate Roof Unit Thickness, H (m)	**10.0**	**10.0**	**10.0**	**10.0**	**10.0**	**10.0**	**10.0**	**10.0**	**10.0**	**10.0**	**10.0**
Upper Roof Unit UCS, 2*cu2 (MPa)	**40.0**	**40.0**	**40.0**	**40.0**	**40.0**	**40.0**	**40.0**	**40.0**	**40.0**	**40.0**	**40.0**
cu1/cu2	**1.0**	**1.0**	**1.0**	**1.0**	**1.0**	**1.0**	**1.0**	**1.0**	**1.0**	**1.0**	**1.0**
H/B	**0.31**	**0.31**	**0.31**	**0.31**	**0.31**	**0.03**	**0.31**	**0.31**	**0.32**	**0.32**	**0.33**
N*1	**5.14**	**5.14**	**5.14**	**5.14**	**5.14**	**5.14**	**5.14**	**5.14**	**5.14**	**5.14**	**5.14**
N*2	5.14	5.14	5.14	5.14	5.14	5.14	5.14	5.14	5.14	5.14	5.14
Roof Bearing Capacity (MPa)	102.8	102.8	102.8	102.8	102.8	102.8	102.8	102.8	102.8	102.8	102.8
Pillar Stress (MPa)	**15.0**	**14.8**	**14.3**	**13.7**	**13.4**	**6.0**	**15.3**	**15.0**	**15.0**	**14.9**	**14.6**
Effective Roof Bearing Failure FoS	**6.85**	**6.95**	**7.21**	**7.48**	**7.66**	**17.27**	**6.71**	**6.85**	**6.85**	**6.88**	**7.06**
FTA Roof Bearing Failure FoS	**18.05**	**18.24**	**18.76**	**19.30**	**19.64**	**20.78**	**17.76**	**18.05**	**18.26**	**18.42**	**18.90**
Voussoir Beam Deflection (m)	**0.005**	**0.044**	**0.065**	**0.011**	**0.021**	**0.010**	**0.038**	**0.887**	**0.887**	**0.913**	**0.765**
System Settlement at Base of beam (m)	0.000	0.000	0.000	0.000	0.000	0.000	0.000	0.000	0.000	0.000	0.000
Applied Pillar Stress/FTA Stress Ratio (Mpa)	1.00	1.00	1.00	1.00	1.00	1.00	1.00	1.00	1.00	1.00	1.00
Effective Pillar Stress (Mpa)	15.00	14.79	14.27	13.74	13.43	5.95	15.32	15.00	15.00	14.94	14.56
Multi-Seam Stress Inc (min)											
Multi-Seam Stress Inc (max)											
Effective Pillar FoS	**2.24**	**2.27**	**2.36**	**2.45**	**2.50**	**355.04**	**2.20**	**2.24**	**2.15**	**2.11**	**2.12**
Eresidual coal(GPa)	**0.27**	**0.27**	**0.27**	**0.27**	**0.27**	**0.38**	**0.27**	**0.27**	**0.26**	**0.26**	**0.25**

UNSW Pillar Design Spreadsheet											
Chain Valley XL.Panel#	6.1	6.2	6.3	6.4	6.5	6.6	6.7	6.8	6.9	6.10	6.11
INPUT DATA											
Depth of Cover (m)	**170**	**165**	**160**	**185**	**178**	**175**	**173**	**168**	**163**	**160**	**158**
Mining Height (m)	**3.2**	**3.2**	**3.2**	**3.2**	**3.2**	**3.2**	**3.2**	**3.2**	**3.2**	**3.2**	**3.2**
Pillar Length - centres (m)	100.7	100.7	100.2	100.7	100.7	100.7	100.7	100.7	100.7	100.7	100.7
Pillar Width - centres (m)	35.3	34.7	34.7	38.0	37.0	36.5	36.0	35.3	34.7	34.7	34.7
Roadway Width for maximum pillar dimension	5.4	5.4	5.4	5.4	5.4	5.4	5.4	5.4	5.4	5.4	5.4
Roadway Width for minimum pillar dimension	5.4	5.4	5.4	5.4	5.4	5.4	5.4	5.4	5.4	5.4	5.4
Cut-Through Angle (degrees)	**90**	**90**	**90**	**90**	**90**	**90**	**90**	**90**	**90**	**90**	**90**
Average Panel Span (m) {rib-rib width}	**97**	**97**	97	97	97	97	97	97	97	97	97
SG (tonnes/m^3)	2.5	2.5	2.5	2.5	2.5	2.5	2.5	2.5	2.5	2.5	2.5
Conversion (tonnes to N)	10000	10000	10000	10000	10000	10000	10000	10000	10000	10000	10000
Abutment Angle (^{0})	21	21	21	21	21	21	21	21	21	21	21
W/H	0.57	0.59	0.61	0.52	0.54	0.55	0.56	0.58	0.60	0.61	0.61
PRELIMINARY CALCULATIONS											
Maximum Rib to Rib Pillar Length (w_2)	**95.3**	**95.3**	**94.8**	**95.3**	**95.3**	**95.3**	**95.3**	**95.3**	**95.3**	**95.3**	**95.3**
Minimum Rib to Rib Pillar Width (w_1)	**29.90**	**29.30**	**29.30**	**32.60**	**31.60**	**31.10**	**30.60**	**29.90**	**29.30**	**29.30**	**29.30**
w, Minimum Rib to Rib Pillar Width (ie $w_1 \sin\theta$)	**29.90**	**29.30**	**29.30**	**32.60**	**31.60**	**31.10**	**30.60**	**29.90**	**29.30**	**29.30**	**29.30**
Minimum Pillar Width/Height Ratio	**9.3**	**9.2**	**9.2**	**10.2**	**9.9**	**9.7**	**9.6**	**9.3**	**9.2**	**9.2**	**9.2**
Extraction Ratio (%)	**19.8%**	**20.1%**	**20.1%**	**18.8%**	**19.2%**	**19.4%**	**19.6%**	**19.8%**	**20.1%**	**20.1%**	**20.1%**
Abutment Angle (Radians)	0.367	0.367	0.367	0.367	0.367	0.367	0.367	0.367	0.367	0.367	0.367
Cut-Through Angle (Radians)	1.571	1.571	1.571	1.571	1.571	1.571	1.571	1.571	1.571	1.571	1.571
Is the Panel Super-Critical?	No	No	No	No	No	No	No	No	No	No	No
D (Peng & Chiang Loading Factor)	66.887	65.896	64.890	69.776	68.443	67.864	67.475	66.492	65.495	64.890	64.483
R (Pillar 2nd Abutment Component)	0.89	0.89	0.90	0.91	0.90	0.90	0.90	0.90	0.90	0.90	0.90
Dimensionless Pillar 'Rectangularity'	1.52	1.53	1.53	1.49	1.50	1.51	1.51	1.52	1.53	1.53	1.53
Width/Height Ratio Exponent	1.00	1.00	1.00	1.00	1.00	1.00	1.00	1.00	1.00	1.00	1.00
Effective Width Factor (Omega)	1.52	1.53	1.53	1.49	1.50	1.51	1.51	1.52	1.53	1.53	1.53
Effective Width Interim	45.52	44.82	44.76	48.58	47.46	46.90	46.33	45.52	44.82	44.82	44.82
Effective Pillar Width (m)	45.52	44.82	44.76	48.58	47.46	46.90	46.33	45.52	44.82	44.82	44.82
Effective Pillar Loading Height (m)	170.00	165.00	160.00	185.00	178.00	175.00	173.00	168.00	163.00	160.00	158.00
RESULTS											
Tributary Area Loading (MPa)	**5.30**	**5.16**	**5.01**	**5.70**	**5.51**	**5.43**	**5.38**	**5.24**	**5.10**	**5.01**	**4.94**
Pillar Strength (UNSW Squat Pillar 1999)	**29.88**	**29.10**	**29.08**	**33.62**	**32.18**	**31.49**	**30.81**	**29.88**	**29.10**	**29.10**	**29.10**
Pillar Strength (UNSW w/h<5)	**N/A**	**N/A**	**N/A**	**N/A**	**N/A**	**N/A**	**N/A**	**N/A**	**N/A**	**N/A**	**N/A**
Safety Factor under FTA Loading (Squat Pillar)	**5.63**	**5.64**	**5.81**	**5.90**	**5.85**	**5.80**	**5.73**	**5.70**	**5.71**	**5.81**	**5.89**
Safety Factor under FTA Loading (w/h<5)	**N/A**	**N/A**	**N/A**	**N/A**	**N/A**	**N/A**	**N/A**	**N/A**	**N/A**	**N/A**	**N/A**
Single Abutment Loading (3D) - full	4.46	4.35	4.14	4.65	4.53	4.49	4.48	4.38	4.27	4.14	4.06
Single Abutment Loading (3D) - pillar	**3.99**	**3.89**	**3.73**	**4.21**	**4.09**	**4.04**	**4.03**	**3.93**	**3.82**	**3.73**	**3.66**
Single Abutment Loading (3D) - solid	0.47	0.46	0.42	0.44	0.44	0.44	0.45	0.45	0.44	0.42	0.40
Design Abutment Load Multiplier	1.00	1.00	1.00	1.00	1.00	1.00	1.00	1.00	1.00	1.00	1.00
Total Pillar Loading with Single Abutment Loading	10.30	10.05	9.73	10.91	10.60	10.47	10.40	10.17	9.92	9.73	9.60
Safety Factor (under Single Abutment Loading)	**2.90**	**2.90**	**2.99**	**3.08**	**3.04**	**3.01**	**2.96**	**2.94**	**2.93**	**2.99**	**3.03**
Total Pillar Loading @ nA	**9.77**	**9.51**	**9.15**	**10.35**	**10.04**	**9.91**	**9.86**	**9.62**	**9.37**	**9.15**	**9.00**
Safety Factor @ nA	**3.06**	**3.06**	**3.18**	**3.25**	**3.21**	**3.18**	**3.13**	**3.10**	**3.11**	**3.18**	**3.23**
Total Pillar Loading under Double Abutment Loading	14.23	13.86	13.30	15.00	14.57	14.40	14.34	14.01	13.63	13.29	13.06
Safety Factor (under Double Abutment Loading)	**2.10**	**2.10**	**2.19**	**2.24**	**2.21**	**2.19**	**2.15**	**2.13**	**2.13**	**2.19**	**2.23**
Elastic Model Subsidence											
Ecoal(GPa)	**0.75**	**0.75**	**0.75**	**0.75**	**0.75**	**0.75**	**0.75**	**0.75**	**0.75**	**0.75**	**0.75**
E1floor(GPa)	**0.30**	**0.30**	**0.30**	**0.30**	**0.30**	**0.30**	**0.30**	**0.30**	**0.30**	**0.30**	**0.30**
E2floor(GPa)	**1.50**	**1.50**	**1.50**	**1.50**	**1.50**	**1.50**	**1.50**	**1.50**	**1.50**	**1.50**	**1.50**
E1roof(GPa)	**1.00**	**1.00**	**1.00**	**1.00**	**1.00**	**1.00**	**1.00**	**1.00**	**1.00**	**1.00**	**1.00**
E2roof(GPa)	**1.20**	**1.20**	**1.20**	**1.20**	**1.20**	**1.20**	**1.20**	**1.20**	**1.20**	**1.20**	**1.20**
Poissons Ratio floor/roof	**0.25**	**0.25**	**0.25**	**0.25**	**0.25**	**0.25**	**0.25**	**0.25**	**0.25**	**0.25**	**0.25**
initial vertical stress (MPa)	**4.25**	**4.13**	**4.00**	**4.63**	**4.45**	**4.38**	**4.33**	**4.20**	**4.08**	**4.00**	**3.95**
increase in vertical stress for DA (MPa)	**9.98**	**9.74**	**9.30**	**10.38**	**10.12**	**10.02**	**10.01**	**9.81**	**9.56**	**9.29**	**9.11**
Roof t1	**2.00**	**2.00**	**2.00**	**2.00**	**2.00**	**2.00**	**2.00**	**2.00**	**2.00**	**2.00**	**2.00**
Roof t2	**27.90**	**27.30**	**27.30**	**30.60**	**29.60**	**29.10**	**28.60**	**27.90**	**27.30**	**27.30**	**27.30**
Roof sig1	**9.98**	**9.74**	**9.30**	**10.37**	**10.12**	**10.02**	**10.01**	**9.81**	**9.56**	**9.29**	**9.11**
Roof sig2	**8.94**	**8.72**	**8.32**	**9.31**	**9.07**	**8.99**	**8.97**	**8.78**	**8.56**	**8.32**	**8.16**
Floor t1	**6.00**	**6.00**	**6.00**	**6.00**	**6.00**	**6.00**	**6.00**	**6.00**	**6.00**	**6.00**	**6.00**
Floor t2	**23.9**	**23.3**	**23.3**	**26.6**	**25.6**	**25.1**	**24.6**	**23.9**	**23.3**	**23.3**	**23.3**
Floor sig1	**9.97**	**9.73**	**9.29**	**10.37**	**10.11**	**10.02**	**10.01**	**9.80**	**9.55**	**9.28**	**9.11**
Floor sig2	**9.74**	**9.49**	**9.06**	**10.18**	**9.91**	**9.81**	**9.79**	**9.57**	**9.32**	**9.06**	**8.88**
Pillar Compression (m)	**0.040**	**0.039**	**0.037**	**0.042**	**0.040**	**0.040**	**0.040**	**0.039**	**0.038**	**0.037**	**0.036**
Roof Compression (m)	**0.214**	**0.204**	**0.195**	**0.242**	**0.229**	**0.223**	**0.219**	**0.210**	**0.200**	**0.195**	**0.191**
Floor Compression (m)	**0.333**	**0.321**	**0.306**	**0.364**	**0.348**	**0.342**	**0.338**	**0.327**	**0.315**	**0.306**	**0.300**
Total Compression (m)	**0.586**	**0.564**	**0.538**	**0.647**	**0.617**	**0.605**	**0.597**	**0.576**	**0.553**	**0.538**	**0.528**
Total Effective Compression (m)	**0.586**	**0.564**	**0.538**	**0.647**	**0.617**	**0.605**	**0.597**	**0.576**	**0.553**	**0.538**	**0.528**
1.5 times Effective Compression (m)	**0.879**	**0.846**	**0.807**	**0.971**	**0.926**	**0.907**	**0.896**	**0.864**	**0.830**	**0.807**	**0.792**
Total Yielded Panel Subs (m)	**0.65**	**0.63**	**0.60**	**0.72**	**0.69**	**0.67**	**0.67**	**0.64**	**0.62**	**0.60**	**0.59**
5 x Effective Predictions (m)	**2.930**	**2.819**	**2.691**	**3.235**	**3.087**	**3.024**	**2.987**	**2.879**	**2.767**	**2.690**	**2.639**
Bearing Capacity											
Upper Floor Unit UCS, 2*cu1 (MPa)	**20.0**	**20.0**	**20.0**	**20.0**	**20.0**	**20.0**	**20.0**	**20.0**	**20.0**	**20.0**	**20.0**
Upper Unit Thickness, H (m)	**6.0**	**6.0**	**6.0**	**6.0**	**6.0**	**6.0**	**6.0**	**6.0**	**6.0**	**6.0**	**6.0**
Lower Floor Unit UCS, 2*cu2 (MPa)	**40.0**	**40.0**	**40.0**	**40.0**	**40.0**	**40.0**	**40.0**	**40.0**	**40.0**	**40.0**	**40.0**
cu1/cu2	**0.5**	**0.5**	**0.5**	**0.5**	**0.5**	**0.5**	**0.5**	**0.5**	**0.5**	**0.5**	**0.5**
H/B	**0.20**	**0.20**	**0.20**	**0.18**	**0.19**	**0.19**	**0.20**	**0.20**	**0.20**	**0.20**	**0.20**
N*1	**6.63**	**6.58**	**6.58**	**6.86**	**6.77**	**6.73**	**6.69**	**6.63**	**6.58**	**6.58**	**6.58**
N*2	**3.32**	**3.29**	**3.29**	**3.43**	**3.39**	**3.37**	**3.35**	**3.32**	**3.29**	**3.29**	**3.29**
Floor Bearing Capacity (MPa)	**66.3**	**65.8**	**65.8**	**68.6**	**67.7**	**67.3**	**66.9**	**66.3**	**65.8**	**65.8**	**65.8**
Eff Pillar Stress (MPa)	**14.2**	**13.9**	**13.3**	**15.0**	**14.6**	**14.4**	**14.3**	**14.0**	**13.6**	**13.3**	**13.1**
Eff Floor Bearing Failure FoS	**4.66**	**4.75**	**4.95**	**4.57**	**4.65**	**4.68**	**4.67**	**4.74**	**4.83**	**4.95**	**5.04**
FTA Floor Bearing Failure FoS	**12.51**	**12.75**	**13.15**	**12.04**	**12.31**	**12.41**	**12.45**	**12.66**	**12.91**	**13.15**	**13.32**
Immediate Roof Unit UCS, 2*cu1 (MPa)	**40.0**	**40.0**	**40.0**	**40.0**	**40.0**	**40.0**	**40.0**	**40.0**	**40.0**	**40.0**	**40.0**
Immediate Roof Unit Thickness, H (m)	**10.0**	**10.0**	**10.0**	**10.0**	**10.0**	**10.0**	**10.0**	**10.0**	**10.0**	**10.0**	**10.0**
Upper Roof Unit UCS, 2*cu2 (MPa)	**40.0**	**40.0**	**40.0**	**40.0**	**40.0**	**40.0**	**40.0**	**40.0**	**40.0**	**40.0**	**40.0**
cu1/cu2	**1.0**	**1.0**	**1.0**	**1.0**	**1.0**	**1.0**	**1.0**	**1.0**	**1.0**	**1.0**	**1.0**
H/B	**0.33**	**0.34**	**0.34**	**0.31**	**0.32**	**0.32**	**0.33**	**0.33**	**0.34**	**0.34**	**0.34**
N*1	**5.14**	**5.14**	**5.14**	**5.14**	**5.14**	**5.14**	**5.14**	**5.14**	**5.14**	**5.14**	**5.14**
N*2	5.14	5.14	5.14	5.14	5.14	5.14	5.14	5.14	5.14	5.14	5.14
Roof Bearing Capacity (MPa)	102.8	102.8	102.8	102.8	102.8	102.8	102.8	102.8	102.8	102.8	102.8
Pillar Stress (MPa)	**14.2**	**13.9**	**13.3**	**15.0**	**14.6**	**14.4**	**14.3**	**14.0**	**13.6**	**13.3**	**13.1**
Effective Roof Bearing Failure FoS	**7.22**	**7.42**	**7.73**	**6.85**	**7.06**	**7.14**	**7.17**	**7.34**	**7.54**	**7.73**	**7.87**
FTA Roof Bearing Failure FoS	**19.39**	**19.91**	**20.53**	**18.05**	**18.67**	**18.95**	**19.12**	**19.62**	**20.16**	**20.54**	**20.80**
Voussoir Beam Deflection (m)	**0.691**	**1.072**	**0.957**	**0.957**	**0.957**	**0.957**	**0.957**	**0.957**	**0.957**	**0.957**	**0.957**
System Settlement at Base of beam (m)	0.000	0.000	0.000	0.000	0.000	0.000	0.000	0.000	0.000	0.000	0.000
Applied Pillar Stress/FTA Stress Ratio (Mpa)	1.00	1.00	1.00	1.00	1.00	1.00	1.00	1.00	1.00	1.00	1.00
Effective Pillar Stress (Mpa)	14.23	13.86	13.30	15.00	14.57	14.40	14.34	14.01	13.63	13.29	13.06
Multi-Seam Stress Inc (min)											
Multi-Seam Stress Inc (max)											
Effective Pillar FoS	**2.10**	**2.10**	**2.19**	**2.24**	**2.21**	**2.19**	**2.15**	**2.13**	**2.13**	**2.19**	**2.23**
Eresidual coal(GPa)	**0.25**	**0.25**	**0.25**	**0.27**	**0.26**	**0.26**	**0.25**	**0.25**	**0.25**	**0.25**	**0.25**

UNSW Pillar Design Spreadsheet											
Chain Valley XL.Panel#	6.12	6.13	7.1	7.2	7.3	7.4	7.5	7.6	7.7	7.8	7.9
INPUT DATA											
Depth of Cover (m)	**156**	**153**	**150**	**148**	**167**	**168**	**169**	**187**	**188**	**189**	**190**
Mining Height (m)	**3.2**	**3.2**	**3.2**	**3.2**	**3.2**	**3.2**	**3.2**	**3.2**	**3.2**	**3.2**	**3.2**
Pillar Length - centres (m)	100.7	100.2	100.2	100.2	100.7	100.7	100.7	100.7	100.7	100.7	100.7
Pillar Width - centres (m)	34.7	34.7	34.7	305.4	36.4	36.4	305.4	36.4	36.4	36.4	36.4
Roadway Width for maximum pillar dimension	5.4	5.4	5.4	5.4	5.4	5.4	5.4	5.4	5.4	5.4	5.4
Roadway Width for minimum pillar dimension	5.4	5.4	5.4	5.4	5.4	5.4	5.4	5.4	5.4	5.4	5.4
Cut-Through Angle (degrees)	**90**	**90**	**90**	**90**	**90**	**90**	**90**	**90**	**90**	**90**	**90**
Average Panel Span (m) {rib-rib width}	97	97	97	97	97	97	97	97	97	97	97
SG (tonnes/m^3)	2.5	2.5	2.5	2.5	2.5	2.5	2.5	2.5	2.5	2.5	2.5
Conversion (tonnes to N)	10000	10000	10000	10000	10000	10000	10000	10000	10000	10000	10000
Abutment Angle (^{0})	21	21	21	21	21	21	21	21	21	21	21
W/H	0.62	0.63	0.65	0.66	0.58	0.58	0.57	0.52	0.52	0.51	0.51
PRELIMINARY CALCULATIONS											
Maximum Rib to Rib Pillar Length (w_2)	**95.3**	**94.8**	**94.8**	**94.8**	**95.3**	**95.3**	**95.3**	**95.3**	**95.3**	**95.3**	**95.3**
Minimum Rib to Rib Pillar Width (w_1)	**29.30**	**29.30**	**29.30**	**300.00**	**31.00**	**31.00**	**300.00**	**31.00**	**31.00**	**31.00**	**31.00**
w, Minimum Rib to Rib Pillar Width (ie $w_1 \sin\theta$)	**29.30**	**29.30**	**29.30**	**300.00**	**31.00**	**31.00**	**300.00**	**31.00**	**31.00**	**31.00**	**31.00**
Minimum Pillar Width/Height Ratio	**9.2**	**9.2**	**9.2**	**29.6**	**9.7**	**9.7**	**29.8**	**9.7**	**9.7**	**9.7**	**9.7**
Extraction Ratio (%)	**20.1%**	**20.1%**	**20.1%**	**7.1%**	**19.4%**	**19.4%**	**7.0%**	**19.4%**	**19.4%**	**19.4%**	**19.4%**
Abutment Angle (Radians)	0.367	0.367	0.367	0.367	0.367	0.367	0.367	0.367	0.367	0.367	0.367
Cut-Through Angle (Radians)	1.571	1.571	1.571	1.571	1.571	1.571	1.571	1.571	1.571	1.571	1.571
Is the Panel Super-Critical?	No	No	No	No	No	No	No	No	No	No	No
D (Peng & Chiang Loading Factor)	64.074	63.455	62.829	62.409	66.294	66.492	66.690	70.152	70.339	70.526	70.712
R (Pillar 2nd Abutment Component)	0.90	0.91	0.91	1.00	0.91	0.91	1.00	0.89	0.89	0.89	0.89
Dimensionless Pillar 'Rectangularity'	1.53	1.53	1.53	0.48	1.51	1.51	0.48	1.51	1.51	1.51	1.51
Width/Height Ratio Exponent	1.00	1.00	1.00	1.00	1.00	1.00	1.00	1.00	1.00	1.00	1.00
Effective Width Factor (Omega)	1.53	1.53	1.53	0.48	1.51	1.51	0.48	1.51	1.51	1.51	1.51
Effective Width Interim	44.82	44.76	44.76	144.07	46.78	46.78	144.65	46.78	46.78	46.78	46.78
Effective Pillar Width (m)	44.82	44.76	44.76	144.07	46.78	46.78	144.65	46.78	46.78	46.78	46.78
Effective Pillar Loading Height (m)	156.00	153.00	150.00	148.00	167.00	168.00	169.00	187.00	188.00	189.00	190.00
RESULTS											
Tributary Area Loading (MPa)	**4.88**	**4.79**	**4.69**	**3.98**	**5.18**	**5.21**	**4.54**	**5.80**	**5.83**	**5.86**	**5.89**
Pillar Strength (UNSW Squat Pillar 1999)	**29.10**	**29.08**	**29.08**	**2108.59**	**31.35**	**31.35**	**2112.89**	**31.35**	**31.35**	**31.35**	**31.35**
Pillar Strength (UNSW w/h<5)	**N/A**	**N/A**	**N/A**	**N/A**	**N/A**	**N/A**	**N/A**	**N/A**	**N/A**	**N/A**	**N/A**
Safety Factor under FTA Loading (Squat Pillar)	**5.96**	**6.07**	**6.20**	**529.64**	**6.05**	**6.02**	**464.91**	**5.40**	**5.38**	**5.35**	**5.32**
Safety Factor under FTA Loading (w/h<5)	**N/A**	**N/A**	**N/A**	**N/A**	**N/A**	**N/A**	**N/A**	**N/A**	**N/A**	**N/A**	**N/A**
Single Abutment Loading (3D) - full	3.98	3.86	3.73	0.36	4.19	4.23	0.44	4.97	5.01	5.05	5.09
Single Abutment Loading (3D) - pillar	**3.59**	**3.50**	**3.40**	**0.36**	**3.81**	**3.84**	**0.44**	**4.42**	**4.45**	**4.48**	**4.51**
Single Abutment Loading (3D) - solid	0.38	0.36	0.33	0.00	0.38	0.39	0.00	0.55	0.56	0.57	0.58
Design Abutment Load Multiplier	1.00	1.00	1.00	1.00	1.00	1.00	1.00	1.00	1.00	1.00	1.00
Total Pillar Loading with Single Abutment Loading	9.48	9.28	9.09	5.34	9.99	10.05	5.99	11.22	11.28	11.34	11.40
Safety Factor (under Single Abutment Loading)	**3.07**	**3.13**	**3.20**	**395.05**	**3.14**	**3.12**	**352.99**	**2.79**	**2.78**	**2.76**	**2.75**
Total Pillar Loading @ nA	**8.86**	**8.64**	**8.43**	**4.34**	**9.37**	**9.44**	**4.99**	**10.77**	**10.84**	**10.91**	**10.98**
Safety Factor @ nA	**3.28**	**3.36**	**3.45**	**486.13**	**3.35**	**3.32**	**423.79**	**2.91**	**2.89**	**2.87**	**2.86**
Total Pillar Loading under Double Abutment Loading	12.84	12.50	12.16	4.69	13.56	13.67	5.43	15.74	15.85	15.96	16.07
Safety Factor (under Double Abutment Loading)	**2.27**	**2.33**	**2.39**	**449.22**	**2.31**	**2.29**	**389.35**	**1.99**	**1.98**	**1.96**	**1.95**
Elastic Model Subsidence											
Ecoal(GPa)	**0.75**	**0.75**	**0.75**	**0.75**	**0.75**	**0.75**	**0.75**	**0.75**	**0.75**	**0.75**	**0.75**
E1floor(GPa)	**0.30**	**0.30**	**0.30**	**0.30**	**0.30**	**0.30**	**0.30**	**0.30**	**0.30**	**0.30**	**0.30**
E2floor(GPa)	**1.50**	**1.50**	**1.50**	**1.50**	**1.50**	**1.50**	**1.50**	**1.50**	**1.50**	**1.50**	**1.50**
E1roof(GPa)	**1.00**	**1.00**	**1.00**	**1.00**	**1.00**	**1.00**	**1.00**	**1.00**	**1.00**	**1.00**	**1.00**
E2roof(GPa)	**1.20**	**1.20**	**1.20**	**1.20**	**1.20**	**1.20**	**1.20**	**1.20**	**1.20**	**1.20**	**1.20**
Poissons Ratio floor/roof	**0.25**	**0.25**	**0.25**	**0.25**	**0.25**	**0.25**	**0.25**	**0.25**	**0.25**	**0.25**	**0.25**
initial vertical stress (MPa)	**3.90**	**3.83**	**3.75**	**3.70**	**4.18**	**4.20**	**4.23**	**4.68**	**4.70**	**4.73**	**4.75**
increase in vertical stress for DA (MPa)	**8.94**	**8.67**	**8.41**	**0.99**	**9.38**	**9.47**	**1.20**	**11.07**	**11.15**	**11.23**	**11.32**
Roof t1	**2.00**	**2.00**	**2.00**	**2.00**	**2.00**	**2.00**	**2.00**	**2.00**	**2.00**	**2.00**	**2.00**
Roof t2	**27.30**	**27.30**	**27.30**	**298.00**	**29.00**	**29.00**	**298.00**	**29.00**	**29.00**	**29.00**	**29.00**
Roof sig1	**8.94**	**8.67**	**8.41**	**0.99**	**9.38**	**9.47**	**1.20**	**11.07**	**11.15**	**11.23**	**11.32**
Roof sig2	**8.00**	**7.77**	**7.53**	**0.90**	**8.41**	**8.49**	**1.09**	**9.92**	**9.99**	**10.07**	**10.14**
Floor t1	**6.00**	**6.00**	**6.00**	**6.00**	**6.00**	**6.00**	**6.00**	**6.00**	**6.00**	**6.00**	**6.00**
Floor t2	**23.3**	**23.3**	**23.3**	**294.0**	**25.0**	**25.0**	**294.0**	**25.0**	**25.0**	**25.0**	**25.0**
Floor sig1	**8.93**	**8.66**	**8.40**	**0.99**	**9.38**	**9.46**	**1.20**	**11.06**	**11.14**	**11.22**	**11.31**
Floor sig2	**8.71**	**8.45**	**8.19**	**0.99**	**9.18**	**9.26**	**1.20**	**10.83**	**10.91**	**10.99**	**11.07**
Pillar Compression (m)	**0.036**	**0.035**	**0.034**	**0.004**	**0.038**	**0.038**	**0.005**	**0.044**	**0.045**	**0.045**	**0.045**
Roof Compression (m)	**0.187**	**0.182**	**0.176**	**0.212**	**0.208**	**0.210**	**0.257**	**0.245**	**0.247**	**0.249**	**0.251**
Floor Compression (m)	**0.294**	**0.286**	**0.277**	**0.201**	**0.319**	**0.322**	**0.243**	**0.376**	**0.379**	**0.382**	**0.385**
Total Compression (m)	**0.517**	**0.502**	**0.487**	**0.417**	**0.565**	**0.570**	**0.505**	**0.666**	**0.671**	**0.676**	**0.681**
Total Effective Compression (m)	**0.517**	**0.502**	**0.487**	**0.417**	**0.565**	**0.570**	**0.505**	**0.666**	**0.671**	**0.676**	**0.681**
1.5 times Effective Compression (m)	**0.776**	**0.753**	**0.730**	**0.626**	**0.847**	**0.855**	**0.757**	**0.999**	**1.007**	**1.014**	**1.022**
Total Yielded Panel Subs (m)	**0.58**	**0.56**	**0.55**	**0.45**	**0.63**	**0.64**	**0.54**	**0.74**	**0.74**	**0.75**	**0.75**
5 x Effective Predictions (m)	**2.587**	**2.511**	**2.434**	**2.087**	**2.825**	**2.850**	**2.524**	**3.331**	**3.356**	**3.381**	**3.407**
Bearing Capacity											
Upper Floor Unit UCS, 2*cu1 (MPa)	**20.0**	**20.0**	**20.0**	**20.0**	**20.0**	**20.0**	**20.0**	**20.0**	**20.0**	**20.0**	**20.0**
Upper Unit Thickness, H (m)	**6.0**	**6.0**	**6.0**	**6.0**	**6.0**	**6.0**	**6.0**	**6.0**	**6.0**	**6.0**	**6.0**
Lower Floor Unit UCS, 2*cu2 (MPa)	**40.0**	**40.0**	**40.0**	**40.0**	**40.0**	**40.0**	**40.0**	**40.0**	**40.0**	**40.0**	**40.0**
cu1/cu2	**0.5**	**0.5**	**0.5**	**0.5**	**0.5**	**0.5**	**0.5**	**0.5**	**0.5**	**0.5**	**0.5**
H/B	**0.20**	**0.20**	**0.20**	**0.02**	**0.19**	**0.19**	**0.02**	**0.19**	**0.19**	**0.19**	**0.19**
N*1	**6.58**	**6.58**	**6.58**	**29.14**	**6.72**	**6.72**	**29.14**	**6.72**	**6.72**	**6.72**	**6.72**
N*2	**3.29**	**3.29**	**3.29**	**14.57**	**3.36**	**3.36**	**14.57**	**3.36**	**3.36**	**3.36**	**3.36**
Floor Bearing Capacity (MPa)	**65.8**	**65.8**	**65.8**	**291.4**	**67.2**	**67.2**	**291.4**	**67.2**	**67.2**	**67.2**	**67.2**
Eff Pillar Stress (MPa)	**12.8**	**12.5**	**12.2**	**4.7**	**13.6**	**13.7**	**5.4**	**15.7**	**15.8**	**16.0**	**16.1**
Eff Floor Bearing Failure FoS	**5.13**	**5.27**	**5.41**	**62.08**	**4.96**	**4.92**	**53.70**	**4.27**	**4.24**	**4.21**	**4.19**
FTA Floor Bearing Failure FoS	**13.49**	**13.75**	**14.02**	**73.20**	**12.98**	**12.90**	**64.12**	**11.59**	**11.53**	**11.47**	**11.41**
Immediate Roof Unit UCS, 2*cu1 (MPa)	**40.0**	**40.0**	**40.0**	**40.0**	**40.0**	**40.0**	**40.0**	**40.0**	**40.0**	**40.0**	**40.0**
Immediate Roof Unit Thickness, H (m)	**10.0**	**10.0**	**10.0**	**10.0**	**10.0**	**10.0**	**10.0**	**10.0**	**10.0**	**10.0**	**10.0**
Upper Roof Unit UCS, 2*cu2 (MPa)	**40.0**	**40.0**	**40.0**	**40.0**	**40.0**	**40.0**	**40.0**	**40.0**	**40.0**	**40.0**	**40.0**
cu1/cu2	**1.0**	**1.0**	**1.0**	**1.0**	**1.0**	**1.0**	**1.0**	**1.0**	**1.0**	**1.0**	**1.0**
H/B	**0.34**	**0.34**	**0.34**	**0.03**	**0.32**	**0.32**	**0.03**	**0.32**	**0.32**	**0.32**	**0.32**
N*1	**5.14**	**5.14**	**5.14**	**5.14**	**5.14**	**5.14**	**5.14**	**5.14**	**5.14**	**5.14**	**5.14**
N*2	5.14	5.14	5.14	5.14	5.14	5.14	5.14	5.14	5.14	5.14	5.14
Roof Bearing Capacity (MPa)	102.8	102.8	102.8	102.8	102.8	102.8	102.8	102.8	102.8	102.8	102.8
Pillar Stress (MPa)	**12.8**	**12.5**	**12.2**	**4.7**	**13.6**	**13.7**	**5.4**	**15.7**	**15.8**	**16.0**	**16.1**
Effective Roof Bearing Failure FoS	**8.01**	**8.22**	**8.46**	**21.90**	**7.58**	**7.52**	**18.94**	**6.53**	**6.49**	**6.44**	**6.40**
FTA Roof Bearing Failure FoS	**21.06**	**21.47**	**21.90**	**25.82**	**19.85**	**19.73**	**22.62**	**17.72**	**17.63**	**17.54**	**17.44**
Voussoir Beam Deflection (m)	**0.957**	**0.957**	**0.957**	**0.957**	**0.957**	**0.957**	**0.957**	**0.957**	**0.957**	**0.957**	**0.957**
System Settlement at Base of beam (m)	0.000	0.000	0.000	0.000	0.000	0.000	0.000	0.000	0.000	0.000	0.000
Applied Pillar Stress/FTA Stress Ratio (Mpa)	1.00	1.00	1.00	1.00	1.00	1.00	1.00	1.00	1.00	1.00	1.00
Effective Pillar Stress (Mpa)	12.84	12.50	12.16	4.69	13.56	13.67	5.43	15.74	15.85	15.96	16.07
Multi-Seam Stress Inc (min)											
Multi-Seam Stress Inc (max)											
Effective Pillar FoS	**2.27**	**2.33**	**2.39**	**449.22**	**2.31**	**2.29**	**389.35**	**1.99**	**1.98**	**1.96**	**1.95**
Eresidual coal(GPa)	**0.25**	**0.25**	**0.25**	**0.38**	**0.26**	**0.26**	**0.38**	**0.26**	**0.26**	**0.26**	**0.26**

UNSW Pillar Design Spreadsheet											
Chain Valley XL.Panel#	7.10	7.11	7.12	7.13	7.14	7.15	8.1	8.2	8.3	8.4	8.5
INPUT DATA											
Depth of Cover (m)	**190**	**190**	**219**	**218**	**221**	**220**	**217**	**229**	**230**	**231**	**232**
Mining Height (m)	**3.2**	**3.2**	**3.2**	**3.2**	**3.2**	**3.2**	**3.2**	**3.2**	**3.2**	**3.2**	**3.2**
Pillar Length - centres (m)	100.7	100.7	100.7	100.7	100.7	100.7	100.7	100.7	100.7	100.7	100.7
Pillar Width - centres (m)	36.4	36.4	36.0	36.0	36.0	36.0	36.0	36.0	36.0	36.0	36.0
Roadway Width for maximum pillar dimension	5.4	5.4	5.4	5.4	5.4	5.4	5.4	5.4	5.4	5.4	5.4
Roadway Width for minimum pillar dimension	5.4	5.4	5.4	5.4	5.4	5.4	5.4	5.4	5.4	5.4	5.4
Cut-Through Angle (degrees)	**90**	**90**	**90**	**90**	**90**	**90**	**90**	**90**	**90**	**90**	**90**
Average Panel Span (m) {rib-rib width}	97	97	97	97	97	97	97	97	97	97	97
SG (tonnes/m^3)	2.5	2.5	2.5	2.5	2.5	2.5	2.5	2.5	2.5	2.5	2.5
Conversion (tonnes to N)	10000	10000	10000	10000	10000	10000	10000	10000	10000	10000	10000
Abutment Angle (^{0})	21	21	21	21	21	21	21	21	21	21	21
W/H	0.51	0.51	0.44	0.44	0.44	0.44	0.45	0.42	0.42	0.42	0.42
PRELIMINARY CALCULATIONS											
Maximum Rib to Rib Pillar Length (w_2)	**95.3**	**95.3**	**95.3**	**95.3**	**95.3**	**95.3**	**95.3**	**95.3**	**95.3**	**95.3**	**95.3**
Minimum Rib to Rib Pillar Width (w_1)	**31.00**	**31.00**	**30.60**	**30.60**	**30.60**	**30.60**	**30.60**	**30.60**	**30.60**	**30.60**	**30.60**
w, Minimum Rib to Rib Pillar Width (ie $w_1 \sin\theta$)	**31.00**	**31.00**	**30.60**	**30.60**	**30.60**	**30.60**	**30.60**	**30.60**	**30.60**	**30.60**	**30.60**
Minimum Pillar Width/Height Ratio	**9.7**	**9.7**	**9.6**	**9.6**	**9.6**	**9.6**	**9.6**	**9.6**	**9.6**	**9.6**	**9.6**
Extraction Ratio (%)	**19.4%**	**19.4%**	**19.6%**	**19.6%**	**19.6%**	**19.6%**	**19.6%**	**19.6%**	**19.6%**	**19.6%**	**19.6%**
Abutment Angle (Radians)	0.367	0.367	0.367	0.367	0.367	0.367	0.367	0.367	0.367	0.367	0.367
Cut-Through Angle (Radians)	1.571	1.571	1.571	1.571	1.571	1.571	1.571	1.571	1.571	1.571	1.571
Is the Panel Super-Critical?	No	No	No	No	No	No	No	No	No	No	No
D (Peng & Chiang Loading Factor)	70.712	70.712	75.917	75.744	76.263	76.090	75.570	77.631	77.800	77.969	78.138
R (Pillar 2nd Abutment Component)	0.89	0.89	0.85	0.86	0.85	0.85	0.86	0.85	0.84	0.84	0.84
Dimensionless Pillar 'Rectangularity'	1.51	1.51	1.51	1.51	1.51	1.51	1.51	1.51	1.51	1.51	1.51
Width/Height Ratio Exponent	1.00	1.00	1.00	1.00	1.00	1.00	1.00	1.00	1.00	1.00	1.00
Effective Width Factor (Omega)	1.51	1.51	1.51	1.51	1.51	1.51	1.51	1.51	1.51	1.51	1.51
Effective Width Interim	46.78	46.78	46.33	46.33	46.33	46.33	46.33	46.33	46.33	46.33	46.33
Effective Pillar Width (m)	46.78	46.78	46.33	46.33	46.33	46.33	46.33	46.33	46.33	46.33	46.33
Effective Pillar Loading Height (m)	190.00	190.00	219.00	218.00	221.00	220.00	217.00	229.00	230.00	231.00	232.00
RESULTS											
Tributary Area Loading (MPa)	**5.89**	**5.89**	**6.81**	**6.78**	**6.87**	**6.84**	**6.74**	**7.12**	**7.15**	**7.18**	**7.21**
Pillar Strength (UNSW Squat Pillar 1999)	**31.35**	**31.35**	**30.81**	**30.81**	**30.81**	**30.81**	**30.81**	**30.81**	**30.81**	**30.81**	**30.81**
Pillar Strength (UNSW w/h<5)	**N/A**	**N/A**	**N/A**	**N/A**	**N/A**	**N/A**	**N/A**	**N/A**	**N/A**	**N/A**	**N/A**
Safety Factor under FTA Loading (Squat Pillar)	**5.32**	**5.32**	**4.53**	**4.55**	**4.49**	**4.51**	**4.57**	**4.33**	**4.31**	**4.29**	**4.27**
Safety Factor under FTA Loading (w/h<5)	**N/A**	**N/A**	**N/A**	**N/A**	**N/A**	**N/A**	**N/A**	**N/A**	**N/A**	**N/A**	**N/A**
Single Abutment Loading (3D) - full	5.09	5.09	6.30	6.26	6.38	6.34	6.22	6.70	6.74	6.77	6.81
Single Abutment Loading (3D) - pillar	**4.51**	**4.51**	**5.38**	**5.36**	**5.44**	**5.41**	**5.33**	**5.66**	**5.69**	**5.72**	**5.75**
Single Abutment Loading (3D) - solid	0.58	0.58	0.92	0.90	0.94	0.93	0.89	1.03	1.04	1.06	1.07
Design Abutment Load Multiplier	1.00	1.00	1.00	1.00	1.00	1.00	1.00	1.00	1.00	1.00	1.00
Total Pillar Loading with Single Abutment Loading	11.40	11.40	13.19	13.13	13.31	13.25	13.07	13.78	13.84	13.90	13.96
Safety Factor (under Single Abutment Loading)	**2.75**	**2.75**	**2.34**	**2.35**	**2.31**	**2.33**	**2.36**	**2.24**	**2.23**	**2.22**	**2.21**
Total Pillar Loading @ nA	**10.98**	**10.98**	**13.11**	**13.04**	**13.25**	**13.18**	**12.97**	**13.81**	**13.88**	**13.95**	**14.02**
Safety Factor @ nA	**2.86**	**2.86**	**2.35**	**2.36**	**2.33**	**2.34**	**2.38**	**2.23**	**2.22**	**2.21**	**2.20**
Total Pillar Loading under Double Abutment Loading	16.07	16.07	19.41	19.30	19.63	19.52	19.19	20.51	20.62	20.73	20.84
Safety Factor (under Double Abutment Loading)	**1.95**	**1.95**	**1.59**	**1.60**	**1.57**	**1.58**	**1.61**	**1.50**	**1.49**	**1.49**	**1.48**
Elastic Model Subsidence											
Ecoal(GPa)	**0.75**	**0.75**	**0.75**	**0.75**	**0.75**	**0.75**	**0.75**	**0.75**	**0.75**	**0.75**	**0.75**
E1floor(GPa)	**0.30**	**0.30**	**0.30**	**0.30**	**0.30**	**0.30**	**0.30**	**0.30**	**0.30**	**0.30**	**0.30**
E2floor(GPa)	**1.50**	**1.50**	**1.50**	**1.50**	**1.50**	**1.50**	**1.50**	**1.50**	**1.50**	**1.50**	**1.50**
E1roof(GPa)	**1.00**	**1.00**	**1.00**	**1.00**	**1.00**	**1.00**	**1.00**	**1.00**	**1.00**	**1.00**	**1.00**
E2roof(GPa)	**1.20**	**1.20**	**1.20**	**1.20**	**1.20**	**1.20**	**1.20**	**1.20**	**1.20**	**1.20**	**1.20**
Poissons Ratio floor/roof	**0.25**	**0.25**	**0.25**	**0.25**	**0.25**	**0.25**	**0.25**	**0.25**	**0.25**	**0.25**	**0.25**
initial vertical stress (MPa)	**4.75**	**4.75**	**5.48**	**5.45**	**5.53**	**5.50**	**5.43**	**5.73**	**5.75**	**5.78**	**5.80**
increase in vertical stress for DA (MPa)	**11.32**	**11.32**	**13.93**	**13.85**	**14.10**	**14.02**	**13.76**	**14.78**	**14.87**	**14.95**	**15.04**
Roof t1	**2.00**	**2.00**	**2.00**	**2.00**	**2.00**	**2.00**	**2.00**	**2.00**	**2.00**	**2.00**	**2.00**
Roof t2	**29.00**	**29.00**	**28.60**	**28.60**	**28.60**	**28.60**	**28.60**	**28.60**	**28.60**	**28.60**	**28.60**
Roof sig1	**11.32**	**11.32**	**13.93**	**13.85**	**14.10**	**14.02**	**13.76**	**14.78**	**14.87**	**14.95**	**15.04**
Roof sig2	**10.14**	**10.14**	**12.48**	**12.41**	**12.64**	**12.56**	**12.33**	**13.25**	**13.32**	**13.40**	**13.48**
Floor t1	**6.00**	**6.00**	**6.00**	**6.00**	**6.00**	**6.00**	**6.00**	**6.00**	**6.00**	**6.00**	**6.00**
Floor t2	**25.0**	**25.0**	**24.6**	**24.6**	**24.6**	**24.6**	**24.6**	**24.6**	**24.6**	**24.6**	**24.6**
Floor sig1	**11.31**	**11.31**	**13.92**	**13.83**	**14.09**	**14.00**	**13.75**	**14.77**	**14.85**	**14.94**	**15.02**
Floor sig2	**11.07**	**11.07**	**13.62**	**13.54**	**13.79**	**13.70**	**13.45**	**14.45**	**14.53**	**14.62**	**14.70**
Pillar Compression (m)	**0.045**	**0.045**	**0.056**	**0.055**	**0.056**	**0.056**	**0.055**	**0.059**	**0.059**	**0.060**	**0.060**
Roof Compression (m)	**0.251**	**0.251**	**0.305**	**0.303**	**0.309**	**0.307**	**0.301**	**0.324**	**0.326**	**0.327**	**0.329**
Floor Compression (m)	**0.385**	**0.385**	**0.470**	**0.467**	**0.476**	**0.473**	**0.465**	**0.499**	**0.502**	**0.505**	**0.508**
Total Compression (m)	**0.681**	**0.681**	**0.831**	**0.826**	**0.841**	**0.836**	**0.821**	**0.882**	**0.887**	**0.892**	**0.897**
Total Effective Compression (m)	**0.681**	**0.681**	**0.831**	**0.826**	**0.841**	**0.836**	**0.821**	**0.882**	**0.887**	**0.892**	**0.897**
1.5 times Effective Compression (m)	**1.022**	**1.022**	**1.247**	**1.239**	**1.262**	**1.254**	**1.231**	**1.323**	**1.331**	**1.338**	**1.346**
Total Yielded Panel Subs (m)	**0.75**	**0.75**	**0.92**	**0.91**	**0.93**	**0.92**	**0.91**	**0.97**	**0.98**	**0.98**	**0.99**
5 x Effective Predictions (m)	**3.407**	**3.407**	**4.156**	**4.130**	**4.207**	**4.181**	**4.105**	**4.410**	**4.435**	**4.461**	**4.486**
Bearing Capacity											
Upper Floor Unit UCS, 2*cu1 (MPa)	**20.0**	**20.0**	**20.0**	**20.0**	**20.0**	**20.0**	**20.0**	**20.0**	**20.0**	**20.0**	**20.0**
Upper Unit Thickness, H (m)	**6.0**	**6.0**	**6.0**	**6.0**	**6.0**	**6.0**	**6.0**	**6.0**	**6.0**	**6.0**	**6.0**
Lower Floor Unit UCS, 2*cu2 (MPa)	**40.0**	**40.0**	**40.0**	**40.0**	**40.0**	**40.0**	**40.0**	**40.0**	**40.0**	**40.0**	**40.0**
cu1/cu2	**0.5**	**0.5**	**0.5**	**0.5**	**0.5**	**0.5**	**0.5**	**0.5**	**0.5**	**0.5**	**0.5**
H/B	**0.19**	**0.19**	**0.20**	**0.20**	**0.20**	**0.20**	**0.20**	**0.20**	**0.20**	**0.20**	**0.20**
N*1	**6.72**	**6.72**	**6.69**	**6.69**	**6.69**	**6.69**	**6.69**	**6.69**	**6.69**	**6.69**	**6.69**
N*2	**3.36**	**3.36**	**3.35**	**3.35**	**3.35**	**3.35**	**3.35**	**3.35**	**3.35**	**3.35**	**3.35**
Floor Bearing Capacity (MPa)	**67.2**	**67.2**	**66.9**	**66.9**	**66.9**	**66.9**	**66.9**	**66.9**	**66.9**	**66.9**	**66.9**
Eff Pillar Stress (MPa)	**16.1**	**16.1**	**19.4**	**19.3**	**19.6**	**19.5**	**19.2**	**20.5**	**20.6**	**20.7**	**20.8**
Eff Floor Bearing Failure FoS	**4.19**	**4.19**	**3.45**	**3.47**	**3.41**	**3.43**	**3.49**	**3.26**	**3.25**	**3.23**	**3.21**
FTA Floor Bearing Failure FoS	**11.41**	**11.41**	**9.83**	**9.88**	**9.74**	**9.79**	**9.92**	**9.40**	**9.36**	**9.32**	**9.28**
Immediate Roof Unit UCS, 2*cu1 (MPa)	**40.0**	**40.0**	**40.0**	**40.0**	**40.0**	**40.0**	**40.0**	**40.0**	**40.0**	**40.0**	**40.0**
Immediate Roof Unit Thickness, H (m)	**10.0**	**10.0**	**10.0**	**10.0**	**10.0**	**10.0**	**10.0**	**10.0**	**10.0**	**10.0**	**10.0**
Upper Roof Unit UCS, 2*cu2 (MPa)	**40.0**	**40.0**	**40.0**	**40.0**	**40.0**	**40.0**	**40.0**	**40.0**	**40.0**	**40.0**	**40.0**
cu1/cu2	**1.0**	**1.0**	**1.0**	**1.0**	**1.0**	**1.0**	**1.0**	**1.0**	**1.0**	**1.0**	**1.0**
H/B	**0.32**	**0.32**	**0.33**	**0.33**	**0.33**	**0.33**	**0.33**	**0.33**	**0.33**	**0.33**	**0.33**
N*1	**5.14**	**5.14**	**5.14**	**5.14**	**5.14**	**5.14**	**5.14**	**5.14**	**5.14**	**5.14**	**5.14**
N*2	5.14	5.14	5.14	5.14	5.14	5.14	5.14	5.14	5.14	5.14	5.14
Roof Bearing Capacity (MPa)	102.8	102.8	102.8	102.8	102.8	102.8	102.8	102.8	102.8	102.8	102.8
Pillar Stress (MPa)	**16.1**	**16.1**	**19.4**	**19.3**	**19.6**	**19.5**	**19.2**	**20.5**	**20.6**	**20.7**	**20.8**
Effective Roof Bearing Failure FoS	**6.40**	**6.40**	**5.30**	**5.33**	**5.24**	**5.27**	**5.36**	**5.01**	**4.99**	**4.96**	**4.93**
FTA Roof Bearing Failure FoS	**17.44**	**17.44**	**15.10**	**15.17**	**14.97**	**15.04**	**15.24**	**14.44**	**14.38**	**14.32**	**14.26**
Voussoir Beam Deflection (m)	**0.957**	**0.957**	**0.957**	**0.957**	**0.957**	**0.957**	**0.957**	**0.957**	**0.957**	**0.957**	**0.957**
System Settlement at Base of beam (m)	0.000	0.000	0.000	0.000	0.000	0.000	0.000	0.000	0.000	0.000	0.000
Applied Pillar Stress/FTA Stress Ratio (Mpa)	1.00	1.00	1.00	1.00	1.00	1.00	1.00	1.00	1.00	1.00	1.00
Effective Pillar Stress (Mpa)	16.07	16.07	19.41	19.30	19.63	19.52	19.19	20.51	20.62	20.73	20.84
Multi-Seam Stress Inc (min)											
Multi-Seam Stress Inc (max)											
Effective Pillar FoS	**1.95**	**1.95**	**1.59**	**1.60**	**1.57**	**1.58**	**1.61**	**1.50**	**1.49**	**1.49**	**1.48**
Eresidual coal(GPa)	**0.26**	**0.26**	**0.25**	**0.25**	**0.25**	**0.25**	**0.25**	**0.25**	**0.25**	**0.25**	**0.25**

UNSW Pillar Design Spreadsheet											
Chain Valley XL.Panel#	8.6	9.1	9.2	9.3	9.4	9.5	10.1	10.2	10.3	10.4	10.5
INPUT DATA											
Depth of Cover (m)	**228**	**219**	**218**	**221**	**220**	**217**	**229**	**230**	**231**	**232**	**228**
Mining Height (m)	**3.2**	**3.2**	**3.2**	**3.2**	**3.2**	**3.2**	**3.2**	**3.2**	**3.2**	**3.2**	**3.2**
Pillar Length - centres (m)	100.7	100.7	100.7	100.7	100.7	100.7	100.7	100.7	100.7	100.7	100.7
Pillar Width - centres (m)	36.0	36.0	36.0	36.0	36.0	36.0	36.0	36.0	36.0	36.0	36.0
Roadway Width for maximum pillar dimension	5.4	5.4	5.4	5.4	5.4	5.4	5.4	5.4	5.4	5.4	5.4
Roadway Width for minimum pillar dimension	5.4	5.4	5.4	5.4	5.4	5.4	5.4	5.4	5.4	5.4	5.4
Cut-Through Angle (degrees)	**90**	**90**	**90**	**90**	**90**	**90**	**90**	**90**	**90**	**90**	**90**
Average Panel Span (m) {rib-rib width}	97	97	97	97	97	97	97	**97**	**97**	**97**	**97**
SG (tonnes/m^3)	2.5	2.5	2.5	2.5	2.5	2.5	2.5	2.5	2.5	2.5	2.5
Conversion (tonnes to N)	10000	10000	10000	10000	10000	10000	10000	10000	10000	10000	10000
Abutment Angle (^{0})	21	21	21	21	21	21	21	21	21	21	21
W/H	0.43	0.44	0.44	0.44	0.44	0.45	0.42	0.42	0.42	0.42	0.43
PRELIMINARY CALCULATIONS											
Maximum Rib to Rib Pillar Length (w_2)	**95.3**	**95.3**	**95.3**	**95.3**	**95.3**	**95.3**	**95.3**	**95.3**	**95.3**	**95.3**	**95.3**
Minimum Rib to Rib Pillar Width (w_1)	**30.60**	**30.60**	**30.60**	**30.60**	**30.60**	**30.60**	**30.60**	**30.60**	**30.60**	**30.60**	**30.60**
w, Minimum Rib to Rib Pillar Width (ie $w_1 \sin\theta$)	**30.60**	**30.60**	**30.60**	**30.60**	**30.60**	**30.60**	**30.60**	**30.60**	**30.60**	**30.60**	**30.60**
Minimum Pillar Width/Height Ratio	**9.6**	**9.6**	**9.6**	**9.6**	**9.6**	**9.6**	**9.6**	**9.6**	**9.6**	**9.6**	**9.6**
Extraction Ratio (%)	**19.6%**	**19.6%**	**19.6%**	**19.6%**	**19.6%**	**19.6%**	**19.6%**	**19.6%**	**19.6%**	**19.6%**	**19.6%**
Abutment Angle (Radians)	0.367	0.367	0.367	0.367	0.367	0.367	0.367	0.367	0.367	0.367	0.367
Cut-Through Angle (Radians)	1.571	1.571	1.571	1.571	1.571	1.571	1.571	1.571	1.571	1.571	1.571
Is the Panel Super-Critical?	No	No	No	No	No	No	No	No	No	No	No
D (Peng & Chiang Loading Factor)	77.461	75.917	75.744	76.263	76.090	75.570	77.631	77.800	77.969	78.138	77.461
R (Pillar 2nd Abutment Component)	0.85	0.85	0.86	0.85	0.85	0.86	0.85	0.84	0.84	0.84	0.85
Dimensionless Pillar 'Rectangularity'	1.51	1.51	1.51	1.51	1.51	1.51	1.51	1.51	1.51	1.51	1.51
Width/Height Ratio Exponent	1.00	1.00	1.00	1.00	1.00	1.00	1.00	1.00	1.00	1.00	1.00
Effective Width Factor (Omega)	1.51	1.51	1.51	1.51	1.51	1.51	1.51	1.51	1.51	1.51	1.51
Effective Width Interim	46.33	46.33	46.33	46.33	46.33	46.33	46.33	46.33	46.33	46.33	46.33
Effective Pillar Width (m)	46.33	46.33	46.33	46.33	46.33	46.33	46.33	46.33	46.33	46.33	46.33
Effective Pillar Loading Height (m)	228.00	219.00	218.00	221.00	220.00	217.00	229.00	230.00	231.00	232.00	228.00
RESULTS											
Tributary Area Loading (MPa)	**7.09**	**6.81**	**6.78**	**6.87**	**6.84**	**6.74**	**7.12**	**7.15**	**7.18**	**7.21**	**7.09**
Pillar Strength (UNSW Squat Pillar 1999)	**30.81**	**30.81**	**30.81**	**30.81**	**30.81**	**30.81**	**30.81**	**30.81**	**30.81**	**30.81**	**30.81**
Pillar Strength (UNSW w/h<5)	**N/A**	**N/A**	**N/A**	**N/A**	**N/A**	**N/A**	**N/A**	**N/A**	**N/A**	**N/A**	**N/A**
Safety Factor under FTA Loading (Squat Pillar)	**4.35**	**4.53**	**4.55**	**4.49**	**4.51**	**4.57**	**4.33**	**4.31**	**4.29**	**4.27**	**4.35**
Safety Factor under FTA Loading (w/h<5)	**N/A**	**N/A**	**N/A**	**N/A**	**N/A**	**N/A**	**N/A**	**N/A**	**N/A**	**N/A**	**N/A**
Single Abutment Loading (3D) - full	6.66	6.30	6.26	6.38	6.34	6.22	6.70	6.74	6.77	6.81	6.66
Single Abutment Loading (3D) - pillar	**5.64**	**5.38**	**5.36**	**5.44**	**5.41**	**5.33**	**5.66**	**5.69**	**5.72**	**5.75**	**5.64**
Single Abutment Loading (3D) - solid	1.02	0.92	0.90	0.94	0.93	0.89	1.03	1.04	1.06	1.07	1.02
Design Abutment Load Multiplier	1.00	1.00	1.00	1.00	1.00	1.00	1.00	1.00	1.00	1.00	1.00
Total Pillar Loading with Single Abutment Loading	13.72	13.19	13.13	13.31	13.25	13.07	13.78	13.84	13.90	13.96	13.72
Safety Factor (under Single Abutment Loading)	**2.25**	**2.34**	**2.35**	**2.31**	**2.33**	**2.36**	**2.24**	**2.23**	**2.22**	**2.21**	**2.25**
Total Pillar Loading @ nA	**13.74**	**13.11**	**13.04**	**13.25**	**13.18**	**12.97**	**13.81**	**13.88**	**13.95**	**14.02**	**13.74**
Safety Factor @ nA	**2.24**	**2.35**	**2.36**	**2.33**	**2.34**	**2.38**	**2.23**	**2.22**	**2.21**	**2.20**	**2.24**
Total Pillar Loading under Double Abutment Loading	20.40	19.41	19.30	19.63	19.52	19.19	20.51	20.62	20.73	20.84	20.40
Safety Factor (under Double Abutment Loading)	**1.51**	**1.59**	**1.60**	**1.57**	**1.58**	**1.61**	**1.50**	**1.49**	**1.49**	**1.48**	**1.51**
Elastic Model Subsidence											
Ecoal(GPa)	**0.75**	**0.75**	**0.75**	**0.75**	**0.75**	**0.75**	**0.75**	**0.75**	**0.75**	**0.75**	**0.75**
E1floor(GPa)	**0.30**	**0.30**	**0.30**	**0.30**	**0.30**	**0.30**	**0.30**	**0.30**	**0.30**	**0.30**	**0.30**
E2floor(GPa)	**1.50**	**1.50**	**1.50**	**1.50**	**1.50**	**1.50**	**1.50**	**1.50**	**1.50**	**1.50**	**1.50**
E1roof(GPa)	**1.00**	**1.00**	**1.00**	**1.00**	**1.00**	**1.00**	**1.00**	**1.00**	**1.00**	**1.00**	**1.00**
E2roof(GPa)	**1.20**	**1.20**	**1.20**	**1.20**	**1.20**	**1.20**	**1.20**	**1.20**	**1.20**	**1.20**	**1.20**
Poissons Ratio floor/roof	**0.25**	**0.25**	**0.25**	**0.25**	**0.25**	**0.25**	**0.25**	**0.25**	**0.25**	**0.25**	**0.25**
initial vertical stress (MPa)	**5.70**	**5.48**	**5.45**	**5.53**	**5.50**	**5.43**	**5.73**	**5.75**	**5.78**	**5.80**	**5.70**
increase in vertical stress for DA (MPa)	**14.70**	**15.43**	**15.35**	**14.50**	**15.52**	**15.26**	**16.28**	**16.37**	**16.45**	**16.54**	**16.20**
Roof t1	**2.00**	**2.00**	**2.00**	**2.00**	**2.00**	**2.00**	**2.00**	**2.00**	**2.00**	**2.00**	**2.00**
Roof t2	**28.60**	**28.60**	**28.60**	**28.60**	**28.60**	**28.60**	**28.60**	**28.60**	**28.60**	**28.60**	**28.60**
Roof sig1	**14.70**	**15.43**	**15.35**	**14.50**	**15.52**	**15.26**	**16.28**	**16.37**	**16.45**	**16.54**	**16.20**
Roof sig2	**13.17**	**13.83**	**13.75**	**12.99**	**13.90**	**13.68**	**14.59**	**14.67**	**14.74**	**14.82**	**14.51**
Floor t1	**6.00**	**6.00**	**6.00**	**6.00**	**6.00**	**6.00**	**6.00**	**6.00**	**6.00**	**6.00**	**6.00**
Floor t2	**24.6**	**24.6**	**24.6**	**24.6**	**24.6**	**24.6**	**24.6**	**24.6**	**24.6**	**24.6**	**24.6**
Floor sig1	**14.68**	**15.42**	**15.33**	**14.49**	**15.50**	**15.25**	**16.27**	**16.35**	**16.44**	**16.52**	**16.18**
Floor sig2	**14.37**	**15.08**	**15.00**	**14.18**	**15.17**	**14.92**	**15.92**	**16.00**	**16.08**	**16.17**	**15.83**
Pillar Compression (m)	**0.059**	**0.062**	**0.061**	**0.058**	**0.062**	**0.061**	**0.065**	**0.065**	**0.066**	**0.066**	**0.065**
Roof Compression (m)	**0.322**	**0.338**	**0.336**	**0.318**	**0.340**	**0.334**	**0.357**	**0.358**	**0.360**	**0.362**	**0.355**
Floor Compression (m)	**0.496**	**0.521**	**0.518**	**0.490**	**0.524**	**0.515**	**0.550**	**0.553**	**0.556**	**0.558**	**0.547**
Total Compression (m)	**0.877**	**0.921**	**0.916**	**0.865**	**0.926**	**0.910**	**0.971**	**0.977**	**0.982**	**0.987**	**0.966**
Total Effective Compression (m)	**0.877**	**0.921**	**0.916**	**0.865**	**0.926**	**0.910**	**0.971**	**0.977**	**0.982**	**0.987**	**0.966**
1.5 times Effective Compression (m)	**1.315**	**1.381**	**1.373**	**1.298**	**1.389**	**1.366**	**1.457**	**1.465**	**1.472**	**1.480**	**1.450**
Total Yielded Panel Subs (m)	**0.97**	**1.01**	**1.00**	**0.95**	**1.01**	**1.00**	**1.06**	**1.07**	**1.07**	**1.08**	**1.06**
5 x Effective Predictions (m)	**4.384**	**4.603**	**4.578**	**4.326**	**4.629**	**4.552**	**4.857**	**4.883**	**4.908**	**4.933**	**4.832**
Bearing Capacity											
Upper Floor Unit UCS, 2*cu1 (MPa)	**20.0**	**20.0**	**20.0**	**20.0**	**20.0**	**20.0**	**20.0**	**20.0**	**20.0**	**20.0**	**20.0**
Upper Unit Thickness, H (m)	**6.0**	**6.0**	**6.0**	**6.0**	**6.0**	**6.0**	**6.0**	**6.0**	**6.0**	**6.0**	**6.0**
Lower Floor Unit UCS, 2*cu2 (MPa)	**40.0**	**40.0**	**40.0**	**40.0**	**40.0**	**40.0**	**40.0**	**40.0**	**40.0**	**40.0**	**40.0**
cu1/cu2	**0.5**	**0.5**	**0.5**	**0.5**	**0.5**	**0.5**	**0.5**	**0.5**	**0.5**	**0.5**	**0.5**
H/B	**0.20**	**0.20**	**0.20**	**0.20**	**0.20**	**0.20**	**0.20**	**0.20**	**0.20**	**0.20**	**0.20**
N*1	**6.69**	**6.69**	**6.69**	**6.69**	**6.69**	**6.69**	**6.69**	**6.69**	**6.69**	**6.69**	**6.69**
N*2	**3.35**	**3.35**	**3.35**	**3.35**	**3.35**	**3.35**	**3.35**	**3.35**	**3.35**	**3.35**	**3.35**
Floor Bearing Capacity (MPa)	**66.9**	**66.9**	**66.9**	**66.9**	**66.9**	**66.9**	**66.9**	**66.9**	**66.9**	**66.9**	**66.9**
Eff Pillar Stress (MPa)	**20.4**	**20.9**	**20.8**	**20.0**	**21.0**	**20.7**	**22.0**	**22.1**	**22.2**	**22.3**	**21.9**
Eff Floor Bearing Failure FoS	**3.28**	**3.20**	**3.22**	**3.34**	**3.18**	**3.23**	**3.04**	**3.03**	**3.01**	**3.00**	**3.06**
FTA Floor Bearing Failure FoS	**9.44**	**9.83**	**9.88**	**9.74**	**9.79**	**9.92**	**9.40**	**9.36**	**9.32**	**9.28**	**9.44**
Immediate Roof Unit UCS, 2*cu1 (MPa)	**40.0**	**40.0**	**40.0**	**40.0**	**40.0**	**40.0**	**40.0**	**40.0**	**40.0**	**40.0**	**40.0**
Immediate Roof Unit Thickness, H (m)	**10.0**	**10.0**	**10.0**	**10.0**	**10.0**	**10.0**	**10.0**	**10.0**	**10.0**	**10.0**	**10.0**
Upper Roof Unit UCS, 2*cu2 (MPa)	**40.0**	**40.0**	**40.0**	**40.0**	**40.0**	**40.0**	**40.0**	**40.0**	**40.0**	**40.0**	**40.0**
cu1/cu2	**1.0**	**1.0**	**1.0**	**1.0**	**1.0**	**1.0**	**1.0**	**1.0**	**1.0**	**1.0**	**1.0**
H/B	**0.33**	**0.33**	**0.33**	**0.33**	**0.33**	**0.33**	**0.33**	**0.33**	**0.33**	**0.33**	**0.33**
N*1	**5.14**	**5.14**	**5.14**	**5.14**	**5.14**	**5.14**	**5.14**	**5.14**	**5.14**	**5.14**	**5.14**
N*2	5.14	5.14	5.14	5.14	5.14	5.14	5.14	5.14	5.14	5.14	5.14
Roof Bearing Capacity (MPa)	102.8	102.8	102.8	102.8	102.8	102.8	102.8	102.8	102.8	102.8	102.8
Pillar Stress (MPa)	**20.4**	**20.9**	**20.8**	**20.0**	**21.0**	**20.7**	**22.0**	**22.1**	**22.2**	**22.3**	**21.9**
Effective Roof Bearing Failure FoS	**5.04**	**4.92**	**4.94**	**5.13**	**4.89**	**4.97**	**4.67**	**4.65**	**4.62**	**4.60**	**4.69**
FTA Roof Bearing Failure FoS	**14.51**	**15.10**	**15.17**	**14.97**	**15.04**	**15.24**	**14.44**	**14.38**	**14.32**	**14.26**	**14.51**
Voussoir Beam Deflection (m)	**0.957**	**0.957**	**0.957**	**0.957**	**0.957**	**0.957**	**0.957**	**0.957**	**0.957**	**0.957**	**0.957**
System Settlement at Base of beam (m)	0.000	0.000	0.000	0.000	0.000	0.000	0.000	0.000	0.000	0.000	0.000
Applied Pillar Stress/FTA Stress Ratio (Mpa)	1.00	1.00	1.00	1.00	1.00	1.00	1.00	1.00	1.00	1.00	1.00
Effective Pillar Stress (Mpa)	20.40	**20.91**	**20.80**	**20.03**	**21.02**	**20.69**	**22.01**	**22.12**	**22.23**	**22.34**	**21.90**
Multi-Seam Stress Inc (min)		**0.84**	**0.84**	**-0.40**	**0.84**	**0.84**	**0.84**	**0.84**	**0.84**	**0.84**	**0.84**
Multi-Seam Stress Inc (max)		**1.50**	**1.50**	**0.40**	**1.50**	**1.50**	**1.50**	**1.50**	**1.50**	**1.50**	**1.50**
Effective Pillar FoS	**1.51**	**1.47**	**1.48**	**1.54**	**1.47**	**1.49**	**1.40**	**1.39**	**1.39**	**1.38**	**1.41**
Eresidual coal(GPa)	**0.25**	**0.25**	**0.25**	**0.25**	**0.25**	**0.25**	**0.25**	**0.25**	**0.25**	**0.25**	**0.25**

UNSW Pillar Design Spreadsheet										
Chain Valley XL.Panel#	9.1	9.2	9.3	9.4	9.5	10.1	10.2	10.3	10.4	10.5
INPUT DATA										
Depth of Cover (m)	**219**	**218**	**221**	**220**	**217**	**229**	**230**	**231**	**232**	**228**
Mining Height (m)	**3.2**	**3.2**	**3.2**	**3.2**	**3.2**	**3.2**	**3.2**	**3.2**	**3.2**	**3.2**
Pillar Length - centres (m)	100.7	100.7	100.7	100.7	100.7	100.7	100.7	100.7	100.7	100.7
Pillar Width - centres (m)	36.0	36.0	36.0	36.0	36.0	36.0	36.0	36.0	36.0	36.0
Roadway Width for maximum pillar dimension	5.4	5.4	5.4	5.4	5.4	5.4	5.4	5.4	5.4	5.4
Roadway Width for minimum pillar dimension	5.4	5.4	5.4	5.4	5.4	5.4	5.4	5.4	5.4	5.4
Cut-Through Angle (degrees)	**90**	**90**	**90**	**90**	**90**	**90**	**90**	**90**	**90**	**90**
Average Panel Span (m) {rib-rib width}	97	97	97	97	97	97	97	97	97	97
SG (tonnes/m^3)	2.5	2.5	2.5	2.5	2.5	2.5	2.5	2.5	2.5	2.5
Conversion (tonnes to N)	10000	10000	10000	10000	10000	10000	10000	10000	10000	10000
Abutment Angle (^{o})	21	21	21	21	21	21	21	21	21	21
W/H	0.44	0.44	0.44	0.44	0.45	0.42	0.42	0.42	0.42	0.43
PRELIMINARY CALCULATIONS										
Maximum Rib to Rib Pillar Length (w_2)	**95.3**	**95.3**	**95.3**	**95.3**	**95.3**	**95.3**	**95.3**	**95.3**	**95.3**	**95.3**
Minimum Rib to Rib Pillar Width (w_1)	**30.60**	**30.60**	**30.60**	**30.60**	**30.60**	**30.60**	**30.60**	**30.60**	**30.60**	**30.60**
w, Minimum Rib to Rib Pillar Width (ie $w_1 \sin\theta$)	**30.60**	**30.60**	**30.60**	**30.60**	**30.60**	**30.60**	**30.60**	**30.60**	**30.60**	**30.60**
Minimum Pillar Width/Height Ratio	**9.6**	**9.6**	**9.6**	**9.6**	**9.6**	**9.6**	**9.6**	**9.6**	**9.6**	**9.6**
Extraction Ratio (%)	**19.6%**	**19.6%**	**19.6%**	**19.6%**	**19.6%**	**19.6%**	**19.6%**	**19.6%**	**19.6%**	**19.6%**
Abutment Angle (Radians)	0.367	0.367	0.367	0.367	0.367	0.367	0.367	0.367	0.367	0.367
Cut-Through Angle (Radians)	1.571	1.571	1.571	1.571	1.571	1.571	1.571	1.571	1.571	1.571
Is the Panel Super-Critical?	No	No	No	No	No	No	No	No	No	No
D (Peng & Chiang Loading Factor)	75.917	75.744	76.263	76.090	75.570	77.631	77.800	77.969	78.138	77.461
R (Pillar 2nd Abutment Component)	0.85	0.86	0.85	0.85	0.86	0.85	0.84	0.84	0.84	0.85
Dimensionless Pillar 'Rectangularity'	1.51	1.51	1.51	1.51	1.51	1.51	1.51	1.51	1.51	1.51
Width/Height Ratio Exponent	1.00	1.00	1.00	1.00	1.00	1.00	1.00	1.00	1.00	1.00
Effective Width Factor (Omega)	1.51	1.51	1.51	1.51	1.51	1.51	1.51	1.51	1.51	1.51
Effective Width Interim	46.33	46.33	46.33	46.33	46.33	46.33	46.33	46.33	46.33	46.33
Effective Pillar Width (m)	46.33	46.33	46.33	46.33	46.33	46.33	46.33	46.33	46.33	46.33
Effective Pillar Loading Height (m)	219.00	218.00	221.00	220.00	217.00	229.00	230.00	231.00	232.00	228.00
RESULTS										
Tributary Area Loading (MPa)	**6.81**	**6.78**	**6.87**	**6.84**	**6.74**	**7.12**	**7.15**	**7.18**	**7.21**	**7.09**
Pillar Strength (UNSW Squat Pillar 1999)	**30.81**	**30.81**	**30.81**	**30.81**	**30.81**	**30.81**	**30.81**	**30.81**	**30.81**	**30.81**
Pillar Strength (UNSW w/h<5)	**N/A**	**N/A**	**N/A**	**N/A**	**N/A**	**N/A**	**N/A**	**N/A**	**N/A**	**N/A**
Safety Factor under FTA Loading (Squat Pillar)	**4.53**	**4.55**	**4.49**	**4.51**	**4.57**	**4.33**	**4.31**	**4.29**	**4.27**	**4.35**
Safety Factor under FTA Loading (w/h<5)	**N/A**	**N/A**	**N/A**	**N/A**	**N/A**	**N/A**	**N/A**	**N/A**	**N/A**	**N/A**
Single Abutment Loading (3D) - full	6.30	6.26	6.38	6.34	6.22	6.70	6.74	6.77	6.81	6.66
Single Abutment Loading (3D) - pillar	**5.38**	**5.36**	**5.44**	**5.41**	**5.33**	**5.66**	**5.69**	**5.72**	**5.75**	**5.64**
Single Abutment Loading (3D) - solid	0.92	0.90	0.94	0.93	0.89	1.03	1.04	1.06	1.07	1.02
Design Abutment Load Multiplier	1.00	1.00	1.00	1.00	1.00	1.00	1.00	1.00	1.00	1.00
Total Pillar Loading with Single Abutment Loading	13.19	13.13	13.31	13.25	13.07	13.78	13.84	13.90	13.96	13.72
Safety Factor (under Single Abutment Loading)	**2.34**	**2.35**	**2.31**	**2.33**	**2.36**	**2.24**	**2.23**	**2.22**	**2.21**	**2.25**
Total Pillar Loading @ nA	**13.11**	**13.04**	**13.25**	**13.18**	**12.97**	**13.81**	**13.88**	**13.95**	**14.02**	**13.74**
Safety Factor @ nA	**2.35**	**2.36**	**2.33**	**2.34**	**2.38**	**2.23**	**2.22**	**2.21**	**2.20**	**2.24**
Total Pillar Loading under Double Abutment Loading	19.41	19.30	19.63	19.52	19.19	20.51	20.62	20.73	20.84	20.40
Safety Factor (under Double Abutment Loading)	**1.59**	**1.60**	**1.57**	**1.58**	**1.61**	**1.50**	**1.49**	**1.49**	**1.48**	**1.51**
Elastic Model Subsidence										
Ecoal(GPa)										
E1floor(GPa)										
E2floor(GPa)										
E1roof(GPa)										
E2roof(GPa)										
Poissons Ratio floor/roof	**0.25**	**0.25**	**0.25**	**0.25**	**0.25**	**0.25**	**0.25**	**0.25**	**0.25**	**0.25**
initial vertical stress (MPa)	**5.48**	**5.45**	**5.53**	**5.50**	**5.43**	**5.73**	**5.75**	**5.78**	**5.80**	**5.70**
increase in vertical stress for DA (MPa)	**15.43**	**15.35**	**14.50**	**15.52**	**15.26**	**16.28**	**16.37**	**16.45**	**16.54**	**16.20**
Roof t1	**2.00**	**2.00**	**2.00**	**2.00**	**2.00**	**2.00**	**2.00**	**2.00**	**2.00**	**2.00**
Roof t2	**28.60**	**28.60**	**28.60**	**28.60**	**28.60**	**28.60**	**28.60**	**28.60**	**28.60**	**28.60**
Roof sig1	**15.43**	**15.35**	**14.50**	**15.52**	**15.26**	**16.28**	**16.37**	**16.45**	**16.54**	**16.20**
Roof sig2	**13.83**	**13.75**	**12.99**	**13.90**	**13.68**	**14.59**	**14.67**	**14.74**	**14.82**	**14.51**
Floor t1	**6.00**	**6.00**	**6.00**	**6.00**	**6.00**	**6.00**	**6.00**	**6.00**	**6.00**	**6.00**
Floor t2	**24.6**	**24.6**	**24.6**	**24.6**	**24.6**	**24.6**	**24.6**	**24.6**	**24.6**	**24.6**
Floor sig1	**15.42**	**15.33**	**14.49**	**15.50**	**15.25**	**16.27**	**16.35**	**16.44**	**16.52**	**16.18**
Floor sig2	**15.08**	**15.00**	**14.18**	**15.17**	**14.92**	**15.92**	**16.00**	**16.08**	**16.17**	**15.83**
Pillar Compression (m)	**#DIV/0!**	**#DIV/0!**	**#DIV/0!**	**#DIV/0!**	**#DIV/0!**	**#DIV/0!**	**#DIV/0!**	**#DIV/0!**	**#DIV/0!**	**#DIV/0!**
Roof Compression (m)	**#DIV/0!**	**#DIV/0!**	**#DIV/0!**	**#DIV/0!**	**#DIV/0!**	**#DIV/0!**	**#DIV/0!**	**#DIV/0!**	**#DIV/0!**	**#DIV/0!**
Floor Compression (m)	**#DIV/0!**	**#DIV/0!**	**#DIV/0!**	**#DIV/0!**	**#DIV/0!**	**#DIV/0!**	**#DIV/0!**	**#DIV/0!**	**#DIV/0!**	**#DIV/0!**
Total Compression (m)	**#DIV/0!**	**#DIV/0!**	**#DIV/0!**	**#DIV/0!**	**#DIV/0!**	**#DIV/0!**	**#DIV/0!**	**#DIV/0!**	**#DIV/0!**	**#DIV/0!**
Total Effective Compression (m)	**#DIV/0!**	**#DIV/0!**	**#DIV/0!**	**#DIV/0!**	**#DIV/0!**	**#DIV/0!**	**#DIV/0!**	**#DIV/0!**	**#DIV/0!**	**#DIV/0!**
1.5 times Effective Compression (m)	**#DIV/0!**	**#DIV/0!**	**#DIV/0!**	**#DIV/0!**	**#DIV/0!**	**#DIV/0!**	**#DIV/0!**	**#DIV/0!**	**#DIV/0!**	**#DIV/0!**
Total Yielded Panel Subs (m)	**#DIV/0!**	**#DIV/0!**	**#DIV/0!**	**#DIV/0!**	**#DIV/0!**	**#DIV/0!**	**#DIV/0!**	**#DIV/0!**	**#DIV/0!**	**#DIV/0!**
5 x Effective Predictions (m)	**#DIV/0!**	**#DIV/0!**	**#DIV/0!**	**#DIV/0!**	**#DIV/0!**	**#DIV/0!**	**#DIV/0!**	**#DIV/0!**	**#DIV/0!**	**#DIV/0!**
Bearing Capacity										
Upper Floor Unit UCS, 2*cu1 (MPa)	**20.0**	**20.0**	**20.0**	**20.0**	**20.0**	**20.0**	**20.0**	**20.0**	**20.0**	**20.0**
Upper Unit Thickness, H (m)	**6.0**	**6.0**	**6.0**	**6.0**	**6.0**	**6.0**	**6.0**	**6.0**	**6.0**	**6.0**
Lower Floor Unit UCS, 2*cu2 (MPa)	**40.0**	**40.0**	**40.0**	**40.0**	**40.0**	**40.0**	**40.0**	**40.0**	**40.0**	**40.0**
cu1/cu2	**0.5**	**0.5**	**0.5**	**0.5**	**0.5**	**0.5**	**0.5**	**0.5**	**0.5**	**0.5**
H/B	**0.20**	**0.20**	**0.20**	**0.20**	**0.20**	**0.20**	**0.20**	**0.20**	**0.20**	**0.20**
N*1	**6.69**	**6.69**	**6.69**	**6.69**	**6.69**	**6.69**	**6.69**	**6.69**	**6.69**	**6.69**
N*2	**3.35**	**3.35**	**3.35**	**3.35**	**3.35**	**3.35**	**3.35**	**3.35**	**3.35**	**3.35**
Floor Bearing Capacity (MPa)	**66.9**	**66.9**	**66.9**	**66.9**	**66.9**	**66.9**	**66.9**	**66.9**	**66.9**	**66.9**
Eff Pillar Stress (MPa)	**20.9**	**20.8**	**20.0**	**21.0**	**20.7**	**22.0**	**22.1**	**22.2**	**22.3**	**21.9**
Eff Floor Bearing Failure FoS	**3.20**	**3.22**	**3.34**	**3.18**	**3.23**	**3.04**	**3.03**	**3.01**	**3.00**	**3.06**
FTA Floor Bearing Failure FoS	**9.83**	**9.88**	**9.74**	**9.79**	**9.92**	**9.40**	**9.36**	**9.32**	**9.28**	**9.44**
Immediate Roof Unit UCS, 2*cu1 (MPa)	**40.0**	**40.0**	**40.0**	**40.0**	**40.0**	**40.0**	**40.0**	**40.0**	**40.0**	**40.0**
Immediate Roof Unit Thickness, H (m)	**10.0**	**10.0**	**10.0**	**10.0**	**10.0**	**10.0**	**10.0**	**10.0**	**10.0**	**10.0**
Upper Roof Unit UCS, 2*cu2 (MPa)	**40.0**	**40.0**	**40.0**	**40.0**	**40.0**	**40.0**	**40.0**	**40.0**	**40.0**	**40.0**
cu1/cu2	**1.0**	**1.0**	**1.0**	**1.0**	**1.0**	**1.0**	**1.0**	**1.0**	**1.0**	**1.0**
H/B	**0.33**	**0.33**	**0.33**	**0.33**	**0.33**	**0.33**	**0.33**	**0.33**	**0.33**	**0.33**
N*1	**5.14**	**5.14**	**5.14**	**5.14**	**5.14**	**5.14**	**5.14**	**5.14**	**5.14**	**5.14**
N*2	5.14	5.14	5.14	5.14	5.14	5.14	5.14	5.14	5.14	5.14
Roof Bearing Capacity (MPa)	102.8	102.8	102.8	102.8	102.8	102.8	102.8	102.8	102.8	102.8
Pillar Stress (MPa)	**20.9**	**20.8**	**20.0**	**21.0**	**20.7**	**22.0**	**22.1**	**22.2**	**22.3**	**21.9**
Effective Roof Bearing Failure FoS	**4.92**	**4.94**	**5.13**	**4.89**	**4.97**	**4.67**	**4.65**	**4.62**	**4.60**	**4.69**
FTA Roof Bearing Failure FoS	**15.10**	**15.17**	**14.97**	**15.04**	**15.24**	**14.44**	**14.38**	**14.32**	**14.26**	**14.51**
Voussoir Beam Deflection (m)	**0.957**	**0.957**	**0.957**	**0.957**	**0.957**	**0.957**	**0.957**	**0.957**	**0.957**	**0.957**
System Settlement at Base of beam (m)	#DIV/0!	#DIV/0!	#DIV/0!	#DIV/0!	#DIV/0!	#DIV/0!	#DIV/0!	#DIV/0!	#DIV/0!	#DIV/0!
Applied Pillar Stress/FTA Stress Ratio (Mpa)	#DIV/0!	#DIV/0!	#DIV/0!	#DIV/0!	#DIV/0!	#DIV/0!	#DIV/0!	#DIV/0!	#DIV/0!	#DIV/0!
Effective Pillar Stress (Mpa)	**20.91**	**20.80**	**20.03**	**21.02**	**20.69**	**22.01**	**22.12**	**22.23**	**22.34**	**21.90**
Multi-Seam Stress Inc (min)	**0.84**	**0.84**	**-0.40**	**0.84**	**0.84**	**0.84**	**0.84**	**0.84**	**0.84**	**0.84**
Multi-Seam Stress Inc (max)	**1.50**	**1.50**	**0.40**	**1.50**	**1.50**	**1.50**	**1.50**	**1.50**	**1.50**	**1.50**
Effective Pillar FoS	**1.47**	**1.48**	**1.54**	**1.47**	**1.49**	**1.40**	**1.39**	**1.39**	**1.38**	**1.41**
Eresidual coal(GPa)	**0.25**	**0.25**	**0.25**	**0.25**	**0.25**	**0.25**	**0.25**	**0.25**	**0.25**	**0.25**

UNSW Pillar Design Spreadsheet	30.6	30.4	32.6	32.6	32.6	32.6	32.6	40.0	186.0	32.6	32.6
	1.1	**1.2**	**1.3**	**1.4**	**1.5**	**1.6**	**1.7**	**2.1**	**2.2**	**3.1**	**3.2**
Chain Valley XL.Panel#	1.1	1.2	1.3	1.4	1.5	1.6	2.1	2.2	3.1	3.2	4.1
INPUT DATA	95.3	95.3	95.3	95.3	95.3	95.3	95.3	95.3	95.3	95.3	95.3
Depth of Cover (m)	**200**	**200**	**200**	**198**	**195**	**193**	**191**	**196**	**200**	**190**	**188**
Mining Height (m)	**3.2**	**3.2**	**3.2**	**3.2**	**3.2**	**3.2**	**3.2**	**3.2**	**3.2**	**3.2**	**3.2**
Pillar Length - centres (m)	100.7	100.7	100.7	100.7	100.7	100.7	100.7	100.7	100.7	100.7	100.7
Pillar Width - centres (m)	36.0	35.8	38.0	38.0	38.0	38.0	38.0	45.4	191.4	38.0	38.0
Roadway Width for maximum pillar dimension	5.4	5.4	5.4	5.4	5.4	5.4	5.4	5.4	5.4	5.4	5.4
Roadway Width for minimum pillar dimension	5.4	5.4	5.4	5.4	5.4	5.4	5.4	5.4	5.4	5.4	5.4
Cut-Through Angle (degrees)	**90**	**90**	**90**	**90**	**90**	**90**	**90**	**90**	**90**	**90**	**90**
Average Panel Span (m) {rib-rib width}	72	72	97	97	97	97	**97**	**97**	**97**	**97**	**97**
SG (tonnes/m^3)	2.5	2.5	2.5	2.5	2.5	2.5	2.5	2.5	2.5	2.5	2.5
Conversion (tonnes to N)	10000	10000	10000	10000	10000	10000	10000	10000	10000	10000	10000
Abutment Angle (^{0})	21	21	21	21	21	21	21	21	21	21	21
W/H	0.36	0.36	0.49	0.49	0.50	0.50	0.51	0.49	0.49	0.51	0.52
PRELIMINARY CALCULATIONS											
Maximum Rib to Rib Pillar Length (w_2)	**95.3**	**95.3**	**95.3**	**95.3**	**95.3**	**95.3**	**95.3**	**95.3**	**95.3**	**95.3**	**95.3**
Minimum Rib to Rib Pillar Width (w_1)	**30.6**	**30.4**	**32.6**	**32.6**	**32.6**	**32.6**	**32.6**	**40.0**	**186.0**	**32.6**	**32.6**
w, Minimum Rib to Rib Pillar Width (ie $w_1 \sin\theta$)	**30.6**	**30.4**	**32.6**	**32.6**	**32.6**	**32.6**	**32.6**	**40.0**	**186.0**	**32.6**	**32.6**
Minimum Pillar Width/Height Ratio	**9.6**	**9.5**	**10.2**	**10.2**	**10.2**	**10.2**	**10.2**	**12.5**	**29.8**	**10.2**	**10.2**
Extraction Ratio (%)	**19.6%**	**19.6%**	**18.8%**	**18.8%**	**18.8%**	**18.8%**	**18.8%**	**16.6%**	**8.0%**	**18.8%**	**18.8%**
Abutment Angle (Radians)	0.367	0.367	0.367	0.367	0.367	0.367	0.367	0.367	0.367	0.367	0.367
Cut-Through Angle (Radians)	1.571	1.571	1.571	1.571	1.571	1.571	1.571	1.571	1.571	1.571	1.571
Is the Panel Super-Critical?	No	No	No	No	No	No	No	No	No	No	No
D (Peng & Chiang Loading Factor)	72.549	72.549	72.549	72.185	71.637	71.268	70.898	71.820	72.549	70.712	70.339
R (Pillar 2nd Abutment Component)	0.87	0.87	0.89	0.89	0.90	0.90	0.90	0.95	1.00	0.90	0.90
Dimensionless Pillar 'Rectangularity'	1.51	1.52	1.49	1.49	1.49	1.49	1.49	1.41	0.68	1.49	1.49
Width/Height Ratio Exponent	1.00	1.00	1.00	1.00	1.00	1.00	1.00	1.00	1.00	1.00	1.00
Effective Width Factor (Omega)	1.51	1.52	1.49	1.49	1.49	1.49	1.49	1.41	0.68	1.49	1.49
Effective Width Interim	46.33	46.10	48.58	48.58	48.58	48.58	48.58	56.35	126.03	48.58	48.58
Effective Pillar Width (m)	46.33	46.10	48.58	48.58	48.58	48.58	48.58	56.35	126.03	48.58	48.58
Effective Pillar Loading Height (m)	200.00	200.00	200.00	198.00	195.00	193.00	191.00	196.00	200.00	190.00	188.00
RESULTS											
Tributary Area Loading (MPa)	**6.22**	**6.22**	**6.16**	**6.10**	**6.00**	**5.94**	**5.88**	**5.88**	**5.44**	**5.85**	**5.79**
Pillar Strength (UNSW Squat Pillar 1999)	**30.81**	**30.54**	**33.62**	**33.62**	**33.62**	**33.62**	**33.62**	**45.99**	**848.18**	**33.62**	**33.62**
Pillar Strength (UNSW w/h<5)	**N/A**	**N/A**	**N/A**	**N/A**	**N/A**	**N/A**	**N/A**	**N/A**	**N/A**	**N/A**	**N/A**
Safety Factor under FTA Loading (Squat Pillar)	**4.96**	**4.91**	**5.46**	**5.51**	**5.60**	**5.66**	**5.72**	**7.83**	**156.01**	**5.75**	**5.81**
Safety Factor under FTA Loading (w/h<5)	**N/A**	**N/A**	**N/A**	**N/A**	**N/A**	**N/A**	**N/A**	**N/A**	**N/A**	**N/A**	**N/A**
Single Abutment Loading (3D) - full	4.50	4.54	5.21	5.13	5.02	4.95	4.87	4.12	0.91	4.84	4.76
Single Abutment Loading (3D) - pillar	**3.93**	**3.95**	**4.65**	**4.59**	**4.50**	**4.45**	**4.39**	**3.92**	**0.91**	**4.36**	**4.30**
Single Abutment Loading (3D) - solid	0.58	0.59	0.56	0.55	0.52	0.50	0.49	0.21	0.00	0.48	0.46
Design Abutment Load Multiplier	1.00	1.00	1.00	1.50	1.50	1.00	1.00	1.00	1.00	1.00	1.00
Total Pillar Loading with Single Abutment Loading	11.14	11.17	11.80	12.19	12.01	11.39	11.27	10.80	7.35	11.21	11.09
Safety Factor (under Single Abutment Loading)	**2.76**	**2.73**	**2.85**	**2.76**	**2.80**	**2.95**	**2.98**	**4.26**	**115.41**	**3.00**	**3.03**
Total Pillar Loading @ nA	10.72	10.76	11.37	13.80	13.54	10.89	10.76	10.00	6.35	10.69	10.55
Safety Factor @ nA	**2.87**	**2.84**	**2.96**	**2.44**	**2.48**	**3.09**	**3.13**	**4.60**	**133.58**	**3.15**	**3.19**
Total Pillar Loading under Double Abutment Loading	15.22	15.31	16.58	16.37	16.05	15.84	15.63	14.12	7.26	15.53	15.32
Safety Factor (under Double Abutment Loading)	**2.02**	**2.00**	**2.03**	**2.05**	**2.09**	**2.12**	**2.15**	**3.26**	**116.79**	**2.17**	**2.20**
Elastic Model Subsidence											
Ecoal(GPa)	**1.50**	**1.50**	**1.50**	**1.50**	**1.50**	**1.50**	**1.50**	**1.50**	**1.50**	**1.50**	**1.50**
E1floor(GPa)	**0.75**	**0.75**	**0.75**	**0.75**	**0.75**	**0.75**	**0.75**	**0.75**	**0.75**	**0.75**	**0.75**
E2floor(GPa)	**4.00**	**4.00**	**4.00**	**4.00**	**4.00**	**4.00**	**4.00**	**4.00**	**4.00**	**4.00**	**4.00**
E1roof(GPa)	**0.75**	**0.75**	**0.75**	**0.75**	**0.75**	**0.75**	**0.75**	**0.75**	**0.75**	**0.75**	**0.75**
E2roof(GPa)	**5.00**	**5.00**	**5.00**	**5.00**	**5.00**	**5.00**	**5.00**	**5.00**	**5.00**	**5.00**	**5.00**
Poissons Ratio floor/roof	**0.25**	**0.25**	**0.25**	**0.25**	**0.25**	**0.25**	**0.25**	**0.25**	**0.25**	**0.25**	**0.25**
initial vertical stress (MPa)	**5.00**	**5.00**	**5.00**	**4.95**	**4.88**	**4.83**	**4.78**	**4.90**	**5.00**	**4.75**	**4.70**
increase in vertical stress for DA (MPa)	**10.22**	**10.31**	**11.58**	**11.42**	**11.18**	**11.02**	**10.86**	**9.22**	**2.26**	**10.78**	**10.62**
Roof t1	**3.00**	**3.00**	**2.00**	**2.00**	**2.00**	**2.00**	**2.00**	**2.00**	**2.00**	**2.00**	**2.00**
Roof t2	**27.60**	**27.40**	**30.60**	**30.60**	**30.60**	**30.60**	**30.60**	**38.00**	**184.00**	**30.60**	**30.60**
Roof sig1	**10.22**	**10.30**	**11.58**	**11.42**	**11.18**	**11.02**	**10.86**	**9.22**	**2.26**	**10.78**	**10.62**
Roof sig2	**9.08**	**9.16**	**10.38**	**10.24**	**10.02**	**9.88**	**9.74**	**8.30**	**2.05**	**9.67**	**9.52**
Floor t1	**3.00**	**3.00**	**3.00**	**3.00**	**3.00**	**3.00**	**3.00**	**3.00**	**3.00**	**3.00**	**3.00**
Floor t2	**27.6**	**27.4**	**29.6**	**29.6**	**29.6**	**29.6**	**29.6**	**37.0**	**183.0**	**29.6**	**29.6**
Floor sig1	**10.22**	**10.30**	**11.57**	**11.41**	**11.17**	**11.01**	**10.85**	**9.22**	**2.26**	**10.77**	**10.61**
Floor sig2	**10.19**	**10.27**	**11.55**	**11.39**	**11.15**	**10.99**	**10.83**	**9.21**	**2.26**	**10.75**	**10.59**
Pillar Compression (m)	**0.020**	**0.021**	**0.023**	**0.023**	**0.022**	**0.022**	**0.022**	**0.018**	**0.005**	**0.022**	**0.021**
Roof Compression (m)	**0.085**	**0.086**	**0.089**	**0.087**	**0.085**	**0.084**	**0.083**	**0.082**	**0.077**	**0.082**	**0.081**
Floor Compression (m)	**0.104**	**0.105**	**0.124**	**0.122**	**0.119**	**0.118**	**0.116**	**0.114**	**0.106**	**0.115**	**0.113**
Total FTA Compression (m)	**0.210**	**0.211**	**0.235**	**0.232**	**0.227**	**0.224**	**0.221**	**0.215**	**0.187**	**0.219**	**0.216**
Total Effective Compression (m)	**0.210**	**0.211**	**0.235**	**0.232**	**0.227**	**0.224**	**0.221**	**0.215**	**0.187**	**0.219**	**0.216**
2 times Effective Compression (m)	**0.420**	**0.422**	**0.470**	**0.464**	**0.454**	**0.448**	**0.441**	**0.430**	**0.373**	**0.438**	**0.431**
Total Yielded Panel Subs (m)	**0.29**	**0.29**	**0.31**	**0.31**	**0.30**	**0.30**	**0.29**	**0.28**	**0.23**	**0.29**	**0.29**
5 x Effective Predictions (m)	**1.050**	**1.055**	**1.176**	**1.160**	**1.135**	**1.119**	**1.103**	**1.076**	**0.933**	**1.095**	**1.078**
Bearing Capacity											
Upper Floor Unit UCS, 2*cu1 (MPa)	**8.0**	**8.0**	**8.0**	**8.0**	**8.0**	**8.0**	**8.0**	**8.0**	**8.0**	**8.0**	**8.0**
Upper Unit Thickness, H (m)	**3.0**	**3.0**	**3.0**	**3.0**	**3.0**	**3.0**	**3.0**	**3.0**	**3.0**	**3.0**	**3.0**
Lower Floor Unit UCS, 2*cu2 (MPa)	**40.0**	**40.0**	**40.0**	**40.0**	**40.0**	**40.0**	**40.0**	**40.0**	**40.0**	**40.0**	**40.0**
cu1/cu2	**0.2**	**0.2**	**0.2**	**0.2**	**0.2**	**0.2**	**0.2**	**0.2**	**0.2**	**0.2**	**0.2**
H/B	**0.10**	**0.10**	**0.09**	**0.09**	**0.09**	**0.09**	**0.09**	**0.08**	**0.02**	**0.09**	**0.09**
N*1	**9.24**	**9.21**	**9.57**	**9.57**	**9.57**	**9.57**	**9.57**	**10.81**	**35.14**	**9.57**	**9.57**
N*2	**1.85**	**1.84**	**1.91**	**1.91**	**1.91**	**1.91**	**1.91**	**2.16**	**7.03**	**1.91**	**1.91**
Floor Bearing Capacity (MPa)	**37.0**	**36.8**	**38.3**	**38.3**	**38.3**	**38.3**	**38.3**	**43.2**	**140.6**	**38.3**	**38.3**
Eff Pillar Stress (MPa)	**15.2**	**15.3**	**16.6**	**16.4**	**16.1**	**15.8**	**15.6**	**14.1**	**7.3**	**15.5**	**15.3**
Eff Floor Bearing Failure FoS	**2.43**	**2.41**	**2.31**	**2.34**	**2.39**	**2.42**	**2.45**	**3.06**	**19.36**	**2.47**	**2.50**
FTA Floor Bearing Failure FoS	**5.95**	**5.92**	**6.22**	**6.28**	**6.38**	**6.44**	**6.51**	**7.36**	**25.86**	**6.55**	**6.62**
Immediate Roof Unit UCS, 2*cu1 (MPa)	**8.0**	**8.0**	**8.0**	**8.0**	**8.0**	**8.0**	**8.0**	**8.0**	**8.0**	**8.0**	**8.0**
Immediate Roof Unit Thickness, H (m)	**3.0**	**3.0**	**3.0**	**3.0**	**3.0**	**3.0**	**3.0**	**3.0**	**3.0**	**3.0**	**3.0**
Upper Roof Unit UCS, 2*cu2 (MPa)	**40.0**	**40.0**	**40.0**	**40.0**	**40.0**	**40.0**	**40.0**	**40.0**	**40.0**	**40.0**	**40.0**
cu1/cu2	**0.2**	**0.2**	**0.2**	**0.2**	**0.2**	**0.2**	**0.2**	**0.2**	**0.2**	**0.2**	**0.2**
H/B	**0.10**	**0.10**	**0.09**	**0.09**	**0.09**	**0.09**	**0.09**	**0.08**	**0.02**	**0.09**	**0.09**
N*1	**9.24**	**9.21**	**9.57**	**9.57**	**9.57**	**9.57**	**9.57**	**10.81**	**35.14**	**9.57**	**9.57**
N*2	1.85	1.84	1.91	1.91	1.91	1.91	1.91	2.16	7.03	1.91	1.91
Roof Bearing Capacity (MPa)	37.0	36.8	38.3	38.3	38.3	38.3	38.3	43.2	140.6	38.3	38.3
Pillar Stress (MPa)	**15.2**	**15.3**	**16.6**	**16.4**	**16.1**	**15.8**	**15.6**	**14.1**	**7.3**	**15.5**	**15.3**
Effective Roof Bearing Failure FoS	**2.43**	**2.41**	**2.31**	**2.34**	**2.39**	**2.42**	**2.45**	**3.06**	**19.36**	**2.47**	**2.50**
FTA Roof Bearing Failure FoS	**5.95**	**5.92**	**6.22**	**6.28**	**6.38**	**6.44**	**6.51**	**7.36**	**25.86**	**6.55**	**6.62**
Voussoir Beam Deflection (m)	**0.004**	**0.004**	**0.004**	**0.001**	**0.001**	**0.419**	**0.006**	**0.011**	**0.282**	**0.005**	**0.065**
System Settlement at Base of beam (m)	0.000	0.000	0.000	0.000	0.000	0.000	0.000	0.000	0.000	0.000	0.000
Applied Pillar Stress/FTA Stress Ratio (Mpa)	1.00	1.00	1.00	1.00	1.00	1.00	1.00	1.00	1.00	1.00	1.00
Effective Pillar Stress (Mpa)	15.22	15.31	16.58	16.37	16.05	15.84	15.63	14.12	7.26	15.53	15.32
Multi-Seam Stress Inc (min)											
Multi-Seam Stress Inc (max)											
Effective Pillar FoS	**2.02**	**2.00**	**2.03**	**2.05**	**2.09**	**2.12**	**2.15**	**3.26**	**116.79**	**2.17**	**2.20**
Eresidual coal(GPa)	**0.25**	**0.25**	**0.27**	**0.27**	**0.27**	**0.27**	**0.27**	**0.30**	**0.38**	**0.27**	**0.27**

UNSW Pillar Design Spreadsheet	32.6	32.6	32.6	32.6	32.6	300.0	32.6	32.6	31.6	31.1	30.6
	3.3	3.4	3.5	3.6	4.1	4.2	5.1	5.2	5.3	5.4	5.5
Chain Valley XL.Panel#	4.2	4.3	4.4	4.5	5.1	5.2	6.1	6.2	6.3	6.4	6.5
INPUT DATA	95.3	95.3	95.3	95.3	95.3	95.3	95.3	95.3	95.3	95.3	95.3
Depth of Cover (m)	185	183	178	173	170	184	188	185	182	180	175
Mining Height (m)	3.2	3.2	3.2	3.2	3.2	3.2	3.2	3.2	3.2	3.2	3.2
Pillar Length - centres (m)	100.7	100.7	100.7	100.7	100.7	100.7	100.7	100.7	100.7	100.7	100.7
Pillar Width - centres (m)	38.0	38.0	38.0	38.0	38.0	305.4	38.0	38.0	37.0	36.5	36.0
Roadway Width for maximum pillar dimension	5.4	5.4	5.4	5.4	5.4	5.4	5.4	5.4	5.4	5.4	5.4
Roadway Width for minimum pillar dimension	5.4	5.4	5.4	5.4	5.4	5.4	5.4	5.4	5.4	5.4	5.4
Cut-Through Angle (degrees)	90	90	90	90	90	90	90	90	90	90	90
Average Panel Span (m) {rib-rib width}	97	97	97	97	97	97	97	97	97	97	97
SG (tonnes/m^3)	2.5	2.5	2.5	2.5	2.5	2.5	2.5	2.5	2.5	2.5	2.5
Conversion (tonnes to N)	10000	10000	10000	10000	10000	10000	10000	10000	10000	10000	10000
Abutment Angle (^{0})	21	21	21	21	21	21	21	21	21	21	21
W/H	0.52	0.53	0.54	0.56	0.57	0.53	0.52	0.52	0.53	0.54	0.55
PRELIMINARY CALCULATIONS											
Maximum Rib to Rib Pillar Length (w_2)	95.3	95.3	95.3	95.3	95.3	95.3	95.3	95.3	95.3	95.3	95.3
Minimum Rib to Rib Pillar Width (w_1)	32.6	32.6	32.6	32.6	32.6	300.0	32.60	32.60	31.60	31.10	30.60
w, Minimum Rib to Rib Pillar Width (ie $w_1 \sin\theta$)	32.6	32.6	32.6	32.6	32.6	300.0	32.60	32.60	31.60	31.10	30.60
Minimum Pillar Width/Height Ratio	10.2	10.2	10.2	10.2	10.2	29.8	10.2	10.2	9.9	9.7	9.6
Extraction Ratio (%)	18.8%	18.8%	18.8%	18.8%	18.8%	7.0%	18.8%	18.8%	19.2%	19.4%	19.6%
Abutment Angle (Radians)	0.367	0.367	0.367	0.367	0.367	0.367	0.367	0.367	0.367	0.367	0.367
Cut-Through Angle (Radians)	1.571	1.571	1.571	1.571	1.571	1.571	1.571	1.571	1.571	1.571	1.571
Is the Panel Super-Critical?	No	No	No	No	No	No	No	No	No	No	No
D (Peng & Chiang Loading Factor)	69.776	69.397	68.443	67.475	66.887	69.587	70.339	69.776	69.207	68.826	67.864
R (Pillar 2nd Abutment Component)	0.91	0.91	0.91	0.92	0.92	1.00	0.90	0.91	0.90	0.90	0.90
Dimensionless Pillar 'Rectangularity'	1.49	1.49	1.49	1.49	1.49	0.48	1.49	1.49	1.50	1.51	1.51
Width/Height Ratio Exponent	1.00	1.00	1.00	1.00	1.00	1.00	1.00	1.00	1.00	1.00	1.00
Effective Width Factor (Omega)	1.49	1.49	1.49	1.49	1.49	0.48	1.49	1.49	1.50	1.51	1.51
Effective Width Interim	48.58	48.58	48.58	48.58	48.58	144.65	48.58	48.58	47.46	46.90	46.33
Effective Pillar Width (m)	48.58	48.58	48.58	48.58	48.58	144.65	48.58	48.58	47.46	46.90	46.33
Effective Pillar Loading Height (m)	185.00	183.00	178.00	173.00	170.00	184.00	188.00	185.00	182.00	180.00	175.00
RESULTS											
Tributary Area Loading (MPa)	5.70	5.63	5.48	5.33	5.23	4.95	5.79	5.70	5.63	5.58	5.44
Pillar Strength (UNSW Squat Pillar 1999)	33.62	33.62	33.62	33.62	33.62	2112.89	33.62	33.62	32.18	31.49	30.81
Pillar Strength (UNSW w/h<5)	N/A	N/A	N/A	N/A	N/A	N/A	N/A	N/A	N/A	N/A	N/A
Safety Factor under FTA Loading (Squat Pillar)	5.90	5.97	6.13	6.31	6.42	427.01	5.81	5.90	5.72	5.64	5.66
Safety Factor under FTA Loading (w/h<5)	N/A	N/A	N/A	N/A	N/A	N/A	N/A	N/A	N/A	N/A	N/A
Single Abutment Loading (3D) - full	4.65	4.58	4.39	4.21	4.10	0.50	4.76	4.65	4.68	4.68	4.56
Single Abutment Loading (3D) - pillar	4.21	4.15	4.01	3.86	3.77	0.50	4.30	4.21	4.21	4.20	4.09
Single Abutment Loading (3D) - solid	0.44	0.42	0.39	0.35	0.33	0.00	0.46	0.44	0.47	0.49	0.47
Design Abutment Load Multiplier	1.00	1.00	1.00	1.00	1.00	1.00	1.00	1.00	1.00	1.00	1.00
Total Pillar Loading with Single Abutment Loading	10.91	10.79	10.49	10.18	10.00	6.45	11.09	10.91	10.84	10.78	10.53
Safety Factor (under Single Abutment Loading)	3.08	3.12	3.21	3.30	3.36	327.60	3.03	3.08	2.97	2.92	2.93
Total Pillar Loading @ nA	10.35	10.21	9.87	9.53	9.33	5.45	10.55	10.35	10.31	10.26	10.00
Safety Factor @ nA	3.25	3.29	3.41	3.53	3.60	387.71	3.19	3.25	3.12	3.07	3.08
Total Pillar Loading under Double Abutment Loading	15.00	14.79	14.27	13.74	13.43	5.95	15.32	15.00	15.00	14.94	14.56
Safety Factor (under Double Abutment Loading)	2.24	2.27	2.36	2.45	2.50	355.04	2.20	2.24	2.15	2.11	2.12
Elastic Model Subsidence											
Ecoal(GPa)	1.50	1.50	1.50	1.50	1.50	1.50	1.50	1.50	1.50	1.50	1.50
E1floor(GPa)	0.75	0.75	0.75	0.75	0.75	0.75	0.75	0.75	0.75	0.75	0.75
E2floor(GPa)	4.00	4.00	4.00	4.00	4.00	4.00	4.00	4.00	4.00	4.00	4.00
E1roof(GPa)	0.75	0.75	0.75	0.75	0.75	0.75	0.75	0.75	0.75	0.75	0.75
E2roof(GPa)	5.00	5.00	5.00	5.00	5.00	5.00	5.00	5.00	5.00	5.00	5.00
Poissons Ratio floor/roof	0.25	0.25	0.25	0.25	0.25	0.25	0.25	0.25	0.25	0.25	0.25
initial vertical stress (MPa)	4.63	4.58	4.45	4.33	4.25	4.60	4.70	4.63	4.55	4.50	4.38
increase in vertical stress for DA (MPa)	10.38	10.22	9.82	9.42	9.18	1.35	10.62	10.38	10.45	10.44	10.18
Roof t1	2.00	2.00	2.00	2.00	2.00	2.00	2.00	2.00	2.00	2.00	2.00
Roof t2	30.60	30.60	30.60	30.60	30.60	298.00	30.60	30.60	29.60	29.10	28.60
Roof sig1	10.37	10.21	9.81	9.41	9.17	1.35	10.62	10.37	10.45	10.44	10.18
Roof sig2	9.31	9.16	8.80	8.45	8.23	1.23	9.52	9.31	9.37	9.36	9.13
Floor t1	3.00	3.00	3.00	3.00	3.00	3.00	3.00	3.00	3.00	3.00	3.00
Floor t2	29.6	29.6	29.6	29.6	29.6	297.0	29.6	29.6	28.6	28.1	27.6
Floor sig1	10.37	10.21	9.81	9.41	9.17	1.35	10.61	10.37	10.45	10.44	10.18
Floor sig2	10.35	10.19	9.79	9.39	9.15	1.35	10.59	10.35	10.42	10.41	10.15
Pillar Compression (m)	0.021	0.020	0.020	0.019	0.018	0.003	0.021	0.021	0.021	0.021	0.020
Roof Compression (m)	0.079	0.078	0.075	0.072	0.070	0.072	0.081	0.079	0.078	0.077	0.074
Floor Compression (m)	0.111	0.109	0.105	0.100	0.098	0.099	0.113	0.111	0.109	0.108	0.104
Total FTA Compression (m)	0.211	0.208	0.199	0.191	0.186	0.174	0.216	0.211	0.208	0.206	0.199
Total Effective Compression (m)	0.211	0.208	0.199	0.191	0.186	0.174	0.216	0.211	0.208	0.206	0.199
2 times Effective Compression (m)	0.422	0.415	0.399	0.383	0.373	0.348	0.431	0.422	0.416	0.412	0.397
Total Yielded Panel Subs (m)	0.28	0.28	0.27	0.26	0.25	0.22	0.29	0.28	0.28	0.28	0.27
5 x Effective Predictions (m)	1.054	1.038	0.997	0.956	0.932	0.869	1.078	1.054	1.040	1.029	0.993
Bearing Capacity											
Upper Floor Unit UCS, 2*cu1 (MPa)	8.0	8.0	8.0	8.0	8.0	8.0	8.0	8.0	8.0	8.0	8.0
Upper Unit Thickness, H (m)	3.0	3.0	3.0	3.0	3.0	3.0	3.0	3.0	3.0	3.0	3.0
Lower Floor Unit UCS, 2*cu2 (MPa)	40.0	40.0	40.0	40.0	40.0	40.0	40.0	40.0	40.0	40.0	40.0
cu1/cu2	0.2	0.2	0.2	0.2	0.2	0.2	0.2	0.2	0.2	0.2	0.2
H/B	0.09	0.09	0.09	0.09	0.09	0.01	0.09	0.09	0.09	0.10	0.10
N*1	9.57	9.57	9.57	9.57	9.57	54.14	9.57	9.57	9.41	9.32	9.24
N*2	1.91	1.91	1.91	1.91	1.91	10.83	1.91	1.91	1.88	1.86	1.85
Floor Bearing Capacity (MPa)	38.3	38.3	38.3	38.3	38.3	216.6	38.3	38.3	37.6	37.3	37.0
Eff Pillar Stress (MPa)	15.0	14.8	14.3	13.7	13.4	6.0	15.3	15.0	15.0	14.9	14.6
Eff Floor Bearing Failure FoS	2.55	2.59	2.68	2.79	2.85	36.39	2.50	2.55	2.51	2.50	2.54
FTA Floor Bearing Failure FoS	6.72	6.80	6.99	7.19	7.32	43.77	6.62	6.72	6.69	6.68	6.80
Immediate Roof Unit UCS, 2*cu1 (MPa)	8.0	8.0	8.0	8.0	8.0	8.0	8.0	8.0	8.0	8.0	8.0
Immediate Roof Unit Thickness, H (m)	3.0	3.0	3.0	3.0	3.0	3.0	3.0	3.0	3.0	3.0	3.0
Upper Roof Unit UCS, 2*cu2 (MPa)	40.0	40.0	40.0	40.0	40.0	40.0	40.0	40.0	40.0	40.0	40.0
cu1/cu2	0.2	0.2	0.2	0.2	0.2	0.2	0.2	0.2	0.2	0.2	0.2
H/B	0.09	0.09	0.09	0.09	0.09	0.01	0.09	0.09	0.09	0.10	0.10
N*1	9.57	9.57	9.57	9.57	9.57	54.14	9.57	9.57	9.41	9.32	9.24
N*2	1.91	1.91	1.91	1.91	1.91	10.83	1.91	1.91	1.88	1.86	1.85
Roof Bearing Capacity (MPa)	38.3	38.3	38.3	38.3	38.3	216.6	38.3	38.3	37.6	37.3	37.0
Pillar Stress (MPa)	15.0	14.8	14.3	13.7	13.4	6.0	15.3	15.0	15.0	14.9	14.6
Effective Roof Bearing Failure FoS	2.55	2.59	2.68	2.79	2.85	36.39	2.50	2.55	2.51	2.50	2.54
FTA Roof Bearing Failure FoS	6.72	6.80	6.99	7.19	7.32	43.77	6.62	6.72	6.69	6.68	6.80
Voussoir Beam Deflection (m)	0.011	0.021	0.010	0.038	0.887	0.913	0.691	1.072	0.957	0.957	0.957
System Settlement at Base of beam (m)	0.000	0.000	0.000	0.000	0.000	0.000	0.000	0.000	0.000	0.000	0.000
Applied Pillar Stress/FTA Stress Ratio (Mpa)	1.00	1.00	1.00	1.00	1.00	1.00	1.00	1.00	1.00	1.00	1.00
Effective Pillar Stress (Mpa)	15.00	14.79	14.27	13.74	13.43	5.95	15.32	15.00	15.00	14.94	14.56
Multi-Seam Stress Inc (min)											
Multi-Seam Stress Inc (max)											
Effective Pillar FoS	2.24	2.27	2.36	2.45	2.50	355.04	2.20	2.24	2.15	2.11	2.12
Eresidual coal(GPa)	0.27	0.27	0.27	0.27	0.27	0.38	0.27	0.27	0.26	0.26	0.25

UNSW Pillar Design Spreadsheet	29.9	29.3	29.3	32.6	31.6	31.1	30.6	29.9	29.3	29.3	29.3
	5.6	**5.7**	**5.8**	**6.1**	**6.2**	**6.3**	**6.4**	**6.5**	**6.6**	**6.7**	**6.8**
Chain Valley XL.Panel#	6.6	6.7	6.8	6.9	6.10	6.11	6.12	7.1	7.2	7.3	7.4
INPUT DATA	95.3	95.3	94.8	95.3	95.3	95.3	95.3	95.3	95.3	95.3	95.3
Depth of Cover (m)	**170**	**165**	**160**	**185**	**178**	**175**	**173**	**168**	**163**	**160**	**158**
Mining Height (m)	**3.2**	**3.2**	**3.2**	**3.2**	**3.2**	**3.2**	**3.2**	**3.2**	**3.2**	**3.2**	**3.2**
Pillar Length - centres (m)	100.7	100.7	100.2	100.7	100.7	100.7	100.7	100.7	100.7	100.7	100.7
Pillar Width - centres (m)	35.3	34.7	34.7	38.0	37.0	36.5	36.0	35.3	34.7	34.7	34.7
Roadway Width for maximum pillar dimension	5.4	5.4	5.4	5.4	5.4	5.4	5.4	5.4	5.4	5.4	5.4
Roadway Width for minimum pillar dimension	5.4	5.4	5.4	5.4	5.4	5.4	5.4	5.4	5.4	5.4	5.4
Cut-Through Angle (degrees)	**90**	**90**	**90**	**90**	**90**	**90**	**90**	**90**	**90**	**90**	**90**
Average Panel Span (m) {rib-rib width}	97	97	97	97	97	97	97	97	97	97	97
SG (tonnes/m^3)	2.5	2.5	2.5	2.5	2.5	2.5	2.5	2.5	2.5	2.5	2.5
Conversion (tonnes to N)	10000	10000	10000	10000	10000	10000	10000	10000	10000	10000	10000
Abutment Angle (^{0})	21	21	21	21	21	21	21	21	21	21	21
W/H	0.57	0.59	0.61	0.52	0.54	0.55	0.56	0.58	0.60	0.61	0.61
PRELIMINARY CALCULATIONS											
Maximum Rib to Rib Pillar Length (w_2)	**95.3**	**95.3**	**94.8**	**95.3**	**95.3**	**95.3**	**95.3**	**95.3**	**95.3**	**95.3**	**95.3**
Minimum Rib to Rib Pillar Width (w_1)	**29.90**	**29.30**	**29.30**	**32.60**	**31.60**	**31.10**	**30.60**	**29.90**	**29.30**	**29.30**	**29.30**
w, Minimum Rib to Rib Pillar Width (ie $w_1 \sin\theta$)	**29.90**	**29.30**	**29.30**	**32.60**	**31.60**	**31.10**	**30.60**	**29.90**	**29.30**	**29.30**	**29.30**
Minimum Pillar Width/Height Ratio	**9.3**	**9.2**	**9.2**	**10.2**	**9.9**	**9.7**	**9.6**	**9.3**	**9.2**	**9.2**	**9.2**
Extraction Ratio (%)	**19.8%**	**20.1%**	**20.1%**	**18.8%**	**19.2%**	**19.4%**	**19.6%**	**19.8%**	**20.1%**	**20.1%**	**20.1%**
Abutment Angle (Radians)	0.367	0.367	0.367	0.367	0.367	0.367	0.367	0.367	0.367	0.367	0.367
Cut-Through Angle (Radians)	1.571	1.571	1.571	1.571	1.571	1.571	1.571	1.571	1.571	1.571	1.571
Is the Panel Super-Critical?	No	No	No	No	No	No	No	No	No	No	No
D (Peng & Chiang Loading Factor)	66.887	65.896	64.890	69.776	68.443	67.864	67.475	66.492	65.495	64.890	64.483
R (Pillar 2nd Abutment Component)	0.89	0.89	0.90	0.91	0.90	0.90	0.90	0.90	0.90	0.90	0.90
Dimensionless Pillar 'Rectangularity'	1.52	1.53	1.53	1.49	1.50	1.51	1.51	1.52	1.53	1.53	1.53
Width/Height Ratio Exponent	1.00	1.00	1.00	1.00	1.00	1.00	1.00	1.00	1.00	1.00	1.00
Effective Width Factor (Omega)	1.52	1.53	1.53	1.49	1.50	1.51	1.51	1.52	1.53	1.53	1.53
Effective Width Interim	45.52	44.82	44.76	48.58	47.46	46.90	46.33	45.52	44.82	44.82	44.82
Effective Pillar Width (m)	45.52	44.82	44.76	48.58	47.46	46.90	46.33	45.52	44.82	44.82	44.82
Effective Pillar Loading Height (m)	170.00	165.00	160.00	185.00	178.00	175.00	173.00	168.00	163.00	160.00	158.00
RESULTS											
Tributary Area Loading (MPa)	**5.30**	**5.16**	**5.01**	**5.70**	**5.51**	**5.43**	**5.38**	**5.24**	**5.10**	**5.01**	**4.94**
Pillar Strength (UNSW Squat Pillar 1999)	**29.88**	**29.10**	**29.08**	**33.62**	**32.18**	**31.49**	**30.81**	**29.88**	**29.10**	**29.10**	**29.10**
Pillar Strength (UNSW w/h<5)	**N/A**	**N/A**	**N/A**	**N/A**	**N/A**	**N/A**	**N/A**	**N/A**	**N/A**	**N/A**	**N/A**
Safety Factor under FTA Loading (Squat Pillar)	**5.63**	**5.64**	**5.81**	**5.90**	**5.85**	**5.80**	**5.73**	**5.70**	**5.71**	**5.81**	**5.89**
Safety Factor under FTA Loading (w/h<5)	**N/A**	**N/A**	**N/A**	**N/A**	**N/A**	**N/A**	**N/A**	**N/A**	**N/A**	**N/A**	**N/A**
Single Abutment Loading (3D) - full	4.46	4.35	4.14	4.65	4.53	4.49	4.48	4.38	4.27	4.14	4.06
Single Abutment Loading (3D) - pillar	**3.99**	**3.89**	**3.73**	**4.21**	**4.09**	**4.04**	**4.03**	**3.93**	**3.82**	**3.73**	**3.66**
Single Abutment Loading (3D) - solid	0.47	0.46	0.42	0.44	0.44	0.44	0.45	0.45	0.44	0.42	0.40
Design Abutment Load Multiplier	1.00	1.00	1.00	1.00	1.00	1.00	1.00	1.00	1.00	1.00	1.00
Total Pillar Loading with Single Abutment Loading	10.30	10.05	9.73	10.91	10.60	10.47	10.40	10.17	9.92	9.73	9.60
Safety Factor (under Single Abutment Loading)	**2.90**	**2.90**	**2.99**	**3.08**	**3.04**	**3.01**	**2.96**	**2.94**	**2.93**	**2.99**	**3.03**
Total Pillar Loading @ nA	**9.77**	**9.51**	**9.15**	**10.35**	**10.04**	**9.91**	**9.86**	**9.62**	**9.37**	**9.15**	**9.00**
Safety Factor @ nA	**3.06**	**3.06**	**3.18**	**3.25**	**3.21**	**3.18**	**3.13**	**3.10**	**3.11**	**3.18**	**3.23**
Total Pillar Loading under Double Abutment Loading	14.23	13.86	13.30	15.00	14.57	14.40	14.34	14.01	13.63	13.29	13.06
Safety Factor (under Double Abutment Loading)	**2.10**	**2.10**	**2.19**	**2.24**	**2.21**	**2.19**	**2.15**	**2.13**	**2.13**	**2.19**	**2.23**
Elastic Model Subsidence											
Ecoal(GPa)	**1.50**	**1.50**	**1.50**	**1.50**	**1.50**	**1.50**	**1.50**	**1.50**	**1.50**	**1.50**	**1.50**
E1floor(GPa)	**0.75**	**0.75**	**0.75**	**0.75**	**0.75**	**0.75**	**0.75**	**0.75**	**0.75**	**0.75**	**0.75**
E2floor(GPa)	**4.00**	**4.00**	**4.00**	**4.00**	**4.00**	**4.00**	**4.00**	**4.00**	**4.00**	**4.00**	**4.00**
E1roof(GPa)	**0.75**	**0.75**	**0.75**	**0.75**	**0.75**	**0.75**	**0.75**	**0.75**	**0.75**	**0.75**	**0.75**
E2roof(GPa)	**5.00**	**5.00**	**5.00**	**5.00**	**5.00**	**5.00**	**5.00**	**5.00**	**5.00**	**5.00**	**5.00**
Poissons Ratio floor/roof	**0.25**	**0.25**	**0.25**	**0.25**	**0.25**	**0.25**	**0.25**	**0.25**	**0.25**	**0.25**	**0.25**
initial vertical stress (MPa)	**4.25**	**4.13**	**4.00**	**4.63**	**4.45**	**4.38**	**4.33**	**4.20**	**4.08**	**4.00**	**3.95**
increase in vertical stress for DA (MPa)	**9.98**	**9.74**	**9.30**	**10.38**	**10.12**	**10.02**	**10.01**	**9.81**	**9.56**	**9.29**	**9.11**
Roof t1	**2.00**	**2.00**	**2.00**	**2.00**	**2.00**	**2.00**	**2.00**	**2.00**	**2.00**	**2.00**	**2.00**
Roof t2	**27.90**	**27.30**	**27.30**	**30.60**	**29.60**	**29.10**	**28.60**	**27.90**	**27.30**	**27.30**	**27.30**
Roof sig1	**9.98**	**9.74**	**9.30**	**10.37**	**10.12**	**10.02**	**10.01**	**9.81**	**9.56**	**9.29**	**9.11**
Roof sig2	**8.94**	**8.72**	**8.32**	**9.31**	**9.07**	**8.99**	**8.97**	**8.78**	**8.56**	**8.32**	**8.16**
Floor t1	**3.00**	**3.00**	**3.00**	**3.00**	**3.00**	**3.00**	**3.00**	**3.00**	**3.00**	**3.00**	**3.00**
Floor t2	**26.9**	**26.3**	**26.3**	**29.6**	**28.6**	**28.1**	**27.6**	**26.9**	**26.3**	**26.3**	**26.3**
Floor sig1	**9.98**	**9.74**	**9.30**	**10.37**	**10.12**	**10.02**	**10.01**	**9.81**	**9.56**	**9.29**	**9.11**
Floor sig2	**9.95**	**9.70**	**9.26**	**10.35**	**10.09**	**10.00**	**9.98**	**9.78**	**9.53**	**9.26**	**9.08**
Pillar Compression (m)	**0.020**	**0.019**	**0.019**	**0.021**	**0.020**	**0.020**	**0.020**	**0.020**	**0.019**	**0.019**	**0.018**
Roof Compression (m)	**0.072**	**0.069**	**0.066**	**0.079**	**0.076**	**0.074**	**0.073**	**0.070**	**0.068**	**0.066**	**0.065**
Floor Compression (m)	**0.100**	**0.096**	**0.092**	**0.111**	**0.106**	**0.103**	**0.102**	**0.098**	**0.095**	**0.092**	**0.090**
Total FTA Compression (m)	**0.192**	**0.185**	**0.176**	**0.211**	**0.201**	**0.198**	**0.195**	**0.188**	**0.181**	**0.176**	**0.173**
Total Effective Compression (m)	**0.192**	**0.185**	**0.176**	**0.211**	**0.201**	**0.198**	**0.195**	**0.188**	**0.181**	**0.176**	**0.173**
2 times Effective Compression (m)	**0.384**	**0.370**	**0.353**	**0.422**	**0.403**	**0.395**	**0.391**	**0.377**	**0.363**	**0.353**	**0.346**
Total Yielded Panel Subs (m)	**0.26**	**0.25**	**0.24**	**0.28**	**0.27**	**0.27**	**0.26**	**0.26**	**0.25**	**0.24**	**0.24**
5 x Effective Predictions (m)	**0.959**	**0.924**	**0.882**	**1.054**	**1.007**	**0.988**	**0.977**	**0.942**	**0.907**	**0.882**	**0.865**
Bearing Capacity											
Upper Floor Unit UCS, 2*cu1 (MPa)	**8.0**	**8.0**	**8.0**	**8.0**	**8.0**	**8.0**	**8.0**	**8.0**	**8.0**	**8.0**	**8.0**
Upper Unit Thickness, H (m)	**3.0**	**3.0**	**3.0**	**3.0**	**3.0**	**3.0**	**3.0**	**3.0**	**3.0**	**3.0**	**3.0**
Lower Floor Unit UCS, 2*cu2 (MPa)	**40.0**	**40.0**	**40.0**	**40.0**	**40.0**	**40.0**	**40.0**	**40.0**	**40.0**	**40.0**	**40.0**
cu1/cu2	**0.2**	**0.2**	**0.2**	**0.2**	**0.2**	**0.2**	**0.2**	**0.2**	**0.2**	**0.2**	**0.2**
H/B	**0.10**	**0.10**	**0.10**	**0.09**	**0.09**	**0.10**	**0.10**	**0.10**	**0.10**	**0.10**	**0.10**
N*1	**9.12**	**9.02**	**9.02**	**9.57**	**9.41**	**9.32**	**9.24**	**9.12**	**9.02**	**9.02**	**9.02**
N*2	**1.82**	**1.80**	**1.80**	**1.91**	**1.88**	**1.86**	**1.85**	**1.82**	**1.80**	**1.80**	**1.80**
Floor Bearing Capacity (MPa)	**36.5**	**36.1**	**36.1**	**38.3**	**37.6**	**37.3**	**37.0**	**36.5**	**36.1**	**36.1**	**36.1**
Eff Pillar Stress (MPa)	**14.2**	**13.9**	**13.3**	**15.0**	**14.6**	**14.4**	**14.3**	**14.0**	**13.6**	**13.3**	**13.1**
Eff Floor Bearing Failure FoS	**2.56**	**2.60**	**2.71**	**2.55**	**2.58**	**2.59**	**2.58**	**2.61**	**2.65**	**2.72**	**2.76**
FTA Floor Bearing Failure FoS	**6.88**	**6.99**	**7.21**	**6.72**	**6.84**	**6.87**	**6.88**	**6.97**	**7.08**	**7.21**	**7.30**
Immediate Roof Unit UCS, 2*cu1 (MPa)	**8.0**	**8.0**	**8.0**	**8.0**	**8.0**	**8.0**	**8.0**	**8.0**	**8.0**	**8.0**	**8.0**
Immediate Roof Unit Thickness, H (m)	**3.0**	**3.0**	**3.0**	**3.0**	**3.0**	**3.0**	**3.0**	**3.0**	**3.0**	**3.0**	**3.0**
Upper Roof Unit UCS, 2*cu2 (MPa)	**40.0**	**40.0**	**40.0**	**40.0**	**40.0**	**40.0**	**40.0**	**40.0**	**40.0**	**40.0**	**40.0**
cu1/cu2	**0.2**	**0.2**	**0.2**	**0.2**	**0.2**	**0.2**	**0.2**	**0.2**	**0.2**	**0.2**	**0.2**
H/B	**0.10**	**0.10**	**0.10**	**0.09**	**0.09**	**0.10**	**0.10**	**0.10**	**0.10**	**0.10**	**0.10**
N*1	**9.12**	**9.02**	**9.02**	**9.57**	**9.41**	**9.32**	**9.24**	**9.12**	**9.02**	**9.02**	**9.02**
N*2	1.82	1.80	1.80	1.91	1.88	1.86	1.85	1.82	1.80	1.80	1.80
Roof Bearing Capacity (MPa)	36.5	36.1	36.1	38.3	37.6	37.3	37.0	36.5	36.1	36.1	36.1
Pillar Stress (MPa)	**14.2**	**13.9**	**13.3**	**15.0**	**14.6**	**14.4**	**14.3**	**14.0**	**13.6**	**13.3**	**13.1**
Effective Roof Bearing Failure FoS	**2.56**	**2.60**	**2.71**	**2.55**	**2.58**	**2.59**	**2.58**	**2.61**	**2.65**	**2.72**	**2.76**
FTA Roof Bearing Failure FoS	**6.88**	**6.99**	**7.21**	**6.72**	**6.84**	**6.87**	**6.88**	**6.97**	**7.08**	**7.21**	**7.30**
Voussoir Beam Deflection (m)	**0.957**	**0.957**	**0.957**	**0.957**	**0.957**	**0.957**	**0.957**	**0.957**	**0.957**	**0.957**	**0.957**
System Settlement at Base of beam (m)	0.000	0.000	0.000	0.000	0.000	0.000	0.000	0.000	0.000	0.000	0.000
Applied Pillar Stress/FTA Stress Ratio (Mpa)	1.00	1.00	1.00	1.00	1.00	1.00	1.00	1.00	1.00	1.00	1.00
Effective Pillar Stress (Mpa)	14.23	13.86	13.30	15.00	14.57	14.40	14.34	14.01	13.63	13.29	13.06
Multi-Seam Stress Inc (min)											
Multi-Seam Stress Inc (max)											
Effective Pillar FoS	**2.10**	**2.10**	**2.19**	**2.24**	**2.21**	**2.19**	**2.15**	**2.13**	**2.13**	**2.19**	**2.23**
Eresidual coal(GPa)	**0.25**	**0.25**	**0.25**	**0.27**	**0.26**	**0.26**	**0.25**	**0.25**	**0.25**	**0.25**	**0.25**

UNSW Pillar Design Spreadsheet	29.3	29.3	29.3	300.0	31.0	31.0	300.0	31.0	31.0	31.0	31.0
	6.9	**6.1**	**6.11**	**6.12**	**7.1**	**7.2**	**7.3**	**8.1**	**8.2**	**8.3**	**8.4**
Chain Valley XL.Panel#	7.5	7.6	7.7	7.8	7.9	7.10	7.11	7.12	7.13	7.14	8.1
INPUT DATA	95.3	94.8	94.8	94.8	95.3	95.3	95.3	95.3	95.3	95.3	95.3
Depth of Cover (m)	**156**	**153**	**150**	**148**	**167**	**168**	**169**	**187**	**188**	**189**	**190**
Mining Height (m)	**3.2**	**3.2**	**3.2**	**3.2**	**3.2**	**3.2**	**3.2**	**3.2**	**3.2**	**3.2**	**3.2**
Pillar Length - centres (m)	100.7	100.2	100.2	100.2	100.7	100.7	100.7	100.7	100.7	100.7	100.7
Pillar Width - centres (m)	34.7	34.7	34.7	305.4	36.4	36.4	305.4	36.4	36.4	36.4	36.4
Roadway Width for maximum pillar dimension	5.4	5.4	5.4	5.4	5.4	5.4	5.4	5.4	5.4	5.4	5.4
Roadway Width for minimum pillar dimension	5.4	5.4	5.4	5.4	5.4	5.4	5.4	5.4	5.4	5.4	5.4
Cut-Through Angle (degrees)	**90**	**90**	**90**	**90**	**90**	**90**	**90**	**90**	**90**	**90**	**90**
Average Panel Span (m) {rib-rib width}	97	97	97	97	97	97	97	97	97	97	97
SG (tonnes/m^3)	2.5	2.5	2.5	2.5	2.5	2.5	2.5	2.5	2.5	2.5	2.5
Conversion (tonnes to N)	10000	10000	10000	10000	10000	10000	10000	10000	10000	10000	10000
Abutment Angle (^{0})	21	21	21	21	21	21	21	21	21	21	21
W/H	0.62	0.63	0.65	0.66	0.58	0.58	0.57	0.52	0.52	0.51	0.51
PRELIMINARY CALCULATIONS											
Maximum Rib to Rib Pillar Length (w_2)	**95.3**	**94.8**	**94.8**	**94.8**	**95.3**	**95.3**	**95.3**	**95.3**	**95.3**	**95.3**	**95.3**
Minimum Rib to Rib Pillar Width (w_1)	**29.30**	**29.30**	**29.30**	**300.00**	**31.00**	**31.00**	**300.00**	**31.00**	**31.00**	**31.00**	**31.00**
w, Minimum Rib to Rib Pillar Width (ie $w_1 \sin\theta$)	**29.30**	**29.30**	**29.30**	**300.00**	**31.00**	**31.00**	**300.00**	**31.00**	**31.00**	**31.00**	**31.00**
Minimum Pillar Width/Height Ratio	**9.2**	**9.2**	**9.2**	**29.6**	**9.7**	**9.7**	**29.8**	**9.7**	**9.7**	**9.7**	**9.7**
Extraction Ratio (%)	**20.1%**	**20.1%**	**20.1%**	**7.1%**	**19.4%**	**19.4%**	**7.0%**	**19.4%**	**19.4%**	**19.4%**	**19.4%**
Abutment Angle (Radians)	0.367	0.367	0.367	0.367	0.367	0.367	0.367	0.367	0.367	0.367	0.367
Cut-Through Angle (Radians)	1.571	1.571	1.571	1.571	1.571	1.571	1.571	1.571	1.571	1.571	1.571
Is the Panel Super-Critical?	No	No	No	No	No	No	No	No	No	No	No
D (Peng & Chiang Loading Factor)	64.074	63.455	62.829	62.409	66.294	66.492	66.690	70.152	70.339	70.526	70.712
R (Pillar 2nd Abutment Component)	0.90	0.91	0.91	1.00	0.91	0.91	1.00	0.89	0.89	0.89	0.89
Dimensionless Pillar 'Rectangularity'	1.53	1.53	1.53	0.48	1.51	1.51	0.48	1.51	1.51	1.51	1.51
Width/Height Ratio Exponent	1.00	1.00	1.00	1.00	1.00	1.00	1.00	1.00	1.00	1.00	1.00
Effective Width Factor (Omega)	1.53	1.53	1.53	0.48	1.51	1.51	0.48	1.51	1.51	1.51	1.51
Effective Width Interim	44.82	44.76	44.76	144.07	46.78	46.78	144.65	46.78	46.78	46.78	46.78
Effective Pillar Width (m)	44.82	44.76	44.76	144.07	46.78	46.78	144.65	46.78	46.78	46.78	46.78
Effective Pillar Loading Height (m)	156.00	153.00	150.00	148.00	167.00	168.00	169.00	187.00	188.00	189.00	190.00
RESULTS											
Tributary Area Loading (MPa)	**4.88**	**4.79**	**4.69**	**3.98**	**5.18**	**5.21**	**4.54**	**5.80**	**5.83**	**5.86**	**5.89**
Pillar Strength (UNSW Squat Pillar 1999)	**29.10**	**29.08**	**29.08**	**2108.59**	**31.35**	**31.35**	**2112.89**	**31.35**	**31.35**	**31.35**	**31.35**
Pillar Strength (UNSW w/h<5)	**N/A**	**N/A**	**N/A**	**N/A**	**N/A**	**N/A**	**N/A**	**N/A**	**N/A**	**N/A**	**N/A**
Safety Factor under FTA Loading (Squat Pillar)	**5.96**	**6.07**	**6.20**	**529.64**	**6.05**	**6.02**	**464.91**	**5.40**	**5.38**	**5.35**	**5.32**
Safety Factor under FTA Loading (w/h<5)	**N/A**	**N/A**	**N/A**	**N/A**	**N/A**	**N/A**	**N/A**	**N/A**	**N/A**	**N/A**	**N/A**
Single Abutment Loading (3D) - full	3.98	3.86	3.73	0.36	4.19	4.23	0.44	4.97	5.01	5.05	5.09
Single Abutment Loading (3D) - pillar	**3.59**	**3.50**	**3.40**	**0.36**	**3.81**	**3.84**	**0.44**	**4.42**	**4.45**	**4.48**	**4.51**
Single Abutment Loading (3D) - solid	0.38	0.36	0.33	0.00	0.38	0.39	0.00	0.55	0.56	0.57	0.58
Design Abutment Load Multiplier	1.00	1.00	1.00	1.00	1.00	1.00	1.00	1.00	1.00	1.00	1.00
Total Pillar Loading with Single Abutment Loading	9.48	9.28	9.09	5.34	9.99	10.05	5.99	11.22	11.28	11.34	11.40
Safety Factor (under Single Abutment Loading)	**3.07**	**3.13**	**3.20**	**395.05**	**3.14**	**3.12**	**352.99**	**2.79**	**2.78**	**2.76**	**2.75**
Total Pillar Loading @ nA	**8.86**	**8.64**	**8.43**	**4.34**	**9.37**	**9.44**	**4.99**	**10.77**	**10.84**	**10.91**	**10.98**
Safety Factor @ nA	**3.28**	**3.36**	**3.45**	**486.13**	**3.35**	**3.32**	**423.79**	**2.91**	**2.89**	**2.87**	**2.86**
Total Pillar Loading under Double Abutment Loading	12.84	12.50	12.16	4.69	13.56	13.67	5.43	15.74	15.85	15.96	16.07
Safety Factor (under Double Abutment Loading)	**2.27**	**2.33**	**2.39**	**449.22**	**2.31**	**2.29**	**389.35**	**1.99**	**1.98**	**1.96**	**1.95**
Elastic Model Subsidence											
Ecoal(GPa)	**1.50**	**1.50**	**1.50**	**1.50**	**1.50**	**1.50**	**1.50**	**1.50**	**1.50**	**1.50**	**1.50**
E1floor(GPa)	**0.75**	**0.75**	**0.75**	**0.75**	**0.75**	**0.75**	**0.75**	**0.75**	**0.75**	**0.75**	**0.75**
E2floor(GPa)	**4.00**	**4.00**	**4.00**	**4.00**	**4.00**	**4.00**	**4.00**	**4.00**	**4.00**	**4.00**	**4.00**
E1roof(GPa)	**0.75**	**0.75**	**0.75**	**0.75**	**0.75**	**0.75**	**0.75**	**0.75**	**0.75**	**0.75**	**0.75**
E2roof(GPa)	**5.00**	**5.00**	**5.00**	**5.00**	**5.00**	**5.00**	**5.00**	**5.00**	**5.00**	**5.00**	**5.00**
Poissons Ratio floor/roof	**0.25**	**0.25**	**0.25**	**0.25**	**0.25**	**0.25**	**0.25**	**0.25**	**0.25**	**0.25**	**0.25**
initial vertical stress (MPa)	**3.90**	**3.83**	**3.75**	**3.70**	**4.18**	**4.20**	**4.23**	**4.68**	**4.70**	**4.73**	**4.75**
increase in vertical stress for DA (MPa)	**8.94**	**8.67**	**8.41**	**0.99**	**9.38**	**9.47**	**1.20**	**11.07**	**11.15**	**11.23**	**11.32**
Roof t1	**2.00**	**2.00**	**2.00**	**2.00**	**2.00**	**2.00**	**2.00**	**2.00**	**2.00**	**2.00**	**2.00**
Roof t2	**27.30**	**27.30**	**27.30**	**298.00**	**29.00**	**29.00**	**298.00**	**29.00**	**29.00**	**29.00**	**29.00**
Roof sig1	**8.94**	**8.67**	**8.41**	**0.99**	**9.38**	**9.47**	**1.20**	**11.07**	**11.15**	**11.23**	**11.32**
Roof sig2	**8.00**	**7.77**	**7.53**	**0.90**	**8.41**	**8.49**	**1.09**	**9.92**	**9.99**	**10.07**	**10.14**
Floor t1	**3.00**	**3.00**	**3.00**	**3.00**	**3.00**	**3.00**	**3.00**	**3.00**	**3.00**	**3.00**	**3.00**
Floor t2	**26.3**	**26.3**	**26.3**	**297.0**	**28.0**	**28.0**	**297.0**	**28.0**	**28.0**	**28.0**	**28.0**
Floor sig1	**8.94**	**8.67**	**8.41**	**0.99**	**9.38**	**9.47**	**1.20**	**11.06**	**11.15**	**11.23**	**11.32**
Floor sig2	**8.91**	**8.64**	**8.38**	**0.99**	**9.36**	**9.44**	**1.20**	**11.03**	**11.12**	**11.20**	**11.28**
Pillar Compression (m)	**0.018**	**0.017**	**0.017**	**0.002**	**0.019**	**0.019**	**0.002**	**0.022**	**0.022**	**0.022**	**0.023**
Roof Compression (m)	**0.063**	**0.061**	**0.060**	**0.053**	**0.069**	**0.070**	**0.064**	**0.082**	**0.082**	**0.083**	**0.083**
Floor Compression (m)	**0.088**	**0.086**	**0.083**	**0.073**	**0.097**	**0.097**	**0.088**	**0.114**	**0.115**	**0.116**	**0.116**
Total FTA Compression (m)	**0.170**	**0.165**	**0.160**	**0.128**	**0.185**	**0.186**	**0.155**	**0.218**	**0.219**	**0.221**	**0.223**
Total Effective Compression (m)	**0.170**	**0.165**	**0.160**	**0.128**	**0.185**	**0.186**	**0.155**	**0.218**	**0.219**	**0.221**	**0.223**
2 times Effective Compression (m)	**0.339**	**0.329**	**0.319**	**0.256**	**0.369**	**0.372**	**0.309**	**0.435**	**0.439**	**0.442**	**0.445**
Total Yielded Panel Subs (m)	**0.23**	**0.23**	**0.22**	**0.16**	**0.25**	**0.25**	**0.19**	**0.29**	**0.29**	**0.29**	**0.30**
5 x Effective Predictions (m)	**0.848**	**0.823**	**0.798**	**0.639**	**0.923**	**0.931**	**0.773**	**1.088**	**1.096**	**1.105**	**1.113**
Bearing Capacity											
Upper Floor Unit UCS, 2*cu1 (MPa)	**8.0**	**8.0**	**8.0**	**8.0**	**8.0**	**8.0**	**8.0**	**8.0**	**8.0**	**8.0**	**8.0**
Upper Unit Thickness, H (m)	**3.0**	**3.0**	**3.0**	**3.0**	**3.0**	**3.0**	**3.0**	**3.0**	**3.0**	**3.0**	**3.0**
Lower Floor Unit UCS, 2*cu2 (MPa)	**40.0**	**40.0**	**40.0**	**40.0**	**40.0**	**40.0**	**40.0**	**40.0**	**40.0**	**40.0**	**40.0**
cu1/cu2	**0.2**	**0.2**	**0.2**	**0.2**	**0.2**	**0.2**	**0.2**	**0.2**	**0.2**	**0.2**	**0.2**
H/B	**0.10**	**0.10**	**0.10**	**0.01**	**0.10**	**0.10**	**0.01**	**0.10**	**0.10**	**0.10**	**0.10**
N*1	**9.02**	**9.02**	**9.02**	**54.14**	**9.31**	**9.31**	**54.14**	**9.31**	**9.31**	**9.31**	**9.31**
N*2	**1.80**	**1.80**	**1.80**	**10.83**	**1.86**	**1.86**	**10.83**	**1.86**	**1.86**	**1.86**	**1.86**
Floor Bearing Capacity (MPa)	**36.1**	**36.1**	**36.1**	**216.6**	**37.2**	**37.2**	**216.6**	**37.2**	**37.2**	**37.2**	**37.2**
Eff Pillar Stress (MPa)	**12.8**	**12.5**	**12.2**	**4.7**	**13.6**	**13.7**	**5.4**	**15.7**	**15.8**	**16.0**	**16.1**
Eff Floor Bearing Failure FoS	**2.81**	**2.89**	**2.97**	**46.14**	**2.75**	**2.72**	**39.91**	**2.37**	**2.35**	**2.33**	**2.32**
FTA Floor Bearing Failure FoS	**7.40**	**7.54**	**7.69**	**54.40**	**7.19**	**7.14**	**47.65**	**6.42**	**6.38**	**6.35**	**6.32**
Immediate Roof Unit UCS, 2*cu1 (MPa)	**8.0**	**8.0**	**8.0**	**8.0**	**8.0**	**8.0**	**8.0**	**8.0**	**8.0**	**8.0**	**8.0**
Immediate Roof Unit Thickness, H (m)	**3.0**	**3.0**	**3.0**	**3.0**	**3.0**	**3.0**	**3.0**	**3.0**	**3.0**	**3.0**	**3.0**
Upper Roof Unit UCS, 2*cu2 (MPa)	**40.0**	**40.0**	**40.0**	**40.0**	**40.0**	**40.0**	**40.0**	**40.0**	**40.0**	**40.0**	**40.0**
cu1/cu2	**0.2**	**0.2**	**0.2**	**0.2**	**0.2**	**0.2**	**0.2**	**0.2**	**0.2**	**0.2**	**0.2**
H/B	**0.10**	**0.10**	**0.10**	**0.01**	**0.10**	**0.10**	**0.01**	**0.10**	**0.10**	**0.10**	**0.10**
N*1	**9.02**	**9.02**	**9.02**	**54.14**	**9.31**	**9.31**	**54.14**	**9.31**	**9.31**	**9.31**	**9.31**
N*2	1.80	1.80	1.80	10.83	1.86	1.86	10.83	1.86	1.86	1.86	1.86
Roof Bearing Capacity (MPa)	36.1	36.1	36.1	216.6	37.2	37.2	216.6	37.2	37.2	37.2	37.2
Pillar Stress (MPa)	**12.8**	**12.5**	**12.2**	**4.7**	**13.6**	**13.7**	**5.4**	**15.7**	**15.8**	**16.0**	**16.1**
Effective Roof Bearing Failure FoS	**2.81**	**2.89**	**2.97**	**46.14**	**2.75**	**2.72**	**39.91**	**2.37**	**2.35**	**2.33**	**2.32**
FTA Roof Bearing Failure FoS	**7.40**	**7.54**	**7.69**	**54.40**	**7.19**	**7.14**	**47.65**	**6.42**	**6.38**	**6.35**	**6.32**
Voussoir Beam Deflection (m)	**0.957**	**0.957**	**0.957**	**0.957**	**0.957**	**0.957**	**0.957**	**0.957**	**0.957**	**0.957**	**0.957**
System Settlement at Base of beam (m)	0.000	0.000	0.000	0.000	0.000	0.000	0.000	0.000	0.000	0.000	0.000
Applied Pillar Stress/FTA Stress Ratio (Mpa)	1.00	1.00	1.00	1.00	1.00	1.00	1.00	1.00	1.00	1.00	1.00
Effective Pillar Stress (Mpa)	12.84	12.50	12.16	4.69	13.56	13.67	5.43	15.74	15.85	15.96	16.07
Multi-Seam Stress Inc (min)											
Multi-Seam Stress Inc (max)											
Effective Pillar FoS	**2.27**	**2.33**	**2.39**	**449.22**	**2.31**	**2.29**	**389.35**	**1.99**	**1.98**	**1.96**	**1.95**
Eresidual coal(GPa)	**0.25**	**0.25**	**0.25**	**0.38**	**0.26**	**0.26**	**0.38**	**0.26**	**0.26**	**0.26**	**0.26**

UNSW Pillar Design Spreadsheet	31.0	31.0	30.6	30.6	30.6	30.6	30.6	30.6	30.6	30.6	30.6
	8.5	**8.6**	**9.1**	**9.2**	**9.3**	**9.4**	**9.5**	**10.1**	**10.2**	**10.3**	**10.4**
Chain Valley XL.Panel#	8.2	8.3	8.4	8.5	9.1	9.2	9.3	9.4	10.1	10.2	10.3
INPUT DATA	95.3	95.3	95.3	95.3	95.3	95.3	95.3	95.3	95.3	95.3	95.3
Depth of Cover (m)	**190**	**190**	**219**	**218**	**221**	**220**	**217**	**229**	**230**	**231**	**232**
Mining Height (m)	**3.2**	**3.2**	**3.2**	**3.2**	**3.2**	**3.2**	**3.2**	**3.2**	**3.2**	**3.2**	**3.2**
Pillar Length - centres (m)	100.7	100.7	100.7	100.7	100.7	100.7	100.7	100.7	100.7	100.7	100.7
Pillar Width - centres (m)	36.4	36.4	36.0	36.0	36.0	36.0	36.0	36.0	36.0	36.0	36.0
Roadway Width for maximum pillar dimension	5.4	5.4	5.4	5.4	5.4	5.4	5.4	5.4	5.4	5.4	5.4
Roadway Width for minimum pillar dimension	5.4	5.4	5.4	5.4	5.4	5.4	5.4	5.4	5.4	5.4	5.4
Cut-Through Angle (degrees)	**90**	**90**	**90**	**90**	**90**	**90**	**90**	**90**	**90**	**90**	**90**
Average Panel Span (m) {rib-rib width}	97	97	97	97	97	97	97	97	97	**97**	**97**
SG (tonnes/m^3)	2.5	2.5	2.5	2.5	2.5	2.5	2.5	2.5	2.5	2.5	2.5
Conversion (tonnes to N)	10000	10000	10000	10000	10000	10000	10000	10000	10000	10000	10000
Abutment Angle (^{0})	21	21	21	21	21	21	21	21	21	21	21
W/H	0.51	0.51	0.44	0.44	0.44	0.44	0.45	0.42	0.42	0.42	0.42
PRELIMINARY CALCULATIONS											
Maximum Rib to Rib Pillar Length (w_2)	**95.3**	**95.3**	**95.3**	**95.3**	**95.3**	**95.3**	**95.3**	**95.3**	**95.3**	**95.3**	**95.3**
Minimum Rib to Rib Pillar Width (w_1)	**31.00**	**31.00**	**30.60**	**30.60**	**30.60**	**30.60**	**30.60**	**30.60**	**30.60**	**30.60**	**30.60**
w, Minimum Rib to Rib Pillar Width (ie $w_1 \sin\theta$)	**31.00**	**31.00**	**30.60**	**30.60**	**30.60**	**30.60**	**30.60**	**30.60**	**30.60**	**30.60**	**30.60**
Minimum Pillar Width/Height Ratio	**9.7**	**9.7**	**9.6**	**9.6**	**9.6**	**9.6**	**9.6**	**9.6**	**9.6**	**9.6**	**9.6**
Extraction Ratio (%)	**19.4%**	**19.4%**	**19.6%**	**19.6%**	**19.6%**	**19.6%**	**19.6%**	**19.6%**	**19.6%**	**19.6%**	**19.6%**
Abutment Angle (Radians)	0.367	0.367	0.367	0.367	0.367	0.367	0.367	0.367	0.367	0.367	0.367
Cut-Through Angle (Radians)	1.571	1.571	1.571	1.571	1.571	1.571	1.571	1.571	1.571	1.571	1.571
Is the Panel Super-Critical?	No	No	No	No	No	No	No	No	No	No	No
D (Peng & Chiang Loading Factor)	70.712	70.712	75.917	75.744	76.263	76.090	75.570	77.631	77.800	77.969	78.138
R (Pillar 2nd Abutment Component)	0.89	0.89	0.85	0.86	0.85	0.85	0.86	0.85	0.84	0.84	0.84
Dimensionless Pillar 'Rectangularity'	1.51	1.51	1.51	1.51	1.51	1.51	1.51	1.51	1.51	1.51	1.51
Width/Height Ratio Exponent	1.00	1.00	1.00	1.00	1.00	1.00	1.00	1.00	1.00	1.00	1.00
Effective Width Factor (Omega)	1.51	1.51	1.51	1.51	1.51	1.51	1.51	1.51	1.51	1.51	1.51
Effective Width Interim	46.78	46.78	46.33	46.33	46.33	46.33	46.33	46.33	46.33	46.33	46.33
Effective Pillar Width (m)	46.78	46.78	46.33	46.33	46.33	46.33	46.33	46.33	46.33	46.33	46.33
Effective Pillar Loading Height (m)	190.00	190.00	219.00	218.00	221.00	220.00	217.00	229.00	230.00	231.00	232.00
RESULTS											
Tributary Area Loading (MPa)	**5.89**	**5.89**	**6.81**	**6.78**	**6.87**	**6.84**	**6.74**	**7.12**	**7.15**	**7.18**	**7.21**
Pillar Strength (UNSW Squat Pillar 1999)	**31.35**	**31.35**	**30.81**	**30.81**	**30.81**	**30.81**	**30.81**	**30.81**	**30.81**	**30.81**	**30.81**
Pillar Strength (UNSW w/h<5)	**N/A**	**N/A**	**N/A**	**N/A**	**N/A**	**N/A**	**N/A**	**N/A**	**N/A**	**N/A**	**N/A**
Safety Factor under FTA Loading (Squat Pillar)	**5.32**	**5.32**	**4.53**	**4.55**	**4.49**	**4.51**	**4.57**	**4.33**	**4.31**	**4.29**	**4.27**
Safety Factor under FTA Loading (w/h<5)	**N/A**	**N/A**	**N/A**	**N/A**	**N/A**	**N/A**	**N/A**	**N/A**	**N/A**	**N/A**	**N/A**
Single Abutment Loading (3D) - full	5.09	5.09	6.30	6.26	6.38	6.34	6.22	6.70	6.74	6.77	6.81
Single Abutment Loading (3D) - pillar	**4.51**	**4.51**	**5.38**	**5.36**	**5.44**	**5.41**	**5.33**	**5.66**	**5.69**	**5.72**	**5.75**
Single Abutment Loading (3D) - solid	0.58	0.58	0.92	0.90	0.94	0.93	0.89	1.03	1.04	1.06	1.07
Design Abutment Load Multiplier	1.00	1.00	1.00	1.00	1.00	1.00	1.00	1.00	1.00	1.00	1.00
Total Pillar Loading with Single Abutment Loading	11.40	11.40	13.19	13.13	13.31	13.25	13.07	13.78	13.84	13.90	13.96
Safety Factor (under Single Abutment Loading)	**2.75**	**2.75**	**2.34**	**2.35**	**2.31**	**2.33**	**2.36**	**2.24**	**2.23**	**2.22**	**2.21**
Total Pillar Loading @ nA	**10.98**	**10.98**	**13.11**	**13.04**	**13.25**	**13.18**	**12.97**	**13.81**	**13.88**	**13.95**	**14.02**
Safety Factor @ nA	**2.86**	**2.86**	**2.35**	**2.36**	**2.33**	**2.34**	**2.38**	**2.23**	**2.22**	**2.21**	**2.20**
Total Pillar Loading under Double Abutment Loading	16.07	16.07	19.41	19.30	19.63	19.52	19.19	20.51	20.62	20.73	20.84
Safety Factor (under Double Abutment Loading)	**1.95**	**1.95**	**1.59**	**1.60**	**1.57**	**1.58**	**1.61**	**1.50**	**1.49**	**1.49**	**1.48**
Elastic Model Subsidence											
Ecoal(GPa)	**1.50**	**1.50**	**1.50**	**1.50**	**1.50**	**1.50**	**1.50**	**1.50**	**1.50**	**1.50**	**1.50**
E1floor(GPa)	**0.75**	**0.75**	**0.75**	**0.75**	**0.75**	**0.75**	**0.75**	**0.75**	**0.75**	**0.75**	**0.75**
E2floor(GPa)	**4.00**	**4.00**	**4.00**	**4.00**	**4.00**	**4.00**	**4.00**	**4.00**	**4.00**	**4.00**	**4.00**
E1roof(GPa)	**0.75**	**0.75**	**0.75**	**0.75**	**0.75**	**0.75**	**0.75**	**0.75**	**0.75**	**0.75**	**0.75**
E2roof(GPa)	**5.00**	**5.00**	**5.00**	**5.00**	**5.00**	**5.00**	**5.00**	**5.00**	**5.00**	**5.00**	**5.00**
Poissons Ratio floor/roof	**0.25**	**0.25**	**0.25**	**0.25**	**0.25**	**0.25**	**0.25**	**0.25**	**0.25**	**0.25**	**0.25**
initial vertical stress (MPa)	**4.75**	**4.75**	**5.48**	**5.45**	**5.53**	**5.50**	**5.43**	**5.73**	**5.75**	**5.78**	**5.80**
increase in vertical stress for DA (MPa)	**11.32**	**11.32**	**13.93**	**13.85**	**14.10**	**14.02**	**13.76**	**14.78**	**14.87**	**14.95**	**15.04**
Roof t1	**2.00**	**2.00**	**2.00**	**2.00**	**2.00**	**2.00**	**2.00**	**2.00**	**2.00**	**2.00**	**2.00**
Roof t2	**29.00**	**29.00**	**28.60**	**28.60**	**28.60**	**28.60**	**28.60**	**28.60**	**28.60**	**28.60**	**28.60**
Roof sig1	**11.32**	**11.32**	**13.93**	**13.85**	**14.10**	**14.02**	**13.76**	**14.78**	**14.87**	**14.95**	**15.04**
Roof sig2	**10.14**	**10.14**	**12.48**	**12.41**	**12.64**	**12.56**	**12.33**	**13.25**	**13.32**	**13.40**	**13.48**
Floor t1	**3.00**	**3.00**	**3.00**	**3.00**	**3.00**	**3.00**	**3.00**	**3.00**	**3.00**	**3.00**	**3.00**
Floor t2	**28.0**	**28.0**	**27.6**	**27.6**	**27.6**	**27.6**	**27.6**	**27.6**	**27.6**	**27.6**	**27.6**
Floor sig1	**11.32**	**11.32**	**13.93**	**13.84**	**14.10**	**14.02**	**13.76**	**14.78**	**14.87**	**14.95**	**15.04**
Floor sig2	**11.28**	**11.28**	**13.89**	**13.80**	**14.06**	**13.97**	**13.72**	**14.74**	**14.82**	**14.91**	**14.99**
Pillar Compression (m)	**0.023**	**0.023**	**0.028**	**0.028**	**0.028**	**0.028**	**0.028**	**0.030**	**0.030**	**0.030**	**0.030**
Roof Compression (m)	**0.083**	**0.083**	**0.102**	**0.101**	**0.103**	**0.102**	**0.101**	**0.108**	**0.109**	**0.109**	**0.110**
Floor Compression (m)	**0.116**	**0.116**	**0.142**	**0.141**	**0.144**	**0.143**	**0.140**	**0.151**	**0.152**	**0.153**	**0.153**
Total FTA Compression (m)	**0.223**	**0.223**	**0.272**	**0.270**	**0.275**	**0.273**	**0.268**	**0.288**	**0.290**	**0.292**	**0.293**
Total Effective Compression (m)	**0.223**	**0.223**	**0.272**	**0.270**	**0.275**	**0.273**	**0.268**	**0.288**	**0.290**	**0.292**	**0.293**
2 times Effective Compression (m)	**0.445**	**0.445**	**0.543**	**0.540**	**0.550**	**0.547**	**0.537**	**0.577**	**0.580**	**0.583**	**0.587**
Total Yielded Panel Subs (m)	**0.30**	**0.30**	**0.36**	**0.36**	**0.36**	**0.36**	**0.35**	**0.38**	**0.38**	**0.38**	**0.38**
5 x Effective Predictions (m)	**1.113**	**1.113**	**1.359**	**1.350**	**1.375**	**1.367**	**1.342**	**1.442**	**1.450**	**1.458**	**1.467**
Bearing Capacity											
Upper Floor Unit UCS, 2*cu1 (MPa)	**8.0**	**8.0**	**8.0**	**8.0**	**8.0**	**8.0**	**8.0**	**8.0**	**8.0**	**8.0**	**8.0**
Upper Unit Thickness, H (m)	**3.0**	**3.0**	**3.0**	**3.0**	**3.0**	**3.0**	**3.0**	**3.0**	**3.0**	**3.0**	**3.0**
Lower Floor Unit UCS, 2*cu2 (MPa)	**40.0**	**40.0**	**40.0**	**40.0**	**40.0**	**40.0**	**40.0**	**40.0**	**40.0**	**40.0**	**40.0**
cu1/cu2	**0.2**	**0.2**	**0.2**	**0.2**	**0.2**	**0.2**	**0.2**	**0.2**	**0.2**	**0.2**	**0.2**
H/B	**0.10**	**0.10**	**0.10**	**0.10**	**0.10**	**0.10**	**0.10**	**0.10**	**0.10**	**0.10**	**0.10**
N*1	**9.31**	**9.31**	**9.24**	**9.24**	**9.24**	**9.24**	**9.24**	**9.24**	**9.24**	**9.24**	**9.24**
N*2	**1.86**	**1.86**	**1.85**	**1.85**	**1.85**	**1.85**	**1.85**	**1.85**	**1.85**	**1.85**	**1.85**
Floor Bearing Capacity (MPa)	**37.2**	**37.2**	**37.0**	**37.0**	**37.0**	**37.0**	**37.0**	**37.0**	**37.0**	**37.0**	**37.0**
Eff Pillar Stress (MPa)	**16.1**	**16.1**	**19.4**	**19.3**	**19.6**	**19.5**	**19.2**	**20.5**	**20.6**	**20.7**	**20.8**
Eff Floor Bearing Failure FoS	**2.32**	**2.32**	**1.90**	**1.92**	**1.88**	**1.89**	**1.93**	**1.80**	**1.79**	**1.78**	**1.77**
FTA Floor Bearing Failure FoS	**6.32**	**6.32**	**5.43**	**5.46**	**5.38**	**5.41**	**5.48**	**5.19**	**5.17**	**5.15**	**5.13**
Immediate Roof Unit UCS, 2*cu1 (MPa)	**8.0**	**8.0**	**8.0**	**8.0**	**8.0**	**8.0**	**8.0**	**8.0**	**8.0**	**8.0**	**8.0**
Immediate Roof Unit Thickness, H (m)	**3.0**	**3.0**	**3.0**	**3.0**	**3.0**	**3.0**	**3.0**	**3.0**	**3.0**	**3.0**	**3.0**
Upper Roof Unit UCS, 2*cu2 (MPa)	**40.0**	**40.0**	**40.0**	**40.0**	**40.0**	**40.0**	**40.0**	**40.0**	**40.0**	**40.0**	**40.0**
cu1/cu2	**0.2**	**0.2**	**0.2**	**0.2**	**0.2**	**0.2**	**0.2**	**0.2**	**0.2**	**0.2**	**0.2**
H/B	**0.10**	**0.10**	**0.10**	**0.10**	**0.10**	**0.10**	**0.10**	**0.10**	**0.10**	**0.10**	**0.10**
N*1	**9.31**	**9.31**	**9.24**	**9.24**	**9.24**	**9.24**	**9.24**	**9.24**	**9.24**	**9.24**	**9.24**
N*2	1.86	1.86	1.85	1.85	1.85	1.85	1.85	1.85	1.85	1.85	1.85
Roof Bearing Capacity (MPa)	37.2	37.2	37.0	37.0	37.0	37.0	37.0	37.0	37.0	37.0	37.0
Pillar Stress (MPa)	**16.1**	**16.1**	**19.4**	**19.3**	**19.6**	**19.5**	**19.2**	**20.5**	**20.6**	**20.7**	**20.8**
Effective Roof Bearing Failure FoS	**2.32**	**2.32**	**1.90**	**1.92**	**1.88**	**1.89**	**1.93**	**1.80**	**1.79**	**1.78**	**1.77**
FTA Roof Bearing Failure FoS	**6.32**	**6.32**	**5.43**	**5.46**	**5.38**	**5.41**	**5.48**	**5.19**	**5.17**	**5.15**	**5.13**
Voussoir Beam Deflection (m)	**0.957**	**0.957**	**0.957**	**0.957**	**0.957**	**0.957**	**0.957**	**0.957**	**0.957**	**0.957**	**0.957**
System Settlement at Base of beam (m)	0.000	0.000	0.000	0.000	0.000	0.000	0.000	0.000	0.000	0.000	0.000
Applied Pillar Stress/FTA Stress Ratio (Mpa)	1.00	1.00	1.00	1.00	1.00	1.00	1.00	1.00	1.00	1.00	1.00
Effective Pillar Stress (Mpa)	16.07	16.07	19.41	19.30	**19.63**	**19.52**	**19.19**	**20.51**	**20.62**	**20.73**	**20.84**
Multi-Seam Stress Inc (min)											
Multi-Seam Stress Inc (max)											
Effective Pillar FoS	**1.95**	**1.95**	**1.59**	**1.60**	**1.57**	**1.58**	**1.61**	**1.50**	**1.49**	**1.49**	**1.48**
Eresidual coal(GPa)	**0.26**	**0.26**	**0.25**	**0.25**	**0.25**	**0.25**	**0.25**	**0.25**	**0.25**	**0.25**	**0.25**

UNSW Pillar Design Spreadsheet	300.0										
	10.5										
Chain Valley XL.Panel#	10.4	9.1	9.2	9.3	9.4	9.5	10.1	10.2	10.3	10.4	10.5
INPUT DATA	95.3	95.3	95.3	95.3	95.3	95.3	95.3	95.3	95.3	95.3	95.3
Depth of Cover (m)	228	219	218	221	220	217	229	230	231	232	228
Mining Height (m)	3.2	3.2	3.2	3.2	3.2	3.2	3.2	3.2	3.2	3.2	3.2
Pillar Length - centres (m)	100.7	100.7	100.7	100.7	100.7	100.7	100.7	100.7	100.7	100.7	100.7
Pillar Width - centres (m)	36.0	36.0	36.0	36.0	36.0	36.0	36.0	36.0	36.0	36.0	36.0
Roadway Width for maximum pillar dimension	5.4	5.4	5.4	5.4	5.4	5.4	5.4	5.4	5.4	5.4	5.4
Roadway Width for minimum pillar dimension	5.4	5.4	5.4	5.4	5.4	5.4	5.4	5.4	5.4	5.4	5.4
Cut-Through Angle (degrees)	90	90	90	90	90	90	90	90	90	90	90
Average Panel Span (m) {rib-rib width}	97	97	97	97	97	97	97	97	97	97	97
SG (tonnes/m^3)	2.5	2.5	2.5	2.5	2.5	2.5	2.5	2.5	2.5	2.5	2.5
Conversion (tonnes to N)	10000	10000	10000	10000	10000	10000	10000	10000	10000	10000	10000
Abutment Angle (^{0})	21	21	21	21	21	21	21	21	21	21	21
W/H	0.43	0.44	0.44	0.44	0.44	0.45	0.42	0.42	0.42	0.42	0.43
PRELIMINARY CALCULATIONS											
Maximum Rib to Rib Pillar Length (w_2)	95.3	95.3	95.3	95.3	95.3	95.3	95.3	95.3	95.3	95.3	95.3
Minimum Rib to Rib Pillar Width (w_1)	30.60	30.60	30.60	30.60	30.60	30.60	30.60	30.60	30.60	30.60	30.60
w, Minimum Rib to Rib Pillar Width (ie $w_1 \sin\theta$)	30.60	30.60	30.60	30.60	30.60	30.60	30.60	30.60	30.60	30.60	30.60
Minimum Pillar Width/Height Ratio	9.6	9.6	9.6	9.6	9.6	9.6	9.6	9.6	9.6	9.6	9.6
Extraction Ratio (%)	19.6%	19.6%	19.6%	19.6%	19.6%	19.6%	19.6%	19.6%	19.6%	19.6%	19.6%
Abutment Angle (Radians)	0.367	0.367	0.367	0.367	0.367	0.367	0.367	0.367	0.367	0.367	0.367
Cut-Through Angle (Radians)	1.571	1.571	1.571	1.571	1.571	1.571	1.571	1.571	1.571	1.571	1.571
Is the Panel Super-Critical?	No	No	No	No	No	No	No	No	No	No	No
D (Peng & Chiang Loading Factor)	77.461	75.917	75.744	76.263	76.090	75.570	77.631	77.800	77.969	78.138	77.461
R (Pillar 2nd Abutment Component)	0.85	0.85	0.86	0.85	0.85	0.86	0.85	0.84	0.84	0.84	0.85
Dimensionless Pillar 'Rectangularity'	1.51	1.51	1.51	1.51	1.51	1.51	1.51	1.51	1.51	1.51	1.51
Width/Height Ratio Exponent	1.00	1.00	1.00	1.00	1.00	1.00	1.00	1.00	1.00	1.00	1.00
Effective Width Factor (Omega)	1.51	1.51	1.51	1.51	1.51	1.51	1.51	1.51	1.51	1.51	1.51
Effective Width Interim	46.33	46.33	46.33	46.33	46.33	46.33	46.33	46.33	46.33	46.33	46.33
Effective Pillar Width (m)	46.33	46.33	46.33	46.33	46.33	46.33	46.33	46.33	46.33	46.33	46.33
Effective Pillar Loading Height (m)	228.00	219.00	218.00	221.00	220.00	217.00	229.00	230.00	231.00	232.00	228.00
RESULTS											
Tributary Area Loading (MPa)	7.09	6.81	6.78	6.87	6.84	6.74	7.12	7.15	7.18	7.21	7.09
Pillar Strength (UNSW Squat Pillar 1999)	30.81	30.81	30.81	30.81	30.81	30.81	30.81	30.81	30.81	30.81	30.81
Pillar Strength (UNSW w/h<5)	N/A	N/A	N/A	N/A	N/A	N/A	N/A	N/A	N/A	N/A	N/A
Safety Factor under FTA Loading (Squat Pillar)	4.35	4.53	4.55	4.49	4.51	4.57	4.33	4.31	4.29	4.27	4.35
Safety Factor under FTA Loading (w/h<5)	N/A	N/A	N/A	N/A	N/A	N/A	N/A	N/A	N/A	N/A	N/A
Single Abutment Loading (3D) - full	6.66	6.30	6.26	6.38	6.34	6.22	6.70	6.74	6.77	6.81	6.66
Single Abutment Loading (3D) - pillar	5.64	5.38	5.36	5.44	5.41	5.33	5.66	5.69	5.72	5.75	5.64
Single Abutment Loading (3D) - solid	1.02	0.92	0.90	0.94	0.93	0.89	1.03	1.04	1.06	1.07	1.02
Design Abutment Load Multiplier	1.00	1.00	1.00	1.00	1.00	1.00	1.00	1.00	1.00	1.00	1.00
Total Pillar Loading with Single Abutment Loading	13.72	13.19	13.13	13.31	13.25	13.07	13.78	13.84	13.90	13.96	13.72
Safety Factor (under Single Abutment Loading)	2.25	2.34	2.35	2.31	2.33	2.36	2.24	2.23	2.22	2.21	2.25
Total Pillar Loading @ nA	13.74	13.11	13.04	13.25	13.18	12.97	13.81	13.88	13.95	14.02	13.74
Safety Factor @ nA	2.24	2.35	2.36	2.33	2.34	2.38	2.23	2.22	2.21	2.20	2.24
Total Pillar Loading under Double Abutment Loading	20.40	19.41	19.30	19.63	19.52	19.19	20.51	20.62	20.73	20.84	20.40
Safety Factor (under Double Abutment Loading)	1.51	1.59	1.60	1.57	1.58	1.61	1.50	1.49	1.49	1.48	1.51
Elastic Model Subsidence											
Ecoal(GPa)	1.50	1.50	1.50	1.50	1.50	1.50	1.50	1.50	1.50	1.50	1.50
E1floor(GPa)	0.75	0.75	0.75	0.75	0.75	0.75	0.75	0.75	0.75	0.75	0.75
E2floor(GPa)	4.00	4.00	4.00	4.00	4.00	4.00	4.00	4.00	4.00	4.00	4.00
E1roof(GPa)	0.75	0.75	0.75	0.75	0.75	0.75	0.75	0.75	0.75	0.75	0.75
E2roof(GPa)	5.00	5.00	5.00	5.00	5.00	5.00	5.00	5.00	5.00	5.00	5.00
Poissons Ratio floor/roof	0.25	0.25	0.25	0.25	0.25	0.25	0.25	0.25	0.25	0.25	0.25
initial vertical stress (MPa)	5.70	5.48	5.45	5.53	5.50	5.43	5.73	5.75	5.78	5.80	5.70
increase in vertical stress for DA (MPa)	14.70	13.93	13.85	14.10	14.02	13.76	14.78	14.87	14.95	15.04	14.70
Roof t1	2.00	2.00	2.00	2.00	2.00	2.00	2.00	2.00	2.00	2.00	2.00
Roof t2	28.60	28.60	28.60	28.60	28.60	28.60	28.60	28.60	28.60	28.60	28.60
Roof sig1	14.70	13.93	13.85	14.10	14.02	13.76	14.78	14.87	14.95	15.04	14.70
Roof sig2	13.17	12.48	12.41	12.64	12.56	12.33	13.25	13.32	13.40	13.48	13.17
Floor t1	3.00	3.00	3.00	3.00	3.00	3.00	3.00	3.00	3.00	3.00	3.00
Floor t2	27.6	27.6	27.6	27.6	27.6	27.6	27.6	27.6	27.6	27.6	27.6
Floor sig1	14.70	13.93	13.84	14.10	14.02	13.76	14.78	14.87	14.95	15.04	14.70
Floor sig2	14.65	13.89	13.80	14.06	13.97	13.72	14.74	14.82	14.91	14.99	14.65
Pillar Compression (m)	0.029	0.028	0.028	0.028	0.028	0.028	0.030	0.030	0.030	0.030	0.029
Roof Compression (m)	0.107	0.102	0.101	0.103	0.102	0.101	0.108	0.109	0.109	0.110	0.107
Floor Compression (m)	0.150	0.142	0.141	0.144	0.143	0.140	0.151	0.152	0.153	0.153	0.150
Total FTA Compression (m)	0.287	0.272	0.270	0.275	0.273	0.268	0.288	0.290	0.292	0.293	0.287
Total Effective Compression (m)	0.287	0.272	0.270	0.275	0.273	0.268	0.288	0.290	0.292	0.293	0.287
2 times Effective Compression (m)	0.573	0.543	0.540	0.550	0.547	0.537	0.577	0.580	0.583	0.587	0.573
Total Yielded Panel Subs (m)	0.38	0.36	0.36	0.36	0.36	0.35	0.38	0.38	0.38	0.38	0.38
5 x Effective Predictions (m)	1.433	1.359	1.350	1.375	1.367	1.342	1.442	1.450	1.458	1.467	1.433
Bearing Capacity											
Upper Floor Unit UCS, 2*cu1 (MPa)	8.0	8.0	8.0	8.0	8.0	8.0	8.0	8.0	8.0	8.0	8.0
Upper Unit Thickness, H (m)	3.0	3.0	3.0	3.0	3.0	3.0	3.0	3.0	3.0	3.0	3.0
Lower Floor Unit UCS, 2*cu2 (MPa)	40.0	40.0	40.0	40.0	40.0	40.0	40.0	40.0	40.0	40.0	40.0
cu1/cu2	0.2	0.2	0.2	0.2	0.2	0.2	0.2	0.2	0.2	0.2	0.2
H/B	0.10	0.10	0.10	0.10	0.10	0.10	0.10	0.10	0.10	0.10	0.10
N*1	9.24	9.24	9.24	9.24	9.24	9.24	9.24	9.24	9.24	9.24	9.24
N*2	1.85	1.85	1.85	1.85	1.85	1.85	1.85	1.85	1.85	1.85	1.85
Floor Bearing Capacity (MPa)	37.0	37.0	37.0	37.0	37.0	37.0	37.0	37.0	37.0	37.0	37.0
Eff Pillar Stress (MPa)	20.4	19.4	19.3	19.6	19.5	19.2	20.5	20.6	20.7	20.8	20.4
Eff Floor Bearing Failure FoS	1.81	1.90	1.92	1.88	1.89	1.93	1.80	1.79	1.78	1.77	1.81
FTA Floor Bearing Failure FoS	5.22	5.43	5.46	5.38	5.41	5.48	5.19	5.17	5.15	5.13	5.22
Immediate Roof Unit UCS, 2*cu1 (MPa)	8.0	8.0	8.0	8.0	8.0	8.0	8.0	8.0	8.0	8.0	8.0
Immediate Roof Unit Thickness, H (m)	3.0	3.0	3.0	3.0	3.0	3.0	3.0	3.0	3.0	3.0	3.0
Upper Roof Unit UCS, 2*cu2 (MPa)	40.0	40.0	40.0	40.0	40.0	40.0	40.0	40.0	40.0	40.0	40.0
cu1/cu2	0.2	0.2	0.2	0.2	0.2	0.2	0.2	0.2	0.2	0.2	0.2
H/B	0.10	0.10	0.10	0.10	0.10	0.10	0.10	0.10	0.10	0.10	0.10
N*1	9.24	9.24	9.24	9.24	9.24	9.24	9.24	9.24	9.24	9.24	9.24
N*2	1.85	1.85	1.85	1.85	1.85	1.85	1.85	1.85	1.85	1.85	1.85
Roof Bearing Capacity (MPa)	37.0	37.0	37.0	37.0	37.0	37.0	37.0	37.0	37.0	37.0	37.0
Pillar Stress (MPa)	20.4	19.4	19.3	19.6	19.5	19.2	20.5	20.6	20.7	20.8	20.4
Effective Roof Bearing Failure FoS	1.81	1.90	1.92	1.88	1.89	1.93	1.80	1.79	1.78	1.77	1.81
FTA Roof Bearing Failure FoS	5.22	5.43	5.46	5.38	5.41	5.48	5.19	5.17	5.15	5.13	5.22
Voussoir Beam Deflection (m)	0.957	0.957	0.957	0.957	0.957	0.957	0.957	0.957	0.957	0.957	0.957
System Settlement at Base of beam (m)	0.000	0.000	0.000	0.000	0.000	0.000	0.000	0.000	0.000	0.000	0.000
Applied Pillar Stress/FTA Stress Ratio (Mpa)	1.00	1.00	1.00	1.00	1.00	1.00	1.00	1.00	1.00	1.00	1.00
Effective Pillar Stress (Mpa)	20.40	19.41	19.30	19.63	19.52	19.19	20.51	20.62	20.73	20.84	20.40
Multi-Seam Stress Inc (min)											
Multi-Seam Stress Inc (max)											
Effective Pillar FoS	1.51	1.59	1.60	1.57	1.58	1.61	1.50	1.49	1.49	1.48	1.51
Eresidual coal(GPa)	0.25	0.25	0.25	0.25	0.25	0.25	0.25	0.25	0.25	0.25	0.25

UNSW Pillar Design Spreadsheet											
Chain Valley XL.Panel#	1.1	1.2	1.3	1.4	1.5	1.6	1.7	2.1	2.2	2.3	3.1
INPUT DATA											
Depth of Cover (m)	**200**	**200**	**200**	**198**	**195**	**193**	**191**	**196**	**200**	**190**	**188**
Mining Height (m)	**3.2**	**3.2**	**3.2**	**3.2**	**3.2**	**3.2**	**3.2**	**3.2**	**3.2**	**3.2**	**3.2**
Pillar Length - centres (m)	100.7	100.7	100.7	100.7	100.7	100.7	100.7	100.7	100.7	100.7	100.7
Pillar Width - centres (m)	36.0	35.8	38.0	38.0	38.0	38.0	38.0	45.4	191.4	38.0	38.0
Roadway Width for maximum pillar dimension	5.4	5.4	5.4	5.4	5.4	5.4	5.4	5.4	5.4	5.4	5.4
Roadway Width for minimum pillar dimension	5.4	5.4	5.4	5.4	5.4	5.4	5.4	5.4	5.4	5.4	5.4
Cut-Through Angle (degrees)	**90**	**90**	**90**	**90**	**90**	**90**	**90**	**90**	**90**	**90**	**90**
Average Panel Span (m) {rib-rib width}	72	72	97	97	97	97	97	97	97	97	97
SG (tonnes/m^3)	2.5	2.5	2.5	2.5	2.5	2.5	2.5	2.5	2.5	2.5	2.5
Conversion (tonnes to N)	10000	10000	10000	10000	10000	10000	10000	10000	10000	10000	10000
Abutment Angle (^{0})	21	21	21	21	21	21	21	21	21	21	21
W/H	0.36	0.36	0.49	0.49	0.50	0.50	0.51	0.49	0.49	0.51	0.52
PRELIMINARY CALCULATIONS											
Maximum Rib to Rib Pillar Length (w_2)	**95.3**	**95.3**	**95.3**	**95.3**	**95.3**	**95.3**	**95.3**	**95.3**	**95.3**	**95.3**	**95.3**
Minimum Rib to Rib Pillar Width (w_1)	**30.6**	**30.4**	**32.6**	**32.6**	**32.6**	**32.6**	**32.6**	**40.0**	**186.0**	**32.6**	**32.6**
w, Minimum Rib to Rib Pillar Width (ie $w_1 \sin\theta$)	**30.6**	**30.4**	**32.6**	**32.6**	**32.6**	**32.6**	**32.6**	**40.0**	**186.0**	**32.6**	**32.6**
Minimum Pillar Width/Height Ratio	**9.6**	**9.5**	**10.2**	**10.2**	**10.2**	**10.2**	**10.2**	**12.5**	**29.8**	**10.2**	**10.2**
Extraction Ratio (%)	**19.6%**	**19.6%**	**18.8%**	**18.8%**	**18.8%**	**18.8%**	**18.8%**	**16.6%**	**8.0%**	**18.8%**	**18.8%**
Abutment Angle (Radians)	0.367	0.367	0.367	0.367	0.367	0.367	0.367	0.367	0.367	0.367	0.367
Cut-Through Angle (Radians)	1.571	1.571	1.571	1.571	1.571	1.571	1.571	1.571	1.571	1.571	1.571
Is the Panel Super-Critical?	No	No	No	No	No	No	No	No	No	No	No
D (Peng & Chiang Loading Factor)	72.549	72.549	72.549	72.185	71.637	71.268	70.898	71.820	72.549	70.712	70.339
R (Pillar 2nd Abutment Component)	0.87	0.87	0.89	0.89	0.90	0.90	0.90	0.95	1.00	0.90	0.90
Dimensionless Pillar 'Rectangularity'	1.51	1.52	1.49	1.49	1.49	1.49	1.49	1.41	0.68	1.49	1.49
Width/Height Ratio Exponent	1.00	1.00	1.00	1.00	1.00	1.00	1.00	1.00	1.00	1.00	1.00
Effective Width Factor (Omega)	1.51	1.52	1.49	1.49	1.49	1.49	1.49	1.41	0.68	1.49	1.49
Effective Width Interim	46.33	46.10	48.58	48.58	48.58	48.58	48.58	56.35	126.03	48.58	48.58
Effective Pillar Width (m)	46.33	46.10	48.58	48.58	48.58	48.58	48.58	56.35	126.03	48.58	48.58
Effective Pillar Loading Height (m)	200.00	200.00	200.00	198.00	195.00	193.00	191.00	196.00	200.00	190.00	188.00
RESULTS											
Tributary Area Loading (MPa)	**6.22**	**6.22**	**6.16**	**6.10**	**6.00**	**5.94**	**5.88**	**5.88**	**5.44**	**5.85**	**5.79**
Pillar Strength (UNSW Squat Pillar 1999)	**30.81**	**30.54**	**33.62**	**33.62**	**33.62**	**33.62**	**33.62**	**45.99**	**848.18**	**33.62**	**33.62**
Pillar Strength (UNSW w/h<5)	**N/A**	**N/A**	**N/A**	**N/A**	**N/A**	**N/A**	**N/A**	**N/A**	**N/A**	**N/A**	**N/A**
Safety Factor under FTA Loading (Squat Pillar)	**4.96**	**4.91**	**5.46**	**5.51**	**5.60**	**5.66**	**5.72**	**7.83**	**156.01**	**5.75**	**5.81**
Safety Factor under FTA Loading (w/h<5)	**N/A**	**N/A**	**N/A**	**N/A**	**N/A**	**N/A**	**N/A**	**N/A**	**N/A**	**N/A**	**N/A**
Single Abutment Loading (3D) - full	4.50	4.54	5.21	5.13	5.02	4.95	4.87	4.12	0.91	4.84	4.76
Single Abutment Loading (3D) - pillar	**3.93**	**3.95**	**4.65**	**4.59**	**4.50**	**4.45**	**4.39**	**3.92**	**0.91**	**4.36**	**4.30**
Single Abutment Loading (3D) - solid	0.58	0.59	0.56	0.55	0.52	0.50	0.49	0.21	0.00	0.48	0.46
Design Abutment Load Multiplier	1.00	1.00	1.00	1.50	1.50	1.00	1.00	1.00	1.00	1.00	1.00
Total Pillar Loading with Single Abutment Loading	11.14	11.17	11.80	12.19	12.01	11.39	11.27	10.80	7.35	11.21	11.09
Safety Factor (under Single Abutment Loading)	**2.76**	**2.73**	**2.85**	**2.76**	**2.80**	**2.95**	**2.98**	**4.26**	**115.41**	**3.00**	**3.03**
Total Pillar Loading @ nA	10.72	10.76	11.37	13.80	13.54	10.89	10.76	10.00	6.35	10.69	10.55
Safety Factor @ nA	**2.87**	**2.84**	**2.96**	**2.44**	**2.48**	**3.09**	**3.13**	**4.60**	**133.58**	**3.15**	**3.19**
Total Pillar Loading under Double Abutment Loading	15.22	15.31	16.58	16.37	16.05	15.84	15.63	14.12	7.26	15.53	15.32
Safety Factor (under Double Abutment Loading)	**2.02**	**2.00**	**2.03**	**2.05**	**2.09**	**2.12**	**2.15**	**3.26**	**116.79**	**2.17**	**2.20**
Elastic Model Subsidence											
Ecoal(GPa)	**1.20**	**1.20**	**1.20**	**1.20**	**1.20**	**1.20**	**1.20**	**1.20**	**1.20**	**1.20**	**1.20**
E1floor(GPa)	**1.50**	**1.50**	**1.50**	**1.50**	**1.50**	**1.50**	**1.50**	**1.50**	**1.50**	**1.50**	**1.50**
E2floor(GPa)	**4.00**	**4.00**	**4.00**	**4.00**	**4.00**	**4.00**	**4.00**	**4.00**	**4.00**	**4.00**	**4.00**
E1roof(GPa)	**2.50**	**2.50**	**2.50**	**2.50**	**2.50**	**2.50**	**2.50**	**2.50**	**2.50**	**2.50**	**2.50**
E2roof(GPa)	**4.00**	**4.00**	**4.00**	**4.00**	**4.00**	**4.00**	**4.00**	**4.00**	**4.00**	**4.00**	**4.00**
Poissons Ratio floor/roof	**0.25**	**0.25**	**0.25**	**0.25**	**0.25**	**0.25**	**0.25**	**0.25**	**0.25**	**0.25**	**0.25**
initial vertical stress (MPa)	**5.00**	**5.00**	**5.00**	**4.95**	**4.88**	**4.83**	**4.78**	**4.90**	**5.00**	**4.75**	**4.70**
increase in vertical stress for DA (MPa)	**10.22**	**10.31**	**11.58**	**11.42**	**11.18**	**11.02**	**10.86**	**9.22**	**2.26**	**10.78**	**10.62**
Roof t1	**10.00**	**2.00**	**2.00**	**2.00**	**2.00**	**2.00**	**2.00**	**2.00**	**2.00**	**2.00**	**2.00**
Roof t2	**20.60**	**28.40**	**30.60**	**30.60**	**30.60**	**30.60**	**30.60**	**38.00**	**184.00**	**30.60**	**30.60**
Roof sig1	**10.18**	**10.31**	**11.58**	**11.42**	**11.18**	**11.02**	**10.86**	**9.22**	**2.26**	**10.78**	**10.62**
Roof sig2	**8.49**	**9.23**	**10.38**	**10.24**	**10.02**	**9.88**	**9.74**	**8.30**	**2.05**	**9.67**	**9.52**
Floor t1	**6.00**	**6.00**	**6.00**	**6.00**	**6.00**	**6.00**	**6.00**	**6.00**	**6.00**	**6.00**	**6.00**
Floor t2	**24.6**	**24.4**	**26.6**	**26.6**	**26.6**	**26.6**	**26.6**	**34.0**	**180.0**	**26.6**	**26.6**
Floor sig1	**10.21**	**10.30**	**11.57**	**11.41**	**11.17**	**11.01**	**10.85**	**9.22**	**2.26**	**10.77**	**10.61**
Floor sig2	**9.99**	**10.07**	**11.36**	**11.20**	**10.96**	**10.81**	**10.65**	**9.13**	**2.26**	**10.57**	**10.42**
Pillar Compression (m)	**0.026**	**0.026**	**0.029**	**0.029**	**0.028**	**0.028**	**0.027**	**0.023**	**0.006**	**0.027**	**0.027**
Roof Compression (m)	**0.079**	**0.069**	**0.083**	**0.082**	**0.080**	**0.079**	**0.078**	**0.081**	**0.090**	**0.077**	**0.076**
Floor Compression (m)	**0.096**	**0.096**	**0.114**	**0.113**	**0.110**	**0.109**	**0.107**	**0.107**	**0.104**	**0.106**	**0.105**
Total Compression (m)	**0.201**	**0.191**	**0.226**	**0.223**	**0.218**	**0.215**	**0.212**	**0.211**	**0.200**	**0.211**	**0.207**
Total Effective Compression (m)	**0.201**	**0.191**	**0.226**	**0.223**	**0.218**	**0.215**	**0.212**	**0.211**	**0.200**	**0.211**	**0.207**
1.5 times Effective Compression (m)	**0.301**	**0.287**	**0.339**	**0.335**	**0.328**	**0.323**	**0.318**	**0.317**	**0.300**	**0.316**	**0.311**
Total Yielded Panel Subs (m)	**0.28**	**0.27**	**0.30**	**0.30**	**0.29**	**0.29**	**0.28**	**0.27**	**0.25**	**0.28**	**0.28**
5 x Effective Predictions (m)	**1.003**	**0.956**	**1.131**	**1.116**	**1.092**	**1.077**	**1.061**	**1.056**	**0.999**	**1.053**	**1.037**
Bearing Capacity											
Upper Floor Unit UCS, 2*cu1 (MPa)	**20.0**	**20.0**	**20.0**	**20.0**	**20.0**	**20.0**	**20.0**	**20.0**	**20.0**	**20.0**	**20.0**
Upper Unit Thickness, H (m)	**6.0**	**6.0**	**6.0**	**6.0**	**6.0**	**6.0**	**6.0**	**6.0**	**6.0**	**6.0**	**6.0**
Lower Floor Unit UCS, 2*cu2 (MPa)	**40.0**	**40.0**	**40.0**	**40.0**	**40.0**	**40.0**	**40.0**	**40.0**	**40.0**	**40.0**	**40.0**
cu1/cu2	**0.5**	**0.5**	**0.5**	**0.5**	**0.5**	**0.5**	**0.5**	**0.5**	**0.5**	**0.5**	**0.5**
H/B	**0.20**	**0.20**	**0.18**	**0.18**	**0.18**	**0.18**	**0.18**	**0.15**	**0.03**	**0.18**	**0.18**
N*1	**6.69**	**6.67**	**6.86**	**6.86**	**6.86**	**6.86**	**6.86**	**7.47**	**19.64**	**6.86**	**6.86**
N*2	**3.35**	**3.34**	**3.43**	**3.43**	**3.43**	**3.43**	**3.43**	**3.74**	**9.82**	**3.43**	**3.43**
Floor Bearing Capacity (MPa)	**66.9**	**66.7**	**68.6**	**68.6**	**68.6**	**68.6**	**68.6**	**74.7**	**196.4**	**68.6**	**68.6**
Eff Pillar Stress (MPa)	**15.2**	**15.3**	**16.6**	**16.4**	**16.1**	**15.8**	**15.6**	**14.1**	**7.3**	**15.5**	**15.3**
Eff Floor Bearing Failure FoS	**4.40**	**4.36**	**4.14**	**4.19**	**4.27**	**4.33**	**4.39**	**5.29**	**27.05**	**4.42**	**4.48**
FTA Floor Bearing Failure FoS	**10.77**	**10.73**	**11.14**	**11.25**	**11.42**	**11.54**	**11.66**	**12.72**	**36.13**	**11.72**	**11.85**
Immediate Roof Unit UCS, 2*cu1 (MPa)	**40.0**	**40.0**	**40.0**	**40.0**	**40.0**	**40.0**	**40.0**	**40.0**	**40.0**	**40.0**	**40.0**
Immediate Roof Unit Thickness, H (m)	**10.0**	**10.0**	**10.0**	**10.0**	**10.0**	**10.0**	**10.0**	**10.0**	**10.0**	**10.0**	**10.0**
Upper Roof Unit UCS, 2*cu2 (MPa)	**40.0**	**40.0**	**40.0**	**40.0**	**40.0**	**40.0**	**40.0**	**40.0**	**40.0**	**40.0**	**40.0**
cu1/cu2	**1.0**	**1.0**	**1.0**	**1.0**	**1.0**	**1.0**	**1.0**	**1.0**	**1.0**	**1.0**	**1.0**
H/B	**0.33**	**0.33**	**0.31**	**0.31**	**0.31**	**0.31**	**0.31**	**0.25**	**0.05**	**0.31**	**0.31**
N*1	**5.14**	**5.14**	**5.14**	**5.14**	**5.14**	**5.14**	**5.14**	**5.14**	**5.14**	**5.14**	**5.14**
N*2	5.14	5.14	5.14	5.14	5.14	5.14	5.14	5.14	5.14	5.14	5.14
Roof Bearing Capacity (MPa)	102.8	102.8	102.8	102.8	102.8	102.8	102.8	102.8	102.8	102.8	102.8
Pillar Stress (MPa)	**15.2**	**15.3**	**16.6**	**16.4**	**16.1**	**15.8**	**15.6**	**14.1**	**7.3**	**15.5**	**15.3**
Effective Roof Bearing Failure FoS	**6.75**	**6.72**	**6.20**	**6.28**	**6.40**	**6.49**	**6.58**	**7.28**	**14.15**	**6.62**	**6.71**
FTA Roof Bearing Failure FoS	**16.54**	**16.52**	**16.69**	**16.86**	**17.12**	**17.30**	**17.48**	**17.49**	**18.91**	**17.57**	**17.76**
Voussoir Beam Deflection (m)	**0.004**	**0.004**	**0.004**	**0.001**	**0.001**	**0.419**	**0.042**	**0.006**	**0.011**	**0.821**	**0.282**
System Settlement at Base of beam (m)	0.000	0.000	0.000	0.000	0.000	0.000	0.000	0.000	0.000	0.000	0.000
Applied Pillar Stress/FTA Stress Ratio (Mpa)	1.00	1.00	1.00	1.00	1.00	1.00	1.00	1.00	1.00	1.00	1.00
Effective Pillar Stress (Mpa)	15.22	15.31	16.58	16.37	16.05	15.84	15.63	14.12	7.26	15.53	15.32
Multi-Seam Stress Inc (min)											
Multi-Seam Stress Inc (max)											
Effective Pillar FoS	**2.02**	**2.00**	**2.03**	**2.05**	**2.09**	**2.12**	**2.15**	**3.26**	**116.79**	**2.17**	**2.20**
Eresidual coal(GPa)	**0.25**	**0.25**	**0.27**	**0.27**	**0.27**	**0.27**	**0.27**	**0.30**	**0.38**	**0.27**	**0.27**

UNSW Pillar Design Spreadsheet											
Chain Valley XL.Panel#	3.2	3.3	4.1	4.2	4.3	4.4	4.5	4.6	5.1	5.2	5.3
INPUT DATA											
Depth of Cover (m)	**185**	**183**	**178**	**173**	**170**	**184**	**188**	**185**	**182**	**180**	**175**
Mining Height (m)	**3.2**	**3.2**	**3.2**	**3.2**	**3.2**	**3.2**	**3.2**	**3.2**	**3.2**	**3.2**	**3.2**
Pillar Length - centres (m)	100.7	100.7	100.7	100.7	100.7	100.7	100.7	100.7	100.7	100.7	100.7
Pillar Width - centres (m)	38.0	38.0	38.0	38.0	38.0	305.4	38.0	38.0	37.0	36.5	36.0
Roadway Width for maximum pillar dimension	5.4	5.4	5.4	5.4	5.4	5.4	5.4	5.4	5.4	5.4	5.4
Roadway Width for minimum pillar dimension	5.4	5.4	5.4	5.4	5.4	5.4	5.4	5.4	5.4	5.4	5.4
Cut-Through Angle (degrees)	**90**	**90**	**90**	**90**	**90**	**90**	**90**	**90**	**90**	**90**	**90**
Average Panel Span (m) {rib-rib width}	**97**	**97**	**97**	**97**	**97**	**97**	**97**	**97**	**97**	**97**	**97**
SG (tonnes/m^3)	2.5	2.5	2.5	2.5	2.5	2.5	2.5	2.5	2.5	2.5	2.5
Conversion (tonnes to N)	10000	10000	10000	10000	10000	10000	10000	10000	10000	10000	10000
Abutment Angle (^{0})	21	21	21	21	21	21	21	21	21	21	21
W/H	0.52	0.53	0.54	0.56	0.57	0.53	0.52	0.52	0.53	0.54	0.55
PRELIMINARY CALCULATIONS											
Maximum Rib to Rib Pillar Length (w_2)	**95.3**	**95.3**	**95.3**	**95.3**	**95.3**	**95.3**	**95.3**	**95.3**	**95.3**	**95.3**	**95.3**
Minimum Rib to Rib Pillar Width (w_1)	**32.6**	**32.6**	**32.6**	**32.6**	**32.6**	**300.0**	**32.6**	**32.6**	**31.6**	**31.1**	**30.6**
w, Minimum Rib to Rib Pillar Width (ie $w_1 \sin\theta$)	**32.6**	**32.6**	**32.6**	**32.6**	**32.6**	**300.0**	**32.6**	**32.6**	**31.6**	**31.1**	**30.6**
Minimum Pillar Width/Height Ratio	**10.2**	**10.2**	**10.2**	**10.2**	**10.2**	**29.8**	**10.2**	**10.2**	**9.9**	**9.7**	**9.6**
Extraction Ratio (%)	**18.8%**	**18.8%**	**18.8%**	**18.8%**	**18.8%**	**7.0%**	**18.8%**	**18.8%**	**19.2%**	**19.4%**	**19.6%**
Abutment Angle (Radians)	0.367	0.367	0.367	0.367	0.367	0.367	0.367	0.367	0.367	0.367	0.367
Cut-Through Angle (Radians)	1.571	1.571	1.571	1.571	1.571	1.571	1.571	1.571	1.571	1.571	1.571
Is the Panel Super-Critical?	No	No	No	No	No	No	No	No	No	No	No
D (Peng & Chiang Loading Factor)	69.776	69.397	68.443	67.475	66.887	69.587	70.339	69.776	69.207	68.826	67.864
R (Pillar 2nd Abutment Component)	0.91	0.91	0.91	0.92	0.92	1.00	0.90	0.91	0.90	0.90	0.90
Dimensionless Pillar 'Rectangularity'	1.49	1.49	1.49	1.49	1.49	0.48	1.49	1.49	1.50	1.51	1.51
Width/Height Ratio Exponent	1.00	1.00	1.00	1.00	1.00	1.00	1.00	1.00	1.00	1.00	1.00
Effective Width Factor (Omega)	1.49	1.49	1.49	1.49	1.49	0.48	1.49	1.49	1.50	1.51	1.51
Effective Width Interim	48.58	48.58	48.58	48.58	48.58	144.65	48.58	48.58	47.46	46.90	46.33
Effective Pillar Width (m)	48.58	48.58	48.58	48.58	48.58	144.65	48.58	48.58	47.46	46.90	46.33
Effective Pillar Loading Height (m)	185.00	183.00	178.00	173.00	170.00	184.00	188.00	185.00	182.00	180.00	175.00
RESULTS											
Tributary Area Loading (MPa)	**5.70**	**5.63**	**5.48**	**5.33**	**5.23**	**4.95**	**5.79**	**5.70**	**5.63**	**5.58**	**5.44**
Pillar Strength (UNSW Squat Pillar 1999)	**33.62**	**33.62**	**33.62**	**33.62**	**33.62**	**2112.89**	**33.62**	**33.62**	**32.18**	**31.49**	**30.81**
Pillar Strength (UNSW w/h<5)	**N/A**	**N/A**	**N/A**	**N/A**	**N/A**	**N/A**	**N/A**	**N/A**	**N/A**	**N/A**	**N/A**
Safety Factor under FTA Loading (Squat Pillar)	**5.90**	**5.97**	**6.13**	**6.31**	**6.42**	**427.01**	**5.81**	**5.90**	**5.72**	**5.64**	**5.66**
Safety Factor under FTA Loading (w/h<5)	**N/A**	**N/A**	**N/A**	**N/A**	**N/A**	**N/A**	**N/A**	**N/A**	**N/A**	**N/A**	**N/A**
Single Abutment Loading (3D) - full	4.65	4.58	4.39	4.21	4.10	0.50	4.76	4.65	4.68	4.68	4.56
Single Abutment Loading (3D) - pillar	**4.21**	**4.15**	**4.01**	**3.86**	**3.77**	**0.50**	**4.30**	**4.21**	**4.21**	**4.20**	**4.09**
Single Abutment Loading (3D) - solid	0.44	0.42	0.39	0.35	0.33	0.00	0.46	0.44	0.47	0.49	0.47
Design Abutment Load Multiplier	1.00	1.00	1.00	1.00	1.00	1.00	1.00	1.00	1.00	1.00	1.00
Total Pillar Loading with Single Abutment Loading	10.91	10.79	10.49	10.18	10.00	6.45	11.09	10.91	10.84	10.78	10.53
Safety Factor (under Single Abutment Loading)	**3.08**	**3.12**	**3.21**	**3.30**	**3.36**	**327.60**	**3.03**	**3.08**	**2.97**	**2.92**	**2.93**
Total Pillar Loading @ nA	10.35	10.21	9.87	9.53	9.33	5.45	10.55	10.35	10.31	10.26	10.00
Safety Factor @ nA	**3.25**	**3.29**	**3.41**	**3.53**	**3.60**	**387.71**	**3.19**	**3.25**	**3.12**	**3.07**	**3.08**
Total Pillar Loading under Double Abutment Loading	15.00	14.79	14.27	13.74	13.43	5.95	15.32	15.00	15.00	14.94	14.56
Safety Factor (under Double Abutment Loading)	**2.24**	**2.27**	**2.36**	**2.45**	**2.50**	**355.04**	**2.20**	**2.24**	**2.15**	**2.11**	**2.12**
Elastic Model Subsidence											
Ecoal(GPa)	**1.20**	**1.20**	**1.20**	**1.20**	**1.20**	**1.20**	**1.20**	**1.20**	**1.20**	**1.20**	**1.20**
E1floor(GPa)	**1.50**	**1.50**	**1.50**	**1.50**	**1.50**	**1.50**	**1.50**	**1.50**	**1.50**	**1.50**	**1.50**
E2floor(GPa)	**4.00**	**4.00**	**4.00**	**4.00**	**4.00**	**4.00**	**4.00**	**4.00**	**4.00**	**4.00**	**4.00**
E1roof(GPa)	**2.50**	**2.50**	**2.50**	**2.50**	**2.50**	**2.50**	**2.50**	**2.50**	**2.50**	**2.50**	**2.50**
E2roof(GPa)	**4.00**	**4.00**	**4.00**	**4.00**	**4.00**	**4.00**	**4.00**	**4.00**	**4.00**	**4.00**	**4.00**
Poissons Ratio floor/roof	**0.25**	**0.25**	**0.25**	**0.25**	**0.25**	**0.25**	**0.25**	**0.25**	**0.25**	**0.25**	**0.25**
initial vertical stress (MPa)	**4.63**	**4.58**	**4.45**	**4.33**	**4.25**	**4.60**	**4.70**	**4.63**	**4.55**	**4.50**	**4.38**
increase in vertical stress for DA (MPa)	**10.38**	**10.22**	**9.82**	**9.42**	**9.18**	**1.35**	**10.62**	**10.38**	**10.45**	**10.44**	**10.18**
Roof t1	**2.00**	**2.00**	**2.00**	**2.00**	**2.00**	**2.00**	**2.00**	**2.00**	**2.00**	**2.00**	**2.00**
Roof t2	**30.60**	**30.60**	**30.60**	**30.60**	**30.60**	**298.00**	**30.60**	**30.60**	**29.60**	**29.10**	**28.60**
Roof sig1	**10.37**	**10.21**	**9.81**	**9.41**	**9.17**	**1.35**	**10.62**	**10.37**	**10.45**	**10.44**	**10.18**
Roof sig2	**9.31**	**9.16**	**8.80**	**8.45**	**8.23**	**1.23**	**9.52**	**9.31**	**9.37**	**9.36**	**9.13**
Floor t1	**6.00**	**6.00**	**6.00**	**6.00**	**6.00**	**6.00**	**6.00**	**6.00**	**6.00**	**6.00**	**6.00**
Floor t2	**26.6**	**26.6**	**26.6**	**26.6**	**26.6**	**294.0**	**26.6**	**26.6**	**25.6**	**25.1**	**24.6**
Floor sig1	**10.37**	**10.21**	**9.81**	**9.41**	**9.17**	**1.35**	**10.61**	**10.37**	**10.44**	**10.43**	**10.18**
Floor sig2	**10.18**	**10.02**	**9.63**	**9.24**	**9.00**	**1.35**	**10.42**	**10.18**	**10.23**	**10.22**	**9.96**
Pillar Compression (m)	**0.026**	**0.026**	**0.025**	**0.024**	**0.023**	**0.003**	**0.027**	**0.026**	**0.026**	**0.026**	**0.025**
Roof Compression (m)	**0.075**	**0.073**	**0.071**	**0.068**	**0.066**	**0.087**	**0.076**	**0.075**	**0.073**	**0.072**	**0.069**
Floor Compression (m)	**0.102**	**0.101**	**0.097**	**0.093**	**0.091**	**0.098**	**0.105**	**0.102**	**0.101**	**0.099**	**0.096**
Total Compression (m)	**0.203**	**0.200**	**0.192**	**0.184**	**0.179**	**0.188**	**0.207**	**0.203**	**0.199**	**0.197**	**0.190**
Total Effective Compression (m)	**0.203**	**0.200**	**0.192**	**0.184**	**0.179**	**0.188**	**0.207**	**0.203**	**0.199**	**0.197**	**0.190**
1.5 times Effective Compression (m)	**0.304**	**0.300**	**0.288**	**0.276**	**0.269**	**0.283**	**0.311**	**0.304**	**0.299**	**0.296**	**0.285**
Total Yielded Panel Subs (m)	**0.27**	**0.27**	**0.26**	**0.25**	**0.24**	**0.23**	**0.28**	**0.27**	**0.27**	**0.27**	**0.26**
5 x Effective Predictions (m)	**1.014**	**0.998**	**0.959**	**0.920**	**0.897**	**0.942**	**1.037**	**1.014**	**0.997**	**0.985**	**0.949**
Bearing Capacity											
Upper Floor Unit UCS, 2*cu1 (MPa)	**20.0**	**20.0**	**20.0**	**20.0**	**20.0**	**20.0**	**20.0**	**20.0**	**20.0**	**20.0**	**20.0**
Upper Unit Thickness, H (m)	**6.0**	**6.0**	**6.0**	**6.0**	**6.0**	**6.0**	**6.0**	**6.0**	**6.0**	**6.0**	**6.0**
Lower Floor Unit UCS, 2*cu2 (MPa)	**40.0**	**40.0**	**40.0**	**40.0**	**40.0**	**40.0**	**40.0**	**40.0**	**40.0**	**40.0**	**40.0**
cu1/cu2	**0.5**	**0.5**	**0.5**	**0.5**	**0.5**	**0.5**	**0.5**	**0.5**	**0.5**	**0.5**	**0.5**
H/B	**0.18**	**0.18**	**0.18**	**0.18**	**0.18**	**0.02**	**0.18**	**0.18**	**0.19**	**0.19**	**0.20**
N*1	**6.86**	**6.86**	**6.86**	**6.86**	**6.86**	**29.14**	**6.86**	**6.86**	**6.77**	**6.73**	**6.69**
N*2	**3.43**	**3.43**	**3.43**	**3.43**	**3.43**	**14.57**	**3.43**	**3.43**	**3.39**	**3.37**	**3.35**
Floor Bearing Capacity (MPa)	**68.6**	**68.6**	**68.6**	**68.6**	**68.6**	**291.4**	**68.6**	**68.6**	**67.7**	**67.3**	**66.9**
Eff Pillar Stress (MPa)	**15.0**	**14.8**	**14.3**	**13.7**	**13.4**	**6.0**	**15.3**	**15.0**	**15.0**	**14.9**	**14.6**
Eff Floor Bearing Failure FoS	**4.57**	**4.64**	**4.81**	**4.99**	**5.11**	**48.97**	**4.48**	**4.57**	**4.52**	**4.51**	**4.60**
FTA Floor Bearing Failure FoS	**12.04**	**12.17**	**12.51**	**12.87**	**13.10**	**58.89**	**11.85**	**12.04**	**12.03**	**12.07**	**12.30**
Immediate Roof Unit UCS, 2*cu1 (MPa)	**40.0**	**40.0**	**40.0**	**40.0**	**40.0**	**40.0**	**40.0**	**40.0**	**40.0**	**40.0**	**40.0**
Immediate Roof Unit Thickness, H (m)	**10.0**	**10.0**	**10.0**	**10.0**	**10.0**	**10.0**	**10.0**	**10.0**	**10.0**	**10.0**	**10.0**
Upper Roof Unit UCS, 2*cu2 (MPa)	**40.0**	**40.0**	**40.0**	**40.0**	**40.0**	**40.0**	**40.0**	**40.0**	**40.0**	**40.0**	**40.0**
cu1/cu2	**1.0**	**1.0**	**1.0**	**1.0**	**1.0**	**1.0**	**1.0**	**1.0**	**1.0**	**1.0**	**1.0**
H/B	**0.31**	**0.31**	**0.31**	**0.31**	**0.31**	**0.03**	**0.31**	**0.31**	**0.32**	**0.32**	**0.33**
N*1	**5.14**	**5.14**	**5.14**	**5.14**	**5.14**	**5.14**	**5.14**	**5.14**	**5.14**	**5.14**	**5.14**
N*2	5.14	5.14	5.14	5.14	5.14	5.14	5.14	5.14	5.14	5.14	5.14
Roof Bearing Capacity (MPa)	102.8	102.8	102.8	102.8	102.8	102.8	102.8	102.8	102.8	102.8	102.8
Pillar Stress (MPa)	**15.0**	**14.8**	**14.3**	**13.7**	**13.4**	**6.0**	**15.3**	**15.0**	**15.0**	**14.9**	**14.6**
Effective Roof Bearing Failure FoS	**6.85**	**6.95**	**7.21**	**7.48**	**7.66**	**17.27**	**6.71**	**6.85**	**6.85**	**6.88**	**7.06**
FTA Roof Bearing Failure FoS	**18.05**	**18.24**	**18.76**	**19.30**	**19.64**	**20.78**	**17.76**	**18.05**	**18.26**	**18.42**	**18.90**
Voussoir Beam Deflection (m)	**0.005**	**0.044**	**0.065**	**0.011**	**0.021**	**0.010**	**0.038**	**0.887**	**0.887**	**0.913**	**0.765**
System Settlement at Base of beam (m)	0.000	0.000	0.000	0.000	0.000	0.000	0.000	0.000	0.000	0.000	0.000
Applied Pillar Stress/FTA Stress Ratio (Mpa)	1.00	1.00	1.00	1.00	1.00	1.00	1.00	1.00	1.00	1.00	1.00
Effective Pillar Stress (Mpa)	15.00	14.79	14.27	13.74	13.43	5.95	15.32	15.00	15.00	14.94	14.56
Multi-Seam Stress Inc (min)											
Multi-Seam Stress Inc (max)											
Effective Pillar FoS	**2.24**	**2.27**	**2.36**	**2.45**	**2.50**	**355.04**	**2.20**	**2.24**	**2.15**	**2.11**	**2.12**
Eresidual coal(GPa)	**0.27**	**0.27**	**0.27**	**0.27**	**0.27**	**0.38**	**0.27**	**0.27**	**0.26**	**0.26**	**0.25**

UNSW Pillar Design Spreadsheet											
Chain Valley XL.Panel#	6.1	6.2	6.3	6.4	6.5	6.6	6.7	6.8	6.9	6.10	6.11
INPUT DATA											
Depth of Cover (m)	**170**	**165**	**160**	**185**	**178**	**175**	**173**	**168**	**163**	**160**	**158**
Mining Height (m)	**3.2**	**3.2**	**3.2**	**3.2**	**3.2**	**3.2**	**3.2**	**3.2**	**3.2**	**3.2**	**3.2**
Pillar Length - centres (m)	100.7	100.7	100.2	100.7	100.7	100.7	100.7	100.7	100.7	100.7	100.7
Pillar Width - centres (m)	35.3	34.7	34.7	38.0	37.0	36.5	36.0	35.3	34.7	34.7	34.7
Roadway Width for maximum pillar dimension	5.4	5.4	5.4	5.4	5.4	5.4	5.4	5.4	5.4	5.4	5.4
Roadway Width for minimum pillar dimension	5.4	5.4	5.4	5.4	5.4	5.4	5.4	5.4	5.4	5.4	5.4
Cut-Through Angle (degrees)	**90**	**90**	**90**	**90**	**90**	**90**	**90**	**90**	**90**	**90**	**90**
Average Panel Span (m) {rib-rib width}	**97**	**97**	97	97	97	97	97	97	97	97	97
SG (tonnes/m^3)	2.5	2.5	2.5	2.5	2.5	2.5	2.5	2.5	2.5	2.5	2.5
Conversion (tonnes to N)	10000	10000	10000	10000	10000	10000	10000	10000	10000	10000	10000
Abutment Angle (^{0})	21	21	21	21	21	21	21	21	21	21	21
W/H	0.57	0.59	0.61	0.52	0.54	0.55	0.56	0.58	0.60	0.61	0.61
PRELIMINARY CALCULATIONS											
Maximum Rib to Rib Pillar Length (w_2)	**95.3**	**95.3**	**94.8**	**95.3**	**95.3**	**95.3**	**95.3**	**95.3**	**95.3**	**95.3**	**95.3**
Minimum Rib to Rib Pillar Width (w_1)	**29.90**	**29.30**	**29.30**	**32.60**	**31.60**	**31.10**	**30.60**	**29.90**	**29.30**	**29.30**	**29.30**
w, Minimum Rib to Rib Pillar Width (ie $w_1 \sin\theta$)	**29.90**	**29.30**	**29.30**	**32.60**	**31.60**	**31.10**	**30.60**	**29.90**	**29.30**	**29.30**	**29.30**
Minimum Pillar Width/Height Ratio	**9.3**	**9.2**	**9.2**	**10.2**	**9.9**	**9.7**	**9.6**	**9.3**	**9.2**	**9.2**	**9.2**
Extraction Ratio (%)	**19.8%**	**20.1%**	**20.1%**	**18.8%**	**19.2%**	**19.4%**	**19.6%**	**19.8%**	**20.1%**	**20.1%**	**20.1%**
Abutment Angle (Radians)	0.367	0.367	0.367	0.367	0.367	0.367	0.367	0.367	0.367	0.367	0.367
Cut-Through Angle (Radians)	1.571	1.571	1.571	1.571	1.571	1.571	1.571	1.571	1.571	1.571	1.571
Is the Panel Super-Critical?	No	No	No	No	No	No	No	No	No	No	No
D (Peng & Chiang Loading Factor)	66.887	65.896	64.890	69.776	68.443	67.864	67.475	66.492	65.495	64.890	64.483
R (Pillar 2nd Abutment Component)	0.89	0.89	0.90	0.91	0.90	0.90	0.90	0.90	0.90	0.90	0.90
Dimensionless Pillar 'Rectangularity'	1.52	1.53	1.53	1.49	1.50	1.51	1.51	1.52	1.53	1.53	1.53
Width/Height Ratio Exponent	1.00	1.00	1.00	1.00	1.00	1.00	1.00	1.00	1.00	1.00	1.00
Effective Width Factor (Omega)	1.52	1.53	1.53	1.49	1.50	1.51	1.51	1.52	1.53	1.53	1.53
Effective Width Interim	45.52	44.82	44.76	48.58	47.46	46.90	46.33	45.52	44.82	44.82	44.82
Effective Pillar Width (m)	45.52	44.82	44.76	48.58	47.46	46.90	46.33	45.52	44.82	44.82	44.82
Effective Pillar Loading Height (m)	170.00	165.00	160.00	185.00	178.00	175.00	173.00	168.00	163.00	160.00	158.00
RESULTS											
Tributary Area Loading (MPa)	**5.30**	**5.16**	**5.01**	**5.70**	**5.51**	**5.43**	**5.38**	**5.24**	**5.10**	**5.01**	**4.94**
Pillar Strength (UNSW Squat Pillar 1999)	**29.88**	**29.10**	**29.08**	**33.62**	**32.18**	**31.49**	**30.81**	**29.88**	**29.10**	**29.10**	**29.10**
Pillar Strength (UNSW w/h<5)	**N/A**	**N/A**	**N/A**	**N/A**	**N/A**	**N/A**	**N/A**	**N/A**	**N/A**	**N/A**	**N/A**
Safety Factor under FTA Loading (Squat Pillar)	**5.63**	**5.64**	**5.81**	**5.90**	**5.85**	**5.80**	**5.73**	**5.70**	**5.71**	**5.81**	**5.89**
Safety Factor under FTA Loading (w/h<5)	**N/A**	**N/A**	**N/A**	**N/A**	**N/A**	**N/A**	**N/A**	**N/A**	**N/A**	**N/A**	**N/A**
Single Abutment Loading (3D) - full	4.46	4.35	4.14	4.65	4.53	4.49	4.48	4.38	4.27	4.14	4.06
Single Abutment Loading (3D) - pillar	**3.99**	**3.89**	**3.73**	**4.21**	**4.09**	**4.04**	**4.03**	**3.93**	**3.82**	**3.73**	**3.66**
Single Abutment Loading (3D) - solid	0.47	0.46	0.42	0.44	0.44	0.44	0.45	0.45	0.44	0.42	0.40
Design Abutment Load Multiplier	1.00	1.00	1.00	1.00	1.00	1.00	1.00	1.00	1.00	1.00	1.00
Total Pillar Loading with Single Abutment Loading	10.30	10.05	9.73	10.91	10.60	10.47	10.40	10.17	9.92	9.73	9.60
Safety Factor (under Single Abutment Loading)	**2.90**	**2.90**	**2.99**	**3.08**	**3.04**	**3.01**	**2.96**	**2.94**	**2.93**	**2.99**	**3.03**
Total Pillar Loading @ nA	**9.77**	**9.51**	**9.15**	**10.35**	**10.04**	**9.91**	**9.86**	**9.62**	**9.37**	**9.15**	**9.00**
Safety Factor @ nA	**3.06**	**3.06**	**3.18**	**3.25**	**3.21**	**3.18**	**3.13**	**3.10**	**3.11**	**3.18**	**3.23**
Total Pillar Loading under Double Abutment Loading	14.23	13.86	13.30	15.00	14.57	14.40	14.34	14.01	13.63	13.29	13.06
Safety Factor (under Double Abutment Loading)	**2.10**	**2.10**	**2.19**	**2.24**	**2.21**	**2.19**	**2.15**	**2.13**	**2.13**	**2.19**	**2.23**
Elastic Model Subsidence											
Ecoal(GPa)	**1.20**	**1.20**	**1.20**	**1.20**	**1.20**	**1.20**	**1.20**	**1.20**	**1.20**	**1.20**	**1.20**
E1floor(GPa)	**1.50**	**1.50**	**1.50**	**1.50**	**1.50**	**1.50**	**1.50**	**1.50**	**1.50**	**1.50**	**1.50**
E2floor(GPa)	**4.00**	**4.00**	**4.00**	**4.00**	**4.00**	**4.00**	**4.00**	**4.00**	**4.00**	**4.00**	**4.00**
E1roof(GPa)	**2.50**	**2.50**	**2.50**	**2.50**	**2.50**	**2.50**	**2.50**	**2.50**	**2.50**	**2.50**	**2.50**
E2roof(GPa)	**4.00**	**4.00**	**4.00**	**4.00**	**4.00**	**4.00**	**4.00**	**4.00**	**4.00**	**4.00**	**4.00**
Poissons Ratio floor/roof	**0.25**	**0.25**	**0.25**	**0.25**	**0.25**	**0.25**	**0.25**	**0.25**	**0.25**	**0.25**	**0.25**
initial vertical stress (MPa)	**4.25**	**4.13**	**4.00**	**4.63**	**4.45**	**4.38**	**4.33**	**4.20**	**4.08**	**4.00**	**3.95**
increase in vertical stress for DA (MPa)	**9.98**	**9.74**	**9.30**	**10.38**	**10.12**	**10.02**	**10.01**	**9.81**	**9.56**	**9.29**	**9.11**
Roof t1	**2.00**	**2.00**	**2.00**	**2.00**	**2.00**	**2.00**	**2.00**	**2.00**	**2.00**	**2.00**	**2.00**
Roof t2	**27.90**	**27.30**	**27.30**	**30.60**	**29.60**	**29.10**	**28.60**	**27.90**	**27.30**	**27.30**	**27.30**
Roof sig1	**9.98**	**9.74**	**9.30**	**10.37**	**10.12**	**10.02**	**10.01**	**9.81**	**9.56**	**9.29**	**9.11**
Roof sig2	**8.94**	**8.72**	**8.32**	**9.31**	**9.07**	**8.99**	**8.97**	**8.78**	**8.56**	**8.32**	**8.16**
Floor t1	**6.00**	**6.00**	**6.00**	**6.00**	**6.00**	**6.00**	**6.00**	**6.00**	**6.00**	**6.00**	**6.00**
Floor t2	**23.9**	**23.3**	**23.3**	**26.6**	**25.6**	**25.1**	**24.6**	**23.9**	**23.3**	**23.3**	**23.3**
Floor sig1	**9.97**	**9.73**	**9.29**	**10.37**	**10.11**	**10.02**	**10.01**	**9.80**	**9.55**	**9.28**	**9.11**
Floor sig2	**9.74**	**9.49**	**9.06**	**10.18**	**9.91**	**9.81**	**9.79**	**9.57**	**9.32**	**9.06**	**8.88**
Pillar Compression (m)	**0.025**	**0.024**	**0.023**	**0.026**	**0.025**	**0.025**	**0.025**	**0.025**	**0.024**	**0.023**	**0.023**
Roof Compression (m)	**0.066**	**0.063**	**0.060**	**0.075**	**0.071**	**0.069**	**0.068**	**0.065**	**0.062**	**0.060**	**0.059**
Floor Compression (m)	**0.092**	**0.088**	**0.084**	**0.102**	**0.097**	**0.095**	**0.094**	**0.090**	**0.087**	**0.084**	**0.083**
Total Compression (m)	**0.183**	**0.176**	**0.168**	**0.203**	**0.193**	**0.189**	**0.187**	**0.180**	**0.173**	**0.168**	**0.165**
Total Effective Compression (m)	**0.183**	**0.176**	**0.168**	**0.203**	**0.193**	**0.189**	**0.187**	**0.180**	**0.173**	**0.168**	**0.165**
1.5 times Effective Compression (m)	**0.274**	**0.264**	**0.252**	**0.304**	**0.290**	**0.284**	**0.280**	**0.270**	**0.259**	**0.252**	**0.247**
Total Yielded Panel Subs (m)	**0.25**	**0.24**	**0.23**	**0.27**	**0.26**	**0.26**	**0.25**	**0.25**	**0.24**	**0.23**	**0.23**
5 x Effective Predictions (m)	**0.914**	**0.879**	**0.839**	**1.014**	**0.966**	**0.946**	**0.933**	**0.898**	**0.863**	**0.839**	**0.823**
Bearing Capacity											
Upper Floor Unit UCS, 2*cu1 (MPa)	**20.0**	**20.0**	**20.0**	**20.0**	**20.0**	**20.0**	**20.0**	**20.0**	**20.0**	**20.0**	**20.0**
Upper Unit Thickness, H (m)	**6.0**	**6.0**	**6.0**	**6.0**	**6.0**	**6.0**	**6.0**	**6.0**	**6.0**	**6.0**	**6.0**
Lower Floor Unit UCS, 2*cu2 (MPa)	**40.0**	**40.0**	**40.0**	**40.0**	**40.0**	**40.0**	**40.0**	**40.0**	**40.0**	**40.0**	**40.0**
cu1/cu2	**0.5**	**0.5**	**0.5**	**0.5**	**0.5**	**0.5**	**0.5**	**0.5**	**0.5**	**0.5**	**0.5**
H/B	**0.20**	**0.20**	**0.20**	**0.18**	**0.19**	**0.19**	**0.20**	**0.20**	**0.20**	**0.20**	**0.20**
N*1	**6.63**	**6.58**	**6.58**	**6.86**	**6.77**	**6.73**	**6.69**	**6.63**	**6.58**	**6.58**	**6.58**
N*2	**3.32**	**3.29**	**3.29**	**3.43**	**3.39**	**3.37**	**3.35**	**3.32**	**3.29**	**3.29**	**3.29**
Floor Bearing Capacity (MPa)	**66.3**	**65.8**	**65.8**	**68.6**	**67.7**	**67.3**	**66.9**	**66.3**	**65.8**	**65.8**	**65.8**
Eff Pillar Stress (MPa)	**14.2**	**13.9**	**13.3**	**15.0**	**14.6**	**14.4**	**14.3**	**14.0**	**13.6**	**13.3**	**13.1**
Eff Floor Bearing Failure FoS	**4.66**	**4.75**	**4.95**	**4.57**	**4.65**	**4.68**	**4.67**	**4.74**	**4.83**	**4.95**	**5.04**
FTA Floor Bearing Failure FoS	**12.51**	**12.75**	**13.15**	**12.04**	**12.31**	**12.41**	**12.45**	**12.66**	**12.91**	**13.15**	**13.32**
Immediate Roof Unit UCS, 2*cu1 (MPa)	**40.0**	**40.0**	**40.0**	**40.0**	**40.0**	**40.0**	**40.0**	**40.0**	**40.0**	**40.0**	**40.0**
Immediate Roof Unit Thickness, H (m)	**10.0**	**10.0**	**10.0**	**10.0**	**10.0**	**10.0**	**10.0**	**10.0**	**10.0**	**10.0**	**10.0**
Upper Roof Unit UCS, 2*cu2 (MPa)	**40.0**	**40.0**	**40.0**	**40.0**	**40.0**	**40.0**	**40.0**	**40.0**	**40.0**	**40.0**	**40.0**
cu1/cu2	**1.0**	**1.0**	**1.0**	**1.0**	**1.0**	**1.0**	**1.0**	**1.0**	**1.0**	**1.0**	**1.0**
H/B	**0.33**	**0.34**	**0.34**	**0.31**	**0.32**	**0.32**	**0.33**	**0.33**	**0.34**	**0.34**	**0.34**
N*1	**5.14**	**5.14**	**5.14**	**5.14**	**5.14**	**5.14**	**5.14**	**5.14**	**5.14**	**5.14**	**5.14**
N*2	5.14	5.14	5.14	5.14	5.14	5.14	5.14	5.14	5.14	5.14	5.14
Roof Bearing Capacity (MPa)	102.8	102.8	102.8	102.8	102.8	102.8	102.8	102.8	102.8	102.8	102.8
Pillar Stress (MPa)	**14.2**	**13.9**	**13.3**	**15.0**	**14.6**	**14.4**	**14.3**	**14.0**	**13.6**	**13.3**	**13.1**
Effective Roof Bearing Failure FoS	**7.22**	**7.42**	**7.73**	**6.85**	**7.06**	**7.14**	**7.17**	**7.34**	**7.54**	**7.73**	**7.87**
FTA Roof Bearing Failure FoS	**19.39**	**19.91**	**20.53**	**18.05**	**18.67**	**18.95**	**19.12**	**19.62**	**20.16**	**20.54**	**20.80**
Voussoir Beam Deflection (m)	**0.691**	**1.072**	**0.957**	**0.957**	**0.957**	**0.957**	**0.957**	**0.957**	**0.957**	**0.957**	**0.957**
System Settlement at Base of beam (m)	0.000	0.000	0.000	0.000	0.000	0.000	0.000	0.000	0.000	0.000	0.000
Applied Pillar Stress/FTA Stress Ratio (Mpa)	1.00	1.00	1.00	1.00	1.00	1.00	1.00	1.00	1.00	1.00	1.00
Effective Pillar Stress (Mpa)	14.23	13.86	13.30	15.00	14.57	14.40	14.34	14.01	13.63	13.29	13.06
Multi-Seam Stress Inc (min)											
Multi-Seam Stress Inc (max)											
Effective Pillar FoS	**2.10**	**2.10**	**2.19**	**2.24**	**2.21**	**2.19**	**2.15**	**2.13**	**2.13**	**2.19**	**2.23**
Eresidual coal(GPa)	**0.25**	**0.25**	**0.25**	**0.27**	**0.26**	**0.26**	**0.25**	**0.25**	**0.25**	**0.25**	**0.25**

UNSW Pillar Design Spreadsheet											
Chain Valley XL.Panel#	6.12	6.13	7.1	7.2	7.3	7.4	7.5	7.6	7.7	7.8	7.9
INPUT DATA											
Depth of Cover (m)	**156**	**153**	**150**	**148**	**167**	**168**	**169**	**187**	**188**	**189**	**190**
Mining Height (m)	**3.2**	**3.2**	**3.2**	**3.2**	**3.2**	**3.2**	**3.2**	**3.2**	**3.2**	**3.2**	**3.2**
Pillar Length - centres (m)	100.7	100.2	100.2	100.2	100.7	100.7	100.7	100.7	100.7	100.7	100.7
Pillar Width - centres (m)	34.7	34.7	34.7	305.4	36.4	36.4	305.4	36.4	36.4	36.4	36.4
Roadway Width for maximum pillar dimension	5.4	5.4	5.4	5.4	5.4	5.4	5.4	5.4	5.4	5.4	5.4
Roadway Width for minimum pillar dimension	5.4	5.4	5.4	5.4	5.4	5.4	5.4	5.4	5.4	5.4	5.4
Cut-Through Angle (degrees)	**90**	**90**	**90**	**90**	**90**	**90**	**90**	**90**	**90**	**90**	**90**
Average Panel Span (m) {rib-rib width}	97	97	97	97	97	97	97	97	97	97	97
SG (tonnes/m^3)	2.5	2.5	2.5	2.5	2.5	2.5	2.5	2.5	2.5	2.5	2.5
Conversion (tonnes to N)	10000	10000	10000	10000	10000	10000	10000	10000	10000	10000	10000
Abutment Angle (^{0})	21	21	21	21	21	21	21	21	21	21	21
W/H	0.62	0.63	0.65	0.66	0.58	0.58	0.57	0.52	0.52	0.51	0.51
PRELIMINARY CALCULATIONS											
Maximum Rib to Rib Pillar Length (w_2)	**95.3**	**94.8**	**94.8**	**94.8**	**95.3**	**95.3**	**95.3**	**95.3**	**95.3**	**95.3**	**95.3**
Minimum Rib to Rib Pillar Width (w_1)	**29.30**	**29.30**	**29.30**	**300.00**	**31.00**	**31.00**	**300.00**	**31.00**	**31.00**	**31.00**	**31.00**
w, Minimum Rib to Rib Pillar Width (ie $w_1 \sin\theta$)	**29.30**	**29.30**	**29.30**	**300.00**	**31.00**	**31.00**	**300.00**	**31.00**	**31.00**	**31.00**	**31.00**
Minimum Pillar Width/Height Ratio	**9.2**	**9.2**	**9.2**	**29.6**	**9.7**	**9.7**	**29.8**	**9.7**	**9.7**	**9.7**	**9.7**
Extraction Ratio (%)	**20.1%**	**20.1%**	**20.1%**	**7.1%**	**19.4%**	**19.4%**	**7.0%**	**19.4%**	**19.4%**	**19.4%**	**19.4%**
Abutment Angle (Radians)	0.367	0.367	0.367	0.367	0.367	0.367	0.367	0.367	0.367	0.367	0.367
Cut-Through Angle (Radians)	1.571	1.571	1.571	1.571	1.571	1.571	1.571	1.571	1.571	1.571	1.571
Is the Panel Super-Critical?	No	No	No	No	No	No	No	No	No	No	No
D (Peng & Chiang Loading Factor)	64.074	63.455	62.829	62.409	66.294	66.492	66.690	70.152	70.339	70.526	70.712
R (Pillar 2nd Abutment Component)	0.90	0.91	0.91	1.00	0.91	0.91	1.00	0.89	0.89	0.89	0.89
Dimensionless Pillar 'Rectangularity'	1.53	1.53	1.53	0.48	1.51	1.51	0.48	1.51	1.51	1.51	1.51
Width/Height Ratio Exponent	1.00	1.00	1.00	1.00	1.00	1.00	1.00	1.00	1.00	1.00	1.00
Effective Width Factor (Omega)	1.53	1.53	1.53	0.48	1.51	1.51	0.48	1.51	1.51	1.51	1.51
Effective Width Interim	44.82	44.76	44.76	144.07	46.78	46.78	144.65	46.78	46.78	46.78	46.78
Effective Pillar Width (m)	44.82	44.76	44.76	144.07	46.78	46.78	144.65	46.78	46.78	46.78	46.78
Effective Pillar Loading Height (m)	156.00	153.00	150.00	148.00	167.00	168.00	169.00	187.00	188.00	189.00	190.00
RESULTS											
Tributary Area Loading (MPa)	**4.88**	**4.79**	**4.69**	**3.98**	**5.18**	**5.21**	**4.54**	**5.80**	**5.83**	**5.86**	**5.89**
Pillar Strength (UNSW Squat Pillar 1999)	**29.10**	**29.08**	**29.08**	**2108.59**	**31.35**	**31.35**	**2112.89**	**31.35**	**31.35**	**31.35**	**31.35**
Pillar Strength (UNSW w/h<5)	**N/A**	**N/A**	**N/A**	**N/A**	**N/A**	**N/A**	**N/A**	**N/A**	**N/A**	**N/A**	**N/A**
Safety Factor under FTA Loading (Squat Pillar)	**5.96**	**6.07**	**6.20**	**529.64**	**6.05**	**6.02**	**464.91**	**5.40**	**5.38**	**5.35**	**5.32**
Safety Factor under FTA Loading (w/h<5)	**N/A**	**N/A**	**N/A**	**N/A**	**N/A**	**N/A**	**N/A**	**N/A**	**N/A**	**N/A**	**N/A**
Single Abutment Loading (3D) - full	3.98	3.86	3.73	0.36	4.19	4.23	0.44	4.97	5.01	5.05	5.09
Single Abutment Loading (3D) - pillar	**3.59**	**3.50**	**3.40**	**0.36**	**3.81**	**3.84**	**0.44**	**4.42**	**4.45**	**4.48**	**4.51**
Single Abutment Loading (3D) - solid	0.38	0.36	0.33	0.00	0.38	0.39	0.00	0.55	0.56	0.57	0.58
Design Abutment Load Multiplier	1.00	1.00	1.00	1.00	1.00	1.00	1.00	1.00	1.00	1.00	1.00
Total Pillar Loading with Single Abutment Loading	9.48	9.28	9.09	5.34	9.99	10.05	5.99	11.22	11.28	11.34	11.40
Safety Factor (under Single Abutment Loading)	**3.07**	**3.13**	**3.20**	**395.05**	**3.14**	**3.12**	**352.99**	**2.79**	**2.78**	**2.76**	**2.75**
Total Pillar Loading @ nA	**8.86**	**8.64**	**8.43**	**4.34**	**9.37**	**9.44**	**4.99**	**10.77**	**10.84**	**10.91**	**10.98**
Safety Factor @ nA	**3.28**	**3.36**	**3.45**	**486.13**	**3.35**	**3.32**	**423.79**	**2.91**	**2.89**	**2.87**	**2.86**
Total Pillar Loading under Double Abutment Loading	12.84	12.50	12.16	4.69	13.56	13.67	5.43	15.74	15.85	15.96	16.07
Safety Factor (under Double Abutment Loading)	**2.27**	**2.33**	**2.39**	**449.22**	**2.31**	**2.29**	**389.35**	**1.99**	**1.98**	**1.96**	**1.95**
Elastic Model Subsidence											
Ecoal(GPa)	**1.20**	**1.20**	**1.20**	**1.20**	**1.20**	**1.20**	**1.20**	**1.20**	**1.20**	**1.20**	**1.20**
E1floor(GPa)	**1.50**	**1.50**	**1.50**	**1.50**	**1.50**	**1.50**	**1.50**	**1.50**	**1.50**	**1.50**	**1.50**
E2floor(GPa)	**4.00**	**4.00**	**4.00**	**4.00**	**4.00**	**4.00**	**4.00**	**4.00**	**4.00**	**4.00**	**4.00**
E1roof(GPa)	**2.50**	**2.50**	**2.50**	**2.50**	**2.50**	**2.50**	**2.50**	**2.50**	**2.50**	**2.50**	**2.50**
E2roof(GPa)	**4.00**	**4.00**	**4.00**	**4.00**	**4.00**	**4.00**	**4.00**	**4.00**	**4.00**	**4.00**	**4.00**
Poissons Ratio floor/roof	**0.25**	**0.25**	**0.25**	**0.25**	**0.25**	**0.25**	**0.25**	**0.25**	**0.25**	**0.25**	**0.25**
initial vertical stress (MPa)	**3.90**	**3.83**	**3.75**	**3.70**	**4.18**	**4.20**	**4.23**	**4.68**	**4.70**	**4.73**	**4.75**
increase in vertical stress for DA (MPa)	**8.94**	**8.67**	**8.41**	**0.99**	**9.38**	**9.47**	**1.20**	**11.07**	**11.15**	**11.23**	**11.32**
Roof t1	**2.00**	**2.00**	**2.00**	**2.00**	**2.00**	**2.00**	**2.00**	**2.00**	**2.00**	**2.00**	**2.00**
Roof t2	**27.30**	**27.30**	**27.30**	**298.00**	**29.00**	**29.00**	**298.00**	**29.00**	**29.00**	**29.00**	**29.00**
Roof sig1	**8.94**	**8.67**	**8.41**	**0.99**	**9.38**	**9.47**	**1.20**	**11.07**	**11.15**	**11.23**	**11.32**
Roof sig2	**8.00**	**7.77**	**7.53**	**0.90**	**8.41**	**8.49**	**1.09**	**9.92**	**9.99**	**10.07**	**10.14**
Floor t1	**6.00**	**6.00**	**6.00**	**6.00**	**6.00**	**6.00**	**6.00**	**6.00**	**6.00**	**6.00**	**6.00**
Floor t2	**23.3**	**23.3**	**23.3**	**294.0**	**25.0**	**25.0**	**294.0**	**25.0**	**25.0**	**25.0**	**25.0**
Floor sig1	**8.93**	**8.66**	**8.40**	**0.99**	**9.38**	**9.46**	**1.20**	**11.06**	**11.14**	**11.22**	**11.31**
Floor sig2	**8.71**	**8.45**	**8.19**	**0.99**	**9.18**	**9.26**	**1.20**	**10.83**	**10.91**	**10.99**	**11.07**
Pillar Compression (m)	**0.022**	**0.022**	**0.021**	**0.002**	**0.023**	**0.024**	**0.003**	**0.028**	**0.028**	**0.028**	**0.028**
Roof Compression (m)	**0.058**	**0.056**	**0.054**	**0.064**	**0.064**	**0.065**	**0.077**	**0.076**	**0.076**	**0.077**	**0.077**
Floor Compression (m)	**0.081**	**0.079**	**0.076**	**0.072**	**0.089**	**0.090**	**0.087**	**0.105**	**0.106**	**0.106**	**0.107**
Total Compression (m)	**0.161**	**0.157**	**0.152**	**0.139**	**0.177**	**0.178**	**0.168**	**0.208**	**0.210**	**0.211**	**0.213**
Total Effective Compression (m)	**0.161**	**0.157**	**0.152**	**0.139**	**0.177**	**0.178**	**0.168**	**0.208**	**0.210**	**0.211**	**0.213**
1.5 times Effective Compression (m)	**0.242**	**0.235**	**0.228**	**0.208**	**0.265**	**0.267**	**0.251**	**0.312**	**0.315**	**0.317**	**0.320**
Total Yielded Panel Subs (m)	**0.22**	**0.22**	**0.21**	**0.17**	**0.24**	**0.24**	**0.21**	**0.28**	**0.28**	**0.28**	**0.29**
5 x Effective Predictions (m)	**0.806**	**0.783**	**0.759**	**0.693**	**0.883**	**0.891**	**0.838**	**1.041**	**1.049**	**1.057**	**1.065**
Bearing Capacity											
Upper Floor Unit UCS, 2*cu1 (MPa)	**20.0**	**20.0**	**20.0**	**20.0**	**20.0**	**20.0**	**20.0**	**20.0**	**20.0**	**20.0**	**20.0**
Upper Unit Thickness, H (m)	**6.0**	**6.0**	**6.0**	**6.0**	**6.0**	**6.0**	**6.0**	**6.0**	**6.0**	**6.0**	**6.0**
Lower Floor Unit UCS, 2*cu2 (MPa)	**40.0**	**40.0**	**40.0**	**40.0**	**40.0**	**40.0**	**40.0**	**40.0**	**40.0**	**40.0**	**40.0**
cu1/cu2	**0.5**	**0.5**	**0.5**	**0.5**	**0.5**	**0.5**	**0.5**	**0.5**	**0.5**	**0.5**	**0.5**
H/B	**0.20**	**0.20**	**0.20**	**0.02**	**0.19**	**0.19**	**0.02**	**0.19**	**0.19**	**0.19**	**0.19**
N*1	**6.58**	**6.58**	**6.58**	**29.14**	**6.72**	**6.72**	**29.14**	**6.72**	**6.72**	**6.72**	**6.72**
N*2	**3.29**	**3.29**	**3.29**	**14.57**	**3.36**	**3.36**	**14.57**	**3.36**	**3.36**	**3.36**	**3.36**
Floor Bearing Capacity (MPa)	**65.8**	**65.8**	**65.8**	**291.4**	**67.2**	**67.2**	**291.4**	**67.2**	**67.2**	**67.2**	**67.2**
Eff Pillar Stress (MPa)	**12.8**	**12.5**	**12.2**	**4.7**	**13.6**	**13.7**	**5.4**	**15.7**	**15.8**	**16.0**	**16.1**
Eff Floor Bearing Failure FoS	**5.13**	**5.27**	**5.41**	**62.08**	**4.96**	**4.92**	**53.70**	**4.27**	**4.24**	**4.21**	**4.19**
FTA Floor Bearing Failure FoS	**13.49**	**13.75**	**14.02**	**73.20**	**12.98**	**12.90**	**64.12**	**11.59**	**11.53**	**11.47**	**11.41**
Immediate Roof Unit UCS, 2*cu1 (MPa)	**40.0**	**40.0**	**40.0**	**40.0**	**40.0**	**40.0**	**40.0**	**40.0**	**40.0**	**40.0**	**40.0**
Immediate Roof Unit Thickness, H (m)	**10.0**	**10.0**	**10.0**	**10.0**	**10.0**	**10.0**	**10.0**	**10.0**	**10.0**	**10.0**	**10.0**
Upper Roof Unit UCS, 2*cu2 (MPa)	**40.0**	**40.0**	**40.0**	**40.0**	**40.0**	**40.0**	**40.0**	**40.0**	**40.0**	**40.0**	**40.0**
cu1/cu2	**1.0**	**1.0**	**1.0**	**1.0**	**1.0**	**1.0**	**1.0**	**1.0**	**1.0**	**1.0**	**1.0**
H/B	**0.34**	**0.34**	**0.34**	**0.03**	**0.32**	**0.32**	**0.03**	**0.32**	**0.32**	**0.32**	**0.32**
N*1	**5.14**	**5.14**	**5.14**	**5.14**	**5.14**	**5.14**	**5.14**	**5.14**	**5.14**	**5.14**	**5.14**
N*2	5.14	5.14	5.14	5.14	5.14	5.14	5.14	5.14	5.14	5.14	5.14
Roof Bearing Capacity (MPa)	102.8	102.8	102.8	102.8	102.8	102.8	102.8	102.8	102.8	102.8	102.8
Pillar Stress (MPa)	**12.8**	**12.5**	**12.2**	**4.7**	**13.6**	**13.7**	**5.4**	**15.7**	**15.8**	**16.0**	**16.1**
Effective Roof Bearing Failure FoS	**8.01**	**8.22**	**8.46**	**21.90**	**7.58**	**7.52**	**18.94**	**6.53**	**6.49**	**6.44**	**6.40**
FTA Roof Bearing Failure FoS	**21.06**	**21.47**	**21.90**	**25.82**	**19.85**	**19.73**	**22.62**	**17.72**	**17.63**	**17.54**	**17.44**
Voussoir Beam Deflection (m)	**0.957**	**0.957**	**0.957**	**0.957**	**0.957**	**0.957**	**0.957**	**0.957**	**0.957**	**0.957**	**0.957**
System Settlement at Base of beam (m)	0.000	0.000	0.000	0.000	0.000	0.000	0.000	0.000	0.000	0.000	0.000
Applied Pillar Stress/FTA Stress Ratio (Mpa)	1.00	1.00	1.00	1.00	1.00	1.00	1.00	1.00	1.00	1.00	1.00
Effective Pillar Stress (Mpa)	12.84	12.50	12.16	4.69	13.56	13.67	5.43	15.74	15.85	15.96	16.07
Multi-Seam Stress Inc (min)											
Multi-Seam Stress Inc (max)											
Effective Pillar FoS	**2.27**	**2.33**	**2.39**	**449.22**	**2.31**	**2.29**	**389.35**	**1.99**	**1.98**	**1.96**	**1.95**
Eresidual coal(GPa)	**0.25**	**0.25**	**0.25**	**0.38**	**0.26**	**0.26**	**0.38**	**0.26**	**0.26**	**0.26**	**0.26**

UNSW Pillar Design Spreadsheet											
Chain Valley XL.Panel#	7.10	7.11	7.12	7.13	7.14	7.15	8.1	8.2	8.3	8.4	8.5
INPUT DATA											
Depth of Cover (m)	**190**	**190**	**219**	**218**	**221**	**220**	**217**	**229**	**230**	**231**	**232**
Mining Height (m)	**3.2**	**3.2**	**3.2**	**3.2**	**3.2**	**3.2**	**3.2**	**3.2**	**3.2**	**3.2**	**3.2**
Pillar Length - centres (m)	100.7	100.7	100.7	100.7	100.7	100.7	100.7	100.7	100.7	100.7	100.7
Pillar Width - centres (m)	36.4	36.4	36.0	36.0	36.0	36.0	36.0	36.0	36.0	36.0	36.0
Roadway Width for maximum pillar dimension	5.4	5.4	5.4	5.4	5.4	5.4	5.4	5.4	5.4	5.4	5.4
Roadway Width for minimum pillar dimension	5.4	5.4	5.4	5.4	5.4	5.4	5.4	5.4	5.4	5.4	5.4
Cut-Through Angle (degrees)	**90**	**90**	**90**	**90**	**90**	**90**	**90**	**90**	**90**	**90**	**90**
Average Panel Span (m) {rib-rib width}	97	97	97	97	97	97	97	97	97	97	97
SG (tonnes/m^3)	2.5	2.5	2.5	2.5	2.5	2.5	2.5	2.5	2.5	2.5	2.5
Conversion (tonnes to N)	10000	10000	10000	10000	10000	10000	10000	10000	10000	10000	10000
Abutment Angle (^{0})	21	21	21	21	21	21	21	21	21	21	21
W/H	0.51	0.51	0.44	0.44	0.44	0.44	0.45	0.42	0.42	0.42	0.42
PRELIMINARY CALCULATIONS											
Maximum Rib to Rib Pillar Length (w_2)	**95.3**	**95.3**	**95.3**	**95.3**	**95.3**	**95.3**	**95.3**	**95.3**	**95.3**	**95.3**	**95.3**
Minimum Rib to Rib Pillar Width (w_1)	**31.00**	**31.00**	**30.60**	**30.60**	**30.60**	**30.60**	**30.60**	**30.60**	**30.60**	**30.60**	**30.60**
w, Minimum Rib to Rib Pillar Width (ie $w_1 \sin\theta$)	**31.00**	**31.00**	**30.60**	**30.60**	**30.60**	**30.60**	**30.60**	**30.60**	**30.60**	**30.60**	**30.60**
Minimum Pillar Width/Height Ratio	**9.7**	**9.7**	**9.6**	**9.6**	**9.6**	**9.6**	**9.6**	**9.6**	**9.6**	**9.6**	**9.6**
Extraction Ratio (%)	**19.4%**	**19.4%**	**19.6%**	**19.6%**	**19.6%**	**19.6%**	**19.6%**	**19.6%**	**19.6%**	**19.6%**	**19.6%**
Abutment Angle (Radians)	0.367	0.367	0.367	0.367	0.367	0.367	0.367	0.367	0.367	0.367	0.367
Cut-Through Angle (Radians)	1.571	1.571	1.571	1.571	1.571	1.571	1.571	1.571	1.571	1.571	1.571
Is the Panel Super-Critical?	No	No	No	No	No	No	No	No	No	No	No
D (Peng & Chiang Loading Factor)	70.712	70.712	75.917	75.744	76.263	76.090	75.570	77.631	77.800	77.969	78.138
R (Pillar 2nd Abutment Component)	0.89	0.89	0.85	0.86	0.85	0.85	0.86	0.85	0.84	0.84	0.84
Dimensionless Pillar 'Rectangularity'	1.51	1.51	1.51	1.51	1.51	1.51	1.51	1.51	1.51	1.51	1.51
Width/Height Ratio Exponent	1.00	1.00	1.00	1.00	1.00	1.00	1.00	1.00	1.00	1.00	1.00
Effective Width Factor (Omega)	1.51	1.51	1.51	1.51	1.51	1.51	1.51	1.51	1.51	1.51	1.51
Effective Width Interim	46.78	46.78	46.33	46.33	46.33	46.33	46.33	46.33	46.33	46.33	46.33
Effective Pillar Width (m)	46.78	46.78	46.33	46.33	46.33	46.33	46.33	46.33	46.33	46.33	46.33
Effective Pillar Loading Height (m)	190.00	190.00	219.00	218.00	221.00	220.00	217.00	229.00	230.00	231.00	232.00
RESULTS											
Tributary Area Loading (MPa)	**5.89**	**5.89**	**6.81**	**6.78**	**6.87**	**6.84**	**6.74**	**7.12**	**7.15**	**7.18**	**7.21**
Pillar Strength (UNSW Squat Pillar 1999)	**31.35**	**31.35**	**30.81**	**30.81**	**30.81**	**30.81**	**30.81**	**30.81**	**30.81**	**30.81**	**30.81**
Pillar Strength (UNSW w/h<5)	**N/A**	**N/A**	**N/A**	**N/A**	**N/A**	**N/A**	**N/A**	**N/A**	**N/A**	**N/A**	**N/A**
Safety Factor under FTA Loading (Squat Pillar)	**5.32**	**5.32**	**4.53**	**4.55**	**4.49**	**4.51**	**4.57**	**4.33**	**4.31**	**4.29**	**4.27**
Safety Factor under FTA Loading (w/h<5)	**N/A**	**N/A**	**N/A**	**N/A**	**N/A**	**N/A**	**N/A**	**N/A**	**N/A**	**N/A**	**N/A**
Single Abutment Loading (3D) - full	5.09	5.09	6.30	6.26	6.38	6.34	6.22	6.70	6.74	6.77	6.81
Single Abutment Loading (3D) - pillar	**4.51**	**4.51**	**5.38**	**5.36**	**5.44**	**5.41**	**5.33**	**5.66**	**5.69**	**5.72**	**5.75**
Single Abutment Loading (3D) - solid	0.58	0.58	0.92	0.90	0.94	0.93	0.89	1.03	1.04	1.06	1.07
Design Abutment Load Multiplier	1.00	1.00	1.00	1.00	1.00	1.00	1.00	1.00	1.00	1.00	1.00
Total Pillar Loading with Single Abutment Loading	11.40	11.40	13.19	13.13	13.31	13.25	13.07	13.78	13.84	13.90	13.96
Safety Factor (under Single Abutment Loading)	**2.75**	**2.75**	**2.34**	**2.35**	**2.31**	**2.33**	**2.36**	**2.24**	**2.23**	**2.22**	**2.21**
Total Pillar Loading @ nA	**10.98**	**10.98**	**13.11**	**13.04**	**13.25**	**13.18**	**12.97**	**13.81**	**13.88**	**13.95**	**14.02**
Safety Factor @ nA	**2.86**	**2.86**	**2.35**	**2.36**	**2.33**	**2.34**	**2.38**	**2.23**	**2.22**	**2.21**	**2.20**
Total Pillar Loading under Double Abutment Loading	16.07	16.07	19.41	19.30	19.63	19.52	19.19	20.51	20.62	20.73	20.84
Safety Factor (under Double Abutment Loading)	**1.95**	**1.95**	**1.59**	**1.60**	**1.57**	**1.58**	**1.61**	**1.50**	**1.49**	**1.49**	**1.48**
Elastic Model Subsidence											
Ecoal(GPa)	**1.20**	**1.20**	**1.20**	**1.20**	**1.20**	**1.20**	**1.20**	**1.20**	**1.20**	**1.20**	**1.20**
E1floor(GPa)	**1.50**	**1.50**	**1.50**	**1.50**	**1.50**	**1.50**	**1.50**	**1.50**	**1.50**	**1.50**	**1.50**
E2floor(GPa)	**4.00**	**4.00**	**4.00**	**4.00**	**4.00**	**4.00**	**4.00**	**4.00**	**4.00**	**4.00**	**4.00**
E1roof(GPa)	**2.50**	**2.50**	**2.50**	**2.50**	**2.50**	**2.50**	**2.50**	**2.50**	**2.50**	**2.50**	**2.50**
E2roof(GPa)	**4.00**	**4.00**	**4.00**	**4.00**	**4.00**	**4.00**	**4.00**	**4.00**	**4.00**	**4.00**	**4.00**
Poissons Ratio floor/roof	**0.25**	**0.25**	**0.25**	**0.25**	**0.25**	**0.25**	**0.25**	**0.25**	**0.25**	**0.25**	**0.25**
initial vertical stress (MPa)	**4.75**	**4.75**	**5.48**	**5.45**	**5.53**	**5.50**	**5.43**	**5.73**	**5.75**	**5.78**	**5.80**
increase in vertical stress for DA (MPa)	**11.32**	**11.32**	**13.93**	**13.85**	**14.10**	**14.02**	**13.76**	**14.78**	**14.87**	**14.95**	**15.04**
Roof t1	**2.00**	**2.00**	**2.00**	**2.00**	**2.00**	**2.00**	**2.00**	**2.00**	**2.00**	**2.00**	**2.00**
Roof t2	**29.00**	**29.00**	**28.60**	**28.60**	**28.60**	**28.60**	**28.60**	**28.60**	**28.60**	**28.60**	**28.60**
Roof sig1	**11.32**	**11.32**	**13.93**	**13.85**	**14.10**	**14.02**	**13.76**	**14.78**	**14.87**	**14.95**	**15.04**
Roof sig2	**10.14**	**10.14**	**12.48**	**12.41**	**12.64**	**12.56**	**12.33**	**13.25**	**13.32**	**13.40**	**13.48**
Floor t1	**6.00**	**6.00**	**6.00**	**6.00**	**6.00**	**6.00**	**6.00**	**6.00**	**6.00**	**6.00**	**6.00**
Floor t2	**25.0**	**25.0**	**24.6**	**24.6**	**24.6**	**24.6**	**24.6**	**24.6**	**24.6**	**24.6**	**24.6**
Floor sig1	**11.31**	**11.31**	**13.92**	**13.83**	**14.09**	**14.00**	**13.75**	**14.77**	**14.85**	**14.94**	**15.02**
Floor sig2	**11.07**	**11.07**	**13.62**	**13.54**	**13.79**	**13.70**	**13.45**	**14.45**	**14.53**	**14.62**	**14.70**
Pillar Compression (m)	**0.028**	**0.028**	**0.035**	**0.035**	**0.035**	**0.035**	**0.034**	**0.037**	**0.037**	**0.037**	**0.038**
Roof Compression (m)	**0.077**	**0.077**	**0.094**	**0.094**	**0.095**	**0.095**	**0.093**	**0.100**	**0.100**	**0.101**	**0.102**
Floor Compression (m)	**0.107**	**0.107**	**0.131**	**0.130**	**0.132**	**0.132**	**0.129**	**0.139**	**0.140**	**0.140**	**0.141**
Total Compression (m)	**0.213**	**0.213**	**0.260**	**0.258**	**0.263**	**0.261**	**0.256**	**0.276**	**0.277**	**0.279**	**0.280**
Total Effective Compression (m)	**0.213**	**0.213**	**0.260**	**0.258**	**0.263**	**0.261**	**0.256**	**0.276**	**0.277**	**0.279**	**0.280**
1.5 times Effective Compression (m)	**0.320**	**0.320**	**0.390**	**0.387**	**0.394**	**0.392**	**0.385**	**0.413**	**0.416**	**0.418**	**0.420**
Total Yielded Panel Subs (m)	**0.29**	**0.29**	**0.35**	**0.34**	**0.35**	**0.35**	**0.34**	**0.37**	**0.37**	**0.37**	**0.37**
5 x Effective Predictions (m)	**1.065**	**1.065**	**1.298**	**1.290**	**1.314**	**1.306**	**1.282**	**1.378**	**1.386**	**1.394**	**1.402**
Bearing Capacity											
Upper Floor Unit UCS, 2*cu1 (MPa)	**20.0**	**20.0**	**20.0**	**20.0**	**20.0**	**20.0**	**20.0**	**20.0**	**20.0**	**20.0**	**20.0**
Upper Unit Thickness, H (m)	**6.0**	**6.0**	**6.0**	**6.0**	**6.0**	**6.0**	**6.0**	**6.0**	**6.0**	**6.0**	**6.0**
Lower Floor Unit UCS, 2*cu2 (MPa)	**40.0**	**40.0**	**40.0**	**40.0**	**40.0**	**40.0**	**40.0**	**40.0**	**40.0**	**40.0**	**40.0**
cu1/cu2	**0.5**	**0.5**	**0.5**	**0.5**	**0.5**	**0.5**	**0.5**	**0.5**	**0.5**	**0.5**	**0.5**
H/B	**0.19**	**0.19**	**0.20**	**0.20**	**0.20**	**0.20**	**0.20**	**0.20**	**0.20**	**0.20**	**0.20**
N*1	**6.72**	**6.72**	**6.69**	**6.69**	**6.69**	**6.69**	**6.69**	**6.69**	**6.69**	**6.69**	**6.69**
N*2	**3.36**	**3.36**	**3.35**	**3.35**	**3.35**	**3.35**	**3.35**	**3.35**	**3.35**	**3.35**	**3.35**
Floor Bearing Capacity (MPa)	**67.2**	**67.2**	**66.9**	**66.9**	**66.9**	**66.9**	**66.9**	**66.9**	**66.9**	**66.9**	**66.9**
Eff Pillar Stress (MPa)	**16.1**	**16.1**	**19.4**	**19.3**	**19.6**	**19.5**	**19.2**	**20.5**	**20.6**	**20.7**	**20.8**
Eff Floor Bearing Failure FoS	**4.19**	**4.19**	**3.45**	**3.47**	**3.41**	**3.43**	**3.49**	**3.26**	**3.25**	**3.23**	**3.21**
FTA Floor Bearing Failure FoS	**11.41**	**11.41**	**9.83**	**9.88**	**9.74**	**9.79**	**9.92**	**9.40**	**9.36**	**9.32**	**9.28**
Immediate Roof Unit UCS, 2*cu1 (MPa)	**40.0**	**40.0**	**40.0**	**40.0**	**40.0**	**40.0**	**40.0**	**40.0**	**40.0**	**40.0**	**40.0**
Immediate Roof Unit Thickness, H (m)	**10.0**	**10.0**	**10.0**	**10.0**	**10.0**	**10.0**	**10.0**	**10.0**	**10.0**	**10.0**	**10.0**
Upper Roof Unit UCS, 2*cu2 (MPa)	**40.0**	**40.0**	**40.0**	**40.0**	**40.0**	**40.0**	**40.0**	**40.0**	**40.0**	**40.0**	**40.0**
cu1/cu2	**1.0**	**1.0**	**1.0**	**1.0**	**1.0**	**1.0**	**1.0**	**1.0**	**1.0**	**1.0**	**1.0**
H/B	**0.32**	**0.32**	**0.33**	**0.33**	**0.33**	**0.33**	**0.33**	**0.33**	**0.33**	**0.33**	**0.33**
N*1	**5.14**	**5.14**	**5.14**	**5.14**	**5.14**	**5.14**	**5.14**	**5.14**	**5.14**	**5.14**	**5.14**
N*2	5.14	5.14	5.14	5.14	5.14	5.14	5.14	5.14	5.14	5.14	5.14
Roof Bearing Capacity (MPa)	102.8	102.8	102.8	102.8	102.8	102.8	102.8	102.8	102.8	102.8	102.8
Pillar Stress (MPa)	**16.1**	**16.1**	**19.4**	**19.3**	**19.6**	**19.5**	**19.2**	**20.5**	**20.6**	**20.7**	**20.8**
Effective Roof Bearing Failure FoS	**6.40**	**6.40**	**5.30**	**5.33**	**5.24**	**5.27**	**5.36**	**5.01**	**4.99**	**4.96**	**4.93**
FTA Roof Bearing Failure FoS	**17.44**	**17.44**	**15.10**	**15.17**	**14.97**	**15.04**	**15.24**	**14.44**	**14.38**	**14.32**	**14.26**
Voussoir Beam Deflection (m)	**0.957**	**0.957**	**0.957**	**0.957**	**0.957**	**0.957**	**0.957**	**0.957**	**0.957**	**0.957**	**0.957**
System Settlement at Base of beam (m)	0.000	0.000	0.000	0.000	0.000	0.000	0.000	0.000	0.000	0.000	0.000
Applied Pillar Stress/FTA Stress Ratio (Mpa)	1.00	1.00	1.00	1.00	1.00	1.00	1.00	1.00	1.00	1.00	1.00
Effective Pillar Stress (Mpa)	16.07	16.07	19.41	19.30	19.63	19.52	19.19	20.51	20.62	20.73	20.84
Multi-Seam Stress Inc (min)											
Multi-Seam Stress Inc (max)											
Effective Pillar FoS	**1.95**	**1.95**	**1.59**	**1.60**	**1.57**	**1.58**	**1.61**	**1.50**	**1.49**	**1.49**	**1.48**
Eresidual coal(GPa)	**0.26**	**0.26**	**0.25**	**0.25**	**0.25**	**0.25**	**0.25**	**0.25**	**0.25**	**0.25**	**0.25**

UNSW Pillar Design Spreadsheet											
Chain Valley XL.Panel#	8.6	9.1	9.2	9.3	9.4	9.5	10.1	10.2	10.3	10.4	10.5
INPUT DATA											
Depth of Cover (m)	**228**	**219**	**218**	**221**	**220**	**217**	**229**	**230**	**231**	**232**	**228**
Mining Height (m)	**3.2**	**3.2**	**3.2**	**3.2**	**3.2**	**3.2**	**3.2**	**3.2**	**3.2**	**3.2**	**3.2**
Pillar Length - centres (m)	100.7	100.7	100.7	100.7	100.7	100.7	100.7	100.7	100.7	100.7	100.7
Pillar Width - centres (m)	36.0	36.0	36.0	36.0	36.0	36.0	36.0	36.0	36.0	36.0	36.0
Roadway Width for maximum pillar dimension	5.4	5.4	5.4	5.4	5.4	5.4	5.4	5.4	5.4	5.4	5.4
Roadway Width for minimum pillar dimension	5.4	5.4	5.4	5.4	5.4	5.4	5.4	5.4	5.4	5.4	5.4
Cut-Through Angle (degrees)	**90**	**90**	**90**	**90**	**90**	**90**	**90**	**90**	**90**	**90**	**90**
Average Panel Span (m) {rib-rib width}	97	97	97	97	97	97	97	97	97	97	97
SG (tonnes/m^3)	2.5	2.5	2.5	2.5	2.5	2.5	2.5	2.5	2.5	2.5	2.5
Conversion (tonnes to N)	10000	10000	10000	10000	10000	10000	10000	10000	10000	10000	10000
Abutment Angle (^{0})	21	21	21	21	21	21	21	21	21	21	21
W/H	0.43	0.44	0.44	0.44	0.44	0.45	0.42	0.42	0.42	0.42	0.43
PRELIMINARY CALCULATIONS											
Maximum Rib to Rib Pillar Length (w_2)	**95.3**	**95.3**	**95.3**	**95.3**	**95.3**	**95.3**	**95.3**	**95.3**	**95.3**	**95.3**	**95.3**
Minimum Rib to Rib Pillar Width (w_1)	**30.60**	**30.60**	**30.60**	**30.60**	**30.60**	**30.60**	**30.60**	**30.60**	**30.60**	**30.60**	**30.60**
w, Minimum Rib to Rib Pillar Width (ie $w_1 \sin\theta$)	**30.60**	**30.60**	**30.60**	**30.60**	**30.60**	**30.60**	**30.60**	**30.60**	**30.60**	**30.60**	**30.60**
Minimum Pillar Width/Height Ratio	**9.6**	**9.6**	**9.6**	**9.6**	**9.6**	**9.6**	**9.6**	**9.6**	**9.6**	**9.6**	**9.6**
Extraction Ratio (%)	**19.6%**	**19.6%**	**19.6%**	**19.6%**	**19.6%**	**19.6%**	**19.6%**	**19.6%**	**19.6%**	**19.6%**	**19.6%**
Abutment Angle (Radians)	0.367	0.367	0.367	0.367	0.367	0.367	0.367	0.367	0.367	0.367	0.367
Cut-Through Angle (Radians)	1.571	1.571	1.571	1.571	1.571	1.571	1.571	1.571	1.571	1.571	1.571
Is the Panel Super-Critical?	No	No	No	No	No	No	No	No	No	No	No
D (Peng & Chiang Loading Factor)	77.461	75.917	75.744	76.263	76.090	75.570	77.631	77.800	77.969	78.138	77.461
R (Pillar 2nd Abutment Component)	0.85	0.85	0.86	0.85	0.85	0.86	0.85	0.84	0.84	0.84	0.85
Dimensionless Pillar 'Rectangularity'	1.51	1.51	1.51	1.51	1.51	1.51	1.51	1.51	1.51	1.51	1.51
Width/Height Ratio Exponent	1.00	1.00	1.00	1.00	1.00	1.00	1.00	1.00	1.00	1.00	1.00
Effective Width Factor (Omega)	1.51	1.51	1.51	1.51	1.51	1.51	1.51	1.51	1.51	1.51	1.51
Effective Width Interim	46.33	46.33	46.33	46.33	46.33	46.33	46.33	46.33	46.33	46.33	46.33
Effective Pillar Width (m)	46.33	46.33	46.33	46.33	46.33	46.33	46.33	46.33	46.33	46.33	46.33
Effective Pillar Loading Height (m)	228.00	219.00	218.00	221.00	220.00	217.00	229.00	230.00	231.00	232.00	228.00
RESULTS											
Tributary Area Loading (MPa)	**7.09**	**6.81**	**6.78**	**6.87**	**6.84**	**6.74**	**7.12**	**7.15**	**7.18**	**7.21**	**7.09**
Pillar Strength (UNSW Squat Pillar 1999)	**30.81**	**30.81**	**30.81**	**30.81**	**30.81**	**30.81**	**30.81**	**30.81**	**30.81**	**30.81**	**30.81**
Pillar Strength (UNSW w/h<5)	**N/A**	**N/A**	**N/A**	**N/A**	**N/A**	**N/A**	**N/A**	**N/A**	**N/A**	**N/A**	**N/A**
Safety Factor under FTA Loading (Squat Pillar)	**4.35**	**4.53**	**4.55**	**4.49**	**4.51**	**4.57**	**4.33**	**4.31**	**4.29**	**4.27**	**4.35**
Safety Factor under FTA Loading (w/h<5)	**N/A**	**N/A**	**N/A**	**N/A**	**N/A**	**N/A**	**N/A**	**N/A**	**N/A**	**N/A**	**N/A**
Single Abutment Loading (3D) - full	6.66	6.30	6.26	6.38	6.34	6.22	6.70	6.74	6.77	6.81	6.66
Single Abutment Loading (3D) - pillar	**5.64**	**5.38**	**5.36**	**5.44**	**5.41**	**5.33**	**5.66**	**5.69**	**5.72**	**5.75**	**5.64**
Single Abutment Loading (3D) - solid	1.02	0.92	0.90	0.94	0.93	0.89	1.03	1.04	1.06	1.07	1.02
Design Abutment Load Multiplier	1.00	1.00	1.00	1.00	1.00	1.00	1.00	1.00	1.00	1.00	1.00
Total Pillar Loading with Single Abutment Loading	13.72	13.19	13.13	13.31	13.25	13.07	13.78	13.84	13.90	13.96	13.72
Safety Factor (under Single Abutment Loading)	**2.25**	**2.34**	**2.35**	**2.31**	**2.33**	**2.36**	**2.24**	**2.23**	**2.22**	**2.21**	**2.25**
Total Pillar Loading @ nA	**13.74**	**13.11**	**13.04**	**13.25**	**13.18**	**12.97**	**13.81**	**13.88**	**13.95**	**14.02**	**13.74**
Safety Factor @ nA	**2.24**	**2.35**	**2.36**	**2.33**	**2.34**	**2.38**	**2.23**	**2.22**	**2.21**	**2.20**	**2.24**
Total Pillar Loading under Double Abutment Loading	20.40	19.41	19.30	19.63	19.52	19.19	20.51	20.62	20.73	20.84	20.40
Safety Factor (under Double Abutment Loading)	**1.51**	**1.59**	**1.60**	**1.57**	**1.58**	**1.61**	**1.50**	**1.49**	**1.49**	**1.48**	**1.51**
Elastic Model Subsidence											
Ecoal(GPa)	**1.20**	**1.20**	**1.20**	**1.20**	**1.20**	**1.20**	**1.20**	**1.20**	**1.20**	**1.20**	**1.20**
E1floor(GPa)	**1.50**	**1.50**	**1.50**	**1.50**	**1.50**	**1.50**	**1.50**	**1.50**	**1.50**	**1.50**	**1.50**
E2floor(GPa)	**4.00**	**4.00**	**4.00**	**4.00**	**4.00**	**4.00**	**4.00**	**4.00**	**4.00**	**4.00**	**4.00**
E1roof(GPa)	**2.50**	**2.50**	**2.50**	**2.50**	**2.50**	**2.50**	**2.50**	**2.50**	**2.50**	**2.50**	**2.50**
E2roof(GPa)	**4.00**	**4.00**	**4.00**	**4.00**	**4.00**	**4.00**	**4.00**	**4.00**	**4.00**	**4.00**	**4.00**
Poissons Ratio floor/roof	**0.25**	**0.25**	**0.25**	**0.25**	**0.25**	**0.25**	**0.25**	**0.25**	**0.25**	**0.25**	**0.25**
initial vertical stress (MPa)	**5.70**	**5.48**	**5.45**	**5.53**	**5.50**	**5.43**	**5.73**	**5.75**	**5.78**	**5.80**	**5.70**
increase in vertical stress for DA (MPa)	**14.70**	**15.43**	**15.35**	**14.50**	**15.52**	**15.26**	**16.28**	**16.37**	**16.45**	**16.54**	**16.20**
Roof t1	**2.00**	**2.00**	**2.00**	**2.00**	**2.00**	**2.00**	**2.00**	**2.00**	**2.00**	**2.00**	**2.00**
Roof t2	**28.60**	**28.60**	**28.60**	**28.60**	**28.60**	**28.60**	**28.60**	**28.60**	**28.60**	**28.60**	**28.60**
Roof sig1	**14.70**	**15.43**	**15.35**	**14.50**	**15.52**	**15.26**	**16.28**	**16.37**	**16.45**	**16.54**	**16.20**
Roof sig2	**13.17**	**13.83**	**13.75**	**12.99**	**13.90**	**13.68**	**14.59**	**14.67**	**14.74**	**14.82**	**14.51**
Floor t1	**6.00**	**6.00**	**6.00**	**6.00**	**6.00**	**6.00**	**6.00**	**6.00**	**6.00**	**6.00**	**6.00**
Floor t2	**24.6**	**24.6**	**24.6**	**24.6**	**24.6**	**24.6**	**24.6**	**24.6**	**24.6**	**24.6**	**24.6**
Floor sig1	**14.68**	**15.42**	**15.33**	**14.49**	**15.50**	**15.25**	**16.27**	**16.35**	**16.44**	**16.52**	**16.18**
Floor sig2	**14.37**	**15.08**	**15.00**	**14.18**	**15.17**	**14.92**	**15.92**	**16.00**	**16.08**	**16.17**	**15.83**
Pillar Compression (m)	**0.037**	**0.039**	**0.038**	**0.036**	**0.039**	**0.038**	**0.041**	**0.041**	**0.041**	**0.041**	**0.040**
Roof Compression (m)	**0.099**	**0.104**	**0.104**	**0.098**	**0.105**	**0.103**	**0.110**	**0.111**	**0.111**	**0.112**	**0.109**
Floor Compression (m)	**0.138**	**0.145**	**0.144**	**0.136**	**0.146**	**0.143**	**0.153**	**0.154**	**0.154**	**0.155**	**0.152**
Total Compression (m)	**0.274**	**0.288**	**0.286**	**0.270**	**0.289**	**0.284**	**0.304**	**0.305**	**0.307**	**0.308**	**0.302**
Total Effective Compression (m)	**0.274**	**0.288**	**0.286**	**0.270**	**0.289**	**0.284**	**0.304**	**0.305**	**0.307**	**0.308**	**0.302**
1.5 times Effective Compression (m)	**0.411**	**0.431**	**0.429**	**0.405**	**0.434**	**0.427**	**0.455**	**0.458**	**0.460**	**0.462**	**0.453**
Total Yielded Panel Subs (m)	**0.36**	**0.37**	**0.37**	**0.36**	**0.38**	**0.37**	**0.39**	**0.40**	**0.40**	**0.40**	**0.39**
5 x Effective Predictions (m)	**1.370**	**1.438**	**1.430**	**1.352**	**1.446**	**1.422**	**1.518**	**1.525**	**1.533**	**1.541**	**1.510**
Bearing Capacity											
Upper Floor Unit UCS, 2*cu1 (MPa)	**20.0**	**20.0**	**20.0**	**20.0**	**20.0**	**20.0**	**20.0**	**20.0**	**20.0**	**20.0**	**20.0**
Upper Unit Thickness, H (m)	**6.0**	**6.0**	**6.0**	**6.0**	**6.0**	**6.0**	**6.0**	**6.0**	**6.0**	**6.0**	**6.0**
Lower Floor Unit UCS, 2*cu2 (MPa)	**40.0**	**40.0**	**40.0**	**40.0**	**40.0**	**40.0**	**40.0**	**40.0**	**40.0**	**40.0**	**40.0**
cu1/cu2	**0.5**	**0.5**	**0.5**	**0.5**	**0.5**	**0.5**	**0.5**	**0.5**	**0.5**	**0.5**	**0.5**
H/B	**0.20**	**0.20**	**0.20**	**0.20**	**0.20**	**0.20**	**0.20**	**0.20**	**0.20**	**0.20**	**0.20**
N*1	**6.69**	**6.69**	**6.69**	**6.69**	**6.69**	**6.69**	**6.69**	**6.69**	**6.69**	**6.69**	**6.69**
N*2	**3.35**	**3.35**	**3.35**	**3.35**	**3.35**	**3.35**	**3.35**	**3.35**	**3.35**	**3.35**	**3.35**
Floor Bearing Capacity (MPa)	**66.9**	**66.9**	**66.9**	**66.9**	**66.9**	**66.9**	**66.9**	**66.9**	**66.9**	**66.9**	**66.9**
Eff Pillar Stress (MPa)	**20.4**	**20.9**	**20.8**	**20.0**	**21.0**	**20.7**	**22.0**	**22.1**	**22.2**	**22.3**	**21.9**
Eff Floor Bearing Failure FoS	**3.28**	**3.20**	**3.22**	**3.34**	**3.18**	**3.23**	**3.04**	**3.03**	**3.01**	**3.00**	**3.06**
FTA Floor Bearing Failure FoS	**9.44**	**9.83**	**9.88**	**9.74**	**9.79**	**9.92**	**9.40**	**9.36**	**9.32**	**9.28**	**9.44**
Immediate Roof Unit UCS, 2*cu1 (MPa)	**40.0**	**40.0**	**40.0**	**40.0**	**40.0**	**40.0**	**40.0**	**40.0**	**40.0**	**40.0**	**40.0**
Immediate Roof Unit Thickness, H (m)	**10.0**	**10.0**	**10.0**	**10.0**	**10.0**	**10.0**	**10.0**	**10.0**	**10.0**	**10.0**	**10.0**
Upper Roof Unit UCS, 2*cu2 (MPa)	**40.0**	**40.0**	**40.0**	**40.0**	**40.0**	**40.0**	**40.0**	**40.0**	**40.0**	**40.0**	**40.0**
cu1/cu2	**1.0**	**1.0**	**1.0**	**1.0**	**1.0**	**1.0**	**1.0**	**1.0**	**1.0**	**1.0**	**1.0**
H/B	**0.33**	**0.33**	**0.33**	**0.33**	**0.33**	**0.33**	**0.33**	**0.33**	**0.33**	**0.33**	**0.33**
N*1	**5.14**	**5.14**	**5.14**	**5.14**	**5.14**	**5.14**	**5.14**	**5.14**	**5.14**	**5.14**	**5.14**
N*2	5.14	5.14	5.14	5.14	5.14	5.14	5.14	5.14	5.14	5.14	5.14
Roof Bearing Capacity (MPa)	102.8	102.8	102.8	102.8	102.8	102.8	102.8	102.8	102.8	102.8	102.8
Pillar Stress (MPa)	**20.4**	**20.9**	**20.8**	**20.0**	**21.0**	**20.7**	**22.0**	**22.1**	**22.2**	**22.3**	**21.9**
Effective Roof Bearing Failure FoS	**5.04**	**4.92**	**4.94**	**5.13**	**4.89**	**4.97**	**4.67**	**4.65**	**4.62**	**4.60**	**4.69**
FTA Roof Bearing Failure FoS	**14.51**	**15.10**	**15.17**	**14.97**	**15.04**	**15.24**	**14.44**	**14.38**	**14.32**	**14.26**	**14.51**
Voussoir Beam Deflection (m)	**0.957**	**0.957**	**0.957**	**0.957**	**0.957**	**0.957**	**0.957**	**0.957**	**0.957**	**0.957**	**0.957**
System Settlement at Base of beam (m)	0.000	0.000	0.000	0.000	0.000	0.000	0.000	0.000	0.000	0.000	0.000
Applied Pillar Stress/FTA Stress Ratio (Mpa)	1.00	1.00	1.00	1.00	1.00	1.00	1.00	1.00	1.00	1.00	1.00
Effective Pillar Stress (Mpa)	20.40	**20.91**	**20.80**	**20.03**	**21.02**	**20.69**	**22.01**	**22.12**	**22.23**	**22.34**	**21.90**
Multi-Seam Stress Inc (min)		**0.84**	**0.84**	**-0.40**	**0.84**	**0.84**	**0.84**	**0.84**	**0.84**	**0.84**	**0.84**
Multi-Seam Stress Inc (max)		**1.50**	**1.50**	**0.40**	**1.50**	**1.50**	**1.50**	**1.50**	**1.50**	**1.50**	**1.50**
Effective Pillar FoS	**1.51**	**1.47**	**1.48**	**1.54**	**1.47**	**1.49**	**1.40**	**1.39**	**1.39**	**1.38**	**1.41**
Eresidual coal(GPa)	**0.25**	**0.25**	**0.25**	**0.25**	**0.25**	**0.25**	**0.25**	**0.25**	**0.25**	**0.25**	**0.25**

UNSW Pillar Design Spreadsheet										
Chain Valley XL.Panel#	9.1	9.2	9.3	9.4	9.5	10.1	10.2	10.3	10.4	10.5
INPUT DATA										
Depth of Cover (m)	**219**	**218**	**221**	**220**	**217**	**229**	**230**	**231**	**232**	**228**
Mining Height (m)	**3.2**	**3.2**	**3.2**	**3.2**	**3.2**	**3.2**	**3.2**	**3.2**	**3.2**	**3.2**
Pillar Length - centres (m)	100.7	100.7	100.7	100.7	100.7	100.7	100.7	100.7	100.7	100.7
Pillar Width - centres (m)	36.0	36.0	36.0	36.0	36.0	36.0	36.0	36.0	36.0	36.0
Roadway Width for maximum pillar dimension	5.4	5.4	5.4	5.4	5.4	5.4	5.4	5.4	5.4	5.4
Roadway Width for minimum pillar dimension	5.4	5.4	5.4	5.4	5.4	5.4	5.4	5.4	5.4	5.4
Cut-Through Angle (degrees)	**90**	**90**	**90**	**90**	**90**	**90**	**90**	**90**	**90**	**90**
Average Panel Span (m) {rib-rib width}	97	97	97	97	97	97	97	97	97	97
SG (tonnes/m^3)	2.5	2.5	2.5	2.5	2.5	2.5	2.5	2.5	2.5	2.5
Conversion (tonnes to N)	10000	10000	10000	10000	10000	10000	10000	10000	10000	10000
Abutment Angle (^{o})	21	21	21	21	21	21	21	21	21	21
W/H	0.44	0.44	0.44	0.44	0.45	0.42	0.42	0.42	0.42	0.43
PRELIMINARY CALCULATIONS										
Maximum Rib to Rib Pillar Length (w_2)	**95.3**	**95.3**	**95.3**	**95.3**	**95.3**	**95.3**	**95.3**	**95.3**	**95.3**	**95.3**
Minimum Rib to Rib Pillar Width (w_1)	**30.60**	**30.60**	**30.60**	**30.60**	**30.60**	**30.60**	**30.60**	**30.60**	**30.60**	**30.60**
w, Minimum Rib to Rib Pillar Width (ie $w_1 \sin\theta$)	**30.60**	**30.60**	**30.60**	**30.60**	**30.60**	**30.60**	**30.60**	**30.60**	**30.60**	**30.60**
Minimum Pillar Width/Height Ratio	**9.6**	**9.6**	**9.6**	**9.6**	**9.6**	**9.6**	**9.6**	**9.6**	**9.6**	**9.6**
Extraction Ratio (%)	**19.6%**	**19.6%**	**19.6%**	**19.6%**	**19.6%**	**19.6%**	**19.6%**	**19.6%**	**19.6%**	**19.6%**
Abutment Angle (Radians)	0.367	0.367	0.367	0.367	0.367	0.367	0.367	0.367	0.367	0.367
Cut-Through Angle (Radians)	1.571	1.571	1.571	1.571	1.571	1.571	1.571	1.571	1.571	1.571
Is the Panel Super-Critical?	No	No	No	No	No	No	No	No	No	No
D (Peng & Chiang Loading Factor)	75.917	75.744	76.263	76.090	75.570	77.631	77.800	77.969	78.138	77.461
R (Pillar 2nd Abutment Component)	0.85	0.86	0.85	0.85	0.86	0.85	0.84	0.84	0.84	0.85
Dimensionless Pillar 'Rectangularity'	1.51	1.51	1.51	1.51	1.51	1.51	1.51	1.51	1.51	1.51
Width/Height Ratio Exponent	1.00	1.00	1.00	1.00	1.00	1.00	1.00	1.00	1.00	1.00
Effective Width Factor (Omega)	1.51	1.51	1.51	1.51	1.51	1.51	1.51	1.51	1.51	1.51
Effective Width Interim	46.33	46.33	46.33	46.33	46.33	46.33	46.33	46.33	46.33	46.33
Effective Pillar Width (m)	46.33	46.33	46.33	46.33	46.33	46.33	46.33	46.33	46.33	46.33
Effective Pillar Loading Height (m)	219.00	218.00	221.00	220.00	217.00	229.00	230.00	231.00	232.00	228.00
RESULTS										
Tributary Area Loading (MPa)	**6.81**	**6.78**	**6.87**	**6.84**	**6.74**	**7.12**	**7.15**	**7.18**	**7.21**	**7.09**
Pillar Strength (UNSW Squat Pillar 1999)	**30.81**	**30.81**	**30.81**	**30.81**	**30.81**	**30.81**	**30.81**	**30.81**	**30.81**	**30.81**
Pillar Strength (UNSW w/h<5)	**N/A**	**N/A**	**N/A**	**N/A**	**N/A**	**N/A**	**N/A**	**N/A**	**N/A**	**N/A**
Safety Factor under FTA Loading (Squat Pillar)	**4.53**	**4.55**	**4.49**	**4.51**	**4.57**	**4.33**	**4.31**	**4.29**	**4.27**	**4.35**
Safety Factor under FTA Loading (w/h<5)	**N/A**	**N/A**	**N/A**	**N/A**	**N/A**	**N/A**	**N/A**	**N/A**	**N/A**	**N/A**
Single Abutment Loading (3D) - full	6.30	6.26	6.38	6.34	6.22	6.70	6.74	6.77	6.81	6.66
Single Abutment Loading (3D) - pillar	**5.38**	**5.36**	**5.44**	**5.41**	**5.33**	**5.66**	**5.69**	**5.72**	**5.75**	**5.64**
Single Abutment Loading (3D) - solid	0.92	0.90	0.94	0.93	0.89	1.03	1.04	1.06	1.07	1.02
Design Abutment Load Multiplier	1.00	1.00	1.00	1.00	1.00	1.00	1.00	1.00	1.00	1.00
Total Pillar Loading with Single Abutment Loading	13.19	13.13	13.31	13.25	13.07	13.78	13.84	13.90	13.96	13.72
Safety Factor (under Single Abutment Loading)	**2.34**	**2.35**	**2.31**	**2.33**	**2.36**	**2.24**	**2.23**	**2.22**	**2.21**	**2.25**
Total Pillar Loading @ nA	**13.11**	**13.04**	**13.25**	**13.18**	**12.97**	**13.81**	**13.88**	**13.95**	**14.02**	**13.74**
Safety Factor @ nA	**2.35**	**2.36**	**2.33**	**2.34**	**2.38**	**2.23**	**2.22**	**2.21**	**2.20**	**2.24**
Total Pillar Loading under Double Abutment Loading	19.41	19.30	19.63	19.52	19.19	20.51	20.62	20.73	20.84	20.40
Safety Factor (under Double Abutment Loading)	**1.59**	**1.60**	**1.57**	**1.58**	**1.61**	**1.50**	**1.49**	**1.49**	**1.48**	**1.51**
Elastic Model Subsidence										
Ecoal(GPa)	**1.20**	**1.20**	**1.20**	**1.20**	**1.20**	**1.20**	**1.20**	**1.20**	**1.20**	**1.20**
E1floor(GPa)	**1.50**	**1.50**	**1.50**	**1.50**	**1.50**	**1.50**	**1.50**	**1.50**	**1.50**	**1.50**
E2floor(GPa)	**4.00**	**4.00**	**4.00**	**4.00**	**4.00**	**4.00**	**4.00**	**4.00**	**4.00**	**4.00**
E1roof(GPa)	**2.50**	**2.50**	**2.50**	**2.50**	**2.50**	**2.50**	**2.50**	**2.50**	**2.50**	**2.50**
E2roof(GPa)	**4.00**	**4.00**	**4.00**	**4.00**	**4.00**	**4.00**	**4.00**	**4.00**	**4.00**	**4.00**
Poissons Ratio floor/roof	**0.25**	**0.25**	**0.25**	**0.25**	**0.25**	**0.25**	**0.25**	**0.25**	**0.25**	**0.25**
initial vertical stress (MPa)	**5.48**	**5.45**	**5.53**	**5.50**	**5.43**	**5.73**	**5.75**	**5.78**	**5.80**	**5.70**
increase in vertical stress for DA (MPa)	**15.43**	**15.35**	**14.50**	**15.52**	**15.26**	**16.28**	**16.37**	**16.45**	**16.54**	**16.20**
Roof t1	**2.00**	**2.00**	**2.00**	**2.00**	**2.00**	**2.00**	**2.00**	**2.00**	**2.00**	**2.00**
Roof t2	**28.60**	**28.60**	**28.60**	**28.60**	**28.60**	**28.60**	**28.60**	**28.60**	**28.60**	**28.60**
Roof sig1	**15.43**	**15.35**	**14.50**	**15.52**	**15.26**	**16.28**	**16.37**	**16.45**	**16.54**	**16.20**
Roof sig2	**13.83**	**13.75**	**12.99**	**13.90**	**13.68**	**14.59**	**14.67**	**14.74**	**14.82**	**14.51**
Floor t1	**6.00**	**6.00**	**6.00**	**6.00**	**6.00**	**6.00**	**6.00**	**6.00**	**6.00**	**6.00**
Floor t2	**24.6**	**24.6**	**24.6**	**24.6**	**24.6**	**24.6**	**24.6**	**24.6**	**24.6**	**24.6**
Floor sig1	**15.42**	**15.33**	**14.49**	**15.50**	**15.25**	**16.27**	**16.35**	**16.44**	**16.52**	**16.18**
Floor sig2	**15.08**	**15.00**	**14.18**	**15.17**	**14.92**	**15.92**	**16.00**	**16.08**	**16.17**	**15.83**
Pillar Compression (m)	**0.039**	**0.038**	**0.036**	**0.039**	**0.038**	**0.041**	**0.041**	**0.041**	**0.041**	**0.040**
Roof Compression (m)	**0.104**	**0.104**	**0.098**	**0.105**	**0.103**	**0.110**	**0.111**	**0.111**	**0.112**	**0.109**
Floor Compression (m)	**0.145**	**0.144**	**0.136**	**0.146**	**0.143**	**0.153**	**0.154**	**0.154**	**0.155**	**0.152**
Total Compression (m)	**0.288**	**0.286**	**0.270**	**0.289**	**0.284**	**0.304**	**0.305**	**0.307**	**0.308**	**0.302**
Total Effective Compression (m)	**0.288**	**0.286**	**0.270**	**0.289**	**0.284**	**0.304**	**0.305**	**0.307**	**0.308**	**0.302**
1.5 times Effective Compression (m)	**0.431**	**0.429**	**0.405**	**0.434**	**0.427**	**0.455**	**0.458**	**0.460**	**0.462**	**0.453**
Total Yielded Panel Subs (m)	**0.37**	**0.37**	**0.36**	**0.38**	**0.37**	**0.39**	**0.40**	**0.40**	**0.40**	**0.39**
5 x Effective Predictions (m)	**1.438**	**1.430**	**1.352**	**1.446**	**1.422**	**1.518**	**1.525**	**1.533**	**1.541**	**1.510**
Bearing Capacity										
Upper Floor Unit UCS, 2*cu1 (MPa)	**20.0**	**20.0**	**20.0**	**20.0**	**20.0**	**20.0**	**20.0**	**20.0**	**20.0**	**20.0**
Upper Unit Thickness, H (m)	**6.0**	**6.0**	**6.0**	**6.0**	**6.0**	**6.0**	**6.0**	**6.0**	**6.0**	**6.0**
Lower Floor Unit UCS, 2*cu2 (MPa)	**40.0**	**40.0**	**40.0**	**40.0**	**40.0**	**40.0**	**40.0**	**40.0**	**40.0**	**40.0**
cu1/cu2	**0.5**	**0.5**	**0.5**	**0.5**	**0.5**	**0.5**	**0.5**	**0.5**	**0.5**	**0.5**
H/B	**0.20**	**0.20**	**0.20**	**0.20**	**0.20**	**0.20**	**0.20**	**0.20**	**0.20**	**0.20**
N*1	**6.69**	**6.69**	**6.69**	**6.69**	**6.69**	**6.69**	**6.69**	**6.69**	**6.69**	**6.69**
N*2	**3.35**	**3.35**	**3.35**	**3.35**	**3.35**	**3.35**	**3.35**	**3.35**	**3.35**	**3.35**
Floor Bearing Capacity (MPa)	**66.9**	**66.9**	**66.9**	**66.9**	**66.9**	**66.9**	**66.9**	**66.9**	**66.9**	**66.9**
Eff Pillar Stress (MPa)	**20.9**	**20.8**	**20.0**	**21.0**	**20.7**	**22.0**	**22.1**	**22.2**	**22.3**	**21.9**
Eff Floor Bearing Failure FoS	**3.20**	**3.22**	**3.34**	**3.18**	**3.23**	**3.04**	**3.03**	**3.01**	**3.00**	**3.06**
FTA Floor Bearing Failure FoS	**9.83**	**9.88**	**9.74**	**9.79**	**9.92**	**9.40**	**9.36**	**9.32**	**9.28**	**9.44**
Immediate Roof Unit UCS, 2*cu1 (MPa)	**40.0**	**40.0**	**40.0**	**40.0**	**40.0**	**40.0**	**40.0**	**40.0**	**40.0**	**40.0**
Immediate Roof Unit Thickness, H (m)	**10.0**	**10.0**	**10.0**	**10.0**	**10.0**	**10.0**	**10.0**	**10.0**	**10.0**	**10.0**
Upper Roof Unit UCS, 2*cu2 (MPa)	**40.0**	**40.0**	**40.0**	**40.0**	**40.0**	**40.0**	**40.0**	**40.0**	**40.0**	**40.0**
cu1/cu2	**1.0**	**1.0**	**1.0**	**1.0**	**1.0**	**1.0**	**1.0**	**1.0**	**1.0**	**1.0**
H/B	**0.33**	**0.33**	**0.33**	**0.33**	**0.33**	**0.33**	**0.33**	**0.33**	**0.33**	**0.33**
N*1	**5.14**	**5.14**	**5.14**	**5.14**	**5.14**	**5.14**	**5.14**	**5.14**	**5.14**	**5.14**
N*2	5.14	5.14	5.14	5.14	5.14	5.14	5.14	5.14	5.14	5.14
Roof Bearing Capacity (MPa)	102.8	102.8	102.8	102.8	102.8	102.8	102.8	102.8	102.8	102.8
Pillar Stress (MPa)	**20.9**	**20.8**	**20.0**	**21.0**	**20.7**	**22.0**	**22.1**	**22.2**	**22.3**	**21.9**
Effective Roof Bearing Failure FoS	**4.92**	**4.94**	**5.13**	**4.89**	**4.97**	**4.67**	**4.65**	**4.62**	**4.60**	**4.69**
FTA Roof Bearing Failure FoS	**15.10**	**15.17**	**14.97**	**15.04**	**15.24**	**14.44**	**14.38**	**14.32**	**14.26**	**14.51**
Voussoir Beam Deflection (m)	**0.957**	**0.957**	**0.957**	**0.957**	**0.957**	**0.957**	**0.957**	**0.957**	**0.957**	**0.957**
System Settlement at Base of beam (m)	0.000	0.000	0.000	0.000	0.000	0.000	0.000	0.000	0.000	0.000
Applied Pillar Stress/FTA Stress Ratio (Mpa)	1.00	1.00	1.00	1.00	1.00	1.00	1.00	1.00	1.00	1.00
Effective Pillar Stress (Mpa)	**20.91**	**20.80**	**20.03**	**21.02**	**20.69**	**22.01**	**22.12**	**22.23**	**22.34**	**21.90**
Multi-Seam Stress Inc (min)	**0.84**	**0.84**	**-0.40**	**0.84**	**0.84**	**0.84**	**0.84**	**0.84**	**0.84**	**0.84**
Multi-Seam Stress Inc (max)	**1.50**	**1.50**	**0.40**	**1.50**	**1.50**	**1.50**	**1.50**	**1.50**	**1.50**	**1.50**
Effective Pillar FoS	**1.47**	**1.48**	**1.54**	**1.47**	**1.49**	**1.40**	**1.39**	**1.39**	**1.38**	**1.41**
Eresidual coal(GPa)	**0.25**	**0.25**	**0.25**	**0.25**	**0.25**	**0.25**	**0.25**	**0.25**	**0.25**	**0.25**

UNSW Pillar Design Spreadsheet										
GN Seam Workings	FWs	newer	newer	newer	old	FWs	newer	newer	newer	old
INPUT DATA										
Depth of Cover (m)	180	180	185	190	190	180	180	185	190	190
Mining Height (m)	2.5	2.5	2.5	2.5	2.5	3.3	3.3	3.3	3.3	3.3
Pillar Length - centres (m)	31.5	34.1	31.5	29.5	24.6	31.5	34.1	31.5	29.5	24.6
Pillar Width - centres (m)	22.2	22.9	23.6	29.5	24.6	22.2	22.9	23.6	29.5	24.6
Roadway Width for maximum pillar dimension	5.5	5.5	5.5	5.5	5.5	5.5	5.5	5.5	5.5	5.5
Roadway Width for minimum pillar dimension	5.5	5.5	5.5	5.5	5.5	5.5	5.5	5.5	5.5	5.5
Cut-Through Angle (degrees)	90	90	90	90	90	90	90	90	90	90
Average Panel Span (m) (rib-rib width)	142	142	188	188	188	142	142	188	188	188
SG (tonnes/m^3)	2.5	2.5	2.5	2.5	2.5	2.5	2.5	2.5	2.5	2.5
Conversion (tonnes to N)	10000	10000	10000	10000	10000	10000	10000	10000	10000	10000
Abutment Angle (^{o})	21	21	21	21	21	21	21	21	21	21
W/H	0.79	0.79	1.02	0.99	0.99	0.79	0.79	1.02	0.99	0.99
PRELIMINARY CALCULATIONS										
Maximum Rib to Rib Pillar Length (w_2)	26.0	28.6	26.0	24.0	19.1	26.0	28.6	26.0	24.0	19.1
Minimum Rib to Rib Pillar Width (w_1)	16.7	17.4	18.1	24.0	19.1	16.7	17.4	18.1	24.0	19.1
w, Minimum Rib to Rib Pillar Width (ie $w_1 \sin\theta$)	16.7	17.4	18.1	24.0	19.1	16.7	17.4	18.1	24.0	19.1
Minimum Pillar Width/Height Ratio	6.7	7.0	7.2	9.6	7.6	5.1	5.3	5.5	7.3	5.8
Extraction Ratio (%)	37.9%	36.3%	36.7%	33.8%	39.7%	37.9%	36.3%	36.7%	33.8%	39.7%
Abutment Angle (Radians)	0.367	0.367	0.367	0.367	0.367	0.367	0.367	0.367	0.367	0.367
Cut-Through Angle (Radians)	1.571	1.571	1.571	1.571	1.571	1.571	1.571	1.571	1.571	1.571
Is the Panel Super-Critical?	Yes	Yes	Yes	Yes	Yes	Yes	Yes	Yes	Yes	Yes
D (Peng & Chiang Loading Factor)	68.826	68.826	69.776	70.712	70.712	68.826	68.826	69.776	70.712	70.712
R (Pillar 2nd Abutment Component)	0.69	0.70	0.71	0.80	0.72	0.69	0.70	0.71	0.80	0.72
Dimensionless Pillar 'Rectangularity'	1.22	1.24	1.18	1.00	1.00	1.22	1.24	1.18	1.00	1.00
Width/Height Ratio Exponent	1.00	1.00	1.00	1.00	1.00	0.69	0.76	0.83	1.00	0.93
Effective Width Factor (Omega)	1.22	1.24	1.18	1.00	1.00	1.14	1.18	1.15	1.00	1.00
Effective Width Interim	20.34	21.64	21.34	24.00	19.10	19.12	20.52	20.75	24.00	19.10
Effective Pillar Width (m)	20.34	21.64	21.34	24.00	19.10	19.12	20.52	20.75	24.00	19.10
Effective Pillar Loading Height (m)	180.00	180.00	185.00	190.00	190.00	180.00	180.00	185.00	190.00	190.00
RESULTS										
Tributary Area Loading (MPa)	7.25	7.06	7.31	7.18	7.88	7.25	7.06	7.31	7.18	7.88
Pillar Strength (UNSW Squat Pillar 1999)	19.45	20.45	20.71	27.21	20.20	14.10	14.64	14.77	17.46	14.28
Pillar Strength (UNSW w/h<5)	N/A	N/A	N/A	N/A	N/A	N/A	N/A	N/A	N/A	N/A
Safety Factor under FTA Loading (Squat Pillar)	2.68	2.90	2.84	3.79	2.56	1.95	2.07	2.02	2.43	1.81
Safety Factor under FTA Loading (w/h<5)	N/A	N/A	N/A	N/A	N/A	N/A	N/A	N/A	N/A	N/A
Single Abutment Loading (3D) - full	11.28	10.65	10.99	8.87	11.68	11.28	10.65	10.99	8.87	11.68
Single Abutment Loading (3D) - pillar	7.77	7.49	7.81	7.12	8.44	7.77	7.49	7.81	7.12	8.44
Single Abutment Loading (3D) - solid	3.51	3.17	3.19	1.76	3.24	3.51	3.17	3.19	1.76	3.24
Design Abutment Load Multiplier	1.00	1.00	1.00	1.50	1.00	1.00	1.00	1.00	1.50	1.00
Total Pillar Loading with Single Abutment Loading	16.02	15.55	16.11	15.79	17.32	16.02	15.55	16.11	15.79	17.32
Safety Factor (under Single Abutment Loading)	1.21	1.31	1.29	1.72	1.17	0.88	0.94	0.92	1.11	0.82
Total Pillar Loading @ nA	18.53	17.71	18.30	20.48	19.56	18.53	17.71	18.30	20.48	19.56
Safety Factor @ nA	1.05	1.15	1.13	1.33	1.03	0.76	0.83	0.81	0.85	0.73
Total Pillar Loading under Double Abutment Loading	29.80	28.37	29.29	24.92	31.24	29.80	28.37	29.29	24.92	31.24
Safety Factor (under Double Abutment Loading)	0.65	0.72	0.71	1.09	0.65	0.47	0.52	0.50	0.70	0.46
Elastic Model Subsidence										
Ecoal(GPa)	1.25	1.25	1.25	1.25	1.25	1.25	1.25	1.25	1.25	1.25
E1floor(GPa)	1.50	1.50	1.50	1.50	1.50	1.50	1.50	1.50	1.50	1.50
E2floor(GPa)	4.00	4.00	4.00	4.00	4.00	4.00	4.00	4.00	4.00	4.00
E1roof(GPa)	2.50	2.50	2.50	2.50	2.50	2.50	2.50	2.50	2.50	2.50
E2roof(GPa)	4.00	4.00	4.00	4.00	4.00	4.00	4.00	4.00	4.00	4.00
Poissons Ratio floor/roof	0.25	0.25	0.25	0.25	0.25	0.25	0.25	0.25	0.25	0.25
initial vertical stress (MPa)	4.50	4.50	4.63	4.75	4.75	4.50	4.50	4.63	4.75	4.75
increase in vertical stress for DA (MPa)	2.75	2.56	2.68	2.43	3.13	2.75	2.56	2.68	2.43	3.13
Roof t1	10.00	2.00	2.00	2.00	10.00	10.00	2.00	2.00	2.00	10.00
Roof t2	6.70	15.40	16.10	22.00	9.10	6.70	15.40	16.10	22.00	9.10
Roof sig1	2.68	2.56	2.68	2.43	3.08	2.68	2.56	2.68	2.43	3.08
Roof sig2	2.08	2.27	2.37	2.16	2.43	2.08	2.27	2.37	2.16	2.43
Floor t1	6.00	6.00	6.00	6.00	6.00	6.00	6.00	6.00	6.00	6.00
Floor t2	10.7	11.4	12.1	18.0	13.1	10.7	11.4	12.1	18.0	13.1
Floor sig1	2.73	2.55	2.67	2.42	3.12	2.73	2.55	2.67	2.42	3.12
Floor sig2	2.45	2.31	2.44	2.32	2.89	2.45	2.31	2.44	2.32	2.89
Pillar Compression (m)	0.005	0.005	0.005	0.005	0.006	0.007	0.006	0.007	0.006	0.008
Roof Compression (m)	0.013	0.010	0.011	0.013	0.017	0.013	0.010	0.011	0.013	0.017
Floor Compression (m)	0.016	0.016	0.017	0.019	0.021	0.016	0.016	0.017	0.019	0.021
Total FTA Compression (m)	0.035	0.031	0.033	0.036	0.043	0.037	0.032	0.035	0.038	0.045
Total Effective Compression (m)	0.035	0.031	0.033	0.036	0.043	0.037	0.032	0.035	0.038	0.045
1.5 times Effective Compression (m)	0.052	0.046	0.049	0.055	0.065	0.055	0.048	0.052	0.057	0.068
Total Yielded Panel Subs (m)	0.14	0.13	0.13	0.11	0.14	0.30	0.25	0.24	0.16	0.24
5 x Effective Predictions (m)	0.174	0.153	0.165	0.182	0.216	0.183	0.161	0.173	0.189	0.225
Bearing Capacity										
Upper Floor Unit UCS, 2*cu1 (MPa)	20.0	20.0	20.0	20.0	20.0	20.0	20.0	20.0	20.0	20.0
Upper Unit Thickness, H (m)	6.0	6.0	6.0	6.0	6.0	6.0	6.0	6.0	6.0	6.0
Lower Floor Unit UCS, 2*cu2 (MPa)	40.0	40.0	40.0	40.0	40.0	40.0	40.0	40.0	40.0	40.0
cu1/cu2	0.5	0.5	0.5	0.5	0.5	0.5	0.5	0.5	0.5	0.5
H/B	0.36	0.34	0.33	0.25	0.31	0.36	0.34	0.33	0.25	0.31
N*1	5.53	5.59	5.65	6.14	5.73	5.53	5.59	5.65	6.14	5.73
N*2	2.77	2.80	2.82	3.07	2.87	2.77	2.80	2.82	3.07	2.87
Floor Bearing Capacity (MPa)	55.3	55.9	56.5	61.4	57.3	55.3	55.9	56.5	61.4	57.3
Eff Pillar Stress (MPa)	7.2	7.1	7.3	7.2	7.9	7.2	7.1	7.3	7.2	7.9
Eff Floor Bearing Failure FoS	7.63	7.92	7.73	8.56	7.28	7.63	7.92	7.73	8.56	7.28
FTA Floor Bearing Failure FoS	7.63	7.92	7.73	8.56	7.28	7.63	7.92	7.73	8.56	7.28
Immediate Roof Unit UCS, 2*cu1 (MPa)	40.0	40.0	40.0	40.0	40.0	40.0	40.0	40.0	40.0	40.0
Immediate Roof Unit Thickness, H (m)	10.0	10.0	10.0	10.0	10.0	10.0	10.0	10.0	10.0	10.0
Upper Roof Unit UCS, 2*cu2 (MPa)	40.0	40.0	40.0	40.0	40.0	40.0	40.0	40.0	40.0	40.0
cu1/cu2	1.0	1.0	1.0	1.0	1.0	1.0	1.0	1.0	1.0	1.0
H/B	0.60	0.57	0.55	0.42	0.52	0.60	0.57	0.55	0.42	0.52
N*1	5.14	5.14	5.14	5.14	5.14	5.14	5.14	5.14	5.14	5.14
N*2	5.14	5.14	5.14	5.14	5.14	5.14	5.14	5.14	5.14	5.14
Roof Bearing Capacity (MPa)	102.8	102.8	102.8	102.8	102.8	102.8	102.8	102.8	102.8	102.8
Pillar Stress (MPa)	7.2	7.1	7.3	7.2	7.9	7.2	7.1	7.3	7.2	7.9
Effective Roof Bearing Failure FoS	14.18	14.56	14.07	14.32	13.05	14.18	14.56	14.07	14.32	13.05
FTA Roof Bearing Failure FoS	14.18	14.56	14.07	14.32	13.05	14.18	14.56	14.07	14.32	13.05
Voussoir Beam Deflection (m)		0.004	0.004	0.001			0.004	0.004	0.001	
System Settlement at Base of beam (m)	0.000	0.000	0.000	0.000	0.000	0.000	0.000	0.000	0.000	0.000
Applied Pillar Stress/FTA Stress Ratio (Mpa)	1.00	1.00	1.00	1.00	1.00	1.00	1.00	1.00	1.00	1.00
Effective Pillar Stress (Mpa)	7.25	7.06	7.31	7.18	7.88	7.25	7.06	7.31	7.18	7.88
Multi-Seam Stress Inc (min)										
Multi-Seam Stress Inc (max)										
Eresidual coal(GPa)	0.18	0.19	0.20	0.25	0.21	0.09	0.11	0.12	0.20	0.13
Effective Pillar FoS	2.68	2.90	2.84	3.79	2.56	1.95	2.07	2.02	2.43	1.81
Single Seam FoS	2.68	2.90	2.84	3.79	2.56	1.95	2.07	2.02	2.43	1.81
w/h	6.68	6.96	7.24	9.60	7.64	5.06	5.27	5.48	7.27	5.79

UNSW Pillar Design Spreadsheet										
Chain Valley	FWs	newer	newer	newer	old	FWs	newer	newer	newer	old
INPUT DATA										
Depth of Cover (m)	180	180	190	190	190	180	180	185	190	190
Mining Height (m)	2.5	2.5	2.5	2.5	2.5	3.3	3.3	3.3	3.3	3.3
Pillar Length - centres (m)	31.5	34.1	31.5	29.5	24.6	31.5	34.1	31.5	29.5	24.6
Pillar Width - centres (m)	22.2	22.9	23.6	29.5	24.6	22.2	22.9	23.6	29.5	24.6
Roadway Width for maximum pillar dimension	5.5	5.5	5.5	5.5	5.5	5.5	5.5	5.5	5.5	5.5
Roadway Width for minimum pillar dimension	5.5	5.5	5.5	5.5	5.5	5.5	5.5	5.5	5.5	5.5
Cut-Through Angle (degrees)	90	90	90	90	90	90	90	90	90	90
Average Panel Span (m) (rib-rib width)	186	186	186	186	186	186	186	186	186	186
SG (tonnes/m^3)	2.5	2.5	2.5	2.5	2.5	2.5	2.5	2.5	2.5	2.5
Conversion (tonnes to N)	10000	10000	10000	10000	10000	10000	10000	10000	10000	10000
Abutment Angle (^{o})	21	21	21	21	21	21	21	21	21	21
W/H	1.03	1.03	0.98	0.98	0.98	1.03	1.03	1.01	0.98	0.98
PRELIMINARY CALCULATIONS										
Maximum Rib to Rib Pillar Length (w_2)	26.0	28.6	26.0	24.0	19.1	26.0	28.6	26.0	24.0	19.1
Minimum Rib to Rib Pillar Width (w_1)	16.7	17.4	18.1	24.0	19.1	16.7	17.4	18.1	24.0	19.1
w, Minimum Rib to Rib Pillar Width (ie $w_1 \sin\theta$)	16.7	17.4	18.1	24.0	19.1	16.7	17.4	18.1	24.0	19.1
Minimum Pillar Width/Height Ratio	6.7	7.0	7.2	9.6	7.6	5.1	5.3	5.5	7.3	5.8
Extraction Ratio (%)	37.9%	36.3%	36.7%	33.8%	39.7%	37.9%	36.3%	36.7%	33.8%	39.7%
Abutment Angle (Radians)	0.367	0.367	0.367	0.367	0.367	0.367	0.367	0.367	0.367	0.367
Cut-Through Angle (Radians)	1.571	1.571	1.571	1.571	1.571	1.571	1.571	1.571	1.571	1.571
Is the Panel Super-Critical?	Yes	Yes	Yes	Yes	Yes	Yes	Yes	Yes	Yes	Yes
D (Peng & Chiang Loading Factor)	68.826	68.826	70.712	70.712	70.712	68.826	68.826	69.776	70.712	70.712
R (Pillar 2nd Abutment Component)	0.69	0.70	0.70	0.80	0.72	0.69	0.70	0.71	0.80	0.72
Dimensionless Pillar 'Rectangularity'	1.22	1.24	1.18	1.00	1.00	1.22	1.24	1.18	1.00	1.00
Width/Height Ratio Exponent	1.00	1.00	1.00	1.00	1.00	0.69	0.76	0.83	1.00	0.93
Effective Width Factor (Omega)	1.22	1.24	1.18	1.00	1.00	1.14	1.18	1.15	1.00	1.00
Effective Width Interim	20.34	21.64	21.34	24.00	19.10	19.12	20.52	20.75	24.00	19.10
Effective Pillar Width (m)	20.34	21.64	21.34	24.00	19.10	19.12	20.52	20.75	24.00	19.10
Effective Pillar Loading Height (m)	180.00	180.00	190.00	190.00	190.00	180.00	180.00	185.00	190.00	190.00
RESULTS										
Tributary Area Loading (MPa)	7.25	7.06	7.50	7.18	7.88	7.25	7.06	7.31	7.18	7.88
Pillar Strength (UNSW Squat Pillar 1999)	19.45	20.45	20.71	27.21	20.20	14.10	14.64	14.77	17.46	14.28
Pillar Strength (UNSW w/h<5)	N/A	N/A	N/A	N/A	N/A	N/A	N/A	N/A	N/A	N/A
Safety Factor under FTA Loading (Squat Pillar)	2.68	2.90	2.76	3.79	2.56	1.95	2.07	2.02	2.43	1.81
Safety Factor under FTA Loading (w/h<5)	N/A	N/A	N/A	N/A	N/A	N/A	N/A	N/A	N/A	N/A
Single Abutment Loading (3D) - full	11.28	10.65	11.59	8.87	11.68	11.28	10.65	10.99	8.87	11.68
Single Abutment Loading (3D) - pillar	7.77	7.49	8.17	7.12	8.44	7.77	7.49	7.81	7.12	8.44
Single Abutment Loading (3D) - solid	3.51	3.17	3.43	1.76	3.24	3.51	3.17	3.19	1.76	3.24
Design Abutment Load Multiplier	1.00	1.00	1.00	1.50	1.00	1.00	1.00	1.00	1.50	1.00
Total Pillar Loading with Single Abutment Loading	16.02	15.55	16.67	15.79	17.32	16.02	15.55	16.11	15.79	17.32
Safety Factor (under Single Abutment Loading)	1.21	1.31	1.24	1.72	1.17	0.88	0.94	0.92	1.11	0.82
Total Pillar Loading @ nA	18.53	17.71	19.10	20.48	19.56	18.53	17.71	18.30	20.48	19.56
Safety Factor @ nA	1.05	1.15	1.08	1.33	1.03	0.76	0.83	0.81	0.85	0.73
Total Pillar Loading under Double Abutment Loading	29.80	28.37	30.69	24.92	31.24	29.80	28.37	29.29	24.92	31.24
Safety Factor (under Double Abutment Loading)	0.65	0.72	0.67	1.09	0.65	0.47	0.52	0.50	0.70	0.46
Elastic Model Subsidence										
Ecoal(GPa)	1.20	1.20	1.20	1.20	1.20	1.20	1.20	1.20	1.20	1.20
E1floor(GPa)	1.50	1.50	1.50	1.50	1.50	1.50	1.50	1.50	1.50	1.50
E2floor(GPa)	4.00	4.00	4.00	4.00	4.00	4.00	4.00	4.00	4.00	4.00
E1roof(GPa)	2.50	2.50	2.50	2.50	2.50	2.50	2.50	2.50	2.50	2.50
E2roof(GPa)	4.00	4.00	4.00	4.00	4.00	4.00	4.00	4.00	4.00	4.00
Poissons Ratio floor/roof	0.25	0.25	0.25	0.25	0.25	0.25	0.25	0.25	0.25	0.25
initial vertical stress (MPa)	4.50	4.50	4.75	4.75	4.75	4.50	4.50	4.63	4.75	4.75
increase in vertical stress for DA (MPa)	9.35	9.16	9.35	9.03	9.73	9.35	9.16	9.28	9.03	9.73
Roof t1	10.00	2.00	2.00	2.00	10.00	10.00	2.00	2.00	2.00	10.00
Roof t2	6.70	15.40	16.10	22.00	9.10	6.70	15.40	16.10	22.00	9.10
Roof sig1	9.13	9.16	9.35	9.03	9.57	9.13	9.16	9.28	9.03	9.57
Roof sig2	7.07	8.10	8.28	8.05	7.56	7.07	8.10	8.22	8.05	7.56
Floor t1	6.00	6.00	6.00	6.00	6.00	6.00	6.00	6.00	6.00	6.00
Floor t2	10.7	11.4	12.1	18.0	13.1	10.7	11.4	12.1	18.0	13.1
Floor sig1	9.30	9.12	9.31	9.01	9.69	9.30	9.12	9.24	9.01	9.69
Floor sig2	8.35	8.27	8.53	8.64	8.98	8.35	8.27	8.46	8.64	8.98
Pillar Compression (m)	0.018	0.018	0.018	0.018	0.019	0.024	0.024	0.024	0.023	0.025
Roof Compression (m)	0.045	0.036	0.038	0.048	0.052	0.045	0.036	0.038	0.048	0.052
Floor Compression (m)	0.056	0.056	0.059	0.070	0.064	0.056	0.056	0.059	0.070	0.064
Total FTA Compression (m)	0.119	0.110	0.116	0.136	0.135	0.125	0.116	0.121	0.142	0.141
Total Effective Compression (m)	0.119	0.110	0.116	0.136	0.135	0.125	0.116	0.121	0.142	0.141
1.5 times Effective Compression (m)	0.179	0.165	0.173	0.204	0.202	0.188	0.174	0.181	0.213	0.212
Total Yielded Panel Subs (m)	0.22	0.21	0.21	0.21	0.23	0.39	0.34	0.32	0.26	0.33
5 x Effective Predictions (m)	0.597	0.552	0.578	0.681	0.675	0.626	0.580	0.603	0.709	0.705
Bearing Capacity										
Upper Floor Unit UCS, 2*cu1 (MPa)	20.0	20.0	20.0	20.0	20.0	20.0	20.0	20.0	20.0	20.0
Upper Unit Thickness, H (m)	6.0	6.0	6.0	6.0	6.0	6.0	6.0	6.0	6.0	6.0
Lower Floor Unit UCS, 2*cu2 (MPa)	40.0	40.0	40.0	40.0	40.0	40.0	40.0	40.0	40.0	40.0
cu1/cu2	0.5	0.5	0.5	0.5	0.5	0.5	0.5	0.5	0.5	0.5
H/B	0.36	0.34	0.33	0.25	0.31	0.36	0.34	0.33	0.25	0.31
N*1	5.53	5.59	5.65	6.14	5.73	5.53	5.59	5.65	6.14	5.73
N*2	2.77	2.80	2.82	3.07	2.87	2.77	2.80	2.82	3.07	2.87
Floor Bearing Capacity (MPa)	55.3	55.9	56.5	61.4	57.3	55.3	55.9	56.5	61.4	57.3
Eff Pillar Stress (MPa)	13.8	13.7	14.1	13.8	14.5	13.8	13.7	13.9	13.8	14.5
Eff Floor Bearing Failure FoS	4.00	4.09	4.01	4.46	3.96	4.00	4.09	4.06	4.46	3.96
FTA Floor Bearing Failure FoS	7.63	7.92	7.53	8.56	7.28	7.63	7.92	7.73	8.56	7.28
Immediate Roof Unit UCS, 2*cu1 (MPa)	40.0	40.0	40.0	40.0	40.0	40.0	40.0	40.0	40.0	40.0
Immediate Roof Unit Thickness, H (m)	10.0	10.0	10.0	10.0	10.0	10.0	10.0	10.0	10.0	10.0
Upper Roof Unit UCS, 2*cu2 (MPa)	40.0	40.0	40.0	40.0	40.0	40.0	40.0	40.0	40.0	40.0
cu1/cu2	1.0	1.0	1.0	1.0	1.0	1.0	1.0	1.0	1.0	1.0
H/B	0.60	0.57	0.55	0.42	0.52	0.60	0.57	0.55	0.42	0.52
N*1	5.14	5.14	5.14	5.14	5.14	5.14	5.14	5.14	5.14	5.14
N*2	5.14	5.14	5.14	5.14	5.14	5.14	5.14	5.14	5.14	5.14
Roof Bearing Capacity (MPa)	102.8	102.8	102.8	102.8	102.8	102.8	102.8	102.8	102.8	102.8
Pillar Stress (MPa)	13.8	13.7	14.1	13.8	14.5	13.8	13.7	13.9	13.8	14.5
Effective Roof Bearing Failure FoS	7.42	7.52	7.29	7.46	7.10	7.42	7.52	7.39	7.46	7.10
FTA Roof Bearing Failure FoS	14.18	14.56	13.70	14.32	13.05	14.18	14.56	14.07	14.32	13.05
Voussoir Beam Deflection (m)		0.004	0.004	0.001			0.004	0.004	0.001	
System Settlement at Base of beam (m)	0.000	0.000	0.000	0.000	0.000	0.000	0.000	0.000	0.000	0.000
Applied Pillar Stress/FTA Stress Ratio (Mpa)	1.00	1.00	1.00	1.00	1.00	1.00	1.00	1.00	1.00	1.00
Effective Pillar Stress (Mpa)	13.85	13.66	14.10	13.78	14.48	13.85	13.66	13.91	13.78	14.48
Multi-Seam Stress Inc (min)	-3	-3	-3	-3	-3	-3	-3	-3	-3	-3
Multi-Seam Stress Inc (max)	6.60	6.60	6.60	6.60	6.60	6.60	6.60	6.60	6.60	6.60
Eresidual coal(GPa)	0.18	0.19	0.20	0.25	0.21	0.09	0.11	0.12	0.20	0.13
Effective Pillar FoS	1.40	1.50	1.47	1.97	1.39	1.02	1.07	1.06	1.27	0.99
Single Seam FoS	2.68	2.90	2.76	3.79	2.56	1.95	2.07	2.02	2.43	1.81
w/h	6.68	6.96	7.24	9.60	7.64	5.06	5.27	5.48	7.27	5.79

UNSW Pillar Design Spreadsheet										
Chain Valley	FWs				SWs	FWs				SWs
INPUT DATA										
Depth of Cover (m)	**150**	**150**	**150**	**160**	**160**	**150**	**150**	**150**	**160**	**160**
Mining Height (m)	**3**	**3**	**3**	**3**	**3**	**3.5**	**3.5**	**3.5**	**3.5**	**3.5**
Pillar Length - centres (m)	33.8	29.5	61.5	34.0	33.9	33.8	29.5	61.5	34.0	33.9
Pillar Width - centres (m)	24.0	25.1	25.5	30.7	33.9	24.0	25.1	25.5	30.7	33.9
Roadway Width for maximum pillar dimension	**5.5**	**5.5**	**5.5**	**5.5**	**5.5**	**5.5**	**5.5**	**5.5**	**5.5**	**5.5**
Roadway Width for minimum pillar dimension	**5.5**	**5.5**	**5.5**	**5.5**	**5.5**	**5.5**	**5.5**	**5.5**	**5.5**	**5.5**
Cut-Through Angle (degrees)	**90**	**90**	**90**	**90**	**90**	**90**	**90**	**90**	**90**	**90**
Average Panel Span (m) (rib-rib width)	**188**	**160**	**160**	**188**	**60**	**188**	**160**	**160**	**188**	**60**
SG (tonnes/m^3)	2.5	2.5	2.5	2.5	2.5	2.5	2.5	2.5	2.5	2.5
Conversion (tonnes to N)	10000	10000	10000	10000	10000	10000	10000	10000	10000	10000
Abutment Angle (^{o})	21	21	21	21	21	21	21	21	21	21
W/H	1.25	1.07	1.07	1.18	0.38	1.25	1.07	1.07	1.18	0.38
PRELIMINARY CALCULATIONS										
Maximum Rib to Rib Pillar Length (w_2)	**28.3**	**24.0**	**56.0**	**28.5**	**28.4**	**28.3**	**24.0**	**56.0**	**28.5**	**28.4**
Minimum Rib to Rib Pillar Width (w_1)	**18.5**	**19.6**	**20.0**	**25.2**	**28.4**	**18.5**	**19.6**	**20.0**	**25.2**	**28.4**
w, Minimum Rib to Rib Pillar Width (ie $w_1 \sin\theta$)	**18.5**	**19.6**	**20.0**	**25.2**	**28.4**	**18.5**	**19.6**	**20.0**	**25.2**	**28.4**
Minimum Pillar Width/Height Ratio	**6.2**	**6.5**	**6.7**	**8.4**	**9.5**	**5.3**	**5.6**	**5.7**	**7.2**	**8.1**
Extraction Ratio (%)	**35.5%**	**36.5%**	**28.6%**	**31.2%**	**29.8%**	**35.5%**	**36.5%**	**28.6%**	**31.2%**	**29.8%**
Abutment Angle (Radians)	0.367	0.367	0.367	0.367	0.367	0.367	0.367	0.367	0.367	0.367
Cut-Through Angle (Radians)	1.571	1.571	1.571	1.571	1.571	1.571	1.571	1.571	1.571	1.571
Is the Panel Super-Critical?	Yes	Yes	Yes	Yes	No	Yes	Yes	Yes	Yes	No
D (Peng & Chiang Loading Factor)	62.829	62.829	62.829	64.890	64.890	62.829	62.829	62.829	64.890	64.890
R (Pillar 2nd Abutment Component)	0.76	0.78	0.79	0.85	0.89	0.76	0.78	0.79	0.85	0.89
Dimensionless Pillar 'Rectangularity'	1.21	1.10	1.47	1.06	1.00	1.21	1.10	1.47	1.06	1.00
Width/Height Ratio Exponent	1.00	1.00	1.00	1.00	1.00	0.76	0.87	0.90	1.00	1.00
Effective Width Factor (Omega)	1.21	1.10	1.47	1.06	1.00	1.16	1.09	1.42	1.06	1.00
Effective Width Interim	22.37	21.58	29.47	26.75	28.40	21.38	21.30	28.41	26.75	28.40
Effective Pillar Width (m)	22.37	21.58	29.47	26.75	28.40	21.38	21.30	28.41	26.75	28.40
Effective Pillar Loading Height (m)	150.00	150.00	150.00	160.00	160.00	150.00	150.00	150.00	160.00	160.00
RESULTS										
Tributary Area Loading (MPa)	**5.81**	**5.90**	**5.25**	**5.81**	**5.70**	**5.81**	**5.90**	**5.25**	**5.81**	**5.70**
Pillar Strength (UNSW Squat Pillar 1999)	**17.04**	**17.05**	**20.15**	**21.98**	**25.10**	**14.23**	**14.29**	**16.61**	**17.47**	**19.40**
Pillar Strength (UNSW w/h<5)	**N/A**	**N/A**	**N/A**	**N/A**	**N/A**	**N/A**	**N/A**	**N/A**	**N/A**	**N/A**
Safety Factor under FTA Loading (Squat Pillar)	**2.93**	**2.89**	**3.84**	**3.78**	**4.40**	**2.45**	**2.42**	**3.16**	**3.00**	**3.40**
Safety Factor under FTA Loading (w/h<5)	**N/A**	**N/A**	**N/A**	**N/A**	**N/A**	**N/A**	**N/A**	**N/A**	**N/A**	**N/A**
Single Abutment Loading (3D) - full	6.97	6.77	5.93	5.82	3.56	6.97	6.77	5.93	5.82	3.56
Single Abutment Loading (3D) - pillar	**5.32**	**5.30**	**4.68**	**4.96**	**3.18**	**5.32**	**5.30**	**4.68**	**4.96**	**3.18**
Single Abutment Loading (3D) - solid	1.65	1.47	1.24	0.85	0.39	1.65	1.47	1.24	0.85	0.39
Design Abutment Load Multiplier	1.00	1.00	1.00	1.50	1.50	1.00	1.00	1.00	1.50	1.50
Total Pillar Loading with Single Abutment Loading	12.14	12.21	10.94	12.28	10.38	12.14	12.21	10.94	12.28	10.38
Safety Factor (under Single Abutment Loading)	**1.40**	**1.40**	**1.84**	**1.79**	**2.42**	**1.17**	**1.17**	**1.52**	**1.42**	**1.87**
Total Pillar Loading @ nA	12.78	12.67	11.18	14.54	11.05	12.78	12.67	11.18	14.54	11.05
Safety Factor @ nA	**1.33**	**1.35**	**1.80**	**1.51**	**2.27**	**1.11**	**1.13**	**1.49**	**1.20**	**1.76**
Total Pillar Loading under Double Abutment Loading	19.75	19.44	17.11	17.44	12.83	19.75	19.44	17.11	17.44	12.83
Safety Factor (under Double Abutment Loading)	**0.86**	**0.88**	**1.18**	**1.26**	**1.96**	**0.72**	**0.74**	**0.97**	**1.00**	**1.51**
Elastic Model Subsidence										
Ecoal(GPa)	**1.20**	**1.20**	**1.20**	**1.20**	**1.20**	**1.20**	**1.20**	**1.20**	**1.20**	**1.20**
E1floor(GPa)	**1.50**	**1.50**	**1.50**	**1.50**	**1.50**	**1.50**	**1.50**	**1.50**	**1.50**	**1.50**
E2floor(GPa)	**4.00**	**4.00**	**4.00**	**4.00**	**4.00**	**4.00**	**4.00**	**4.00**	**4.00**	**4.00**
E1roof(GPa)	**2.50**	**2.50**	**2.50**	**2.50**	**2.50**	**2.50**	**2.50**	**2.50**	**2.50**	**2.50**
E2roof(GPa)	**4.00**	**4.00**	**4.00**	**4.00**	**4.00**	**4.00**	**4.00**	**4.00**	**4.00**	**4.00**
Poissons Ratio floor/roof	**0.25**	**0.25**	**0.25**	**0.25**	**0.25**	**0.25**	**0.25**	**0.25**	**0.25**	**0.25**
initial vertical stress (MPa)	**3.75**	**3.75**	**3.75**	**4.00**	**4.00**	**3.75**	**3.75**	**3.75**	**4.00**	**4.00**
increase in vertical stress for DA (MPa)	**2.06**	**2.15**	**1.50**	**1.81**	**8.83**	**2.06**	**2.15**	**1.50**	**1.81**	**8.83**
Roof t1	**10.00**	**2.00**	**2.00**	**2.00**	**2.00**	**10.00**	**2.00**	**2.00**	**2.00**	**2.00**
Roof t2	**8.50**	**17.60**	**18.00**	**23.20**	**26.40**	**8.50**	**17.60**	**18.00**	**23.20**	**26.40**
Roof sig1	**2.02**	**2.15**	**1.50**	**1.81**	**8.83**	**2.02**	**2.15**	**1.50**	**1.81**	**8.83**
Roof sig2	**1.59**	**1.91**	**1.33**	**1.62**	**7.90**	**1.59**	**1.91**	**1.33**	**1.62**	**7.90**
Floor t1	**6.00**	**6.00**	**6.00**	**6.00**	**6.00**	**6.00**	**6.00**	**6.00**	**6.00**	**6.00**
Floor t2	**12.5**	**13.6**	**14.0**	**19.2**	**22.4**	**12.5**	**13.6**	**14.0**	**19.2**	**22.4**
Floor sig1	**2.05**	**2.15**	**1.50**	**1.81**	**8.82**	**2.05**	**2.15**	**1.50**	**1.81**	**8.82**
Floor sig2	**1.89**	**2.00**	**1.40**	**1.74**	**8.59**	**1.89**	**2.00**	**1.40**	**1.74**	**8.59**
Pillar Compression (m)	**0.005**	**0.005**	**0.004**	**0.004**	**0.021**	**0.006**	**0.006**	**0.004**	**0.005**	**0.024**
Roof Compression (m)	**0.011**	**0.009**	**0.007**	**0.010**	**0.056**	**0.011**	**0.009**	**0.007**	**0.010**	**0.056**
Floor Compression (m)	**0.013**	**0.014**	**0.010**	**0.015**	**0.078**	**0.013**	**0.014**	**0.010**	**0.015**	**0.078**
Total FTA Compression (m)	**0.029**	**0.029**	**0.020**	**0.029**	**0.154**	**0.030**	**0.030**	**0.021**	**0.030**	**0.158**
Total Effective Compression (m)	**0.029**	**0.029**	**0.020**	**0.029**	**0.154**	**0.030**	**0.030**	**0.021**	**0.030**	**0.158**
1.5 times Effective Compression (m)	**0.043**	**0.043**	**0.031**	**0.044**	**0.232**	**0.044**	**0.045**	**0.032**	**0.045**	**0.237**
Total Yielded Panel Subs (m)	**0.14**	**0.13**	**0.11**	**0.11**	**0.22**	**0.22**	**0.20**	**0.16**	**0.13**	**0.25**
5 x Effective Predictions (m)	**0.144**	**0.145**	**0.102**	**0.145**	**0.772**	**0.148**	**0.149**	**0.105**	**0.149**	**0.789**
Bearing Capacity										
Upper Floor Unit UCS, 2*cu1 (MPa)	**20.0**	**20.0**	**20.0**	**20.0**	**20.0**	**20.0**	**20.0**	**20.0**	**20.0**	**20.0**
Upper Unit Thickness, H (m)	**6.0**	**6.0**	**6.0**	**6.0**	**6.0**	**6.0**	**6.0**	**6.0**	**6.0**	**6.0**
Lower Floor Unit UCS, 2*cu2 (MPa)	**40.0**	**40.0**	**40.0**	**40.0**	**40.0**	**40.0**	**40.0**	**40.0**	**40.0**	**40.0**
cu1/cu2	**0.5**	**0.5**	**0.5**	**0.5**	**0.5**	**0.5**	**0.5**	**0.5**	**0.5**	**0.5**
H/B	**0.32**	**0.31**	**0.30**	**0.24**	**0.21**	**0.32**	**0.31**	**0.30**	**0.24**	**0.21**
N*1	**5.68**	**5.77**	**5.81**	**6.24**	**6.51**	**5.68**	**5.77**	**5.81**	**6.24**	**6.51**
N*2	**2.84**	**2.89**	**2.90**	**3.12**	**3.25**	**2.84**	**2.89**	**2.90**	**3.12**	**3.25**
Floor Bearing Capacity (MPa)	**56.8**	**57.7**	**58.1**	**62.4**	**65.1**	**56.8**	**57.7**	**58.1**	**62.4**	**65.1**
Eff Pillar Stress (MPa)	**5.8**	**5.9**	**5.3**	**5.8**	**12.8**	**5.8**	**5.9**	**5.3**	**5.8**	**12.8**
Eff Floor Bearing Failure FoS	**9.78**	**9.78**	**11.06**	**10.74**	**5.07**	**9.78**	**9.78**	**11.06**	**10.74**	**5.07**
FTA Floor Bearing Failure FoS	**9.78**	**9.78**	**11.06**	**10.74**	**11.42**	**9.78**	**9.78**	**11.06**	**10.74**	**11.42**
Immediate Roof Unit UCS, 2*cu1 (MPa)	**40.0**	**40.0**	**40.0**	**40.0**	**40.0**	**40.0**	**40.0**	**40.0**	**40.0**	**40.0**
Immediate Roof Unit Thickness, H (m)	**10.0**	**10.0**	**10.0**	**10.0**	**10.0**	**10.0**	**10.0**	**10.0**	**10.0**	**10.0**
Upper Roof Unit UCS, 2*cu2 (MPa)	**40.0**	**40.0**	**40.0**	**40.0**	**40.0**	**40.0**	**40.0**	**40.0**	**40.0**	**40.0**
cu1/cu2	**1.0**	**1.0**	**1.0**	**1.0**	**1.0**	**1.0**	**1.0**	**1.0**	**1.0**	**1.0**
H/B	**0.54**	**0.51**	**0.50**	**0.40**	**0.35**	**0.54**	**0.51**	**0.50**	**0.40**	**0.35**
N*1	**5.14**	**5.14**	**5.14**	**5.14**	**5.14**	**5.14**	**5.14**	**5.14**	**5.14**	**5.14**
N*2	5.14	5.14	5.14	5.14	5.14	5.14	5.14	5.14	5.14	5.14
Roof Bearing Capacity (MPa)	102.8	102.8	102.8	102.8	102.8	102.8	102.8	102.8	102.8	102.8
Pillar Stress (MPa)	**5.8**	**5.9**	**5.3**	**5.8**	**12.8**	**5.8**	**5.9**	**5.3**	**5.8**	**12.8**
Effective Roof Bearing Failure FoS	**17.69**	**17.42**	**19.58**	**17.68**	**8.01**	**17.69**	**17.42**	**19.58**	**17.68**	**8.01**
FTA Roof Bearing Failure FoS	**17.69**	**17.42**	**19.58**	**17.68**	**18.04**	**17.69**	**17.42**	**19.58**	**17.68**	**18.04**
Voussoir Beam Deflection (m)		**0.004**	**0.004**	**0.001**	**0.001**		**0.004**	**0.004**	**0.001**	**0.001**
System Settlement at Base of beam (m)	0.000	0.000	0.000	0.000	0.000	0.000	0.000	0.000	0.000	0.000
Applied Pillar Stress/FTA Stress Ratio (Mpa)	1.00	1.00	1.00	1.00	1.00	1.00	1.00	1.00	1.00	1.00
Effective Pillar Stress (Mpa)	5.81	5.90	5.25	5.81	12.83	5.81	5.90	5.25	5.81	12.83
Multi-Seam Stress Inc (min)										
Multi-Seam Stress Inc (max)										
Eresidual coal(GPa)	**0.15**	**0.17**	**0.17**	**0.23**	**0.25**	**0.11**	**0.12**	**0.13**	**0.19**	**0.22**
Effective Pillar FoS	**2.93**	**2.89**	**3.84**	**3.78**	**1.96**	**2.45**	**2.42**	**3.16**	**3.00**	**1.51**
Single Seam FoS	**2.93**	**2.89**	**3.84**	**3.78**	**4.40**	**2.45**	**2.42**	**3.16**	**3.00**	**3.40**
w/h	**6.17**	**6.53**	**6.67**	**8.40**	**9.47**	**5.29**	**5.60**	**5.71**	**7.20**	**8.11**

UNSW Pillar Design Spreadsheet										
Wallarah Seam Workings	FWs				SWs	FWs				SWs
INPUT DATA										
Depth of Cover (m)	**150**	**150**	**150**	**160**	**160**	**150**	**150**	**150**	**150**	**150**
Mining Height (m)	**3**	**3**	**3**	**3**	**3**	**3.5**	**3.5**	**3.5**	**3.5**	**3.5**
Pillar Length - centres (m)	33.8	29.5	61.5	34.0	33.9	33.8	29.5	61.5	34.0	33.9
Pillar Width - centres (m)	24.0	25.1	25.5	30.7	33.9	24.0	25.1	25.5	30.7	33.9
Roadway Width for maximum pillar dimension	**5.5**	**5.5**	**5.5**	**5.5**	**5.5**	**5.5**	**5.5**	**5.5**	**5.5**	**5.5**
Roadway Width for minimum pillar dimension	**5.5**	**5.5**	**5.5**	**5.5**	**5.5**	**5.5**	**5.5**	**5.5**	**5.5**	**5.5**
Cut-Through Angle (degrees)	**90**	**90**	**90**	**90**	**90**	**90**	**90**	**90**	**90**	**90**
Average Panel Span (m) (rib-rib width)	**188**	**160**	**160**	**188**	**60**	**188**	**160**	**160**	**188**	**60**
SG (tonnes/m^3)	2.5	2.5	2.5	2.5	2.5	2.5	2.5	2.5	2.5	2.5
Conversion (tonnes to N)	10000	10000	10000	10000	10000	10000	10000	10000	10000	10000
Abutment Angle (^{o})	21	21	21	21	21	21	21	21	21	21
W/H	1.25	1.07	1.07	1.18	0.38	1.25	1.07	1.07	1.25	0.40
PRELIMINARY CALCULATIONS										
Maximum Rib to Rib Pillar Length (w_2)	**28.3**	**24.0**	**56.0**	**28.5**	**28.4**	**28.3**	**24.0**	**56.0**	**28.5**	**28.4**
Minimum Rib to Rib Pillar Width (w_1)	**18.5**	**19.6**	**20.0**	**25.2**	**28.4**	**18.5**	**19.6**	**20.0**	**25.2**	**28.4**
w, Minimum Rib to Rib Pillar Width (ie $w_1 \sin\theta$)	**18.5**	**19.6**	**20.0**	**25.2**	**28.4**	**18.5**	**19.6**	**20.0**	**25.2**	**28.4**
Minimum Pillar Width/Height Ratio	**6.2**	**6.5**	**6.7**	**8.4**	**9.5**	**5.3**	**5.6**	**5.7**	**7.2**	**8.1**
Extraction Ratio (%)	**35.5%**	**36.5%**	**28.6%**	**31.2%**	**29.8%**	**35.5%**	**36.5%**	**28.6%**	**31.2%**	**29.8%**
Abutment Angle (Radians)	0.367	0.367	0.367	0.367	0.367	0.367	0.367	0.367	0.367	0.367
Cut-Through Angle (Radians)	1.571	1.571	1.571	1.571	1.571	1.571	1.571	1.571	1.571	1.571
Is the Panel Super-Critical?	Yes	Yes	Yes	Yes	No	Yes	Yes	Yes	Yes	No
D (Peng & Chiang Loading Factor)	62.829	62.829	62.829	64.890	64.890	62.829	62.829	62.829	62.829	62.829
R (Pillar 2nd Abutment Component)	0.76	0.78	0.79	0.85	0.89	0.76	0.78	0.79	0.87	0.90
Dimensionless Pillar 'Rectangularity'	1.21	1.10	1.47	1.06	1.00	1.21	1.10	1.47	1.06	1.00
Width/Height Ratio Exponent	1.00	1.00	1.00	1.00	1.00	0.76	0.87	0.90	1.00	1.00
Effective Width Factor (Omega)	1.21	1.10	1.47	1.06	1.00	1.16	1.09	1.42	1.06	1.00
Effective Width Interim	22.37	21.58	29.47	26.75	28.40	21.38	21.30	28.41	26.75	28.40
Effective Pillar Width (m)	22.37	21.58	29.47	26.75	28.40	21.38	21.30	28.41	26.75	28.40
Effective Pillar Loading Height (m)	150.00	150.00	150.00	160.00	160.00	150.00	150.00	150.00	150.00	150.00
RESULTS										
Tributary Area Loading (MPa)	**5.81**	**5.90**	**5.25**	**5.81**	**5.70**	**5.81**	**5.90**	**5.25**	**5.45**	**5.34**
Pillar Strength (UNSW Squat Pillar 1999)	**17.04**	**17.05**	**20.15**	**21.98**	**25.10**	**14.23**	**14.29**	**16.61**	**17.47**	**19.40**
Pillar Strength (UNSW w/h<5)	**N/A**	**N/A**	**N/A**	**N/A**	**N/A**	**N/A**	**N/A**	**N/A**	**N/A**	**N/A**
Safety Factor under FTA Loading (Squat Pillar)	**2.93**	**2.89**	**3.84**	**3.78**	**4.40**	**2.45**	**2.42**	**3.16**	**3.21**	**3.63**
Safety Factor under FTA Loading (w/h<5)	**N/A**	**N/A**	**N/A**	**N/A**	**N/A**	**N/A**	**N/A**	**N/A**	**N/A**	**N/A**
Single Abutment Loading (3D) - full	6.97	6.77	5.93	5.82	3.56	6.97	6.77	5.93	5.11	3.28
Single Abutment Loading (3D) - pillar	**5.32**	**5.30**	**4.68**	**4.96**	**3.18**	**5.32**	**5.30**	**4.68**	**4.43**	**2.96**
Single Abutment Loading (3D) - solid	1.65	1.47	1.24	0.85	0.39	1.65	1.47	1.24	0.68	0.32
Design Abutment Load Multiplier	1.00	1.00	1.00	1.50	1.50	1.00	1.00	1.00	1.50	1.50
Total Pillar Loading with Single Abutment Loading	12.14	12.21	10.94	12.28	10.38	12.14	12.21	10.94	11.38	9.80
Safety Factor (under Single Abutment Loading)	**1.40**	**1.40**	**1.84**	**1.79**	**2.42**	**1.17**	**1.17**	**1.52**	**1.54**	**1.98**
Total Pillar Loading @ nA	12.78	12.67	11.18	14.54	11.05	12.78	12.67	11.18	13.12	10.26
Safety Factor @ nA	**1.33**	**1.35**	**1.80**	**1.51**	**2.27**	**1.11**	**1.13**	**1.49**	**1.33**	**1.89**
Total Pillar Loading under Double Abutment Loading	19.75	19.44	17.11	17.44	12.83	19.75	19.44	17.11	15.67	11.90
Safety Factor (under Double Abutment Loading)	**0.86**	**0.88**	**1.18**	**1.26**	**1.96**	**0.72**	**0.74**	**0.97**	**1.11**	**1.63**
Elastic Model Subsidence										
Ecoal(GPa)	**1.20**	**1.20**	**1.20**	**1.20**	**1.20**	**1.20**	**1.20**	**1.20**	**1.20**	**1.20**
E1floor(GPa)	**1.50**	**1.50**	**1.50**	**1.50**	**1.50**	**1.50**	**1.50**	**1.50**	**1.50**	**1.50**
E2floor(GPa)	**4.00**	**4.00**	**4.00**	**4.00**	**4.00**	**4.00**	**4.00**	**4.00**	**4.00**	**4.00**
E1roof(GPa)	**2.50**	**2.50**	**2.50**	**2.50**	**2.50**	**2.50**	**2.50**	**2.50**	**2.50**	**2.50**
E2roof(GPa)	**4.00**	**4.00**	**4.00**	**4.00**	**4.00**	**4.00**	**4.00**	**4.00**	**4.00**	**4.00**
Poissons Ratio floor/roof	**0.25**	**0.25**	**0.25**	**0.25**	**0.25**	**0.25**	**0.25**	**0.25**	**0.25**	**0.25**
initial vertical stress (MPa)	**3.75**	**3.75**	**3.75**	**4.00**	**4.00**	**3.75**	**3.75**	**3.75**	**3.75**	**3.75**
increase in vertical stress for DA (MPa)	**4.56**	**4.65**	**4.00**	**4.31**	**11.33**	**6.06**	**6.15**	**5.50**	**5.70**	**5.59**
Roof t1	**10.00**	**2.00**	**2.00**	**2.00**	**2.00**	**10.00**	**2.00**	**2.00**	**2.00**	**2.00**
Roof t2	**8.50**	**17.60**	**18.00**	**23.20**	**26.40**	**8.50**	**17.60**	**18.00**	**23.20**	**26.40**
Roof sig1	**4.48**	**4.65**	**4.00**	**4.31**	**11.33**	**5.95**	**6.15**	**5.50**	**5.70**	**5.59**
Roof sig2	**3.52**	**4.13**	**3.55**	**3.85**	**10.14**	**4.68**	**5.46**	**4.89**	**5.09**	**5.01**
Floor t1	**6.00**	**6.00**	**6.00**	**6.00**	**6.00**	**6.00**	**6.00**	**6.00**	**6.00**	**6.00**
Floor t2	**12.5**	**13.6**	**14.0**	**19.2**	**22.4**	**12.5**	**13.6**	**14.0**	**19.2**	**22.4**
Floor sig1	**4.54**	**4.64**	**3.99**	**4.31**	**11.32**	**6.04**	**6.13**	**5.48**	**5.69**	**5.59**
Floor sig2	**4.18**	**4.31**	**3.72**	**4.15**	**11.02**	**5.55**	**5.71**	**5.12**	**5.48**	**5.44**
Pillar Compression (m)	**0.011**	**0.011**	**0.009**	**0.010**	**0.027**	**0.017**	**0.017**	**0.015**	**0.016**	**0.015**
Roof Compression (m)	**0.024**	**0.021**	**0.018**	**0.024**	**0.071**	**0.032**	**0.027**	**0.025**	**0.032**	**0.035**
Floor Compression (m)	**0.029**	**0.031**	**0.027**	**0.035**	**0.100**	**0.039**	**0.041**	**0.037**	**0.046**	**0.050**
Total FTA Compression (m)	**0.064**	**0.063**	**0.055**	**0.069**	**0.198**	**0.087**	**0.085**	**0.077**	**0.094**	**0.100**
Total Effective Compression (m)	**0.064**	**0.063**	**0.055**	**0.069**	**0.198**	**0.087**	**0.085**	**0.077**	**0.094**	**0.100**
1.5 times Effective Compression (m)	**0.096**	**0.094**	**0.082**	**0.104**	**0.297**	**0.131**	**0.128**	**0.116**	**0.140**	**0.150**
Total Yielded Panel Subs (m)	**0.18**	**0.17**	**0.14**	**0.15**	**0.27**	**0.28**	**0.25**	**0.22**	**0.19**	**0.18**
5 x Effective Predictions (m)	**0.319**	**0.313**	**0.273**	**0.346**	**0.990**	**0.436**	**0.426**	**0.386**	**0.468**	**0.500**
Bearing Capacity										
Upper Floor Unit UCS, 2*cu1 (MPa)	**20.0**	**20.0**	**20.0**	**20.0**	**20.0**	**20.0**	**20.0**	**20.0**	**20.0**	**20.0**
Upper Unit Thickness, H (m)	**6.0**	**6.0**	**6.0**	**6.0**	**6.0**	**6.0**	**6.0**	**6.0**	**6.0**	**6.0**
Lower Floor Unit UCS, 2*cu2 (MPa)	**40.0**	**40.0**	**40.0**	**40.0**	**40.0**	**40.0**	**40.0**	**40.0**	**40.0**	**40.0**
cu1/cu2	**0.5**	**0.5**	**0.5**	**0.5**	**0.5**	**0.5**	**0.5**	**0.5**	**0.5**	**0.5**
H/B	**0.32**	**0.31**	**0.30**	**0.24**	**0.21**	**0.32**	**0.31**	**0.30**	**0.24**	**0.21**
N*1	**5.68**	**5.77**	**5.81**	**6.24**	**6.51**	**5.68**	**5.77**	**5.81**	**6.24**	**6.51**
N*2	**2.84**	**2.89**	**2.90**	**3.12**	**3.25**	**2.84**	**2.89**	**2.90**	**3.12**	**3.25**
Floor Bearing Capacity (MPa)	**56.8**	**57.7**	**58.1**	**62.4**	**65.1**	**56.8**	**57.7**	**58.1**	**62.4**	**65.1**
Eff Pillar Stress (MPa)	**8.3**	**8.4**	**7.8**	**8.3**	**15.3**	**9.8**	**9.9**	**9.3**	**9.5**	**9.3**
Eff Floor Bearing Failure FoS	**6.84**	**6.87**	**7.49**	**7.51**	**4.25**	**5.79**	**5.83**	**6.28**	**6.60**	**6.97**
FTA Floor Bearing Failure FoS	**9.78**	**9.78**	**11.06**	**10.74**	**11.42**	**9.78**	**9.78**	**11.06**	**11.45**	**12.18**
Immediate Roof Unit UCS, 2*cu1 (MPa)	**40.0**	**40.0**	**40.0**	**40.0**	**40.0**	**40.0**	**40.0**	**40.0**	**40.0**	**40.0**
Immediate Roof Unit Thickness, H (m)	**10.0**	**10.0**	**10.0**	**10.0**	**10.0**	**10.0**	**10.0**	**10.0**	**10.0**	**10.0**
Upper Roof Unit UCS, 2*cu2 (MPa)	**40.0**	**40.0**	**40.0**	**40.0**	**40.0**	**40.0**	**40.0**	**40.0**	**40.0**	**40.0**
cu1/cu2	**1.0**	**1.0**	**1.0**	**1.0**	**1.0**	**1.0**	**1.0**	**1.0**	**1.0**	**1.0**
H/B	**0.54**	**0.51**	**0.50**	**0.40**	**0.35**	**0.54**	**0.51**	**0.50**	**0.40**	**0.35**
N*1	**5.14**	**5.14**	**5.14**	**5.14**	**5.14**	**5.14**	**5.14**	**5.14**	**5.14**	**5.14**
N*2	5.14	5.14	5.14	5.14	5.14	5.14	5.14	5.14	5.14	5.14
Roof Bearing Capacity (MPa)	102.8	102.8	102.8	102.8	102.8	102.8	102.8	102.8	102.8	102.8
Pillar Stress (MPa)	**8.3**	**8.4**	**7.8**	**8.3**	**15.3**	**9.8**	**9.9**	**9.3**	**9.5**	**9.3**
Effective Roof Bearing Failure FoS	**12.37**	**12.23**	**13.26**	**12.37**	**6.71**	**10.48**	**10.38**	**11.11**	**10.88**	**11.00**
FTA Roof Bearing Failure FoS	**17.69**	**17.42**	**19.58**	**17.68**	**18.04**	**17.69**	**17.42**	**19.58**	**18.86**	**19.24**
Voussoir Beam Deflection (m)		**0.004**	**0.004**	**0.001**	**0.001**		**0.004**	**0.004**	**0.001**	**0.001**
System Settlement at Base of beam (m)	0.000	0.000	0.000	0.000	0.000	0.000	0.000	0.000	0.000	0.000
Applied Pillar Stress/FTA Stress Ratio (Mpa)	1.00	1.00	1.00	1.00	1.00	1.00	1.00	1.00	1.00	1.00
Effective Pillar Stress (Mpa)	8.31	8.40	7.75	8.31	15.33	9.81	9.90	9.25	9.45	9.34
Multi-Seam Stress Inc (min)	**-3**	**-3**	**-3**	**-3**	**-3**	**4**	**4**	**4**	**4**	**4**
Multi-Seam Stress Inc (max)	**2.50**	**2.50**	**2.50**	**2.50**	**2.50**	**4.00**	**4.00**	**4.00**	**4.00**	**4.00**
Eresidual coal(GPa)	**0.15**	**0.17**	**0.17**	**0.23**	**0.25**	**0.11**	**0.12**	**0.13**	**0.19**	**0.22**
Effective Pillar FoS	**2.05**	**2.03**	**2.60**	**2.64**	**1.64**	**1.45**	**1.44**	**1.80**	**1.85**	**2.08**
Single Seam FoS	**2.93**	**2.89**	**3.84**	**3.78**	**4.40**	**2.45**	**2.42**	**3.16**	**3.21**	**3.63**
w/h	**6.17**	**6.53**	**6.67**	**8.40**	**9.47**	**5.29**	**5.60**	**5.71**	**7.20**	**8.11**



EMM
EMGA Mitchell McLennan

www.emgamm.com

SYDNEY
Ground Floor, Suite 1, 20 Chandos Street
St Leonards NSW 2065
T 02 9493 9500 F 02 9493 9599

NEWCASTLE
Level 5, 21 Bolton Street
Newcastle NSW 2300
T 02 4927 0506 F 02 4926 1312

BRISBANE
Suite 1, Level 4, 87 Wickham Terrace
Spring Hill Queensland 4000
T 07 3839 1800 F 07 3839 1866

LakeCoal